John D. Clayton

Nonlinear Mechanics of Crystals

Springer

Nonlinear Mechanics of Crystals

SOLID MECHANICS AND ITS APPLICATIONS
Volume 177

Aims and Scope of the Series

The fundamental questions arising in mechanics are: *Why?*, *How?*, and *How much?* The aim of this series is to provide lucid accounts written by authoritative researchers giving vision and insight in answering these questions on the subject of mechanics as it relates to solids.

The scope of the series covers the entire spectrum of solid mechanics. Thus it includes the foundation of mechanics; variational formulations; computational mechanics; statics, kinematics and dynamics of rigid and elastic bodies: vibrations of solids and structures; dynamical systems and chaos; the theories of elasticity, plasticity and viscoelasticity; composite materials; rods, beams, shells and membranes; structural control and stability; soils, rocks and geomechanics; fracture; tribology; experimental mechanics; biomechanics and machine design.

The median level of presentation is the first year graduate student. Some texts are monographs defining the current state of the field; others are accessible to final year undergraduates; but essentially the emphasis is on readability and clarity.

John D. Clayton

Nonlinear Mechanics
of Crystals

Springer

John D. Clayton
US Army Research Laboratory
RDRL-WMP-B
Bldg 390, Room 212
Aberdeen Proving Ground
Maryland 21005-5066
USA
jdclayt@comcast.net

Cover design: SPI Publisher Services

Printed on acid-free paper

Springer is part of Springer Science+Business Media (www.springer.com)

Preface

This book presents mathematical descriptions of behavior of crystalline solids following theoretical methods of modern continuum mechanics. Emphasis is placed on geometrically nonlinear descriptions, i.e., finite or large deformations. Topics include elasticity, plasticity, and ways of representing effects of distributions of defects or flaws in the solid on the material's thermomechanical response. Defects may include crystal dislocations, point defects such as vacancies or interstitial atoms, rotational defects, deformation twins, voids or pores, and micro-cracks. Representative substances towards which modeling techniques forwarded here may be applied are single crystalline and polycrystalline metals and alloys, ceramics, minerals, and other geologic materials and their constituents.

An early and substantial part of the text is devoted to kinematics of finite deformations, multiplicative inelasticity, and representations of lattice defects in a differential-geometric setting. An accurate depiction of kinematics is deemed necessary in order to accompany rigorous models of thermodynamics and kinetics of material behavior, since kinematic assumptions tend to enter, implicitly or explicitly, subsequent thermodynamic and kinetic relations. Descriptions and derivations of fundamental mechanical and thermodynamic balance laws and inequalities are then given. Constitutive frameworks are provided for representing thermomechanical behaviors of various classes of crystalline materials: elastic solids, elastic-plastic solids, generalized inelastic solids with lattice defects, and dielectric solids. In each case, material responses corresponding to large deformations are emphasized, though complementary geometrically linear theories are included in some cases for completeness and for comparison with their nonlinear counterparts. General kinetic concepts are described, but relatively less attention is directed towards development of specific kinetic relations, since these tend to be more strongly dependent upon microstructures of particular materials (e.g., crystal structure or chemical composition) within each general class of materials considered. Appendices provide supporting discussion on crystal symmetry and material coefficients, atomistic methods (i.e., lattice statics and origins of stress and elastic coefficients), and elastic models of discrete line and point defects in crystals. The content of this book consists of a combination of the author's

interpretation and consolidation of existing science from historic and more recent literature, as well as a number of novel—and sometimes less conventional—theoretical modeling concepts, the latter often presented, developed, or refined by the author (and collaborators in many cases) in a number of archival publications over the past ten years. With a few exceptions, the text is written in the context of generalized (e.g., curvilinear) coordinates, a rarity among other recent texts and monographs dealing with similar subject matter.

This book is intended for use by scientists and engineers involved in advanced constitutive modeling of nonlinear mechanical behavior of crystalline materials. Knowledge of fundamentals of continuum mechanics and tensor calculus is a prerequisite for accessing much of the material in the text. The book could conceivably be used as supplemental material in graduate-level courses in continuum mechanics, elasticity, plasticity, micromechanics, or dislocation mechanics, for students in various disciplines of engineering, materials science, applied mathematics, or condensed matter physics.

A number of individuals have contributed, directly or indirectly, to the content or production of this work; a number have suggested specific changes to early drafts resulting in significant overall improvement to the final manuscript. Technical discussions, interactions, and/or close collaborations with the following individuals over the past decade are gratefully acknowledged (in alphabetical order): Doug Bammann, Peter Chung, Datta Dandekar, Misha Grinfeld, Jarek Knap, Dave McDowell, Rich Regueiro, Mike Scheidler, and Tim Wright. However, any technical inconsistencies, unjust omissions, or errors that may remain are entirely my own. I also appreciate support and resources of the U.S. Army Research Laboratory (formerly known as U.S. Army Ballistics Research Laboratories), including a diligent library staff that was able to efficiently provide or obtain a number of historical works referenced in this text. Finally, I am most appreciative of my wife and daughter, who have remained supportive and patient during the many hours I have spent working on this book over the past 3½ years.

John D. Clayton
Aberdeen, Maryland, USA
2010

Contents

1 Introduction

1.1 Objectives and Scope

This book presents modeling techniques, primarily from the standpoint of modern continuum mechanics, for describing the nonlinear response of crystalline solids subjected to mechanical loading or deformation. This response may be deformation induced by applied loading, or the forces required to induce such deformation. Nonlinearity may emerge in the geometric sense, pertaining to finite deformations, and/or in the material sense, pertaining to nonlinear relationships among independent and dependent state variables, for example relationships between strain and stress. Though mechanical behavior is of primary interest in this book, thermodynamic principles are exercised for developing descriptions of material behavior also dependent on temperature and internal state variables and consistent with known balance laws or inequalities such as conservation of energy and production of entropy.

Though some physical and mathematical principles applicable towards descriptions of all kinds of materials are supplied in early Chapters, the content of this book is primarily focused on crystalline solids. A crystal refers to a body whose atoms occupy an ordered, repeating structure called a lattice. Defects in the crystal may disrupt the regularity of the lattice, and certain types of point, line, and surface defects are addressed explicitly in this book. A body with defects is still considered here to be crystalline so long as a large percentage of its atoms maintain a repeating, ordered structure. In various instances throughout the text, single- or polycrystalline materials are considered, as are homogeneous and heterogeneous solids. In a single crystal, the lattice is for the most part aligned in a uniform orientation, whereas a polycrystal consists of multiple single crystals or grains aligned in potentially different directions, with constituent crystals separated by grain boundaries. Heterogeneous materials exhibit spatial variations in material properties, for example composites consisting of different phases with different chemical compositions or different crystal

structures. Specific examples of heterogeneous solids include metal-matrix composites and geologic and cementious materials with several crystalline constituents, e.g., minerals of various crystal structures. In contrast, single crystals are conventionally idealized as homogeneous, at least when their defect content is low. During the course of deformation or a change in environment, initially homogeneous single crystals can become heterogeneous. For example, misoriented subgranular regions can emerge within metallic crystals deformed plastically to large strains.

Detailed consideration of material nonlinearity requires a description of microstructure and defects in the solid, including effects of such defects on kinematics of deformation and on the thermodynamic state of the material. Furthermore, kinetic relations are often required to dictate the temporal evolution of defect distributions and to account for their motions and dissipated energy during time-dependent problems. Defects considered explicitly in this text include distributions of dislocations, rotational line defects, deformation twins, vacancies, and voids.

Chapter 2 provides mathematical background used subsequently throughout the text. Chapter 2 begins with a description of general curvilinear coordinates and related definitions from differential geometry and tensor algebra on manifolds. Such definitions emerge frequently later in presentations of theories of continuously distributed lattice defects. A thorough treatment of the deformation gradient, a fundamental kinematic variable used in continuum mechanical descriptions of constitutive behavior, is provided. This treatment includes discussion of push-forward and pull-back operations, useful identities associated with the deformation gradient, and deformation measures derived from it. Chapter 2 also presents two identities from tensor calculus used often later in the text: Gauss's theorem—a particular version of which is often called the divergence theorem—and Stokes's theorem. Compatibility conditions for finite deformation are discussed, and anholonomic spaces are introduced.

Chapter 3 focuses on descriptions of deformation kinematics of crystalline bodies. This Chapter begins with the fundamental hypothesis of Cauchy and Born describing homogeneous deformations of Bravais lattice vectors and basis vectors comprising the structure of a perfect crystal. Kinematics of multiplicative inelasticity is then considered. The intermediate configuration that emerges under the assumption of multiplicative deformation gradient kinematics is addressed from a general geometric point of view, regardless of the physical origin of inelastic response. Then particular physical sources of non-recoverable deformation are treated in various kinematic descriptions. These include dislocation-based large deformation plasticity of single- and polycrystalline materials, generation and motion of point defects, porosity evolution, and sources of residual elastic

deformation of the lattice emerging from multiscale considerations. Chapter 3 then addresses generalized continua embedded with additional kinematic degrees of freedom that describe spatial gradients of deformation of lattice director vectors, whereby locally inhomogeneous deformations can often be associated with the presence of lattice defects. These additional degrees of freedom are introduced in the differential-geometric context of a linear connection on a spatial manifold whose tangent bundle is spanned by a field of deformed director vectors. Geometric properties of the connection enable physical characterization of deformation incompatibilities resulting from continuous distributions of line and point defects.

Chapter 4 features general, traditional thermodynamic relationships and balance laws governing nonlinear behaviors of continuous bodies. The discussion begins with presentation of traditional mass, momentum, and energy balances. Mappings of balance equations among configurations or deformation states are given. Thermodynamic potentials are defined. The internal state variable concept is introduced, enabling representation of effects of defects or evolving microstructure in the description of the thermodynamic state of the material. The dissipation inequality is presented, followed by a brief introduction to kinetic relations and dissipation potentials. Governing equations for generalized continua supporting higher-order stresses (e.g., couple stresses) and those incorporating electromechanical effects are addressed on a case-by-case basis in later Chapters.

Chapter 5 considers elastically deforming solids, a description most applicable to defect-free crystals or to those wherein any effects of defects are not considered explicitly. Constitutive functions and thermodynamic relationships are presented for crystals displaying a hyperelastic response with temperature changes. Thermoelastic material coefficients pertinent to arbitrary three-dimensional stress states, and then those specifically applicable to (but not always limited to) spherical stress states, are defined or derived. Reductions of the general theory of nonlinear anisotropic thermoelasticity under conditions of material linearity, geometric linearity, and isotropic symmetry are described. A thorough presentation of symmetry operations, anisotropy, and material coefficients for all thirty-two crystal classes is provided as supplementary supporting material in Appendix A. An alternative version of finite elasticity with explicitly delineated mechanical and thermal deformations is then developed. Next, Lagrangian field theory of elasticity is presented, wherein governing equations are deduced from Hamilton's principle. Chapter 5 concludes with a discussion of second-grade hyperelasticity, a kind of generalized continuum theory.

Chapter 6 deals with elastoplastic materials. The kinematic description consists of a multiplicative decomposition of the deformation gradient into two terms: the lattice-altering thermoelastic deformation associated with

mechanical stresses and temperature changes, and the lattice-preserving plastic deformation resulting from glide of dislocations. Thermodynamic relationships are derived via consideration of thermodynamic potentials on a per-unit-volume basis in the thermoelastically unloaded intermediate configuration. A variant of the so-called Eshelby stress emerges as a work conjugate stress measure to the plastic velocity gradient. This stress measure is examined in some detail in a later Section of Chapter 6. The stored energy of cold working—reflected via internal state variables related to defects and microstructural features—is considered. Specific applications of the general finite deformation theory towards describing plasticity resulting from distributed line defects (i.e., dislocation dynamics) and crystallographic slip on discrete glide systems (i.e., crystal plasticity) are discussed in turn. Kinetic equations for plastic flow and time rates of internal variables are considered briefly in each case. Reduction of the finite deformation theory to geometrically linear elastoplasticity is presented for completeness. Chapter 6 concludes with description of a generalized continuum theory incorporating second-grade elasticity with multiplicative elastic-plastic kinematics.

Chapter 7 addresses large deformation kinematics and internal forces arising from defects in crystalline solids by combining a nonlinear kinematic description with multiscale averaging concepts. An element of material containing defects such as dislocation lines and loops is considered. The average deformation gradient for this element is decomposed multiplicatively into terms accounting for effects of dislocation flux, recoverable elastic stretch and rotation, and residual elastic deformation associated with self-equilibrating internal forces induced by defects. Two methods are considered for quantifying the average residual elastic deformation gradient: continuum nonlinear elasticity and discrete lattice statics. Volume changes resulting from point defects such as vacancies are discussed in the final Section of Chapter 7. Supporting background information on lattice statics pertinent to the content of Chapter 7, including atomic origins of elasticity coefficients, is provided in Appendix B. Pertinent supporting information on residual elastic stress fields and strain energies induced by line and point defects is provided in Appendix C.

Chapter 8 extends the introductory treatment of crystal plasticity developed in Chapter 6 to encompass thermoelasticity, residual elastic volume changes, plastic slip, and mechanical twinning in anisotropic single crystals subjected to arbitrarily large deformations. Dislocation glide and deformation twinning are treated as dissipative mechanisms, while energy storage mechanisms associated with dislocation lines and twin boundaries are described via internal state variables. Shear strain rates for discrete glide and twinning systems are modeled explicitly. Residual elastic vol-

ume changes, predicted from nonlinear elasticity using theoretical methods developed in Chapter 7, are proportional to dislocation line length per unit volume and twin boundary area per unit volume.

Chapter 9 broadens the constitutive description of elastoplastic materials to encompass a number of more general modes of inelastic deformation. The kinematic description forwarded in Chapter 9 features a three-term decomposition of the deformation gradient into recoverable elastic deformation, lattice-preserving plastic deformation, and an intermediate term associated with irreversible lattice rearrangements. A general thermodynamic analysis proceeds with the intermediate term of the deformation gradient entering the thermodynamic potentials as a generic independent state variable, leading to general constitutive relationships and a reduced dissipation inequality. Particular versions of this generic framework for inelasticity are then developed to address physics of isotropic void growth, pore compaction, and residual lattice deformation from defects. The last Section of Chapter 9 describes a second-grade theory of elastoplasticity accounting for geometrically necessary dislocations and disclinations. Micropolar kinematics and microscopic balance laws featuring higher-order stresses enter the description. This nonlocal theory is intended to represent the constitutive response of ductile crystals exhibiting drastic microstructural changes such as grain refinement occurring during severe plastic deformation processes.

Chapter 10 depicts the geometrically nonlinear response of dielectric crystalline solids. A dielectric crystal is defined as an insulator (i.e., a non-conductor of electricity) that may exhibit electric polarization. Maxwell's complete set of electrodynamic equations are presented; however, electrodynamics and magnetization are not formally addressed in the constitutive theory developed later in Chapter 10. Rather, mechanical, thermal, and quasi-electrostatic behaviors, and their couplings, are considered simultaneously. Forces of electromechanical origin contribute to balance laws of momentum and energy and the dissipation inequality, resulting in discrepancies from the traditional continuum mechanical description of Chapter 4. In particular, the presence of Maxwell's stress associated with nonlinear electromechanics can render the Cauchy stress, as defined in the present context, non-symmetric. A thermodynamic treatment is developed that addresses dielectric, piezoelectric, pyroelectric, and electrostrictive phenomena. Material coefficients of various orders, and relationships among these coefficients, are defined or derived. Reduction of the nonlinear theory to the traditional geometrically and materially linear theory of piezoelectric materials is presented for completeness.

The following topics are not addressed extensively in this book: viscoelastic behavior, lattice vibrations, acoustic wave propagation, electrody-

namics (including optics), electrical conduction, magnetism, phase transformations, mass transport, liquid crystals, or fracture mechanics of discrete cracks. Brief coverage of atomic lattice statics and dynamics is given in Appendix B; this Appendix does not, however, contain a complete description of classical particle mechanics, nor does it include discussion of electronic structure or fundamental topics in quantum mechanics.

Because of the inherent nonlinearity of many of the models presented, numerical methods become necessary for obtaining solutions of the governing equations of mechanics when used in conjunction with many constitutive relationships discussed in this book. Methods for numerically approximating solutions of governing equations (with requisite boundary and initial conditions) of thermomechanical problems involving nonlinear constitutive models are beyond the scope of this book. Discussions of solutions of specific boundary value problems are primarily limited, in this book, to those considered in the context of discrete, elastic defect models of Appendix C.

1.2 Background

An attempt to provide adequate historical perspective for the content of this book would require an entire volume in itself. Instead, a brief collection of books and review articles is suggested below, and presumably adequate historical context can be found, collectively, in these references. The list is limited to books and review articles published in the 20th century or later, and is divided into relevant categories. Some of the listed references clearly could belong to multiple categories. Omission of other relevant references is certain but is not intentional; those references listed below have been particularly useful during preparation of this book.

- Mathematics and geometry: Eisenhart (1926), Schouten (1954), Brillouin (1964), Marsden and Hughes (1983), Epstein and Elzanowski (2007)
- Continuum mechanics: Eringen (1962), Sedov (1966), Malvern (1969), Gurtin (1981)
- Elasticity: Love (1927), Landau and Lifshitz (1959), Wang and Truesdell (1973), Thurston (1974)
- Plasticity: Hill (1950), Schmid and Boas (1950), Kocks et al. (1975), Lubliner (1990), Havner (1992), Khan and Huang (1995), Nemat-Nasser (2004)

- Defect mechanics and micromechanics: Eshelby (1956), Nabarro (1967), Hirth and Lothe (1982), Mura (1982), Teodosiu (1982), Nemat-Nasser and Hori (1999), Phillips (2001), Buryachenko (2007)
- Electromechanics: Stratton (1941), Landau and Lifshitz (1960), Maugin (1988), Jackson (1999)

Also notable are books of Born and Huang (1954), Maradudin et al. (1971), and Wallace (1972) that consider atomic, and in some instances quantum mechanical, origins of thermoelastic and/or electromechanical behavior in crystals. Finally, works by Truesdell and Toupin (1960) and Truesdell and Noll (1965), the former with an Appendix by Ericksen (1960), address many relevant topics in mechanics and provide an extensive bibliography of historical contributions to the field.

1.3 Notation

Throughout the text, boldface type is generally used to denote vectors and tensors of higher order, while italic type is usually used for scalars and individual components of vectors and tensors. Notable exceptions are the zero vector and null tensor, both of which are simply written in Roman font (i.e., not boldface).

The index notation is used frequently for describing vector and tensor variables. The index notation complements the direct or boldface notation, often providing increased clarification. Another advantage of the index notation is that it is straightforwardly converted to computer programming languages enabling matrix operations (e.g., addition and multiplication) often involved in numerical solutions of boundary value problems. The Einstein summation convention is followed unless noted otherwise, with summation implied over repeated contravariant (superscript) and covariant (subscript) pairs. For example, a scalar or dot product is computed as $V^a W_a = V^1 W_1 + V^2 W_2 + V^3 W_3$ for components of contravariant vector **V** and covariant vector **W** in three-dimensional vector space.

In the index notation, fonts used for indices of vectors and higher-order tensors also follow a certain convention. Specifically, indices associated with the spatial (i.e., deformed or current) configuration are usually written in lower case Roman font, e.g., V^a. Indices associated with the reference (i.e., undeformed or initial) configuration are usually written in upper case Roman font, e.g., V^A. Indices associated with other configurations (for example, one or more intermediate configuration(s) of multiplicative inelasticity) are usually written in Greek font, e.g., V^α.

Regarding higher-order tensors, indices in parentheses are symmetric, and indices in braces are anti-symmetric (i.e., skew). For example, let A_{ab} be covariant components of an arbitrary second-order tensor **A**. Then $A_{(ab)} = (1/2)(A_{ab} + A_{ba})$, $A_{[ab]} = (1/2)(A_{ab} - A_{ba})$, and $A_{(ab)} + A_{[ab]} = A_{ab}$.

Following the usual notation scheme of continuum mechanics, labels "order" and "rank" are used interchangeably throughout the text to denote the total number of associated indices (both contravariant and covariant) of tensors, matrices, and more general mathematical objects. For example, a tensor **A** with contravariant components A^{ab} is said to be of second order, or rank two. A vector can be interpreted as a tensor of rank one, and a scalar can be considered a tensor of rank zero. The term "rank" as used here differs from formal definitions often encountered in linear algebra, wherein the rank of a matrix can depend on the number of linearly independent rows or columns in that matrix.

Another notational scheme concerns the differentiability of mathematical functions. Terms "sufficiently differentiable" and "sufficiently smooth" are used interchangeably throughout the text to specify that derivatives of adequate order exist, enabling validity of mathematical formulae or definitions in a given context. Formally, the term "smooth" usually refers to a function of class C^{∞}, while "sufficiently smooth" as used herein can be a weaker, i.e., less stringent, requirement.

An additional point of clarification involves notation for the square root operation. Let x denote a scalar. Then the square root and its reciprocal are written in this book as $\sqrt{x} = x^{1/2}$ and $\sqrt[-2]{x} = 1/\sqrt{x} = x^{-1/2}$, respectively. Hence, $\sqrt[-1]{x} \neq x^{-1}$ for any x. To avoid confusion, roots other than the second are written as exponents, i.e., as $x^{1/n}$ ($n \neq \pm 2$) rather than as $\sqrt[n]{x}$.

In many cases, derivations of equations and relationships are written out in full, including algebraic and indicial manipulations that experienced readers may find routine. While such a presentation results in some rather lengthy equations, it is hoped that the derivations will provide insight, for the novice, into the final expressions so obtained and enable the reader to easily verify correctness of the results. An attempt is made to minimize use of the same symbol to represent quantities with different meanings; when such duplication is unavoidable, the meaning of a given symbol is clarified either explicitly or implicitly from the context in which it is used.

Certain literary conventions are used throughout the text, and some of these should be clear to the reader already. References are labeled in (author year) format and are compiled alphabetically at the end of the book, rather than in footnotes or on a chapter-by-chapter basis. References to historical works published prior to year 1900 are omitted. Author's names

of non-Anglican origin are written in standard English language, with special characters replaced in some cases by letters most similar in appearance. A subject index is provided at the end of the book, following the list of references.

2 Mathematical Foundations

Chapter 2 includes notation, definitions, and a number of identities that are applied subsequently in later Chapters of the text. Emphasized are differential-geometric aspects of kinematics of finite deformations, linear connections and covariant differentiation, the deformation gradient of continuum mechanics, time derivatives and rate kinematics, theorems of Gauss and Stokes, and compatibility conditions.

As will be clear in later Chapters, from the standpoint of crystals with defects, a geometric approach is advantageous for dealing with incompatible material configurations not globally homeomorphic to, i.e., configurations topologically inequivalent to, three-dimensional Euclidean space (Eckart 1948; Kondo 1949, 1964; Bilby et al. 1955; Truesdell and Noll 1965; Noll 1967; Teodosiu 1967a, b). Detailed descriptions invoking formalisms of tensor algebra and tensor calculus on differential manifolds have been devoted elsewhere to elasticity theory (Marsden and Hughes 1983; Yavari et al. 2006) and general nonlinear continuum mechanics (Van der Giessen and Kollmann 1996; Stumpf and Hoppe 1997; Clayton et al. 2005; Epstein and Elzanowski 2007). In many instances, the differential-geometric approach is favored over conventional Cartesian formulations for the former's generality in terms of available choices of coordinates (e.g., curvilinear coordinates in the former versus rectangular coordinates in the latter) and representation of spaces with non-vanishing curvature (e.g., curved surfaces such as shells). Compact, coordinate-free (i.e., component-free) representations are possible for many mathematical expressions and identities, and have become popular among many authors in recent literature. However, coordinate-based representations are frequently exercised in this text for clarity of presentation and for drawing comparisons with other treatments from historic and more recent literature. Hence, the index notation is used often in Chapter 2, especially in the context of geometric objects such as connections, torsion, curvature, and important properties and mathematical identities for these objects.

Included in Chapter 2 is only that content deemed relevant and necessary for development of theories of material behavior in later Chapters. Comprehensive supplementary treatment of topics in differential geometry can be found in historical texts of Eisenhart (1926) and Schouten (1954),

while more modern presentations can be found in monographs of Boothby (1975) and Kosinski (1993). In-depth descriptions of continuum mechanics in the setting of general curvilinear coordinates and finite deformations can be found in a number of texts, including those of Truesdell and Toupin (1960), Eringen (1962), Sedov (1966), Malvern (1969), Wang and Truesdell (1973), and Marsden and Hughes (1983).

2.1 Geometric Description of a Deformable Body

Section 2.1 addresses the following topics: terminology of geometric spaces in the context of continuum mechanics; configurations of a body subjected to large deformations; manifolds and associated tangent and cotangent spaces; coordinate systems; basis vectors and their reciprocal vectors; and metric tensors.

2.1.1 Terminology

The definitions given immediately below are free of notation and hence are somewhat qualitative. More precise mathematical formulae and supplementary figures follow in Section 2.1.2 and later in Section 2.2.

A configuration denotes a time-dependent realization of a body. A body is said to consist of a number of material particles, each encompassing a representative set of atoms or molecules pertinent to the scale of resolution afforded by the continuum description. A configuration may be actual or virtual (i.e., real or fictitious). In finite deformation continuum mechanics, the terms reference, initial, undeformed, or Lagrangian configuration most often refer to a description of the body at zero time, though broader definitions enabling multiple and evolving reference configurations are possible. Similarly, the current, spatial, deformed, or Eulerian configuration usually corresponds to the current instant of time. In the absence of discontinuities, reference and current configurations are holonomic to one another, implying that current coordinates of a material particle can be written as single-valued functions of reference coordinates of that particle, and vice-versa. In contrast, as will be demonstrated in Chapter 3, a virtual intermediate, relaxed, or unloaded configuration is often introduced, for example to describe crystals with distributions of defects or those undergoing large inelastic deformations. Such an intermediate configuration is anholonomic when its "coordinates" cannot be prescribed as single-valued functions of reference or current coordinates of material particles. The term placement

(Noll 1967; Maugin 1993) has also been used to refer to a configuration of a deformable body.

A connection is a rank three construct that enables evaluation of the co-variant derivative of vectors and tensors of higher rank. The covariant derivative operation defines the connection coefficients, also called Christof-fel symbols of the connection in the context of Riemannian geometry. The content of this book only deals with linear connections, also called affine connections. Nonlinear connections can arise in more generalized spaces such as Finsler spaces (Rund 1959; Bejancu 1990) and are not addressed in this text.

A metric tensor, or simply a metric, is a rank two covariant tensor that defines the scalar product of contravariant vectors, and consequently, the squared length of a vector. A metric tensor that is both symmetric and positive definite is called a Riemannian metric tensor[1]; non-Riemannian metrics are not considered explicitly in this text. Metric tensors perform other consequential functions, such as raising and lowering of vector and tensor indices and defining scalar products of higher-order tensors.

A particular configuration can be assigned more than one connection, just as it can be assigned more than one metric tensor. The pair of {configuration, connection} or triplet of {configuration, connection, metric tensor} can often be classified as one or more of the following five types of geometric spaces: Euclidean, anholonomic, non-metric, Cartan, and/or Riemannian.

For a space to be classified as Euclidean or non-Euclidean, it must include a configuration, a metric tensor, and a connection. A Euclidean space satisfies three requirements: (i) the torsion tensor of the connection vanishes, (ii) the covariant derivative of the metric tensor vanishes, and (iii) the Riemann-Christoffel curvature tensor constructed from the connection coefficients vanishes. A Euclidean *n*-space permits at each location a transformation from local, possibly curvilinear *n*-dimensional coordinates to a global *n*-dimensional Cartesian coordinate system. In continuum mechanics, both the reference and current configurations are typically viewed as three-dimensional Euclidean spaces, with the motion acting as a diffeomorphism, i.e., a differentiable homeomorphism, or a differentiable one-to-one, invertible mapping, between these two configurations (Stumpf and Hoppe 1997). Notice the distinction between Euclidean

---

[1] A non-Riemannian metric tensor need not be positive definite. Such metrics can arise in more general geometric settings such as Finsler spaces, or for example Minkowski's spacetime (Rund 1959; Synge 1960) wherein the determinant of the metric in 4-space can be negative in sign. A non-symmetric fundamental tensor was suggested in Einstein's unified field theory (Einstein 1945; Schouten 1954).

and Cartesian: a general coordinate system in the former, for example spherical coordinates in three dimensions, admits a global transformation to a more specific kind of coordinate system in the latter, i.e., coordinate axes consisting of three constant orthonormal basis vectors.

An anholonomic space is a configuration associated with a non-integrable, two-point deformation map. For example, in multiplicative elastoplasticity theory, since elastic and plastic deformation maps (i.e., tangent maps) taken individually are generally non-integrable or anholonomic functions of current and reference coordinates, respectively, the corresponding intermediate configuration is generally anholonomic. Continuous coordinates on such an anholonomic space do not exist; rather, anholonomic coordinates can be regarded as discontinuous, multi-valued functions of holonomic coordinates of the current or reference configuration. Anholonomicity is related to Cartan's torsion tensor of a special connection constructed from the non-integrable, two-point deformation map. Anholonomic coordinates are analyzed at length by Schouten (1954), and to a lesser extent, by Ericksen (1960).

Designation of a general space as metric or non-metric requires that the configuration be assigned both a linear connection and a metric tensor; i.e., one must examine the triad of {configuration, connection, metric tensor}. In a non-metric space, the covariant derivative of the metric tensor taken with respect to the connection is nonzero. On the other hand, in a metric space the covariant derivative of the metric tensor vanishes identically.

A configuration with a connection admitting a non-vanishing torsion tensor is labeled a Cartan space, sometimes called a non-symmetric space. Only the pair {configuration, connection} need be considered to enable labeling a space as Cartan or non-Cartan. A space with vanishing torsion is called a symmetric space.

For a space to be labeled as Riemannian or non-Riemannian, it must include the pair {configuration, connection}—a metric is not needed for such a designation as defined herein. A Riemannian space is defined here as a configuration with connection coefficients whose components yield a nonzero Riemann-Christoffel curvature tensor[2]. A space with non-vanishing curvature is necessarily non-Euclidean. For example, a global two-dimensional Cartesian coordinate system cannot be used to parameterize a shell unless the shell is flat. Conversely, a space with vanishing curvature is non-Riemannian and is said to be flat, and the connection in a non-Riemannian space is said to be integrable.

---

[2] The mathematical field of study traditionally referred to as Riemannian geometry considers metric spaces with vanishing torsion, but in general non-vanishing curvature (Eisenhart 1926; Schouten 1954).

Euclidean spaces by definition exclude the other four types of (non-Euclidean) spaces: anholonomic, non-metric, Cartan, and Riemannian spaces. On the other hand, the four types of non-Euclidean spaces are not mutually exclusive. The above terminology is not always consistent in the literature (Schouten 1954; Bilby et al. 1955; Kondo 1964; Noll 1967; Marsden and Hughes 1983; Steinmann 1996; Clayton et al. 2005). However, definitions given here are deemed as those used either most frequently or most logically for describing kinematics of deformable crystalline solids, as will become clear later in Chapter 3.

2.1.2 Manifolds, Coordinates, and Metrics

Denoted by $\chi_t(\mathcal{B}):\mathcal{B} \to \mathrm{E}^3$ is a smooth, invertible, time-dependent embedding of a material body $\mathcal{B}$ into three-dimensional Euclidean space E^3. The configuration of body $\mathcal{B}$ at time t is denoted by $B_t = \chi_t(\mathcal{B})$, henceforth written simply as B for $t > 0$. Initially, i.e., at $t = 0$, material particles $\mathcal{X} \in \mathcal{B}$ are said to occupy reference configuration $B_0 = \chi_0(\mathcal{B})$ and are assigned reference coordinates $X^A = \chi_0^A(\mathcal{X})$. Particles of material mapped to current configuration B are assigned spatial coordinates $x^a = \chi_t^a(\mathcal{X})$. A description of the motion of all material particles is furnished by the continuous, invertible mapping $\varphi = \chi_t \circ \chi_0^{-1}:B_0 \to B$. The $\circ$ operator denotes the composition, such that for two functions f and g, $(f \circ g)(X) = f(g(X))$. The inverse obeys $f \circ f^{-1} = i$, with i the identity operator. The local motion for a material particle identified by particular reference coordinates $X^A = \chi_0^A(\mathcal{X})$ is written φ_X. Restricting the motion so that no two material particles occupy the same spatial location may limit the domain of $\varphi(X,t)$ to open regions of the body, e.g., when two points at different referential locations of the boundary of a body may come into contact as a result of deformation. Mappings χ_0, χ_t, and φ can be applied pointwise or globally and are not vector fields. For this reason, and since these mappings may operate without explicit introduction of coordinate basis vectors, boldface notation is not used to symbolically represent these functions. As indicated implicitly already and as will be made clear later, contravariant indices (i.e., indices in the upper position) are appended to such mappings as needed when coordinate systems are involved.

A point in space occupied by the body in the reference configuration is denoted by $X \in B_0$, while a point in space occupied by the body in the

current configuration is denoted by $x \in B$. Functions depending on position in the reference configuration are denoted by $f(X)$, while functions depending on position in the current configuration are written $f(x)$. No distinction is made here between functions depending on material particle, e.g., a material description $f(X)$ (Malvern 1969), and those depending on the reference coordinates X^A of that particle, e.g., a Lagrangian description $f(\mathbf{X})$. Because the reference configuration is embedded in Euclidean space, a unique vector of coordinates $\mathbf{X}$ can always be assigned to each material particle at X. Similar arguments hold for the spatial description, since at any given time t, each location x can be assigned a unique vector of coordinates $\mathbf{x}$. Thus the notation for a function of spatial position, $f(x)$, is hereafter used interchangeably with $f(\mathbf{x})$.

In indicial notation, time-dependent components of the motion and its inverse, respectively, are expressed in functional form as

$$x^a = x^a(X,t), \ X^A = X^A(x,t). \tag{2.1}$$

The first of (2.1) implies that spatial coordinates x^a of each material particle depend upon the choice of point X, or equivalently the material particle located at that point in the reference configuration, and time t. The second of (2.1) assigns a set of reference coordinates X^A to a material particle that occupies spatial location x at time t. Spatial coordinates x^a of a material particle corresponding to location X will generally change with time as a result of motion, and spatial locations x occupied by the body at one instance of time may not coincide with those occupied at a different instance.

The manifold concept, in the context of differential geometry, is now formally introduced (Boothby 1975). An n-manifold is a set $\mathcal{M}$ such that for each point $P \in \mathcal{M}$ there is a subset $\mathcal{U}$ of $\mathcal{M}$ containing P, and a one-to-one mapping called a chart or coordinate system from $\mathcal{U}$ onto an open set in the n-dimensional space of real numbers $\mathbb{R}^n$. Multiple charts or coordinate systems may be introduced on (regions of) a given manifold. Transformations between different coordinate systems over (regions of) the manifold are assumed to be infinitely differentiable if the manifold is smooth; i.e., such changes in coordinates are of continuity class C^∞ for smooth manifolds. A collection of charts covering $\mathcal{M}$ is called an atlas. As will be discussed in Section 2.2.4, the chart of a smooth n-manifold can be embedded in n-dimensional Euclidean space E^n if and only if the curvature tensor of its corresponding Levi-Civita connection vanishes.
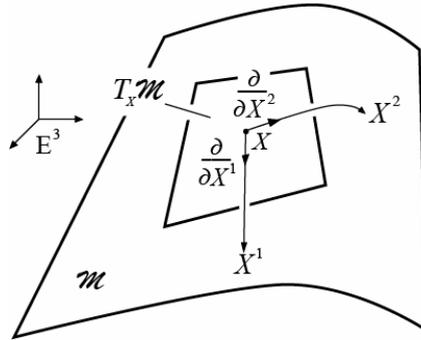
Fig. 2.1 Two-dimensional manifold embedded in 3-D Euclidean space

The tangent space of $\mathcal{M}$ at P is the n-dimensional space of contravariant vectors emanating from P, written as $T_P\mathcal{M}$. The collection of base points P and tangent vectors at all P comprises the tangent bundle $T\mathcal{M}$ (i.e., the tangent bundle is the union of tangent spaces over all points P on $\mathcal{M}$), and the map $\pi_{\mathcal{M}}$ from a tangent vector to its base point is called that vector's projection. Inverse mappings $\pi_{\mathcal{M}}^{-1}$ comprise sections of the tangent bundle. Similarly, the cotangent space of $\mathcal{M}$ at P, written as $T_P^*\mathcal{M}$, is the n-dimensional space of covariant vectors—also called covectors, one-forms, reciprocal vectors, or dual vectors—emanating from P. The cotangent bundle, denoted by $T^*\mathcal{M}$, is defined analogously to the tangent bundle, i.e., the cotangent bundle is the union of cotangent spaces over manifold $\mathcal{M}$. Shown in Fig. 2.1 is a two-dimensional manifold $\mathcal{M}$ with nonvanishing curvature embedded in E^3, with a point X described by a pair of coordinates $\mathbf{X} = (X^1, X^2)$. Tangent space $T_X\mathcal{M}$ is also shown.

Each time-dependent configuration of a deformable body can be regarded as a manifold, with locations of particles of material in that configuration identified in a one-to-one manner with points $\mathcal{X}$ of $\mathcal{B}$; the latter itself can also be viewed as a manifold since charts of smooth coordinates (e.g., $\mathcal{X}^a$) can, in principle, be introduced to cover $\mathcal{B}$. Referential locations X and spatial locations x can be associated with base points on corresponding manifolds B_0 and B, respectively. Tangent spaces to reference and current manifolds at points X and x are written $T_X B_0$ and $T_x B$, respectively. Body $\mathcal{B}$, configurations B_0 and B, and tangent spaces $T_X B_0$ and $T_x B$ are illustrated in Fig. 2.2. Reference and current tangent bundles are

$TB_0 = \cup_{X \in B_0} T_X B_0$ and $TB = \cup_{x \in B} T_x B$, respectively. Analogously, cotangent spaces are written as $T_X^* B_0$ and $T_x^* B$, with $T^* B_0 = \cup_{X \in B_0} T_X^* B_0$ and $T^* B = \cup_{x \in B} T_x^* B$ the corresponding cotangent bundles in reference and current configurations, respectively.
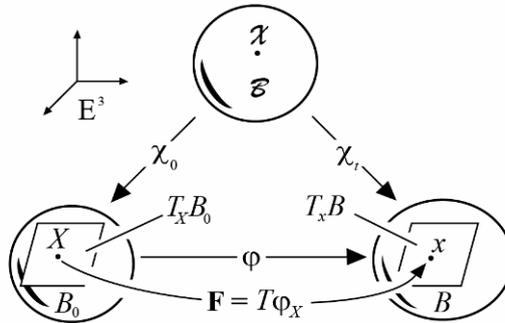
Fig. 2.2 Configurations, mappings, and tangent spaces

Natural or holonomic basis vectors in reference and current configurations are defined, respectively, by

$$\mathbf{G}_A = \frac{\partial}{\partial X^A} \in T_X B_0 \,, \quad \mathbf{g}_a = \frac{\partial}{\partial x^a} \in T_x B \,, \tag{2.2}$$

and are tangent to local coordinate curves at X or x; for example, see Fig. 2.1 in which $\mathcal{M}$ can represent the reference configuration B_0. Sometimes the basis vectors in (2.2) are called covariant basis vectors because their indices occupy lower positions, though this can cause confusion because these vectors act as the basis for general contravariant vectors. Basis vectors in (2.2) are sometimes written as $\mathbf{G}_A = \partial_A \mathbf{X} = \mathbf{X}_{,A}$ and $\mathbf{g}_a = \partial_a \mathbf{x} = \mathbf{x}_{,a}$. Dual or reciprocal bases to (2.2) are written as

$$\mathbf{G}^A = \mathbf{d}X^A \in T_X^* B_0 \,, \quad \mathbf{g}^a = \mathbf{d}x^a \in T_x^* B \,. \tag{2.3}$$

Basis vectors (2.2) and their duals (2.3) satisfy the orthonormality relations

$$\left\langle \mathbf{G}^A, \mathbf{G}_B \right\rangle_{B_0} = \delta_{.B}^A \,, \quad \left\langle \mathbf{g}^a, \mathbf{g}_b \right\rangle_B = \delta_{.b}^a \,. \tag{2.4}$$

In (2.4), dual pairings (i.e., scalar product of vector and covector) in reference and spatial configurations correspond to the respective operations $\left\langle . \,, . \right\rangle_{B_0} : T_X^* B_0 \times T_X B_0 \to \mathbb{R}$ and $\left\langle . \,, . \right\rangle_B : T_x^* B \times T_x B \to \mathbb{R}$. The dual basis vectors are sometimes called contravariant basis vectors because their indices occupy upper positions. Also introduced in (2.4), Kronecker delta symbols satisfy

$$\delta_{.B}^{A} = \begin{cases} 1 \ \forall \ A = B, \\ 0 \ \forall \ A \neq B, \end{cases} \quad \delta_{.b}^{a} = \begin{cases} 1 \ \forall \ a = b, \\ 0 \ \forall \ a \neq b. \end{cases} \tag{2.5}$$

Location of the placeholder (index) denoted by the period is arbitrary in the special symbols defined in (2.5), but such placeholders are not always arbitrary for general tensor-valued quantities defined later in this book. Henceforward, subscripts on scalar product operations as in (2.4) denoting configuration(s) of arguments in angled brackets are omitted since the appropriate configuration(s) can always be inferred from the arguments. Summation over repeated indices produces $\delta_{.A}^{A} = \delta_{.a}^{a} = \delta_{.1}^{1} + \delta_{.2}^{2} + \delta_{.3}^{3} = 3$.

From (2.2)-(2.4), $T_X B_0$ is the linear vector space of all contravariant vectors $\mathbf{V} = V^A \mathbf{G}_A$ emanating from point $X \in B_0$. Cotangent space $T_X^* B_0$ is the linear vector space of all one-forms $\boldsymbol{\alpha} = \alpha_A \mathbf{G}^A$ emanating from point $X \in B_0$. In the context of dual products, vectors and one-forms are linear functions, $\mathbf{V}: T_X^* B_0 \to \mathbb{R}$ and $\boldsymbol{\alpha}: T_X B_0 \to \mathbb{R}$, and correspondingly

$$\langle \boldsymbol{\alpha}, \mathbf{V} \rangle = \boldsymbol{\alpha}(\mathbf{V}) = \alpha_A V^A = V^A \alpha_A = \mathbf{V}(\boldsymbol{\alpha}) = \langle \mathbf{V}, \boldsymbol{\alpha} \rangle, \tag{2.6}$$

invoking the symmetry property of the scalar product operation. Similar arguments hold for vectors and one-forms on respective tangent and cotangent spaces referred to current configuration B. Contravariant component V^A of vector $\mathbf{V}$ can be obtained via the scalar product operation as $\langle \mathbf{V}, \mathbf{G}^A \rangle = \langle V^B \mathbf{G}_B, \mathbf{G}^A \rangle = V^B \delta_{.B}^A = V^A$, where (2.4) has been used.

Let $\mathbf{G}: (\mathbf{V} \in T_X B_0, \mathbf{W} \in T_X B_0) \to \mathbb{R}$ be a symmetric, positive definite bilinear form assigning a real number to any two vectors $\mathbf{V}$ and $\mathbf{W}$ in $T_X B_0$. Object $\mathbf{G}$ is called a metric tensor, or simply a metric. Since $\mathbf{G}$ is symmetric, its components obey $G_{AB} = G_{(AB)}$, where indices in parentheses are symmetric: $2A_{(AB)} = A_{AB} + A_{BA}$ for arbitrary second-order tensor $\mathbf{A}$. Metric $\mathbf{G}$ maps a contravariant vector $\mathbf{V}$ into its associated covariant vector $\mathbf{V}_\#$:

$$\mathbf{V}_\# = \mathbf{G}\mathbf{V} = \left(G_{AB} \mathbf{G}^A \otimes \mathbf{G}^B \right)\left(V^B \mathbf{G}_B \right) = V_A \mathbf{G}^A, \ V_A = G_{AB} V^B. \tag{2.7}$$

The outer product (also called tensor product) of vectors and/or covectors, corresponding to a juxtaposition of indices, is denoted by $\otimes$ and satisfies the identity $(\mathbf{G}^A \otimes \mathbf{G}^B)\mathbf{G}_C = \mathbf{G}^A \langle \mathbf{G}^B, \mathbf{G}_C \rangle$.

The inverse of the metric tensor $\mathbf{G}^{-1}$, or simply the inverse metric, maps covectors $\boldsymbol{\alpha}$ into associated vectors $\boldsymbol{\alpha}^\#$:

$$\boldsymbol{\alpha}^\# = \mathbf{G}^{-1}\boldsymbol{\alpha} = \left(G^{AB} \mathbf{G}_A \otimes \mathbf{G}_B \right)\left(\alpha_B \mathbf{G}^B \right) = \alpha^A \mathbf{G}_A, \ \alpha^A = G^{AB} \alpha_B. \tag{2.8}$$

The standard notational convention of denoting components of $\mathbf{G}^{-1}$ with G^{AB} (i.e., $(\mathbf{G}^{-1})^{AB} = G^{AB}$) is followed henceforth.

On vector space $T_X B_0$, metric tensor $\mathbf{G}$ enables evaluation of the inner product or dot product of vectors:

$$\mathbf{V} \cdot \mathbf{W} = \langle \mathbf{V}, \mathbf{G} \mathbf{W} \rangle = V^A G_{AB} W^B. \tag{2.9}$$

Covariant component V_A of vector $\mathbf{V}$ can be obtained via use of the dot product operation as follows: $\mathbf{V} \cdot \mathbf{G}_A = V^B \mathbf{G}_B \cdot \mathbf{G}_A = V^B G_{BA} = V_A$. Similarly to (2.9), the inverse of the metric tensor, i.e., its contravariant form, enables evaluation of the inner product or dot product of covectors:

$$\boldsymbol{\alpha} \cdot \boldsymbol{\beta} = \langle \boldsymbol{\alpha}, \mathbf{G}^{-1} \boldsymbol{\beta} \rangle = \alpha_A G^{AB} \beta_B. \tag{2.10}$$

In the current configuration B, the metric tensor associated with spatial coordinates $\mathbf{x}$ is denoted by $\mathbf{g}: (\mathbf{v} \in T_x B, \mathbf{w} \in T_x B) \to \mathbb{R}$, with inverse $\mathbf{g}^{-1}$. Equations analogous to (2.7)-(2.10) apply for spatial metric $\mathbf{g}$ and its inverse in the current configuration.

From (2.4), (2.9), and (2.10), it is implied that matrix components of metric tensors and their inverses in reference and current configurations are given, respectively, by

$$G_{AB} = \mathbf{G}_A \cdot \mathbf{G}_B, \ G^{AB} = \mathbf{G}^A \cdot \mathbf{G}^B; \tag{2.11}$$

$$g_{ab} = \mathbf{g}_a \cdot \mathbf{g}_b, \ g^{ab} = \mathbf{g}^a \cdot \mathbf{g}^b. \tag{2.12}$$

Metrics and their inverses are related, by definition, as follows:

$$G^{AB} G_{BC} = \delta^A_{.C}, \ g^{ab} g_{bc} = \delta^a_{.c}. \tag{2.13}$$

Relationships between basis vectors and their reciprocal vectors are

$$\mathbf{G}^A = G^{AB} \mathbf{G}_B, \ \mathbf{G}_A = G_{AB} \mathbf{G}^B, \ \mathbf{g}^a = g^{ab} \mathbf{g}_b, \ \mathbf{g}_a = g_{ab} \mathbf{g}^b. \tag{2.14}$$

In addition to their role in scalar product operations, metric tensors (or their inverses) may be used to lower (or raise) indices of tensors of arbitrarily higher order. For example, let $\mathbf{A} = A^{AB} \mathbf{G}_A \otimes \mathbf{G}_B$ be a generic contravariant tensor of order two. The fully covariant representation of $\mathbf{A}$ is

$$\mathbf{A}_\# = G_{AC} G_{BD} A^{CD} \mathbf{G}^A \otimes \mathbf{G}^B = A_{AB} \mathbf{G}^A \otimes \mathbf{G}^B. \tag{2.15}$$

When considering multiple configurations, it often becomes necessary to express components of vectors or tensors introduced in one configuration, with one set of coordinates, with respect to bases in another configuration with a different set of coordinates. For example, a vector $\mathbf{V}$ defined in a parallel manner on $T_X B_0$ and $T_x B$ is written (Eringen 1962)

$$\mathbf{V} = V^A \mathbf{G}_A(X) = V^a \mathbf{g}_a(x). \tag{2.16}$$

Taking the inner product with dual basis vectors in each configuration, it follows that

$$V^B = V^A \left\langle \mathbf{G}_A, \mathbf{G}^B \right\rangle = V^a \left\langle \mathbf{g}_a, \mathbf{G}^B \right\rangle = V^a g_{.a}^B, \quad \mathbf{g}_a = g_a^A \mathbf{G}_A; \qquad (2.17)$$

$$V^b = V^a \left\langle \mathbf{g}_a, \mathbf{g}^b \right\rangle = V^A \left\langle \mathbf{G}_A, \mathbf{g}^b \right\rangle = V^A g_{.A}^b, \quad \mathbf{G}_A = g_A^a \mathbf{g}_a; \qquad (2.18)$$

where mixed-variant components of shifters, examples of two-point tensors, are defined as

$$g_{.a}^A(x, X) = \left\langle \mathbf{G}^A, \mathbf{g}_a \right\rangle = g_{.a}^A, \quad g_{.A}^a(x, X) = \left\langle \mathbf{g}^a, \mathbf{G}_A \right\rangle = g_{.A}^a. \qquad (2.19)$$

Similarly, fully covariant and fully contravariant components of shifter tensors are, respectively,

$$g_{Aa}(x, X) = \mathbf{G}_A \cdot \mathbf{g}_a = g_{aA}, \quad g^{Aa}(x, X) = \mathbf{G}^A \cdot \mathbf{g}^a = g^{aA}. \qquad (2.20)$$

From (2.14), it follows that components of the shifters are raised and lowered by components of metric tensors of the corresponding configuration:

$$g_{Aa} = g_{ab} g_{.A}^b = G_{AB} g_{.a}^B = g_{ab} G_{AB} g^{Bb}. \qquad (2.21)$$

Moreover, summation over one set of indices leads to the identities

$$g_{.b}^A g_{.A}^a = \delta_{.b}^a, \quad g_{.a}^A g_{.B}^a = \delta_{.B}^A. \qquad (2.22)$$

It follows that $\det(g_{.a}^A) = 1/\det(g_{.A}^a) = \sqrt{\det(g_{ab})/\det(G_{AB})}$, where det is the usual determinant of a second-order tensor. Shifters can also be used to express components of vectors and tensors introduced in one frame of coordinates with respect to a different coordinate frame in the same configuration via parallel transport (Toupin 1956; Ericksen 1960). Differentiation indices cannot usually be shifted; e.g., generally $\partial_a \neq g_{.a}^A \partial_A$.

Components of metric tensors on Euclidean spaces can be defined equivalently in terms of transformations to Cartesian coordinates and the dot product of vectors. For example, let X^A denote general curvilinear coordinates on B_0, and let $Z^A = Z^A(X)$ denote Cartesian coordinates on B_0. Since tangent vectors to Z^A are orthonormal by definition,

$$G_{AB} = \frac{\partial}{\partial X^A} \cdot \frac{\partial}{\partial X^B} = \frac{\partial Z^C}{\partial X^A} \frac{\partial Z^D}{\partial X^B} \left(\frac{\partial}{\partial Z^C} \cdot \frac{\partial}{\partial Z^D} \right) = \frac{\partial Z^C}{\partial X^A} \frac{\partial Z^D}{\partial X^B} \delta_{CD}, \qquad (2.23)$$

with δ_{CD} covariant Kronecker delta symbols. From (2.23), the determinant of the matrix of metric tensor components is always non-negative: $\det(G_{AB}) = [\det(\partial Z^A / \partial X^B)]^2 \geq 0$. Similarly for the inverse metric tensor, $\det(G^{AB}) = 1/\det(G_{AB}) = [\det(\partial X^A / \partial Z^B)]^2 \geq 0$. The metric tensor (or its inverse) may have zero determinant along certain singular points or curves (e.g., at $R = 0$ in cylindrical or spherical coordinates) but is non-singular over any volume (Malvern 1969). In Cartesian space, the metric is simply $G_{AB} = \delta_{AB}$, and distinction between covariant and contravariant indices is not necessary. Analogously for a shifter, components can be computed via

$$g_{Aa} = \frac{\partial}{\partial X^A} \bullet \frac{\partial}{\partial x^a} = \frac{\partial Z^B}{\partial X^A} \frac{\partial z^b}{\partial x^a} \left(\frac{\partial}{\partial Z^B} \bullet \frac{\partial}{\partial z^b} \right) = \frac{\partial Z^B}{\partial X^A} \frac{\partial z^b}{\partial x^a} \delta_{Bb} , \quad (2.24)$$

where x^a and $z^a = z^a(x)$ denote curvilinear and Cartesian coordinates, respectively, in spatial configuration B, and δ_{Bb} reduces to Kronecker's delta when coincident Cartesian coordinate frames for Z^A and z^a are prescribed, respectively, in reference and current configurations.

   Generally non-vanishing components of metric tensors for several common three-dimensional coordinate systems are listed in Table 2.1. Metric tensor components listed in Table 2.1 can be applied towards representations in either of the reference or current configurations.

Table 2.1 Metric tensors for common three-dimensional coordinate systems

Coordinate system	Non-vanishing components of G_{AB}
Cartesian: $(X^1, X^2, X^3) \rightarrow (X, Y, Z)$	$G_{XX} = G_{YY} = G_{ZZ} = 1$
Cylindrical: $(X^1, X^2, X^3) \rightarrow (R, \theta, Z)$	$G_{RR} = G_{ZZ} = 1$, $G_{\theta\theta} = R^2$
$X = R\cos\theta$, $Y = R\sin\theta$, $Z = Z$	
$R \geq 0$, $\theta \in (-\pi, \pi]$	
Spherical: $(X^1, X^2, X^3) \rightarrow (R, \theta, \varphi)$	$G_{RR} = 1$, $G_{\theta\theta} = R^2$, $G_{\varphi\varphi} = R^2 \sin^2\theta$
$X = R\sin\theta\cos\varphi$, $Y = R\sin\theta\sin\varphi$, $Z = R\cos\theta$	
$R \geq 0$, $\theta \in [0, \pi]$, $\varphi \in (-\pi, \pi]$	

2.2 Linear Connections

The following topics are addressed in Section 2.2: the definition of a generic linear connection, its covariant derivative, and connection coefficients; torsion and curvature of a connection; identities from differential geometry describing properties of the connection and its torsion and curvature; and a special kind of connection called the Levi-Civita connection.

2.2.1 The Covariant Derivative and Connection Coefficients

A linear connection, also often called an affine connection, on a manifold B_0 induces an operation ∇ that assigns to two vector fields $\mathbf{V}, \mathbf{W} \in TB_0$ a third vector field $\nabla_{\mathbf{V}} \mathbf{W} \in TB_0$, called the covariant derivative of $\mathbf{W}$ along $\mathbf{V}$, such that

(i) $\nabla_{\mathbf{V}}\mathbf{W}$ is linear in both $\mathbf{V}$ and $\mathbf{W}$;

(ii) $\nabla_{f\mathbf{V}}\mathbf{W} = f\nabla_{\mathbf{V}}\mathbf{W}$ for scalar function f;   (2.25)

(iii) $\nabla_{\mathbf{V}}(f\,\mathbf{W}) = f\nabla_{\mathbf{V}}\mathbf{W} + \langle \mathbf{V},\mathbf{D}f\rangle \mathbf{W}$.

The derivative of f is $\mathbf{D}f$, and in coordinates the derivative of f in the direction of $\mathbf{V}$ is $\langle \mathbf{V},\mathbf{D}f\rangle = V^A f_{,A} = V^A \partial_A f = V^A \partial f/\partial X^A$. The covariant derivative of $\mathbf{W}$ along $\mathbf{V}$ is written in indicial notation as

$$\nabla_{\mathbf{V}}\mathbf{W} = (V^B \partial_B W^A + \Gamma_{BC}^{\;\;A} V^B W^C)\mathbf{G}_A = (V^B W^A_{\;\;,B} + \Gamma_{BC}^{\;\;A} V^B W^C)\mathbf{G}_A,\quad (2.26)$$

where the notation $(\,.\,)_{,B} = \partial_B(\,.\,) = \partial(\,.\,)/\partial X^B$ is used interchangeably throughout this text for partial coordinate differentiation. The n^3 coefficients of the connection in n-dimensional space are written $\Gamma_{BC}^{\;\;A}$. Connection coefficients do not follow conventional coordinate transformation laws for third-order tensors. Consider a coordinate transformation $X^A \to \widehat{X}^{\bar{A}}$. Since vector field $\nabla_{\mathbf{V}}\mathbf{W}$ of (2.26) transforms conventionally under a change of basis as (Schouten 1954)

$$
\begin{aligned}
\left(\nabla_V W\right)^A &= V^B \frac{\partial W^A}{\partial X^B} + \Gamma_{BC}^{\;\;A} V^B W^C \\[4pt]
&= \widehat{V}^{\bar{B}} \frac{\partial X^B}{\partial \widehat{X}^{\bar{B}}} \frac{\partial}{\partial X^B}\left(\widehat{W}^{\bar{C}} \frac{\partial X^A}{\partial \widehat{X}^{\bar{C}}}\right) + \Gamma_{BC}^{\;\;A} \widehat{V}^{\bar{B}} \frac{\partial X^B}{\partial \widehat{X}^{\bar{B}}} \widehat{W}^{\bar{C}} \frac{\partial X^C}{\partial \widehat{X}^{\bar{C}}} \\[4pt]
&= \widehat{V}^{\bar{B}} \frac{\partial}{\partial \widehat{X}^{\bar{B}}}\left(\widehat{W}^{\bar{C}} \frac{\partial X^A}{\partial \widehat{X}^{\bar{C}}}\right) + \Gamma_{BC}^{\;\;A} \frac{\partial X^B}{\partial \widehat{X}^{\bar{B}}} \frac{\partial X^C}{\partial \widehat{X}^{\bar{C}}} \widehat{V}^{\bar{B}} \widehat{W}^{\bar{C}} \\[4pt]
&= \widehat{V}^{\bar{B}} \frac{\partial \widehat{W}^{\bar{C}}}{\partial \widehat{X}^{\bar{B}}} \frac{\partial X^A}{\partial \widehat{X}^{\bar{C}}} + \left(\Gamma_{BC}^{\;\;A} \frac{\partial X^B}{\partial \widehat{X}^{\bar{B}}} \frac{\partial X^C}{\partial \widehat{X}^{\bar{C}}} + \frac{\partial}{\partial \widehat{X}^{\bar{B}}} \frac{\partial X^A}{\partial \widehat{X}^{\bar{C}}}\right)\widehat{V}^{\bar{B}} \widehat{W}^{\bar{C}} \quad (2.27) \\[4pt]
&= \frac{\partial X^A}{\partial \widehat{X}^{\bar{A}}} \widehat{V}^{\bar{B}} \frac{\partial \widehat{W}^{\bar{A}}}{\partial \widehat{X}^{\bar{B}}} + \frac{\partial X^A}{\partial \widehat{X}^{\bar{A}}}\left(\Gamma_{BC}^{\;\;D} \frac{\partial \widehat{X}^{\bar{A}}}{\partial X^D} \frac{\partial X^B}{\partial \widehat{X}^{\bar{B}}} \frac{\partial X^C}{\partial \widehat{X}^{\bar{C}}}\right. \\[4pt]
&\qquad\qquad\qquad \left. + \frac{\partial \widehat{X}^{\bar{A}}}{\partial X^C} \frac{\partial}{\partial \widehat{X}^{\bar{B}}} \frac{\partial X^C}{\partial \widehat{X}^{\bar{C}}}\right)\widehat{V}^{\bar{B}} \widehat{W}^{\bar{C}} \\[4pt]
&= \frac{\partial X^A}{\partial \widehat{X}^{\bar{A}}}\left(\widehat{V}^{\bar{B}} \frac{\partial \widehat{W}^{\bar{A}}}{\partial \widehat{X}^{\bar{B}}} + \widehat{\Gamma}_{\bar{B}\bar{C}}^{\;\;\bar{A}} \widehat{V}^{\bar{B}} \widehat{W}^{\bar{C}}\right) = \frac{\partial X^A}{\partial \widehat{X}^{\bar{A}}}(\nabla_{\hat{V}}\widehat{W})^{\bar{A}},
\end{aligned}
$$

transformation formulae for the connection coefficients are deduced as

$$\hat{\varGamma}^{\bar{A}}_{\bar{B}\bar{C}} = \frac{\partial X^B}{\partial \hat{X}^{\bar{B}}} \frac{\partial X^C}{\partial \hat{X}^{\bar{C}}} \frac{\partial \hat{X}^{\bar{A}}}{\partial X^A} \varGamma^{..A}_{BC} + \frac{\partial \hat{X}^{\bar{A}}}{\partial X^C} \frac{\partial}{\partial \hat{X}^{\bar{B}}} \frac{\partial X^C}{\partial \hat{X}^{\bar{C}}}$$

$$= \frac{\partial X^B}{\partial \hat{X}^{\bar{B}}} \frac{\partial X^C}{\partial \hat{X}^{\bar{C}}} \left(\frac{\partial \hat{X}^{\bar{A}}}{\partial X^A} \varGamma^{..A}_{BC} - \frac{\partial}{\partial X^B} \frac{\partial \hat{X}^{\bar{A}}}{\partial X^C} \right), \tag{2.28}$$

with the second equality in (2.28) following readily from the identity $(\partial_C \hat{X}^{\bar{A}} \partial_{\bar{C}} X^C)_{,\bar{B}} = (\delta^{\bar{A}}_{.\bar{C}})_{,\bar{B}} = 0$. Furthermore, the covariant derivative of a vector field, $\nabla \mathbf{W}(X)$, is a $\{^1_1\}$ tensor field, expressed in components as

$$\nabla \mathbf{W}(X) = (\partial_B W^A + \varGamma^{..A}_{BC} W^C) \mathbf{G}_A \otimes \mathbf{G}^B$$

$$= (W^A_{,B} + \varGamma^{..A}_{BC} W^C) \mathbf{G}_A \otimes \mathbf{G}^B. \tag{2.29}$$

An affine connection on tangent bundle TB_0 enables parallel transport of vectors across different tangent spaces in TB_0. A vector is said to undergo parallel transport with respect to a connection with covariant derivative ∇ along paths for which its covariant derivative vanishes. For example, a vector $\mathbf{W}$ is considered to be parallel along a curve $\lambda(t)$ if $\nabla_{\mathbf{V}} \mathbf{W} = 0$, where $\mathbf{V} = \partial \lambda / \partial t$ is tangent to the curve parameterized by t. A vector $\mathbf{W}$ is then parallel transported along λ if it is extended to a parallel vector field $\mathbf{W}(t)$ for all values of t.

The covariant derivative is applied to covector fields and to tensor fields of higher order as follows (Schouten 1954):

$$\nabla_N A^{A...F}_{G...M} = A^{A...F}_{G...M,N}$$

$$+ \varGamma^{..A}_{NR} A^{RB...F}_{G...M} + ... + \varGamma^{..F}_{NR} A^{A...ER}_{G...M} \tag{2.30}$$

$$- \varGamma^{..R}_{NG} A^{A...F}_{RH...M} - ... - \varGamma^{..R}_{NM} A^{A...F}_{G...LR},$$

where the index of covariant differentiation is a subscript immediately following the ∇-operator. Notice that the first covariant index of the connection coefficients corresponds to that of the differentiation. The covariant derivative of an absolute or true scalar function is defined in the same way as its ordinary partial derivative: $\nabla_N A = \partial_N A = A_{,N}$. Hence the covariant derivative of a constant scalar vanishes identically. Another useful identity is $\nabla_N \delta^A_{.B} = \delta^A_{.B,N} + \varGamma^{..A}_{NC} \delta^C_{.B} - \varGamma^{..C}_{NB} \delta^A_{.C} = \delta^A_{.B,N} + \varGamma^{..A}_{NB} - \varGamma^{..A}_{NB} = \delta^A_{.B,N} = 0$. From the linearity property of the connection, the covariant derivative of a sum of objects is equal to the sum of the covariant derivatives of these objects. Covariant differentiation obeys the product rule of Leibniz; e.g., $\nabla_C (V^A W^B) = V^A \nabla_C W^B + W^B \nabla_C V^A$. Analogous to terminology for parallel

transport of vectors, a tensor is said to be parallel transported along a curve if its covariant derivative vanishes as the tensor is dragged along the curve.

2.2.2 Torsion and Curvature

The torsion tensor **T** of a connection is defined by the operation

$$2\mathbf{T}(\mathbf{V}, \mathbf{W}) = \nabla_{\mathbf{V}}\mathbf{W} - \nabla_{\mathbf{W}}\mathbf{V} - [\mathbf{V}, \mathbf{W}], \tag{2.31}$$

where the Lie bracket of vector fields **V** and **W** on TB_0 is

$$[\mathbf{V}, \mathbf{W}] = \left(V^B W^A_{.,B} - W^B V^A_{.,B}\right)\mathbf{G}_A. \tag{2.32}$$

From (2.26), (2.31), and (2.32), the torsion tensor is

$$\mathbf{T} = \Gamma^{..A}_{[BC]} \mathbf{G}^B \otimes \mathbf{G}^C \otimes \mathbf{G}_A, \tag{2.33}$$

where pairs of indices in square brackets are anti-symmetric, e.g., for a second-rank tensor $2A_{[AB]} = A_{AB} - A_{BA}$. A connection is torsion-free when its torsion tensor vanishes, or equivalently, when its connection coefficients are symmetric in covariant indices. The torsion tensor of a linear connection on a manifold is often called Cartan's torsion, by association with geometer E. Cartan (Cartan 1922). A connection with vanishing torsion is said to be symmetric. Sometimes twice the quantity in (2.31) and (2.33) is used as the definition of the torsion (Marsden and Hughes 1983; Clayton et al. 2004a, b, 2005, 2006, 2008). One may verify that the torsion transforms like a true tensor of order $\left\{ {1 \atop 2} \right\}$ under a change of holonomic coordinate basis, by direct substitution of (2.33) into (2.28).

The Riemann-Christoffel curvature tensor associated with a linear connection with covariant derivative ∇, **R**: $T^*_X B_0 \times T_X B_0 \times T_X B_0 \times T_X B_0 \to \mathbb{R}$, is a $\left\{ {1 \atop 3} \right\}$ tensor with component representation

$$\begin{aligned} R^{..A}_{BCD} &= \Gamma^{..A}_{CD,B} - \Gamma^{..A}_{BD,C} + \Gamma^{..A}_{BE}\Gamma^{..E}_{CD} - \Gamma^{..A}_{CE}\Gamma^{..E}_{BD} \\ &= 2\partial_{[B}\Gamma^{..A}_{C]D} + 2\Gamma^{..A}_{[B|E|}\Gamma^{..E}_{C]D}, \end{aligned} \tag{2.34}$$

where indices in vertical bars are excluded from the anti-symmetry operation. Order and placement of indices used in the definition of **R** vary among authors (Schouten 1954; Fosdick 1966; Marsden and Hughes 1983; Clayton et al. 2005); conventions adopted in this book for the Riemann-Christoffel curvature tensor and quantities derived from it follow those of Schouten (1954) and Minagawa (1979). The Riemann-Christoffel curvature tensor transforms like a true tensor of order $\left\{ {1 \atop 3} \right\}$ under a change of holonomic coordinates (Schouten 1954). From definition (2.34), **R** is al-

ways anti-symmetric in the first two covariant indices. Definitions, in indicial components, of several quantities constructed from the Riemann-Christoffel curvature tensor include its fully covariant version

$$R_{BCDA} = R_{BCD}^{\cdots E} G_{EA}, \tag{2.35}$$

called simply the curvature tensor by Eringen (1962) and the Riemann tensor by Fosdick (1966), though again the placement of indices varies among authors. Components of the Ricci curvature are

$$R_{CD} = R_{ACD}^{\cdots A}. \tag{2.36}$$

Recalling that n is the dimensionality of the space, scalar curvature κ is defined as

$$\kappa = \frac{1}{n(n-1)} R_{AB} G^{AB} = \frac{1}{n(n-1)} R, \tag{2.37}$$

with R the trace of the Ricci curvature. For $n = 2$, R of (2.37) is equivalent to the Gaussian curvature. Finally, Einstein's tensor $\boldsymbol{\theta}$ has components

$$4\theta^{AB} = \varepsilon^{ACD} \varepsilon^{BEF} R_{CDEF}, \tag{2.38}$$

where components of the permutation tensor ε^{ACD} are introduced formally later in (2.64).

The skew second covariant derivatives of a contravariant vector $\mathbf{V}$ and covariant vector $\boldsymbol{\alpha}$ can be expressed as (Schouten 1954)

$$\nabla_{[B}\nabla_{C]}V^A = \frac{1}{2} R_{BCD}^{\cdots A} V^D - T_{BC}^{\cdots D} \nabla_D V^A, \tag{2.39}$$

$$\nabla_{[B}\nabla_{C]}\alpha_D = -\frac{1}{2} R_{BCD}^{\cdots A} \alpha_A - T_{BC}^{\cdots A} \nabla_A \alpha_D. \tag{2.40}$$

Skew differential operator $\nabla_{[B}\nabla_{C]}$ obeys the product rule of Leibniz, e.g.,

$$\nabla_{[B}\nabla_{C]}(V^A \alpha_D) = \alpha_D \nabla_{[B}\nabla_{C]}V^A + V^A \nabla_{[B}\nabla_{C]}\alpha_D. \tag{2.41}$$

2.2.3 Identities for the Connection Coefficients and Curvature

Coefficients of an arbitrary linear connection can be written in the form (Schouten 1954)

$$\Gamma_{BC}^{\cdot\cdot A} = \left\{ {}_{BC}^{\cdot\cdot A} \right\} + T_{BC}^{\cdot\cdot A} - T_{C.B}^{A\cdot\cdot} + T_{.BC}^{A\cdot\cdot} + \frac{1}{2}(M_{BC}^{\cdot\cdot A} + M_{C.B}^{A\cdot\cdot} - M_{.BC}^{A\cdot\cdot}), \tag{2.42}$$

where for a symmetric, three times differentiable, and invertible but otherwise arbitrary second-rank tensor with components G_{AB} and inverse components G^{AB}, the quantities

$$\left\{{}^{..A}_{BC}\right\} = \frac{1}{2}G^{AD}(G_{CD,B} + G_{BD,C} - G_{BC,D}) \qquad (2.43)$$

are called Christoffel symbols[3] of the tensor G_{AB}. Christoffel symbols in (2.43) are symmetric in covariant indices. Also in (2.42), the third-order object

$$M^{..A}_{BC} = G^{AD}M_{BCD} = -G^{AD}\nabla_B G_{CD} = G_{CD}\nabla_B G^{AD}, \qquad (2.44)$$

with the final equality following from identity $\nabla_B(G_{CD}G^{AD}) = \nabla_B \delta^A_{.C} = 0$. The covariant derivative of G_{AB} is, from (2.30) and coefficients in (2.42),

$$\nabla_A G_{BC} = G_{BC,A} - \Gamma^{..D}_{AB}G_{DC} - \Gamma^{..D}_{AC}G_{BD} = -M_{ABC}. \qquad (2.45)$$

Symmetry conditions $M_{ABC} = M_{A(BC)}$ follow immediately from conditions $G_{AB} = G_{BA}$. When $\nabla_A G_{BC} = 0$, or equivalently when $M_{ABC} = 0$, the connection is said to be metric with respect to G_{AB}. In that case, covariant differentiation via ∇ and raising (or lowering) of indices via G^{AB} (or G_{AB}) or commute. In general, G_{AB} of (2.43)-(2.45) need not be the metric tensor used to define scalar products of vectors. However, when the connection of (2.42) is metric, and when G_{AB} is in fact the metric tensor of the space with connection (2.42), then G_{AB} is called the fundamental tensor of the space (Schouten 1954). In the particular case of Riemannian geometry, by definition the connection is simultaneously symmetric ($T^{..A}_{BC} = 0$) and metric ($M^{..A}_{BC} = 0$), leading to

$$\Gamma^{..A}_{BC} = \left\{{}^{..A}_{BC}\right\} \text{ (Riemannian geometry).} \qquad (2.46)$$

Returning now to the general case in (2.42) with possibly non-vanishing torsion and non-metric connection, the Riemann-Christoffel curvature tensor of (2.34) exhibits the following properties (Schouten 1954):

$$R^{...A}_{(BC)D} = 0, \qquad (2.47)$$

$$R^{...A}_{[BCD]} = 2\nabla_{[B}T^{..A}_{CD]} - 4T^{..E}_{[BC}T^{..A}_{D]E}, \qquad (2.48)$$

$$R_{AB(CD)} = \nabla_{[A}M_{B]CD} + T^{..E}_{AB}M_{ECD}, \qquad (2.49)$$

$$\nabla_{[E}R^{...A}_{BC]D} = 2T^{..F}_{[EB}R^{...A}_{C]FD}, \qquad (2.50)$$

where anti-symmetry over three indices is expressed as

$$6A_{[ABC]} = A_{ABC} + A_{BCA} + A_{CAB} - A_{BAC} - A_{CBA} - A_{ACB}. \qquad (2.51)$$

---

[3] In tensor analysis, $\left\{{}^{..A}_{BC}\right\}$ are often labeled Christoffel symbols of the second kind, and $[{}_{BC,A}] = G_{AD}\left\{{}^{..D}_{BC}\right\}$ are often labeled Christoffel symbols of the first kind.

Relation (2.50) is often called Bianchi's identity. For a symmetric connection the right sides of (2.48) and (2.50) vanish, and for a metric connection the right side of (2.49) vanishes. For a Riemannian connection of the type (2.46) that is both symmetric and metric,

$$R_{(BC)DA} = 0, \; R_{[BCD]A} = 0, \; R_{BC(DA)} = 0, \; R_{BCDA} = R_{DABC}, \qquad (2.52)$$

and the number of independent components of **R** is $n^2(n^2-1)/12$, for example one independent component for a two-dimensional space and six independent components for a three-dimensional space. In Riemannian geometry, the Ricci tensor of (2.36) and Einstein's tensor of (2.38) are both symmetric and satisfy

$$\theta_{AB} = R_{AB} - \frac{1}{2}RG_{AB}, \; \nabla_A\theta^A_{.B} = \nabla_A\left(R_{CB}G^{AC} - \frac{1}{2}R\delta^A_{.B}\right) = 0. \quad (2.53)$$

A space with connection for which the covariant derivative of the Ricci tensor of (2.36) vanishes, i.e., for which $\nabla_A R_{CD} = 0$, is called a Ricci space. A space in Riemannian geometry—that is a symmetric space with connection and metric in which (2.46) applies—in which the Ricci curvature and metric differ only by a scalar factor as

$$R_{CD} = \frac{1}{n}RG_{CD} = (n-1)\kappa G_{CD} \qquad (2.54)$$

is called an Einstein space. From vanishing of the right side of Bianchi's identity (2.50) for a symmetric space, it follows that the scalar curvature of an Einstein space is constant, i.e., $\nabla_A\kappa = 0$ (Schouten 1954).

2.2.4 The Levi-Civita Connection

For a smooth manifold B_0 with metric tensor $\mathbf{G} = (\mathbf{G}_A \cdot \mathbf{G}_B)\mathbf{G}^A \otimes \mathbf{G}^B$, there is a unique affine connection with the covariant derivative operator $\overset{G}{\nabla}$ on B_0 that is torsion-free ($\overset{G}{\mathbf{T}} = 0$) and metric ($\overset{G}{\nabla}\mathbf{G} = 0$), i.e., for which parallel transport preserves the dot products of vectors. It is called the Levi-Civita connection (Marsden and Hughes 1983). The Levi-Civita connection is a particular example of (2.46) and hence is often called the Riemannian connection (Hou and Hou 1997). In this book the term Levi-Civita connection is reserved for the particular Riemannian connection whose curvature tensor vanishes as discussed below. Coefficients of $\overset{G}{\nabla}$ are defined as

$$\overset{G}{\Gamma}{}^{..A}_{BC} = \frac{1}{2}G^{AD}(G_{BD,C} + G_{CD,B} - G_{BC,D}) = \overset{G}{\Gamma}{}^{..A}_{CB}. \qquad (2.55)$$

Superscript $\mathbf{G}$ (or G) of the Levi-Civita connection and its corresponding covariant derivative or gradient operator is not subject to the summation convention. The Riemann-Christoffel curvature tensor formed by inserting Christoffel symbols of Levi-Civita connection (2.55) into definition (2.34) is denoted by $\overset{G}{\mathbf{R}}$. This curvature tensor can be expressed completely in terms of metric $\mathbf{G}$ and its first and second partial derivatives with respect to coordinates X^A. A space B_0 with metric $\mathbf{G}$ and having $\overset{G}{\mathbf{R}} = 0$ is called flat. One may show (Schouten 1954) that $\overset{G}{\mathbf{R}} = 0$ if and only if one may assign parallel orthonormal coordinate basis vectors at each point $X \in B_0$ such that $G_{AB} \to \delta_{AB}$. Thus, the curvature tensor vanishes identically and the space is flat when B_0 is Euclidean. In fact, $\overset{G}{\mathbf{R}} = 0$ are compatibility conditions for the existence of connection coefficients $\overset{G}{\Gamma}{}^{\ ..A}_{\ \ BC}$ derived from a Euclidean metric tensor $\mathbf{G}$ via (2.55) (Schouten 1954; Ciarlet 1998). Henceforward in this book, space B_0 with metric $\mathbf{G}$ and associated connection (2.55) is always assumed Euclidean, meaning that $\overset{G}{\mathbf{R}} = 0$ by definition. Thus, the notation $\overset{G}{\Gamma}{}^{\ ..A}_{\ \ BC}$ is used to denote components of $\left\{{}^{\ ..A}_{\ BC}\right\}$ of (2.46) when $G_{AB} = \mathbf{G}_A \cdot \mathbf{G}_B$ and when the Riemann Christoffel curvature tensor formed from $\left\{{}^{\ ..A}_{\ BC}\right\}$ vanishes. On the other hand, on a curved surface—for example a two-dimensional shell parameterized by a pair of coordinates $X^A : \mathcal{M} \to \mathbb{R}^2$ embedded in E^3 such as shown in Fig. 2.1—the single independent component of the curvature from $\left\{{}^{\ ..A}_{\ BC}\right\}$ does not vanish.

In terms of Levi-Civita connection (2.55), partial coordinate derivatives of natural basis vectors and dual basis vectors are

$$\mathbf{G}^A_{\ ,B} = -\overset{G}{\Gamma}{}^{\ ..A}_{\ \ BC}\mathbf{G}^C, \ \ \mathbf{G}_{A,B} = \overset{G}{\Gamma}{}^{\ ..C}_{\ \ BA}\mathbf{G}_C = \mathbf{G}_{B,A}, \tag{2.56}$$

and partial derivatives of components of the metric tensor are

$$G_{AB,C} = (\mathbf{G}_A \cdot \mathbf{G}_B)_{,C} = \overset{G}{\Gamma}{}^{\ ..D}_{\ \ CB}G_{AD} + \overset{G}{\Gamma}{}^{\ ..D}_{\ \ CA}G_{BD}. \tag{2.57}$$

Viewed another way, (2.56) and (2.57) imply that the basis vectors, dual basis vectors, and metric tensor are all parallel (i.e., have vanishing covariant derivatives) with respect to the Levi-Civita connection. Since the curvature and torsion of the connection (2.55) vanish by definition, (2.39) implies that skew second covariant derivatives vanish, i.e., $\overset{G}{\nabla}_{[B}\overset{G}{\nabla}_{C]}V^A = 0$

for a vector field with components $V^A(X)$. From the second of (2.56), $\mathbf{G}_{[A,B]} = 0$. However, in general $\partial_{[B} \overset{G}{\nabla}_{C]} V^A \neq 0$, meaning that partial and covariant differentiation do not always commute. From the first of (2.4) and the second of (2.56), referential Christoffel symbols of (2.55) can also be computed as $\overset{G}{\Gamma}{}^{..C}_{BA} = \overset{G}{\Gamma}{}^{..D}_{BA} \delta^C_{.D} = \overset{G}{\Gamma}{}^{..D}_{BA} \langle \mathbf{G}_D, \mathbf{G}^C \rangle = \langle \mathbf{G}_{A,B}, \mathbf{G}^C \rangle$.

In the context of geometrically nonlinear continuum mechanics, (2.55)-(2.57) may be formulated in spatial configuration B by replacing reference coordinates X^A with current coordinates x^a, replacing reference metric $\mathbf{G}$ with spatial metric $\mathbf{g}$, and replacing reference configuration basis (co)vectors with current configuration basis (co)vectors. Christoffel symbols of the second kind for covariant derivative operator $\overset{\mathbf{g}}{\nabla}$ on B are

$$\overset{g}{\Gamma}{}^{..a}_{bc} = \frac{1}{2} g^{ad} (g_{bd,c} + g_{cd,b} - g_{bc,d}) = \overset{g}{\Gamma}{}^{..a}_{cb}, \qquad (2.58)$$

and the curvature tensor derived from $\overset{g}{\Gamma}{}^{..a}_{bc}$ using (2.34) is denoted by $\overset{\mathbf{g}}{\mathbf{R}}$. Configuration B with connection (2.58) and metric $\mathbf{g}$ is always assumed a Euclidean space. Since the set $\{ B, \overset{g}{\Gamma}{}^{..a}_{bc}, g_{ab} \}$ constitutes a Euclidean space, torsion and curvature tensors formed from (2.58) vanish identically. Analogs of (2.56) and (2.57) in the current configuration are

$$\mathbf{g}^a_{,b} = -\overset{g}{\Gamma}{}^{..a}_{bc} \mathbf{g}^c, \quad \mathbf{g}_{a,b} = \overset{g}{\Gamma}{}^{..c}_{ba} \mathbf{g}_c = \mathbf{g}_{b,a}; \qquad (2.59)$$

$$g_{ab,c} = (\mathbf{g}_a \cdot \mathbf{g}_b)_{,c} = \overset{g}{\Gamma}{}^{..d}_{cb} g_{ad} + \overset{g}{\Gamma}{}^{..d}_{ca} g_{bd}; \qquad (2.60)$$

and $\overset{g}{\nabla}_{[b} \overset{g}{\nabla}_{c]} V^a = 0$ for a spatial vector field with components $V^a(x)$. From the symmetry properties evident in (2.58), $\mathbf{g}_{[a,b]} = 0$. From the second of (2.4) and the second of (2.59), spatial Christoffel symbols of (2.58) can also be computed as $\overset{g}{\Gamma}{}^{..c}_{ba} = \overset{g}{\Gamma}{}^{..d}_{ba} \delta^c_{.d} = \overset{g}{\Gamma}{}^{..d}_{ba} \langle \mathbf{g}_d, \mathbf{g}^c \rangle = \langle \mathbf{g}_{a,b}, \mathbf{g}^c \rangle$.

In terms of transformation formulae to Cartesian coordinates introduced in (2.23) and (2.24), coefficients in (2.55) and (2.58) satisfy

$$\overset{G}{\Gamma}{}^{..A}_{BC} = \frac{\partial^2 Z^D}{\partial X^B \partial X^C} \frac{\partial X^A}{\partial Z^D}, \quad \overset{g}{\Gamma}{}^{..a}_{bc} = \frac{\partial^2 z^d}{\partial x^b \partial x^c} \frac{\partial x^a}{\partial z^d}. \qquad (2.61)$$

Levi-Civita connection coefficients for cylindrical and spherical coordinate systems are listed in Table 2.2, where the superscript G has been dropped for brevity.

Since metric tensor components $G_{AB} = \delta_{AB} = \text{constant}$ in Cartesian coordinates, Christoffel symbols obtained from G_{AB} all vanish by (2.55) in Cartesian coordinates. So long as basis vectors $\mathbf{G}_A$ are spatially constant (but not necessarily orthogonal), Christoffel symbols formed from $G_{AB} = \mathbf{G}_A \cdot \mathbf{G}_B$ vanish identically, and covariant differentiation via $\overset{G}{\nabla}_A$ and partial differentiation via $\partial_A = \partial / \partial X^A$ are equivalent operations.

Table 2.2 Connection coefficients for common coordinate systems

Coordinate system	Nonzero components of $\varGamma_{BC}^{\cdot\cdot A}$
Cartesian: $(X^1, X^2, X^3) \to (X, Y, Z)$	None
Cylindrical: $(X^1, X^2, X^3) \to (R, \theta, Z)$	$\varGamma_{R\theta}^{\cdot\cdot\theta} = \varGamma_{\theta R}^{\cdot\cdot\theta} = 1/R$, $\varGamma_{\theta\theta}^{\cdot\cdot R} = -R$
$X = R\cos\theta$, $Y = R\sin\theta$, $Z = Z$	
Spherical: $(X^1, X^2, X^3) \to (R, \theta, \varphi)$	$\varGamma_{R\theta}^{\cdot\cdot\theta} = \varGamma_{\theta R}^{\cdot\cdot\theta} = \varGamma_{R\varphi}^{\cdot\cdot\varphi} = \varGamma_{\varphi R}^{\cdot\cdot\varphi} = 1/R$,
$X = R\sin\theta\cos\varphi$, $Y = R\sin\theta\sin\varphi$, $Z = R\cos\theta$	$\varGamma_{\theta\theta}^{\cdot\cdot R} = -R$, $\varGamma_{\varphi\varphi}^{\cdot\cdot R} = -R\sin^2\theta$,
	$\varGamma_{\varphi\varphi}^{\cdot\cdot\theta} = -\sin\theta\cos\theta$,
	$\varGamma_{\theta\varphi}^{\cdot\cdot\varphi} = \varGamma_{\varphi\theta}^{\cdot\cdot\varphi} = \cot\theta$

2.3 Notation, Differential Operators, and Other Identities

To avoid frequent writing of the gradient operator for covariant derivatives, the following compact notation is used henceforward for covariant differentiation with respect to associated Levi-Civita connections with coefficients in (2.55) and (2.58):

$$\overset{G}{\nabla}_N A(X)^{A...H}{}_{I...M} = A^{A...H}{}_{I...M;N} , \tag{2.62}$$

$$\overset{g}{\nabla}_n B(x)^{a...h}{}_{i...m} = B^{a...h}{}_{i...m;n} , \tag{2.63}$$

where $\mathbf{A}(X)$ and $\mathbf{B}(x)$ are tensors of arbitrary order referred to reference and current coordinate systems, respectively. From (2.55)-(2.60), it follows that $\mathbf{G}_{;B}^A = 0$, $\mathbf{G}_{A;B} = 0$, $G_{AB;C} = 0$, $\mathbf{g}_{;b}^a = 0$, $\mathbf{g}_{a;b} = 0$, and $g_{ab;c} = 0$.

Contravariant and covariant components of third rank permutation tensors on configurations B_0 and B, respectively, are defined by

$$\varepsilon^{ABC} = \sqrt[-1]{G}e^{ABC} , \quad \varepsilon_{ABC} = \sqrt{G}e_{ABC} ; \tag{2.64}$$

$$\varepsilon^{abc} = \sqrt[-1]{g}e^{abc} , \quad \varepsilon_{abc} = \sqrt{g}e_{abc} ; \tag{2.65}$$

where henceforth the standard abbreviated notation $G = \det \mathbf{G} = \det(G_{AB})$ and $g = \det \mathbf{g} = \det(g_{ab})$ is used for determinants of metric tensors. Recall also the compact notation used in this text for reciprocals of square roots: $\sqrt[-1]{G} = 1/\sqrt{G}$ and $\sqrt[-1]{g} = 1/\sqrt{g}$. Permutation symbols, also often called Levi-Civita symbols, satisfy

$$e^{ABC} = e_{ABC} = \begin{cases} 0 \text{ when any two indices are equal} \\ +1 \text{ for } ABC = 123, 231, 312 \\ -1 \text{ for } ABC = 132, 213, 321; \end{cases} \qquad (2.66)$$

$$e^{abc} = e_{abc} = \begin{cases} 0 \text{ when any two indices are equal} \\ +1 \text{ for } abc = 123, 231, 312 \\ -1 \text{ for } abc = 132, 213, 321. \end{cases} \qquad (2.67)$$

Permutation tensors and symbols in (2.64)-(2.67) are anti-symmetric in all pairs and triplets of indices, e.g., $\varepsilon^{ABC} = \varepsilon^{[AB]C} = \varepsilon^{A[BC]} = \varepsilon^{[A|B|C]} = \varepsilon^{[ABC]}$ (refer to (2.51)). Covariant derivatives of permutation tensors in (2.64) and (2.65) with respect to Levi-Civita connections vanish since $G_{;A} = 0$ and $g_{;a} = 0$ (Malvern 1969). However, in general, $G_{,A} \neq 0$ and $g_{,a} \neq 0$ since $G(X)$ and $g(x)$ are not invariant under general changes of coordinates and hence are not absolute scalars. Identities for symbols of (2.66) are tabulated in Table 2.3. Analogous identities apply for spatial symbols e^{abc} and e_{abc} of (2.67) and for the permutation tensors of (2.64) and (2.65).

Table 2.3 Identities for permutation symbols

Identity	Identity
$e^{ABC} e_{DEF} = \det \begin{bmatrix} \delta^A_{.D} & \delta^A_{.E} & \delta^A_{.F} \\ \delta^B_{.D} & \delta^B_{.E} & \delta^B_{.F} \\ \delta^C_{.D} & \delta^C_{.E} & \delta^C_{.F} \end{bmatrix}$	$e^{ABC} e_{ADE} = \delta^B_{.D} \delta^C_{.E} - \delta^B_{.E} \delta^C_{.D}$
$e^{ABC} e_{ABE} = 2\delta^C_{.E}$	$e^{ABC} e_{ABC} = 2\delta^A_{.A} = 6$

Several mathematical operations are now introduced in reference coordinates. Analogous definitions apply for spatial coordinates. The trace of a second-order tensor $\mathbf{A}$ is defined as summation over its mixed-variant indices:

$$\text{tr}\mathbf{A} = A^A_{.A} = A^{AB} G_{AB} = A_{AB} G^{AB}. \qquad (2.68)$$

The transpose is identified as a horizontal switch of indices:

$$A^T_{AB} = A_{BA} \,, \ (A^T)^{AB} = A^{BA} \,. \tag{2.69}$$

The gradient of a scalar function f is equivalent to its partial or covariant derivative:

$$\overset{G}{\nabla} f = f_{;A} \mathbf{G}^A = f_{,A} \mathbf{G}^A \,. \tag{2.70}$$

From (2.56) and (2.62), the gradient of a contravariant vector field $\mathbf{V}$ is

$$
\begin{aligned}
\overset{G}{\nabla} \mathbf{V} &= \mathbf{V}_{,B} \otimes \mathbf{G}^B = (V^A \mathbf{G}_A)_{,B} \otimes \mathbf{G}^B \\
&= (V^A_{,B} \mathbf{G}_A + V^A \mathbf{G}_{A,B}) \otimes \mathbf{G}^B \\
&= V^A_{,B} \mathbf{G}_A \otimes \mathbf{G}^B + V^A \overset{G}{\Gamma}{}^{\ .C}_{BA} \mathbf{G}_C \otimes \mathbf{G}^B \\
&= (V^A_{,B} + V^C \overset{G}{\Gamma}{}^{\ .A}_{BC}) \mathbf{G}_A \otimes \mathbf{G}^B = V^A_{;B} \mathbf{G}_A \otimes \mathbf{G}^B \,.
\end{aligned}
\tag{2.71}
$$

The divergence of a contravariant vector field $\mathbf{V}$ satisfies

$$
\begin{aligned}
\left\langle \overset{G}{\nabla}, \mathbf{V} \right\rangle &= \mathrm{tr} \, \overset{G}{\nabla} \mathbf{V} = \left\langle \mathbf{V}_{,A}, \mathbf{G}^A \right\rangle \\
&= \left\langle (V^B \mathbf{G}_B)_{,A}, \mathbf{G}^A \right\rangle = V^A_{;A} = \sqrt[-1]{G} \left(\sqrt{G} V^A \right)_{,A}.
\end{aligned}
\tag{2.72}
$$

The final equality in (2.72) follows from the identity (Eringen 1962)

$$\left(\ln \sqrt{G} \right)_{,A} = \overset{G}{\Gamma}{}^{\ .B}_{AB} = \overset{G}{\Gamma}{}^{\ .B}_{BA} \,. \tag{2.73}$$

The curl of a covariant vector field $\boldsymbol{\alpha}$ satisfies

$$\overset{G}{\nabla} \times \boldsymbol{\alpha} = \mathbf{G}^A \times (\alpha_B \mathbf{G}^B)_{,A} = \mathbf{G}^A \times \mathbf{G}^B \alpha_{B;A} = \varepsilon^{ABC} \alpha_{C;B} \mathbf{G}_A \,, \tag{2.74}$$

where the vector cross product of two contravariant or covariant vectors, respectively, is

$$\mathbf{V} \times \mathbf{W} = \varepsilon_{ABC} V^B W^C \mathbf{G}^A \,, \ \boldsymbol{\alpha} \times \boldsymbol{\beta} = \varepsilon^{ABC} \alpha_B \beta_C \mathbf{G}_A \,. \tag{2.75}$$

Since the Levi-Civita connection is symmetric, the covariant derivative in (2.74) can be replaced with a partial derivative:

$$\varepsilon^{ABC} \alpha_{C;B} = \varepsilon^{ABC} \alpha_{C,B} - \varepsilon^{ABC} \overset{G}{\Gamma}{}^{\ .A}_{[BC]} \alpha_A = \varepsilon^{ABC} \alpha_{C,B} = \varepsilon^{ABC} \partial_B \alpha_C \,. \tag{2.76}$$

The Laplacian of a scalar function f is computed in general curvilinear coordinates as

$$\overset{G}{\nabla}{}^2 f = \left(G^{AB} f_{,A} \right)_{;B} = G^{AB} \left(f_{,A} \right)_{;B} = \sqrt[-1]{G} \left(\sqrt{G} G^{AB} f_{,A} \right)_{,B} \,. \tag{2.77}$$

A number of other identities can be derived immediately from definitions in (2.68)-(2.77). For example,

$$\left\langle \overset{G}{\nabla}, \overset{G}{\nabla} \times \boldsymbol{\alpha} \right\rangle = \varepsilon^{ABC} \alpha_{C;BA} = \varepsilon^{ABC} \alpha_{C;(BA)} = 0 \,, \tag{2.78}$$

$$\overset{G}{\nabla} \times \overset{G}{\nabla} f = \varepsilon^{ABC} f_{;CB} \mathbf{G}_A = \varepsilon^{ABC} f_{;(CB)} \mathbf{G}_A = 0 \,. \tag{2.79}$$

Many others can be found in books on vector calculus, electromagnetism (Stratton 1941; Jackson 1999), or continuum mechanics (Malvern 1969).

Two mathematical operations for second- and higher-order tensors are defined next: the generalized dual product and the double-dot product. These operations will become particularly useful in Chapter 4 (and in subsequent Chapters) for defining energetic quantities in the context of the continuum thermodynamics of deformable bodies. The generalized dual product written for rank two tensors extends (2.4) to second-order tensors, providing a scalar product of two such quantities. For example,

$$\langle \mathbf{A}, \mathbf{B} \rangle = A^{AB} B_{BA} \quad \left\{ \forall \mathbf{A} \in T_X B_0 \times T_X B_0, \mathbf{B} \in T_X^* B_0 \times T_X^* B_0 \right\}, \tag{2.80}$$

$$\langle \mathbf{a}, \mathbf{b} \rangle = a^{ab} b_{ba} \quad \left\{ \forall \mathbf{a} \in T_x B \times T_x B, \mathbf{b} \in T_x^* B \times T_x^* B \right\}, \tag{2.81}$$

$$\langle \mathbf{C}, \mathbf{D} \rangle = C^a_{\cdot A} D^A_{\cdot a} \quad \left\{ \forall \mathbf{C} \in T_x B \times T_X^* B_0, \mathbf{D} \in T_X B_0 \times T_x^* B \right\}. \tag{2.82}$$

In (2.82), $\mathbf{C}$ and $\mathbf{D}$ are examples of two-point tensors. The double-dot product, denoted by boldface colon $\boldsymbol{:}$, implies summation over two sets of adjacent indices of second- and higher-order tensors. As with the generalized dual product, the double-dot product may be applied to quantities defined on the tangent and/or cotangent spaces of one or more configurations, i.e., two-point tensors. For example,

$$\mathbf{A} : \mathbf{B} = A^{AB} B_{AB} \quad \left\{ \forall \mathbf{A} \in T_X B_0 \times T_X B_0, \mathbf{B} \in T_X^* B_0 \times T_X^* B_0 \right\}, \tag{2.83}$$

$$\mathbf{a} : \mathbf{b} = a^{ab} b_{ab} \quad \left\{ \forall \mathbf{a} \in T_x B \times T_x B, \mathbf{b} \in T_x^* B \times T_x^* B \right\}, \tag{2.84}$$

$$\mathbf{C} : \mathbf{D} = C^{aA} D_{aA} \quad \left\{ \forall \mathbf{C} \in T_x B \times T_X B_0, \mathbf{D} \in T_x^* B \times T_x^* B_0 \right\}, \tag{2.85}$$

$$\mathbf{E} : \mathbf{F} = E^{abcd} F_{cd} \mathbf{g}_a \otimes \mathbf{g}_b \left\{ \forall \mathbf{E} \in T_x B \times T_x B \times T_x B \times T_x B, \mathbf{F} \in T_x^* B \times T_x^* B \right\}. \tag{2.86}$$

Notice from (2.86) that when tensors of rank greater than two are involved, the double-dot product operation does not yield a scalar as the result. In situations where there is no chance for confusion, e.g., scalar products of mixed contravariant-covariant pairs along the lines of (2.82), the dual product and double-dot product notations may be used interchangeably. In terms of the trace operation of (2.68),

$$\langle \mathbf{A}, \mathbf{B} \rangle = \mathrm{tr}\left(\mathbf{AB} \right) = \mathrm{tr}\left(\mathbf{A}^T \mathbf{B}^T \right), \quad \mathbf{A} : \mathbf{B} = \mathrm{tr}\left(\mathbf{AB}^T \right) = \mathrm{tr}\left(\mathbf{A}^T \mathbf{B} \right). \tag{2.87}$$

2.4 Physical Components

Components of vectors and tensors expressed in general curvilinear coordinates generally do not all exhibit the same dimensional units. In general curvilinear systems, basis vectors need not be dimensionless. Physical components of these objects can be introduced so that all components exhibit the same dimensions, and so that all basis vectors are dimensionless and of unit length. Developments that follow in Section 2.4 are expressed with respect to the reference configuration; analogous expressions apply for spatial coordinates.

Physical components are referred to dimensionless basis vectors $\mathbf{E}_A$ obtained by normalizing basis vectors of a general curvilinear coordinate system by their lengths:

$$\mathbf{E}_A = \frac{\mathbf{G}_A}{(\mathbf{G}_A \bullet \mathbf{G}_A)^{1/2}} = \mathbf{G}_A \sqrt[-1]{G_{\underline{AA}}} , \qquad (2.88)$$

where underlined indices are not subject to the summation convention. An arbitrary vector $\mathbf{V} \in T_X B_0$ can be written as

$$\mathbf{V} = V^A \mathbf{G}_A = V^A \sqrt{G_{\underline{AA}}} \mathbf{E}_A = V^{\langle A \rangle} \mathbf{E}_A , \qquad (2.89)$$

where contravariant physical components of $\mathbf{V}$ are

$$V^{\langle A \rangle} = V^A \sqrt{G_{\underline{AA}}} . \qquad (2.90)$$

Covariant components satisfy

$$V_A = G_{AB} V^B = G_{AB} \sqrt[-1]{G_{\underline{BB}}} V^{\langle B \rangle} . \qquad (2.91)$$

Physical components of a tensor of higher order can be defined by considering the way the tensor represents phenomena in physics; however, transformation formulae for higher-order tensors from general curvilinear components to physical components often involve lengthy manipulations (Malvern 1969). Listed next are useful expressions for general orthogonal curvilinear coordinates, cylindrical coordinates, and spherical coordinates. Other kinds of curvilinear coordinate systems—elliptic, parabolic, bipolar, spheroidal, paraboloidal, and ellipsoidal—are addressed by Stratton (1941).

2.4.1 General Orthogonal Coordinates

General orthogonal coordinates are defined by the requirement that at each point X, the coordinate curves X^A passing through X are mutually orthogonal. This requirement results in a diagonal metric tensor

$$G_{AB} = \mathbf{G}_A \cdot \mathbf{G}_B = \begin{cases} G_{AA} & \forall A = B, \\ 0 & \forall A \neq B. \end{cases} \tag{2.92}$$

Thus

$$d\mathbf{X} \cdot d\mathbf{X} = dX^A G_{AB} dX^B = G_{11}(dX^1)^2 + G_{22}(dX^2)^2 + G_{33}(dX^3)^2, \tag{2.93}$$

$$G_{AA} = 1/G^{AA}, \tag{2.94}$$

$$G = G_{11}G_{22}G_{33}, \quad G^{-1} = G^{11}G^{22}G^{33}. \tag{2.95}$$

Non-vanishing Christoffel symbols are

$$\overset{G}{\Gamma}{}^{..B}_{AA} = -\frac{1}{2G_{BB}} G_{AA,B}, \quad \overset{G}{\Gamma}{}^{..B}_{BA} = \overset{G}{\Gamma}{}^{..B}_{AB} = (\ln\sqrt{G_{BB}})_{,A}, \quad \overset{G}{\Gamma}{}^{..A}_{AA} = (\ln\sqrt{G_{AA}})_{,A}, \tag{2.96}$$

and otherwise

$$\overset{G}{\Gamma}{}^{..A}_{BC} = 0 \ (A \neq B \neq C). \tag{2.97}$$

In contravariant physical components of orthogonal coordinates, the gradient and Laplacian of a scalar function $f(X)$ and the divergence and curl of a vector field $\mathbf{V}(X)$ are, respectively (Eringen 1962)

$$\overset{G}{\nabla} f = \sqrt[-]{G_{11}} f_{,1} \mathbf{E}_1 + \sqrt[-]{G_{22}} f_{,2} \mathbf{E}_2 + \sqrt[-]{G_{33}} f_{,3} \mathbf{E}_3, \tag{2.98}$$

$$\overset{G}{\nabla}{}^2 f = \sqrt[-]{G}\Big[(\sqrt[-]{G_{11}}\sqrt{G_{22}G_{33}} f_{,1})_{,1} + (\sqrt[-]{G_{22}}\sqrt{G_{33}G_{11}} f_{,2})_{,2} + (\sqrt[-]{G_{33}}\sqrt{G_{11}G_{22}} f_{,3})_{,3} \Big], \tag{2.99}$$

$$\Big\langle \overset{G}{\nabla}, \mathbf{V} \Big\rangle = \sqrt[-]{G}\Big[(\sqrt{G_{22}G_{33}} V^{\langle 1 \rangle})_{,1} + (\sqrt{G_{33}G_{11}} V^{\langle 2 \rangle})_{,2} + (\sqrt{G_{11}G_{22}} V^{\langle 3 \rangle})_{,3} \Big], \tag{2.100}$$

$$\overset{G}{\nabla} \times \mathbf{V} = \sqrt[-]{G_{22}G_{33}}\Big[(\sqrt{G_{33}} V^{\langle 3 \rangle})_{,2} - (\sqrt{G_{22}} V^{\langle 2 \rangle})_{,3} \Big] \mathbf{E}_1$$
$$+ \sqrt[-]{G_{33}G_{11}}\Big[(\sqrt{G_{11}} V^{\langle 1 \rangle})_{,3} - (\sqrt{G_{33}} V^{\langle 3 \rangle})_{,1} \Big] \mathbf{E}_2 \tag{2.101}$$
$$+ \sqrt[-]{G_{11}G_{22}}\Big[(\sqrt{G_{22}} V^{\langle 2 \rangle})_{,1} - (\sqrt{G_{11}} V^{\langle 1 \rangle})_{,2} \Big] \mathbf{E}_3.$$

2.4.2 Cylindrical Coordinates

Cylindrical coordinates $(X^1, X^2, X^3) \rightarrow (R, \theta, Z)$ are a particular kind of orthogonal curvilinear coordinates. Transformation formulae to Cartesian coordinates and metric tensor components are listed in Table 2.1, and Christoffel symbols are listed in Table 2.2. In particular, a squared increment of distance is

$$dX \cdot dX = dX^A G_{AB} dX^B = G_{RR}(dR)^2 + G_{\theta\theta}(d\theta)^2 + G_{ZZ}(dZ)^2$$
$$= (dR)^2 + R^2(d\theta)^2 + (dZ)^2. \tag{2.102}$$

In physical components of cylindrical coordinates, the gradient and Laplacian of a scalar $f(X)$ and the divergence and curl of a vector field $\mathbf{V}(X)$ are, respectively,

$$\overset{G}{\nabla} f = f_{,R} \mathbf{E}_R + R^{-1} f_{,\theta} \mathbf{E}_\theta + f_{,Z} \mathbf{E}_Z, \tag{2.103}$$

$$\overset{G}{\nabla}^2 f = f_{,RR} + R^{-1} f_{,R} + R^{-2} f_{,\theta\theta} + f_{,ZZ}, \tag{2.104}$$

$$\left\langle \overset{G}{\nabla}, \mathbf{V} \right\rangle = R^{-1}(RV_R)_{,R} + R^{-1}V_{\theta,\theta} + V_{Z,Z}, \tag{2.105}$$

$$\overset{G}{\nabla} \times \mathbf{V} = \left[R^{-1}V_{Z,\theta} - V_{\theta,Z} \right] \mathbf{E}_R + \left[V_{R,Z} - V_{Z,R} \right] \mathbf{E}_\theta$$
$$+ R^{-1} \left[(RV_\theta)_{,R} - V_{R,\theta} \right] \mathbf{E}_Z. \tag{2.106}$$

By convention, indices of physical components of a vector in cylindrical coordinates are written in the subscript position, with angled brackets on indices omitted: $V^{\langle 1 \rangle} = V^{\langle R \rangle} = V_R$, $V^{\langle 2 \rangle} = V^{\langle \theta \rangle} = V_\theta$, and $V^{\langle 3 \rangle} = V^{\langle Z \rangle} = V_Z$.

2.4.3 Spherical Coordinates

Spherical coordinates $(X^1, X^2, X^3) \rightarrow (R, \theta, \varphi)$ are a second particular kind of orthogonal curvilinear coordinates. Transformation formulae to Cartesian coordinates and metric tensor components are listed in Table 2.1; Christoffel symbols are listed in Tables 2.2. In particular, a squared increment of distance is

$$dX \cdot dX = dX^A G_{AB} dX^B = G_{RR}(dR)^2 + G_{\theta\theta}(d\theta)^2 + G_{\varphi\varphi}(d\varphi)^2$$
$$= (dR)^2 + R^2(d\theta)^2 + R^2 \sin^2\theta(d\varphi)^2. \tag{2.107}$$

In physical components of spherical coordinates, the gradient and Laplacian of a scalar $f(X)$ and the divergence and curl of a vector field $\mathbf{V}(X)$ are computed, respectively, as follows:

$$\overset{G}{\nabla} f = f_{,R} \mathbf{E}_R + R^{-1} f_{,\theta} \mathbf{E}_\theta + (R\sin\varphi)^{-1} f_{,\varphi} \mathbf{E}_\varphi, \tag{2.108}$$

$$\overset{G}{\nabla}^2 f = R^{-2}(R^2 f_{,R})_{,R} + (R^2 \sin\theta)^{-1}(f_{,\theta}\sin\theta)_{,\theta} + (R\sin\theta)^{-2} f_{,\varphi\varphi}, \tag{2.109}$$

$$\left\langle \overset{G}{\nabla}, \mathbf{V} \right\rangle = R^{-2}(R^2 V_R)_{,R} + (R\sin\theta)^{-1} \left[(V_\theta \sin\theta)_{,\theta} + V_{\varphi,\varphi} \right], \tag{2.110}$$

$$\overset{\mathbf{G}}{\nabla} \times \mathbf{V} = (R\sin\theta)^{-1}\left[(V_\varphi \sin\theta)_{,\theta} - V_{\theta,\vartheta}\right]\mathbf{E}_R$$
$$+ R^{-1}\left[(\sin\theta)^{-1}V_{R,\varphi} - (RV_\varphi)_{,R}\right]\mathbf{E}_\theta \qquad (2.111)$$
$$+ R^{-1}\left[(RV_\theta)_{,R} - V_{R,\theta}\right]\mathbf{E}_\varphi.$$

By convention, indices of physical components of a vector in spherical co-ordinates are written in the subscript position, with angled brackets on indices omitted: $V^{\langle 1 \rangle} = V^{\langle R \rangle} = V_R$, $V^{\langle 2 \rangle} = V^{\langle \theta \rangle} = V_\theta$, and $V^{\langle 3 \rangle} = V^{\langle \varphi \rangle} = V_\varphi$.

2.5 The Deformation Gradient

The deformation gradient is a fundamental descriptor of kinematics of deformable bodies, and is of particular importance in the context of nonlinear solid mechanics. In Section 2.5, the definition and interpretation of the deformation gradient are provided, followed by definitions and identities for key quantities derived from the deformation gradient.

2.5.1 Fundamentals

Recall from Section 2.1.2 that motion from the reference configuration to the current configuration of a deformable body is denoted by continuous, invertible, one-to-one function $\varphi = \chi_t \circ \chi_0^{-1} : B_0 \to B$. The deformation gradient field is defined as the tangent of φ, mapping vectors in TB_0 to vectors in TB, or locally at material point X, $\mathbf{F}(X) = T\varphi_X : T_X B_0 \to T_x B$. A visual interpretation is provided in Fig. 2.2. When coordinate systems x^a and X^a are introduced on B_0 and B, respectively, such that $x^a = \varphi^a(X^A, t)$, then deformation gradient $\mathbf{F}$ can be written as

$$\mathbf{F} = F_{.A}^a \mathbf{g}_a \otimes \mathbf{G}^A = \frac{\partial \varphi^a}{\partial X^A}\mathbf{g}_a \otimes \mathbf{G}^A \in T_x B \times T_X^* B_0. \qquad (2.112)$$

In components, the deformation gradient is often written[4] $F_{.A}^a(X,t) = x_{.A}^a$. At any particular time t, spatial coordinates x^a occupied by the body are assumed one-to-one functions of X^A and (usually) differential of class C^r ($r \geq 1$) with respect to X^A. Also at any time t, reference locations occupied by the body with coordinates X^A are assumed one-to-one and of

---

[4] Partial differentiation proceeds as $\partial_A(\cdot) = (\cdot)_{,A} = (\cdot)_{,a}\partial_A x^a = (\cdot)_{,a}x_{.A}^a = \partial_a(\cdot)F_{.A}^a$.

class C^r with respect to spatial coordinates x^a. Thus $\det(x^a_{.,A}) \neq 0$. If $r = 0$ across certain singular surfaces within an otherwise "smooth" body, then **F** may be discontinuous across such surfaces. Because it is referred to (possibly) distinct coordinate systems in different configurations, **F** is said to be a two-point tensor or double tensor (Ericksen 1960) whose components each transform like those of a vector (upper index) or covector (lower index) under transformations of only one set of coordinates. The deformation gradient operates on an arbitrary vector $\mathbf{V} = V^B \mathbf{G}_B \in T_X B_0$ as

$$\mathbf{F}\mathbf{V} = F^a_{.A} \mathbf{g}_a \otimes \mathbf{G}^A \left(V^B \mathbf{G}_B \right)$$
$$= F^a_{.A} V^B \mathbf{g}_a \left\langle \mathbf{G}^A, \mathbf{G}_B \right\rangle = F^a_{.A} V^A \mathbf{g}_a \in T_x B, \tag{2.113}$$

where the first of (2.4) has been used. From (2.113) it is clear why the deformation gradient is called a tangent map: **F** maps a reference vector **V** that is a linear combination of tangent basis vectors at a point X on the reference configuration to a spatial vector **FV** that is a linear combination of tangent basis vectors at a point x on the current configuration.

The deformation gradient provides the first-order approximation of the length and direction of a differential line element $d\mathbf{x} \in T_x B$ mapped to the current configuration from its referential representation $d\mathbf{X} \in T_X B_0$. For example, a Taylor-like series expansion can be written (Toupin 1964)

$$dx^a = x^a(X') - x^a(X)$$

$$= \underbrace{x^a_{.,A}\Big|_X}_{F^a_{.A}} dX^A + \frac{1}{2!} \underbrace{x^a_{.,AB}\Big|_X}_{F^a_{.AB}} dX^A dX^B + \frac{1}{3!} \underbrace{x^a_{.,ABC}\Big|_X}_{F^a_{.ABC}} dX^A dX^B dX^C + ... , \tag{2.114}$$

with $dX^A = X'^A - X^A$ an infinitesimal vector between reference points X and X'. Section D.1 of Appendix D contains a complete tensor derivation of (2.114), to second order in $d\mathbf{X}$. To first order in $d\mathbf{X}$,

$$d\mathbf{x} = \mathbf{F}d\mathbf{X}, \quad dx^a = F^a_{.A} dX^A = x^a_{.,A} dX^A. \tag{2.115}$$

In (2.114), the total covariant derivative of the deformation gradient, i.e., the second-order position gradient, obeys (Eringen 1962; Toupin 1964)

$$x^a_{:AB} = F^a_{.A:B} = F^a_{.A,B} - \overset{G}{\Gamma}{}^{.C}_{BA} F^a_{.C} + \overset{g}{\Gamma}{}^{.a}_{bc} F^c_{.A} F^b_{.B}$$
$$= x^a_{.,AB} - \overset{G}{\Gamma}{}^{.C}_{BA} x^a_{.,C} + \overset{g}{\Gamma}{}^{.a}_{bc} x^c_{.,A} x^b_{.,B}. \tag{2.116}$$

The total covariant derivative of a generic two-point or double tensor of arbitrary order, $\mathbf{A}(X, x)$, is defined as (Ericksen 1960; Eringen 1962)

$$(A^{A...C\ a...c}_{D...F\ d...f})_{:K} = (A^{A...C\ a...c}_{D...F\ d...f})_{;K} + (A^{A...C\ a...c}_{D...F\ d...f})_{;k} F^k_{.K}$$
$$= (A^{A...C\ a...c}_{D...F\ d...f})_{:k} F^k_{.K} = (A^{A...C\ a...c}_{D...F\ d...f})_{:k} x^k_{.,K}. \tag{2.117}$$

Partial covariant derivatives of **A** are found by applying the usual rules of covariant differentiation in (2.30) to only one index. For example,

$$A^a_{.A;B} = A^a_{.A,B} - \overset{G}{\Gamma}{}^{.C}_{BA} A^a_{.C}, \quad A^a_{.A;b} = A^a_{.A,b} + \overset{g}{\Gamma}{}^{.a}_{bc} A^c_{.A}. \tag{2.118}$$

In (2.116), regarding $x^a_{.,A} = x^a_{.,A}(X)$ leads to inclusion of only one second-order partial derivative in the total covariant derivative of **F** (Eringen 1962; Toupin 1964), though in general $F^a_{.A,b} = F^a_{.A,B} F^{-1B}_{.b} \neq 0$. From the chain rule, $F^a_{.A:B} = F^a_{.A:b} F^b_{.B}$ and $F^a_{.A:b} = F^a_{.A:B} F^{-1B}_{.b}$ (Ericksen 1960). Third-order position gradient $x^a_{:ABC}$ can be computed by taking the total covariant derivative of $F^a_{.A:B}$ via another iteration of (2.117). Partial covariant derivatives of two-point shifter tensors vanish: $g^A_{.a;b} = 0$, $g^a_{.A;B} = 0$, $g^a_{.A;b} = 0$, and $g^A_{.a;B} = 0$ (Toupin 1956; Ericksen 1960). For example, $g^A_{.a;b} = \mathbf{G}^A \cdot \mathbf{g}_{a;b} = 0$. Then from (2.117), total covariant derivatives of shifters must vanish: $g^A_{.a:b} = 0$, $g^a_{.A:B} = 0$, $g^a_{.A:b} = 0$, and $g^A_{.a:B} = 0$. Thus it follows that partial covariant differentiation and total covariant differentiation both commute with shifting, raising, and lowering of indices.

The dual map $\mathbf{F}^*$ of the two-point tensor **F** is defined by

$$\left\langle \mathbf{F}^*\boldsymbol{\alpha}, \mathbf{V} \right\rangle = \left\langle \boldsymbol{\alpha}, \mathbf{F}\mathbf{V} \right\rangle \; \forall \; \boldsymbol{\alpha} \in T^*_x B, \mathbf{V} \in T_X B_0. \tag{2.119}$$

From the properties of the mapping φ, deformation gradient tensor **F** is non-singular, and its inverse satisfies

$$\mathbf{F}^{-1}\mathbf{F} = \mathbf{1}_0, \; X^A_{.,a} x^a_{.,B} = \delta^A_{.B}; \; \mathbf{F}\mathbf{F}^{-1} = \mathbf{1}, \; x^a_{.,A} X^A_{.,b} = \delta^a_{.b}; \tag{2.120}$$

where $\mathbf{1}_0 = \delta^A_{.B} \mathbf{G}_A \otimes \mathbf{G}^B$ and $\mathbf{1} = \delta^a_{.b} \mathbf{g}_a \otimes \mathbf{g}^b$ are identity tensors on B_0 and B. In components, the inverse $F^{-1A}_{.a}(x,t) = X^A_{.,a}$, and partial differentiation $\partial_a(.) = \partial_A(.) F^{-1A}_{.a}$. The dual and inverse commute: $\mathbf{F}^{*-1} = \mathbf{F}^{-1*} = \mathbf{F}^{-*}$. In components, the dual, inverse, and dual-inverse of **F** are, respectively,

$$\mathbf{F}^* = F^{.a}_A \mathbf{G}^A \otimes \mathbf{g}_a \in T^*_X B_0 \times T_x B, \tag{2.121}$$

$$\mathbf{F}^{-1} = F^{-1\;A}_{.a} \mathbf{G}_A \otimes \mathbf{g}^a \in T_X B_0 \times T^*_x B, \tag{2.122}$$

$$\mathbf{F}^{-*} = F^{-*\;A}_{.a} \mathbf{g}^a \otimes \mathbf{G}_A \in T^*_x B \times T_X B_0. \tag{2.123}$$

The transpose map $\mathbf{F}^T$ between metric vector spaces $(T_X B_0, \mathbf{G})$ and $(T_x B, \mathbf{g})$ is defined by the operation

$$(\mathbf{F}^T\mathbf{w}) \cdot \mathbf{V} = \mathbf{w} \cdot (\mathbf{F}\mathbf{V}) \; \forall \; \mathbf{w} \in T_x B, \mathbf{V} \in T_X B_0. \tag{2.124}$$

Upon inspection of (2.119) and (2.124), the relationship between the transpose and dual maps is apparent:

$$\mathbf{F}^T = \mathbf{G}^{-1}\mathbf{F}^*\mathbf{g}\,. \tag{2.125}$$

Notice that the transpose map depends on the metric tensors of each configuration, while the dual map is defined independently of the metric in either configuration. In index notation, the dual map corresponds to a horizontal switch of indices, while the transpose corresponds to a diagonal switch. In coordinates, transpose and inverse-transpose maps are written

$$\mathbf{F}^T = G^{AB} F_B^{*.b} g_{ba} \, \mathbf{G}_A \otimes \mathbf{g}^a \in T_X B_0 \times T_x^* B\,, \tag{2.126}$$

$$\mathbf{F}^{-T} = g^{ab} F_{\ b}^{-*.B} G_{BA} \, \mathbf{g}_a \otimes \mathbf{G}^A \in T_x B \times T_X^* B_0\,. \tag{2.127}$$

Two specific kinds of coordinate representation of the motion (and hence the deformation gradient) are common: convected coordinate representations and Cartesian coordinate representations.

For one kind of representation in convected coordinates, basis vectors of the spatial frame are updated with the motion in such a way that numerical values of the coordinates of a material particle in reference and spatial descriptions always coincide:

$$x^a(X,t) = \delta_{.A}^a X^A\,, \ F_{.A}^a = \delta_{.A}^a\,, \ \mathbf{F} = \mathbf{g}_a(x,t) \otimes \mathbf{G}^A(X)\,. \tag{2.128}$$

Alternatively, convected coordinates can be expressed in terms of spatial basis vectors fixed in time and updated reference basis vectors, again resulting in coincident numerical values of coordinates of a material particle:

$$x^a(X,t) = \delta_{.A}^a X^A\,, \ F_{.A}^a = \delta_{.A}^a\,, \ \mathbf{F} = \mathbf{g}_a(x) \otimes \mathbf{G}^A(X,t)\,. \tag{2.129}$$

Because basis vectors for spatial and reference coordinates, respectively, in (2.128) and (2.129) evolve with time, associated metric tensors will also change with time as the body deforms. Convected coordinates of types (2.128) and (2.129) will not be used henceforward in this book for describing the relationship between reference and spatial coordinates of a material particle. Definition (2.112)—which is applicable in general curvilinear coordinates—is used this book, but it is henceforth restricted to non-deforming, inertial coordinate systems on B_0 and B, thus ruling out use of convected coordinates. Accordingly, natural basis vectors and metric tensors do not depend explicitly on time: in the reference configuration $\mathbf{G}_A = \mathbf{G}_A(X)$, $\mathbf{G}^A = \mathbf{G}^A(X)$, and hence $G_{AB} = G_{AB}(X)$. Likewise in the current configuration, $\mathbf{g}_a = \mathbf{g}_a(x)$, $\mathbf{g}^a = \mathbf{g}^a(x)$, and $g_{ab} = g_{ab}(x)$. Thus in the remainder of this book, holonomic basis vectors can change with position (X or x) as is the case for curvilinear coordinates, but the origin of each coordinate system for X^A and x^a remains fixed in both time and space.

The presentation of kinematics of deformable bodies simplifies considerably in Cartesian coordinates, also often called rectangular coordinates, rectilinear coordinates, or flat coordinates. If coincident Cartesian coordi-

nate axes[5] are specified with $\mathbf{e}_A = \mathbf{G}_A = \delta^a_{.A}\mathbf{g}_a$, $\mathbf{e}^A = \mathbf{G}^A = \delta^A_{.a}\mathbf{g}^a$, $G_{AB} = \delta_{AB}$, $g_{ab} = \delta_{ab}$, $g^a_{.A} = \delta^a_{.A}$, and $g^A_{.a} = \delta^A_{.a}$, then (2.112) becomes, quite simply,

$$\mathbf{F} = F^A_{.B}\mathbf{e}_A \otimes \mathbf{e}^B . \tag{2.130}$$

Occasionally Cartesian representation (2.130) is used in this book, again assuming that the orientation of each basis vector remains fixed in time. Restriction of validity of a corresponding expression to Cartesian coordinates will be stated explicitly. In (2.130), notice $F^A_{.B} = \delta^A_{.a}x^a_{.,B} \neq X^A_{.,B} = \delta^A_{.B}$.

Push-forward and pull-back operations are now defined. The push forward of a scalar $f : B_0 \rightarrow \mathbb{R}$ is defined by $\varphi_* f = f \circ \varphi^{-1}$. The pull-back of a scalar $h : B \rightarrow \mathbb{R}$ is defined by $\varphi^* h = h \circ \varphi$. The push-forward $\varphi_* \mathbf{V}$ of a vector $\mathbf{V} \in T_X B_0$, the pull-back $\varphi^* \mathbf{w}$ of a vector $\mathbf{w} \in T_x B$, the push-forward $\varphi_* \boldsymbol{\alpha}$ of a covector $\boldsymbol{\alpha} \in T^*_X B_0$, and the pull-back $\varphi^* \boldsymbol{\beta}$ of a covector $\boldsymbol{\beta} \in T^*_x B$ are defined by

$$\varphi_* \mathbf{V} = T\varphi_X(\mathbf{V}) \circ \varphi^{-1} = \mathbf{F}\mathbf{V} \circ \varphi^{-1} \in T_x B , \tag{2.131}$$

$$\varphi^* \mathbf{w} = (T\varphi_X)^{-1}(\mathbf{w}) \circ \varphi = \mathbf{F}^{-1}\mathbf{w} \circ \varphi \in T_X B_0 , \tag{2.132}$$

$$\varphi_* \boldsymbol{\alpha} = (T\varphi_X)^{-*}(\boldsymbol{\alpha}) \circ \varphi^{-1} = \mathbf{F}^{-*}\boldsymbol{\alpha} \circ \varphi^{-1} \in T^*_x B , \tag{2.133}$$

$$\varphi^* \boldsymbol{\beta} = (T\varphi_X)^*(\boldsymbol{\beta}) \circ \varphi = \mathbf{F}^*\boldsymbol{\beta} \circ \varphi \in T^*_X B_0 . \tag{2.134}$$

By extension, the push-forward to the current configuration of arbitrary tensor $\mathbf{A}$ of rank $\{^N_M\}$ referred to the reference configuration is defined as

$$\varphi_* \mathbf{A}(\mathbf{w}_1, ... \mathbf{w}_M, \boldsymbol{\beta}_1, ... \boldsymbol{\beta}_N) = \mathbf{A}(\mathbf{F}^{-1}\mathbf{w}_1, ... \mathbf{F}^{-1}\mathbf{w}_M, \mathbf{F}^*\boldsymbol{\beta}_1, ... \mathbf{F}^*\boldsymbol{\beta}_N) \tag{2.135}$$
$$\forall \, \mathbf{w}_i \in T_x B, \, \boldsymbol{\beta}_i \in T^*_x B.$$

Similarly, the pull-back from the spatial configuration of arbitrary tensor $\mathbf{b}$ of order $\{^N_M\}$ to the reference configuration is defined as

$$\varphi^* \mathbf{b}(\mathbf{V}_1, ... \mathbf{V}_M, \boldsymbol{\alpha}_1, ... \boldsymbol{\alpha}_N) = \mathbf{b}(\mathbf{F}\mathbf{V}_1, ... \mathbf{F}\mathbf{V}_M, \mathbf{F}^{-*}\boldsymbol{\alpha}_1, ... \mathbf{F}^{-*}\boldsymbol{\alpha}_N) \tag{2.136}$$
$$\forall \, \mathbf{V}_i \in T_X B_0, \, \boldsymbol{\alpha}_i \in T^*_X B_0.$$

Composition with φ^{-1} and φ for respective push-forward and pull-back operations in (2.131)-(2.134) is often implied rather than written explicitly and is omitted henceforth when there is no chance of confusion.

---

[5] This is a stricter requirement than non-coincident Cartesian coordinates, wherein the metric tensors reduce to Kronecker delta symbols, but the shifters represent rigid rotations independent of location.

Since reference and current configurations are embedded in Euclidean space, it is possible to introduce, for each material particle, a displacement function **u** with spatial components (Eringen 1962)

$$u^a = x^a - X^a + \xi^a , \qquad (2.137)$$

where x^a are spatial components of the vector from the origin of a fixed Cartesian coordinate frame to the particle in the deformed body, $X^a = g^a_{.A} X^A$ are spatial components of the vector from the origin of a different fixed Cartesian coordinate frame to the same particle in the undeformed body, and ξ^a are spatial components of the vector extending from the origin of the Cartesian frame in the reference configuration to the origin of the Cartesian frame in the current configuration. Using shifters and metric tensors of Section 2.1.2,

$$u^A = g^A_{.a} u^a = g^{Aa} u_a = G^{AB} u_B . \qquad (2.138)$$

Since ξ^a are components of a constant vector, deformation gradient components $F^a_{.A}(X,t)$ can be represented as (Toupin 1956; Suhubi and Eringen 1964)

$$F^a_{.A} = x^a_{,A} = (u^a + X^a - \xi^a)_{,A} = (u^B g^a_{.B})_{,A} + (X^B g^a_{.B})_{,A} - (\xi^B g^a_{.B})_{,A}$$

$$= (u^B_{,A} + X^B_{,A} - \xi^B_{,A}) g^a_{.B} + (X^B + u^B - \xi^B)(\mathbf{g}^a \cdot \mathbf{G}_{B,A}) \qquad (2.139)$$

$$= (u^B_{;A} + \delta^B_{.A}) g^a_{.B}.$$

Similarly, components of the inverse deformation gradient, $F^{-1A}_{\ \ .a}(x,t)$, can be expressed as

$$F^{-1A}_{\ \ .a} = X^A_{,a} = (\delta^b_{.a} - u^b_{;a}) g^A_{.b}. \qquad (2.140)$$

It is emphasized that the deformation gradient and its inverse cannot be represented by (2.139) and (2.140) when reference and current configurations are non-Euclidean spaces, in which case (2.137) does not apply.

2.5.2 Derived Kinematic Quantities and Identities

The Jacobian determinant of **F** provides the relationship between a differential reference volume element $dV = \sqrt{G} dX^1 dX^2 dX^3 \subset B_0$ and its deformed counterpart in the current configuration $dv = \sqrt{g} dx^1 dx^2 dx^3 \subset B$:

$$J dV = dv . \qquad (2.141)$$

In coordinates (Truesdell and Toupin 1960; Eringen 1962; Marsden and Hughes 1983; Dluzewski 1996), the Jacobian determinate is computed as follows:

$$J = \frac{1}{6}\varepsilon_{abc}\varepsilon^{ABC}F^a_{.A}F^b_{.B}F^c_{.C} = \frac{1}{6}\sqrt{g/G}e_{abc}e^{ABC}F^a_{.A}F^b_{.B}F^c_{.C}$$

$$= \frac{1}{6}\det\mathbf{F}\sqrt{g/G} = \frac{1}{6}\det(x^a_{.,A})\sqrt{\det(g_{ab})/\det(G_{AB})}, \qquad (2.142)$$

where (2.64) and (2.65) have been used. For the inverse deformation[6],

$$6J^{-1} = \varepsilon^{abc}\varepsilon_{ABC}F^{-1A}_{.a}F^{-1B}_{.b}F^{-1C}_{.c} = \sqrt{G/g}\det\mathbf{F}^{-1}.$$ From (2.64)-(2.67) and

Table 2.3, it follows that permutation tensors map between configurations

via $\varepsilon^{abc} = J^{-1}\varepsilon^{ABC}F^a_{.A}F^b_{.B}F^c_{.C}$ and $\varepsilon_{abc} = J\varepsilon_{ABC}F^{-1A}_{.a}F^{-1B}_{.b}F^{-1C}_{.c}$. Jacobian

$J(X,t)$, unlike $\det\mathbf{F}$, is an absolute scalar, invariant under coordinate transformations (Marsden and Hughes 1983). Since volume v remains positive and bounded, $0 < J < \infty$. When there is no deformation, e.g., when a body undergoes only rigid translation, then $\mathbf{F} = \mathbf{1} = g^a_{.A}\mathbf{g}_a \otimes \mathbf{G}^A$,

and in that case $J = \sqrt{g/G}\det(g^a_{.A}) = 1$ follows from (2.142).

The following identity applies for the derivative of the determinant of a non-singular, second-order matrix $\mathbf{A}$ (Ericksen 1960; Thurston 1974):

$$\frac{\partial(\det\mathbf{A})}{\partial A^A_{.B}} = A^{-1B}_{.A}\det\mathbf{A}. \qquad (2.143)$$

Applying (2.143) to J and J^{-1} produces the following identities:

$$\frac{\partial J}{\partial F^a_{.A}} = JF^{-1A}_{.a}, \quad \frac{\partial J^{-1}}{\partial F^{-1A}_{.a}} = J^{-1}F^a_{.A}, \qquad (2.144)$$

as can be verified directly via inspection of (2.142). The total covariant derivative of the second of (2.144), using (2.73) and the chain rule (see the full derivation in Section D.2 of Appendix D), is

$$(\partial J^{-1}/\partial F^{-1A}_{.a})_{:a} = (J^{-1}F^a_{.A})_{:a} = \sqrt[3]{g}(\sqrt{g}J^{-1}F^a_{.A})_{,a} - J^{-1}F^a_{.C}\overset{G}{\Gamma}^{.C}_{BA}F^{-1B}_{.a} \qquad (2.145)$$

$$= J^{-1}F^{-1B}_{.a}\left[x^a_{.,AB} - x^a_{.,BA}\right] = 0.$$

Analogously, the divergence of the first of (2.144) produces the identity

$$(\partial J/\partial F^a_{.A})_{:A} = (JF^{-1A}_{.a})_{:A} = \sqrt[3]{G}(\sqrt{G}JF^{-1A}_{.a})_{,A} - J\overset{g}{\Gamma}^{.b}_{ba} = 0. \qquad (2.146)$$

Relations (2.145) and (2.146) are often called Piola identities. Using the definition of the determinant and (2.139), the Jacobian satisfies

$$J = \sqrt{g/G}\det(g^a_{.A})\det\left[u^A_{;B} + \delta^A_{.B}\right] = \det\left[u^A_{;B} + \delta^A_B\right]$$

$$\approx 1 + u^A_{;A} + (1/2)\left[(u^A_{;A})^2 - u^A_{;B}u^B_{;A}\right]. \qquad (2.147)$$

---

[6] Recall that for two generic, non-singular square matrices $\mathbf{A}$ and $\mathbf{B}$ the following identities apply: $\det(\mathbf{AB}) = (\det\mathbf{A})(\det\mathbf{B})$ and $\det(\mathbf{A}^{-1}) = (\det\mathbf{A})^{-1}$.

Terms of order three in referential displacement gradients are omitted in the final approximation in (2.147).

Let oriented differential area elements referred to configurations B_0 and B be labeled $\mathbf{N}dS$ and $\mathbf{n}ds$, respectively, where unit normal covariant vectors $\mathbf{N} \in T_X^* B_0$ and $\mathbf{n} \in T_x^* B$. These area elements are related by the transformation formula

$$\mathbf{n}ds = J\varphi_* \mathbf{N}dS, \ n_a ds = JF_{\cdot a}^{-*A} N_A dS = JF_{\cdot a}^{-1A} N_A dS . \qquad (2.148)$$

Relation (2.148) is called Nanson's formula (Malvern 1969) and represents the Piola transformation between differential forms $\mathbf{N}dS$ and $\mathbf{n}ds$ (Marsden and Hughes 1983). Let $n_a ds = \varepsilon_{abc} dx^{[b} dx^{c]} = \varepsilon_{abc} dx^b \wedge dx^c / 2$ and $N_A dS = \varepsilon_{ABC} dX^{[B} dX^{C]} = \varepsilon_{ABC} dX^B \wedge dX^C / 2$, where for two rank-one objects, the wedge product satisfies $(\alpha \wedge \beta)^{AB} = \alpha^A \wedge \beta^B = \alpha^A \beta^B - \alpha^B \beta^A$. Schouten (1954) calls $dx^a \wedge dx^b$ an infinitesimal bivector. From the above definitions of oriented differential area elements and the properties of the permutation tensor in Table 2.3, it follows that $dx^a \wedge dx^b = \varepsilon^{abc} n_c ds$ and $dX^A \wedge dX^B = \varepsilon^{ABC} N_C dS$. Notice that dx^a and dx^b are treated as components of distinct vectors in the definition of the area element; otherwise the dyad $dx^a dx^b$ would be symmetric. Notice also that the oriented area element $n_a ds = \varepsilon_{abc} dx^{[b} dx^{c]} = \varepsilon_{abc} dx^b dx^c$.

Decomposition of the deformation gradient into the product of two tensors—a rotation and a symmetric positive definite tensor called a stretch tensor—is always possible since $\mathbf{F}$ is non-singular. This separation into stretch and rotation is called the polar decomposition and is written as

$$\mathbf{F} = \mathbf{R}\mathbf{U} = \mathbf{V}\mathbf{R} , \qquad (2.149)$$

where rotation $\mathbf{R} : T_X B_0 \to T_x B$ is a proper orthogonal two-point tensor, i.e., $\mathbf{R}^{-1} = \mathbf{R}^T$ and $\mathbf{R}$ has positive Jacobian determinant of unit magnitude:

$$\mathbf{R}^T \mathbf{R} = \mathbf{1}_0, \ \mathbf{R}\mathbf{R}^T = \mathbf{1}, \ \varepsilon_{abc} \varepsilon^{ABC} R_{\cdot A}^a R_{\cdot B}^b R_{\cdot C}^c = 6 . \qquad (2.150)$$

Right stretch tensor $\mathbf{U} : T_X B_0 \to T_X B_0$ and left stretch tensor $\mathbf{V} : T_x B \to T_x B$ satisfy the following symmetry conditions:

$$G_{AB} U_{\cdot C}^B = G_{CB} U_{\cdot A}^B, \ g_{ab} V_{\cdot c}^b = g_{cb} V_{\cdot a}^b . \qquad (2.151)$$

The stretch tensors in (2.151) are determined uniquely by the polar decomposition of $\mathbf{F}$, and are related to the right and left Cauchy-Green deformation tensors, $\mathbf{C}$ and $\mathbf{B}$ respectively, as

$$\mathbf{C} = \mathbf{F}^T \mathbf{F} = \mathbf{U}^2, \ \mathbf{B} = \mathbf{F}\mathbf{F}^T = \mathbf{V}^2 . \qquad (2.152)$$

Since $\det \mathbf{R} = \sqrt{G/g} > 0$ by convention (2.150), $J = \det \mathbf{U} = \det \mathbf{V} > 0$.

The covariant version of $\mathbf{C}$ is the pull-back of spatial metric $\mathbf{g}$, and the contravariant version of $\mathbf{B}$ is the push-forward of reference metric $\mathbf{G}^{-1}$:

$$\mathbf{C} = \varphi^*(\mathbf{g}), \quad C_{AB} = F_{.A}^a g_{ab} F_{.B}^b = C_{(AB)}; \qquad (2.153)$$

$$\mathbf{B} = \varphi_*(\mathbf{G}^{-1}), \quad B^{ab} = F_{.A}^a G^{AB} F_{.B}^b = B^{(ab)}. \qquad (2.154)$$

The tensors defined in (2.153) and (2.154) are clearly symmetric. From (2.115) and (2.153), $\mathbf{C}$ assigns, to first order, the length of an infinitesimal line element after deformation:

$$|d\mathbf{x}| = |\mathbf{F}d\mathbf{X}| = \sqrt{\langle d\mathbf{X}, \mathbf{C}d\mathbf{X} \rangle}. \qquad (2.155)$$

Furthermore, the right Cauchy-Green strain tensor

$$\mathbf{E} = \frac{1}{2}(\mathbf{C} - \mathbf{G}), \quad E_{AB} = \frac{1}{2}(C_{AB} - G_{AB}) = E_{(AB)}, \qquad (2.156)$$

provides a relationship for the difference in squared lengths of deformed and undeformed line elements as

$$d\mathbf{x} \cdot d\mathbf{x} - d\mathbf{X} \cdot d\mathbf{X} = 2\langle d\mathbf{X}, \mathbf{E}d\mathbf{X} \rangle. \qquad (2.157)$$

A number of other finite strain measures not described here may be constructed from $\mathbf{F}$ or its inverse (Malvern 1969; Marsden and Hughes 1983). Notice that it is customary to represent the rotation $\mathbf{R}$ of (2.149) and (2.150) as a two-point tensor. If instead $\mathbf{R}$ is referred exclusively to reference coordinates, for example, then a shifter must be introduced into the deformation gradient, e.g., $F_{.A}^a = R_{.C}^a U_{.A}^C = g_{.B}^a R_{.C}^B U_{.A}^C = g_{.B}^a R_{.C}^B (C^{1/2})_{.A}^C$.

More kinematic identities emerge from straightforward differentiation[7]:

$$\frac{\partial C_{AB}}{\partial g_{ab}} = F_{.A}^a F_{.B}^b, \quad \frac{\partial C_{AB}}{\partial F_{.C}^a} = 2g_{ab}\delta_{.(A}^C F_{.B)}^b, \quad \frac{\partial E_{AB}}{\partial C_{CD}} = \frac{1}{2}\delta_{.(A}^{(C}\delta_{.B)}^{D)}. \qquad (2.158)$$

The following identity is derived from (2.143) and the symmetry of $\mathbf{C}$:

$$\frac{\partial(\det \mathbf{C})}{\partial C_{AB}} = C^{-1BA}\det\mathbf{C} = C^{-1AB}\det\mathbf{C}. \qquad (2.159)$$

Then because $\det\mathbf{C} = \det(C_{.B}^A) = \det(G^{AC}F_{.C}^c g_{cb}F_{.B}^b) = (g/G)(\det\mathbf{F})^2 = J^2$,

$$\frac{\partial J}{\partial E_{AB}} = 2\frac{\partial J}{\partial C_{AB}} = \frac{1}{J}\frac{\partial J^2}{\partial C_{AB}} = \frac{1}{J}\frac{\partial(\det\mathbf{C})}{\partial C_{AB}} \qquad (2.160)$$

$$= JC^{-1AB} = JF_{.a}^{-1A}g^{ab}F_{.b}^{-1B} = JX_{.,a}^A g^{ab} X_{.,b}^B.$$

---

[7] Additionally, from (2.120), $\dfrac{\partial F_{.B}^a}{\partial F_{.b}^{-1A}} = -F_{.A}^a F_{.B}^b$ and $\dfrac{\partial F_{.b}^{-1A}}{\partial F_{.B}^a} = -F_{.a}^{-1A}F_{.b}^{-1B}$.

2.5.3 Linearization

It is instructive to consider the small deformation, i.e., geometrically linear or infinitesimal, kinematic description often applied in engineering practice. In the usual linear theory, displacements and displacement gradients are assumed small so that configurations B_0 and B nearly coincide, and the same coordinate system is used in both configurations. Thus the shifter degenerates to $g^a_{.A} = \delta^a_{.A}$, and partial coordinate differentiation with respect to either configuration is nearly the same operation, e.g., $\partial_a(.) \approx \delta^A_{.a} \partial_A(.)$. Since there is only one coordinate system, lower case indices are used in this book for representation of mathematical objects the linear theory, by default. Covariant differentiation with respect to the Levi-Civita connection is represented by $\overset{g}{\nabla}$, Christoffel symbols by $\overset{g}{\Gamma}{}^{.a}_{bc}(x)$, and metric by $g_{ab}(x)$. In Euclidean space, spatial and reference coordinates are related in the linear theory by the vector addition rule

$$\mathbf{x} = \mathbf{X} + \mathbf{u} , \tag{2.161}$$

where $\mathbf{u}$ is the displacement vector. Components of the right Cauchy-Green strain tensor $\mathbf{E}(X,t)$ of (2.156) are related to spatial covariant derivatives of $\mathbf{u}(x,t)$ as (Eringen 1962)

$$2F^{-1A}_{.a} E_{AB} F^{-1B}_{.b} = u_{a;b} + u_{b;a} - u^c_{.a} u_{c;b} . \tag{2.162}$$

Components of the infinitesimal strain tensor $\boldsymbol{\varepsilon}(x,t)$ (also called the linear or small strain tensor) are defined as

$$\varepsilon_{ab} = u_{(a;b)} = \frac{1}{2}(u_{a;b} + u_{b;a}) , \tag{2.163}$$

and clearly differ from those of finite strain tensor $\mathbf{E}$ by terms of order two in displacement gradients. Such terms are assumed negligibly small with respect to the displacement gradient itself in the linear theory. Volume changes in the linear theory are computed after omitting terms of orders two and higher in displacement gradients in (2.147) as

$$J \approx 1 + u^a_{;a} = 1 + \mathrm{tr}(\overset{g}{\nabla}\mathbf{u}) , \quad J^{-1} \approx 1 - u^a_{;a} = 1 - \mathrm{tr}(\overset{g}{\nabla}\mathbf{u}) . \tag{2.164}$$

The skew rotation tensor $\boldsymbol{\Omega}$ is also introduced in the linear theory:

$$\Omega_{ab} = u_{[a;b]} = u_{[a,b]} - \overset{g}{\Gamma}{}^{.c}_{[ba]} u_c = u_{[a,b]} , \tag{2.165}$$

which itself can be reduced to a vector $\mathbf{w}$ via the axial transformation

$$w^a = -\frac{1}{2}\varepsilon^{abc}\Omega_{bc} = -\frac{1}{2}\varepsilon^{abc}u_{[b,c]} , \quad \Omega_{ab} = -\varepsilon_{abc}w^c . \tag{2.166}$$

Tensor $\boldsymbol{\Omega}$, when acting on differential element $d\mathbf{x}$, produces the relative displacement $\boldsymbol{\Omega}d\mathbf{x} = \mathbf{w} \times d\mathbf{x}$, where $(\mathbf{w} \times d\mathbf{x})_a = \varepsilon_{abc} w^b dx^c$. When all components of $\boldsymbol{\Omega}$ are small compared to one radian, this relative displacement represents a true rotation, and in Cartesian coordinates, $\mathbf{R} = \mathbf{1} + \boldsymbol{\Omega}$ is the corresponding rotation tensor appearing in (2.149).

2.6 Velocities and Time Differentiation

Material velocity $\mathbf{V}(X,t)$ and spatial velocity $\mathbf{v}(x,t)$ satisfy the following definitions in direct and indicial notation, respectively:

$$\mathbf{V} = \frac{\partial \mathbf{x}}{\partial t} = \left.\frac{\partial \varphi^a}{\partial t}\right|_X \mathbf{g}_a, \; V^a(X,t) = \frac{\partial}{\partial t}\varphi^a(X,t) = v^a(\varphi(X,t),t); \quad (2.167)$$

$$\mathbf{v}_t = \mathbf{V}_t \circ \varphi_t^{-1}, \; v^a(x,t) = V^a\left(\varphi^{-1}(x,t),t\right). \quad (2.168)$$

Recall the notation $x = \varphi(X,t)$ and $X = \varphi^{-1}(x,t)$ from Sections 2.1.2 and 2.5.1. Subscript t in the first of (2.168) denotes a spatial field quantity at a particular (fixed) time t. Notice that components of both velocity fields are referred to spatial coordinates. In each definition, the material particle at X is held constant during time differentiation, meaning that velocity is the time rate of change of position of a given material particle. The composition operation in (2.168) is often implicitly assumed rather than written explicitly, and is omitted later in the text when no confusion arises.

2.6.1 The Material Time Derivative

The material time derivative measures the rate of change of a quantity associated with given a material particle at X. Because spatial position x of a given particle may change with time, the material time derivative and the partial time derivative of a function expressed in terms of spatial position x can differ. The material time derivative of a differentiable scalar function f of time t and spatial position x is defined as

$$\begin{aligned}
\dot{f}(x,t) = \frac{df}{dt} &= \left.\frac{\partial f}{\partial t}\right|_x + \frac{\delta f}{\delta t} \\
&= \left.\frac{\partial f}{\partial t}\right|_x + \left.\frac{\partial f}{\partial x^a}\right|_t \left.\frac{\partial x^a}{\partial t}\right|_X \\
&= \left.\frac{\partial f}{\partial t}\right|_x + f_{;a}v^a,
\end{aligned} \qquad (2.169)$$

where the partial time derivative is taken with spatial coordinates $\mathbf{x}$ (i.e., position x) held constant, and the intrinsic derivative that accounts for convective changes of scalar function f resulting from the velocity field is

$$\frac{\delta f}{\delta t} = \overset{g}{\nabla}_{\mathbf{v}} f = f_{;a} v^a = (f v^a)_{;a} - f v^a_{;a} = f_{,a} v^a. \qquad (2.170)$$

It follows that for differentiable functions f and g, $d(f+g)/dt = \dot{f} + \dot{g}$ and $d(fg)/dt = \dot{f}g + f\dot{g}$. The material time derivative is applied in an analogous way to vectors and tensors of higher order as, for example,

$$\dot{f}^a(x,t) = \left.\frac{\partial f^a}{\partial t}\right|_x + f^a_{;b} v^b, \quad \dot{f}^{a...c}_{d...f}(x,t) = \left.\frac{\partial f^{a...c}_{d...f}}{\partial t}\right|_x + f^{a...c}_{d...f;k} v^k. \qquad (2.171)$$

The material time derivative of a time-dependent function of position in the reference configuration, with all indices referred to reference coordinates[8], by definition equals its partial time derivative:

$$\dot{f}(X,t) = \left.\frac{\partial f}{\partial t}\right|_X, \quad \dot{f}^A(X,t) = \left.\frac{\partial f^A}{\partial t}\right|_X, \quad \dot{f}^{A...C}_{D...F}(X,t) = \left.\frac{\partial f^{A...C}_{D...F}}{\partial t}\right|_X. \qquad (2.172)$$

One application of (2.171) for a spatial vector is the spatial acceleration:

$$
\begin{aligned}
\mathbf{a}(x,t) = a^a \mathbf{g}_a = \dot{\mathbf{v}} &= \left.\frac{\partial \mathbf{v}}{\partial t}\right|_x + \overset{g}{\nabla}_{\mathbf{v}} \mathbf{v} \\
&= \left.\frac{\partial v^a}{\partial t}\right|_x \mathbf{g}_a + (\mathbf{v}_{,b} \mathbf{g}^b)\mathbf{v} \\
&= \left.\frac{\partial v^a}{\partial t}\right|_x \mathbf{g}_a + [(v^c \mathbf{g}_c)_{,b} \mathbf{g}^b)][v^d \mathbf{g}_d] \qquad (2.173) \\
&= \left.\frac{\partial v^a}{\partial t}\right|_x \mathbf{g}_a + \left(v^c_{,b} \mathbf{g}_c + v^c \overset{g}{\Gamma}{}^{\;a}_{bc} \mathbf{g}_a\right) v^b \\
&= \left[\left.\frac{\partial v^a}{\partial t}\right|_x + \left(v^a_{,b} + \overset{g}{\Gamma}{}^{\;a}_{bc} v^c\right) v^b\right] \mathbf{g}_a.
\end{aligned}
$$

----

[8] For a function f of reference position with one or more indices referred to spatial coordinates, letting D/Dt denote the partial derivative with both $\mathbf{X}$ and $\mathbf{g}$ constant, the material time derivative is defined by (Truesdell and Toupin 1960)

$$\dot{f}^{A...C\;a...c}_{D...F\;d...f}(X,t) = \frac{Df^{A...C\;a...c}_{D...F\;d...f}}{Dt} + \left(\overset{g}{\Gamma}{}^{\;a}_{bk} f^{A...C\;k...c}_{D...F\;d...f} + ... - \overset{g}{\Gamma}{}^{\;k}_{bd} f^{A...C\;a...c}_{D...F\;k...f} - ...\right) V^b.$$

On the other hand, the material acceleration, i.e., the material time derivative of material velocity (2.167) referred to spatial coordinates, satisfies

$$
\mathbf{A}(X,t) = A^a \mathbf{g}_a = \left.\frac{\partial \mathbf{V}}{\partial t}\right|_X = \left.\frac{\partial (V^a \mathbf{g}_a)}{\partial t}\right|_X
$$

$$
= \left.\frac{\partial V^a}{\partial t}\right|_X \mathbf{g}_a + V^a \left.\frac{\partial \mathbf{g}_a(x)}{\partial t}\right|_X
$$

$$
= \left.\frac{\partial V^a}{\partial t}\right|_X \mathbf{g}_a + V^c \mathbf{g}_{c,b} \left.\frac{\partial x^b}{\partial t}\right|_X \tag{2.174}
$$

$$
= \left(\left.\frac{\partial V^a}{\partial t}\right|_X + \overset{g}{\Gamma}{}^{.a}_{bc} V^c V^b \right) \mathbf{g}_a,
$$

noting that $(\partial V^a / \partial t)|_X = (\partial v^a / \partial t)|_x + v^a_{,b} v^b$ from (2.167). Expressed as material time derivatives, contravariant velocity components are written as $V^a(X,t) = v^a(x,t) = \dot{x}^a(X,t)$ and contravariant acceleration components are written as $A^a(X,t) = a^a(x,t) = \ddot{x}^a(X,t)$.

Using (2.118) and (2.171), the material time derivative of the deformation gradient $\mathbf{F} = F^a_{.A} \mathbf{g}_a \otimes \mathbf{G}^A = x^a_{.,A} \mathbf{g}_a \otimes \mathbf{G}^A$ of (2.112), an example of a two-point tensor, is calculated in components as follows (Eringen 1962):

$$
\dot{F}^a_{.A} = \left.\frac{\partial F^a_{.A}}{\partial t}\right|_x + \frac{\delta F^a_{.A}}{\delta t} = \left.\frac{\partial F^a_{.A}}{\partial t}\right|_x + F^a_{.A;b} v^b
$$

$$
= \left.\frac{\partial F^a_{.A}}{\partial t}\right|_x + \left(F^a_{.A,b} + \overset{g}{\Gamma}{}^{.a}_{bc} F^c_{.A} \right) v^b \tag{2.175}
$$

$$
= \frac{D F^a_{.A}}{Dt} + \overset{g}{\Gamma}{}^{.a}_{bc} F^c_{.A} V^b = V^a_{.,A} + \overset{g}{\Gamma}{}^{.a}_{bc} F^c_{.A} V^b
$$

$$
= \left(v^a_{.,c} + \overset{g}{\Gamma}{}^{.a}_{cb} v^b \right) F^c_{.A} = v^a_{;c} F^c_{.A}.
$$

The spatial velocity gradient tensor $\mathbf{L}(x,t)$, i.e., the covariant spatial derivative of the velocity vector $\mathbf{v}(x,t)$, is

$$
\mathbf{L} = \mathbf{v}_{,b} \otimes \mathbf{g}^b = v^a_{;b} \mathbf{g}_a \otimes \mathbf{g}^b = \dot{\mathbf{F}} \mathbf{F}^{-1},
$$
$$
L^a_{.b} = v^a_{;b} = (\dot{x}^a)_{;b} = \dot{F}^a_{.A} F^{-1A}_{.b}. \tag{2.176}
$$

Noting that $d(F^a_{.A} F^{-1A}_{.b}) / dt = d(\delta^a_b)/dt = 0$, the material time derivative of the inverse deformation gradient satisfies $(\dot{F}^{-1})^A_{.a} = -F^{-1A}_{.b} L^b_{.a} = -X^A_{.,b} (\dot{x}^b)_{;a}$.

The covariant derivative of a metric tensor with respect to its Levi-Civita connection always vanishes identically; thus the material time derivative of spatial metric tensor with components $g_{ab}(x)$ vanishes:

$$\dot{g}_{ab}(x) = \left.\frac{\partial g_{ab}}{\partial t}\right|_x + g_{ab;c}v^c = 0, \ \dot{g}^{ab}(x) = \left.\frac{\partial g^{ab}}{\partial t}\right|_x + g^{ab}_{\ ;c}v^c = 0. \quad (2.177)$$

Furthermore, $\dot{G}_{AB}(X) = (\partial G_{AB}/\partial t)\big|_X = 0$. Thus, raising or lowering of indices commutes with material time differentiation in either configuration.

2.6.2 The Lie Derivative

The Lie derivative of a differentiable but otherwise arbitrary function $f(x,t)$ on spatial manifold B taken with respect to the velocity field $\mathbf{v}(x,t)$ of (2.168) is computed by

$$\mathcal{L}_\mathbf{v} f = \varphi_* \left[\frac{d}{dt}(\varphi^* f) \right], \quad (2.178)$$

where φ^* and φ_* denote pull-back and push-forward operations with respect to the motion. The notation d/dt denotes a material time derivative, as implied already by (2.169). In this text, particular Lie derivative (2.178) is considered exclusively. However, more general definitions of Lie derivatives taken with respect to time-dependent vector fields, e.g., fields other than velocity $\mathbf{v}$, exist (Schouten 1954; Marsden and Hughes 1983). Lie derivatives are useful for positing constitutive equations in rate form because objective rates of second-rank tensors have objective Lie derivatives. The component representation of Lie derivative (2.178) for a scalar function f equals its material time derivative:

$$\mathcal{L}_\mathbf{v} f = \dot{f} = \left.\frac{\partial f}{\partial t}\right|_X = \left.\frac{\partial f}{\partial t}\right|_x + v^a f_{;a} = \left.\frac{\partial f}{\partial t}\right|_x + (f v^a)_{;a} - f v^a_{\ ;a}. \quad (2.179)$$

For vectors and tensors of higher order, the Lie derivative in components is

$$\mathcal{L}_{\mathbf{v}} f^{a...h}{}_{i...r} = \left.\frac{\partial f^{a...h}{}_{i...r}}{\partial t}\right|_x + v^s f^{a...h}{}_{i...r;s}$$

$$- v^a{}_{;s} f^{s...h}{}_{i...r} - ... - v^h{}_{;s} f^{a...s}{}_{i...r}$$

$$+ v^t{}_{;i} f^{s...h}{}_{t...r} + ... + v^t{}_{;r} f^{a...s}{}_{i...t}$$

$$= \left.\frac{\partial f^{a...h}{}_{i...r}}{\partial t}\right|_x + v^s f^{a...h}{}_{i...r,s}$$ (2.180)

$$- v^a{}_{,s} f^{s...h}{}_{i...r} - ... - v^h{}_{,s} f^{a...s}{}_{i...r}$$

$$+ v^t{}_{,i} f^{s...h}{}_{t...r} + ... + v^t{}_{,r} f^{a...s}{}_{i...t}$$

since terms involving Christoffel symbols in the covariant derivatives cancel by the symmetry of the Levi-Civita connection on B. For the scalar $J(X,t)$, a direct calculation with the chain rule, (2.144), and (2.176) gives

$$\mathcal{L}_{\mathbf{v}} J(F^a_{.A}(X,t), g(x), G(X)) = \dot{J} = \frac{\partial J}{\partial F^a_{.A}} \dot{F}^a_{.A} = J F^{-1A}{}_{.a} \dot{F}^a_{.A}$$ (2.181)

$$= J L^a_{.a} = J D^a_{.a} = J v^a_{;a} = J(\dot{x}^a)_{;a}.$$

In components, the Lie derivative of the spatial metric tensor $g_{ab}(x)$ is

$$(\mathcal{L}_{\mathbf{v}} g)_{ab} = \underbrace{\left.\partial g_{ab}/\partial t\right|_x}_{=0} + v^c g_{ab;c} + v^c_{;a} g_{cb} + v^c_{;b} g_{ac} = 2L_{(ab)} = 2D_{ab},$$ (2.182)

where D_{ab} are components of the symmetric deformation rate tensor.

2.6.3 Rate Kinematics

Velocity gradient **L** provides, to first order, the difference $d\mathbf{v}$ in spatial velocities of two particles in the spatial frame separated by a small vector $d\mathbf{x}$. The material time derivative applied to (2.115) results in

$$d\mathbf{v} = \mathbf{L}d\mathbf{x}, \quad dv^a = d\dot{x}^a = \dot{F}^a_{.A} dX^A = \dot{F}^a_{.A} F^{-1A}{}_{.b} dx^b = v^a_{;b} dx^b = L^a_{.b} dx^b.$$ (2.183)

Deformation rate tensor **D** provides the material time derivative of the squared length of a differential line element $d\mathbf{x}$:

$$d(d\mathbf{x} \cdot d\mathbf{x})/dt = 2d\mathbf{x} \cdot d\mathbf{v} = 2L_{ab} dx^a dx^b$$

$$= 2L_{(ab)} dx^a dx^b = 2D_{ab} dx^a dx^b$$ (2.184)

because $dx^a dx^b = dx^{(a} dx^{b)}$. Since from (2.115),

$$d(d\mathbf{x} \cdot d\mathbf{x})/dt = d(F^a_{.A} dX^A g_{ab} F^b_{.B} dX^B)/dt = \dot{C}_{AB} dX^A dX^B,$$ (2.185)

time rates of right Cauchy-Green strain and deformation tensors satisfy

$$\dot{E}_{AB} = \frac{1}{2}\dot{C}_{AB} = F_{.A}^{a} D_{ab} F_{.B}^{b}, \tag{2.186}$$

relationships that can also be derived directly from (2.153), (2.156), (2.176), and (2.182), without resorting to use of first-order approximation (2.115). The skew covariant part of **L**, called the spin tensor or vorticity tensor and labeled **W**, provides the time rate of rotation of a differential line element $d\mathbf{x}$. In components,

$$W_{ab} = L_{[ab]} = L_{ab} - D_{ab} = v_{a;b} - v_{(a;b)} = v_{[a;b]} = v_{[a,b]}, \tag{2.187}$$

with the final equality following from the symmetry of the connection coefficients. Appealing to the polar decomposition in the first of (2.149) and (2.176), the velocity gradient can be written

$$\mathbf{L} = \dot{\mathbf{R}}\mathbf{R}^{T} + \mathbf{R}\dot{\mathbf{U}}\mathbf{U}^{-1}\mathbf{R}^{T}. \tag{2.188}$$

From time differentiation of (2.150), the covariant version of the first term on the right of (2.188) is always skew:

$$g_{ac}\dot{R}_{.A}^{c}R_{.b}^{TA} = -g_{bc}\dot{R}_{.A}^{c}R_{.a}^{TA}, \tag{2.189}$$

meaning that the spatial deformation rate is comprised of the symmetric part of the second term on the right of (2.188):

$$2D_{ab} = g_{ac}R_{.A}^{c}\dot{U}_{.B}^{A}U_{.C}^{-1B}R_{.b}^{TC} + g_{bc}R_{.A}^{c}\dot{U}_{.B}^{A}U_{.C}^{-1B}R_{.a}^{TC}. \tag{2.190}$$

Noting that $\dot{\mathbf{u}} = \mathbf{v}$, in the context of the geometrically linear theory of Section 2.5.3, the deformation rate is equivalent to the time rate of the small strain tensor, and the spin is equivalent to the rate of rotation:

$$\begin{aligned} D_{ab} &= v_{(a;b)} = \dot{u}_{(a;b)} = \dot{\varepsilon}_{ab}, \\ W_{ab} &= \dot{u}_{[a;b]} = \dot{u}_{[a,b]} = \dot{\Omega}_{ab} = -\varepsilon_{abc}\dot{w}^{c}. \end{aligned} \tag{2.191}$$

2.7 Theorems of Gauss and Stokes

Two fundamental theorems of vector calculus associated with integration are used frequently later in the text. The first, known as Gauss's theorem or Green's theorem, relates volume and surface integrals. A particular case is the well-known divergence theorem. The second is Stokes's theorem, and it relates surface and line integrals.

2.7.1 Gauss's Theorem

The generalized Gauss's theorem exhibits the form (Malvern 1969)

$$\int_{V} \mathbf{A} * \nabla \, dV = \int_{S} \mathbf{A} * \mathbf{N} \, dS, \tag{2.192}$$

where **A** is a scalar, vector, or tensor of arbitrary order that has continuous first derivatives with respect to local coordinates, ∇ is the covariant derivative operator with respect to the Levi-Civita connection of these coordinates, and **N** is the outward unit normal covariant vector to differential surface area element dS. Surface S, which encloses volume V, is required to be piecewise smooth and exhibit a topological outside and inside, such that **N** may be clearly assigned to point from the inside to the outside of V for each surface element dS. Volume V must be simply connected for a single continuous surface S to suffice[9]; otherwise, (2.192) may be applied over the union of disjoint surfaces completely enclosing a volume that is not simply connected. The $*$ operator—not to be confused with the push-forward φ_* or pull-back φ^* introduced in Section 2.5.1 that feature asterisks written in respective subscript or superscript positions—represents a general product that exhibits the distributive property. Examples include the dual product $\langle \, , \, \rangle$, the dot product $\bullet$, the vector cross product $\times$, and the tensor (outer) product $\otimes$. The familiar divergence theorem of vector calculus is obtained from (2.192) when $*$ is the dual or dot product, e.g., for a spatial vector field $\hat{\mathbf{a}}(x,t)$,

$$\int_v \hat{a}^a_{;a} \, dv = \int_s \hat{a}^a n_a \, ds \,. \tag{2.193}$$

As a second example (Hill 1972, 1984; Clayton and McDowell 2003a), consider cases wherein the body is simply connected, enclosed by a single continuous surface. In (2.192), let $\mathbf{A} \rightarrow \mathbf{x}(X,t)$ and let V be the volume of the body in the reference configuration enclosed by surface S, with local outward normal **N**. The $*$ operator is chosen to be the outer product $\otimes$, giving

$$\int_V x^a_{;A} dV = \int_S x^a N_A dS \,. \tag{2.194}$$

Since (2.194) involves integration of a two-point tensor field, for the integrals to represent valid quantities at any location in Euclidean space[10], basis vectors $\mathbf{g}_a(x)$ and $\mathbf{G}_A(X)$ should be chosen as constant with respect to changes in position. This requirement leads to vanishing of the Christoffel

---

[9] In many texts, integration over a closed surface in (2.192) or closed curve in (2.197) is delineated by the explicit notation $\oint$. Throughout this text, domains of integration are simply defined as they appear.

[10] Alternatively, the integral of a vector or tensor field can be defined in a valid manner at a single point in space by parallel transporting all position-dependent quantities within the integrand to that point using a shifter (Toupin 1956). This approach is pursued explicitly in Chapter 3 in the context of the Burgers circuit.

symbols in each configuration. This restriction does not require that basis vectors in the two configurations must coincide, nor does it require that basis vectors in each configuration must be orthogonal. In other words, (2.194) requires $g_{ab,c} = 0$ and $G_{AB,C} = 0$, but one can still have $g_{ab} \neq \delta_{ab}$, $G_{AB} \neq \delta_{AB}$, and $g_{.A}^a \neq \delta_{.A}^a$, as considered by Sedov (1966). Thus, (2.194) reduces to

$$\int_V x_{,A}^a dV = \int_V F_{.A}^a dV = \int_S x^a N_A dS .$$
(2.195)

Dividing (2.195) by V gives the volume average of the deformation gradient in terms of spatial position and reference orientation of surface S:

$$V^{-1} \int_V \mathbf{F} dV = V^{-1} \int_S \mathbf{x} \otimes \mathbf{N} dS .$$
(2.196)

Strict application of (2.196) requires C^1-continuity of $\mathbf{x}(X,t)$.

2.7.2 Stokes's Theorem

The generalized Stokes's theorem is written (Malvern 1969)

$$\int_S (\mathbf{N} \times \nabla) * \mathbf{A} \, dS = \int_C d\mathbf{X} * \mathbf{A} ,$$
(2.197)

where quantities introduced already in (2.192) have the same definitions, and where C is a closed curve with coordinates $\mathbf{X}$ encircling an oriented surface S with normal $\mathbf{N}$. Again, $\mathbf{A}$ must have continuous first derivatives with respect to coordinates corresponding to covariant derivative with gradient operator ∇. Surface S must be simply connected for a single curve C to suffice; otherwise the line integration must proceed over the collection of bounding curves interior and exterior to S. When path C of the line integral is taken in a counterclockwise sense, the positive direction of normal $\mathbf{N}$ is defined according to the usual right-hand rule of vector calculus. Stokes's theorem, like Gauss's theorem, can be applied in either configuration of the body. For example, when $\mathbf{A} \to \mathbf{v}(x,t)$ (the spatial velocity field) and $* \to \langle . , . \rangle_x$, the following equality applies:

$$\int_s \varepsilon^{abc} n_b \overset{g}{\nabla}_c v_a ds = \int_s \varepsilon^{abc} v_{a;c} n_b ds = \int_s \varepsilon^{abc} (v_{a,c} - \overset{g}{\Gamma}_{ca}^{.d} v_d) n_b ds$$
$$= -\int_s \varepsilon^{abc} v_{a,b} n_c ds = -\int_s v_{a,b} dx^a \wedge dx^b = \int_c v_a dx^a ,$$
(2.198)

where s and c denote, respectively, surfaces and bounding curves on a body in the spatial description. When the curl or skew gradient of $\mathbf{v}$ van-

ishes, i.e., when $v_{[a;c]} = v_{[a,c]} = W_{ac} = 0$, the integrand in (2.198) is identically zero, and the velocity field is said to be irrotational.

Consider now the deformation gradient in the context of Stokes's theorem. Let S and C denote, respectively, surfaces and bounding curves on a body in the reference description, let $\mathbf{A} \to \mathbf{F}(X,t)$, and let $* \to \langle ., . \rangle_X$. Then in indicial notation,

$$\int_S \varepsilon^{ABC} F^a_{.A;C} N_B dS = -\int_S \varepsilon^{ABC} F^a_{.A,B} N_C dS$$

$$= -\int_S F^a_{.A,B} dX^A \wedge dX^B = \int_C F^a_{.A} dX^A. \qquad (2.199)$$

where symmetry properties of the Christoffel symbols $\overset{G}{\Gamma}{}^{.A}_{BC} = \overset{G}{\Gamma}{}^{.A}_{(BC)}$ have been exploited. Likewise, in the spatial description,

$$\int_s \varepsilon^{abc} F^{-1A}_{.a;c} n_b ds = -\int_s \varepsilon^{abc} F^{-1A}_{.a,b} n_c ds$$

$$= -\int_s F^{-1A}_{.a,b} dx^a \wedge dx^b = \int_c F^{-1A}_{.a} dx^a. \qquad (2.200)$$

Restrictions on coordinate systems may apply since (2.199) and (2.200) involve integration of vector fields. Specifically, basis vectors $\mathbf{g}_a$ must be constant for all points x in the domain of integration in global equation (2.199), while basis vectors $\mathbf{G}_A$ must be constant for all points X in the domain of integration of (2.200). Otherwise, integrands in (2.199) and (2.200) must be parallel transported to a single point (x or X) using the appropriate shifter, and the integral then evaluated at that point (Toupin 1956). Furthermore, $\mathbf{F}(X,t)$ and $\mathbf{F}^{-1}(x,t)$ must have continuous first derivatives with respect to reference and spatial coordinates, respectively. From (2.115), since the line integral of position about a closed loop on the surface of or within a simply connected body vanishes,

$$0 = \int_c dx^a = \int_C F^a_{.A} dX^A = -\int_S \varepsilon^{ABC} F^a_{.A,B} N_C dS, \qquad (2.201)$$

$$0 = \int_C dX^A = \int_c F^{-1A}_{.a} dx^a = -\int_s \varepsilon^{abc} F^{-1A}_{.a,b} n_c ds. \qquad (2.202)$$

Since (2.201) and (2.202) must hold for any path within the body,

$$F^a_{[A,B]} = F^a_{[A;B]} = F^a_{.[A:B]} = 0, \quad F^{-1A}_{.[a,b]} = F^{-1A}_{.[a;b]} = F^{-1A}_{.[a:b]} = 0. \qquad (2.203)$$

As discussed further in Section 2.8, (2.203) can be interpreted as local compatibility conditions for the deformation gradient and its inverse.

2.8 Anholonomic Spaces and Compatibility

The following topics associated with compatibility, or lack thereof, of arbitrary tangent maps and linear connections are discussed in Section 2.8: anholonomic deformations and anholonomic configurations, strain compatibility, connection compatibility, and the Jacobian determinant.

2.8.1 Anholonomicity

Consider a field of covariant basis vectors $\tilde{\mathbf{g}}_\alpha$ ($\alpha = 1, 2, 3$), spanning a tangent bundle $T\tilde{B}$ associated with arbitrary configuration $\tilde{B}$. By introducing the two-point map $\tilde{\mathbf{F}}(X,t) = \tilde{F}^\alpha_{.A}\, \tilde{\mathbf{g}}_\alpha \otimes \mathbf{G}^A$ that is assumed to be differentiable and invertible, generic vectors $\mathbf{V} \in T_X B_0$ are pushed forward to $T_{\tilde{x}}\tilde{B}$:

$$
\begin{aligned}
\tilde{\mathbf{F}}\mathbf{V} &= \tilde{F}^\alpha_{.A}\, \tilde{\mathbf{g}}_\alpha \otimes \mathbf{G}^A \left(V^B \mathbf{G}_B\right) = \tilde{F}^\alpha_{.A} V^B \tilde{\mathbf{g}}_\alpha \left\langle \mathbf{G}^A, \mathbf{G}_B \right\rangle \\
&= \tilde{F}^\alpha_{.A} V^B \delta^A_{.B} \tilde{\mathbf{g}}_\alpha = \tilde{F}^\alpha_{.A} V^A \tilde{\mathbf{g}}_\alpha \in T_{\tilde{x}}\tilde{B}.
\end{aligned}
\tag{2.204}
$$

Basis vectors are tangent to globally continuous coordinate curves $\tilde{x}^\alpha$ (i.e., $\tilde{\mathbf{g}}_\alpha = \partial / \partial \tilde{x}^\alpha$ for some coordinate parameterization $\tilde{x}^\alpha(X,t)$) if and only if the following integrability conditions hold for $\tilde{\mathbf{F}}$ (Schouten 1954):

$$
\tilde{F}^\alpha_{.A,B} = \tilde{F}^\alpha_{.B,A} \Leftrightarrow \frac{\partial^2 \tilde{x}^\alpha}{\partial X^A \partial X^B} = \frac{\partial^2 \tilde{x}^\alpha}{\partial X^B \partial X^A}.
\tag{2.205}
$$

If conditions (2.205) are not satisfied, then $\tilde{\mathbf{g}}_\alpha$ is called an anholonomic basis vector, the tangent map $\tilde{\mathbf{F}}$ is called an incompatible map, and $\tilde{B}$ is called an incompatible configuration or an anholonomic space[11]. In such a case, anholonomic coordinates $\tilde{x}^\alpha$, sometimes called non-holonomic coordinates (Stojanovitch 1969), are available as one-to-one functions of location X only over local patches of $\tilde{B}$, if at all. Anholonomic spaces can be interpreted as containing regions where coordinates $\tilde{x}^\alpha$ may be multivalued (overlaps) or undefined (holes) functions of X (Kondo 1964). From another perspective, when anholonomic, $\tilde{B}$ can be considered a nine-dimensional space (nine independent components of $\tilde{F}^\alpha_{.A}$) in contrast to

---

[11] When $\tilde{\mathbf{F}}$ does not have continuous first partial derivatives, (2.205) does not apply. For example, a piecewise linear field of coordinates $\tilde{x}^\alpha(X)$ can result in a piecewise constant deformation gradient $\tilde{x}^\alpha_{.,A}(X)$ with discontinuities, as can occur physically in crystals in the context of deformation twinning (James 1981).

holonomic configuration B_0 parameterized by three independent coordinates X^A. Since the deformation gradient and its inverse are integrable, $F^a_{[A,B]} = 0$ and $F^{-1A}_{[a,b]} = 0$, as indicated in (2.203) in the context of Stokes's theorem.

Because conventional differentiation with respect to anholonomic coordinates does not apply, partial differentiation with respect to anholonomic $\tilde{x}^\alpha$ is defined in a special manner:

$$\partial_\alpha(\,.\,) = (\,.\,)_{,\alpha} = \frac{\partial(\,.\,)}{\partial \tilde{x}^\alpha} = \frac{\partial(\,.\,)}{\partial X^A} \tilde{F}^{-1A}_{\quad.\alpha}$$
$$= \partial_A(\,.\,)\tilde{F}^{-1A}_{\quad.\alpha} = \partial_a(\,.\,)F^a_{.A}\tilde{F}^{-1A}_{\quad.\alpha}. \tag{2.206}$$

The anholonomic object $\tilde{\boldsymbol{\kappa}}$ is introduced (Schouten 1954; Kondo 1964):

$$\tilde{\kappa}^{\cdot.\alpha}_{\beta\chi} = \tilde{F}^{-1A}_{\quad.\beta}\tilde{F}^{-1B}_{\quad.\chi}\partial_{[A}\tilde{F}^\alpha_{.B]} = \tilde{F}^{-1A}_{\quad.\beta}\tilde{F}^{-1B}_{\quad.\chi}\tilde{F}^\alpha_{[B,A]} = \tilde{\kappa}^{\cdot.\alpha}_{[\beta\chi]}, \tag{2.207}$$

a geometric construct whose components vanish if and only if $\tilde{\mathbf{F}}$ is integrable. Consider the transformation law for the connection coefficients given by (2.28), but now applied with respect to a change from holonomic to anholonomic coordinates $X^A \to \tilde{x}^\alpha$, where (2.206) is used to define partial differentiation with respect to $\tilde{x}^\alpha$. Arbitrary connection coefficients $\Gamma^{\cdot.A}_{BC}$ on B_0 then transform to coefficients $\tilde{\Gamma}^{\cdot.\alpha}_{\beta\chi}$ on $\tilde{B}$ as

$$\tilde{\Gamma}^{\cdot.\alpha}_{\beta\chi} = \tilde{F}^{-1B}_{\quad.\beta}\tilde{F}^{-1C}_{\quad.\chi}\tilde{F}^\alpha_{.A}\Gamma^{\cdot.A}_{BC} + \tilde{F}^{-1C}_{\quad.\chi,\beta}\tilde{F}^\alpha_{.C}$$
$$= \tilde{F}^{-1B}_{\quad.\beta}\tilde{F}^{-1C}_{\quad.\chi}\tilde{F}^\alpha_{.A}\Gamma^{\cdot.A}_{BC} - \tilde{F}^{-1B}_{\quad.\beta}\tilde{F}^{-1C}_{\quad.\chi}\tilde{F}^\alpha_{.C,B}. \tag{2.208}$$

Torsion tensor $\mathbf{T}$ of (2.33) pushed forward to $\tilde{B}$ becomes, in components

$$\tilde{T}^{\cdot.\alpha}_{\beta\chi} = \tilde{F}^{-1B}_{\quad.\beta}\tilde{F}^{-1C}_{\quad.\chi}\tilde{F}^\alpha_{.A}T^{\cdot.A}_{BC} = \tilde{\Gamma}^{\cdot.\alpha}_{[\beta\chi]} + \tilde{\kappa}^{\cdot.\alpha}_{\beta\chi}, \tag{2.209}$$

implying that $\tilde{\Gamma}^{\cdot.\alpha}_{[\beta\chi]}$ need not vanish for covariant components of $\Gamma^{\cdot.A}_{BC}$ to be symmetric. Partial derivatives of basis vectors with respect to an arbitrary connection on $\tilde{B}$ are defined as analogs of (2.56):

$$\tilde{\mathbf{g}}^\alpha_{,\beta} = -\tilde{\Gamma}^{\cdot.\alpha}_{\beta\chi}\tilde{\mathbf{g}}^\chi, \quad \tilde{\mathbf{g}}_{\alpha,\beta} = \tilde{\Gamma}^{\cdot.\chi}_{\beta\alpha}\tilde{\mathbf{g}}_\chi. \tag{2.210}$$

Relations (2.210) are treated here as general postulates, applicable regardless of whether or not (2.208) is used to define connection coefficients on $\tilde{B}$. However, when (2.208) does specifically apply, skew partial derivatives of covariant basis vectors in (2.210) need not always vanish even if $\tilde{T}^{\cdot.\alpha}_{\beta\chi} = 0$, since

$$\tilde{\mathbf{g}}_{[\alpha,\beta]} = \tilde{\Gamma}^{\cdot.\chi}_{[\beta\alpha]}\tilde{\mathbf{g}}_\chi = (\tilde{T}^{\cdot.\chi}_{\beta\alpha} - \tilde{\kappa}^{\cdot.\chi}_{\beta\alpha})\tilde{\mathbf{g}}_\chi. \tag{2.211}$$

The expression for the Riemann-Christoffel curvature tensor of a linear connection, defined with respect to holonomic coordinates in B_0 as $R_{BCD}^{...A}$ in (2.34) and pushed forward to anholonomic coordinates $\tilde{x}^\alpha$, is (Schouten 1954; Kondo 1964)

$$\tilde{R}_{\beta\chi\delta}^{..\alpha} = \tilde{F}_{.\beta}^{-1B}\tilde{F}_{.\chi}^{-1C}\tilde{F}_{.\delta}^{-1D}\tilde{F}_{.A}^{\alpha}R_{BCD}^{...A}$$

$$= \frac{\partial\tilde{\Gamma}_{\chi\delta}^{..\alpha}}{\partial\tilde{x}^\beta} - \frac{\partial\tilde{\Gamma}_{\beta\delta}^{..\alpha}}{\partial\tilde{x}^\chi} + \tilde{\Gamma}_{\beta\varepsilon}^{..\alpha}\tilde{\Gamma}_{\chi\delta}^{..\varepsilon} - \tilde{\Gamma}_{\chi\varepsilon}^{..\alpha}\tilde{\Gamma}_{\beta\delta}^{..\varepsilon} + 2\tilde{\kappa}_{\beta\chi}^{..\varepsilon}\tilde{\Gamma}_{\varepsilon\delta}^{..\alpha} \qquad (2.212)$$

$$= 2\partial_{[\beta}\tilde{\Gamma}_{\chi]\delta}^{..\alpha} + 2\tilde{\Gamma}_{[\beta|\varepsilon|}^{..\alpha}\tilde{\Gamma}_{\chi]\delta}^{..\varepsilon} + 2\tilde{\kappa}_{[\beta\chi]}^{..\varepsilon}\tilde{\Gamma}_{\varepsilon\delta}^{..\alpha},$$

which, upon comparison with the holonomic representation in (2.34), differs only by the rightmost term that includes the anholonomic object.

2.8.2 Strain Compatibility

A second interpretation of compatibility follows from consideration of the Riemann-Christoffel curvature tensor. From (2.43), Christoffel symbols of the second kind in the context of Riemannian geometry formed from the symmetric right Cauchy-Green deformation tensor $\mathbf{C}(X,t)$ are

$$\overset{C}{\Gamma}_{BC}^{..A} = \frac{1}{2}C^{-1AD}(C_{BD,C} + C_{CD,B} - C_{BC,D}) = \overset{C}{\Gamma}_{CB}^{..A}. \qquad (2.213)$$

A curvature tensor $\overset{\mathbf{C}}{\mathbf{R}}$ can be constructed by substituting components $\overset{C}{\Gamma}_{BC}^{..A}$ into (2.34). Since $\mathbf{C} = \varphi^*(\mathbf{g})$, $\overset{\mathbf{C}}{\mathbf{R}} = \varphi^*(\overset{\mathbf{g}}{\mathbf{R}})$ follows from properties of the connection and curvature (Marsden and Hughes 1983). Thus, if the deformation tensor field $\mathbf{C}$ is derivable from a motion $\varphi(X,t)$, and since $\overset{\mathbf{g}}{\mathbf{R}} = 0$, it follows that $\overset{\mathbf{C}}{\mathbf{R}} = \varphi^*(0) = 0$ and $\mathbf{C}$ is compatible. Section D.3 of Appendix D contains an alternative derivation worked out in convected coordinates, demonstrating vanishing of the curvature tensor formed from $C_{AB} = F_{.A}^a g_{ab} F_{.B}^b$ noting that conditions $F_{.A}^a = x_{,A}^a$ and $F_{.A,B}^a = F_{.B,A}^a$ apply.

Notice that $\mathbf{C}$-compatibility does not require specification of a unique spatial configuration, since $\mathbf{C}$ is independent of the rotation tensor associated with the right polar decomposition in (2.149). Furthermore, even if $\mathbf{C}$ is compatible, integrability of an arbitrary field $\mathbf{F}$ generating the field $\mathbf{C} = \mathbf{F}^T\mathbf{F}$ may be precluded by rotations $\mathbf{R}$ that do not arise from rigid-body transformations of φ. For example, consider the field $F_{.A}^a = R_{.A}^a$ with $R_{.A}^a R_{.b}^{TA} = \delta_{.b}^a$, such that $C_{AB} = F_{.A}^a g_{ab} F_{.B}^b = R_{.A}^C G_{CD} R_{.B}^D = G_{AB}$. Integrability of

F is violated by a rotation field for which $R^a_{[A,B]} \neq 0$, even though the curvature tensor constructed from $C_{AB} = G_{AB}$ vanishes identically in this case. A material in such a condition is said to be in a state of contorted aleotropy (Noll 1967). The converse of the previous theorem has also been proven, albeit only locally (Eisenhart 1926). In other words, given a positive definite, symmetric, second-order tensor **C** whose curvature vanishes (i.e., $\overset{c}{\mathbf{R}} = 0$) then at any point $X \in B_0$ there exists a neighborhood U_0 of X endowed with a mapping $\varphi : B_0 \supset U_0 \rightarrow U \subset B$ whose deformation tensor is **C**. A more extensive discussion of compatibility in terms of **C** is given by Fosdick (1966), who notes that vanishing of the Ricci tensor or the Einstein tensor constructed from $\overset{c}{\mathbf{R}}$ is sufficient to ensure compatibility of **C**. One can consider **C**-compatibility an outcome of deformation gradient compatibility (i.e., **F**-compatibility): if $F^a_{.A}(X,t)$ is compatible, then it follows that $C_{AB}(X,t) = F^a_{.A} g_{ab} F^b_{.B}$ is also compatible, as demonstrated in Section D.3 of Appendix D.

It is emphasized that a Levi-Civita connection—a connection both torsion-free and metric with respect to $\tilde{\mathbf{g}}$, where the metric has components $\tilde{g}_{\alpha\beta} = \tilde{\mathbf{g}}_\alpha \cdot \tilde{\mathbf{g}}_\beta$—on anholonomic space $\tilde{B}$ may not exist, since the field of vectors $\tilde{\mathbf{g}}_\alpha$ may not be sufficiently smooth over all of $\tilde{B}$ to admit coordinate differentiation with respect to coordinates that may in fact be discontinuous or multi-valued, i.e., anholonomic coordinates. However, in anholonomic (e.g., intermediate or natural) configurations of elastoplasticity theory, each local volume element of material is often referred to an external system of coordinates with Euclidean metric tensor, typically taken as Kronecker's delta for convenience (Teodosiu 1967a, b; Simo and Ortiz 1985), though the assumption $\tilde{g}_{\alpha\beta} = \delta_{\alpha\beta}$ is not always necessary (Maugin 1995; Clayton et al. 2004a). This issue is discussed in more detail in Section 3.2.2. Notice also that the Riemann-Christoffel curvature tensor formed from the generally incompatible covariant deformation measure $\tilde{C}_{AB} = \tilde{F}^\alpha_{.A} \tilde{g}_{\alpha\beta} \tilde{F}^\beta_{.B}$ does not necessarily vanish unless $\tilde{x}^\alpha$ are holonomic, in contrast to the vanishing curvature tensor derived from connection (2.213) formed from the compatible deformation tensor **C**.

Compatibility equations for the small strain tensor of (2.163) are typically expressed somewhat differently than those for **C** (Malvern 1969; Mura 1982; Teodosiu 1982). The former are derived from differentiation

of the right side of (2.163) and a sequence of indicial manipulations, leading to vanishing of the incompatibility tensor with components s^{cf}:

$$s^{cf} = s^{(cf)} = g^{-1} e^{abc} e^{def} \varepsilon_{bd;ae} = -g^{-1} e^{cab} e^{fed} \varepsilon_{bd;ae} = 0 . \qquad (2.214)$$

The six independent equations in (2.214) ensure that symmetric tensor $\varepsilon(x,t)$ with continuous second derivatives with respect to holonomic coordinates x^a is integrable; i.e., (2.214) ensures that a continuously differentiable displacement field $\mathbf{u}(x,t)$ exists such that (2.163) applies. Analogously to (2.203), $u_{a,[bc]} = 0$ from the commutative property the of the mixed second partial derivative with respect to holonomic coordinates, and vanishing of the curvature and torsion of the Levi-Civita connection results in $u_{a;[bc]} = 0$, as concluded from (2.40).

2.8.3 Connection Compatibility

Consider coefficients of a special linear connection formed by spatial differentiation of a smooth, possibly anholonomic tangent map with inverse $\bar{\mathbf{F}}^{-1}(x,t)$: $T_x B \to T_{\bar{x}} \bar{B}$, defined as follows:

$$\begin{aligned}
\bar{\Gamma}_{cb}^{..a} &= \bar{F}_{.\alpha}^{a} \partial_c \bar{F}_{.b}^{-1\alpha} = \bar{F}_{.\alpha}^{a} \bar{F}_{.b,c}^{-1\alpha} \\
&= -\bar{F}_{.\alpha,c}^{a} \bar{F}_{.b}^{-1\alpha} = -\bar{F}_{.\alpha,\beta}^{a} \bar{F}_{.b}^{-1\alpha} \bar{F}_{.c}^{-1\beta} ,
\end{aligned} \qquad (2.215)$$

where the third of (2.215) follows from $(\bar{F}_{.\alpha}^{a} \bar{F}_{.b}^{-1\alpha})_{,c} = \delta_{.b,c}^{a} = 0$ and the final equality follows from (2.206). Connections of the form (2.215) have special meaning in field theories of lattice defects (Bilby et al. 1955; Kroner 1960) and are said to exhibit the property of teleparallelism or absolute parallelism (Einstein 1928; Schouten 1954).

Partial differentiation of (2.215) yields

$$(\bar{F}_{.a}^{-1\alpha} \bar{\Gamma}_{bc}^{..a})_{,d} = \bar{F}_{.c,bd}^{-1\alpha} , \qquad (2.216)$$

the left side of which is expanded as

$$\bar{F}_{.a,d}^{-1\alpha} \bar{\Gamma}_{bc}^{..a} + \bar{F}_{.a}^{-1\alpha} \bar{\Gamma}_{bc,d}^{..a} = \bar{F}_{.a}^{-1\alpha} (\bar{\Gamma}_{de}^{..a} \bar{\Gamma}_{bc}^{..e} + \bar{\Gamma}_{bc,d}^{..a}) . \qquad (2.217)$$

Since the order of partial differentiation on the right side of (2.216) is arbitrary (Schouten 1954; Le and Stumpf 1996a),

$$\begin{aligned}
0 = 2\partial_{[b}\partial_{d]}\bar{F}_{.c}^{-1\alpha} &= \bar{F}_{.a}^{-1\alpha} (\bar{\Gamma}_{dc,b}^{..a} - \bar{\Gamma}_{bc,d}^{..a} + \bar{\Gamma}_{be}^{..a} \bar{\Gamma}_{dc}^{..e} - \bar{\Gamma}_{de}^{..a} \bar{\Gamma}_{bc}^{..e}) \\
&= \bar{F}_{.a}^{-1\alpha} \bar{R}_{bdc}^{...a} ,
\end{aligned} \qquad (2.218)$$

where $\bar{R}_{bdc}^{...a}$ are components of the Riemann-Christoffel curvature tensor derived from $\bar{\Gamma}_{cb}^{..a}$ of (2.215) using definition (2.34). Upon multiplication

of (2.218) through by $\overline{\mathbf{F}}$, it is evident that $\overline{R}_{cdb}^{\ \ \ a} = 0$ are conditions ensuring satisfaction of (2.215). In that case (i.e., null curvature), the connection with coefficients $\overline{\Gamma}_{cb}^{\ \ a}$ is said to be integrable (Schouten 1954).

Secondly, if the connection with coefficients in (2.215) is symmetric, then its torsion vanishes by definition, and it follows from arguments analogous to those accompanying (2.205) that $\overline{\mathbf{F}}^{-1}(x,t)$ is itself integrable:

$$\overline{T}_{cb}^{\ \ a} = \overline{\Gamma}_{[cb]}^{\ \ a} = \overline{F}_{.\alpha}^{a}\overline{F}_{[b,c]}^{-1\alpha} = 0 \Leftrightarrow \overline{F}_{.a}^{-1\alpha} = \overline{x}_{.,a}^{\alpha} = \partial_a \overline{x}^{\alpha} . \qquad (2.219)$$

When (2.219) applies,

$$\overline{\Gamma}_{bc}^{\ \ a} = \frac{1}{2}\overline{C}^{-1ad}(\overline{C}_{bd,c} + \overline{C}_{cd,b} - \overline{C}_{bc,d}) , \ \overline{\nabla}_a\overline{C}_{bc} = 0 , \qquad (2.220)$$

meaning that $\overline{\Gamma}_{cb}^{\ \ a}$ are Levi-Civita coefficients formed from a metric tensor with components $\overline{C}_{ab}(x,t) = \overline{F}_{.a}^{-1\alpha}\overline{g}_{\alpha\beta}\overline{F}_{.b}^{-1\beta}$, and the set $\{\overline{B},\overline{\Gamma}_{cb}^{\ \ a},\overline{C}_{ab}\}$ constitutes a Euclidean space since $\overline{R}_{bdc}^{\ \ \ a} = 0$. Components of a second metric tensor on $\overline{B}$ are denoted by $\overline{g}_{\alpha\beta}$ and can be chosen as $\overline{g}_{\alpha\beta} = \delta_{\alpha\beta}$ for convenience. The first equality in (2.220) follows from direct calculation and (2.219) as

$$2\overline{\Gamma}_{bc}^{\ \ a} = \overline{C}^{-1ad}(\overline{C}_{bd,c} + \overline{C}_{cd,b} - \overline{C}_{bc,d})$$
$$= 2\overline{F}_{.\alpha}^{a}\overline{F}_{.(c,b)}^{-1\alpha} + 2\overline{F}_{.\alpha}^{a}\overline{g}^{\alpha\beta}\overline{F}_{.\beta}^{d}\left[\overline{F}_{.b}^{-1\chi}\overline{F}_{[d,c]}^{-1\delta} + \overline{F}_{.c}^{-1\chi}\overline{F}_{[d,b]}^{-1\delta}\right]\overline{g}_{\chi\delta} \qquad (2.221)$$
$$= 2\overline{F}_{.\alpha}^{a}\overline{F}_{.(c,b)}^{-1\alpha},$$

and the second of (2.220) is verified by substituting the first of (2.220) into

$$\overline{\nabla}_a\overline{C}_{bc} = \overline{C}_{bc,a} - \overline{\Gamma}_{ab}^{\ \ d}\overline{C}_{dc} - \overline{\Gamma}_{ac}^{\ \ d}\overline{C}_{bd} = 0 . \qquad (2.222)$$

2.8.4 The Jacobian Determinant for Anholonomic Mappings

The Jacobian determinant of anholonomic mapping $\tilde{\mathbf{F}}$ introduced in (2.204) provides, by definition, the relationship between a differential reference volume element $dV \subset B_0$ and its deformed counterpart in the anholonomic space, $d\tilde{V} \subset \tilde{B}$:

$$\tilde{J}dV = d\tilde{V} . \qquad (2.223)$$

Analogously to (2.142), the function $\tilde{J}(X,t)$, regarded as a true scalar under coordinate transformations, is calculated in coordinates as

$$\tilde{J} = \frac{1}{6}\varepsilon_{\alpha\beta\chi}\varepsilon^{ABC}\tilde{F}^{\alpha}_{.A}\tilde{F}^{\beta}_{.B}\tilde{F}^{\chi}_{.C} = \frac{1}{6}\sqrt{\tilde{g}/G}e_{\alpha\beta\chi}e^{ABC}\tilde{F}^{\alpha}_{.A}\tilde{F}^{\beta}_{.B}\tilde{F}^{\chi}_{.C}$$
$$= \frac{1}{6}\det\tilde{\mathbf{F}}\sqrt{\tilde{g}/G} = \frac{1}{6}\det(\tilde{F}^{\alpha}_{.A})\sqrt{\det(\tilde{g}_{\alpha\beta})/\det(G_{AB})}, \qquad (2.224)$$

where $\tilde{g} = \det(\tilde{g}_{\alpha\beta}) = \det(\tilde{\mathbf{g}}_{\alpha}\cdot\tilde{\mathbf{g}}_{\beta}) \geq 0$. Requiring that the volume of any element must remain positive and finite implies bounds $\infty > \tilde{J} > 0$. Differentiation of (2.224) produces an identity like (2.144):

$$\frac{\partial \tilde{J}}{\partial \tilde{F}^{\alpha}_{.A}} = \frac{1}{2}\varepsilon_{\alpha\beta\chi}\varepsilon^{ABC}\tilde{F}^{\beta}_{.B}\tilde{F}^{\chi}_{.C} = \tilde{J}F^{-1A}_{.\alpha}. \qquad (2.225)$$

Taking the total covariant derivative of the first of (2.225) then gives

$$2(\tilde{J}\tilde{F}^{-1A}_{.\alpha})_{:A} = \varepsilon_{\alpha\beta\chi}\varepsilon^{ABC}(\tilde{F}^{\beta}_{.B:A}\tilde{F}^{\chi}_{.C} + \tilde{F}^{\beta}_{.B}\tilde{F}^{\chi}_{.C:A})$$
$$= \varepsilon_{\alpha\beta\chi}\varepsilon^{ABC}(\tilde{F}^{\beta}_{.[B:A]}\tilde{F}^{\chi}_{.C} + \tilde{F}^{\beta}_{.B}\tilde{F}^{\chi}_{.[C:A]}). \qquad (2.226)$$

When (2.205) is not satisfied, meaning anholonomic object $\tilde{\boldsymbol{\kappa}}$ in (2.207) does not vanish, the right side of (2.226) may be nonzero and Piola identities such as those in (2.145) and (2.146) for holonomic mapping $\mathbf{F}$ and its inverse do not always hold for anholonomic mappings.

Let oriented differential area elements referred to configurations B_0 and $\tilde{B}$ be labeled $\mathbf{N}dS$ and $\tilde{\mathbf{n}}d\tilde{s}$, respectively. Analogously to (2.148), these elements are related by Nanson's formula or a Piola transformation:

$$\tilde{\mathbf{n}}d\tilde{s} = \tilde{J}\tilde{F}^{-*}\mathbf{N}dS, \quad \tilde{n}_{\alpha}d\tilde{s} = \tilde{J}\tilde{F}^{-*.A}_{.\alpha}N_{A}dS = \tilde{J}\tilde{F}^{-1A}_{.\alpha}N_{A}dS. \qquad (2.227)$$

In terms of the wedge product, $\tilde{n}_{\alpha}d\tilde{s} = \varepsilon_{\alpha\beta\chi}d\tilde{x}^{[\beta}d\tilde{x}^{\chi]} = \varepsilon_{\alpha\beta\chi}d\tilde{x}^{\beta}\wedge d\tilde{x}^{\chi}/2$ and $d\tilde{x}^{a}\wedge d\tilde{x}^{b} = \varepsilon^{\alpha\beta\chi}\tilde{n}_{\chi}d\tilde{s}$, with $d\tilde{x}^{a}$ and $d\tilde{x}^{b}$ components of two different infinitesimal vectors so their tensor product is not identically symmetric.

Relation (2.227) can be obtained directly from (2.224), noting that

$$6 = (\varepsilon_{\alpha\beta\chi})(\tilde{J}^{-1}\varepsilon^{ABC}\tilde{F}^{\alpha}_{.A}\tilde{F}^{\beta}_{.B}\tilde{F}^{\chi}_{.C})$$
$$= (\sqrt{\tilde{g}}e_{\alpha\beta\chi})(\tilde{J}^{-1}\sqrt[-1]{G}e^{ABC}\tilde{F}^{\alpha}_{.A}\tilde{F}^{\beta}_{.B}\tilde{F}^{\chi}_{.C})$$
$$= \varepsilon_{\alpha\beta\chi}\varepsilon^{\alpha\beta\chi} = \varepsilon_{ABC}\varepsilon^{ABC} \qquad (2.228)$$
$$= (\tilde{J}^{-1}\sqrt{\tilde{g}}e_{\alpha\beta\chi}\tilde{F}^{\alpha}_{.A}\tilde{F}^{\beta}_{.B}\tilde{F}^{\chi}_{.C})(\sqrt[-1]{G}e^{ABC}).$$

Therefore, permutation tensors referred to configurations $\tilde{B}$ and B_0 satisfy

$$\varepsilon^{\alpha\beta\chi} = \tilde{J}^{-1}\varepsilon^{ABC}\tilde{F}^{\alpha}_{.A}\tilde{F}^{\beta}_{.B}\tilde{F}^{\chi}_{.C}, \quad \varepsilon_{ABC} = \tilde{J}^{-1}\varepsilon_{\alpha\beta\chi}\tilde{F}^{\alpha}_{.A}\tilde{F}^{\beta}_{.B}\tilde{F}^{\chi}_{.C}. \qquad (2.229)$$

Letting $d\tilde{x}^{\alpha} = \tilde{F}^{\alpha}_{.A}dX^{A}$, it follows that an oriented area element in B_0 is

$$N_A dS = \varepsilon_{ABC} dX^B dX^C = \varepsilon_{ABC} \tilde{F}^{-1B}_{.\varepsilon} \tilde{F}^{-1C}_{.\phi} d\tilde{x}^\varepsilon d\tilde{x}^\phi$$
$$= \tilde{J}^{-1} \tilde{F}^\alpha_{.A} \varepsilon_{\alpha\beta\chi} d\tilde{x}^\beta d\tilde{x}^\chi = \tilde{J}^{-1} \tilde{F}^\alpha_{.A} \tilde{n}_\alpha d\tilde{s},$$

(2.230)

the inverse of which yields the final result in (2.227). The same approach can be used to derive (2.148) directly from (2.142), as demonstrated in Section D.2 of Appendix D.

3 Kinematics of Crystalline Solids

Chapter 3 provides descriptions of kinematics of crystalline materials undergoing various deformation mechanisms at the microscopic scale. Specifically, such deformation mechanisms can include recoverable and residual elasticity, thermal expansion or contraction, plasticity manifesting from dislocation glide, and volume changes resulting from point defects and voids. A description of kinematics of deformation twinning is postponed until Chapter 8.

The treatment of kinematics is developed in the context of geometric nonlinearity; i.e., finite strains and rotations are addressed. Finite deformation theory is considered more applicable than linear or infinitesimal deformation theory for a number of reasons. From a physical standpoint, a nonlinear theory permits consideration of the sequence of deformation mechanisms occurring in a crystalline solid in terms of a multiplicative series of tangent maps. Such a description is naturally associated with a series of configurations or manifolds corresponding to real or virtual states of the deforming body. For example, application of the inverse elastic tangent map to a deformed crystal leads to a stress-free, unloaded state. Such configurations are possibly incompatible, or anholonomic in the terminology of Chapter 2, and their geometric description can be directly related to physical features such as defect content in a crystal. In addition to the increased generality and physical insight afforded by a finite deformation description, a nonlinear theory is essential for obtaining accurate depictions of material behavior in applications of solid mechanics wherein strains are inevitably large, for example in ballistic impact, crashworthiness scenarios, metal forming, and high pressure phenomena, with the latter encountered, for example, in geologic settings and shock physics experiments. Such nonlinear problems often require numerical solutions because of their complexity. Even when average deformations remain small, large deformations may still arise locally in many micromechanical problems of interest, for example studies of defect core structures, crack tip mechanics, and strain localization phenomena. Furthermore, since nearly all natural single crystals are anisotropic, large rotations of the lattice may be of importance even when strains are small. Finally, reduction of the finite deformation description to the infinitesimal deformation the-

ory via linearization is usually straightforward (though it is noted that methods of linearization are often not unique), while extension of a linear description to the nonlinear regime is often not. For completeness, occasional comparisons are drawn in Chapter 3 with complementary geometrically linear theories.

Chapter 3 begins with an introductory description of crystal structures. The usual fourteen Bravais lattices comprising the seven crystal systems are introduced. The Cauchy-Born hypothesis (Born and Huang 1954; Ericksen 1984)—a fundamental postulate stating that primitive Bravais lattice vectors of a crystal structure deform according to the action of a spatially constant deformation gradient acting over a homogeneously deforming volume element of crystal—is then discussed. Deformations of the solid induced explicitly by changes in temperature are described.

Multiplicative inelasticity (Bilby et al. 1957; Kroner 1960; Lee and Liu 1967) is presented next. Characterizations of plastic deformation in the context of dislocation flux (i.e., discrete dislocation dynamics), slip system activity in single crystals (i.e., crystal plasticity), and flow in polycrystals (i.e., macroscopic plasticity) are presented in turn. While plasticity manifesting from dislocation glide is volume-preserving, inelastic deformation attributed to the generation and motion of point defects, including vacancies associated with dislocation climb, is generally not (Teodosiu and Sidoroff 1976; Kroner 1990). At a somewhat larger length scale, damage mechanisms such as porosity evolution (e.g., void growth or pore compaction) can engender inelastic volume changes. Such phenomena are all addressed in the kinematic descriptions of Chapter 3. Coarse-graining principles (Clayton and McDowell 2003a) enabling quantification of heterogeneous local elastic and plastic deformations within a volume element of crystalline material are also presented.

Defect densities, typically tensor-valued quantities (Nye 1953), are considered next, from a differential-geometric viewpoint. In Chapter 3, defects are frequently treated as continuous distributions rather than as discrete entities with singularities in displacement gradients, and elastic and plastic tangent maps are assumed suitably smooth; specifically, these maps are assumed at least twice differentiable with respect to local coordinates. The multiplicative decomposition of elastoplasticity is used to describe the possibly large deformation of a volume element of crystalline material, and a complementary linear connection is introduced to describe spatial gradients of stretch and rotation of a field of lattice director vectors at a finer scale of resolution. Geometric properties of the connection enable characterization of dislocations (Bilby et al. 1955; Kroner 1960; Kondo 1963; Noll 1967), disclinations (Lardner 1973, 1974; Minagawa 1979, 1981; Clayton et al. 2005, 2006), point defects (Minagawa 1979; Kroner 1981,

1990; Clayton et al. 2008a), and physical origins of incompatibility of a more generic nature (Clayton et al. 2005).

3.1 Crystals and Lattice Deformation

Section 3.1 begins with an introductory description of crystal structures and related terminology. This is followed by discussion of homogeneous deformation of an element of the crystal, i.e., the Cauchy-Born hypothesis, under isothermal conditions and in the absence of defects in the crystal. The description is then generalized to account for effects of temperature change, for example expansion of the lattice with increasing temperature.

3.1.1 Crystal Structures

In this book, a crystal is defined as a material whose majority of atoms occupies a periodically repeating arrangement called a lattice. A crystal structure consists of a Bravais lattice and a basis for atoms decorating that lattice. A Bravais lattice is an infinite array of points generated by repeated translation of a set of vectors called primitive lattice vectors. A point on a three-dimensional Bravais lattice can be identified by its position in three-dimensional vector space via the vector summation

$$\mathbf{R}(l) = \sum_{i=1}^{3} l^i \mathbf{A}_i = l^1 \mathbf{A}_1 + l^2 \mathbf{A}_2 + l^3 \mathbf{A}_3, \ (l^1, l^2, l^3 \in \mathbb{Z}), \qquad (3.1)$$

where $\mathbf{R}(l)$ denotes the Bravais lattice vector directed from the origin of a global Cartesian coordinate system to the lattice point corresponding to primitive unit cell l, $\mathbf{A}_i$ are the primitive Bravais lattice vectors, and l^i are integers. By convention, a lattice point is placed at the origin of the global coordinate system. Each primitive unit cell contains exactly one lattice point, and each primitive unit cell occupies volume $\Omega_P = \mathbf{A}_1 \cdot (\mathbf{A}_2 \times \mathbf{A}_3)$. An entire perfect lattice, i.e., one free of defects, can be reconstructed by stacking the primitive unit cells.

   In three spatial dimensions, crystals are assigned to one of fourteen distinct kinds of Bravais lattices. Symmetry considerations enable each of the fourteen Bravais lattices to be grouped into one of seven crystal systems. Similarities among different Bravais lattices comprising a single crystal system become evident upon examination of conventional unit cells. Conventional unit cells may be non-primitive, i.e., they may contain more than one lattice point per cell; equivalently, the volume of a conventional cell is an integer number of primitive cell volumes. Conventional unit cells may,

like primitive unit cells, be translated to exactly reconstruct an entire (infinite) lattice. The location of a corner point of any conventional unit cell in the lattice can be described by a linear combination of three vectors labeled **a**, **b**, and **c**. In a non-primitive cell, however, all points of the Bravais lattice are not necessarily included in the set of corner points. For example, lattice points may be centered inside a conventional cell or on its faces, in addition to those points at the corners. Conventional lattice parameters consist of the magnitudes of conventional cell vectors:

$$a = (\mathbf{a} \cdot \mathbf{a})^{1/2}, \ b = (\mathbf{b} \cdot \mathbf{b})^{1/2}, \ c = (\mathbf{c} \cdot \mathbf{c})^{1/2}, \tag{3.2}$$

and of the three angles describing their relative orientations, denoted by α, β, and γ. Vectors **a**, **b**, and **c** and angles α, β, and γ are shown in Fig. 3.1 for a conventional unit cell. The volume of the conventional unit cell is $\Omega_C = \mathbf{a} \cdot (\mathbf{b} \times \mathbf{c}) = N\Omega_P$, with N the number of lattice points per conventional unit cell.
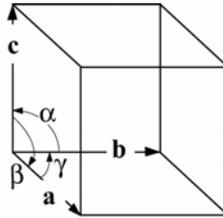
Fig. 3.1 Conventional lattice parameters

In a crystal structure, each Bravais lattice point, i.e., the lattice point of each primitive unit cell, is decorated by an identical basis of one or more atoms. A basis is a set of one or more atoms with the same stoichiometry (i.e., chemical composition) as the overall material. When each lattice point corresponds to a single atom, the basis is said to be monatomic. On the other hand, a polyatomic basis consists of multiple atoms per point on the Bravais lattice. These atoms may or may not be of different elemental species. The simplest example of a polyatomic structure is a diatomic crystal, which consists of two monatomic lattices, one differing from the other by a uniform translation (Ericksen 1970). The position of each atom k of a polyatomic basis relative to the Bravais lattice point centered at the origin of a local coordinate system for each primitive unit cell is specified by the basis vector for atom k, labeled as $\mathbf{R}\binom{0}{k}$. Since each atom is located within its own unit cell, its basis vector can be expressed in terms of fractional components of the primitive Bravais lattice vectors:

$$\mathbf{R}\binom{0}{k} = \sum_{i=1}^{3} m^i \mathbf{A}_i = m^1 \mathbf{A}_1 + m^2 \mathbf{A}_2 + m^3 \mathbf{A}_3, \ (0 \le m^i < 1), \tag{3.3}$$

The position of any atom (e.g., any one atom's nuclear coordinates) in Cartesian space in a perfect lattice is then the sum of the basis vector for that atom and the Bravais lattice vector for that atom's primitive unit cell:

$$\mathbf{R}\begin{pmatrix} l \\ k \end{pmatrix} = \mathbf{R}\begin{pmatrix} 0 \\ k \end{pmatrix} + \mathbf{R}(l) = \sum_{i=1}^{3} (m^i + l^i)\mathbf{A}_i \;, \qquad (3.4)$$

where $\mathbf{R}\binom{l}{k}$ denotes the global position of atom k within primitive unit cell l. When the structure is monatomic, basis vector $\mathbf{R}\binom{0}{k}$ is redundant and the location of the an atom is simply $\mathbf{R}(l)$, since the number of primitive unit cells and number of atoms then coincide. A measure of atomic volume in an infinitely extended lattice is $\Omega_0 = \Omega_P / K = \Omega_C / (NK)$, where K is the number of atoms in the basis (i.e., the number of atoms per primitive cell). The total number of atoms per conventional unit cell is the product NK. Note that a polyatomic basis—and hence a primitive unit cell in a polyatomic structure—can contain more than one formula unit.

The fourteen Bravais lattices are organized into crystal systems in Table 3.1 and Fig. 3.2, following the notational scheme of Rohrer (2001). Conventional unit cells are drawn in Fig. 3.2; those labeled with a P are also primitive (one lattice point per cell), while those labeled with an I, F, or C are not. Specifically, I refers to an inner centered lattice, F refers to a face centered lattice, and C refers to a lattice with a lattice point centered only on faces normal to conventional unit cell vector **c**. Lattice points of primitive unit cells are represented by spheres in Fig. 3.2; when the basis is monatomic, each sphere corresponds to (the nucleus of) an atom in the crystal.

Table 3.1 Crystal systems and symmetry restrictions (Rohrer 2001)

Crystal system	Number of lattices	Conventional cell parameters
Cubic	3	$a = b = c$; $\alpha = \beta = \gamma = 90°$
Tetragonal	2	$a = b \neq c$; $\alpha = \beta = \gamma = 90°$
Orthorhombic	4	$a \neq b \neq c$; $\alpha = \beta = \gamma = 90°$
Monoclinic	2	$a \neq b \neq c$; $\alpha = \gamma = 90° \neq \beta$
Triclinic	1	$a \neq b \neq c$; $\alpha \neq \beta \neq \gamma$
Rhombohedral	1	$a = b = c$; $\alpha = \beta = \gamma < 120°, \neq 90°$
Hexagonal	1	$a = b \neq c$; $\alpha = \beta = 90°, \gamma = 120°$

cubic

tetragonal

ortho-
rhombic

mono-
clinic

triclinic

rhombohedral
(trigonal)

hexagonal
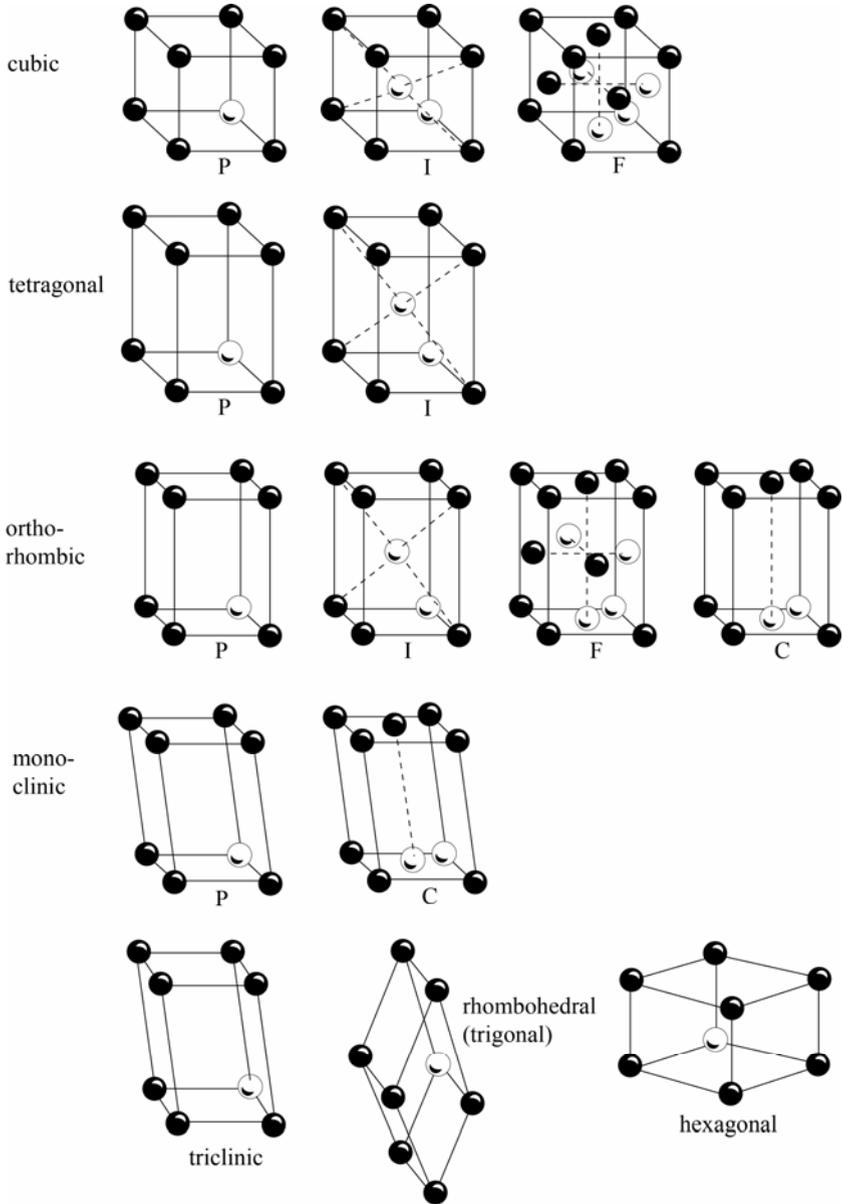
Fig. 3.2 Bravais lattices

When a monatomic basis is added to each site of a lattice, a common crystal structure is often recovered. For example, a cubic P lattice with a monatomic basis forms a simple cubic (SC) structure. A cubic I lattice with a monatomic basis produces a body centered cubic (BCC) structure. A cubic F lattice with a monatomic basis produces a face centered cubic (FCC) structure. On the other hand, the hexagonal close packed (HCP) structure consists of a basis of two atoms at each point on a hexagonal Bravais lattice, the first located, for example, at a corner point of the conventional cell and the second in a plane spaced midway between two faces of the cell perpendicular to **c** (i.e., perpendicular to the c-axis).

Table 3.2 lists several geometric parameters for each of the SC, BCC, FCC, and HCP structures wherein all atoms are of identical size (e.g., of the same species). Radius r is used to denote the size of an atom in the structure when that atom is idealized as a rigid sphere in exact (i.e., non-penetrating) contact with its nearest neighbors. The coordination number is the number of nearest neighbors, i.e., the number of sphere centers located at a distance $2r$ from the center of a given sphere. The packing factor P is defined as the volume occupied by the spheres contained in a conventional unit cell divided by the total volume of the conventional unit cell: $P = 4\pi r^3 NK/(3\Omega_C) = 4\pi r^3 K/(3\Omega_P) = 4\pi r^3/(3\Omega_0)$. It follows that the volume of each hard sphere is the product of the atomic volume and the packing factor. Often the c/a ratio in a material classified as HCP differs from the ideal value of 1.633 because of effects of atomic bonding.

Table 3.2 Geometric characteristics of several common crystal structures

Structure	Atomic radius r	No. atoms NK	Coord. no.	Packing P
SC	$r = a/2$	1	6	0.52
BCC	$r = \sqrt{3}a/4$	2	8	0.68
FCC	$r = \sqrt{2}a/4$	4	12	0.74
HCP	$r = a/2 = 0.306c$	2	12	0.74

Locations of atoms within a unit cell are written, in terms of fractional components of primitive Bravais lattice vectors in (3.4), by the notational convention $(m^1, m^2, m^3) \Leftrightarrow (x, y, z)$. Directions in the unit cell are written in terms of coefficients of the primitive Bravais lattice vectors by the notational convention $[l^1 l^2 l^3] \Leftrightarrow [uvw]$, with over-bars denoting negative values. Families of directions, i.e., directions that are indistinguishable because of particular values of the indices $[uvw]$ and symmetry of the lattice, are denoted by $\langle uvw \rangle$. Planes are denoted by Miller indices (hkl), with

families of crystallographically equivalent planes denoted by $\{hkl\}$. Miller indices of planes are reciprocals of intercepts of directional axes intersecting those planes. A zero is assigned to a Miller index when a plane does not intersect that axis. In cubic crystals, Miller indices of a plane are the same as the indices of the direction normal to that plane. It is common for one to denote corner points on the lattice of conventional unit cells by the position vector

$$\mathbf{R}(c) = c^1\mathbf{a} + c^2\mathbf{b} + c^3\mathbf{c}, \ (c^1, c^2, c^3 \in \mathbb{Z}). \tag{3.5}$$

In terms of conventional unit cell vectors, directions in Miller's notation then obey the correspondence $[c^1 c^2 c^3] \Leftrightarrow [uvw]$. Miller indices of planes in the conventional unit cell description are defined as reciprocals of intercepts of the $[c^1 c^2 c^3]$ directions. For non-primitive unit cells, $\mathbf{R}(c)$ does not describe every point on the Bravais lattice.

Miller-Bravais indices of type $[uvtw]$ are conventionally used for directions in hexagonal crystal systems, subject to the constraint $u + v + t = 0$. This four-index notational scheme is also often used for crystals of the rhombohedral or trigonal system (Kronberg 1957). Indices u, v, and t correspond to directions in the basal plane spaced 120° apart, while w corresponds to translation along the c-axis. Families of directions are denoted by $\langle uvtw \rangle$. Individual planes and families of planes are denoted, respectively, by the notation $(hkil)$ and $\{hkil\}$, with the constraint $h + k + i = 0$.

The reciprocal lattice concept is often useful, especially for study of lattice vibrations. Coordinates of a point in the primitive reciprocal lattice are

$$\mathbf{R}'_{hkl}(l) = h\mathbf{A}^1 + k\mathbf{A}^2 + l\mathbf{A}^3, \ (h, k, l \in \mathbb{Z}), \tag{3.6}$$

where reciprocal primitive Bravais lattice vectors are expressed in terms of primitive Bravais lattice vectors by (Maradudin et al. 1971)

$$\mathbf{A}^1 = \frac{2\pi(\mathbf{A}_2 \times \mathbf{A}_3)}{\Omega_P}, \ \mathbf{A}^2 = \frac{2\pi(\mathbf{A}_3 \times \mathbf{A}_1)}{\Omega_P}, \ \mathbf{A}^3 = \frac{2\pi(\mathbf{A}_1 \times \mathbf{A}_2)}{\Omega_P}, \tag{3.7}$$

or more succinctly in Cartesian space,

$$A^i_A \Omega_P = \pi e_{ABC} e^{ijk} A^B_j A^C_k, \tag{3.8}$$

where upper case indices denote components of each vector referred to the reference coordinate system and lower case indices are placeholders. Notice that the primitive Bravais lattice vectors are contravariant (indices in upper positions), while the primitive reciprocal lattice vectors are covariant (indices in lower positions). The primitive lattice vectors and their reciprocals satisfy the orthogonality conditions

$$\left\langle \mathbf{A}^i, \mathbf{A}_j, \right\rangle = 2\pi \delta^i_{\cdot j} , \tag{3.9}$$

and locations of points on the primitive Bravais lattice and the primitive reciprocal lattice satisfy

$$\left\langle \mathbf{R}(l), \mathbf{R}'_{hkl}(l) \right\rangle = 2\pi \left(l^1 h + l^2 k + l^3 l \right) = 2\pi n , \; (n \in \mathbb{Z}). \tag{3.10}$$

For each set of parallel planes in the primitive Bravais lattice specified by Miller indices h, k, and l, there exists a point on the primitive reciprocal lattice. The direction of the reciprocal vector $\mathbf{R}'_{hkl}(l)$ of (3.6) is normal to the plane with Miller indices (hkl). The factor of 2π in (3.7) is omitted in alternative definitions by some authors (Born and Huang 1954).

Conventional unit cell vectors can also be used to define a reciprocal lattice. In that case, analogs of (3.6), (3.7), and (3.10) are

$$\mathbf{R}'_{hkl}(c) = h\mathbf{a}' + k\mathbf{b}' + l\mathbf{c}' , \; (h,k,l \in \mathbb{Z}), \tag{3.11}$$

$$\mathbf{a}' = \frac{2\pi (\mathbf{b} \times \mathbf{c})}{\Omega_C}, \; \mathbf{b}' = \frac{2\pi (\mathbf{c} \times \mathbf{a})}{\Omega_C}, \; \mathbf{c}' = \frac{2\pi (\mathbf{a} \times \mathbf{b})}{\Omega_C}; \tag{3.12}$$

$$\left\langle \mathbf{R}(c), \mathbf{R}'_{hkl}(c) \right\rangle = 2\pi \left(c^1 h + c^2 k + c^3 l \right) = 2\pi n , \; (n \in \mathbb{Z}). \tag{3.13}$$

The direction of $\mathbf{R}'_{hkl}(c)$ of (3.11) is normal to the plane with Miller indices (hkl), though some values of h, k, and l will produce reciprocal lattice vectors that do not correspond to points on the reciprocal lattice, and not all points on the primitive reciprocal lattice are described by $\mathbf{R}'_{hkl}(c)$. For cubic, tetragonal, and orthorhombic Bravais lattices, conventional unit cell vectors and their reciprocals are parallel: $\mathbf{a}' \| \mathbf{a}$, $\mathbf{b}' \| \mathbf{b}$, and $\mathbf{c}' \| \mathbf{c}$.

Table 3.3 lists formulae for metric tensors, unit cell volumes, and interplanar spacings for each of the seven crystal systems, all in terms of conventional unit cell parameters. The metric tensor $\mathbf{G}$ in Table 3.3 is used to determine lengths of vectors $\mathbf{R}(c)$ in (3.5):

$$\mathbf{R}(c) \cdot \mathbf{R}(c) = \sum_{i,j=1}^{3} c^i G_{ij} c^j , \tag{3.14}$$

where components of the metric are denoted by $G_{ij} = G_{ji}$ and satisfy

$$\begin{bmatrix} G_{11} & G_{12} & G_{13} \\ G_{21} & G_{22} & G_{23} \\ G_{31} & G_{32} & G_{33} \end{bmatrix} = \begin{bmatrix} \mathbf{a} \cdot \mathbf{a} & \mathbf{a} \cdot \mathbf{b} & \mathbf{a} \cdot \mathbf{c} \\ \mathbf{b} \cdot \mathbf{a} & \mathbf{b} \cdot \mathbf{b} & \mathbf{b} \cdot \mathbf{c} \\ \mathbf{c} \cdot \mathbf{a} & \mathbf{c} \cdot \mathbf{b} & \mathbf{c} \cdot \mathbf{c} \end{bmatrix}. \tag{3.15}$$

Table 3.3 Metrics, unit cell volumes, and interplanar spacings (Rohrer 2001)

System	Metric $\mathbf{G}$	Unit cell volume Ω_C	Spacing $1/d_{hkl}^2$
Cubic	$\begin{bmatrix} a^2 & 0 & 0 \\ 0 & a^2 & 0 \\ 0 & 0 & a^2 \end{bmatrix}$	a^3	$\dfrac{h^2 + k^2 + l^2}{a^2}$
Tetragonal	$\begin{bmatrix} a^2 & 0 & 0 \\ 0 & a^2 & 0 \\ 0 & 0 & c^2 \end{bmatrix}$	$a^2 c$	$\dfrac{h^2 + k^2}{a^2} + \dfrac{l^2}{c^2}$
Ortho-rhombic	$\begin{bmatrix} a^2 & 0 & 0 \\ 0 & b^2 & 0 \\ 0 & 0 & c^2 \end{bmatrix}$	abc	$\dfrac{h^2}{a^2} + \dfrac{k^2}{b^2} + \dfrac{l^2}{c^2}$
Monoclinic	$\begin{bmatrix} a^2 & 0 & ac\cos\beta \\ 0 & b^2 & 0 \\ ac\cos\beta & 0 & c^2 \end{bmatrix}$	$abc\sin\beta$	$\dfrac{1}{\sin^2\beta}\left[\dfrac{h^2}{a^2} + \dfrac{k^2\sin^2\beta}{b^2} + \dfrac{l^2}{c^2} - \dfrac{2hl\cos\beta}{ac} \right]$
Triclinic	$\begin{bmatrix} a^2 & ab\cos\gamma & ac\cos\beta \\ ab\cos\gamma & b^2 & bc\cos\alpha \\ ac\cos\beta & bc\cos\alpha & c^2 \end{bmatrix}$	$abc\left[1 - \cos^2\alpha - \cos^2\beta - \cos^2\gamma + 2\cos\alpha\cos\beta\cos\gamma \right]^{1/2}$	$\dfrac{1}{\Omega_C^2}\big[h^2 b^2 c^2 \sin^2\alpha + k^2 a^2 c^2 \sin^2\beta + l^2 a^2 b^2 \sin^2\gamma + 2hk\,abc^2 \times (\cos\alpha\cos\beta - \cos\gamma) + 2kl\,a^2 bc \times (\cos\beta\cos\gamma - \cos\alpha) + 2lh\,ab^2 c \times (\cos\gamma\cos\alpha - \cos\beta) \big]$
Rhombo-hedral	$\begin{bmatrix} a^2 & a^2\cos\alpha & a^2\cos\alpha \\ a^2\cos\alpha & a^2 & a^2\cos\alpha \\ a^2\cos\alpha & a^2\cos\alpha & a^2 \end{bmatrix}$	$a^3\left[1 - 3\cos^2\alpha + 2\cos^3\alpha \right]^{1/2}$	$\dfrac{a^4}{\Omega_C^2} \times \big[(h^2 + k^2 + l^2) \times \sin^2\alpha + 2(hk + kl + hl) \times (\cos^2\alpha - \cos\alpha) \big]$
Hexagonal	$\begin{bmatrix} a^2 & -a^2/2 & 0 \\ -a^2/2 & a^2 & 0 \\ 0 & 0 & c^2 \end{bmatrix}$	$\dfrac{\sqrt{3}}{2} a^2 c$	$\dfrac{4(h^2 + hk + k^2)}{3a^2} + \dfrac{l^2}{c^2}$

The conventional unit cell volume is $\Omega_C = \mathbf{a} \cdot (\mathbf{b} \times \mathbf{c})$, as noted following (3.2). Magnitudes of reciprocal lattice vectors $\mathbf{R}'_{hkl}(c)$ are inversely proportional to separation distances between planes (hkl), written as d_{hkl}:

$$\frac{1}{d_{hkl}^{2}} = \frac{\mathbf{R}'_{hkl} \cdot \mathbf{R}'_{hkl}}{4\pi^{2}} = \frac{1}{4\pi^{2}} \begin{bmatrix} hkl \end{bmatrix} \begin{bmatrix} \mathbf{a}' \cdot \mathbf{a}' & \mathbf{a}' \cdot \mathbf{b}' & \mathbf{a}' \cdot \mathbf{c}' \\ \mathbf{b}' \cdot \mathbf{a}' & \mathbf{b}' \cdot \mathbf{b}' & \mathbf{b}' \cdot \mathbf{c}' \\ \mathbf{c}' \cdot \mathbf{a}' & \mathbf{c}' \cdot \mathbf{b}' & \mathbf{c}' \cdot \mathbf{c}' \end{bmatrix} \begin{bmatrix} h \\ k \\ l \end{bmatrix}, \tag{3.16}$$

where the 3×3 matrix in (3.16) is the metric of the reciprocal space. Analogous formulae apply when primitive Bravais lattice vectors of the primitive unit cell are used.

For a more comprehensive treatment of crystallographic terminology, structures of various crystalline substances, and lattice orientation characterization, the reader is referred to books dealing with topics in crystallography (Schmid and Boas 1950; Wyckoff 1963; Buerger 1965; Senechal 1990; Rohrer 2001) and texture analysis (Bunge 1982; Randle and Engler 2000).

3.1.2 The Cauchy-Born Hypothesis

The Cauchy-Born hypothesis (Born and Huang 1954), also often called the Cauchy-Born rule or Cauchy-Born approximation, states that under a homogeneous deformation, the primitive Bravais lattice vectors of a crystal in the reference configuration, $\mathbf{A}_i \in TB_0$ of (3.1), deform in an affine manner via a 3×3 matrix $\mathbf{F}$ to spatial vectors $\mathbf{a}_i \in TB$:

$$\mathbf{a}_i = \mathbf{F} \mathbf{A}_i, \quad a_i^a = F_{.A}^a A_i^A, \quad (i = 1, 2, 3). \tag{3.17}$$

Accordingly, coordinates of points on the Bravais lattice in (3.1) are updated under a homogeneous deformation as

$$\mathbf{r}(l) = \sum_{i=1}^{3} l^i \mathbf{a}_i = \sum_{i=1}^{3} l^i \mathbf{F} \mathbf{A}_i = \mathbf{F} \mathbf{R}(l). \tag{3.18}$$

In an elastic body, $\mathbf{F}$ of (3.17) is often identified with the deformation gradient of (2.112). By the polar decomposition (2.149), stretch and rotation of the primitive Bravais lattice vectors are included in (3.17). Stretch $\mathbf{U}$ or $\mathbf{V}$ induces a change in the lattice parameters of the primitive unit cell, and thus a (probable) change in inter-atomic forces sustained by the crystal.

A homogeneous deformation for a crystal with a polyatomic basis, in the sense of Born and Huang (1954), is

$$\mathbf{r}\binom{l}{k} = \mathbf{q}\binom{0}{k} + \mathbf{F} \mathbf{R}\binom{l}{k}. \tag{3.19}$$

Vector $\mathbf{q}\binom{0}{k}$ represents a uniform displacement (translation) of all atoms of type k, as might occur for example when an ionic crystal becomes polarized under an electric field. Substituting from (3.4) and (3.18),

$$
\begin{aligned}
\mathbf{r}\binom{l}{k} &= \mathbf{q}\binom{0}{k} + \mathbf{FR}\binom{l}{k} = \mathbf{q}\binom{0}{k} + \mathbf{F}\left[\mathbf{R}\binom{0}{k} + \mathbf{R}(l)\right] \\
&= \sum_{i=1}^{3} \Delta m^i\binom{0}{k}\mathbf{a}_i + \mathbf{FR}\binom{0}{k} + \mathbf{r}(l) = \sum_{i=1}^{3}[\Delta m^i\binom{0}{k} + m^i + l^i]\mathbf{a}_i \quad (3.20) \\
&= \mathbf{F}\left[\mathbf{F}^{-1}\mathbf{q}\binom{0}{k} + \mathbf{R}\binom{0}{k} + \mathbf{R}(l)\right] = \mathbf{F}\left[\mathbf{Q}\binom{0}{k} + \mathbf{R}\binom{l}{k}\right],
\end{aligned}
$$

with $\Delta m^i\binom{0}{k}$ a scalar translation parameter for all atoms of type k in the crystal structure. In the context of coincident Cartesian coordinate systems in reference and deformed crystal lattices, Born and Huang (1954) call $\mathbf{q}\binom{0}{k}$ the internal displacement and $\mathbf{F} - \mathbf{1}_0$ the external strain. The former, i.e., the inner displacement or internal displacement, can arise in complex crystal structures subject to external deformation $\mathbf{F}$ via relative displacements of sub-lattices, even in the absence of electric polarization (Ericksen 1970; Wallace 1972; Cousins 1978). A rotationally invariant version of inner displacement of basis atom k is represented by vector $\mathbf{Q}\binom{0}{k} = \mathbf{F}^{-1}\mathbf{q}\binom{0}{k}$ (Tadmor et al. 1999). Vector $\mathbf{Q}\binom{0}{k}$ generally depends on the applied (i.e., far-field) deformation; in practice the set of particular values of all internal displacement vectors k for a given applied deformation gradient $\mathbf{F}$ tend to minimize the energy of the crystal. Inner displacements also arise in the context of optical vibrations (Chen and Lee 2005). Rigid translation of the entire structure is omitted in (3.19) and (3.20); such motion can be included by adding a translation vector, independent of position, to $\mathbf{r}\binom{l}{k}$.

Now consider the reciprocal lattice. Assuming that in the deformed configuration, primitive Bravais lattice vectors and their reciprocals $\mathbf{a}^j$ remain orthogonal:

$$
\langle \mathbf{a}^i, \mathbf{a}_j \rangle = a^i_a a^a_j = 2\pi \delta^i_{\cdot j}, \quad (3.21)
$$

reciprocal Bravais lattice vectors transform like dual vectors according to

$$
\mathbf{a}^i = \mathbf{F}^{-*}\mathbf{A}^i, \quad a^i_a = F^{-1A}_{\cdot a} A^i_A, \quad (i = 1, 2, 3) . \quad (3.22)
$$

A point on the primitive reciprocal lattice has spatial coordinates

$$
\mathbf{r}'_{hkl}(l) = h\mathbf{a}^1 + k\mathbf{a}^2 + l\mathbf{a}^3 = \mathbf{F}^{-*}\mathbf{R}'_{hkl}(l) , \quad (3.23)
$$

from which it follows that, analogously to (3.10), in a homogeneously deformed primitive Bravais lattice,

$$
\langle \mathbf{r}(l), \mathbf{r}'_{hkl}(l) \rangle = 2\pi\left(l^1 h + l^2 k + l^3 l\right) = 2\pi n , \ (n \in \mathbb{Z}) . \quad (3.24)
$$

Quantities introduced in (3.17)-(3.20) are depicted in Fig. 3.3 for primitive unit cell l of a triclinic Bravais lattice with diatomic basis ($k = 0,1$). In Fig. 3.3, parallel Cartesian coordinate systems are used for reference (X^A) and deformed (x^a) configurations of the crystal structure, and ξ is a vector directed from the origin of the reference frame to the origin of the spatial frame.
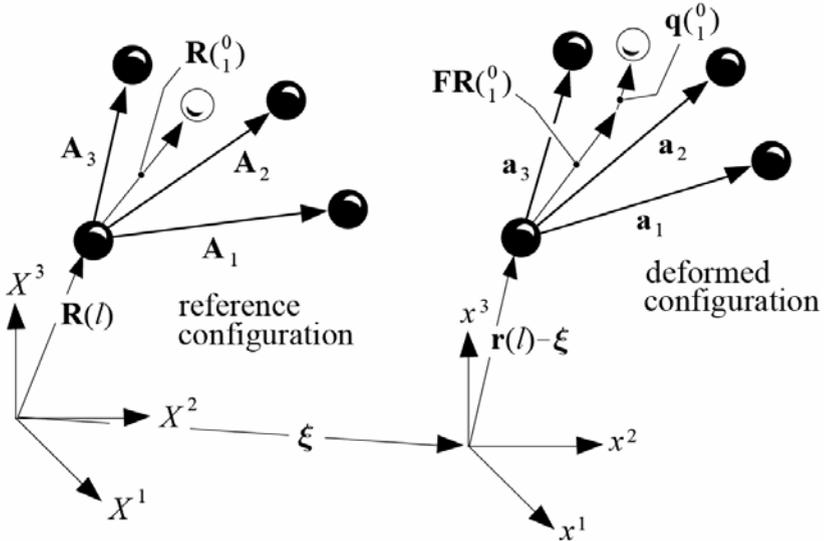
Fig. 3.3 Homogeneous deformation in the sense of Born and Huang (1954)

In an elastic crystal, the following notation is used in this book to indicate that the local deformation gradient of the material in the continuum sense, $\mathbf{F}$ of (2.112), and the local deformation of the lattice $\mathbf{F^L}$, coincide:

$$\mathbf{F}(X,t) = \mathbf{F^L}(X,t),\tag{3.25}$$

where dependence on position and time indicates that the deformation gradient need not be homogeneous in space or static in time. For example, with this notation (3.18) becomes

$$\mathbf{r}(l) = \sum_{i=1}^{3} l^i \mathbf{a}_i = \sum_{i=1}^{3} l^i \mathbf{F^L A}_i = \mathbf{F^L R}(l).\tag{3.26}$$

On the other hand, as will be demonstrated later in Chapter 3, when a crystalline substance deforms inelastically, for example via dislocation plasticity, $\mathbf{F}$ and $\mathbf{F^L}$ do not coincide. In the remainder of this book, $\mathbf{F^L}$ is referred to as the lattice deformation. Substituting (3.25) into (3.17)-(3.20), $\mathbf{F^L}(X,t)$ stretches and rotates the primitive Bravais lattice vectors and ba-

sis vectors of a primitive unit cell or a collection of primitive unit cells assigned to "material point" X. When a differential volume element in the reference configuration $dV(X)$ is assumed to consist of multiple primitive cells, then lattice vectors and basis vectors of each cell of that volume element deform homogeneously according to the value of $\mathbf{F}^L(X,t)$ for that material point centered at X. Lattice vectors and basis vectors of unit cells assigned to different locations X deform heterogeneously when $\mathbf{F}^L(X,t)$ varies with position. Further exposition on the Cauchy-Born rule, its extensions, and related applications in crystal mechanics and multiscale modeling can be found in a number of references (Ericksen 1970, 1984, 2005, 2008; Zanzotto 1992, 1996; Tadmor et al. 1996, 1999; Knap and Ortiz 2001; Arroyo and Belytschko 2002; Chung and Namburu 2003; Curtin and Miller 2003; Sunyk and Steinmann 2003; Clayton and Chung 2006).

3.1.3 Elastic Deformation and Thermal Deformation

In crystalline solids, lattice deformations may be introduced by forces of purely mechanical origin (e.g., elasticity due to bond stretching[1]), temperature changes, and applied electromagnetic fields (e.g., piezoelectricity, electrostriction, piezomagnetism, or magnetostriction). Consider a crystalline solid subjected to mechanical loading and temperature variations. With increasing temperature, the equilibrium spacing of atomic nuclei tends to increase as a result of increasing vibrational energy that accompanies local thermal oscillations. This leads to thermal expansion, specifically stretching of the Bravais lattice vectors and basis vectors, even when no mechanical forces are applied from external agents. Thorough discussion of atomic and quantum mechanical origins of thermal expansion in solids can be found in treatments of condensed matter physics (Slater 1939; Brillouin 1964). Cooling will usually lead to the opposite effect, i.e., thermal contraction. However, at a given pressure, contraction with increasing temperature is not impossible (Hanson et al. 1974), even in the absence of phase transformations. In continuum thermoelasticity, contributions from temperature change and those from mechanical stress are not usually explicitly delineated within lattice deformation $\mathbf{F}^L$ (Thurston 1974; Marsden and Hughes 1983; Rosakis et al. 2000), as described in de-

---

[1] At the scale of electronic and nuclear resolution, even "mechanical" forces associated with atomic bonds result from Coulomb-type electrostatic interactions among electrons and nuclei. Dynamic exchange forces associated with phonons, photons, protons, and electrons can also contribute to mechanical stiffness (Gilman 2003).

tail later in Chapter 5. However, in some cases it is useful to make the distinction (Stojanovitch 1969; Lu and Pister 1975; Imam and Johnson 1998; Clayton 2005a, b, 2006a)

$$\mathbf{F}^{\mathbf{L}} = \mathbf{F}^{\mathbf{E}}\mathbf{F}^{\boldsymbol{\theta}}, \ F^{La}_{\ .A} = F^{Ea}_{\ .B}F^{\theta B}_{\ .A}, \tag{3.27}$$

where $\mathbf{F}^{\mathbf{E}}$ is associated with mechanical loading and possible rigid body rotation of the lattice, and where $\mathbf{F}^{\boldsymbol{\theta}}$ is attributed to stress-free thermal expansion or contraction. For simplicity, both indices of the thermal deformation are referred to the reference coordinate system in (3.27). Introducing the absolute temperature θ and its material time derivative $\dot{\theta}$, a rate expression for thermal deformation can be written as[2]

$$\dot{\mathbf{F}}^{\boldsymbol{\theta}}\mathbf{F}^{\boldsymbol{\theta}-1} = \boldsymbol{\alpha}_{\mathbf{T}}\dot{\theta}, \ \dot{F}^{\theta A}_{\ .C}F^{\theta-1C}_{\ .B} = \alpha^{\ A}_{T.B}\dot{\theta}, \tag{3.28}$$

where $\boldsymbol{\alpha}_{\mathbf{T}}(X,t)$ is a second-order tensor of thermal expansion that is generally symmetric (Nye 1957), since thermal expansion does not induce any spin of the lattice. The coefficient of thermal expansion $\boldsymbol{\alpha}_{\mathbf{T}}$ can be treated as a polar tensor of rank two in the terminology of Thurston (1974), with independent components listed for crystal classes in Table A.4 of Appendix A. For cubic crystals and isotropic materials, thermal deformation is isotropic: $\boldsymbol{\alpha}_{\mathbf{T}} = \alpha_T \mathbf{1}_0$, where α_T is a scalar coefficient of thermal expansion. In that case, and when thermal expansion/contraction is the only deformation mode,

$$\dot{J}^\theta J^{\theta-1} = \left(d(\sqrt[-1]{G}\det\mathbf{F}^{\boldsymbol{\theta}})/dt\right)\left(\sqrt{G}\det\mathbf{F}^{\boldsymbol{\theta}-1}\right) = d\dot{v}/dv = 3\alpha_T\dot{\theta}, \tag{3.29}$$

with $dv = J^\theta dV$ the volume of a material element after thermal deformation. In the geometrically linear theory (i.e., the small deformation theory of Section 2.5.3), an analog of (3.27) is

$$\boldsymbol{\varepsilon}^{\mathbf{L}} = \boldsymbol{\varepsilon}^{\mathbf{E}} + \boldsymbol{\varepsilon}^{\boldsymbol{\theta}} = \boldsymbol{\varepsilon}^{\mathbf{E}} + \boldsymbol{\alpha}_{\mathbf{T}}\Delta\theta, \tag{3.30}$$

where $\boldsymbol{\varepsilon}^{\mathbf{L}}$ is a symmetric total lattice strain, $\boldsymbol{\varepsilon}^{\mathbf{E}}$ is the mechanical elastic strain, the coefficient of thermal expansion $\boldsymbol{\alpha}_{\mathbf{T}}$ is symmetric with the same meaning as in (3.28), and $\Delta\theta$ is the change in temperature from a reference state at which thermal strain $\boldsymbol{\varepsilon}^{\boldsymbol{\theta}}$ vanishes.

---

[2] Kinematic prescription (3.28) is not unique. Another reasonable possibility consistent with (3.30) is $F^{\theta A}_{\ .B}(X,t) = \delta^A_{.B} + \alpha^{\ A}_{T.B}\Delta\theta$, where $\boldsymbol{\alpha}_{\mathbf{T}}$ has a similar meaning and $\Delta\theta$ is the change in temperature from an undeformed reference state.

3.2 Multiplicative Inelasticity

Finite deformation inelasticity theory is predicated on the existence of a re-
laxed configuration of the body free of internal and/or external forces at
some length scale of observation. For example, a crystal may attain a
globally unloaded state upon removal of traction along its external sur-
faces. However, a heterogeneous crystalline solid supporting residual
stresses such as those arising from defects may simultaneously be globally
relaxed and locally or microscopically stressed. In such cases the body
must be cut into small pieces, or in geometric terminology mapped to an
anholonomic state as defined in Section 2.8, in order to relieve such inter-
nal stress fields. From an atomic perspective, it may be physically impos-
sible to define a configuration of a defective lattice free of all internal
forces without breaking stretched or distorted bonds in the vicinity of de-
fects.

3.2.1 Background

The concept of a locally relaxed, generally anholonomic state was posited
by Eckart (1948), who introduced a metric tensor describing lengths of
material elements in such an unloaded state and used this construction in a
thermodynamic theory of anelasticity. Kondo (1949) invoked the concept
of a metric with non-vanishing curvature tensor to describe plastic yield-
ing. Bilby et al. (1955) forwarded the idea of using a generally incompati-
ble, two-point lattice deformation map to describe the Bravais lattice vec-
tors of a crystal containing dislocations, purely from the perspective of
crystallography and independent of the notion of stress relaxation or re-
moval of mechanical forces.

   The multiplicative decomposition of the deformation gradient (formally
introduced in (3.31)) is perhaps the most popular postulate used to describe
the deformation kinematics of elastic-plastic crystals subjected to large
strains and rotations. Bilby et al. (1957) are often credited with first ex-
plicitly proposing the two-term multiplicative decomposition for elastic-
plastic crystals, using the terminology "shape deformation", "lattice de-
formation", and "dislocation deformation" to describe the total deforma-
tion gradient, its elastic part, and its plastic or lattice-preserving (i.e., "lat-
tice invariant" in their terminology) part, respectively (see also Bilby and
Smith (1956)). Kroner (1960) posited a similar model for kinematics of
elastic-plastic crystals. Teodosiu (1967a, 1968) developed a generalized
continuum theory of elasto-plasticity incorporating a multiplicative de-
composition of the deformation gradient into a product of two incompati-

ble maps, generalizing Toupin's theory of hyperelastic materials of grade two (Toupin 1964). Fox (1968), Lardner (1969), and Teodosiu (1970) postulated continuum theories of finite deformation plasticity from consideration of dynamics of mobile dislocation lines or loops. The above-mentioned studies were generally conducted in the context of continuously distributed dislocations, whereby internal stress fields resulting from defects were of primary interest in practical applications of the theory involving solutions of boundary value problems (Kroner and Seeger 1959; Teodosiu 1967b; Willis 1967).

The multiplicative decomposition emerged somewhat independently in the context of macroscopic continuum plasticity theory of engineering and structural mechanics, a context wherein evolution of mechanical stresses and macroscopic state variables of solid bodies, usually polycrystalline, subjected to large external forces is of primary concern. Acknowledging prior work by Eckart, Bilby, and Sedov, Lee and Liu (1967) introduced a two-term multiplicative decomposition to describe deformations of metals subjected to large pressures occurring in impact problems. This early study of kinematics and thermodynamics was extended to general deformation histories by Lee (1969), popularizing the multiplicative decomposition among the engineering mechanics community. Shock waves in elastic-plastic solids were studied using finite strain approaches by Lee and Wierzbicki (1967), Foltz and Grace (1969), and Germain and Lee (1973).

In decades since, the multiplicative decomposition is the standard prescription used for the nonlinear kinematics of crystal plasticity (Rice 1971; Teodosiu and Sidoroff 1976; Asaro 1983), wherein the generally anisotropic mechanical response of single crystals is modeled via consideration of dislocation glide along preferred directions in the crystal lattice on a number of discrete slip planes. The decomposition has also become popular for describing macroscopic plasticity (Kratochvil 1971; Simo and Ortiz 1985; Bammann and Aifantis 1987; Moran et al. 1990; Scheidler and Wright 2001; Wright 2002), whereby at each volume element centered at a point X within a body, the response of a large number of grains, typically metallic, is modeled in an average sense. Issues regarding material symmetries and multiple, evolving natural configurations have been addressed by Rajagopal and Srinivasa (1998) and Epstein and Elzanowski (2007).

3.2.2 The Multiplicative Decomposition

The two-term multiplicative decomposition of the deformation gradient for elastic-plastic solids is written

$$\mathbf{F} = \mathbf{F^L}\mathbf{F^P} , \quad F^a_{.A} = F^{La}_{.\alpha}F^{P\alpha}_{.A} , \tag{3.31}$$

where $\mathbf{F^L}$ is the lattice deformation first mentioned in (3.25) and $\mathbf{F^P}$ is the plastic deformation. Accompanying (3.31) are the following requirements: $\det \mathbf{F^P} > 0$, $\det \mathbf{F^L} > 0$, and inverses $\mathbf{F^{L-1}}$ and $\mathbf{F^{P-1}}$ exist that satisfy

$$F^{La}_{.\alpha} F^{L-1\alpha}_{.b} = \delta^a_{.b}, \quad F^{L-1\alpha}_{.a} F^{La}_{.\beta} = \delta^\alpha_{.\beta},$$
$$F^{P-1A}_{.\alpha} F^{P\alpha}_{.B} = \delta^A_{.B}, \quad F^{P\alpha}_{.A} F^{P-1A}_{.\beta} = \delta^\alpha_{.\beta}. \tag{3.32}$$

Decomposition (3.31) suggests existence of an additional configuration of the body, called the intermediate configuration and labeled $\tilde{B}$ in Fig. 3.3, such that globally, $\mathbf{F^P}:TB_0 \to T\tilde{B}$ and $\mathbf{F^L}:T\tilde{B} \to TB$. Although $\mathbf{F^L}$ and $\mathbf{F^P}$ are referred to as elastic and plastic "deformation gradients", these two tangent maps need not be integrable; i.e., elastic and plastic deformation gradients and their inverses need not be true gradients of vector fields taken with respect to any spatial or material coordinates.
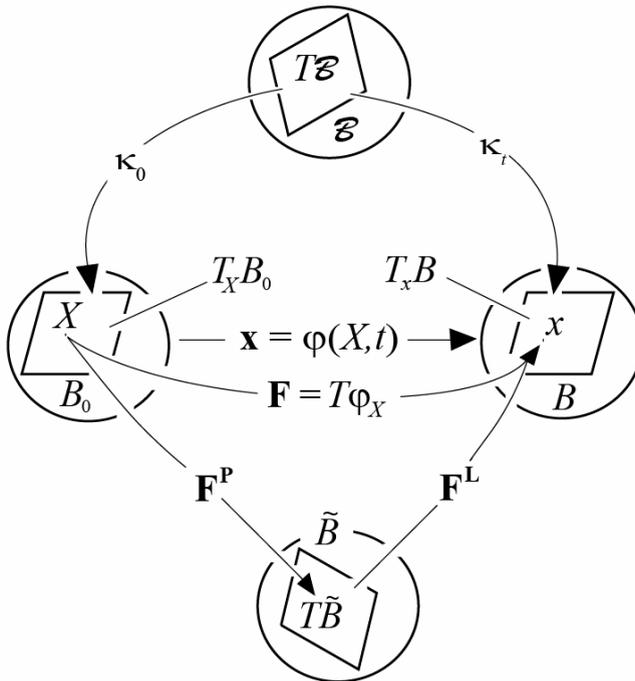
Fig. 3.4 Tangent maps and configurations

Plastic deformation $\mathbf{F^P}$ as defined here is engendered by cumulative motions of defects that are said to be lattice-preserving or lattice invariant

(Bilby et al. 1957), in other words phenomena that do not significantly alter the crystal structure from the length scale of resolution of the external observer. In crystalline solids, $\mathbf{F^P}$ is most often attributed to collective motion of dislocations when the solid is observed at a length scale coarse enough that local microscopic stretch and rotation fields associated with individual defects may be neglected. Such typically omitted fields may encompass, for example, stretch and rotation of primitive Bravais lattice vectors and basis vectors of the crystal structure in the immediate vicinity of cores of individual dislocation lines.

From an atomistic perspective, reference configuration B_0 can be related to intermediate configuration $\tilde{B}$ as follows (Clayton and Chung 2006) when mapping $\mathbf{F^P}$ represents the cumulative deformation of the material, but not the lattice, attributed to dislocation glide through a local volume element of a crystalline body. Consider a fixed control volume (i.e., a Eulerian representation centered at spatial point x) and initially containing of a large number of atoms, for example the number of atoms occupying a basis decorating at least 10^3 primitive unit cells. Once atoms have passed through this control volume as a result of dislocation glide, B_0 and $\tilde{B}$ appear identical in terms of atomic coordinates if no defects remain within the volume element and if elastic fields of dislocations that have passed through this element are excluded in configuration $\tilde{B}$. Yet deformation of the material will have taken place because of dislocation motion. For a purely plastic process with $\mathbf{F^L} = \mathbf{1}$, new atoms would enter the control volume in identical locations as the old, to replace those that exited due to plastic flow, and the mass of material contained within the control volume element would be conserved. The concept is illustrated in Fig. 3.5 for a cubic lattice, in which atoms that exit the volume are denoted by filled circles, and those that enter the cell by open circles, with the underlying material undergoing pure "plastic" shear. Boundaries of the fixed control volume through which atoms may pass are denoted by dashed lines, and boundaries of a Lagrangian material element (e.g., centered at X) and associated with a fixed set of atoms are denoted by solid lines. The mass of the Lagrangian element remains fixed because dislocation glide does not involve mass transport, and the volume occupied by the Lagrangian element remains fixed because dislocation glide is isochoric. The magnitude of the plastic shear shown in Fig. 3.5, upon prescription of parallel rectangular coordinate frames in each configuration, is $F^{P1}_{.2} = (2/5)(b/d)$.
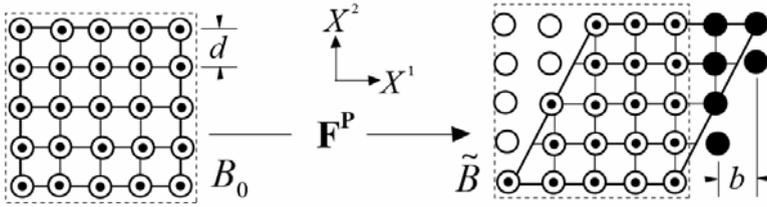
Fig. 3.5 Plastic deformation from atomic perspective

The lattice deformation $\mathbf{F^L}$ in turn encompasses all remaining physical mechanisms that do affect the underlying crystal structure. This includes rigid rotations of the entire solid body, as well as local rotations and local stretching of the Bravais lattice vectors associated with mechanical stresses and thermal expansion or contraction.

The majority of theoretical developments in finite deformation inelasticity seem to address plasticity in crystalline metals, perhaps since historically, inelastic behavior of these materials has garnered utmost interest in structural mechanics and manufacturing sciences. However, multiplicative kinematics of (3.31) have been extended to describe deformations of a variety of non-metallic (poly)crystalline solids, whereby $\mathbf{F^L}$ accounts for stretch and rotation of some aspect of the microstructure of the particular material under consideration. Decomposition (3.31), or variations of it, has been used to describe finite inelasticity in brittle crystalline solids such as geological materials (Krajcinovic 1996; Barton and Wenk 2007; Clayton 2010a) and dielectric and piezoelectric ceramics (Clayton 2009a, b, 2010b), granular media such as soils (Ortiz and Pandolfi 2004), heterogeneous structural solids such as concrete (Clayton 2008), energetic crystals (Barton et al. 2009), and crystalline- and semi-crystalline polymers (Shepherd et al. 2006). Multiplicative kinematics have also been used to model amorphous solids (Anand and Gurtin 2003). However, rotation of the microstructure within an element of isotropic amorphous material, relative to the total rotation of that element, is of presumably less consequence to the mechanical response than would be expected for an anisotropic crystalline solid wherein the directions of the lattice vectors of the structure dictate thermomechanical properties such as elastic constants and thermal expansion coefficients.

The polar decomposition (2.149) applied to each of $\mathbf{F^L}$ and $\mathbf{F^P}$ yields

$$\mathbf{F} = \mathbf{V^L R^L R^P U^P} = \mathbf{R^L U^L V^P R^P}, \qquad (3.33)$$

where $\mathbf{V^L}$ is the left lattice stretch, $\mathbf{R^L}$ is the lattice rotation that includes rigid body rotations of the entire body, $\mathbf{R^P}$ is the plastic rotation, and $\mathbf{U^P}$

is the right plastic stretch. In the second of (3.33), $\mathbf{U}^{\mathbf{L}}$ is the right lattice stretch and $\mathbf{V}^{\mathbf{P}}$ is the left plastic stretch. In many interpretations, deformation mapping $\mathbf{F}^{\mathbf{L}}$, rather than being linked explicitly to the deformation of Bravais lattice vectors and basis vectors (Born and Huang 1954), is defined in terms of a reversible or elastic unloading from a stressed configuration to an unstressed configuration. In other words, unloading via $\mathbf{V}^{\mathbf{L}-1}$ maps the solid body from the stressed current configuration to an unloaded intermediate configuration. In continuum plasticity models, depending on the constitutive formulation used to specify the evolution of plastic deformation, this operation may leave the unloaded state indeterminate by a rotation, as discussed more in Section 3.2.7. Reverse decompositions, i.e., $\mathbf{F} = \mathbf{F}^{\mathbf{P}}\mathbf{F}^{\mathbf{L}}$, have also been forwarded (Bilby et al. 1957; Clifton 1972; Lubarda 1999). While such a reverse decomposition may pose no formal difficulties from a mathematical standpoint, an apparent benefit of original decomposition (3.31) is that unloading occurs most realistically from the actual (current) configuration of the body, as opposed to unloading from a stressed intermediate configuration as in the case of the reverse decomposition. In the former case, from (3.33) and for a compatible stretch field $\mathbf{V}^{\mathbf{L}}$, an entire stressed crystalline body could conceivably be unloaded to an intermediate configuration in one piece, simply by removal of traction along its external boundaries.

However, since $\mathbf{F}^{\mathbf{L}}$ and $\mathbf{F}^{\mathbf{P}}$ and their inverses are generally not compatible or integrable, configuration $\tilde{B}$ is generally anholonomic or non-holonomic. As demonstrated later in Section 3.3.2, the mathematical anholonomicity conditions imply, physically, the presence of geometrically necessary dislocations in the crystal, induced by the incompatible nature of $\mathbf{F}^{\mathbf{L}-1}$ or $\mathbf{F}^{\mathbf{P}}$. These defects differ from those dislocations that pass through the crystal in a relatively homogenous manner, contributing to the compatible or integrable part of $\mathbf{F}^{\mathbf{P}}$. From the perspective of local mechanical unloading, the incompatibility of $\mathbf{V}^{\mathbf{L}-1}$ implies that the body must be cut into pieces to relieve internal stresses associated with heterogeneous local elastic deformations (Eckart 1948).

As depicted in Fig. 3.4, tangent mappings from the material body $\mathcal{B}$ to the reference or current configuration, $\boldsymbol{\kappa}_t : T\mathcal{B} \to TB_t$ $(t \geq 0)$, need not be integrable, implying that $\boldsymbol{\chi}_t$ $(t \geq 0)$ of Fig. 2.2 could be an anholonomic function of reference coordinates $(t = 0)$ or spatial coordinates $(t > 0)$, and that natural configuration $\mathcal{B}$, like $\tilde{B}$, could be anholonomic. Incompatibility of $\boldsymbol{\kappa}_0$ implies that the defect content differs between the actual mate-

rial body $\mathcal{B}$ and its initial representation in Euclidean space B_0. For example, it often becomes convenient to treat the body at $t = 0$ as a perfect crystal. If the real body $\mathcal{B}$ contains defects, then κ_0 may be used to remove the effects of defects from the mathematical representation of the body at $t = 0$, or vice-versa. While some authors simultaneously introduce both κ_t and $\mathbf{F}^\mathbf{P}$ (Teodosiu 1970; Rice 1971; Tigoiu and Soos 1990; Le and Stumpf 1996a; Clayton et al. 2004a) in an independent manner similar to Fig. 3.4 (with possible differences in notation), in practice the distinction between reference configuration B_0 and natural configuration $\mathcal{B}$ is usually omitted. In this way, contributions of all defects towards the deformation gradient kinematics are embedded in $\mathbf{F}^\mathbf{L}$ and $\mathbf{F}^\mathbf{P}$, even though the crystal may be imperfect at $t = 0$. For the most part, henceforward in this book, this practical viewpoint will be used, meaning that mappings κ_0 and κ_t and material manifold $\mathcal{B}$ will not be considered explicitly.

Returning now to decomposition (3.31), lattice and plastic deformations are written fully in component form as, respectively,

$$\mathbf{F}^\mathbf{L} = F^{La}_{.\alpha}\mathbf{g}_a \otimes \tilde{\mathbf{g}}^\alpha , \; \mathbf{F}^\mathbf{P} = F^{P\beta}_{.A}\tilde{\mathbf{g}}_\beta \otimes \mathbf{G}^A , \tag{3.34}$$

where the anholonomic basis vectors $\tilde{\mathbf{g}}_\alpha$ and their reciprocals $\tilde{\mathbf{g}}^\alpha$ obey

$$\left\langle \tilde{\mathbf{g}}^\alpha , \tilde{\mathbf{g}}_\beta \right\rangle = \delta^\alpha_{.\beta} . \tag{3.35}$$

Unless noted otherwise, it is assumed that $\mathbf{F}^\mathbf{L}(X,t)$ and $\mathbf{F}^\mathbf{P}(X,t)$ are at least twice differentiable with respect to reference coordinates X^A, and that their inverses $\mathbf{F}^{\mathbf{L}-1}(x,t)$ and $\mathbf{F}^{\mathbf{P}-1}(x,t)$ are at least twice differentiable with respect to spatial coordinates x^a. Applying definition (2.206) for anholonomic partial differentiation with respect to lattice and plastic deformations, along with definition (2.112) and identity (3.31), leads to

$$\partial_\alpha (\cdot) = (\cdot)_{,\alpha} = \frac{\partial (\cdot)}{\partial X^A} F^{P-1A}_{.\alpha} = \frac{\partial (\cdot)}{\partial x^a} x^a_{.,A} F^{P-1A}_{.\alpha} = \frac{\partial (\cdot)}{\partial x^a} F^{La}_{.\alpha} . \tag{3.36}$$

Partial coordinate derivatives of anholonomic basis vectors and reciprocal basis vectors, following verbatim from postulates (2.210), are

$$\tilde{\mathbf{g}}^\alpha_{,\beta} = -\tilde{\Gamma}^{..\alpha}_{\beta\chi}\tilde{\mathbf{g}}^\chi , \; \tilde{\mathbf{g}}_{\alpha,\beta} = \tilde{\Gamma}^{..\chi}_{\beta\alpha}\tilde{\mathbf{g}}_\chi , \tag{3.37}$$

where from (2.208), either of the following definitions, not necessarily equivalent or exclusive[3], can be used for connection coefficients on $\tilde{B}$:

---

[3] Symbols in (3.38) and (3.39) are derived in Appendix D (Section D.4) via use of convected anholonomic basis vectors. Others are possible (e.g., (3.51) later).

$$\tilde{\Gamma}^{..\alpha}_{\beta\chi} = F^{P-1B}_{.\beta} F^{P-1C}_{.\chi} F^{P\alpha}_{.A} \overset{G}{\Gamma}^{..A}_{BC} + F^{P-1C}_{.\chi,\beta} F^{P\alpha}_{.C}$$

$$= F^{P-1B}_{.\beta} F^{P-1C}_{.\chi} F^{P\alpha}_{.A} \overset{G}{\Gamma}^{..A}_{BC} - F^{P-1B}_{.\beta} F^{P-1C}_{.\chi} F^{P\alpha}_{.C,B} ,\tag{3.38}$$

$$\tilde{\Gamma}^{..\alpha}_{\beta\chi} = F^{Lb}_{.\beta} F^{Lc}_{.\chi} F^{L-1\alpha}_{.a} \overset{g}{\Gamma}^{..a}_{bc} + F^{Lc}_{.\chi,\beta} F^{L-1\alpha}_{.c}$$

$$= F^{Lb}_{.\beta} F^{Lc}_{.\chi} F^{L-1\alpha}_{.a} \overset{g}{\Gamma}^{..a}_{bc} - F^{Lb}_{.\beta} F^{Lc}_{.\chi} F^{L-1\alpha}_{.c,b} .\tag{3.39}$$

Since Levi-Civita connections with Christoffel symbols $\overset{G}{\Gamma}^{..A}_{BC}$ and $\overset{g}{\Gamma}^{..a}_{bc}$ are symmetric, $\tilde{T}^{..\chi}_{\beta\alpha} = 0$ in (2.209) and the skew part of the second of (3.37) is

$$\tilde{\mathbf{g}}_{[\alpha,\beta]} = \tilde{\Gamma}^{..\chi}_{[\beta\alpha]} \tilde{\mathbf{g}}_\chi = -\tilde{\kappa}^{.\chi}_{\beta\alpha} \tilde{\mathbf{g}}_\chi ,\tag{3.40}$$

where anholonomic objects (2.207) obtained from (3.38) and (3.39) are identical[4]:

$$\tilde{\kappa}^{.\alpha}_{\beta\chi} = F^{La}_{.\beta} F^{Lb}_{.\chi} F^{L-1\alpha}_{.[b,a]} = F^{P-1A}_{.\beta} F^{P-1B}_{.\chi} F^{P\alpha}_{.[B,A]} .\tag{3.41}$$

On the other hand, only when $\tilde{B}$ is holonomic, meaning that coordinates $\tilde{x}^\alpha$ exist that are continuously (twice) differentiable functions of x^a or X^A, are all of the following conditions satisfied simultaneously:

$$F^{L-1\alpha}_{.a} = \frac{\partial \tilde{x}^\alpha}{\partial x^a} , \; F^{P\alpha}_{.A} = \frac{\partial \tilde{x}^\alpha}{\partial X^A} , \; \tilde{\mathbf{g}}_\alpha = \frac{\partial}{\partial \tilde{x}^\alpha} , \; \tilde{\kappa}^{.\alpha}_{\beta\chi} = 0 , \; \tilde{\mathbf{g}}_{[\alpha,\beta]} = 0 .\tag{3.42}$$

3.2.3 The Metric Tensor in the Intermediate Configuration

A generic metric tensor on anholonomic space $\tilde{B}$ is expressed as $\tilde{\mathbf{g}} = \tilde{g}_{\alpha\beta} \tilde{\mathbf{g}}^\alpha \otimes \tilde{\mathbf{g}}^\beta$ and is positive definite and symmetric by definition. Components of this metric tensor satisfy

$$\tilde{g}_{\alpha\beta} = \tilde{\mathbf{g}}_\alpha \bullet \tilde{\mathbf{g}}_\beta = \tilde{\mathbf{g}}_\beta \bullet \tilde{\mathbf{g}}_\alpha = \tilde{g}_{\beta\alpha} ,\tag{3.43}$$

where $\bullet$ denotes the scalar product of vectors akin to (2.9). The scalar product of two arbitrary vectors $\tilde{\mathbf{a}}, \tilde{\mathbf{b}} \in T\tilde{B}$ then becomes

$$\tilde{\mathbf{a}} \bullet \tilde{\mathbf{b}} = \tilde{a}^\alpha \tilde{\mathbf{g}}_\alpha \bullet \tilde{b}^\beta \tilde{\mathbf{g}}_\beta = \tilde{a}^\alpha \tilde{b}^\beta \tilde{\mathbf{g}}_\alpha \bullet \tilde{\mathbf{g}}_\beta = \tilde{a}^\alpha \tilde{g}_{\alpha\beta} \tilde{b}^\beta .\tag{3.44}$$

---

[4] A different anholonomic object defined as $\tilde{\kappa}^{.\alpha}_{\beta\chi} = F^{La}_{.\beta} F^{Lb}_{.\chi} F^{L-1\alpha}_{.[a,b]}$ was used in previous work (Clayton et al. 2004a), but implications regarding the vanishing or non-vanishing of the Riemann-Christoffel curvature tensor introduced in anholonomic coordinates in (36) of that paper remain the same.

Components of metric tensor $\tilde{\mathbf{g}}$ are also used to lower indices in the conventional manner, for example a contravariant vector is converted to a dual or covariant vector via

$$\tilde{a}_\alpha = \tilde{g}_{\alpha\beta}\tilde{a}^\beta . \tag{3.45}$$

Transposes (see e.g., (2.125) and (2.126)) of lattice and plastic deformations are given, respectively, by

$$F^{LT\alpha}_{\ \ .a} = \tilde{g}^{\alpha\beta}F^{Lb}_{\ \ .\beta}g_{ab} = \tilde{g}^{\alpha\beta}F^{L*\ .b}_{\ \ \beta}g_{ba} , \tag{3.46}$$

$$F^{PT A}_{\ \ .\alpha} = \tilde{g}_{\alpha\beta}F^{P\beta}_{\ \ .B}G^{AB} = \tilde{g}_{\alpha\beta}F^{P*\ \beta}_{\ \ B}G^{BA} , \tag{3.47}$$

where $\tilde{g}^{\alpha\beta}$ are components of the inverse intermediate metric $\tilde{\mathbf{g}}^{-1}$. Jacobian invariants of deformation mappings $\mathbf{F^L}$ and $\mathbf{F^P}$ providing relationships among volume elements $dv \subset B$, $d\tilde{V} \subset \tilde{B}$, and $dV \subset B_0$ also depend upon $\tilde{\mathbf{g}}$, as in (2.141), (2.142), (2.223), and (2.224). Letting z^a, $\tilde{z}^\alpha$, and Z^A denote coordinates referred to local Cartesian axes associated with material elements in B, $\tilde{B}$, and B_0, respectively, Jacobian determinants are found as (Teodosiu 1967b; Clayton et al. 2004a)

$$J^L = \frac{dv}{d\tilde{V}} = \det\left(\frac{\partial z^a}{\partial x^b}F^{Lb}_{\ \ .\beta}\frac{\partial \tilde{x}^\beta}{\partial \tilde{z}^\alpha}\right) = \det(F^{Lb}_{\ \ .\beta})\sqrt{\det(g_{ab})/\det(\tilde{g}_{\alpha\beta})} , \tag{3.48}$$

$$J^P = \frac{d\tilde{V}}{dV} = \det\left(\frac{\partial \tilde{z}^\alpha}{\partial \tilde{x}^\beta}F^{P\beta}_{\ \ .B}\frac{\partial X^B}{\partial Z^A}\right) = \det(F^{P\beta}_{\ \ .B})\sqrt{\det(\tilde{g}_{\alpha\beta})/\det(G_{AB})} , \tag{3.49}$$

where $\det(\tilde{g}_{\alpha\beta}) = [\det(\partial \tilde{z}^\alpha/\partial \tilde{x}^\beta)]^2$ has been used. Introducing permutation tensors $\tilde{\varepsilon}_{\alpha\beta\chi} = \sqrt{\tilde{g}}e_{\alpha\beta\chi}$ and $\tilde{\varepsilon}^{\alpha\beta\chi} = {}^{-1}\!\sqrt{\tilde{g}}e^{\alpha\beta\chi}$ and setting $\tilde{g} = \det(\tilde{g}_{\alpha\beta})$,

$$J^L = \frac{1}{6}\tilde{\varepsilon}^{\alpha\beta\chi}\varepsilon_{abc}F^{La}_{\ \ .\alpha}F^{Lb}_{\ \ .\beta}F^{Lc}_{\ \ .\chi} , \quad J^P = \frac{1}{6}\tilde{\varepsilon}_{\alpha\beta\chi}\varepsilon^{ABC}F^{P\alpha}_{\ \ .A}F^{P\beta}_{\ \ .B}F^{P\chi}_{\ \ .C} , \tag{3.50}$$

a form consistent with (2.224). Since $\mathbf{F^L}$ and $\mathbf{F^P}$ are required to have positive determinants as mentioned following (3.31), and since $\tilde{\mathbf{g}}$ is positive definite, $J^L > 0$, $J^P > 0$, and $d\tilde{V} > 0$.

Conceivable choices for metric tensor $\tilde{\mathbf{g}}$ and basis vectors $\tilde{\mathbf{g}}_\alpha$ in (3.43) are now discussed (Clayton et al. 2004a). The simplest and most prevalent option from the literature is (Teodosiu 1967a, b; Simo and Ortiz 1985)

$$\tilde{\mathbf{g}} = \delta_{\alpha\beta}\mathbf{e}^\alpha \otimes \mathbf{e}^\beta , \ \mathbf{e}_{\alpha,A} = \mathbf{e}_{\alpha,\beta}F^{P\beta}_{\ \ .A} = \tilde{\Gamma}^{.\delta}_{\beta\alpha}\mathbf{e}_\delta F^{P\beta}_{\ \ .A} = 0 , \ \tilde{\Gamma}^{.\delta}_{\beta\alpha} = 0 . \tag{3.51}$$

where intermediate metric tensor components are $\tilde{g}_{\alpha\beta} = \delta_{\alpha\beta}$. Intermediate Kronecker delta symbols $\delta_{\alpha\beta} = 1 \forall \alpha = \beta$ and $\delta_{\alpha\beta} = 0 \forall \alpha \neq \beta$, and $\tilde{\mathbf{g}}_\alpha = \mathbf{e}_\alpha$

are constant orthonormal (Cartesian) basis vectors[5]. The last of (3.51) applies in the present context, instead of alternatives (3.38) or (3.39).

Prescription (3.51) indicates that contravariant vectors defined on $\tilde{B}$ are referred to a single global Cartesian frame, or equivalently, a parallel Cartesian frame attached to each local relaxed volume $d\tilde{V} \subset \tilde{B}$. This implies either that (i) $\tilde{B}$ is a Euclidean space or that (ii) the $\tilde{\mathbf{g}}_\alpha$ are not actually tangent to any coordinate lines inscribed on base manifold $\tilde{B}$ since such coordinates do not exist, but instead correspond to some external reference frame. Statement (i) is ruled out in general by a non-vanishing anholonomic object in (3.40), physically indicating the presence of crystal defects such as dislocations that render $\tilde{B}$ anholonomic. This leaves statement (ii): indices of vectors on $T\tilde{B}$ are not referred to the actual tangent spaces of any deformed material manifold but are instead referred to the fixed external Cartesian frame. The intermediate metric $\delta_{\alpha\beta}$ (or equivalently, the external Cartesian frame) is introduced somewhat artificially as an additional modeling assumption, accompanying introduction of kinematic variables $\mathbf{F}^L$ and $\mathbf{F}^P$. Along similar lines, Simo (1988) posited an intermediate configuration metric $\tilde{g}_{\alpha\beta} = \delta_{.\alpha}^A G_{AB} \delta_{.\beta}^B$, implying a Cartesian metric for $\tilde{B}$ when B_0 is described using Cartesian coordinates, and requiring introduction of the two-point Kronecker delta (i.e., shifter) $\delta_{.\alpha}^A$.

Several alternatives have been proposed (Moran et al. 1990; Maugin 1994, 1995; Le and Stumpf 1998; Miehe 1998; Clayton et al. 2004a) that, in contrast to (3.51), do not embed non-Euclidean space $\tilde{B}$ within a global Cartesian space equipped with a Euclidean metric tensor $\delta_{\alpha\beta}$. It should be noted, however, that (3.48) and (3.49), wherein Cartesian $\tilde{z}^\alpha$ are assigned to each volume element $d\tilde{V} \subset \tilde{B}$, do rely on the pointwise assumption that transformation formulae to intermediate Cartesian coordinates $\tilde{z}^\alpha$ are available.

One such alternative is specification of an alternative kind of intermediate metric tensor $\tilde{\mathbf{g}}'$ as the covariant lattice deformation tensor $\tilde{\mathbf{C}}^L$ (Moran et al. 1990; Maugin 1994; Clayton et al. 2004a):

---

[5] Conditions $\tilde{g}_{\alpha\beta} = \tilde{\mathbf{g}}_\alpha \cdot \tilde{\mathbf{g}}_\beta = \delta_{\alpha\beta}$ can still be imposed without requiring $\tilde{\mathbf{g}}_\alpha(X)$ remain parallel for all X. For example, basis vectors $\tilde{\mathbf{g}}_\alpha(X)$ of unit length could differ by a (jump in) rotation at distinct points; conditions $\tilde{\mathbf{g}}_{\alpha,A} = 0$ and $\tilde{\Gamma}_{\beta\alpha}^{.\delta} = 0$ would not hold everywhere in that case, and the second of (3.51) would not apply.

$$\tilde{g}'_{\alpha\beta}(x,t) = \tilde{C}^L_{\alpha\beta} = F^{La}_{.\alpha} g_{ab} F^{Lb}_{.\beta} = F^{La}_{.\alpha}\mathbf{g}_a \cdot F^{Lb}_{.\beta}\mathbf{g}_b = \tilde{\mathbf{g}}'_\alpha \cdot \tilde{\mathbf{g}}'_\beta, \qquad (3.52)$$

implying that an alternative set of anholonomic basis vectors can be defined by

$$\tilde{\mathbf{g}}'_\alpha(x,t) = F^{La}_{.\alpha}(x,t)\mathbf{g}_a(x). \qquad (3.53)$$

Requiring that $\left\langle \tilde{\mathbf{g}}'^\alpha, \tilde{\mathbf{g}}'_\beta \right\rangle = \delta^\alpha_\beta$ leads to the corresponding reciprocal vectors

$$\tilde{\mathbf{g}}'^\alpha(x,t) = F^{L-1\alpha}_{.a}(x,t)\mathbf{g}^a(x). \qquad (3.54)$$

Since components $F^{La}_{.\alpha}$ and $\tilde{C}^L_{\alpha\beta}$ evolve with time along with changes in crystal structure (i.e., stretch and/or rotation of Bravais lattice vectors), basis vectors in (3.53) and (3.54) represent a kind of convected coordinates. Most generally, $\tilde{\mathbf{g}}'_\alpha \neq \tilde{\mathbf{g}}_\alpha$ meaning that basis vectors in (3.43) and (3.52) do not coincide[6]. However, letting $\tilde{\mathbf{g}}_\alpha(x) = g^a_{.\alpha}\mathbf{g}_a$, the first of (3.34) becomes

$$\begin{aligned}\mathbf{F}^L(x,t) &= F^{La}_{.\alpha}\mathbf{g}_a \otimes \tilde{\mathbf{g}}^\alpha \\ &= F^{La}_{.\alpha}\mathbf{g}_a \otimes g^\alpha_{.b}\mathbf{g}^b = g^\alpha_{.a}(x)\tilde{\mathbf{g}}'_\alpha(x,t) \otimes \mathbf{g}^a(x),\end{aligned} \qquad (3.55)$$

and is analogous to the convected coordinate representation of the deformation gradient (2.128) when coordinate systems are chosen such that the shifter is $g^\alpha_{.a} = \left\langle \tilde{\mathbf{g}}^\alpha, \mathbf{g}_a \right\rangle = \delta^\alpha_{.a}$. Maugin (1995) suggested an analogous form of (3.52) as a metric tensor on possibly anholonomic material manifold $\mathcal{B}$. The covariant plastic deformation $\tilde{\mathbf{C}}^P$ can likewise be employed as a metric on $\tilde{B}$ (Miehe 1998):

$$\begin{aligned}\tilde{g}'_{\alpha\beta}(X,t) &= \tilde{C}^P_{\alpha\beta} = F^{P-1A}_{.\alpha} G_{AB} F^{P-1B}_{.\beta} \\ &= F^{P-1A}_{.\alpha}\mathbf{G}_A \cdot F^{P-1B}_{.\beta}\mathbf{G}_B = \tilde{\mathbf{g}}'_\alpha \cdot \tilde{\mathbf{g}}'_\beta,\end{aligned} \qquad (3.56)$$

implying anholonomic basis vectors obey $\tilde{\mathbf{g}}'_\alpha(X,t) = F^{P-1A}_{.\alpha}(X,t)\mathbf{G}_A(X)$. In (3.52) and (3.56), respectively, the standard Euclidean relations $g_{ab} = \mathbf{g}_a \cdot \mathbf{g}_b$ and $G_{AB} = \mathbf{G}_A \cdot \mathbf{G}_B$ are used.

---

[6] In a previous paper (Clayton et al. 2004a), the same notation was used for $\tilde{\mathbf{g}}'_\alpha$ and $\tilde{\mathbf{g}}_\alpha$ in different sections, an ambiguity that could cause confusion. In that paper, the intended implication was that anholonomic basis vectors used in definitions of elastic and plastic deformation gradients differ from those used in metric tensors (3.52) and (3.56). Otherwise, setting $\tilde{\mathbf{g}}'^\alpha = \tilde{\mathbf{g}}^\alpha$ in (3.34) results, recursively, in null lattice deformation: $\mathbf{F}^L = F^{La}_{.\alpha}\mathbf{g}_a \otimes F^{L-1\alpha}_{.b}\mathbf{g}^b = \delta^a_{.b}\mathbf{g}_a \otimes \mathbf{g}^b$.

The $\tilde{\mathbf{g}}'_\alpha$ in (3.52) or (3.56) are not tangent to any global coordinate curves $\tilde{x}^\alpha$ since such coordinates are precluded by the anholonomicity of $\tilde{B}$, but they do exist in a one-to-one manner with the set $\mathbf{g}_a(x)$ and the map $F^{La}_{\ \ \cdot\alpha}(x,t)$ or with the set $\mathbf{G}_A(X)$ and the map $F^{P-1A}_{\quad\ \cdot\alpha}(X,t)$, respectively. In this sense, $\tilde{\mathbf{C}}^{\mathbf{L}}$ and $\tilde{\mathbf{C}}^{\mathbf{P}}$ are well-defined, but time-dependent, geometric quantities referred to space $\tilde{B}$, in contrast to $\delta_{\alpha\beta}$ of (3.51) that cannot be derived from components of lattice or plastic deformation maps and holonomic basis vectors on B_0 or B. Regardless, basis vectors $\tilde{\mathbf{g}}_\alpha$ and their reciprocals $\tilde{\mathbf{g}}^\alpha$ must always be prescribed by the modeler in the context of (3.34) so that components of $F^{La}_{\ \ \cdot\alpha}$ and $F^{P\alpha}_{\ \ \cdot A}$ can be defined. In later parts of this book (e.g., (3.64), (3.65), and thermodynamic treatments in Chapters 6, 8, and 9), to avoid unnecessary complexity, time-independent (extrinsic) basis vectors $\tilde{\mathbf{g}}_\alpha$ with metric tensor components $\tilde{g}_{\alpha\beta} = \tilde{\mathbf{g}}_\alpha \cdot \tilde{\mathbf{g}}_\beta$ are prescribed. Practical sets of time-independent intermediate {basis vectors, metric tensor components} include, but are not limited to, the following: $\{\tilde{\mathbf{g}}_\alpha = \mathbf{e}_\alpha, \tilde{g}_{\alpha\beta} = \delta_{\alpha\beta}\}$, $\{\tilde{\mathbf{g}}_\alpha = \delta^A_{\cdot\alpha}\mathbf{G}_A, \tilde{g}_{\alpha\beta} = \delta^A_{\cdot\alpha}G_{AB}\delta^B_{\cdot\beta}\}$, and $\{\tilde{\mathbf{g}}_\alpha = \delta^a_{\cdot\alpha}\mathbf{g}_a, \tilde{g}_{\alpha\beta} = \delta^a_{\cdot\alpha}g_{ab}\delta^b_{\cdot\beta}\}$. Two-point Kronecker delta symbols obey $\delta^A_{\cdot\alpha} = 1$ for $\alpha = A$ and $\delta^A_{\cdot\alpha} = 0$ for $\alpha \neq A$, where $\alpha, A = 1,2,3$. Analogous relationships apply for Kronecker delta symbols $\delta^a_{\cdot\alpha}$.

Consider now the rank four Riemann-Christoffel curvature tensor formed from connection coefficients (3.38) on anholonomic space $\tilde{B}$, with components found from (2.212):

$$\tilde{R}^{\cdot\cdot\alpha}_{\beta\chi\delta} = F^{Lb}_{\ \ \cdot\beta}F^{Lc}_{\ \ \cdot\chi}F^{Ld}_{\ \ \cdot\delta}F^{L-1\alpha}_{\quad\ \cdot a}\overset{g}{R}^{\cdot\cdot a}_{bcd}$$

$$= 2\partial_{[\beta}\tilde{\Gamma}^{\cdot\cdot\alpha}_{\chi]\delta} + 2\tilde{\Gamma}^{\cdot\cdot\alpha}_{[\beta|\varepsilon|}\tilde{\Gamma}^{\cdot\cdot\varepsilon}_{\chi]\delta} + 2\tilde{\kappa}^{\cdot\cdot\varepsilon}_{[\beta\chi]}\tilde{\Gamma}^{\cdot\cdot\alpha}_{\varepsilon\delta}. \tag{3.57}$$

Recall that $\overset{g}{R}^{\cdot\cdot a}_{bcd} = 0$ identically since B is a Euclidean space; hence, $\tilde{R}^{\cdot\cdot\alpha}_{\beta\chi\delta} = 0$ regardless of the vanishing of $F^{L-1\alpha}_{\quad\ [a,b]}$. However, integrability conditions $\tilde{R}^{\cdot\cdot\alpha}_{\beta\chi\delta} = 0$ and $\tilde{\kappa}^{\cdot\cdot\varepsilon}_{\beta\chi} = 0$ hold identically and simultaneously when $F^{L-1\alpha}_{\quad\ \cdot a}(x,t) = \tilde{x}^\alpha_{,a}$, i.e., when $\tilde{B}$ is homeomorphic to Euclidean space B and $\tilde{x}^\alpha = \tilde{x}^\alpha(x,t)$ are holonomic coordinates with respect to which partial coordinate differentiation can be defined as usual. Under such conditions, the anholonomic object in the first of (3.41) reduces to

$\tilde{\kappa}^{..\alpha}_{\beta\chi} = x^a_{.,\beta} x^b_{.,\chi} \tilde{x}^{\alpha}_{.,[ba]} = 0$. When $F^{L a}_{.\alpha}(x,t) = x^a_{.,\alpha}$, the curvature tensor formed from the symmetric Riemannian connection with metric coefficients $\tilde{C}^{L-1\alpha\delta}(\tilde{C}^L_{\beta\delta,\chi} + \tilde{C}^L_{\chi\delta,\beta} - \tilde{C}^L_{\beta\chi,\delta})/2$ vanishes identically since this curvature tensor is the pull-back by a continuously differentiable motion $\tilde{x}^{\alpha}$, to the intermediate configuration, of $\overset{g}{R}{}^{..a}_{bcd}$ formed from components of the Euclidean spatial metric g_{ab} , analogously to the situation discussed in Section 2.8.2. Similar statements apply for (3.39): the Riemann-Christoffel curvature tensor from coefficients in (3.39) vanishes identically; anholonomic object following the second equality of (3.41) vanishes if

$F^{P\alpha}_{.A}(X,t) = \tilde{x}^{\alpha}_{.,A}$, giving $\tilde{\kappa}^{..\alpha}_{\beta\chi} = X^A_{.,\beta} X^B_{.,\chi} \tilde{x}^{\alpha}_{.,[BA]} = 0$; and since $\overset{G}{R}{}^{..A}_{BCD} = 0$, the Riemann-Christoffel curvature tensor constructed from coefficients $\tilde{C}^{P-1\alpha\delta}(\tilde{C}^P_{\beta\delta,\chi} + \tilde{C}^P_{\chi\delta,\beta} - \tilde{C}^P_{\beta\chi,\delta})/2$ vanishes identically when $F^{P\alpha}_{.A} = \tilde{x}^{\alpha}_{.,A}$.

3.2.4 Kinematics, Rates, and Kinematic Approximations

Taking the material time derivative[7] of (3.31), applying the product rule, and post-multiplying the result by the inverse of deformation gradient **F** leads to

$$\mathbf{L} = \dot{\mathbf{F}}\mathbf{F}^{-1} = \dot{\mathbf{F}}^{\mathbf{L}}\mathbf{F}^{\mathbf{L}-1} + \mathbf{F}^{\mathbf{L}}\dot{\mathbf{F}}^{\mathbf{P}}\mathbf{F}^{\mathbf{P}-1}\mathbf{F}^{\mathbf{L}-1} = \mathbf{L}^{\mathbf{L}} + \mathbf{F}^{\mathbf{L}}\mathbf{L}^{\mathbf{P}}\mathbf{F}^{\mathbf{L}-1} , \qquad (3.58)$$

where **L** is the spatial velocity gradient of (2.176) with mixed-variant components $L^a_{.b} = v^a_{;b}$. The quantity $\mathbf{L}^{\mathbf{L}} = \dot{\mathbf{F}}^{\mathbf{L}}\mathbf{F}^{\mathbf{L}-1}$ is a mixed-variant tensor with components referred to spatial configuration B and is called the lattice velocity gradient, and $\mathbf{L}^{\mathbf{P}} = \dot{\mathbf{F}}^{\mathbf{P}}\mathbf{F}^{\mathbf{P}-1}$ is a mixed-variant tensor referred to intermediate configuration $\tilde{B}$ and is called the plastic velocity gradient. Using (3.33), the following definitions are introduced, where subscripts *skew* and *symm* refer to anti-symmetric and symmetric parts of covariant ingredients in (3.58), i.e., skew and symmetric parts of $L_{ab} = g_{ac}\dot{F}^c_{.A}F^{-1A}_{.b}$:

$$\dot{\mathbf{F}}\mathbf{F}^{-1} = \mathbf{W}^{\mathbf{L}} + \mathbf{D}^{\mathbf{L}} + \mathbf{F}^{\mathbf{L}}\left(\mathbf{W}^{\mathbf{P}} + \mathbf{D}^{\mathbf{P}}\right)\mathbf{F}^{\mathbf{L}-1} , \qquad (3.59)$$

$$\mathbf{W}^{\mathbf{L}} = \left(\mathbf{L}^{\mathbf{L}}\right)_{skew} = \dot{\mathbf{R}}^{\mathbf{L}}\mathbf{R}^{\mathbf{L}T} + \left(\mathbf{R}^{\mathbf{L}}\dot{\mathbf{U}}^{\mathbf{L}}\mathbf{U}^{\mathbf{L}-1}\mathbf{R}^{\mathbf{L}T}\right)_{skew} , \qquad (3.60)$$

$$\mathbf{D}^{\mathbf{L}} = \left(\mathbf{L}^{\mathbf{L}}\right)_{symm} = \left(\mathbf{R}^{\mathbf{L}}\dot{\mathbf{U}}^{\mathbf{L}}\mathbf{U}^{\mathbf{L}-1}\mathbf{R}^{\mathbf{L}T}\right)_{symm} , \qquad (3.61)$$

---

[7] From Section 2.6.1, $\dot{F}^{P\alpha}_{.A}(X,t) = \left.\dfrac{\partial F^{P\alpha}_{.A}}{\partial t}\right|_X$ and $\dot{F}^{L a}_{.\alpha}(x,t) = \left.\dfrac{\partial F^{L a}_{.\alpha}}{\partial t}\right|_x + F^{L a}_{.\alpha;b}v^b$.

$$\mathbf{W^P} = \left(\mathbf{L^P} \right)_{skew} = \dot{\mathbf{R}}^{\mathbf{P}} \mathbf{R}^{\mathbf{P}T} + \left(\mathbf{R^P} \dot{\mathbf{U}}^{\mathbf{P}} \mathbf{U}^{\mathbf{P}-1} \mathbf{R}^{\mathbf{P}T} \right)_{skew}, \qquad (3.62)$$

$$\mathbf{D^P} = \left(\mathbf{L^P} \right)_{symm} = \left(\mathbf{R^P} \dot{\mathbf{U}}^{\mathbf{P}} \mathbf{U}^{\mathbf{P}-1} \mathbf{R}^{\mathbf{P}T} \right)_{symm}. \qquad (3.63)$$

Above, $\mathbf{W^L}$ is the lattice spin, $\mathbf{D^L}$ is the lattice deformation rate, $\mathbf{W^P}$ is the plastic spin, and $\mathbf{D^P}$ is the plastic deformation rate. Another strain rate relation analogous to (2.186) that will become useful later is

$$\dot{\tilde{\mathbf{E}}}^{\mathbf{L}} = \mathbf{F^{L*}} \mathbf{D^L} \mathbf{F^L} , \quad \dot{\tilde{E}}^L_{\alpha\beta} = F^{La}_{.\alpha} D^L_{ab} F^{Lb}_{.\beta} , \qquad (3.64)$$

where lattice strain referred to the intermediate configuration, $\tilde{\mathbf{E}}^{\mathbf{L}}$, is defined analogously to the right Cauchy-Green strain introduced in (2.156):

$$\tilde{\mathbf{E}}^{\mathbf{L}} = \frac{1}{2} (\tilde{\mathbf{C}}^{\mathbf{L}} - \tilde{\mathbf{g}}), \quad \tilde{E}^L_{\alpha\beta} = \frac{1}{2} (\tilde{C}^L_{\alpha\beta} - \tilde{g}_{\alpha\beta}) = \tilde{E}^L_{(\alpha\beta)}, \qquad (3.65)$$

with symmetric lattice deformation tensor $\tilde{C}^L_{\alpha\beta} = F^{La}_{.\alpha} g_{ab} F^{Lb}_{.\beta}$ as first introduced in (3.52). Conditions $\dot{\tilde{g}}_{\alpha\beta} = 0$ are assumed in (3.64).

Analogously to (2.114), lattice and plastic deformation gradients provide first-order approximations of the length and direction of a differential line element $d\tilde{\mathbf{x}} \in T\tilde{B}$ mapped to the intermediate configuration. For example, for the plastic deformation:

$$d\tilde{x}^\alpha = \tilde{x}^\alpha (X') - \tilde{x}^\alpha (X)$$

$$= F^{P\alpha}_{.A} \Big|_X dX^A + \frac{1}{2!} F^{P\alpha}_{.A:B} \Big|_X dX^A dX^B \qquad (3.66)$$

$$+ \frac{1}{3!} F^{P\alpha}_{.A:BC} \Big|_X dX^A dX^B dX^C + ...,$$

where $dX^A = X'^A - X^A$ is the infinitesimal vector between two reference points X and X', and the total covariant derivative, similar to (2.116), is

$$F^{P\alpha}_{.A:B} = F^{P\alpha}_{.A,B} - \overset{G}{\Gamma}{}^{.C}_{BA} F^{P\alpha}_{.C} + \tilde{\Gamma}^{.\alpha}_{\beta\chi} F^{P\chi}_{.A} F^{P\beta}_{.B}, \qquad (3.67)$$

where $\tilde{\Gamma}^{.\alpha}_{\beta\chi}$ are connection coefficients associated with basis vectors on $\tilde{B}$. Noting $dX^A dX^B = dX^B dX^A$, skew terms $F^{P\alpha}_{.[A:B]}$, while generally nonzero, will not contribute to (3.66). Similarly for the lattice deformation,

$$d\tilde{x}^\alpha = \tilde{x}^\alpha (x') - \tilde{x}^\alpha (x)$$

$$= F^{L-1\alpha}_{.a} \Big|_x dx^a + \frac{1}{2!} F^{L-1\alpha}_{.a:b} \Big|_x dx^a dx^b \qquad (3.68)$$

$$+ \frac{1}{3!} F^{L-1\alpha}_{.a:bc} \Big|_x dx^a dx^b dx^c + ...,$$

where $dx^a = x'^a - x^a$ is the infinitesimal vector between two spatial points x and x', and analogously to (2.116), the total covariant derivative

$$F^{L-1\alpha}_{\quad .a:b} = F^{L-1\alpha}_{\quad .a,b} - \overset{g}{\Gamma}^{..c}_{ba}F^{L-1\alpha}_{\quad .c} + \tilde{\Gamma}^{..\alpha}_{\beta\chi}F^{L-1\chi}_{\quad .a}F^{L-1\beta}_{\quad .b}. \qquad (3.69)$$

Skew terms $F^{L-1\alpha}_{\quad [a:b]}$ are nonzero when $\mathbf{F}^{L-1}$ is not integrable, but will not affect the quadratic term in (3.68). From (3.66) and (3.68), to first order,

$$d\tilde{\mathbf{x}} = \mathbf{F}^{P}d\mathbf{X} = \mathbf{F}^{L-1}d\mathbf{x}, \quad d\tilde{x}^{\alpha} = F^{P\alpha}_{\quad .A}dX^A = F^{L-1\alpha}_{\quad .a}dx^a. \qquad (3.70)$$

Because lattice and plastic deformation gradients are generally not integrable, $d\tilde{\mathbf{x}}$ is generally not an exact differential and is sometimes referred to as a Pfaffian (Stojanovitch 1969). The role of the lattice deformation and lattice strain tensors in the context of first-order deformed lengths of differential line elements is thus

$$|d\mathbf{x}| = |\mathbf{F}^{L}d\tilde{\mathbf{x}}| = \sqrt{\langle d\tilde{\mathbf{x}}, \tilde{\mathbf{C}}^{L}d\tilde{\mathbf{x}} \rangle}, \qquad (3.71)$$

$$d\mathbf{x} \cdot d\mathbf{x} - d\tilde{\mathbf{x}} \cdot d\tilde{\mathbf{x}} = 2\langle d\tilde{\mathbf{x}}, \tilde{\mathbf{E}}^{L}d\tilde{\mathbf{x}} \rangle. \qquad (3.72)$$

Two approximations are commonly encountered pertaining to relative magnitudes of lattice and plastic deformations. The first is the small lattice strain assumption:

$$\mathbf{V}^{L} = \mathbf{1} + \boldsymbol{\varepsilon}^{L}, \quad |\boldsymbol{\varepsilon}^{L}| = (\boldsymbol{\varepsilon}^{L} : \boldsymbol{\varepsilon}^{L})^{1/2} \ll 1, \qquad (3.73)$$

where terms of the symmetric tensor $g_{ac}\varepsilon^{Lc}_{\quad .b}$ are small relative to unity as indicated. This assumption is often deemed relevant for ductile metallic crystals that deform by dislocation motion before large elastic strains are attained (Bammann and Johnson 1987). The contribution of the plastic velocity gradient in (3.58) is then often approximated as

$$\mathbf{F}^{L}\mathbf{L}^{P}\mathbf{F}^{L-1} = (\mathbf{1} + \boldsymbol{\varepsilon}^{L})\mathbf{R}^{L}\mathbf{L}^{P}\mathbf{R}^{LT}(\mathbf{1} + \boldsymbol{\varepsilon}^{L})^{-1} \approx \mathbf{R}^{L}\mathbf{L}^{P}\mathbf{R}^{LT}. \qquad (3.74)$$

Neither $\mathbf{W}^{L}$ nor $\mathbf{D}^{L}$ necessarily vanishes according to approximation (3.73), since lattice rotation and stretch rates may still be arbitrarily large.

The second approximation is the small deformation assumption, as introduced in Section 2.5.3, with rate kinematics listed in (2.191). The analog of (3.31) in the geometrically linear theory is

$$\mathbf{F} \approx \mathbf{1} + \boldsymbol{\beta}^{L} + \boldsymbol{\beta}^{P}, \quad F^{a}_{.A} \approx g^{ab}\delta^{c}_{.A}(g_{bc} + \beta^{L}_{bc} + \beta^{P}_{bc}), \qquad (3.75)$$

where the lattice displacement gradient is denoted by $\boldsymbol{\beta}^{L}$ and the plastic displacement gradient is denoted by $\boldsymbol{\beta}^{P}$, such that an additive decomposition of the total covariant displacement gradient applies:

$$u_{a;b} = \beta^{L}_{ab} + \beta^{P}_{ab}. \qquad (3.76)$$

Displacement gradients in (3.76) are sometimes called distortions (Mura 1982). Like the lattice and plastic deformation maps of (3.31), the lattice and plastic distortions of (3.75) are generally incompatible, i.e.

$$\beta^L_{a[b,c]} \neq 0, \ \beta^P_{a[b,c]} \neq 0, \tag{3.77}$$

even though the total distortion, since it is a true covariant derivative of a continuous displacement field, must satisfy $u_{a,[bc]} = u_{a;[bc]} = 0$. Distortions are separated into skew rotational and symmetric strain tensors as follows:

$$\varepsilon_{ab} = u_{(a;b)} = \varepsilon^L_{ab} + \varepsilon^P_{ab}, \ \Omega_{ab} = u_{[a,b]} = \Omega^L_{ab} + \Omega^P_{ab}; \tag{3.78}$$

$$\beta^L_{ab} = \varepsilon^L_{ab} + \Omega^L_{ab}, \ \varepsilon^L_{ab} = \beta^L_{(ab)}, \ \Omega^L_{ab} = \beta^L_{[ab]}; \tag{3.79}$$

$$\beta^P_{ab} = \varepsilon^P_{ab} + \Omega^P_{ab}, \ \varepsilon^P_{ab} = \beta^P_{(ab)}, \ \Omega^P_{ab} = \beta^P_{[ab]}. \tag{3.80}$$

Upon taking time derivatives of (3.78)-(3.80), linearized lattice and plastic rotation and strain rates are obtained:

$$\dot{u}_{a;b} = \dot{\Omega}^L_{ab} + \dot{\varepsilon}^L_{ab} + \dot{\Omega}^P_{ab} + \dot{\varepsilon}^P_{ab}; \tag{3.81}$$

$$\dot{\Omega}^L_{ab} = \dot{\beta}^L_{[ab]} \approx W^L_{ab}, \ \dot{\varepsilon}^L_{ab} = \dot{\beta}^L_{(ab)} \approx D^L_{ab}; \tag{3.82}$$

$$\dot{\Omega}^P_{ab} = \dot{\beta}^P_{[ab]} \approx W^P_{ab}, \ \dot{\varepsilon}^P_{ab} = \dot{\beta}^P_{(ab)} \approx D^P_{ab}; \tag{3.83}$$

where approximations in (3.82) and (3.83) hold when both lattice and plastic distortions are small so that, in Cartesian coordinates, $\mathbf{W^L} \approx \dot{\mathbf{R}}^L$, $\mathbf{D^L} \approx \dot{\mathbf{U}}^L$, $\mathbf{W^P} \approx \dot{\mathbf{R}}^P$, $\mathbf{D^P} \approx \dot{\mathbf{U}}^P$, $\mathbf{R^L} \approx 1 + \mathbf{\Omega^L}$, $\mathbf{U^L} \approx 1 + \mathbf{\varepsilon^L}$, $\mathbf{R^P} \approx 1 + \mathbf{\Omega^P}$, $\mathbf{U^P} \approx 1 + \mathbf{\varepsilon^P}$, and $\mathbf{F} = \mathbf{F^L F^P} \approx 1 + \mathbf{\Omega^L} + \mathbf{\varepsilon^L} + \mathbf{\Omega^P} + \mathbf{\varepsilon^P}$, consistent with (3.75).

3.2.5 Dislocation Plasticity

Dislocations are elementary line defects in crystalline solids, and their motion is often the primary source of plastic deformation in crystalline materials. Dislocations are characterized by a tangent line and Burgers vector (Burgers 1939; Frank 1951). The dimensionless tangent line $\tilde{\xi}(X,t) \in T\tilde{B}$, which may be straight or curved, indicates the direction of the defect and is typically assigned a unit magnitude. At any point along the dislocation line L, the tangent line defines the normal to a plane perpendicular to the defect. Dislocation lines may intersect with other defects or free surfaces of the crystal, and may form loops, but do not end abruptly within an otherwise perfect crystal lattice. The Burgers vector $\tilde{\mathbf{b}}(X,t) \in T\tilde{B}$ (dimensions of length) indicates the magnitude and direction of the closure failure, or step in the lattice, induced by mapping a closed loop in a defective crystal to a perfect crystal or vice-versa (Hirth and Lothe 1982; Teodosiu

1982; Hull and Bacon 1984). The corresponding closed loop is called a Burgers circuit. Straight dislocation lines may be of screw, edge, or mixed character. Screw dislocations have parallel tangent lines and Burgers vectors, while edge dislocations have perpendicular tangent lines and Burgers vectors. Mixed dislocations are neither parallel nor perpendicular to their tangent lines. Partial dislocations, dislocation loops, helical dislocations, disclinations (Frank 1958; De Wit 1973), and other more general defect structures such as Somigliana dislocations (Eshelby 1956; Asaro 1976) are also observed in some kinds of crystals. Dislocation-like defects can also emerge in geologic solids (Eshelby 1973) and porous media (Pan 1991).

The magnitude of the Burgers vector of a full (complete) dislocation is equal to the distance between two atoms in a perfect crystal in the direction of the atomic displacement, e.g., a lattice parameter in a primitive unit cell. In contrast, the magnitude of a partial dislocation may differ from the distance between two atoms in a perfect crystal. The movement of an isolated partial dislocation through a region of crystal leaves behind a stacking fault in that region, but a perfect lattice can be restored by collective movement of partial dislocations (e.g., leading and trailing partial dislocations separated by a stacking fault). Mechanical twinning can also involve coordinated motion of partial dislocations (Christian and Mahajan 1995; Bernstein and Tadmor 2004). Full dislocations tend to dissociate into partial dislocations if the energy of the full dislocation exceeds the sum of energies of the partial dislocations (including their core and elastic interaction energies) and the energy of the stacking fault between the partials (Hull and Bacon 1984).
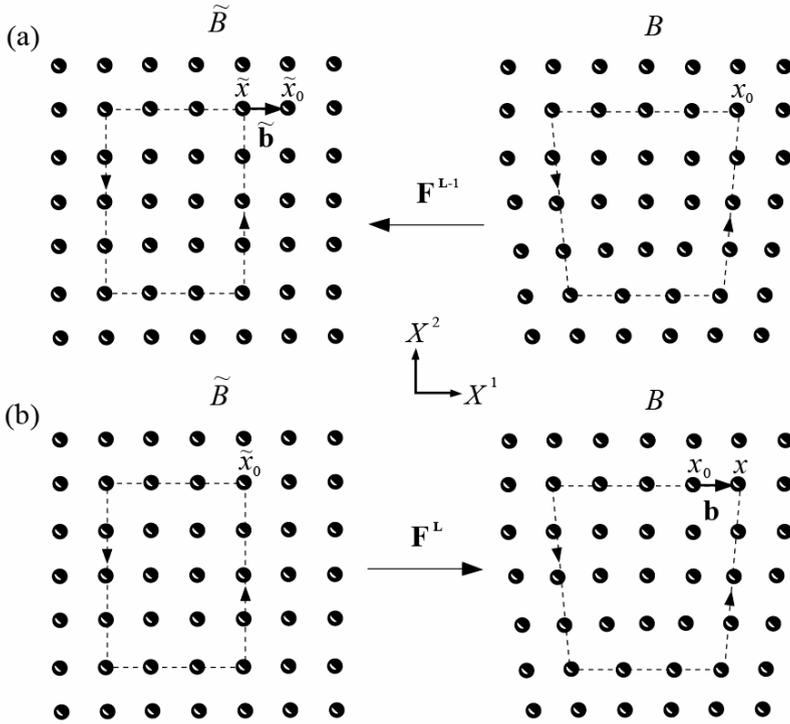
Fig. 3.6 Burgers circuit surrounding single edge dislocation in cubic crystal

The Burgers circuit concept is illustrated explicitly in Fig. 3.6 for a cubic crystal containing a single edge dislocation. The tangent line of the dislocation is directed in a positive sense out of the plane of the figure, i.e., $\tilde{\xi} \parallel \mathbf{G}_3$. Two kinds of Burgers circuits are typically considered. In the first, shown in Fig. 3.6(a), a closed circuit about the defect line in the current configuration on the right, beginning and ending at point x_0, is mapped to an open circuit by counting the same steps in a perfect lattice in the intermediate configuration on the left. By convention the circuit is taken in a clockwise sense from an observer viewing in the direction of the tangent line, or equivalently, via the usual right-hand rule of vector calculus. In the perfect lattice, the circuit does not close. The Burgers vector in Fig. 3.6(a) is then the vector $\tilde{\mathbf{b}} = \tilde{\mathbf{x}}_0 - \tilde{\mathbf{x}}$ directed from the point $\tilde{x}$ at the end of the circuit to the point $\tilde{x}_0$ at the start. In the second kind of Burgers circuit shown in Fig. 3.6(b), a closed circuit about the defect line in the in-

termediate configuration on the left, beginning and ending at point $\tilde{x}_0$, is mapped to an open circuit by counting the same steps in the defective lattice in the current configuration on the right. By convention, the circuit is again taken in the right-handed sense. In the dislocated lattice, the circuit does not close. The Burgers vector in Fig. 3.6(b) is $\mathbf{b} = \mathbf{x} - \mathbf{x}_0$, directed from point x_0 at the start of the circuit to point x at the end. Kondo (1963) calls the circuit of Fig. 3.6(a) "Frank's disturbance", and the circuit of 3.6(b) "Read's disturbance". Using a nonlinear elastic model based on Volterra's construction (Volterra 1907) in which $\mathbf{F} = \mathbf{F^L}$, Teodosiu (1982) demonstrates that after neglecting terms on the order of the square of $\tilde{\mathbf{b}}$, the two Burgers vectors are related by

$$\mathbf{b}(X,t) = \mathbf{F^L}(X,t)\tilde{\mathbf{b}}(X,t) \,, \quad b^a = F^{La}_{.\alpha}\tilde{b}^\alpha \,. \qquad (3.84)$$

Willis (1967) and Teodosiu (1982) note that $\tilde{\mathbf{b}}$ does not depend upon the choice of starting point x_0, while $\mathbf{b}$ does depend upon choice of starting point $\tilde{x}_0$ as a result of the local lattice deformation $\mathbf{F^L}(X = \tilde{x}_0)$. Different conventions exist for algebraic signs of Burgers vectors and tangent lines and for the positive sense of circulation about the Burgers circuit; those used here follow from Willis (1967) and Hull and Bacon (1984). Volterra-type elasticity models of discrete dislocation lines and disclination lines are provided in Appendix C, Section C.1. Linear elastic models of dislocation and disclination loops are discussed in Section C.2 of Appendix C. The Burgers circuit concept can be used for dislocation lines of screw and mixed character, and can be extended to describe the total summed Burgers vector of a number of dislocation lines passing through an oriented surface in the crystal enclosed by a circuit.

Mobile dislocations engender plastic stretch and rotation. When acted on by external forces, dislocations tend to move directions normal to their tangent vectors. For a single mobile dislocation, the direction of movement of atoms is in the same direction as the Burgers vector. For an edge dislocation, atoms move in the same direction as the motion (i.e., the velocity) of the dislocation line and perpendicular to the tangent vector. For a screw dislocation, atoms move parallel to the tangent line but normal to the velocity vector of the dislocation line. Dislocation motion may proceed by glide or climb. Dislocations that undergo glide are often labeled glissile, while dislocations that are immobile, or locked in place due to constraints imposed by other defects for example, are often labeled sessile.

Glide is dislocation motion whereby the movement of the dislocation is restricted to a surface called the glide plane that contains both the Burgers vector and tangent line. Glide is often referred to as slip, and terms glide

and slip are used interchangeably in this book. Dislocation glide is an example of conservative motion, meaning that the local volume of the crystal is unaffected by the process. The surface on which the dislocation glides is called the slip plane or glide plane. Unlike edge dislocations, screw dislocations do not exhibit a mathematically unique slip plane since the latter's Burgers vector and tangent line are parallel. However, in crystals a finite set of discrete planes upon which screw dislocations usually move is often dictated by the crystal structure. Cross slip, or a change of slip planes, may occur during the course of plastic deformation as screw dislocations seek paths of least resistance (Hirth and Lothe 1982). The usual thermodynamic driving force for dislocation glide is a shear stress component acting on the slip plane in the direction of the Burgers vector, as demonstrated in explicit detail in Sections 6.2 and 6.3 of Chapter 6.

The combination of Burgers vector or its orientation—with the latter denoting the slip direction—and the slip plane constitute a slip system. Typical slip systems for cubic and hexagonal crystal structures are illustrated in Fig. 3.7 and are listed in Table 3.4. The direction of the Burgers vector is always parallel to the slip direction. Dislocations tend to move in close-packed directions on close-packed planes, though exceptions exist among certain kinds of materials. Depending on the particular material (e.g., element or compound), its purity, and environmental conditions (e.g., temperature), the most common slip system, or that with the least resistance to slip, may vary. More extensive lists of slip systems in different materials—including for example secondary systems activated at higher temperatures as well as slip systems for other crystal structures not listed in Table 3.4—can be found in books by Schmid and Boas (1950) and Hirth and Lothe (1982). Exceptions to the slip systems in Fig. 3.7 are common among polyatomic structures and nonmetals, especially ionic solids wherein electrostatic interactions (e.g., charge imbalances) among ions strongly affect defect structures and mobilities (Sprackling 1976). For example, primary slip systems in alkali halide crystals (rock salt structure) are of type $\langle 110 \rangle \{1\bar{1}0\}$. Pure ionic crystals are often very ductile, with high dislocation mobilities (Gilman 2003). For hexagonal structures, direction X^1 is often chosen parallel to $\langle 2\bar{1}\bar{1}0 \rangle$ rather than $\langle \bar{1}2\bar{1}0 \rangle$ as shown in Fig. 3.7, though in the present context the choice is arbitrary.
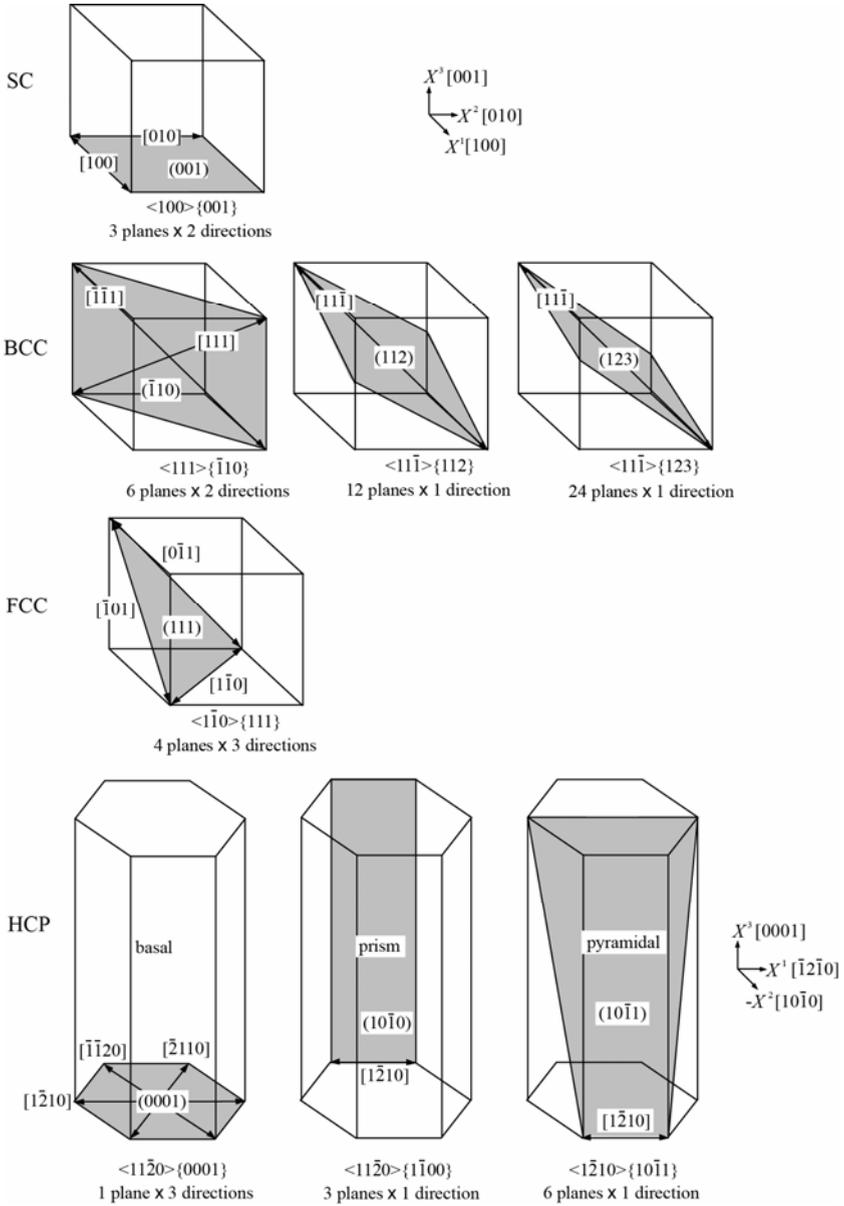
Fig. 3.7 Slip systems for cubic and hexagonal crystal structures

Table 3.4 Slip systems and Burgers vectors for several crystal structures

Structure	Primary slip systems	Burgers vector, magnitude
SC	$\langle 100 \rangle \{010\}$	$\langle 100 \rangle$, a
BCC	$\langle 111 \rangle \{1\,\overline{1}0\}$, $\langle 111 \rangle \{11\overline{2}\}$, $\langle 111 \rangle \{12\overline{3}\}$	$1/2\langle 111 \rangle$, $a\sqrt{3}/2$
FCC	$\langle 110 \rangle \{1\,\overline{1}1\}$	$1/2\langle 110 \rangle$, $a\sqrt{2}/2$
HCP	$\langle 11\overline{2}0 \rangle \{0001\}$, $\langle 11\overline{2}0 \rangle \{1\,\overline{1}00\}$, $\langle 11\overline{2}0 \rangle \{1\,\overline{1}01\}$	$1/3\langle 11\overline{2}0 \rangle$, a

Climb occurs when an edge dislocation moves out of the surface containing its Burgers vector and tangent line, and is a generally nonconservative motion since the volume of the solid is changed locally by the process. Dislocation climb often involves the motion of point defects such as vacancies or interstitials to accommodate volume changes. Conservative climb of prismatic dislocation loops is possible, however (Hull and Bacon 1984). In engineering metals deformed at low temperatures or high strain rates, glide tends to prevail over climb, since diffusion mechanisms often require higher temperatures and longer time scales to contribute substantially to inelastic deformation.

The intermediate configuration $\tilde{B}$ in Fig. 3.4 differs from B_0 due to the influence of cumulative motion of lattice defects through the volume element under consideration and perturbations of atomic positions resulting from defects contained within that volume. Defects considered in what follows next in the present Section are displacement discontinuities tangential to an internal surface (i.e., crystallographic plane) in the material. These include gliding straight or curved dislocation lines, dislocation loops, and partial dislocations. Configuration $\tilde{B}$ is considered free of external traction and free of all internal stresses, and hence is fictitious in the sense that local stress fields of defects are absent. In the context of continuum elasticity, one could view the volume element in configuration $\tilde{B}$ at the stage of the Volterra process (see e.g., Appendix C) after discontinuities in displacement have been introduced, but prior to the stage of resealing the body and introduction of self-stresses (Eshelby 1956; Toupin and Rivlin 1960; De Wit 1973; Mura 1982).

For a crystal containing a single dislocation, a singular plastic deformation map can be defined in the vicinity of the defect in Cartesian coordinates as follows (Teodosiu 1970; Rice 1971; Ortiz and Repetto 1999):

$$\mathbf{F}^{\mathbf{P}} = \mathbf{1} + \tilde{\mathbf{b}} \otimes \mathbf{M}\delta\big(\langle \mathbf{X}, \mathbf{M}\rangle\big)\chi, \qquad (3.85)$$

where $\mathbf{1}$ is the unit tensor, $\mathbf{M}$ is the normal to the slip plane in the reference configuration, $\delta(.)$ is Dirac's delta function, and χ is a characteristic

function equal to unity at reference coordinates $\mathbf{X}$ on a slipped surface (i.e., surface of singularity) Σ and zero elsewhere. The coordinate system for $\mathbf{X}$ is chosen with its origin in the slip plane so that along the surface of displacement discontinuity $X^A M_A = 0$. Plastic deformation (3.85) is singular on Σ and vanishes elsewhere. A dislocation density tensor corresponding to the discrete dislocation line described by (3.85) is (Teodosiu 1970)

$$\boldsymbol{\alpha}_0 = \tilde{\mathbf{b}} \otimes \boldsymbol{\xi}_0 \delta(L), \tag{3.86}$$

where $\boldsymbol{\xi}_0 \in TB_0$ is tangent to dislocation line L in the reference configuration. From (3.85) and (3.86),

$$\tilde{\mathbf{b}} = -\int_{\mathbf{X}^+}^{\mathbf{X}^-} \mathbf{F^P} d\mathbf{X} = \int_A \boldsymbol{\alpha}_0 \mathbf{N} dA. \tag{3.87}$$

Line integration in the first of (3.87) takes place between limiting coordinates immediately above ($\mathbf{X}^+$) and below ($\mathbf{X}^-$) the slipped singular surface Σ ($\mathbf{X}^+ \cong \mathbf{X}^-$). Area integration in the second of (3.87) proceeds over the union of oriented reference elements $\mathbf{N} dA$ pierced once by the dislocation line, and $\langle \boldsymbol{\xi}_0, \mathbf{N} \rangle dA = dA$ by definition at the intersection of L and A.

Now consider the average plastic deformation gradient for a volume element containing multiple dislocation lines. If the dislocations are introduced into the volume element sequentially, a logical non-singular extension of (3.85) is

$$\mathbf{F^P} = \prod_{m=1}^{n} \left(\mathbf{1} + V^{-1} \int \tilde{\mathbf{b}} \otimes \mathbf{M} \delta(\Sigma) dV \right) = \prod_{m=1}^{n} \left(\mathbf{1} + V^{-1} \tilde{\mathbf{b}} \otimes \mathbf{M} \Sigma \right), \tag{3.88}$$

where the product is taken over n dislocations, each with a possibly different Burgers vector $\tilde{\mathbf{b}}$ and constant normal vector $\mathbf{M}$ to an assumed flat slipped surface (i.e., glide plane) of reference area Σ. The volume of the element in the reference configuration is denoted by V. Note that (3.88) depends upon the sequence in which each dislocation is introduced ($m=1$ corresponds to the most recently generated dislocation) and hence cannot be used effectively if dislocations with different Burgers vectors or slip surfaces are generated simultaneously. Since $\tilde{\mathbf{b}} \perp \mathbf{M}$ from the definition of a glide plane, (3.88) consists of a product of simple shears and volume is conserved, i.e., $J^P = 1$. For a collection of $i = 1, 2, ... j$ straight dislocation line populations of density $\rho_0^i = \lim_{V \to 0} (L^i / V) = dL^i / dV \geq 0$, Burgers vector $\tilde{\mathbf{b}}^i$, reference tangent $\boldsymbol{\xi}_0^i$, and plane normal $\mathbf{M}^i$, dislocation density in (3.86) and Burgers integral in (3.87) can be extended as

$$\boldsymbol{\alpha}_0 = V^{-1} \int_L \tilde{\mathbf{b}} \otimes \boldsymbol{\xi}_0 dL = \sum_{i=1}^{j} \rho_0^i \tilde{\mathbf{b}}^i \otimes \boldsymbol{\xi}_0^i, \tag{3.89}$$

$$\tilde{\mathbf{B}} = \int_A \langle \boldsymbol{\alpha}_0, \mathbf{N} \rangle dA = \int_A \sum_{i=1}^{j} \rho_0^i \tilde{\mathbf{b}}^i \langle \boldsymbol{\xi}_0^i, \mathbf{N} dA \rangle, \tag{3.90}$$

with $\tilde{\mathbf{B}}$ the summed projection of all local Burgers vectors of dislocation lines passing through area A contributing to the closure failure of the Burgers circuit corresponding to the boundary of A. Line integration in (3.89) proceeds over all dislocations of total length L. The second equation in (3.90) pertains to j discrete dislocation populations with the same tangent line and local Burgers vector for each value of i. Using a version of Nanson's formula (2.227), a differential Burgers vector from (3.90) can be defined completely in terms of quantities in the intermediate configuration as follows:

$$d\tilde{B}^\alpha = \alpha_0^{\alpha A} N_A dA = \sum_{i=1}^{j} \rho_0^i \tilde{b}^{i\alpha} \xi_0^{iA} N_A dA$$

$$= \sum_{i=1}^{j} \rho_0^i \tilde{b}^{i\alpha} \xi_0^{iA} J^{P-1} F^{P\beta}_{.A} \tilde{n}_\beta d\tilde{a} = \sum_{i=1}^{j} \tilde{\rho}^i \tilde{b}^{i\alpha} \xi^{i\beta} \tilde{n}_\beta d\tilde{a} = \tilde{\alpha}^{\alpha\beta} \tilde{n}_\beta d\tilde{a}, \tag{3.91}$$

where the intermediate tangent line, number of dislocations per unit volume in $\tilde{B}$, and intermediate dislocation density tensor, are respectively,

$$\xi^{i\alpha} = F^{P\alpha}_{.A} \xi_0^{iA}, \ \ \tilde{\rho}^i J^P = \rho_0^i, \ \ \tilde{\alpha}^{\alpha\beta} = J^{P-1} \alpha_0^{\alpha A} F^{P\beta}_{.A}, \tag{3.92}$$

and the differential area element maps from reference to intermediate configuration according to (see e.g., Cermelli and Gurtin (2001) and (2.227))

$$\tilde{n}_\alpha d\tilde{a} = J^P F^{P-1A}_{.\alpha} N_A dA. \tag{3.93}$$

Integration of (3.91) then gives

$$\tilde{B}^\alpha = \int_{\tilde{a}} d\tilde{B}^\alpha = \int_{\tilde{a}} \tilde{\alpha}^{\alpha\beta} \tilde{n}_\beta d\tilde{a}. \tag{3.94}$$

From the first of (3.92), the intermediate tangent vector with components $\xi^{i\alpha}$ need not be of unit length when $\xi_0^{iA} \xi_{0A}^i = 1$. As discussed in Section 3.2.3, the assignment of Cartesian basis vectors to intermediate configuration $\tilde{B}$ is not always necessary, and is not geometrically natural when the plastic deformation gradient is not integrable. However, (3.87), (3.89), (3.90), and (3.94) are integrals of vector fields whose components are referred to $T\tilde{B}$. Thus, these integral equations are valid globally, in component form, only when basis vectors $\tilde{\mathbf{g}}_\alpha$ are independent of position within the domains of integration, e.g., when these basis vectors are spatially constant, but not necessarily orthonormal. On the other hand, following Toupin (1956), such integrals can be evaluated numerically at a single point X by parallel transporting the integrands to that point using a shifter $g^A_{.\alpha}(X, X')$ that is assumed to exist everywhere within the domain of integration. For example, (3.94) evaluated at X is

$$\tilde{B}^A(X) = \int_{\tilde{a}} g_{.\alpha}^A(X, X') d\tilde{B}^\alpha(X') = \int_{\tilde{a}} g_{.\alpha}^A(X, X') \tilde{\alpha}^{\alpha\beta}(X') \tilde{n}_\beta(X') d\tilde{a} . \quad (3.95)$$

The resultant can then be transported back to any point X' via

$$\tilde{B}^\beta(X') = g_{.A}^\beta(X', X) \tilde{B}^A(X) = g_{.A}^\beta(X', X) \int_{\tilde{a}} g_{.\alpha}^A(X, X') d\tilde{B}^\alpha(X') . \quad (3.96)$$

Steps such as (3.95) and (3.96) are implied henceforth in this book for integrals of vector and tensor fields when curvilinear coordinates are involved, and are usually not written out explicitly.

A more general definition of the average plastic deformation of a volume element accounts for the time history of generation and motion of mobile defects within it, in which case $\mathbf{F^P}$ is defined as the solution of the following differential equation with initial conditions:

$$\dot{\mathbf{F}}^{\mathbf{P}} = \mathbf{L^P F^P} , \quad \mathbf{F^P}\big|_{t=0} = \mathbf{1} . \quad (3.97)$$

The average plastic velocity gradient $\mathbf{L^P}$ in (3.58) for the volume element, including both rate of deformation and spin, is dictated by the flux $\tilde{\mathbf{\zeta}}$ of mobile dislocations (Mura 1968; Lardner 1969; Lempriere 1970; Zbib et al. 2002; Clayton et al. 2006):

$$\mathbf{L^P} = \tilde{\mathbf{\zeta}} : \mathbf{\varepsilon} , \quad L_{.\beta}^{P\alpha} = \tilde{\zeta}^{\alpha\chi\delta} \varepsilon_{\chi\delta\beta} ; \quad (3.98)$$

$$\tilde{\mathbf{\zeta}} = V^{-1} \int_L \tilde{\mathbf{b}}^i \otimes \tilde{\mathbf{\xi}}^i \otimes \tilde{\mathbf{v}}^i dL = \sum_{i=1}^j \tilde{\rho}^i \tilde{\mathbf{b}}^i \otimes \tilde{\mathbf{\xi}}^i \otimes \tilde{\mathbf{v}}^i , \quad (3.99)$$

where $\varepsilon_{\chi\delta\beta}$ are covariant permutation tensor components first introduced in (2.224) and $\tilde{\mathbf{\xi}}^i = \xi^{\alpha i}/|\xi^{\alpha i}|\tilde{\mathbf{g}}_\alpha$ and $\tilde{\mathbf{v}}^i$ are respectively the normalized unit tangent vector and velocity of dislocation population i, all referred to configuration $\tilde{B}$. Since dislocation segments exhibit perpendicular velocities and tangent lines, $\tilde{\mathbf{\xi}}^i \perp \tilde{\mathbf{v}}^i$ and $\tilde{\mathbf{b}}^i \perp (\tilde{\mathbf{\xi}}^i \times \tilde{\mathbf{v}}^i)$, $\dot{J}^P = J^P \text{tr} \mathbf{L^P} = 0$ and $J^P = 1$, meaning volume is conserved by (3.98). Relation (3.99) applies for straight dislocation lines; similar expressions can be formulated for dislocation loops (Kroupa 1962; Teodosiu 1970), or curved lines can simply be discretized into a number of smaller straight segments (Zbib et al. 1998; Arsenlis and Parks 2002; Zbib and De La Rubia 2002). Introducing the notation $\tilde{\mathbf{\xi}}^i \times \tilde{\mathbf{v}}^i = \tilde{\mathbf{m}}^i \tilde{v}^i$, $\tilde{v}^i = |\tilde{\mathbf{v}}^i|$, $\tilde{\mathbf{b}}^i = \tilde{b}^i \tilde{\mathbf{s}}^i$, and $\tilde{b}^i = |\tilde{\mathbf{b}}^i|$, where $\tilde{\mathbf{m}}^i$ is the unit normal to the slip plane in configuration $\tilde{B}$ and $\tilde{\mathbf{s}}^i$ is a unit vector in the direction of slip, the plastic velocity gradient of (3.98) reduces to the form most often encountered in crystal plasticity (Rice 1971; Asaro 1983):

$$\mathbf{L^P} = \sum_i \tilde{\rho}^i \tilde{b}^i \tilde{v}^i \tilde{\mathbf{s}}^i \otimes \tilde{\mathbf{m}}^i = \sum_i \dot{\gamma}^i \tilde{\mathbf{s}}^i \otimes \tilde{\mathbf{m}}^i , \quad \dot{\gamma}^i = \tilde{\rho}^i \tilde{b}^i \tilde{v}^i . \quad (3.100)$$

The definition of the slip rate $\dot{\gamma}^i$ in (3.100) is often attributed to Orowan (1934, 1940), Polanyi (1934), and Taylor (1934). Implicit in (3.100) is the idea that only mobile dislocations ($\tilde{v}^i \neq 0$) contribute. Since the product $\dot{\gamma}^i \tilde{\mathbf{s}}^i \otimes \tilde{\mathbf{m}}^i$ does not depend upon the orientation of the Burgers vector relative to the tangent line, summation in (3.100) can be reduced to a sum over i slip systems identified by slip direction and slip plane normal, and $\dot{\gamma}^i$ then accounts for all mobile screw, edge, partial, and mixed dislocations, including loops, with an effective scalar Burgers vector $\tilde{b}^i$, average velocity $\tilde{v}^i$, and total mobile density $\tilde{\rho}^i$ on that slip system. Since $\tilde{\mathbf{s}}^i \perp \tilde{\mathbf{m}}^i$, again $\dot{J}^P = J^P \mathrm{tr}\mathbf{L}^P = 0$ and $J^P = 1$. Thus the scalar line densities are equal in intermediate and reference configurations: $\tilde{\rho}^i = \rho_0^i$. Some authors switch positions of the tangent line and dislocation velocity in the dislocation flux; in that case, (3.100) can still be recovered by defining the slip plane as the negative of that used in (3.100), i.e., $\tilde{\mathbf{m}}^i = (\tilde{\mathbf{v}}^i \times \tilde{\boldsymbol{\xi}}^i)/\tilde{v}^i$. Regardless, the contravariant index of $\mathbf{L}^P$ always corresponds to the direction of atomic motion, i.e., the Burgers vector or the slip direction. Kinematic relationship (3.100) is considered again in Section 3.2.6 dealing with continuum crystal plasticity theory. Consideration of kinematics of mechanical twinning resulting from the collective motion of partial dislocations and atomic shuffling (Christian and Mahajan 1995; Zanzotto 1996; Clayton 2009a, 2010c) is deferred until Chapter 8.
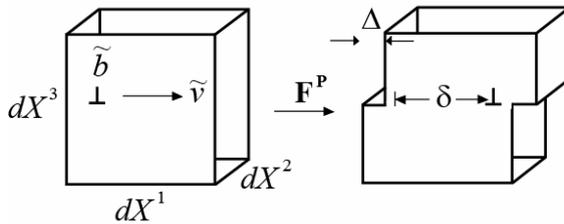
Fig. 3.8 Plastic shear resulting from a single edge dislocation

Slip rate equation $\dot{\gamma}^i = \tilde{\rho}^i \tilde{b}^i \tilde{v}^i$ in (3.100) can be derived intuitively as follows. First consider the glide of a single edge dislocation with Burgers vector of magnitude $\tilde{b}$, as shown in Fig. 3.8, where the volume of the element of crystal prior to plastic deformation is $dV = dX^1 dX^2 dX^3$. The velocity of the dislocation line is $\tilde{v} = \dot{\delta}$, where δ is the distance the dislo-

cation moves during the course of plastic deformation. The plastic shear experienced by the volume element is

$$\gamma = \frac{\Delta}{dX^3} = \frac{\tilde{b}\delta}{dX^1 dX^3} \ . \tag{3.101}$$

When n parallel edge dislocations of the same configuration shown in Fig. 3.8 are superposed, the plastic shear becomes

$$\gamma = \sum_{m=1}^{n} \frac{\Delta^m}{dX^3} = \sum_{m=1}^{n} \frac{\tilde{b}\delta^m}{dX^1 dX^3} = \frac{n}{dX^1 dX^3} \tilde{b}\overline{\delta} = \rho_0 \tilde{b}\overline{\delta} = \tilde{\rho}\tilde{b}\overline{\delta} \ , \tag{3.102}$$

where $\overline{\delta}$ is an average distance moved by the dislocations, $\tilde{\rho} = J^{P-1}\rho_0$ is the scalar mobile dislocation density, and $J^P = 1$. Since $\tilde{b}$ is a constant, time differentiation of (3.102) leads to

$$\dot{\gamma} = \tilde{\rho}\tilde{b}\tilde{v} + \dot{\tilde{\rho}}\tilde{b}\overline{\delta} \ . \tag{3.103}$$

Typically the second term on the right side, which can be attributed to dislocation generation or annihilation, is not treated explicitly. However, in some constitutive models for plasticity (see e.g., Zerilli and Armstrong (1987)) the contribution of dislocation generation to the total inelastic strain rate is considered substantial. When the second term on the right of (3.103) is omitted, Orowan's slip rate equation written in the second of (3.100) is recovered for the case of a single set of parallel edge dislocations.

Relation (3.103) was modified to account for the motion of disclinations, or rotational dislocations, by Li and Gilman (1970):

$$\dot{\gamma} = \kappa\tilde{\eta}R\tilde{\omega}\tilde{v} \ , \tag{3.104}$$

where κ is a scalar geometry factor, $\tilde{\eta}$ is the line density of mobile disclination loops per unit reference or intermediate volume of the material, $\tilde{\omega}$ is the magnitude of the Frank vector representing the strength of the disclination, R is an effective scalar disclination radius, and $\tilde{v}$ is again the mean line velocity of the defects. Das et al. (1973) and Kossecka and De Wit (1977) considered kinematics of mobile disclinations in the setting of geometric linearity. Disclinations are further examined in the context of geometric theories of continuous defect distributions in Section 3.3.3, and elastic solutions for disclination lines and loops are given in Appendix C.

Returning now to the plastic velocity gradient resulting only from the dislocation flux, (3.98) can be written as (Werne and Kelly 1978)

$$\mathbf{L^P} = \left(\sum_{i=1}^{j} \tilde{\boldsymbol{\alpha}}_\mathbf{T}^i \otimes \tilde{\mathbf{v}}_+^i \right) : \boldsymbol{\varepsilon} \ , \tag{3.105}$$

with summation applied over j populations of straight dislocation lines, each with velocity vector $\tilde{\mathbf{v}}_+^j$. The total dislocation density tensor $\tilde{\boldsymbol{\alpha}}_\mathbf{T}^i$ is

$$\tilde{\boldsymbol{\alpha}}_{\mathbf{T}}^i = \left(\tilde{\rho}_+^i + \tilde{\rho}_-^i \right) \tilde{\mathbf{b}}_+^i \otimes \tilde{\boldsymbol{\xi}}^i , \tag{3.106}$$

with $\tilde{\rho}_+^i$ and $\tilde{\rho}_-^i$ the densities (line length per unit volume in $\tilde{B}$) of posi-tively and negatively signed dislocations, where, for each value of i, posi-tive and negative dislocations share the same tangent $\tilde{\boldsymbol{\xi}}^i$ but oppositely oriented Burgers vectors $\tilde{\mathbf{b}}_+^i = -\tilde{\mathbf{b}}_-^i$ and velocities $\tilde{\mathbf{v}}_+^i = -\tilde{\mathbf{v}}_-^i$. Using (3.104), Clayton et al. (2006) generalized (3.105) to account for contribu-tions of total densities of mobile dislocation and disclination lines to the plastic velocity gradient.

Deformations of primitive Bravais lattice vectors and basis vectors of crystal structures are now considered in the context of decomposition (3.31) and (3.26). Let a volume element of crystalline material of suffi-cient size as discussed in Section 3.2.2 deform via $\mathbf{F} = \mathbf{F}^{\mathbf{L}}\mathbf{F}^{\mathbf{P}}$, where the plastic deformation from dislocation flux $\mathbf{F}^{\mathbf{P}}$ results from time integration of (3.98)-(3.99) or (3.100). Let $\tilde{\mathbf{a}}_i$ denote primitive Bravais lattice vectors of (3.1) mapped to $\tilde{B}$:

$$\tilde{a}_i^\alpha = g_{.A}^\alpha A_i^A , \ (i = 1, 2, 3) . \tag{3.107}$$

Basis vectors in (3.3) likewise map only via the shifter

$$\tilde{R}\left(\begin{smallmatrix} 0 \\ k \end{smallmatrix}\right)^\alpha = \sum_{i=1}^3 m^i g_{.A}^\alpha A_i^A , \ (0 \le m^i < 1). \tag{3.108}$$

Relations (3.107) and (3.108) imply that primitive lattice vectors and the basis vectors of the crystal structure are not affected by $\mathbf{F}^{\mathbf{P}}$, in accordance with continuous dislocation theory (Bilby et al. 1957; Kroner 1960). However, primitive Bravais lattice vectors deform from configuration $\tilde{B}$ to configuration B according to

$$\mathbf{a}_i = \mathbf{F}^{\mathbf{L}} \tilde{\mathbf{a}}_i , \ a_i^a = F_{.\alpha}^{La} \tilde{a}_i^\alpha = F_{.\alpha}^{La} g_{.A}^\alpha A_i^A , \tag{3.109}$$

and correspondingly, in the absence of inner displacements $q\left(\begin{smallmatrix} 0 \\ k \end{smallmatrix}\right)^a$ and Δm^i of the sort described in (3.19) and (3.20), deformed basis vectors satisfy

$$r\left(\begin{smallmatrix} 0 \\ k \end{smallmatrix}\right)^a = F_{.\alpha}^{La} g_{.A}^\alpha R\left(\begin{smallmatrix} 0 \\ k \end{smallmatrix}\right)^A = F_{.\alpha}^{La} \sum_{i=1}^3 m^i g_{.A}^\alpha A_i^A . \tag{3.110}$$

However, because of plastic deformation, (3.26) cannot be used to specify absolute spatial coordinates of (the nucleus of) a particular atom occupying a point on the Bravais lattice with reference position $\mathbf{R}(l)$. This is because atoms are translated in space by moving dislocations, even though primi-tive Bravais lattice vectors and basis vectors remain fixed in magnitude and direction while the material undergoes plastic flow.

Reference Bravais lattice vectors $\mathbf{A}_i$ are uniform in a perfect homoge-neous lattice. However, when defects are contained within the volume, the

deformed primitive lattice vectors $\mathbf{a}_i$ represent suitable averages (Naghdi and Srinivasa 1993) of local primitive lattice vectors $\mathbf{a}_i'$ that may not be spatially constant within the deformed element of material:

$$\mathbf{a}_i = V^{-1} \int_V \mathbf{a}_i' dV \ . \tag{3.111}$$

The lattice deformation and lattice strain tensors in (3.65) thus provide first-order deformed lengths of primitive Bravais lattice vectors and basis vectors of the crystal structure:

$$\left| \mathbf{a}_i \right| = \left| \mathbf{F}^{\mathbf{L}} \tilde{\mathbf{a}}_i \right| = \sqrt{\left\langle \tilde{\mathbf{a}}_i, \tilde{\mathbf{C}}^{\mathbf{L}} \tilde{\mathbf{a}}_i \right\rangle} = \left[A_i^A g_{.A}^\alpha \tilde{C}_{\alpha\beta}^L g_{.B}^\beta A_i^B \right]^{1/2} , \tag{3.112}$$

$$\left| \mathbf{r} \begin{pmatrix} 0 \\ k \end{pmatrix} \right| = \left[\left(\sum_{i=1}^3 m^i g_{.A}^\alpha A_i^A \right) \tilde{C}_{\alpha\beta}^L \left(\sum_{i=1}^3 m^i g_{.B}^\beta A_i^B \right) \right]^{1/2} , \tag{3.113}$$

$$\mathbf{a}_i \bullet \mathbf{a}_i - \mathbf{A}_i \bullet \mathbf{A}_i = g_{.A}^\alpha A_i^A (\tilde{C}_{\alpha\beta}^L - \tilde{g}_{\alpha\beta}) A_i^B g_{.B}^\beta = 2\tilde{E}_{\alpha\beta}^L g_{.A}^\alpha A_i^A A_i^B g_{.B}^\beta . \tag{3.114}$$

From (3.112)-(3.114), it is evident that $\tilde{\mathbf{C}}^{\mathbf{L}}$ and $\tilde{\mathbf{E}}^{\mathbf{L}}$ provide a first-order accurate measure of the stretch of the interatomic bond vectors in a crystal structure.

3.2.6 Crystal Plasticity

In what is referred to in this book as crystal plasticity theory, plastic deformation of single crystals is represented by slip on a finite number of glide planes, but lengths and directions of individual dislocation lines are not resolved explicitly. Early studies, in this context, of potentially finite distortions of cubic metallic crystals were conducted by Taylor and co-workers in the first half of the 20th century (Taylor and Elam 1923; Taylor 1927; Taylor 1938). A detailed account of these studies is given by Havner (1992). More modern treatments of finite deformation crystal plasticity that follow a notational scheme similar to that used here include those of Rice (1971), Hill and Rice (1972), Teodosiu and Sidoroff (1976), Peirce et al. (1982), and Asaro (1983).
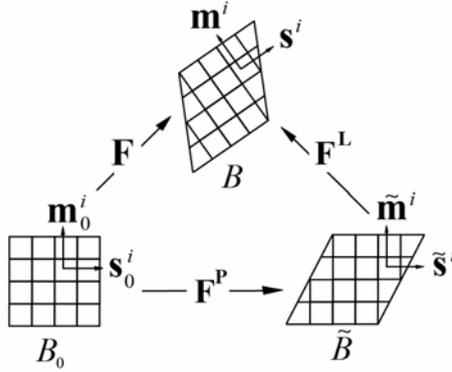
Fig. 3.9 Crystal plasticity kinematics

Fundamental variables entering the kinematic description of crystal plasticity theory are shown in Fig. 3.9. Multiplicative decomposition (3.31) applies, with the same general premise of Fig. 3.5 implied: plastic deformation resulting from dislocation glide is lattice-preserving (Bilby et al. 1957). Slip director unit vectors $\mathbf{s}_0^i(X) \in T_X B_0$ give the direction of dislocation motion on glide planes with unit normal covectors $\mathbf{m}_0^i(X) \in T_X^* B_0$. Index i refers to a slip system comprised of $\mathbf{s}_0^i$ and $\mathbf{m}_0^i$ for a particular value of i, where $i = 1, 2, \ldots n$, with n the total number of slip systems. Upon designation of a coordinate system, numerical values of $\mathbf{s}_0^i$ and $\mathbf{m}_0^i$ can be assigned for particular crystal structures; for example, slip systems for cubic and hexagonal structures are listed in Table 3.4 and illustrated in Fig. 3.7. In FCC metals, slip systems are usually of type $\langle 110 \rangle \{1\,\overline{1}1\}$, in which case $n = 12$ if positive and negative slip are both allowed on a single system[8]. By definition, $\mathbf{s}_0^i$ and $\mathbf{m}_0^i$ are orthonormal for each value of i:

$$\left\langle \mathbf{s}_0^i, \mathbf{m}_0^i \right\rangle = s_0^{iA} m_{0A}^i = 0. \tag{3.115}$$

From Fig. 3.9, since $\mathbf{F}^\mathbf{P}$ is lattice-preserving, slip vectors and slip plane covectors have parallel representations in intermediate configuration $\tilde{B}$:

$$\tilde{s}^{i\alpha} = g_{.A}^\alpha s_0^{iA}, \quad \tilde{m}_{.\alpha}^i = g_{.\alpha}^A m_{0A}^i; \tag{3.116}$$

$$\left\langle \tilde{\mathbf{s}}^i, \tilde{\mathbf{m}}^i \right\rangle = s^{i\alpha} m_\alpha^i = g_{.A}^\alpha s_0^{iA} g_{.\alpha}^B m_{0B}^i = s_0^{iA} \delta_{.A}^B m_{0B}^i = 0. \tag{3.117}$$

---

[8] If on the other hand positive and negative slip are described by mathematically distinct slip systems, $n = 24$ in FCC crystals.

However, these quantities are pushed forward to the current configuration via the lattice deformation gradient:

$$\mathbf{s}^i(x,t) = \mathbf{F}^\mathbf{L}\tilde{\mathbf{s}}^i \in T_x B \,, \quad \mathbf{m}^i(x,t) = \mathbf{F}^{\mathbf{L}-*}\tilde{\mathbf{m}}^i = \tilde{\mathbf{m}}^i \mathbf{F}^{\mathbf{L}-1} \in T_x^* B \,. \quad (3.118)$$

The transformation law for a slip direction is analogous to that of a primitive Bravais lattice vector in (3.109), and the transformation law for a slip plane normal is analogous to that of a reciprocal Bravais lattice vector in (3.22) with $\mathbf{F}$ replaced by the lattice deformation. For a particular slip system i, $\mathbf{s}^i$ and $\mathbf{m}^i$ are orthogonal:

$$\left\langle \mathbf{s}^i, \mathbf{m}^i \right\rangle = F^{La}_{.\alpha} \tilde{s}^{i\alpha} F^{L-1\beta}_{.a} \tilde{m}^i_\beta = \tilde{s}^{i\alpha} \delta^\beta_{.\alpha} \tilde{m}^i_\beta = 0 \,. \quad (3.119)$$

However, neither $\mathbf{s}^i$ nor $\mathbf{m}^i$ is necessarily of unit length.

Scalar slip rates or shearing rates $\dot{\gamma}^i$ are introduced on each system so that the plastic velocity gradient entering (3.58) is written as in (3.100):

$$\mathbf{L}^\mathbf{P} = \sum_i \dot{\gamma}^i \tilde{\mathbf{s}}^i \otimes \tilde{\mathbf{m}}^i \,, \quad (3.120)$$

though Orowan's relation in (3.100) need not be formally enforced. Scalar $\dot{\gamma}^i$ need not be a material time derivative of the cumulative slip on a particular glide system i. From (3.117), plastic deformation is isochoric:

$$\dot{J}^P = J^P L^{P\alpha}_{.\alpha} = J^P \sum_i \dot{\gamma}^i \left\langle \tilde{\mathbf{s}}^i, \tilde{\mathbf{m}}^i \right\rangle = 0 \,, \quad (3.121)$$

in agreement with the microscopic observation that dislocation glide is volume-conservative. From (3.118) and (3.120), the contribution from slip to the spatial velocity gradient of (3.58) is simply

$$\mathbf{F}^\mathbf{L} \mathbf{L}^\mathbf{P} \mathbf{F}^{\mathbf{L}-1} = \sum_i \dot{\gamma}^i \mathbf{s}^i \otimes \mathbf{m}^i \,, \quad (3.122)$$

and plastic spin $\mathbf{W}^\mathbf{P}$ and plastic deformation rate $\mathbf{D}^\mathbf{P}$ tensors are computed in covariant form as

$$2\mathbf{W}^\mathbf{P} = \sum_i \dot{\gamma}^i \left[(\tilde{\mathbf{g}}\tilde{\mathbf{s}}^i) \otimes \tilde{\mathbf{m}}^i - \tilde{\mathbf{m}}^i \otimes (\tilde{\mathbf{g}}\tilde{\mathbf{s}}^i) \right], \quad (3.123)$$

$$2\mathbf{D}^\mathbf{P} = \sum_i \dot{\gamma}^i \left[(\tilde{\mathbf{g}}\tilde{\mathbf{s}}^i) \otimes \tilde{\mathbf{m}}^i + \tilde{\mathbf{m}}^i \otimes (\tilde{\mathbf{g}}\tilde{\mathbf{s}}^i) \right]. \quad (3.124)$$

In the geometrically linear theory, stretch and rotation of the slip vectors are typically omitted, i.e., $\mathbf{s}^i$ and $\mathbf{m}^i$ are assumed of constant (unit) length and orthonormal for all $t \geq 0$. In such a linear theory, using $\mathbf{g}$ to denote the metric tensor of the coordinate system, time rates of plastic distortion, rotation, and strain (refer to (3.81)-(3.83)) are computed, respectively, as

$$\dot{\boldsymbol{\beta}}^\mathbf{P} = \sum_i \dot{\gamma}^i \mathbf{s}^i \otimes \mathbf{m}^i \,, \quad (3.125)$$

$$2\dot{\boldsymbol{\Omega}}^\mathbf{P} = \sum_i \dot{\gamma}^i \left[(\mathbf{g}\mathbf{s}^i) \otimes \mathbf{m}^i - \mathbf{m}^i \otimes (\mathbf{g}\mathbf{s}^i) \right], \quad (3.126)$$

$$2\dot{\boldsymbol{\varepsilon}}^{\mathbf{P}} = \sum_i \dot{\gamma}^i \left[(\mathbf{gs}^i) \otimes \mathbf{m}^i + \mathbf{m}^i \otimes (\mathbf{gs}^i) \right]. \qquad (3.127)$$

3.2.7 Macroscopic Plasticity

In what is labeled in this book as macroscopic plasticity, a volume element of material undergoing inelastic deformation is assumed to contain a large number of single crystals or grains. Deformation map $\mathbf{F}^{\mathbf{P}}$ thus depicts the net contribution of local plastic responses of individual grains to that of the aggregate. In this representation of macroscopic plasticity, evolution of plastic deformation is prescribed without explicit consideration of individual grains and hence, without explicit consideration of individual glide systems or discrete defects corresponding to those systems.

Macroscopic plasticity is distinguishable from what is termed typically as polycrystal plasticity. In polycrystal plasticity, various averaging or homogenization schemes are used to construct the response of the aggregate from that of its constituent single crystals (Taylor 1938; Bishop and Hill 1951; Kocks 1970).

Consider the polar decompositions entering (3.33). Often the following requirements are stipulated for individual terms entering this kinematic description, in the context of macroscopic plasticity: plastic deformation $\mathbf{F}^{\mathbf{P}}$ is lattice-preserving (i) and hence is volume-preserving (ii). Some measure of applied stress is work conjugate to $\mathbf{V}^{\mathbf{L}}$ (iii), such that a relaxed intermediate configuration $\tilde{B}$ can be achieved via local unloading of the volume element by $\mathbf{V}^{\mathbf{L}-1}$ (iv). This unloading scenario (iv) is in agreement with lattice preservation requirement (i), since mechanical stresses are associated with stretch of the interatomic bond vectors (primitive Bravais lattice vectors and basis vectors) at the atomistic level, as discussed at the end of Section 3.2.5. Requirement (ii) that $J^P = 1$ is in agreement with the microscopic observation that dislocation glide is a conservative motion.

Regarding the first equality of (3.33), if total deformation $\mathbf{F}$ is applied, and if symmetric plastic stretch $\mathbf{U}^{\mathbf{P}}$ is known from a constitutive or kinetic relation, then since $\mathbf{F}\mathbf{U}^{\mathbf{P}-1} = \mathbf{V}^{\mathbf{L}}\mathbf{R}^{\mathbf{L}}\mathbf{R}^{\mathbf{P}}$, it follows that $\mathbf{R}^{\mathbf{L}}$ and $\mathbf{R}^{\mathbf{P}}$ are not known uniquely (Bammann and Johnson 1987), but their product $\mathbf{R}^{\mathbf{L}}\mathbf{R}^{\mathbf{P}}$ is. In such circumstances, elastically unloaded intermediate configuration $\tilde{B}$ is non-unique up to a rotation. Uniqueness of $\tilde{B}$ can only be ensured by prescription of skew rotation rate $\dot{\mathbf{R}}^{\mathbf{P}}\mathbf{R}^{\mathbf{P}T}$ for all $t \geq 0$ or plastic spin $\mathbf{W}^{\mathbf{P}}$ of (3.62), in addition to the symmetric plastic deformation rate $\mathbf{D}^{\mathbf{P}}$ of

$(3.63)^9$. However, in implementations of macroscopic plasticity wherein the stress-strain response of the material of interest is isotropic, plastic spin is often not prescribed explicitly since the stress state can be deduced from knowledge of elastic and plastic stretch tensors and/or their time derivatives. This is in contrast to single crystal plasticity, wherein the plastic spin is prescribed explicitly by (3.123) and the intermediate configuration $\tilde{B}$ is always defined uniquely. In particular, the choice of orientation of intermediate configuration and corresponding plastic rotation is usually thought unimportant for isotropic polycrystals, e.g., large numbers of randomly oriented grains whose individual anisotropies have no net effect on the mechanical response of the polycrystal. Kratochvil (1971) and Mandel (1973) suggested the intermediate configuration be associated with the substructure or a representative lattice in the polycrystalline material; Mandel (1973) labeled one such relaxed intermediate configuration an isoclinic space. Proper choices of constitutive functions or kinetic relationships for the plastic spin have been addressed by a number of researchers (Bammann and Aifantis 1987; Dafalias 1998; Scheidler and Wright 2003).

3.2.8 Inelastic Volumetric Deformation

While dislocation glide is volume-preserving, in general the contribution of other kinds of lattice defects to the deformation gradient need not be. Consider a volume element of solid material containing a uniformly distributed collection of spherical defects, which could include isotropic point defects of local dimensions on the order of the lattice spacing: vacancies, interstitial atoms, or substitutional atoms. At a coarser scale of resolution, spherical defects could also include voids, defined as holes in the material of volume much greater than the atomic volume, or inclusions, defined as embedded inhomogeneities of dimensions much greater than the atomic volume. These defects can induce an isotropic, i.e. spherical or purely volumetric, deformation in the crystal, as modeled in what follows, though in general the deformation resulting from point defects, voids, or inclusions of arbitrary shape will be anisotropic.

Finite deformation kinematics of crystalline solids with point defects was modeled by Teodosiu and Sidoroff (1976) and Kroner (1990), while large deformation kinematics of void growth in metallic crystals was ad-

---

^{9} Alternatively, one could prescribe a separate constitutive equation for skew lattice spin tensors $\dot{\mathbf{R}}^L \mathbf{R}^{LT}$ or $\mathbf{W}^L$ in order to specify a unique intermediate configuration, but this approach seems rarely used since $\mathbf{R}^L$ is usually presumed to include rigid body rotations of the entire solid.

dressed by Bammann and Aifantis (1989). Nunziato and Cowin (1979) formulated a geometrically nonlinear model of elastic solids with voids incorporating a multiplicative decomposition of the mass density. In solids of geologic origin such as many crystalline rocks, pore compaction (i.e., void shrinkage and collapse accompanying pressure loading) and dilatancy (i.e., inelastic volumetric expansion accompanying shear loading) are frequently observed (Brace et al. 1966; Rudnicki and Rice 1976; Goodman 1989). The pore compaction mechanism occurring in crushable brittle solids has been modeled with finite multiplicative kinematics (Clayton 2008).

Unlike lattice-preserving dislocation glide, the deformation induced by volumetric mechanisms generally does affect the lattice spacing in the (poly)crystal and hence is embedded in lattice deformation gradient $\mathbf{F}^L$:

$$\mathbf{F}^L = \mathbf{F}^E \mathbf{F}^V , \tag{3.128}$$

where $\mathbf{F}^E = \mathbf{V}^E \mathbf{R}^E$ is the elastic deformation associated with mechanical loading introduced in (3.27) and $\mathbf{F}^V(X,t)$ accounts for volume changes from the reference configuration that remain in an element of the solid after mechanical loads are removed. Stresses applied to the volume element are associated with the stretch $\mathbf{V}^E$, so that unloading by $\mathbf{V}^{E-1}$ maps the element to a new stress-free intermediate configuration $\bar{B}$. Proper orthogonal tensor $\mathbf{R}^E$ includes rigid body rotation of the entire body. Deformation $\mathbf{F}^V$ is not reversed when mechanical loads are removed from the volume element, e.g., when traction on the surface of the element is relaxed.

The contribution of defects to mechanically irreversible volume changes of the solid may be written as (Bammann and Aifantis 1989; Clayton et al. 2005; Clayton 2009b)

$$\mathbf{F}^V = \bar{\upsilon}\delta_{\beta}^{\alpha}\mathbf{g}_{\alpha} \otimes \mathbf{g}^{\beta} , \tag{3.129}$$

with the scalar $\bar{\upsilon}(X,t)$ given by

$$\bar{\upsilon} = (1-\bar{\phi})^{-1/3} , \tag{3.130}$$

where $\bar{\phi}(X,t)$ will be defined shortly. Requiring $0 < \bar{\upsilon} < \infty$ leads to the limits $-\infty < \bar{\phi} < 1$. Consider differential volume elements $d\tilde{V} \subset \tilde{B}$ and $d\bar{V} \subset \bar{B}$, where the generally anholonomic tangent map $\mathbf{F}^V : T\tilde{B} \to T\bar{B}$. The relationship between volume elements is

$$d\bar{V} = J^V d\tilde{V} = \sqrt{\frac{\det \bar{\mathbf{g}}}{\det \tilde{\mathbf{g}}}} \ \det \mathbf{F}^V d\tilde{V} = \frac{1}{1-\bar{\phi}} d\tilde{V} , \tag{3.131}$$

upon assuming coincident coordinate systems and equivalent metric tensors $\tilde{\mathbf{g}}$ and $\bar{\mathbf{g}}$ in $\tilde{B}$ and $\bar{B}$, respectively, as implied by $g^{\alpha}_{.\beta} = \delta^{\alpha}_{.\beta}$ in (3.129). Thus the scalar $\bar{\phi}$ is defined by

$$\bar{\phi} = \frac{d\bar{V} - d\tilde{V}}{d\bar{V}} . \tag{3.132}$$

When defects are introduced into a volume element of fixed mass within the body, $\bar{\phi}$ is interpreted as a fraction of defects in the intermediate configuration $\bar{B}$, per unit intermediate configuration volume:

$$\bar{\phi} \, d\bar{V} = d\bar{V} - d\tilde{V} = (\alpha \bar{\xi} \, d\bar{V} + d\tilde{V}) - d\tilde{V} = \alpha \bar{\xi} \, d\bar{V} , \tag{3.133}$$

where $\bar{\xi}(X,t)$ and $\alpha(X,t)$ are the number of defects per unit volume and the volume change induced by each defect, respectively, contained within $d\bar{V}$. When volume increases as a result of defects, for example from nucleation and growth of voids, then $\alpha > 0$. This condition is not required, however. For example, for an isotropic distribution of interstitial atoms, there could result a net decrease in volume due to $\mathbf{F}^{V}$, since the volume occupied per atom can decrease with increasing number density of interstitial atoms if the mass of the volume element is held fixed. Volume could also decrease if voids present in the reference configuration are compacted irreversibly as a result of applied pressure. In such cases $\alpha < 0$. Thus by (3.133), defects decrease the mass density of the solid when $\alpha > 0$, while defects increase the mass density when $\alpha < 0$.

A different interpretation of deformation induced by vacancies or interstitials is possible if the mass of the volume element is not required to remain constant when such defects are introduced (Kroner 1990; Clayton et al. 2005). In such instances, introduction of a vacancy by removal of an atom from the crystal structure will typically cause contraction of the remaining atoms towards the defect as a result of attractive interatomic forces among atoms surrounding the vacancy, and the introduction of an interstitial atom into an otherwise perfect crystal will typically engender expansion of the remaining atoms away from the defect as a result of repulsive interatomic forces between the interstitial atom and its neighbors.
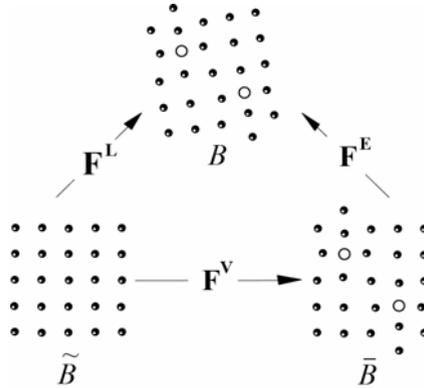
Fig. 3.10 Kinematics of crystal element of fixed mass containing vacancies

Models of discrete point defects based on continuum linear elasticity are described in Section C.3 of Appendix C. A general expression for the total volume change per vacancy defect, when modeled as a rigid sphere in an isotropic elastic medium, is

$$\alpha = \Omega_0 + (1+\Gamma)\Delta v, \text{ (vacancy)}, \qquad (3.134)$$

where $\Omega_0 > 0$ is the atomic volume introduced in Section 3.1.1, $\Delta v \leq 0$ is the relaxation volume introduced in (C.188) or (C.195), and $\Gamma(X,t)$ is a scalar correction factor, ordinarily satisfying $|\Gamma| < 1$, accounting for elastic nonlinearity (Eshelby 1954; Holder and Granato 1969) formally derived later in Section 7.4 of Chapter 7. Often for vacancies, $-0.1 \leq \Delta v/\Omega_0 \leq 0$ (Hull and Bacon 1984), though in materials with strong interatomic forces $\alpha < 0$ is possible, leading to a net increase in mass density (Garikipati et al. 2006). For insertion of an interstitial atom of the same species as the surrounding medium, (3.134) is replaced with

$$\alpha = -\Omega_0 + (1+\Gamma)\Delta v, \text{ (interstitial)}, \qquad (3.135)$$

where typically $0.1 \leq \Delta v/\Omega_0 \leq 1.0$ (Hull and Bacon 1984). Decomposition (3.128) is illustrated in Fig. 3.10 for a cubic crystal with vacancies. Dark circles represent atoms and open circles represent vacancies. Mass is conserved since the volume element in each configuration contains the same number of atoms. Atoms neighboring each vacancy exhibit attraction towards the defect, leading to negative relaxation $\Delta v < 0$ in (3.134). For a substitutional atom, the net volume change is simply $\alpha = (1+\Gamma)\Delta v$, with Δv positive in algebraic sign when the volume of the substitutional atom exceeds the atomic volume of the atom it replaces and negative when the

volume of the substitutional atom is less than that of the atom it replaces. Insertion of a substitutional atom almost always involves a mass change.

The preceding discussion applies primarily towards monatomic structures. In polyatomic crystals, distinct volumes are associated with defects (e.g., missing or extra atoms) of each species. In ionic crystals, defects often carry an electric charge that can significantly affect the imparted volume change (Mott and Littleton 1938; Sprackling 1976). For example, it is possible that a charged vacancy can induce local expansion ($\Delta v > 0$) as a result of repulsive Coulomb interactions among surrounding ions.

Vacancies can arise in several ways that involve multiple atoms (Mott and Gurney 1948). Consider a simple monatomic lattice. A Frenkel defect consists of an interstitial atom together with a vacant lattice site, with these two individual defects spaced far enough apart so that their interaction is negligible. A Schottky defect consists of a vacancy and corresponding missing atom placed at a normal lattice site on a free surface of the crystal. The total volume of a crystal with Schottky defects will be greater than that of a perfect crystal with the same number of atoms provided that contraction of neighboring atoms towards each vacancy is not too large.

From (3.129) and (3.130), the contribution to the time rate of deformation from inelastic volumetric deformation is also spherical:

$$\dot{\mathbf{F}}^{\mathbf{V}}\mathbf{F}^{\mathbf{V}-1} = \frac{\dot{\bar{\phi}}}{3(1-\bar{\phi})}\mathbf{1}, \quad \dot{F}^{V\,\alpha}_{.\,\chi}F^{V-1\chi}_{.\,\beta} = \frac{\dot{\bar{\phi}}}{3(1-\bar{\phi})}\delta^{\alpha}_{.\,\beta}. \tag{3.136}$$

Since $\mathbf{F}^{\mathbf{V}}$ is generally incompatible, conditions $\delta^{\alpha}_{[\beta}\bar{\phi}_{,\chi]} \neq 0$ may apply.

3.2.9 Residual Deformation and a Multiscale Description

As introduced in (3.26) and (3.31), lattice deformation $\mathbf{F}^{\mathbf{L}}$ accounts for all mechanisms that affect the primitive Bravais lattice vectors. When applied to an element of finite volume of a single crystalline or polycrystalline solid, deformation of the lattice may consist of contributions from multiple sources. Following Kratochvil (1972) and Clayton and McDowell (2003a), (3.31) may be expanded as a sequence of three terms:

$$\mathbf{F} = \mathbf{F}^{\mathbf{E}}\mathbf{F}^{\mathbf{I}}\mathbf{F}^{\mathbf{P}}, \quad \mathbf{F}^{\mathbf{L}} = \mathbf{F}^{\mathbf{E}}\mathbf{F}^{\mathbf{I}} = \mathbf{V}^{\mathbf{E}}\mathbf{R}^{\mathbf{E}}\mathbf{F}^{\mathbf{I}}, \tag{3.137}$$

where intermediate deformation map $\mathbf{F}^{\mathbf{I}}(X,t)$ accounts in some way for residual lattice deformation, distinct from the recoverable elastic stretch $\mathbf{V}^{\mathbf{E}}$ associated with mechanical loading, and also distinct from the average rigid body rotation of the element embedded within elastic rotation $\mathbf{R}^{\mathbf{E}}$. Mapping $\mathbf{F}^{\mathbf{I}}$ is attributed to deformation induced by defects or microscopic heterogeneities within the element of crystal distinct from lattice-

preserving plastic flow associated with $\mathbf{F}^\mathbf{P}$. These defects may include deformation twins, dislocation substructures and subgrain boundaries, and point defect or void distributions of the sort described already by (3.128) and (3.129). Thermal deformation can be distinguished from mechanical elastic deformation via a similar decomposition, as discussed in Section 3.1.3. Even a single dislocation, in isolation, will contribute to the local positions of atoms, as indicated in Fig. 3.11, which depicts the physics behind (3.137) in the context of a simple cubic lattice.
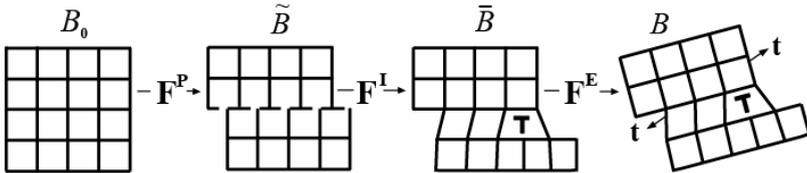
Fig. 3.11 Volume element of cubic crystal containing a single edge dislocation

In Fig. 3.11, traction applied to the volume in B is denoted by vector $\mathbf{t}(x,t)$, formally defined later in (4.2) of Chapter 4. The displacement discontinuity in the wake of the dislocation is sealed by residual lattice deformation $\mathbf{F}^\mathbf{I}$. Prior to the application of $\mathbf{F}^\mathbf{I}$, for the body labeled $\tilde{B}$, elastic strain fields are absent, and plastic deformation $\mathbf{F}^\mathbf{P}$ is associated with relative rigid motion of the two halves of the lattice on opposite sides of the slip plane (dotted line). Note also that $\tilde{B}$ is anholonomic in the vicinity of the slip plane: lattice vectors are discontinuous across this plane. The element in this configuration contains displacement (slip) discontinuities but no lattice strains, and is considered free of internal residual stress fields. This is in contrast to $\bar{B}$, which may contain residual stress and strain fields but includes no discontinuities in displacements or displacement gradients except for those in the immediate vicinity of the individual defect line (i.e., the dislocation core) contained within the volume.

Though not necessary, some authors make the additional assumption that $\mathbf{F}^\mathbf{E}$, but not $\mathbf{F}^\mathbf{L}$, be integrable at some scale of observation, or physically that its stretch be associated with external loads applied to solid body at that scale (Bilby and Smith 1956). Similar ideas have been forwarded in more recent strain gradient plasticity formulations (Bammann 2001; Regueiro et al. 2002). In that case, the contribution to the anholonomicity of $\mathbf{F}^{\mathbf{L}-1}(x,t)$ arises strictly from skew gradients of $\mathbf{F}^{\mathbf{I}-1}(x,t)$ (Clayton et al. 2004b):

$$2F^{L-1\alpha}_{[a,b]} = (F^{I-1\alpha}_{.\beta}F^{E-1\beta}_{.a})_{,b} - (F^{I-1\alpha}_{.\beta}F^{E-1\beta}_{.b})_{,a}$$
$$= 2F^{E-1\beta}_{.[a}F^{I-1\alpha}_{|\beta|,b]},$$

(3.138)

since $F^{E-1\beta}_{[a,b]} = 0$ are compatibility conditions for $\mathbf{F^{E-1}}$. Other authors have suggested that $\mathbf{F^I}$ be limited to a rotation $\mathbf{R^I} = \mathbf{R^{I-T}}$, for example accounting for irreversible rotations of Bravais lattice vectors attributed to disclination defects (Lardner 1973, 1974; Pecherski 1983, 1985), as discussed in greater depth in Section 3.3.3.

An explicit expression for $\mathbf{F^I}$ can be derived in terms of volume averages—over an element of crystalline material of finite size—of microscopic residual lattice and plastic deformations, following multiscale analysis (Clayton and McDowell 2003a; Clayton et al. 2004b). In such a multiscale interpretation of (3.137), continuous elastic and plastic deformation mappings describe the motion of the material at two length scales: a larger scale corresponding to the average or coarse-grained behavior of the volume element, and a smaller scale corresponding to sub-volumes within this larger volume element.

Continuum elements serving as domains for volume integration are shown in Fig. 3.12. Symbols V, $\bar{V}$, and v describe respective crystalline volume elements in reference, unloaded intermediate, and current configurations. The lineal size of V is denoted by ℓ, the latter presumed to far exceed the lattice parameters. However, the upper bound of ℓ is left unspecified, such that V may encompass a region within a single crystal or numerous grains within a polycrystal. Corresponding reference, intermediate, and current configurations of the element are labeled B_0, $\bar{B}$, and B, respectively. All of these configurations are described in more detail later in the text. Local, scalar differential volume elements within reference, intermediate, and current configurations are labeled dV, $d\bar{V}$, and dv, respectively. These so-called differential elements are required to be smaller than their associated volume elements and should consist of no more than one grain of a polycrystalline aggregate, but should still be of dimensions larger than the atomic spacing in a perfect crystal.
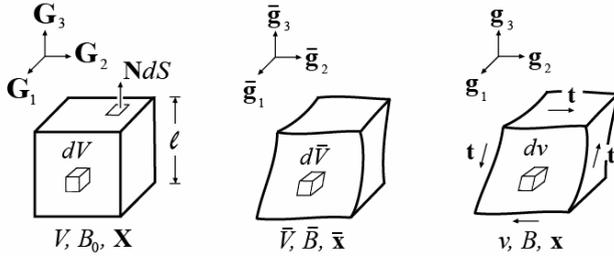
Fig. 3.12 Configurations, local volumes, and coordinate systems in reference configuration B_0, intermediate configuration $\bar{B}$, and current configuration B

The motion of material points within element V from reference to current configurations is written $x^a = \varphi^a(X,t)$, where $\varphi : B_0 \to B$ is continuously differentiable within V. Local intermediate configuration coordinates $\bar{x}^\alpha = \bar{x}^\alpha(X,t)$ are also assumed to be continuously differentiable within $\bar{V}$. Additional remarks on availability of continuously differentiable coordinates $\bar{x}^\alpha$ follow later. In what follows, basis vectors, basis covectors, and metric tensors are restricted to be constant, but not necessarily Cartesian, within each element in each configuration, such that covariant and partial differentiation are equivalent operations. However, these objects are permitted to vary smoothly across neighboring macroscopic volume elements V, $\bar{V}$, and v if curvilinear coordinates are useful at the macroscale, and also from configuration to configuration.

Configurations shown in Fig. 3.12 are now defined precisely. The referential volume V consists of the crystal structure as it existed prior to application of external forces, i.e., at initial time $t = 0$, such that it is free of traction along its external boundary S. It may or may not contain dislocations, internal residual elastic strains, or residual plastic deformation. The current configuration volume element, v, is the elastically and plastically deformed single crystal or polycrystal, supporting possibly non-vanishing traction vector $\mathbf{t}$ on its external boundary s. The local or nested microscopic deformation gradient $\mathbf{f}$ for material points with coordinates X^A within volume element V is defined as the tangent mapping

$$\mathbf{f} = T\varphi_X = \frac{\partial \varphi^a}{\partial X^A} \mathbf{g}_a \otimes \mathbf{G}^A . \tag{3.139}$$

The volume averaged deformation gradient $\mathbf{F}$ for the macroscopic element of volume V is then defined by the motion of its external boundary,

equivalent to the volume averaged local deformation gradient upon use of Gauss's theorem as in (2.194)-(2.196), with a slight change in notation:

$$F^a_{.A} = V^{-1}\int_S x^a N_A dS = V^{-1}\int_V x^a_{.,A} dV = V^{-1}\int_V f^a_{.A} dV . \qquad (3.140)$$

In (3.140), $N_A dS$ is an oriented differential surface element of S, with $\mathbf{N}$ an outward unit covector normal to the surface, as shown in Fig. 3.12.

An elastic stretch tensor $\mathbf{V^E}$ is associated with the traction or stress applied to s. A new intermediate configuration $\hat{B}$ is reached upon hypothetical instantaneous unloading via the inverse of the elastic stretch $\mathbf{V^{E-1}}$, corresponding to null traction conditions on the external boundary of the element $\hat{V}$ (i.e., the traction $\hat{\mathbf{t}} = 0$ along $\hat{s}$), as shown in Fig. 3.13. The left elastic stretch tensor $\mathbf{V^E}$ is determined explicitly from

$$\mathbf{V^E} = \left(\int_S \mathbf{x} \otimes \mathbf{N} dS\right)\left(\int_S \hat{\mathbf{x}} \otimes \mathbf{N} dS\right)^{-1} , \qquad (3.141)$$

where $\hat{\mathbf{x}}$ are local coordinates of the external boundary of the element in configuration $\hat{B}$. Thus, configuration $\hat{B}$ arises from instantaneous removal of traction along the boundary of $\hat{V}$, constrained in such a way that global rotation of the volume element, $\mathbf{R^{E-1}}$, does not occur upon stress relaxation. Furthermore, during unloading by $\mathbf{V^{E-1}}$, plastic rearrangements of the solid are idealized as rate independent and inertial effects are excluded.

Elastic rotation tensor $\mathbf{R^E}$ is determined from solution of the following integro-differential equation arising purely from local lattice rotations along with the following initial conditions:

$$\dot{\mathbf{R}}^{\mathbf{E}}\mathbf{R^{E-1}} = V^{-1}\int_V \dot{\mathbf{r}}^{\mathbf{E}}\mathbf{r^{E-1}} dV , \quad \mathbf{R^E}\big|_{t=0} = \mathbf{r^E}\big|_{t=0} = \mathbf{1} . \qquad (3.142)$$

Denoted by $\mathbf{r^E}$ is the local elastic and rigid body rotation exhibited by microscopic element of volume dV as it is deformed to its current representation dv. Note that $\mathbf{R}^{\mathbf{E}T} = \mathbf{R^{E-1}}$ and $\mathbf{r}^{\mathbf{E}T} = \mathbf{r^{E-1}}$, since the anti-symmetric property of the spin is preserved by volume averaging.
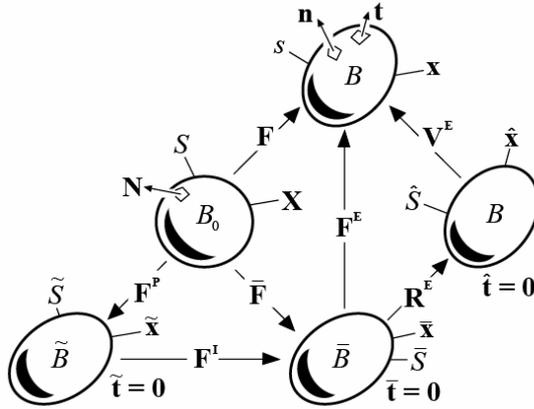
Fig. 3.13 Configurations of macroscopic material element in context of multiscale three-term decomposition of macroscopic deformation gradient

Intermediate configuration $\hat{B}$ is achieved by the net unloading procedure $\mathbf{F}^{E-1} = \mathbf{R}^{ET}\mathbf{V}^{E-1}$, i.e., unloading of the macroscopic element in the current configuration by removal of external forces then and subsequent rotation by the inverse (equivalently, the transpose) of the elastic rotation. After this unloading procedure, local coordinates $\bar{x}^{\alpha}$ describe positions of material particles within volume element $\bar{V}$. The microscopic residual deformation gradient $\bar{\mathbf{f}}$ is the tangent mapping

$$\bar{\mathbf{f}} = T\bar{\varphi}_X = \frac{\partial \bar{\varphi}^{\alpha}}{\partial X^A}\bar{\mathbf{g}}_{\alpha} \otimes \mathbf{G}^A , \tag{3.143}$$

with $\bar{x}^{\alpha} = \bar{\varphi}^{\alpha}(X,t): B_0 \rightarrow \bar{B}$ the local motion for differential volume elements between reference and intermediate configurations. The volume averaged residual deformation $\bar{\mathbf{F}}$ for the macroscopic crystal element is deduced from intermediate configuration coordinates of its external boundary. This definition of $\bar{\mathbf{F}}$ is equivalent to the volume-averaged residual local deformation gradient upon invocation of Gauss's theorem, analogously to (3.140):

$$\bar{F}^{\alpha}_{.A} = V^{-1}\int_S \bar{x}^{\alpha} N_A dS = V^{-1}\int_V \bar{x}^{\alpha}_{,A}dV = V^{-1}\int_V \bar{f}^{\alpha}_{.A}dV . \tag{3.144}$$

Two additional assumptions, following kinematics of single crystalline elastoplasticity in Section 3.2.6, are made on a pointwise basis, for each differential volume element (Bilby et al. 1957):

$$\mathbf{f} = \mathbf{f}^E\mathbf{f}^P , \quad \bar{\mathbf{f}} = \bar{\mathbf{f}}^E\bar{\mathbf{f}}^P . \tag{3.145}$$

Denoted by $\mathbf{f}^{\mathbf{E}} = \mathbf{v}^{\mathbf{E}}\mathbf{r}^{\mathbf{E}}$ is the total lattice stretch ($\mathbf{v}^{\mathbf{E}}$) and rotation ($\mathbf{r}^{\mathbf{E}}$) for a differential volume element deformed to the current configuration, and $\mathbf{f}^{\mathbf{P}}$ is the remaining plastic deformation attributed to the history of motion of dislocations within or traversing that local element. Local elastic rotation $\mathbf{r}^{\mathbf{E}}$ was first introduced in (3.142). In the second equality listed in (3.145), $\overline{\mathbf{f}}^{\mathbf{E}}$ embodies residual elastic stretch and rotation for a sub-volume $d\overline{V}$ contained within externally unloaded volume $\overline{V}$, and $\overline{\mathbf{f}}^{\mathbf{P}}$ is the residual plastic deformation arising from dislocation motion. Microscopic volumes $dV \subset V$, $d\overline{V} \subset \overline{V}$, and $dv \subset v$ are shown in Fig. 3.14, each visually enlarged relative to its surrounding macroscopic volume element for clarity. Local deformations of (3.145) then are interpreted as mappings between tangent spaces of local configurations associated with each microscopic element. Of the six tangent mappings entering (3.145), only $\mathbf{f}$ and $\overline{\mathbf{f}}$ are necessarily compatible deformation gradient fields, as is clear from the integrands in (3.140) and (3.144). Furthermore, these six mappings are each regarded as constant (e.g., spatial averages) over their corresponding microscopic or differential volumes. Volumes whose boundary coordinates are generally anholonomic are denoted by dashed curves in Fig. 3.14, while holonomic coordinates are presumed available over external boundaries of elements depicted by solid curves in Fig. 3.14.

Macroscopic plastic deformation $\mathbf{F}^{\mathbf{P}}$ emerges in the present multiscale context from the following integro-differential equation written in terms of the volume averaged local plastic velocity gradient (Clayton et al. 2004b):

$$\dot{\mathbf{F}}^{\mathbf{P}}\mathbf{F}^{\mathbf{P}-1} = V^{-1}\int_V \dot{\mathbf{f}}^{\mathbf{P}}\mathbf{f}^{\mathbf{P}-1}dV \;, \quad \mathbf{F}^{\mathbf{P}}\big|_{t=0} = \mathbf{f}^{\mathbf{P}}\big|_{t=0} = \mathbf{1}\,. \tag{3.146}$$

Initial conditions in (3.146) presume that plastic deformation vanishes at the initial time. Notice that if the local plastic flow is isochoric such that $\dot{f}^{P\alpha}_{.A}f^{P-1A}_{.\alpha} = 0$, then the volume averaged plastic flow of (3.146) is volume-conserving as well, since $\dot{J}^P = J^P\dot{F}^{P\alpha}_{.A}F^{P-1A}_{.\alpha} = 0$ then follows automatically from (3.146). In an earlier work (Clayton and McDowell 2003a), alternative definition $\mathbf{F}^{\mathbf{P}} = V^{-1}\int \overline{\mathbf{f}}^{\mathbf{P}}dV$ was suggested; however, according to that definition, $\mathbf{F}^{\mathbf{P}}$ is isochoric only to first order in terms of local plastic distortions if $\overline{\mathbf{f}}^{\mathbf{P}}$ is isochoric but heterogeneous because volume averaging and the determinant operation do not generally commute.
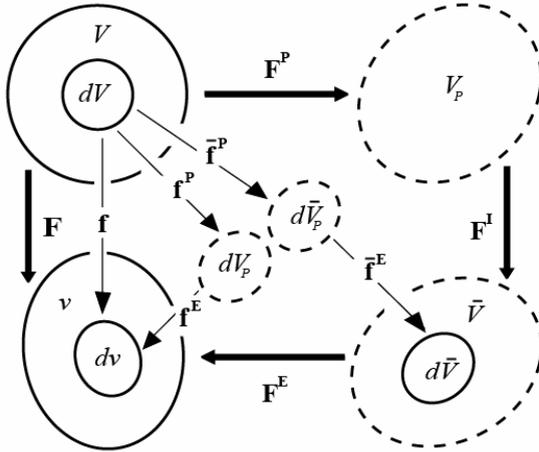
Fig. 3.14 Volumes, tangent maps, and configurations at two length scales

Upon assuming a three-term multiplicative decomposition along the lines of (3.137) for total macroscopic deformation gradient $\mathbf{F}$:

$$\mathbf{F} = \mathbf{F}^{\mathbf{E}}\mathbf{F}^{\mathbf{I}}\mathbf{F}^{\mathbf{P}} = \mathbf{F}^{\mathbf{E}}\overline{\mathbf{F}} , \qquad (3.147)$$

net residual deformation gradient $\overline{\mathbf{F}}$ enters the decomposition in accordance with (3.140), (3.141), and (3.144). Combining (3.144), (3.145), and (3.147) then leads to a representation of $\mathbf{F}^{\mathbf{I}}$ (Clayton and McDowell 2003a; Clayton et al. 2004b):

$$\mathbf{F}^{\mathbf{I}} = \overline{\mathbf{F}}\mathbf{F}^{\mathbf{P}-1} = V^{-1}\left(\int_V \overline{\mathbf{f}}^{\mathbf{E}}\overline{\mathbf{f}}^{\mathbf{P}} dV\right)\mathbf{F}^{\mathbf{P}-1} . \qquad (3.148)$$

Deformation map $\mathbf{F}^{\mathbf{I}}$ can be interpreted as an indicator of residual elasticity in configuration $\overline{B}$, along with corresponding residual stresses and stored elastic strain energy in the solid (Clayton et al. 2004b). Two-point deformation tensor $\mathbf{F}^{\mathbf{I}}$ defined according to (3.148) contains both residual elastic ($\overline{\mathbf{f}}^{\mathbf{E}}$) and plastic ($\overline{\mathbf{f}}^{\mathbf{P}}$, $\mathbf{F}^{\mathbf{P}-1}$) contributions.

It is clear from (3.148) that $\mathbf{F}^{\mathbf{I}} \rightarrow \mathbf{1}$ as $\overline{\mathbf{f}}^{\mathbf{E}} \rightarrow \mathbf{1}$ and $\overline{\mathbf{f}}^{\mathbf{P}} \rightarrow \mathbf{F}^{\mathbf{P}}$, as would be the case for homogeneous deformation of the entire macroscopic (poly)crystalline element, such that external unloading by $\mathbf{V}^{\mathbf{E}-1}$ relieves all local internal stresses and plastic rearrangements do not occur upon instantaneous unloading. On the other hand, if elastic and plastic deformation fields are heterogeneous throughout the macroscopic volume element, $\mathbf{F}^{\mathbf{I}}$ and commensurate residual stresses may not vanish. This is the usual circumstance when V encompasses a polycrystalline sample whose grains are

misoriented by a non-negligible amount (Clayton and McDowell 2003a). Such heterogeneity may arise within single crystals when cellular or laminar dislocation substructures misoriented from one other by finite lattice rotations, embodied here by the orthogonal part $\overline{\mathbf{r}}^{\mathbf{E}}$ of $\overline{\mathbf{f}}^{\mathbf{E}}$, evolve and refine for example in FCC metals (Hughes et al. 1997; Kuhlmann-Wilsdorf 1999; Ortiz and Repetto 1999; Ortiz et al. 2000) and BCC metals (Valiev et al. 2002) deformed to very large strains. Thus, when volume element V encompasses an entire single crystal, $\mathbf{F}^{\mathbf{I}}$ can represent the contribution of grain subdivision processes to the total deformation gradient $\mathbf{F}$, as proposed by Butler and McDowell (1998). Additionally, if heterogeneity of local deformation and stresses (e.g., increased slip system activity and stress concentrations) are intensified in the vicinity of misoriented grain and subgrain boundaries—see for example experimental and numerical results for polycrystalline copper subjected to finite strains (Clayton et al. 2002; Clayton and McDowell 2003a)—then the largest contributions to $\mathbf{F}^{\mathbf{I}}$ would presumably emerge from these regions.

Deformation tensor $\mathbf{F}^{\mathbf{I}}$ represents, in an average sense, the incompatibility of local microelastic deformation $\mathbf{f}^{\mathbf{E}-1}$ within an element of reference volume V. If local elastic unloading $\mathbf{f}^{\mathbf{E}-1}$ is uniform and hence integrable throughout spatial volume v, then $\mathbf{f}^{\mathbf{E}} = \mathbf{F}^{\mathbf{E}}$, $\overline{\mathbf{f}}^{\mathbf{E}} = \mathbf{1}$, and if plasticity is locally homogeneous so that $\overline{\mathbf{F}} = \overline{\mathbf{f}} = \overline{\mathbf{f}}^{\mathbf{P}} = \mathbf{f}^{\mathbf{P}} = \mathbf{F}^{\mathbf{P}}$, then $\mathbf{F}^{\mathbf{I}} = \mathbf{1}$ (refer to Fig. 3.14). However, $\mathbf{F}^{\mathbf{I}}$ reveals nothing about the compatibility, or lack thereof, of the average recoverable elastic deformation $\mathbf{F}^{\mathbf{E}-1}(x,t)$ from macroscopic volume element to neighboring macroscopic volume element. If each macroscopic volume element V is regarded as an entire single crystal, then the incompatibility of $\mathbf{F}^{\mathbf{E}-1}$ measures intergranular incompatibility among neighboring grains, while if each V is regarded as a subgrain, then incompatibility of $\mathbf{F}^{\mathbf{E}-1}$ is an intragranular measure. Here incompatibility of $\mathbf{F}^{\mathbf{E}-1}$ refers to a lack of continuous, single valued coordinates $\overline{x}^{\alpha}(x,t)$ spanning the union of i intermediate configuration volume elements $\cup \overline{V}^{(i)}$. Thus, while the $\overline{x}^{\alpha}$ are assumed to be available and differentiable within each volume element $\overline{V}^{(i)}$, they may not be so over global configuration $\overline{B}$. If in fact $\overline{x}^{\alpha}$ are multi-valued or discontinuous over this global configuration, they are anholonomic in the sense of Section 2.8.1.

An alternative definition of residual lattice deformation tensor $\mathbf{F}^{\mathbf{I}}$ is derived in Chapter 7. In the approach of Chapter 7, $\mathbf{F}^{\mathbf{I}}$ is defined in covariant Cartesian indices as the sum of the unit tensor and the average taken

over a reference volume element of material displacement gradients associated with residual stress fields of defects. Self-equilibrium conditions provide analytical expressions for the symmetric part of $\mathbf{F}^{I}$ in the context of continuum nonlinear elasticity or anharmonic lattice statics. The nonlinear elastic approach of Chapter 7 builds on previous work of a number of authors (Zener 1942; Seeger and Haasen 1958; Toupin and Rivlin 1960). A detailed discussion of the approach is deferred until later (Chapter 7) because the derivation requires elements of thermomechanics and nonlinear elasticity developed in Chapters 4 and 5, respectively. This is in contrast to the derivation of $\mathbf{F}^{I}$ in (3.148) that is purely kinematical.

3.2.10 Multiplicative Atomistic Plasticity

An alternative perspective of finite crystal kinematics is achieved upon consideration of motions of individual atoms (Clayton and Chung 2006; Chung and Clayton 2007). Assume that in reference configuration B_0, the representative Lagrangian volume element under consideration consists of a majority of atoms arranged on a lattice, but perhaps imperfectly due to the presence of defects within that volume element. Furthermore, assume that in configuration $\tilde{B}$ of Fig. 3.4, the same mass and number of atoms exist in this representative volume, for example after propagation of dislocations across the volume. Atomic coordinates in B_0 and $\tilde{B}$ may not coincide, even though the crystal structure may look the same to an external observer in each of these two configurations because of the lattice-preserving nature of dislocation glide. For simplicity, considered in the present Section are monatomic crystal structures for which basis vectors of the crystal structure vanish. Generalization of the present approach to polyatomic lattices is straightforward but requires introduction of additional mathematical machinery and notation. Furthermore, the treatment of Section 3.2.10 is restricted to coincident Cartesian coordinates in all configurations. Generalization to curvilinear coordinates is possible but requires additional cumbersome notation, e.g., shifter tensors.

The position vector for arbitrary atom i in evolving intermediate configuration $\tilde{B}$ is denoted by $\tilde{\mathbf{r}}_{\langle i \rangle}$, where angled brackets are reserved for atomic labels, and $i = 1, 2, ... n$, with n the total number of atoms contained within the volume element. Spatial positions of atoms (e.g., nuclear coordinates) in current configuration B, written as $\mathbf{r}_{\langle i \rangle}$, are then found as

$$r_{\langle i \rangle}^{a} = \delta_{.\alpha}^{a} \tilde{R}_{\langle i \rangle}^{\alpha} + q_{\langle i \rangle}^{a}, \tag{3.149}$$

with $\mathbf{q}_{\langle i \rangle}$ the Cartesian displacement vector between intermediate and current locations of atom i. Vectors separating atoms i and j in respective configurations $\tilde{B}$ and B are denoted by

$$\tilde{\mathbf{R}}_{\langle i \backslash j \rangle} = \tilde{\mathbf{R}}_{\langle j \rangle} - \tilde{\mathbf{R}}_{\langle i \rangle}, \quad \mathbf{r}_{\langle i \backslash j \rangle} = \mathbf{r}_{\langle j \rangle} - \mathbf{r}_{\langle i \rangle}. \tag{3.150}$$

Let the spatial position of atom i be updated according to

$$r^a_{\langle i \rangle} = \sum_{j=1}^{n} \overline{F}^{L\,a}_{\langle ij \rangle \alpha} \tilde{R}^\alpha_{\langle j \rangle} + \Delta r^a_{\langle i \rangle}. \tag{3.151}$$

The first term on the right side of (3.151) accounts for the projection, over the volume element of atoms, of the macroscopic lattice deformation field to each atom within.

Assuming that the Cauchy-Born approximation of (3.26) applies only for the first term on the right side of (3.151), operator $\overline{F}^{L\,a}_{\langle ij \rangle \alpha}$ can be decomposed multiplicatively into the product of a continuum tangent map $F^{L\,a}_{.\alpha}(X,t)$ akin to that in (3.31) and a discrete Kronecker delta operator $\delta_{\langle ij \rangle}$, with the latter satisfying $\delta_{\langle ij \rangle} = 1$ for $i = j$ and $\delta_{\langle ij \rangle} = 0$ otherwise:

$$\overline{F}^{L\,a}_{\langle ij \rangle \alpha} = F^{L\,a}_{.\alpha} \delta_{\langle ij \rangle}. \tag{3.152}$$

The second term on the right side of (3.151), $\Delta \mathbf{r}_{\langle i \rangle}$, is the atomic scale perturbation in displacement attributed to microscopic heterogeneity in the vicinity of lattice defects, written here for atom i. This perturbation measures discrepancies in local atomic coordinates from those that would be predicted under homogeneous deformation of a monatomic crystal structure under the Cauchy-Born hypothesis such as given in (3.109) for the primitive Bravais lattice vectors. From (3.151) and (3.152), spatial separation vectors introduced in (3.150) are updated according to

$$\mathbf{r}_{\langle i \backslash j \rangle} = \overline{\mathbf{F}}^{\mathbf{L}} \tilde{\mathbf{R}}_{\langle i \backslash j \rangle} + \Delta \mathbf{r}_{\langle j \rangle} - \Delta \mathbf{r}_{\langle i \rangle}. \tag{3.153}$$

The perturbation in atomic displacement from an atom's position in the intermediate configuration $\tilde{B}$ is measured by $\Delta \mathbf{r}_{\langle i \rangle}$. However, if $\mathbf{F}^{\mathbf{P}}$, the plastic deformation gradient of (3.31), is assumed to leave the geometry of the lattice unaltered as illustrated in the periodic domain of Fig. 3.5, then displacement perturbation $\Delta \mathbf{r}_{\langle i \rangle}$ may be considered equivalent, from the standpoint of mechanical properties of the crystal, to a displacement perturbation measured from reference configuration B_0. The perturbation in this case would correspond to that of a different atom that may have entered a corresponding Eulerian control volume (dotted boundary in Fig. 3.5) during the course of plastic slip. Immobile defects such as pinned dis-

locations, grain or subgrain boundaries, and fixed point defects may also be present in configurations B_0 and $\tilde{B}$; such defects are represented mathematically by perturbed atomic coordinates in the reference configuration.

The description afforded by (3.149)-(3.153) has been used to study effects of point, line, and surface defects upon stored energy and tangent elastic stiffness of the lattice in BCC crystals in the context of single slip (Clayton and Chung 2006) and to facilitate comparisons between predictions of molecular statics calculations (see Section B.2 of Appendix B) and continuum theories of lattice defects (Chung and Clayton 2007). The atomistic description follows from earlier work (Chung and Namburu 2003; Chung 2004) that considered perturbations in atomic displacements from their predicted positions under the Cauchy-Born approximation in elastic solids—for example perturbations attributed to point defects—without recourse to introduction of an evolving intermediate configuration $\tilde{B}$ needed to describe dislocation-based plasticity at finite deformations.

3.3 A Linear Connection for Lattice Defects

The two-term multiplicative decomposition of the deformation gradient of (3.31), $\mathbf{F} = \mathbf{F}^{\mathbf{L}}\mathbf{F}^{\mathbf{P}}$, was proposed by Bilby et al. (1957) and Kroner (1960) for modeling the deformation of single crystals within the framework of continuously distributed dislocations. Here in Section 3.3, the description afforded by (3.31) is enhanced via consideration of a special class of linear connection (Section 2.2) describing physics of crystalline solids at a length scale more refined than that associated with (3.31). Such connections enable description of higher-order gradients of stretch and rotation in the lattice, or equivalently, enable more accurate approximation of atomic positions at microscopic spatial locations between two representative volume elements of crystal, each of whose average set of deformed, primitive Bravais lattice vectors is encapsulated by the nine degrees of freedom corresponding to a particular value of $\mathbf{F}^{\mathbf{L}}(X,t)$ according to (3.109)-(3.114).

Discovery of the relationship between the density of continuously distributed dislocations and Cartan's torsion tensor of the crystal connection is usually credited to Kondo (1953, 1963), Bilby et al. (1955), and Kroner (1960). The crystal connection is defined in terms of a spatial gradient of the lattice deformation. Specifically, $\bar{\Gamma}_{cb}^{\,.a} = F^{La}_{\,.\alpha}F^{L-1\alpha}_{\,.b,c} = -F^{La}_{\,.\alpha,c}F^{L-1\alpha}_{\,.b}$ are coefficients of the crystal connection, integrable according to (2.218) as will be later demonstrated explicitly. The non-Riemannian geometric

space associated with the crystal connection is said to possess a distant parallelism or a teleparallelism (Einstein 1928; Schouten 1954), and exhibits the special property that covariant derivatives of vectors taken with respect to this connection vanish if these vectors comprise a spatially constant vector field when pulled back to the intermediate configuration. The null curvature property of the crystal connection, together with knowledge of its torsion and a certain covariant plastic or elastic strain tensor is sufficient to uniquely specify the relaxed intermediate configuration (Le and Stumpf 1996a). Berdichevski and Sedov (1967), Noll (1967), Teodosiu (1967a), De Wit (1968), Toupin (1968), and Steinmann (1996) provided detailed viewpoints of dislocation kinematics using linear connections and geometric ideas.

Since dislocations associated with the crystal connection are required to sustain compatibility of the total deformation, they are often labeled geometrically necessary dislocations in the sense of Ashby (1970). This is in contrast to absolute dislocations (Lardner 1969; Werne and Kelly 1978) that, when mobile, enable a nonzero dislocation flux and hence a nonzero rate of plastic deformation in (3.105). Nye (1953) associated a dislocation density tensor with the gradient of lattice rotation, i.e., the stress-free lattice curvature. Lardner (1969) showed that vanishing of the torsion tensor of the crystal connection corresponds to vanishing of excess dislocations of the same sign. Grain boundary, surface, and interface dislocations have been investigated from the standpoint of differential geometry and/or compatibility conditions (Bullough and Bilby 1956; Marcinkowski and Sadananda 1975; Hartley and Blachon 1978; Cermelli and Gurtin 1994; Dluzewski 1996; Gupta et al. 2007). Experimental techniques for measuring lattice curvature, redundant defect populations associated with geometrically necessary dislocations, and statistically stored dislocations have emerged and advanced in recent years (El-Dasher et al. 2003; Hughes et al. 2003; Taheri et al. 2006)

Kondo (1949, 1953, 1963, 1964) proposed general frameworks for yielding and plastic deformation allowing nonzero Riemann-Christoffel curvature associated with a connection different from the crystal connection. Kondo's frameworks admit different non-unique anholonomic (i.e., incompatible) intermediate configurations, or "tearings" in his terminology, for the same crystal. These configurations differ from the unique intermediate configuration favored by Bilby et al. (1955), for which the curvature tensor of the associated crystal connection vanishes and teleparallelism is enforced. Kondo (1964) associated nonzero curvature with the presence of rotational anomalies in the lattice, which can be interpreted as disclinations (Nabarro 1967; De Wit 1971, 1973). Connections admitting non-vanishing curvature tensors have since been used by many

for modeling disclinations in Bravais lattices (Anthony 1970; Lardner 1973, 1974; Minagawa 1979, 1981; Amari 1981; De Wit 1981). Rotational defects falling under the general category of Somigliana dislocations (Eshelby 1951, 1956; Asaro 1976; Teodosiu 1981) were addressed in terms of a path-dependent integral of a non-vanishing curvature tensor by Pecherski (1983; 1985). Non-metric connections admitting extra-matter defects (e.g., interstitial atoms, vacancies, or other point defects) were introduced in continuum theories by Kroner (1960, 1980, 1983), Minagawa (1979), and De Wit (1981). A brief early history of generalized continuum theories—for example theories with kinematic descriptions addressing orientations in addition to positions of material particles—was given by Eringen (1968).

The remainder of Section 3.3 is organized as follows. First, a general linear connection is introduced in Section 3.3.1, capable of describing a variety of defects in the crystal in its deformed configuration. Particular forms of this connection, corresponding to various classes of admitted defects, are then examined in detail. The crystal connection and geometrically necessary dislocations are described in Section 3.3.2. The representation of distributions of disclinations in terms of a linear connection is developed in Section 3.3.3. Isotropic defects are considered in a differential-geometric context in Section 3.3.4. Finally, the geometric description of kinematics of crystals with defects is summarized in Section 3.3.5. The remaining content of Section 3.3 parallels, refines, and substantially extends earlier work for modeling lattice defects (Clayton et al. 2005, 2006, 2008a).

3.3.1 General Form and Properties of the Connection

Consider a volume element of a crystalline solid whose average deformation gradient $\mathbf{F}$ follows decomposition $\mathbf{F} = \mathbf{F}^L \mathbf{F}^P$ of (3.31). As was the case in Section 3.2, this volume element is required to be of lineal dimensions much larger than the lattice parameters of the unit cell of the crystal structure, so that many dislocations or other defects may be contained within it. However, in Section 3.3, the volume element is restricted to either be embedded within a single crystal, or to consist of an entire single crystal. This restriction implies that when defects are absent, the orientation of each of the primitive Bravais lattice vectors in (3.1) does not vary with position within the element in its undistorted reference configuration. Recall from Section 3.2.2 that intermediate configuration $\tilde{B}$ is generally anholonomic, with associated anholonomic coordinates $\tilde{x}^\alpha$, while refer-

ence and spatial configurations B_0 and B are holonomic, spanned by continuously differentiable coordinates $X^A(x,t)$ and $x^a(X,t)$, respectively. Note that (3.137) also applies here in general, though in Section 3.3 no decomposition of the total lattice deformation into recoverable and residual parts is necessary.

Introduced next are continuously differentiable vector fields of director triads (Fox 1966) referred to tangent spaces of each configuration:

$$\mathbf{d}_A \in TB_0, \ \mathbf{d}_\alpha \in T\tilde{B}, \ \mathbf{d}_a(x,t) \in TB, \ (A,\alpha,a=1,2,3). \qquad (3.154)$$

Vectors of each triad in (3.154) are all dimensionless. From the last of (3.154), within a single crystal only the deformed directors referred to the spatial configuration are assumed to vary with position and time. Directors are mapped across configurations via the relations

$$\mathbf{d}_\alpha = \delta_{.\alpha}^A \mathbf{d}_A, \ \mathbf{d}_a = F^{L-1\,\alpha}_{\quad .a}(x,t)\mathbf{d}_\alpha = F^{L-1\,\alpha}_{\quad .a}\delta_{.\alpha}^A \mathbf{d}_A, \qquad (3.155)$$

with summation implied over repeated indices. Plastic deformation $\mathbf{F}^{\mathbf{P}}$ is assumed lattice-preserving as discussed in Section 3.2.1 such that the directors are physically the same in reference and intermediate configurations, as is clear from the first of (3.155). According to the second of (3.155), each director vector $\mathbf{d}_\alpha$ is pushed forward to the current configuration by the lattice deformation as the individual component of a covariant vector, analogously to (2.133). Reciprocal directors to (3.154) are introduced, satisfying

$$\mathbf{d}^A \in T^*B_0, \ \mathbf{d}^\alpha \in T^*\tilde{B}, \ \mathbf{d}^a(x,t) \in T^*B, \ (A,\alpha,a=1,2,3); \qquad (3.156)$$

$$\left\langle \mathbf{d}^A, \mathbf{d}_B \right\rangle = \delta_{.B}^A, \ \left\langle \mathbf{d}^\alpha, \mathbf{d}_\beta \right\rangle = \delta_{.\beta}^\alpha, \ \left\langle \mathbf{d}^a, \mathbf{d}_b \right\rangle = \delta_{.b}^a. \qquad (3.157)$$

It follows that transformation formulae for the reciprocal directors are

$$\mathbf{d}^\alpha = \delta_{.A}^\alpha \mathbf{d}^A, \ \mathbf{d}^a = F^{La}_{\ .\alpha}(x,t)\mathbf{d}^\alpha = F^{La}_{\ .\alpha}\delta_{.A}^\alpha \mathbf{d}^A. \qquad (3.158)$$

Thus, each reciprocal director is pushed forward by the lattice deformation like the component of a contravariant vector analogously to (2.131). By analogy with basis vectors of coordinate systems in (2.2) and (2.3), director vectors with indices in lower positions (3.154) are referred to as covariant director vectors or covariant lattice directors, while those with indices in upper positions (3.158) are referred to as contravariant director vectors or contravariant lattice directors.

It is assumed that director vectors in configuration $\tilde{B}$ are of unit length and are orthogonal:

$$\mathbf{d}_\alpha \bullet \mathbf{d}_\beta = d_\alpha^\chi \tilde{g}_{\chi\delta} d_\beta^\delta = \delta_{\alpha\beta}, \qquad (3.159)$$

with $\delta_{\alpha\beta}$ emerging as a natural Euclidean metric on $\tilde{B}$. A generally non-Euclidean metric $\mathbf{C}^{\mathbf{L}}(x,t)$ with components referred to spatial configura-

tion B and associated with the director strain is obtained from (3.155) and (3.156) as

$$C_{ab}^{L} = \mathbf{d}_a \bullet \mathbf{d}_b = F^{L-1\alpha}_{.a} \mathbf{d}_\alpha \bullet \mathbf{d}_\beta F^{L-1\beta}_{.b} = F^{L-1\alpha}_{.a} \delta_{\alpha\beta} F^{L-1\beta}_{.b}. \qquad (3.160)$$

The contravariant version of (3.160) provides the inverse metric:

$$C^{L-1ab} = \mathbf{d}^a \bullet \mathbf{d}^b = F^{La}_{.\alpha} \mathbf{d}^\alpha \bullet \mathbf{d}^\beta F^{Lb}_{.\beta} = F^{La}_{.\alpha} \delta^{\alpha\beta} F^{Lb}_{.\beta}, \qquad (3.161)$$

where the following orthonormality conditions have been applied:

$$\mathbf{d}^\alpha \bullet \mathbf{d}^\beta = d^\alpha_\chi \tilde{g}^{\chi\delta} d^\beta_\delta = \delta^{\alpha\beta}. \qquad (3.162)$$

It follows that covariant and contravariant lattice directors are related by

$$\mathbf{d}_A = \delta_{AB} \mathbf{d}^B, \quad \mathbf{d}_\alpha = \delta_{\alpha\beta} \mathbf{d}^\beta, \quad \mathbf{d}_a = C_{ab}^{L} \mathbf{d}^b, \quad \mathbf{d}^a = C^{L-1ab} \mathbf{d}_b. \qquad (3.163)$$

In crystals with cubic, orthorhombic, or tetragonal structures (refer to Table 3.1 and Fig. 3.2), it is instructive to assign each reference director parallel to a reciprocal lattice vector, e.g., $\mathbf{d}_A \parallel \delta_{Ai} \mathbf{A}^i$, and to assign a coincident Cartesian coordinate system in each configuration with axes aligned with the referential reciprocal lattice vectors. In that case,

$$\begin{aligned}\mathbf{d}_a &= F^{L-1\,\alpha}_{.a} \delta^A_{.\alpha} \mathbf{d}_A = F^{L-1\,\alpha}_{.a} \delta_{\alpha i} \mathbf{A}^i \left| \mathbf{A}^i \right|^{-1} \\ &= F^{L-1\,\alpha}_{.a} \delta^B_{.\alpha} A^i_B \left| \mathbf{A}^i \right|^{-1} \mathbf{g}^a = \mathbf{a}^i \left| \mathbf{A}^i \right|^{-1}.\end{aligned} \qquad (3.164)$$

From (3.164), director vectors in the current configuration $\mathbf{d}_a$ are equivalent to reciprocal basis vectors $\mathbf{a}^i$ in the current configuration, normalized by their original lengths. In crystal structures wherein primitive reciprocal vectors are not necessarily orthogonal, directors of (3.154) are not necessarily parallel to the primitive translation vectors of the unit cell, but are instead an external construct. In that case, directors $\mathbf{d}_a$ and strain metric (3.160) still provide a measure of the lattice deformation. Components of lattice deformation and its inverse can be recovered directly from the scalar products

$$F^{La}_{.\alpha} = F^{La}_{.\beta} \left\langle \mathbf{d}^\beta, \mathbf{d}_\alpha \right\rangle = \mathbf{d}^a \bullet \mathbf{d}_\alpha, \quad F^{L-1\alpha}_{.a} = F^{L-1\alpha}_{.b} \left\langle \mathbf{d}^b, \mathbf{d}_a \right\rangle = \mathbf{d}^\alpha \bullet \mathbf{d}_a, \qquad (3.165)$$

implying that knowledge of the vector fields in (3.155) and (3.156) is sufficient to characterize the first-order deformation of the lattice.

At a microscopic scale of resolution, absolute changes in lattice directors $\mathbf{d}_a$ are described in terms of a covariant derivative executed with respect to a linear connection with coefficients $\hat{\Gamma}^{..a}_{bc}(x,t)$. The absolute change of director vector $\mathbf{d}_a$ with spatial position is defined in terms of the corresponding covariant derivative operation $\hat{\nabla}$, treating the index of the director as that of a component of a covector in (2.30):

$$\hat{\nabla}_b \mathbf{d}_a = \mathbf{d}_{a,b} - \hat{\Gamma}^{..c}_{ba} \mathbf{d}_c = \partial_b \mathbf{d}_a - \hat{\Gamma}^{..c}_{ba} \mathbf{d}_c, \qquad (3.166)$$

with the subscripted comma denoting partial differentiation with respect to spatial coordinates $x^a(X,t)$. Similarly, for a contravariant director $\mathbf{d}^a$,

$$\hat{\nabla}_b \mathbf{d}^a = \mathbf{d}^a_{,b} + \hat{\varGamma}^{..a}_{bc} \mathbf{d}^c = \partial_b \mathbf{d}^a + \hat{\varGamma}^{..a}_{bc} \mathbf{d}^c . \tag{3.167}$$

Coefficients of the connection in (3.166) and (3.167) are defined by (Minagawa 1979, 1981; Clayton et al. 2005, 2006, 2008a)

$$\hat{\varGamma}^{..a}_{cb} = F^{La}_{.\alpha} F^{L-1\alpha}_{.b,c} + Q^{.a}_{cb} = \bar{\varGamma}^{..a}_{cb} + Q^{.a}_{cb} , \tag{3.168}$$

where $\bar{\varGamma}^{..a}_{cb} = F^{La}_{.\alpha} F^{L-1\alpha}_{.b,c} = -F^{La}_{.\alpha,c} F^{L-1\alpha}_{.b}$ are coefficients of the crystal connection of non-Riemannian dislocation theories (Bilby et al. 1955; Noll 1967; Le and Stumpf 1996a), and $Q^{.a}_{cb}$ are micromorphic degrees of freedom representing additional contributions of defects to spatial gradients of the lattice director fields. Upon assuming $\hat{\nabla}_b \mathbf{d}_a = 0$ (Minagawa 1981; Clayton et al. 2006), the connection of (3.166)-(3.168) enables one to interpolate for directions and magnitudes of lattice directors at spatial locations between centroids of neighboring volume elements within a crystalline solid. In the trivial situation when $\hat{\varGamma}^{..a}_{cb} = 0$, lattice directors are spatially constant since in that case $\mathbf{d}_{a,b} = 0$. The crystal connection ($\bar{\varGamma}^{..a}_{cb}$) component of (3.168) accounts for effects of first-order spatial gradients of (the inverse of) $\mathbf{F^L}$, while micromorphic variable $\mathbf{Q}$ of (3.168) accounts for additional spatial variations of lattice directors not captured by the first-order gradient of $\mathbf{F^{L-1}}$. The deformation of a representative set of director vectors located at spatial position x corresponding to the volume element's centroid is determined by $\mathbf{F^L}$, as indicated by (3.155). Stretch and rotation gradients of the lattice at spatial position x, for example at the scale of sub-grain cells and cell blocks within a severely deformed single crystal (Seefeldt 2001; Hughes et al. 2003), are represented by coefficients of (3.168).

Covariant components of $\mathbf{Q}$ are defined via lowering by the metric $\mathbf{C^L}$:

$$Q_{cba} = Q^{.d}_{cb} C^L_{da} . \tag{3.169}$$

The covariant derivative of $\mathbf{C^L}$ with respect to the connection coefficients in (3.168) is found by direct invocation of (2.30) as

$$\begin{aligned}
\hat{\nabla}_c C^L_{ab} &= C^L_{ab,c} - \bar{\varGamma}^{..d}_{ca} C^L_{db} - \bar{\varGamma}^{..d}_{cb} C^L_{ad} - Q^{.d}_{ca} C^L_{db} - Q^{.d}_{cb} C^L_{ad} \\
&= -2Q_{c(ab)} + \delta_{\alpha\beta} \Big[F^{L-1\alpha}_{.a} F^{L-1\beta}_{.b,c} + F^{L-1\alpha}_{.a,c} F^{L-1\beta}_{.b} \\
&\quad - F^{Ld}_{.\chi} F^{L-1\chi}_{.a,c} F^{L-1\alpha}_{.d} F^{L-1\beta}_{.b} - F^{Ld}_{.\chi} F^{L-1\chi}_{.b,c} F^{L-1\alpha}_{.a} F^{L-1\beta}_{.d} \Big] \\
&= -2Q_{c(ab)}.
\end{aligned} \tag{3.170}$$

Components of the torsion tensor of the connection are obtained from application of (2.33):

$$\hat{T}_{cb}^{..a} = \hat{\Gamma}_{[cb]}^{..a} = \overline{T}_{cb}^{..a} + Q_{[cb]}^{.a}, \tag{3.171}$$

where $\overline{T}_{cb}^{..a} = \overline{\Gamma}_{[cb]}^{..a}$ are components of the torsion of the crystal connection. Mixed-variant components of the Riemann-Christoffel curvature tensor, $\hat{R}_{bcd}^{...a}$, formed from connection coefficients $\hat{\Gamma}_{cb}^{..a}$ are computed from (2.34):

$$\hat{R}_{bcd}^{...a} = \hat{\Gamma}_{cd,b}^{..a} - \hat{\Gamma}_{bd,c}^{..a} + \hat{\Gamma}_{be}^{..a}\hat{\Gamma}_{cd}^{..e} - \hat{\Gamma}_{ce}^{..a}\hat{\Gamma}_{bd}^{..e}$$
$$= 2\partial_{[b}\hat{\Gamma}_{c]d}^{..a} + 2\hat{\Gamma}_{[b|e|}^{..a}\hat{\Gamma}_{c]d}^{..e}, \tag{3.172}$$

which, because of additive decomposition (3.168), can be expressed as the following sum (Schouten 1954):

$$\hat{R}_{bcd}^{...a} = \overline{R}_{bcd}^{...a} + 2\hat{\nabla}_{[b}Q_{c]d}^{.a} + 2\hat{T}_{bc}^{..e}Q_{ed}^{.a} - 2Q_{[b|d|}^{.e}Q_{c]e}^{.a}$$
$$= 2F_{.a}^{La}\partial_{[b}\partial_{c]}F_{.d}^{L-1\alpha} + 2\hat{\nabla}_{[b}Q_{c]d}^{.a} + 2\hat{T}_{bc}^{..e}Q_{ed}^{.a} - 2Q_{[b|d|}^{.e}Q_{c]e}^{.a} \tag{3.173}$$
$$= 2\hat{\nabla}_{[b}Q_{c]d}^{.a} + 2\hat{T}_{bc}^{..e}Q_{ed}^{.a} + Q_{cd}^{.e}Q_{be}^{.a} - Q_{bd}^{.e}Q_{ce}^{.a}.$$

In (3.173), the curvature from the crystal connection, $\overline{R}_{bcd}^{...a}$, vanishes identically since the crystal connection is integrable, as follows from the generic derivation in (2.215)-(2.218). The fully covariant curvature tensor corresponding to (3.173) is obtained directly using (3.170) and the product rule as follows:

$$\hat{R}_{bcda} = 2\hat{\nabla}_{[b}Q_{c]d}^{.e}C_{ae}^{L} + 2\hat{T}_{bc}^{..e}Q_{eda} - 2Q_{[b|d|}^{.e}Q_{c]e}^{.f}C_{af}^{L}$$
$$= 2\hat{\nabla}_{[b}Q_{c]da} + 2\hat{T}_{bc}^{..e}Q_{eda} - 2Q_{[c|d|}^{.e}\hat{\nabla}_{b]}C_{ae}^{L} - 2Q_{[b|d|}^{.e}Q_{c]ea}$$
$$= 2\hat{\nabla}_{[b}Q_{c]da} + 2\hat{T}_{bc}^{..e}Q_{eda} + 4Q_{[b|d|}^{.e}Q_{c](ae)} - 2Q_{[b|d|}^{.e}Q_{c]ea} \tag{3.174}$$
$$= 2\hat{\nabla}_{[b}Q_{c]da} + 2\hat{T}_{bc}^{..e}Q_{eda} + 2Q_{[b|d|}^{.e}Q_{c]ae}.$$

From (3.173) and (3.174), curvature tensor $\hat{\mathbf{R}}$ vanishes identically when the supplementary degrees of freedom vanish, i.e., when $\mathbf{Q} = 0$. Decomposing (3.174) into an antisymmetric part over the final two indices gives

$$\hat{R}_{[bc][da]} = 2\hat{\nabla}_{[b}Q_{c][da]} + 2\hat{T}_{bc}^{..e}Q_{e[da]} + C^{L-1ef}\left[Q_{[b|df|}Q_{c]ae} - Q_{[b|af|}Q_{c]de}\right]$$
$$= 2\hat{\nabla}_{[b}Q_{c][da]} + 2\hat{T}_{bc}^{..e}Q_{e[da]} + C^{L-1ef}\left[Q_{[b|de|}Q_{c]af} - Q_{[b|af|}Q_{c]de}\right]$$
$$= 2\hat{\nabla}_{[b}Q_{c][da]} + 2\hat{T}_{bc}^{..e}Q_{e[da]} - C^{L-1fe}\left[Q_{[c|af|}Q_{b]de} - Q_{[c|af|}Q_{b]de}\right] \tag{3.175}$$
$$= 2\hat{\nabla}_{[b}Q_{c][da]} + 2\hat{T}_{bc}^{..e}Q_{e[da]}.$$

The symmetric part of (3.174) over the final two covariant indices is obtained from identity (2.49) and (3.170):

$$\hat{R}_{[bc](da)} = -\hat{\nabla}_{[b}\hat{\nabla}_{c]}C^L_{da} - \hat{T}^{..e}_{bc}\hat{\nabla}_e C^L_{da} = 2\hat{\nabla}_{[b}Q_{c](da)} + 2\hat{T}^{..e}_{bc}Q_{e(da)}. \qquad (3.176)$$

The notion of a Cartan displacement (Schouten 1954; Brillouin 1964; Wang and Truesdell 1973; Minagawa 1979) is often used to provide a geometric interpretation of non-integrability of a space or manifold with possibly non-vanishing torsion and curvature. Cartan's displacement about a curve c encircling area a with differential element $dx^a \wedge dx^b = \varepsilon^{abc}n_c da$ is derived using Stokes's theorem of Section 2.7.2. While the general treatment of Section 3.3 permits arbitrary curvilinear coordinates in the spatial configuration, the derivation given immediately below in (3.177) in indicial notation is restricted to spatial coordinates x^a wherein corresponding Christoffel symbols $\overset{g}{\Gamma}{}^{..a}_{bc}=0$ by definition (e.g., Cartesian coordinates), since integration of a vector field is involved. Cartan's displacement is defined as the following line integral:

$$
\begin{aligned}
\hat{B}^a &= -\int_c (\delta^a_{.e} + x^a_{.,e})dx^e = -\int_c \delta^a_{.e}dx^e - \int_c x^a_{.,e}dx^e \\
&= \int_a \delta^a_{.e,b}dx^e \wedge dx^b + \int_c \hat{\Gamma}^{..a}_{ec}x^c dx^e \\
&= \int_a \delta^a_{.e,b}dx^e \wedge dx^b - \int_a (\hat{\Gamma}^{..a}_{ec}x^c)_{,b}dx^e \wedge dx^b \\
&= -\int_a \hat{\Gamma}^{..a}_{eb}dx^e \wedge dx^b + \int_a (\hat{\Gamma}^{..a}_{ec}x^c)_{,b}dx^e \wedge dx^b \\
&= -\int_a \hat{T}^{..a}_{eb}dx^e \wedge dx^b + \int_a (\hat{\Gamma}^{..a}_{ec,b}x^c + \hat{\Gamma}^{..a}_{ec}x^c_{.,b})dx^e \wedge dx^b \\
&= -\int_a \hat{T}^{..a}_{eb}dx^e \wedge dx^b + \int_a (\hat{\Gamma}^{..a}_{ec,b}x^c - \hat{\Gamma}^{..a}_{ec}\hat{\Gamma}^{..c}_{bd}x^d)dx^e \wedge dx^b \\
&= -\int_a \hat{T}^{..a}_{eb}dx^e \wedge dx^b + \int_a (\partial_{[b}\hat{\Gamma}^{..a}_{e]d} + \hat{\Gamma}^{..a}_{[b|c|}\hat{\Gamma}^{..c}_{e]d})x^d dx^e \wedge dx^b \\
&= -\int_a (\hat{T}^{..a}_{be} + \frac{1}{2}\hat{R}^{..a}_{bed}x^d)dx^b \wedge dx^e = -\varepsilon^{bec}\int_a (\hat{T}^{..a}_{be} + \frac{1}{2}\hat{R}^{..a}_{bed}x^d)n_c da.
\end{aligned}
\qquad (3.177)
$$

The following special definitions[10] that presume a kind of modified parallel transport of Kronecker's delta $\delta^a_{.e}$ and spatial position x^d with respect to (3.168) are also used to compute the Cartan displacement in (3.177):

$$\hat{\nabla}'_b \delta^a_{.e} = \delta^a_{.e,b} - \hat{\Gamma}^{..a}_{bc}\delta^c_{.e} = \delta^a_{.e,b} - \hat{\Gamma}^{..a}_{be} = 0, \quad \hat{\nabla}'_b x^c = x^c_{.,b} + \hat{\Gamma}^{..c}_{bd}x^d = 0. \quad (3.178)$$

Using (3.174)-(3.177), the Cartan displacement can be written as the sum

---

[10] Notice that $\hat{\nabla}'_a$ as defined in (3.178) does not obey (2.30); i.e., $\hat{\nabla}'_a \neq \hat{\nabla}_a$.

$$\hat{B}^a = -\int_a \left[\hat{T}_{bc}^{..a} + \frac{1}{2} C^{L-1ae} (\hat{R}_{bc[de]} + \hat{R}_{bc(de)}) x^d \right] dx^b \wedge dx^c . \qquad (3.179)$$

Cartan displacement $\hat{B}^a$ will be associated later in Sections 3.3.2, 3.3.3, and 3.3.4 with a total Burgers vector (i.e., incompatibility measure) resulting from effects of all defects (e.g., dislocations, disclinations, and point defects) threading or situated on oriented area a encircled by circuit c. Application of Stokes's theorem in (3.177) requires that connection coefficients have continuous first derivatives with respect to spatial coordinates, implying that lattice deformation and its inverse must have continuous second derivatives with respect to spatial coordinates.

It is often instructive to consider a linearized theory. In that case, the distinction between intermediate and spatial coordinate systems is omitted, and the lattice deformation gradient and lattice distortion are related by

$$F^{La}_{.b} = \delta^a_{.b} + \beta^{La}_{.b}, \ F^{L-1a}_{.b} = \delta^a_{.b} - \beta^{La}_{.b} . \qquad (3.180)$$

Clayton et al. (2008a) considered a partially nonlinear regime wherein approximation (3.180) applies for lattice deformation, but wherein gradients of lattice directors may be arbitrarily large, thus retaining fully nonlinear forms of connection (3.168), torsion (3.171), and curvature (3.172). On the other hand, a fully linear description omits all second-order terms in the connection coefficients, torsion, and curvature. In the context of such a fully linear theory, the connection (3.168) becomes

$$\hat{\Gamma}^{..a}_{cb} = -(\delta^a_{.d} + \beta^{La}_{.d}) \beta^{Ld}_{.b,c} + Q^{.a}_{cb} \approx -\beta^{La}_{.b,c} + Q^{.a}_{cb} = \overline{\Gamma}^{..a}_{cb} + Q^{.a}_{cb} , \qquad (3.181)$$

where the linearized crystal connection and its torsion are, respectively,

$$\overline{\Gamma}^{..a}_{cb} = -\beta^{La}_{.b,c}, \ \overline{T}^{..a}_{cb} = -\beta^{La}_{.[b,c]} . \qquad (3.182)$$

The linearized metric of (3.160) is

$$C^L_{ab} = F^{L-1\alpha}_{.a} \delta_{\alpha\beta} F^{L-1\beta}_{.b} = (\delta^d_{.a} - \beta^{Ld}_{.a}) \delta_{de} (\delta^e_{.b} - \beta^{Le}_{.b})$$

$$= (\delta_{ab} - \beta^L_{ab} - \beta^L_{ba} + \beta^L_{ea} \beta^{Le}_{.b}) \approx \delta_{ab} - 2\beta^L_{(ab)} . \qquad (3.183)$$

Similarly, the linearized inverse metric of (3.161) is

$$C^{L-1ab} = F^{La}_{.\alpha} \delta^{\alpha\beta} F^{Lb}_{.\beta} = (\delta^a_{.d} + \beta^{La}_{.d}) \delta^{de} (\delta^b_{.e} + \beta^{Lb}_{.e})$$

$$= (\delta^{ab} + \beta^{Lab} + \beta^{Lba} + \beta^{Lae} \beta^{Lb}_{.e}) \approx \delta^{ab} + 2\beta^{L(ab)} . \qquad (3.184)$$

Covariant components of connection (3.181) are then approximated as

$$\hat{\Gamma}_{cba} \approx (-\beta^{Ld}_{.b,c} + Q^{.d}_{cb}) C^L_{da} \approx (-\beta^{Ld}_{.b,c} + Q^{.d}_{cb})(\delta_{da} - 2\beta^L_{(da)})$$

$$\approx -\partial_c \beta^L_{ab} + Q^{.d}_{cb} \delta_{da} . \qquad (3.185)$$

Connection coefficients in (3.185) can then be partitioned as

$$\hat{\Gamma}_{c(ba)} \approx \frac{1}{2} \partial_c C^L_{(ba)} + Q_{c(ba)} , \ \hat{\Gamma}_{c[ba]} \approx \partial_c \beta^L_{[ba]} + Q_{c[ba]} . \qquad (3.186)$$

The torsion tensor of (3.181) is simply

$$\hat{T}_{cb}^{..a} \approx \beta^{La}_{\ \ [c,b]} + Q^{..a}_{[cb]}.$$ (3.187)

The curvature tensor of (3.172) is approximated successively as follows by neglecting products of two and higher in the connection coefficients:

$$\hat{R}_{bcd}^{...a} \approx 2\partial_{[b}\hat{\Gamma}^{..a}_{c]d} = 2\partial_{[c}\partial_{b]}\beta^{La}_{\ \ .e} + 2\partial_{[b}Q^{.a}_{c]d} = 2\partial_{[b}Q^{.a}_{c]d}.$$ (3.188)

Fully covariant approximations of the curvature tensor are then

$$\hat{R}_{bcda} \approx 2\partial_{[b}Q_{c]da} \ , \ \hat{R}_{bc[da]} \approx 2\partial_{[b}Q_{c][da]} \ , \ \hat{R}_{bc(da)} \approx 2\partial_{[b}Q_{c](da)} \ .$$ (3.189)

The Cartan displacement in (3.177) can then be obtained in the linear approximation via use of (3.187) and (3.188).

Association of the mathematical framework of Section 3.3.1 is made with the physics of continuous distributions of lattice defects in what follows in the remainder of Section 3.3. This association is accomplished by considering three limiting cases: traditional (geometrically necessary) dislocation theory in Section 3.3.2, characterized by $Q_{cba} = 0$; disclination theory in Section 3.3.3, characterized by $Q_{cba} = Q_{c[ba]}$; and a theory for isotropically distributed point defects in Section 3.3.4, characterized by $Q_{cba} = \Upsilon_c C^L_{ba}$. Superposition of ideas set forth in each of the three cases then enables description of crystals containing dislocations, disclinations, and point defects.

3.3.2 Dislocations and the Crystal Connection

The description of Section 3.3.1 encompasses only traditional, translational dislocations if $Q_{cba} = 0$, for which (3.168) reduces to the crystal connection (Bilby et al. 1955; Kroner 1960; Noll 1967):

$$\hat{\Gamma}_{cb}^{..a} = \bar{\Gamma}_{cb}^{..a} = F^{La}_{\ .\alpha}F^{L-1\alpha}_{\ \ .b,c}$$

$$= -F^{La}_{\ .\alpha,c}F^{L-1\alpha}_{\ \ .b} = -F^{La}_{\ .\alpha,\beta}F^{L-1\beta}_{\ \ .c}F^{L-1\alpha}_{\ \ .b},$$ (3.190)

where the third equality follows from $(F^{La}_{\ .\alpha}F^{L-1\alpha}_{\ \ .b})_{,c} = \delta^a_{.b,c} = 0$. The torsion tensor obtained from connection coefficients in (3.190) is then

$$\hat{T}_{cb}^{..a} = \bar{T}_{cb}^{..a} = F^{La}_{\ .\alpha}F^{L-1\alpha}_{\ \ [b,c]} = F^{La}_{\ .\alpha}\partial_{[c}F^{L-1\alpha}_{\ \ .b]},$$ (3.191)

The torsion in (3.191) vanishes by (2.219) when the lattice deformation is integrable:

$$\bar{T}_{cb}^{..a} = 0 \leftrightarrow F^{L-1\alpha}_{\ \ [b,c]} = 0 \Leftrightarrow F^{L-1\alpha}_{\ \ .a} = \tilde{x}^\alpha_{.,a},$$ (3.192)

in which case $\tilde{x}^\alpha = \tilde{x}^\alpha(x,t)$. Recall from (3.170) that the connection is metric, $\bar{\nabla}_a C^L_{bc} = 0$, and from (3.173) that the connection is integrable, $\bar{R}^{...a}_{bcd} = 0$, both following from prescription $Q_{cba} = 0$ in (3.190).

Consider partial derivatives of the lattice director vectors and their reciprocals obtained following (3.155) and (3.158):

$$\mathbf{d}_{a,b} = F^{L-1\alpha}_{.a,b}\mathbf{d}_\alpha = F^{L-1\alpha}_{.a,b}F^{Lc}_{.\alpha}\mathbf{d}_c = \bar{\Gamma}^{..c}_{ba}\mathbf{d}_c , \qquad (3.193)$$

$$\mathbf{d}^a_{,b} = F^{La}_{.\alpha,b}\mathbf{d}^\alpha = F^{La}_{.\alpha,b}F^{L-1\alpha}_{.c}\mathbf{d}^c = -F^{La}_{.\alpha}F^{L-1\alpha}_{.c,b}\mathbf{d}^c = -\bar{\Gamma}^{..a}_{bc}\mathbf{d}^c , \qquad (3.194)$$

since by definition, $\mathbf{d}_{\alpha,b} = 0$ and $\mathbf{d}^\alpha_{,b} = 0$. Relations (3.193) and (3.194) denote parallel transport of the lattice directors with respect to the crystal connection:

$$\bar{\nabla}_b\mathbf{d}_a = \mathbf{d}_{a,b} - \bar{\Gamma}^{..c}_{ba}\mathbf{d}_c = 0, \ \bar{\nabla}_b\mathbf{d}^a = \mathbf{d}^a_{,b} + \bar{\Gamma}^{..a}_{bc}\mathbf{d}^c = 0, \qquad (3.195)$$

and are analogous to relationships for partial coordinate derivatives of holonomic basis vectors in (2.59).
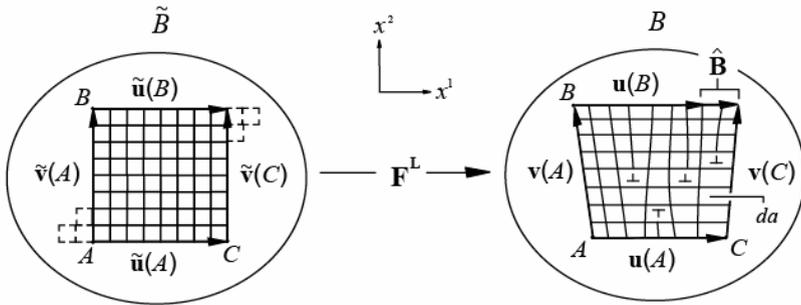
Fig. 3.15 Defective cubic lattice as described by the crystal connection

A two-dimensional visual interpretation of the crystal connection is given in Fig. 3.15 for a simple cubic lattice. Inscribed on the image of the body on the left side of Fig. 3.15 are two orthogonal fields of constant contravariant vectors in configuration $\tilde{B}$—denoted by $\tilde{\mathbf{u}}$ and $\tilde{\mathbf{v}}$—that form a rectilinear grid representative of the field of primitive Bravais lattice vectors. More specifically, each vector $\tilde{\mathbf{u}}$ or $\tilde{\mathbf{v}}$ is parallel to a primitive Bravais lattice vector of (3.1), but is of magnitude of a Bravais lattice vector multiplied by a factor of eight. In a simple cubic lattice, $\tilde{\mathbf{u}}$ and $\tilde{\mathbf{v}}$ are also parallel to slip directions and perpendicular to slip planes, as deduced from Table 3.4. The representation of a perfect lattice in $\tilde{B}$ is in agreement with dislocation-based plasticity theory (Section 3.2.5) and crystal plastic-

ity theory (Section 3.2.6), for example, wherein $\mathbf{F}^{\mathbf{P}} : TB_0 \to T\tilde{B}$ is assumed to leave the slip directions and slip planes unperturbed. Notice that the crystal may have undergone slip with respect to its position relative to reference configuration B_0, as indicated by the dotted unit cell boundaries on the left side of Fig. 3.15. For clarity, these slip steps are not shown on the right side of Fig. 3.15, though they do exist in configuration B. Since vectors $\tilde{\mathbf{u}}$ and $\tilde{\mathbf{v}}$ are independent of position in the intermediate configuration,

$$\tilde{\mathbf{u}}(A) = \tilde{\mathbf{u}}(B), \ \tilde{\mathbf{v}}(A) = \tilde{\mathbf{v}}(B), \tag{3.196}$$

where A and B are two points on the lattice in the relaxed configuration separated by a small distance $d\mathbf{x} = \mathbf{x}(B) - \mathbf{x}(A)$ when their positions are mapped onto the deformed image of the crystal. Focusing for the moment on the field $\tilde{\mathbf{u}}$, both sides of the first of (3.196) are pre-multiplied by $\mathbf{F}^{\mathbf{L}}(B)$, the value of the deformation at the location corresponding to point B on the lattice, to obtain

$$F^{La}_{\ \ .\alpha}(B)\tilde{u}^{\alpha}(A) = F^{La}_{\ \ .\alpha}(B)\tilde{u}^{\alpha}(B). \tag{3.197}$$

Expanding $\mathbf{F}^{\mathbf{L}}(B)$ with a first-order (i.e., linear) approximation in $\mathbf{x}$ gives

$$F^{La}_{\ \ .\alpha}(B) \approx F^{La}_{\ \ .\alpha}(A) + F^{La}_{\ \ .\alpha,b}(A)dx^b, \tag{3.198}$$

which is then substituted into (3.197) to yield

$$u^a(B) = u^a(A) + F^{La}_{\ \ .\alpha,b}(A)F^{L-1\alpha}_{\ \ \ .c}(A)u^c(A)dx^b, \tag{3.199}$$

where vectors $\tilde{\mathbf{u}}$ are pushed forward via

$$u^a(A) = F^{La}_{\ \ .\alpha}(A)\tilde{u}^{\alpha}(A), \ u^a(B) = F^{La}_{\ \ .\alpha}(B)\tilde{u}^{\alpha}(B). \tag{3.200}$$

Using the identity $(F^{La}_{\ \ .\alpha}F^{L-1\alpha}_{\ \ \ .c})_{,b} = 0$, (3.199) is rewritten as

$$0 = u^a(B) - u^a(A) + F^{La}_{\ \ .\alpha}(A)F^{L-1\alpha}_{\ \ \ .c,b}(A)dx^b u^c(A). \tag{3.201}$$

Making the linear approximation

$$u^a(B) - u^a(A) \approx \partial_b u^a(A)\left[x^b(B) - x^b(A)\right] = u^a_{\ .b}(A)dx^b, \tag{3.202}$$

and dropping notation signaling localization to point A, (3.201) becomes

$$0 = u^a_{\ .b}dx^b + F^{La}_{\ \ .\alpha}F^{L-1\alpha}_{\ \ \ .c,b}dx^b u^c. \tag{3.203}$$

This is the structure of a null covariant derivative, i.e., parallel transport with respect to the crystal connection of (3.190):

$$\bar{\nabla}_b u^a = u^a_{\ .b} + \bar{\Gamma}^{..a}_{bc} u^c = 0, \tag{3.204}$$

because dx^b is now arbitrary. Since connection coefficients corresponding to $\bar{\nabla}$ in (3.204) are equivalent to those given in (3.190), parallel transport of vectors $\mathbf{u}$ with respect to the crystal connection physically corresponds

to a reconstruction of the deformed lattice from a rectilinear grid in relaxed configuration $\tilde{B}$. Analogously, field **v** in Fig. 3.15 obeys

$$\overline{\nabla}_b v^a = v^a_{\ ,b} + \overline{\Gamma}^{\ ..a}_{bc} v^c = 0, \qquad (3.205)$$

i.e., the vector field $\mathbf{v} = \mathbf{F}^L \tilde{\mathbf{v}} \in TB$ constructed by pushing forward from the uniform reference grid $\tilde{\mathbf{v}} \in T\tilde{B}$ obeys the rule of parallel transport with respect to the connection in (3.190). It is now clear why the crystal connection is said to possess the property of teleparallelism in the context of geometric field theories (Einstein 1928; Schouten 1954).

The closure failure or Cartan displacement $\hat{\mathbf{B}}$ of the area a shown in Fig. 3.15—i.e., the area of the parallelogram enclosed by $\mathbf{u}(A)$, $\mathbf{u}(B)$, $\mathbf{v}(A)$, and $\mathbf{v}(C)$, with C a third location in the deformed crystal—is equivalent to the integral of a field of local Burgers vectors $\mathbf{b}(x,t)$ (Kroner 1980). Consider first the vector addition relation that follows from visual inspection of Fig. 3.15:

$$\hat{B}^a = u^a(A) - u^a(B) + v^a(C) - v^a(A). \qquad (3.206)$$

Comparison with Fig. 3.6(b) demonstrates that $\hat{\mathbf{B}}$ represents the sum of local Burgers vectors of dislocations traversing area a, when the tangent lines of dislocations are defined in a right-handed sense when the Burgers circuit is taken as counterclockwise. In configuration B in Fig. 3.15,

$$x^b(B) - x^b(A) = v^b(A), \ x^b(C) - x^b(A) = u^b(A). \qquad (3.207)$$

Upon making the linear approximations

$$u^a(B) - u^a(A) \approx u^a_{\ ,b}(A)v^b(A), \ v^a(C) - v^a(A) \approx v^a_{\ ,b}(A)u(A)^b, \quad (3.208)$$

and invoking (3.204) and (3.205), the closure failure of (3.206) becomes

$$\hat{B}^a = -u^a_{\ ,b}(A)v^b(A) + v^a_{\ ,b}(A)u^b(A) = \overline{\Gamma}^{\ ..a}_{bc}v^b u^c - \overline{\Gamma}^{\ ..a}_{bc}u^b v^c, \qquad (3.209)$$

which can be written as

$$\hat{B}^a = 2\overline{\Gamma}^{\ ..a}_{[bc]}v^b u^c = 2\overline{T}^{\ ..a}_{bc}u^{[c}v^{b]}. \qquad (3.210)$$

Making the identification

$$u^{[c}v^{b]} = \frac{1}{2}(u^c v^b - u^b v^c) = \frac{1}{2}\int_a dx^c \wedge dx^b$$

$$= \frac{1}{2}\varepsilon^{cbd}\int_a n_d da = \frac{1}{2}\varepsilon^{cbd}n_d a, \qquad (3.211)$$

equality (3.210) is then rewritten as

$$\hat{B}^a = -\varepsilon^{bcd}\overline{T}^{\ ..a}_{bc}n_d a, \qquad (3.212)$$

which is identical to the Cartan displacement in (3.177) when the curvature tensor vanishes (recall that $\tilde{R}^{\ ..a}_{bcd} = 0$ is always true for the integrable crys-

tal connection) and when the normal to the area enclosed by the Burgers circuit is constant, as is the case in the two-dimensional scenario shown in Fig. 3.15.

More generally, the Cartan displacement or total Burgers vector in (3.177) is written as

$$
\begin{aligned}
\hat{B}^a &= \int_a b^a \, da = -\int_a \overline{T}_{cd}^{..a} \, dx^c \wedge dx^d \\
&= -\int_a \overline{T}_{cd}^{..a} \varepsilon^{bcd} n_b \, da = \int_a \alpha^{ab} n_b \, da,
\end{aligned}
\tag{3.213}
$$

with the geometrically necessary dislocation density tensor[11] referred to B:

$$
\alpha^{ab} = \varepsilon^{bcd} \overline{T}_{dc}^{..a} = F_{.\alpha}^{La} \varepsilon^{bcd} F_{.c,d}^{L-1\alpha}, \ 2\overline{T}_{dc}^{..a} = \varepsilon_{cdb} \alpha^{ab}.
\tag{3.214}
$$

Formally, field $b^a(x,t)$ is assumed continuous and differentiable, in the context of theories of continuously distributed dislocations (Bilby et al. 1955; Willis 1967; Teodosiu 1982). On the other hand, Burgers vectors in real crystals measure discrete steps in the lattice. In continuum field theories (Bilby et al. 1955; Willis 1967; Teodosiu 1982), one often considers a volume element of a body in which the number of discrete dislocations tends towards infinity while the Burgers vector of each tends to zero such that their product remains finite. In this limiting process, the radius of each dislocation core, and the total volume occupied by core regions is also assumed to approach zero (Willis 1967).

In terms of straight defect lines, analogously to (3.89), the dislocation density tensor in the spatial configuration is written (Lardner 1974)

$$
\boldsymbol{\alpha} = \sum_{i=1}^{j} \rho^i \mathbf{b}^i \otimes \boldsymbol{\xi}^i , \ \alpha^{ab} = \sum_{i=1}^{j} \rho^i b^{ia} \xi^{ib} ,
\tag{3.215}
$$

with ρ^i, $\mathbf{b}^i$, and $\boldsymbol{\xi}^i$ the non-negative line length per unit current volume, Burgers vector, and tangent line in the spatial configuration for dislocation population i. Complete and partial dislocations may contribute to (3.214) and (3.215). Nye (1953) is credited with equating the dislocation density tensor of (3.215) with that of (3.214) when the lattice deformation reduces to a small rotation:

---

[11] Depending on the sign convention used to define the Burgers circuit, positive line direction of dislocations, and positive orientation of the area enclosed by the circuit, the algebraic sign of the total Burgers vector and dislocation density tensor may vary (Minagawa 1979; Teodosiu 1982; Clayton et al. 2005). The relationship between the dislocation density tensor and torsion may differ by a factor of two depending on the definition used for the torsion tensor. The transpose of (3.214) is often used as a definition of the dislocation density tensor (Minagawa 1979).

$$\alpha^{ab} = -(\delta^a_{.e} + \beta^{La}_{.e})\varepsilon^{bcd}\beta^{Le}_{.c,d} \approx -\varepsilon^{bcd}\beta^{La}_{.c,d} \approx -g^{ae}\varepsilon^{bcd}\Omega^L_{[ec],d}$$
$$= g^{ae}\varepsilon^{cdb}\varepsilon_{cfe}w^{Lf}_{.,d} = g^{ab}w^{Ld}_{.,d} - g^{ad}w^{Lb}_{.,d}, \tag{3.216}$$

where $w^{La} = -\varepsilon^{abc}\Omega^L_{bc}/2$ is a lattice rotation vector obtained via an axial transformation such as (2.166).

Now consider relaxed intermediate configuration $\tilde{B}$, which is generally anholonomic as discussed in Section 3.2.2. The anholonomicity of $\tilde{B}$ may be represented in terms of the non-integrability of either of tangent maps $\mathbf{F}^{\mathbf{L}-1}$ or $\mathbf{F}^{\mathbf{P}}$ via a non-vanishing anholonomic object in (3.41), or equivalently, with a net Burgers vector $\tilde{\mathbf{B}} \in T\tilde{B}$, defined in terms of closure failure of the line integral of pseudo-differential vector element (i.e., Pfaffian) $d\tilde{\mathbf{x}} = \mathbf{F}^{\mathbf{L}-1}d\mathbf{x} = \mathbf{F}^{\mathbf{P}}d\mathbf{X}$ over a loop $\tilde{c}$ in $\tilde{B}$ (Bilby et al. 1955; Kroner 1960):

$$\tilde{\mathbf{B}} = -\int_{\tilde{c}} d\tilde{\mathbf{x}} = -\int_c \mathbf{F}^{\mathbf{L}-1}d\mathbf{x} = -\int_C \mathbf{F}^{\mathbf{P}}d\mathbf{X}, \tag{3.217}$$

where c and C are closed images of Burgers circuit $\tilde{c}$ mapped to current and reference configurations, respectively[12]. The opposite sign convention for $\tilde{\mathbf{B}}$ is used by some authors (Teodosiu 1970, 1982; Clayton et al. 2004a). Comments regarding integration of vector fields over $T\tilde{B}$ in the context of (3.95) and (3.96) and general curvilinear coordinates apply here as well. Using the generalized Stokes's theorem of Section 2.7.2, and replacing $\mathbf{F}$ with $\mathbf{F}^{\mathbf{P}}$ in (2.199) and $\mathbf{F}^{-1}$ with $\mathbf{F}^{\mathbf{L}-1}$ in (2.200), leads to

$$-\int_C F^{P\alpha}_{.A}dX^A = \int_A F^{P\alpha}_{.[A;B]}dX^A \wedge dX^B = \int_A \varepsilon^{CAB}F^{P\alpha}_{.A,B}N_C dA, \tag{3.218}$$

$$-\int_c F^{L-1\alpha}_{.a}dx^a = \int_a F^{L-1\alpha}_{.[a;b]}dx^a \wedge dx^b = \int_a \varepsilon^{cab}F^{L-1\alpha}_{.a,b}n_c da. \tag{3.219}$$

Similarity of (3.219) with the geometric interpretation (3.213) is evident:

$$\tilde{B}^\alpha = \int_a \varepsilon^{dab}F^{L-1\alpha}_{.[a,b]}n_d da$$
$$= \int_a \varepsilon^{dab}F^{L-1\alpha}_{.c}\bar{T}^{.c}_{ba}n_d da = \int_a F^{L-1\alpha}_{.c}\alpha^{cd}n_d da. \tag{3.220}$$

Two-point dislocation density tensors $\boldsymbol{\alpha}_0$ and $\boldsymbol{\alpha}_{\mathbf{L}}$ are introduced as

$$\tilde{\mathbf{B}} = \int_A \boldsymbol{\alpha}_0 \mathbf{N}dA = \int_a \boldsymbol{\alpha}_{\mathbf{L}}\mathbf{n}da; \tag{3.221}$$

$$\alpha^{\alpha A}_0 = \varepsilon^{ABC}F^{P\alpha}_{.B;C} = \varepsilon^{ABC}F^{P\alpha}_{.B,C}, \quad \alpha^{\alpha a}_L = \varepsilon^{abc}F^{L-1\alpha}_{.b;c} = \varepsilon^{abc}F^{L-1\alpha}_{.b,c}. \tag{3.222}$$

---

[12] Designation of $\tilde{c}$ as "closed" is somewhat abstract since configuration $\tilde{B}$ is anholonomic. The first equality in (3.217) can be omitted without consequence.

Symmetries of Levi-Civita connections are exercised in (3.218), (3.219), and (3.222). The first of (3.222) exhibits a discrete version (3.89), analogously to (3.215). Using Nanson's formula (2.227), surface integrals in (3.221) are mapped to integrals over area $\tilde{a}$ in configuration $\tilde{B}$:

$$\tilde{B}^\alpha = \int_{\tilde{a}} \alpha_0^{\alpha A} J^{P-1} F^{P\beta}_{.A} \tilde{n}_\beta \, d\tilde{a} = \int_{\tilde{a}} \alpha_L^{\alpha a} J^L F^{L-1\beta}_{.a} \tilde{n}_\beta \, d\tilde{a} = \int_{\tilde{a}} \tilde{\alpha}^{\alpha\beta} \tilde{n}_\beta \, d\tilde{a} , \quad (3.223)$$

where J^L and J^P are defined in (3.48) and (3.49), and where components of the dislocation density tensor referred to the intermediate configuration

$$\tilde{\alpha}^{\alpha\beta} = J^{P-1} \alpha_0^{\alpha A} F^{P\beta}_{.A} = J^L \alpha_L^{\alpha a} F^{L-1\beta}_{.a} . \quad (3.224)$$

The first of (3.224) is consistent with the last of (3.92). The second equality in (3.224) can be derived directly from (2.142) and (3.31) as follows:

$$\begin{aligned}
J^{P-1} F^{P\beta}_{.A} \varepsilon^{ABC} F^{P\alpha}_{.B,C} &= J^{-1} J^L F^{L-1\beta}_{.a} F^a_{.A} \varepsilon^{ABC} (F^{L-1\alpha}_{.b} F^b_{.B})_{,C} \\
&= J^L F^{L-1\beta}_{.a} \left[J^{-1} F^a_{.A} \varepsilon^{ABC} F^{L-1\alpha}_{.b,C} F^b_{.B} \right] \\
&= J^L F^{L-1\beta}_{.a} \left[(J^{-1} \varepsilon^{ABC} F^a_{.A} F^b_{.B} F^c_{.C}) F^{L-1\alpha}_{.b,c} \right] \\
&= J^L F^{L-1\beta}_{.a} \varepsilon^{abc} F^{L-1\alpha}_{.b,c} .
\end{aligned} \quad (3.225)$$

In terms of discrete lines, terms entering various intermediate and spatial dislocation densities are related by

$$\begin{aligned}
d\tilde{B}^\alpha = \alpha_L^{\alpha a} n_a da &= \sum_{i=1}^j \rho^i \tilde{b}^{i\alpha} \xi^{ia} n_a da \\
&= \tilde{\alpha}^{\alpha\beta} \tilde{n}_\beta d\tilde{a} = \sum_{i=1}^j \tilde{\rho}^i \tilde{b}^{i\alpha} \xi^{i\beta} \tilde{n}_\beta d\tilde{a} \quad (3.226) \\
&= \alpha^{ba} n_a da = \sum_{i=1}^j \rho^i b^{ib} \xi^{ia} n_a da,
\end{aligned}$$

where tangent lines, scalar numbers of dislocations per unit volume, and local Burgers vectors are mapped across configurations as

$$\xi^{ia} = F^{La}_{.\alpha} \xi^{i\alpha} = F^a_{.A} \xi^{iA}_0 , \ \rho^i = J^{L-1} \tilde{\rho}^i = J^{-1} \rho_0^i, \ b^{ib} = F^{Lb}_{.\alpha} \tilde{b}^{i\alpha} . \quad (3.227)$$

From the first of (3.227), the tangent vector is generally only of unit length in one configuration. From the second of (3.227), since $J^P = 1$ when slip is lattice-preserving, the scalar densities satisfy $\rho^i J^L = \tilde{\rho}^i = \rho_0^i$. The third of (3.227) is consistent with the relationship between intermediate and spatial Burgers vectors in (3.84).

In the context of the geometrically linear theory, all line and surface integrals effectively take place in the same (e.g., spatial) configuration; a total Burgers vector $\tilde{\mathbf{B}}$ in this configuration is found in terms of plastic distortion $\boldsymbol{\beta}^P = \mathbf{F}^P - \mathbf{1}$ as

$$\tilde{B}^a = -\int_c (\delta^a_{.b} + \beta^{Pa}_{.b})dx^b = \int_c \beta^{Pa}_{.b;c}dx^b \wedge dx^c$$

$$= \int_c (\beta^{Pa}_{.b,c} + \overset{g}{\Gamma}{}^{..a}_{(cd)}\beta^{Pd}_{.b} - \overset{g}{\Gamma}{}^{.d}_{(cb)}\beta^{Pa}_{.d})\varepsilon^{bcd}n_d da. \qquad (3.228)$$

$$= \int_c \varepsilon^{bcd}\beta^{Pa}_{.b,c}n_d da = \int_c \alpha^{ad}n_d da.$$

Similarly, the total Burgers vector in terms of the elastic distortion is

$$\tilde{B}^a = -\int_c (\delta^a_{.b} - \beta^{La}_{.b})dx^b = -\int_c \beta^{La}_{.b;c}dx^b \wedge dx^c$$

$$= -\int_c \varepsilon^{bcd}\beta^{La}_{.b,c}n_d da = \int_c \alpha^{ad}n_d da. \qquad (3.229)$$

Comparing (3.228) and (3.229), the linearized dislocation density tensor satisfies

$$\alpha^{ad} = \varepsilon^{bcd}\beta^{Pa}_{.b,c} = -\varepsilon^{bcd}\beta^{La}_{.b,c}. \qquad (3.230)$$

The dislocation density in terms of the skew gradient of the elastic distortion is consistent with derivation (3.216). Analogously to (3.225), the second of (3.230) can be derived directly from the compatibility conditions:

$$\varepsilon^{bcd}\beta^{Pa}_{.b,c} = \varepsilon^{bcd}\beta^{Pa}_{.b;c} = \varepsilon^{bcd}(\beta^a_{.b;c} - \beta^{La}_{.b;c}) = \varepsilon^{bcd}(u^a_{;bc} - \beta^{La}_{.b;c})$$

$$= \varepsilon^{bcd}(u^a_{;(bc)} - \beta^{La}_{.b;c}) = -\varepsilon^{bcd}\beta^{La}_{.b;c} = -\varepsilon^{bcd}\beta^{La}_{.b,c}. \qquad (3.231)$$

Returning to the nonlinear description, continuity equations for the two-point dislocation densities defined in (3.221) are deduced by integrating the fields of local Burgers vectors over closed oriented surfaces with area elements $N_A dS$ and $n_a ds$ enclosing volume elements dV and dv in B_0 and B, respectively:

$$\int_S \alpha^{\alpha A}_0 N_A dS = \int_V \alpha^{\alpha A}_{0;A}dV \,, \quad \int_s \alpha^{\alpha a}_L n_a ds = \int_v \alpha^{\alpha a}_{L;a}dv \,, \qquad (3.232)$$

where Gauss's theorem of Section 2.7.1 has been used to convert from surface to volume integration. Considering definitions (3.222), localized continuity equations become

$$\alpha^{\alpha A}_{0;A} = \varepsilon^{ABC}F^{P\alpha}_{.B;(CA)} = 0 \,, \quad \alpha^{\alpha a}_{L;a} = \varepsilon^{abc}F^{L-1\alpha}_{.b;(ca)} = 0 \,, \qquad (3.233)$$

where symmetries of torsion-free Christoffel symbols $\overset{G}{\Gamma}{}^{..A}_{BC}$ and $\overset{g}{\Gamma}{}^{..a}_{bc}$ have been exploited. Since dislocation density tensors are divergence-free, (3.233) implies that dislocation lines cannot terminate abruptly inside the crystal (De Wit 1971, 1981), but instead must terminate at other defects or at free surfaces (Teodosiu 1982; Hull and Bacon 1984). Linearized global and local continuity equations are, respectively,

$$\int_s \alpha^{ad} n_d ds = \int_v \alpha^{ad}_{;d} dv = \int_s \varepsilon^{bcd} \beta^{Pa}_{.b;(cd)} ds = 0 \, , \quad \alpha^{ad}_{;d} = 0 \, . \tag{3.234}$$

Following Lardner (1969, 1974) the fully intermediate dislocation density tensor $\tilde{\boldsymbol{\alpha}}$ is readily decomposed into contributions from positively signed dislocations ($\tilde{\boldsymbol{\alpha}}_+$) and negatively signed dislocations ($\tilde{\boldsymbol{\alpha}}_-$):

$$\tilde{\boldsymbol{\alpha}} = \tilde{\boldsymbol{\alpha}}_+ + \tilde{\boldsymbol{\alpha}}_- = \sum_{i=1}^{j} \left(\tilde{\rho}^i_+ - \tilde{\rho}^i_- \right) \tilde{\mathbf{b}}^i_+ \otimes \tilde{\boldsymbol{\xi}}^i \, , \tag{3.235}$$

$$\tilde{\boldsymbol{\alpha}}_+ = \sum_{i=1}^{j} \tilde{\rho}^i_+ \tilde{\mathbf{b}}^i_+ \otimes \tilde{\boldsymbol{\xi}}^i \, , \quad \tilde{\boldsymbol{\alpha}}_- = \sum_{i=1}^{j} \tilde{\rho}^i_- \tilde{\mathbf{b}}^i_- \otimes \tilde{\boldsymbol{\xi}}^i \, , \tag{3.236}$$

with $\tilde{\rho}^i_+$ and $\tilde{\rho}^i_-$ the densities (line length per unit volume in $\tilde{B}$) of positively and negatively signed dislocations, where, for each value of i, positive and negative dislocations share the same unit tangent $\tilde{\boldsymbol{\xi}}^i$ (defined following (3.99)) but opposite Burgers vectors $\tilde{\mathbf{b}}^i_+ = -\tilde{\mathbf{b}}^i_-$ and line velocities $\tilde{\mathbf{v}}^i_+ = -\tilde{\mathbf{v}}^i_-$. Recall also from Section 3.2.5 that edge dislocations are characterized by $\tilde{\mathbf{b}} \perp \tilde{\boldsymbol{\xi}}$, while screw dislocations are characterized by $\tilde{\mathbf{b}} \| \tilde{\boldsymbol{\xi}}$. Thus when a set of dislocations all sharing the same tangent line $\tilde{\boldsymbol{\xi}}^i$ (but different Burgers vectors $\tilde{\mathbf{b}}^i$) is considered, and when orthogonal coordinate axes are introduced in $\tilde{B}$ with one axis aligned along $\tilde{\boldsymbol{\xi}}^i$, screw dislocations comprise the diagonal components of $\tilde{\boldsymbol{\alpha}}$ and edge dislocations comprise the off-diagonal components of $\tilde{\boldsymbol{\alpha}}$.

Werne and Kelly (1978) call $\tilde{\boldsymbol{\alpha}}$ the net dislocation density tensor. In contrast, the absolute or total dislocation density tensor $\tilde{\boldsymbol{\alpha}}_{\mathbf{T}}$ is defined as

$$\tilde{\boldsymbol{\alpha}}_{\mathbf{T}} = \tilde{\boldsymbol{\alpha}}_+ - \tilde{\boldsymbol{\alpha}}_- = \sum_{i=1}^{j} \left(\tilde{\rho}^i_+ + \tilde{\rho}^i_- \right) \tilde{\mathbf{b}}^i_+ \otimes \tilde{\boldsymbol{\xi}}^i = \sum_{i=1}^{j} \tilde{\boldsymbol{\alpha}}^i_{\mathbf{T}} \, , \tag{3.237}$$

where $\tilde{\boldsymbol{\alpha}}^i_{\mathbf{T}}$, the absolute dislocation density for straight dislocation line population i, is defined in (3.106). Notice from (3.105) the explicit dependence of the plastic velocity gradient $\mathbf{L}^{\mathbf{P}} = \dot{\mathbf{F}}^{\mathbf{P}} \mathbf{F}^{\mathbf{P}-1}$ on the summation of contributions from mobile dislocations comprising absolute dislocation density tensors $\tilde{\boldsymbol{\alpha}}^i_{\mathbf{T}}$. Net and absolute dislocation density tensors can be further decomposed into contributions from mobile and immobile dislocations (Lardner 1969), with the latter characterized by $\tilde{\mathbf{v}}^i_{+/-} = 0$ and thus not affecting dislocation flux (3.99) or plastic velocity gradient (3.105). When the conditions $\tilde{\boldsymbol{\alpha}} = \tilde{\boldsymbol{\alpha}}_+ + \tilde{\boldsymbol{\alpha}}_- = 0$, then $\tilde{\boldsymbol{\alpha}}_{\mathbf{T}} = 2\tilde{\boldsymbol{\alpha}}_+ = -2\tilde{\boldsymbol{\alpha}}_-$. When such conditions hold for all $t > 0$, then the dislocation flux of (3.99) and plastic velocity gradient of (3.105) may be nonzero, but the geometrically necessary

dislocation density vanishes. In such cases, dislocation content of the crystal is limited to statistically stored dislocations (Ashby 1970; Arsenlis and Parks 1999). Statistically stored dislocations, also called redundant dislocations (Arsenlis and Parks 1999), consist of closed loops, dislocation dipoles, and other self-terminating dislocation structures that give no contribution to the total Burgers vector of (3.217) or the dislocation density tensor (3.235). A formal definition extending that given in a linear framework by Arsenlis and Parks (1999) is

$$\tilde{\rho}_S^i = \tilde{\rho}_T^i - \tilde{\rho}^i , \ \rho_S^i = \rho_T^i - \rho^i = J^{L-1}\tilde{\rho}_S^i = J^{L-1}(\tilde{\rho}_T^i - \tilde{\rho}^i), \qquad (3.238)$$

where $\tilde{\rho}_S^i$ is the scalar statistically stored dislocation density per unit intermediate volume for dislocation population i, and the total scalar density of segments of orientation i and length L^i is

$$\tilde{\rho}_T^i = \lim_{\tilde{V} \to 0}\frac{1}{\tilde{V}}\int_L dL^i = \frac{dL^i}{d\tilde{V}} \geq 0. \qquad (3.239)$$

Summation over all populations leads to the following definitions:

$$\tilde{\rho}_T = \sum_{i=1}^{j}\tilde{\rho}_T^i = \lim_{\tilde{V}\to 0}\frac{1}{\tilde{V}}\int_L dL = \tilde{\rho} + \tilde{\rho}_S, \ \tilde{\rho} = \sum_{i=1}^{j}\tilde{\rho}^i, \ \tilde{\rho}_S = \sum_{i=1}^{j}\tilde{\rho}_S^i . \qquad (3.240)$$

The scalar $\tilde{\rho}_T$ measures the total line density of all dislocations per unit volume in the intermediate configuration.

Returning to the crystal connection of (3.190), note that by (2.218),

$$\bar{R}_{bdc}^{\ \ \ a}F^{L-1\alpha}_{\quad .a} = -2F^{L-1\alpha}_{\quad .c,[bd]} = 0, \qquad (3.241)$$

where $\bar{R}_{bdc}^{\ \ \ a}$ are the components of the Riemann-Christoffel curvature tensor derived from $\bar{\Gamma}_{bc}^{\ ..a}$. Conditions $\bar{R}_{bdc}^{\ \ \ a} = 0$ ensure satisfaction of (3.241), meaning that the crystal connection is integrable (Schouten 1954). Since the crystal connection is also metric (Section 2.1.3) with respect to $\mathbf{C^L}$ from (3.170) with $Q_{bca} = 0$, and since its curvature tensor vanishes identically, the set $\{B, \bar{\Gamma}_{cd}^{\ ..a}, C_{ab}^L\}$ constitutes a metric, non-Riemannian space. From (2.221),

$$2C_{ab}^L\bar{\Gamma}_{(cd)}^{\ ..a} = C_{cb,d}^L + C_{db,c}^L - C_{dc,b}^L . \qquad (3.242)$$

In the particular instance wherein the torsion vanishes, i.e., $\bar{T}_{cd}^{\ ..a} = 0$ such that $\bar{\Gamma}_{cd}^{\ ..a} = \bar{\Gamma}_{(cd)}^{\ ..a}$, the following statements apply: the crystal connection is symmetric (i.e., $\{B, \bar{\Gamma}_{cd}^{\ ..a}, C_{ab}^L\}$ becomes a non-Cartan space), geometrically necessary dislocations are absent, (3.242) defines a set of Levi-Civita connection coefficients akin to (2.58) on the current configuration with associated metric tensor $\mathbf{C^L}$, and the set $\{B, \bar{\Gamma}_{cd}^{\ ..a}, C_{ab}^L\}$ constitutes a Euclid-

ean space. In that case, (3.192) applies, meaning $F^{L-1\alpha}_{\quad .a} = \tilde{x}^{\alpha}_{.,a}$. The lattice director vectors then satisfy $\mathbf{d}_{a,b} = \bar{\Gamma}^{..c}_{(ba)}\mathbf{d}_c = \mathbf{d}_{b,a}$ and $\mathbf{d}_{[a,b]} = 0$, and are tangents to holonomic curves $\lambda^a(x,t)$: $\mathbf{d}_a = \tilde{x}^{\alpha}_{.,a}\mathbf{d}_{\alpha} = \tilde{x}^{\alpha}_{.,a}\partial/\partial\tilde{\lambda}^{\alpha} = \partial/\partial\lambda^a$.

3.3.3 Disclinations

The disclination concept is used to describe rotational defects in crystals. In a general sense, such defects may encompass low-angle, high-angle, and twin boundaries. Disclinations can be interpreted as equivalent arrays of dislocations with net Burgers vectors that collectively can be used to represent grain and phase boundaries. Limiting these boundaries to finite strain energy necessitates that they be composed of disclinations of finite size, i.e., partial disclinations compensated by disclination dipoles, termed disclination structural units by Nazarov et al. (2000). Finite elastoplasticity theory has been extended (Clayton et al. 2006) to incorporate continuous distributions of disclinations since such defects can describe size effects and self-organization of dislocation substructure, physical phenomena becoming increasingly evident in experimental characterization of ductile metallic crystals at finer length scales (Pantleon 1996; Hughes et al. 1998; Valiev et al. 2002). By including both dislocations and disclinations in a geometric modeling framework, distinctions naturally emerge among different classes of geometrically necessary defect densities reflecting incompatible deformation modes at multiple length scales. For example, Hughes and co-workers (Hughes et al. 1997, 1998) observed, within deforming ductile FCC metals, the formation of cells of relatively small misorientation organized collectively into larger cell blocks, with average misorientations between blocks usually greater in magnitude than those between cells. With increasing applied strain, cell block sizes generally decrease at a faster rate than do cell sizes (Hughes et al. 1997). In the context of the present geometric theory, the disclination concept can be used to capture gradients of lattice rotation (or alternatively, smoothed variations in orientations of Bravais lattice vectors) in the vicinity of cell block boundaries that arise from organization and superposition of relatively small misorientations between cells. Lattice curvature (i.e., rotation gradients) resulting from the latter (small) misorientations are reflected by geometrically necessary dislocations (Nye 1953). The disclination concept has also been used (Clayton et al. 2008a) to describe misorientations across domain walls in polarized dielectric solids such as ferroelectric ceramic crystals wherein gradients of the polarization field may reflect domain wall energies (Maugin 1988; Shu and Bhattacharya 2001; Xiao et al. 2005).

In the early 20th century, Volterra (1907) introduced six fundamental types of defects in elastic bodies: three types of translational displacement discontinuities, known as edge and screw dislocations, and three types of rotational incompatibilities, later termed disclinations by Frank (1958) and further classified as either wedge or twist disclinations. A detailed treatment of Volterra models of straight dislocation and disclination lines is given in Section C.1 of Appendix C, including linear elastic solutions for isolated line defects embedded in isotropic bodies of infinite extent.

Disclination theory has been applied to numerous problems of interest. These include descriptions of micropolar rotations in liquid crystals (Frank 1958; Cermelli and Fried 2002), rotational defect substructures and strain hardening in metal forming (Romanov 1993; Valiev et al. 2002), grain boundary structure in crystalline solids (Li 1972; Gertsman et al. 1989), deformation twins (Mullner and Romanov 1994; Christian and Mahajan 1995), and polycrystalline triple junctions (Bollmann 1991). Disclinations have also been recognized as characteristic defects in polymers (Li and Gilman 1970) and nanocrystals (Nazarov et al. 1993; Konstantinidis and Aifantis 1998). Molecular dynamics simulations incorporating disclination concepts (Shenderova and Brenner 1999; Nazarov et al. 2000) have been undertaken to characterize grain boundary energy distributions over a range of intergranular misorientations. Spearot et al. (2005) proposed a partial disclination dipole model of distorted lattices in the vicinity of metallic grain boundaries undergoing dislocation emission.

Continuum theories of distributed disclinations can be found in geometrically oriented works of Anthony (1970), Lardner (1973), Kossecka and De Wit (1977), Minagawa (1979, 1981), Amari (1981), and De Wit (1981). In a series of three papers, De Wit (1973) provides a comprehensive account of linear elastic solutions for discrete disclination lines and loops in isotropic and anisotropic solids. Texts of Nabarro (1967), Lardner (1974), Mura (1982), Maugin (1993), and Zubov (1997) also include mathematical descriptions or elastic solutions. Lazar and Maugin (2004) describe the stress field of a wedge disclination using higher gradient elasticity theory. Pecherski (1983, 1985) employs disclination concepts in continuum formulations describing finite elastic-plastic kinematics, strain hardening, dislocation substructure development, and geometrical softening, the latter resulting from local lattice rotations and acting as a potential precursor to shear localization. An extensive review of disclination theory focusing upon kinetics and contributions to plastic strain hardening is provided by Seefeldt (2001), who suggests partial disclination dipoles be used to describe the collective effects of dislocations comprising misoriented subgranular interfaces (i.e., cell block boundaries) manifesting with dislocation substructure refinement in advanced stages of plastic deformation.

Seefeldt et al. (2001) use dislocation-disclination models to predict texture diffusion and cellular refinement commensurate with grain subdivision. Panin (1998) and Makarov et al. (2000) emphasize the role of disclination structures accompanying finite rotations of the microstructure in metals often occurring in conjunction with shear localization triggered by microscopic heterogeneity.

Classification of disclinations as fundamental defects in Bravais crystals has been an occasional subject of debate in the literature (Kroner 1983; Marcinkowski 1990; Kroner and Lagoudas 1992). This argument arises because one generally must consider a larger length scale of observation— e.g., in a discrete disclination model the distance R from the axis of rotation to the point where the discontinuity in displacement is measured—to define the displacement jump associated with a single disclination in a solid crystal than is required for an isolated dislocation, whose effects manifest at a scale on the order of the lattice parameter (i.e., the Burgers vector of a single dislocation). In fact, one may construct a nearly equivalent lattice configuration by replacing disclinations with organized arrays of translational dislocations (Li 1972; De Wit 1981; Seefeldt 2001). While such a reconstruction in terms of dislocations may be capable of capturing the stress fields associated with the original distribution of disclinations, the lattice curvature may not always be identically reproduced (De Wit 1981).

Figure 3.16 shows how a simple tilt boundary may be represented either in terms of edge dislocations (Li 1960; Hull and Bacon 1984) or partial disclination dipoles (Li 1972). In Fig. 3.16, θ is the angle of misorientation, b is the magnitude of the Burgers vector, ω is the magnitude of the Frank vector (i.e., the strength of the individual disclination), h is the spacing between edge dislocations, l is the spacing between disclination dipoles, and $2R$ is the characteristic spacing between partial wedge disclinations comprising each disclination dipole. The tangent line of each defect, directed out of the plane of the figure, is denoted by ξ. Pure twist boundaries may be constructed from either screw dislocations or partial twist disclination dipoles in an analogous fashion (Seefeldt 2001), and general grain boundaries—including all types of coincident-site interfaces such as deformation twins—can be built up from a mixture of dislocation or disclination types.
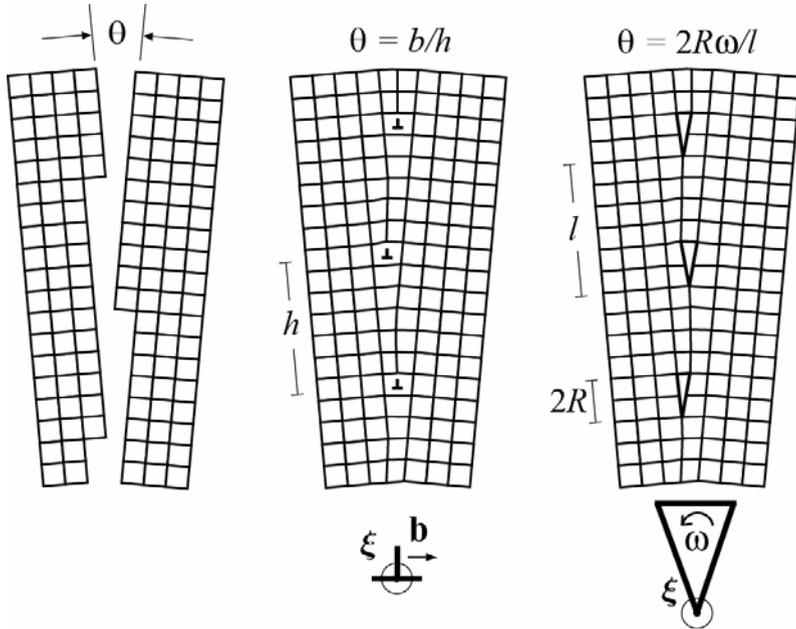
Fig. 3.16 Tilt boundary (left) comprised of edge dislocations (center) or partial disclination dipoles (right)

Partial disclinations are needed to describe lattice misorientations of strength less than 90° in cubic crystal structures and of strength less than 60° in hexagonal crystal structures. Full wedge disclinations ($\omega = \pi/3$) with tangent lines normal to basal planes have been observed experimentally in hexagonal structures (Anthony et al. 1968).

In Fig. 3.17, director vector $\mathbf{d}_a$ is parallel transported about a closed loop to a new vector $\mathbf{d}'_a$ that differs from $\mathbf{d}_a$ by a finite rotation (Lardner 1974). The Cartan displacement about a Burgers circuit corresponding to the dashed line in Fig. 3.17 measures incompatibility induced by the disclination. The disclinated crystal structure exhibits a characteristic pentagonal shape for both (i) a negative wedge disclination with tangent line normal to a {001} plane in a cubic lattice (shown in Fig. 3.17), corresponding to insertion of a 90° wedge of material and (ii) a positive wedge disclination with tangent line normal to a basal {0001} plane in a hexagonal lattice (not shown), corresponding to removal of a 60° wedge of material (De Wit 1971; Clayton et al. 2006). Atomic coordinates differ in these two cases, however, as do elastic stress and strain fields induced by the de-

fect since the algebraic sign and magnitude of ω are different in each case (as are anisotropic elastic constants).

Disclination dipole descriptions are generally required to allow termination of misoriented interfaces over finite distances, providing for bounded elastic energies (Li 1972; Seefeldt 2001). Since the strain energy of a disclination line or loop is proportional to $(R\omega)^2$ —see, e.g., the linear elastic isotropic solutions (C.149), (C.167), and (C.170) in Sections C.1 and C.2 of Appendix C—disclinations tend to organize into dipoles to minimize (i.e., screen) the contribution of R to this energy, and tend to disocciate into partials (De Wit 1981) to minimize the contribution of ω to this energy. Partial disclinations have an associated surface energy (Li 1972), analogous to the stacking fault energy associated with partial dislocations.
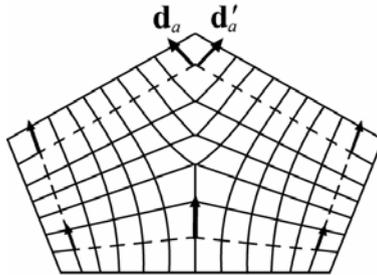
Fig. 3.17 Full negative (90°) wedge disclination in cubic lattice (Lardner 1974)

A differential-geometric description of crystalline solids containing both dislocations and disclinations, based on general concepts introduced in Section 3.3.1, is given in what follows. The linear connection coefficients $\hat{\Gamma}_{cb}^{\;\;a}$ in the dislocation-disclination version of the present framework are given by (3.168), with the covariant components of **Q** restricted to be anti-symmetric (Minagawa 1979, 1981; Clayton et al. 2006):

$$Q_{cba} = Q_{cb}^{\;\;d} C_{da}^L = -Q_{cab} = Q_{c[ba]}, \; Q_{c(ba)} = 0 . \qquad (3.243)$$

Kinematic variable **Q**, termed here a micro-rotation or micropolar rotation, describes spatial gradients of lattice rotation within a crystalline volume element arising from distributed disclinations. The absolute change of director vector $\mathbf{d}_a$ is then expressed in terms of the corresponding covariant derivative $\hat{\nabla}$ as in (3.166):

$$\hat{\nabla}_b \mathbf{d}_a = \partial_b \mathbf{d}_a - F^{Lc}_{\;\;.\alpha} \partial_b F^{L-1\alpha}_{\;\;\;\;.a} \mathbf{d}_c - Q_{b[ac]} \mathbf{d}^c , \qquad (3.244)$$

where (3.163) has been used. Similarly, for contravariant field $\mathbf{d}^a(x,t)$,

$$\hat{\nabla}_b \mathbf{d}^a = \partial_b \mathbf{d}^a + F^{La}_{.\alpha} \partial_b F^{L-1\alpha}_{.c} \mathbf{d}^c + C^{L-1ad} Q_{b[cd]} \mathbf{d}^c . \qquad (3.245)$$

Although (3.154) and (3.155) apply for representative sets of director vectors at the centroid of the volume element under consideration, differential equations (3.193) and (3.194) do not apply when $\mathbf{Q}$ is non-zero. Instead, micro-polar rotation $\mathbf{Q}$ augments the description of spatial gradients of the director vectors obtained from direct differentiation of (3.154) and (3.155).

Consider parallel transport of a covariant lattice director $\mathbf{d}_a$, over small oriented distance $d\mathbf{x}$ to a new orientation $\mathbf{d}'_a$, conducted with respect to covariant derivative (3.244). For illustrative purposes, attention is temporarily restricted to the special case when $\mathbf{F}^L \approx \mathbf{1}$ and spatial gradients of lattice deformation tensor $\mathbf{F}^L$ are negligible. In that case, $\partial_b \mathbf{d}_a = Q_{b[ac]} \mathbf{d}^c$, and

$$\mathbf{d}'_a = \mathbf{d}_a + \mathbf{d}_{a,b} dx^b = \mathbf{d}_a + Q_{b[ac]} dx^b \mathbf{d}^c = (\delta_{ac} + dx^b Q_{b[ac]}) \mathbf{d}^c = \Phi_{ac} \mathbf{d}_c , \quad (3.246)$$

where rotation matrix Φ_{ac} satisfies $\mathbf{\Phi}^T \approx \mathbf{\Phi}^{-1}$ and $\det \mathbf{\Phi} \approx 1$ for small magnitudes of $dx^b Q_{b[ac]}$, i.e., small relative lattice rotations such as those occurring across low-angle grain or subgrain boundaries (Brandon 1966). Notice from (3.246) that Q_{bac} acts in effect as a gradient of rotation in the direction of x^b. However, since $\mathbf{Q}$ is not required to satisfy the following compatibility conditions, it is not a true gradient:

$$Q_{b[ac],d} - Q_{d[ac],b} \neq 0 \rightarrow Q_{b[ac]} \neq \psi_{[ac],b} , \qquad (3.247)$$

where $\psi_{[ac]}$ is a skew matrix that exists only when $Q_{b[ac],d} = Q_{d[ac],b}$.

In general situations, components of $\mathbf{F}^L$ and its spatial gradient may be arbitrarily large. From (3.170), connection (3.168) restricted by conditions (3.243) is metric, since the covariant derivative of $\mathbf{C}^L$ vanishes:

$$\hat{\nabla}_c C^L_{ab} = -2Q_{c(ab)} = 0 . \qquad (3.248)$$

Components of the torsion tensor of connection $\hat{\Gamma}^{.a}_{bc}$ are given by

$$\hat{T}^{.a}_{bc} = \overline{T}^{.a}_{bc} + Q^{.a}_{[bc]} = F^{La}_{.\alpha} F^{L-1\alpha}_{.[c,b]} + Q^{.a}_{[bc]} , \qquad (3.249)$$

where $\overline{T}^{.a}_{cb}$ is the torsion of the crystal connection discussed in Section 3.3.2. Covariant components of the Riemann-Christoffel curvature tensor are, from (3.175) and (3.176),

$$\begin{aligned}
\hat{R}_{ab[cd]} &= 2\hat{\nabla}_{[a} Q_{b][cd]} + 2\hat{T}^{.e}_{ab} Q_{e[cd]}, \\
\hat{R}_{ab(cd)} &= 2\hat{\nabla}_{[a} Q_{b](cd)} + 2\hat{T}^{.e}_{ab} Q_{e(cd)} = 0.
\end{aligned} \qquad (3.250)$$

Thus, from the second of (3.250), the curvature tensor of the connection with micropolar rotations consists of up to nine independent components: $\hat{R}_{abcd} = \hat{R}_{[ab][cd]}$.

Consider a Burgers circuit c in the current configuration, enclosing area a comprised of oriented differential elements $\varepsilon^{bcf} n_f da = dx^b \wedge dx^c$. A total Burgers vector accounting for incompatibility induced by torsion and curvature may be identified with the Cartan displacement of (3.179) (Kondo 1964; Lardner 1973; Minagawa 1979):

$$
\begin{aligned}
\hat{B}^a &= -\int_a \hat{T}_{bc}^{..a} dx^b \wedge dx^c - \frac{1}{2} \int_a C^{L-1ae} \hat{R}_{bc[de]} x^d dx^b \wedge dx^c \\
&= -\varepsilon^{bcf} \int_a \hat{T}_{bc}^{..a} n_f da - \frac{1}{2} \varepsilon^{bcf} \int_a C^{L-1ae} \hat{R}_{bc[de]} x^d n_f da.
\end{aligned}
\tag{3.251}
$$

Total Burgers vector (3.251) reduces to that of (3.213) when disclinations are absent (i.e., when $\hat{T}_{bc}^{..a} = \bar{T}_{bc}^{..a}$, $Q_{bc}^{..a} = 0$, and $\hat{R}_{bcd}^{...a} = 0$). One can re-write (3.251) in terms of the second-order geometrically necessary dislocation tensor $\boldsymbol{\alpha}$ and second-order geometrically necessary disclination tensor $\boldsymbol{\theta}$, each referred to spatial configuration B:

$$
\hat{B}^a = \int_a (\alpha^{af} + C^{L-1ae} \varepsilon_{ehd} \theta^{hf} x^d) n_f da ,
\tag{3.252}
$$

where components of the defect density tensors are, in indicial notation[13],

$$
\alpha^{af} = \varepsilon^{fbc} \hat{T}_{cb}^{..a} , \quad \theta^{gf} = \frac{1}{4} \varepsilon^{gde} \varepsilon^{fbc} \hat{R}_{cbde} .
\tag{3.253}
$$

The disclination density tensor of the second of (3.253) becomes equivalent to the negative transpose of Einstein's tensor of (2.38) when $\varepsilon^{cab} \Rightarrow e^{cab} (\det \mathbf{C}^{\mathbf{L}})^{-1/2}$. Rank two defect density tensors $\boldsymbol{\alpha}$ and $\boldsymbol{\theta}$ of (3.253) enable full reconstruction of rank three torsion tensor $\hat{\mathbf{T}}$ and rank four curvature tensor $\hat{\mathbf{R}}$:

$$
\hat{T}_{cb}^{..a} = \hat{T}_{[cb]}^{..a} = \frac{1}{2} \varepsilon_{bcd} \alpha^{ad} , \quad \hat{R}_{abcd} = \hat{R}_{[ab][cd]} = \varepsilon_{bae} \varepsilon_{cdf} \theta^{fe} .
\tag{3.254}
$$

The tensors of (3.252) are related to summed contributions of discrete defects as

$$
\boldsymbol{\alpha} = \sum_{i=1}^{j} \rho^i \mathbf{b}^i \otimes \boldsymbol{\xi}^i , \quad \boldsymbol{\theta} = \sum_{k=1}^{l} \eta^k \boldsymbol{\omega}^k \otimes \boldsymbol{\xi}^k .
\tag{3.255}
$$

---

[13] As with the dislocation density, the algebraic sign and placement of indices used to define the disclination density tensor vary among authors (Minagawa 1979, 1981; De Wit 1981; Clayton et al. 2005, 2006, 2008).

In (3.255), ρ^i, $\mathbf{b}^i$, and ξ^i are the scalar dislocation line density, Burgers vector, and tangent line, respectively, for dislocation population $i = 1, 2, \ldots j$, while η^k, $\mathbf{\omega}^k$, and ξ^k are the scalar disclination line density, Frank vector, and tangent line, respectively, for disclination population $k = 1, 2, \ldots l$. Complete and partial disclinations may contribute to $\mathbf{\theta}$. The physical definition of the dislocation density tensor $\mathbf{\alpha}$ in the first of (3.255) is identical to (3.215), but the mathematical definition in the first of (3.253) differs from that in (3.214) when $Q_{[cb]}^{\;\;a} \neq 0$. For an element of crystal containing a single dislocation population with uniform Burgers vector and tangent line, and a single disclination population with uniform Frank vector and tangent line, substitution of (3.255) into (3.252) gives

$$\hat{B}^a = \int_a b^a (\rho \xi^f n_f) da + \int_a \varepsilon_{ehd} \omega^h x^d (C^{L-1ae} \eta \xi^f n_f) da , \qquad (3.256)$$

which in turn is the nonlinear analog of displacement jump relation (C.5) for a single Volterra line defect given in Section C.1 of Appendix C.

Complete pull-backs of $\mathbf{\alpha}$ and $\mathbf{\theta}$ to the intermediate configuration $\tilde{B}$ are written

$$\tilde{\alpha}^{\alpha\beta} = J^L F^{L-1\alpha}_{\;\;.a} \alpha^{ab} F^{L-1\beta}_{\;\;.b}$$
$$= J^L \varepsilon^{bcd} F^{L-1\alpha}_{\;\;.c,d} F^{L-1\beta}_{\;\;.b} + J^L F^{L-1\alpha}_{\;\;.a} \varepsilon^{bcd} Q^{\;\;a}_{[dc]} F^{L-1\beta}_{\;\;.b}, \qquad (3.257)$$

$$\tilde{\theta}^{\alpha\beta} = J^L F^{L-1\alpha}_{\;\;.a} \theta^{ab} F^{L-1\beta}_{\;\;.b} = \frac{1}{4} J^L F^{L-1\alpha}_{\;\;.a} \varepsilon^{adg} \varepsilon^{bce} \hat{R}_{[ce][gd]} F^{L-1\beta}_{\;\;.b} , \qquad (3.258)$$

with J^L the Jacobian determinant of $\mathbf{F^L}$ found from (3.48). Notice that (3.257) is consistent with (3.224), and hence (3.226) and (3.227) apply as transformation formulae for dislocation tangent lines, scalar numbers of dislocations per unit volume, and local Burgers vectors. Analogous transformation formulae can be assigned to disclination tangent lines, scalar numbers of disclinations per unit volume, and local Frank vectors in (3.255):

$$\xi^{ka} = F^{La}_{\;\;.\alpha} \tilde{\xi}^{k\alpha} = F^a_{\;.A} \xi^{kA}_0 , \; \eta^k = J^{L-1} \tilde{\eta}^k = J^{-1} \eta^k_0 , \; \omega^{kb} = F^{Lb}_{\;\;.\alpha} \tilde{\omega}^{k\alpha} , \quad (3.259)$$

where tilded quantities are defined on $\tilde{B}$, and quantities with zero subscripts are defined in reference configuration B_0. The analog of (3.226) is then

$$\theta^{ba} n_a da = \sum_{k=1}^l \eta^k \omega^{kb} \xi^{ka} n_a da = \sum_{k=1}^l \tilde{\eta}^k \tilde{\omega}^{k\beta} \tilde{\xi}^{k\alpha} \tilde{n}_\alpha d\tilde{a} = \tilde{\theta}^{\beta\alpha} \tilde{n}_\alpha d\tilde{a} . \qquad (3.260)$$

Kinematic variables $\tilde{\mathbf{\alpha}}$ and $\tilde{\mathbf{\theta}}$ may be regarded as "elastic" in the sense that they are derived completely from lattice kinematic quantities $\mathbf{F^L}$ and

Q and/or spatial gradients of $\mathbf{F}^L$ and **Q,** and not from plastic deformation $\mathbf{F}^P$ or its higher-order gradients.

As discussed in Section 3.3.2, $\tilde{\boldsymbol{\alpha}}$ does not account for curved defect segments and combinations of defect lines that do not contribute to the total Burgers vector. Hence, the same definitions introduced in (3.235)-(3.240) can be used to define total dislocation density tensors, scalar total dislocation densities, and scalar statistically stored dislocation densities. The same statements apply to the geometrically necessary disclination density tensor $\tilde{\boldsymbol{\theta}}$: this tensor does not account for combinations of defect lines and loops whose local Frank vectors cancel and hence do not contribute to the total Burgers vector (3.252). The disclination density can be decomposed into contributions from positively signed disclinations ($\tilde{\boldsymbol{\theta}}_+$) and negatively signed disclinations ($\tilde{\boldsymbol{\theta}}_-$):

$$\tilde{\boldsymbol{\theta}} = \tilde{\boldsymbol{\theta}}_+ + \tilde{\boldsymbol{\theta}}_- = \sum_{k=1}^{l} \left(\tilde{\eta}_+^k - \tilde{\eta}_-^k \right) \tilde{\boldsymbol{\omega}}_+^k \otimes \tilde{\boldsymbol{\xi}}^k , \qquad (3.261)$$

where

$$\tilde{\boldsymbol{\theta}}_+ = \sum_{k=1}^{l} \tilde{\eta}_+^k \tilde{\boldsymbol{\omega}}_+^k \otimes \tilde{\boldsymbol{\xi}}^k , \ \tilde{\boldsymbol{\theta}}_- = \sum_{k=1}^{l} \tilde{\eta}_-^k \tilde{\boldsymbol{\omega}}_-^k \otimes \tilde{\boldsymbol{\xi}}^k , \qquad (3.262)$$

with $\tilde{\eta}_+^k$ and $\tilde{\eta}_-^k$ the densities (line length per unit volume in $\tilde{B}$) of positively and negatively signed disclinations, where, for each value of k, positive and negative disclinations share the same tangent $\tilde{\boldsymbol{\xi}}^k$ but opposite Frank vectors $\tilde{\boldsymbol{\omega}}_+^k = -\tilde{\boldsymbol{\omega}}_-^k$ and if mobile, line velocities $\tilde{\mathbf{v}}_+^k = -\tilde{\mathbf{v}}_-^k$. As explained in Section C.1 of Appendix C, twist disclinations are characterized by $\tilde{\boldsymbol{\omega}} \perp \tilde{\boldsymbol{\xi}}$, while wedge disclinations are characterized by $\tilde{\boldsymbol{\omega}} \parallel \tilde{\boldsymbol{\xi}}$. Thus when a set of disclinations all sharing the same tangent line $\tilde{\boldsymbol{\xi}}^k$ (but different Frank vectors $\tilde{\boldsymbol{\omega}}^k$) is considered, and when orthogonal coordinate axes are introduced in $\tilde{B}$ with one axis aligned along $\tilde{\boldsymbol{\xi}}^k$, wedge disclinations comprise the diagonal components of $\tilde{\boldsymbol{\theta}}$ and twist disclinations comprise the off-diagonal components of $\tilde{\boldsymbol{\theta}}$.

In contrast to (3.261), an absolute or total disclination density tensor $\tilde{\boldsymbol{\theta}}_T$ is defined as (Clayton et al. 2006)

$$\tilde{\boldsymbol{\theta}}_T = \tilde{\boldsymbol{\theta}}_+ - \tilde{\boldsymbol{\theta}}_- = \sum_{k=1}^{l} (\tilde{\eta}_+^k + \tilde{\eta}_-^k) \tilde{\boldsymbol{\omega}}_+^k \otimes \tilde{\boldsymbol{\xi}}^k . \qquad (3.263)$$

When the conditions $\tilde{\boldsymbol{\theta}} = \tilde{\boldsymbol{\theta}}_+ + \tilde{\boldsymbol{\theta}}_- = 0$ apply, then $\tilde{\boldsymbol{\theta}}_T = 2\tilde{\boldsymbol{\theta}}_+ = -2\tilde{\boldsymbol{\theta}}_-$. When such conditions hold, then the total disclination line length L in the crystal

may be nonzero, but the geometrically necessary disclination density vanishes. In such cases, the disclination content of the crystal is limited to statistically stored disclinations, analogous to statistically stored dislocations (Ashby 1970; Arsenlis and Parks 1999) discussed in Section 3.3.2. Statistically stored disclinations give no contribution to the total Burgers vector of (3.252) or the disclination density tensor (3.261). A formal definition for the scalar density $\tilde{\eta}_S^k$ of statistically stored disclinations of population k per unit intermediate volume is

$$\tilde{\eta}_S^k = \tilde{\eta}_T^k - \tilde{\eta}^k \,, \; \eta_S^k = \eta_T^k - \eta^k = J^{L-1}\tilde{\eta}_S^k = J^{L-1}(\tilde{\eta}_T^k - \tilde{\eta}^k) \,, \quad (3.264)$$

where the total scalar density of segments of orientation k and length L^k is

$$\tilde{\eta}_T^k = \lim_{\tilde{V}\to 0}\frac{1}{\tilde{V}}\int_L dL^k = \frac{dL^k}{d\tilde{V}} \geq 0 \,. \quad (3.265)$$

Summation over all l populations leads to the following definitions analogous to those given for scalar dislocation densities in (3.240):

$$\tilde{\eta}_T = \sum_{k=1}^{l}\tilde{\eta}_T^k = \lim_{\tilde{V}\to 0}\frac{1}{\tilde{V}}\int_L dL = \tilde{\eta} + \tilde{\eta}_S \,, \; \tilde{\eta} = \sum_{k=1}^{l}\tilde{\eta}^k \,, \; \tilde{\eta}_S = \sum_{k=1}^{l}\tilde{\eta}_S^k \,. \quad (3.266)$$

Notice that disclination dipoles, when summed over a finite volume, give no contribution to the value of $\tilde{\boldsymbol{\theta}}$ or $\boldsymbol{\theta}$ for that volume, and hence no contribution to the total Burgers vector. In order to measure the misorientation attributed to a wall of disclination dipoles as in Fig. 3.16, one must consider in (3.252) the local field $\boldsymbol{\theta}(x)$ consisting of contributions of infinitesimal Frank vectors $\boldsymbol{\omega}(x)$ with tangent lines $\boldsymbol{\zeta}(x)$ piercing area a enclosed by the Burgers circuit. Even though the average Frank vector of the disclination density tensor may vanish over the entire area, e.g., $\int \theta^{ab}n_b da = 0$, the distribution of disclinations within the area can still produce a nonzero total Burgers vector because of the presence of coordinates x^d in (3.252). Alternatively, by treating each dipole as a single disclination with terminated radius of influence and effective Frank vector of magnitude $2R\omega/l$ (refer to Fig. 3.16), one can use an average value of (3.261) to compute the non-zero contribution of an array of disclination dipoles to the total Burgers vector or to the lattice misorientation across a boundary, as discussed at the conclusion of Section 3.3.3. The stress field and strain energy of such an array of dipoles would differ from that of a distribution of disclinations of the same sign producing the same total Burgers vector.

Continuity equations for dislocation and disclination density tensors in the current configuration follow from Schouten's identity (2.48) and Bianchi's identity (2.50):

$$\hat{R}_{[bcd]}^{\;\;\;a} = 2\hat{\nabla}_{[b}\hat{T}_{cd]}^{\;\;\;a} - 4\hat{T}_{[bc}^{\;\;\;e}\hat{T}_{d]e}^{\;\;\;a}, \;\; \hat{\nabla}_{[e}\hat{R}_{bc]d}^{\;\;\;\;a} = 2\hat{T}_{[eb}^{\;\;\;f}\hat{R}_{c]fd}^{\;\;\;\;a}. \tag{3.267}$$

Substitution of (3.254) gives for the first of (3.267):

$$C^{L-1ae}\varepsilon_{[bc|g|}\varepsilon_{d]ef}\theta^{fg} = \hat{\nabla}_{[b}\alpha^{\;ae}\varepsilon_{cd]e} + \varepsilon_{[bc|f|}\varepsilon_{d]eg}\alpha^{ag}\alpha^{ef}, \tag{3.268}$$

and for the second of (3.267):

$$\hat{\nabla}_{[e}(C^{L-1ag}\varepsilon_{cb]h}\varepsilon_{dgf}\theta^{fh}) = \varepsilon_{[be|k|}\alpha^{fk}C^{L-1ag}\varepsilon_{c]hf}\varepsilon_{dgm}\theta^{mh}. \tag{3.269}$$

The geometrically linear dislocation-disclination theory is now formally considered. From (3.181), (3.186), (3.187), and (3.189), using (3.243):

$$\hat{\Gamma}_{cb}^{\;\;a} \approx -\beta_{\;\;b,c}^{La} + Q_{cb}^{\;\;a}; \tag{3.270}$$

$$\hat{\Gamma}_{c(ba)} \approx \frac{1}{2}\partial_c C_{\;(ba)}^{L}, \;\; \hat{\Gamma}_{c[ba]} \approx \partial_c\beta_{\;[ba]}^{L} + Q_{c[ba]}; \tag{3.271}$$

$$\hat{T}_{cb}^{\;\;a} \approx \beta_{\;[c,b]}^{La} + Q_{[cb]}^{\;\;a}; \tag{3.272}$$

$$\hat{R}_{bc[da]} \approx 2\partial_{[b}Q_{c][da]}, \;\; \hat{R}_{bc(da)} = 0. \tag{3.273}$$

The second of (3.271) can be written as

$$\hat{\Gamma}_c^{[ba]} \approx \partial_c\Omega^{L[ba]} + Q_c^{[ba]} = \varepsilon^{abd}\kappa_{dc}^{L}, \tag{3.274}$$

where elastic bend-twist $\kappa^{\mathbf{L}}$ and micropolar rotation $\boldsymbol{\varphi}$ are defined by

$$\kappa_{ab}^{L} = -\frac{1}{2}\varepsilon_{acd}\Omega_{\;\;,b}^{L[cd]} - \varphi_{ab}, \;\; \varphi_{ab} = \frac{1}{2}\varepsilon_{acd}Q_b^{[cd]}. \tag{3.275}$$

The dislocation density tensor of (3.253) becomes

$$\alpha^{af} = \varepsilon^{fbc}(\beta_{\;.c,b}^{La} + Q_{cb}^{\;.a}) = \varepsilon^{fbc}(\beta_{\;.c,b}^{La} + \delta_{bd}\varepsilon^{dae}\varphi_{ec}), \tag{3.276}$$

while the disclination density tensor in (3.253) can be expressed as

$$\theta^{gf} = \frac{1}{2}\varepsilon^{gde}\varepsilon^{fbc}\partial_{[c}Q_{b][de]} = \frac{1}{2}\varepsilon^{gde}\varepsilon^{fbc}\varepsilon_{deh}\partial_{[c}\varphi_{.b]}^{h} = \varepsilon^{fbc}\varphi_{.b,c}^{g}. \tag{3.277}$$

Continuity equations in the linearized case can then be obtained by direct substitution into (3.268) and (3.269), replacing covariant derivatives with partial derivatives and omitting higher-order terms:

$$\delta^{ae}\varepsilon_{[bc|g|}\varepsilon_{d]ef}\theta^{fg} = \partial_{[b}\alpha^{\;ae}\varepsilon_{cd]e}, \tag{3.278}$$

$$\varepsilon_{daf}\partial_{[e}\theta^{fh}\varepsilon_{bc]h} = 0. \tag{3.279}$$

In the context of a geometrically linear formulation, De Wit (1981) inferred from equations analogous to (3.279) that disclination lines cannot end abruptly within a crystalline body, and from equations analogous to (3.278) that disclinations may act as sources or sinks for dislocations.

Consider now the three-term decomposition of (3.137), wherein the lattice deformation is decomposed as $\mathbf{F^L} = \mathbf{F^E}\mathbf{F^I} = \mathbf{V^E}\mathbf{R^E}\mathbf{R^I}\mathbf{U^I}$. Following Lardner (1973, 1974), the rotational part $\mathbf{R^I}$ of $\mathbf{F^I}$, when the former is at-

tributed solely to disclinations within a volume element of crystal, can be associated with the change in orientation of a vector with unit components ($x^d \to 1$ in (3.251)) upon parallel transport around a closed circuit of area a containing a non-vanishing disclination density $\boldsymbol{\theta}$ (Clayton et al. 2006):

$$
R^{I\alpha}_{\cdot\beta} = g^{\alpha}_{\cdot a}\left(\delta^{a}_{\cdot d} - \frac{1}{2}\int_a \hat{R}^{\cdot\cdot a}_{bcd} dx^b \wedge dx^c \right) g^{d}_{\cdot\beta}
$$

$$
= \delta^{\alpha}_{\cdot\beta} + g^{\alpha}_{\cdot a} g^{d}_{\cdot\beta} \int_a C^{L-1ae}\varepsilon_{ehd}\theta^{hf} n_f\, da
$$

$$
\approx \delta^{\alpha}_{\cdot\beta} + g^{\alpha}_{\cdot a} g^{d}_{\cdot\beta} C^{L-1ae}\varepsilon_{ehd} \int_a \theta^{hf} n_f\, da \qquad (3.280)
$$

$$
= \delta^{\alpha}_{\cdot\beta} + g^{\alpha}_{\cdot a} g^{d}_{\cdot\beta} C^{L-1ae}\varepsilon_{deh}\hat{\Omega}^{h}
$$

$$
\approx g^{\alpha e} g^{d}_{\cdot\beta}(\delta_{de} + \varepsilon_{deh}\hat{\Omega}^{h}),
$$

and where in the third equality of (3.280), a constant lattice stretch has been assumed over a, such that the net Frank vector $\hat{\Omega}^{h} = \int \theta^{hf} n_f\, da$ acts in Cartesian coordinates as the axial vector of $\mathbf{R}^{I} - \mathbf{1}$, meaning that $\mathbf{R}^{I}$ is truly orthogonal only in the limit of small lattice stretch and small rotations as implied in the final expression. Notice that (3.280) is non-unique in the sense that $\mathbf{R}^{I}$ depends on choice of oriented area element $\mathbf{n}da$. In a crystal plasticity framework (Section 3.2.6), one possible means of addressing this integral involves a discrete sum over area elements on representative set of crystallographic planes (e.g., low-index or slip planes) (Clayton et al. 2006). A more general approach advocated here, accounting for all possible orientations $\mathbf{n}$, is prescription of the domain of integration in (3.280) as a spherical half-shell (in orientation space) of radius ℓ :

$$
R^{I\alpha}_{\cdot\beta} = \delta^{\alpha}_{\cdot\beta} + \ell^2 g^{\alpha}_{\cdot a} g^{d}_{\cdot\beta} \int_0^{\pi}\int_0^{\pi} C^{L-1ae}\varepsilon_{ehd}\theta^{hf} n_f (\sin\phi)(d\phi)(d\varphi), \qquad (3.281)
$$

where θ^{hf} is expressed in rectangular coordinates, unit normal components are $n_1 = \sin^2\phi\cos^2\varphi$, $n_2 = \sin^2\phi\sin^2\varphi$, and $n_3 = \cos^2\phi$, and ℓ^2 corresponds to the effective area over which the disclinations act. In the limit that the crystal volume element shrinks to infinitesimal size (see Fig. 3.12), $\ell \to 0$, and effects of disclinations cannot be resolved by the multiplicative decomposition of the deformation gradient (3.137).

Dislocation-disclination theory may be applied to describe evolution of cellular defect substructures observed in ductile metallic crystals deformed at low homologous temperatures to relatively large total strains (Stout and Rollett 1990; Pantleon 1996; Hughes et al. 1997, 1998; Valiev et al. 2002).

As shown in the left part of Fig. 3.18, this substructure consists of nearly equiaxed cells with interiors of relatively low defect density, separated by incidental dislocation boundaries (IDBs) across which lattice misorientations are generally of the low-angle variety, for example, limited to less than 10° in aluminum and nickel cold-rolled to 100% effective strain (Hughes et al. 2003). With increasing applied strain, the cells tend to organize collectively into bands or cell blocks, often elongated in shape in a direction depending upon the initial texture and loading conditions. The cell blocks are separated by dislocation walls termed geometrically necessary boundaries (GNBs), across which misorientations can reach high-angle magnitudes, i.e., in excess of 15°. Both GNBs and IDBs are thought to contain mixed populations of statistically stored and geometrically necessary dislocations (Hughes et al. 2003).
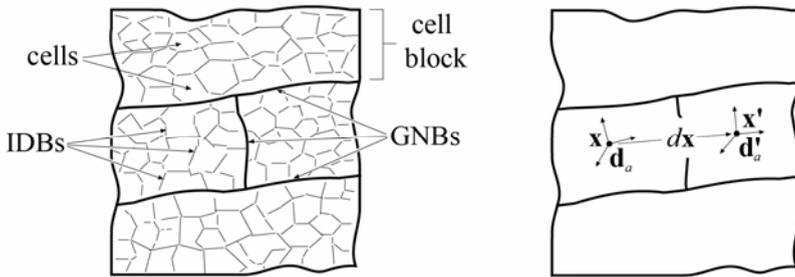
Fig. 3.18 Dislocation substructure (left) and lattice director vectors (right) in a severely plastically deformed (SPD) single crystal

In the context of the present geometric framework, kinematics of defect substructure can be described as follows. Redundant dislocations and disclinations that contribute no net misorientation are grouped collectively into statistically stored dislocation and disclination scalars: line lengths per unit spatial volume ρ_S and η_S, respectively, as introduced following (3.238) and (3.264), respectively. Geometrically necessary dislocations comprising $\boldsymbol{\alpha}$ represent non-redundant defects corresponding to fluctuations in lattice orientation in the vicinity of the cell boundaries, i.e., IDBs. Micropolar rotation variable $\mathbf{Q}$ (in conjunction with associated net disclination density tensor $\boldsymbol{\theta}$) measures the non-redundant defect content of the cell block boundaries, i.e., GNBs. Fractions of dislocations and disclinations that are non-redundant or geometrically necessary as opposed to redundant or statistically stored may differ since they represent different features of the microstructure.

The general theory developed in Section 3.3.3 places no restriction on characteristic spacing or strength (i.e., magnitude of angle) of the misoriented boundary to which is attributed a particular type of defect density. For example, dislocations could alternatively comprise GNBs and disclinations could comprise IDBs, or a mixture of defect types could comprise each kind of boundary. The decision to model GNBs with the disclination density and IDBs with the dislocation density stems from both convenience and from physical considerations in agreement with models set forth in prior literature (Panin 1998; Seefeldt 2001). Thus, the rotational units that serve to accommodate inelastic deformation and subgranular incompatibility seen at comparatively large strains are associated with disclinations (GNBs), with geometrically necessary dislocations capturing the local misorientations across IDBs arising at a smaller length scale. From this standpoint, with inelastic straining, dislocations accumulate first, and then later organize into disclination structures at larger applied deformations (Seefeldt 2001; Valiev et al. 2002).

The micro-rotation concept in the context of GNBs and IDBs is illustrated on the right side of Fig. 3.18. Let $\mathbf{x}$ and $\mathbf{x}'$ be spatial coordinates of material points in neighboring cell blocks, with corresponding lattice director vectors $\mathbf{d}_a$ and $\mathbf{d}'_a$. Recall that by definition, in configuration $\tilde{B}$ director vector triads are parallel, leading to

$$\mathbf{d}_\alpha = \mathbf{d}'_\alpha . \tag{3.282}$$

Let $\mathbf{F^L}$ and $\mathbf{F^{L'}}$ denote the local lattice deformations at $\mathbf{x}$ and $\mathbf{x}'$, respectively. Pre-multiplying both sides of (3.282) by $\mathbf{F^{L'-1}}$ results in

$$\mathbf{d}'_a = \left[F^{L-1\alpha}_{.a} + \frac{F^{L'-1\alpha}_{.a} - F^{L-1\alpha}_{.a}}{x'^c - x^c}(x'^c - x^c) \right] F^{Lb}_{.\alpha} \mathbf{d}_b . \tag{3.283}$$

From (3.166), (3.168), and assertion of parallel transport (i.e., $\hat{\nabla}_b \mathbf{d}_a = 0$),

$$\mathbf{d}'_a = (F^{L-1\alpha}_{.a} + F^{L-1\alpha}_{.a,c} dx^c + F^{L-1\alpha}_{.d} Q^{.d}_{ca} dx^c) F^{Lb}_{.\alpha} \mathbf{d}_b , \tag{3.284}$$

where $dx^c = x'^c - x^c$ and $\mathbf{d}'_a - \mathbf{d}_a \approx \mathbf{d}_{a,b} dx^b$. Comparing (3.283) and (3.284), $\mathbf{Q}$ reflects the possible inability of the first spatial gradient of $\mathbf{F^{L-1}}$ to capture the change in the directors over small distance dx^c:

$$Q^{.d}_{ca} = F^{Ld}_{.\alpha} \left(\frac{F^{L'-1\alpha}_{.a} - F^{L-1\alpha}_{.a}}{dx^c} - F^{L-1\alpha}_{.a,c} \right). \tag{3.285}$$

One can think of $\mathbf{Q}$ as implicitly representative of cumulative effects of all higher than first-order gradients of the (inverse) lattice deformation $\mathbf{F^{L-1}}$ on the spatial variation of the lattice directors. In many higher-order gra-

dient crystal plasticity theories from the more recent literature (Naghdi and Srinivasa 1993; Le and Stumpf 1996a, b, c; Shizawa and Zbib 1999; Acharya 2001; Bammann 2001; Regueiro et al. 2002; Garikipati 2003; Clayton et al. 2004b), the first-order gradient of the elastic or plastic deformation influences the material response, for example through its manifestation in the dislocation density tensor. However, by including the micro-rotation variable $\mathbf{Q}$, potentially nonlinear spatial variations in lattice directors between neighboring material points are captured. This nonlinearity arises in the dislocation density $\boldsymbol{\alpha}$ and in the disclination density $\boldsymbol{\theta}$ through variable $\mathbf{Q}$ and its spatial gradient, respectively. It is noted that $Q_{bc}^{.a}$ is not an explicit function of higher-order lattice deformation gradients $F^{L-1\alpha}_{.a,bc}$, $F^{L-1\alpha}_{.a,bcd}, \dots$; rather, $\mathbf{Q}$ is an independent kinematic variable.

The disclination concept has been extended to describe domain boundaries in spontaneously polar perovskite crystals (Clayton et al. 2008a). Consider a finite wedge disclination density—e.g., a set of partial wedge disclination dipoles (Li 1972)—with net nonzero component $\theta^{11} = \eta\omega$, meaning both the axis of rotation ($\boldsymbol{\zeta}$) and the effective rotation vector ($\boldsymbol{\omega}$) are aligned along the x^1-direction in the sample. An effective disclination density tensor in this case can be used to represent a tilt boundary with misorientation vector aligned along the x^1-direction. In this construction, each dipole is replaced with a single disclination line of strength ω whose Frank vector terminates at a distance R from the core of the defect, i.e., at the position of the other disclination line comprising the dipole in Fig. 3.16. To represent domain walls in barium strontium titanate (BST), for example, let $\eta \propto 1/\ell_D^2$ where ℓ_D is the typical domain or grain size, on the order of 50 nm in representative BST thin films (Cole et al. 2003). Referring to Fig. 3.16, for a standard low-angle boundary, $\theta \leq \pi/12$ (Brandon 1966), while $\theta = \pi/2$ and $\theta = \pi$ are energetically favorable misorientations across domain walls in non-cubic phases of some kinds of ferroelectric crystals (Shu and Bhattacharya 2001). For closely packed disclination dipoles, $2R = l$ and $\theta = \omega$ in Fig. 3.16.

3.3.4 Point Defects

Attention is now focused on a geometric representation of uniformly distributed point defects within a volume element of a crystal structure. Recall that the contribution $\mathbf{F}^{\mathbf{V}}$ of such defects to the lattice deformation $\mathbf{F}^{\mathbf{L}}$ of the total deformation gradient $\mathbf{F}$ for such an element is described in Section 3.2.8, specifically in (3.128)-(3.136). The corresponding micro-

scopic description, at a more refined length scale of explicitly resolved gradients in the lattice directors, is given in what follows. The same connection coefficients $\hat{\Gamma}^{..a}_{bc}(x,t)$ listed in (3.168) are used, but the form of $\mathbf{Q}$ is restricted as (Minagawa 1979, 1981; Clayton et al. 2005, 2008a)

$$\hat{\Gamma}^{..a}_{cb} = F^{La}_{.\alpha}F^{L-1\alpha}_{.b,c} + Q^{..a}_{cb} = \bar{\Gamma}^{..a}_{cb} + \Upsilon_c\delta^a_{.b}, \quad Q^{..a}_{cb} = \Upsilon_c\delta^a_{.b}, \quad (3.286)$$

while the covariant version of $\mathbf{Q}$ is $Q_{cba} = \Upsilon_c C^L_{ba} = \Upsilon_c C^L_{(ba)}$. From (3.166),

$$\hat{\nabla}_c\mathbf{d}_a dx^c = \mathbf{d}_{a,c} dx^c - \bar{\Gamma}^{..b}_{ca} dx^c\mathbf{d}_b - \Upsilon_c dx^c\mathbf{d}_a, \quad (3.287)$$

implying that the contribution from point defects to derivative $\hat{\nabla}_c\mathbf{d}_a$ is an isotropic stretch of magnitude $|\Upsilon_c dx^c|$. Considering for the moment the case when the crystal connection coefficients vanish and the directors undergo parallel transport, and letting $dx^c = x'^c - x^c$, (3.287) results in

$$\mathbf{d}'_a = \mathbf{d}_a + \mathbf{d}_{a,c} dx^c = (1 + \Upsilon_c dx^c)\mathbf{d}_a, \quad \partial_c\mathbf{d}_a = \Upsilon_c\mathbf{d}_a. \quad (3.288)$$

The connection in (3.286) is non-metric, since by (3.170),

$$\hat{\nabla}_c C^L_{ab} = -2\Upsilon_c C^L_{ab}, \quad (3.289)$$

meaning physically that vacancies, interstitials, or voids alter the counting of atomic steps in the crystal (Kroner 1981, 1990). The torsion tensor is, upon substitution of (3.286) into (3.171),

$$\hat{T}^{..a}_{cb} = \bar{T}^{..a}_{cb} + \Upsilon_{[c}\delta^a_{.b]}, \quad (3.290)$$

From (3.174) or (3.175), skew components of the covariant Riemann-Christoffel curvature tensor vanish identically since C^L_{ab} is symmetric:

$$\hat{R}_{[bc][da]} = 2\hat{\nabla}_{[b}\Upsilon_{c]}C^L_{[da]} + 2\hat{T}^{..e}_{bc}\Upsilon_e C^L_{[da]} = 0. \quad (3.291)$$

From (3.176), symmetric components of the curvature tensor are

$$\hat{R}_{[bc](da)} = 2(\hat{\nabla}_{[b}\Upsilon_{c]} + \hat{T}^{..e}_{bc}\Upsilon_e)C^L_{da} = 2(\partial_{[b}\Upsilon_{c]} - \hat{\Gamma}^{..e}_{[bc]}\Upsilon_e + \hat{T}^{..e}_{bc}\Upsilon_e)C^L_{da}$$
$$= 2\partial_{[b}\Upsilon_{c]}C^L_{da}. \quad (3.292)$$

The total Burgers vector resulting from Cartan displacement (3.179) is

$$\hat{B}^a = -\int_a\left[\hat{T}^{..a}_{bc} + \frac{1}{2}C^{L-1ae}\hat{R}_{bc(de)}x^d\right]dx^b \wedge dx^c$$
$$= -\int_a(\bar{T}^{..a}_{bc} + \Upsilon_{[b}\delta^a_{.c]})dx^b \wedge dx^c + \int_a\Upsilon_{[b,c]}x^a dx^b \wedge dx^c$$
$$= -\varepsilon^{bce}\int_a(\bar{T}^{..a}_{bc} + \Upsilon_{[b}\delta^a_{.c]})n_e da + \varepsilon^{bce}\int_a\Upsilon_{[b,c]}x^a n_e da \quad (3.293)$$
$$= \int_a\alpha^{ae}n_e da + \int_a x^a \vartheta^e n_e da,$$

where the dislocation density tensor $\boldsymbol{\alpha}$ is defined in terms of the torsion in the same way as in (3.253) and (3.254):

$$\alpha^{ae} = \varepsilon^{cbe}\hat{T}_{bc}^{..a} = \varepsilon^{cbe}F^{La}_{.\alpha}F^{L-1\alpha}_{.c,b} - \varepsilon^{cbe}\Upsilon_c\delta^a_{.b}, \quad 2\hat{T}_{bc}^{..a} = \varepsilon_{cbe}\alpha^{ae}, \qquad (3.294)$$

and components of the point defect vector (Clayton et al. 2008a) satisfy[14]

$$\mathcal{G}^e = \varepsilon^{ebc}\Upsilon_{b,c} = \varepsilon^{ecb}(\hat{\nabla}_{[b}\Upsilon_{c]} + \hat{T}_{bc}^{..e}\Upsilon_e)$$

$$= \frac{1}{3}\delta^a_{.a}\varepsilon^{ecb}(\hat{\nabla}_{[b}\Upsilon_{c]} + \hat{T}_{bc}^{..e}\Upsilon_e)$$

$$= \frac{1}{6}C^{L-1ad}\varepsilon^{ecb}(2\hat{\nabla}_{[b}\Upsilon_{c]} + 2\hat{T}_{bc}^{..e}\Upsilon_e)C^L_{(da)} \qquad (3.295)$$

$$= \frac{1}{6}C^{L-1ad}\varepsilon^{ecb}\hat{R}_{[bc](ad)}.$$

When (3.291) applies, the disclination density of (3.253) and (3.254) vanishes. Dislocation density $\boldsymbol{\alpha}$ has the same physical interpretation as that given in (3.215) of Section 3.3.2, but differs mathematically from (3.214) by the term $\varepsilon^{bce}\Upsilon_{[c}\delta^a_{.b]}$. From (3.295), it follows that $2\Upsilon_{[b,c]} = \varepsilon_{bcd}\mathcal{G}^d$.

A local differential Burgers vector induced by the point defect vector is

$$d\hat{B}^a = x^a\Upsilon_{b,c}dx^b \wedge dx^c = x^a\mathcal{G}^e n_e da = x^a\left[\frac{\delta\chi^e}{dx^b dx_b}\right]n_e da = x^a\delta\chi, \quad (3.296)$$

where the following definitions apply:

$$\delta\chi^e = n^e\delta\chi = \mathcal{G}^e da = \mathcal{G}^e dx^b dx_b, \quad \delta\chi = \sqrt{\delta\chi^e\delta\chi_e}, \quad da = \sqrt{dx^b dx_b}. \quad (3.297)$$

From (3.296) and (3.297), one then may write

$$x^a + d\hat{B}^a = (1+\delta\chi)x^a = (1+\mathcal{G}^e n_e da)x^a, \qquad (3.298)$$

where $\delta\chi$ represents a microscopic isotropic expansion ($\delta\chi > 0$) or contraction ($\delta\chi < 0$). Consider the case when the point defects correspond to atomic vacancies in the lattice. Analogous to the situation for continuous distributions of dislocations discussed in Section 3.3.2, let the radius of each vacancy shrink to zero and the number of vacancies in each volume element tend to infinity, such that their product remains finite. Let $\delta\chi$ represent a constant spherical stretch of the lattice produced by a concentration of vacancies at the origin $x^a = 0$. Coordinates of a nearby point x' after application of this microstretch are then $(1+\delta\chi)x'^a$. A ,simple physically motivated assumption is that $\delta\chi$ is equivalent to the vacancy concen-

---

[14] A factor of 1/6 was unintentionally omitted in (23)₁ of Clayton et al. (2008a). That misprint is corrected here in (3.295). The opposite sign convention was used in that work for the Cartan displacement.

tration at x minus that at x' (Clayton et al. 2008a). Bianchi's identity in the second of (3.267) becomes for the present case

$$\hat{\nabla}_{[e}\Upsilon_{c,b]} = \hat{T}_{[eb}^{..f}\partial_{c]}\Upsilon_f \Leftrightarrow \hat{\nabla}_{[e}\vartheta^a\varepsilon_{cb]a} = \varepsilon_{[be|a|}\alpha^{fa}\partial_{c]}\Upsilon_f, \qquad (3.299)$$

providing a continuity equation for the point defect vector.

The geometrically linear theory is now reconsidered for crystals with dislocations and point defects. From (3.181), (3.186), (3.187), and (3.189), using (3.286):

$$\hat{\Gamma}_{cb}^{..a} \approx -\beta^{La}_{.b,c} + \Upsilon_c\delta^a_{.b}; \qquad (3.300)$$

$$\hat{\Gamma}_{c(ba)} \approx \frac{1}{2}\partial_c C^L_{(ba)} + \Upsilon_c C^L_{(ba)}, \quad \hat{\Gamma}_{c[ba]} \approx \partial_c \beta^L_{[ba]}; \qquad (3.301)$$

$$\hat{T}_{cb}^{..a} \approx \beta^{La}_{[c,b]} + \Upsilon_{[c}\delta^a_{.b]}; \qquad (3.302)$$

$$\hat{R}_{bc[da]} = 0, \quad \hat{R}_{bc(da)} \approx 2\partial_{[b}\Upsilon_{c]}\delta_{da}. \qquad (3.303)$$

The dislocation density tensor of (3.294) and point defect vector of (3.295) are

$$\alpha^{af} \approx \varepsilon^{fbc}(\beta^{La}_{.c,b} + \Upsilon_{[c}\delta^a_{.b]}), \quad \vartheta^e = \varepsilon^{ebc}\Upsilon_{[b,c]}, \qquad (3.304)$$

where the latter evidently is the same in both linear and nonlinear descriptions. The linear disclination density tensor in (3.277) vanishes. The continuity equation (3.299) in linearized form is

$$\partial_{[e}\Upsilon_{c,b]} = 0 \Leftrightarrow \partial_{[e}\vartheta^a\varepsilon_{cb]a} = 0. \qquad (3.305)$$

Consider now a linear connection formed by superposition of components of the crystal connection with skew and symmetric components of **Q** introduced, respectively, in (3.243) and (3.286):

$$\hat{\Gamma}_{cb}^{..a} = \overline{\Gamma}_{cb}^{..a} + C^{L-1ad}Q_{c[bd]} + \Upsilon_c\delta^a_{.b}, \qquad (3.306)$$

where $C^{L-1ad}Q_{c[bd]}$ accounts for disclinations according to Section 3.3.3 and $\Upsilon_c\delta^a_{.b}$ accounts for point defects as discussed above. In this case,

$$\hat{\nabla}_c C^L_{ab} = -2\Upsilon_c C^L_{ab}, \qquad (3.307)$$

$$\hat{T}_{cb}^{..a} = \overline{T}_{cb}^{..a} + \frac{1}{4}C^{L-1ae}(Q_{cbe} - Q_{bce} - Q_{ceb} + Q_{bec}) + \Upsilon_{[c}\delta^a_{.b]}. \qquad (3.308)$$

Skew components of the covariant Riemann-Christoffel curvature tensor are identical to the first of (3.250):

$$\hat{R}_{[bc][da]} = 2\hat{\nabla}_{[b}Q_{c][da]} + 2\hat{T}_{bc}^{..e}Q_{e[da]} + \Upsilon_{[b}\Upsilon_{c]}C^L_{[da]}$$
$$= 2\hat{\nabla}_{[b}Q_{c][da]} + 2\hat{T}_{bc}^{..e}Q_{e[da]}. \qquad (3.309)$$

From (3.176), symmetric components of the curvature tensor are identical to (3.292):

$$\hat{R}_{[bc](da)} = 2(\hat{\nabla}_{[b}\Upsilon_{c]} + \hat{T}_{bc}^{..e}\Upsilon_e)C_{da}^L = 2\partial_{[b}\Upsilon_{c]}C_{da}^L. \tag{3.310}$$

The total Burgers vector resulting from Cartan displacement (3.179) is

$$\hat{B}^a = -\int_a \left[\hat{T}_{bc}^{..a} + \frac{1}{2}C^{L-1ae}\hat{R}_{bc[de]}x^d + \frac{1}{2}C^{L-1ae}\hat{R}_{bc(de)}x^d \right]dx^b \wedge dx^c$$

$$= -\int_a \hat{T}_{bc}^{..a}dx^b \wedge dx^c - \frac{1}{2}\int_a C^{L-1ae}\hat{R}_{bc[de]}x^d dx^b \wedge dx^c + \int_a \Upsilon_{[b,c]}x^a dx^b \wedge dx^c$$

$$= -\varepsilon^{bcf}\int_a \hat{T}_{bc}^{..a}n_f da - \frac{1}{2}\varepsilon^{bcf}\int_a C^{L-1ae}\hat{R}_{bc[de]}x^d n_f da + \varepsilon^{bcf}\int_a \Upsilon_{[b,c]}x^a n_f da$$

$$= \int_a \alpha^{af}n_f da + \int_a C^{L-1ae}\varepsilon_{ehd}\theta^{hf}x^d n_f da + \int_a x^a \vartheta^f n_f da, \tag{3.311}$$

where spatial components of the defect density tensors are, in indicial notation,

$$\alpha^{af} = \varepsilon^{fbc}\hat{T}_{cb}^{..a}, \quad \theta^{gf} = \frac{1}{4}\varepsilon^{gde}\varepsilon^{fbc}\hat{R}_{cbde}; \tag{3.312}$$

$$\vartheta^f = \varepsilon^{bcf}\Upsilon_{b,c} = \frac{1}{6}C^{L-1de}\varepsilon^{fbc}\hat{R}_{[cb](de)}. \tag{3.313}$$

Definitions (3.312) and (3.313) agree with (3.253) and (3.295), and can be inverted to reconstruct the torsion and curvature tensors:

$$2\hat{T}_{cb}^{..a} = \varepsilon_{bcf}\alpha^{af}, \quad \hat{R}_{cb[de]} = \varepsilon_{fbc}\varepsilon_{gde}\theta^{gf}, \quad \hat{R}_{cb(de)} = \varepsilon_{bcf}\vartheta^f C_{de}^L. \tag{3.314}$$

Substitution of (3.314) into identities (3.267) then provides continuity equations relating dislocation and disclination density tensors, the point defect vector, and their covariant derivatives:

$$C^{L-1ae}\varepsilon_{[bc|g|}\varepsilon_{d]ef}\theta^{fg} + \delta_{[d}^a\varepsilon_{bc]f}\vartheta^f = \hat{\nabla}_{[b}\alpha^{ae}\varepsilon_{cd]e} + \varepsilon_{[bc|f|}\varepsilon_{d]eg}\alpha^{ag}\alpha^{ef}, \tag{3.315}$$

$$\hat{\nabla}_{[e}(C^{L-1ag}\varepsilon_{cb]h}\varepsilon_{dgf}\theta^{fh}) + \hat{\nabla}_{[e}\vartheta^f\varepsilon_{cb]f}\delta_{.d}^a$$

$$= \varepsilon_{[be|k|}\alpha^{fk}C^{L-1ag}\varepsilon_{c]hf}\varepsilon_{dgm}\theta^{mh} + \frac{1}{2}\varepsilon_{[be|k|}\alpha^{fk}\varepsilon_{c]gf}\vartheta^g\delta_{.d}^a. \tag{3.316}$$

3.3.5 Summary

The theory presented in Section 3.3 is founded upon two major assumptions, the first being multiplicative decomposition (3.31), $\mathbf{F} = \mathbf{F^L}\mathbf{F^P}$, of the average deformation gradient $\mathbf{F}$ for a volume element of a crystalline solid, where plastic deformation attributed to the flux of mobile crystal defects, $\mathbf{F^P}$, is lattice-preserving or lattice invariant, and where $\mathbf{F^L}$ accounts for stretch and rotation of the lattice. Lattice deformation $\mathbf{F^L}$ can be further

decomposed into recoverable and residual parts according to (3.137), but such an enhanced description is not necessary in the context of Section 3.3. The second major assumption is an additive decomposition of a linear connection describing spatial gradients of lattice director vectors between neighboring crystalline elements, i.e., a microscopic description. Coefficients of this connection, introduced in (3.168), may be written as

$$\hat{\varGamma}^{..a}_{cb} = \underbrace{F^{La}_{.\alpha}\partial_c F^{L-1\alpha}_{.b}}_{\substack{\text{crystal}\\\text{connection}\\\text{(dislocations)}}} + \underbrace{C^{L-1ad}Q_{c[bd]}}_{\substack{\text{micro-rotation}\\\text{(disclinations)}}} + \underbrace{\delta^a_{.b}\varUpsilon_c}_{\substack{\text{micro-}\\\text{dilatancy}\\\text{(point defects)}}} + \underbrace{C^{L-1ad}(Q_{c(bd)} - \varUpsilon_c C^L_{bd})}_{\substack{\text{micro-strain}\\\text{(Somigliana dislocations)}}} \quad (3.317)$$

where the first term on the right side of (3.317) describes gradients of the director vectors attributed to first-order spatial gradients of the average lattice deformation tensor $\mathbf{F^L}$ at the centroid of the volume element, following Bilby et al. (1955), as discussed in Section 3.3.2. Micromorphic variable $\mathbf{Q}$ (Minagawa 1979; De Wit 1981; Clayton et al. 2005, 2008a) participates in the remaining three terms on the right of (3.317): a micro-rotation associated with disclinations as discussed in Section 3.3.3, a spherical micromorphic expansion or contraction associated with point defects as discussed in Section 3.3.4, and a general micromorphic strain that may be used to represent arbitrary lattice director deformations when combined with the other terms in (3.317). Defect densities then follow from contributions of the torsion and curvature of the connection to the Cartan displacement defined generically in (3.177). When the rightmost term is absent in (3.317) and $Q_{c(bd)} = \varUpsilon_c C^L_{bd}$, then suitable definitions for defect densities are given in (3.312)-(3.313). On the other hand, when $Q_{c(bd)} \neq \varUpsilon_c C^L_{bd}$, alternative definitions of defect densities are possible.

Table 3.5 provides classifications of the affine geometries corresponding to various crystal defects (Clayton et al. 2005), following the geometric terminology of Section 2.1.1 and motivated by Steinmann (1996). The present framework has been developed with the primary intent of describing crystalline solids that deform plastically by dislocation glide, most typically exhibiting a Bravais lattice structure and most often realized in engineering metals in a face centered cubic, body centered cubic, or hexagonal close packed arrangement (Tables 3.2 and 3.4). Concepts that have been forwarded here are most naturally applied to cubic lattices, wherein the director vectors of (3.155) may be assigned parallel to primitive translation vectors of the Bravais lattice as in (3.164) (recall from Section 3.1.1 that primitive Bravais lattice vectors and their reciprocals are parallel in cubic crystals). The framework is valid for crystal structures of lower symmetry (e.g., hexagonal Bravais lattices) so long as the Cauchy-Born rule (Section 3.1.2) applies for deformation of the inter-atomic bond vec-

tors. In such cases, while the covariant directors of relations (3.155) assigned to each crystalline volume element are not parallel to physical edges of primitive or conventional unit cells of the Bravais lattice, they are assumed to fully characterize the stretch and rotation of interatomic vectors comprising the primitive cells contained in that volume element, as is clear from (3.165). On the other hand, for more complex structures wherein recoverable (i.e., elastic) deformation is non-uniform within the unit cell, e.g., polyatomic structures such as non-centrosymmetric crystals with a basis undergoing inner displacements among sub-lattices (Cousins 1978; Garikipati 2003), additional degrees of freedom not included in Section 3.3 may prove useful for characterizing certain kinds of defects that affect the geometry of each sub-lattice differently.

Table 3.5 Geometric classifications, kinematic quantities, and lattice defects

Geometry	Torsion	Curvature	Metric	Defects
Euclidean ($\tilde{B}$ holonomic)	$\hat{\mathbf{T}} = 0$	$\hat{\mathbf{R}} = 0$	$\hat{\nabla}\mathbf{C}^{\mathbf{L}} = 0$	Statistically stored defects [15]
Cartan and non-Riemannian	$\hat{\mathbf{T}} \neq 0$	$\hat{\mathbf{R}} = 0$	$\hat{\nabla}\mathbf{C}^{\mathbf{L}} = 0$	Geometrically necessary dislocations
Riemannian and symmetric	$\hat{\mathbf{T}} = 0$	$\hat{\mathbf{R}} \neq 0$	$\hat{\nabla}\mathbf{C}^{\mathbf{L}} = 0$	Geometrically necessary disclinations
Metric, Cartan, and Riemannian	$\hat{\mathbf{T}} \neq 0$	$\hat{\mathbf{R}} \neq 0$	$\hat{\nabla}\mathbf{C}^{\mathbf{L}} = 0$	Dislocations and disclinations
Non-metric, Cartan, and Riemannian	$\hat{\mathbf{T}} \neq 0$	$\hat{\mathbf{R}} \neq 0$	$\hat{\nabla}\mathbf{C}^{\mathbf{L}} \neq 0$	Any point and line defects

---

[15] Admissible for all geometries in Table 3.5. All straight non-terminating dislocations are geometrically necessary when considered in isolation; collections of SSDs produce no net Burgers vector and no contribution to the torsion tensor.

4 Thermomechanics of Crystalline Solids

Chapter 4 addresses fundamental thermomechanical relationships necessary for describing physical behavior of crystalline materials. Meant by the term thermomechanics are the balance principles from continuum mechanics and thermodynamics that dictate the response of the solid when subjected to mechanical forces, temperature variations, or other physical stimuli. Accordingly, the state of the material, for example equilibrium positions of atoms within a crystal and local vibrations of atoms about these positions, may change reversibly or irreversibly during a thermomechanical process. Complementary to the geometrically nonlinear description of kinematics in Chapter 3, the content of Chapter 4 focuses on descriptions of solid bodies subjected to finite deformations. Reductions of the nonlinear theory to the case of geometric linearity are included in many instances.

The behavior of crystalline solids generally consists of a combination of a (thermo)elastic response corresponding to recoverable deformation and the inelastic response corresponding to plastic deformation such as that resulting from the generation and motion of defects. Elastic materials with viscosity and heat conduction were examined from a continuum thermodynamic viewpoint by Coleman and Noll (1963), who developed a method for exploiting the entropy production inequality to deduce thermodynamic relationships among field variables and restrictions on constitutive laws. Coleman (1964) extended this approach to materials with memory. In earlier work, Eckart applied similar, but apparently less mathematically formal, approaches towards deducing thermodynamic restrictions on behaviors of simple fluids (Eckart 1940) and elastic-anelastic bodies undergoing potentially large deformations (Eckart 1948). Anelasticity in a general sense refers to any thermodynamically irreversible deformation and encompasses viscoelasticity and plasticity, for example. Viscoelastic media, both solid and fluid, were a primary focus of the study of Coleman and Noll (1963).

The internal state variable concept is used in continuum theories to represent features of the material distinct from those addressed by conventional field variables (i.e., external variables) such as deformation and temperature. Internal state variables for crystalline solids often represent

microscopic features of the crystal structure that may evolve with strain or temperature. For example, internal state variables can often include scalar- or tensor-valued measures of defect densities such as the number of point defects per unit volume in (3.133) or the dislocation density tensor of (3.224). Evolution refers to a change of a variable with time. Coleman and Gurtin (1967) developed a formal procedure using the balance of energy and dissipation inequality to impose restrictions on evolution of internal state variables. Internal state variable concepts were applied by Rice (1971) in an examination of inelastic constitutive relationships for crystalline solids. A critical comparison of competing theories of thermodynamics of irreversible processes is outside the scope of this text; a concise overview is given by Maugin (1988, pp. 99-115). Other relevant works that feature treatments of continuum thermodynamics include those of Gurtin (1965), Truesdell and Noll (1965), Malvern (1969), Germain et al. (1983), Ericksen (1991), Grinfeld (1991), and Maugin and Muschik (1994a, b).

Chapter 4 is organized as follows. Continuum concepts of mass density, traction, and stress referred to reference and current configurations are introduced. Thermodynamic potentials are defined. Classical balance equations of thermomechanics in continuous media undergoing potentially large deformations are reviewed: conservation of mass, momentum, and energy. A brief introduction to internal state variable theory is provided, including discussion of possible choices of internal variables for crystalline solids, followed by presentation of the dissipation inequality. Chapter 4 concludes with a short treatment of general kinetic relationships for irreversible processes, including dissipation potentials for inelastic rates. Much of the material presented in Chapter 4 applies to any continuous body in the framework of continuum mechanics; i.e., much of the forthcoming treatment in Chapter 4 is not restricted to crystalline solids and also applies to amorphous solids and fluids, for example.

Developments in Chapter 4 are, however, restricted to classical continua as opposed to generalized continua. Generalized continua do not always obey standard balance laws of momentum and energy presented in Chapter 4. Generalized continua include materials supporting couple stresses (Cosserat and Cosserat 1909; Toupin 1962, 1964; Malvern 1969). Because balance laws of generalized continua differ among various theories, balance laws for generalized continua are addressed in this book on a case-by-case basis. Specifically, governing equations for generalized elasticity (Toupin 1964) are discussed in Section 5.7 of Chapter 5, for generalized elasticity with an evolving intermediate configuration (Teodosiu 1967a, 1968) in Section 6.7 of Chapter 6, and for micropolar elastoplasticity (Clayton et al. 2006) in Section 9.4 of Chapter 9.

Possible electromagnetic contributions to governing equations are omitted from the presentation of Chapter 4 and are deferred until Chapter 10. In continuum electromechanical theories (Stratton 1941; Toupin 1956, 1963; Eringen 1963; Tiersten 1971; Maugin 1988), electromagnetic forces may influence balances of momentum and energy and the reduced entropy inequality.

4.1 Classical Balance Laws and Definitions

The present Section discusses what are termed classical balance laws of continuum mechanics: mass conservation, linear and angular momentum conservation, and the balance of energy. Though applicable to continuous bodies of an arbitrary nature, these relationships are used in later Chapters to enable rigorous descriptions of physical phenomena in crystalline solids deforming by one or more physical mechanisms (e.g., elasticity, dislocation-based plasticity, void growth, fracture, and so forth). Definitions of thermomechanical variables are presented first, followed by the aforementioned conservation and balance laws. Introduction of the dissipation inequality, i.e., the Second Law of Thermodynamics, follows later in Section 4.2.2. For additional insight, the reader is referred to other books dealing with nonlinear continuum mechanics (Truesdell and Toupin 1960; Eringen 1962; Truesdell and Noll 1965; Malvern 1969; Gurtin 1981; Marsden and Hughes 1983). Omitted from the discussion is treatment of surfaces of discontinuity[1] occurring in the context of shock waves (e.g., discontinuous particle velocity, deformation gradient, and stress) or acceleration waves (e.g., discontinuous particle acceleration, velocity gradient, and second-order position gradient). In other words, sufficient differentiability of field variables is presumed unless noted otherwise.

4.1.1 Definitions

Definitions are provided for fundamental local quantities associated with mass, force, energy, and entropy. When forces or energies are measured on a per unit area or per unit volume basis, multiple definitions are needed to represent such quantities corresponding to each configuration of a deformable body. At a minimum, two definitions are needed for completeness: one referred to reference configuration B_0 and another referred to

---

[1] Surfaces of discontinuity are formally addressed by Truesdell and Toupin (1960).

spatial configuration B. For tensor-valued entities such as stress, the number of possible definitions increases because of the possibility of two-point tensors.

Reference mass density $\rho_0(X)$ and current mass density $\rho(x,t)$ of an element of mass $m \geq 0$ are defined by

$$\rho_0 = \lim_{V \to 0} \frac{m}{V} = \frac{dm}{dV}, \quad \rho = \lim_{v \to 0} \frac{m}{v} = \frac{dm}{dv}, \tag{4.1}$$

with V and v that element's volume in configurations B_0 and B, respectively. Mass m (or dm) of a particular material particle, or of a fixed set of atoms, is assumed the same in (4.1) for corresponding reference and deformed volume elements. In continuum mechanics, mass density is subject to the constraints $0 \leq \rho_0 < \infty$ and $0 \leq \rho < \infty$.

Traction vectors measure directed forces per unit area acting on oriented surfaces, either external or internal, to the body. The reference traction $\mathbf{t}_0(X,t)$ and current traction (or simply the traction vector) $\mathbf{t}(x,t)$ satisfy

$$\mathbf{t}_0 dS = \mathbf{t} ds = d\mathbf{P} \in T_x B, \quad t_0^a dS = t^a ds = dP^a, \tag{4.2}$$

where dS and ds are differential area elements in configurations B_0 and B, respectively, and $d\mathbf{P}$ is the force acting on the surface element. The reference traction $\mathbf{t}_0$ is thus the force per unit reference area, while the traction vector $\mathbf{t}$ measures the force per unit spatial area. In either case, the index on the vector is referred to the current configuration. Thus indices of both traction vectors in (4.2) are referred to basis vectors $\mathbf{g}_a(x)$ of spatial tangent bundle TB.
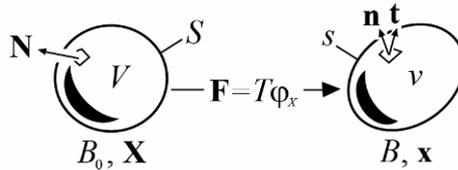
Fig. 4.1 Deforming material element

Stress tensors relate traction vectors of (4.2) and unit normal covectors $\mathbf{N}$ and $\mathbf{n}$ (Fig. 4.1) associated with differential area elements dS and ds, respectively. Cauchy stress tensor $\boldsymbol{\sigma}(x,t) \in T_x B \times T_x B$ and first Piola-Kirchhoff stress tensor $\mathbf{P}(X,t) \in T_x B \times T_X B_0$ satisfy

$$\mathbf{t} = \boldsymbol{\sigma} \mathbf{n}, \quad t^a = \sigma^{ab} n_b; \tag{4.3}$$

$$\mathbf{t}_0 = \mathbf{P} \mathbf{N}, \quad t_0^a = P^{aA} N_A. \tag{4.4}$$

Relations (4.3) and (4.4) are often referred to either as versions or outcomes of Cauchy's theorem (Truesdell and Toupin 1960; Eringen 1962; Marsden and Hughes 1983). The linear function relating traction and the unit normal is the stress tensor. From (4.2)-(4.4) and Piola transform (2.148),

$$t^a ds = \sigma^{ab} n_b ds = J F^{-1A}_{.b} \sigma^{ab} N_A dS = P^{aA} N_A dS = t^a_0 dS \, , \tag{4.5}$$

implying that the two stress tensors in (4.3) and (4.4) are related by

$$\mathbf{P} = J \boldsymbol{\sigma} \mathbf{F}^{-*} \, , \quad P^{aA} = J \sigma^{ab} F^{-1A}_{.b} \, . \tag{4.6}$$

Second Piola-Kirchhoff stress tensor $\boldsymbol{\Sigma}(X,t) \in T_X B_0 \times T_X B_0$ and nominal stress tensor $\mathbf{S}(X,t) \in T_X B_0 \times T_x B$ are defined by pulling back and transposing $\mathbf{P}$, respectively, while Kirchhoff stress tensor $\boldsymbol{\tau}(x,t) \in T_x B \times T_x B$ is simply the Cauchy stress normalized by the Jacobian determinant as an energy per unit reference volume:

$$\boldsymbol{\Sigma} = \mathbf{F}^{-1} \mathbf{P} \, , \quad \mathbf{S} = \mathbf{P}^T \, , \quad \boldsymbol{\tau} = J \boldsymbol{\sigma} \, . \tag{4.7}$$

Relationships among contravariant components of the five stress tensors introduced in (4.3)-(4.7) are listed in Table 4.1 for ease of reference[2]. In the geometrically linear theory of continuum mechanics (i.e., infinitesimal strain theory of Section 2.5.3), distinctions between first Piola-Kirchhoff stress P^{aA} and Kirchhoff stress $\tau^{ab} = P^{aA} F^b_{.A} = P^{aA}(\delta^b_{.A} + u^b_{;A}) \approx P^{aA} \delta^b_{.A}$ are conventionally omitted (Malvern 1969), as explained in more detail in the context of the balance of linear momentum in Section 4.1.3.

Table 4.1 Relationships among stress tensors

Stress	$\boldsymbol{\sigma}$	$\boldsymbol{\tau}$	$\mathbf{P}$	$\boldsymbol{\Sigma}$	$\mathbf{S}$
Cauch. $\boldsymbol{\sigma}$	σ^{ab}	$J^{-1}\tau^{ab}$	$J^{-1}P^{aA}F^b_{.A}$	$J^{-1}F^a_{.B}\Sigma^{BA}F^b_{.A}$	$J^{-1}S^{Aa}F^b_{.A}$
Kirch. $\boldsymbol{\tau}$	$J\sigma^{ab}$	τ^{ab}	$P^{aA}F^b_{.A}$	$F^a_{.B}\Sigma^{BA}F^b_{.A}$	$S^{Aa}F^b_{.A}$
1st PK $\mathbf{P}$	$J\sigma^{ab}F^{-1A}_{.b}$	$\tau^{ab}F^{-1A}_{.b}$	P^{aA}	$F^a_{.B}\Sigma^{BA}$	S^{Aa}
2nd PK $\boldsymbol{\Sigma}$	$JF^{-1A}_{.a}\sigma^{ab}F^{-1B}_{.b}$	$F^{-1A}_{.a}\tau^{ab}F^{-1B}_{.b}$	$F^{-1A}_{.a}P^{aB}$	Σ^{AB}	$S^{Ba}F^{-1A}_{.a}$
Nom. $\mathbf{S}$	$JF^{-1A}_{.b}\sigma^{ab}$	$F^{-1A}_{.b}\tau^{ab}$	P^{aA}	$\Sigma^{BA}F^a_{.B}$	S^{Aa}

---

[2] Placement of indices in stress tensors varies among authors. For example, Eringen (1962) and Malvern (1969) use the transpose of the definition used in this book for the Cauchy stress, expressing (4.3) as $t^a = n_b \sigma^{ba}$. In such cases, the summation convention used for stress divergence in momentum balance (4.17) is modified accordingly. The distinction is irrelevant when the Cauchy stress is symmetric as occurs in classical continuum mechanics, but is important in generalized continuum theories (e.g., Sections 5.7 and 6.7) and nonlinear electromechanical theories (Chapter 10) wherein the Cauchy stress is not always symmetric.

Absolute temperature $\theta(X,t) \geq 0$ and entropy per unit mass $\eta(X,t)$ are introduced. Temperature θ traditionally is associated with local vibrations of atomic nuclei about their equilibrium positions, though the total (e.g., free) energy of an unstrained solid will also contain electronic contributions. Entropy in a qualitative sense measures the disorder of the substance or the ability of a system to perform work; more formal interpretations following from statistical mechanics principles and atomic systems are possible (Slater 1939; Phillips 2001) but are not included here. As will be demonstrated later in Sections 4.2.2 and 4.3, entropy production is associated with dissipative or irreversible thermodynamic processes.

Also introduced are the following thermodynamic potentials, defined on a per unit mass basis: internal energy $e(X,t)$, enthalpy $h(X,t)$, Helmholtz free energy $\psi(X,t)$, and Gibbs function $g(X,t)$. Interrelationships among thermodynamic potentials for elastic bodies are listed in Table 4.2, following the scheme of Thurston (1974). Definitions of enthalpy and the Gibbs function depend upon the appropriate work-conjugate thermodynamic tension or stress (e.g., the second-Piola Kirchhoff stress $\boldsymbol{\Sigma}$ of (4.7)) and deformation (e.g., the right Cauchy-Green strain $\mathbf{E}$ of (2.156)) measures. By allowing each of the thermodynamic potentials to depend on a particular set of independent variables—for example deformation gradient (2.112) and temperature, or stress (4.6) and entropy—additional relationships among thermodynamic quantities can be deduced from partial cross-derivatives of the potentials. In later Chapters dealing with constitutive theory, Helmholtz free energy ψ, often simply called the free energy, is featured prominently since it is conventionally assumed a function of the deformation gradient and temperature in the Gibbs formalism, and since deformation gradient and temperature are variables that are conveniently controllable in solid mechanics experiments, as opposed to entropy and enthalpy, for example (though in certain dynamic experiments, such as those involving wave propagation, that can be idealized as adiabatic, use of internal energy is often more convenient). Different definitions of the various thermodynamic potentials, particularly h and g, are possible for general states of stress (Malvern 1969), and traditional thermodynamic potentials of thermoelasticity (Thurston 1974) may require modification to account for inelastic deformation (Scheidler and Wright 2001; Wright 2002) as well as electromechanical effects (Devonshire 1954; Thurston 1974; McMeeking et al. 2007).

Table 4.2 Thermodynamic potentials for elastic solids

Potential [energy per unit mass]	Relationship to internal energy e
Internal energy e	e
Enthalpy h	$h = e - \rho_0^{-1} \Sigma^{AB} E_{AB}$
Helmholtz free energy ψ	$\psi = e - \theta\eta$
Gibbs function g	$g = e - \rho_0^{-1} \Sigma^{AB} E_{AB} - \theta\eta$

It sometimes becomes useful to define thermodynamic potentials and entropy on a per unit volume basis:

$$N = \rho\eta \,,\; E = \rho e \,,\; H = \rho h \,,\; \Psi = \rho\psi \,,\; G = \rho g \,; \tag{4.8}$$

$$N_0 = \rho_0\eta \,,\; E_0 = \rho_0 e \,,\; H_0 = \rho_0 h \,,\; \Psi_0 = \rho_0\psi \,,\; G_0 = \rho_0 g \,. \tag{4.9}$$

In (4.8), capitalization denotes a quantity defined on a per unit current volume basis in spatial configuration B. The zero subscript introduced in (4.9) is used in conjunction with capitalization for an energetic or entropic quantity measured per unit volume in reference configuration B_0.

4.1.2 Mass Conservation

Mass m of an element of material is said to be conserved when that element's mass does not vary with time, i.e., when m is the same in referential and spatial descriptions. Eliminating dm from (4.1) and using (2.141), mass densities in spatial and reference configurations are related by

$$\rho_0 = \rho J \,. \tag{4.10}$$

Since volume elements are non-negative and of finite size in both configurations, $0 < J < \infty$ as noted already following (2.141), and $0 < J^{-1} < \infty$. Thus $\rho = 0$ if and only if $\rho_0 = 0$ and the mass of the corresponding element vanishes. The continuity equation expresses the time rate of change of current mass density ρ. This equation can be derived in a number of ways, for example integration over a control volume supporting fluxes of mass across its external surfaces followed by localization, or direct time differentiation of local conservation law (4.10). Taking the latter approach and using (2.181),

$$\dot{\rho}_0 = 0 = \dot{\rho}J + \rho\dot{J} = \dot{\rho}J + \rho\mathcal{L}_v J = J(\dot{\rho} + \rho v^a_{;a}) \,, \tag{4.11}$$

where the first equality follows from the assertion that mass density in the reference configuration is time-independent. From the definition of the material time derivative in (2.169), continuity equation (4.11) can be written in either of two forms upon division by J as

$$\dot{\rho} + \rho v^a_{;a} = 0 \,, \quad \left.\frac{\partial \rho}{\partial t}\right|_x + (\rho v^a)_{;a} = 0 \,. \tag{4.12}$$

A material for which $\rho(x(X,t),t) = \rho_0(X)$ at all material points X, and hence for which $J(X,t) = 1$ for all X and for all $t > 0$, is called incompressible. In the geometrically linear theory, use of (2.164) in (4.10) and (4.11) produces the following first-order approximations for mass density and its time rate of change: $\rho_0 \approx \rho(1 + u^a_{;a})$ and $\dot{\rho} + \rho \dot{u}^a_{;a} = 0$.

Reynolds transport theorem accounts for the time rate of change of a given quantity carried by a deformable mass of material occupying an evolving volume v in configuration B. The rate of change of generic quantity $\hat{a}$, which may be any differentiable scalar, vector, or tensor of higher order, is computed as follows:

$$\int_v \frac{\partial}{\partial t}(\rho \hat{a}) dv = \frac{d}{dt} \int_v \rho \hat{a} dv - \int_s \rho \hat{a} \langle \mathbf{v}, \mathbf{n} \rangle ds \,, \tag{4.13}$$

where s is the external surface of v with oriented unit normal covector $\mathbf{n}(x,t)$. Applying the divergence theorem of (2.193) in conjunction with (4.12), Reynolds transport theorem is written more compactly as

$$\frac{d}{dt} \int_v \rho \hat{a} dv = \int_v \frac{\partial}{\partial t}(\rho \hat{a}) dv + \int_s \rho \hat{a} v^a n_a ds = \int_v \frac{\partial}{\partial t}(\rho \hat{a}) dv + \int_v (\rho \hat{a} v^a)_{;a} dv$$

$$= \int_v \left[\frac{\partial \rho}{\partial t} + (\rho v^a)_{;a} \right] \hat{a} dv + \int_v \rho \left[\frac{\partial \hat{a}}{\partial t} + \hat{a}_{;a} v^a \right] dv = \int_v \rho \dot{\hat{a}} dv. \tag{4.14}$$

Recall from Section 2.6.1 that d/dt denotes the material time derivative (i.e., reference particle at X held fixed during time differentiation), and $\partial/\partial t$ denotes the partial time derivative taken with spatial position x held fixed.

4.1.3 Momentum Conservation

Traditional conservation laws of momentum consist of balances of linear and angular momentum. The global spatial balance of linear momentum is

$$\frac{d}{dt} \int_v \rho \mathbf{v} dv = \int_v \bar{\mathbf{b}} dv + \int_s \mathbf{t} ds \,, \tag{4.15}$$

where $\mathbf{v}(x,t)$ is the spatial velocity of (2.168), $\bar{\mathbf{b}}(x,t)$ is the body force vector (measured here as a force per unit spatial volume), and integration proceeds over the body in current configuration B with volume v enclosed

by surface s. From (4.3), (4.14), and application of the divergence theorem, (4.15) can be written as

$$\int_v \rho \dot{v}^a \, dv = \int_v (\sigma^{ab}_{;b} + \bar{b}^a) \, dv . \tag{4.16}$$

Localization of (4.16) and use of (4.12) then provides a spatial balance of linear momentum that can be expressed in two forms:

$$\sigma^{ab}_{;b} + \bar{b}^a = \rho a^a \Leftrightarrow (\sigma^{ab} - \rho v^a v^b)_{;b} + \bar{b}^a = \frac{\partial}{\partial t}(\rho v^a) , \tag{4.17}$$

with $a^a(x,t) = \dot{v}^a$ the spatial acceleration of (2.173).

   The global material balance of linear momentum is written as follows:

$$\frac{d}{dt} \int_V \rho_0 \mathbf{V} dV = \int_V \bar{\mathbf{B}} dV + \int_S \mathbf{t}_0 dS , \tag{4.18}$$

where $\mathbf{V}(X,t)$ is the material velocity of (2.167) and $\bar{\mathbf{B}}(X,t)$ is the body force per unit reference volume. Application of (4.4) and the divergence theorem gives (Eringen 1962; Malvern 1969; Marsden and Hughes 1983)

$$\int_V \rho_0 \dot{V}^a dV = \int_V \bar{B}^a dV + \int_V P^{aA}_{:A} dV , \tag{4.19}$$

with the total covariant derivative (more specifically, divergence) of the first Piola-Kirchhoff stress $\mathbf{P}$ found via application of (2.73), (2.117), and inclusion of only the referential partial derivative of $P^{aA}(X,t)$:

$$
\begin{aligned}
P^{aA}_{:A} &= P^{aA}_{,,A} + \overset{G}{\Gamma}{}^{\;A}_{AB} P^{aB} + \overset{g}{\Gamma}{}^{\;a}_{bc} P^{cA} F^b_{.A} \\
&= P^{aA}_{,,A} + (\ln \sqrt{G})_{,A} P^{aA} + \overset{g}{\Gamma}{}^{\;a}_{bc} P^{cA} F^b_{.A} \\
&= (JF^{-1A}_{\;\;b} \sigma^{ab})_{:A} = (JF^{-1A}_{\;\;b})_{:A} \sigma^{ab} + JF^{-1A}_{\;\;b} \sigma^{ab}_{:A} \\
&= J\sigma^{ab}_{:b} = J\sigma^{ab}_{;b} .
\end{aligned}
\tag{4.20}
$$

Application of Piola's identity (2.146), i.e., $(JF^{-1A}_{\;\;b})_{:A} = 0$, to the stress divergence, and use of properties of the total covariant derivative in (2.117), enable derivation of the final three equalities in (4.20). The local material balance of linear momentum following from (4.19) is

$$P^{aA}_{:A} + \bar{B}^a = \rho_0 A^a , \tag{4.21}$$

where $A^a(X,t)$ is the material acceleration of (2.174). It follows from (4.10), (4.20), and $\bar{B}^a = J\bar{b}^a$ that the local material momentum balance can be obtained from local spatial momentum balance (4.17) via multiplication of the latter by J (Truesdell and Toupin 1960). While local forms of the balance of linear momentum in (4.17) and (4.21) apply for any choice of spatial coordinates, global coordinate forms (4.16) and (4.19) in-

volve integrals of vector fields over the spatial manifold with current tangent bundle *TB*. Thus the latter are valid only for coordinate systems wherein spatial basis vectors $\mathbf{g}_a$ are independent of position x, e.g., Cartesian coordinates. Alternatively, following Toupin (1956) and discussion in Section 3.2.5, resultant forces and total linear momentum can be evaluated at a particular point x via parallel transport of integrands to that point using appropriate shifter tensors.

Table 4.3 Spatial momentum balance in physical cylindrical coordinates

Quantity	R-component	θ–component	Z-component
Momentum	$\sigma_{RR,R} + R^{-1}\sigma_{R\theta,\theta}$	$\sigma_{\theta R,R} + R^{-1}\sigma_{\theta\theta,\theta}$	$\sigma_{ZR,R} + R^{-1}\sigma_{Z\theta,\theta}$
	$+\sigma_{RZ,Z} + R^{-1}(\sigma_{RR} - \sigma_{\theta\theta})$	$+\sigma_{\theta Z,Z} + 2R^{-1}\sigma_{\theta R}$	$+\sigma_{ZZ,Z} + R^{-1}\sigma_{ZR}$
	$= \rho a_R - \bar{b}_R$	$= \rho a_\theta - \bar{b}_\theta$	$= \rho a_z - \bar{b}_z$
Acceleration	$a_R = \partial v_R / \partial t$	$a_\theta = \partial v_\theta / \partial t$	$a_Z = \partial v_Z / \partial t$
	$+v_R v_{R,R} + R^{-1}v_\theta v_{R,\theta}$	$+v_R v_{\theta,R} + R^{-1}v_\theta v_{\theta,\theta}$	$+v_R v_{Z,R} + R^{-1}v_\theta v_{Z,\theta}$
	$+v_Z v_{R,Z} - R^{-1}(v_\theta)^2$	$+v_Z v_{\theta,Z} + R^{-1}v_R v_\theta$	$+v_Z v_{Z,Z}$
Velocity	$v_R = \dot{R}$	$v_\theta = R\dot{\theta}$	$v_Z = \dot{Z}$

Table 4.4 Spatial momentum balance in physical spherical coordinates

Quantity	R-component	θ–component	φ-component
Momentum	$\sigma_{RR,R} + R^{-1}\sigma_{R\theta,\theta}$	$\sigma_{\theta R,R} + R^{-1}\sigma_{\theta\theta,\theta}$	$\sigma_{\varphi R,R} + R^{-1}\sigma_{\varphi\theta,\theta}$
	$+(R\sin\theta)^{-1}\sigma_{R\varphi,\varphi}$	$+(R\sin\theta)^{-1}\sigma_{\theta\varphi,\varphi}$	$+(R\sin\theta)^{-1}\sigma_{\varphi\varphi,\varphi}$
	$+R^{-1}(2\sigma_{RR} - \sigma_{\theta\theta}$	$+R^{-1}[3\sigma_{\theta R} + (\sigma_{\theta\theta}$	$+R^{-1}(3\sigma_{\varphi R}$
	$-\sigma_{\varphi\varphi} + \sigma_{R\theta}\cot\theta)$	$-\sigma_{\varphi\varphi})\cot\theta]$	$+2\sigma_{\varphi\theta}\cot\theta)$
	$= \rho a_R - \bar{b}_R$	$= \rho a_\theta - \bar{b}_\theta$	$= \rho a_\varphi - \bar{b}_\varphi$
Acceleration	$a_R = \partial v_R / \partial t$	$a_\theta = \partial v_\theta / \partial t$	$a_\varphi = \partial v_\varphi / \partial t$
	$+v_R v_{R,R} + R^{-1}v_\theta v_{R,\theta}$	$+v_R v_{\theta,R} + R^{-1}v_\theta v_{\theta,\theta}$	$+v_R v_{\varphi,R} + R^{-1}v_\theta v_{\varphi,\theta}$
	$+(R\sin\theta)^{-1}v_\varphi v_{R,\varphi}$	$+(R\sin\varphi)^{-1}v_\varphi v_{\theta,\varphi}$	$+(R\sin\varphi)^{-1}v_\varphi v_{\varphi,\varphi}$
	$-R^{-1}[(v_\theta)^2 + (v_\varphi)^2]$	$+R^{-1}[v_R v_\theta - (v_\varphi)^2\cot\theta]$	$+R^{-1}v_\varphi[v_R + v_\theta\cot\theta]$
Velocity	$v_R = \dot{R}$	$v_\theta = R\dot{\theta}$	$v_\varphi = \dot{\varphi}R\sin\theta$

Procedures for deriving the balance of linear momentum in terms of physical components of vectors and tensors are given by Eringen (1962) and Malvern (1969). Tables 4.3 and 4.4 provide spatial balances of linear momentum in cylindrical coordinates of Section 2.4.2 and spherical coordinates of Section 2.4.3. Components of velocity (2.168) and acceleration (2.173) in corresponding physical components are also listed in Tables 4.3 and 4.4. In Table 4.5, components of velocity gradient (2.176) that enter

the convective part of the spatial acceleration are listed, following Malvern (1969). In contrast to Section 2.4 in which physical components correspond to the reference configuration, indices of cylindrical and spherical coordinates are referred to the spatial configuration B in Tables 4.3-4.5. The summation convention does not apply over repeated indices in Tables 4.3-4.5.

Table 4.5 Velocity gradient components in cylindrical and spherical coordinates

Coordinate system	Velocity gradient $L_{<ab>} = \overset{g}{\nabla}_{<b>} v^{<a>}$		
Cylindrical	$L_{RR} = v_{R,R}$	$L_{R\theta} = R^{-1}(v_{R,\theta} - v_\theta)$	$L_{RZ} = v_{R,Z}$
	$L_{\theta R} = v_{\theta,R}$	$L_{\theta\theta} = R^{-1}(v_{\theta,\theta} + v_R)$	$L_{\theta Z} = v_{\theta,Z}$
	$L_{ZR} = v_{Z,R}$	$L_{Z\theta} = R^{-1}v_{Z,\theta}$	$L_{ZZ} = v_{Z,Z}$
Spherical	$L_{RR} = v_{R,R}$	$L_{R\theta} = R^{-1}(v_{R,\theta} - v_\theta)$	$L_{R\varphi} = (R\sin\theta)^{-1}v_{R,\varphi} - R^{-1}v_\varphi$
	$L_{\theta R} = v_{\theta,R}$	$L_{\theta\theta} = R^{-1}(v_{\theta,\theta} + v_R)$	$L_{\theta\varphi} = (R\sin\theta)^{-1}v_{\theta,\varphi} - R^{-1}v_\varphi \cot\varphi$
	$L_{\varphi R} = v_{\varphi,R}$	$L_{\varphi\theta} = R^{-1}v_{\varphi,\theta}$	$L_{\varphi\varphi} = (R\sin\theta)^{-1}v_{\varphi,\varphi} + R^{-1}(v_\theta \cot\theta + v_R)$

The global balance of angular momentum referred to the spatial configuration is

$$\frac{d}{dt}\int_v \mathbf{x} \times \rho\mathbf{v}\,dv = \int_v \mathbf{x} \times \bar{\mathbf{b}}\,dv + \int_s \mathbf{x} \times \mathbf{t}\,ds , \qquad (4.22)$$

where $\times$ is the vector cross product. In indicial notation, (4.22) is written

$$\frac{d}{dt}\int_v \varepsilon_{abc}x^b \rho v^c\,dv = \int_v \varepsilon_{abc}x^b \bar{b}^c\,dv + \int_s \varepsilon_{abc}x^b t^c\,ds . \qquad (4.23)$$

Using divergence theorem (2.193), Cauchy's theorem (4.3), and Reynolds transport theorem (4.14), (4.23) becomes

$$\int_v \varepsilon_{abc}(\rho v^b v^c + \rho x^b \dot{v}^c - x^b \bar{b}^c)\,dv = \int_s \varepsilon_{abc}x^b \sigma^{cd}n_d\,ds$$
$$= \int_v \varepsilon_{abc}(x^b \sigma^{cd})_{;d}\,dv = \int_v \varepsilon_{abc}(\sigma^{cb} + x^b \sigma^{cd}_{;d})\,dv. \qquad (4.24)$$

Collecting terms gives

$$\int_v \varepsilon_{abc}x^b(\rho\dot{v}^c - \bar{b}^c - \sigma^{cd}_{;d})\,dv = \int_v \varepsilon_{abc}(\sigma^{cb} - \rho v^b v^c)\,dv . \qquad (4.25)$$

The left side of (4.25) vanishes by (4.17), and the last term in the integrand on the right of (4.25) vanishes from symmetry of the dyad $v^b v^c = v^{(b}v^{c)}$. This leaves the local requirement

$$\varepsilon_{abc}\sigma^{cb} = 0 \Leftrightarrow \sigma^{ab} = \sigma^{(ab)}, \ \sigma^{[ab]} = 0 , \qquad (4.26)$$

i.e., the Cauchy stress tensor is symmetric in classical continuum mechanics. From (4.6) and (4.7), the local balance of angular momentum can also be expressed in any of the following forms as

$$F_{.A}^a P^{bA} = P^{aA} F_{.A}^b , \; \Sigma^{AB} = \Sigma^{BA} , \; S^{Ab} F_{.A}^a = F_{.A}^b S^{Aa} , \; \tau^{ab} = \tau^{ba} . \quad (4.27)$$

In geometrically linear theories of continuum mechanics, with the assumption $P^{aA} \approx \tau^{ab} \delta_{.b}^A$ (Malvern 1969), the balance of linear momentum (4.21) in terms of force per unit reference volume is $\tau_{;b}^{ab} + \bar{B}^a = \rho_0 \ddot{u}^a$. Similarly, $\sigma_{;b}^{ab} + \bar{b}^a = \rho \ddot{u}^a$ in terms of force per unit current volume (4.17). Together, $J \sigma_{;b}^{ab} = J(J^{-1} \tau^{ab})_{;b} = \tau_{;b}^{ab} - J_{;b} \sigma^{ab} \approx \tau_{;b}^{ab}$ is implied if both momentum balances are assumed to apply simultaneously in the linear theory. Thus, formally, two linear momentum balances would seem necessary in the linear theory even though the distinction between reference and spatial coordinates is not enforced explicitly. This issue arises when mass density is permitted to change with deformation in the linear theory, as noted following (4.12). In the geometrically linear theory, angular momentum balances (4.26) and (4.27) remain unchanged from those of the nonlinear theory: $\sigma^{ab} = \sigma^{ba}$ and $\tau^{ab} = \tau^{ba}$.

Like the coordinate form of the global balance of linear momentum, the indicial expression of the global balance of angular momentum is restricted to spatial coordinate systems for which holonomic basis vectors are independent of position. Local forms (4.26) and (4.27), however, apply for any choice of coordinate system, e.g., curvilinear coordinates. Local forms of conservation of mass (4.12), balance of linear momentum (4.17), and balance of angular momentum (4.26) can be obtained without resorting to the global (i.e., integral) forms via prescription of an energy balance that is presumed invariant under rigid body motions (Green and Rivlin 1964a). This alternative approach towards derivation of local balance laws, which does not require assignment of particular kinds of coordinate systems, is formally discussed by Marsden and Hughes (1983).

4.1.4 Energy Conservation

The global form of the balance of energy or First Law of Thermodynamics for a continuous body is written

$$\frac{d}{dt}(\mathcal{E} + \mathcal{K}) = \mathcal{P} + \mathcal{Q} , \quad (4.28)$$

where $\mathcal{E}$ is the global internal energy, $\mathcal{K}$ is the global kinetic energy, $\mathcal{P}$ is the mechanical rate of working, and $\mathcal{Q}$ is the rate of work of non-mechanical sources. These quantities are defined as follows for a body in

spatial configuration B occupying volume v and enclosed by surface s, with the latter's orientation defined by outward unit normal covector $\mathbf{n}$:

$$\mathcal{E} = \int_v \rho e \, dv , \tag{4.29}$$

$$\mathcal{K} = \int_v (\rho/2) \mathbf{v} \cdot \mathbf{v} \, dv , \tag{4.30}$$

$$\mathcal{P} = \int_v \overline{\mathbf{b}} \cdot \mathbf{v} \, dv + \int_s \mathbf{t} \cdot \mathbf{v} \, ds , \tag{4.31}$$

$$\mathcal{Q} = \int_v \rho r \, dv - \int_s \langle \mathbf{q}, \mathbf{n} \rangle \, ds . \tag{4.32}$$

In (4.32), $r(x,t)$ is the scalar heat source per unit mass that may arise from non-mechanical phenomena (e.g., a radiation field), and $\mathbf{q}(x,t) \in T_x B$ is the heat flux vector associated with heat conduction. Source r vanishes identically in most typical boundary value problems. The sign convention for $\mathbf{q}$ is specified such that when $\langle \mathbf{q}, \mathbf{n} \rangle = q^a n_a > 0$, energy flows out of the body so that the contribution from heat flux to energy rate $\mathcal{Q}$ is negative.

The local version of (4.28) is derived as follows. Using (4.14) and the divergence theorem to convert surface integrals in (4.31) and (4.32) to volume integrals,

$$\int_v \rho(\dot{e} + \dot{v}^b v_b) \, dv = \int_v \overline{b}^b v_b \, dv + \int_v (\sigma^{ba} v_b - q^a)_{;a} \, dv + \int_v \rho r \, dv$$
$$= \int_v v_b (\overline{b}^b + \sigma^{ba}_{;a}) \, dv + \int_v (\sigma^{ba} v_{b;a} - q^a_{;a}) \, dv + \int_v \rho r \, dv. \tag{4.33}$$

Then from (4.17), terms associated with stress divergence, linear momentum, and body forces cancel. Localizing, the remaining terms comprise the spatial balance of energy:

$$\rho \dot{e} = \sigma^{ab} v_{a;b} - q^a_{;a} + \rho r , \tag{4.34}$$

or in direct notation

$$\rho \dot{e} = \langle \boldsymbol{\sigma}, \mathbf{D} \rangle - \left\langle \overset{g}{\nabla}, \mathbf{q} \right\rangle + \rho r , \tag{4.35}$$

where (4.26) has been used and $\mathbf{D} = (1/2)\mathcal{L}_v \mathbf{g}$ is the deformation rate tensor of (2.182). The skew part of the velocity gradient, i.e., the spin tensor $\mathbf{W}$ of (2.187), does not contribute to balance of energy (4.35) because of the symmetry of the Cauchy stress tensor.

The local balance of energy is expressed in material form as follows. Heat flux $\mathbf{q}$ is mapped to $\mathbf{Q}(X,t) \in T_X B_0$ via Nanson's formula (2.148):

$$Q^A N_A dS = Q^A J^{-1} F^a_{.A} n_a ds = q^a n_a ds \rightarrow Q^A = J F^{-1A}_{.a} q^a . \tag{4.36}$$

Using Piola's identity (2.145), the divergence of the heat flux satisfies

$$q_{;a}^{a} = (J^{-1}F_{.A}^{a}Q^{A})_{;a} = (J^{-1}F_{.A}^{a})_{;a}Q^{A} + J^{-1}F_{.A}^{a}Q_{:a}^{A} = J^{-1}Q_{;A}^{A} . \qquad (4.37)$$

Scalars e and r are defined on a per unit mass basis and hence remain stationary with respect to changes in configuration, while the mass density changes according to (4.10). From (2.186), (4.6), and (4.7), the stress power per unit current volume can be written

$$\sigma^{ab}D_{ab} = \sigma^{ab}F_{.a}^{-1A}\dot{E}_{AB}F_{.b}^{-1B} = J^{-1}\Sigma^{AB}\dot{E}_{AB} , \qquad (4.38)$$

where the right Cauchy-Green strain tensor **E** is defined in (2.156). Multiplying (4.35) by J and using (4.10), (4.37), and (4.38) gives the local material balance of energy:

$$\rho_0\dot{e} = \Sigma^{AB}\dot{E}_{AB} - Q_{;A}^{A} + \rho_0 r . \qquad (4.39)$$

In the context of the geometrically linear theory of (2.191), deformation rate and strain rate are equivalent, and the local balance of energy of (4.34) reduces to

$$\rho\dot{e} = \sigma^{ab}\dot{\varepsilon}_{ab} - q_{;a}^{a} + \rho r . \qquad (4.40)$$

When body forces are conservative, global energy balance (4.28) can be expressed in an illustrative form (Eringen 1962). Conservative forces are derivable from a local potential energy function $\Phi(x)$ that depends only on position, and not explicitly on time:

$$\rho\overline{b}_a \Rightarrow b_a(x) = -\Phi_{,a}(x), \ \overline{\Phi} = \int_v \rho\Phi dv . \qquad (4.41)$$

In the first of (4.41), **b** is a body force per unit mass, and the dimensions of the local potential energy $\Phi(x)$ are energy per unit mass. The second of (4.41) defines a global potential energy. From (4.41) the latter's rate is

$$\dot{\overline{\Phi}} = \int_v \rho\dot{\Phi}dv = \int_v \rho\left(\left.\frac{\partial\Phi}{\partial t}\right|_x + \Phi_{,a}v^a\right)dv = \int_v \rho\Phi_{,a}v^a dv = -\int_v \rho b_a v^a dv . \qquad (4.42)$$

The global rate of mechanical working in (4.31) becomes

$$\mathcal{P} = \int_v \rho b_a v^a dv + \int_s t^a v_a ds = \int_s t^a v_a ds - \dot{\overline{\Phi}} . \qquad (4.43)$$

Global energy balance (4.28) then becomes

$$\dot{\mathcal{E}} + \dot{\mathcal{K}} + \dot{\overline{\Phi}} = \int_s t^a v_a ds + \mathcal{Q} . \qquad (4.44)$$

When the right side of (4.44) vanishes, $\mathcal{E} + \mathcal{K} + \overline{\Phi} = \text{constant}$, meaning that the sum of internal, kinetic, and potential energies is conserved. Specific scenarios for which this holds are conditions in which the body is insulated (i.e., adiabatic or vanishing heat flux **q** with no heat sources r) and when either velocities or tractions vanish on boundary surface s. The analogous situation for conservative discrete particle systems is derived in

Section B.1, specifically relations (B.13) and (B.15), in the context of the Hamiltonian representation of governing equations of molecular dynamics.

4.2 Internal State Variables and the Dissipation Inequality

A number of formal philosophical interpretations exist regarding consideration of thermodynamic quantities, balance equations, and fundamental inequalities in the context of modern continuum mechanics (Germain et al. 1983; Maugin and Muschik 1994a). What is often called classical thermodynamics deals with equilibrium states of materials. A system is said to be in thermodynamic equilibrium if it is isolated, does not evolve with time, and hence contains no unbalanced internal forces. Classical thermodynamics is thus sometimes referred to as thermostatics (Thurston 1974). In thermostatics, temperature and entropy of a material and thermodynamic potentials introduced in Section 4.1.1 have clear origins in statistical mechanics (Slater 1939; Malvern 1969). On the other hand, in many physical problems of interest the situation is more complex, and one often seeks descriptions of the condition of the material as it attains various non-equilibrated states, i.e., descriptions afforded by non-equilibrium thermodynamics. In such circumstances, traditional thermostatic definitions do not readily apply, and the system cannot be adequately described by a finite collection of state variables. To overcome this difficulty, the notion of local accompanying equilibrium states or constrained equilibrium states is often introduced (De Groot and Mazur 1962; Lubliner 1990; Kestin 1992). In this context, the material is treated as if it were in local equilibrium at any given instant, even when undergoing an irreversible process, and thus can be described by the thermodynamic temperature, thermodynamic potentials, and a finite set of state variables. This is often deemed an appropriate assumption when time scales for irreversible processes are fast relative to those for incremental changes in driving forces such as mechanical stresses or temperature gradients (Rice 1971; McDowell 2005). The concept is also appropriate when such driving forces change rapidly enough that changes in internal variables associated with irreversibility do not have time to occur. Though the formal definition of constrained equilibrium states does not apply in situations wherein time scales associated with internal variables and their driving forces are similar, the state variable concept is still used regularly in modern applications of continuum thermomechanics, albeit in the context of non-equilibrium thermodynamics, to describe various behaviors of deformable continuous bodies (Maugin and Muschik 1994a, b).

The condition or state of the material, for example its energy content and constitutive response, is assumed from a mathematical perspective to depend upon a number of independent state variables. These may include kinematic variables such as volume or strain, intrinsic field variables such as temperature or entropy, and any number of internal state variables. An internal state variable refers to an intrinsic quantity that is required to fully characterize the state of the material and that can be varied, albeit often irreversibly, without changing the other independent state variables. In crystalline solids, such variables are typically used to reflect influences of the microstructure on the state of the system, for example energies attributed to lattice defects, or phenomena at a finer length scale not represented by strain or temperature fields at the coarser scale of immediate consideration. For example, dislocation densities were treated as internal state variables in an early continuum plasticity theory of Kroner (1963a). The transition of the material from one state (i.e., one particular set of values of state variables) to another is called a thermodynamic process. If application of the inverse of the external stimuli invoked during a given thermodynamic process returns the material to its original state, such a process is said to be reversible. On the other hand, if the inverted stimuli do not return the material to its original condition, the material is said to have undergone an irreversible process. Irreversible processes involve dissipation of energy and production of entropy. The reversibility of a thermodynamic process, or lack thereof, may depend upon the scale at which the observer views the process (Germain et al. 1983). For example, a crystal structure undergoing small, slow deformations may appear reversible (i.e., elastic) at the macroscale, but could be irreversible at the scale of the motion of some individual atoms, particularly those in the vicinity of imperfections (i.e., defects) in the material.

The Clausius-Duhem inequality and various renditions of it are alternatively referred to as the Second Law of Thermodynamics, the entropy production inequality, or the dissipation inequality. This relationship reduces to an equality for thermodynamically reversible processes. In solids undergoing irreversible processes, a local version of this inequality, in combination with the local balance of energy, provides an indication of contributions of various mechanisms to energy stored in the material and to energy dissipated by the material. Constitutive equalities and thermodynamic restrictions on constitutive and kinetic relationships can be derived by appealing to the First and Second Laws of Thermodynamics, as formally demonstrated for heat conducting media with viscosity by Coleman and Noll (1963) and continua with generic internal state variables by Coleman and Gurtin (1967). Such methods of thermodynamic analysis have become commonplace for constructing nonlinear theories of elasto-

plasticity of crystalline solids (Scheidler and Wright 2001), including those incorporating internal variables associated with higher-order deformation gradients reflecting dislocation content (Teodosiu 1970; Steinmann 1996; Bammann 2001; Regueiro et al. 2002; Clayton et al. 2004b, 2006).

Section 4.2.1 describes considerations for selection of constitutive variables (including both dependent and independent variables) and internal state variables that together describe the thermodynamic state of a body. Particular attention is paid to variables appropriate for crystalline solids undergoing potentially large deformations.

4.2.1 Constitutive and Internal Variables for Crystalline Solids

Constitutive laws are mathematical relationships that describe properties of particular materials or particular classes of materials. Such relationships emerge from the constitution of the material, e.g., its composition and structure, hence the term "constitutive law". In the context of continuum thermomechanics, constitutive laws describe relationships between independent and dependent state variables and/or their rates of change. A number of possibilities exist with regards to selection of which variables should be used as independent quantities and which should be dependent quantities. For example, various formulations treating temperature, entropy, or internal energy as either independent or dependent variables exist (Eringen 1962; Coleman and Noll 1963; Coleman and Gurtin 1967; Malvern 1969; Thurston 1974; Wright 2002), all of which are mathematically and physically valid.

Selections of independent and dependent variables in thermodynamic processes are labeled in this book as constitutive assumptions. Though more general assumptions are possible, for crystalline solids under consideration in this text the following forms are perhaps most common[3]:

$$\psi = \psi\left(\mathbf{F}^{\mathbf{L}}, \alpha, \theta, \overset{g}{\nabla}\theta, X, \mathbf{G}_A\right), \ \psi = \psi\left(F^{La}_{.\alpha}, \alpha, \theta, \theta_{,a}, X, \mathbf{G}_A\right); \qquad (4.45)$$

$$\eta = \eta\left(\mathbf{F}^{\mathbf{L}}, \alpha, \theta, \overset{g}{\nabla}\theta, X, \mathbf{G}_A\right), \ \eta = \eta\left(F^{La}_{.\alpha}, \alpha, \theta, \theta_{,a}, X, \mathbf{G}_A\right); \qquad (4.46)$$

---

[3] Not included in (4.45)-(4.49) is a dependence on higher-order deformation gradients, e.g., $F^a_{A:B} = x^a_{.AB}$ of (2.116). A material is often said to be of grade N, where N is the highest order of deformation gradient present in the list of dependent state variables (Toupin 1964). Thus, when $F^{La}_{.\alpha} = x^a_{.A} g^A_{.\alpha}$ such as in an elastic solid described by (3.25), relations (4.45)-(4.49) describe a material of grade 1.

$$\boldsymbol{\sigma} = \boldsymbol{\sigma}\left(\mathbf{F^L}, \alpha, \theta, \overset{g}{\nabla}\theta, X, \mathbf{G}_A\right), \quad \sigma^{ab} = \sigma^{ab}\left(F^{La}_{.\alpha}, \alpha, \theta, \theta_{,a}, X, \mathbf{G}_A\right); \quad (4.47)$$

$$\mathbf{q} = \mathbf{q}\left(\mathbf{F^L}, \alpha, \theta, \overset{g}{\nabla}\theta, X, \mathbf{G}_A\right), \quad q^a = q^a\left(F^{La}_{.\alpha}, \alpha, \theta, \theta_{,a}, X, \mathbf{G}_A\right); \quad (4.48)$$

$$\dot{\alpha} = \dot{\alpha}\left(\mathbf{F^L}, \alpha, \theta, \overset{g}{\nabla}\theta, X, \mathbf{G}_A\right), \quad \dot{\alpha} = \dot{\alpha}\left(F^{La}_{.\alpha}, \alpha, \theta, \theta_{,a}, X, \mathbf{G}_A\right). \quad (4.49)$$

Dependent variables in (4.45)-(4.49) are Helmholtz free energy per unit mass ψ, entropy per unit mass η, Cauchy stress $\boldsymbol{\sigma}$, heat flux vector $\mathbf{q}$, and the material time derivative of a generic scalar internal state variable $\alpha(X,t)$. Extension of the treatment to multiple state variables of scalar, vector, or tensor character is straightforward, and is pursued by example later in Chapters 8 and 9. Independent variables are lattice deformation gradient $\mathbf{F^L}$ of (3.31), absolute temperature θ and its spatial gradient $\theta_{,a}$, and internal state variable α. Additionally, dependence on position of material particle X is included, as is dependence on basis vectors $\mathbf{G}_A(X)$ in the reference configuration. Dependence on X is required to describe variations, with changes in position, of properties in a heterogeneous material, while dependence on $\mathbf{G}_A$ is required to describe anisotropy, or dependence of the response on orientation of a body with certain symmetries (see Appendix A) relative to the chosen system of coordinates[4].

As discussed in Section 3.1.2, in defect-free elastic crystals $\mathbf{F^L}$ corresponds to deformation gradient $\mathbf{F}$. More generally, as indicated in (3.31), for a crystal featuring inelastic deformation, $\mathbf{F^L} = \mathbf{FF^{P-1}} \neq \mathbf{F}$. The rationale for dependence of free energy and stress upon lattice deformation follows from (3.109)-(3.114): lattice deformation provides a first-order accurate measure of stretch and rotation of interatomic bond vectors in a crystal structure. In dielectric solids, the list of independent variables may be supplemented with a measure of the electric polarization (e.g., measuring relative translations among charged nuclei in a polyatomic ionic crystal), and dependent variables then may include the electric field or electric displacement, as described in detail in Chapter 10.

It is possible to write (4.45)-(4.49) in terms of variables defined partially or entirely with respect to coordinate charts of different configurations

---

[4] Often dependence on X and $\mathbf{G}_A$ is not written out explicitly, but rather is included implicitly in the material coefficients (e.g., thermoelastic moduli) entering series expansions of the thermodynamic potentials. This will become clear in Chapter 5 in the context of thermoelastic crystalline solids.

(e.g., spatial configuration B or reference configuration B_0), and with dependent energetic and entropic variables measured on a per-unit-volume basis following (4.8) or (4.9), as opposed to a per-unit-mass basis. Certain choices of configuration may result in different constitutive laws or different predicted behaviors, and some choices may be more physically motivated than others, as considered later for elastic-plastic crystals in Chapters 6, 8, and 9.

Response functions (4.45)-(4.49) are often presumed to adhere to a collection of formal, fundamental principles or postulates. These include the principle of equipresence (Truesdell 1951) that suggests that all independent variables should be present in each constitutive equation unless contradicted by physical laws or symmetry properties of the material. The latter requirement is often delineated as a separate principle, that is functions (4.45)-(4.49) should respect symmetry properties of the substance, as addressed explicitly here by presence of basis vectors $\mathbf{G}_A$ (Eringen 1962).

The response should also satisfy an objectivity, frame-indifference, or covariance principle, versions of which have been considered for a number of years in the mathematical mechanics literature (Noll 1958; Coleman and Noll 1963; Coleman and Gurtin 1967; Marsden and Hughes 1983; Yavari et al. 2006). Objectivity as defined here implies that physical behavior is independent of the reference frame of the observer. Specifically, the physical behavior of an event should not change under a change of spatial coordinate system (Coleman and Noll 1963; Coleman and Gurtin 1967). Objective constitutive functions can be formulated in a number of ways. Perhaps the easiest way involves replacing the list of independent variables by constructs of these variables that are invariant under appropriate rigid body motions (i.e., rigid rotations and translations) of the spatial coordinate system, and by choosing complementary forms of dependent variables that are likewise spatially invariant.

Consider the choice of lattice deformation gradient $\mathbf{F}^L$ as an independent variable entering functions (4.45)-(4.49). Under a change of spatial frame $\mathbf{x} \to \hat{\mathbf{Q}}\mathbf{x} + \mathbf{c}$, where $\hat{\mathbf{Q}}(t) = \hat{\mathbf{Q}}^{-T}(t)$ is a spatially constant, proper orthogonal rotation matrix and $\mathbf{c}(t)$ is a spatially constant translation vector, the deformation gradient $\mathbf{F} \to \hat{\mathbf{Q}}\mathbf{F}$ and the lattice deformation $\mathbf{F}^L \to \hat{\mathbf{Q}}\mathbf{F}^L$. More general kinds of space-time transformations involving time shifts and additional translations are possible (Malvern 1969; Gurtin 1981; Maugin 1988), but consideration of $\mathbf{x} \to \hat{\mathbf{Q}}\mathbf{x} + \mathbf{c}$ is sufficient for the present discussion. Often, a number of possible sets of reduced constitutive equations exist that fulfill the objectivity requirement. For example, re-

placing dependent variable $\mathbf{F^L}(X,t)$ with $\tilde{\mathbf{C}}^L(X,t)$ of (3.52) satisfies the objectivity requirement that is not unequivocally satisfied by use of independent variable $\mathbf{F^L}$, since under a change of frame,

$$
\begin{aligned}
\tilde{C}^L_{\alpha\beta} &= F^{La}_{.\alpha} g_{ab} F^{Lb}_{.\beta} = F^{La}_{.\alpha} F^{LT}_{\beta a} \rightarrow (\hat{Q}^a_{.c} F^{Lc}_{.\alpha})(\hat{Q}^{Td}_{.a} F^{LT}_{\beta d}) \\
&= \hat{Q}^{Td}_{.a} \hat{Q}^a_{.c} F^{Lc}_{.\alpha} F^L_{.d\beta} = \delta^d_{.c} F^{Lc}_{.\alpha} F^L_{.d\beta} = F^{Ld}_{.\alpha} F^L_{.d\beta} = \tilde{C}^L_{\alpha\beta}.
\end{aligned}
\tag{4.50}
$$

Spatial metric tensor $\mathbf{g}(x)$ is unaffected by such an orthogonal transformation since $g_{ab} \rightarrow \hat{Q}^c_{.a} g_{cd} \hat{Q}^d_{.b} = \hat{Q}^c_{.a} \hat{Q}_{cb} = \hat{Q}^T_{bc} \hat{Q}^c_{.a} = g_{ba} = g_{ab}$.

Similarly, spatial temperature gradient $\theta_{,a}(X,t)$ is not frame indifferent. One of several possible substitutions that fulfills the objectivity requirement is the reference gradient $\theta_{,A} = \theta_{,a} x^a_{.,A}$ (Coleman and Noll 1963):

$$
\begin{aligned}
\theta_{,A} &= \theta_{,a} x^a_{.,A} = \theta^{.a} F^T_{Aa} \rightarrow \hat{Q}^a_{.c} \theta^{.c} F^T_{Ad} \hat{Q}^{Td}_{.a} \\
&= \hat{Q}^{Td}_{.a} \hat{Q}^a_{.c} \theta^{.c} F^T_{Ad} = \theta^{.c} F^T_{Ac} = \theta_{,c} x^c_{.,A} = \theta_{,A}.
\end{aligned}
\tag{4.51}
$$

In classical continuum mechanics, response functions (4.45)-(4.49) are also required to satisfy a principle of locality, meaning that dependent variables corresponding to a particular material particle at X are functions of independent variables at point X and not values of independent variables at other material points X'. However, in many generalized continuum theories, the assertion of locality is relaxed (Eringen 1972; Bazant 1991). As an example, consider a material that exhibits time evolution of internal state variable α. Classes of nonlocal internal variable theories include those with evolution equations of the general type

$$
\dot{\alpha}(X,t) = f\left(F^{La}_{.\alpha}, \alpha, \theta, \theta_{,a}, \mathbf{G}_A, X, X'\right),
\tag{4.52}
$$

where the value of $\dot{\alpha}$ at X is affected by the values of state quantities at different points $X' \in B_0$ entering function f. Integral formulations, inherently nonlocal, are also possible, e.g.

$$
\dot{\alpha}(X,t) = V^{-1} \int_V f'\left(F^{La}_{.\alpha}, \alpha, \theta, \theta_{,a}, \mathbf{G}_A, X, X'\right) dV,
\tag{4.53}
$$

where the domain of integration may encompass some local region (e.g., volume V) in the vicinity of point X in the body (Hall and Hayhurst 1991), or may engulf the entire solid. Finally, theories of the higher-gradient type are often labeled nonlocal in character (Voyiadjis and Deliktas 2009). For example, consider an evolution equation of the form

$$
\dot{\alpha}(X,t) = f\left(F^{La}_{.\alpha}, \alpha, \alpha_{,A}, \theta, \theta_{,a}, \mathbf{G}_A, X\right).
\tag{4.54}
$$

Expanding α in a Taylor series approximation about point X gives

$$\alpha\big|_{X'} = \alpha\big|_X + \alpha_{,A}\big|_X \, dX^A + \frac{1}{2!}\alpha_{,AB}\big|_X \, dX^A dX^B$$

$$+ \frac{1}{3!}\alpha_{,ABC}\big|_X \, dX^A dX^B dX^C + ..., \tag{4.55}$$

where $dX^A = X'^A - X^A$. Omitting second- and higher-order terms in $d\mathbf{X}$, the material gradient of α is expressed via local and nonlocal values of α:

$$\alpha_{,A}(X,t)dX^A = \alpha(X',t) - \alpha(X,t), \tag{4.56}$$

implying that (4.54) exhibits a particular form encompassed by nonlocal equation (4.52). Constitutive functions depending on first-order, but not higher-order, spatial gradients of position and temperature are considered to describe materials categorized as classical rather than generalized continua. Elastic solids of grade 2 (see Section 5.7), as a matter of semantics, can be labeled local (Epstein and Elzanowski 2007) or nonlocal.

Particular choices of internal state variables should satisfy physical and practical considerations. Internal state variables may be directly measurable or observable to allow straightforward construction of evolution laws such as (4.49) from experimental data, or they can be "hidden" variables that influence the response in a measurable way but lack a precise microscopic interpretation. Examples of the former include measures of dislocation density in plastically deforming crystals (Kroner 1963a; Teodosiu 1970) and direct measures of porosity or crack density in damaged media (Bammann and Aifantis 1989; Kachanov 1992; Nemat-Nasser and Horii 1998). Examples of the latter include generic variables representing strain hardening in plastic crystals (e.g., thermodynamic conjugate variables to a yield stress or back stress) and generic scalar or tensor damage measures that reflect mechanical stiffness reduction, for example (Germain et al. 1983; Lemaitre 1985). However, while an internal variable or its effects should be measurable, its value should not be controllable simply by immediate application of external boundary conditions (e.g., mechanical traction and heat flux), since in that case it would be an external as opposed to internal variable. In such a case, the so-called internal variable would not be independent of other state variables such as stress, strain, and temperature, and would be redundant for characterizing the state of the material. Instead, instantaneous values of internal state variables tend to depend on initial conditions and the cumulative history of boundary conditions applied to the body.

Internal state variables should be chosen to adhere to underlying physics of the microstructure of the material, and their evolution should reflect corresponding changes in forces or energies supported in the substance. For example, accumulating dislocations tend to increase the energy stored in

the crystal as a result of their local stress and strain fields, and damage mechanisms such as voids or cracks tend to affect the energy of a strained crystal via a reduction in the effective elastic stiffness. On the other hand, non-cumulative measures of plastic flow such as plastic deformation gradient $\mathbf{F^P}$ of (3.31) or plastic strain tensor $\boldsymbol{\varepsilon^P}$ of (3.80) are not always realistic choices for internal state variables. From a microscopic perspective (Sections 3.2.1, 3.2.2, and 3.2.5-3.2.7), plastic deformation is regarded as lattice-preserving or lattice invariant (Bilby et al. 1957), and dislocations may pass completely through a volume element of the crystal, engendering significant plastic deformation without leaving behind any defects that would render the energetic state of the crystal different from that of an initially perfect lattice. From a macroscopic perspective, prescription of $\mathbf{F^P}$ (or, for example, $\boldsymbol{\varepsilon^P}$ in the linear case) as a state variable fails in applications wherein external loading is not monotonic. For example, a crystalline specimen can be deformed plastically and then deformed plastically again to its original shape. Under such a sequence, the material in its final state will often contain larger internal residual stresses, more defects, and greater energy of cold work (Farren and Taylor 1925; Taylor and Quinney 1934; Rosakis et al. 2000) than the specimen in its initial state, yet such changes will not be reflected by $\mathbf{F^P}$ or $\boldsymbol{\varepsilon^P}$, since these variables are negligible both at the start and the end of the cyclic experiment.

Finally, particular forms of constitutive assumptions (4.45)-(4.49) should not lead to violations of the fundamental balance principles of continuum thermomechanics: balances of mass, momentum, and energy. In addition, thermodynamic processes should be thermodynamically admissible, meaning they should satisfy the Clausius-Duhem inequality.

4.2.2 The Clausius-Duhem Inequality

The Clausius-Duhem inequality, alternatively referred to as the entropy production inequality or dissipation inequality, is the particular form of the Second Law of Thermodynamics usually considered in continuum mechanics. The global form of the Clausius-Duhem inequality is written for a continuous body in spatial configuration B as

$$\frac{d}{dt}\int_v \rho\eta\,dv \geq \int_v \frac{\rho r}{\theta}\,dv - \int_s \frac{\langle\mathbf{q},\mathbf{n}\rangle}{\theta}\,ds \,, \qquad (4.57)$$

where heat flux vector $\mathbf{q}(x,t)$ and heat source scalar $r(x,t)$ were introduced in (4.32). Applying the divergence theorem to the rightmost term,

$$\int_s \frac{\langle \mathbf{q}, \mathbf{n} \rangle}{\theta} ds = \int_v \left\langle \overset{\mathbf{g}}{\nabla}, \frac{\mathbf{q}}{\theta} \right\rangle dv = \int_v \frac{1}{\theta} \left\langle \overset{\mathbf{g}}{\nabla}, \mathbf{q} \right\rangle dv - \int_v \frac{1}{\theta^2} \left\langle \overset{\mathbf{g}}{\nabla} \theta, \mathbf{q} \right\rangle dv, \quad (4.58)$$

or in indicial notation,

$$\int_s \theta^{-1} q^a n_a ds = \int_v (\theta^{-1} q^a)_{;a} dv = \int_v \theta^{-1} q^a_{;a} dv - \int_v \theta^{-2} \theta_{,a} q^a dv. \quad (4.59)$$

The local form of (4.57) becomes, upon using Reynolds transport theorem (4.14) and (4.59),

$$\Gamma = \rho \dot{\eta} + \theta^{-1}(q^a_{;a} - \rho r - \theta^{-1} q^a \theta_{,a}) \geq 0. \quad (4.60)$$

Above, Γ is the total entropy production rate per unit spatial volume that, according to the Second Law of Thermodynamics, must be non-negative. The entropy production rate is often written on a per unit mass basis by dividing (4.60) by mass density $\rho(x,t) > 0$ (Malvern 1969). When $\Gamma = 0$, the corresponding thermodynamic process is said to be thermodynamically reversible or conservative; when $\Gamma > 0$, the process is said to be irreversible or dissipative.

Entropy production law (4.60) is often partitioned into two separate, more restrictive inequalities (Truesdell and Noll 1965):

$$\Gamma_L = \rho \dot{\eta} + \theta^{-1}(q^a_{;a} - \rho r) \geq 0, \quad \Gamma_C = -\theta^{-2} q^a \theta_{,a} \geq 0, \quad (4.61)$$

where Γ_L is the rate of local entropy production and Γ_C is the rate of entropy production attributed to heat conduction. The first inequality in (4.61) is often referred to as the strong form of the Clausius-Duhem inequality, and it requires that the specific entropy rate $\dot{\eta}$ be non-negative in the absence of heat supply r and heat conduction $\mathbf{q}$. The second inequality of (4.61) prevents heat from spontaneously flowing from regions of low temperature to high temperature. Though more general constitutive equations for heat flux are possible (Truesdell and Noll 1965), the following constitutive assumption in the spatial frame is standard for many solids:

$$\mathbf{q} = -\mathbf{k} \overset{\mathbf{g}}{\nabla} \theta, \quad q^a = -k^{ab} \theta_{,b}, \quad \Gamma_C = \theta^{-2} \theta_{,a} k^{ab} \theta_{,b} \geq 0, \quad (4.62)$$

where $\mathbf{k}(x,t) \in T_x B \times T_x B$ is the contravariant tensor of thermal conductivity, assumed symmetric and positive semi-definite. Conductivity $\mathbf{k}$ may generally depend on temperature, deformation, other state variables, position, and orientation of the material element. When all entries of k^{ab} are constants, (4.62) is often referred to as Fourier's law of heat conduction.

From differentiation of the free energy in Table 4.2, $\theta \dot{\eta} = \dot{e} - \dot{\psi} - \dot{\theta} \eta$, so that after multiplying by θ, (4.60) can be written

$$\rho\theta\dot{\eta} + (q^a_{;a} - \rho r - \theta^{-1}q^a\theta_{,a})$$
$$= \rho(\dot{e} - \dot{\psi} - \dot{\theta}\eta - r) + q^a_{;a} - \theta^{-1}q^a\theta_{,a} \geq 0. \quad (4.63)$$

For classical continua, substitution of energy balance (4.35) into (4.63) then gives

$$\sigma^{ab}D_{ab} - \rho\dot{\psi} - \rho\dot{\theta}\eta - \theta^{-1}q^a\theta_{,a} \geq 0. \quad (4.64)$$

Expanding the rate of free energy ψ of (4.45) using the chain rule (Coleman and Noll 1963) gives

$$\dot{\psi} = \frac{\partial\psi}{\partial F^{La}_{.\alpha}}\dot{F}^{La}_{.\alpha} + \frac{\partial\psi}{\partial\theta}\dot{\theta} + \frac{\partial\psi}{\partial\theta_{,a}}\gamma_a + \frac{\partial\psi}{\partial\alpha}\dot{\alpha}, \quad (4.65)$$

where as noted following (2.129), $\mathbf{G}_A(X) = 0$ since convected reference coordinates are not considered. The rate of temperature gradient is

$$\gamma_a = d(\theta_{,a})/dt = d(\theta_{,A}F^{-1A}_{.a})/dt = \dot{\theta}_{,a} + \theta_{,b}F^b_A\dot{F}^{-1A}_{.a}$$
$$= \dot{\theta}_{,a} - \theta_{,b}\dot{F}^b_A F^{-1A}_{.a} = \dot{\theta}_{,a} - \theta_{,b}v^b_{;a} = \dot{\theta}_{,a} - \theta_{,b}L^b_{.a}. \quad (4.66)$$

Substitution of (4.65) into (4.64) then results in a local form of the Clausius-Duhem inequality that accounts for constitutive dependencies allotted in (4.45):

$$\sigma^{ab}D_{ab} - \rho\left[\frac{\partial\psi}{\partial F^{La}_{.\alpha}}\dot{F}^{La}_{.\alpha} + \left(\eta + \frac{\partial\psi}{\partial\theta}\right)\dot{\theta} + \frac{\partial\psi}{\partial\theta_{,a}}\gamma_a + \frac{\partial\psi}{\partial\alpha}\dot{\alpha}\right] \geq \theta^{-1}q^a\theta_{,a}. \quad (4.67)$$

Quantity $-\rho\partial\psi/\partial\alpha$ is often referred to as a conjugate thermodynamic force or conjugate driving force to thermodynamic flux $\dot{\alpha}$. Thermodynamic processes for which $\dot{\theta} = 0$ are called isothermal processes. Processes for which $\dot{\eta} = 0$ are labeled isentropic processes. Processes for which $q^a = 0$ are referred to as adiabatic processes.

The Clausius-Duhem inequality exhibits an analogous representation in reference configuration B_0. The referential representation can be derived starting from a global principle like (4.57), but couched in the reference frame, or by converting local quantities using appropriate pull-back and Piola transform operations. The latter approach is pursued here. Local dissipation inequality (4.60) becomes, upon multiplying by $J(X,t) > 0$,

$$\Gamma_0 = J\Gamma = \rho_0\dot{\eta} + \theta^{-1}(Jq^a_{;a} - \rho_0 r - \theta^{-1}Jq^a\theta_{,a})$$
$$= \rho_0\dot{\eta} + \theta^{-1}(Q^A_{;A} - \rho_0 r - \theta^{-1}Q^A\theta_{,A}) \geq 0, \quad (4.68)$$

where mass density $\rho_0 = \rho J$ by (4.10), heat flux $Q^A = JF^{-1A}_{.a}q^a$ by (4.36), and $Jq^a_{;a} = Q^A_{;A}$ by (4.37). A heat conduction law of the following form in

the reference configuration can be prescribed, so that the rightmost term in (4.68) associated with conduction is always non-negative:

$$\mathbf{Q} = -\mathbf{K} \overset{G}{\nabla} \theta, \quad Q^A = -K^{AB}\theta_{,B}, \quad -\theta^{-2}Q^A\theta_{,A} = \theta^{-2}\theta_{,A}K^{AB}\theta_{,B} \geq 0, \quad (4.69)$$

where $\mathbf{K}(X,t) \in T_X B_0 \times T_X B_0$ is a symmetric and positive semi-definite matrix of thermal conductivity. Similarly to $\mathbf{k}$ of (4.62), $\mathbf{K}$ of (4.69) may depend on temperature as is often the case in crystalline solids, strain, location and orientation of the material element (heterogeneity and anisotropy), as well as internal state variables. Consistency with (4.62) implies that spatial and referential matrices of thermal conductivity are related by $k^{ab} = J^{-1}F_{.A}^a K^{AB}F_{.B}^b$.

From (4.68) and $\psi = e - \theta\eta$, an analog of (4.63) measured as an energy rate per unit reference volume is

$$\rho_0(\dot{e} - \dot{\psi} - \dot{\theta}\eta - r) + Q_{;A}^A - \theta^{-1}Q^A\theta_{,A} \geq 0. \quad (4.70)$$

Substituting referential energy balance (4.39) into (4.70) gives

$$\Sigma^{AB}\dot{E}_{AB} - \rho_0\dot{\psi} - \rho_0\dot{\theta}\eta - \theta^{-1}Q^A\theta_{,A} \geq 0. \quad (4.71)$$

Then upon expanding the rate of free energy per unit mass $\dot{\psi}$ using (4.65), the referential form of (4.67) is

$$\Sigma^{AB}\dot{E}_{AB} - \rho_0\left[\frac{\partial\psi}{\partial F_{.\alpha}^{La}}\dot{F}_{.\alpha}^{La} + \left(\eta + \frac{\partial\psi}{\partial\theta}\right)\dot{\theta}\right.$$
$$\left. + \frac{\partial\psi}{\partial\theta_{,a}}\gamma_a + \frac{\partial\psi}{\partial\alpha}\dot{\alpha}\right] \geq \theta^{-1}Q^A\theta_{,A}. \quad (4.72)$$

In the case of geometric linearity, i.e., small deformations with (4.40), dissipation inequality (4.67) is simply

$$\sigma^{ab}\dot{\varepsilon}_{ab} - \rho\left[\frac{\partial\psi}{\partial\beta_{ab}^L}\dot{\beta}_{ab}^L + \left(\eta + \frac{\partial\psi}{\partial\theta}\right)\dot{\theta} + \frac{\partial\psi}{\partial\theta_{,a}}\gamma_a + \frac{\partial\psi}{\partial\alpha}\dot{\alpha}\right] \geq \theta^{-1}q^a\theta_{,a}, \quad (4.73)$$

where dependence of free energy ψ on lattice distortion β_{ab}^L of (3.75) replaces dependence of free energy on lattice deformation gradient $F_{.\alpha}^{La}$ in constitutive assumption (4.45).

4.3 Kinetics and Inelastic Rates

The term kinetics is used generically in this book to denote thermodynamically irreversible processes involving rates or fluxes of matter or energy. For example, kinetic processes in crystals include defect generation and

motion, such as dislocation nucleation and glide or vacancy production and diffusion. Other irreversible processes include damage evolution in the form of micro-cracking in brittle solids or pore collapse in crushable solids. Kinetic processes are contrasted to reversible processes in crystalline solids such as mechanically elastic deformation in the absence of viscosity or internal friction. Kinetic processes involve dissipation of energy, for example heat produced by the conjugate pair of dislocation velocity and lattice friction (Kocks et al. 1975), or the rate of work of crack sliding conjugate to frictional forces along fracture surfaces in contact.

In the context of (4.67) or (4.72), dissipation may result from three physical mechanisms: heat conduction, mechanical deformation, and time rates of internal state variables. As noted in Section 4.2.1, internal state variables typically account for irreversible structural rearrangements within crystalline solids, often at a microscopic scale of resolution. Regardless of mechanism or physical origin, dissipative energy changes in the solid can often be written in the generic form

$$d = \sum_{i=1}^{k} \lambda^i \left\langle \mathbf{Z}^i, \mathbf{J}^i \right\rangle , \tag{4.74}$$

where d is the time rate of energy change or dissipation, $\mathbf{J}^i$ is a generalized rate or flux, $\mathbf{Z}^i$ is a generalized conjugate force to $\mathbf{J}^i$, and $\lambda^i \geq 0$ is a scalar multiplier, each for flux-force pair i. Summation in (4.74) runs over $i = 1, 2, \ldots k$ generalized flux-force pairs that may be scalars, vectors, or tensors of higher order. To ensure that energetic changes associated with (4.74) are always dissipative, or always contribute positively to the rate of entropy production Γ in (4.60) for example, the dissipation potential concept is often invoked (Ziegler 1963; Germain et al. 1983):

$$\mathbf{Z}^i = \frac{\partial \Theta}{\partial \mathbf{J}^i}, \ \ \mathbf{J}^i = \frac{\partial \Omega}{\partial \mathbf{Z}^i} , \tag{4.75}$$

where scalar potentials Θ and Ω are constructed such that $d \geq 0$ in (4.74). A straightforward way to guarantee positive dissipation is prescription of the quadratic forms

$$\Theta = \frac{1}{2} \sum_{i,j=1}^{k} \left\langle \mathbf{J}^i, \mathbf{O}^{ij} \mathbf{J}^j \right\rangle, \ \ \Omega = \frac{1}{2} \sum_{i,j=1}^{k} \left\langle \mathbf{Z}^i, \mathbf{o}^{ij} \mathbf{Z}^j \right\rangle , \tag{4.76}$$

where operators $\mathbf{O}$ and $\mathbf{o}$ are symmetric with respect to i and j and are positive definite. Potentials (4.76) lead to linear relationships between fluxes and forces known as Onsager's relations (Onsager 1931a, b):

$$\mathbf{Z}^i = \sum_{j=1}^{k} \mathbf{O}^{ij} \mathbf{J}^j , \ \ \mathbf{J}^i = \sum_{j=1}^{k} \mathbf{o}^{ij} \mathbf{Z}^j . \tag{4.77}$$

The rate of dissipated energy of (4.74) in these cases is

$$d = \sum_{i,j=1}^{k} \lambda^i \left\langle \mathbf{J}^i, \mathbf{O}^{ij} \mathbf{J}^j \right\rangle = \sum_{i,j=1}^{k} \lambda^i \left\langle \mathbf{Z}^i, \mathbf{o}^{ij} \mathbf{Z}^j \right\rangle \geq 0 . \tag{4.78}$$

Kinetic relations of the form (4.77) are convenient and physically realistic in some, but not all, circumstances (Onsager 1931a, b). Ziegler (1963) demonstrated that Onsager's relations correspond to a principle of maximum entropy production or maximum dissipated energy, an appealing concept if one follows the viewpoint that kinetic processes in materials take place in such a way that stored energy in the substance tends to evolve towards a minimum value. However, linear relations of the form (4.77) are not the most general kinetic laws that simply ensure positive entropy production, and in many cases more physically realistic alternatives exist.

Energetic changes attributed to heat conduction often follow the scheme outlined in (4.74)-(4.78). From (4.61), dissipation from conduction is

$$d = \theta \Gamma_C = -\frac{1}{\theta} q^a \theta_{,a} . \tag{4.79}$$

In the scheme of (4.74), $\lambda = \theta^{-1} > 0$, heat flux $J^a = q^a$, and $Z_a = -\theta_{,a}$ is a conjugate thermodynamic force. A dissipation potential can be defined:

$$\Omega = \frac{1}{2} \theta_{,a} k^{ab} \theta_{,b} , \tag{4.80}$$

where in the context of (4.76), $\mathbf{o} = \mathbf{k}$ is the symmetric thermal conductivity. Using (4.75), this potential leads to Fourier conduction:

$$q^a = \frac{\partial \Omega}{\partial (-\theta_{,a})} = -\frac{\partial \Omega}{\partial \theta_{,a}} = -k^{ab} \theta_{,b} , \tag{4.81}$$

and to unconditionally non-negative dissipation in (4.78):

$$d = \frac{1}{\theta} \theta_{,a} k^{ab} \theta_{,b} \geq 0 . \tag{4.82}$$

Next consider energetic changes associated with evolution of internal state variables. Following (4.67), the time rate of change of a single internal state variable α produces a rate of change in free energy

$$d = -\rho \frac{\partial \psi}{\partial \alpha} \dot{\alpha} , \tag{4.83}$$

where in the notation of (4.74), $\lambda = 1$, the flux is the rate of the internal variable $J = \dot{\alpha}$, and the conjugate force is the negative free energy derivative $Z = -\rho \partial \psi / \partial \alpha$. In this context, $d > 0$ implies that the material dissipates energy as a result of structural rearrangements associated with rates of internal variables, leading to a decrease in Helmholtz free energy ψ. Structural rearrangements need not always be dissipative, however, and in many cases lead to an increase in free energy of the solid, such that $d < 0$.

An example of such an energetic storage process in a crystal is an increase in defect density and corresponding increase in residual elastic energy associated with stress fields of individual defects. However, to ensure positive dissipation when physically appropriate, a dissipation potential can still be used along the lines of (4.74)-(4.78) to dictate rates of internal variables or their conjugate thermodynamic forces.

Finally, consider energetic changes stemming from rates of inelastic deformation. For illustrative purposes, consider specifically the time rate of plastic deformation gradient $\mathbf{F^P}$ of multiplicative decomposition (3.31), and its work conjugate stress measure labeled here as $\mathbf{Z^P}$. More precise definitions of appropriate inelastic rates and conjugate stress measures are derived in Chapter 6 dealing with elastoplasticity, but a generic description suffices for now. The dissipation associated with this stress-deformation rate pair is

$$d = \left\langle \mathbf{Z^P}, \dot{\mathbf{F}}^\mathbf{P} \right\rangle = Z^{PA}_{.\alpha} \dot{F}^{P\alpha}_{.A} , \qquad (4.84)$$

or in the terminology of (4.74), $\lambda = 1$, flux $\mathbf{J} = \dot{\mathbf{F}}^\mathbf{P}$, and the driving force $\mathbf{Z} = \mathbf{Z^P}$. A dissipation potential can be constructed to ensure positive dissipation, i.e.,

$$2\Omega = \left\langle \mathbf{Z^P}, \boldsymbol{\lambda}^\mathbf{P} : \mathbf{Z^P} \right\rangle^N = (Z^{PA}_{.\alpha} \lambda^{P\alpha\beta}_{AB} Z^{PB}_{.\beta})^N = \bar{Z}^N , \qquad (4.85)$$

where $\boldsymbol{\lambda}^\mathbf{P}$ is a positive semi-definite operator of order four and is clearly a two-point tensor. Exponent N (subject to constraint $N > 0$), when given a value other than unity, accounts for situations when a linear dependence of the dissipation potential on scalar product $\bar{Z}$ is physically inappropriate. The rate of plastic deformation becomes, from the second of (4.75),

$$\dot{\mathbf{F}}^\mathbf{P} = \frac{\partial \Omega}{\partial \mathbf{Z^P}} = N\bar{Z}^{N-1}\boldsymbol{\lambda}^\mathbf{P} : \mathbf{Z^P} , \; \dot{F}^{P\alpha}_{.A} = \frac{\partial \Omega}{\partial Z^{PA}_{.\alpha}} = N\bar{Z}^{N-1}\lambda^{P\alpha\beta}_{AB} Z^{PB}_{.\beta} , \qquad (4.86)$$

and the dissipation of (4.78) is always non-negative:

$$d = N\bar{Z}^{N-1} \left\langle \mathbf{Z^P}, \boldsymbol{\lambda}^\mathbf{P} : \mathbf{Z^P} \right\rangle = N\bar{Z}^N \geq 0 . \qquad (4.87)$$

When the matrix $\boldsymbol{\lambda}^\mathbf{P}$ is isotropic, i.e., $\lambda^{P\alpha\beta}_{AB} = \lambda^P g^{\alpha\beta} G_{AB}$, the rate of plastic deformation gradient is coaxial with driving stress $\mathbf{Z^P}$:

$$\dot{\mathbf{F}}^\mathbf{P} = N\bar{Z}^{N-1}\lambda^P \mathbf{Z^P} , \; \dot{F}^{P\alpha}_{.A} = N\bar{Z}^{N-1}\lambda^P g^{\alpha\beta} G_{AB} Z^{PB}_{.\beta} , \qquad (4.88)$$

and λ^P is the plastic multiplier found by squaring both sides of (4.88):

$$\lambda^P = N^{-2}\bar{Z}^{1-2N}\dot{\mathbf{F}}^\mathbf{P} : \dot{\mathbf{F}}^\mathbf{P} = N^{-2}\bar{Z}^{1-2N}\dot{F}^{P\alpha}_{.A} \tilde{g}_{\alpha\beta} G^{AB} \dot{F}^{P\beta}_{.B} , \qquad (4.89)$$

As demonstrated by example in Section 6.4 of Chapter 6, a description similar to (4.88) is often used in macroscopic plasticity theories for ductile metals, such that the time rate of plastic deformation and its driving force

always share the same direction. A distinct kinetic relation, or a constitutive assumption such as the consistency condition of associative plasticity (see Section 6.4), specifies the magnitude of the plastic deformation gradient rate via the instantaneous value of $\lambda^P(X,t)$. In plasticity theory, the explicit prescription of the rate of plastic deformation is often labeled a flow rule. When derived from the gradient of a plastic potential, e.g., Ω of (4.86), plastic deformation is said to obey a normality principle.

When each rate $\dot{\alpha}$ of an internal variable representing a microscopic structural rearrangement—for example dislocation position or cumulative slip—is dictated solely by its conjugate driving force $-\rho \partial \psi / \partial \alpha$, the temperature θ, and the current values of the set of such structural variables, a generalized normality structure similar to that depicted in (4.86) emerges for increments of plastic strain (Rice 1971). However, derivation of such a normality structure seems to require that the increment of plastic deformation gradient (or plastic strain) be characterized by a kinematic equation of the form $\delta \mathbf{F}^\mathbf{P} = \sum_\alpha (\partial \mathbf{F}^\mathbf{P} / \partial \alpha) \delta \alpha$, with summation applied over all structural variables α, an equation which may not always be physically realistic if α are interpreted as internal state variables in the usual energetic sense of continuum thermomechanics. Recall that plastic slip is often not a valid internal state variable associated with energetic changes in the crystal, as explained in Section 4.2.1, so a direct correspondence between $\mathbf{F}^\mathbf{P}$ and usual internal state variable(s) may not always exist[5].

---

[5] More precisely, Rice (1971) defines an increment in a symmetric plastic strain tensor as the change in total strain resulting from changes in microscopic structural variable(s) with macroscopic stress and temperature held constant. The number of such structural variables may thus far exceed the number of internal state variables of the averaging type (i.e., α) needed to characterize the average free energy of a volume element of the solid.

5 Thermoelasticity

Deformation of a crystalline solid is labeled, in this book, as purely elastic in the absence of defect motion and temperature changes. In an elastic material of grade one, the mechanical stress supported by a material particle located at a particular point in space and the deformation gradient or strain in the material at that point are related by a constitutive law, e.g., a local tensor-valued version of Hooke's law relating force and stretch. A hyperelastic material of grade one can be defined as a material possessing a strain energy density function depending on the first-order deformation gradient, or on a symmetric deformation tensor or strain tensor constructed from this deformation gradient (Truesdell and Noll 1965). In such a material, the partial derivative of strain energy density with respect to a deformation gradient component produces a corresponding stress component, more precisely a component of the first Piola-Kirchhoff stress tensor. Thermoelasticity by definition addresses recoverable mechanical deformation (i.e., elastic deformation from body and surface forces) and thermal effects (e.g., temperature rates, temperature gradients, heat sources, and heat flux) as well as their couplings (e.g., thermal expansion or contraction).

Two alternative formulations of finite deformation thermoelasticity of grade one are presented in Chapter 5. In both cases, following the theme of this book, the focus is geared towards crystalline solids, though many aspects of these theories apply for arbitrary solid bodies, regardless of crystallinity. Both formulations rely on balance laws for classical continua presented in Section 4.1 and the general treatment of dissipation in Section 4.2. Viscoelasticity, a rate-dependent elastic response that may involve local entropy production (i.e., entropy production even in the absence of heat conduction), is not addressed in this book. Discussion of electromechanical coupling effects present in elastic dielectric crystals is deferred until later in Chapter 10.

In the first formulation—which can best be labeled traditional nonlinear thermoelasticity—presented in Sections 5.1-5.4, the contribution to the deformation gradient arising from temperature changes is not explicitly delineated in the kinematic description, and independent, time-dependent variables entering constitutive response functions consist of the total deformation gradient and temperature. Dependence of strain energy of the

material upon the first-order deformation gradient, and not higher-order gradients of position or strain, indicates a hyperelastic response of grade one, as noted in Section 4.2.1. As explained in Section 4.2.1 and discussed explicitly later in Chapter 5, objectivity requirements reduce dependence of thermodynamic potentials and response functions on deformation gradient to a dependence on a stretch tensor (or a symmetric deformation or strain tensor) derived from the deformation gradient. This formulation follows classical treatments of hyperelasticity with temperature changes (Truesdell and Noll 1965; Thurston 1974; Marsden and Hughes 1983; Rosakis et al. 2000). Materially nonlinear and materially linear constitutive models are discussed. Relationships among material coefficients derived from thermodynamic potentials are presented in Section 5.2 for general three-dimensional stress states (Section 5.2.1) as well as hydrostatic stress states (Section 5.2.2), following earlier work of Thurston (1974). Symmetry properties of material coefficients are discussed, with a brief focus on isotropic behavior representative of non-textured polycrystals; the reader is directed to Appendix A for an extensive treatment of symmetry properties of all thirty-two crystal classes. In Section 5.3, a free energy function accounting for large thermoelastic volume changes but small elastic shape changes, applicable for example at large hydrostatic pressures observed in some shock physics experiments, is described. In Section 5.4, reduction of the finite strain theory to the geometrically linear case is considered for completeness.

In a second, alternative or non-traditional formulation of nonlinear thermoelasticity presented in Section 5.5, purely thermal deformation induced by temperature changes is explicitly delineated in the kinematic description from the mechanical deformation associated with applied stresses. Independent state variables in thermodynamic potentials consist of mechanical elastic deformation and temperature. The deformation gradient is decomposed multiplicatively into an elastic part associated with mechanical loading and a thermal part associated with temperature changes, following the qualitative discussion of Section 3.2.2. Such a formulation, while not following what may be termed classical thermoelasticity, offers a more detailed depiction of the kinematics and provides different thermodynamic relationships among independent and dependent state variables (Stojanovitch 1969; Lu and Pister 1975; Imam and Johnson 1998; Clayton 2005a, b, 2006a). Thermal strain can be expressed via an evolution equation associated with the temperature rate (Lee et al. 1997), and additional thermoelastic couplings emerge via higher-order thermal stress coefficients, e.g., those reflecting dependence of elastic moduli on temperature.

Dissipative effects are omitted in the final two Sections of Chapter 5. Section 5.6 presents the Lagrangian field theory of elasticity, wherein the

linear momentum balance and constitutive laws of hyperelasticity of grade one are deduced from Euler-Lagrange equations of the appropriate action integral. Section 5.7 discusses hyperelastic bodies of grade two, following the variational approach of Toupin (1964). Such materials may support hyperstresses (including couple stresses) and do not obey the classical balance laws of continuum mechanics presented in Chapter 4 apart from the conservation of mass of Section 4.1.2 which is presumed identical for elastic materials of grades one and two.

   This Chapter, while providing detailed descriptions of selected topics in thermoelasticity, does not provide a comprehensive account of the whole subject of elasticity to which numerous books have been entirely devoted. For completeness, a few other relevant references include Love (1927), Landau and Lifshitz (1959), Marsden and Hughes (1983), and Ogden (1997). References specifically dealing with nonlinear elasticity of anisotropic crystals include Thurston (1974) and Teodosiu (1982).

5.1 Nonlinear Elasticity and Thermoelasticity

In a thermoelastic crystalline material not containing mobile defects, or in which contributions from defects to deformation are negligible, the deformation gradient is asserted to follow (3.25):

$$\mathbf{F}(X,t) = T\varphi_X(t) = \mathbf{F}^{\mathbf{L}}(X,t),$$
$$F^a_{.A} = x^a_{.,A} = F^{La}_{.\alpha}g^\alpha_{.A} = F^{La}_{.B}g^B_{.\alpha}g^\alpha_{.A} = F^{La}_{.A}. \tag{5.1}$$

In this context, there is no need for introduction of an evolving intermediate configuration, since the lattice deformation serves as the local tangent map $\mathbf{F}^{\mathbf{L}}(X,t): T_X B_0 \to T_x B$. Recall that superscript $\mathbf{L}$ indicates deformation of the lattice (e.g., deformation of primitive Bravais lattice vectors and basis vectors in (3.109)-(3.110)) in the volume element of crystal associated, symbolically, with material point X, under the Cauchy-Born hypothesis. From (5.1), this superscript is dropped from the notation for the lattice or total deformation gradient $\mathbf{F}$ in the remainder of Chapter 5 without consequence.

5.1.1 Constitutive Assumptions

Applying (5.1), and prior to consideration of objectivity requirements, appropriate versions of functional dependencies of dependent state variables (4.45)-(4.48) for a hyperelastic material of grade one are

$$\psi = \psi\left(\mathbf{F}, \theta, \overset{\mathrm{g}}{\nabla}\theta, X, \mathbf{G}_A\right), \ \psi = \psi\left(F_{.A}^a, \theta, \theta_{,a}, X, \mathbf{G}_A\right); \qquad (5.2)$$

$$\eta = \eta\left(\mathbf{F}, \theta, \overset{\mathrm{g}}{\nabla}\theta, X, \mathbf{G}_A\right), \ \eta = \eta\left(F_{.A}^a, \theta, \theta_{,a}, X, \mathbf{G}_A\right); \qquad (5.3)$$

$$\boldsymbol{\sigma} = \boldsymbol{\sigma}\left(\mathbf{F}, \theta, \overset{\mathrm{g}}{\nabla}\theta, X, \mathbf{G}_A\right), \ \sigma^{ab} = \sigma^{ab}\left(F_{.A}^a, \theta, \theta_{,a}, X, \mathbf{G}_A\right); \qquad (5.4)$$

$$\mathbf{q} = \mathbf{q}\left(\mathbf{F}, \theta, \overset{\mathrm{g}}{\nabla}\theta, X, \mathbf{G}_A\right), \ q^a = q^a\left(F_{.A}^a, \theta, \theta_{,a}, X, G_A\right). \qquad (5.5)$$

Independent quantities (in parentheses) are deformation gradient, temperature, spatial temperature gradient, position or choice of material particle at X, and reference basis vectors. The present definition of a hyperelastic material includes no internal state variables, meaning that (4.49) is not needed. Dependence on deformation gradient follows arguments given in Section 4.2 and relations (3.109)-(3.114) of Chapter 3. Specifically, $\mathbf{F}$ reflects, to first order, the stretch of interatomic bonds since primitive Bravais lattice and basis vectors in a volume element of a crystal structure at point X deform according to the value of $\mathbf{F}(X,t)$ at that point at time t. Since changes in interatomic bond distances and angles result in mechanical stresses and corresponding changes in energy stored in the crystal, as explained in detail in Appendix B in the context of discrete lattice statics, dependence of Cauchy stress and free energy on $\mathbf{F}$ is appropriate[1]. De-

---

[1] In polyatomic structures, internal (i.e., inner) displacements discussed in Section 3.1.2 also affect bond distances and angles, and hence free energy and other response functions. Recall from (3.20) that $\mathbf{Q}(_k^0)$ denotes the inner displacement vector for basis atom k, with K the total number of atoms in the basis. Without loss of generality, let the primitive Bravais lattice and $k=0$ coincide, so $\mathbf{Q}(_0^0) = 0$. Since $\mathbf{Q}(_k^0)$ can be determined if the other independent state variables (e.g., deformation gradient and temperature) are known, internal displacement(s) need not be included in the list of independent state variables entering (5.2)-(5.5). For example, the free energy of a homogeneous material in the athermal case can be written as $\psi(\mathbf{F}) = \hat{\psi}\left(\mathbf{F}, \mathbf{Q}(_k^0)(\mathbf{F})\right)$. Inner displacement vector(s) at a given deformation gradient $\mathbf{F}$ can then obtained as the solution of (Tadmor et al. 1999)

$$\left.\frac{\partial\hat{\psi}}{\partial\mathbf{Q}(_k^0)}\right|_{\mathbf{F}} = 0 \ \ (\forall k=1,...K-1) \ ; \ \frac{\partial^2\hat{\psi}}{\partial\mathbf{Q}(_k^0)\partial\mathbf{Q}(_l^0)} \ \text{positive definite}.$$

It follows that at the equilibrium conditions corresponding to this solution,

$$\frac{\partial\psi}{\partial\mathbf{F}} = \left.\frac{\partial\hat{\psi}}{\partial\mathbf{F}}\right|_{\mathbf{Q}(_k^0)} + \sum_{k=1}^{K-1}\left.\frac{\partial\hat{\psi}}{\partial\mathbf{Q}(_k^0)}\right|_{\mathbf{F}}\frac{\partial\mathbf{Q}(_k^0)}{\partial\mathbf{F}} = \left.\frac{\partial\hat{\psi}}{\partial\mathbf{F}}\right|_{\mathbf{Q}(_k^0)}.$$

pendence of entropy and heat flux on deformation gradient is written out following the equipresence principle. Dependence of free energy and entropy on temperature depicts well-known phenomena, e.g., from physical chemistry, of the specific heat capacity of the material to account for changes in energy and entropy that accompany local thermal vibrations of atoms as well as possibly significant electronic contributions. Dependence of stress on temperature enables a description of thermal expansion, while dependence of heat flux on temperature enables a description of temperature-dependent conductivity. Dependence of heat flux on temperature gradient enables, for example, use of Fourier's law of (4.62). Dependence of the other state variables on temperature gradient is written out in (5.2)-(5.4) for completeness, but will be eliminated following thermodynamic considerations in Section 5.1.2. As discussed in Section 4.2.1, dependence of response functions on X is included to permit description of a heterogeneous body, that is a body whose properties such as elastic stiffness, mass density, or thermal conductivity vary with position in the undeformed state. Dependence on basis vectors $\mathbf{G}_A(X)$, often implied rather than written out explicitly in other presentations of elasticity theory, is used to describe solids exhibiting an anisotropic response, as explained more in Section 5.1.5.

Under superposed rigid body motions of the spatial frame $\mathbf{x} \to \hat{\mathbf{Q}}\mathbf{x} + \mathbf{c}$, where $\hat{\mathbf{Q}} = \hat{\mathbf{Q}}^{-T}$ is a spatially constant rotation matrix and $\mathbf{c}$ is a spatially constant translation vector, vector- and tensor-valued variables entering (5.2)-(5.5) transform as

$$F_{.A}^a \to \hat{Q}_{.b}^a F_{.A}^b, \quad \sigma^{ab} \to \hat{Q}_{.c}^a \sigma^{cd} \hat{Q}_{.d}^b, \quad q^a \to \hat{Q}_{.b}^a q^b, \quad \theta^{,a} \to \hat{Q}_{.b}^a \theta^{,b}. \quad (5.6)$$

Scalars (i.e., free energy, entropy, and temperature) associated with a given material particle X, as well as reference basis vectors $\mathbf{G}_A(X)$, are all invariant under such spatial coordinate transformations. From (5.6), it is clear that constitutive assumptions of the general form (5.2)-(5.5) are not always objective, since independent and dependent variables transform differently under a change of spatial basis. To conform to objectivity requirements, constitutive assumptions for thermoelastic solids should satisfy the following requirements (Coleman and Noll 1963; Coleman and Gurtin 1967), where the spatial temperature gradient is expressed in contravariant vector form following the last of (5.6):

$$\psi\left(\mathbf{F}, \theta, \overset{\mathrm{g}}{\nabla}\theta, X, \mathbf{G}_A\right) = \psi\left(\hat{\mathbf{Q}}\mathbf{F}, \theta, \hat{\mathbf{Q}}\overset{\mathrm{g}}{\nabla}\theta, X, \mathbf{G}_A\right), \quad (5.7)$$

$$\eta\left(\mathbf{F}, \theta, \overset{\mathrm{g}}{\nabla}\theta, X, \mathbf{G}_A\right) = \eta\left(\hat{\mathbf{Q}}\mathbf{F}, \theta, \hat{\mathbf{Q}}\overset{\mathrm{g}}{\nabla}\theta, X, \mathbf{G}_A\right), \quad (5.8)$$

$$\hat{\mathbf{Q}}\boldsymbol{\sigma}\left(\mathbf{F},\theta\overset{g}{\nabla}\theta,X,\mathbf{G}_A\right)\hat{\mathbf{Q}}^T = \boldsymbol{\sigma}\left(\hat{\mathbf{Q}}\mathbf{F},\theta,\hat{\mathbf{Q}}\overset{g}{\nabla}\theta,X,\mathbf{G}_A\right), \tag{5.9}$$

$$\hat{\mathbf{Q}}\mathbf{q}\left(\mathbf{F},\theta,\overset{g}{\nabla}\theta,X,\mathbf{G}_A\right) = \mathbf{q}\left(\hat{\mathbf{Q}}\mathbf{F},\theta,\hat{\mathbf{Q}}\overset{g}{\nabla}\theta,X,\mathbf{G}_A\right). \tag{5.10}$$

A number of possible variations of (5.2)-(5.5) satisfy (5.7)-(5.10). The forms suggested below are straightforward and are frequently encountered:

$$\psi = \psi\left(\mathbf{C},\theta,\overset{G}{\nabla}\theta,X,\mathbf{G}_A\right), \ \psi = \psi\left(C_{AB},\theta,\theta_{,A},X,\mathbf{G}_A\right); \tag{5.11}$$

$$\eta = \eta\left(\mathbf{C},\theta,\overset{G}{\nabla}\theta,X,\mathbf{G}_A\right), \ \eta = \eta\left(C_{AB},\theta,\theta_{,A},X,\mathbf{G}_A\right); \tag{5.12}$$

$$\boldsymbol{\Sigma} = \boldsymbol{\Sigma}\left(\mathbf{C},\theta,\overset{G}{\nabla}\theta,X,\mathbf{G}_A\right), \ \Sigma^{AB} = \Sigma^{AB}\left(C_{AB},\theta,\theta_{,A},X,\mathbf{G}_A\right); \tag{5.13}$$

$$\mathbf{Q} = \mathbf{Q}\left(\mathbf{C},\theta,\overset{G}{\nabla}\theta,X,\mathbf{G}_A\right), \ Q^A = Q^A\left(C_{AB},\theta,\theta_{,A},X,\mathbf{G}_A\right). \tag{5.14}$$

where symmetric deformation tensor $C_{AB} = F_{.A}^a g_{ab} F_{.B}^b$ by (2.153), symmetric second Piola-Kirchhoff stress tensor $\Sigma^{AB} = J F_{.a}^{-1A} \sigma^{ab} F_{.b}^{-1B}$ according to (4.6)-(4.7) and the identities listed in Table 4.1, referential heat flux vector $Q^A = J F_{.a}^{-1A} q^a$ by (4.36), and referential temperature gradient $\theta_{,A} = F_{.A}^a \theta_{,a}$ as in (4.51). All variables of order one or greater in (5.11)-(5.14) exhibit indicial components referred to reference configuration B_0 and are invariant under spatial coordinate transformations (see e.g., (4.50)-(4.51)).

For purposes of constructing strain energy functions in constitutive models of thermoelastic response, the following versions of (5.11)-(5.14) are often useful, and will be invoked frequently in Chapter 5:

$$\psi = \psi\left(\mathbf{E},\theta,\overset{G}{\nabla}\theta,X,\mathbf{G}_A\right), \ \psi = \psi\left(E_{AB},\theta,\theta_{,A},X,\mathbf{G}_A\right); \tag{5.15}$$

$$\eta = \eta\left(\mathbf{E},\theta,\overset{G}{\nabla}\theta,X,\mathbf{G}_A\right), \ \eta = \eta\left(E_{AB},\theta,\theta_{,A},X,\mathbf{G}_A\right); \tag{5.16}$$

$$\boldsymbol{\Sigma} = \boldsymbol{\Sigma}\left(\mathbf{E},\theta,\overset{G}{\nabla}\theta,X,\mathbf{G}_A\right), \ \Sigma^{AB} = \Sigma^{AB}\left(E_{AB},\theta,\theta_{,A},X,\mathbf{G}_A\right); \tag{5.17}$$

$$\mathbf{Q} = \mathbf{Q}\left(\mathbf{E},\theta,\overset{G}{\nabla}\theta,X,\mathbf{G}_A\right), \ Q^A = Q^A\left(E_{AB},\theta,\theta_{,A},X,\mathbf{G}_A\right); \tag{5.18}$$

where symmetric right Cauchy-Green strain tensor $2E_{AB} = C_{AB} - G_{AB}$ by (2.156) and is also invariant under rigid body transformations of the spatial coordinate system, since

$$2E_{AB} = F_{Aa}^T F_{.B}^a - G_{AB} \rightarrow F_{Ab}^T \hat{Q}_{.a}^{Tb} \hat{Q}_{.c}^a F_{.B}^c - G_{AB}$$

$$= F_{Ab}^T F_{.B}^b - G_{AB} = 2E_{AB}.$$

(5.19)

Dependence of response functions on strain tensor **E** rather than on defor-mation tensor **C** is useful for linearization of the energy density about a strain-free reference state, since $\mathbf{E} = 0$ at a reference state in which $\mathbf{F} = \mathbf{1}$ and $\mathbf{C} = \mathbf{1}$.

5.1.2 Thermodynamics

Using kinematic assumption (5.1) and constitutive assumptions (5.2)-(5.5), dissipation inequality (4.67) referred to spatial configuration B becomes

$$\sigma^{ab} D_{ab} - \rho \left[\frac{\partial \psi}{\partial F_{.A}^a} \dot{F}_{.A}^a + \left(\eta + \frac{\partial \psi}{\partial \theta} \right) \dot{\theta} + \frac{\partial \psi}{\partial \theta_{,a}} \gamma_a \right] - \theta^{-1} q^a \theta_{,a} \geq 0 . \quad (5.20)$$

The stress power per unit current volume can be written as follows:

$$\sigma^{ab} D_{ab} = \sigma^{ab} L_{ab} = \sigma^{ab} \dot{F}_{aA} F_{.b}^{-1A} = J^{-1} P_a^A \dot{F}_{.A}^a , \quad (5.21)$$

with **P** the first Piola-Kirchhoff stress of (4.6). Substituting into (5.20),

$$\left(J^{-1} P_a^A - \rho \frac{\partial \psi}{\partial F_{.A}^a} \right) \dot{F}_{.A}^a - \rho \left(\eta + \frac{\partial \psi}{\partial \theta} \right) \dot{\theta} - \rho \left(\frac{\partial \psi}{\partial \theta_{,a}} \right) \gamma_a - \theta^{-1} q^a \theta_{,a} \geq 0 . \quad (5.22)$$

Presuming that rates of deformation gradient, temperature, and tempera-ture gradient (i.e., $\dot{\mathbf{F}}$, $\dot{\theta}$, and $\boldsymbol{\gamma}$) can be prescribed arbitrarily—i.e., inde-pendently of each other and of their coefficients in a thermodynamic proc-ess—such coefficients (in parentheses in (5.22)) should vanish identically (Coleman and Noll 1963). Presumably, judicious application of body force $\bar{b}^a$ of (4.17) and heat source r of (4.34) enables this arbitrary pre-scriptions of rates $\dot{\mathbf{F}}$, $\dot{\theta}$, and $\boldsymbol{\gamma}$. Such reasoning leads to the constitutive relations

$$P_a^A = \rho_0 \frac{\partial \psi}{\partial F_{.A}^a} , \quad \eta = -\frac{\partial \psi}{\partial \theta} , \quad \frac{\partial \psi}{\partial \theta_{,a}} = 0 . \quad (5.23)$$

Notice from (5.2)-(5.4) that free energy, entropy, and stress do not depend on $\dot{\mathbf{F}}$, $\dot{\theta}$, or $\boldsymbol{\gamma}$. If, on the other hand, the dependent state variables were permitted to depend on rates of deformation gradient, temperature, or tem-perature gradient, it would not be possible to vary such rates independently of their coefficients in (5.22), and hence (5.23) would not necessarily fol-low. Because the heat flux vector and temperature gradient are explicitly related through (5.5), neither can be varied arbitrarily in (5.22), and neither

must vanish in a generic heat conductor. From (4.6), the Cauchy stress tensor satisfies

$$\sigma^{ab} = J^{-1} g^{ac} P_c^A F_{.A}^b = \rho \frac{\partial \psi}{\partial F_{aA}} F_{.A}^b. \tag{5.24}$$

It follows from (5.23) that free energy, entropy, and stress do not depend explicitly on the spatial temperature gradient:

$$\psi = \psi(\mathbf{F}, \theta, X, \mathbf{G}_A), \; \eta = \eta(\mathbf{F}, \theta, X, \mathbf{G}_A), \; \boldsymbol{\sigma} = \boldsymbol{\sigma}(\mathbf{F}, \theta, X, \mathbf{G}_A). \tag{5.25}$$

Since $\theta > 0$, the local entropy production inequality reduces to the conduction inequality in the second of (4.61).

$$\theta \Gamma = \theta \Gamma_C = -\theta^{-1} \theta_{,a} q^a \geq 0. \tag{5.26}$$

The rate of local entropy production vanishes in a hyperelastic material:

$$\theta \Gamma_L = \rho \theta \dot{\eta} + q_{;a}^a - \rho r = \sigma^{ab} D_{ab} - \rho \dot{\psi} - \rho \dot{\theta} \eta = 0. \tag{5.27}$$

A similar procedure can be followed with the entropy inequality (4.72) referred to the reference configuration taken as a starting point, which becomes, using (5.1) and (5.11)-(5.14),

$$\left(\frac{\Sigma^{AB}}{2} - \rho_0 \frac{\partial \psi}{\partial C_{AB}} \right) \dot{C}_{AB} - \rho_0 \left(\eta + \frac{\partial \psi}{\partial \theta} \right) \dot{\theta}$$
$$- \rho_0 \frac{\partial \psi}{\partial \theta_{,A}} \gamma_{0A} - \theta^{-1} \theta_{,A} Q^A \geq 0, \tag{5.28}$$

where $2\dot{E}_{AB} = \dot{C}_{AB}$. The reference rate of temperature gradient satisfies

$$\frac{\partial \psi}{\partial \theta_{,a}} \gamma_a = \frac{\partial \psi}{\partial \theta_{,A}} \frac{\partial \theta_{,A}}{\partial \theta_{,a}} \gamma_a = \frac{\partial \psi}{\partial \theta_{,A}} F_{.A}^a \gamma_a = \frac{\partial \psi}{\partial \theta_{,A}} \gamma_{0A} \Leftrightarrow \gamma_{0A} = F_{.A}^a \gamma_a. \tag{5.29}$$

The following stress-strain and temperature-entropy relations are then deduced for hyperelastic materials, using (2.158):

$$\Sigma^{AB} = 2\rho_0 \frac{\partial \psi}{\partial C_{AB}} = \rho_0 \frac{\partial \psi}{\partial E_{AB}} = \rho_0 \frac{\partial \psi}{\partial E_{BA}} = \Sigma^{BA}, \; \eta = -\frac{\partial \psi}{\partial \theta}, \; \frac{\partial \psi}{\partial \theta_{,A}} = 0. \tag{5.30}$$

It follows that in addition to the free energy, the entropy and stress do not depend explicitly on the referential temperature gradient:

$$\psi = \psi(\mathbf{C}, \theta, X, \mathbf{G}_A), \; \eta = \eta(\mathbf{C}, \theta, X, \mathbf{G}_A), \; \boldsymbol{\Sigma} = \boldsymbol{\Sigma}(\mathbf{C}, \theta, X, \mathbf{G}_A). \tag{5.31}$$

Since $\theta > 0$, the entropy production inequality reduces to the conduction inequality:

$$J\theta \Gamma = J\theta \Gamma_C = -\theta^{-1} \theta_{,A} Q^A \geq 0. \tag{5.32}$$

The rate of local entropy production vanishes:

$$J\theta \Gamma_L = \rho_0 \theta \dot{\eta} + Q_{;A}^A - \rho_0 r = \Sigma^{AB} \dot{E}_{AB} - \rho_0 \dot{\psi} - \rho_0 \dot{\theta} \eta = 0. \tag{5.33}$$

Writing the free energy as $\psi = \psi\left(\mathbf{C}(\mathbf{F}(X,t),\mathbf{g}(x)),\theta,X,\mathbf{G}_A\right)$ and using (2.158) with (5.23) and (5.30), the following relationships emerge:

$$P^{aA} = F_{.B}^{a}\Sigma^{BA} = 2\rho_0 F_{.B}^{a}\frac{\partial\psi}{\partial C_{AB}} = 2\rho_0 F_{.B}^{a}\frac{\partial\psi}{\partial E_{CD}}\frac{\partial E_{CD}}{\partial C_{AB}} = \rho_0 F_{.B}^{a}\frac{\partial\psi}{\partial E_{BA}}, \quad (5.34)$$

$$\frac{\partial\psi}{\partial g_{ab}} = \frac{\partial\psi}{\partial C_{AB}}\frac{\partial C_{AB}}{\partial g_{ab}} = F_{.A}^{a}\frac{\partial\psi}{\partial C_{AB}}F_{.B}^{b} \Leftrightarrow \frac{\partial\psi}{\partial C_{AB}} = F_{.a}^{-1A}\frac{\partial\psi}{\partial g_{ab}}F_{.b}^{-1B}, \quad (5.35)$$

$$\sigma^{ab} = J^{-1}F_{.A}^{a}\Sigma^{AB}F_{.B}^{b} = 2\rho F_{.A}^{a}\frac{\partial\psi}{\partial C_{AB}}F_{.B}^{b} = 2\rho\frac{\partial\psi}{\partial g_{ab}} = 2\rho\frac{\partial\psi}{\partial g_{ba}} = \sigma^{ba}. \quad (5.36)$$

Notice from (5.30) and (5.36) that angular momentum balances (4.26) and (4.27) are satisfied identically: $\Sigma = \Sigma^T$ and $\sigma = \sigma^T$. The first of (5.30) provides the relationship between the reference second Piola-Kirchhoff stress Σ and a pull-back of the spatial metric $\mathbf{g}$, while (5.36) provides the relationship between a push-forward of the reference stress Σ and the spatial metric $\mathbf{g}$. Relation (5.36) is often called the Doyle-Ericksen formula (Doyle and Ericksen 1956; Yavari et al. 2006). From (2.182) and (5.36), in a hyperelastic material the spatial stress power can be expressed compactly in terms of the scalar product of the derivative of the free energy with respect to metric $\mathbf{g}$ and its Lie derivative with respect to the velocity field:

$$\langle\sigma,\mathbf{D}\rangle = \left\langle\rho\frac{\partial\psi}{\partial\mathbf{g}},\mathcal{L}_v\mathbf{g}\right\rangle. \quad (5.37)$$

Relation (5.34) can also be deduced directly from (2.158) and (5.23):

$$P_a^{.A} = \rho_0\frac{\partial\psi}{\partial C_{BC}}\frac{\partial C_{BC}}{\partial F_{.A}^{a}} = 2\rho_0\frac{\partial\psi}{\partial C_{BC}}g_{ab}\delta_{.B}^{A}F_{.C}^{b} = 2\rho_0\frac{\partial\psi}{\partial C_{AB}}g_{ab}F_{.B}^{b}. \quad (5.38)$$

As noted in Section 4.2, alternative choices of independent and dependent state variables are possible. One typical prescription regards the entropy as an independent variable and temperature as a dependent variable, with the internal energy e used as the primary thermodynamic potential:

$$e = e\left(\mathbf{F},\eta,X,\mathbf{G}_A\right), \quad \theta = \theta\left(\mathbf{F},\eta,X,\mathbf{G}_A\right), \quad \sigma = \sigma\left(\mathbf{F},\eta,X,\mathbf{G}_A\right), \quad (5.39)$$

where the partial Legendre transform (Marsden and Hughes 1983)

$$e = \theta\left(\mathbf{F},\eta,X,\mathbf{G}_A\right)\eta + \psi\left(\mathbf{F},\theta,X,\mathbf{G}_A\right). \quad (5.40)$$

From the second of (5.30) and the chain rule,

$$\frac{\partial e}{\partial F_{.A}^{a}} = \frac{\partial\psi}{\partial F_{.A}^{a}} + \frac{\partial\psi}{\partial\theta}\frac{\partial\theta}{\partial F_{.A}^{a}} + \frac{\partial\theta}{\partial F_{.A}^{a}}\eta$$

$$= \frac{\partial\psi}{\partial F_{.A}^{a}} + \frac{\partial\theta}{\partial F_{.A}^{a}}\left(\frac{\partial\psi}{\partial\theta} + \eta\right) = \frac{\partial\psi}{\partial F_{.A}^{a}},$$
$$(5.41)$$

so that constitutive relationships for the first Piola-Kirchhoff stress, second Piola-Kirchhoff stress, and Cauchy stress in terms of internal energy are

$$P_a^{\,A} = \rho_0 \frac{\partial e}{\partial F_{\cdot A}^a}, \quad \Sigma^{AB} = 2\rho_0 \frac{\partial e}{\partial C_{AB}} = \rho_0 \frac{\partial e}{\partial E_{AB}}, \quad \sigma^{ab} = 2\rho \frac{\partial e}{\partial g_{ab}}. \quad (5.42)$$

The thermodynamic analysis of (5.20)-(5.42) is often labeled the Coleman-Noll procedure, after Coleman and Noll (1963). In the present Section, this procedure is applied to hyperelastic crystalline solids, following Teodosiu (1982) for example, though formal analytical methods of Coleman and co-workers have been applied to numerous classes of materials (Coleman and Noll 1963; Coleman 1964; Coleman and Mizel 1964; Coleman and Gurtin 1967; Maugin 1988). It is also noted that constitutive relations among stress, deformation gradient, free or internal energy, temperature, and entropy need not be derived for hyperelastic bodies using the Second Law of thermodynamics or the Coleman-Noll procedure. For example, Marsden and Hughes (1983) obtain (5.30) by applying principles of locality, the balance of energy, and covariance. Other approaches can be found in Eringen (1962) and Truesdell and Noll (1965). Alternatively, stress and entropy can simply be assigned in hyperelastic solids as derivatives of thermodynamic potentials, taking (5.30) as basic definitions (Thurston 1974).

When temperature rates and temperature gradients are omitted from the description, the body is said to be elastic as opposed to thermoelastic. In such a description, let $\theta = \text{constant}$ such that $\dot{\theta} = 0$ and $\theta_{,A} = 0$, and let the heat flux $\mathbf{q}$ and heat source r vanish. Conduction inequality (5.32) is identically zero, and the entropy production (5.27) becomes

$$\theta\Gamma_L = \rho\theta\dot{\eta} = 0. \quad (5.43)$$

Since temperature and entropy are treated as constants, there is no need to include them explicitly in the thermodynamic description. General expressions (5.31) for free energy and stress become

$$\psi = \psi\left(\mathbf{C}, X, \mathbf{G}_A\right), \quad \mathbf{\Sigma} = \mathbf{\Sigma}\left(\mathbf{C}, X, \mathbf{G}_A\right), \quad (5.44)$$

and the resulting constitutive equations are

$$P_a^{\,A} = \rho_0 \frac{\partial \psi}{\partial F_{\cdot A}^a}, \quad \Sigma^{AB} = 2\rho_0 \frac{\partial \psi}{\partial C_{AB}} = \rho_0 \frac{\partial \psi}{\partial E_{AB}}, \quad \sigma^{ab} = 2\rho \frac{\partial \psi}{\partial g_{ab}}. \quad (5.45)$$

The temperature-independent thermodynamic potential $\psi = \psi(\mathbf{C}, X, \mathbf{G}_A)$ is called the strain energy density. Relations (5.45) along with the balance of linear momentum and boundary conditions can also be obtained from Hamilton's principle of stationary action, as demonstrated later in Section 5.6.

The specific heat capacity at constant deformation gradient $\mathbf{F}$ (i.e., at constant strain $\mathbf{E}$) is introduced as

$$c = \frac{\partial e}{\partial \theta} = \frac{\partial e}{\partial \eta}\frac{\partial \eta}{\partial \theta} = -\frac{\partial e}{\partial \eta}\frac{\partial}{\partial \theta}\left(\frac{\partial \psi}{\partial \theta}\right) = -\theta\frac{\partial^2 \psi}{\partial \theta^2}\,, \tag{5.46}$$

since from the second of (5.23) and (5.40),

$$\frac{\partial e}{\partial \eta} = \frac{\partial}{\partial \eta}(\theta\eta) + \frac{\partial}{\partial \eta}\psi = \theta + \frac{\partial \theta}{\partial \eta}\left(\eta + \frac{\partial \psi}{\partial \theta}\right) = \theta\,. \tag{5.47}$$

Also often used for thermoelastic solids is Fourier's Law of conduction, as first introduced in (4.69), leading to non-negative dissipation from conduction:

$$Q^A = -K^{AB}\theta_{,B}\,, \quad -\theta_{,A}Q^A = \theta_{,A}K^{AB}\theta_{,B} \geq 0\,. \tag{5.48}$$

From (5.33) and (5.48), the local energy balance can be expressed as

$$-\theta\frac{d}{dt}\left(\rho_0\frac{\partial \psi}{\partial \theta}\right) = (K^{AB}\theta_{,B})_{;A} + \rho_0 r\,. \tag{5.49}$$

Note that, by the chain rule,

$$-\theta\frac{d}{dt}\left(\rho_0\frac{\partial \psi}{\partial \theta}\right) = -\theta\rho_0\frac{\partial}{\partial \theta}\left(\frac{\partial \psi}{\partial E_{AB}}\dot{E}_{AB} + \frac{\partial \psi}{\partial \theta}\dot{\theta}\right)$$
$$= \theta\beta^{AB}\dot{E}_{AB} + \rho_0 c\dot{\theta}, \tag{5.50}$$

where (5.15) has been used and where the symmetric contravariant tensor $\boldsymbol{\beta} = -\partial\boldsymbol{\Sigma}/\partial\theta = -\rho_0\partial^2\psi/\partial\theta\partial\mathbf{E}$ accounts for thermoelastic coupling. Equating (5.49) and (5.50) results in a rate equation for the temperature:

$$\rho_0 c\dot{\theta} = (K^{AB}\theta_{,B})_{;A} - \theta\beta^{AB}\dot{E}_{AB} + \rho_0 r\,. \tag{5.51}$$

In the absence of strain rate $\dot{\mathbf{E}}$ (e.g., a rigid body) and heat sources r, and when $K^{AB} = KG^{AB}$ with K a constant (e.g., an isotropic homogeneous conductor), (5.51) becomes the transient heat equation

$$\dot{\theta} = \frac{K}{\rho_0 c}\overset{G}{\nabla}^2\theta = \frac{K}{\rho_0 c}(G^{AB}\theta_{,A})_{;B} = \frac{K}{\rho_0 c}\frac{1}{\sqrt{G}}\left(\sqrt{G}G^{AB}\theta_{,A}\right)_{,B}\,, \tag{5.52}$$

where the Laplacian is given by (2.77).

5.1.3 Materially Nonlinear Hyperelasticity

Differentiation of (5.23) and (5.30) results in definitions of second-order elastic stiffness coefficients:

$$\mathrm{A}^{A.B}_{a.b}(\mathbf{F},\theta,X,\mathbf{G}_A) = \frac{\partial P^A_a}{\partial F^b_{.B}} = \rho_0\frac{\partial^2\psi}{\partial F^a_{.A}\partial F^b_{.B}}\,, \tag{5.53}$$

$$\mathbb{C}^{ABCD}(\mathbf{E},\theta,X,\mathbf{G}_A)=\frac{\partial \Sigma^{AB}}{\partial E_{CD}}=\rho_0 \frac{\partial^2 \psi}{\partial E_{AB}\partial E_{CD}}. \qquad (5.54)$$

Coefficients in (5.53) and (5.54) are generally not constants and are labeled as tangent moduli when evaluated at particular values of the state variables. Third-order coefficients are defined via further differentiation:

$$\mathrm{A}_{a.b.c}^{.A.B.C}(\mathbf{F},\theta,X,\mathbf{G}_A)=\frac{\partial^2 P_a^{.A}}{\partial F_{.B}^b \partial F_{.C}^c}=\rho_0 \frac{\partial^3 \psi}{\partial F_{.A}^a \partial F_{.B}^b \partial F_{.C}^c}, \qquad (5.55)$$

$$\mathbb{C}^{ABCDEF}(\mathbf{E},\theta,X,\mathbf{G}_A)=\frac{\partial^2 \Sigma^{AB}}{\partial E_{CD}\partial E_{EF}}=\rho_0 \frac{\partial^3 \psi}{\partial E_{AB}\partial E_{CD}\partial E_{EF}}. \qquad (5.56)$$

Tangent moduli of orders four and higher can be defined by straightforward extension, i.e., additional differentiation with respect to deformation gradient or strain. The following symmetries follow automatically from definitions (5.53)-(5.54) and symmetry of $E_{AB}=E_{(AB)}$:

$$\mathrm{A}_{a.b}^{.A.B}=\mathrm{A}_{b.a}^{.B.A}, \quad \mathbb{C}^{ABCD}=\mathbb{C}^{(AB)(CD)}=\mathbb{C}^{CDAB}. \qquad (5.57)$$

Tensor $\mathrm{A}_{a.b}^{.A.B}$ consists of 45 independent entries before consideration of material symmetry, while $\mathbb{C}^{ABCD}$ consists of up to 21 independent entries. Similarly,

$$\mathrm{A}_{a.b.c}^{.A.B.C}=\mathrm{A}_{b.a.c}^{.B.A.C}=\mathrm{A}_{a.c.b}^{.A.C.B},$$
$$\mathbb{C}^{ABCDEF}=\mathbb{C}^{(AB)(CD)(EF)}=\mathbb{C}^{CDABEF}=\mathbb{C}^{ABEFCD}. \qquad (5.58)$$

In particular, third-order tangent stiffness $\mathbb{C}^{ABCDEF}$ consists of up to 56 independent entries.

Transformation formulae among elastic coefficients are deduced as follows. Since from (2.158),

$$\mathrm{A}_{a.b}^{.A.B}=\frac{\partial P_a^{.A}}{\partial F_{.B}^b}=\frac{\partial F_{aE}}{\partial F_{.B}^b}\Sigma^{EA}+F_{aE}\frac{\partial \Sigma^{EA}}{\partial E_{CD}}\frac{\partial E_{CD}}{\partial F_{.B}^b}$$

$$=g_{ab}\Sigma^{AB}+F_{aC}\mathbb{C}^{ACBD}F_{bD}, \qquad (5.59)$$

it follows from (5.57) that

$$\mathbb{C}^{ACBD}=F_{.a}^{-1A}\mathrm{A}_{.b}^{aCbD}F_{.b}^{-1B}-\Sigma^{AB}F_{.a}^{-1C}g^{ab}F_{.b}^{-1D}. \qquad (5.60)$$

Similarly, the relationship between third-order tangent elasticity coefficients is, using (5.58),

$$\mathbb{C}^{AEBDCG}=(\mathrm{A}^{aAbBcC}-\mathbb{C}^{ABCF}g^{ab}F_{.F}^c$$
$$-\mathbb{C}^{ACBF}g^{ac}F_{.F}^b-\mathbb{C}^{AFBC}g^{bc}F_{.F}^a)F_{.a}^{-1E}F_{.b}^{-1D}F_{.c}^{-1G}. \qquad (5.61)$$

Expressing free energy (5.31) of a hyperelastic material with thermal effects in a Taylor series of multiple variables (cf. Hoffman (1992)) about a reference state wherein $F_{.A}^a=g_{.A}^a$, $C_{AB}=G_{AB}$, $E_{AB}=0$, and $\theta=\theta_0>0$

produces the following result per unit reference volume, where free energy per unit reference volume Ψ_0 is introduced in (4.9):

$$
\begin{aligned}
\Psi_0 &= \rho_0 \psi\left(E_{AB}, \theta, X, \mathbf{G}_A\right) \\
&= \bar{\Psi}_0 + \bar{\mathbb{C}}^{AB} E_{AB} + \frac{1}{2!} \bar{\mathbb{C}}^{ABCD} E_{AB} E_{CD} + \frac{1}{3!} \bar{\mathbb{C}}^{ABCDEF} E_{AB} E_{CD} E_{EF} \\
&\quad + \frac{1}{4!} \bar{\mathbb{C}}^{ABCDEFGH} E_{AB} E_{CD} E_{EF} E_{GH} + \ldots - \bar{\beta}^{AB} E_{AB} \Delta\theta \\
&\quad - \frac{1}{2!} \bar{\beta}^{ABCD} E_{AB} E_{CD} \Delta\theta - \frac{1}{8} \bar{\beta}^{ABCDEF} E_{AB} E_{CD} E_{EF} \Delta\theta - \ldots \\
&\quad - \frac{1}{2!} \bar{\beta}'^{AB} E_{AB} (\Delta\theta)^2 - \frac{1}{8} \bar{\beta}''^{AB} E_{AB} (\Delta\theta)^3 - \ldots \\
&\quad - \frac{1}{4} \bar{\beta}'^{ABCD} E_{AB} E_{CD} (\Delta\theta)^2 \ldots + Y_0\left(\theta, X\right).
\end{aligned}
\tag{5.62}
$$

Temperature change from the reference state $\Delta\theta = \theta - \theta_0$ can be positive, zero, or negative. Presuming sufficient differentiability of Ψ_0 with respect to independent state variables, quantities in (5.62) are defined as follows:

$$
\Psi_0\left(0, \theta_0, X, \mathbf{G}_A\right) = \bar{\Psi}_0\left(X\right) + Y_0\left(\theta_0, X\right) = 0,
\tag{5.63}
$$

$$
\bar{\mathbb{C}}^{AB}\left(X, \mathbf{G}_A\right) = \left.\frac{\partial \Psi_0}{\partial E_{AB}}\right|_{\substack{\mathbf{E}=0 \\ \theta=\theta_0}} = 0,
\tag{5.64}
$$

$$
\bar{\mathbb{C}}^{ABCD}\left(X, \mathbf{G}_A\right) = \left.\frac{\partial^2 \Psi_0}{\partial E_{AB} \partial E_{CD}}\right|_{\substack{\mathbf{E}=0 \\ \theta=\theta_0}},
\tag{5.65}
$$

$$
\bar{\mathbb{C}}^{ABCDEF}\left(X, \mathbf{G}_A\right) = \left.\frac{\partial^3 \Psi_0}{\partial E_{AB} \partial E_{CD} \partial E_{EF}}\right|_{\substack{\mathbf{E}=0 \\ \theta=\theta_0}},
\tag{5.66}
$$

$$
\bar{\mathbb{C}}^{ABCDEFGH}\left(X, \mathbf{G}_A\right) = \left.\frac{\partial^4 \Psi_0}{\partial E_{AB} \partial E_{CD} \partial E_{EF} \partial E_{GH}}\right|_{\substack{\mathbf{E}=0 \\ \theta=\theta_0}},
\tag{5.67}
$$

$$
\bar{\beta}^{AB}\left(X, \mathbf{G}_A\right) = -\left.\frac{\partial^2 \Psi_0}{\partial \theta \partial E_{AB}}\right|_{\substack{\mathbf{E}=0 \\ \theta=\theta_0}},
\tag{5.68}
$$

$$
\bar{\beta}^{ABCD}\left(X, \mathbf{G}_A\right) = -\left.\frac{\partial^3 \Psi_0}{\partial \theta \partial E_{AB} \partial E_{CD}}\right|_{\substack{\mathbf{E}=0 \\ \theta=\theta_0}} = -\left.\frac{\partial \mathbb{C}^{ABCD}}{\partial \theta}\right|_{\substack{\mathbf{E}=0 \\ \theta=\theta_0}},
\tag{5.69}
$$

$$\bar{\beta}^{ABCDEF}\left(X,\mathbf{G}_A\right)=-\left.\frac{\partial^4\Psi_0}{\partial\theta\partial E_{AB}\partial E_{CD}\partial E_{EF}}\right|_{\substack{\mathbf{E}=0\\\theta=\theta_0}}=-\left.\frac{\partial\mathbb{C}^{ABCDEF}}{\partial\theta}\right|_{\substack{\mathbf{E}=0\\\theta=\theta_0}}, \quad (5.70)$$

$$\bar{\beta}'^{AB}\left(X,\mathbf{G}_A\right)=-\left.\frac{\partial^3\Psi_0}{\partial\theta^2\partial E_{AB}}\right|_{\substack{\mathbf{E}=0\\\theta=\theta_0}}, \quad (5.71)$$

$$\bar{\beta}''^{AB}\left(X,\mathbf{G}_A\right)=-\left.\frac{\partial^4\Psi_0}{\partial\theta^3\partial E_{AB}}\right|_{\substack{\mathbf{E}=0\\\theta=\theta_0}}, \quad (5.72)$$

$$\bar{\beta}'^{ABCD}\left(X,\mathbf{G}_A\right)=-\left.\frac{\partial^4\Psi_0}{\partial\theta^2\partial E_{AB}\partial E_{CD}}\right|_{\substack{\mathbf{E}=0\\\theta=\theta_0}}=-\left.\frac{\partial^2\mathbb{C}^{ABCD}}{\partial\theta^2}\right|_{\substack{\mathbf{E}=0\\\theta=\theta_0}}. \quad (5.73)$$

The total free energy at the reference state is chosen as a zero datum in (5.63) for convenience ($\bar{\Psi}_0(X)=-Y_0(\theta_0,X)$), since from inspection of the derivations in Section 5.1.2, the dependent variables stress, entropy, and heat flux only depend on derivatives of the free energy and not its absolute value. First-order elastic constants $\overline{\mathbb{C}}^{AB}$ are zero by definition in (5.64) so that by (5.30) and (5.34), stress vanishes in the reference state. Coefficients in (5.65)-(5.67) are referred to, respectively, as isothermal second-order elastic constants, isothermal third-order elastic constants, and isothermal fourth-order elastic constants. Stress-temperature coefficients of various orders are defined in (5.68)-(5.73); some of these can be interpreted as temperature derivatives of the elastic moduli at the reference state as indicated. All constants in (5.65)-(5.73) can depend on position X in a heterogeneous body as well as orientation $\mathbf{G}_A(X)$, but have fixed values at each point X. Stress-strain and entropy-temperature relations become

$$\Sigma^{AB}=\overline{\mathbb{C}}^{ABCD}E_{CD}+\frac{1}{2}\overline{\mathbb{C}}^{ABCDEF}E_{CD}E_{EF}+\frac{1}{6}\overline{\mathbb{C}}^{ABCDEFGH}E_{CD}E_{EF}E_{GH}+...$$

$$-\bar{\beta}^{AB}\Delta\theta-\bar{\beta}^{ABCD}E_{CD}\Delta\theta-\frac{3}{8}\bar{\beta}^{ABCDEF}E_{CD}E_{EF}\Delta\theta-... \quad (5.74)$$

$$-\frac{1}{2}\bar{\beta}'^{AB}(\Delta\theta)^2-\frac{1}{8}\bar{\beta}''^{AB}(\Delta\theta)^3-...-\frac{1}{2}\bar{\beta}'^{ABCD}E_{CD}(\Delta\theta)^2...,$$

$$N_0 = \rho_0 \eta = -\frac{\partial \Psi_0}{\partial \theta}$$

$$= -\frac{\partial Y_0}{\partial \theta} + \overline{\beta}^{AB} E_{AB} + \frac{1}{2} \overline{\beta}^{ABCD} E_{AB} E_{CD} + \frac{1}{8} \overline{\beta}^{ABCDEF} E_{AB} E_{CD} E_{EF} + \dots \quad (5.75)$$

$$+ \overline{\beta}'^{AB} E_{AB} \Delta\theta - \frac{3}{8} \overline{\beta}''^{AB} E_{AB} (\Delta\theta)^2 - \dots - \frac{1}{2} \overline{\beta}'^{ABCD} E_{AB} E_{CD} \Delta\theta \dots$$

The thermal energy Y_0 is not expanded in a polynomial series in (5.62) since such an expansion is usually deemed more appropriate for internal energy rather than free energy.

Two early models for thermal energy of solids include Einstein's model (Einstein 1907) and Debye's model (Debye 1912). A thermal internal energy is defined as

$$U_0(\theta, X) = Y_0 - \theta \frac{\partial Y_0}{\partial \theta}. \quad (5.76)$$

According to Einstein's model (Born and Huang 1954),

$$U_0 = 3nk_B \theta \left(\frac{\xi}{2} + \frac{\xi}{e^\xi - 1} \right), \quad C_0 = \frac{\partial U_0}{\partial \theta} = 3nk_B \left[\frac{\xi^2 e^\xi}{(e^\xi - 1)^2} \right], \quad (5.77)$$

where $C_0(\theta)$ is a specific heat per unit reference volume and

$$\xi = \Theta_E / \theta, \quad \Theta_E = h\nu_E / k_B, \quad (5.78)$$

with Einstein's temperature Θ_E presently assumed constant for a given substance with characteristic vibrational frequency ν_E, measured here in units of cycles per second. Planck's constant and Boltzmann's constant are written as $h = 2\pi\hbar$ and k_B, respectively. The number of degrees of freedom per unit reference volume is $3n$. For a monatomic crystal $3n = 3/\Omega_0$, with Ω_0 the atomic volume introduced in Section 3.1.1. According to Debye's model, considered more accurate for many crystalline solids (Born and Huang 1954; Brillouin 1964), thermal internal energy and specific heat are given by

$$U_0 = 9nk_B \theta \left[\left(\frac{\theta}{\Theta_D} \right)^3 \int_0^{\Theta_D/\theta} \left(\frac{1}{2} + \frac{1}{e^\xi - 1} \right) \xi^3 d\xi \right], \quad (5.79)$$

$$C_0 = \frac{\partial U_0}{\partial \theta} = 9nk_B \left[\left(\frac{\theta}{\Theta_D} \right)^3 \int_0^{\Theta_D/\theta} \frac{e^\xi \xi^4}{(e^\xi - 1)^2} d\xi \right], \quad (5.80)$$

where Debye's temperature Θ_D is here assumed constant[2] for a substance with characteristic maximum frequency ν_D of vibrational modes:

$$\Theta_D = h\nu_D / k_B. \tag{5.81}$$

At relatively high temperatures $\theta \gg \Theta_D$, the energy U_0 in (5.79) is linear in temperature, and the specific heat in (5.80) is constant:

$$U_0 \approx 9nk_B\theta\left[\left(\frac{\theta}{\Theta_D}\right)^3 \int_0^{\Theta_D/\theta} \xi^2 d\xi\right] = 3nk_B\theta, \; C_0 \approx 3nk_B. \tag{5.82}$$

At relatively low temperatures $\theta \ll \theta_D$, (5.79) and (5.80) become (Brillouin 1964)

$$U_0 = \left(\frac{3\pi^4}{5\Theta_D^3}nk_B\right)\theta^4 + C, \; C_0 = \left(\frac{12\pi^4}{5\Theta_D^3}nk_B\right)\theta^3, \tag{5.83}$$

with C a material constant reflecting the cohesive or total ground state internal energy of the undeformed material at $\theta = 0$.

Methods of derivation of elastic coefficients in (5.53)-(5.61), and elastic constants in (5.65) and (5.66), using atomistic models (i.e., lattice statics) are provided in Sections B.2.4-B.2.6 of Appendix B. Derivations of thermoelastic and thermal properties of matter (e.g., stress-temperature coefficients, thermal conductivity, and caloric equations of state), apart from the brief treatment in (5.76)-(5.83), from atomistic or quantum mechanical models fall outside the scope of this book. Such derivations can instead be found in books by Slater (1939), Born and Huang (1954) and Brillouin (1964), while Slater (1955) gives a historical account of quantum theories of specific heats of condensed matter. Methods of extending or combining Debye and Einstein models for specific heats of polyatomic substances wherein effects of intramolecular vibrations are significant are also discussed by Slater (1939).

---

[2] Debye's temperature Θ_D is constant for a given substance according to the model of (5.79) that omits coupling between vibrational energy and specific volume. Frequency ν_D can be related to sound speeds and hence elastic constants (Hearmon 1956). More generally, $\Theta_D = \Theta_D(J, \theta)$, where dependence on absolute temperature is most evident at very low temperatures (Born and Huang 1954; Bian et al. 2008). Volumetric (i.e., J) dependence of Debye and Einstein temperatures is considered explicitly in Section 5.2.2 in the context of Gruneisen's parameter.

5.1.4 Materially Linear Hyperelasticity

Material coefficients of orders three and higher (e.g., third- and fourth-order elastic constants) can be of importance for crystalline solids in high pressure events such as shock physics experiments wherein elastic deformations can be large, or high temperature events wherein nonlinear thermal expansion can be significant (Thurston 1974; Hiki 1981; Graham 1992). Higher-order elastic constants also affect elastic wave speeds in pressurized media, and provide insight into anharmonic atomic interactions (Appendix B, Section B.2.5).

On the other hand, in many practical applications, higher-order coefficients can be omitted from the series expansion of the free energy while still maintaining a reasonably accurate depiction of thermoelastic behavior. In such cases, (5.62) becomes

$$\Psi_0 = \frac{1}{2}\overline{\mathbb{C}}^{ABCD}E_{AB}E_{CD} - \overline{\beta}^{AB}E_{AB}\Delta\theta - \rho_0\overline{c}\,\theta\ln\frac{\theta}{\theta_0}, \qquad (5.84)$$

where elastic constants $\overline{\mathbb{C}}^{ABCD}$, stress-temperature coefficients $\overline{\beta}^{AB}$, and specific heat $\overline{c}$ are defined as second derivatives of the free energy at null strain and reference temperature:

$$\overline{\mathbb{C}}^{ABCD} = \frac{\partial^2\Psi_0}{\partial E_{AB}\partial E_{CD}}\bigg|_{\substack{\mathbf{E}=\mathbf{0}\\\theta=\theta_0}}, \quad \overline{\beta}^{AB} = -\frac{\partial^2\Psi_0}{\partial\theta\partial E_{AB}}\bigg|_{\substack{\mathbf{E}=\mathbf{0}\\\theta=\theta_0}}, \quad \overline{c} = -\left(\theta\frac{\partial^2\psi}{\partial\theta^2}\right)\bigg|_{\substack{\mathbf{E}=\mathbf{0}\\\theta=\theta_0}}. \quad (5.85)$$

At a particular material point X, parameters in (5.85) are all constants. The thermal energy comprising the rightmost term in (5.84) depends only on temperature. This term (Abeyaratne and Knowles 1993) is consistent with a thermal internal energy U_0 measured per unit reference volume depending linearly on temperature:

$$U_0 = \rho_0\overline{c}\,\theta \Leftrightarrow \overline{c} = \frac{1}{\rho_0}\frac{\partial U_0}{\partial\theta}. \qquad (5.86)$$

Stress and entropy measured in the reference configuration are

$$\Sigma^{AB} = \overline{\mathbb{C}}^{ABCD}E_{CD} - \overline{\beta}^{AB}\Delta\theta, \qquad (5.87)$$

$$N_0 = \rho_0\eta = \overline{\beta}^{AB}E_{AB} + \rho_0\overline{c}\left(\ln\frac{\theta}{\theta_0} + 1\right). \qquad (5.88)$$

In (5.87), the first term on the right accounts for stress due to strain and the second accounts for changes in stress resulting from changes in temperature $\Delta\theta = \theta - \theta_0$. This is a geometrically nonlinear but materially linear constitutive relationship; i.e., second Piola-Kirchhoff stress is linearly related to (finite) right Cauchy-Green strain and the temperature change.

At a fixed reference temperature $\theta = \theta_0$, the requirement that the free energy Ψ_0 be positive for all nonzero strains $\mathbf{E}$ implies that the fourth-rank tensor $\overline{\mathbb{C}}^{ABCD}$ should be positive definite. From the first of (5.85), it follows that at $\theta = \theta_0$, in the material linear case addressed in (5.84), Ψ_0 is a strictly convex function[3] of $\mathbf{E}$.

Stress equation (5.87) applies for any choice of reference configuration coordinate system, including Cartesian coordinates and general curvilinear coordinates. In physical components of orthogonal curvilinear coordinates (Section 2.4), the stress-strain law exhibits the same general form (Malvern 1969):

$$\Sigma_{\langle AB \rangle} = \sum_{C,D=1}^{3} \overline{\mathbb{C}}_{\langle ABCD \rangle} E_{\langle CD \rangle} - \overline{\beta}_{\langle AB \rangle} \Delta \theta, \tag{5.89}$$

where indices in angled brackets are referred to physical components of orthogonal curvilinear coordinates such as cylindrical coordinates of Section 2.4.2 and Table 4.3 or spherical coordinates of Section 2.4.3 and Table 4.4. Transformation formulae relating quantities in (5.89) to their counterparts in Cartesian coordinates are lengthy and are given by Malvern (1969).

5.1.5 Symmetry

Following from (5.65) and (5.68), matrices of second-order elastic constants $\overline{\mathbb{C}}^{ABCD}$ and thermal stress constants $\overline{\beta}^{AB}$ exhibit the following symmetries:

$$\overline{\mathbb{C}}^{ABCD} = \overline{\mathbb{C}}^{CDAB} = \overline{\mathbb{C}}^{BACD} = \overline{\mathbb{C}}^{ABDC}, \quad \overline{\beta}^{AB} = \overline{\beta}^{BA}, \tag{5.90}$$

meaning that $\overline{\mathbb{C}}^{ABCD}$ contains up to 21, as opposed to $3^4 = 81$, independent entries, and $\overline{\beta}^{AB}$ contains up to 6 as opposed to $3^2 = 9$ independent entries. Appealing to such symmetry considerations, (5.87) is often written in reduced matrix form as (Nye 1957; Hirth and Lothe 1982)

---

[3] In nonlinear elasticity in three spatial dimensions, convexity is not always necessary, and may be overly restrictive for addressing certain physical phenomena such as buckling associated with non-uniqueness of solutions (Marsden and Hughes 1983). Less restrictive assumptions such as polyconvexity and quasi-convexity may be more appropriate for strain energy functions of some kinds of materials. Also not addressed in Chapter 5 are non-convex, multi-well strain energy potentials that may emerge in continuum theories of phase transformations (Ericksen 1975; Ball and James 1987; Abeyaratne and Knowles 1993).

$$
\begin{bmatrix} \Sigma^{11} \\ \Sigma^{22} \\ \Sigma^{33} \\ \Sigma^{23} \\ \Sigma^{31} \\ \Sigma^{12} \end{bmatrix} =
\begin{bmatrix}
\overline{\mathbb{C}}^{11} & \overline{\mathbb{C}}^{12} & \overline{\mathbb{C}}^{13} & \overline{\mathbb{C}}^{14} & \overline{\mathbb{C}}^{15} & \overline{\mathbb{C}}^{16} \\
\overline{\mathbb{C}}^{12} & \overline{\mathbb{C}}^{22} & \overline{\mathbb{C}}^{23} & \overline{\mathbb{C}}^{24} & \overline{\mathbb{C}}^{25} & \overline{\mathbb{C}}^{26} \\
\overline{\mathbb{C}}^{13} & \overline{\mathbb{C}}^{23} & \overline{\mathbb{C}}^{33} & \overline{\mathbb{C}}^{34} & \overline{\mathbb{C}}^{35} & \overline{\mathbb{C}}^{36} \\
\overline{\mathbb{C}}^{14} & \overline{\mathbb{C}}^{24} & \overline{\mathbb{C}}^{34} & \overline{\mathbb{C}}^{44} & \overline{\mathbb{C}}^{45} & \overline{\mathbb{C}}^{46} \\
\overline{\mathbb{C}}^{15} & \overline{\mathbb{C}}^{25} & \overline{\mathbb{C}}^{35} & \overline{\mathbb{C}}^{45} & \overline{\mathbb{C}}^{55} & \overline{\mathbb{C}}^{56} \\
\overline{\mathbb{C}}^{16} & \overline{\mathbb{C}}^{26} & \overline{\mathbb{C}}^{36} & \overline{\mathbb{C}}^{46} & \overline{\mathbb{C}}^{56} & \overline{\mathbb{C}}^{66}
\end{bmatrix}
\begin{bmatrix} E_{11} \\ E_{22} \\ E_{33} \\ 2E_{23} \\ 2E_{31} \\ 2E_{12} \end{bmatrix} -
\begin{bmatrix} \overline{\beta}^{11} \\ \overline{\beta}^{22} \\ \overline{\beta}^{33} \\ \overline{\beta}^{23} \\ \overline{\beta}^{31} \\ \overline{\beta}^{12} \end{bmatrix} \Delta\theta ,
\qquad (5.91)
$$

where components of the symmetric 6×6 matrix of elastic constants are

$$
\begin{bmatrix}
\overline{\mathbb{C}}^{11}=\overline{\mathbb{C}}^{1111} & - & - & - & - & - \\
\overline{\mathbb{C}}^{12}=\overline{\mathbb{C}}^{1122} & \overline{\mathbb{C}}^{22}=\overline{\mathbb{C}}^{2222} & - & - & - & - \\
\overline{\mathbb{C}}^{13}=\overline{\mathbb{C}}^{1133} & \overline{\mathbb{C}}^{23}=\overline{\mathbb{C}}^{2233} & \overline{\mathbb{C}}^{33}=\overline{\mathbb{C}}^{3333} & - & - & - \\
\overline{\mathbb{C}}^{14}=\overline{\mathbb{C}}^{1123} & \overline{\mathbb{C}}^{24}=\overline{\mathbb{C}}^{2223} & \overline{\mathbb{C}}^{34}=\overline{\mathbb{C}}^{3323} & \overline{\mathbb{C}}^{44}=\overline{\mathbb{C}}^{2323} & - & - \\
\overline{\mathbb{C}}^{15}=\overline{\mathbb{C}}^{1113} & \overline{\mathbb{C}}^{25}=\overline{\mathbb{C}}^{2213} & \overline{\mathbb{C}}^{35}=\overline{\mathbb{C}}^{3313} & \overline{\mathbb{C}}^{45}=\overline{\mathbb{C}}^{2313} & \overline{\mathbb{C}}^{55}=\overline{\mathbb{C}}^{1313} & - \\
\overline{\mathbb{C}}^{16}=\overline{\mathbb{C}}^{1112} & \overline{\mathbb{C}}^{26}=\overline{\mathbb{C}}^{2212} & \overline{\mathbb{C}}^{36}=\overline{\mathbb{C}}^{3312} & \overline{\mathbb{C}}^{46}=\overline{\mathbb{C}}^{2312} & \overline{\mathbb{C}}^{56}=\overline{\mathbb{C}}^{1312} & \overline{\mathbb{C}}^{66}=\overline{\mathbb{C}}^{1212}
\end{bmatrix} . \qquad (5.92)
$$

The indicial form of (5.92) is often referred to as Voigt's notation (Voigt 1928). Nine components of symmetric second-order tensors reduce to six according to the correspondence

$$
11 \sim 1, \qquad 22 \sim 2, \qquad 33 \sim 3,
$$
$$
23 = 32 \sim 4, \quad 31 = 13 \sim 5, \quad 12 = 21 \sim 6.
$$
$$(5.93)$$

In the compact notation of Brugger (1964), Thurston (1974), and Teodosiu (1982), components of the stress and thermoelastic moduli are re-written to take advantage of these symmetries:

$$
\Sigma^{(AB)} \sim \Sigma^{\overline{A}}, \quad \overline{\mathbb{C}}^{(AB)(CD)} \sim \overline{\mathbb{C}}^{\overline{A}\overline{B}}, \quad \overline{\beta}^{AB} \sim \overline{\beta}^{\overline{A}}. \qquad (5.94)
$$

Barred single indices span 1,2,…6 and correspond to unbarred pairs of indices as indicated in (5.93). Consistent with (5.91) and (5.94), strains are

$$
2E_{(AB)} = (1+\delta_{AB})E_{\overline{A}}. \qquad (5.95)
$$

As a consequence of hyperelasticity, second-order elastic constants have the remaining symmetries

$$
\overline{\mathbb{C}}^{\overline{A}B} = \overline{\mathbb{C}}^{(\overline{A}B)}. \qquad (5.96)
$$

Using (5.94), Helmholtz free energy per unit reference volume in the materially linear case, (5.84), is expressed as

$$
\Psi_0 = \frac{1}{2}\overline{\mathbb{C}}^{\overline{A}B}E_{\overline{A}}E_{\overline{B}} - \overline{\beta}^{\overline{A}}E_{\overline{A}}\Delta\theta - \rho_0\overline{c}\,\theta\ln\frac{\theta}{\theta_0}, \qquad (5.97)
$$

and the second Piola-Kirchhoff stress of (5.87) is written compactly as

$$
\Sigma^{\overline{A}} = \overline{\mathbb{C}}^{\overline{A}B}E_{\overline{B}} - \overline{\beta}^{\overline{A}}\Delta\theta . \qquad (5.98)
$$

Voigt's notation can also be used for tangent moduli $\mathbb{C}^{ABCD}$ of (5.54) in the materially nonlinear regime, since tangent moduli exhibit the same symmetries as the constants in (5.90). Voigt's notation is likewise often ap-

plied to third-order elastic constants, as described in Section A.3 of Appendix A.

In many practical applications, the material axes (e.g., the conventional unit cell (lattice) vectors in a cubic crystal) and the reference coordinate axes do not coincide. In such cases, a rotation or reflection operation is required to represent the matrix of elastic constants in the reference coordinate system as opposed to the crystallographic frame. Let X'^A denote coordinates in the crystallographic frame, and let X^A denote coordinates in the reference configuration. The transformation

$$X^A = \breve{Q}^A_{.B} X'^B \tag{5.99}$$

describes the relationship between coordinate systems, with orthogonal matrix $\breve{\mathbf{Q}}$ satisfying $\breve{Q}^{TA}_{.B} = \breve{Q}^{-1A}_{.B}$ and $|\det \breve{Q}^A_{.B}| = 1$. When $\det \breve{Q}^A_{.B} = +1$, the rotation is said to be proper orthogonal; otherwise, when $\det \breve{Q}^A_{.B} = -1$, the operation is said to be improper orthogonal, i.e., a reflection. The elasticity tensor then transforms from its representation $\overline{\mathbb{C}}'^{ABCD}$ in the crystal coordinate system to its representation $\overline{\mathbb{C}}^{ABCD}$ in the reference coordinate system as a fourth-order tensor, while the thermal stress coefficients transform from $\overline{\beta}'^{AB}$ to $\overline{\beta}^{AB}$ as components of a rank two tensor:

$$\overline{\mathbb{C}}^{ABCD} = \breve{Q}^A_{.E} \breve{Q}^B_{.F} \breve{Q}^C_{.G} \breve{Q}^D_{.H} \overline{\mathbb{C}}'^{EFGH}, \quad \overline{\beta}^{AB} = \breve{Q}^A_{.C} \breve{Q}^B_{.D} \overline{\beta}'^{CD}. \tag{5.100}$$

Analogous formulae apply for tangent moduli in (5.54) and higher-order material coefficients in (5.62). In practice, the 6×6 square matrix of elastic moduli in crystallographic coordinates must often be converted to fourth rank ($3 \times 3 \times 3 \times 3$) form by appealing to (5.92), and then the first of (5.100) can be applied. Finally, the resulting fourth-order elasticity tensor, now based in reference coordinates X^A, can be converted back to 6×6 form by again using (5.92).

In fields of crystallography and texture analysis, the three independent components of the matrix $\breve{\mathbf{Q}}$ are often represented in terms of Euler angles describing successive angular rotations about particular directions in the sample (Bunge 1982; Kocks et al. 1998; Randle and Engler 2000; Cermelli and Gurtin 2001). One particular representation is (Cermelli and Gurtin 2001)

$$\breve{\mathbf{Q}} = \left[\exp\left(-\varphi_1 \boldsymbol{\varepsilon} \mathbf{k}\right) \right] \left[\exp\left(-\psi \boldsymbol{\varepsilon} \mathbf{i}\right) \right] \left[\exp\left(-\varphi_2 \boldsymbol{\varepsilon} \mathbf{k}\right) \right], \tag{5.101}$$

where the Euler angles in Bunge's notation are limited to the range

$$\varphi_1, \varphi_2 \in [0, 2\pi), \quad \psi \in [0, \pi], \tag{5.102}$$

and $(\mathbf{i}, \mathbf{j}, \mathbf{k})$ form an orthonormal basis for the X'^A coordinate system. Arguments of matrix exponentials in (5.101) are skew, e.g.

$$\left(-\varphi_1 \boldsymbol{\varepsilon} \mathbf{k}\right)_{AB} = -\varphi_1 \varepsilon_{ABC} k^C . \tag{5.103}$$

The matrix exponential of a second-order tensor $\mathbf{A}$ is

$$\exp \mathbf{A} = \sum_{k=0}^{\infty} \frac{1}{k!} \mathbf{A}^k = \mathbf{1} + \mathbf{A} + \frac{\mathbf{A}^2}{2} + \dots . \tag{5.104}$$

If $\mathbf{A}$ is skew (i.e., if $A_{AB} = -A_{BA}$), then its matrix exponential $\exp \mathbf{A}$ is a (proper) orthogonal tensor, i.e., a rotation. In that case, to first order in $\mathbf{A}$, the difference $\exp \mathbf{A} - \mathbf{1}$ is also skew.

Recall from (5.7)-(5.18) and (5.31) that the thermodynamic potentials and response functions generally depend on reference basis vectors $\mathbf{G}_A(X)$, following the notational convention of Eringen (1962). Such dependence can be made explicit by considering effects of orthogonal transformations of reference coordinates along the lines of (5.99). Under such rotations or reflections $\breve{\mathbf{Q}}$, basis vector $\mathbf{G}_A$ and metric tensor $\mathbf{G}(X)$ transform as

$$\mathbf{G}_A \rightarrow \mathbf{G}_B \breve{Q}_{.A}^B, \ G_{AB} \rightarrow \breve{Q}_{.A}^C G_{CD} \breve{Q}_{.B}^D = G_{AC} \breve{Q}_{.D}^{TC} \breve{Q}_{.B}^D = G_{AC} \delta_{.B}^C = G_{AB} . \tag{5.105}$$

Dependence of response functions on basis vectors is conventionally assumed to result only from dependence of independent state variables on the basis vectors, so that (5.31) can be written

$$\psi = \psi\left(\mathbf{C}(X,\mathbf{G}_A),\theta,X\right), \ \eta = \eta\left(\mathbf{C}(X,\mathbf{G}_A),\theta,X\right),$$
$$\boldsymbol{\Sigma} = \boldsymbol{\Sigma}\left(\mathbf{C}(X,\mathbf{G}_A),\theta,X\right). \tag{5.106}$$

Similarly, heat flux equation (5.14) becomes

$$\mathbf{Q} = \mathbf{Q}\left(\mathbf{C}(X,\mathbf{G}_A),\theta,\overset{\mathbf{G}}{\nabla}\theta(X,\mathbf{G}_A),X\right). \tag{5.107}$$

Deformation gradient $\mathbf{F}$, right Cauchy-Green deformation tensor $\mathbf{C}$ and Lagrangian strain tensor $\mathbf{E}$ transform as

$$F_{.A}^a \rightarrow \breve{Q}_{.A}^B F_{.B}^a, \ C_{AB} \rightarrow \breve{Q}_{.AC}^T C_{.D}^C \breve{Q}_{.B}^D, \ E_{AB} \rightarrow \breve{Q}_{.AC}^T E_{.D}^C \breve{Q}_{.B}^D . \tag{5.108}$$

Heat flux $\mathbf{Q}$ and reference temperature gradient transform as

$$Q^A \rightarrow \breve{Q}_{.B}^A Q^B, \ \theta_{,A} \rightarrow \theta_{,B} \breve{Q}_{.A}^B = \breve{Q}_{.AB}^T \theta^{.B} . \tag{5.109}$$

It follows that for all rotations and reflections $\breve{\mathbf{Q}} \in \mathbb{Q}$ within symmetry group $\mathbb{Q}$ of the considered material, the following identities apply:

$$\psi(\mathbf{C},\theta,X) = \psi\left(\breve{\mathbf{Q}}^T \mathbf{C} \breve{\mathbf{Q}},\theta,X\right), \tag{5.110}$$

$$\eta(\mathbf{C},\theta,X) = \eta\left(\breve{\mathbf{Q}}^T \mathbf{C} \breve{\mathbf{Q}},\theta,X\right), \tag{5.111}$$

$$\breve{\mathbf{Q}} \boldsymbol{\Sigma}(\mathbf{C},\theta,X) \breve{\mathbf{Q}}^T = \boldsymbol{\Sigma}\left(\breve{\mathbf{Q}}^T \mathbf{C} \breve{\mathbf{Q}},\theta,X\right), \tag{5.112}$$

$$\breve{\mathbf{Q}}\mathbf{Q}\left(\mathbf{C},\theta,\overset{\mathbf{G}}{\nabla}\theta,X\right)=\mathbf{Q}\left(\breve{\mathbf{Q}}^{T}\mathbf{C}\breve{\mathbf{Q}},\theta,\breve{\mathbf{Q}}^{T}\overset{\mathbf{G}}{\nabla}\theta,X\right). \qquad (5.113)$$

Regarding the heat flux vector, when Fourier's law (5.48) applies,

$$Q^{A}=-K^{AB}\theta_{,B}\rightarrow-\breve{Q}_{,C}^{A}(K^{CB}\theta_{,B})=-(\breve{Q}_{,C}^{A}K^{CD}\breve{Q}_{,D}^{E})(\theta_{,B}Q_{,E}^{B}). \quad (5.114)$$

Relations (5.110)-(5.113) may result in a reduction of the number of independent components of material coefficients that can be defined as derivatives of thermodynamic potentials with respect to independent state variables couched in the reference configuration and listed as arguments of these potentials. Without loss of generality, $\mathbf{C}$ can be replaced by $\mathbf{E}$ in (5.110)-(5.113). Such material coefficients include tangent elastic moduli (5.54) and (5.56), thermal stress coefficients, and elastic and thermal stress constants of all orders in (5.62)-(5.73). Symmetric conductivity matrix $\mathbf{K}$, while not the derivative of a thermodynamic potential, transforms in (5.114) as a second-order tensor under changes of reference coordinates and thus should exhibit the same symmetries as material tensors that are second-order derivatives of thermodynamic potentials (e.g., $\overline{\beta}^{AB}$ of (5.100)).

Specifically, when $\mathbb{Q}$ consists only of the identity map and the inversion, there is no reduction in the number of independent elasticity coefficients due to material symmetry; in this case, the crystalline material is said to be triclinic. The crystal class of a given crystal structure determines symmetry properties of thermoelastic material coefficients for that structure. Recall from Section 3.1, Table 3.1, and Fig. 3.2 that the seven crystal systems encompass fourteen different kinds of Bravais lattices. The symmetry of a crystal is further described by its crystal class or point group of symmetry operations comprising $\mathbb{Q}$. Thirty-two crystal classes exist for natural crystal structures, each falling into one of eleven Laue groups. Mechanical elastic properties such as second- and third-order elastic constants depend only on the Laue group of the crystal, while other material coefficients such as vectors and tensors of odd rank (e.g., pyroelectric and piezoelectric coefficients emerging in electromechanical theories, as discussed in Chapter 10) can depend on the particular crystal class within a Laue group. A detailed discussion of symmetry of crystals in the context of material coefficients is provided in Appendix A. In particular, Tables A.3-A.7 list the independent material coefficients for tensors of ranks one, two, three, and four, while Tables A.8 and A.9 list second- and third-order elastic constants for all Laue groups.

When the symmetry group $\mathbb{Q}$ of the material contains all orthogonal transformations, the response is independent of the choice of $\mathbf{G}_{A}$, and the material is said to be isotropic. Isotropy is extremely rare among single

crystalline solids. However, the macroscopic response of polycrystals containing a large number of randomly oriented grains can often be accurately represented as isotropic, so that isotropic behavior is of keen interest in the general study of crystalline solids. In an isotropic solid, (5.52) applies for heat conduction in the context of Fourier's law, and (5.106) reduces to

$$\psi = \psi\left(I_1, I_2, I_3, \theta, X\right), \quad \eta = \eta\left(I_1, I_2, I_3, \theta, X\right),$$

$$\boldsymbol{\Sigma} = \boldsymbol{\Sigma}\left(I_1, I_2, I_3, \theta, X\right). \tag{5.115}$$

Three scalar invariants of $\mathbf{C}$ are defined as

$$I_1 = C_{.A}^A, \quad I_2 = (\det \mathbf{C})\mathrm{tr}(\mathbf{C}^{-1}) = \frac{1}{2}\left[C_{.A}^A C_{.B}^B - C_{.B}^A C_{.A}^B\right], \quad I_3 = \det \mathbf{C}. \tag{5.116}$$

For isotropic materials, it follows from (5.30) and (5.115)-(5.116) that the second Piola-Kirchhoff stress can be written

$$\Sigma^{AB} = 2\rho_0 \frac{\partial \psi}{\partial C_{AB}} = 2\rho_0 \sum_{\lambda=1}^{3} \frac{\partial \psi}{\partial I_\lambda} \frac{\partial I_\lambda}{\partial C_{AB}}$$

$$= \alpha_0 G^{AB} + \alpha_1 C^{AB} + \alpha_2 C^{AD} C_{.D}^B. \tag{5.117}$$

where the scalar functions α_λ generally depend on the invariants of $\mathbf{C}$, the temperature, and location in the material (Marsden and Hughes 1983):

$$\alpha_\lambda = \alpha_\lambda\left(I_1, I_2, I_3, \theta, X\right), \quad (\lambda = 0, 1, 2). \tag{5.118}$$

The tangent elastic stiffness of (5.54) becomes, for an isotropic material,

$$\mathbb{C}^{ABCD} = \rho_0 \frac{\partial^2 \psi}{\partial E_{AB} \partial E_{CD}} = 4\rho_0 \frac{\partial^2 \psi}{\partial C_{AB} \partial C_{CD}}$$

$$= \gamma_1 G^{AB} G^{CD} + \gamma_2 (C^{AB} G^{CD} + G^{AB} C^{CD})$$

$$+ \gamma_3 (C^{2AB} G^{CD} + G^{AB} C^{2CD}) + \gamma_4 C^{AB} C^{CD} \tag{5.119}$$

$$+ \gamma_5 (C^{2AB} C^{CD} + C^{AB} C^{2CD}) + \gamma_6 C^{2AB} C^{2CD}$$

$$+ \gamma_7 (G^{AC} G^{BD} + G^{BC} G^{AD})$$

$$+ \gamma_8 (G^{AC} C^{BD} + G^{BC} C^{AD} + G^{AD} C^{BC} + G^{BD} C^{AC}),$$

where the notation $(\mathbf{C}^2)^{AB} = C^{2AB} = C^{AC} C_C^{.B}$ and coefficients are scalar functions of the following form:

$$\gamma_\chi = \gamma_\chi\left(I_1, I_2, I_3, \theta, X\right), \quad (\chi = 1, 2, \ldots 8). \tag{5.120}$$

Thus the maximum number of independent components of $\mathbb{C}^{ABCD}$ at material point X is reduced from 21 to 8 in a nonlinear isotropic thermoelastic solid.

Now consider a materially linear, isotropic hyperelastic solid. In that case, the second-order elastic constants in (5.85) become

$$\overline{\mathbb{C}}^{ABCD} = \rho_0 \frac{\partial^2 \psi}{\partial E_{AB} \partial E_{CD}}\bigg|_{\substack{\mathbf{E}=\mathbf{0}\\ \theta=\theta_0}} = 4\rho_0 \frac{\partial^2 \psi}{\partial C_{AB} \partial C_{CD}}\bigg|_{\substack{\mathbf{C}=\mathbf{G}\\ \theta=\theta_0}} \qquad (5.121)$$

$$= \mu(G^{AC}G^{BD} + G^{AD}G^{BC}) + \lambda G^{AB}G^{CD},$$

with $\mu(X) = \gamma_7$ the shear modulus and $\lambda(X) = \gamma_1$ Lamé's constant, both evaluated at the reference state. The remaining parameters γ_χ in (5.119) are redundant in the materially linear theory and can be set to zero. Thus, the elasticity tensor consists of two independent components, and in 6×6 matrix form is written as

$$[\overline{\mathbb{C}}] = \begin{bmatrix} 2\mu+\lambda & \lambda & \lambda & 0 & 0 & 0 \\ \lambda & 2\mu+\lambda & \lambda & 0 & 0 & 0 \\ \lambda & \lambda & 2\mu+\lambda & 0 & 0 & 0 \\ 0 & 0 & 0 & \mu & 0 & 0 \\ 0 & 0 & 0 & 0 & \mu & 0 \\ 0 & 0 & 0 & 0 & 0 & \mu \end{bmatrix}. \qquad (5.122)$$

Second-order thermal stress coefficients for an isotropic material exhibit the form

$$\overline{\beta}^{AB} = -\rho_0 \frac{\partial^2 \psi}{\partial \theta \partial E_{AB}}\bigg|_{\substack{\mathbf{E}=\mathbf{0}\\ \theta=\theta_0}} = -2\rho_0 \frac{\partial^2 \psi}{\partial \theta \partial C_{AB}}\bigg|_{\substack{\mathbf{C}=\mathbf{G}\\ \theta=\theta_0}} = \overline{\beta} G^{AB}, \qquad (5.123)$$

with $\overline{\beta}$ a constant. For isotropic solids, transformation formulae are not needed among orthogonal reference coordinate frames since (5.100) degenerates to $\overline{\mathbb{C}}^{ABCD} = \overline{\mathbb{C}}'^{ABCD}$ and $\overline{\beta}^{AB} = \overline{\beta}'^{AB}$. Stress-strain-temperature relations exhibit the form

$$\Sigma^{AB} = 2\mu E^{AB} + (\lambda E_{.C}^{C} - \overline{\beta}\Delta\theta)G^{AB}. \qquad (5.124)$$

Defining the bulk modulus for a materially linear, isotropic elastic solid as $K = 2\mu/3 + \lambda$, (5.124) can be inverted to give

$$2\mu\left(E_{AB} - \frac{1}{3}E_{.C}^{C}G_{AB}\right) = \Sigma_{AB} - \frac{1}{3}\Sigma_{.C}^{C}G_{AB}, \quad E_{.A}^{A} = \frac{\Sigma_{.A}^{A}}{3K} + \frac{\overline{\beta}}{K}\Delta\theta. \qquad (5.125)$$

The first of equality of (5.125) is recognizable as a relationship between the deviatoric (i.e., traceless) stress Σ'_{AB} and deviatoric strain E'_{AB}:

$$\Sigma'_{AB} = 2\mu E'_{AB}, \quad \Sigma'_{AB} = \Sigma_{AB} - \frac{1}{3}\Sigma_{.C}^{C}G_{AB}, \quad E'_{AB} = E_{AB} - \frac{1}{3}E_{.C}^{C}G_{AB}. \qquad (5.126)$$

The second of (5.125) relates traces of strains and stresses and temperature change. When deformations are small, $E_{.A}^{A} \approx J - 1 \approx u_{;a}^{a}$ accurately reflects volume changes in the material, as is clear from (2.162)-(2.164). From in-

version of the second of (5.125) and assuming stress-free strain from isotropic thermal expansion of the form $E_{.A}^{A} = \bar{\alpha}_T \Delta\theta \delta_{.A}^{A} = 3\bar{\alpha}_T \Delta\theta$ with $\Sigma_{.A}^{A} = 0$, the relationship between the coefficient of thermal expansion $\bar{\alpha}_T$ and $\bar{\beta}$ is obtained:

$$\bar{\beta} = 3K\bar{\alpha}_T . \tag{5.127}$$

Elastic isotropy is discussed in more detail in Section A.3.3 of Appendix A, including representations of third-order elastic constants and a complete table of algebraic relationships among various second-order elastic constants (Table A.10).

5.2 Thermostatic Relationships

A number of material coefficients, and relationships among these coefficients, can be derived from thermodynamic potentials of Table 4.2 and results of the analysis of Section 5.1.2. Such derivations are given in Section 5.2, primarily following from the presentation of Thurston (1974). Wallace (1972) offers a similar account. The general situation involving three-dimensional states of stress is considered first in Section 5.2.1, while the special scenario of a spherical state of Cauchy stress (i.e., hydrostatic pressure without deviatoric or shear stresses) is considered in Section 5.2.2.

5.2.1 Three-dimensional Stress States

Consider thermostatic potentials, measured as energy per unit reference volume as in (4.9), of the following functional forms:

$$E_0 = E_0\left(E_{AB}, N_0, X, \mathbf{G}_A\right), \; H_0 = H_0\left(\Sigma^{AB}, N_0, X, \mathbf{G}_A\right), \tag{5.128}$$

$$\Psi_0 = \left(E_{AB}, \theta, X, \mathbf{G}_A\right), \; G_0 = G_0\left(\Sigma^{AB}, \theta, X, \mathbf{G}_A\right), \tag{5.129}$$

where the entropy per unit reference volume is of the functional form

$$N_0 = N_0\left(E_{AB}, E_0, X, \mathbf{G}_A\right). \tag{5.130}$$

In the remainder of Section 5.2, dependence of potentials on material symmetry (e.g., via $\mathbf{G}_A$) and position of material particle X is implied and not written out explicitly, and partial derivatives of functions are assumed to take place with $\mathbf{G}_A$ and X fixed. With this reduction in notation, and using Voigt's notation (5.93)-(5.95) with barred indices spanning $1,2,...6$,

$$E_0 = E_0\left(E_{\bar{A}}, N_0\right), \; H_0 = H_0\left(\Sigma^{\bar{A}}, N_0\right), \tag{5.131}$$

$$\Psi_0 = \Psi_0\left(E_{\bar{A}}, \theta\right), \ G_0 = G_0\left(\Sigma^{\bar{A}}, \theta\right), \tag{5.132}$$

$$N_0 = N_0\left(E_{\bar{A}}, E_0\right). \tag{5.133}$$

Multiplying the relationships in Table 4.2 by $\rho_0(X)$ produces

$$H_0 = E_0 - \Sigma^{AB} E_{AB} = E_0 - \Sigma^{\bar{A}} E_{\bar{A}}, \tag{5.134}$$

$$\Psi_0 = E_0 - \theta N_0, \tag{5.135}$$

$$G_0 = H_0 - \theta N_0. \tag{5.136}$$

Differentials of the potentials are found from (5.131)-(5.136):

$$dE_0 = \Sigma^{\bar{A}} dE_{\bar{A}} + \theta dN_0, \ dH_0 = -E_{\bar{A}} d\Sigma^{\bar{A}} + \theta dN_0, \tag{5.137}$$

$$d\Psi_0 = \Sigma^{\bar{A}} dE_{\bar{A}} - N_0 d\theta, \ dG_0 = -E_{\bar{A}} d\Sigma^{\bar{A}} - N_0 d\theta. \tag{5.138}$$

First derivatives then provide the following thermostatic relationships:

$$N_0 = -\left.\frac{\partial \Psi_0}{\partial \theta}\right|_{\mathbf{E}} = -\left.\frac{\partial G_0}{\partial \theta}\right|_{\Sigma}, \ \theta = \left.\frac{\partial E_0}{\partial N_0}\right|_{\mathbf{E}} = \left.\frac{\partial H_0}{\partial N_0}\right|_{\Sigma}, \tag{5.139}$$

$$\Sigma^{\bar{A}} = \left.\frac{\partial E_0}{\partial E_{\bar{A}}}\right|_{N_0} = \left.\frac{\partial \Psi_0}{\partial E_{\bar{A}}}\right|_{\theta}, \ E_{\bar{A}} = -\left.\frac{\partial H_0}{\partial \Sigma^{\bar{A}}}\right|_{N_0} = -\left.\frac{\partial G_0}{\partial \Sigma^{\bar{A}}}\right|_{\theta}, \tag{5.140}$$

$$\frac{1}{\theta} = \left.\frac{\partial N_0}{\partial E_0}\right|_{\mathbf{E}}, \ \Sigma^{\bar{A}} = -\theta \left.\frac{\partial N_0}{\partial E_{\bar{A}}}\right|_{E_0}. \tag{5.141}$$

Specific heats per unit reference volume at constant strain, C_E, and constant stress, C_Σ are defined respectively as

$$C_E = \left.\frac{\partial E_0}{\partial \theta}\right|_{\mathbf{E}} = \theta \left.\frac{\partial N_0}{\partial \theta}\right|_{\mathbf{E}} = -\theta \left.\frac{\partial^2 \Psi_0}{\partial \theta^2}\right|_{\mathbf{E}}, \tag{5.142}$$

$$C_\Sigma = \left.\frac{\partial H_0}{\partial \theta}\right|_{\Sigma} = \theta \left.\frac{\partial N_0}{\partial \theta}\right|_{\Sigma} = -\theta \left.\frac{\partial^2 G_0}{\partial \theta^2}\right|_{\Sigma}. \tag{5.143}$$

From (5.46), C_E is related to specific heat per unit mass c via $C_E = \rho_0 c$. Subscripts on specific heat coefficients in (5.142) and (5.143) are labels of scalar quantities and are not subject to the Einstein summation convention.

Second derivatives provide isothermal and isentropic elastic stiffness coefficients (i.e., tangent moduli) of second order:

$$\mathbb{C}^{\bar{A}\bar{B}} = \left.\frac{\partial \Sigma^{\bar{A}}}{\partial E_{\bar{B}}}\right|_{\theta} = \left.\frac{\partial^2 \Psi_0}{\partial E_{\bar{A}} \partial E_{\bar{B}}}\right|_{\theta}, \ \mathbb{C}^{ABCD} = \left.\frac{\partial \Sigma^{AB}}{\partial E_{CD}}\right|_{\theta} = \left.\frac{\partial^2 \Psi_0}{\partial E_{AB} \partial E_{CD}}\right|_{\theta}; \tag{5.144}$$

$$\underline{\mathbb{C}}^{\bar{A}\bar{B}} = \left.\frac{\partial \Sigma^{\bar{A}}}{\partial E_{\bar{B}}}\right|_{N_0} = \left.\frac{\partial^2 E_0}{\partial E_{\bar{A}} \partial E_{\bar{B}}}\right|_{N_0}, \ \underline{\mathbb{C}}^{ABCD} = \left.\frac{\partial \Sigma^{AB}}{\partial E_{CD}}\right|_{N_0} = \left.\frac{\partial^2 E_0}{\partial E_{AB} \partial E_{CD}}\right|_{N_0}. \tag{5.145}$$

Isothermal second-order coefficients are identical to those introduced in Section 5.1.3. Isentropic coefficients are denoted by an underscore and are sometimes referred to as adiabatic coefficients (e.g., adiabatic elastic moduli) in applications wherein heat conduction and (radiative) heat supply do not arise, since in that case, (5.27) results in $\dot{N}_0 = \rho_0 \dot{\eta} = J\rho\dot{\eta} = 0$. Notice the symmetry conditions $\mathbb{C}^{\overline{AB}} = \mathbb{C}^{\overline{BA}}$ and $\underline{\mathbb{C}}^{\overline{AB}} = \underline{\mathbb{C}}^{\overline{BA}}$ follow identically from the assumption of hyperelasticity. Isothermal coefficients are typically used for elastostatic problems, while isentropic coefficients are typically deemed appropriate for studies of wave propagation (Thurston 1974).

Isothermal and isentropic elastic compliances are defined, respectively, as

$$S_{\overline{AB}} = \frac{\partial E_{\overline{A}}}{\partial \Sigma^{\overline{B}}}\bigg|_{\theta} = -\frac{\partial^2 G_0}{\partial \Sigma^{\overline{A}}\partial \Sigma^{\overline{B}}}\bigg|_{\theta} \,, \; S_{ABCD} = \frac{\partial E_{AB}}{\partial \Sigma^{CD}}\bigg|_{\theta} = -\frac{\partial^2 G_0}{\partial \Sigma^{AB}\partial \Sigma^{CD}}\bigg|_{\theta} \,; \quad (5.146)$$

$$\underline{S}_{\overline{AB}} = \frac{\partial E_{\overline{A}}}{\partial \Sigma^{\overline{B}}}\bigg|_{N_0} = -\frac{\partial^2 H_0}{\partial \Sigma^{\overline{A}}\partial \Sigma^{\overline{B}}}\bigg|_{N_0} \,, \; \underline{S}_{ABCD} = \frac{\partial E_{AB}}{\partial \Sigma^{CD}}\bigg|_{N_0} = -\frac{\partial^2 H_0}{\partial \Sigma^{AB}\partial \Sigma^{CD}}\bigg|_{N_0} \,. \quad (5.147)$$

Symmetry relations $S_{\overline{AB}} = S_{\overline{BA}}$ and $\underline{S}_{\overline{AB}} = \underline{S}_{\overline{BA}}$ apply. Second-order elastic stiffness and compliance tensors are related by

$$\mathbb{C}^{\overline{AB}}S_{\overline{BC}} = \frac{\partial \Sigma^{\overline{A}}}{\partial E_{\overline{B}}}\bigg|_{\theta} \frac{\partial E_{\overline{B}}}{\partial \Sigma^{\overline{C}}}\bigg|_{\theta} = \delta^A_{.C} \,, \; \underline{\mathbb{C}}^{\overline{AB}}\underline{S}_{\overline{BC}} = \frac{\partial \Sigma^{\overline{A}}}{\partial E_{\overline{B}}}\bigg|_{N_0} \frac{\partial E_{\overline{B}}}{\partial \Sigma^{\overline{C}}}\bigg|_{N_0} = \delta^A_{.C} \,; \quad (5.148)$$

$$2\mathbb{C}^{ABCD}S_{CDEF} = \delta^A_{.E}\delta^B_{.F} + \delta^A_{.F}\delta^B_{.E} \,, \; 2\underline{\mathbb{C}}^{ABCD}\underline{S}_{CDEF} = \delta^A_{.E}\delta^B_{.F} + \delta^A_{.F}\delta^B_{.E} \,. \quad (5.149)$$

Third-order elastic stiffness coefficients are defined via further differentiation of (5.144)-(5.145) with respect to strain:

$$\mathbb{C}^{\overline{ABC}} = \frac{\partial^2 \Sigma^{\overline{A}}}{\partial E_{\overline{B}}E_{\overline{C}}}\bigg|_{\theta} = \frac{\partial^3 \Psi_0}{\partial E_{\overline{A}}\partial E_{\overline{B}}\partial E_{\overline{C}}}\bigg|_{\theta} \,, \; \mathbb{C}^{ABCDEF} = \frac{\partial^3 \Psi_0}{\partial E_{AB}\partial E_{CD}\partial E_{EF}}\bigg|_{\theta} \,; \quad (5.150)$$

$$\underline{\mathbb{C}}^{\overline{ABC}} = \frac{\partial^2 \Sigma^{\overline{A}}}{\partial E_{\overline{B}}\partial E_{\overline{C}}}\bigg|_{N_0} = \frac{\partial^3 E_0}{\partial E_{\overline{A}}\partial E_{\overline{B}}\partial E_{\overline{C}}}\bigg|_{N_0} \,, \; \underline{\mathbb{C}}^{ABCDEF} = \frac{\partial^3 E_0}{\partial E_{AB}\partial E_{CD}\partial E_{EF}}\bigg|_{N_0} \,. \quad (5.151)$$

Isothermal third-order elastic stiffness coefficients are identical to those of Section 5.1.3. Notice the symmetry conditions $\mathbb{C}^{\overline{ABC}} = \mathbb{C}^{\overline{BAC}} = \mathbb{C}^{\overline{ACB}}$ and $\underline{\mathbb{C}}^{\overline{ABC}} = \underline{\mathbb{C}}^{\overline{BAC}} = \underline{\mathbb{C}}^{\overline{ACB}}$. Isothermal and isentropic third-order compliances are, respectively,

$$S_{\overline{ABC}} = -\frac{\partial^3 G_0}{\partial \Sigma^{\overline{A}}\partial \Sigma^{\overline{B}}\partial \Sigma^{\overline{C}}}\bigg|_{\theta} \,, \; S_{ABCDEF} = -\frac{\partial^3 G_0}{\partial \Sigma^{AB}\partial \Sigma^{CD}\partial \Sigma^{EF}}\bigg|_{\theta} \,; \quad (5.152)$$

$$\underline{S}_{\overline{AB}\overline{C}} = -\left.\frac{\partial^3 H_0}{\partial \Sigma^{\overline{A}} \partial \Sigma^{\overline{B}} \partial \Sigma^{\overline{C}}}\right|_{N_0} , \quad \underline{S}_{ABCDEF} = -\left.\frac{\partial^3 H_0}{\partial \Sigma^{AB} \partial \Sigma^{CD} \partial \Sigma^{EF}}\right|_{N_0} . \quad (5.153)$$

Symmetry relations $S_{\overline{AB}\overline{C}} = S_{\overline{BA}\overline{C}} = S_{\overline{AC}\overline{B}}$ and $\underline{S}_{\overline{AB}\overline{C}} = \underline{S}_{\overline{BA}\overline{C}} = \underline{S}_{\overline{AC}\overline{B}}$ apply.

Relationships among third-order stiffness and compliance coefficients can be derived as follows. Differentiation of the first of (5.148) by the strain tensor leads to

$$\frac{\partial}{\partial E_{\overline{D}}}(\mathbb{C}^{\overline{AB}} S_{\overline{BC}}) = \mathbb{C}^{\overline{ABD}} S_{\overline{BC}} + \mathbb{C}^{\overline{AB}} \frac{\partial S_{\overline{BC}}}{\partial \Sigma^{\overline{E}}} \frac{\partial \Sigma^{\overline{E}}}{\partial E_{\overline{D}}}$$

$$= \mathbb{C}^{\overline{ABD}} S_{\overline{BC}} + \mathbb{C}^{\overline{AB}} \mathbb{C}^{\overline{ED}} S_{\overline{BCE}} = 0. \quad (5.154)$$

Multiplying (5.154) by $\mathbb{C}^{\overline{CF}}$ and using (5.148) and symmetry properties of the elastic coefficients gives

$$\mathbb{C}^{\overline{ABC}} = -\mathbb{C}^{\overline{AD}} \mathbb{C}^{\overline{BE}} \mathbb{C}^{\overline{CF}} S_{\overline{DEF}} , \quad \underline{\mathbb{C}}^{\overline{ABC}} = -\underline{\mathbb{C}}^{\overline{AD}} \underline{\mathbb{C}}^{\overline{BE}} \underline{\mathbb{C}}^{\overline{CF}} S_{\overline{DEF}} , \quad (5.155)$$

where the second of (5.155) applies analogously for the isentropic coefficients. Analogous differentiation of (5.148) by the stress leads to

$$S_{\overline{ABC}} = -S_{\overline{AD}} S_{\overline{BE}} S_{\overline{CF}} \mathbb{C}^{\overline{DEF}} , \quad \underline{S}_{\overline{ABC}} = -\underline{S}_{\overline{AD}} \underline{S}_{\overline{BE}} \underline{S}_{\overline{CF}} \underline{\mathbb{C}}^{\overline{DEF}} . \quad (5.156)$$

Second-order thermal expansion coefficients are defined as

$$\alpha_{T\overline{A}} = \left.\frac{\partial E_{\overline{A}}}{\partial \theta}\right|_{\Sigma} = -\frac{\partial^2 G_0}{\partial \theta \partial \Sigma^{\overline{A}}} , \quad (\alpha_T)_{AB} = \left.\frac{\partial E_{AB}}{\partial \theta}\right|_{\Sigma} = -\frac{\partial^2 G_0}{\partial \theta \partial \Sigma^{AB}} , \quad (5.157)$$

and second-order thermal stress coefficients are defined as

$$\beta^{\overline{A}} = -\left.\frac{\partial \Sigma^{\overline{A}}}{\partial \theta}\right|_{\mathbf{E}} = -\frac{\partial^2 \Psi_0}{\partial \theta \partial E_{\overline{A}}} , \quad \beta^{AB} = -\left.\frac{\partial \Sigma^{AB}}{\partial \theta}\right|_{\mathbf{E}} = -\frac{\partial^2 \Psi_0}{\partial \theta \partial E_{AB}} . \quad (5.158)$$

Thermal stress coefficients in (5.158) are identical to those introduced in (5.50). The T subscript on thermal expansion coefficients in (5.157) is used as a label and is not subject to the Einstein summation convention.

Maxwell equations provide additional relationships among thermostatic coefficients. For example, using (5.143) and (5.157),

$$\left.\frac{\partial E_{\overline{A}}}{\partial N_0}\right|_{\Sigma} = \left.\frac{\partial E_{\overline{A}}}{\partial \theta}\right|_{\Sigma} \left.\frac{\partial \theta}{\partial N_0}\right|_{\Sigma} = \frac{\alpha_{T\overline{A}}\theta}{C_{\Sigma}} . \quad (5.159)$$

Similarly, from (5.142) and (5.158),

$$\left.\frac{\partial \Sigma^{\overline{A}}}{\partial N_0}\right|_{\mathbf{E}} = \left.\frac{\partial \Sigma^{\overline{A}}}{\partial \theta}\right|_{\mathbf{E}} \left.\frac{\partial \theta}{\partial N_0}\right|_{\mathbf{E}} = -\frac{\beta^{\overline{A}}\theta}{C_E} . \quad (5.160)$$

From the chain rule, thermal stress coefficients and thermal expansion coefficients are related by the following identity that incorporates isothermal second-order elastic coefficients:

$$
\beta^{\bar{A}} = -\frac{\partial \Sigma^{\bar{A}}}{\partial \theta}\bigg|_{\mathbf{E}} = \frac{\partial N_0}{\partial E_{\bar{A}}}\bigg|_{\theta} = \frac{\partial N_0}{\partial \Sigma^{\bar{B}}}\bigg|_{\theta}\frac{\partial \Sigma^{\bar{B}}}{\partial E^{\bar{A}}}\bigg|_{\theta} = \frac{\partial E_{\bar{B}}}{\partial \theta}\bigg|_{\Sigma}\frac{\partial \Sigma^{\bar{B}}}{\partial E^{\bar{A}}}\bigg|_{\theta} = \alpha_{T\bar{B}}\mathbb{C}^{\overline{BA}} . \quad (5.161)
$$

Multiplying (5.159) by the second-order isentropic elastic stiffness coefficients gives

$$
-\underline{\mathbb{C}}^{\overline{BA}}\frac{\alpha_{T\bar{A}}\theta}{C_\Sigma} = \frac{\partial \Sigma^{\bar{B}}}{\partial E_{\bar{A}}}\bigg|_{N_0}\frac{\partial E_{\bar{A}}}{\partial N_0}\bigg|_{\Sigma} = \frac{\partial \Sigma^{\bar{A}}}{\partial E_{\bar{B}}}\bigg|_{N_0}\frac{\partial \theta}{\partial \Sigma^{\bar{A}}}\bigg|_{N_0}
$$

$$
= \frac{\partial \theta}{\partial E_{\bar{B}}}\bigg|_{N_0} = \frac{\partial \Sigma^{\bar{B}}}{\partial N_0}\bigg|_{\mathbf{E}} = -\frac{\beta^{\bar{B}}\theta}{C_E}. \quad (5.162)
$$

Relation (5.162) can be written as

$$
\alpha_{T\bar{A}}\underline{\mathbb{C}}^{\overline{AB}} = \frac{C_\Sigma}{C_E}\beta^{\bar{A}} = C_R\beta^{\bar{A}}, \quad (5.163)
$$

where the ratio of specific heats satisfies, from (5.161),

$$
C_R\alpha_{T\bar{A}}\mathbb{C}^{\overline{AB}} = \alpha_{T\bar{A}}\underline{\mathbb{C}}^{\overline{AB}} . \quad (5.164)
$$

It can be shown (Thurston 1974) from Maxwell relations that the difference between specific heats at constant stress and constant strain is

$$
C_\Sigma - C_E = \theta\beta^{\bar{A}}\alpha_{T\bar{A}} = \theta\alpha_{T\bar{A}}\alpha_{T\bar{B}}\mathbb{C}^{\overline{AB}} = \frac{\theta}{C_R}\alpha_{T\bar{A}}\alpha_{T\bar{B}}\underline{\mathbb{C}}^{\overline{AB}} . \quad (5.165)
$$

Isentropic and isothermal second-order elastic stiffnesses are related by

$$
\underline{\mathbb{C}}^{\overline{AB}} = \frac{\partial \Sigma^{\bar{A}}}{\partial E_{\bar{B}}}\bigg|_{N_0} = \frac{\partial \Sigma^{\bar{A}}}{\partial E_{\bar{B}}}\bigg|_{\theta} + \frac{\partial \Sigma^{\bar{A}}}{\partial \theta}\bigg|_{\mathbf{E}}\frac{\partial \theta}{\partial E_{\bar{B}}}\bigg|_{N_0} = \mathbb{C}^{\overline{AB}} + \frac{\theta}{C_E}\beta^{\bar{A}}\beta^{\bar{B}} . \quad (5.166)
$$

Similarly, for isentropic and isothermal second-order elastic compliances,

$$
\underline{\mathbf{S}}_{\overline{AB}} = \frac{\partial E_{\bar{A}}}{\partial \Sigma^{\bar{B}}}\bigg|_{N_0} = \frac{\partial E_{\bar{A}}}{\partial \Sigma^{\bar{B}}}\bigg|_{\theta} + \frac{\partial E_{\bar{A}}}{\partial \theta}\bigg|_{\Sigma}\frac{\partial \theta}{\partial \Sigma^{\bar{B}}}\bigg|_{N_0} = \mathbf{S}_{\overline{AB}} - \frac{\theta}{C_\Sigma}\alpha_{T\bar{A}}\alpha_{T\bar{B}} . \quad (5.167)
$$

Thus, differences between isentropic and isothermal second-order elastic coefficients result from the dyadic (tensor) product of thermal expansion or thermal stress coefficients. Such differences are often overlooked in practical applications at low to moderate temperatures, since differences between isentropic and isothermal constants can typically be of the same order of magnitude as uncertainties in experimental measurements of the elastic coefficients.

Gruneisen numbers (i.e., Gruneisen's tensor components) are dimensionless quantities written in full as

$$
\Gamma^{AB} = -\frac{1}{\theta}\frac{\partial \theta}{\partial E_{AB}}\bigg|_{N_0} = \frac{1}{\theta}\frac{\partial \theta}{\partial N_0}\bigg|_{\mathbf{E}}\frac{\partial N_0}{\partial E_{AB}}\bigg|_{\theta} = -\frac{1}{C_E}\frac{\partial \Sigma^{AB}}{\partial \theta}\bigg|_{\mathbf{E}} = \frac{\beta^{AB}}{C_E}, \quad (5.168)
$$

or in reduced Voigt notation, using (5.161)-(5.164),

$$\Gamma^{\bar{A}} = -\frac{1}{\theta}\frac{\partial\theta}{\partial E_{\bar{A}}}\bigg|_{N_0} = \frac{\beta^{\bar{A}}}{C_E} = \frac{\alpha_{T\bar{B}}\mathbb{C}^{\overline{BA}}}{C_E} = \frac{\alpha_{T\bar{B}}\underline{\mathbb{C}}^{\overline{BA}}}{C_{\Sigma}}.$$ (5.169)

It follows from Maxwell's relations that Gruneisen parameters satisfy the following equalities:

$$\Gamma^{\bar{A}} = -\frac{1}{\theta}\frac{\partial\Sigma^{\bar{A}}}{\partial N_0}\bigg|_{\mathbf{E}} = -\frac{1}{\theta}\frac{\partial\theta}{\partial E_{\bar{A}}}\bigg|_{N_0} = -\frac{1}{C_E}\frac{\partial\Sigma^{\bar{A}}}{\partial\theta}\bigg|_{\mathbf{E}} = \frac{1}{C_E}\frac{\partial N_0}{\partial E_{\bar{A}}}\bigg|_{\theta},$$ (5.170)

and the ratio of specific heats at constant strain to constant stress can be expressed in terms of absolute temperature, thermal expansion coefficients, and Gruneisen numbers as

$$C_R = \frac{C_{\Sigma}}{C_E} = 1 + \frac{\theta}{C_{\Sigma}}\alpha_{T\bar{A}}\alpha_{T\bar{B}}\underline{\mathbb{C}}^{\overline{AB}}$$

$$= 1 + \theta\Gamma^{\bar{A}}\alpha_{T\bar{A}} = 1 + \theta\Gamma^{AB}(\alpha_T)_{AB},$$ (5.171)

where (5.165) and (5.169) have been used.

The number of independent components of all tensor-valued material coefficients, defined specifically as derivatives with respect to thermodynamic potentials evaluated at some undistorted reference state (i.e., polar tensors in the terminology of Thurston (1974)), can be reduced as a result of material symmetries of the particular crystal class (i.e., the point group) to which the substance under consideration belongs, as discussed in Appendix A. Forms of symmetric second-rank polar tensors such as thermal stress constants, thermal expansion constants, and Gruneisen's constants for all eleven Laue groups encompassing the 32 crystal classes are provided in Table A.5. Forms of second-order elastic constants (which include isothermal and isentropic moduli and compliances) are listed in Table A.8. Forms of third-order elastic stiffness constants (which include isothermal and adiabatic moduli only) are listed in Table A.9.

5.2.2 Hydrostatic Stress States

In certain applications, the pressure-volume response of a material may be of great importance while deviatoric (i.e., shear) stresses may not be. Such situations occur in some fluids that cannot support significant shear stresses, for example. Furthermore, in many high pressure applications, the deviatoric stress response may be insignificant compared to the hydrostatic stress response. The Cauchy pressure $p(x,t)$, which will often be called the hydrostatic pressure or simply the pressure, is defined as

$$p = -\frac{1}{3}\text{tr}\boldsymbol{\sigma} = -\frac{1}{3}\sigma^a_{.a}. \tag{5.172}$$

The relationship between pressure and Piola-Kirchhoff stresses is

$$p = -\frac{1}{3J}P^{aA}F_{aA} = -\frac{1}{3J}F^a_{.B}\Sigma^{BA}F_{aA}. \tag{5.173}$$

Using kinematic identity (2.144) and constitutive relationship (5.42), for a hyperelastic material, holding the deviatoric part of $\mathbf{F}$ constant,

$$\begin{aligned}
p &= -\frac{1}{3}\frac{\partial E_0}{\partial F_{aA}}J^{-1}F_{aA} = -\frac{1}{3}\frac{\partial E_0}{\partial J}\bigg|_{J^{-1/3}\mathbf{F}}\frac{\partial J}{\partial F_{aA}}J^{-1}F_{aA}\\
&= -\frac{1}{3}\frac{\partial E_0}{\partial J}\bigg|_{J^{-1/3}\mathbf{F}}JF^{-1Aa}J^{-1}F_{aA} = -\frac{1}{3}\frac{\partial E_0}{\partial J}\bigg|_{J^{-1/3}\mathbf{F}}\delta^A_{.A} = -\frac{\partial E_0}{\partial J}\bigg|_{J^{-1/3}\mathbf{F}}.
\end{aligned} \tag{5.174}$$

Similarly from (5.23), in terms of Helmholtz free energy per unit reference volume, the pressure satisfies

$$p = -\frac{\partial \Psi_0}{\partial J}\bigg|_{J^{-1/3}\mathbf{F}}. \tag{5.175}$$

Relations (5.172)-(5.175) hold regardless of dimensionality of the stress state. In the remainder of Section 5.2.2, the focus is on hydrostatic stress states for which the Cauchy stress tensor satisfies, by definition,

$$\sigma^{ab} = -pg^{ab}, \quad \sigma'^{ab} = \sigma^{ab} - \frac{1}{3}\sigma^c_{.c}g^{ab} = \sigma^{ab} + pg^{ab} = 0, \tag{5.176}$$

where $\boldsymbol{\sigma}'$ is the deviatoric part of the Cauchy stress. Piola-Kirchhoff stresses are generally not spherical under conditions (5.176):

$$P^{aA} = -JpF^{-1A}_{.b}g^{ab}, \quad \Sigma^{AB} = -JpF^{-1A}_{.a}g^{ab}F^{-1B}_{.b} = -JpC^{-1AB}. \tag{5.177}$$

Using (5.176), the stress power per unit reference volume becomes

$$J\sigma^{ab}D_{ab} = -JpL^a_{.a} = -Jpv^a_{;a} = -p\dot{J}. \tag{5.178}$$

In general anisotropic materials, no particular strain components E_{AB} need vanish when the Cauchy stress state is hydrostatic; only in elastic materials with isotropic or cubic symmetry does a spherical deformation gradient $F^a_{.A} = J^{1/3}g^a_{.A}$ with $C_{AB} = J^{2/3}G_{AB}$ always result in a hydrostatic state of stress. For example, for an isotropic, nonlinear hyperelastic material, (5.117) results in $\sigma^{ab} = J^{-1/3}g^a_{.A}\Sigma^{AB}g^b_{.B} = (\alpha_0 J^{-1/3} + \alpha_1 J^{1/3} + \alpha_2 J)g^{ab}$ when the deformation gradient is spherical.

Thermostatic potentials of Section 5.2.1 are redefined for spherical stress states with $-p$ replacing $\boldsymbol{\Sigma}$ and J replacing $\mathbf{E}$. In this context, all independent and dependent state variables in the thermostatic framework are scalars, and (5.131)-(5.133) are replaced with

$$E_0 = E_0\left(J, N_0\right), \; H_0 = H_0\left(p, N_0\right), \tag{5.179}$$

$$\Psi_0 = \Psi_0\left(J, \theta\right), \; G_0 = G_0\left(p, \theta\right), \tag{5.180}$$

$$N_0 = N_0\left(J, E_0\right). \tag{5.181}$$

The relationships in Table 4.2 are redefined as

$$H_0 = E_0 + pJ, \; \Psi_0 = E_0 - \theta N_0, \; G_0 = H_0 - \theta N_0, \tag{5.182}$$

where in general, enthalpies in (5.134) and (5.182) do not coincide since $pJ \neq -\Sigma^{AB} E_{AB}$. Differentials of the potentials are

$$dE_0 = -p\,dJ + \theta\,dN_0, \; dH_0 = J\,dp + \theta\,dN_0, \tag{5.183}$$

$$d\Psi_0 = -p\,dJ - N_0\,d\theta, \; dG_0 = J\,dp - N_0\,d\theta. \tag{5.184}$$

First derivatives then provide the following thermostatic relationships:

$$N_0 = -\left.\frac{\partial \Psi_0}{\partial \theta}\right|_J = -\left.\frac{\partial G_0}{\partial \theta}\right|_p, \; \theta = \left.\frac{\partial E_0}{\partial N_0}\right|_J = \left.\frac{\partial H_0}{\partial N_0}\right|_p, \tag{5.185}$$

$$p = -\left.\frac{\partial E_0}{\partial J}\right|_{N_0} = -\left.\frac{\partial \Psi_0}{\partial J}\right|_\theta, \; J = \left.\frac{\partial H_0}{\partial p}\right|_{N_0} = \left.\frac{\partial G_0}{\partial p}\right|_\theta. \tag{5.186}$$

$$\frac{1}{\theta} = \left.\frac{\partial N_0}{\partial E_0}\right|_J, \; p = \theta\left.\frac{\partial N_0}{\partial J}\right|_{E_0}. \tag{5.187}$$

Isothermal (B) and isentropic ($\underline{B}$) bulk moduli are defined as follows:

$$B = -J\left.\frac{\partial p}{\partial J}\right|_\theta = J\left.\frac{\partial^2 \Psi_0}{\partial J^2}\right|_\theta, \; \underline{B} = -J\left.\frac{\partial p}{\partial J}\right|_{N_0} = J\left.\frac{\partial^2 E_0}{\partial J^2}\right|_{N_0}, \tag{5.188}$$

Isothermal and isentropic compressibilities are defined, respectively, as

$$\chi = \frac{1}{B} = -\frac{1}{J}\left.\frac{\partial J}{\partial p}\right|_\theta, \; \underline{\chi} = \frac{1}{\underline{B}} = -\frac{1}{J}\left.\frac{\partial J}{\partial p}\right|_{N_0}. \tag{5.189}$$

Recalling from the conservation of mass (4.10) that $\rho_0 = \rho J$, partial derivatives with respect to Jacobian determinant J can be expressed as

$$J\frac{\partial(.)}{\partial J} = J\frac{\partial(.)}{\partial \rho}\frac{\partial \rho}{\partial J} = \rho_0 J\frac{\partial(.)}{\partial \rho}\frac{\partial J^{-1}}{\partial J} = -\rho_0 J^{-1}\frac{\partial(.)}{\partial \rho} = -\rho\frac{\partial(.)}{\partial \rho}. \tag{5.190}$$

Defining specific volume as $\upsilon = \rho^{-1} = J\rho_0^{-1}$, derivatives can also be written

$$J\frac{\partial(.)}{\partial J} = -\frac{1}{\upsilon}\frac{\partial(.)}{\partial \upsilon}\frac{\partial \upsilon}{\partial \rho} = -\frac{1}{\upsilon}\frac{\partial(.)}{\partial \upsilon}\frac{\partial \rho^{-1}}{\partial \rho} = \frac{1}{\upsilon}\rho^{-2}\frac{\partial(.)}{\partial \upsilon} = \upsilon\frac{\partial(.)}{\partial \upsilon}. \tag{5.191}$$

The absolute spatial volume v can be substituted for the specific volume:

$$J\frac{\partial(.)}{\partial J}=\frac{dv}{dV}\frac{\partial(.)}{\partial(dv/dV)}=\frac{v}{V}\frac{\partial(.)}{\partial v/V}=v\frac{\partial(.)}{\partial v}\,. \tag{5.192}$$

Thus isothermal and isentropic bulk moduli in (5.188) can be written

$$B=\rho\frac{\partial p}{\partial \rho}\bigg|_{\theta}=-\upsilon\frac{\partial p}{\partial \upsilon}\bigg|_{\theta}=-v\frac{\partial p}{\partial v}\bigg|_{\theta}\,,\quad \underline{B}=\rho\frac{\partial p}{\partial \rho}\bigg|_{N_0}=-\upsilon\frac{\partial p}{\partial \upsilon}\bigg|_{N_0}=-v\frac{\partial p}{\partial v}\bigg|_{N_0}\,. \tag{5.193}$$

A volumetric expansion coefficient at constant pressure, i.e., an isotropic coefficient of thermal expansion, is defined as

$$A=\frac{1}{J}\frac{\partial J}{\partial \theta}\bigg|_{p}=\frac{1}{J}\frac{\partial^2 G_0}{\partial \theta \partial p}\,. \tag{5.194}$$

It follows from mass conservation that

$$A=\frac{1}{J}\frac{\partial J}{\partial \theta}\bigg|_{p}=\rho\frac{\partial \rho^{-1}}{\partial \theta}\bigg|_{p}=-\frac{1}{\rho}\frac{\partial \rho}{\partial \theta}\bigg|_{p}=-\frac{\partial \ln \rho}{\partial \theta}\bigg|_{p}\,. \tag{5.195}$$

From (5.193) and (5.195) and noting that $p=p[\rho(p,\theta),\theta]$,

$$0=\frac{\partial p}{\partial \theta}\bigg|_{p}=\frac{\partial p}{\partial \theta}\bigg|_{\rho}+\frac{\partial p}{\partial \rho}\bigg|_{\theta}\frac{\partial \rho}{\partial \theta}\bigg|_{p}=\frac{\partial p}{\partial \theta}\bigg|_{\rho}-AB\Rightarrow\frac{\partial p}{\partial \theta}\bigg|_{\rho}=AB=\frac{\partial p}{\partial \theta}\bigg|_{J}\,. \tag{5.196}$$

Definitions at a reference state of null strain and zero stress are instructive and useful for formulating constitutive models in terms of measured thermoelastic properties. In this state, the deformation gradient, strain, and Jacobian determinant are

$$F^{a}_{.A}=g^{a}_{.A}\,,\ C_{AB}=G_{AB}\,,\ E_{AB}=0\,,\ J=1\,, \tag{5.197}$$

and the stress state is, by definition,

$$\Sigma^{AB}=0\,,\ P^{aB}=0\,,\ \sigma^{ab}=0\,,\ p=0\,. \tag{5.198}$$

Let the temperature at the reference state be θ_0, which can be of arbitrary positive value. From the second of (5.177),

$$\frac{\partial \Sigma^{AB}}{\partial p}\bigg|_{\substack{p=0\\\theta=\theta_0}}=-JC^{-1AB}\bigg|_{\substack{p=0\\\theta=\theta_0}}=-G^{AB}\,. \tag{5.199}$$

Also from (2.160), in the reference state

$$\frac{\partial J}{\partial E_{AB}}\bigg|_{\substack{p=0\\\theta=\theta_0}}=2\frac{\partial J}{\partial C_{AB}}\bigg|_{\substack{p=0\\\theta=\theta_0}}=JC^{-1AB}\bigg|_{\substack{p=0\\\theta=\theta_0}}=G^{AB}\,. \tag{5.200}$$

Tensors of thermal expansion coefficients (5.157) and thermal stress coefficients (5.158) evaluated at the reference state are then

$$(\alpha_{T0})_{AB}=\frac{\partial E_{AB}}{\partial \theta}\bigg|_{\substack{\Sigma=0\\\theta=\theta_0}}=\frac{\partial E_{AB}}{\partial \theta}\bigg|_{\substack{p=0\\\theta=\theta_0}}\,,\quad \beta_0^{AB}=-\frac{\partial \Sigma^{AB}}{\partial \theta}\bigg|_{\substack{E=0\\\theta=\theta_0}}=-\frac{\partial \Sigma^{AB}}{\partial \theta}\bigg|_{\substack{J=1\\\theta=\theta_0}}\,. \tag{5.201}$$

From (5.194) and (5.200), the scalar expansion coefficient at null pressure and reference temperature is the trace of the corresponding tensor coefficient of thermal expansion:

$$A_0 = \left(\frac{1}{J} \frac{\partial J}{\partial \theta} \bigg|_p \right)\bigg|_{\substack{p=0 \\ \theta=\theta_0}} = \left(\frac{1}{J} \frac{\partial J}{\partial E_{AB}} \bigg|_p \frac{\partial E_{AB}}{\partial \theta} \bigg|_\Sigma \right)\bigg|_{\substack{p=0 \\ \theta=\theta_0}} = G^{AB} \alpha_{T0AB} = \alpha_{T0.A}{}^{A}. \quad (5.202)$$

For the isothermal compressibility of the first of (5.189) at the reference state, from (5.199) and (5.200),

$$\chi_0 = \frac{1}{B_0} = -\left(\frac{1}{J} \frac{\partial J}{\partial p} \bigg|_\theta \right)\bigg|_{\substack{p=0 \\ \theta=\theta_0}} = -\left(\frac{1}{J} \frac{\partial J}{\partial E_{AB}} \frac{\partial E_{AB}}{\partial \Sigma^{CD}} \frac{\partial \Sigma^{CD}}{\partial p} \right)\bigg|_{\substack{p=0 \\ \theta=\theta_0}}$$

$$= G^{AB} \left(S_{ABCD} \big|_{\substack{p=0 \\ \theta=\theta_0}} \right) G^{CD} = G^{AB} G^{CD} \overline{S}_{ABCD}. \quad (5.203)$$

An analogous relationship applies for the isentropic compressibility and isentropic elastic compliance coefficients:

$$\underline{\chi}_0 = \frac{1}{\underline{B}_0} = -\left(\frac{1}{J} \frac{\partial J}{\partial p} \bigg|_{N_0} \right)\bigg|_{\substack{p=0 \\ \theta=\theta_0}} = G^{AB} G^{CD} \underline{S}_{ABCD} \big|_{\substack{p=0 \\ \theta=\theta_0}}. \quad (5.204)$$

Relations (5.202)-(5.204) apply regardless of material symmetry. For an isotropic materially linear thermoelastic solid, in the context of (5.127) and holding shear strains fixed, the isothermal bulk modulus satisfies

$$B_0 = -\left(J \frac{\partial p}{\partial J} \bigg|_\theta \right)\bigg|_{\substack{p=0 \\ \theta=\theta_0}} = \frac{K}{3}\left[J \frac{\partial}{\partial J}\left(C_{.A}^{A} E_{.B}^{B} \right) \right]\bigg|_{\substack{p=0 \\ \theta=\theta_0}}$$

$$= \frac{K}{6}\left[J \frac{\partial}{\partial J}\left(C_{.A}^{A} C_{.B}^{B} - C_{.A}^{A} \delta_{.B}^{B} \right) \right]\bigg|_{\substack{p=0 \\ \theta=\theta_0}}$$

$$= \frac{K}{6}\left[J \left(2C_{.B}^{B} - 3 \right) \frac{\partial C_{.A}^{A}}{\partial J} \right]\bigg|_{\substack{p=0 \\ \theta=\theta_0}} = \frac{K}{2} \frac{\partial (3J^{2/3})}{\partial J}\bigg|_{\substack{p=0 \\ \theta=\theta_0}}$$

$$= K J^{-1/3} \big|_{\substack{p=0 \\ \theta=\theta_0}} = K. \quad (5.205)$$

Thus, from (5.127) and (5.205), isothermal thermoelastic coupling coefficients are related in isotropic solids by the relationships $(\alpha_{T0})_{.B}^{A} = (\bar{\alpha}_T)\delta_{.B}^{A}$, $A_0 = 3\bar{\alpha}_T = \bar{\beta}/K$, and $K = B_0 = 1/\chi_0$. Similar relationships hold for crystals with cubic symmetry, but not for general anisotropic bodies.

Definitions of specific heats per unit reference volume at constant volume C_v and constant pressure C_p, i.e., isochoric and isobaric specific heats, are, respectively,

$$C_v = \left.\frac{\partial E_0}{\partial \theta}\right|_J = \left.\theta\frac{\partial N_0}{\partial \theta}\right|_J = \left.-\theta\frac{\partial^2 \Psi_0}{\partial \theta^2}\right|_J, \tag{5.206}$$

$$C_p = \left.\frac{\partial H_0}{\partial \theta}\right|_p = \left.\theta\frac{\partial N_0}{\partial \theta}\right|_p = \left.-\theta\frac{\partial^2 G_0}{\partial \theta^2}\right|_p. \tag{5.207}$$

At the reference state, since both pressure and stress vanish by (5.198),

$$C_{p0} = \left.\frac{\partial H_0}{\partial \theta}\right|_{\substack{p=0 \\ \theta=\theta_0}} = \left.\frac{\partial H_0}{\partial \theta}\right|_{\substack{\Sigma=0 \\ \theta=\theta_0}} = C_{\Sigma 0}. \tag{5.208}$$

Noting that

$$\left.\frac{\partial N_0}{\partial \theta}\right|_p = \left.\frac{\partial N_0}{\partial \theta}\right|_J + \left.\frac{\partial N_0}{\partial J}\right|_\theta \left.\frac{\partial J}{\partial \theta}\right|_p, \tag{5.209}$$

specific heats at constant pressure and constant volume are related at any equilibrium state by

$$\begin{aligned} C_p &= \left.\theta\frac{\partial N_0}{\partial \theta}\right|_J + \left.\theta\frac{\partial N_0}{\partial J}\right|_\theta \left.\frac{\partial J}{\partial \theta}\right|_p = C_v + \left.\theta J A\frac{\partial N_0}{\partial J}\right|_\theta \\ &= C_v + \left.\theta J A\frac{\partial N_0}{\partial p}\right|_\theta \left.\frac{\partial p}{\partial J}\right|_\theta = C_v - \left.\theta A B\frac{\partial N_0}{\partial p}\right|_\theta \\ &= C_v + AB\theta\frac{\partial^2 G_0}{\partial p\partial\theta} = C_v + \left.AB\theta\frac{\partial J}{\partial \theta}\right|_p = C_v + J A^2 B\theta. \end{aligned} \tag{5.210}$$

From (5.165) and (5.210),

$$C_p - C_\Sigma - C_v + C_E = \theta(J A^2 B - \alpha_{TAB}\alpha_{TCD}\mathbb{C}^{ABCD}). \tag{5.211}$$

At the reference state, from (5.208), this reduces to

$$C_{E0} - C_{v0} = \theta(A_0^2 B_0 - \alpha_{T0AB}\alpha_{T0CD}\overline{\mathbb{C}}^{ABCD}). \tag{5.212}$$

Thurston (1974) noted that the difference in (5.212) vanishes identically in isotropic materials and crystals of cubic symmetry, but that $C_{E0} \neq C_{v0}$ in general for materials of greater anisotropy.

As explained by Thurston (1974), thermostatic potentials can be redefined at an alternative state of nonzero constant hydrostatic pressure, and relationships among their derivatives can be calculated at this alternative reference state. Choice of zero pressure for the reference state is not necessary, but is convenient if one assigns for the physical environment (e.g., laboratory) a datum of zero gauge pressure.

The following relationships can be derived from the thermostatic potentials:

$$\frac{\partial J}{\partial N_0}\bigg|_p = \frac{J\theta A}{C_p}, \quad \frac{\partial p}{\partial N_0}\bigg|_J = \frac{\theta AB}{C_v}. \tag{5.213}$$

Noting that $p = p[J, \theta(J, N_0)]$,

$$\frac{\partial p}{\partial J}\bigg|_{N_0} = \frac{\partial p}{\partial J}\bigg|_\theta + \frac{\partial p}{\partial \theta}\bigg|_J \frac{\partial \theta}{\partial J}\bigg|_{N_0}. \tag{5.214}$$

Dividing both sides of (5.214) by isothermal bulk modulus B and using (5.196), isentropic and isothermal bulk moduli are related by

$$\frac{\underline{B}}{B} = 1 + \frac{\partial J}{\partial p}\bigg|_\theta \frac{\partial p}{\partial \theta}\bigg|_J \frac{\partial \theta}{\partial J}\bigg|_{N_0} = 1 + \left(\frac{-J}{B}\right)(AB)\left(\frac{-\partial p}{\partial N_0}\bigg|_J\right) = 1 + \frac{JA^2 B\theta}{C_v}. \tag{5.215}$$

Comparing (5.210) and (5.215),

$$\underline{B}/B = C_p/C_v. \tag{5.216}$$

The Gruneisen parameter (scalar) is defined as

$$\Gamma = -\frac{J}{\theta}\frac{\partial \theta}{\partial J}\bigg|_{N_0} = -\frac{\partial \ln \theta}{\partial \ln J}\bigg|_{N_0}. \tag{5.217}$$

It follows from (5.216) and the thermostatic potentials that the Gruneisen "gamma" satisfies the following identities:

$$\Gamma = \frac{J}{C_v}\frac{\partial N_0}{\partial J}\bigg|_\theta = \frac{J}{C_v}\frac{\partial p}{\partial \theta}\bigg|_J = J\frac{\partial p}{\partial E_0}\bigg|_J = \frac{JAB}{C_v} = \frac{JA\underline{B}}{C_p}. \tag{5.218}$$

Furthermore from (5.189), (5.210), and (5.216),

$$\frac{\underline{B}}{B} = \frac{C_p}{C_v} = \frac{\chi}{\underline{\chi}} = 1 + A\Gamma\theta. \tag{5.219}$$

From (5.168) and (5.217), three-dimensional Gruneisen numbers are related to scalar Gruneisen parameter by

$$\Gamma = \frac{J}{C_v}\frac{\partial N_0}{\partial E_{AB}}\bigg|_\theta \frac{\partial E_{AB}}{\partial J}\bigg|_\theta = \frac{J}{C_v}\theta\frac{\partial N_0}{\partial \theta}\bigg|_E \Gamma^{AB}\frac{\partial E_{AB}}{\partial J}\bigg|_\theta$$

$$= \frac{JC_E}{C_v}\Gamma^{AB}\frac{\partial E_{AB}}{\partial J}\bigg|_\theta. \tag{5.220}$$

Under a hydrostatic stress state, the following identity holds:

$$\frac{\partial E_{AB}}{\partial J}\bigg|_\theta = \frac{\partial E_{AB}}{\partial \Sigma^{CD}}\bigg|_\theta \frac{\partial \Sigma^{CD}}{\partial p}\bigg|_\theta \frac{\partial p}{\partial J}\bigg|_\theta = -\frac{B}{J}S_{ABCD}\frac{\partial \Sigma^{CD}}{\partial p}\bigg|_\theta, \tag{5.221}$$

which, when substituted into (5.220), leads to the relationship

$$\Gamma = -\frac{BC_E}{C_v}\Gamma^{AB}\mathbf{S}_{ABCD}\frac{\partial \Sigma^{CD}}{\partial p}\bigg|_\theta, \tag{5.222}$$

and at the stress-free undeformed reference state, from (5.199),

$$\Gamma_0 = \frac{B_0 C_{E0}}{C_{v0}}\Gamma_0^{AB}\overline{\mathbf{S}}_{ABCD}G^{CD}. \tag{5.223}$$

Recall from discussion following (5.212) that $C_{E0} = C_{v0}$ for isotropic solids and for crystals with cubic symmetry, in which case (5.223) yields $\Gamma_0^{AB} = \Gamma_0 G^{AB}$ and $3\Gamma_0 = \Gamma_{0.A}^A$.

A number of theoretical models for the Gruneisen parameter have been developed using macroscopic arguments or atomic treatments of lattice vibrations. According to Einstein's model (Einstein 1907; Born and Huang 1954), when the internal energy of (5.77) is extended to include effects of volume change,

$$E_0(J,\theta) = U_S(J) + U_V(J,\theta) = U_S(J) + 3nk_B\theta\left(\frac{\xi}{2} + \frac{\xi}{e^\xi - 1}\right), \tag{5.224}$$

where

$$\xi(J,\theta) = \Theta_E(J)/\theta, \ \Theta_E = h\nu_E(J)/k_B. \tag{5.225}$$

Einstein's temperature Θ_E and characteristic frequency ν_E are not constant as was the case in (5.78), but are instead here assumed to depend on volume via J, but not on absolute temperature θ. Static internal energy per unit reference volume is written U_S, and U_V is the vibrational energy. The free energy per unit reference volume corresponding to (5.224) is

$$\Psi_0 = E_0 - N_0\theta = U_S(J) + 3nk_B\theta\left[\frac{\xi}{2} + \ln\left(1 - e^{-\xi}\right)\right]. \tag{5.226}$$

Similarly, for Debye's model (Debye 1912), the total internal energy can be expressed as (Born and Huang 1954)

$$E_0(J,\theta) = U_S(J) + U_V(J,\theta)$$

$$= U_S(J) + 9nk_B\theta\left[\left(\frac{\theta}{\Theta_D}\right)^3 \int_0^{\Theta_D/\theta}\left(\frac{1}{2} + \frac{1}{e^\xi - 1}\right)\xi^3 d\xi\right], \tag{5.227}$$

with the corresponding definitions

$$\xi(J,\theta) = \Theta_D(J)/\theta, \ \Theta_D(J) = h\nu_D(J)/k_B. \tag{5.228}$$

The free energy per unit reference volume in Debye's theory is (Born and Huang 1954)

$$\Psi_0 = E_0 - N_0\theta$$

$$= U_S(J) + 9nk_B\theta\left\{\left(\frac{\theta}{\Theta_D}\right)^{\Theta_D/\theta}\int_0^{\Theta_D/\theta}\left[\frac{1}{2}\xi + \ln\left(1 - e^{-\xi}\right)\right]\xi^2 d\xi\right\}. \tag{5.229}$$

Writing Θ to describe either the Einstein temperature or the Debye temperature, it can be shown (Born and Huang 1954)

$$J\frac{\partial\xi}{\partial J}\bigg|_\theta = v\frac{\partial\xi}{\partial v}\bigg|_\theta = \frac{v}{\Theta}\frac{d\Theta}{dv}\frac{\partial\xi}{\partial\ln\Theta}\bigg|_\theta = \frac{d\ln\Theta}{d\ln v}\frac{\partial\xi}{\partial\ln\Theta}\bigg|_\theta = -\Gamma\frac{\partial\xi}{\partial\ln\Theta}\bigg|_\theta, \tag{5.230}$$

so that for Einstein's model,

$$\Gamma_E = -\frac{d\ln\Theta_E}{d\ln v} = -\frac{J}{\Theta_E}\frac{d\Theta_E}{dJ} = -\frac{d\ln\Theta_E}{d\ln J} = -\frac{J}{v_E}\frac{dv_E}{dJ} = -\frac{v}{v_E}\frac{dv_E}{dv}, \tag{5.231}$$

and for Debye's model,

$$\Gamma_D = -\frac{d\ln\Theta_D}{d\ln v} = -\frac{J}{\Theta_D}\frac{d\Theta_D}{dJ} = -\frac{d\ln\Theta_D}{d\ln J} = -\frac{J}{v_D}\frac{dv_D}{dJ} = -\frac{v}{v_D}\frac{dv_D}{dv}. \tag{5.232}$$

Using (5.224) or (5.227),

$$-J\frac{\partial\Psi_0}{\partial J}\bigg|_\theta + J\frac{dU_S}{dJ} = \Gamma U_V, \tag{5.233}$$

from which dividing by J and using (5.186) gives a functional form for the equation of state of Mie and Gruneisen (1926):

$$p(J,\theta) = -\frac{dU_S}{dJ} + \Gamma J^{-1}U_V. \tag{5.234}$$

Consider now the pressure derivative of the isothermal bulk modulus B at constant temperature:

$$\frac{\partial B}{\partial p}\bigg|_\theta = \frac{\partial J}{\partial p}\bigg|_\theta\frac{\partial B}{\partial J}\bigg|_\theta = -\frac{J}{B}\frac{\partial B}{\partial J}\bigg|_\theta = \frac{J}{B}\frac{\partial}{\partial J}\left(J\frac{\partial p}{\partial J}\right)\bigg|_\theta = \frac{J}{B}\left(\frac{-B}{J} + J\frac{\partial^2 p}{\partial J^2}\bigg|_\theta\right)$$

$$= -1 + \frac{J^2}{B}\frac{\partial^2 p}{\partial J^2}\bigg|_\theta = -1 - \frac{J(\partial^2 p/\partial J^2)\big|_\theta}{(\partial p/\partial J)\big|_\theta} = -1 - \frac{v(\partial^2 p/\partial v^2)\big|_\theta}{(\partial p/\partial v)\big|_\theta}. \tag{5.235}$$

One may also write

$$\frac{\partial B}{\partial p}\bigg|_\theta = -\frac{J}{B}\frac{\partial B}{\partial J}\bigg|_\theta = -\frac{\partial\ln B}{\partial\ln J}\bigg|_\theta = -\frac{v}{B}\frac{\partial B}{\partial v}\bigg|_\theta = -\frac{\partial\ln B}{\partial\ln v}\bigg|_\theta. \tag{5.236}$$

The relationship between Gruneisen's coefficient and the isothermal pressure derivatives in (5.235) and (5.236) is often expressed as

$$\Gamma = -C_\Gamma - \frac{v}{2}\frac{(\partial^2 p/\partial v^2)\big|_\theta}{(\partial p/\partial v)\big|_\theta} = \frac{1}{2}\frac{\partial B}{\partial p}\bigg|_\theta + \frac{1}{2} - C_\Gamma, \tag{5.237}$$

where C_Γ is a constant. Slater (1939) suggested $C_\Gamma = 2/3$ following a Debye-type analysis in which Poisson's ratio is assumed independent of volume. Dugdale and MacDonald (1953) suggested $C_\Gamma = 1$ for isothermal conditions based on analysis of plane wave velocities in a monatomic lattice, leading to vanishing of Γ when interatomic forces are harmonic. Value $C_\Gamma = 7/6$ has also been widely suggested (Slater 1940; Eshelby 1954). Notice that the reference Gruneisen parameter Γ_0 can be determined from (5.237) when the pressure derivative of the isothermal bulk modulus is evaluated at the reference state.

A number of other functional forms of Gruneisen's parameter have been suggested. Segletes and Walters (1998) developed a power-law model for Gruneisen's parameter that encompasses several historical models (Slater 1940; Dugdale and MacDonald 1953). Murnaghan (1944) developed a simple model in which the bulk modulus varies linearly with pressure. Birch (1978) developed a popular nonlinear equation of state for crystalline solids undergoing potentially large volume changes. Vinet et al. (1989) developed a universal form for equations of state of covalent and metallic solids. Zhou (2005) postulated a free energy function similar to (5.229) by additively decomposing atomic velocities into high frequency terms associated with thermal oscillations and low frequency terms associated with bulk structural motion.

5.3 Finite Elastic Volume Changes

Consider applications wherein large elastic volume changes are of interest, but large elastic deviatoric deformations are not. In many ductile crystalline solids such as engineering metals, large deviatoric deformations are sustained by dislocation glide which is assumed to be lattice-preserving (i.e., inelastic), as explained in Sections 3.2.2 and 3.2.5. In more brittle solids such as many ceramic crystals at low to moderate temperatures, driving forces necessary for dislocation motion exceed those for fracture, and large deviatoric deformations are sustained by damage mechanisms (e.g., micro-cracking) when mechanical stresses exceed some threshold. Inelastic tensile volumetric deformations are accommodated by damage mechanisms such as voids in ductile materials and mode I cracks in brittle materials. On the other hand, large compressive volumetric deformations are accommodated in fully dense (i.e., non-porous) crystalline solids by elastic contraction of the lattice. Tensile damage mechanisms of void growth and mode I fracture are impeded by large compressive pressures.

Such confining pressures are attained in shock physics experiments, for example, under dynamic impact situations (Graham and Brooks 1971; Graham 1992; Vogler and Clayton 2008), as well as in more general scenarios of ballistic impact or high pressure/blast loading, or geological activity involving significant confinement.

The model framework that follows is appropriate for thermoelastic behavior of isotropic solids (e.g., polycrystals with random grain orientations) undergoing large volume changes but small shape changes. The framework is a reduction of the more general one of Section 5.1.3, but is based on a series expansion of the internal energy rather than the free energy. Specifically, internal energy per unit reference volume is written

$$E_0\left(\mathbf{E},\theta,X\right)=E_S\left(\mathbf{E}',X\right)+E_V\left(\zeta(J),\theta,X\right), \qquad (5.238)$$

where the deviatoric right Cauchy-Green strain and measure of volumetric deformation are, respectively,

$$E'_{AB}=E_{AB}-\frac{1}{3}E^C_{.C}G_{AB}\,,\ \zeta=\frac{\rho}{\rho_0}-1=J^{-1}-1\,. \qquad (5.239)$$

Kinematic variable $\zeta(X,t)$ contains the same information as J so that volume changes are measured exactly to the extent permitted by the deformation gradient itself. From the second of (5.239), $\zeta=0$ at the reference state with $J=1$, $\zeta>0$ when the material is spherically compressed, and $\zeta<0$ when the material is spherically expanded. The deviatoric energy is usually taken as a quadratic function of $\mathbf{E}'$, while the term E_V is generally a nonlinear function of ζ and θ, accounting for the equation of state of the material, a generally nonlinear pressure-volume-temperature relationship. Using (5.238) in (5.42), the second Piola-Kirchhoff stress satisfies, from (2.160),

$$\begin{aligned}
\Sigma^{AB} &= \frac{\partial E_0}{\partial E_{AB}} = \frac{\partial E_S}{\partial E'_{CD}}\frac{\partial E'_{CD}}{\partial E_{AB}} + \frac{\partial E_V}{\partial \zeta}\frac{\partial \zeta}{\partial J}\frac{\partial J}{\partial E_{AB}} \\
&= \frac{\partial E_S}{\partial E'_{CD}}\left(\delta^A_{.C}\delta^B_{.D}-\frac{1}{3}G^{AB}G_{CD}\right)-\frac{1}{J}\frac{\partial E_V}{\partial \zeta}C^{-1AB}.
\end{aligned} \qquad (5.240)$$

Cauchy stress and Cauchy pressure are computed, respectively, as

$$\sigma^{ab}=\frac{1}{J}\frac{\partial E_S}{\partial E'_{CD}}\left(F^a_{.C}F^b_{.D}-\frac{1}{3}F^a_{.A}F^b_{.B}G^{AB}G_{CD}\right)-\frac{1}{J^2}\frac{\partial E_V}{\partial \zeta}g^{ab}, \quad (5.241)$$

$$p=-\frac{1}{3J}\frac{\partial E_S}{\partial E'_{CD}}\left(C_{CD}-\frac{1}{3}C^A_{.A}G_{CD}\right)+\frac{1}{J^2}\frac{\partial E_V}{\partial \zeta}\,. \qquad (5.242)$$

For illustrative purposes, let the internal energy (5.238) be written at material point X as

$$E_0 = \mu E'^{AB} E'_{AB} + \left(\frac{1}{2} B_0 \zeta^2 + \frac{1}{3} B_1 \zeta^3 + ... \right) + A_0 B_0 \zeta \Delta\theta + \bar{C} \Delta\theta . \quad (5.243)$$

The first term on the right of (5.243) accounts for the deviatoric response, with μ a constant shear modulus. Terms in parentheses account for the nonlinear pressure-volume response at constant temperature, with B_0 and B_1 material constants. The next term accounts for thermoelastic coupling, with A_0 a constant. The final term accounts for the purely thermal energy, with $\bar{C}$ a constant specific heat per unit reference volume and $\Delta\theta = \theta - \theta_0$, with θ_0 a reference temperature at which this thermal energy vanishes. Material constants satisfy

$$\mu = \frac{1}{2} \frac{\partial^2 E_S}{\partial E'^{AB} \partial E'_{AB}} \bigg|_{\substack{\mathbf{E}=0 \\ \theta=\theta_0}}, \quad B_0 = \frac{\partial^2 E_V}{\partial \zeta^2} \bigg|_{\substack{\mathbf{E}=0 \\ \theta=\theta_0}}, \quad B_1 = \frac{1}{2} \frac{\partial^3 E_V}{\partial \zeta^3} \bigg|_{\substack{\mathbf{E}=0 \\ \theta=\theta_0}}, \quad (5.244)$$

$$A_0 = \frac{1}{B_0} \frac{\partial^2 E_0}{\partial\theta \partial\zeta} \bigg|_{\substack{\mathbf{E}=0 \\ \theta=\theta_0}}, \quad \bar{C} = \frac{\partial E_0}{\partial\theta} \bigg|_{\substack{\mathbf{E}=0 \\ \theta=\theta_0}} . \quad (5.245)$$

From (5.240)-(5.242), stress components and Cauchy pressure are

$$\Sigma^{AB} = 2\mu E'^{AB} - \frac{1}{J} C^{-1AB} \left[\left(B_0 \zeta + B_1 \zeta^2 + ... \right) + A_0 B_0 \Delta\theta \right], \quad (5.246)$$

$$\sigma^{ab} = \frac{2}{J} \mu E'^{AB} F^a_{.A} F^b_{.B} - \frac{1}{J^2} \left[\left(B_0 \zeta + B_1 \zeta^2 + ... \right) + A_0 B_0 \Delta\theta \right] g^{ab}, \quad (5.247)$$

$$p = -\frac{2}{3J} \mu E'^{AB} C_{AB} + \frac{1}{J^2} \left[\left(B_0 \zeta + B_1 \zeta^2 + ... \right) + A_0 B_0 \Delta\theta \right]. \quad (5.248)$$

Consider the volume derivative of the pressure at the reference state when the contribution from the first term on the right side of (5.248) vanishes (e.g., null shear stress):

$$-\left(J \frac{\partial p}{\partial J} \right) \bigg|_{\substack{\mathbf{E}=0 \\ \theta=\theta_0}} = \left(\frac{1}{J} \frac{\partial p}{\partial \zeta} \right) \bigg|_{\substack{\mathbf{E}=0 \\ \theta=\theta_0}} = \left[\frac{1}{J} \left(B_0 + 2B_1 \zeta + ... \right) \right] \bigg|_{\substack{\zeta=0 \\ \theta=\theta_0}} = B_0 . \quad (5.249)$$

Thus B_0 is equivalent to isothermal bulk modulus at the reference state in the context of hydrostatic stress conditions, as introduced in (5.203). Now consider the relationship

$$\frac{\partial p}{\partial\theta} \bigg|_{\substack{\mathbf{E}=0 \\ \theta=\theta_0}} = \left[\left(\frac{1}{J} \frac{\partial J}{\partial\theta} \right) \left(-J \frac{\partial p}{\partial J} \right) \right] \bigg|_{\substack{\mathbf{E}=0 \\ \theta=\theta_0}} = (AB)|_{\substack{\mathbf{E}=0 \\ \theta=\theta_0}} = A_0 B_0 , \quad (5.250)$$

implying that A_0 is equivalent to the spherical thermal expansion coefficient of (5.202) at the reference state for hydrostatic stress conditions:

$$A_0 = \left(\frac{1}{J} \frac{\partial J}{\partial \theta} \right)\Bigg|_{\substack{\mathbf{E}=0 \\ \theta=\theta_0}}. \tag{5.251}$$

For isotropic solids, the right side of (5.212) vanishes (Thurston 1974). Thus the specific heat at constant volume or constant strain at the reference state satisfies $C_{E0} = C_{v0} = \bar{C}$, and the product

$$A_0 B_0 \Delta\theta = J^{-1} \Gamma \bar{C} \Delta\theta = J^{-1} \Gamma U_0, \tag{5.252}$$

where $\Gamma = J A_0 B_0 \bar{C}^{-1}$ is Gruneisen's parameter of (5.218), and $U_0 = \bar{C}\Delta\theta$ is the thermal energy in (5.243). For negligible shape changes, note that $C_{AB} \approx J^{2/3} G_{AB}$ and the first term on the right of (5.248) vanishes, leaving the following equation of state for the hydrostatic pressure:

$$p(J,\theta) = \frac{1}{J^2} \left[\left(B_0 \zeta + B_1 \zeta^2 + \dots \right) + \Gamma J^{-1} U_0 \right], \tag{5.253}$$

which is similar in appearance to the Mie-Gruneisen form given in (5.234).

5.4 Geometrically Linear Elasticity

In geometrically linear elasticity theory, the distinction between reference and current configurations is not made explicit, and the displacement gradient (i.e., distortion) of (3.76) is used as the fundamental kinematic descriptor as opposed to the deformation gradient. In the geometrically linear theory, the analog of (5.1) is

$$u_{a;b} = \beta_{ab}^L, \tag{5.254}$$

with $\mathbf{u}(x,t)$ the displacement and $\boldsymbol{\beta}^{\mathbf{L}}(x,t)$ the lattice distortion. Strains and rotations are, respectively, the symmetric and skew parts of (5.254):

$$\begin{aligned} u_{(a;b)} &= \varepsilon_{ab} = \beta_{(ab)}^L = \varepsilon_{ab}^L, \\ u_{[a;b]} = u_{[a,b]} &= \beta_{[ab]}^L = \Omega_{ab}^L = \Omega_{ab} = -\varepsilon_{abc} w^c, \end{aligned} \tag{5.255}$$

with $\mathbf{w}(x,t)$ the rotation vector of (2.166).

5.4.1 Constitutive Assumptions

Applying (5.254), and prior to consideration of objectivity requirements, appropriate versions of functional dependencies of dependent state variables (4.45)-(4.48) for a hyperelastic material of grade one are

$$\psi = \psi\left(u_{a;b}, \theta, \theta_{,a}, x, \mathbf{g}_a \right), \tag{5.256}$$

$$\eta = \eta\left(u_{a;b}, \theta, \theta_{,a}, x, \mathbf{g}_a\right), \tag{5.257}$$

$$\sigma^{ab} = \sigma^{ab}\left(u_{a;b}, \theta, \theta_{,a}, x, \mathbf{g}_a\right), \tag{5.258}$$

$$q^a = q^a\left(u_{a;b}, \theta, \theta_{,a}, x, \mathbf{g}_a\right). \tag{5.259}$$

Independent variables are displacement gradient, temperature, temperature gradient, position or choice of material particle at x, and basis vectors. The dependence on displacement gradient replaces that of the deformation gradient in Section 5.1.1. Dependence of response functions other than heat flux $\mathbf{q}$ on temperature gradient is written out in (5.256)-(5.259) for completeness, but will be eliminated following thermodynamic considerations in Section 5.4.2. Dependence of response functions on position x (analogous to dependence on X in the nonlinear case) is included to permit description of a heterogeneous body. Dependence on basis vectors $\mathbf{g}_a(x)$ enables description of solids exhibiting an anisotropic response, as explained in Section 5.4.5.

Under superposed small rigid body motions, $\mathbf{x} \to (\mathbf{1} + \hat{\mathbf{\Omega}})\mathbf{x} + \mathbf{c}$, where $\hat{\mathbf{\Omega}}(t) = -\hat{\mathbf{\Omega}}^T$ is a skew rotation matrix and $\mathbf{c}(t)$ is a spatially constant translation vector, to first order the displacement gradient and its skew and symmetric parts transform as

$$u_{a;b} \to u_{a;b} + \hat{\Omega}_{ab}, \ u_{[a,b]} \to u_{[a,b]} + \hat{\Omega}_{ab}, \ \varepsilon_{ab} = u_{(a;b)} \to u_{(a;b)}. \tag{5.260}$$

Thus, the skew part of the displacement gradient (2.254) should not enter the list of independent variables since the response (e.g., thermodynamic potentials) should not be affected by rigid body motions of the frame of observation. The temperature gradient transforms under small rigid body rotations as

$$\theta_{,a} \to (\delta_{,a}^b + \hat{\Omega}_{,a}^b)\theta_{,b} = \theta_{,a} + \hat{\Omega}_{,a}^b\theta_{,b} \approx \theta_{,a}, \tag{5.261}$$

so that dependence of response functions on $\theta_{,a}$ is not considered a violation of objectivity, in contrast to the nonlinear theory of Section 5.1.1. Similarly to (5.261), heat flux $\mathbf{q}$ and stress $\boldsymbol{\sigma}$ remain approximately unchanged when rigid rotations are small. Thus, appropriate analogs of (5.15)-(5.18) in the geometrically linear regime are

$$\psi = \psi\left(\varepsilon_{ab}, \theta, \theta_{,a}, x, \mathbf{g}_a\right), \tag{5.262}$$

$$\eta = \eta\left(\varepsilon_{ab}, \theta, \theta_{,a}, x, \mathbf{g}_a\right), \tag{5.263}$$

$$\sigma^{ab} = \sigma^{ab}\left(\varepsilon_{ab}, \theta, \theta_{,a}, x, \mathbf{g}_a\right), \tag{5.264}$$

$$q^a = q^a\left(\varepsilon_{ab}, \theta, \theta_{,a}, x, \mathbf{g}_a\right). \tag{5.265}$$

5.4.2 Thermodynamics

Using kinematic assumption (5.254) and constitutive assumptions (5.262)-(5.265), dissipation inequality (4.73) becomes

$$\left(\sigma^{ab} - \rho \frac{\partial \psi}{\partial \varepsilon_{ab}} \right) \dot{\varepsilon}_{ab} - \rho \left(\eta + \frac{\partial \psi}{\partial \theta} \right) \dot{\theta} - \rho \frac{\partial \psi}{\partial \theta_{,a}} \gamma_a - \theta^{-1} q^a \theta_{,a} \geq 0 . \quad (5.266)$$

To ensure thermodynamic admissibility, coefficients of $\dot{\boldsymbol{\varepsilon}}$, $\dot{\theta}$, and $\boldsymbol{\gamma}$ must vanish identically in (5.266). This leads to the constitutive relationships

$$\sigma^{ab} = \rho \frac{\partial \psi}{\partial \varepsilon_{ab}}, \quad \eta = -\frac{\partial \psi}{\partial \theta}, \quad \frac{\partial \psi}{\partial \theta_{,a}} = 0 . \quad (5.267)$$

It follows that free energy, entropy, and stress do not depend explicitly on the spatial temperature gradient:

$$\psi = \psi \left(\boldsymbol{\varepsilon}, \theta, x, \mathbf{g}_a \right), \quad \eta = \eta \left(\boldsymbol{\varepsilon}, \theta, x, \mathbf{g}_a \right), \quad \boldsymbol{\sigma} = \boldsymbol{\sigma} \left(\boldsymbol{\varepsilon}, \theta, x, \mathbf{g}_a \right) . \quad (5.268)$$

The entropy production inequality reduces to the conduction inequality in (4.60):

$$\theta \Gamma = \theta \Gamma_C = -\theta^{-1} \theta_{,a} q^a \geq 0 . \quad (5.269)$$

The rate of local entropy production vanishes:

$$\theta \Gamma_L = \rho \theta \dot{\eta} + q^a_{;a} - \rho r = \sigma^{ab} \dot{\varepsilon}_{ab} - \rho \dot{\psi} - \rho \dot{\theta} \eta = 0 . \quad (5.270)$$

Treating the entropy as an independent variable and temperature as a dependent variable, with the internal energy e used as the primary thermodynamic potential gives

$$e = e \left(\boldsymbol{\varepsilon}, \eta, x, \mathbf{g}_a \right), \quad \theta = \theta \left(\boldsymbol{\varepsilon}, \eta, x, \mathbf{g}_a \right), \quad \boldsymbol{\sigma} = \boldsymbol{\sigma} \left(\boldsymbol{\varepsilon}, \eta, x, \mathbf{g}_a \right), \quad (5.271)$$

where the partial Legendre transform

$$e = \theta \left(\boldsymbol{\varepsilon}, \eta, x, \mathbf{g}_a \right) \eta + \psi \left(\boldsymbol{\varepsilon}, \theta, x, \mathbf{g}_a \right) . \quad (5.272)$$

From the second of (5.267) and the chain rule,

$$\rho \frac{\partial e}{\partial \varepsilon_{ab}} = \rho \left(\frac{\partial \psi}{\partial \varepsilon_{ab}} + \frac{\partial \psi}{\partial \theta} \frac{\partial \theta}{\partial \varepsilon_{ab}} + \frac{\partial \theta}{\partial \varepsilon_{ab}} \eta \right) = \rho \frac{\partial \psi}{\partial \varepsilon_{ab}} = \sigma^{ab} . \quad (5.273)$$

When temperature and temperature gradients are held fixed or are omitted from the description, the body is said to be elastic as opposed to thermoelastic. In such a description, let $\theta = \text{constant}$ such that $\dot{\theta} = 0$ and $\theta_{,a} = 0$, and let heat flux $\mathbf{q}$ and heat sources r vanish. The conduction inequality (5.269) is identically zero, and the rate of entropy production becomes

$$\theta \Gamma = \rho \theta \dot{\eta} = 0 . \quad (5.274)$$

Since temperature and entropy are treated constants, there is no need to include them explicitly in the description. Expressions (5.268) for free energy and stress become

$$\psi = \psi(\varepsilon, x, \mathbf{g}_a), \quad \boldsymbol{\sigma} = \boldsymbol{\sigma}(\varepsilon, x, \mathbf{g}_a), \qquad (5.275)$$

and the constitutive equations are given by (5.273). Temperature-independent thermodynamic potential $\psi = \psi(\varepsilon, x, \mathbf{g}_a)$ is then referred to as the strain energy density.

The specific heat capacity per unit mass at constant strain ε is

$$c = \frac{\partial e}{\partial \theta} = \frac{\partial e}{\partial \eta} \frac{\partial \eta}{\partial \theta} = -\frac{\partial e}{\partial \eta} \frac{\partial}{\partial \theta}\left(\frac{\partial \psi}{\partial \theta}\right) = -\theta \frac{\partial^2 \psi}{\partial \theta^2}. \qquad (5.276)$$

Fourier's Law of conduction, as introduced in (4.62), leads to non-negative dissipation:

$$q^a = -k^{ab}\theta_{,b}, \quad -\theta_{,a}q^a = \theta_{,a}k^{ab}\theta_{,b} \geq 0. \qquad (5.277)$$

From (5.270) and (5.277), the local energy balance can be expressed as

$$-\rho\theta \frac{d}{dt}\left(\frac{\partial \psi}{\partial \theta}\right) = \left(k^{ab}\theta_{,b}\right)_{;a} + \rho r. \qquad (5.278)$$

Note that, by the chain rule,

$$-\rho\theta \frac{d}{dt}\left(\frac{\partial \psi}{\partial \theta}\right) = -\rho\theta \frac{\partial}{\partial \theta}\left(\frac{\partial \psi}{\partial \varepsilon_{ab}}\dot{\varepsilon}_{ab} + \frac{\partial \psi}{\partial \theta}\dot{\theta}\right) = \theta\beta^{ab}\dot{\varepsilon}_{ab} + \rho c\dot{\theta}, \qquad (5.279)$$

where $\beta^{ab} = -\rho\partial^2\psi / \partial\theta\partial\varepsilon_{ab}$ accounts for thermoelastic coupling. Equating (5.278) and (5.279) results in

$$\rho c\dot{\theta} = (k^{ab}\theta_{,b})_{;a} - \theta\beta^{ab}\dot{\varepsilon}_{ab} + \rho r. \qquad (5.280)$$

In the absence of heat sources, in a homogeneous isotropic rigid conductor with $k^{ab} = kg^{ab}$, (5.280) becomes the transient heat equation

$$\dot{\theta} = \frac{k}{\rho c}\overset{g}{\nabla}^2\theta = \frac{k}{\rho c}(g^{ab}\theta_{,a})_{;b} = \frac{k}{\rho c}\sqrt[\eta]{g}\left(\sqrt{g}\,g^{ab}\theta_{,a}\right)_{,b}. \qquad (5.281)$$

5.4.3 Materially Nonlinear Hyperelasticity

Differentiation of (5.267) with respect to strain results in the following definition of second-order elastic stiffness coefficients:

$$\mathbb{C}^{abcd}(\varepsilon, \theta, x, \mathbf{g}_a) = \frac{\partial\sigma^{ab}}{\partial\varepsilon_{cd}} = \rho\frac{\partial^2\psi}{\partial\varepsilon_{ab}\partial\varepsilon_{cd}}. \qquad (5.282)$$

From (2.162), finite Lagrangian strain $\mathbf{E}$ and linear strain ε are related by

$$E_{AB} = u_{(a;b)}\left(\delta^a_{.A} + u^a_{.,A}\right)\left(\delta^b_{.B} + u^b_{.,B}\right) - \frac{1}{2}u^c_{;a}u_{c;b}\left(\delta^a_{.A} + u^a_{.,A}\right)\left(\delta^b_{.B} + u^b_{.,B}\right). \qquad (5.283)$$

It follows that

$$
\frac{\partial E_{AB}}{\partial u_{(d;e)}} = \delta_{(A}^{(d}\delta_{B)}^{e)} + \left[\left(u_{(a;b)} - \frac{1}{2}u_{;a}^{c}u_{c;b} \right) \frac{\partial}{\partial u_{(d;e)}} \left(\delta_{.A}^{a}u_{.,B}^{b} + \delta_{.B}^{b}u_{.,A}^{a} + u_{.,A}^{a}u_{.,B}^{b} \right) \right.
$$
$$
\left. - \frac{1}{2}\left(\frac{\partial u_{;a}^{c}}{\partial u_{(d;e)}}u_{c;b} + \frac{\partial u_{c;b}}{\partial u_{(d;e)}}u_{;a}^{c} \right)\left(\delta_{.A}^{a} + u_{.,A}^{a} \right)\left(\delta_{.B}^{b} + u_{.,B}^{b} \right) \right].
$$

(5.284)

Thus, tangent moduli in (5.54) and (5.282) are related, at the same temperature and material point, by

$$
\mathbb{C}^{abcd} = \rho \frac{\partial}{\partial \varepsilon_{ab}}\left(\frac{\partial \psi}{\partial \varepsilon_{cd}} \right) = J^{-1}\rho_0 \frac{\partial}{\partial E_{AB}}\left(\frac{\partial \psi}{\partial E_{CD}} \right) \frac{\partial E_{CD}}{\partial \varepsilon_{cd}} \frac{\partial E_{AB}}{\partial \varepsilon_{ab}}
$$
$$
= \mathbb{C}^{ABCD}\delta_{(A}^{(a}\delta_{.B)}^{b)}\delta_{(C}^{(c}\delta_{.D)}^{d)}\left\{ 1 + \left[o(u_{a;b}) + o(u_{a;b})^2 + o(u_{a;b})^3 + ... \right] \right\},
$$

(5.285)

where terms in square braces correspond to products of those of orders one and higher in displacement gradients in (5.284). The following natural symmetries apply for the linear coefficients:

$$
\mathbb{C}^{abcd} = \mathbb{C}^{(ab)(cd)} = \mathbb{C}^{(cd)(ab)},
$$

(5.286)

meaning that the tangent elastic stiffness contains up to 21 independent entries. Third-order coefficients can be defined in a similar manner:

$$
\mathbb{C}^{abcdef}(\varepsilon,\theta,x,\mathbf{g}_a) = \frac{\partial^2 \sigma^{ab}}{\partial \varepsilon_{cd}\partial \varepsilon_{ef}} = \rho \frac{\partial^3 \psi}{\partial \varepsilon_{ab}\partial \varepsilon_{cd}\partial \varepsilon_{ef}}.
$$

(5.287)

From (5.287), symmetry conditions limit the number of independent third-order coefficients in $\mathbb{C}^{abcdef}$ to 56.

Analogously to (5.62), expanding free energy of the first of (5.268) for a hyperelastic material with thermal effects in a Taylor series about a reference state wherein $u_{a;b} = \varepsilon_{ab} = 0$ and $\theta = \theta_0 > 0$ produces the following result per unit reference volume, where temperature variation $\Delta\theta = \theta - \theta_0$:

$$
\rho_0\psi(\varepsilon_{ab},\theta,x,\mathbf{g}_a) = \bar{\Psi}_0 + \bar{\mathbb{C}}^{ab}\varepsilon_{ab} + \frac{1}{2!}\bar{\mathbb{C}}^{abcd}\varepsilon_{ab}\varepsilon_{cd} + \frac{1}{3!}\bar{\mathbb{C}}^{abcdef}\varepsilon_{ab}\varepsilon_{cd}\varepsilon_{ef}
$$
$$
+ \frac{1}{4!}\bar{\mathbb{C}}^{abcdefgh}\varepsilon_{ab}\varepsilon_{cd}\varepsilon_{ef}\varepsilon_{gh} + ... - \bar{\beta}^{ab}\varepsilon_{ab}\Delta\theta
$$
$$
- \frac{1}{2!}\bar{\beta}^{abcd}\varepsilon_{ab}\varepsilon_{cd}\Delta\theta - \frac{1}{8}\bar{\beta}^{abcdef}\varepsilon_{ab}\varepsilon_{cd}\varepsilon_{ef}\Delta\theta - ...
$$
$$
- \frac{1}{2!}\bar{\beta}'^{ab}\varepsilon_{ab}(\Delta\theta)^2 - \frac{1}{8}\bar{\beta}''^{ab}\varepsilon_{ab}(\Delta\theta)^3 - ...
$$
$$
- \frac{1}{4}\bar{\beta}'^{abcd}\varepsilon_{ab}\varepsilon_{cd}(\Delta\theta)^2 ... + Y_0(\theta,x).
$$

(5.288)

Quantities in (5.288) are defined as

$$\rho_0 \psi\left(0, \theta_0, x, \mathbf{g}_a\right) = \bar{\Psi}_0\left(x\right) + Y_0\left(\theta_0, x\right) = 0 , \tag{5.289}$$

$$\overline{\mathbb{C}}^{ab}\left(x, \mathbf{g}_a\right) = \rho_0 \left.\frac{\partial \psi}{\partial \varepsilon_{ab}}\right|_{\substack{\varepsilon=0 \\ \theta=\theta_0}} = 0 , \tag{5.290}$$

$$\overline{\mathbb{C}}^{abcd}\left(x, \mathbf{g}_a\right) = \rho_0 \left.\frac{\partial^2 \psi}{\partial \varepsilon_{ab} \partial \varepsilon_{cd}}\right|_{\substack{\varepsilon=0 \\ \theta=\theta_0}} , \tag{5.291}$$

$$\overline{\mathbb{C}}^{abcdef}\left(x, \mathbf{g}_a\right) = \rho_0 \left.\frac{\partial^3 \psi}{\partial \varepsilon_{ab} \partial \varepsilon_{cd} \partial \varepsilon_{ef}}\right|_{\substack{\varepsilon=0 \\ \theta=\theta_0}} , \tag{5.292}$$

$$\overline{\mathbb{C}}^{abcdefgh}\left(x, \mathbf{g}_a\right) = \rho_0 \left.\frac{\partial^4 \psi}{\partial \varepsilon_{ab} \partial \varepsilon_{cd} \partial \varepsilon_{ef} \partial \varepsilon_{gh}}\right|_{\substack{\varepsilon=0 \\ \theta=\theta_0}} , \tag{5.293}$$

$$\overline{\beta}^{ab}\left(x, \mathbf{g}_a\right) = -\rho_0 \left.\frac{\partial^2 \psi}{\partial \theta \partial \varepsilon_{ab}}\right|_{\substack{\varepsilon=0 \\ \theta=\theta_0}} , \tag{5.294}$$

$$\overline{\beta}^{abcd}\left(x, \mathbf{g}_a\right) = -\rho_0 \left.\frac{\partial^3 \psi}{\partial \theta \partial \varepsilon_{ab} \partial \varepsilon_{cd}}\right|_{\substack{\varepsilon=0 \\ \theta=\theta_0}} = -\left.\frac{\partial \mathbb{C}^{abcd}}{\partial \theta}\right|_{\substack{\varepsilon=0 \\ \theta=\theta_0}} , \tag{5.295}$$

$$\overline{\beta}^{abcdef}\left(x, \mathbf{g}_a\right) = -\rho_0 \left.\frac{\partial^4 \psi}{\partial \theta \partial \varepsilon_{ab} \partial \varepsilon_{cd} \partial \varepsilon_{ef}}\right|_{\substack{\varepsilon=0 \\ \theta=\theta_0}} = -\left.\frac{\partial \mathbb{C}^{abcdef}}{\partial \theta}\right|_{\substack{\varepsilon=0 \\ \theta=\theta_0}} , \tag{5.296}$$

$$\overline{\beta}'^{ab}\left(x, \mathbf{g}_a\right) = -\rho_0 \left.\frac{\partial^3 \psi}{\partial \theta^2 \partial \varepsilon_{ab}}\right|_{\substack{\varepsilon=0 \\ \theta=\theta_0}} , \tag{5.297}$$

$$\overline{\beta}''^{ab}\left(x, \mathbf{g}_a\right) = -\rho_0 \left.\frac{\partial^4 \psi}{\partial \theta^3 \partial E_{ab}}\right|_{\substack{\varepsilon=0 \\ \theta=\theta_0}} , \tag{5.298}$$

$$\overline{\beta}'^{abcd}\left(x, \mathbf{g}_a\right) = -\rho_0 \left.\frac{\partial^4 \psi}{\partial \theta^2 \partial \varepsilon_{ab} \partial \varepsilon_{cd}}\right|_{\substack{\varepsilon=0 \\ \theta=\theta_0}} = -\left.\frac{\partial^2 \mathbb{C}^{abcd}}{\partial \theta^2}\right|_{\substack{\varepsilon=0 \\ \theta=\theta_0}} . \tag{5.299}$$

Thermal free energy $Y_0(\theta, x)$ can be defined in the same way as $Y_0(\theta, X)$ in Section 5.1.3, noting that x and X refer to the same material particle in the linear theory of the present Section. Definitions (5.289) and (5.290) provide for zero free energy and stress at the reference state. Isothermal elastic constants of orders two, three, and four are defined in (5.291)-

(5.293). Stress-temperature coefficients of various orders are listed in (5.294)-(5.299). Stress-strain-temperature relations become, from (5.267),

$$\sigma^{ab} = \rho \frac{\partial \psi}{\partial \varepsilon_{ab}} = J^{-1} \rho_0 \frac{\partial \psi}{\partial \varepsilon_{ab}}$$

$$= J^{-1} \left[\overline{\mathbb{C}}^{abcd} \varepsilon_{cd} + \frac{1}{2} \overline{\mathbb{C}}^{abcdef} \varepsilon_{cd} \varepsilon_{ef} + \frac{1}{6} \overline{\mathbb{C}}^{abcdefgh} \varepsilon_{cd} \varepsilon_{ef} \varepsilon_{gh} + ... \right.$$

$$- \overline{\beta}^{ab} \Delta \theta - \overline{\beta}^{abcd} \varepsilon_{cd} \Delta \theta - \frac{3}{8} \overline{\beta}^{abcdef} \varepsilon_{cd} \varepsilon_{ef} \Delta \theta - ...$$

$$\left. - \frac{1}{2} \overline{\beta}'^{ab} (\Delta \theta)^2 - \frac{1}{8} \overline{\beta}''^{ab} (\Delta \theta)^3 - ... - \frac{1}{2} \overline{\beta}'^{abcd} \varepsilon_{cd} (\Delta \theta)^2 ... \right]. \tag{5.300}$$

In the geometrically linear theory, terms of orders two and higher in the strain $\boldsymbol{\varepsilon}$ are typically omitted from (5.300) since displacement gradients are assumed small. Such an omission is consistent with the use of infinitesimal strain measure $\boldsymbol{\varepsilon}$ as opposed to finite strain measure $\mathbf{E}$ as a state variable, since $\boldsymbol{\varepsilon}$ differs from $\mathbf{E}$ by terms quadratic in displacement gradients in (2.162). Furthermore, if the distinction between the Kirchhoff stress and Cauchy stress is omitted, then $\tau^{ab} = J\sigma^{ab} \approx \sigma^{ab}$, with σ^{ab} thus used as the exclusive measure of stress in the linear theory, then (5.300) becomes

$$\sigma^{ab} = \overline{\mathbb{C}}^{abcd} \varepsilon_{cd} - \overline{\beta}^{ab} \Delta \theta - \overline{\beta}^{abcd} \varepsilon_{cd} \Delta \theta - \frac{1}{2} \overline{\beta}'^{ab} (\Delta \theta)^2$$

$$- \frac{1}{8} \overline{\beta}''^{ab} (\Delta \theta)^3 - ... - \frac{1}{2} \overline{\beta}'^{abcd} \varepsilon_{cd} (\Delta \theta)^2 .... \tag{5.301}$$

Notice also that at the reference state, from (5.65) and (5.285), second-order elastic constants of nonlinear and linear theories are equal since terms of orders one and higher in displacement gradients vanish from (5.284) and (5.285) at the reference state:

$$\overline{\mathbb{C}}^{abcd} = \left(J\rho \frac{\partial^2 \psi}{\partial \varepsilon_{ab} \partial \varepsilon_{cd}} \right) \Bigg|_{\substack{\boldsymbol{\varepsilon}=0 \\ \theta=\theta_0}} = \rho_0 \frac{\partial^2 \psi}{\partial E_{AB} \partial E_{CD}} \Bigg|_{\substack{\mathbf{E}=0 \\ \theta=\theta_0}} \delta^{(a}_{.(A} \delta^{b)}_{.B)} \delta^{(c}_{.(C} \delta^{d)}_{.D)}$$

$$= \overline{\mathbb{C}}^{ABCD} \delta^{(a}_{.(A} \delta^{b)}_{.B)} \delta^{(c}_{.(C} \delta^{d)}_{.D)}. \tag{5.302}$$

Similarly, thermal stress coefficients in (5.68) and (5.294) are equal at the reference state:

$$\overline{\beta}^{ab} = - \left(J\rho \frac{\partial^2 \psi}{\partial \theta \partial \varepsilon_{ab}} \right) \Bigg|_{\substack{\boldsymbol{\varepsilon}=0 \\ \theta=\theta_0}} = -\rho_0 \frac{\partial^2 \psi}{\partial \theta \partial E_{AB}} \Bigg|_{\substack{\mathbf{E}=0 \\ \theta=\theta_0}} \delta^{(a}_{.(A} \delta^{b)}_{.B)} = \overline{\beta}^{AB} \delta^{(a}_{.(A} \delta^{b)}_{.B)}. \tag{5.303}$$

5.4.4 Materially Linear Hyperelasticity

Omitting terms of orders two and higher in strains and temperature variations, (5.288) becomes

$$\rho_0 \psi = \frac{1}{2} \overline{\mathbb{C}}^{abcd} \varepsilon_{ab} \varepsilon_{cd} - \overline{\beta}^{ab} \varepsilon_{ab} \Delta\theta - \rho_0 \overline{c} \theta \ln \frac{\theta}{\theta_0}, \qquad (5.304)$$

where elastic coefficients $\overline{\mathbb{C}}^{abcd}$, stress-temperature coefficients $\overline{\beta}^{ab}$, and specific heat $\overline{c}$ are defined as second derivatives of the free energy at null strain and reference temperature:

$$\overline{\mathbb{C}}^{abcd} = \rho_0 \left. \frac{\partial^2 \psi}{\partial \varepsilon_{ab} \partial \varepsilon_{cd}} \right|_{\substack{\varepsilon=0 \\ \theta=\theta_0}}, \quad \overline{\beta}^{ab} = -\rho_0 \left. \frac{\partial^2 \psi}{\partial \theta \partial \varepsilon_{ab}} \right|_{\substack{\varepsilon=0 \\ \theta=\theta_0}}, \quad \overline{c} = -\left. \left(\theta \frac{\partial^2 \psi}{\partial \theta^2} \right) \right|_{\substack{\varepsilon=0 \\ \theta=\theta_0}}. \quad (5.305)$$

At a particular material point x, parameters in (5.305) are all constants. The thermal energy comprising the rightmost term in (5.304) depends only on temperature. This term is consistent with a thermal internal energy U_0 measured per unit reference volume depending linearly on temperature:

$$U_0 = \rho_0 \overline{c} \theta \Leftrightarrow \overline{c} = \frac{1}{\rho_0} \frac{\partial U_0}{\partial \theta}. \qquad (5.306)$$

Stress and entropy are, from (5.304) and (5.267)

$$\sigma^{ab} \approx \tau^{ab} = \overline{\mathbb{C}}^{abcd} \varepsilon_{cd} - \overline{\beta}^{ab} \Delta\theta, \qquad (5.307)$$

$$\rho_0 \eta = \overline{\beta}^{ab} \varepsilon_{ab} + \rho_0 \overline{c} \left(\ln \frac{\theta}{\theta_0} + 1 \right). \qquad (5.308)$$

At a fixed reference temperature $\theta = \theta_0$, the requirement that the free energy be positive for all non-negligible strains $\varepsilon^{ab} \neq 0$ implies that the fourth-order tensor $\overline{\mathbb{C}}^{abcd}$ should be positive definite. From (5.304), it follows that at $\theta = \theta_0$, $\rho_0 \psi$ is a strictly convex function of $\boldsymbol{\varepsilon}$.

Stress equation (5.307) applies for any choice of coordinate system, including Cartesian coordinates and general curvilinear coordinates. In physical components of orthogonal curvilinear coordinates (Section 2.4), the stress-strain law exhibits the same form (Malvern 1969):

$$\sigma_{\langle ab \rangle} = \sum_{c,d=1}^{3} \overline{\mathbb{C}}_{\langle abcd \rangle} \varepsilon_{\langle cd \rangle} - \overline{\beta}_{\langle ab \rangle} \Delta\theta, \qquad (5.309)$$

where indices in angled brackets are referred to physical components of orthogonal curvilinear coordinates such as cylindrical coordinates of Section 2.4.2 and Table 4.3 or spherical coordinates of Section 2.4.3 and Table 4.4. Transformation formulae relating quantities in (5.309) to their counterparts in Cartesian coordinates are listed by Malvern (1969).

5.4.5 Symmetry

Analogously to (5.90), matrices of second-order elastic constants and thermal stress constants exhibit the following symmetries:

$$\overline{\mathbb{C}}^{abcd} = \overline{\mathbb{C}}^{cdab} = \overline{\mathbb{C}}^{bacd} = \overline{\mathbb{C}}^{abdc}, \quad \overline{\beta}^{ab} = \overline{\beta}^{ba}, \tag{5.310}$$

meaning that $\overline{\mathbb{C}}^{abcd}$ contains up to 21 independent entries and $\overline{\beta}^{ab}$ contains up to 6 independent entries. Thus (5.307) is often written in reduced matrix form as

$$
\begin{bmatrix} \sigma^{11} \\ \sigma^{22} \\ \sigma^{33} \\ \sigma^{23} \\ \sigma^{31} \\ \sigma^{12} \end{bmatrix}
=
\begin{bmatrix}
\overline{\mathbb{C}}^{11} & \overline{\mathbb{C}}^{12} & \overline{\mathbb{C}}^{13} & \overline{\mathbb{C}}^{14} & \overline{\mathbb{C}}^{15} & \overline{\mathbb{C}}^{16} \\
\overline{\mathbb{C}}^{12} & \overline{\mathbb{C}}^{22} & \overline{\mathbb{C}}^{23} & \overline{\mathbb{C}}^{24} & \overline{\mathbb{C}}^{25} & \overline{\mathbb{C}}^{26} \\
\overline{\mathbb{C}}^{13} & \overline{\mathbb{C}}^{23} & \overline{\mathbb{C}}^{33} & \overline{\mathbb{C}}^{34} & \overline{\mathbb{C}}^{35} & \overline{\mathbb{C}}^{36} \\
\overline{\mathbb{C}}^{14} & \overline{\mathbb{C}}^{24} & \overline{\mathbb{C}}^{34} & \overline{\mathbb{C}}^{44} & \overline{\mathbb{C}}^{45} & \overline{\mathbb{C}}^{46} \\
\overline{\mathbb{C}}^{15} & \overline{\mathbb{C}}^{25} & \overline{\mathbb{C}}^{35} & \overline{\mathbb{C}}^{45} & \overline{\mathbb{C}}^{55} & \overline{\mathbb{C}}^{56} \\
\overline{\mathbb{C}}^{16} & \overline{\mathbb{C}}^{26} & \overline{\mathbb{C}}^{36} & \overline{\mathbb{C}}^{46} & \overline{\mathbb{C}}^{56} & \overline{\mathbb{C}}^{66}
\end{bmatrix}
\begin{bmatrix} \varepsilon_{11} \\ \varepsilon_{22} \\ \varepsilon_{33} \\ 2\varepsilon_{23} \\ 2\varepsilon_{31} \\ 2\varepsilon_{12} \end{bmatrix}
-
\begin{bmatrix} \overline{\beta}^{11} \\ \overline{\beta}^{22} \\ \overline{\beta}^{33} \\ \overline{\beta}^{23} \\ \overline{\beta}^{31} \\ \overline{\beta}^{12} \end{bmatrix}
\Delta\theta, \tag{5.311}
$$

where components of the symmetric 6×6 matrix of second-order elastic constants are identical to those in (5.92):

$$
\begin{bmatrix}
\overline{\mathbb{C}}^{11} = \overline{\mathbb{C}}^{1111} & - & - & - & - & - \\
\overline{\mathbb{C}}^{12} = \overline{\mathbb{C}}^{1122} & \overline{\mathbb{C}}^{22} = \overline{\mathbb{C}}^{2222} & - & - & - & - \\
\overline{\mathbb{C}}^{13} = \overline{\mathbb{C}}^{1133} & \overline{\mathbb{C}}^{23} = \overline{\mathbb{C}}^{2233} & \overline{\mathbb{C}}^{33} = \overline{\mathbb{C}}^{3333} & - & - & - \\
\overline{\mathbb{C}}^{14} = \overline{\mathbb{C}}^{1123} & \overline{\mathbb{C}}^{24} = \overline{\mathbb{C}}^{2223} & \overline{\mathbb{C}}^{34} = \overline{\mathbb{C}}^{3323} & \overline{\mathbb{C}}^{44} = \overline{\mathbb{C}}^{2323} & - & - \\
\overline{\mathbb{C}}^{15} = \overline{\mathbb{C}}^{1113} & \overline{\mathbb{C}}^{25} = \overline{\mathbb{C}}^{2213} & \overline{\mathbb{C}}^{35} = \overline{\mathbb{C}}^{3313} & \overline{\mathbb{C}}^{45} = \overline{\mathbb{C}}^{2313} & \overline{\mathbb{C}}^{55} = \overline{\mathbb{C}}^{1313} & - \\
\overline{\mathbb{C}}^{16} = \overline{\mathbb{C}}^{1112} & \overline{\mathbb{C}}^{26} = \overline{\mathbb{C}}^{2212} & \overline{\mathbb{C}}^{36} = \overline{\mathbb{C}}^{3312} & \overline{\mathbb{C}}^{46} = \overline{\mathbb{C}}^{2312} & \overline{\mathbb{C}}^{56} = \overline{\mathbb{C}}^{1312} & \overline{\mathbb{C}}^{66} = \overline{\mathbb{C}}^{1212}
\end{bmatrix}
. \tag{5.312}
$$

Voigt's notation in (5.93)-(5.98) applies. Components of the stress and moduli are written in reduced form to take advantage of symmetries:

$$\sigma^{(ab)} \sim \sigma^{\overline{a}}, \quad \overline{\mathbb{C}}^{(ab)(cd)} \sim \overline{\mathbb{C}}^{\overline{a}\overline{b}}, \quad \overline{\beta}^{ab} \sim \overline{\beta}^{\overline{a}}. \tag{5.313}$$

Barred indices span 1,2,…6 and correspond to unbarred pairs of indices as noted in (5.93). Consistent with (5.311) and (5.313), strains in Voigt's notation satisfy

$$2\varepsilon_{(ab)} = (1 + \delta_{ab})\varepsilon_{\overline{a}}. \tag{5.314}$$

As a consequence of hyperelasticity, second-order elastic constants exhibit the remaining symmetries

$$\overline{\mathbb{C}}^{\overline{a}\overline{b}} = \overline{\mathbb{C}}^{(\overline{a}\overline{b})}. \tag{5.315}$$

Free energy in the materially linear case, (5.304), is

$$\rho_0 \psi = \frac{1}{2} \overline{\mathbb{C}}^{\overline{a}\overline{b}} \varepsilon_{\overline{a}} \varepsilon_{\overline{b}} - \overline{\beta}^{\overline{a}} \varepsilon_{\overline{a}} \Delta\theta - \rho_0 \overline{c}\theta \ln\frac{\theta}{\theta_0}, \tag{5.316}$$

and the stress of (5.307) is written compactly as

$$\sigma^{\overline{a}} = \overline{\mathbb{C}}^{\overline{a}\overline{b}} \varepsilon_{\overline{b}} - \overline{\beta}^{\overline{a}} \Delta\theta. \tag{5.317}$$

Arguments pertaining to transformations of material coefficients under rotations of the coordinate system in (5.99)-(5.104) apply likewise in the geometrically linear theory. Furthermore, since (5.302) and (5.303) indicate that elastic constants and thermal stress coefficients measured at the reference state in linear and nonlinear theories are equal, these particular material coefficients share the same symmetries in linear and nonlinear theories. Since in a rigid heat conductor, the reference and current configurations coincide, it follows that conductivity coefficients in the linear theory, k^{ab} of (5.277), are related to those of the nonlinear theory, K^{AB} in (5.48), at material point X in the undeformed reference state by

$$k^{ab}\Big|_{\substack{\varepsilon=0 \\ \theta=\theta_0}} = \delta_{.A}^{a}\delta_{.B}^{b} K^{AB}\Big|_{\substack{E=0 \\ \theta=\theta_0}} . \tag{5.318}$$

Thus, thermal conductivities in linear and nonlinear descriptions should exhibit the same symmetries when evaluated at the same reference state.

Now consider a geometrically linear and materially linear, isotropic hyperelastic solid. Second-order elastic constants in (5.310) become

$$\overline{\mathbb{C}}^{abcd} = \mu(g^{ac}g^{bd} + g^{ad}g^{cb}) + \lambda g^{ab}g^{cd}, \tag{5.319}$$

with $\mu(x)$ the shear modulus and $\lambda(x)$ Lamé's constant. Thus, the elasticity tensor in 6×6 matrix form is identical to that of (5.122). Thermal stress coefficients for an isotropic material are

$$\overline{\beta}^{ab} = \overline{\beta}g^{ab} . \tag{5.320}$$

Stress-strain-temperature relations then exhibit the form

$$\sigma^{ab} = 2\mu\varepsilon^{ab} + (\lambda\varepsilon_{.c}^{c} - \overline{\beta}\Delta\theta)g^{ab} . \tag{5.321}$$

Local balance of linear momentum (4.17), per unit spatial volume, is

$$\sigma_{;b}^{ab} = (2\mu\varepsilon^{ab})_{;b} + (\lambda\varepsilon_{.c}^{c} - \overline{\beta}\Delta\theta)_{;b}g^{ab} = \rho\ddot{u}^{a} - \overline{b}^{a} . \tag{5.322}$$

Under isothermal conditions ($\Delta\theta = 0$) and when elastic constants are independent of position (i.e., a homogeneous body), (5.322) reduces to

$$2\mu\varepsilon_{;b}^{ab} + \lambda\varepsilon_{.c;b}^{c}g^{ab} = \rho\ddot{u}^{a} - \overline{b}^{a} . \tag{5.323}$$

In rectangular Cartesian coordinates, the covariant derivatives become partial derivatives. In general curvilinear coordinates, (5.323) is cumbersome. Tables 5.1 and 5.2 list (5.323) in physical components of cylindrical coordinates (see Section 2.4.2 and Table 4.3) and spherical coordinates (see Section 2.4.3 and Table 4.4), following Malvern (1969).

Table 5.1 Momentum balance of linear isotropic elasticity: cylindrical coordinates

Quantity	R-component	θ–component	Z-component
Momentum	$(2\mu+\lambda)e_{,R}-2\mu R^{-1}w_{Z,\theta}$	$(2\mu+\lambda)R^{-1}e_{,\theta}-2\mu w_{R,Z}$	$(2\mu+\lambda)e_{,Z}-2\mu R^{-1}(rw_\theta)_{,R}$
	$+2\mu w_{\theta,Z}=\rho a_R-\bar{b}_R$	$+2\mu w_{Z,R}=\rho a_\theta-\bar{b}_\theta$	$+2\mu R^{-1}w_{R,\theta}=\rho a_Z-\bar{b}_Z$
Rotation	$2w_R=R^{-1}u_{Z,\theta}-u_{\theta,Z}$	$2w_\theta=u_{R,Z}-u_{Z,R}$	$2w_Z=R^{-1}[(Ru_\theta)_{,R}-u_{R,\theta}]$
Dilatation	$e=R^{-1}[(Ru_R)_{,R}+u_{\theta,\theta}]+u_{Z,Z}$		

Table 5.2 Momentum balance of linear isotropic elasticity: spherical coordinates

Quantity	R-component	θ–component	φ-component
Momentum	$(2\mu+\lambda)e_{,R}$	$(2\mu+\lambda)R^{-1}e_{,\theta}$	$(2\mu+\lambda)e_{,\varphi}R^{-1}\sin^{-1}\theta$
	$-2\mu R^{-1}\sin^{-1}\theta\times$	$+2\mu R^{-1}\sin^{-1}\theta\times$	$-2\mu R^{-1}[(Rw_\theta)_{,R}-w_{R,\theta}]$
	$[(w_\varphi\sin\theta)_{,\theta}-w_{\theta,\varphi}]$	$[(Rw_\varphi\sin\theta)_{,R}-w_{R,\varphi}]$	$=\rho a_\varphi-\bar{b}_\varphi$
	$=\rho a_R-\bar{b}_R$	$=\rho a_\theta-\bar{b}_\theta$	
Rotation	$2w_R=R^{-1}\sin^{-1}\theta$	$2w_\theta=R^{-1}[u_{R,\varphi}\sin^{-1}\theta$	$2w_\varphi=R^{-1}[(Ru_\theta)_{,R}-u_{R,\theta}]$
	$\times[(u_\varphi\sin\theta)_{,\theta}-u_{\theta,\varphi}]$	$-(Ru_\varphi)_{,R}]$	
Dilatation	$e=R^{-2}\sin^{-1}\theta[(R^2u_R\sin\theta)_{,R}+(Ru_\theta\sin\theta)_{,\theta}+(Ru_\varphi)_{,\varphi}]$		

5.5 Explicitly Resolved Thermal Deformation

An alternative formulation of finite hyperelasticity with temperature changes addresses the kinematics of deformation in a more refined or explicit manner (Stojanovitch 1969; Lu and Pister 1975; Imam and Johnson 1998; Clayton 2005a, b, 2006a) that proves useful in certain experimental and computational settings. Extending (5.1), the total deformation gradient and lattice deformation gradient remain equivalent, but each is further decomposed into mechanically recoverable elastic and thermal parts, following (3.27):

$$\mathbf{F}=\mathbf{F}^{\mathbf{L}}=\mathbf{F}^{\mathbf{E}}\mathbf{F}^{\boldsymbol{\theta}}, \tag{5.324}$$

$$F^a_{.A}=x^a_{,A}=F^{La}_{.\alpha}g^\alpha_{.A}=F^{Ea}_{.B}F^{\theta B}_{.A}=F^{Ea}_{.B}g^B_{.\alpha}F^{\theta\alpha}_{.A}=F^{Ea}_{.\alpha}F^{\theta\alpha}_{.A}, \tag{5.325}$$

where $\mathbf{F}^{\mathbf{E}}$ is associated with purely mechanical loads, and where $\mathbf{F}^{\boldsymbol{\theta}}$ is the deformation attributed solely to temperature changes in the absence of mechanical forces. The form after the final equality in (5.325) is introduced for convenience in keeping track of indices during manipulation of the thermodynamic relations later in Section 5.5.2, even though all indices of $\mathbf{F}^{\boldsymbol{\theta}}$ are referred to reference coordinates, meaning $g^\alpha_{.A}=\delta^\alpha_{.A}$. Though alternative prescriptions are possible (see the footnote in Section 3.1.3), evolution of $\mathbf{F}^{\boldsymbol{\theta}}$ is assumed to follow (3.28):

$$\dot{\mathbf{F}}^{\boldsymbol{\theta}}\mathbf{F}^{\boldsymbol{\theta}-1} = \boldsymbol{\alpha}_{\mathbf{T}}\dot{\theta}, \quad \dot{F}^{\theta\alpha}_{.A}F^{\theta-1A}_{.\beta} = \alpha^{\alpha}_{T.\beta}\dot{\theta} = \alpha^{A}_{T.B}g^{\alpha}_{.A}g^{B}_{.\beta}\dot{\theta}, \quad (5.326)$$

where $\boldsymbol{\alpha}_{\mathbf{T}}(\theta, X, \mathbf{G}_A)$ is a symmetric second-order tensor of thermal expansion coefficients that, by definition, may depend on temperature θ, location X of material particle (for a heterogeneous solid), and material symmetry via dependence on reference basis vectors $\mathbf{G}_A(X)$. Thermal expansion coefficients in (5.326) are assumed to possess material symmetries of generic symmetric rank two polar tensors listed in Table A.5. The form of (5.325) applicable for cubic crystals, i.e., $\alpha^{\alpha}_{T.\beta} = \alpha_T\delta^{\alpha}_{.\beta}$, has been used for computational modeling of thermoelastic-plastic behavior of cubic metals deformed at high strain rates (Lee et al. 1997; Clayton 2005a, b, 2006a; Vogler and Clayton 2008).

5.5.1 Constitutive Assumptions

In the context of (5.324), constitutive assumptions (5.2)-(5.5) are replaced by the following, meaning that the state of the material at point X is determined by the elastic deformation, temperature, and temperature gradient:

$$\psi = \psi\left(\mathbf{F}^{\mathbf{E}}, \theta, \overset{\mathbf{g}}{\nabla}\theta, X, \mathbf{G}_A\right), \quad \psi = \psi\left(F^{Ea}_{.\alpha}, \theta, \theta_{,a}, X, \mathbf{G}_A\right); \quad (5.327)$$

$$\eta = \eta\left(\mathbf{F}^{\mathbf{E}}, \theta, \overset{\mathbf{g}}{\nabla}\theta, X, \mathbf{G}_A\right), \quad \eta = \eta\left(F^{Ea}_{.\alpha}, \theta, \theta_{,a}, X, \mathbf{G}_A\right); \quad (5.328)$$

$$\boldsymbol{\sigma} = \boldsymbol{\sigma}\left(\mathbf{F}^{\mathbf{E}}, \theta, \overset{\mathbf{g}}{\nabla}\theta, X, \mathbf{G}_A\right), \quad \sigma^{ab} = \sigma^{ab}\left(F^{Ea}_{.\alpha}, \theta, \theta_{,a}, X, \mathbf{G}_A\right); \quad (5.329)$$

$$\mathbf{q} = \mathbf{q}\left(\mathbf{F}^{\mathbf{E}}, \theta, \overset{\mathbf{g}}{\nabla}\theta, X, \mathbf{G}_A\right), \quad q^a = q^a\left(F^{Ea}_{.\alpha}, \theta, \theta_{,a}, X, \mathbf{G}_A\right). \quad (5.330)$$

Like (5.2)-(5.5), relations (5.327)-(5.330) are not always objective under a rigid body transformation of spatial coordinates. Let such a transformation be described by $\mathbf{x} \to \hat{\mathbf{Q}}\mathbf{x} + \mathbf{c}$, where $\hat{\mathbf{Q}} = \hat{\mathbf{Q}}^{-T}$. Then the elastic deformation is assumed to transform in the same manner as the total deformation gradient, i.e., $\mathbf{F}^{\mathbf{E}} \to \hat{\mathbf{Q}}\mathbf{F}^{\mathbf{E}}$. The recoverable (symmetric) elastic deformation tensor $\mathbf{C}^{\mathbf{E}}$ and strain tensor $\mathbf{E}^{\mathbf{E}}$, defined in covariant form by

$$C^{E}_{\alpha\beta} = F^{Ea}_{.\alpha}g_{ab}F^{Eb}_{.\beta}, \quad E^{E}_{\alpha\beta} = \frac{1}{2}(C^{E}_{\alpha\beta} - \tilde{g}_{\alpha\beta}), \quad (5.331)$$

thus remain invariant under such rigid body motions, following the same analysis procedure considered in (4.50). Hence, a possible set of objective constitutive assumptions is

$$\psi = \psi\left(\mathbf{E^E}, \theta, \overset{G}{\nabla}\theta, X, \mathbf{G}_A\right) , \ \psi = \psi\left(E^E_{\alpha\beta}, \theta, \theta_{,A}, X, \mathbf{G}_A\right); \qquad (5.332)$$

$$\eta = \eta\left(\mathbf{E^E}, \theta, \overset{G}{\nabla}\theta, X, \mathbf{G}_A\right), \ \eta = \eta\left(E^E_{\alpha\beta}, \theta, \theta_{,A}, X, \mathbf{G}_A\right); \qquad (5.333)$$

$$\overline{\mathbf{\Sigma}} = \overline{\mathbf{\Sigma}}\left(\mathbf{E^E}, \theta, \overset{G}{\nabla}\theta, X, \mathbf{G}_A\right), \ \overline{\Sigma}^{\alpha\beta} = \overline{\Sigma}^{\alpha\beta}\left(E^E_{\alpha\beta}, \theta, \theta_{,A}, X, \mathbf{G}_A\right); \quad (5.334)$$

$$\mathbf{Q} = \mathbf{Q}\left(\mathbf{E^E}, \theta, \overset{G}{\nabla}\theta, X, \mathbf{G}_A\right), \ Q^A = Q^A\left(E^E_{\alpha\beta}, \theta, \theta_{,A}, X, \mathbf{G}_A\right); \qquad (5.335)$$

immediately recognizable as (5.15)-(5.18) with the total strain $\mathbf{E}$ replaced by the elastic strain $\mathbf{E^E}$ and the second Piola-Kirchhoff stress replaced by

$$\overline{\Sigma}^{\alpha\beta} = J^E F^{E-1\alpha}_{.a} \sigma^{ab} F^{E-1\beta}_{.b}, \qquad (5.336)$$

where $J^E = \sqrt{g/\tilde{g}} \det \mathbf{F^E}$. The stress in (5.336), referred to as an elastic second Piola-Kirchhoff stress or simply an elastic stress, is symmetric and is invariant under rigid body motions of the spatial coordinate frame:

$$\overline{\Sigma}^{\alpha\beta} \to J^{E-1} F^{E-1\alpha}_{.a} \hat{Q}^{-1a}_{.c} \hat{Q}^c_{.e} \sigma^{ef} \hat{Q}^d_{.f} \hat{Q}^{-1b}_{.d} F^{E-1\beta}_{.b} = J^{E-1} F^{E-1\alpha}_{.a} \sigma^{ef} F^{E-1\beta}_{.f}. \quad (5.337)$$

As a result of different constitutive assumptions used in (5.332)-(5.335), thermodynamic and thermostatic relationships derived in Sections 5.1-5.4 generally do not apply when thermal deformation is non-negligible.

5.5.2 Thermodynamics

From (5.324) and (5.326), spatial velocity gradient $\mathbf{L}$ of (2.176) is

$$L^a_{.b} = v^a_{;b} = \dot{F}^a_{.A} F^{-1A}_{.b} = \dot{F}^{Ea}_{.\alpha} F^{E-1\alpha}_{.b} + F^{Ea}_{.\alpha} \alpha^\alpha_{T.\beta} F^{E-1\beta}_{.b} \dot{\theta}. \qquad (5.338)$$

The material time derivative of the elastic strain tensor is computed directly from (5.331), leading to a relationship similar to (3.64):

$$2\dot{E}^E_{\alpha\beta} = \dot{F}^{Ea}_{.\alpha} g_{ab} F^{Eb}_{.\beta} + F^{Ea}_{.\alpha} g_{ab} \dot{F}^{Eb}_{.\beta} = 2F^{Ea}_{.\alpha} D^E_{ab} F^{Eb}_{.\beta}, \qquad (5.339)$$

with the symmetric rate of elastic deformation referred to the spatial frame

$$2D^E_{ab} = g_{ac} \dot{F}^{Ec}_{.\alpha} F^{E-1\alpha}_{.b} + g_{bc} \dot{F}^{Ec}_{.\alpha} F^{E-1\alpha}_{.a} = 2D^E_{(ab)}. \qquad (5.340)$$

Stress power per unit reference volume entering (4.39) can then be written as follows, using symmetry of the Cauchy stress:

$$\Sigma^{AB} \dot{E}_{AB} = J\sigma^{ab} L_{ab} = J\sigma^{ab}(D^E_{ab} + g_{ac} F^{Ec}_{.\alpha} \alpha^\alpha_{T.\beta} F^{E-1\beta}_{.b} \dot{\theta})$$
$$= J\sigma^{ab}(F^{E-1\alpha}_{.a} \dot{E}^E_{\alpha\beta} F^{E-1\beta}_{.b} + g_{ac} F^{Ec}_{.\alpha} \alpha^\alpha_{T.\beta} F^{E-1\beta}_{.b} \dot{\theta}). \qquad (5.341)$$

Using constitutive assumption (5.332) along with (5.339), the appropriate version of dissipation inequality (4.72) is

$$\left(JF^{E-1\alpha}_{.a}\sigma^{ab}F^{E-1\beta}_{.b} - \rho_0\frac{\partial\psi}{\partial E^E_{\alpha\beta}} \right)\dot{E}^E_{\alpha\beta}$$

$$-\rho_0\left(\eta + \frac{\partial\psi}{\partial\theta} - J\rho_0^{-1}\sigma^{ab}g_{ac}F^{Ec}_{.a}\alpha^{\alpha}_{T.\beta}F^{E-1\beta}_{.b} \right)\dot{\theta} \qquad (5.342)$$

$$-\rho_0\frac{\partial\psi}{\partial\theta_{,A}}\gamma_{0A} - \theta^{-1}\theta_{,A}Q^A \geq 0,$$

where the referential rate of temperature gradient γ_{0A} is defined in (5.29). Appealing to arguments analogous to those immediately following (5.22) regarding thermodynamic admissibility, the following constitutive equations for the Cauchy stress tensor, the elastic stress measure (5.336), and the specific entropy emerge:

$$\sigma^{ab} = \rho F^{Ea}_{.\alpha}\frac{\partial\psi}{\partial E^E_{\alpha\beta}}F^{Eb}_{.\beta}, \qquad (5.343)$$

$$\overline{\Sigma}^{\alpha\beta} = J^E\rho\frac{\partial\psi}{\partial E^E_{\alpha\beta}}, \qquad (5.344)$$

$$\eta = -\frac{\partial\psi}{\partial\theta} + \rho_0^{-1}J\sigma^{ab}g_{ac}F^{Ec}_{.\alpha}\alpha^{\alpha}_{T.\beta}F^{E-1\beta}_{.b}$$

$$= -\frac{\partial\psi}{\partial\theta} + C^E_{\alpha\chi}\alpha^{\alpha}_{T.\beta}\frac{\partial\psi}{\partial E^E_{\chi\beta}} = -\frac{\partial\psi}{\partial\theta} + \varsigma. \qquad (5.345)$$

Scalar quantity $\varsigma(\mathbf{E}^E,\theta,X)$, with dimensions of entropy per unit mass, does not emerge in the classical theory of thermoelasticity of Section 5.1. For the case of isotropic thermal expansion $\alpha^{\alpha}_{T.\beta} = \alpha_T\delta^{\alpha}_{.\beta}$, this term reduces to $\varsigma = -3\alpha_T p/\rho$, where p is the Cauchy pressure (Clayton 2005a). From (5.340)-(5.342), $\partial\psi/\partial\theta_{,A} = 0$, and the response functions reduce to

$$\psi = \psi\left(\mathbf{E}^E,\theta,X,\mathbf{G}_A\right), \ \eta = \eta\left(\mathbf{E}^E,\theta,X,\mathbf{G}_A\right), \ \overline{\Sigma} = \overline{\Sigma}\left(\mathbf{E}^E,\theta,X,\mathbf{G}_A\right). \ (5.346)$$

The conduction inequality remains identical to that of (5.32):

$$-\theta^{-1}\theta_{,A}Q^A \geq 0, \qquad (5.347)$$

and the local rate of entropy production vanishes as in (5.33).

The specific heat capacity per unit mass at constant elastic strain is defined similarly, but not identically, to that in (5.46):

$$c = \frac{\partial e}{\partial\eta}\bigg|_{\varsigma=0}\frac{\partial\eta}{\partial\theta} = -\theta\frac{\partial}{\partial\theta}\left(\frac{\partial\psi}{\partial\theta} - \varsigma \right) = -\theta\frac{\partial^2\psi}{\partial\theta^2} + \theta\frac{\partial\varsigma}{\partial\theta}, \qquad (5.348)$$

following the definition of the free energy $\psi = e - \theta \eta$ in Table 4.2 which still applies in the present context. Using Fourier's law (5.48), energy balance (4.39) reduces to

$$\rho_0 \theta \dot{\eta} = (K^{AB} \theta_{,B})_{;A} + \rho_0 r . \tag{5.349}$$

By the chain rule, (5.332), and (5.348),

$$\rho_0 \theta \dot{\eta} = \rho_0 \theta \frac{d}{dt}\left(\varsigma - \frac{\partial \psi}{\partial \theta} \right)$$

$$= \rho_0 \theta \dot{\varsigma} - \rho_0 \theta \frac{\partial}{\partial \theta}\left(\frac{\partial \psi}{\partial E_{\alpha\beta}^E} \dot{E}_{\alpha\beta}^E + \frac{\partial \psi}{\partial \theta} \dot{\theta} \right)$$

$$= \rho_0 \theta \dot{\varsigma} + \theta \beta^{\alpha\beta} \dot{E}_{\alpha\beta}^E - \rho_0 \theta \frac{\partial^2 \psi}{\partial \theta^2} \dot{\theta} \tag{5.350}$$

$$= \rho_0 c \dot{\theta} + \theta \beta^{\alpha\beta} \dot{E}_{\alpha\beta}^E - \rho_0 \theta \frac{\partial \varsigma}{\partial \theta} \dot{\theta} + \rho_0 \theta \dot{\varsigma}$$

$$= \rho_0 c \dot{\theta} + \theta \left(\beta^{\alpha\beta} + \rho_0 \frac{\partial \varsigma}{\partial E_{\alpha\beta}^E} \right) \dot{E}_{\alpha\beta}^E ,$$

where symmetric contravariant tensor $\beta^{\alpha\beta} = -\rho_0 \partial^2 \psi / \partial \theta \partial E_{\alpha\beta}^E$ accounts for thermoelastic coupling. Equating (5.349) and (5.350) results in a rate equation for the temperature analogous to (5.51):

$$\rho_0 c \dot{\theta} = (K^{AB} \theta_{,B})_{;A} - \theta \hat{\beta}^{\alpha\beta} \dot{E}_{\alpha\beta}^E + \rho_0 r , \tag{5.351}$$

where the modified thermal stress coefficients[4] are defined according to

$$\hat{\beta}^{\alpha\beta} = \rho_0 \frac{\partial \varsigma}{\partial E_{\alpha\beta}^E} + \beta^{\alpha\beta} = \rho_0 \left(\frac{\partial \varsigma}{\partial E_{\alpha\beta}^E} - \frac{\partial^2 \psi}{\partial \theta \partial E_{\alpha\beta}^E} \right). \tag{5.352}$$

5.5.3 Representative Free Energy

An apparent advantage of the present formulation (Section 5.5) over classical nonlinear thermoelasticity (Section 5.1) is that in the former, deformations and deformation rates attributed to temperature rise can easily be delineated from those due to mechanical stresses. The free energy in the first of (5.346) is expanded in a Taylor series about a reference state characterized by the conditions $F^{Ea}_{.\alpha} = g^a_{.\alpha}$, $E^E_{\alpha\beta} = 0$, $\theta = \theta_0 > 0$ as follows:

---

[4] In prior work (Clayton 2005a, b; Vogler and Clayton 2008) the distinction between thermal stress coefficients was omitted, i.e., it was assumed $\beta^{\alpha\beta} = \hat{\beta}^{\alpha\beta}$.

$$\Psi_0 = \rho_0 \psi\left(E_{\alpha\beta}^E, \theta, X, \mathbf{G}_A\right)$$

$$= \bar{\Psi}_0 + \overline{\mathbb{C}}^{\alpha\beta} E_{\alpha\beta}^E + \frac{1}{2!}\overline{\mathbb{C}}^{\alpha\beta\chi\delta} E_{\alpha\beta}^E E_{\chi\delta}^E + \frac{1}{3!}\overline{\mathbb{C}}^{\alpha\beta\chi\delta\varepsilon\phi} E_{\alpha\beta}^E E_{\chi\delta}^E E_{\varepsilon\phi}^E$$

$$+ \frac{1}{4!}\overline{\mathbb{C}}^{\alpha\beta\chi\delta\varepsilon\phi\gamma} E_{\alpha\beta}^E E_{\chi\delta}^E E_{\varepsilon\phi}^E E_{\varphi\gamma}^E + ... - \bar{\beta}^{\alpha\beta} E_{\alpha\beta}^E \Delta\theta$$

$$- \frac{1}{2!}\bar{\beta}^{\alpha\beta\chi\delta} E_{\alpha\beta}^E E_{\chi\delta}^E \Delta\theta - \frac{1}{8}\bar{\beta}^{\alpha\beta\chi\delta\varepsilon\phi} E_{\alpha\beta}^E E_{\chi\delta}^E E_{\varepsilon\phi}^E \Delta\theta - ... \qquad (5.353)$$

$$- \frac{1}{2!}\bar{\beta}'^{\alpha\beta} E_{\alpha\beta}^E (\Delta\theta)^2 - \frac{1}{8}\bar{\beta}''^{\alpha\beta} E_{\alpha\beta}^E (\Delta\theta)^3 - ...$$

$$- \frac{1}{4}\bar{\beta}'^{\alpha\beta\chi\delta} E_{\alpha\beta}^E E_{\chi\delta}^E (\Delta\theta)^2 ... + Y_0\left(\theta, X\right).$$

The temperature change from the reference state is $\Delta\theta = \theta - \theta_0$. Material properties in (5.353) are defined as follows:

$$\Psi_0\left(0, \theta_0, X, \mathbf{G}_A\right) = \bar{\Psi}_0\left(X\right) + Y_0\left(\theta_0, X\right) = 0, \qquad (5.354)$$

$$\overline{\mathbb{C}}^{\alpha\beta}\left(X, \mathbf{G}_A\right) = \left.\frac{\partial \Psi_0}{\partial E_{\alpha\beta}^E}\right|_{\substack{\mathbf{E}^{\mathbf{E}}=0 \\ \theta=\theta_0}} = 0, \qquad (5.355)$$

$$\overline{\mathbb{C}}^{\alpha\beta\chi\delta}\left(X, \mathbf{G}_A\right) = \left.\frac{\partial^2 \Psi_0}{\partial E_{\alpha\beta}^E \partial E_{\chi\delta}^E}\right|_{\substack{\mathbf{E}^{\mathbf{E}}=0 \\ \theta=\theta_0}}, \qquad (5.356)$$

$$\overline{\mathbb{C}}^{\alpha\beta\chi\delta\varepsilon\phi}\left(X, \mathbf{G}_A\right) = \left.\frac{\partial^3 \Psi_0}{\partial E_{\alpha\beta}^E \partial E_{\chi\delta}^E \partial E_{\varepsilon\phi}^E}\right|_{\substack{\mathbf{E}^{\mathbf{E}}=0 \\ \theta=\theta_0}}, \qquad (5.357)$$

$$\overline{\mathbb{C}}^{\alpha\beta\chi\delta\varepsilon\phi\gamma}\left(X, \mathbf{G}_A\right) = \left.\frac{\partial^4 \Psi_0}{\partial E_{\alpha\beta}^E \partial E_{\chi\delta}^E \partial E_{\varepsilon\phi}^E \partial E_{\varphi\gamma}^E}\right|_{\substack{\mathbf{E}^{\mathbf{E}}=0 \\ \theta=\theta_0}}, \qquad (5.358)$$

$$\bar{\beta}^{\alpha\beta}\left(X, \mathbf{G}_A\right) = -\left.\frac{\partial^2 \Psi_0}{\partial\theta\partial E_{\alpha\beta}^E}\right|_{\substack{\mathbf{E}^{\mathbf{E}}=0 \\ \theta=\theta_0}}, \qquad (5.359)$$

$$\bar{\beta}^{\alpha\beta\chi\delta}\left(X, \mathbf{G}_A\right) = -\left.\frac{\partial^3 \Psi_0}{\partial\theta\partial E_{\alpha\beta}^E \partial E_{\chi\delta}^E}\right|_{\substack{\mathbf{E}^{\mathbf{E}}=0 \\ \theta=\theta_0}} = -\left.\frac{\partial\mathbb{C}^{\alpha\beta\chi\delta}}{\partial\theta}\right|_{\substack{\mathbf{E}^{\mathbf{E}}=0 \\ \theta=\theta_0}}, \qquad (5.360)$$

$$\bar{\beta}^{\alpha\beta\chi\delta\varepsilon\phi}\left(X, \mathbf{G}_A\right) = -\left.\frac{\partial^4 \Psi_0}{\partial\theta\partial E_{\alpha\beta}^E \partial E_{\chi\delta}^E \partial E_{\varepsilon\phi}^E}\right|_{\substack{\mathbf{E}^{\mathbf{E}}=0 \\ \theta=\theta_0}} = -\left.\frac{\partial\mathbb{C}^{\alpha\beta\chi\delta\varepsilon\phi}}{\partial\theta}\right|_{\substack{\mathbf{E}^{\mathbf{E}}=0 \\ \theta=\theta_0}}, \qquad (5.361)$$

$$\bar{\beta}'^{\alpha\beta}\left(X,\mathbf{G}_A\right)=-\left.\frac{\partial^3\Psi_0}{\partial\theta^2\partial E^E_{\alpha\beta}}\right|_{\substack{\mathbf{E}^{\mathbf{E}}=0\\\theta=\theta_0}}, \tag{5.362}$$

$$\bar{\beta}''^{\alpha\beta}\left(X,\mathbf{G}_A\right)=-\left.\frac{\partial^4\Psi_0}{\partial\theta^3\partial E^E_{\alpha\beta}}\right|_{\substack{\mathbf{E}^{\mathbf{E}}=0\\\theta=\theta_0}}, \tag{5.363}$$

$$\bar{\beta}'^{\alpha\beta\chi\delta}\left(X,\mathbf{G}_A\right)=-\left.\frac{\partial^4\Psi_0}{\partial\theta^2\partial E^E_{\alpha\beta}\partial E^E_{\chi\delta}}\right|_{\substack{\mathbf{E}^{\mathbf{E}}=0\\\theta=\theta_0}}=-\left.\frac{\partial^2\mathbb{C}^{\alpha\beta\chi\delta}}{\partial\theta^2}\right|_{\substack{\mathbf{E}^{\mathbf{E}}=0\\\theta=\theta_0}}. \tag{5.364}$$

Definitions (5.354) and (5.355) result in null free energy and null stress at the reference state. Isothermal elastic constants of orders two, three, and four are defined in (5.356)-(5.358). Isothermal stress-temperature coefficients of various orders are listed in (5.359)-(5.364). Since coefficients in (5.356)-(5.364) are all derivatives of thermodynamic potentials, these coefficients exhibit the same material symmetries as polar tensors of the same orders in (5.65)-(5.73) and Section 5.1.5. If the reference state is chosen as one in which $F^{\theta\alpha}_{.A}=g^{\alpha}_{.A}$ (i.e., thermal deformation vanishes at $\theta=\theta_0$), then reference states in (5.62) and (5.353) coincide.

From (5.344) and (5.353), the elastic second Piola-Kirchhoff stress is

$$\begin{aligned}\bar{\Sigma}^{\alpha\beta}&=J^E\rho\frac{\partial\psi}{\partial E^E_{\alpha\beta}}=J^EJ^{-1}\rho_0\frac{\partial\psi}{\partial E^E_{\alpha\beta}}=J^{\theta-1}\rho_0\frac{\partial\psi}{\partial E^E_{\alpha\beta}}\\&=J^{\theta-1}\left[\bar{\mathbb{C}}^{\alpha\beta\chi\delta}E^E_{\chi\delta}+\frac{1}{2}\bar{\mathbb{C}}^{\alpha\beta\chi\delta\varepsilon\phi}E^E_{\chi\delta}E^E_{\varepsilon\phi}+\frac{1}{6}\bar{\mathbb{C}}^{\alpha\beta\chi\delta\varepsilon\phi\varphi\gamma}E^E_{\chi\delta}E^E_{\varepsilon\phi}E^E_{\varphi\gamma}+...\right.\\&\quad-\bar{\beta}^{\alpha\beta}\Delta\theta-\bar{\beta}^{\alpha\beta\chi\delta}E^E_{\chi\delta}\Delta\theta-\frac{3}{8}\bar{\beta}^{\alpha\beta\chi\delta\varepsilon\phi}E^E_{\chi\delta}E^E_{\varepsilon\phi}\Delta\theta-...\\&\quad\left.-\frac{1}{2}\bar{\beta}'^{\alpha\beta}(\Delta\theta)^2-\frac{1}{8}\bar{\beta}''^{\alpha\beta}(\Delta\theta)^3-...-\frac{1}{2}\bar{\beta}'^{\alpha\beta\chi\delta}E^E_{\chi\delta}(\Delta\theta)^2\right].\end{aligned} \tag{5.365}$$

The Jacobian determinant of thermal deformation is $J^\theta=\sqrt{\tilde{g}/G}\det\mathbf{F}^\theta$. Recall that stress-free thermal expansion to first order in strain is included in kinematic description (5.324)-(5.326), since $\boldsymbol{\alpha}_{\mathbf{T}}=\boldsymbol{\alpha}_{\mathbf{T}}(\theta,X,\mathbf{G}_A)$. Rank two stress-temperature coefficients $\bar{\beta}^{\alpha\beta}$, $\bar{\beta}'^{\alpha\beta}$, $\bar{\beta}''^{\alpha\beta}$, ... will also induce thermal expansion of the same physical origin. Thus, experimental delineation of second-order stress-temperature coefficients in (5.365) from second-order temperature-dependent thermal expansion coefficients in (5.326) becomes problematic. This ambiguity can be eliminated by assuming that $\bar{\beta}^{\alpha\beta}$, $\bar{\beta}'^{\alpha\beta}$, $\bar{\beta}''^{\alpha\beta}$, ... vanish by definition:

$$\overline{\beta}^{\alpha\beta} = -\frac{\partial^2 \Psi_0}{\partial\theta\partial E^E_{\alpha\beta}}\Bigg|_{\substack{\mathbf{E}^E=0 \\ \theta=\theta_0}} = 0 \,, \tag{5.366}$$

$$\overline{\beta}'^{\alpha\beta} = -\frac{\partial^3 \Psi_0}{\partial\theta^2 \partial E^E_{\alpha\beta}}\Bigg|_{\substack{\mathbf{E}^E=0 \\ \theta=\theta_0}} = 0 \,, \tag{5.367}$$

$$\overline{\beta}''^{\alpha\beta} = -\frac{\partial^4 \Psi_0}{\partial\theta^3 \partial E^E_{\alpha\beta}}\Bigg|_{\substack{\mathbf{E}^E=0 \\ \theta=\theta_0}} = 0 \,. \tag{5.368}$$

Thermal stress coefficients of orders four and higher are retained since $\boldsymbol{\alpha}_T$ is, by definition, independent of elastic strain. The stress becomes

$$\begin{aligned}
\overline{\Sigma}^{\alpha\beta} = J^{\theta-1}\Bigg[&\overline{\mathbb{C}}^{\alpha\beta\chi\delta} E^E_{\chi\delta} + \frac{1}{2}\overline{\mathbb{C}}^{\alpha\beta\chi\delta\varepsilon\phi} E^E_{\chi\delta} + \frac{1}{6}\overline{\mathbb{C}}^{\alpha\beta\chi\delta\varepsilon\phi\varphi\gamma} E^E_{\chi\delta}E^E_{\varepsilon\phi}E^E_{\varphi\gamma} + \dots \\
&-\overline{\beta}^{\alpha\beta\chi\delta} E^E_{\chi\delta}\Delta\theta - \frac{3}{8}\overline{\beta}^{\alpha\beta\chi\delta\varepsilon\phi} E^E_{\chi\delta}E^E_{\varepsilon\phi}\Delta\theta - \dots - \frac{1}{2}\overline{\beta}'^{\alpha\beta\chi\delta} E^E_{\chi\delta}(\Delta\theta)^2 \Bigg].
\end{aligned} \tag{5.369}$$

Thermal free energy $Y_0(\theta, X)$ in (5.353) can be defined in the same way as in Section 5.1.3.

In the materially linear, but geometrically nonlinear, regime the appropriate reduction of (5.353), using (5.366), is

$$\Psi_0 = \frac{1}{2}\overline{\mathbb{C}}^{\alpha\beta\chi\delta} E^E_{\alpha\beta}E^E_{\chi\delta} - \rho_0\overline{c}\theta\ln\frac{\theta}{\theta_0} \,, \tag{5.370}$$

where a constant specific heat capacity is defined as in the last of (5.85):

$$\overline{c} = -\left(\theta\frac{\partial^2 \psi}{\partial\theta^2}\right)\Bigg|_{\substack{\mathbf{E}^E=0 \\ \theta=\theta_0}} . \tag{5.371}$$

The elastic second Piola-Kirchhoff stress and Cauchy stress then become, respectively,

$$\overline{\Sigma}^{\alpha\beta} = J^{\theta-1}\overline{\mathbb{C}}^{\alpha\beta\chi\delta} E^E_{\chi\delta} \,, \quad \sigma^{ab} = J^{-1}F^{Ea}_{.\alpha}\overline{\mathbb{C}}^{\alpha\beta\chi\delta} E^E_{\chi\delta}F^{Eb}_{.\beta} \,. \tag{5.372}$$

5.6 Lagrangian Field Theory of Elasticity

Hamilton's principle applied to the appropriate action integral for hyperelastic bodies can be used to obtain a local form of the balance of linear momentum as well as constitutive equations relating stress, deformation gradient, and strain energy. The treatment of Section 5.6 is restricted to the athermal case with no dissipation, meaning heat flux, heat sources,

temperature gradients, and temperature rates are not addressed. Prior to presentation of Hamilton's principle in the context of nonlinear elasticity of grade one, the variational derivative is introduced.

5.6.1 The Variational Derivative

A family of deformations is denoted by $x^a = x^a(X^A, \Lambda)$, where Λ is a scalar parameter. At a reference state characterized by conditions $\Lambda = 0$ and $x^a = g^a_{\cdot A} X^A$, field $x^a = x^a(X^A, 0)$ is known. The first variation of $\mathbf{x}$ is then defined by (Toupin 1956, 1962; Eringen 1962):

$$\delta x^a = \left. \frac{\partial x^a}{\partial \Lambda} \right|_{\substack{X \\ \Lambda=0}} d\Lambda, \tag{5.373}$$

where reference coordinates X^A of material particle at X are held fixed during the variation. For a scalar function $f = f(x^a, x^a_{\cdot,A}, x^a_{\cdot:AB}, ...)$ depending on spatial position, deformation gradient, and higher-order total covariant derivatives of position (see e.g., (2.116)), the first variation of f is

$$\delta f = \left. \frac{\partial f}{\partial \Lambda} \right|_{\substack{X \\ \Lambda=0}} d\Lambda. \tag{5.374}$$

Since reference coordinates are held fixed in the variation, partial differentiation of a scalar with respect to reference coordinates commutes with the variational derivative:

$$\delta(f_{,A}) = (\delta f)_{,A} = \delta f_{,A}. \tag{5.375}$$

The first variation does not commute with partial differentiation in the spatial frame $\partial_a = \partial/\partial x^a$. Similarities between the variational derivative and the material time derivative of Section 2.6.1 are evident (Eringen 1962). In particular, δx^a is analogous to $v^a dt$, and δf is analogous to $\dot{f} dt$.

The following formulae for variations of kinematic quantities are often useful (Toupin 1956; Eringen 1962):

$$\delta F^a_{\cdot A} = \delta(x^a_{\cdot,A}) = (\delta x^a)_{,A} + F^a_{\cdot A;b} \delta x^b$$
$$= (\delta x^a)_{;b} F^b_{\cdot A} = (\delta x^a)_{;b} x^b_{\cdot,A} = (\delta x^a)_{;A}, \tag{5.376}$$

$$\delta F^{-1A}_{\cdot\cdot a} = \delta(X^A_{\cdot,a}) = -F^{-1A}_{\cdot\cdot b} F^{-1B}_{\cdot\cdot a} (\delta x^b)_{;B} = -F^{-1A}_{\cdot\cdot b}(\delta x^b)_{;a}, \tag{5.377}$$

$$\delta J = J(\delta F^a_{\cdot A}) F^{-1A}_{\cdot\cdot a} = J(\delta x^a)_{;a}. \tag{5.378}$$

Notice that (5.376) is analogous to (2.175), and (5.378) is analogous to (2.181). It follows from (5.375), (5.377), and the chain rule that

$$\delta(f_{,a}) = \delta(f_{,A}F^{-1A}_{.a}) = F^{-1A}_{.a}\delta(f_{,A}) + f_{,A}\delta F^{-1A}_{.a}$$
$$= F^{-1A}_{.a}(\delta f)_{,A} - f_{,b}F^{-1A}_{.a}(\delta x^b)_{,A} = (\delta f)_{,a} - f_{,b}(\delta x^b)_{;a}. \tag{5.379}$$

5.6.2 Hamilton's Principle in Nonlinear Elasticity

A general version of Hamilton's principle incorporating boundary conditions and external forces can be written as (Toupin 1964)

$$\delta\mathcal{A} + \int_{t_1}^{t_2}\left[\int_V\left(\rho_0\hat{\mathbf{b}}\bullet\delta\mathbf{x}\right)dV\right]dt + \int_{t_1}^{t_2}\left[\int_S\left(\hat{\mathbf{t}}\bullet\delta\mathbf{x}\right)dS\right]dt = \int_V\left(\hat{\mathbf{P}}\bullet\delta\mathbf{x}\right)dV\bigg|_{t_1}^{t_2}, \tag{5.380}$$

where $\hat{\mathbf{b}}(X,t)$ is a vector of generalized body forces per unit mass, $\hat{\mathbf{t}}(X,t)$ is a generalized traction vector prescribed per unit reference area, $\hat{\mathbf{P}}$ is a vector of generalized momenta, and the action integral is

$$\mathcal{A} = \int_{t_1}^{t_2}\mathcal{L}dt . \tag{5.381}$$

The Lagrangian functional $\mathcal{L}$ is given by the volume integral

$$\mathcal{L} = \int_V L_0 dV , \tag{5.382}$$

where L_0 is the Lagrangian energy density per unit reference volume of the following functional form for hyperelastic solids of grade one (Yavari et al. 2006):

$$L_0 = L_0\left(x^a, \dot{x}^a, x^a_{,A}, g_{ab}, X^A, \mathbf{G}_A\right). \tag{5.383}$$

Computation of the variation in (5.380) leads to

$$\delta\mathcal{A} = \delta\int_{t_1}^{t_2}\mathcal{L}dt = \delta\int_{t_1}^{t_2}\left(\int_V L_0 dV\right)dt =$$

$$= \int_{t_1}^{t_2}\int_V\left(\frac{\partial L_0}{\partial x^a}\delta x^a + \frac{\partial L_0}{\partial\dot{x}^a}\delta\dot{x}^a + \frac{\partial L_0}{\partial F^a_{.A}}\delta F^a_{.A} + \frac{\partial L_0}{\partial g_{ab}}\delta g_{ab}\right.$$

$$\left. + \frac{\partial L_0}{\partial X^A}\delta X^A + \frac{\partial L_0}{\partial\mathbf{G}_A}\bullet\delta\mathbf{G}_A + L_0\delta(dV)\right)dVdt \tag{5.384}$$

$$= \int_{t_1}^{t_2}\int_V\left(\frac{\partial L_0}{\partial x^a}\delta x^a + \frac{\partial L_0}{\partial\dot{x}^a}\delta\dot{x}^a + \frac{\partial L_0}{\partial F^a_{.A}}\delta F^a_{.A} + \frac{\partial L_0}{\partial g_{ab}}\delta g_{ab}\right)dVdt,$$

since L_0 does not depend explicitly on time and since, by the definition of the variational derivative used here,

$$\delta X^A = 0 , \ \delta \mathbf{G}_A(X) = 0 , \ \delta V(X) = 0 , \ \delta t = 0 , \qquad (5.385)$$

thereby enabling the variational operator to be brought inside the integration over time and reference volume. Integrating the remaining terms by parts, noting that $d(\delta x^a)/dt = \delta(dx^a/dt) = \delta \dot{x}^a$, and applying the divergence theorem of (2.193) of Section 2.7.1 in material coordinates results in

$$\int_{t_1}^{t_2}\int_V \frac{\partial L_0}{\partial \dot{x}^a}\delta\dot{x}^a dVdt = \int_{t_1}^{t_2}\int_V \left[\frac{d}{dt}\left(\frac{\partial L_0}{\partial \dot{x}^a}\delta x^a\right) - \frac{d}{dt}\left[\frac{\partial L_0}{\partial \dot{x}^a}\right]\delta x^a\right]dVdt$$

$$= \left[\int_V \left(\frac{\partial L_0}{\partial \dot{x}^a}\delta x^a\right)dV\right]\Bigg|_{t_1}^{t_2} - \int_{t_1}^{t_2}\int_V \frac{d}{dt}\left[\frac{\partial L_0}{\partial \dot{x}^a}\right]\delta x^a dVdt, \qquad (5.386)$$

$$\int_{t_1}^{t_2}\int_V \frac{\partial L_0}{\partial F^a_{.A}}\delta F^a_{.A}dVdt = \int_{t_1}^{t_2}\left[\int_V \frac{\partial L_0}{\partial F^a_{.A}}(\delta x^a)_{;A}dV\right]dt$$

$$= \int_{t_1}^{t_2}\int_V \left[\left(\frac{\partial L_0}{\partial F^a_{.A}}\delta x^a\right)_{;A} - \left(\frac{\partial L_0}{\partial F^a_{.A}}\right)_{;A}\delta x^a\right]dVdt \qquad (5.387)$$

$$= \int_{t_1}^{t_2}\int_S \left(\frac{\partial L_0}{\partial F^a_{.A}}N_A\delta x^a\right)dSdt - \int_{t_1}^{t_2}\int_V \left(\frac{\partial L_0}{\partial F^a_{.A}}\right)_{;A}\delta x^a dVdt,$$

$$\int_{t_1}^{t_2}\int_V \frac{\partial L_0}{\partial g_{ab}}\delta g_{ab}dVdt = \int_{t_1}^{t_2}\int_V \frac{\partial L_0}{\partial g_{ab}}g_{ab,c}\delta x^c dVdt$$

$$= \int_{t_1}^{t_2}\int_V 2\frac{\partial L_0}{\partial g_{ab}}\left(\overset{g}{\Gamma}{}^{.d}_{cb}g_{ad}\right)\delta x^c dVdt, \qquad (5.388)$$

appealing to symmetry properties of the spatial Christoffel symbols and their spatial derivatives from (2.60):

$$\delta g_{ab}(x) = g_{ab,c}\delta x^c = \left(\overset{g}{\Gamma}{}^{.d}_{cb}g_{ad} + \overset{g}{\Gamma}{}^{.d}_{ca}g_{bd}\right)\delta x^c. \qquad (5.389)$$

Collecting terms, the first variation of the action integral in (5.384) is

$$\delta \mathcal{A} = \int_{t_1}^{t_2}\int_V \left[\frac{\partial L_0}{\partial x^a} - \frac{d}{dt}\left(\frac{\partial L_0}{\partial \dot{x}^a}\right) - \left(\frac{\partial L_0}{\partial F^a_{.A}}\right)_{;A} + 2\frac{\partial L_0}{\partial g_{cb}}\left(\overset{g}{\Gamma}{}^{.d}_{ab}g_{cd}\right)\right]\delta x^a dVdt$$

$$+ \int_{t_1}^{t_2}\int_S \left(\frac{\partial L_0}{\partial F^a_{.A}}N_A\right)\delta x^a dSdt + \left[\int_V \left(\frac{\partial L_0}{\partial \dot{x}^a}\right)\delta x^a dV\right]\Bigg|_{t_1}^{t_2}. \qquad (5.390)$$

Substitution of (5.390) into (5.380), localizing the result, and requiring that Hamilton's principle be satisfied for arbitrary variations δx^a gives the

field equations within reference domain V, also called Euler-Lagrange equations:

$$-\left(\frac{\partial L_0}{\partial F^a_{.A}}\right)_{;A} + \rho_0 \hat{b}_a + \frac{\partial L_0}{\partial x^a} = \frac{d}{dt}\left(\frac{\partial L_0}{\partial \dot{x}^a}\right) - 2\frac{\partial L_0}{\partial g_{cb}}\left(\overset{g}{\Gamma}{}^{..d}_{ab} g_{cd}\right), \quad (5.391)$$

traction boundary conditions on reference surface S:

$$-\frac{\partial L_0}{\partial F^a_{.A}} N_A = \hat{t}_a, \qquad (5.392)$$

with $\mathbf{N}$ the outward unit normal to S, and endpoint conditions on linear momentum per unit reference volume:

$$\frac{\partial L_0}{\partial \dot{x}^a} = \hat{P}_a, \text{ (at } t = t_1, t_2 \text{)}. \qquad (5.393)$$

For a hyperelastic solid of grade one, the following Lagrangian is assumed to apply:

$$\mathcal{L} = \mathcal{K} - \mathcal{E} - \bar{\Phi} = \int_v \rho\left(\frac{1}{2}v^a v_a - e - \Phi\right)dv$$

$$= \int_V \left(\frac{\rho_0}{2}\dot{x}^a \dot{x}_a - E_0 - \Phi_0\right)dV, \qquad (5.394)$$

where kinetic energy $\mathcal{K}$ and global internal energy $\mathcal{E}$ are introduced in (4.28)-(4.30) and global potential energy $\bar{\Phi}$ is given by (4.41), with local potential energy per unit reference volume $\Phi_0(x) = \rho_0(X)\Phi(x)$. Since in the present Section, entropy production and temperature rates are assumed to vanish, internal energy per unit reference volume E_0 and free energy per unit reference volume $\Psi_0 = E_0 - \theta N_0$ differ by an arbitrary additive constant. Letting this constant vanish for convenience, and denoting the strain energy density by $\rho_0 \psi = \Psi_0 = E_0$, the Lagrangian density becomes

$$L_0 = \frac{\rho_0}{2}\dot{x}^a \dot{x}_a - \Psi_0\left(F^a_{.A}, X, \mathbf{G}_A\right) - \Phi_0(x), \qquad (5.395)$$

where the dependence on $\mathbf{F}$ temporarily replaces that on $\mathbf{C}$ in (5.44). Notice that (5.395) is a particular form of (5.383).

The partial covariant derivative in the first term on the left side of (5.391), using (5.395), becomes

$$-\left(\frac{\partial L_0}{\partial F^a_{.A}}\right)_{;A} = \left(\frac{\partial \Psi_0}{\partial F^a_{.A}}\right)_{;A} = \left(\frac{\partial \Psi_0}{\partial F^a_{.A}}\right)_{:A} - \left(\frac{\partial \Psi_0}{\partial F^a_{.A}}\right)_{;c} F^c_{.A}$$

$$= \left(\frac{\partial \Psi_0}{\partial F^a_{.A}}\right)_{:A} + \overset{g}{\Gamma}{}^{..b}_{ca}\left(\frac{\partial \Psi_0}{\partial F^b_{.A}}\right) F^c_{.A}, \qquad (5.396)$$

where the total covariant derivative of two point tensor $\partial \Psi_0 / \partial F_{.A}^a$ is defined similarly to (2.116)-(2.118) and (4.20). The third term on the left side of (5.391) becomes

$$\frac{\partial L_0}{\partial x^a} = -\frac{\partial \Phi_0}{\partial x^a} = -\rho_0 \Phi_{,a} = -J\rho\Phi_{,a} = J\rho b_a = \rho_0 b_a, \qquad (5.397)$$

where the conservative body force per unit mass with covariant components b_a is introduced in (4.41). The first term on the right of (5.391) becomes (Yavari et al. 2006)

$$\begin{aligned}
\frac{d}{dt}\left(\frac{\partial L_0}{\partial \dot{x}^a}\right) &= \frac{\rho_0}{2}\frac{d}{dt}\left[\frac{\partial}{\partial \dot{x}^a}\left(\dot{x}^b g_{bc}\dot{x}^c\right)\right] \\
&= \frac{\rho_0}{2}g_{bc}\frac{d}{dt}\left[\frac{\partial}{\partial \dot{x}^a}(\dot{x}^b \dot{x}^c)\right] + \frac{\rho_0}{2}\dot{x}^b\dot{x}^c\frac{d}{dt}\left[\frac{\partial}{\partial \dot{x}^a}g_{bc}\right] \\
&= \frac{\rho_0}{2}g_{bc}\frac{d}{dt}\left[\dot{x}^b\delta_{.a}^c + \dot{x}^c\delta_{.a}^b\right] + \frac{\rho_0}{2}\dot{x}^b\dot{x}^c g_{bc,a} \qquad (5.398) \\
&= \frac{\rho_0}{2}g_{bc}\left(A^b\delta_{.a}^c + A^c\delta_{.a}^b\right) + \frac{\rho_0}{2}\dot{x}^b\dot{x}^c\left(\overset{g}{\Gamma}_{.ac}^{.d}g_{bd} + \overset{g}{\Gamma}_{.ab}^{.d}g_{cd}\right) \\
&= \rho_0\left(g_{ab}A^b + \dot{x}^b\dot{x}^c\overset{g}{\Gamma}_{.ab}^{.d}g_{cd}\right),
\end{aligned}$$

with $A^b(X,t)$ contravariant components of the material acceleration of (2.174). The rightmost term of (5.391) is

$$\begin{aligned}
-2\frac{\partial L_0}{\partial g_{cb}}\left(\overset{g}{\Gamma}_{.ab}^{.d}g_{cd}\right) &= \left[2\frac{\partial \Psi_0}{\partial g_{cb}} - \rho_0\frac{\partial}{\partial g_{cb}}(\dot{x}^e g_{ef}\dot{x}^f)\right]\overset{g}{\Gamma}_{.ab}^{.d}g_{cd} \\
&= \left[2\frac{\partial \Psi_0}{\partial g_{cb}} - \rho_0\dot{x}^c\dot{x}^b\right]\overset{g}{\Gamma}_{.ab}^{.d}g_{cd}.
\end{aligned} \qquad (5.399)$$

Substituting (5.396)-(5.399) into (5.391) and collecting terms results in the following reduced set of Euler-Lagrange equations:

$$\left(\frac{\partial \Psi_0}{\partial F_{.A}^a}\right)_{:A} + \rho_0(\hat{b}_a + b_a) - \rho_0 g_{ab}A^b = \left(2\frac{\partial \Psi_0}{\partial g_{cb}}g_{cd} - \frac{\partial \Psi_0}{\partial F_{.A}^d}F_{.A}^b\right)\overset{g}{\Gamma}_{.ba}^{.d}. \quad (5.400)$$

The first Piola-Kirchhoff stress tensor and total body force per unit reference volume are defined respectively as

$$P_a^A = \frac{\partial \Psi_0}{\partial F_{.A}^a}, \quad \overline{B}_a = \rho_0(\hat{b}_a + b_a). \qquad (5.401)$$

Now following invariance arguments of (5.34)-(5.36), let the strain energy density depend on the deformation gradient **F** and spatial metric **g** only through the symmetric deformation tensor **C**:

$$\Psi_0\left(F^a_{.A},\mathbf{G}_A,X\right)=\Psi_0\left(C_{AB}(F^a_{.A},g_{ab}),\mathbf{G}_A,X\right), \tag{5.402}$$

where $C_{AB}=F^a_{.A}g_{ab}F^b_{.B}$. It follows that

$$\frac{\partial\Psi_0}{\partial g_{bc}}=\frac{\partial\Psi_0}{\partial C_{BC}}\frac{\partial C_{BC}}{\partial g_{bc}}=F^b_{.B}\frac{\partial\Psi_0}{\partial C_{BC}}F^c_{.C}, \tag{5.403}$$

$$\frac{\partial\Psi_0}{\partial F^d_{.A}}=\frac{\partial\Psi_0}{\partial C_{BC}}\frac{\partial C_{BC}}{\partial F^d_{.A}}=\frac{\partial\Psi_0}{\partial C_{BC}}(\delta^b_{.d}\delta^A_{.B}g_{bc}F^c_{.C}+\delta^c_{.d}\delta^A_{.C}g_{bc}F^b_{.B})$$
$$=\frac{\partial\Psi_0}{\partial C_{BC}}\left(\delta^A_{.B}g_{dc}F^c_{.C}+\delta^A_{.C}g_{bd}F^b_{.B}\right)=2\frac{\partial\Psi_0}{\partial C_{AB}}g_{ad}F^a_{.B}, \tag{5.404}$$

from which the right side of (5.400) vanishes:

$$2\frac{\partial\Psi_0}{\partial g_{cb}}g_{cd}=2F^b_{.B}\frac{\partial\Psi_0}{\partial C_{BC}}F^c_{.C}g_{cd}$$
$$=F^b_{.B}\left(\frac{\partial\Psi_0}{\partial F^e_{.B}}F^{-1C}_{.a}g^{ae}\right)F^c_{.C}g_{cd}=F^b_{.B}\frac{\partial\Psi_0}{\partial F^d_{.B}}. \tag{5.405}$$

Substituting from (5.401), the left side of (5.400) is identical to the material balance of linear momentum of (4.21):

$$P^{aA}_{:A}+\bar{B}^a=\rho_0A^a. \tag{5.406}$$

Traction boundary conditions (5.392) are identical to those entering Cauchy's theorem in (4.4):

$$\hat{t}_a=-\frac{\partial L_0}{\partial F^a_{.A}}N_A=\frac{\partial\Psi_0}{\partial F^a_{.A}}N_A=P^A_aN_A=t_{0a}, \tag{5.407}$$

where by definition $\hat{t}_a=t_{0a}$ is the traction per unit reference area. The conditions (5.393) on initial and final momentum density are

$$\hat{P}_a=\frac{\partial L_0}{\partial\dot{x}^a}=\frac{\rho_0}{2}g_{bc}\left[\frac{\partial}{\partial\dot{x}^a}(\dot{x}^b\dot{x}^c)\right]=\rho_0g_{ab}\dot{x}^b,\ (\text{at }t=t_1,t_2). \tag{5.408}$$

Invariance of free energy density under rigid rotations of the spatial frame provides the local balance of angular momentum. Consider a finite rotation $F^a_{.A}\rightarrow\hat{Q}^a_{.b}F^b_{.A}$ as discussed in Section 4.2.1. An infinitesimal rotation can be expressed in the form $\hat{Q}^a_{.b}\approx\delta^a_{.b}+g_{bc}\hat{\Omega}^{ac}$, where $\hat{\Omega}^{ac}=\hat{\Omega}^{[ac]}$. According to Toupin (1964), invariance of the free energy density under infinitesimal rotations is sufficient to ensure invariance under finite rotations. Let the differential change of free energy under such small rotations be (Eringen 1962)

$$dΨ_0 = \frac{∂Ψ_0}{∂(\hat{Q}^a_{.e}F^e_{.A})} \frac{∂(\hat{Q}^a_{.b}F^b_{.A})}{∂\hat{Q}^c_{.d}} d\hat{Q}^c_{.d} = \frac{∂Ψ_0}{∂(\hat{Q}^a_{.e}F^e_{.A})} F^b_{.A} d\hat{Q}^a_{.b}$$

$$= \frac{∂Ψ_0}{∂F^a_{.A}} F^b_{.A} g_{bc} d\hat{Ω}^{[ac]} = P^A_a F_{cA} d\hat{Ω}^{[ac]}.$$

(5.409)

Requiring that (5.409) vanish under arbitrary rotations $d\hat{Ω}^{[ac]}$ leads to a local balance of angular momentum identical to the first of (4.27):

$$dΨ_0 = 0 \Rightarrow P^A_{[a}F_{c]A} = 0 \Leftrightarrow P^{aA}F^c_{.A} = F^a_{.A}P^{cA}.$$

(5.410)

Notice that no global balance of linear or angular momentum has been posited in Section 5.6.2, and that the derivations apply for any choice of generalized spatial or referential coordinates, including curvilinear coordinates. The procedure followed in (5.380)-(5.406) is somewhat analogous to that sketched in Section B.1.2 of Appendix B dealing with dynamic particle systems.

5.7 Elasticity of Grade Two

Recall from kinematic relations (2.114) and (2.115) that deformation gradient $\mathbf{F}$ provides a first-order accurate approximation of the length and direction of a differential line element mapped to the current configuration: $d\mathbf{x} = \mathbf{F}d\mathbf{X}$. This approximation can be interpreted as exact for the case of homogeneous deformations. On the other hand, a second-order accurate approximation is obtained by retaining the second-order term in (2.114), leading to

$$dx^a(X) = F^a_{.A}\big|_X dX^A + \frac{1}{2}F^a_{.A:B}\big|_X dX^A dX^B,$$

(5.411)

where the total covariant derivative of $\mathbf{F}$ with components $F^a_{.A:B} = x^a_{.AB}$ satisfies, from (2.57), (2.59), and (2.116),

$$\mathbf{F}_{,B} \otimes \mathbf{G}^B = (F^a_{.A}\mathbf{g}_a \otimes \mathbf{G}^A)_{,B} \otimes \mathbf{G}^B = F^a_{.A:B}\mathbf{g}_a \otimes \mathbf{G}^A \otimes \mathbf{G}^B$$

$$= (F^a_{.A,B} + \overset{g}{Γ}^{.a}_{bc}F^c_{.A}F^b_{.B} - \overset{G}{Γ}^{.C}_{BA}F^a_{.C})\mathbf{g}_a \otimes \mathbf{G}^A \otimes \mathbf{G}^B.$$

(5.412)

It follows from local compatibility conditions (2.203) and symmetries of spatial and referential Christoffel symbols that $F^a_{.A:B} = F^a_{.B:A}$, meaning that

the total covariant derivative of **F** consists of at most $3 \times 6 = 18$ independent entries. Eringen (1962) shows that[5]

$$F^a_{.A:B} = F^a_{.A,B} + \overset{g}{\Gamma}{}^{.a}_{bc} F^c_{.A} F^b_{.B} = (F^a_{.A,b} + \overset{g}{\Gamma}{}^{.a}_{bc} F^c_{.A}) F^b_{.B} = F^a_{.A;b} F^b_{.B};$$

$$F^a_{.A:B} = F^a_{.A;b} F^b_{.B} \Leftrightarrow x^a_{.,AB} = (x^a_{.,A})_{;b} x^b_{.,B}, \tag{5.413}$$

from which it follows that for the inverse of the deformation gradient,

$$0 = (F^a_{.A} F^{-1A}_{.c})_{;b} \Rightarrow F^{-1B}_{.c;b} = -F^{-1A}_{.c} F^{-1B}_{.a} F^{-1C}_{.b} F^a_{.A:C}. \tag{5.414}$$

The first variation of $F^a_{.A:B}$ is found using (5.376), (5.377), and (5.413) as

$$\begin{aligned}
\delta(F^a_{.A:B}) &= \delta(F^a_{.A;b} F^b_{.B}) = F^b_{.B} \delta(F^a_{.A;b}) + F^a_{.A;b} \delta(F^b_{.B}) \\
&= F^b_{.B}\left[\delta(F^a_{.A;C} F^{-1C}_{.b}) \right] + F^a_{.A;b}(\delta x^b)_{;B} \\
&= F^b_{.B}\left[\delta(F^a_{.A;C}) F^{-1C}_{.b} + F^a_{.A;C}(\delta F^{-1C}_{.b}) \right] + F^a_{.A;b}(\delta x^b)_{;B} \\
&= F^b_{.B}\left[\delta(F^a_{.A})_{;C} F^{-1C}_{.b} - F^a_{.A;C} F^{-1C}_{.c}(\delta x^c)_{;b} \right] + F^a_{.A;c}(\delta x^c)_{;B} \\
&= \delta(F^a_{.A})_{;B}.
\end{aligned} \tag{5.415}$$

In what follows in Section 5.7, concepts of surface gradient and normal derivative of a differentiable function at a surface are used. For a differentiable function $f(x,t)$ defined on spatial surface s, the covariant derivative, normal derivative, and surface gradient are related by (Toupin 1962):

$$f_{;a} = n_a D(f) + D_a(f), \quad D(f) = f_{;a} n^a, \quad D_a(f) = (\delta^b_a - n_a n^b) f_{;b}, \tag{5.416}$$

where $n_a(x,t)$ is the unit outward normal to s, the first term on the right accounts for the normal derivative $Df(x,t)$, and the second accounts for the tangential derivative $D_a f(x,t)$. The following integral identity applies for the tangential derivative of f over surface s bounded by closed curve c:

$$\int_s D_a(f) n_b \, ds = \int_s (\kappa^c_{.c} n_a n_b - \kappa_{ab}) f \, ds - \int_c f \varepsilon_{acd} n^c n_b \, dx^d, \tag{5.417}$$

where boundary s is assumed sufficiently smooth (i.e., no sharp edges or corners) and $f(x,t)$ is assumed to have continuous first partial derivatives with respect to x^a. The second fundamental form of a smooth surface is defined as (Toupin 1962)

$$\kappa_{ab}(x) = -D_a n_b = -D_b n_a = \kappa_{ba}. \tag{5.418}$$

Consider a hyperelastic material of grade two, in which stress and strain energy depend on the total covariant derivative of **F** in addition to the deformation gradient, reference position of a material particle (in the case of

---

[5] It is assumed in (5.413) and in the remainder of Section 5.7 that a coordinate system is chosen such that referential Christoffel symbols vanish, i.e., $\overset{G}{\Gamma}{}^{.C}_{BA} = 0$.

heterogeneity) and reference basis vectors (in the case of anisotropy). The strain energy density is written in functional form as

$$\rho_0 \psi = \Psi_0 = \Psi_0 \left(F^a_{.A}, F^a_{.A:B}, X, \mathbf{G}_A \right). \tag{5.419}$$

By assertion, the balance of mass in (4.10)-(4.12) still applies for materials of grade two: $\rho_0 = \rho J$ with $J = dv/dV = \sqrt{g/G} \det \mathbf{F}$ from (2.141)-(2.142), despite (5.411). On the other hand, stress and traction definitions in Section 4.1.1, linear and angular momentum balances in Section 4.1.3, and the treatment of thermodynamics in Sections 4.1.4 and 4.2 do not generally apply for the theory of elasticity of grade two presented in what follows in the present Section.

As was assumed in Section 5.6, in the present Section entropy production and temperature rates are assumed to vanish, and free energy and internal energy are equivalent to the strain energy. Heat conduction, heat sources, and temperature gradients are not considered in the present Section. Furthermore, considered for simplicity in what follows is the quasi-static case, in which velocities and accelerations are omitted. Potential energies from conservative body forces are also omitted for simplicity of presentation, but these forces could be incorporated easily by subtracting the appropriate term from the Lagrangian. Thus, the Lagrangian density function and the Lagrangian functional of (5.394) simply become, respectively,

$$L_0 = -\Psi_0, \quad \mathcal{L} = \int_V L_0 dV = -\mathcal{E} = -\int_V \Psi_0 dV = -\int_V \rho_0 \psi \, dV = -\int_v \rho \psi \, dv , \tag{5.420}$$

since kinetic energy $\mathcal{K} = 0$ and global potential energy $\bar{\Phi} = 0$ by definition in the present simplified case.

The appropriate generalization of Hamilton's principle (5.380) for elastic materials of grade two (Toupin 1962, 1964) with vanishing inertia is written as follows in the spatial configuration:

$$\delta \mathcal{A} + \int_{t_1}^{t_2} \left[\int_v \left(\bar{\mathbf{b}} \cdot \delta \mathbf{x} \right) dv \right] dt + \int_{t_1}^{t_2} \left[\int_s \left(\mathbf{t} \cdot \delta \mathbf{x} + \mathbf{h} \cdot D \delta \mathbf{x} \right) ds \right] dt = 0 , \tag{5.421}$$

with $\mathbf{h}(x,t)$ a generalized surface traction introduced as a work conjugate to the normal derivative of the variation of spatial motion at the surface, $D\delta \mathbf{x} = (\delta x^a)_{;b} n^b \mathbf{g}_a = (\delta x^a)^{;b} n_b \mathbf{g}_a$. Body force per unit current volume is written as $\bar{\mathbf{b}}(x,t)$, and $\mathbf{t}(x,t)$ is a surface traction, i.e., a force vector per unit spatial area. Substituting from (5.420),

$$\delta\mathcal{A} = \delta\int_{t_1}^{t_2}\mathcal{L}dt = \delta\int_{t_1}^{t_2}\left(\int_V L_0 dV\right)dt$$

$$= -\int_{t_1}^{t_2}\left(\int_V \delta\Psi_0 dV\right)dt = -\int_{t_1}^{t_2}\left(\int_v \delta\Psi_0(J^{-1}dv)\right)dt. \tag{5.422}$$

Thus the equality

$$-\int_v J^{-1}\delta\Psi_0 dv + \int_v \bar{b}_a\delta x^a dv + \int_s\left[t_a\delta x^a + h_a D(\delta x^a)\right]ds = 0 \tag{5.423}$$

should hold at any time in (arbitrary) interval $t_1 \leq t \leq t_2$. The first integral on the left side of (5.423) can be written using (5.419) as

$$-\int_v J^{-1}\delta\Psi_0 dv = -\int_v J^{-1}\left[\frac{\partial\Psi_0}{\partial F^a_{.A}}\delta F^a_{.A} + \frac{\partial\Psi_0}{\partial F^a_{.A:B}}\delta(F^a_{.A:B})\right]dv, \tag{5.424}$$

where from (5.376), (5.415), and the product rule,

$$J^{-1}\frac{\partial\Psi_0}{\partial F^a_{.A}}\delta F^a_{.A} + J^{-1}\frac{\partial\Psi_0}{\partial F^a_{.A:B}}\delta(F^a_{.A:B})$$

$$= \left[J^{-1}\frac{\partial\Psi_0}{\partial F^a_{.A}} - \left(J^{-1}\frac{\partial\Psi_0}{\partial F^a_{.A:B}}F^b_{.B}\right)_{;b}\right]\delta F^a_{.A} + \left[J^{-1}\frac{\partial\Psi_0}{\partial F^a_{.A:B}}F^b_{.B}\delta F^a_{.A}\right]_{;b}$$

$$= \left[J^{-1}\frac{\partial\Psi_0}{\partial F^a_{.A}} - \left(J^{-1}\frac{\partial\Psi_0}{\partial F^a_{.A:B}}F^b_{.B}\right)_{;b}\right]F^c_{.A}(\delta x^a)_{;c} \tag{5.425}$$

$$+ \left[J^{-1}\frac{\partial\Psi_0}{\partial F^a_{.A:B}}F^b_{.B}F^c_{.A}(\delta x^a)_{;c}\right]_{;b},$$

since by (5.413) and (5.415),

$$\left[J^{-1}\frac{\partial\Psi_0}{\partial F^a_{.A:B}}F^b_{.B}\delta F^a_{.A}\right]_{;b} = \left[J^{-1}\frac{\partial\Psi_0}{\partial F^a_{.A:B}}F^b_{.B}\right]_{;b}\delta F^a_{.A} + J^{-1}\frac{\partial\Psi_0}{\partial F^a_{.A:B}}\delta(F^a_{.A:B}). \tag{5.426}$$

Noting from (2.145) that $(J^{-1}F^a_{.A})_{;a} = 0$ when $\overset{G}{\Gamma}{}^{.B}_{BA} = 0$, the rank two stress tensor $\sigma^{dc}(x,t)$ and rank three hyperstress tensor $H^{bdc}(x,t)$ are defined, respectively, as

$$\sigma^{dc} = g^{da}\sigma^{.c}_a = g^{da}\left[J^{-1}\frac{\partial\Psi_0}{\partial F^a_{.A}} - \left(J^{-1}\frac{\partial\Psi_0}{\partial F^a_{.A:B}}F^b_{.B}\right)_{;b}\right]F^c_{.A}$$

$$= g^{da}J^{-1}\left[\frac{\partial\Psi_0}{\partial F^a_{.A}} - F^b_{.B}\left(\frac{\partial\Psi_0}{\partial F^a_{.A:B}}\right)_{;b}\right]F^c_{.A}, \tag{5.427}$$

$$H^{bdc} = g^{da} H_a^{b.c} = J^{-1} g^{da} \frac{\partial \Psi_0}{\partial F^a_{.A:B}} F^b_{.B} F^c_{.A} = J^{-1} g^{da} \frac{\partial \Psi_0}{\partial F^a_{.B:A}} F^c_{.B} F^b_{.A} = H^{cdb} . \quad (5.428)$$

In physical components, the stress in (5.427) exhibits dimensions of force per unit spatial area or energy per unit spatial volume, while the hyperstress in (5.428) exhibits dimensions of force per unit spatial length or energy per unit spatial area. The hyperstress consists of up to 18, as opposed to 27, independent entries as a consequence of compatibility conditions $F^a_{[A:B]} = 0$. The stress tensor of (5.427) consists of up to 9 independent entries, and is generally not symmetric, in contrast to the Cauchy stress tensor of classical continuum mechanics defined in Chapter 4. Substituting these stress definitions into (5.425),

$$J^{-1} \delta \Psi_0 = \sigma_a^c (\delta x^a)_{;c} + \left[H_a^{b.c} (\delta x^a)_{;c} \right]_{;b}$$
$$= (\sigma_a^c \delta x^a)_{;c} - (\sigma_a^c)_{;c} \delta x^a + \left[H_a^{b.c} (\delta x^a)_{;c} \right]_{;b} . \quad (5.429)$$

Applying the divergence theorem of (2.193) in spatial coordinates to (5.424) gives

$$-\int_v J^{-1} \delta \Psi_0 dv = -\int_v \left\{ (\sigma_a^c \delta x^a)_{;c} - \sigma_{a;c}^c \delta x^a + \left[H_a^{b.c} (\delta x^a)_{;c} \right]_{;b} \right\} dv$$
$$= \int_v \sigma_{a;c}^c \delta x^a dv - \int_s \left[\sigma_a^c \delta x^a + H_a^{b.c} (\delta x^a)_{;b} \right] n_c ds . \quad (5.430)$$

Using (5.416)-(5.418), Stokes's theorem (2.198), and integration by parts, the rightmost term in the surface integral in (5.430) can be expressed as follows (Teodosiu 1967a), appealing to the symmetry of $H_a^{b.c} = H_a^{c.b}$:

$$\int_s H_a^{b.c} (\delta x^a)_{;b} n_c ds = \int_s H_a^{b.c} [D(\delta x^a) n_b + D_b(\delta x^a)] n_c ds$$

$$= \int_s H_a^{b.c} n_b n_c D(\delta x^a) ds + \int_s H_a^{b.c} (\kappa_{.d}^d n_b n_c - \kappa_{bc}) \delta x^a ds$$

$$- \int_c H_a^{b.c} \varepsilon_{bde} n^d n_c \delta x^a dx^e$$

$$= \int_s H_a^{b.c} n_b n_c D(\delta x^a) ds + \int_s H_a^{b.c} (\kappa_{.d}^d n_b n_c - \kappa_{bc}) \delta x^a ds \quad (5.431)$$

$$- \int_s (H_a^{b.c} \varepsilon_{bde} n^d n_c \delta x^a)_{;g} n_f \varepsilon^{efg}$$

$$= \int_s H_a^{b.c} n_b n_c D(\delta x^a) ds - \int_s H_a^{b.c} (\kappa_{.d}^d n_b n_c - \kappa_{bc}) \delta x^a ds$$

$$- \int_s D_b(H_a^{b.c}) n_c \delta x^a ds,$$

where $D_b(H_a^{b.c}) = H_{a;b}^{b.c} - D(H_a^{b.c})n_b = H_{a;b}^{b.c} - H_a^{b.c;d}n_d n_b$ is the surface gradient of the hyperstress, with normal derivative $D(H_a^{b.c}) = H_{a;d}^{b.c}n^d$. Finally, substituting (5.430) and (5.431) into (5.423) and collecting terms,

$$\int_v (\sigma_{a;c}^c + \bar{b}_a)\delta x^a dv = \int_S \left[H_a^{b.c} n_b n_c - h_a \right] D(\delta x^a) ds$$

$$+ \int_S \left[\sigma_a^c n_c - H_a^{b.c}(\kappa_{.d}^d n_b n_c - \kappa_{bc}) - D_b(H_a^{b.c})n_c - t_a \right]\delta x^a ds. \tag{5.432}$$

Presuming (5.432) must hold for arbitrary variations δx^a and normal surface variations $D(\delta x^a)$, the following equilibrium equations and boundary conditions are obtained:

$$\sigma_{a;c}^c + \bar{b}_a = 0, \tag{5.433}$$

$$t_a = \sigma_a^c n_c - H_a^{b.c}(\kappa_{.d}^d n_b n_c - \kappa_{bc}) - D_b(H_a^{b.c})n_c, \tag{5.434}$$

$$h_a = H_a^{b.c} n_b n_c. \tag{5.435}$$

Relation (5.433) is the static balance of linear momentum. Relation (5.434) is the boundary condition for the traction. Relation (5.435) is the boundary condition for the hypertraction. Spatial relations (5.433)-(5.435) were first derived by Toupin (1962) using the virtual work procedure outlined above, and were presented later in material coordinates by Toupin (1964).

For the particular case when free energy (5.419) does not depend on second-order position gradient $F_{.A:B}^a$, i.e., when $\Psi_0 = \Psi_0(F_{.A}^a, X, \mathbf{G}_A)$, stress σ^{dc} becomes identical to the Cauchy stress of classical nonlinear elasticity (e.g., (5.24) and (5.427) become equivalent), and the hyperstress $H^{bdc} = 0$ in (5.428). Thus, in that particular case, (5.433) becomes equivalent to linear momentum balance (4.17) in the absence of spatial acceleration, boundary condition (5.434) becomes equivalent to Cauchy's relation (4.3), and the right side of (5.435) vanishes identically. In the general theory, however, i.e., when the free energy depends on $F_{.A:B}^a$, the stress in (5.427) depends, in part, on the derivative of the free energy with respect to $F_{.A:B}^a$. Such dependence can be interpreted from (5.411) as resulting from second-order effects on stretch of interatomic bond vectors (e.g., possibly interpreted as anharmonic or nonlinear effects), thereby influencing interatomic forces and the resulting stress tensor of (5.427), and giving rise to the hyperstress tensor of (5.428).

As was the case in Section 5.6, a local balance of angular momentum can be obtained by restricting the strain energy density to be invariant under rigid body rotations of the spatial frame. Consider a finite rotation

$F^a_{.A} \to \hat{Q}^a_{.b} F^b_{.A}$ as discussed in Sections 4.2.1 and 5.6.2. The total covariant derivative transforms in this situation as $F^a_{.A:B} \to \hat{Q}^a_{.b} F^b_{.A:B}$. An infinitesimal rotation is then written in the form $\hat{Q}^a_{.b} = \delta^a_{.b} + g_{bc}\hat{\Omega}^{ac}$, where the skew matrix $\hat{\Omega}^{ac} = \hat{\Omega}^{[ac]}$. According to Toupin (1964), invariance of the strain energy density under infinitesimal rotations is sufficient to ensure invariance under finite rotations. Extending (5.409), the variational change of strain energy under such small rotations is

$$J^{-1} d\Psi_0 = J^{-1}\left[\frac{\partial \Psi_0}{\partial(\hat{Q}^a_{.e} F^e_{.A})} F^b_{.A} + \frac{\partial \Psi_0}{\partial(\hat{Q}^a_{.e} F^e_{.A:B})} F^b_{.A:B} \right] d\hat{Q}^a_{.b}$$

$$= J^{-1}\left[\frac{\partial \Psi_0}{\partial F^a_{.A}} F^b_{.A} + \frac{\partial \Psi_0}{\partial F^a_{.A:B}} F^b_{.A:B} \right] d\hat{\Omega}^a_{.b} \qquad (5.436)$$

$$= J^{-1}\left[\frac{\partial \Psi_0}{\partial F^a_{.A}} F_{bA} + \frac{\partial \Psi_0}{\partial F^a_{.A:B}} F_{bA:B} \right] d\hat{\Omega}^{ab}.$$

Requiring that (5.436) vanish under small but otherwise arbitrary rotations $d\hat{\Omega}^{[ab]}$ leads to the local balance of angular momentum for elastic materials of grade two:

$$d\Psi_0 = 0 \to J^{-1}\left[\frac{\partial \Psi_0}{\partial F^{[a}_{.A}} F_{b]A} + \frac{\partial \Psi_0}{\partial F^{[a}_{.A:B}} F_{b]A:B} \right] = 0 . \qquad (5.437)$$

Components of the second-order stress tensor in (5.427) can be expressed as (Toupin 1964)

$$\sigma^{.b}_a = J^{-1}\left[\frac{\partial \Psi_0}{\partial F^a_{.A}} - F^c_{.B}\left(\frac{\partial \Psi_0}{\partial F^a_{.A:B}} \right)_{;c} \right] F^b_{.A}$$

$$= J^{-1}\frac{\partial \Psi_0}{\partial F^a_{.A}} F^b_{.A} - \left(J^{-1}F^c_{.B}\frac{\partial \Psi_0}{\partial F^a_{.A:B}} \right)_{;c} F^b_{.A}$$

$$= J^{-1}\frac{\partial \Psi_0}{\partial F^a_{.A}} F^b_{.A} + J^{-1}F^c_{.B}\frac{\partial \Psi_0}{\partial F^a_{.A:B}} F^b_{.A;c} - \left(J^{-1}F^c_{.B}\frac{\partial \Psi_0}{\partial F^a_{.A:B}} F^b_{.A} \right)_{;c} \qquad (5.438)$$

$$= J^{-1}\left[\frac{\partial \Psi_0}{\partial F^a_{.A}} F^b_{.A} + \frac{\partial \Psi_0}{\partial F^a_{.A:B}} F^b_{.A:B} \right] - H^{b.c}_{.a;c} .$$

Substituting the antisymmetric part from (5.437) into (5.438),

$$\sigma^{[ab]} = J^{-1}\left(\frac{\partial \Psi_0}{\partial F_{[a|A|}} F^{b]}_{.A} + \frac{\partial \Psi_0}{\partial F_{[a|A:B|}} F^{b]}_{.A:B} \right) - H^{[ba]c}_{...;c} = H^{[ab]c}_{...;c} = M^{abc}_{...}, \qquad (5.439)$$

where rank three tensor (i.e., third-order tensor) of couple stresses M^{abc} and rank two couple stress tensor m_d^c are constructed from the antisymmetric part of the hyperstress[6]:

$$M^{abc} = \frac{1}{2}\varepsilon^{abd}m_d^c = H^{[ab]c}, \; m_d^c = \varepsilon_{dab}M^{abc} = \varepsilon_{dab}H^{abc}. \quad (5.440)$$

Local angular momentum balance (5.439) becomes

$$\sigma^{[ab]} - M^{abc}_{\dots;c} = \sigma^{[ab]} - \frac{1}{2}\varepsilon^{abd}m_{d;c}^c = 0 \Leftrightarrow \varepsilon_{abc}\sigma^{ab} - m_{c;d}^d = 0. \quad (5.441)$$

The symmetric part of the hyperstress $H^{(ab)c} = H^{abc} - M^{abc}$, while not affecting the angular momentum balance (5.441), does not always vanish identically and has been interpreted as resulting from a distribution of self-equilibrating forces (Toupin 1964).

A frame indifferent version of strain energy function (5.419) is

$$\Psi_0 = \Psi_0\left(E_{AB}, B_{ABC}, X, \mathbf{G}_A\right), \quad (5.442)$$

where the right Cauchy-Green strain $2E_{AB} = F_{.A}^a g_{ab} F_{.B}^b - G_{AB}$ as in (2.156), and the covariant strain gradient referred to the reference configuration satisfies

$$B_{ABC} = F_{aA}F_{.B:C}^a = \frac{1}{2}(C_{AB;C} + C_{AC;B} - C_{CB;A})$$
$$= E_{AB;C} + E_{AC;B} - E_{CB;A}. \quad (5.443)$$

Clearly, the strain gradient tensor $B_{ABC} = B_{A(BC)}$, like $F_{.B:C}^b = F_{.C:B}^b$, contains 18 independent entries. Contravariant hyperstress and stress tensors are then computed, respectively, from the chain rule as follows:

$$H^{bdc} = J^{-1}g^{da}\frac{\partial \Psi_0}{\partial B_{CDE}}\frac{\partial(F_{eC}F_{D:E}^e)}{\partial F_{.A:B}^a}F_{.B}^b F_{.A}^c = J^{-1}\frac{\partial \Psi_0}{\partial B_{CAB}}F_{.B}^b F_{.C}^d F_{.A}^c, \quad (5.444)$$

---

[6] The second-order couple stress defined in (5.440) is consistent with the definition of Toupin (1964) but is the negative transpose of the couple stress defined by Malvern (1969).

$$\sigma^{dc} = g^{da} J^{-1} \left[\frac{\partial \Psi_0}{\partial F^a_{.A}} - F^b_{.B} \left(\frac{\partial \Psi_0}{\partial F^a_{.A:B}} \right)_{;b} \right] F^c_{.A}$$

$$= g^{da} J^{-1} F^c_{.A} \left[\frac{\partial \Psi_0}{\partial E_{CD}} \frac{\partial E_{CD}}{\partial F^a_{.A}} + \frac{\partial \Psi_0}{\partial B_{CDE}} \frac{\partial B_{CDE}}{\partial F^a_{.A}} - F^b_{.B} \left(\frac{\partial \Psi_0}{\partial B_{CDE}} \frac{\partial B_{CDE}}{\partial F^a_{.A:B}} \right)_{;b} \right]$$

$$= g^{da} J^{-1} F^c_{.A} \left[\frac{\partial \Psi_0}{\partial E_{AC}} F_{aC} + \frac{\partial \Psi_0}{\partial B_{ACB}} F_{aC:B} - F^b_{.B} \left(\frac{\partial \Psi_0}{\partial B_{CAB}} F_{aC} \right)_{;b} \right]$$

$$= J^{-1} F^c_{.A} \left[\frac{\partial \Psi_0}{\partial E_{AC}} F^d_{.C} - F^b_{.B} \left(\frac{\partial \Psi_0}{\partial B_{CAB}} \right)_{;b} F^d_{.C} + \left(\frac{\partial \Psi_0}{\partial B_{[AC]B}} \right) F^d_{.C:B} \right].$$

(5.445)

Expanding strain energy density (5.442) in a Taylor expansion to second order in strains and strain gradients about a reference state at which $F^a_{.A} = g^a_{.A}$ and $F^a_{.A:B} = 0$ gives

$$\Psi_0 = \bar{\Psi}_0 + \bar{\mathbb{C}}^{AB} E_{AB} + \bar{\mathrm{D}}^{ABC} B_{ABC} + \frac{1}{2} \bar{\mathbb{C}}^{ABCD} E_{AB} E_{CD}$$
$$+ \frac{1}{2} \bar{\mathrm{D}}^{ABCDEF} B_{ABC} B_{DEF} + \bar{\mathrm{K}}^{ABCDE} E_{AB} B_{CDE},$$

(5.446)

where $\bar{\Psi}_0 = \Psi_0(0,0,X,\mathbf{G}_A)$ is the strain energy density at the reference state, and where constant material coefficients at a material point X are defined as follows:

$$\bar{\mathbb{C}}^{AB} = \left. \frac{\partial \Psi_0}{\partial E_{AB}} \right|_{\substack{\mathbf{E}=0 \\ \mathbf{B}=0}}, \quad \bar{\mathrm{D}}^{ABC} = \left. \frac{\partial \Psi_0}{\partial B_{ABC}} \right|_{\substack{\mathbf{E}=0 \\ \mathbf{B}=0}}, \quad \bar{\mathbb{C}}^{ABCD} = \left. \frac{\partial^2 \Psi_0}{\partial E_{AB} \partial E_{CD}} \right|_{\substack{\mathbf{E}=0 \\ \mathbf{B}=0}}, \quad (5.447)$$

$$\bar{\mathrm{D}}^{ABCDEF} = \left. \frac{\partial^2 \Psi_0}{\partial B_{ABC} \partial B_{DEF}} \right|_{\substack{\mathbf{E}=0 \\ \mathbf{B}=0}}, \quad \bar{\mathrm{K}}^{ABCDE} = \left. \frac{\partial^2 \Psi_0}{\partial E_{AB} \partial B_{CDE}} \right|_{\substack{\mathbf{E}=0 \\ \mathbf{B}=0}}. \quad (5.448)$$

As noted by Toupin (1964), a natural state in which both the stress and hyperstress vanish everywhere may not exist for a given material, and such a state may be an exceptional case rather than the norm. None of the constants in (5.447) and (5.448) need vanish in general for an arbitrary (i.e., fully anisotropic) material of grade two.

Since choice (5.442) is invariant under spatial rotations, (5.437) and hence angular momentum balance (5.441), are satisfied identically. Linear momentum balance (5.433) provides three equations in three unknowns $x^a(X)$, $(a = 1,2,3)$, subject to boundary conditions (5.434) and (5.435).

The theory of hyperelastic materials of grade two presented heretofore in Section 5.7 is a particular kind of generalized continuum theory with

higher-order stresses (i.e., hyperstresses). More general theories have been formulated accounting for dynamics and deformations of microstructures (i.e., director vectors), as summarized by Toupin (1964). Elastic materials of grade two are a particular class of director theory in which a set of directors at X is constrained to deform in conjunction with material particles (i.e., first- and higher-order deformation gradients) at X. More general theories of oriented (micropolar) or micromorphic elastic solids were developed by Cosserat and Cosserat (1909), Ericksen and Truesdell (1958), Toupin (1962, 1964), Mindlin (1964), Eringen and Suhubi (1964), and Eringen (1968), among others. Mindlin (1965) considered elastic bodies whose strain energy density depends on strain and first and second gradients of strain (corresponding to elasticity of grade three in the terminology used in this Chapter), while Green and Rivlin (1964b) considered bodies supporting higher-order stresses work conjugate to velocity gradients of first and arbitrarily higher order. Cosserat and Cosserat (1909) developed a theory of elasticity for a continuum embedded with a triad of rigid directors that may rotate independently of the macroscopic displacement field of material particles, and angular momentum balance (5.441) is often credited to these authors. Eringen (1968) provided some historical references and remarks on early generalized continuum theories. Truesdell and Noll (1965) offered an in-depth analysis of director theories and second-grade elasticity. Green and Naghdi (1995) developed a general procedure for obtaining balance laws for generalized continua using an energy balance, invariance arguments, and thermodynamic principles. Yavari and Marsden (2009) obtained balance laws and constitutive relations for generalized continua (e.g., elastic materials with microstructure) using covariance principles.

Recall that in the case of elasticity, (5.1) applies ($\mathbf{F}(X,t) = \mathbf{F}^{\mathrm{L}}(X,t)$), implying that the (total) covariant derivative of $\mathbf{F}$ reflects material gradients of stretch and rotation of interatomic bond vectors among atoms in a crystal structure. The hyperstress—or its antisymmetric part, the couple stress of (5.440)—reflects moments induced by distributions of interatomic forces and interatomic moments corresponding to these gradients of interatomic bond vectors. Physical origins of higher-order stresses in the context of atomistic force or moment interactions were suggested by Kroner (1963b), Mindlin (1964, 1968a, 1972), Zhou and McDowell (2002), and Sunyk and Steinmann (2003). Kroner (1963b) and Bammann (2001) gave arguments supporting the presence of couple stresses resulting from the stress fields of dislocations in crystals.

If the viewpoint in (5.411) is adopted, elasticity of grade two can be interpreted as providing additional accuracy over elasticity of grade one in

terms of description of the kinematics of deformation. This does not imply that the total covariant derivative of **F** vanishes in elasticity of grade one; rather, this quantity simply does not explicitly enter the thermodynamic potentials in the classical theory. It is noted, however, that series expansion (5.411) is written only to provide physical interpretation of the total covariant derivative of the deformation gradient and does not explicitly enter the subsequent constitutive theory in Section 5.7.

Elasticity of grade two also provides a number of other possible advantages over classical nonlinear elasticity. Strain gradient theories enable numerical solution of certain kinds of boundary value problems without mesh sensitivity that may emerge in classical theories (Menzel and Steinmann 2000; Abu Al-Rub and Voyiadjis 2005). Second- and higher-grade elasticity provides analytical solutions for stress and strain fields produced by dislocation or disclination lines without singularities in these fields near defect cores (Lazar and Maugin 2004, 2005; Deng et al. 2007). Such singularities inevitably arise in solutions obtained from the classical theory of elasticity of grade one, as exemplified by linear elastic solutions for straight line defects listed in Section C.1 of Appendix C. Drawbacks of second-grade elasticity, relative to classical elasticity of grade one, are complex hyperelastic constitutive relations (5.427)-(5.428) and traction boundary conditions (5.434), boundary conditions for the hyperstress (5.435) that may be difficult to interpret physically, and the large number of material constants arising even in the lowest order (quadratic) approximation of the strain energy in (5.446). The latter point is in contrast to classical nonlinear elasticity of grade one, wherein for the lowest degree of symmetry (e.g., a triclinic crystal structure) only 21 distinct second-order elastic constants are required. As a counter-example, Mindlin's geometrically linear theory of elastic materials of grade two with unconstrained micro-deformations (Mindlin 1964) requires 903 independent material coefficients to describe a material of maximum anisotropy, following a Taylor series expansion of the strain energy of quadratic accuracy akin to (5.446).

6 Elastoplasticity

Plasticity attributed to dislocation motion in crystals is considered in detail in Chapter 6. In many crystalline solids, large deformations are not sustainable by thermomechanically recoverable deformation alone. Deviatoric elastic deformations generate shear stresses, which, when large enough, facilitate generation and motion of lattice defects. More specifically, ductile crystals tend to exhibit plastic deformation arising from generation and glide of dislocations (e.g., dislocation lines and loops) when subjected to deviatoric stresses exceeding some mechanical threshold, elastic limit, or yield point. Thermally activated dislocation motion (e.g., kink migration) is possible even when resistance in isolated locations (e.g., in the vicinity of obstacles such as heterogeneities) to glide exceeds the magnitude of average resolved stress acting on a glide plane in the slip direction.

Thermodynamics and kinetics of dislocation-based plasticity have been studied since the early twentieth century. Fundamental restrictions on plastic work or plastic dissipation in the context of the entropy inequality were posited by Drucker (1951) and Ilyushin (1961). These restrictions were generalized to the case of finite deformations, i.e., geometric nonlinearity, by Lee (1969) and Kratochvil (1971). In the context of crystal plasticity theory, Bishop and Hill (1951) suggested a maximum plastic work postulate for determining active slip systems in crystals subjected to small deformations, while Rice (1971), Hill and Rice (1972, 1973), and Havner (1986) studied aspects of the normality structure of finite deformation inelasticity. Kocks et al. (1975) developed a systematic framework for describing thermodynamics and kinetics of slip across a range of length scales spanning from behaviors of individual dislocation segments to large groups of dislocations represented in slip rate variables of continuum crystal plasticity.

Changes in microstructure of crystalline materials occur as lattice defects are generated and propagated, manifesting in changes in the thermodynamic state of the solid. For example, stored energy associated with residual, self-equilibrated stress fields attributed to defects in crystals, often referred to as stored energy of cold working, has been investigated for some time (Farren and Taylor 1925; Taylor and Quinney 1934; Zener

1942; Toupin and Rivlin 1960; Wright 1982; Rosakis et al. 2000; Longere and Dragon 2008). This energy is properly reflected in the thermodynamic potentials via prescription of dependence of such potentials on evolving internal state variables representing densities of defects in the solid.

In geometrically nonlinear elastoplasticity, a naturally arising conjugate thermodynamic force to the plastic velocity gradient is a variant of the so-called Eshelby stress tensor (Maugin 1994; Svendsen 2001; Clayton et al. 2004b). The divergence of the Eshelby stress is a material force, i.e., an energy gradient, associated with explicit changes in position of heterogeneities, as demonstrated in the context of linear elasticity (Eshelby 1951) and nonlinear elasticity (Eshelby 1975; Epstein and Maugin 1990; Maugin 1994, 1995). Tensors of similar nature but often not identical mathematical form, often referred to as energy-momentum tensors or chemical potential tensors depending on context, have been used to describe a number of phenomena in continuum physics (Bowen 1967; Grinfeld 1981, 1991; Hill 1986; Maugin and Epstein 1991; Gurtin 1995; Maugin 1994, 1995; Cermelli and Fried 1997).

Chapter 6 is organized as follows. A general formulation of finite deformation elastoplasticity is presented in Section 6.1, following the formalism of the internal state variable framework described in Section 4.2, and in the context of balance laws for classical continua given in Section 4.1. Most aspects of the kinematic and thermodynamic description are now standard in the finite deformation plasticity literature (Lee 1969; Bammann and Aifantis 1987; Lubliner 1990; Scheidler and Wright 2001), with the deformation gradient decomposed into lattice and plastic parts according to (3.31), $\mathbf{F} = \mathbf{F}^{\mathbf{L}}\mathbf{F}^{\mathbf{P}}$, and the Helmholtz free energy density dependent upon the stretch associated with the lattice deformation $\mathbf{F}^{\mathbf{L}}$, the temperature, and one or more internal state variables accounting for stored energy associated with lattice defects. The formulation presented here differs from many others, however, via its consideration of thermodynamic potentials measured per unit volume in an unstressed intermediate configuration, as opposed to thermodynamic potentials measured per unit mass. This difference turns out to be inconsequential, however, when inelastic deformation is isochoric, as is the case with pure slip as defined by (3.97)-(3.100) and demonstrated in (3.121) in the context of crystal plasticity.

Specialization of the general formulation to discrete dislocation-based plasticity of Section 3.2.5 and crystal plasticity of Section 3.2.6 then follow in Sections 6.2 and 6.3, respectively. In the former, a vector measure of force per unit length analogous to the Peach-Koehler force (Peach and Koehler 1950) emerges as the conjugate force to the velocity of mobile line defects, i.e., glissile dislocation segments. In the latter, the dissipative

part of the stress power can be decomposed into a sum of products of slip rates and conjugate shear stresses acting on each glide system. Kinetic equations for inelastic deformation rates (i.e., dislocation velocities and slip rates), both thermodynamically admissible and physically motivated, are discussed, primarily following the scheme of Kocks et al. (1975). A concise summary of general kinetic relations encountered in classical macroscopic plasticity theory is then presented in Section 6.4, wherein the notion of a dissipation potential first introduced in Section 4.3 proves useful. Reduction of the nonlinear theory of elastoplasticity to the geometrically linear case is given in Section 6.5.

In the thermodynamic analysis of Section 6.1, a stress tensor similar in appearance to several proposed by Eshelby (Eshelby 1951, 1975) is found to act as a conjugate driving force to the time rate of plastic deformation. This stress quantity is considered in Section 6.6 from the perspective of material forces in continuum elasticity theory.

Chapter 6 concludes, in Section 6.7, with an extension of elasticity of grade two of Section 5.7 to the context of multiplicative elastoplasticity. The presentation of Section 6.7 focuses on large elastic deformations from a stationary, but possibly anholonomic, intermediate configuration in the athermal case. Dissipative processes associated with evolution of the intermediate configuration are not explicitly considered, nor are temperature effects. Governing equations and boundary conditions are derived using a variational principle, following Teodosiu (1967a, b).

The content of Chapter 6 by no means constitutes a complete treatment of the field of plasticity; entire texts have been devoted to sub-disciplines addressed in individual Sections of Chapter 6. A few relevant general references on plasticity theory include books of Hill (1950), Nadai (1950), Schmid and Boas (1950), Lubliner (1990), Khan and Huang (1995), and Nemat-Nasser (2004). Texts including treatments of dislocation kinetics and single crystal slip include those of Friedel (1964), Nabarro (1967), Hirth and Lothe (1982), and Havner (1992), and the extensive article of Kocks, Argon, and Ashby (1975).

6.1 Two-term Multiplicative Elastoplasticity

Early investigations (Lee 1969; Teodosiu 1970; Kratochvil 1971) of thermomechanics of crystalline bodies in the context of the two-term multiplicative decomposition followed a scheme similar to that posited here, apart from the distinction that the present analysis is conducted with energetic

quantities measured on a per-unit-volume basis as opposed to a per-unit-mass basis. According to (3.31), let

$$\mathbf{F} = \mathbf{F}^{\mathbf{L}}\mathbf{F}^{\mathbf{P}}, \; F^a_{.A} = F^{La}_{.\alpha}F^{P\alpha}_{.A}, \tag{6.1}$$

whereby total deformation gradient $\mathbf{F}$ is decomposed multiplicatively into lattice deformation $\mathbf{F}^{\mathbf{L}}$ and plastic deformation $\mathbf{F}^{\mathbf{P}}$, neither of which necessarily satisfies integrability conditions (3.42). Recall from Fig. 3.4 that (6.1) implies the existence of a number of configurations for each material element: reference configuration B_0, intermediate configuration $\tilde{B}$, and current or spatial configuration B. The intermediate configuration is anholonomic unless conditions (3.42) are satisfied. Terms entering decomposition (6.1) act as mappings between tangent bundles on each configuration, i.e., $\mathbf{F}:TB_0 \to TB$, $\mathbf{F}^{\mathbf{P}}:TB_0 \to T\tilde{B}$, and $\mathbf{F}^{\mathbf{L}}:T\tilde{B} \to TB$. The lattice deformation $\mathbf{F}^{\mathbf{L}}$ encompasses both mechanical elastic deformation and thermal deformation following the theory of traditional thermoelasticity outlined in Sections 5.1-5.4; mechanical and thermal origins of lattice deformation are not explicitly delineated in the kinematic description of Chapter 6, in contrast to the treatment of Section 5.5.

As illustrated in Fig. 3.5 and discussed at length in Sections 3.2.2, 3.2.5, 3.2.6, and 3.2.7, plastic deformation $\mathbf{F}^{\mathbf{P}}$ is by definition lattice-preserving, meaning that $\mathbf{F}^{\mathbf{P}}$ does not alter the arrangement of the lattice, such as distances between atoms and angles between atomic bonds; i.e., lattice parameters and bond vectors are not changed by plastic deformation. For example, when $\mathbf{F}^{\mathbf{P}}$ is attributed to glide of full (as opposed to partial) dislocations and loops, relative tangential displacements of planes of atoms occur in discrete steps corresponding to scalar multiples of the Burgers vector. After the crystal has been affected by $\mathbf{F}^{\mathbf{P}}$ alone, its shape may have changed (e.g., steps may exist on the surface of a crystal with initially flat faces), but the structure of its interior is assumed to remain unchanged presuming no dislocations remain within its volume. Of course, in real crystals, plastic deformation does not occur in isolation without some accompanying deformation of the lattice $\mathbf{F}^{\mathbf{L}}$, so that consideration of $\mathbf{F}^{\mathbf{P}}$ in isolation is a hypothetical exercise conducted only to lend physical interpretation to (6.1). Because of the lattice-preserving property of $\mathbf{F}^{\mathbf{P}}$, the kinematic state (i.e., orientation and stretch) of the bulk lattice in intermediate configuration $\tilde{B}$ appears identical to the kinematic state of the bulk lattice in reference configuration B_0. Inverse lattice tangent map $\mathbf{F}^{\mathbf{L}-1}:TB \to T\tilde{B}$ returns the crystal from its possibly stretched and rotated condition to the unstressed intermediate configuration. The thermal constituent of $\mathbf{F}^{\mathbf{L}-1}$ corresponds to deformation of the crystal from its current

temperature to a reference temperature at which the contribution to stress from thermoelastic coupling (i.e., thermal expansion or contraction) vanishes. Vice-versa, action of the lattice deformation $\mathbf{F^L}$ takes the crystal from its evolving unloaded state at a reference temperature to its current stressed and rotated state at the current temperature. Thus, intermediate configuration $\tilde{B}$ serves as an updated reference configuration for the instantaneous thermoelastic response. Hence, a thermodynamic analysis analogous to that performed for elastic bodies in Chapter 5 with reference configuration B_0 serving as the reference state for thermoelastic response is conducted in what follows in Chapter 6 for elastic-plastic bodies with evolving intermediate configuration $\tilde{B}$ serving as the reference state for thermoelastic response. Following the formulation of Section 5.1 of Chapter 5, the elastic response addressed in Section 6.1 is treated as hyperelastic of grade one, with full account of geometric and material nonlinearities and material anisotropy appropriate to the particular crystal class under consideration. Viscoelastic phenomena are not addressed.

6.1.1 Constitutive Assumptions

A number of variables defined with respect to intermediate configuration $\tilde{B}$ are introduced:

$$\tilde{\rho} = \rho_0 J^{P-1} = \rho J^L, \tag{6.2}$$

$$\tilde{\Psi} = \tilde{\rho}\psi, \; \tilde{E} = \tilde{\rho}e, \; \tilde{N} = \tilde{\rho}\eta, \tag{6.3}$$

$$2\tilde{E}^L_{\alpha\beta} = \tilde{C}^L_{\alpha\beta} - \tilde{g}_{\alpha\beta} = F^{La}_{.\alpha}g_{ab}F^{Lb}_{.\beta} - \tilde{g}_{\alpha\beta}, \tag{6.4}$$

$$\tilde{\Sigma}^{\alpha\beta} = J^{P-1}F^{P\alpha}_{.A}\Sigma^{AB}F^{P\beta}_{.B} = J^L F^{L-1\alpha}_{.a}\sigma^{ab}F^{L-1\beta}_{.b}, \tag{6.5}$$

$$\theta_{,\alpha} = \theta_{,A}F^{P-1A}_{.\alpha} = \theta_{,a}F^{La}_{.\alpha} = \tilde{\nabla}_\alpha\theta, \tag{6.6}$$

$$\tilde{q}^\alpha = J^{P-1}F^{P\alpha}_{.A}Q^A = J^L F^{L-1\alpha}_{.a}q^a. \tag{6.7}$$

Mass density per unit intermediate volume $\tilde{\rho}$ in (6.2) follows from (3.48), (3.49), and (4.10), noting that $J = J^L J^P$. While plastic deformation is usually assumed to be isochoric following arguments that dislocation glide is lattice-preserving and hence volume conservative (Sections 3.2.2 and 3.2.5), for illustrative purposes the requirement $J^P = 1$ is not enforced in the present mathematical developments. The Helmholtz free energy $\tilde{\Psi}$, internal energy $\tilde{E}$, and specific entropy $\tilde{N}$ are defined on a per unit intermediate configuration volume basis in (6.3). Definitions in (6.4) of symmetric covariant lattice deformation and symmetric lattice strain, both with indices referred to the span of cotangent spaces $T^*\tilde{B} \times T^*\tilde{B}$, follow

from (3.52) and (3.65). Relationships among contravariant lattice stress $\tilde{\boldsymbol{\Sigma}} \in T\tilde{B} \times T\tilde{B}$ (symmetric automatically by (4.26), (4.27), and (6.5)), second Piola-Kirchhoff stress $\boldsymbol{\Sigma}$ of (4.7), and Cauchy stress $\boldsymbol{\sigma}$ of (4.3) and (4.6) are analogous to those between the latter two in Table 4.1, but with coordinate transformations conducted here only with respect to either plastic or lattice parts of the total deformation gradient $\mathbf{F}$. The intermediate temperature gradient in (6.6) follows from the definition of the anholonomic partial derivative given in (3.36). The covariant derivative in intermediate coordinates in the last of (6.6) is valid only for a scalar function. In contrast, the covariant derivative of a vector or tensor will depend on the particular definition used for the anholonomic covariant derivative (e.g., see later (6.38)) and may depend on the choice of coordinate basis $\tilde{\mathbf{g}}_{\alpha}$ and coefficients $\tilde{\Gamma}^{..\alpha}_{\beta\chi}$ introduced for configuration $\tilde{B}$. These coefficients could be defined as anholonomic transformations from reference or spatial Christoffel symbols, using (3.38) or (3.39), respectively. However, in practice, following discussion in Section 3.2.3 and (3.51), an external Cartesian coordinate frame is usually assigned to $\tilde{B}$, leading to $\tilde{g}_{\alpha\beta} = \delta_{\alpha\beta}$ in (6.4) and $\tilde{\Gamma}^{..\alpha}_{\beta\chi} = 0$. In the first of (6.7), the heat flux vector $\mathbf{Q}$ transforms from reference to intermediate configuration in a similar manner as in (4.36), and the second of (6.7) then follows automatically from the first of (6.7) and (6.1).

Under rigid body motions of the spatial frame of the form $\mathbf{x} \to \hat{\mathbf{Q}}\mathbf{x} + \mathbf{c}$, where $\hat{\mathbf{Q}} = \hat{\mathbf{Q}}^{-T}$ is a rotation matrix and $\mathbf{c}$ is a translation vector independent of position, the following transformation laws are assumed to hold, with intermediate and reference configurations held fixed (Bammann and Johnson 1987):

$$\mathbf{F} \to \hat{\mathbf{Q}}\mathbf{F}, \ \mathbf{F^L} \to \hat{\mathbf{Q}}\mathbf{F^L}, \ \mathbf{F^P} \to \mathbf{F^P}, \tag{6.8}$$

and since $\det\hat{\mathbf{Q}} = 1$, it follows that scalars $J^L \to J^L$ and $J^P \to J^P$. Following from (6.8), variables defined with respect to the intermediate configuration in (6.2)-(6.7) all remain invariant under such rigid rotation and translation. Invariance of scalar quantities in (6.2) and (6.3) follows trivially from conservation of mass (i.e., invariance of the reference mass density ρ_0) and invariance of J^P. Invariance of $\tilde{\mathbf{C}}^{\mathbf{L}}$ and $\tilde{\mathbf{E}}^{\mathbf{L}}$ follows from direct calculation using the second of (6.8). Invariance of $\tilde{\boldsymbol{\Sigma}}$, $\tilde{\nabla}\theta$, and $\tilde{\mathbf{q}}$ follow, respectively, from invariance of reference quantities $\boldsymbol{\Sigma}$, $\theta_{,A}$, and $\mathbf{Q}$ entering (6.5)-(6.7) (see (4.50)-(4.51)) and from invariance of $\mathbf{F^P}$ in the last of (6.8).

Objective forms of constitutive assumptions (4.45)-(4.49) are specified as follows for elastic-plastic solids:

$$\tilde{\varPsi} = \tilde{\varPsi}\left(\tilde{\mathbf{E}}^{\mathbf{L}}, \alpha, \theta, \tilde{\nabla}\theta, X, \tilde{\mathbf{g}}_{\alpha}\right), \ \tilde{\varPsi} = \tilde{\varPsi}\left(\tilde{E}^{L}_{\alpha\beta}, \alpha, \theta, \tilde{\nabla}_{\alpha}\theta, X, \tilde{\mathbf{g}}_{\alpha}\right); \qquad (6.9)$$

$$\tilde{N} = \tilde{N}\left(\tilde{\mathbf{E}}^{\mathbf{L}}, \alpha, \theta, \tilde{\nabla}\theta, X, \tilde{\mathbf{g}}_{\alpha}\right), \ \tilde{N} = \tilde{N}\left(\tilde{E}^{L}_{\alpha\beta}, \alpha, \theta, \tilde{\nabla}_{\alpha}\theta, X, \tilde{\mathbf{g}}_{\alpha}\right); \qquad (6.10)$$

$$\tilde{\boldsymbol{\Sigma}} = \tilde{\boldsymbol{\Sigma}}\left(\tilde{\mathbf{E}}^{\mathbf{L}}, \alpha, \theta, \tilde{\nabla}\theta, X, \tilde{\mathbf{g}}_{\alpha}\right), \ \tilde{\Sigma}^{\alpha\beta} = \tilde{\Sigma}^{\alpha\beta}\left(\tilde{E}^{L}_{\alpha\beta}, \alpha, \theta, \tilde{\nabla}_{\alpha}\theta, X, \tilde{\mathbf{g}}_{\alpha}\right); \quad (6.11)$$

$$\tilde{\mathbf{q}} = \tilde{\mathbf{q}}\left(\tilde{\mathbf{E}}^{\mathbf{L}}, \alpha, \theta, \tilde{\nabla}\theta, X, \tilde{\mathbf{g}}_{\alpha}\right), \ \tilde{q}^{\alpha} = \tilde{q}^{\alpha}\left(\tilde{E}^{L}_{\alpha\beta}, \alpha, \theta, \tilde{\nabla}_{\alpha}\theta, X, \tilde{\mathbf{g}}_{\alpha}\right); \qquad (6.12)$$

$$\dot{\alpha} = \dot{\alpha}\left(\tilde{\mathbf{E}}^{\mathbf{L}}, \alpha, \theta, \tilde{\nabla}\theta, X, \tilde{\mathbf{g}}_{\alpha}\right), \ \dot{\alpha} = \dot{\alpha}\left(\tilde{E}^{L}_{\alpha\beta}, \alpha, \theta, \tilde{\nabla}_{\alpha}\theta, X, \tilde{\mathbf{g}}_{\alpha}\right); \qquad (6.13)$$

where $\alpha(X,t)$ denotes a scalar internal state variable of the sort discussed in Section 4.2.1, accounting for changes in the thermodynamic potentials or response functions of the crystalline solid attributed to sources other than changes in the lattice strain, temperature, and temperature gradient. For simplicity of presentation, only a single scalar internal state variable is considered here, though multiple internal state variables, including scalars and/or vector- or tensor-valued internal variables of higher order, can be included without conceptual difficulty, as demonstrated by example later in Chapters 8 and 9. Constitutive assumptions (6.9)-(6.12) are analogous to those of thermoelasticity theory in (5.15)-(5.18). Dependence of response functions on lattice strain accounts for changes in energy and stress associated with stretching of atomic bonds, for example. The same arguments given in Section 5.1.1 apply here (and in subsequent Chapters 8, 9, and 10) with regards to possible inner displacements that may implicitly affect strain energy in polyatomic crystals: such inner displacements are presumed obtainable (e.g., via energy minimization) when other state variables are prescribed, and hence are not independent state variables (though conceivably, inner displacements could be addressed via internal state variables (Garikipati 2003)). Dependence of response functions on temperature and temperature gradient follows the same arguments given in Section 5.1.1. Dependence of response functions on reference position X of a material particle accounts for heterogeneity (e.g., variations in material properties with position), while dependence on intermediate basis vectors $\tilde{\mathbf{g}}_{\alpha}$ is written out explicitly to account for elastic anisotropy that exists in almost all single crystals, following the notational schemes of Chapter 5 and Eringen (1962). Though not explicitly listed in (6.9)-(6.13), an additional relationship is usually required to dictate evolution of plastic deformation $\mathbf{F}^{\mathbf{P}}$, e.g., a kinetic equation for dislocation velocity, slip system shearing, or deviatoric plastic flow, as discussed in more detail in Sections 6.2, 6.3, and 6.4.

Notice that no dependence of free energy, entropy, stress, or other re-sponse functions upon plastic deformation is prescribed explicitly, i.e., the mapping $\mathbf{F}^{\mathbf{P}}(X,t)$ is not included in the list of independent variables en-tering (6.9)-(6.13). Recall from Chapter 3 that plastic deformation $\mathbf{F}^{\mathbf{P}}$ represents the shape change of an element of the crystal that has undergone plastic slip. Because $\mathbf{F}^{\mathbf{P}}$ is lattice-preserving, energetic or stress changes directly associated with changes in atomic arrangement (e.g., bond stretch-ing, bond angle changes, and lattice vibrations) by definition are not re-flected by $\mathbf{F}^{\mathbf{P}}$. Defects such as pinned dislocations may naturally be asso-ciated with residual strain energy of the solid and may accumulate with plastic deformation; in such cases, the corresponding change in the local thermodynamic state of the solid is reflected by a change in the local value of internal variable α. For example, consider a ductile crystalline sample that is deformed plastically by $\mathbf{F}^{\mathbf{P}}$, and then returned via $\mathbf{F}^{\mathbf{P}-1}$ to its origi-nal shape. After this cyclic deformation process, the material may have accumulated defects and stored energy (e.g., energy of cold working), but will exhibit null net plastic strain, i.e., $\mathbf{F}^{\mathbf{P}}=\mathbf{1}$ at the conclusion of the ex-periment. In this case, the (null) change in plastic deformation is unable to indicate energetic changes in the crystal, and hence an internal state vari-able is needed to reflect such changes associated with null net, but nonzero cumulative, plastic strain. In ductile metallic crystals, a typical physically motivated choice of internal variable is the line length per unit volume of dislocations, either scalar or tensor in rank (Kroner 1963a; Teodosiu 1970), though a complete set of internal state variables should logically also include other relevant anomalies in the crystal structure that affect the thermodynamic response functions (Kratochvil 1971, 1972), e.g., densities of point defects, grain and sub-grain boundaries, deformation twins, inclu-sions, voids, micro-cracks, and so forth.

6.1.2 Thermodynamics

According to (4.71), the entropy production inequality can be written as

$$\Sigma^{AB}\dot{E}_{AB} - \rho_0(\dot{\psi} + \eta\dot{\theta}) - \theta^{-1}Q^A\theta_{,A} \geq 0. \tag{6.14}$$

The stress power per unit reference volume can be written

$$\Sigma^{AB}\dot{E}_{AB} = J\sigma_a^{.b}L_{.b}^a = J^P(J^L F_{.b}^{L-1\beta}\sigma_a^{.b}F_{.\alpha}^{La})(F_{.e}^{L-1\alpha}L_{.d}^e F_{.\beta}^{Ld})$$
$$= J^P\tilde{M}_\alpha^{.\beta}\tilde{L}_{.\beta}^\alpha, \tag{6.15}$$

where quantity $\tilde{\mathbf{M}}$, often called the Mandel stress (Mandel 1974), and the velocity gradient pulled back to intermediate configuration $\tilde{B}$ are defined, respectively, by

$$\tilde{M}_{\alpha}^{\cdot\beta} = J^{L} F_{\cdot a}^{La} \sigma_{a}^{\cdot b} F_{\cdot b}^{L-1\beta} = \tilde{C}_{\alpha\delta}^{L} \tilde{\Sigma}^{\delta\beta} , \quad \tilde{L}_{\cdot\beta}^{\alpha} = F^{L-1\alpha} L_{\cdot b}^{a} F_{\cdot\beta}^{Lb} , \qquad (6.16)$$

where (6.4) and (6.5) have been used. Notice that $\tilde{C}_{\alpha\delta}^{L}$ acts as a natural intermediate metric (see Section 3.2.3) for lowering the index of the lattice stress $\tilde{\Sigma}^{\delta\beta}$ in the definition of the Mandel stress. The quantity $\tilde{M}_{\chi}^{\cdot\beta} \tilde{g}^{\alpha\chi}$ is generally not symmetric in contravariant indices. The total velocity gradient of (3.58) is

$$\mathbf{L} = \overset{\mathbf{g}}{\nabla} \mathbf{v} = \dot{\mathbf{F}} \mathbf{F}^{-1} = \dot{\mathbf{F}}^{\mathbf{L}} \mathbf{F}^{\mathbf{L}-1} + \mathbf{F}^{\mathbf{L}} \dot{\mathbf{F}}^{\mathbf{P}} \mathbf{F}^{\mathbf{P}-1} \mathbf{F}^{\mathbf{L}-1} , \qquad (6.17)$$

leading to

$$\tilde{\mathbf{L}} = \mathbf{F}^{\mathbf{L}-1} \dot{\mathbf{F}}^{\mathbf{L}} + \dot{\mathbf{F}}^{\mathbf{P}} \mathbf{F}^{\mathbf{P}-1} . \qquad (6.18)$$

The material time derivative of the free energy per unit intermediate volume is, from (6.2) and (6.3),

$$\dot{\tilde{\Psi}} = \frac{d}{dt}(\tilde{\rho}\psi) = \tilde{\rho}\dot{\psi} + \dot{\tilde{\rho}}\psi = J^{P-1}\rho_{0}\dot{\psi} - \dot{J}^{P} J^{P-2} \rho_{0}\psi$$

$$= \tilde{\rho}(\dot{\psi} - \dot{F}_{\cdot A}^{P\alpha} F_{\cdot\alpha}^{P-1A}\psi) = \tilde{\rho}\dot{\psi} - \tilde{\Psi} L_{\cdot\alpha}^{P\alpha} = \tilde{\rho}\dot{\psi} - \tilde{\Psi} D_{\cdot\alpha}^{P\alpha} , \qquad (6.19)$$

via a relation akin to (2.181)[1]. Substituting (6.2), (6.3), (6.6), (6.7), (6.15), (6.18), and (6.19) into (6.14) and multiplying by J^{P-1} gives the local entropy production inequality referred to intermediate configuration $\tilde{B}$:

$$\tilde{M}_{\alpha}^{\cdot\beta} \tilde{L}_{\cdot\beta}^{\alpha} - \tilde{\Psi} L_{\cdot\beta}^{P\alpha} \delta_{\cdot\alpha}^{\beta} - \dot{\tilde{\Psi}} - \tilde{N}\dot{\theta} - \theta^{-1} \tilde{q}^{\alpha} \theta_{,\alpha} \geq 0 , \qquad (6.20)$$

where $\mathbf{L}^{\mathbf{P}} = \dot{\mathbf{F}}^{\mathbf{P}} \mathbf{F}^{\mathbf{P}-1}$ is the plastic velocity gradient introduced in (3.58). Using (6.16) and (6.18),

$$\tilde{M}_{\alpha}^{\cdot\beta} \tilde{L}_{\cdot\beta}^{\alpha} = \tilde{M}_{\alpha}^{\cdot\beta} F_{\cdot a}^{L-1\alpha} \dot{F}_{\cdot\beta}^{La} + \tilde{M}_{\alpha}^{\cdot\beta} L_{\cdot\beta}^{P\alpha}$$

$$= (F_{\cdot a}^{L-1\delta a} F_{\cdot a}^{L-1\alpha} \tilde{M}_{\alpha}^{\cdot\beta})(F_{\cdot b\delta}^{L} \dot{F}_{\cdot\beta}^{Lb}) + \tilde{M}_{\alpha}^{\cdot\beta} L_{\cdot\beta}^{P\alpha} \qquad (6.21)$$

$$= \tilde{C}^{L-1\delta\alpha} \tilde{C}_{\alpha\chi}^{L} \tilde{\Sigma}^{\beta\chi} \dot{\tilde{E}}_{\delta\beta}^{L} + \tilde{M}_{\alpha}^{\cdot\beta} L_{\cdot\beta}^{P\alpha} = \tilde{\Sigma}^{\beta\delta} \dot{\tilde{E}}_{\delta\beta}^{L} + \tilde{M}_{\alpha}^{\cdot\beta} L_{\cdot\beta}^{P\alpha} ,$$

where $\dot{\tilde{g}}_{\alpha\beta} = d(\tilde{\mathbf{g}}_{\alpha} \cdot \tilde{\mathbf{g}}_{\beta})/dt = 0$ has been assumed. From (6.9) with $\dot{\tilde{\mathbf{g}}}_{\alpha} = 0$,

$$\dot{\tilde{\Psi}} = \frac{\partial \tilde{\Psi}}{\partial \tilde{E}_{\alpha\beta}^{L}} \dot{\tilde{E}}_{\alpha\beta}^{L} + \frac{\partial \tilde{\Psi}}{\partial \theta} \dot{\theta} + \frac{\partial \tilde{\Psi}}{\partial \theta_{,\alpha}} \dot{\tilde{\gamma}}_{\alpha} + \frac{\partial \tilde{\Psi}}{\partial \alpha} \dot{\alpha} , \qquad (6.22)$$

where the intermediate rate of temperature gradient satisfies

---

[1] From (2.225), $\dfrac{d(\ln J^{P})}{dt} = \dfrac{\dot{J}^{P}}{J^{P}} = \dfrac{1}{J^{P}} \dfrac{\partial J^{P}}{\partial F_{\cdot A}^{P\alpha}} \dot{F}_{\cdot A}^{P\alpha} = F_{\cdot\alpha}^{P-1A} \dot{F}_{\cdot A}^{P\alpha} = L_{\cdot\alpha}^{P\alpha} = D_{\cdot\alpha}^{P\alpha} .$

$$\tilde{\gamma}_\alpha = \frac{d\theta_{,\alpha}}{dt} = \frac{d(\theta_{,A}F^{P-1A}_{.\alpha})}{dt} = \dot\theta_{,\alpha} + \theta_{,\beta}F^{P\beta}_{.A}\dot{F}^{P-1A}_{.\alpha} = \dot\theta_{,\alpha} - \theta_{,\beta}L^{P\beta}_{.\alpha}. \quad (6.23)$$

Using (6.21) and (6.22) in (6.20), the local dissipation inequality becomes

$$\left(\tilde{\Sigma}^{\alpha\beta} - \frac{\partial\tilde{\Psi}}{\partial\tilde{E}^L_{\alpha\beta}}\right)\dot{\tilde{E}}^L_{\alpha\beta} - \left(\tilde{N} + \frac{\partial\tilde{\Psi}}{\partial\theta}\right)\dot\theta - \frac{\partial\tilde{\Psi}}{\partial\theta_{,\alpha}}\tilde{\gamma}_\alpha$$

$$+\left(\tilde{M}^{.\beta}_\alpha - \tilde{\Psi}\delta^\beta_{.\alpha}\right)L^{P\alpha}_{.\beta} - \frac{\partial\tilde{\Psi}}{\partial\alpha}\dot\alpha - \theta^{-1}\tilde{q}^\alpha\theta_{,\alpha} \geq 0. \quad (6.24)$$

Extending the logic of Section 5.1.2, coefficients of rates $\dot{\tilde{E}}^L$, $\dot\theta$, and $\tilde{\gamma}$ should vanish identically to ensure thermodynamic admissibility, presuming such rates can be prescribed independently of each other and their coefficients in a thermodynamic process. Constitutive relations

$$\tilde{\Sigma} = \frac{\partial\tilde{\Psi}}{\partial\tilde{E}^L} = \tilde{\Sigma}^T, \quad \tilde{N} = -\frac{\partial\tilde{\Psi}}{\partial\theta}, \quad \frac{\partial\tilde{\Psi}}{\partial(\nabla\theta)} = 0 \quad (6.25)$$

are then deduced immediately from (6.24). Hence, it follows that free energy, entropy, and stress do not depend explicitly on temperature gradient:

$$\tilde{\Psi} = \tilde{\Psi}\left(\tilde{E}^L, \alpha, \theta, X, \tilde{g}_\alpha\right), \quad \tilde{N} = \tilde{N}\left(\tilde{E}^L, \alpha, \theta, X, \tilde{g}_\alpha\right),$$

$$\tilde{\Sigma} = \tilde{\Sigma}\left(\tilde{E}^L, \alpha, \theta, X, \tilde{g}_\alpha\right). \quad (6.26)$$

Cauchy stress and specific entropy per unit mass are found, respectively, from (6.5) and (6.3):

$$\sigma^{ab} = J^{-1}F^{La}_{.\alpha}\frac{\partial\tilde{\Psi}}{\partial\tilde{E}^L_{\alpha\beta}}F^{Lb}_{.\beta} = J^{-1}F^{Lb}_{.\beta}\frac{\partial\tilde{\Psi}}{\partial\tilde{E}^L_{\beta\alpha}}F^{La}_{.\alpha} = \sigma^{ba}, \quad \eta = -\frac{1}{\tilde{\rho}}\frac{\partial\tilde{\Psi}}{\partial\theta}. \quad (6.27)$$

Since $\tilde{E}^L_{\alpha\beta} = \tilde{E}^L_{\beta\alpha}$ identically by definition (6.4), $\tilde{\Sigma}^{\alpha\beta} = \tilde{\Sigma}^{\beta\alpha}$ as in (6.25), and $\sigma^{ab} = \sigma^{ba}$ as indicated in (6.27). Thus the Cauchy stress is consistently symmetric, and angular momentum balance (4.26) holds identically. Using the chain rule and the functional dependency $\tilde{C}^L_{\alpha\beta} = \tilde{C}^L_{\alpha\beta}(F^{La}_{.\alpha}, g_{ab})$,

$$2\frac{\partial\tilde{\Psi}}{\partial g_{ab}} = 2\frac{\partial\tilde{\Psi}}{\partial\tilde{C}^L_{\alpha\beta}}\frac{\partial\tilde{C}^L_{\alpha\beta}}{\partial g_{ab}} = F^{La}_{.\alpha}\frac{\partial\tilde{\Psi}}{\partial\tilde{E}^L_{\alpha\beta}}F^{Lb}_{.\beta}, \quad (6.28)$$

a relationship similar to Doyle-Ericksen formula (5.36) of nonlinear hyperelasticity emerges:

$$\sigma^{ab} = 2J^{L-1}\frac{\partial \tilde{\Psi}}{\partial g_{ab}} = 2\left[\frac{\partial(J^{-1}\Psi_0)}{\partial g_{ab}}\right] - 2\left[\tilde{\Psi}\frac{\partial(J^{L-1})}{\partial g_{ab}}\right]$$

$$= 2\left[J^{-1}\frac{\partial \Psi_0}{\partial g_{ab}} + \Psi_0\frac{\partial J^{-1}}{\partial g_{ab}}\right] - 2\left[\tilde{\Psi}\frac{\partial(J^{L-1})}{\partial g_{ab}}\right]$$

$$= 2J^{-1}\frac{\partial \Psi_0}{\partial g_{ab}} - \Psi_0 J^{-2}\sqrt[-1]{gG}\det(F^a_{.A})\frac{\partial g}{\partial g_{ab}}$$

$$+ \tilde{\Psi}J^{L-2}\sqrt[-1]{g\tilde{g}}\det(F^{La}_{.\alpha})\frac{\partial g}{\partial g_{ab}} \tag{6.29}$$

$$= 2J^{-1}\frac{\partial \Psi_0}{\partial g_{ab}} - \Psi_0 J^{-2}\sqrt{g/G}\det(F^a_{.A})g^{ab}$$

$$+ \tilde{\Psi}J^{L-2}\sqrt{g/\tilde{g}}\det(F^{La}_{.\alpha})g^{ab}$$

$$= 2J^{-1}\frac{\partial \Psi_0}{\partial g_{ab}} - J^{-1}\Psi_0 g^{ab} + J^{L-1}\tilde{\Psi}g^{ab}$$

$$= 2J^{-1}\rho_0\frac{\partial \psi}{\partial g_{ab}} = 2\rho\frac{\partial \psi}{\partial g_{ab}},$$

where (2.142)-(2.144), (3.48), (4.8), (4.9), and (6.3) have been used. A particular version of (6.29) with $\det(g_{ab}) = g = $ constant was derived by Clayton et al. (2004b).

A number of other relations for stresses can be derived using the chain rule in a similar manner[2]. Table 4.1 provides some requisite identities.

---

[2] Because $\mathbf{F^L} = \mathbf{FF^{P-1}}$, $\tilde{\Psi}(\tilde{\mathbf{E}}^L,\alpha,\theta,X,\tilde{\mathbf{g}}_\alpha) = J^{P-1}\Psi_0(\mathbf{F^L}(\mathbf{F},\mathbf{F^P},\mathbf{g}),\alpha,\theta,X,\tilde{\mathbf{g}}_\alpha)$. Holding $(\alpha,\theta,X,g_{ab},\tilde{\mathbf{g}}_\alpha)$ fixed, first Piola-Kirchhoff and Mandel stresses satisfy

$$\frac{\partial \Psi_0}{\partial F^a_{.A}}\bigg|_{\mathbf{F^P}} = \frac{\partial(J^P\tilde{\Psi})}{\partial \tilde{E}^L_{\alpha\beta}}\frac{\partial \tilde{E}^L_{\alpha\beta}}{\partial F^{Lb}_{.\chi}}\frac{\partial F^{Lb}_{.\chi}}{\partial F^a_{.A}}\bigg|_{\mathbf{F^P}} = \frac{1}{2}J^P\tilde{\Sigma}^{\alpha\beta}(\delta^\chi_{.\beta}F^L_{b\alpha} + \delta^\chi_{.\alpha}F^L_{b\beta})\frac{\partial(F^b_{.B}F^{P-1B}_{.\chi})}{\partial F^a_{.A}}\bigg|_{\mathbf{F^P}}$$

$$= J^P\tilde{\Sigma}^{\alpha\chi}F^L_{b\alpha}F^{P-1B}_{.\chi}\delta^b_{.a}\delta^A_{.B} = J^PF^L_{a\alpha}(J^{P-1}F^{P\alpha}_{.B}\Sigma^{BC}F^{P\chi}_{.C})F^{P-1A}_{.\chi}$$

$$= F_{aB}\Sigma^{BA} = P^A_{a.},$$

$$\frac{\partial \Psi_0}{\partial F^{P\alpha}_{.A}}\bigg|_{\mathbf{F}} = \frac{\partial \Psi_0}{\partial F^{P\alpha}_{.A}}\bigg|_{\mathbf{F^L}} + \frac{\partial \Psi_0}{\partial F^{La}_{.\beta}}\bigg|_{\mathbf{F^P}}\frac{\partial F^{La}_{.\beta}}{\partial F^{P\alpha}_{.A}}\bigg|_{\mathbf{F}} = J^P\frac{\partial \tilde{\Psi}}{\partial \tilde{E}^L_{\chi\delta}}\frac{\partial \tilde{E}^L_{\chi\delta}}{\partial F^{La}_{.\beta}}\frac{\partial F^{La}_{.\beta}}{\partial F^{P\alpha}_{.A}}\bigg|_{\mathbf{F}}$$

$$= \frac{1}{2}J^P\tilde{\Sigma}^{\chi\delta}(\delta^\beta_{.\delta}F^L_{a\chi} + \delta^\beta_{.\chi}F^L_{a\delta})F^a_{.B}\frac{\partial F^{P-1B}_{.\beta}}{\partial F^{P\alpha}_{.A}} = -J^PF^L_{a\chi}\tilde{\Sigma}^{\chi\beta}F^a_{.B}F^{P-1B}_{.\alpha}F^{P-1A}_{.\beta}$$

$$= -J^P\tilde{C}^L_{\alpha\chi}\tilde{\Sigma}^{\chi\beta}F^{P-1A}_{.\beta} = -J^P\tilde{M}^{.\beta}_\alpha F^{P-1A}_{.\beta}.$$

Dissipation associated with conduction can be made non-negative upon assuming a Fourier-type conduction law analogous to (5.48), but couched here in the intermediate configuration:

$$\tilde{\mathbf{q}} = -\tilde{\mathbf{K}}\tilde{\nabla}\theta \, , \ \tilde{q}^{\alpha} = -\tilde{K}^{\alpha\beta}\theta_{,\beta} = -\tilde{K}^{\alpha\beta}\theta_{,b}F^{Lb}_{.\beta} = -\tilde{K}^{\alpha\beta}\theta_{,B}F^{PB}_{.\beta} \, , \quad (6.30)$$

with $\tilde{\mathbf{K}}$ a symmetric positive semi-definite matrix of thermal conductivity that, like $\mathbf{K}$ of (5.48), may generally depend on temperature and other state variables:

$$-\theta^{-1}\left\langle \tilde{\nabla}\theta, \tilde{\mathbf{q}} \right\rangle = \theta^{-1}\left\langle \tilde{\nabla}\theta, \tilde{\mathbf{K}}\tilde{\nabla}\theta \right\rangle \geq 0 \, . \quad (6.31)$$

The dissipation inequality consists of the remaining terms in (6.24):

$$\tilde{\mathbf{\Pi}} : \mathbf{L}^{\mathbf{P}} - \frac{\partial \tilde{\Psi}}{\partial \alpha}\dot{\alpha} + \theta^{-1}\left\langle \tilde{\nabla}\theta, \tilde{\mathbf{K}}\tilde{\nabla}\theta \right\rangle \geq 0 \, , \quad (6.32)$$

where

$$\tilde{\mathbf{\Pi}} = \tilde{\mathbf{M}} - \tilde{\Psi}\mathbf{1} \, , \ \tilde{\Pi}^{.\beta}_{\alpha} = \tilde{M}^{.\beta}_{\alpha} - \tilde{\Psi}\delta^{.\beta}_{\alpha} \, . \quad (6.33)$$

Stress measure $\tilde{\mathbf{\Pi}}$, as discussed in detail in Section 6.6, is closely related to a quantity introduced by Eshelby (1951, 1975) whose divergence represents a kind of force on arbitrary heterogeneities in elastic solids[3]. The quantity $\dot{W}^{P} = \tilde{\mathbf{\Pi}} : \mathbf{L}^{\mathbf{P}} = \tilde{\Pi}^{.\beta}_{\alpha}L^{P\alpha}_{.\beta}$ is often referred to as the plastic dissipation or the rate of plastic work. When the material is plastically incompressible—which is always true for lattice-preserving plastic deformation manifesting only from dislocation glide—conditions $J^{P} = 1$ and $\mathrm{tr}(\mathbf{L}^{\mathbf{P}}) = 0$ hold and the plastic dissipation reduces to $\dot{W}^{P} = \tilde{\mathbf{M}} : \mathbf{L}^{\mathbf{P}}$. Variants of stress $\tilde{\mathbf{\Pi}}$ have been used by a number of authors as a conjugate thermodynamic force to plastic velocity gradient $\mathbf{L}^{\mathbf{P}}$ (Maugin 1994; Le and Stumpf 1996b, c; Clayton et al. 2004b, 2006; Clayton 2009a). Use of Mandel stress $\tilde{\mathbf{M}}$ in a similar capacity is also widespread (Moran et al. 1990; Maugin and Epstein 1998; Regueiro et al. 2002). Since $\tilde{\mathbf{\Sigma}}$ is symmetric, from (6.16),

$$\dot{W}^{P} = \tilde{\Pi}^{.\beta}_{\alpha}L^{P\alpha}_{.\beta} = \tilde{M}^{.\beta}_{\alpha}L^{P\alpha}_{.\beta} - \tilde{\Psi}L^{P\alpha}_{.\alpha} = \tilde{\Sigma}^{\beta\delta}\tilde{C}^{L}_{\alpha\delta}L^{P\alpha}_{.\beta} - \tilde{\Psi}L^{P\alpha}_{.\alpha}$$
$$= \tilde{\Sigma}^{\beta\delta}\tilde{C}^{L}_{\alpha\delta}D^{P\alpha}_{.\beta} + \tilde{\Sigma}^{\beta\delta}\tilde{C}^{L}_{\alpha\delta}W^{P\alpha}_{.\beta} - \tilde{\Psi}\dot{J}^{P}J^{P-1} \, , \quad (6.34)$$

where plastic spin $W^{P}_{\alpha\beta} = W^{P}_{[\alpha\beta]}$ and plastic deformation rate $D^{P}_{\alpha\beta} = D^{P}_{(\alpha\beta)}$ referred to the intermediate configuration are introduced in (3.62) and (3.63).

---

[3] Precisely, $\tilde{\mathbf{\Pi}}$ is a negative push-forward to configuration $\tilde{B}$ of one of several so-called energy-momentum tensors introduced by Eshelby (1975). The sign convention used in (6.33) enables both the stress and plastic velocity gradient to share the same (positive) algebraic sign in (6.32) and follows the convention of Epstein and Maugin (1990) and Clayton et al. (2004b, 2006).

As is evident from (6.34), only the symmetric part of $\tilde{\mathbf{C}}^L \mathbf{L}^P$ contributes to $\dot{W}^P$, but both plastic deformation rate $\mathbf{D}^P$ and plastic spin $\mathbf{W}^P$ can contribute to $\dot{W}^P$. In particular, $\tilde{\mathbf{C}}^L \mathbf{W}^P$ is not generally anti-symmetric.

Inequality (6.32) indicates that, in the absence of heat conduction, plastic dissipation should exceed the rate of increase in free energy associated with time rate(s) of internal state variable(s). In crystalline solids such as metals and ceramics, free energy changes attributed to internal state variables are often associated with changes in cumulative defect densities, e.g., energetic changes associated with local residual stresses in the vicinity of dislocation lines and internal boundaries such as grain, sub-grain, and twin boundaries (Kocks et al. 1975).

The specific heat at constant elastic strain and constant internal variable α, measured as energy per degree per unit intermediate volume, is introduced as

$$\tilde{C} = \frac{\partial \tilde{E}}{\partial \theta}\bigg|_{\substack{\tilde{E}^L \\ \alpha}} = \left[\frac{\partial \tilde{E}}{\partial \tilde{N}}\right]\left[\frac{\partial \tilde{N}}{\partial \theta}\right] = \left[\theta + \frac{\partial \theta}{\partial \tilde{N}}\left(\tilde{N} + \frac{\partial \tilde{\Psi}}{\partial \theta}\right)\right]\left[-\frac{\partial^2 \tilde{\Psi}}{\partial \theta^2}\right] = -\theta \frac{\partial^2 \tilde{\Psi}}{\partial \theta^2} , \quad (6.35)$$

where (6.3) and (6.25) have been used. Multiplying (4.39) by J^{P-1}, the energy balance in configuration $\tilde{B}$ is

$$\tilde{\rho}\dot{e} = \dot{\tilde{E}} - \dot{\tilde{\rho}}e = \dot{\tilde{E}} - \dot{J}^{P-1}\rho_0 e = \dot{\tilde{E}} + \dot{J}^P J^{P-1}\tilde{E} = \tilde{M}_\alpha^{\ \beta}\tilde{L}_{\cdot\beta}^\alpha - J^{P-1}Q_{;A}^A + \tilde{\rho}r . \quad (6.36)$$

Substituting from the second of (6.25) leads to

$$\dot{\tilde{E}} = \dot{\tilde{\Psi}} + \dot{\theta}\tilde{N} + \theta\dot{\tilde{N}}$$

$$= \frac{\partial \tilde{\Psi}}{\partial \tilde{E}_{\alpha\beta}^L}\dot{\tilde{E}}_{\alpha\beta}^L + \frac{\partial \tilde{\Psi}}{\partial \alpha}\dot{\alpha} + \theta\dot{\tilde{N}} = \tilde{M}_\alpha^{\ \beta}\tilde{L}_{\cdot\beta}^\alpha - \tilde{L}_{\cdot\alpha}^{P\alpha}\tilde{E} - \check{\nabla}_\alpha \tilde{q}^\alpha + \tilde{\rho}r, \quad (6.37)$$

where, for the heat conduction term, the anholonomic covariant derivative is defined by (Clayton 2009a)

$$\check{\nabla}_\alpha(.) = (.)_{;A}F_{\cdot\alpha}^{P-1A} + J^{P-1}(.)(J^P F_{\cdot\alpha}^{P-1A})_{;A}, \quad (6.38)$$

such that

$$J^{P-1}Q_{;A}^A = J^{P-1}(J^P F_{\cdot\alpha}^{P-1A}\tilde{q}^\alpha)_{;A}$$

$$= (\tilde{q}^\alpha)_{;A}F_{\cdot\alpha}^{P-1A} + J^{P-1}\tilde{q}^\alpha(J^P F_{\cdot\alpha}^{P-1A})_{;A} = \check{\nabla}_\alpha\tilde{q}^\alpha . \quad (6.39)$$

The term $(J^P F_{\cdot\alpha}^{P-1A})_{;A} = 0$ by Piola's identity akin to (2.146) in general only when the plastic deformation gradient satisfies compatibility conditions $F_{[A;B]}^{P\alpha} = 0$. Rearranging (6.37) for the rate of entropy production and using (6.25),

$$\theta\dot{\tilde{N}} = \tilde{M}_\alpha^{.\beta}\tilde{L}_{.\beta}^\alpha - \frac{\partial\tilde{\Psi}}{\partial\tilde{E}_{\alpha\beta}^L}\dot{\tilde{E}}_{\alpha\beta}^L - \frac{\partial\tilde{\Psi}}{\partial\alpha}\dot{\alpha} - \tilde{L}_{.\alpha}^{P\alpha}\tilde{E} - \breve{\nabla}_\alpha\tilde{q}^\alpha + \tilde{\rho}r$$

$$= \left(\tilde{M}_\alpha^{.\beta} - \tilde{E}\delta_{.\alpha}^\beta\right)L_{.\beta}^{P\alpha} - \left(\partial\tilde{\Psi}/\partial\alpha\right)\dot{\alpha} - \breve{\nabla}_\alpha\tilde{q}^\alpha + \tilde{\rho}r$$

$$= \left(\tilde{M}_\alpha^{.\beta} - \tilde{\Psi}\delta_{.\alpha}^\beta - \theta\tilde{N}\delta_{.\alpha}^\beta\right)L_{.\beta}^{P\alpha} - \left(\partial\tilde{\Psi}/\partial\alpha\right)\dot{\alpha} - \breve{\nabla}_\alpha\tilde{q}^\alpha + \tilde{\rho}r \qquad (6.40)$$

$$= \left(\tilde{\Pi}_\alpha^{.\beta} + \delta_{.\alpha}^\beta\theta\frac{\partial\tilde{\Psi}}{\partial\theta}\right)L_{.\beta}^{P\alpha} - \frac{\partial\tilde{\Psi}}{\partial\alpha}\dot{\alpha} - \breve{\nabla}_\alpha\tilde{q}^\alpha + \tilde{\rho}r.$$

Analogously to (5.50),

$$\theta\dot{\tilde{N}} = -\theta\frac{d}{dt}\left(\frac{\partial\tilde{\Psi}}{\partial\theta}\right) = -\theta\left(\frac{\partial^2\tilde{\Psi}}{\partial\theta^2}\dot{\theta} + \frac{\partial^2\tilde{\Psi}}{\partial\theta\partial\tilde{E}_{\alpha\beta}^L}\dot{\tilde{E}}_{\alpha\beta}^L + \frac{\partial^2\tilde{\Psi}}{\partial\theta\partial\alpha}\dot{\alpha}\right)$$

$$= \tilde{C}\dot{\theta} + \theta\tilde{\beta}^{\alpha\beta}\dot{\tilde{E}}_{\alpha\beta}^L - \theta\frac{\partial^2\tilde{\Psi}}{\partial\theta\partial\alpha}\dot{\alpha}, \qquad (6.41)$$

with stress-temperature coefficients referred to intermediate configuration

$$\tilde{\boldsymbol{\beta}} = -\frac{\partial^2\tilde{\Psi}}{\partial\theta\partial\tilde{\mathbf{E}}^L}\bigg|_\alpha. \qquad (6.42)$$

Equating (6.40) and (6.41) and using (6.30), the temperature rate becomes

$$\tilde{C}\dot{\theta} = \left(\tilde{\Pi}_\alpha^{.\beta} + \delta_{.\alpha}^\beta\frac{\partial\tilde{\Psi}}{\partial\theta}\theta\right)L_{.\beta}^{P\alpha} - \left(\frac{\partial\tilde{\Psi}}{\partial\alpha} - \theta\frac{\partial^2\tilde{\Psi}}{\partial\theta\partial\alpha}\right)\dot{\alpha}$$

$$- \theta\tilde{\beta}^{\alpha\beta}\dot{\tilde{E}}_{\alpha\beta}^L + \breve{\nabla}_\alpha(\tilde{K}^{\alpha\beta}\theta_{,\beta}) + \tilde{\rho}r. \qquad (6.43)$$

The first term on the right side of (6.43) represents the effect of the plastic velocity gradient on the rate of temperature increase. It can be written

$$\left(\tilde{\Pi}_\alpha^{.\beta} + \delta_{.\alpha}^\beta\frac{\partial\tilde{\Psi}}{\partial\theta}\theta\right)L_{.\beta}^{P\alpha} = \tilde{\Sigma}^{\beta\delta}\tilde{C}_{\alpha\delta}^L L_{.\beta}^{P\alpha} - \left(\tilde{\Psi} + \theta\frac{\partial\tilde{\Psi}}{\partial\theta}\right)L_{.\alpha}^{P\alpha}$$

$$= \dot{W}^P + \frac{\theta}{J^P}\frac{\partial\tilde{\Psi}}{\partial\theta}\dot{J}^P = \dot{W}^P + \frac{\dot{J}^P}{J^P}\frac{\partial\tilde{\Psi}}{\partial\ln\theta}. \qquad (6.44)$$

From the symmetry of $\tilde{\boldsymbol{\Sigma}}$, again only the symmetric part of the covariant product $\tilde{\mathbf{C}}^L\mathbf{L}^P$ contributes to plastic dissipation $\dot{W}^P$ and hence the temperature change. From (6.32)-(6.34) and (6.43), when plastic deformation is not isochoric, the absolute value of free energy $\tilde{\Psi}$ enters the entropy inequality and energy balance. Thus, the zero datum used to define free energy and other thermodynamic potentials is not inconsequential; e.g., the free energy in this case is not arbitrary to within an additive constant.

Notice that when the plastic deformation is isochoric, $\dot{J}^P = 0$ and the temperature rate equation becomes

$$\tilde{C}\dot{\theta} = \dot{W}^P - \left(\frac{\partial\tilde{\Psi}}{\partial\alpha} - \theta\frac{\partial^2\tilde{\Psi}}{\partial\theta\partial\alpha}\right)\dot{\alpha} - \theta\tilde{\beta}^{\alpha\beta}\dot{\tilde{E}}^L_{\alpha\beta} + \breve{\nabla}_\alpha(\tilde{K}^{\alpha\beta}\theta_{,\beta}) + \tilde{\rho}r. \qquad (6.45)$$

The first term on the right of (6.45), i.e., the rate of plastic work, accounts for dissipation from moving dislocations such as that resulting from lattice friction. The second term on the right of (6.45) represents energetic changes attributed to the rate of change of the internal state variable, for example residual elastic energy accumulation with increases in defect density. The third term represents effects of thermoelastic coupling. The final two terms on the right of (6.45) account for heat conduction (i.e., temperature gradients) and non-mechanical heat sources such as a radiation field, respectively.

Energy balance (6.45) is often written as follows for ductile crystalline metals:

$$\tilde{C}\dot{\theta} = \beta'\dot{W}^P - \theta\tilde{\beta}^{\alpha\beta}\dot{\tilde{E}}^L_{\alpha\beta} + \breve{\nabla}_\alpha(\tilde{K}^{\alpha\beta}\theta_{,\beta}) + \tilde{\rho}r, \qquad (6.46)$$

where

$$\beta'\dot{W}^P = \dot{W}^P - \left(\frac{\partial\tilde{\Psi}}{\partial\alpha} - \theta\frac{\partial^2\tilde{\Psi}}{\partial\theta\partial\alpha}\right)\dot{\alpha}. \qquad (6.47)$$

Scalar β' is often called the Taylor-Quinney parameter. The product $(1-\beta')\dot{W}^P$ measures the rate of energy accumulation in the solid associated with irreversible changes in its internal structure, for example stored energy of cold working. Following measurements of β' on several engineering metals subjected to large deformations (Farren and Taylor 1925; Taylor and Quinney 1934; Havner 1992), analysts often assume a constant value of β' in the range $0.8 \leq \beta' \leq 1.0$ (Bammann et al. 1993; Zhou et al. 1994), though more recent experiments (Rosakis et al. 2000) indicate that for some metallic materials β' may fall outside this range and may change significantly with history of plastic deformation. When $\partial^2\tilde{\Psi}/(\partial\theta\partial\alpha) = 0$, (6.32) requires $\beta' \geq 0$ in the absence of heat conduction, i.e., for an adiabatic process. However, if the energetic change associated with the rate of an internal state variable is dissipative, for example if condition $\partial\tilde{\Psi}/\partial\alpha < 0$ holds over some regime in which $\dot{\alpha} > 0$, thermodynamic admissibility does not preclude $\beta' > 1$.

6.1.3 Representative Free Energy

A specific form of the Helmholtz free energy potential of (6.9) and (6.26) for finite elastoplasticity is now considered. For describing crystalline materials in structural applications, the free energy density is often decomposed additively into a thermoelastic part $\tilde{\Psi}^E$ associated with reversible deformations and temperature changes and a residual part $\tilde{\Psi}^R$ associated with the internal state variable:

$$\tilde{\Psi} = \tilde{\Psi}^E \left(\tilde{\mathbf{E}}^{\mathbf{L}}, \theta, X, \tilde{\mathbf{g}}_\alpha \right) + \tilde{\Psi}^R \left(\alpha, \theta, X, \tilde{\mathbf{g}}_\alpha \right). \qquad (6.48)$$

The additive decoupling of reversible thermoelastic and residual free energies as depicted in (6.48) is common (Bammann 2001; Regueiro et al. 2002; McDowell 2005), though may not always be a physically realistic assumption if free energies associated with the internal state variable (i.e., defect energies) are amplified by external stress fields (Gibeling and Nix 1980; Clayton et al. 2004a; Chung and Clayton 2007), or if elastic moduli are strongly affected by the evolving defect density represented by the internal state variable (Smith 1953; Clayton and Chung 2006). A more general formulation for elastic-plastic crystals with residual elastic strains and residual stresses, posited in Section 9.4.6 of Chapter 9, addresses these issues. Furthermore, as demonstrated in Section 9.2 of Chapter 9, when defects such as interstitials, vacancies, pores, voids, or micro-cracks affect the instantaneous thermoelestic response, internal variables associated with defects should reflect elastic stiffness variations, and hence cannot be decoupled from the lattice strain in the free energy (Mackenzie 1950; Dienes 1952; Grinfeld and Wright 2004; Clayton 2008; Clayton et al. 2008a).

The thermoelastic part of the free energy, $\tilde{\Psi}^E$, is often defined in a similar manner to the corresponding potential Ψ_0 in classical thermoelasticity of Sections 5.1.3 and 5.1.4, but with quantities defined in the intermediate as opposed to the reference configuration, with total strain $\mathbf{E}$ replaced by lattice strain $\tilde{\mathbf{E}}^{\mathbf{L}}$, and with second Piola-Kirchhoff stress $\boldsymbol{\Sigma}$ replaced by symmetric lattice stress $\tilde{\boldsymbol{\Sigma}}$. For example, consider a series expansion of the thermoelastic part free energy density of up to third order in lattice strains (Havner 1973) about a possibly evolving intermediate state—a state that serves as an updated reference configuration for the thermoelastic response—but otherwise analogous to materially linear thermoelasticity of (5.84):

$$\tilde{\Psi}^E = \frac{1}{2}\tilde{\mathbb{C}}^{\alpha\beta\chi\delta}\tilde{E}^L_{\alpha\beta}\tilde{E}^L_{\chi\delta} + \frac{1}{6}\tilde{\mathbb{C}}^{\alpha\beta\chi\delta\varepsilon\phi}\tilde{E}^L_{\alpha\beta}\tilde{E}^L_{\chi\delta}\tilde{E}^L_{\varepsilon\phi}$$
$$-\tilde{\beta}^{\alpha\beta}\tilde{E}^L_{\alpha\beta}\Delta\theta - \tilde{C}\theta\ln\frac{\theta}{\theta_0}. \tag{6.49}$$

The state about which (6.49) is expanded is characterized by conditions $F^{La}_{.\alpha} = g^a_{.\alpha}$, $\tilde{C}^L_{\alpha\beta} = \tilde{g}_{\alpha\beta}$, $\tilde{E}^L_{\alpha\beta} = 0$, and $\theta = \theta_0 > 0$. Temperature change from this reference state $\Delta\theta = \theta - \theta_0$ can be positive, zero, or negative. Material constants referred to configuration $\tilde{B}$ are defined at a material point X with stationary basis $\tilde{\mathbf{g}}_\alpha(X)$ by

$$\tilde{\mathbb{C}}^{\alpha\beta\chi\delta} = \left.\frac{\partial^2\tilde{\Psi}^E}{\partial\tilde{E}^L_{\alpha\beta}\partial\tilde{E}^L_{\chi\delta}}\right|_{\substack{\tilde{\mathbf{E}}^L=0\\\theta=\theta_0}}, \quad \tilde{\mathbb{C}}^{\alpha\beta\chi\delta\varepsilon\phi} = \left.\frac{\partial^3\tilde{\Psi}^E}{\partial\tilde{E}^L_{\alpha\beta}\partial\tilde{E}^L_{\chi\delta}\partial\tilde{E}^L_{\varepsilon\phi}}\right|_{\substack{\tilde{\mathbf{E}}^L=0\\\theta=\theta_0}}, \tag{6.50}$$

$$\tilde{\beta}^{\alpha\beta} = -\left.\frac{\partial^2\tilde{\Psi}^E}{\partial\theta\partial\tilde{E}^L_{\alpha\beta}}\right|_{\substack{\tilde{\mathbf{E}}^L=0\\\theta=\theta_0}}, \quad \tilde{C} = -\left(\theta\frac{\partial^2\tilde{\Psi}^E}{\partial\theta^2}\right)\Bigg|_{\substack{\tilde{\mathbf{E}}^L=0\\\theta=\theta_0}}. \tag{6.51}$$

In (6.51), the thermal stress coefficients and specific heat are constant versions of quantities first introduced in (6.42) and (6.35), respectively. Isothermal second- and third-order elastic constants are introduced in (6.50), the latter important in structural or shock physics applications wherein confining pressures and elastic strains can be large, especially in certain kinds of crystals (e.g., those with covalent and ionic bonding such as ceramics) wherein resistance to dislocation-mediated plastic slip can be high.

Material coefficients in (6.50) and (6.51) are related to those of (5.66) and (5.85) at the same material point X as follows:

$$\tilde{\mathbb{C}}^{\alpha\beta\chi\delta} = J^{P-1}\overline{\mathbb{C}}^{ABCD}g^\alpha_{.A}g^\beta_{.B}g^\chi_{.C}g^\delta_{.D}, \tag{6.52}$$

$$\tilde{\mathbb{C}}^{\alpha\beta\chi\delta\varepsilon\phi} = J^{P-1}\overline{\mathbb{C}}^{ABCDEF}g^\alpha_{.A}g^\beta_{.B}g^\chi_{.C}g^\delta_{.D}g^\varepsilon_{.E}g^\phi_{.F}, \tag{6.53}$$

$$\tilde{\beta}^{\alpha\beta} = J^{P-1}\overline{\beta}^{AB}g^\alpha_{.A}g^\beta_{.B}, \tag{6.54}$$

$$\tilde{C} = \tilde{\rho}\overline{c} = J^{P-1}\rho_0\overline{c} = J^{P-1}\overline{C}_0. \tag{6.55}$$

Since $\dot{\tilde{\mathbf{g}}}_\alpha = 0$ and $\dot{\mathbf{G}}_A = 0$ (e.g., see discussion in Section 2.5.1), the shifter $g^\alpha_{.A} = \langle\tilde{\mathbf{g}}^\alpha, \mathbf{G}_A\rangle$ at X does not depend on time. When plastic deformation is isochoric ($J^P = 1$) and when coincident coordinate systems are used in reference and intermediate configurations so that $g^\alpha_{.A} = \delta^\alpha_{.A}$, numerical values of material coefficients on left and right sides of each of (6.52)-(6.55)

are equal[4]. Hence, all considerations regarding symmetry of reference material coefficients discussed in Section 5.1.5 and Appendix A apply for intermediate elasticity tensors in (6.52) and (6.53) and thermal stress coefficients in (6.54). To convert symmetry relations in Section 5.1.5 and Appendix A to the present context, reference indices in capital Roman font are merely replaced with intermediate indices in Greek font. The thermostatic formalism of Section 5.2 can be applied as well, wherein partial derivatives are taken with respect to lattice strains as opposed to total strains. This enables definitions of isentropic material coefficients, Gruneisen parameters, and Maxwell relations among thermostatic variables. Details of such an approach are given by Scheidler and Wright (2001) and Wright (2002). Like the elastic constants, thermal stress coefficients and specific heat in (6.51) are assumed constant and not dependent upon internal variables representing defect densities, for example. This assumption is standard in plasticity theories, but may not always be physically appropriate since dislocations can affect the specific heat capacity (Gottstein 1973).

Stress-strain-temperature relations following from (6.25) and (6.49) exhibit the form

$$\tilde{\Sigma}^{\alpha\beta} = \tilde{\mathbb{C}}^{\alpha\beta\chi\delta}\tilde{E}_{\chi\delta}^{L} + \frac{1}{2}\tilde{\mathbb{C}}^{\alpha\beta\chi\delta\varepsilon\phi}\tilde{E}_{\chi\delta}^{L}\tilde{E}_{\varepsilon\phi}^{L} - \tilde{\beta}^{\alpha\beta}\Delta\theta\,. \qquad (6.56)$$

Consider a stress-free thermal strain of the form $\tilde{E}_{\alpha\beta}^{L} = \tilde{\alpha}_{\alpha\beta}\Delta\theta$, where $\tilde{\alpha}_{\alpha\beta}$ may generally depend on the thermodynamic state. Setting the left side of (6.56) to zero gives, analogously to (5.161),

$$\tilde{\beta}^{\alpha\beta} = \left(\tilde{\mathbb{C}}^{\alpha\beta\chi\delta}\tilde{\alpha}_{\chi\delta} + \tilde{\mathbb{C}}^{\alpha\beta\chi\delta\varepsilon\phi}\tilde{\alpha}_{\chi\delta}\tilde{\alpha}_{\varepsilon\phi}\Delta\theta/2\right)\Big|_{\theta_0} = \tilde{\mathbb{C}}^{\alpha\beta\chi\delta}\tilde{\alpha}_{\chi\delta}\Big|_{\theta_0}\,, \qquad (6.57)$$

with $\tilde{\alpha}_{\alpha\beta}$ a symmetric rank two tensor of thermal expansion coefficients.

For the case of thermoelastic isotropy, second-order thermoelastic constants become

$$\tilde{\mathbb{C}}^{\alpha\beta\chi\delta} = \mu(\tilde{g}^{\alpha\chi}\tilde{g}^{\beta\delta} + \tilde{g}^{\alpha\delta}\tilde{g}^{\chi\beta}) + \lambda\tilde{g}^{\alpha\beta}\tilde{g}^{\chi\delta}\,, \quad \tilde{\beta}^{\alpha\beta} = \tilde{\beta}\tilde{g}^{\alpha\beta}\,, \qquad (6.58)$$

with μ the shear modulus, λ Lamé's constant, and $\tilde{\beta}$ a thermal stress constant, identical to those entering (5.124) when $J^{P} = 1$. Stress-strain-temperature relations for thermoelastically isotropic solids are, when third-order elastic constants are omitted,

---

[4] When $\dot{J}^{P}(X,t) \neq 0$, then coefficients on both sides of (6.52)-(6.55) cannot all be constant. If the left sides are taken as constant in time, then the elastic coefficients and specific heat per unit reference volume on the right sides increase with increases in plastic volume change. This issue is taken up again in Chapter 8 wherein residual volume changes are incorporated explicitly in the constitutive model framework.

$$\tilde{\Sigma}^{\alpha\beta} = 2\mu\tilde{E}^{L\alpha\beta} + (\lambda\tilde{E}^{L\chi}_{\cdot\chi} - \tilde{\beta}\Delta\theta)\tilde{g}^{\alpha\beta}. \tag{6.59}$$

The form of the residual free energy $\tilde{\Psi}^R$ introduced in (6.48) depends upon the specific choice of internal state variable, and is thus material-specific. A quadratic function akin to the first term in the thermoelastic potential $\tilde{\Psi}^E$ is simple and logical in many instances:

$$\tilde{\Psi}^R = \frac{1}{2}\tilde{\kappa}\alpha^2, \tag{6.60}$$

where material coefficient $\tilde{\kappa}$ may generally depend on temperature, reference position, and orientation of the material element:

$$\tilde{\kappa}(\theta, X, \tilde{\mathbf{g}}_\alpha) = \left.\frac{\partial^2\tilde{\Psi}^R}{\partial\alpha^2}\right|_{\alpha=0}. \tag{6.61}$$

Relations (6.32) and (6.60) yield a thermodynamic force linear in the internal state variable conjugate to the time rate of the internal state variable, i.e., $-\partial\tilde{\Psi}/\partial\alpha = -\tilde{\kappa}\alpha$. When $\tilde{\kappa} > 0$, residual free energy (6.60) is a convex function of internal state variable α. However, for a material whose total free energy consists of contributions from multiple sources—e.g., lattice strains, temperature, and one or more internal state variables representing irreversible lattice rearrangements—the global free energy may not be convex with regards to distributions of field variables (Carstensen et al. 2002; Clayton et al. 2006). In such cases, even when a crystal with uniform initial properties is subjected to affine far-field boundary conditions, heterogeneous distributions of field variables such as localized deformation gradients can emerge as the thermodynamic state of the deforming crystal evolves towards a condition of minimum global energy (Ball and James 1987; Bhattacharya 1991; Ortiz and Repetto 1999). Formation of heterogeneous deformation patterns is expected in anisotropic crystals that favor single slip as a result of strong latent hardening (Conti and Ortiz 2005), i.e., strong hardening on slip systems that are non-coplanar with an active system (see Section 6.3 and (6.110)).

The theoretical description of material behavior is completed via prescription of kinetic laws for evolution of inelastic deformation, i.e., $\dot{\mathbf{F}}^{\mathbf{P}}$, and rate of internal state variable, i.e., $\dot{\alpha}$. Ideally, such kinetic relations should be formulated in such a way that (6.32) is satisfied unequivocally. Such kinetic equations, along with physically descriptive choices of internal state variables, are described in Sections 6.2, 6.3, and 6.4 in the context of discrete dislocation plasticity, crystal plasticity, and macroscopic plasticity, respectively.

6.2 Dislocation Plasticity

Consider a kinematic description further refined to account for motion of discrete dislocation lines as developed in Section 3.2.5. Plastic velocity gradient $\mathbf{L}^{\mathbf{P}}$ can in this case be expressed by combining (3.98) and the last of (3.99):

$$L^{P\alpha}_{\ .\beta} = \dot{F}^{P\alpha}_{\ .A} F^{P-1A}_{\ .\beta} = \zeta^{\alpha\chi\delta} \varepsilon_{\chi\delta\beta} = \sum_{i=1}^{j} \tilde{\rho}^i \tilde{b}^{i\alpha} \tilde{\xi}^{i\chi} \tilde{v}^{i\delta} \varepsilon_{\chi\delta\beta} \ . \qquad (6.62)$$

Summation proceeds over $i = 1, 2, \ldots j$ populations of dislocations with the same tangent line, Burgers vector, and velocity for each value of i; nomenclature entering (6.62) is explained more thoroughly in Section 3.2.5. The plastic dissipation per unit intermediate volume, $\dot{W}^P = \tilde{\mathbf{\Pi}} : \mathbf{L}^{\mathbf{P}}$ of (6.34), is

$$
\begin{aligned}
\tilde{\Pi}^{\ \beta}_{\alpha} L^{P\alpha}_{\ .\beta} &= \sum_{i=1}^{j} \tilde{\rho}^i \tilde{v}^{i\delta} \varepsilon_{\chi\delta\beta} \tilde{\xi}^{i\chi} \tilde{M}^{\ \beta}_{\alpha.} \tilde{b}^{i\alpha} - \sum_{i=1}^{j} \tilde{\rho}^i \tilde{\Psi} \tilde{b}^{i\beta} \varepsilon_{\beta\chi\delta} \tilde{\xi}^{i\chi} \tilde{v}^{i\delta} \\
&= \sum_{i=1}^{j} \tilde{\rho}^i \tilde{v}^{i\delta} \varepsilon_{\chi\delta\beta} \tilde{\xi}^{i\chi} (J^L F^{L-1\beta}_{\ .b} \sigma^{.b}_{a} F^{La}_{\ .a}) F^{L-1\alpha}_{\ .c} b^{ic} \\
&= \sum_{i=1}^{j} \tilde{\rho}^i \tilde{v}^{i\delta} \varepsilon_{\chi\delta\beta} \tilde{\xi}^{i\chi} (J^L F^{L-1\beta}_{\ .b} \sigma^{.b}_{a}) b^{ia} = \sum_{i=1}^{j} \tilde{\rho}^i \tilde{v}^{i\delta} \varepsilon_{\chi\delta\beta} \tilde{\xi}^{i\chi} \tilde{S}^{\ \beta}_{.a} b^{ia} \\
&= -\sum_{i=1}^{j} \tilde{\rho}^i (\varepsilon_{\delta\chi\beta} \tilde{\xi}^{i\chi} \tilde{S}^{\ \beta}_{.a} b^{ia}) \tilde{v}^{i\delta} = \sum_{i=1}^{j} \tilde{\rho}^i \tilde{f}^i_{\delta} \tilde{v}^{i\delta} ,
\end{aligned}
\qquad (6.63)
$$

where since the Burgers vector and normal to the glide plane are always orthogonal, $\tilde{b}^{i\beta} \varepsilon_{\beta\chi\delta} \tilde{\xi}^{i\chi} \tilde{v}^{i\delta} = 0$. The thermodynamic force, with dimensions of force per unit length, acting on dislocation population i is

$$\tilde{\mathbf{f}}^i = -\tilde{\xi}^i \times \tilde{\mathbf{S}} \mathbf{b}^i , \qquad (6.64)$$

where the two-point nominal lattice stress $\tilde{S}^{\ \beta}_{.a} = J^L F^{L-1\beta}_{\ .b} \sigma^{.b}_{a}$. Force $\tilde{\mathbf{f}}^i$ conjugate to dislocation line velocity $\tilde{\mathbf{v}}^i$ is similar in nature to the force acting on a single dislocation line by an external, as opposed to self-induced, stress field in a linear elastic body:

$$\mathbf{f}^i_{\mathbf{PK}} = -\xi^i \times \boldsymbol{\sigma} \mathbf{b}^i , \qquad (6.65)$$

The vector $\mathbf{f}^i_{\mathbf{PK}}$ is known as the Peach-Koehler force (Peach and Koehler 1950; Mura 1968; Zorski 1981; Bammann and Aifantis 1982) acting on dislocation type i with unit tangent ξ^i and Burgers vector $\mathbf{b}^i$. The Peach-Koehler force is the force conjugate entering the expression for the negative energy gradient $-\partial W / \partial s$ attributed to rigidly translating the dislocation line along trajectory $\lambda ds = d\mathbf{s}$ (Peach and Koehler 1950):

$$-\frac{\partial W}{\partial s} = -\int_L b_a \sigma^{ab} \varepsilon_{bcd} \lambda^c d\xi^d = -\int_L \varepsilon_{dbc} \xi^d \sigma^{ba} b_a \lambda^c dL = \int_L (f_{PK})_c \lambda^c dL, \quad (6.66)$$

where $d\boldsymbol{\xi} = \boldsymbol{\xi} dL$ is a segment of the dislocation line. In the limit of small elastic deformations, $\tilde{S}_{.a}^{\beta} \approx g_{.b}^{\beta} \sigma_a^{.b}$, $\tilde{\xi}^{i\chi} \approx g_{.a}^{\chi} \xi^{ia}$, and $(\tilde{f}^i)_\alpha \approx g_{.\alpha}^a (f_{PK}^i)_a$.

In physical descriptions of dislocation kinetics, use of Orowan's (1940) relation in (3.100) is often preferred over (6.62):

$$L_{.\beta}^{P\alpha} = \sum_i \tilde{\rho}^i \tilde{b}^i \tilde{v}^i \tilde{s}^{i\alpha} \tilde{m}_\beta^i, \quad (6.67)$$

where for each slip system i, the magnitude of Burgers vector, direction of atomic motion, dislocation line velocity, and normal to the glide plane, are respectively

$$\tilde{b}^i = |\tilde{\mathbf{b}}^i|, \quad \tilde{s}^i = \tilde{\mathbf{b}}^i / \tilde{b}^i, \quad \tilde{v}^i = |\tilde{\mathbf{v}}^i|, \quad \tilde{\mathbf{m}}^i = \tilde{\boldsymbol{\xi}}^i \times \tilde{\mathbf{v}}^i / \tilde{v}^i. \quad (6.68)$$

Using (6.67) in (6.34), the rate of plastic work per intermediate volume is

$$\tilde{\Pi}_\alpha^{.\beta} L_{.\beta}^{P\alpha} = \sum_i \tilde{\rho}^i \tilde{b}^i \tilde{v}^i \tilde{s}^{i\alpha} \tilde{M}_{\alpha.}^\beta \tilde{m}_\beta^i - \sum_i \tilde{\rho}^i \tilde{b}^i \tilde{v}^i \tilde{\Psi}(\tilde{s}^{i\alpha} \delta_{\alpha.}^\beta \tilde{m}_\beta^i)$$

$$= \sum_i \tilde{\rho}^i \tilde{b}^i \tilde{v}^i \tilde{s}^{i\alpha} (J^L F_{.\alpha}^{La} \sigma_a^{.b} F_{.b}^{L-1\beta}) \tilde{m}_\beta^i \quad (6.69)$$

$$= \sum_i \tilde{\rho}^i \tilde{b}^i \tilde{v}^i (J^L s_a^i \sigma^{ab} m_b^i) = \sum_i \tilde{\rho}^i \tilde{b}^i \tilde{v}^i \tilde{\tau}^i,$$

where the resolved shear stress (more precisely, a resolved lattice Kirchhoff stress) is

$$\tilde{\tau}^i = J^L s_a^i \sigma^{ab} m_b^i = J^L s_a^i \sigma^{ba} m_b^i = J^L \sigma^{ab} s_{(a}^i m_{b)}^i, \quad (6.70)$$

the latter two relations following from the symmetry of the Cauchy stress.

The kinetic relationship between the velocity of a dislocation $\tilde{v}^i$ and its driving stress $\tilde{\tau}^i$ depends upon the thermodynamic state of the crystal, as represented here by lattice strain, temperature, and internal state variable α reflecting contributions from internal structure such as defects or obstacles to dislocation motion. In the remainder of Section 6.2, index i is often dropped, with a focus on kinetic relations for the velocity magnitude $\tilde{v}$ of a representative dislocation or set of dislocations on that system subjected to shear stress magnitude $\tilde{\tau}$. Both $\tilde{v}$ and $\tilde{\tau}$ are assumed to exhibit the same (positive) algebraic sign in this context.

Though supersonic dislocation motion has been posited (Hirth and Lothe 1982) and may be sustainable if a dislocation is nucleated supersonically at a stress concentration in a crystal subjected to very high applied shear stress (Gumbsch and Gao 1999), conventionally the dislocation velocity is assumed to be bounded from above by the speed of transverse elastic waves in the crystal (Eshelby 1949a; Johnston and Gilman 1959). In anisotropic crystals, elastic plane waves can propagate in a given direc-

tion in three distinct, mutually orthogonal modes when no degeneracy occurs (Brugger 1965); these modes are in general neither longitudinal nor transverse. Special directions exist in crystals allowing for propagation of one longitudinal and two transverse modes. These directions, and speeds of propagation of plane waves, depend upon second-order elastic constants in initially unstressed crystals, as listed by Brugger (1965). In the isotropic approximation, the elastic shear wave speed c_S is

$$c_S = \sqrt{\mu / \rho_0} \; , \tag{6.71}$$

with μ the isentropic shear modulus and ρ_0 the reference mass density. The maximum sustainable shear stress is the theoretical strength τ_T of the crystal of Section C.4.1 (Frenkel 1926); when subjected to stresses of this magnitude, all atomic bonds spanning two crystallographic planes undergoing relative shear are broken simultaneously. In an isotropic linear elastic body, the theoretical strength is approximated by (C.209) as $\tau_T \approx \mu / 10$. Thus, upper bounds on dislocation velocity and resolved shear stress are

$$\tilde{v} \le c_S = \sqrt{\mu / \rho_0} \; , \; \tilde{\tau} \le \tau_T \approx \mu / 10 \, . \tag{6.72}$$

Denote the resistance to motion of dislocation population i by the shear stress

$$\hat{\tau}^i = \hat{\tau}^i \left(\tilde{\mathbf{E}}^{\mathbf{L}}, \alpha, \theta, X, \tilde{\mathbf{g}}_\alpha \right), \tag{6.73}$$

with $\hat{\tau} \ge 0$ denoting a characteristic magnitude of dislocation line resistance to motion, sometimes called a mechanical threshold stress.

Steady state dislocation glide can be achieved when the resolved shear stress $\tilde{\tau}$ greatly exceeds threshold stress $\hat{\tau}$, but when the dislocation velocity remains appreciably lower than c_S. In this case, the following kinetic relation applies (Kocks et al. 1975):

$$(\tilde{\tau} - \hat{\tau})\tilde{b} = B\tilde{v} \, , \tag{6.74}$$

where B is the drag coefficient that depends on lattice friction (e.g., the Peierls mechanism of Section C.4.3), phonon drag, and at very low temperatures, electron drag (Kocks et al. 1975). Kocks et al. (1975) define an atomic frequency

$$\omega_A = c_S / \tilde{b} \, , \tag{6.75}$$

and the drag coefficient as

$$B = \frac{k_B \theta}{\omega_A \Omega_0} = \frac{k_B \theta \tilde{b}}{c_S \Omega_0} = \frac{k_B \theta \tilde{b}}{\Omega_0} \sqrt{\frac{\rho_0}{\mu}} \, , \tag{6.76}$$

where k_B is Boltzmann's constant and Ω_0 is the atomic volume introduced in Section 3.1.1. The drag coefficient increases with temperature

because phonon mechanisms become stronger as the temperature rises. The drag-controlled steady state velocity is then, from (6.74) and (6.76),

$$\tilde{v} = \frac{(\tilde{\tau} - \hat{\tau})\tilde{b}}{B} = \frac{\Omega_0 (\tilde{\tau} - \hat{\tau})}{k_B \theta} c_S . \tag{6.77}$$

The rate of plastic work is always non-negative since

$$\tilde{\tau}\tilde{v} = \left[\Omega_0 \tilde{\tau}(\tilde{\tau} - \hat{\tau})/(k_B \theta)\right] c_S \geq 0 . \tag{6.78}$$

Conditions for which (6.74) applies are

$$\hat{\tau} \ll \tilde{\tau} \ll k_B \theta / \Omega_0 . \tag{6.79}$$

When applied stresses vary rapidly, or when obstacles to glide are closely spaced, inertial effects can become important. Such effects are omitted in (6.74), corresponding to a regime in which the dislocation motion is said to be overdamped. As the dislocation velocity approaches the sound speed, say $\tilde{v} \gtrsim 0.7 c_S$, drag forces increase with increasing velocity and (6.74) no longer applies. Because additional dissipation occurs from dislocation-phonon interactions and other radiative mechanisms, the stress-velocity relationship becomes nonlinear in this so-called radiation-controlled regime (Kocks et al. 1975).

When the resistance $\hat{\tau}$ exceeds the applied stress $\tilde{\tau}$ at some locations in the slip plane, thermal oscillations may supply enough energy to enable dislocations to move in a jerky fashion (Kocks et al. 1975). Such jerky glide often involves kink migration between obstacles. The dislocation velocity in this regime can be written (Hull and Bacon 1984)

$$\tilde{v} = y\omega_G \exp\left(\frac{-\Delta G}{k_B \theta}\right), \tag{6.80}$$

where $0 \leq \omega_G \leq \omega_A$ is the vibrational frequency of the dislocation, y is the distance the dislocation moves for each obstacle overcome, and ΔG is the activation energy that may generally depend on stress, temperature, and structure variable α. A phenomenological relation for the activation energy, deemed most appropriate when $\hat{\tau}$ stems from short range obstacles, is (Kocks et al. 1975; Hull and Bacon 1984)

$$\Delta G = F_0 \left[1 - (\tilde{\tau}/\hat{\tau})^p\right]^q , \tag{6.81}$$

where F_0 is the activation free energy and p and q are empirical constants limited to the range $0 < p \leq 1$ and $1 \leq q \leq 2$, with $p = 1/2$ and $q = 3/2$ typical. Relations (6.80) and (6.81) are valid when

$$\Delta G \gg k_B \theta, \ 0 < \tilde{\tau} < \hat{\tau} . \tag{6.82}$$

When $\tilde{\tau} \approx \hat{\tau}$, superposition of effects of drag and thermal activation becomes necessary. In the absence of drag, dislocation velocity would in-

crease rapidly towards its limiting value (i.e., the shear wave speed) as applied shear stress $\tilde{\tau}$ approaches threshold stress $\hat{\tau}$. When $\tilde{\tau} = 0$, (6.80) does not apply since the net dislocation velocity in a particular direction should not be nonzero in an unstressed body. Figure 6.1 summarizes regimes of dislocation velocity versus applied stress, following Kocks et al. (1975). The solid line corresponds to physically realistic behavior over the entire range of shear stress up to the theoretical strength. Dashed and dotted lines correspond to responses associated with individual mechanisms. In particular, drag control corresponds to (6.74), while thermal activation, or obstacle control, corresponds to (6.80).

Plastic velocity gradient (6.63) or (6.67) depends on the mobile dislocation density $\tilde{\rho}^i$. Since the mobile dislocation density decreases as a result of dislocations exiting the crystal at free surfaces, maintenance of a constant mobile density, and hence a constant plastic velocity gradient under conditions of steady state dislocation velocities, requires generation and multiplication of dislocations to offset those that exit the crystal or that are pinned or annihilated via interactions with other defects.
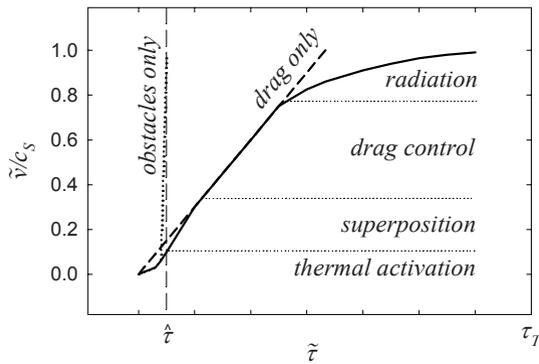
Fig. 6.1 Dislocation velocity-shear stress diagram (Kocks et al. 1975)

A number of functional relationships between dislocation velocities and conjugate driving stresses have been observed or posited (Johnston and Gilman 1959; Lardner 1969; Teodosiu 1970; Bammann and Aifantis 1982), as have evolution equations for mobile and/or immobile dislocation line densities (Bammann and Aifantis 1982; Aifantis 1987; Zikry and Kao 1996; Rezvanian et al. 2007). Dislocation densities, both glissile and sessile, can be viewed as internal state variables, with their evolution equations expressed in the general form of (6.13).

Partial dislocations can be addressed using the same formalism as outlined in (6.62)-(6.82) when the partials move collectively, with a total Burgers vector $\tilde{\mathbf{b}} = \sum \tilde{\mathbf{b}}_{\mathbf{P}}$, with $\tilde{\mathbf{b}}_{\mathbf{P}}$ the Burgers vector of an individual partial. In some cases, mobility of the leading partial may exceed that of the trailing partial, in which case only the Burgers vectors, line densities, and velocities of mobile partials contribute to the plastic velocity gradient. Separation of a full dislocation into partial dislocations in the absence of slip barriers is energetically favorable when the energy of the full dislocation with total Burgers vector exceeds the sum of the energies of the partial dislocations, their interaction energy, and the stacking fault energy of the faulted region between the partials. Dissociation at slip barriers can occur when (Kocks et al. 1975)

$$\hat{\tau} > \tilde{W}_{SF} / \tilde{b} , \tag{6.83}$$

where $\tilde{W}_{SF}$ is the stacking fault energy per unit intermediate area. The shear stress required to move only the leading partial of a dissociated dislocation with partial Burgers vector of magnitude $\tilde{b}_P$ is often estimated as $\hat{\tau} = \tilde{W}_{SF} / \tilde{b}_P$ (Maeda et al. 1988).

6.3 Crystal Plasticity

Consider the description of kinematics of slip on one or more distinct systems i afforded by crystal plasticity theory of Section 3.2.6. The plastic velocity gradient is given by (3.120):

$$\mathbf{L}^{\mathbf{P}} = \dot{\mathbf{F}}^{\mathbf{P}} \mathbf{F}^{\mathbf{P}-1} = \sum_i \dot{\gamma}^i \tilde{\mathbf{s}}^i \otimes \tilde{\mathbf{m}}^i , \tag{6.84}$$

and the plastic work rate per unit intermediate volume is, from (3.117),

$$\dot{W}^P = \tilde{\Pi}_{.\alpha}^{.\beta} L_{.\beta}^{P\alpha} = \sum_i \dot{\gamma}^i \tilde{s}^{i\alpha} \tilde{M}_{\alpha.}^{\beta} \tilde{m}_{\beta}^i - \sum_i \dot{\gamma}^i \tilde{\Psi} (\tilde{s}^{i\alpha} \delta_{\alpha.}^{\beta} \tilde{m}_{\beta}^i)$$

$$= \sum_i \dot{\gamma}^i \tilde{s}^{i\alpha} (J^L F_{.\alpha}^{La} \sigma_a^{.b} F_{.b}^{L-1\beta}) \tilde{m}_{\beta}^i \tag{6.85}$$

$$= \sum_i \dot{\gamma}^i (J^L s_a^i \sigma^{ab} m_b^i) = \sum_i \dot{\gamma}^i \tilde{\tau}^i ,$$

where the resolved lattice Kirchhoff shear stress is

$$\tilde{\tau}^i = J^L s_a^i \sigma^{ab} m_b^i = J^L s_a^i \sigma^{ba} m_b^i = J^L \sigma^{ab} s_{(a}^i m_{b)}^i . \tag{6.86}$$

Symmetrized dyad $s_{(a}^i m_{b)}^i = (s_a^i m_b^i + s_b^i m_a^i)/2$ is sometimes called a Schmid tensor. As explained below, the resolved shear stress $\tilde{\tau}^i$ plays a prominent role in kinetic relations for the slip rates, following Schmid's law that

states that plastic flow initiates in a single crystal at a given temperature and orientation when the applied stress is such that $\tilde{\tau}^i$ reaches a critical magnitude. In uniaxial stress experiments, (6.86) reduces to Schmid's relation $\tau^i = J^{L-1}\tilde{\tau}^i = \sigma\cos(\lambda^i)\cos(\phi^i)$, where σ is the applied true stress, λ^i is the angle between the loading axis and the slip direction, and ϕ^i is the angle between the loading axis and the normal to slip plane i. The product $\cos(\lambda^i)\cos(\phi^i)$ is known as the Schmid factor.

Before addressing slip on multiple systems and their interactions, consider kinetics of slip on a single system, extending the treatment of Section 6.2. In the drag-controlled regime of (6.79), (6.77) gives

$$\dot{\gamma}^i = \tilde{\rho}^i\tilde{b}^i\tilde{v}^i = \frac{\tilde{\rho}^i(\tilde{b}^i)^2(\tilde{\tau}^i - \hat{\tau}^i)}{B} = \frac{\tilde{\rho}^i\tilde{b}^i\Omega_0(\tilde{\tau}^i - \hat{\tau}^i)}{k_B\theta}c_S . \qquad (6.87)$$

In the thermally activated regime of (6.82), (6.80) leads to

$$\dot{\gamma}^i = \tilde{\rho}^i\tilde{b}^i\tilde{v}^i = \tilde{\rho}^i\tilde{b}^i y\omega_G \exp\left(\frac{-\Delta G}{k_B\theta}\right)\frac{\tilde{\tau}^i}{|\tilde{\tau}^i|} = \dot{\gamma}_0^i \exp\left(\frac{-\Delta G}{k_B\theta}\right)\frac{\tilde{\tau}^i}{|\tilde{\tau}^i|} , \qquad (6.88)$$

with $\dot{\gamma}_0^i = \tilde{\rho}^i\tilde{b}^i y\omega_G \geq 0$. Term $\tilde{\tau}^i/|\tilde{\tau}^i|$ ensures that the applied shear stress and dislocation velocity share the same algebraic sign when the convention of Section 3.2.6 adopted. According to that convention, $\dot{\gamma}^i$ may be positive, negative, or zero in algebraic sign. Since $\dot{\gamma}^i = \tilde{\rho}^i\tilde{b}^i\tilde{v}^i$, this implies dislocation velocities $\tilde{v}^i$ may likewise be positive, negative, or zero.

A number of operational parameters are often introduced in the context of thermally activated slip (Kocks et al. 1975). Considering single slip with $\dot{\gamma}^i \Rightarrow \dot{\gamma}$, activation energy parameter Q is defined by

$$Q = \frac{\partial \ln\dot{\gamma}}{\partial[-1/(k_B\theta)]}\bigg|_{\tilde{\tau}} = k_B\theta\frac{\partial \ln\dot{\gamma}}{\partial \ln\theta}\bigg|_{\tilde{\tau}} = k_B\frac{\theta^2}{\dot{\gamma}}\frac{\partial\dot{\gamma}}{\partial\theta}\bigg|_{\tilde{\tau}} . \qquad (6.89)$$

Rate sensitivity m is defined by

$$m = \frac{\partial \ln\dot{\gamma}}{\partial \ln\tilde{\tau}}\bigg|_{\theta} = \frac{\tilde{\tau}}{\dot{\gamma}}\frac{\partial\dot{\gamma}}{\partial\tilde{\tau}}\bigg|_{\theta} . \qquad (6.90)$$

Since

$$\frac{\partial \ln\tilde{\tau}}{\partial \ln\theta}\bigg|_{\tilde{\tau}} = 0 = \frac{\partial \ln\tilde{\tau}}{\partial \ln\theta}\bigg|_{\dot{\gamma}} + \frac{\partial \ln\tilde{\tau}}{\partial \ln\dot{\gamma}}\bigg|_{\theta}\frac{\partial \ln\dot{\gamma}}{\partial \ln\theta}\bigg|_{\tilde{\tau}} , \qquad (6.91)$$

it follows from (6.89) and (6.90) that (Kocks et al. 1975)

$$\frac{\partial \ln\tilde{\tau}}{\partial \ln\theta}\bigg|_{\dot{\gamma}} = -\frac{\partial \ln\dot{\gamma}}{\partial \ln\theta}\bigg|_{\tilde{\tau}}\frac{\partial \ln\tilde{\tau}}{\partial \ln\dot{\gamma}}\bigg|_{\theta} = -\frac{Q}{m k_B\theta} . \qquad (6.92)$$

An activation volume can be described by

$$V^* = k_B \theta \frac{\partial \ln \dot{\gamma}}{\partial \tilde{\tau}} \bigg|_\theta = \frac{k_B \theta}{\tilde{\tau}} \frac{\partial \ln \dot{\gamma}}{\partial \ln \tilde{\tau}} \bigg|_\theta = \frac{m k_B \theta}{\tilde{\tau}} . \qquad (6.93)$$

If $\dot{\gamma}_0^i$ and ΔG are treated as independent of temperature in (6.88), then

$$Q = \frac{\partial \ln \dot{\gamma}}{\partial[-1/(k_B \theta)]} \bigg|_{\tilde{\tau}} = \frac{\partial[-\Delta G/(k_B \theta)]}{\partial[-1/(k_B \theta)]} \bigg|_{\tilde{\tau}} = \Delta G . \qquad (6.94)$$

A simple and common prescription for activation energy in crystal plasticity theory, used at applied stress levels $\tilde{\tau}$ both above and below the mechanical threshold $\hat{\tau}$, is (6.81) with $p = q = 1$:

$$Q = \Delta G = F_0 \left[1 - (\tilde{\tau}/\hat{\tau}) \right], \qquad (6.95)$$

where F_0 and $\hat{\tau}$ are treated as parameters independent of stress and temperature, but possibly dependent on internal state variable α. It follows that

$$\dot{\gamma} = \dot{\gamma}_0 \exp\left[\frac{F_0}{k_B \theta} \left(\frac{\tilde{\tau}}{\hat{\tau}} - 1 \right) \right] \approx \dot{\gamma}_0 \left(\frac{\tilde{\tau}}{\hat{\tau}} \right)^m , \qquad (6.96)$$

where

$$m = \frac{\partial \ln[(\tilde{\tau}/\hat{\tau})^m]}{\partial \ln \tilde{\tau}} \bigg|_\theta = \frac{F_0}{k_B \theta} . \qquad (6.97)$$

Activation volume V^* of (6.93) then becomes

$$V^* = F_0 / \tilde{\tau} . \qquad (6.98)$$

The resistance to dislocation motion, $\hat{\tau}$, consists of short-range barriers associated with lattice friction and long-range barriers associated with interactions between mobile dislocations and other defects, for example (Hull and Bacon 1984; Beltz et al. 1996). A simple way of superposing effects of these barriers at a particular location X in the crystal with particular orientation and elastic constants is the sum (Hull and Bacon 1984)

$$\hat{\tau}(\alpha, \theta, p) = \tau_P(\theta, p) + \tau_D(\alpha, \theta, p) , \qquad (6.99)$$

where τ_P accounts for short-range barriers such as the Peierls stress of (C.237), (C.246), or (C.248) of Section C.4.3, and τ_D is the resisting stress from defects that depends on internal state variable α. Short-range barriers, by definition, manifest approximately at scales on the order of the lattice spacing or smaller. Long-range barriers account for sources of glide resistance separated by distances larger than the lattice spacing, for example forest dislocations or point defects separated by tens of nanometers or more. When other dislocations are the primary long-range obstacle, the following dimensionless internal state variable is often appropriate:

$$\alpha = \tilde{b}\sqrt{\tilde{\rho}_T} \, , \tag{6.100}$$

where $\tilde{\rho}_T(X,t)$ is the total line density of dislocations, both immobile and mobile, per unit volume in the intermediate configuration, as defined in (3.240). At room temperature in many engineering metals, $\tau_D \gg \tau_P$, and the short-range barriers can be overcome by thermal activation (Hull and Bacon 1984), though exceptions exist. At very low temperatures, or in stiff crystals with high concentrations of valence electrons such as ceramics, Peierls stress τ_P can comprise a significant part of the total slip resistance (Friedel 1964; Clayton 2009a, 2010c, d). The slip resistance arising from other dislocations is often expressible in a functional form called Taylor's law (Taylor 1934; Beltz et al. 1996; Clayton 2005a):

$$\tau_D = \hat{a}\mu\alpha = \hat{a}\mu\tilde{b}\sqrt{\tilde{\rho}_T} = \frac{\hat{a}\mu\tilde{b}}{\tilde{l}} \, , \quad 0.05 \leq \hat{a} \leq 1.0 \, , \tag{6.101}$$

with paramter $\hat{a}$ depending on the type of material and $\tilde{l} = \tilde{\rho}_T^{-1/2}$ a mean dislocation spacing. Possible temperature- and pressure-dependencies of τ_D arise only from temperature- and pressure-dependencies of effective (tangent) shear modulus $\mu(\theta, p)$, and are often omitted. In particular, dependence of τ_P and τ_D on hydrostatic pressure p can result from dependence of shear modulus on pressure, since both terms in (6.99) are proportional to the shear modulus. Such pressure effects can be important in shock physics applications (Steinberg et al. 1980; Becker 2004). By definition, $\hat{\tau} \geq 0$, $\tau_P \geq 0$, and $\tau_D \geq 0$. When various dislocation types move simultaneously (e.g., screw, edge, and mixed dislocations and dislocation loops of various orientations), resistances of those types with the largest impedance to motion contribute most strongly to (6.99).

Now consider activity of multiple slip systems in the context of crystal plasticity theory. Phenomenological kinetic laws for slip fall into two categories: rate independent and rate dependent. In the former class of models (Kocks 1970; Hill and Rice 1972; Peirce et al. 1982; Asaro 1983), rate independence occurs when $m \to \infty$ in (6.96), leading to the yield conditions

$$\tilde{\tau}^i = \hat{\tau}^i \Leftrightarrow \dot{\gamma}^i \geq 0,$$
$$\tilde{\tau}^i < \hat{\tau}^i \Leftrightarrow \dot{\gamma}^i = 0. \tag{6.102}$$

In the context of rate independent plasticity, the total number of slip systems n is typically chosen such that slip rates and driving stresses are always non-negative (Peirce et al. 1982). Such a prescription requires distinct assignment of positive and negative directions on a slip plane, as per

the special convention noted in the footnote of Section 3.2.6. Plastic flow occurs on slip system i when the driving stress $\tilde{\tau}^i$ attains a critical value $\hat{\tau}^i$. Systems for which $\dot{\gamma}^i > 0$ are called active slip systems. Shear stresses obey the following hardening laws:

$$\dot{\hat{\tau}}^i = \sum_{j=1}^{n} h^{ij} \dot{\gamma}^j .\tag{6.103}$$

In (6.103), $h^{ij}(\alpha, \theta, p, X)$ is an interaction matrix that accounts for hardening (or softening) and possible interactions among slip systems. Instantaneous values of entries of h^{ij} will generally depend upon defects (e.g., immobile dislocation networks and forest dislocations) that accumulate with inelastic straining, represented by internal state variable α in the present framework, as well as temperature θ. Diagonal entries h^{ii} account for self hardening, and off-diagonal entries $h^{ij} (i \neq j)$ account for latent hardening. In many metals, latent hardening coefficients exceed those for self hardening (Kocks 1970; Conti and Ortiz 2005) in part since dislocations moving and accumulating on the same system do not provide as much obstruction as those on intersecting slip planes. The latter (noncoplanar) defects include forest dislocations, for example. Explicit representations of h^{ij} follow later in the context of rate dependent plasticity.

For actively hardening slip systems, consistency conditions following from (6.102) are

$$\dot{\tilde{\tau}}^i = \dot{\hat{\tau}}^i = \sum_{j=1}^{n} h^{ij} \dot{\gamma}^j > 0 \Leftrightarrow \dot{\gamma}^i > 0 .\tag{6.104}$$

When the rate of resolved shear stress falls below the critical shear stress rate, a formerly active system becomes inactive:

$$\dot{\tilde{\tau}}^i < \dot{\hat{\tau}}^i = \sum_{j=1}^{n} h^{ij} \dot{\gamma}^j \Leftrightarrow \dot{\gamma}^i = 0 ,\tag{6.105}$$

Clearly, dissipation of (6.85) is always non-negative in the context of rate independent crystal plasticity since slip rates are always non-negative in the present description and since $\dot{\gamma}^i \geq 0$ only when $\tilde{\tau}^i = \hat{\tau}^i \geq 0$.

Rate dependent, i.e., viscoplastic, kinetic relations for crystallographic slip are more general and perhaps more commonly encountered (Hutchinson 1976; Teodosiu and Sidoroff 1976; Asaro and Needleman 1985; Nemat-Nasser and Obata 1986; Schoenfeld et al. 1995; Schoenfeld 1998; Horstemeyer et al. 1999; Clayton 2005a, b). The usual sign convention of Section 3.2.6 is prescribed, whereby slip may proceed in either direction on a given system, such that $\dot{\gamma}^i$ may be positive or negative in algebraic sign. A typical functional form for a viscoplastic flow rule is

$$\dot{\gamma}^i = \dot{\gamma}_0 \left| \frac{\tilde{\tau}^i - \hat{\chi}^i}{\hat{\tau}^i} \right|^m \frac{\tilde{\tau}^i - \hat{\chi}^i}{|\tilde{\tau}^i - \hat{\chi}^i|}, \tag{6.106}$$

where parameter $\dot{\gamma}_0$ does not depend on stress and exhibits the same value for all slip systems. Typically $\dot{\gamma}_0$ is imposed as constant (Hutchinson 1976) or a function of temperature alone (Balasubramanian and Anand 2002) for a particular type of crystal. As often prescribed for non-proportional or cyclic loading scenarios, $\hat{\chi}^i$ is an evolving backstress capturing directional hardening effects (McDowell and Moosebrugger 1992; Horstemeyer and McDowell 1998; Horstemeyer et al. 1999; Xie et al. 2004). Backstress $\hat{\chi}^i = 0$ by definition in many traditional models (Asaro 1983; Asaro and Needleman 1985). By inverting and time differentiating (6.106), it is evident that as $m \to \infty$, the limiting case of rate independent behavior is approached. Notice that so long as $\tilde{\tau}^i \geq \hat{\chi}^i$, (6.106) results in unconditionally non-negative dissipation $\dot{W}^P$ in (6.85). When $\hat{\chi}^i = 0$, (6.106) corresponds to a dissipation potential Ω in the context of the second of (4.75):

$$\Omega = \sum_{i=1}^{n} \frac{\dot{\gamma}_0 \hat{\tau}^i}{1+m} \left| \frac{\tilde{\tau}^i}{\hat{\tau}^i} \right|^{1+m}, \quad \tilde{\tau}^i \frac{\partial \Omega}{\partial \tilde{\tau}^i} \geq 0, \tag{6.107}$$

with

$$\dot{\gamma}^i = \begin{cases} \partial \Omega / \partial \tilde{\tau}^i & \forall \tilde{\tau}^i \neq 0, \\ 0 & \forall \tilde{\tau}^i = 0. \end{cases} \tag{6.108}$$

Hardening evolution laws typically exhibit the form

$$\dot{\hat{\tau}}^i = \sum_{j=1}^{n} h^{ij} \left| \dot{\gamma}^j \right|, \tag{6.109}$$

where matrix h^{ij} is defined in the same manner as in (6.103). A standard assumption for many metallic solids is (Hutchinson 1976; Peirce et al. 1982; Asaro 1983)

$$h^{ij} = \tilde{q}h + (1 - \tilde{q})h\delta^{ij}, \quad 1.0 \leq \tilde{q} \leq 1.4, \tag{6.110}$$

where $\tilde{q}$ is the latent hardening ratio that is treated as a constant for a given material. When $\tilde{q} = 1$, all systems harden equally, an assumption used by and often credited to Taylor (1934). Strong latent hardening with $\tilde{q} \approx 1.4$ of non-coplanar systems has been suggested as a typical rule for ductile metallic crystals (Asaro and Needleman 1985). Parameter h in (6.110) is an internal variable that evolves with cumulative plastic shear γ and possibly temperature, e.g.,

$$h = h(\gamma, \theta, p), \quad \gamma = \sum_i \int |\dot{\gamma}^i| \, dt . \tag{6.111}$$

Two different slip system hardening models suggested by Peirce et al. (1982) include

$$h = h_0 \, \text{sech}^2 \left(\frac{h_0 \gamma}{\hat{\tau}_s - \hat{\tau}_0} \right), \tag{6.112}$$

and

$$h = h_0 \left(\frac{h_0 \gamma}{\hat{n} \hat{\tau}_0} + 1 \right)^{\hat{n}-1}, \tag{6.113}$$

where h_0 is a hardening modulus with dimensions of stress, $\hat{\tau}_0$ is an initial value of $\hat{\tau}$, $\hat{\tau}_s$ is a saturation value of $\hat{\tau}$, and $\hat{n}$ is a hardening exponent.

An alternative hardening relation to (6.109) given by Horstemeyer et al. (1999) is

$$\dot{\hat{\tau}}^i = h_0 \sum_{j=1}^{n} \left[\tilde{q} + (1 - \tilde{q}) \delta^{ij} \right] |\dot{\gamma}^j| - r_0 \hat{\tau}^i \sum_{j=1}^{n} |\dot{\gamma}^j|, \tag{6.114}$$

where h_0 is a hardening modulus and r_0 is a dimensionless parameter that accounts for dynamic recovery, leading to eventual saturation of slip resistance $\hat{\tau}^i$. Both h_0 and r_0 may depend on temperature; for example reflecting increased dislocation mobility at observed at higher temperatures in the thermally activated regime of Fig. 6.1. The backstress on a given slip system in (6.106) typically evolves only as a result of slip on that system (Horstemeyer et al. 1999; Clayton and McDowell 2003a):

$$\dot{\hat{\chi}}^i = h_1 \dot{\gamma}^i - r_1 \hat{\chi}^i |\dot{\gamma}^i|, \tag{6.115}$$

where h_1 and r_1 may in general depend on temperature. Regardless of particular formulation, when $\hat{\tau}^i$ and $\hat{\chi}^i$ evolve with changes in deformation and temperature, each can be interpreted as a kind of internal state variable, though $\hat{\tau}^i$ and $\hat{\chi}^i$ do not explicitly enter the thermodynamic potentials and response functions of (6.9)-(6.13).

When dislocations are the primary source of stored energy in the lattice—for example energy of cold working attributed to self-equilibrating stress fields supported by dislocations—the simplest natural choice for a scalar internal state variable is a dimensionless function of the total dislocation density $\tilde{\rho}_T$, as in (6.100). Scalar $\tilde{\rho}_T$ defined in (3.240), with physical dimensions of length of dislocation line per unit intermediate volume, is assumed to encompass energetic effects of both geometrically necessary and statistically stored dislocations (Ashby 1970), or net disloca-

tions and absolute dislocations (Werne and Kelly 1978), as described in Section 3.3.2. More detailed, tensor-based internal variable descriptions delineating energies of geometrically necessary and statistically stored dislocation densities are deferred until Chapters 8 and 9. Using (6.100), residual free energy (6.60) becomes (Clayton 2005a, b; 2009a)

$$\tilde{\Psi}^R = \frac{1}{2}\tilde{\kappa}\tilde{b}^2\tilde{\rho}_T .$$

(6.116)

The linear dependence of stored energy on dislocation density indicated by (6.117) has been used in thermodynamic components of a number of finite deformation plasticity models, particularly with regards to statistically stored dislocations (Bammann 2001; Regueiro et al. 2002; Svendsen 2002). Coefficient $\tilde{\kappa}$ can be assigned a more explicit definition when details regarding the dislocation distribution, such as dislocation orientations and median separation distances, are known. In the simplest approximation, in which all dislocations are treated as non-interacting straight lines of the same type in an infinite elastic medium, the energy per unit length E of dislocation line is given by linear elastic solution (C.152):

$$E = \hat{K}\frac{\tilde{b}^2}{4\pi}\ln\left(\frac{R}{R_C}\right),$$

(6.117)

where, as explained in Section C.1.6 of Appendix C, the energy factor $\hat{K}$ depends on the type (i.e., screw, edge, or mixed) and orientation of the dislocation as well as the second-order elastic coefficients that may depend on temperature. For a pure screw dislocation in the isotropic elastic approximation, energy factor $\hat{K} = \mu$, the elastic shear modulus. Combining (6.116) and (6.117), a typical approximation is (Kocks et al. 1975; Hull and Bacon 1984; Clayton 2009a, 2010c, d)

$$\tilde{\Psi}^R = E\tilde{\rho}_T = \Lambda\hat{K}\tilde{b}^2\tilde{\rho}_T , \ 0.5 \lesssim \Lambda \lesssim 1.0 ,$$

(6.118)

leading to

$$\tilde{\kappa} = 2\frac{\tilde{\Psi}^R}{\tilde{b}^2\tilde{\rho}_T} = 2\Lambda\hat{K} .$$

(6.119)

Using (6.85), (6.100), (6.116), and (6.118), Taylor-Quinney parameter of (6.47) becomes, in the context of crystal plasticity with the (square root of) total scalar dislocation density as an internal variable as in (6.100),

$$\beta' = \left(\sum_i \tilde{\tau}^i\dot{\gamma}^i - \alpha\left(\tilde{\kappa} - \theta\frac{\partial\tilde{\kappa}}{\partial\theta}\right)\dot{\alpha}\right)\left(\sum_i \tilde{\tau}^i\dot{\gamma}^i\right)^{-1}$$

$$= 1 - \Lambda\tilde{b}^2\dot{\tilde{\rho}}_T\left(\hat{K} - \theta\frac{\partial\hat{K}}{\partial\theta}\right)\left(\sum_i \tilde{\tau}^i\dot{\gamma}^i\right)^{-1} .$$

(6.120)

When the dependence of $\hat{K}$ on temperature is negligible, as the rate of dislocation accumulation increases, residual energy storage increases, β' decreases, and the fraction of plastic work converted to temperature rise via (6.46) decreases. A typical, but not universal, trend is that the fraction of plastic work converted to heat energy can be significantly less than unity as a metallic crystal or polycrystal strain hardens, and then later increases towards unity as the material ceases to harden and the strain energy contribution from defect densities saturates (Taylor and Quinney 1934; Foltz and Grace 1969; Lee 1969; Aravas et al. 1990; Wright 2002; Clayton 2005a, 2009c). The conjugate thermodynamic force associated with (6.60), (6.100), and (6.116)-(6.119) is $-\partial \tilde{\Psi}^R / \partial \alpha = -2\Lambda\hat{K}\alpha \approx -\mu\tilde{b}\sqrt{\tilde{\rho}_T}$, which is notably proportional to (the negative of) resistance τ_D to dislocation glide from dislocation interactions in Taylor's hardening rule (6.101).

An evolution equation for $\dot{\tilde{\rho}}_T$ of the general form (6.13) is required to complete the thermodynamic description. Such an equation should be formulated so that relationships between defect content and strain hardening, e.g., (6.99)-(6.101) when applicable, as well as experimentally observed trends for β' for the particular crystalline solid under consideration, are all captured simultaneously (Clayton 2005a, b, 2009a).

6.4 Macroscopic Plasticity

Recall from Section 3.2.7 that macroscopic plasticity refers to a description in which each volume element of material to which kinematic and constitutive models are assigned contains a large number of grains in a polycrystal. A convenient way of ensuring that the rate of working from plastic deformation is non-negative[5] in the context of macroscopic plasticity is specification of a plastic dissipation potential along the lines of that described in a general way in Section 4.3. In the present context, from (6.32), the appropriate thermodynamic flux is the plastic velocity gradient $\mathbf{L}^P$, and the conjugate driving force is the Eshelby stress measure $\tilde{\mathbf{\Pi}}$. Recall that both of these quantities are couched in intermediate configuration $\tilde{B}$.

---

[5] Restricting the rate of plastic working associated with dislocation glide to be dissipative is often a physically realistic assumption. However, in arbitrary solids, the rate of inelastic working need not always dissipate energy if rates of internal variables and heat conduction provide enough dissipation so that the net entropy production (left side of (6.32)) always remains non-negative (Lubliner 1990).

Specifically as an illustrative example, let

$$\mathbf{L^P} = \lambda^P \frac{\partial \Omega}{\partial \tilde{\mathbf{\Pi}}'}, \tag{6.121}$$

where the scalar plastic multiplier $\lambda^P \geq 0$ will be determined later, and the flow potential Ω is constructed such that the generalized scalar product $\tilde{\mathbf{\Pi}} : \partial\Omega/\partial\tilde{\mathbf{\Pi}}' \geq 0$. The deviatoric part of the intermediate Eshelby stress is equivalent to the deviatoric part of the Mandel stress:

$$\begin{aligned}
\tilde{\Pi}_\alpha'^{,\beta} &= \tilde{M}_\alpha^{\,\beta} - \tilde{\Psi}\delta_\alpha^{\,\beta} - \frac{1}{3}(\tilde{M}_\chi^{\,\chi} - \tilde{\Psi}\delta_\chi^{\,\chi})\delta_\alpha^{\,\beta} \\
&= \tilde{M}_\alpha^{\,\beta} - \frac{1}{3}\tilde{M}_\chi^{\,\chi}\delta_\alpha^{\,\beta} = \tilde{M}_\alpha'^{,\beta}.
\end{aligned} \tag{6.122}$$

A simple illustrative example of dissipation potential is

$$\Omega = (\tilde{\Pi}_\alpha'^{,\beta}\tilde{\Pi}_{.\beta}'^{,\alpha})^{1/2} = (\tilde{\Pi}'^{\alpha\beta}\tilde{\Pi}_{\alpha\beta}')^{1/2} \geq 0. \tag{6.123}$$

From (6.121) and (6.123), the plastic velocity gradient becomes

$$L_{.\beta}^{P\alpha} = \frac{\lambda^P}{\Omega}\tilde{\Pi}_{.\beta}'^{,\alpha}, \tag{6.124}$$

and is clearly coaxial (i.e., of the same direction in $T\tilde{B} \times T^*\tilde{B}$) as the driving stress $\tilde{\mathbf{\Pi}}'$. Squaring both sides of (6.124) leads to the consistent definition

$$\lambda^P = (L^{P\alpha\beta}L_{\alpha\beta}^P)^{1/2}. \tag{6.125}$$

The resulting plastic dissipation is always non-negative since

$$\tilde{\Pi}_\alpha^{\,\beta}L_{.\beta}^{P\alpha} = \lambda^P \tilde{\Pi}_\alpha^{\,\beta}\frac{\partial\Omega}{\partial\tilde{\Pi}_{\alpha.}'^{,\beta}} = \frac{\lambda^P}{\Omega}\tilde{\Pi}'^{\alpha\beta}\tilde{\Pi}_{\alpha\beta}' = \lambda^P\Omega \geq 0. \tag{6.126}$$

Relations (6.121)-(6.126) parallel (4.84)-(4.89), with $\mathbf{L^P}$ used here as the thermodynamic flux rather than $\dot{\mathbf{F}}^\mathbf{P}$ used in Section 4.3. Another subtle difference is that in (4.85) and (4.86) of Section 4.3, the plastic multiplier is absorbed into the dissipation potential, whereas λ^P is written distinctly from the dissipation potential in (6.121). Since $\tilde{\Pi}_\alpha'^{,\alpha} = 0$, $\dot{J}^P = J^P L_{.\alpha}^{P\alpha} = 0$ from (6.124), ensuring that macroscopic plastic deformation is isochoric. A constitutive relationship between λ^P and the state variables (e.g., stress or strain, temperature, and internal state variable(s)) then dictates the magnitude of plastic flow.

Typically in engineering practice, as opposed to (6.121), a kinetic equation is specified for the plastic velocity gradient $\hat{\mathbf{L}}^\mathbf{P}$ mapped to the current configuration B, i.e.,

$$\hat{\mathbf{L}}^\mathbf{P} = \mathbf{F^L L^P F^{L-1}}, \quad \hat{\mathbf{D}}^\mathbf{P} = \left(\mathbf{F^L L^P F^{L-1}}\right)_{symm}, \quad \hat{\mathbf{W}}^\mathbf{P} = \left(\mathbf{F^L L^P F^{L-1}}\right)_{skew}, \tag{6.127}$$

where $\hat{\mathbf{D}}^{\mathbf{P}}$ is a symmetric plastic strain rate and $\hat{\mathbf{W}}^{\mathbf{P}}$ is a skew plastic spin. With these definitions, the spatial velocity gradient of (3.58) becomes

$$
\begin{aligned}
L^a_{.b} = v^a_{;b} = \dot{F}^a_{.A} F^{-1A}_{.b} &= \dot{F}^{La}_{.\alpha} F^{L-1\alpha}_{.b} + \hat{L}^{Pa}_{.b} \\
&= L^{La}_{.b} + \hat{W}^{Pa}_{.b} + \hat{D}^{Pa}_{.b} \,.
\end{aligned}
\tag{6.128}
$$

Kinetic equations for the plastic strain rate and plastic spin of (6.127) are usually prescribed separately. The latter is often omitted (i.e., $\hat{W}^{Pa}_{.b} = 0$ by definition) for solids that remain isotropic throughout their deformation history, e.g., polycrystalline metals with randomly oriented grains that do not develop significant texture or anisotropic hardening during plastic flow. In plastically anisotropic polycrystals, anisotropic hardening can be represented by a traceless, symmetric second-order tensor (i.e., a tensor internal state variable) $\hat{\mathbf{a}}$ often labeled a backstress. In such anisotropic materials, the plastic spin can be assigned as (Aifantis 1987; Bammann and Aifantis 1989; Bammann et al. 1993; Regueiro et al. 2002)

$$
\hat{\mathbf{W}}^{\mathbf{P}} = \hat{\lambda}^W (\hat{\mathbf{a}}\hat{\mathbf{D}}^{\mathbf{P}} - \hat{\mathbf{D}}^{\mathbf{P}}\hat{\mathbf{a}}) \,, \quad \hat{\mathbf{a}} = \hat{\mathbf{a}}^T, \ \mathrm{tr}(\hat{\mathbf{a}}) = 0 \,,
\tag{6.129}
$$

with scalar $\hat{\lambda}^W$ related to dislocation interactions (Bammann and Aifantis 1989) or dominant slip system orientations (Regueiro et al. 2002).

The plastic strain rate of the second of (6.127) can be assigned a kinetic law in a number of physically meaningful and mathematically convenient ways, and an immense literature exists on the subject (Hill 1950; Perzyna 1963; Follansbee and Kocks 1988; Lubliner 1990; Bammann et al. 1993; Marin and McDowell 1996; Simo and Hughes 1998; Scheidler and Wright 2001, 2003; Wright 2002; Nemat-Nasser 2004). For example, for nonporous viscoplastic solids, a direct flow rule applicable over a range of strain rates and temperatures can be prescribed as (Bammann et al. 1993)

$$
\hat{\mathbf{D}}^{\mathbf{P}} = \begin{cases} \hat{f}(\theta)\sinh\left[\dfrac{|\hat{\boldsymbol{\xi}}|-\hat{k}-\hat{Y}(\theta)}{\hat{V}(\theta)}\right]\dfrac{\hat{\boldsymbol{\xi}}}{|\hat{\boldsymbol{\xi}}|} & \text{for } |\hat{\boldsymbol{\xi}}| = (\hat{\boldsymbol{\xi}}:\hat{\boldsymbol{\xi}})^{1/2} \geq \hat{k}+\hat{Y}, \\[2ex] 0 & \text{for } |\hat{\boldsymbol{\xi}}| = (\hat{\boldsymbol{\xi}}:\hat{\boldsymbol{\xi}})^{1/2} < \hat{k}+\hat{Y}, \end{cases}
\tag{6.130}
$$

where the stress difference

$$
\hat{\boldsymbol{\xi}} = \boldsymbol{\sigma}' - \frac{2}{3}\hat{\mathbf{a}} \,,
\tag{6.131}
$$

and the deviatoric Cauchy stress is

$$
\sigma'^{ab} = \sigma^{ab} - \frac{1}{3}\sigma^c_{.c}g^{ab} = \sigma^{ab} + pg^{ab} \,,
\tag{6.132}
$$

with p the Cauchy pressure. In (6.130), $\hat{f}$, $\hat{Y}$, and $\hat{V}$ are scalar functions of temperature, $\hat{k}$ reflects isotropic hardening (or softening) and may in-

crease (or decrease) during the deformation history. Similarly, backstress $\hat{\boldsymbol{\alpha}}$ evolves with the deformation history. Evolution equations for $\hat{k}$ and $\hat{\boldsymbol{\alpha}}$ often follow a hardening-dynamic recovery format similar to (6.114) and (6.115) and are available in the literature (Bammann et al. 1993; McDowell et al. 1993; Marin and McDowell 1996).

Described in what follows in (6.133)-(6.143) is the standard engineering approach towards kinetics of macroscopic plasticity based on principles of normality, associativity, and a Von Mises–type yield function. Often, for isotropic and plastically incompressible solids, the normality conditions

$$\hat{\mathbf{D}}^{\mathbf{P}} = \begin{cases} \hat{\lambda}^P (\partial \hat{\Omega} / \partial \boldsymbol{\sigma}') \text{ for } \hat{F} = 0, \\ 0 \qquad \text{for } \hat{F} < 0, \end{cases} \tag{6.133}$$

are assigned, where values of $\hat{\Omega} = $ constant represent a set of flow iso-surfaces in deviatoric stress space, $\hat{\lambda}^P \geq 0$ is a plastic multiplier, and $\hat{F}$ is the yield function . Though many other possible flow functions exist, according to the most prevalent assumption for ductile metals, $\hat{\Omega}$ is defined in terms of the second invariant of the deviatoric stress:

$$\hat{\Omega} = \sqrt{J_2} = \left(\frac{1}{2} \sigma'^{ab} \sigma'_{ab} \right)^{1/2} = \frac{\bar{\sigma}}{\sqrt{3}} = \sqrt{\frac{3}{2}} \bar{\tau} , \tag{6.134}$$

$$J_2 = \frac{1}{2} \sigma'^{ab} \sigma'_{ab} , \tag{6.135}$$

$$\bar{\tau} = \left(\frac{2}{3} J_2 \right)^{1/2} = \frac{\sqrt{2}}{3} \bar{\sigma} , \tag{6.136}$$

$$\bar{\sigma} = \sqrt[1]{2} \left\{ (\sigma^{11} - \sigma^{22})^2 + (\sigma^{22} - \sigma^{33})^2 + (\sigma^{33} - \sigma^{11})^2 \right.$$
$$\left. + 6 \left[(\sigma^{12})^2 + (\sigma^{23})^2 + (\sigma^{31})^2 \right] \right\}^{1/2} \tag{6.137}$$
$$= \left[(3/2) \sigma^{ab} \sigma_{ab} - (1/2) \sigma^a_{.a} \sigma^b_{.b} \right]^{1/2} = \left[(3/2) \sigma'^{ab} \sigma'_{ab} \right]^{1/2} = \left[3 J_2 \right]^{1/2} .$$

Above, $\bar{\sigma}$ is called the Von Mises stress (Von Mises 1913) or effective stress, and $\bar{\tau}$ is called the octahedral shear stress. For a uniaxial normal stress state with nonzero Cauchy stress component σ^{11}, the following conditions apply: $\bar{\sigma} = \sigma^{11}$, $J_2 = 2(\sigma^{11})^2 / 9$, and $\bar{\tau} = \sqrt{2} \sigma^{11} / 3$. For a shear stress state with nonzero component $\sigma^{12} = \sigma^{21}$, the following conditions hold: $J_2 = (\sigma^{12})^2$, $\bar{\sigma} = \sqrt{3} \sigma^{12}$, and $\bar{\tau} = \sqrt{2/3} \sigma^{12}$. The spatial plastic deformation rate following from (6.133) and (6.134) is

$$\hat{\mathbf{D}}^{\mathbf{P}} = \frac{\hat{\lambda}^P}{2\hat{\Omega}}\boldsymbol{\sigma}' = \frac{\hat{\lambda}^P}{2\sqrt{J_2}}\boldsymbol{\sigma}' = \frac{\sqrt{3}\hat{\lambda}^P}{2\bar{\sigma}}\boldsymbol{\sigma}', \text{ (for } \hat{F} = 0\text{)}, \qquad (6.138)$$

clearly traceless and symmetric. From a rudimentary physical standpoint, (6.138) is realistic: the material deforms inelastically in the direction of the applied stress, in agreement with experimental observations. Squaring both sides of (6.133) or (6.138), the plastic multiplier satisfies

$$\hat{\lambda}^P = (\hat{\mathbf{D}}^{\mathbf{P}} : \hat{\mathbf{D}}^{\mathbf{P}})^{1/2}\left[(\partial\hat{\Omega}/\partial\boldsymbol{\sigma}') : (\partial\hat{\Omega}/\partial\boldsymbol{\sigma}')\right]^{-1/2} = (2\hat{\mathbf{D}}^{\mathbf{P}} : \hat{\mathbf{D}}^{\mathbf{P}})^{1/2}. \quad (6.139)$$

Kinetic equations for plastic deformation are often labeled either as associative or non-associative. In an associative flow rule, with a plastic potential of the form (6.134), the yield function is

$$\hat{F} = \hat{\Omega} - \hat{k} = \sqrt{J_2} - \hat{k}, \qquad (6.140)$$

where scalar function $\hat{k}(\{\varsigma\}, X)$ demarcates elastic and plastic domains and $\{\varsigma\}$ is a set of scalars that may include temperature, internal state variable α, and other field variables (e.g., pressure). When the yield and flow functions do not depend upon the time rate of plastic deformation, plastic behavior is said to be rate independent, while in the converse situation, the plastic deformation is said to be rate dependent or viscoplastic.

In many engineering applications, plastic deformation is idealized as rate independent. In such cases, the magnitude of the plastic strain rate for a given thermodynamic state (e.g., state of stress, temperature, and internal variables) is prescribed as follows. Kuhn-Tucker conditions are (Lubliner 1990)

$$\hat{\lambda}^P \hat{F} = 0, \ \hat{\lambda}^P \geq 0, \ \hat{F} \leq 0, \qquad (6.141)$$

with the plastic multiplier

$$\hat{\lambda}^P = \begin{cases} \hat{H}^{-1}\left\langle (\partial\hat{F}/\partial\sigma^{ab})\dot{\sigma}^{ab}\right\rangle & \text{for } \hat{F} = 0 \text{ and } \hat{H} \neq 0, \\ 0 & \text{for } \hat{F} < 0. \end{cases} \qquad (6.142)$$

Macaulay brackets in (6.142) satisfy $\langle A\rangle = 0 \forall A \leq 0$ and $\langle A\rangle = A \forall A > 0$ for scalar function A, and are not to be confused with the dual product operator of (2.4) and (2.80)-(2.82) which acts only on vector and tensor objects of higher order. Hardening modulus $\hat{H}$ satisfies the consistency conditions

$$\dot{\hat{F}} = 0 = \dot{\hat{F}}\Big|_{\boldsymbol{\sigma}} + \frac{\partial\hat{F}}{\partial\sigma^{ab}}\dot{\sigma}^{ab} \quad \text{(when } \hat{F} = 0\text{)}$$

$$\Rightarrow \dot{\hat{F}}\Big|_{\boldsymbol{\sigma}} = -\hat{\lambda}^P \hat{H} = \sum \frac{\partial\hat{F}}{\partial\varsigma}\Big|_{\boldsymbol{\sigma}}\dot{\varsigma} = -\sum \frac{\partial\hat{k}}{\partial\varsigma}\Big|_{\boldsymbol{\sigma}}\dot{\varsigma}, \qquad (6.143)$$

where summation applies over all variables of the set $\{\varsigma\}$. During plastic deformation, the yield surface in stress space represented by $\hat{F} = 0$ and the stress state coincide. During elastic unloading, $\hat{F} < 0$, and one says that the stress state is contained within the yield surface. Typically (6.138) and (6.142) are combined with (3.58) and an objective rate form of (6.29) to provide a relationship between the time derivative of Cauchy stress and the total deformation rate $D_{ab} = L_{(ab)}$. The constitutive description is complete upon prescription of evolution equation(s) for internal state variable(s) α and a functional relationship for $\hat{k}$ in terms of $\{\varsigma\}$ at each location X. When $\hat{k}$ is a constant, $\hat{H} = 0$ in (6.143), and the corresponding mechanical behavior is labeled perfectly plastic. When $\hat{H} = 0$, $\hat{\lambda}^P$ is indeterminate in (6.142), but the plastic deformation rate is still dictated by $\hat{F} = 0$ and $\dot{\hat{F}} = 0$ (Lubliner 1990).

In the case of non-associative plasticity, the yield function and flow function need not be related, i.e., $\hat{F} \neq \hat{\Omega} - \hat{k}$. More generally, for the non-associative case, the direction of plastic deformation and its magnitude can be prescribed independently of any dissipation potential, as in (6.130). Bammann et al. (1993) showed that nonzero function $\hat{V}$ renders direct flow rule (6.130) rate dependent.

The theoretical framework of (6.133)-(6.143) is used frequently in engineering practice for isotropic ductile metals; when the material is plastically incompressible, this framework always provides for unconditionally non-negative dissipation from plastic working in (6.32). From (6.16), (6.34), and (6.127), when $\dot{J}^P = 0$ the plastic work rate per unit intermediate volume is

$$\dot{W}^P = \tilde{\Pi}_\alpha^{\cdot\beta} L_{\cdot\beta}^{P\alpha} = \tilde{M}_\alpha^{\cdot\beta} L_{\cdot\beta}^{P\alpha} = J^L \sigma^{ab} \hat{L}_{ab}^P = J^L \sigma^{ab} \hat{D}_{ab}^P . \tag{6.144}$$

Substituting (6.138) then gives

$$\dot{W}^P = J^L \sigma^{ab} \hat{D}_{ab}^P = J^L \hat{\lambda}^P \frac{\sigma'^{ab} \sigma'_{ab}}{2\hat{\Omega}} = J^L \hat{\lambda}^P \hat{\Omega} = J^L \hat{\lambda}^P \sqrt{J_2} \geq 0 . \tag{6.145}$$

Since the plastic spin referred to the current configuration, $\hat{\mathbf{W}}^P$ of (6.127), is skew by definition, this quantity does no mechanical work in (6.144) and does not contribute to the energy balance or dissipation inequality.

It is emphasized that (6.133)-(6.143) and (6.145) apply only for isotropic (poly)crystalline solids. When inelastic behavior is anisotropic, typically the notion of backstress is introduced to reflect differences in directions of $\hat{\mathbf{D}}^P$ and the deviatoric Cauchy stress $\boldsymbol{\sigma}'$ (Lubliner 1990; Bam-

mann et al. 1993; Marin and McDowell 1996; Voyiadjis and Abu Al-Rub 2003), as indicated for example in (6.130). Furthermore, the lattice spin, and hence the total and plastic spins, require delineation in anisotropic solids, since the representation of the Cauchy stress in a hyperelastic solid depends on the rotational part of the lattice deformation, $\mathbf{R}^{\mathbf{L}} = \mathbf{V}^{\mathbf{L}-1}\mathbf{F}^{\mathbf{L}}$, via the second of (6.5), even when lattice stretch $\mathbf{V}^{\mathbf{L}}$ is small. From (6.138) the spatial plastic velocity gradient $\hat{\mathbf{L}}^{\mathbf{P}} = \mathbf{F}^{\mathbf{L}}\mathbf{L}^{\mathbf{P}}\mathbf{F}^{\mathbf{L}-1}$ is always traceless, though the true plastic volume change $\dot{J}^{P} = J^{P}L_{.\alpha}^{P\alpha} \neq 0$ in general, meaning that (6.144) is not ensured by (6.138). However, in the limit of small lattice strains, (3.73) and (3.74) lead to

$$L_{.\alpha}^{P\alpha} \approx R_{.a}^{LT\alpha}\hat{L}_{.b}^{Pa}R_{.\alpha}^{Lb} = \hat{L}_{.b}^{Pa}\delta_{.a}^{b} = \hat{D}_{.a}^{Pa} = 0 . \qquad (6.146)$$

6.5 Geometrically Linear Elastoplasticity

Linearization of finite deformation kinematics of two-term multiplicative elastoplasticity follows from (3.78)-(3.83). Recall that displacement gradient $\nabla\mathbf{u}$, strain $\boldsymbol{\varepsilon}$, and rotation $\boldsymbol{\Omega}$ are each decomposed additively as

$$u_{a;b} = \beta_{ab}^{L} + \beta_{ab}^{P}, \qquad (6.147)$$

$$\varepsilon_{ab} = u_{(a;b)} = \beta_{(ab)}^{L} + \beta_{(ab)}^{P} = \varepsilon_{ab}^{L} + \varepsilon_{ab}^{P}, \qquad (6.148)$$

$$\Omega_{ab} = u_{[a,b]} = \beta_{[ab]}^{L} + \beta_{[ab]}^{P} = \Omega_{ab}^{L} + \Omega_{ab}^{P}, \qquad (6.149)$$

where superscripts L and P denote lattice-changing and plastic (i.e., lattice-preserving) parts, and the remaining notation is explained in Section 3.2.4. When plastic deformation is isochoric, the resulting kinematic implications are $\text{tr}(\boldsymbol{\varepsilon}^{\mathbf{P}}) = 0$ and $\text{tr}(\dot{\boldsymbol{\varepsilon}}^{\mathbf{P}}) = 0$, though throughout the forthcoming developments of Section 6.5, plastic deformation is not constrained to be volume-preserving unless noted otherwise.

6.5.1 Constitutive Assumptions

In the geometrically linear theory of elastic-plastic solids, (6.9)-(6.13) are replaced by the following constitutive assumptions:

$$\psi = \psi\left(\boldsymbol{\varepsilon}^{\mathbf{L}}, \alpha, \theta, \nabla\theta, x, \mathbf{g}_{a}\right), \ \psi = \psi\left(\varepsilon_{ab}^{L}, \alpha, \theta, \theta_{,a}, x, \mathbf{g}_{a}\right); \qquad (6.150)$$

$$\eta = \eta\left(\boldsymbol{\varepsilon}^{\mathbf{L}}, \alpha, \theta, \nabla\theta, x, \mathbf{g}_{a}\right), \ \eta = \eta\left(\varepsilon_{ab}^{L}, \alpha, \theta, \theta_{,a}, x, \mathbf{g}_{a}\right); \qquad (6.151)$$

$$\boldsymbol{\sigma} = \boldsymbol{\sigma}\left(\boldsymbol{\varepsilon}^{\mathbf{L}}, \alpha, \theta, \nabla\theta, X, \mathbf{g}_{a}\right), \ \sigma^{ab} = \sigma^{ab}\left(\varepsilon_{ab}^{L}, \alpha, \theta, \theta_{,a}, x, \mathbf{g}_{a}\right); \qquad (6.152)$$

$$\mathbf{q} = \mathbf{q}\left(\boldsymbol{\varepsilon}^{\mathrm{L}}, \alpha, \theta, \nabla\theta, x, \mathbf{g}_a\right), \quad q^a = q^a\left(\varepsilon_{ab}^L, \alpha, \theta, \theta_{,a}, x, \mathbf{g}_a\right); \tag{6.153}$$

$$\dot{\alpha} = \dot{\alpha}\left(\boldsymbol{\varepsilon}^{\mathrm{L}}, \alpha, \theta, \nabla\theta, x, \mathbf{g}_a\right), \quad \dot{\alpha} = \dot{\alpha}\left(\varepsilon_{ab}^L, \alpha, \theta, \theta_{,a}, x, \mathbf{g}_a\right); \tag{6.154}$$

Because all volume changes are assumed small in the present linear analysis, thermodynamic potentials are defined, for convenience, on a per unit mass basis as opposed to a per unit (intermediate configuration) volume basis as was considered in Section 6.1. Analogously to those of the nonlinear theory, thermodynamic potentials and response functions in (6.150)-(6.154) do not depend explicitly upon the plastic distortion or plastic strain. Notice that objectivity with respect to small rigid body rotations precludes the use of the lattice rotation $\boldsymbol{\Omega}^{\mathrm{L}}$ of (6.149) as a dependent variable entering (6.150)-(6.154), via the same arguments used in Section 5.4.1 following (5.260).

6.5.2 Thermodynamics

Substituting (6.150) into linearized dissipation inequality (4.73) gives

$$\sigma^{ab}\dot{\varepsilon}_{ab} - \rho\left[\frac{\partial\psi}{\partial\varepsilon_{ab}^L}\dot{\varepsilon}_{ab}^L + \left(\eta + \frac{\partial\psi}{\partial\theta}\right)\dot{\theta} + \frac{\partial\psi}{\partial\theta_{,a}}\gamma_a + \frac{\partial\psi}{\partial\alpha}\dot{\alpha}\right] \geq \theta^{-1}q^a\theta_{,a}. \tag{6.155}$$

From the time derivative of (6.148), $\dot{\varepsilon}_{ab} = \dot{\varepsilon}_{ab}^L + \dot{\varepsilon}_{ab}^P$, so (6.155) becomes

$$\left(\sigma^{ab} - \rho\frac{\partial\psi}{\partial\varepsilon_{ab}^L}\right)\dot{\varepsilon}_{ab}^L - \rho\left(\eta + \frac{\partial\psi}{\partial\theta}\right)\dot{\theta} - \rho\left(\frac{\partial\psi}{\partial\theta_{,a}}\right)\gamma_a$$

$$+ \sigma^{ab}\dot{\varepsilon}_{ab}^P - \rho\frac{\partial\psi}{\partial\alpha}\dot{\alpha} - \theta^{-1}q^a\theta_{,a} \geq 0. \tag{6.156}$$

Following arguments akin to those of Section 5.1.2, coefficients of $\dot{\varepsilon}_{ab}^L$, $\dot{\theta}$, and $\gamma_a = d(\theta_{,a})/dt$ should vanish identically, leading to the equalities

$$\boldsymbol{\sigma} = \rho\frac{\partial\psi}{\partial\boldsymbol{\varepsilon}^{\mathrm{L}}}, \quad \eta = -\frac{\partial\psi}{\partial\theta}, \quad \frac{\partial\psi}{\partial\nabla\theta} = 0, \tag{6.157}$$

and the reduced constitutive forms

$$\psi = \psi\left(\boldsymbol{\varepsilon}^{\mathrm{L}}, \alpha, \theta, x, \mathbf{g}_a\right), \quad \eta = \eta\left(\boldsymbol{\varepsilon}^{\mathrm{L}}, \alpha, \theta, x, \mathbf{g}_a\right),$$

$$\boldsymbol{\sigma} = \boldsymbol{\sigma}\left(\boldsymbol{\varepsilon}^{\mathrm{L}}, \alpha, \theta, x, \mathbf{g}_a\right). \tag{6.158}$$

Assuming Fourier conduction of the kind suggested in (4.62) and (5.277):

$$q^a = -k^{ab}\theta_{,b}, \tag{6.159}$$

where $\mathbf{k}$ is symmetric and positive semi-definite, local entropy production from heat conduction $-\theta^{-2}q^a\theta_{,a}$ is always non-negative. The entropy inequality then consists of the remaining terms in (6.156):

$$\boldsymbol{\sigma}:\dot{\boldsymbol{\varepsilon}}^{\mathbf{P}} - \rho\frac{\partial\psi}{\partial\alpha}\dot{\alpha} + \frac{1}{\theta}\langle\nabla\theta,\mathbf{k}\nabla\theta\rangle \geq 0, \qquad (6.160)$$

demonstrating that in the absence of temperature gradients, the rate of plastic work $\dot{W}^P = \boldsymbol{\sigma}:\dot{\boldsymbol{\varepsilon}}^{\mathbf{P}}$ must exceed the rate of free energy accumulation associated with the time derivative of internal state variable α. When plastic deformation is isochoric, the plastic dissipation can be expressed as

$$\dot{W}^P = \boldsymbol{\sigma}:\dot{\boldsymbol{\varepsilon}}^{\mathbf{P}} = (\boldsymbol{\sigma} - \rho\psi\mathbf{1}):\dot{\boldsymbol{\varepsilon}}^{\mathbf{P}} = \hat{\boldsymbol{\pi}}:\dot{\boldsymbol{\varepsilon}}^{\mathbf{P}}, \qquad (6.161)$$

with $\hat{\boldsymbol{\pi}} = \boldsymbol{\sigma} - \Psi\mathbf{1}$ a symmetric, small deformation analog of the Eshelby-type stress $\tilde{\boldsymbol{\Pi}}$ of the nonlinear theory first defined in (6.33). An equation for the temperature rise, analogous to (6.45), in terms of the plastic work rate, thermoelastic coupling, the rate of the internal variable, heat conduction, and heat sources can be derived immediately in the context of geometric linearity. Plastic rotation rate $\dot{\Omega}^P_{ab} = \dot{\beta}^P_{[ab]}$ does not contribute to (6.160) or $\dot{W}^P$.

6.5.3 Representative Free Energy

A version of free energy function (6.48) describing a geometrically linear thermoelastic response additively decoupled from effects of internal variables, is

$$\psi = \psi^E\left(\boldsymbol{\varepsilon}^{\mathbf{L}},\theta,x,\mathbf{g}_a\right) + \psi^R\left(\alpha,\theta,x,\mathbf{g}_a\right). \qquad (6.162)$$

The thermoelastic part of (6.162), assuming a linear response analogous to (5.304) about a reference state wherein $\boldsymbol{\varepsilon}^{\mathbf{L}} = 0$ and $\Delta\theta = \theta - \theta_0 = 0$, is

$$\rho_0\psi = \frac{1}{2}\overline{\mathbb{C}}^{abcd}\varepsilon^L_{ab}\varepsilon^L_{cd} - \overline{\beta}^{ab}\varepsilon^L_{ab}\Delta\theta - \rho_0\overline{c}\,\theta\ln\frac{\theta}{\theta_0}, \qquad (6.163)$$

where the thermoelastic constants at a point x with basis $\mathbf{g}_a(x)$ are

$$\overline{\mathbb{C}}^{abcd} = \rho_0\frac{\partial^2\psi^E}{\partial\varepsilon^L_{ab}\partial\varepsilon^L_{cd}}\Big|_{\substack{\varepsilon^{\mathbf{L}}=0\\\theta=\theta_0}}, \quad \overline{\beta}^{ab} = -\rho_0\frac{\partial^2\psi^E}{\partial\theta\partial\varepsilon^L_{ab}}\Big|_{\substack{\varepsilon^{\mathbf{L}}=0\\\theta=\theta_0}}, \qquad (6.164)$$

$$\overline{c} = -\left(\theta\frac{\partial^2\psi^E}{\partial\theta^2}\right)\Big|_{\substack{\varepsilon^{\mathbf{L}}=0\\\theta=\theta_0}}. \qquad (6.165)$$

Thermoelastic constants in (6.164) depend on the symmetry of the material (via $\mathbf{g}_a(x)$) and are identical to those of (5.305) so long as the former are measured in a loading regime for which the material undergoes only lattice (thermoelastic) and not plastic deformation. Specific heat per unit mass in (6.165) likewise is identical to that of Section 5.1.4. All considerations regarding symmetry of material coefficients discussed in Section 5.4.5 and Appendix A apply for the elasticity tensor and the thermal stress coefficients in (6.164). Possible effects of evolving densities of defects (i.e., non-stationary internal variables) on material coefficients are omitted in (6.162)-(6.165). From (6.148), (6.157), and (6.163), linearized stress-strain-temperature relations are

$$\sigma^{ab} = J^{-1}\tau^{ab} \approx \tau^{ab} = \overline{\mathbb{C}}^{abcd}\varepsilon_{cd}^L - \overline{\beta}^{ab}\Delta\theta$$
$$= \overline{\mathbb{C}}^{abcd}(\varepsilon_{cd} - \varepsilon_{cd}^P) - \overline{\beta}^{ab}\Delta\theta. \tag{6.166}$$

The residual part of the free energy, ψ^R in (6.162), can be constructed in a manner completely analogous to (6.60) if, for example, a simple quadratic form is used for the energetic contribution from internal state variable α.

6.5.4 Linearized Dislocation Plasticity

In the geometrically linear theory, the rate of plastic distortion can be expressed by linearizing (3.98) and the last of (3.99), leading to (Mura 1968)

$$\dot{\beta}_{ab}^P = \varsigma_a^{.cd}\varepsilon_{cdb} = \sum_{i=1}^j \rho^i b_a^i \xi^{ic} v^{id}\varepsilon_{bcd}. \tag{6.167}$$

Summation proceeds over $i = 1, 2, \ldots j$ populations of dislocations with the same tangent line, Burgers vector, and velocity for each value of i. The spatial dislocation flux, a third-order tensor, is $\varsigma(x,t)$. The length per unit volume, Burgers vector, unit tangent line, and velocity of dislocation population i are, respectively, ρ^i, $\mathbf{b}^i$, $\boldsymbol{\xi}^i$, and $\mathbf{v}^i$. Plastic dissipation per unit volume, $\dot{W}^P = \boldsymbol{\sigma}:\dot{\boldsymbol{\varepsilon}}^P$ of (6.161), is then computed as follows, using the symmetry of the Cauchy stress:

$$\dot{W}^P = \sigma^{ab}\dot{\varepsilon}_{ab}^P = \sigma^{ab}\dot{\beta}_{ab}^P = \sum_{i=1}^j \rho^i(\varepsilon_{cdb}\xi^{ic}\sigma^{ab}b_a^i)v^{id}$$
$$= \sum_{i=1}^j \rho^i(-\varepsilon_{dcb}\xi^{ic}\sigma^{ba}b_a^i)v^{id} = \sum_{i=1}^j \rho^i(f_{PK}^i)_d v^{id}, \tag{6.168}$$

where the Peach-Koehler force (Peach and Koehler 1950; Mura 1968; Bammann and Aifantis 1982) is

$$\mathbf{f}_{PK}^i = -\boldsymbol{\xi}^i \times \boldsymbol{\sigma}\mathbf{b}^i. \tag{6.169}$$

Use of Orowan's (1940) relation instead of (6.167) gives

$$\beta_{ab}^P = \sum_i \rho^i b^i v^i s_a^i m_b^i \ , \tag{6.170}$$

where in the geometrically linear theory, for each slip system i, the magnitude of Burgers vector, slip direction, dislocation line velocity, and unit normal to the glide plane, are respectively

$$b^i = |\mathbf{b}^i| \ , \quad \mathbf{s}^i = \mathbf{b}^i / b^i \ , \quad v^i = |\mathbf{v}^i| \ , \quad \mathbf{m}^i = \boldsymbol{\xi}^i \times \mathbf{v}^i / v^i \ . \tag{6.171}$$

Using (6.171) in (6.161), the rate of plastic work per unit spatial volume is

$$\dot{W}^P = \sigma^{ab} \dot{\varepsilon}_{ab}^P = \sigma^{ab} \dot{\beta}_{ab}^P = \sum_i \rho^i b^i v^i (s_a^i \sigma^{ab} m_b^i) = \sum_i \rho^i b^i v^i \tau^i \ , \tag{6.172}$$

where the resolved shear stress is

$$\tau^i = s_a^i \sigma^{ab} m_b^i = s_{(a}^i \sigma^{ab} m_{b)}^i \ . \tag{6.173}$$

Kinetic relationships between dislocation velocity and resolved shear stress in the geometrically linear case are posited in the same manner as outlined in Section 6.2, simply by replacing $\tilde{v}^i$ of the nonlinear theory with v^i in the second of (6.171), and $\tilde{\tau}^i$ of the nonlinear theory with τ^i of (6.173).

6.5.5 Linearized Crystal Plasticity

In the linearized description of kinematics of slip in crystal plasticity theory of Section 3.2.6, the plastic rate of distortion is given by (3.125):

$$\dot{\boldsymbol{\beta}}^\mathbf{P} = \sum_i \dot{\gamma}^i \mathbf{s}^i \otimes \mathbf{m}^i \ , \tag{6.174}$$

and the plastic work rate per unit volume is, just as in (6.172),

$$\dot{W}^P = \sigma^{ab} \dot{\varepsilon}_{ab}^P = \sigma^{ab} \dot{\beta}_{ab}^P = \sum_i \dot{\gamma}^i (s_a^i \sigma^{ab} m_b^i) = \sum_i \dot{\gamma}^i \tau^i \ , \tag{6.175}$$

where the resolved shear stress τ^i is defined in (6.173). Kinetic relationships between slip rate $\dot{\gamma}^i$ and resolved shear stress τ^i in the geometrically linear case are prescribed in the same way as demonstrated in Section 6.3 for the nonlinear case, simply by replacing the resolved Kirchhoff stress $\tilde{\tau}^i$ of the nonlinear theory with τ^i of (6.173). The quadratic form used as an estimate of the residual free energy in (6.116) can be replaced by

$$\rho \psi^R = \frac{1}{2} \kappa \alpha^2 = \frac{1}{2} \kappa b^2 \rho_T \ , \quad \alpha = b \sqrt{\rho_T} \ , \quad \kappa = 2 \Lambda \hat{K} \ , \quad 0.5 \lesssim \Lambda \lesssim 1.0 \ , \tag{6.176}$$

with ρ_T the total dislocation line length per unit spatial volume and $\hat{K}$, as defined in (C.152), the energy factor for a dislocation line in an anisotropic

elastic body. For a pure screw dislocation in an isotropic solid, the energy factor is equivalent to the temperature-dependent shear modulus.

6.5.6 Linearized Macroscopic Plasticity

Macroscopic plasticity as outlined in the geometrically nonlinear context in Section 6.4 can be described analogously in the linear theory, replacing $\hat{\mathbf{L}}^{\mathbf{P}}$ of (6.127) with plastic distortion rate $\dot{\boldsymbol{\beta}}^{\mathbf{P}}$, $\hat{\mathbf{D}}^{\mathbf{P}}$ of (6.127) with plastic strain rate $\dot{\boldsymbol{\varepsilon}}^{\mathbf{P}}$, and $\hat{\mathbf{W}}^{\mathbf{P}}$ of (6.127) with plastic rotation rate $\dot{\boldsymbol{\Omega}}^{\mathbf{P}}$. For example, relations (6.133)-(6.143) for a plastically incompressible and plastically isotropic material based on concepts of normality, associated flow, and a Von Mises-type (i.e., $\sqrt{J_2}$) yield and flow function are linearized as follows. The flow rule, assuming normality, is

$$\dot{\boldsymbol{\varepsilon}}^{\mathbf{P}} = \begin{cases} \hat{\lambda}^P (\partial \hat{\Omega} / \partial \boldsymbol{\sigma}') \text{ for } \hat{F} = 0, \\ \quad 0 \qquad \text{for } \hat{F} < 0, \end{cases} \tag{6.177}$$

with flow function

$$\hat{\Omega} = \sqrt{J_2} = \left(\sigma'^{ab} \sigma'_{ab} / 2 \right)^{1/2} = \bar{\sigma} / \sqrt{3} = \sqrt{3/2}\,\bar{\tau}\,, \tag{6.178}$$

where the second invariant of the deviatoric stress, the octahedral shear stress, and the Von Mises effective stress are defined identically as in Section 6.4:

$$J_2 = \sigma'^{ab} \sigma'_{ab} / 2\,, \tag{6.179}$$

$$\bar{\tau} = \sqrt{2J_2/3} = \sqrt{2}\bar{\sigma}/3\,, \tag{6.180}$$

$$\bar{\sigma} = \sqrt{3J_2}\,. \tag{6.181}$$

The plastic strain rate then follows as

$$\dot{\boldsymbol{\varepsilon}}^{\mathbf{P}} = \frac{\hat{\lambda}^P}{2\hat{\Omega}} \boldsymbol{\sigma}' = \frac{\hat{\lambda}^P}{2\sqrt{J_2}} \boldsymbol{\sigma}' = \frac{\sqrt{3}\hat{\lambda}^P}{2\bar{\sigma}} \boldsymbol{\sigma}'\,,\ (\hat{F} = 0)\,, \tag{6.182}$$

and the plastic multiplier satisfies

$$\hat{\lambda}^P = (\dot{\boldsymbol{\varepsilon}}^{\mathbf{P}} : \dot{\boldsymbol{\varepsilon}}^{\mathbf{P}})^{1/2} \left[(\partial \hat{\Omega} / \partial \boldsymbol{\sigma}') : (\partial \hat{\Omega} / \partial \boldsymbol{\sigma}') \right]^{-1/2} = (2\dot{\boldsymbol{\varepsilon}}^{\mathbf{P}} : \dot{\boldsymbol{\varepsilon}}^{\mathbf{P}})^{1/2}\,. \tag{6.183}$$

The yield function is

$$\hat{F} = \hat{\Omega} - \hat{k} = \sqrt{J_2} - \hat{k}\,, \tag{6.184}$$

with $\hat{k} = \hat{k}(\{\varsigma\}, X)$ and the constraints

$$\hat{\lambda}^P \hat{F} = 0,\ \hat{\lambda}^P \geq 0, \hat{F} \leq 0\,. \tag{6.185}$$

In rate independent plasticity, the plastic multiplier can be expressed as (Lubliner 1990)

$$\hat{\lambda}^P = \begin{cases} \hat{H}^{-1} \left\langle (\partial \hat{F} / \partial \sigma^{ab}) \dot{\sigma}^{ab} \right\rangle & \text{for } \hat{F} = 0 \text{ and } \hat{H} \neq 0, \\ 0 & \text{for } \hat{F} < 0, \end{cases} \quad (6.186)$$

where hardening modulus $\hat{H}$ is obtained from the consistency condition

$$\dot{F}\Big|_{\sigma} = -\hat{\lambda}^P \hat{H} = \sum \frac{\partial \hat{F}}{\partial \varsigma}\Big|_{\sigma} \dot{\varsigma} = -\sum \frac{\partial \hat{k}}{\partial \varsigma}\Big|_{\sigma} \dot{\varsigma}, \text{ (for } \hat{F} = 0 \text{)}. \quad (6.187)$$

When $\hat{H} = 0$, as occurs in a perfectly plastic material, $\hat{\lambda}^P$ is indeterminate (Lubliner 1990), but the magnitude of the plastic strain rate is still dictated by the constraint that the stress state remain on the yield surface during plastic loading. The rate of plastic work and plastic volume change are respectively

$$\dot{W}^P = \sigma^{ab} \beta_{ab}^P = \sigma^{ab} \dot{\varepsilon}_{ab}^P = \hat{\lambda}^P \sigma'^{ab} \sigma'_{ab} / (2\hat{\Omega}) = \hat{\lambda}^P \hat{\Omega} = \hat{\lambda}^P \sqrt{J_2} \geq 0, \quad (6.188)$$

$$\dot{\varepsilon}_{.a}^{Pa} = (\hat{\lambda}^P / \hat{\Omega}) \sigma_{.a}'^a = 0. \quad (6.189)$$

From (6.188) and (6.189), respectively, it follows that plastic dissipation is always non-negative and the plastic strain rate is always isochoric.

6.6 The Eshelby Stress

The stress tensor $\tilde{\mathbf{\Pi}}$, work conjugate to the plastic velocity gradient in (6.32) in the setting of two-term multiplicative elastoplasticity, can be related to several quantities introduced by Eshelby (1951, 1975) in the context of continuum elasticity theory. This stress measure can be written, using (4.6), (4.7), or Table 4.1, along with (6.1)-(6.5), (6.16), and (6.33), as follows:

$$\tilde{\mathbf{\Pi}} = \tilde{\mathbf{M}} - \tilde{\mathcal{\Psi}}\mathbf{1} = -J^L \mathbf{F}^{\mathbf{L}-\mathbf{1}} \boldsymbol{\pi}^* \mathbf{F}^{\mathbf{L}} = -J^{P-1} \mathbf{F}^{\mathbf{P}} \mathbf{\Pi}^* \mathbf{F}^{\mathbf{P}-\mathbf{1}}, \quad (6.190)$$

where the superposed asterisk denotes the dual of a mixed variant tensor akin to (2.119). Expressed in indicial notation, (6.190) is

$$\tilde{\Pi}_\alpha^{.\beta} = \tilde{M}_\alpha^{.\beta} - \tilde{\mathcal{\Psi}}\delta_\alpha^{.\beta} = -J^L F^{L-1\beta}_{.b} \pi_a^{.b} F^{La}_{.\alpha} = -J^{P-1} F^{P\beta}_{.B} \Pi_A^{.B} F^{P-1A}_{.\alpha}, \quad (6.191)$$

with

$$\pi_a^{.b} = -J^{L-1} F^{Lb}_{.\beta} (\tilde{M}_\alpha^{.\beta} - \tilde{\mathcal{\Psi}}\delta_\alpha^{.\beta}) F^{L-1\alpha}_{.a}$$
$$= \mathcal{\Psi}\delta_a^{.b} - J^{L-1} F^{Lb}_{.\beta} \tilde{M}_\alpha^{.\beta} F^{L-1\alpha}_{.a} = \mathcal{\Psi}\delta_a^{.b} - \sigma_a^{.b}, \quad (6.192)$$

and

$$\Pi_A^{.B} = JF^{-1B}_{.b} (\mathcal{\Psi}\delta_a^{.b} - \sigma_a^{.b}) F^a_{.A}$$
$$= \mathcal{\Psi}_0 \delta_A^{.B} - F^a_{.A} P_a^{.B} = \mathcal{\Psi}_0 \delta_A^{.B} - C_{AC} \Sigma^{CB}. \quad (6.193)$$

According to (6.161), quantity $\hat{\boldsymbol{\pi}} = -\boldsymbol{\pi}$ serves as the conjugate stress to the plastic strain rate in geometrically linear elasto-plasticity, but only when the plastic strain rate is traceless.

Tensors $\boldsymbol{\pi}$, $\boldsymbol{\Pi}$, or variations of them, exhibit interesting characteristics in the context of elastic bodies containing defects and are often referred to as elastic energy-momentum tensors (Eshelby 1951, 1975). Following Maugin (1995), local stress measures $\boldsymbol{\pi} \in T_x^* B \times T_x B$ and $\boldsymbol{\Pi} \in T_X^* B_0 \times T_X B_0$ in (6.192) and (6.193) are labeled spatial and referential Eshelby stresses, respectively. It is noted as a point of clarification that a number of other tensors often differing in mathematical form and/or physical origin from those of Eshelby enter descriptions of thermodynamics of heterogeneous systems (Bowen 1967; Grinfeld 1991) and configurational (Gurtin 1995) or material forces (Maugin 1995). For example, chemical potential tensors (Grinfeld 1981) can emerge in theories of phase transformations.

Consider a nonlinear elastic body in the context of elastostatics (no inertia) and in the absence of body forces and thermal effects. Local balances of linear and angular momentum are, from (4.21) and (4.27),

$$P_{:A}^{aA} = 0 , \quad F_{.A}^a P^{bA} = P^{aA} F_{.A}^b , \tag{6.194}$$

and the constitutive equations of elasticity theory are given by (5.44)-(5.45), written here in terms of the deformation gradient $\mathbf{F}(X,t)$ as independent state variable:

$$P_a^{.A} = \frac{\partial \Psi_0}{\partial F_{.A}^a} , \quad \Psi_0 = \Psi_0\left(\mathbf{F}, \mathbf{G}_A(X), X\right) . \tag{6.195}$$

Strain energy density per unit reference volume can be expressed as a series expansion along the lines of (5.62):

$$\Psi_0 = \frac{1}{2}\overline{\mathbb{C}}^{ABCD} E_{AB} E_{CD} + \frac{1}{6}\overline{\mathbb{C}}^{ABCDEF} E_{AB} E_{CD} E_{EF} + ... , \tag{6.196}$$

where elastic constants $\overline{\mathbb{C}}^{ABCD}$ and $\overline{\mathbb{C}}^{ABCDEF}$ are defined in (5.65) and (5.66) and may depend on orientation (via $\mathbf{G}_A$) in anisotropic crystals as well as choice of material particle X in heterogeneous bodies. Consider the material gradient of the strain energy density:

$$\begin{aligned}
\Psi_{0,A} &= \frac{\partial \Psi_0}{\partial X^A} = \frac{\partial \Psi_0}{\partial F_{.B}^a} F_{.B:A}^a + \frac{\partial \Psi_0}{\partial \mathbf{G}_B} \mathbf{G}_{B;A} + \frac{\partial \Psi_0}{\partial X^A}\bigg|_{\exp} \\
&= \frac{\partial \Psi_0}{\partial F_{.B}^a} F_{.B:A}^a + \frac{\partial \Psi_0}{\partial X^A}\bigg|_{\exp} ,
\end{aligned} \tag{6.197}$$

where the explicit material gradient is defined by (Eshelby 1975)

$$\frac{\partial \Psi_0}{\partial X^A}\bigg|_{\text{exp}} = \frac{\partial \Psi_0}{\partial X^A}\bigg|_{\substack{F^a_{.A}=\text{const.} \\ X^B=\text{const. }(A\neq B)}} = \Psi_{0,A} - \frac{\partial \Psi_0}{\partial F^a_{.B}} F^a_{.B:A}. \qquad (6.198)$$

From (6.193)-(6.197), the divergence of the referential Eshelby stress is

$$\Pi^{.B}_{A;B} = \Psi_{0,B}\delta^{.B}_A - (F^a_{.A}P^{.B}_a)_{;B} = \Psi_{0,A} - P^{.B}_a F^a_{.A;B} - F^a_{.A}P^{.B}_{a;B}$$

$$= \Psi_{0,A} - P^{.B}_a(F^a_{.A;B} + \overset{g}{\Gamma}{}^{.a}_{bc}F^c_{.A}F^b_{.B}) - F^c_{.A}(P^{.B}_{c;B} - \overset{g}{\Gamma}{}^{.a}_{bc}P^{.B}_a F^b_{.B})$$

$$= \Psi_{0,A} - P^{.B}_a F^a_{.A;B} - F^c_{.A}P^{.B}_{c;B} = \Psi_{0,A} - P^{.B}_a F^a_{.A:B} \qquad (6.199)$$

$$= \Psi_{0,A} - \frac{\partial \Psi_0}{\partial F^a_{.B}} F^a_{.A:B} = \frac{\partial \Psi_0}{\partial X^A}\bigg|_{\text{exp}}$$

$$= \frac{1}{2}\overline{\mathbb{C}}^{BCDE}_{....,A} E_{BC}E_{DE} + \frac{1}{6}\overline{\mathbb{C}}^{BCDEFG}_{......,A} E_{BC}E_{DE}E_{FG} + ...,$$

with total covariant derivative of deformation gradient $F^a_{.A:B} = x^a_{.AB} = F^a_{.B:A}$ defined in (2.116) and total covariant derivative of the first Piola-Kirchhoff stress $P^A_a(X,t)$ given in (4.20). The local material force per unit reference volume in a heterogeneous elastic body is then defined by

$$\mathcal{b}_A = -\frac{\partial \Psi_0}{\partial X^A}\bigg|_{\text{exp}} = -\Pi^{.B}_{A;B}, \qquad (6.200)$$

and clearly depends on variations in elastic constants with reference coordinates, as indicated from the last of (6.199). Such variations may arise in crystalline solids, for example, from variations in reference orientation of the crystal lattice (e.g., misoriented grains in a polycrystal or deformation twins), changes in material composition (e.g., inclusions or precipitates with different elastic constants than the surrounding medium), or defects (e.g., a dependence of elastic constants on spatially heterogeneous densities of voids, vacancies, or dislocations). For a homogeneous body, $\mathcal{b}_A = 0$. The sign convention used for the material force is somewhat arbitrary; that of (6.200) parallels the sign convention typically used in particle mechanics (Appendix B), wherein a force is defined as a negative potential energy gradient with respect to position of a particle (see e.g., (B.2)).

A total force acting on a volume V enclosed by surface S with unit normal **N** can be found by integrating (6.200) over the volume and application of the divergence theorem of Section 2.7.1 in reference coordinates:

$$\mathcal{F}_A = \int_V \mathcal{b}_A dV = -\int_V \frac{\partial \Psi_0}{\partial X^A}\bigg|_{\text{exp}} dV = -\int_V \Pi^{.B}_{A;B} dV = -\int_S \Pi^{.B}_A N_B dS, \qquad (6.201)$$

where reference basis vectors $\mathbf{G}_A(X)$ are presumed constant over the domain of integration of covector field $\mathcal{b}_A(X,t)$. When V contains a singular-

ity—for example a discontinuity in elastic constants at the boundary surface between an inclusion or crack and the surrounding medium—energy density Ψ_0 may not be differentiable or even continuous, f_A may not be bounded, and the divergence theorem cannot be applied as in (6.201). In that case, a force acting on a singularity can be defined directly as the surface integral

$$\mathcal{F}_A = -\int_S \Pi_A^{\ B} N_B \, dS \,, \tag{6.202}$$

where S may fully or partially enclose the defect or source of singularity. Two different surfaces S enclosing or bordering the same defect or source of heterogeneity will produce the same force $\mathcal{F}_A$ because f_A vanishes in regions of V where elastic constants are uniform and where defects do not exist. In this sense, surface integral (6.202) is said to be path independent.

Extensions of the Eshelby stress of nonlinear elastostatics have addressed second grade elasticity (Eshelby 1975; Le and Stumpf 1996b, c), Cosserat media (Epstein and Elzanowski 2007), dynamics and inertia (Eshelby 1951; Maugin 1994; Cermelli and Fried 1997), nonlinear electrostatics of dielectrics (Epstein and Maugin 1990), and ductile fracture (Maugin 1994). In the context of a multiplicative decomposition of the deformation gradient, differential-geometric identities for the divergence of $\mathbf{\Pi}$ in terms of connection coefficients formed from a lattice-preserving deformation map were derived by Epstein and Maugin (1990). Entire texts have been devoted to the subject of material forces or mechanics in material space (Maugin 1993; Kienzler and Herrmann 2000). In such treatments (see also Maugin 1995), governing equations of continuum mechanics are written entirely referred to referential or material coordinates, with such equations often involving Eshelby-type stress measures.

A quantity similar, but not identical, to $\mathbf{\pi}$ of (6.192) was introduced by Eshelby (1951) to describe the force per unit volume acting on a singularity in an otherwise linear elastic body. In linear elasticity, (6.194)-(6.202) are replaced by their linearized spatial analogs as follows. Quasi-static momentum balances, in the absence of body forces, are

$$\sigma^{ab}_{\ ;b} = 0 \,, \ \sigma^{ab} = \sigma^{ba} \,, \tag{6.203}$$

constitutive equations (5.273) and (5.275) are

$$\sigma^{ab} = \frac{\partial \Psi}{\partial \varepsilon_{ab}} = \frac{\partial \Psi}{\partial u_{(a;b)}} \,, \ \Psi = \Psi\left(\mathbf{\varepsilon}, \mathbf{g}_a(x), x\right), \tag{6.204}$$

and strain energy density (5.304) in the absence of temperature effects is

$$\Psi = \frac{1}{2}\overline{\mathbb{C}}^{abcd} \varepsilon_{ab} \varepsilon_{cd} = \frac{1}{2}\overline{\mathbb{C}}^{abcd} u_{a;b} u_{c;d} \,, \tag{6.205}$$

where generally anisotropic, second-order elastic constants satisfy symmetry conditions $\overline{\mathbb{C}}^{abcd}(\mathbf{g}_a(x),x) = \overline{\mathbb{C}}^{(ab)(cd)}$. The spatial gradient of the strain energy density is

$$
\begin{aligned}
\Psi_{,a} &= \frac{\partial \Psi}{\partial x^a} = \frac{\partial \Psi}{\partial \varepsilon_{bc}}\varepsilon_{bc;a} + \frac{\partial \Psi}{\partial \mathbf{g}_b}\mathbf{g}_{b;a} + \frac{\partial \Psi}{\partial x^a}\bigg|_{\exp} \\
&= \frac{\partial \Psi}{\partial \varepsilon_{bc}}(u_{b;ca} - u_{[b;c]a}) + \frac{\partial \Psi}{\partial x^a}\bigg|_{\exp} = \frac{\partial \Psi}{\partial u_{b;c}}u_{b;ca} + \frac{\partial \Psi}{\partial x^a}\bigg|_{\exp},
\end{aligned}
\tag{6.206}
$$

where the explicit gradient with respect to position of the particle in question is defined by

$$
\frac{\partial \Psi}{\partial x^a}\bigg|_{\exp} = \frac{\partial \Psi}{\partial x^a}\bigg|_{\substack{u_{a;b}=\text{const.} \\ x^b=\text{const. }(a \neq b)}} = \Psi_{,a} - \frac{\partial \Psi}{\partial u_{b;c}}u_{b;ca}.
\tag{6.207}
$$

From (6.203)-(6.207), and from the compatibility conditions $u_{a;[bc]} = 0$,

$$
\begin{aligned}
\breve{\pi}^{.b}_{a;b} &= \Psi_{,b}\delta^b_a - (\sigma^{bc}u_{c;a})_{;b} = \Psi_{,a} - \sigma^{cb}_{;b}u_{c;a} - \sigma^{bc}u_{c;ab} \\
&= \Psi_{,a} - \frac{\partial \Psi}{\partial u_{b;c}}u_{c;ab} = \Psi_{,a} - \frac{\partial \Psi}{\partial u_{b;c}}u_{c;ba} = \Psi_{,a} - \frac{\partial \Psi}{\partial u_{b;c}}u_{b;ca} \\
&= \frac{\partial \Psi}{\partial x^a}\bigg|_{\exp} = \frac{1}{2}\overline{\mathbb{C}}^{bcde}_{....,a}\varepsilon_{bc}\varepsilon_{de},
\end{aligned}
\tag{6.208}
$$

where the original Eshelby stress measure in linear elastostatics, $\breve{\boldsymbol{\pi}}$, is defined as (Eshelby 1951)

$$
\breve{\boldsymbol{\pi}} = \Psi \mathbf{1} - \boldsymbol{\sigma}\nabla\mathbf{u}, \quad \breve{\pi}^{.b}_a = \Psi\delta^b_a - \sigma^{bc}u_{c;a}.
\tag{6.209}
$$

Notice that $\boldsymbol{\pi}$ of (6.192) differs from $\breve{\boldsymbol{\pi}}$ of (6.209) by the presence of the displacement gradient in the rightmost term of the latter. The local material force per unit volume in a heterogeneous elastic body is defined as

$$
\mathcal{b}_a = -\frac{\partial \Psi}{\partial x^a}\bigg|_{\exp} = -\breve{\pi}^{.b}_{a;b} = -\frac{1}{2}\overline{\mathbb{C}}^{bcde}_{....,a}u_{b;c}u_{d;e},
\tag{6.210}
$$

and depends on variations in elastic constants with coordinates x^a.

A total force acting on volume v enclosed by surface s with unit normal $\mathbf{n}$ can be found by integrating (6.210) over that volume and application of the divergence theorem of Section 2.7.1 in spatial coordinates:

$$
\mathcal{F}_a = \int_v \mathcal{b}_a dv = -\int_v \frac{\partial \Psi}{\partial x^a}\bigg|_{\exp} dv = -\int_v \breve{\pi}^{.b}_{a;b} dv = -\int_s \breve{\pi}^{.b}_a n_b ds,
\tag{6.211}
$$

where basis vectors $\mathbf{g}_a(x)$ are required to be constant over the domain of integration. When volume v contains a singularity (e.g., a jump discontinuity in the gradient of strain energy density across an internal boundary

within v), the divergence theorem cannot be applied as in (6.211). In that case, the material force can be defined as the surface integral

$$\mathcal{F}_a = -\int_s \breve{\pi}_a^{\cdot b} n_b \, ds , \qquad (6.212)$$

where s may fully or partially enclose the defect, heterogeneity, or source of singularity. Because $f_{ba} = 0$ in parts of volume v where elastic constants are uniform and where defects do not exist, (6.212) is path independent.

For situations in which a region of the body contains a singularity, strain energy density may not be differentiable or even continuous within the region. For example, for a stressed region containing a void or crack, a jump in mass density and hence strain energy per unit volume may exist between the elastic medium ($\rho_0 > 0$) and the empty region inside the void or open crack ($\rho_0 = 0$). In such cases, the gradient of the strain energy density is not bounded, and the divergence theorem cannot be applied as in (6.211). Similarly, (6.207) and (6.211) would not apply for a region containing a dislocation or disclination line or loop in the context of linear elasticity (Sections C.1 and C.2 of Appendix C). For example, from (C.152) the energy gradient per unit length of dislocation line is singular as $R \to 0$:

$$\frac{\partial}{\partial x^a} \left[\frac{\hat{K} b^2}{4\pi} \ln\left(\frac{R}{R_C}\right) \right] = \hat{K}_{,a} \frac{b^2}{4\pi} \ln\left(\frac{R}{R_C}\right) + \frac{\hat{K} b^2}{4\pi} \frac{x_a}{R^2} , \qquad (6.213)$$

where the first term on the right of (6.213) is nonzero if elastic coefficient $\hat{K}$ is permitted to vary with x, though the analytical derivation of (C.152) assumes constant elastic moduli. While the total energy of the dislocation will not depend on its position in an infinite medium, this energy can depend on position in a finite medium (Phillips 2001). For the elastic sphere-in-hole models of point defects of Section C.3 (Bitter 1931; Eshelby 1954, 1956; Teodosiu 1982), the divergence theorem used in (6.211) would also not apply, since the strain energy density is not necessarily differentiable or even continuous across the interface between the sphere (defect) and the surrounding medium. In all of these situations involving singularities, one can still define a global material force acting on the singularity via a surface integral of the type (6.212), presuming that the integrand $\breve{\pi}_a^{\cdot b} n_b$ is well defined along the surface of integration. Surface s may or may or may not completely enclose the defect, and the surface integral is path independent so long each path considered bounds the same defect(s).

For a body containing a notch or crack, the projection in the direction of extension $\mathbf{e}_1$ of surface integral $\breve{\pi}_a^{\cdot b} n_b$ along an open contour c (dotted line

in Fig. 6.2) enclosing the notch tip or crack tip can be associated with the J-integral of fracture mechanics (Rice 1968; Maugin 1993, 1994, 1995):

$$\mathscr{J} = \mathbf{e}_1 \cdot \int_c \breve{\boldsymbol{\pi}} \mathbf{n} dc = \int_c (\Psi n_1 - t^a u_{a,1}) dc . \tag{6.214}$$

The quantity $\mathscr{J}$ exhibits dimensions of energy per unit area and is often called an energy release rate. This quantity can be compared to the energy required to generate free surface area, i.e., to extend a sharp crack, within an elastic solid (Griffith 1921): crack extension is predicted when $\mathscr{J}$ attains a threshold value for a particular material. When contour c is collapsed to the free surface of a smooth notch tip c',

$$\mathscr{J} = \lim_{c \to c'} \left[\mathbf{e}_1 \cdot \int_c \breve{\boldsymbol{\pi}} \mathbf{n} dc \right] = \int_{c'} \Psi \mathbf{n} \cdot \mathbf{e}_1 dc' , \tag{6.215}$$

since traction $t^a = \sigma^{ab} n_b$ vanishes along free surface c'. When c is taken as a closed contour about a region containing no defects or heterogeneities, $\mathscr{J}$ vanishes identically for that region, implying path independence of the J-integral of (6.214) (Rice 1968). Extensions of the J-integral to nonlinear and inelastic behavior are possible (Rice 1968; Maugin 1993, 1994, 1995).
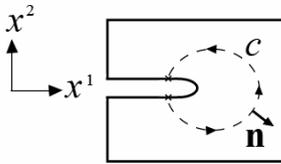
Fig. 6.2 Contour used in evaluation of J-integral about a notch or crack tip

6.7 Elastoplasticity of Grade Two

The present Section generalizes second grade nonlinear elasticity of Section 5.7 to crystals with defects. Specifically, the present kinematic description follows from decomposition (6.1): $x^a_{.,A} = F^a_{.A} = F^{La}_{.\alpha} F^{P\alpha}_{.A}$. A version of Hamilton's principle is employed in which the stress-free intermediate configuration $\tilde{B}$ of Fig. 3.4, and hence components of plastic deformation $F^{P\alpha}_{.A}$, remain stationary with respect to variational derivatives. This version of Hamilton's principle furnishes equilibrium equations and traction boundary conditions for the instantaneous elastic response from the intermediate configuration. Kinetic equations for

evolution of the plastic deformation and relaxed intermediate configuration are not provided by this approach, which deals only with non-dissipative part of the response, in the absence of heat conduction, heat sources, and temperature gradients. Much of what follows in Section 6.7 is based on the theory of Teodosiu (1967a, b, 1968). Similar, but not identical, approaches generalizing Toupin's second grade elasticity theory (Toupin 1962, 1964; see also Section 5.7) to account for plastic slip and multiplicative kinematics were forwarded by Le and Stumpf (1996b, c) and Garikipati (2003).

6.7.1 Covariant and Variational Derivatives

Recall from (3.70) that the lattice deformation gradient $\mathbf{F^L}(X,t)$ provides a first-order accurate approximation of the length and direction of a differential line element mapped from the intermediate configuration to the current configuration: $d\mathbf{x} = \mathbf{F^L}d\tilde{\mathbf{x}}$. A second-order accurate approximation is obtained by writing the inverse of (3.68) and retaining the second-order term in the Taylor series expansion, leading to

$$dx^a(X) = F^{La}_{.\alpha}\Big|_X d\tilde{x}^\alpha + \frac{1}{2}F^{La}_{.\alpha:\beta}\Big|_X d\tilde{x}^\alpha d\tilde{x}^\beta , \qquad (6.216)$$

where the base point of the differential line element is assigned to location X of the material particle. The total covariant derivative of the lattice deformation is, from the inverted form of (3.69) and the definition in the last of (3.36) of partial differentiation with respect to anholonomic coordinates $\tilde{x}^\alpha$,

$$
\begin{aligned}
F^{La}_{.\alpha:\beta} &= F^{La}_{.\alpha,\beta} - \tilde{\Gamma}^{..\chi}_{\beta\alpha}F^{La}_{.\chi} + \overset{g}{\Gamma}^{..a}_{bc}F^{Lc}_{.\alpha}F^{Lb}_{.\beta} \\
&= (F^{La}_{.\alpha,b} + \overset{g}{\Gamma}^{..a}_{bc}F^{Lc}_{.\alpha})F^{Lb}_{.\beta} - \tilde{\Gamma}^{..\chi}_{\beta\alpha}F^{La}_{.\chi} \\
&= (F^{La}_{.\chi,b}F^{L-1\chi}_{.c} + \overset{g}{\Gamma}^{..a}_{bc})F^{Lc}_{.\alpha}F^{Lb}_{.\beta} - \tilde{\Gamma}^{..\chi}_{\beta\alpha}F^{La}_{.\chi} \qquad (6.217) \\
&= (\overset{g}{\Gamma}^{..a}_{bc} - F^{La}_{.\chi}F^{L-1\chi}_{.c,b})F^{Lc}_{.\alpha}F^{Lb}_{.\beta} - \tilde{\Gamma}^{..\chi}_{\beta\alpha}F^{La}_{.\chi} \\
&= (\overset{g}{\Gamma}^{..a}_{bc} - \bar{\Gamma}^{..a}_{bc})F^{Lc}_{.\alpha}F^{Lb}_{.\beta} - \tilde{\Gamma}^{..\chi}_{\beta\alpha}F^{La}_{.\chi} ,
\end{aligned}
$$

where $\bar{\Gamma}^{..a}_{bc}$ are components of the crystal connection of (3.190) and $\overset{g}{\Gamma}^{..a}_{bc}$ and $\tilde{\Gamma}^{..\chi}_{\beta\alpha}$ are coefficients of connection coefficients used for coordinate systems on B and $\tilde{B}$, respectively. In general, $F^{La}_{.\alpha:\beta}$ consists of 27 inde-

pendent entries. When the torsion of crystal connection vanishes corresponding to a vanishing of the dislocation density tensor of (3.214), and when a symmetric connection is used for the intermediate configuration, then the following conditions hold:

$$\bar{\Gamma}^{..a}_{[bc]} = 0, \; \tilde{\Gamma}^{..\chi}_{[\beta\alpha]} = 0, \; F^{La}_{.[\alpha:\beta]} = F^{La}_{.[\alpha;\beta]} = F^{La}_{.[\alpha,\beta]} = 0, \; F^{La}_{.\alpha} = x^a_{.,\alpha}, \quad (6.218)$$

in which case $F^{La}_{.\alpha:\beta} = F^{La}_{.(\alpha:\beta)}$ consists only of up to 18 independent entries. From the last of (6.218), when such conditions hold, the lattice deformation is integrable and the elastic response of grade two becomes identical to that addressed in Section 5.7 of Chapter 5, with reference coordinates X^A of Section 5.7 replaced with (now holonomic) intermediate coordinates $\tilde{x}^\alpha$. However, for the general situation considered in what follows in Section 6.7, (6.218) does not apply, the crystal may contain defects such as dislocations, and the constitutive response may differ from that predicted in the context of holonomic elasticity of grade two discussed in Section 5.7. Extending (5.413) and results of Eringen (1962), and specifying intermediate external basis vectors with vanishing Christoffel symbols (i.e., $\tilde{\Gamma}^{..\chi}_{\beta\alpha} = 0$), the following identity applies:

$$F^{La}_{.\alpha:\beta} = \left(F^{La}_{.\alpha,b} + \overset{g}{\Gamma}^{..a}_{bc} F^{Lc}_{.\alpha} \right) F^{Lb}_{.\beta} = (F^{La}_{.\alpha})_{;b} F^{Lb}_{.\beta}, \quad (6.219)$$

from which it follows that for the inverse of the lattice deformation,

$$0 = (F^{La}_{.\alpha} F^{L-1\alpha}_{.c})_{;b} \Rightarrow F^{L-1\alpha}_{.c;b} = -F^{L-1\alpha}_{.a} F^{L-1\beta}_{.b} F^{L-1\chi}_{.c} F^{La}_{.\chi:\beta}. \quad (6.220)$$

Recall from Section 5.6.1 the definition of the variational derivative. Let $x^a = x^a(X^A, \Lambda)$, where Λ is a scalar parameter. In the present setting, the first variation of **x** is defined as follows, generalizing (5.373):

$$\delta x^a = \frac{\partial x^a}{\partial \Lambda}\bigg|_{\substack{X, \mathbf{F}^\mathbf{P} \\ \Lambda=0}} d\Lambda, \quad (6.221)$$

where by definition, reference coordinates X^A of material particle at X and values of plastic deformation gradient $F^{P\alpha}_{.A}(X) = F^{L-1\alpha}_{.a} F^a_{.A}$ are held fixed during the variation (Teodosiu 1967a). For a scalar function $f = f(x^a, F^{La}_{.\alpha}, F^{La}_{.\alpha:\beta}, ...)$ depending on spatial position, lattice deformation gradient, and total covariant derivatives of lattice deformation, the first variation is

$$\delta f = \frac{\partial f}{\partial \Lambda}\bigg|_{\substack{X, \mathbf{F}^\mathbf{P} \\ \Lambda=0}} d\Lambda. \quad (6.222)$$

Since reference coordinates are held fixed in the variational derivative,

$$\delta(f_{,A}) = (\delta f)_{,A} = \delta f_{,A}. \tag{6.223}$$

The first variation does not commute with partial differentiation in the spatial frame $\partial_a = \partial / \partial x^a$, as indicated in (5.379) which also applies here. For anholonomic partial derivatives,

$$\delta(f_{,a}) = \delta(f_{,A} F^{P-1A}_{.a}) = F^{P-1A}_{.a} \delta(f_{,A}) = F^{P-1A}_{.a} \delta f_{,A} = (\delta f)_{,a}, \tag{6.224}$$

since plastic deformation is stationary during the variation:

$$\delta(F^{P\alpha}_{.A}) = 0, \ \delta(F^{P-1A}_{.a}) = 0, \ \delta J^P = 0, \ \delta J^{P-1} = 0. \tag{6.225}$$

The following formulae for variations of kinematic quantities are useful, following from (5.376)-(5.378), (6.1), and (6.225):

$$\begin{aligned}
\delta F^{La}_{.\alpha} &= \delta(x^a_{,A} F^{P-1A}_{.\alpha}) = F^{P-1A}_{.\alpha}[(\delta x^a)_{,A} + F^a_{.A;b}\delta x^b] \\
&= F^{P-1A}_{.\alpha}(\delta x^a)_{;b} F^b_{.A} = (\delta x^a)_{;b} F^{Lb}_{.\alpha},
\end{aligned} \tag{6.226}$$

$$\begin{aligned}
\delta F^{L-1\alpha}_{.a} &= \delta(F^{P\alpha}_{.A} X^A_{,a}) = F^{P\alpha}_{.A}\delta(X^A_{,a}) \\
&= -F^{P\alpha}_{.A} F^{-1A}_{.b} F^{-1B}_{.a}(\delta x^b)_{;B} = -F^{L-1\alpha}_{.b}(\delta x^b)_{;a},
\end{aligned} \tag{6.227}$$

$$\delta J^L = \delta(J^{P-1}J) = J^{P-1}\delta J = J^{P-1}J(\delta F^a_{.A})F^{-1A}_{.a} = J^L(\delta x^a)_{;a}. \tag{6.228}$$

The first variation of total anholonomic covariant derivative of the lattice deformation, $F^{La}_{.\alpha:\beta}$, is found using (5.376), (6.219), (6.224), (6.226), and (6.227), as given by Teodosiu (1967a):

$$\begin{aligned}
\delta(F^{La}_{.\alpha:\beta}) &= \delta(F^{La}_{.\alpha;b} F^{Lb}_{.\beta}) = F^{Lb}_{.\beta}\delta(F^{La}_{.\alpha;b}) + F^{La}_{.\alpha;b}\delta(F^{Lb}_{.\beta}) \\
&= F^{Lb}_{.\beta}\left[\delta(F^{La}_{.\alpha;\chi} F^{L-1\chi}_{.b})\right] + F^{La}_{.\alpha;b}(\delta x^b)_{;c} F^{Lc}_{.\beta} \\
&= F^{Lb}_{.\beta}\left[\delta(F^{La}_{.\alpha;\chi})F^{L-1\chi}_{.b} + F^{La}_{.\alpha;\chi}(\delta F^{L-1\chi}_{.b})\right] + F^{La}_{.\alpha;b}(\delta x^b)_{;\beta} \\
&= F^{Lb}_{.\beta}\left[\delta(F^{La}_{.\alpha})_{;\chi} F^{L-1\chi}_{.b} - F^{La}_{.\alpha;\chi} F^{L-1\chi}_{.c}(\delta x^c)_{;b}\right] + F^{La}_{.\alpha;b}(\delta x^b)_{;\beta} \\
&= F^{Lb}_{.\beta}\delta(F^{La}_{.\alpha})_{;b} - F^{La}_{.\alpha;b}(\delta x^b)_{;\beta} + F^{La}_{.\alpha;b}(\delta x^b)_{;\beta} \\
&= F^{Lb}_{.\beta}\delta(F^{La}_{.\alpha})_{;b}.
\end{aligned} \tag{6.229}$$

6.7.2 Constitutive Assumptions and Governing Equations

Consider an elastic-plastic material featuring an instantaneous response from the intermediate configuration, with this response characterized by hyperelasticity of grade two. The strain energy of the solid depends on the total covariant derivative of the lattice deformation (6.217) in addition to the lattice deformation gradient, reference position of a material particle (in the case of heterogeneity) and intermediate basis vectors (in the case of anisotropy). The strain energy density is written in functional form as

$$\tilde{\rho}\psi = \tilde{\Psi} = \tilde{\Psi}\left(F^{La}_{\ \cdot\alpha}, F^{La}_{\ \cdot\alpha:\beta}, X, \tilde{\mathbf{g}}_{\alpha}\right). \qquad (6.230)$$

By assertion, the balance of mass in (4.10)-(4.12) applies, as do (3.48)-(3.50) and (6.2):

$$\rho_0 = \rho J = \rho\sqrt{g/G}\det\mathbf{F} = \rho J^L J^P, \quad \tilde{\rho} = \rho J^L = \rho_0 J^{P-1}. \qquad (6.231)$$

Contrarily, stress and traction definitions in Section 4.1.1, linear and angular momentum balances in Section 4.1.3, and the treatment of thermodynamics of crystalline solids in Sections 4.1.4 and 4.2 do not apply for the generalized continuum theory described in what follows in Section 6.7.

In the present Section, entropy production and temperature rates are assumed to vanish; hence free energy and internal energy are considered equivalent to strain energy. Heat conduction, heat sources, and temperature gradients are not considered in the present Section. Internal state variables are not considered explicitly, but it will be demonstrated later in Section 6.7.3 that the skew part of the total covariant derivative of the lattice deformation is directly related to the dislocation density tensor for a crystalline solid and hence can be used to represent the strain energy contribution from dislocations. Furthermore, considered for simplicity in what follows is the quasi-static case, in which velocities and accelerations are omitted. Potential energies from conservative body forces are also omitted for simplicity of presentation, but these forces could be incorporated easily by subtracting the appropriate term from the Lagrangian.

A Lagrangian density function $\tilde{L}$ per unit intermediate volume $\tilde{V}$ and Lagrangian functional $\mathscr{L}$ of (5.394) become simply

$$\tilde{L} = -\tilde{\Psi}, \quad \mathscr{L} = \int_{\tilde{V}}\tilde{L}d\tilde{V} = -\mathscr{E} = -\int_{\tilde{V}}\tilde{\Psi}d\tilde{V} = -\int_{\tilde{V}}\tilde{\rho}\psi d\tilde{V} = -\int_{v}\rho\psi dv, \quad (6.232)$$

since kinetic energy $\mathscr{K} = 0$ and global potential energy $\bar{\Phi} = 0$ by definition in the present simplified case. The appropriate generalization of Hamilton's principle (5.380) is written as follows in the spatial configuration, in accordance with (5.421):

$$\delta\mathscr{A} + \int_{t_1}^{t_2}\left[\int_{v}\left(\bar{\mathbf{b}}\bullet\delta\mathbf{x}\right)dv\right]dt + \int_{t_1}^{t_2}\left[\int_{s}\left(\mathbf{t}\bullet\delta\mathbf{x} + \mathbf{h}\bullet D\delta\mathbf{x}\right)ds\right]dt = 0, \quad (6.233)$$

with $\mathbf{h}(x,t)$ a generalized surface traction (force per unit spatial length) work conjugate to the normal derivative of the variation of spatial motion at the surface, $D\delta x_a = (\delta x_a)_{;b}n^b$ (Teodosiu 1967a). Recall that the normal derivative D of an arbitrary function is introduced in (5.416), along with tangential derivative D_a. The body force vector per unit current volume is $\bar{\mathbf{b}}(x,t)$, and $\mathbf{t}(x,t)$ is a surface traction (force per unit spatial area). Substituting from (6.232),

$$\delta \mathcal{A} = \delta \int_{t_1}^{t_2} \mathcal{L} dt = \delta \int_{t_1}^{t_2} \left(\int_{\tilde{V}} \tilde{L} d\tilde{V} \right) dt$$

$$= -\int_{t_1}^{t_2} \left(\int_{\tilde{V}} \delta \tilde{\Psi} d\tilde{V} \right) dt = -\int_{t_1}^{t_2} \left(\int_{v} \delta \tilde{\Psi} (J^{L-1} dv) \right) dt,$$

(6.234)

since $\delta \tilde{V} = \delta(J^P V) = J^P \delta V = 0$. Thus the equality

$$-\int_{v} J^{L-1} \delta \tilde{\Psi} dv + \int_{v} \bar{b}_a \delta x^a dv + \int_{s} \left[t_a \delta x^a + h_a D(\delta x^a) \right] ds = 0 \qquad (6.235)$$

must hold for each time in the (arbitrary) interval $t_1 \leq t \leq t_2$. The first integral on the left side of (6.235) can be written using (6.230) as

$$-\int_{v} J^{L-1} \delta \tilde{\Psi} dv = -\int_{v} J^{L-1} \left[\frac{\partial \tilde{\Psi}}{\partial F^{La}_{.\alpha}} \delta F^{La}_{.\alpha} + \frac{\partial \tilde{\Psi}}{\partial F^{La}_{.\alpha:\beta}} \delta(F^{La}_{.\alpha:\beta}) \right] dv, \quad (6.236)$$

where the integrand on the right of (6.236) is expressed as follows:

$$J^{L-1} \frac{\partial \tilde{\Psi}}{\partial F^{La}_{.\alpha}} \delta F^{La}_{.\alpha} + J^{L-1} \frac{\partial \tilde{\Psi}}{\partial F^{La}_{.\alpha:\beta}} \delta(F^{La}_{.\alpha:\beta})$$

$$= \left[J^{L-1} \frac{\partial \tilde{\Psi}}{\partial F^{La}_{.\alpha}} - \left(J^{L-1} \frac{\partial \tilde{\Psi}}{\partial F^{La}_{.\alpha:\beta}} F^{Lb}_{.\beta} \right)_{;b} \right] \delta F^{La}_{.\alpha}$$

$$+ \left[J^{L-1} \frac{\partial \tilde{\Psi}}{\partial F^{La}_{.\alpha:\beta}} F^{Lb}_{.\beta} \delta F^{La}_{.\alpha} \right]_{;b} \qquad (6.237)$$

$$= \left[J^{L-1} \frac{\partial \tilde{\Psi}}{\partial F^{La}_{.\alpha}} - \left(J^{L-1} \frac{\partial \tilde{\Psi}}{\partial F^{La}_{.\alpha:\beta}} F^{Lb}_{.\beta} \right)_{;b} \right] F^{Lc}_{.\alpha} (\delta x^a)_{;c}$$

$$+ \left[J^{L-1} \frac{\partial \tilde{\Psi}}{\partial F^{La}_{.\alpha:\beta}} F^{Lb}_{.\beta} F^{Lc}_{.\alpha} (\delta x^a)_{;c} \right]_{;b},$$

which follows from the product rule, (6.219), (6.226), and (6.229), since

$$\left[J^{L-1} \frac{\partial \tilde{\Psi}}{\partial F^{La}_{.\alpha:\beta}} F^{Lb}_{.\beta} \delta F^{La}_{.\alpha} \right]_{;b}$$

$$= \left[J^{L-1} \frac{\partial \tilde{\Psi}}{\partial F^{La}_{.\alpha:\beta}} F^{Lb}_{.\beta} \right]_{;b} \delta F^{La}_{.\alpha} + J^{L-1} \frac{\partial \tilde{\Psi}}{\partial F^{La}_{.\alpha:\beta}} \delta(F^{La}_{.\alpha:\beta}).$$

(6.238)

Second-order stress tensor $\sigma^{dc}(x,t)$ and third-order hyperstress tensor $H^{bdc}(x,t)$ are defined, respectively, as follows:

$$\sigma^{dc} = g^{da}\sigma_{.a}^{.c} = g^{da}\left[J^{L-1}\frac{\partial\tilde{\Psi}}{\partial F^{La}_{.\alpha}} - \left(J^{L-1}\frac{\partial\tilde{\Psi}}{\partial F^{La}_{.\alpha:\beta}}F^{Lb}_{.\beta} \right)_{;b} \right] F^{Lc}_{.\alpha}, \quad (6.239)$$

$$H^{bdc} = g^{da}H_{a}^{b.c} = J^{L-1}g^{da}\frac{\partial\tilde{\Psi}}{\partial F^{La}_{.\alpha:\beta}}F^{Lb}_{.\beta}F^{Lc}_{.\alpha}. \quad (6.240)$$

The stress in (6.239) exhibits, in physical components, dimensions of force per unit spatial area or energy per unit spatial volume, while the hyperstress in (6.240) exhibits dimensions of force per unit spatial length or energy per unit spatial area. When (6.218) applies, $(J^{L-1}F^{La}_{.\alpha})_{;a} = 0$ and $H^{bdc} = H^{cdb}$, but in general the hyperstress (6.240) consists of 27 independent components, in contrast to that of the holonomic theory in (5.428) for which such symmetry conditions hold. The rank two stress of (6.239) consists of up to 9 independent entries. The first and last contravariant indices of the hyperstress in (6.240) are transposed in the definition used by Teodosiu (1967a). Substituting stress definitions (6.239) and (6.240) into (6.236),

$$J^{L-1}\delta\tilde{\Psi} = \sigma_a^{.c}(\delta x^a)_{;c} + \left[H_a^{b.c}(\delta x^a)_{;c} \right]_{;b}$$

$$= (\sigma_a^{.c}\delta x^a)_{;c} - (\sigma_a^{.c})_{;c}\delta x^a + \left[H_a^{b.c}(\delta x^a)_{;c} \right]_{;b}. \quad (6.241)$$

Applying the divergence theorem (2.193) in spatial coordinates leads to

$$-\int_v J^{L-1}\delta\tilde{\Psi}dv = -\int_v \left\{ (\sigma_a^{.c}\delta x^a)_{;c} - \sigma_{a;c}^{.c}\delta x^a + \left[H_a^{b.c}(\delta x^a)_{;c} \right]_{;b} \right\} dv$$

$$= \int_v \sigma_{a;c}^{.c}\delta x^a dv - \int_s \left[\sigma_a^{.c}\delta x^a + H_a^{b.c}(\delta x^a)_{;b} \right] n_c ds. \quad (6.242)$$

Using (5.416)-(5.418), Stokes's theorem (2.198), and integration by parts, the rightmost term in the surface integral in (6.242) can be expressed as follows (Teodosiu 1967a), similarly to (5.431):

$$\int_s H_a^{b.c}(\delta x^a)_{;b}n_c ds = \int_s H_a^{b.c}[D(\delta x^a)n_b + D_b(\delta x^a)]n_c ds$$

$$= \int_s H_a^{b.c}n_b n_c D(\delta x^a)ds - \int_s H_a^{b.c}(\kappa_{.d}^d n_b n_c - \kappa_{bc})\delta x^a ds \quad (6.243)$$

$$- \int_s D_b(H_a^{c.b})n_c\delta x^a ds,$$

where $D_b(H_a^{c.b}) = H_{a;b}^{c.b} - D(H_a^{c.b})n_b$ is the surface gradient of the hyperstress and $\kappa_{bc} = -D_b n_c$ is the symmetric second fundamental form of the oriented surface given in (5.418). Contravariant indices on the hyperstress

in the final integrand of (6.243) are transposed with those of (5.431). Substituting (6.242) and (6.243) into (6.235),

$$
\int_v (\sigma_{a;c}^{.c} + \bar{b}_a)\delta x^a dv = \int_S \left[H_a^{b.c} n_b n_c - h_a \right] D(\delta x^a) ds
$$

$$
+ \int_S \left[\sigma_a^{.c} n_c - H_a^{b.c}(\kappa_{.d}^d n_b n_c - \kappa_{bc}) - D_b(H_a^{c.b})n_c - t_a \right]\delta x^a ds, \tag{6.244}
$$

similarly to (5.432). Requiring that (6.244) must hold for arbitrary variations δx^a and normal surface variations $D(\delta x^a)$, the following equilibrium equations and boundary conditions emerge:

$$
\sigma_{a;c}^{.c} + \bar{b}_a = 0, \tag{6.245}
$$

$$
t_a = \sigma_a^{.c} n_c - H_a^{b.c}(\kappa_{.d}^d n_b n_c - \kappa_{bc}) - D_c(H_a^{b.c})n_b, \tag{6.246}
$$

$$
h_a = H_a^{b.c} n_b n_c. \tag{6.247}
$$

Relation (6.245) is the static balance of linear momentum. Relation (6.246) is the boundary condition for the traction. Relation (6.247) is the boundary condition for the hypertraction. When $H_a^{b.c} = H_a^{c.b}$, (6.245)-(6.247) are identical with (5.433)-(5.435) as originally derived by Toupin (1962) in the context of second grade nonlinear elasticity. However, the stress and hyperstress of (6.239) and (6.240) entering these equilibrium equations and boundary conditions differ from those of Toupin (1962, 1964) and Section 5.7 since those used here are defined as derivatives of strain energy with respect to the lattice deformation and its covariant derivative as opposed to the total deformation and its covariant derivative.

For the particular case when strain energy density does not depend on the total covariant derivative of the lattice deformation gradient, i.e., when (6.230) reduces to $\tilde{\Psi} = \tilde{\Psi}(F_{.\alpha}^{La}, X, \tilde{\mathbf{g}}_\alpha)$, the stress σ^{dc} becomes identical to the Cauchy stress of nonlinear elastoplasticity (i.e., (6.27) and (6.239) become equivalent when the strain energy does not depend on internal state variables or $F_{.\alpha:\beta}^{La}$), and the hyperstress $H^{bdc} = 0$ in (6.240). Thus, in that particular case, (6.245) reduces to linear momentum balance (4.17) in the absence of spatial acceleration, traction boundary condition (6.246) becomes Cauchy's relation (4.3), and the right side of (6.247) vanishes identically.

A local balance of angular momentum can be obtained by forcing the strain energy density to remain invariant under rigid body rotations of the spatial frame, following procedures outlined in Sections 5.6 and 5.7. Consider a finite rotation $F_{.A}^a \to \hat{Q}_{.b}^a F_{.A}^b$ as discussed in Sections 4.2.1 and 5.6.2. From (6.8), the lattice deformation and its total covariant derivative transform in this case as $F_{.\alpha}^{La} \to \hat{Q}_{.b}^a F_{.\alpha}^{Lb}$ and $F_{.\alpha:\beta}^{La} \to \hat{Q}_{.b}^a F_{.\alpha:\beta}^{Lb}$. An infini-

tesimal rotation is $\hat{Q}^a_{.b} = \delta^a_{.b} + g_{bc}\hat{\Omega}^{ac}$, where skew rotation $\hat{\Omega}^{ac} = \hat{\Omega}^{[ac]}$. According to Toupin (1964), invariance of the strain energy density under infinitesimal rotations is sufficient to ensure invariance under finite rotations. Extending (5.409), the differential change of strain energy density under small rotations is

$$J^{L-1}d\tilde{\Psi} = J^{L-1}\left[\frac{\partial\tilde{\Psi}}{\partial(\hat{Q}^a_{.e}F^{Le}_{.\alpha})}F^{Lb}_{.\alpha} + \frac{\partial\tilde{\Psi}}{\partial(\hat{Q}^a_{.e}F^{Le}_{.\alpha:\beta})}F^{Lb}_{.\alpha:\beta}\right]d\hat{Q}^a_{.b}$$

$$= J^{L-1}\left[\frac{\partial\tilde{\Psi}}{\partial F^{La}_{.\alpha}}F^{Lb}_{.\alpha} + \frac{\partial\tilde{\Psi}}{\partial F^{La}_{.\alpha:\beta}}F^{Lb}_{.\alpha:\beta}\right]d\hat{\Omega}^a_{.b} \qquad (6.248)$$

$$= J^{L-1}\left[\frac{\partial\tilde{\Psi}}{\partial F^{La}_{.\alpha}}F^{L}_{.b\alpha} + \frac{\partial\tilde{\Psi}}{\partial F^{La}_{.\alpha:\beta}}F^{L}_{.b\alpha:\beta}\right]d\hat{\Omega}^{ab}.$$

Requiring that (6.248) must vanish under small but otherwise arbitrary rotations $d\hat{\Omega}^{[ab]}$ leads to the local balance of angular momentum for elastic-plastic materials of grade two:

$$J^{L-1}d\tilde{\Psi} = 0 \Rightarrow J^{L-1}\left[\frac{\partial\tilde{\Psi}}{\partial F^{L[a}_{.\alpha}}F^{L}_{.b]\alpha} + \frac{\partial\tilde{\Psi}}{\partial F^{L[a}_{.\alpha:\beta}}F^{L}_{.b]\alpha:\beta}\right] = 0. \qquad (6.249)$$

From the product rule, the rank two stress in (6.239) can be expressed as

$$\sigma^{.b}_a = J^{L-1}\frac{\partial\tilde{\Psi}}{\partial F^{La}_{.\alpha}}F^{Lb}_{.\alpha} + J^{L-1}\frac{\partial\tilde{\Psi}}{\partial F^{La}_{.\alpha:\beta}}F^{Lc}_{.\beta}F^{Lb}_{.\alpha;c}$$

$$-\left(J^{L-1}\frac{\partial\tilde{\Psi}}{\partial F^{La}_{.\alpha:\beta}}F^{Lc}_{.\beta}F^{Lb}_{.\alpha}\right)_{;c} \qquad (6.250)$$

$$= J^{L-1}\left[\frac{\partial\tilde{\Psi}}{\partial F^{La}_{.\alpha}}F^{Lb}_{.\alpha} + \frac{\partial\tilde{\Psi}}{\partial F^{La}_{.\alpha:\beta}}F^{Lb}_{.\alpha:\beta}\right] - H^{c.b}_{.a;c}.$$

Substituting the antisymmetric part from (6.249) into (6.250) gives

$$\sigma^{[ab]} = J^{L-1}\left[\frac{\partial\tilde{\Psi}}{\partial F^{L}_{[a|\alpha|}}F^{Lb]}_{.\alpha} + \frac{\partial\tilde{\Psi}}{\partial F^{L}_{[a|\alpha:\beta|}}F^{Lb]}_{.\alpha:\beta}\right] - H^{c[ab]}_{...;c} \qquad (6.251)$$

$$= H^{c[ba]}_{...;c} = M^{abc}_{...;c},$$

where the rank three couple stress M^{abc} and rank two couple stress $m^{.c}_d$ are constructed from certain antisymmetric parts of the hyperstress:

$$M^{abc} = \frac{1}{2}\varepsilon^{abd}m^{.c}_d = H^{c[ba]}, \quad m^{.c}_d = \varepsilon_{dab}M^{abc} = \varepsilon_{dab}H^{c[ba]} = -\varepsilon_{dab}H^{cab}. \qquad (6.252)$$

Local angular momentum balance (6.251) can thus be written as follows:

$$\sigma^{[ab]} - M^{abc}_{\cdots;c} = \sigma^{[ab]} - \frac{1}{2}\varepsilon^{abd}m^{c}_{d;c} = 0 \Leftrightarrow \varepsilon_{abc}\sigma^{ab} - m^{d}_{c;d} = 0 \,. \qquad (6.253)$$

The symmetric part of the hyperstress, $H^{c(ab)} = H^{cba} - M^{abc}$, while not affecting the angular momentum balance, does not generally vanish and is considered to result from a distribution of self-equilibrating internal forces. Relations (6.252) and (6.253) differ from (5.440) and (5.441) due to different ordering of indices on the definitions of hyperstress and couple stress. Only when $H^{b.c}_{a} = H^{c.b}_{a}$, as would result from compatibility conditions (6.218) on the lattice deformation, do the two sets of relations coincide.

A frame indifferent version of strain energy function (6.230) is (Teodosiu 1968)

$$\tilde{\Psi} = \tilde{\Psi}\left(\tilde{E}^{L}_{\alpha\beta}, \tilde{B}^{L}_{\alpha\beta\chi}, X, \tilde{\mathbf{g}}_{\alpha}\right), \qquad (6.254)$$

where the symmetric lattice strain $2\tilde{E}^{L}_{\alpha\beta} = \tilde{C}^{L}_{\alpha\beta} - \tilde{g}_{\alpha\beta} = F^{La}_{.\alpha}g_{ab}F^{Lb}_{.\beta} - \tilde{g}_{\alpha\beta}$ as in (6.4), and the covariant second lattice gradient (i.e., a kind of strain and rotation gradient) referred to the intermediate configuration satisfies

$$\tilde{B}^{L}_{\alpha\beta\chi} = F^{L}_{.a\alpha}F^{La}_{.\beta:\chi} \qquad (6.255)$$

Contravariant hyperstress and stress tensors are then computed, respectively, from the chain rule as

$$H^{bdc} = J^{L-1}g^{da}\frac{\partial\tilde{\Psi}}{\partial\tilde{B}^{L}_{\chi\delta\varepsilon}}\frac{\partial(F^{L}_{e\chi}F^{Le}_{.\delta:\varepsilon})}{\partial F^{La}_{.\alpha:\beta}}F^{Lb}_{.\beta}F^{Lc}_{.\alpha}$$

$$= J^{L-1}\frac{\partial\tilde{\Psi}}{\partial\tilde{B}^{L}_{\chi\alpha\beta}}F^{Ld}_{.\chi}F^{Lb}_{.\beta}F^{Lc}_{.\alpha}, \qquad (6.256)$$

$$\sigma^{dc} = g^{da}J^{L-1}\left[\frac{\partial\tilde{\Psi}}{\partial\tilde{E}^{L}_{\chi\delta}}\frac{\partial\tilde{E}^{L}_{\chi\delta}}{\partial F^{La}_{.\alpha}} + \frac{\partial\tilde{\Psi}}{\partial\tilde{B}^{L}_{\chi\delta\varepsilon}}\frac{\partial\tilde{B}^{L}_{\chi\delta\varepsilon}}{\partial F^{La}_{.\alpha}}\right]F^{Lc}_{.\alpha}$$

$$- g^{da}\left[\left(J^{L-1}\frac{\partial\tilde{\Psi}}{\partial\tilde{B}^{L}_{\chi\delta\varepsilon}}\frac{\partial\tilde{B}^{L}_{\chi\delta\varepsilon}}{\partial F^{La}_{.\alpha:\beta}}F^{Lb}_{.\beta}\right)_{;b}\right]F^{Lc}_{.\alpha}$$

$$\qquad (6.257)$$

$$= J^{L-1}\left[\frac{\partial\tilde{\Psi}}{\partial\tilde{E}^{L}_{\alpha\chi}}F^{Ld}_{.\chi} + \frac{\partial\tilde{\Psi}}{\partial\tilde{B}^{L}_{\alpha\beta\chi}}F^{Ld}_{.\beta:\chi}\right]F^{Lc}_{.\alpha}$$

$$- \left[\left(J^{L-1}\frac{\partial\tilde{\Psi}}{\partial\tilde{B}^{L}_{\chi\alpha\beta}}F^{Ld}_{.\chi}F^{Lb}_{.\beta}\right)_{;b}\right]F^{Lc}_{.\alpha}\,.$$

As an illustrative simple example, strain energy density (6.254) is written as a Taylor series expansion to second order in lattice strains and sec-

ond-order lattice deformation gradients about a reference state at which $F^{La}_{.\alpha} = g^a_{.\alpha}$ and $F^{La}_{.\alpha:\beta} = 0$:

$$\tilde{\Psi} = \tilde{\Psi}_0 + \overline{\mathbb{C}}^{\alpha\beta} \tilde{E}^L_{\alpha\beta} + \overline{\mathbb{D}}^{\alpha\beta\chi} \tilde{B}^L_{\alpha\beta\chi} + \frac{1}{2} \overline{\mathbb{C}}^{\alpha\beta\chi\delta} \tilde{E}^L_{\alpha\beta} \tilde{E}^L_{\chi\delta}$$

$$+ \frac{1}{2} \overline{\mathbb{D}}^{\alpha\beta\chi\delta\varepsilon\phi} \tilde{B}^L_{\alpha\beta\chi} \tilde{B}^L_{\delta\varepsilon\phi} + \overline{\mathbb{K}}^{\alpha\beta\chi\delta\varepsilon} \tilde{E}^L_{\alpha\beta} \tilde{B}^L_{\chi\delta\varepsilon},$$

(6.258)

where $\tilde{\Psi}_0 = \tilde{\Psi}(0,0,X,\tilde{\mathbf{g}}_\alpha)$ is the strain energy density per unit volume at the reference state and the constant material coefficients at a material point X are defined as

$$\overline{\mathbb{C}}^{\alpha\beta} = \frac{\partial \tilde{\Psi}}{\partial \tilde{E}^L_{\alpha\beta}} \bigg|_{\substack{\tilde{\mathbf{E}}^L=0 \\ \tilde{\mathbf{B}}^L=0}}, \quad \overline{\mathbb{D}}^{\alpha\beta\chi} = \frac{\partial \tilde{\Psi}}{\partial \tilde{B}^L_{\alpha\beta\chi}} \bigg|_{\substack{\tilde{\mathbf{E}}^L=0 \\ \tilde{\mathbf{B}}^L=0}}, \quad \overline{\mathbb{C}}^{\alpha\beta\chi\delta} = \frac{\partial^2 \tilde{\Psi}}{\partial \tilde{E}^L_{\alpha\beta} \partial \tilde{E}^L_{\chi\delta}} \bigg|_{\substack{\tilde{\mathbf{E}}^L=0 \\ \tilde{\mathbf{B}}^L=0}}, \quad (6.259)$$

$$\overline{\mathbb{D}}^{\alpha\beta\chi\delta\varepsilon\phi} = \frac{\partial^2 \tilde{\Psi}}{\partial \tilde{B}^L_{\alpha\beta\chi} \partial \tilde{B}^L_{\delta\varepsilon\phi}} \bigg|_{\substack{\tilde{\mathbf{E}}^L=0 \\ \tilde{\mathbf{B}}^L=0}}, \quad \overline{\mathbb{K}}^{\alpha\beta\chi\delta\varepsilon} = \frac{\partial^2 \tilde{\Psi}}{\partial \tilde{E}^L_{\alpha\beta} \partial \tilde{B}^L_{\chi\delta\varepsilon}} \bigg|_{\substack{\tilde{\mathbf{E}}^L=0 \\ \tilde{\mathbf{B}}^L=0}}. \quad (6.260)$$

A natural state in which both the stress and hyperstress vanish everywhere may not exist for a given material, and such a state may be an exceptional case rather than the norm. None of the constants in (6.259) and (6.260) need vanish entirely in general, though certain symmetry properties result automatically from $\tilde{E}^L_{\alpha\beta} = \tilde{E}^L_{(\alpha\beta)}$. Spatial invariance of (6.254) ensures that (6.249) and angular momentum balance (6.253) are satisfied identically.

6.7.3 Relationship to Dislocation Theory

Recall from Section 3.3.2 the definitions of the second-order geometrically necessary dislocation density tensor referred to $\tilde{B}$, specifically (3.222) and (3.224) that combine to yield

$$\tilde{\alpha}^{\alpha\beta} = J^L \varepsilon^{abc} F^{L-1\alpha}_{.b,c} F^{L-1\beta}_{.a}$$

$$= J^L \varepsilon^{abc} F^{L-1\alpha}_{.d} (F^{Ld}_{.\chi} F^{L-1\chi}_{.b,c}) F^{L-1\beta}_{.a}$$

$$= J^L \varepsilon^{abc} F^{L-1\alpha}_{.d} \overline{\Gamma}^{.d}_{cb} F^{L-1\beta}_{.a}$$

$$= J^L \varepsilon^{abc} F^{L-1\alpha}_{.d} \overline{T}^{.d}_{cb} F^{L-1\beta}_{.a},$$

(6.261)

where the torsion of the crystal connection is, from (3.190) and (3.191),

$$\overline{T}^{..a}_{bc} = \overline{\Gamma}^{..a}_{[bc]} = F^{La}_{.\alpha} \partial_{[b} F^{L-1\alpha}_{.c]}$$

$$= F^{La}_{.\alpha} F^{L-1\alpha}_{.[c,b]} = -F^{La}_{.\alpha,[b} F^{L-1\alpha}_{.c]}.$$

(6.262)

From (6.217), the skew part of the total covariant derivative of the lattice deformation is

$$
\begin{aligned}
F^{La}_{\ .[\alpha:\beta]} &= (\overset{g}{\varGamma}{}^{\ ..a}_{\ bc} - \bar{\varGamma}^{\ ..a}_{\ bc})F^{Lc}_{\ .[\alpha}F^{Lb}_{\ .\beta]} - \tilde{\varGamma}^{\ .\chi}_{\ [\beta\alpha]}F^{La}_{\ .\chi} \\
&= \frac{1}{2}(\overset{g}{\varGamma}{}^{\ ..a}_{\ bc} - \bar{\varGamma}^{\ ..a}_{\ bc})(F^{Lc}_{\ .\alpha}F^{Lb}_{\ .\beta} - F^{Lc}_{\ .\beta}F^{Lb}_{\ .\alpha}) \\
&= \frac{1}{2}(\overset{g}{\varGamma}{}^{\ ..a}_{\ bc} - \overset{g}{\varGamma}{}^{\ ..a}_{\ cb} - \bar{\varGamma}^{\ ..a}_{\ bc} + \bar{\varGamma}^{\ ..a}_{\ cb})(F^{Lc}_{\ .\alpha}F^{Lb}_{\ .\beta}) &&\text{(6.263)} \\
&= (\overset{g}{\varGamma}{}^{\ ..a}_{\ [bc]} - \bar{\varGamma}^{\ ..a}_{\ [bc]})F^{Lc}_{\ .\alpha}F^{Lb}_{\ .\beta} \\
&= \bar{T}^{\ ..a}_{cb}F^{Lc}_{\ .\alpha}F^{Lb}_{\ .\beta},
\end{aligned}
$$

since $\overset{g}{\varGamma}{}^{\ ..a}_{\ [bc]} = 0$ by definition (2.58), and where $\tilde{\varGamma}^{\ .\chi}_{\ [\beta\alpha]} = 0$, i.e., an external intermediate coordinate system with symmetric connection has been assumed. Combining (6.261)-(6.263), the dislocation density tensor can be expressed as

$$
\tilde{\alpha}^{\alpha\beta} = J^L \varepsilon^{abc} F^{L-1\alpha}_{\ .d}(F^{L-1\chi}_{c.}F^{Ld}_{\ [\chi:\delta]}F^{L-1\delta}_{\ .b})F^{L-1\beta}_{\ .a}. \tag{6.264}
$$

Assume next for illustrative purposes that the strain energy density of (6.230) depends on the covariant derivative of the lattice deformation gradient only through the dislocation density tensor:

$$
\tilde{\varPsi} = \tilde{\varPsi}\left(F^{La}_{\ .\alpha}, \tilde{\alpha}^{\alpha\beta}(F^{La}_{\ .\alpha}, F^{La}_{\ .\alpha:\beta}), X, \tilde{\mathbf{g}}_\alpha\right). \tag{6.265}
$$

Stress (6.239) and hyperstress (6.240) then become, in this particular case,

$$
\begin{aligned}
\sigma^{dc} &= g^{da}\left[J^{L-1}\frac{\partial\tilde{\varPsi}}{\partial F^{La}_{\ .\alpha}} - \left(J^{L-1}\frac{\partial\tilde{\varPsi}}{\partial\tilde{\alpha}^{\chi\delta}}\frac{\partial\tilde{\alpha}^{\chi\delta}}{\partial F^{La}_{\ .\alpha:\beta}}F^{Lb}_{\ .\beta}\right)_{;b}\right]F^{Lc}_{\ .\alpha} \\
&= J^{L-1}g^{da}\frac{\partial\tilde{\varPsi}}{\partial F^{La}_{\ .\alpha}}F^{Lc}_{\ .\alpha} \tag{6.266} \\
&\quad -g^{da}\left(\frac{\partial\tilde{\varPsi}}{\partial\tilde{\alpha}^{\chi\delta}}\varepsilon^{fgh}F^{L-1\chi}_{\ .a}F^{L-1[\alpha}_{\ .h}F^{L-1\beta]}_{\ .g}F^{L-1\delta}_{\ .f}F^{Lb}_{\ .\beta}\right)_{;b}F^{Lc}_{\ .\alpha},
\end{aligned}
$$

$$
\begin{aligned}
H^{bdc} &= J^{L-1}g^{da}\frac{\partial\tilde{\varPsi}}{\partial\tilde{\alpha}^{\chi\delta}}\frac{\partial\tilde{\alpha}^{\chi\delta}}{\partial F^{La}_{\ .\alpha:\beta}}F^{Lb}_{\ .\beta}F^{Lc}_{\ .\alpha} \\
&= J^{L-1}g^{da}\frac{\partial\tilde{\varPsi}}{\partial\tilde{\alpha}^{\chi\delta}}(J^L\varepsilon^{fgh}F^{L-1\chi}_{\ .a}F^{L-1[\alpha}_{\ .h}F^{L-1\beta]}_{\ .g}F^{L-1\delta}_{\ .f})F^{Lb}_{\ .\beta}F^{Lc}_{\ .\alpha} \tag{6.267} \\
&= g^{da}\frac{\partial\tilde{\varPsi}}{\partial\tilde{\alpha}^{\chi\delta}}(\varepsilon^{fbc}F^{L-1\chi}_{\ .a}F^{L-1\delta}_{\ .f}) = H^{[b|d|c]},
\end{aligned}
$$

since from (6.264),

$$
\frac{\partial \tilde{\alpha}^{\chi\delta}}{\partial F^{Le}_{.\alpha:\beta}} = \frac{\partial}{\partial F^{Le}_{.\alpha:\beta}}[J^{L}\varepsilon^{abc}F^{L-1\chi}_{.d}(F^{L-1\varepsilon}_{.c}F^{Ld}_{[\varepsilon:\phi]}F^{L-1\phi}_{.b})F^{L-1\delta}_{.a}]
$$

$$
= J^{L}\varepsilon^{abc}F^{L-1\chi}_{.d}F^{L-1\varepsilon}_{.c}\delta^{d}_{.e}\delta^{\alpha}_{[\varepsilon}\delta^{\beta}_{.\phi]}F^{L-1\phi}_{.b}F^{L-1\delta}_{.a} \qquad (6.268)
$$

$$
= J^{L}\varepsilon^{abc}F^{L-1\chi}_{.e}F^{L-1[\alpha}_{.c}F^{L-1\beta]}_{.b}F^{L-1\delta}_{.a}.
$$

From (6.267), the hyperstress consists of only 9 independent components when (6.265) is used in place of (6.230). The hyperstress vanishes when dislocation density (6.261) vanishes, in which case $\partial\tilde{\Psi}/\partial\tilde{\alpha}^{\chi\delta}=0$. Relationships between hyperstress or couple stress and dislocation density were derived by Kroner (1963b). Garikipati (2003) demonstrated relationships among slip gradients, three-body terms in interatomic potentials reflecting bond angle dependence of interatomic forces, and hyperstresses in the context of Toupin's nonlinear elastic theory of grade two (Toupin 1962).

The approach outlined Section 6.7 accounts for the second grade hyperelastic response of the material from intermediate configuration $\tilde{B}$, but does not account for evolution of this intermediate configuration, since kinetic relations for the time rate of plastic deformation, $\dot{\mathbf{F}}^{\mathbf{P}}$, are not addressed. Postulation of such relations in a thermodynamically admissible manner requires consideration of the dissipation equality and thermal effects, phenomena which are excluded by use of Hamilton's principle for conservative systems (Eringen 1962). More recent approaches considering dissipative thermodynamics of materials whose free energy may depend on higher-order gradients of lattice deformation include those of Le and Stumpf (1996b, c), Bammann (2001), Regueiro et al. (2002), and Clayton et al. (2004b, 2006). In these approaches, generalized conservation laws for momentum and energy are often postulated directly rather than derived from the first variation of an action integral. Presumably, the kinetic law for the rate of plastic deformation should include a dependence on tensors $F^{La}_{.\alpha:\beta}$ or $\tilde{\alpha}^{\alpha\beta}$, since geometrically necessary dislocations are thought to affect strain hardening (Ashby 1970; Fleck and Hutchinson 1993; Fleck et al. 1994; Steinmann 1996; Gao et al. 1999; Gurtin 2000, 2002; Acharya 2001; Regueiro et al. 2002; Voyiadjis and Abu Al-Rub 2005; Abu Al-Rub and Voyiadjis 2006). Zubelewicz (2008) developed a constitutive model, based on non-equilibrium thermodynamics and a measure of slip incompatibility, for describing heterogeneous dislocation microstructures and strong dynamic strain hardening that emerge in crystalline metals subjected to shock loading. A complete continuum theory incorporating dependence of thermodynamic potentials and kinetic relations on the dislocation density tensor, as well as the disclination density tensor (see Section

3.3.3), is presented later in Section 9.4 of Chapter 9, a Chapter dealing with inelasticity theories of a more general scope.

7 Residual Deformation from Lattice Defects

An element of crystalline material through which a net flux of dislocations has passed exhibits plastic shape change. Dislocation lines within the element, i.e., displacement discontinuities across the slip plane in the context of Volterra defects may also contribute to this plastic deformation. However, plastic deformation, according to traditional definitions, does not address additional changes in dimensions of the body resulting from residual elastic deformation associated with local stress fields induced by defects. Mura (1982) labels these local, self-equilibrated stresses (i.e., residual stresses) eigenstresses.

Dislocation glide preserves the volume of the crystal, and purely tangential displacement discontinuities such as crystallographic slip do not alter the volume occupied by the material. Yet ample evidence suggests that dislocation lines affect the total volume of crystals (Zener 1942; Schmid and Boas 1950; Holder and Granato 1969; Wright 1982). Stored energies associated with elastic fields of defects are important because they affect recrystallization (Schmid and Boas 1950; Taheri et al. 2006) and the fraction of stress power converted to temperature rise at high deformation rates (Rosakis et al. 2000) that can result in shear localization in metals during dynamic failure events. Large numbers of dislocations, twins, and stacking faults can be generated during shock or impact loading (Rohatgi and Vecchio 2002), and presumably the corresponding volume changes, shape changes, and stored energies associated with local stress fields of these defects affect the observed material response under such conditions (Clayton 2009a, c).

Defects of interest in Sections 7.1-7.3 of Chapter 7 are those that can be described by displacement discontinuities tangential to an internal surface (i.e., crystallographic plane) in a volume element of the solid. These include gliding straight or curved dislocations lines, dislocation loops, as well as partial dislocations. Motion of dislocations through a region of the crystal results in plastic shape change as mentioned above, but preserves the lattice spacing (Bilby and Smith 1956; Bilby et al. 1957), as discussed in detail in Section 3.2 of Chapter 3; this requires cooperative motion of leading and trailing partials for the case of partial dislocations. Residual elastic stress fields from disclination lines and loops are also considered in

Chapter 7, though their contribution to the plastic shape change (Li and Gilman 1970) is not addressed explicitly here. Considered in Section 7.4 are point defects (Eshelby 1954, 1956) that may have finite intrinsic volumes (e.g., volume changes per defect on the order of the atomic volume).

In Chapter 7, a three-term decomposition of the deformation gradient, $\mathbf{F} = \mathbf{F}^E \mathbf{F}^I \mathbf{F}^P$, is assigned to describe the kinematics of a volume element of crystalline material containing lattice defects, following (3.137). In order to delineate residual elastic deformation from recoverable elastic deformation and from plastic deformation, terms entering this decomposition are defined in a precise manner in Section 7.2. Some repetition of definitions given in Chapter 3 is unavoidable. For simplicity, isothermal conditions are assumed throughout Chapter 7, meaning thermal expansion is omitted. Elastic tangent map $\mathbf{F}^E$ accounts for deformation due to applied stresses as well as rigid body rotations of the lattice. Plastic tangent map $\mathbf{F}^P$ results from the cumulative effects of fluxes of dislocations (Orowan 1940; Mura 1968; Lardner 1969) and from slip discontinuities associated with defects within the element (Teodosiu 1970; Rice 1971). Intermediate term $\mathbf{F}^I$ (or its stretch or rotational components) has been introduced in a number of works with various definitions (Kratochvil 1972; Bammann 2001; Regueiro et al. 2002; Clayton and McDowell 2003a; Hartley 2003; Clayton et al. 2004b, 2005, 2006; Gerken and Dawson 2008). In Section 3.2.9, a derivation of $\mathbf{F}^I$ was obtained in (3.148) by volume averaging local continuum fields over an element of a (poly)crystal featuring elastic-plastic responses of the form in (3.145) at a lower length scale. In contrast, $\mathbf{F}^I$ as defined in Chapter 7 represents the average residual elastic deformation of the element of crystal induced by the local stress and strain fields of the defects contained within it. Thus, in Chapter 7, it corresponds exactly to the volume average of the residual elastic deformation in the context of defect field theories (Kroner and Seeger 1959; Willis 1967; Teodosiu 1982).

In Section 7.2, the externally unloaded volume element of crystalline material is treated as a hyperelastic body of grade one with homogeneous elastic constants, in static equilibrium, and containing internal displacement discontinuities across which traction is continuous. The element is free of external traction but may support internal (i.e., residual) stresses. Self-equilibrium conditions result in an integral equation for $\mathbf{F}^I$. For linear elastic constitutive behavior, $\mathbf{F}^I$ reduces to the unit tensor in rectangular Cartesian coordinates, but $\mathbf{F}^I$ does not so reduce for nonlinear constitutive behavior. Analytical elasticity solutions for defect energies (Appendix C) are considered along with experimental data (Clarebrough et al. 1957)

to confirm accuracy of the theory for predicting residual volume changes associated with line defects.

In Section 7.3, the externally unloaded volume element is identified as a set of discrete atoms in static equilibrium and free of external forces. The lattice statics description of Section B.2 in Appendix B applies. According to this description, interatomic forces vanish in a perfect crystal free of defects, but nonzero forces may exist among atoms when they are arranged in an imperfect way (i.e., when defects are present). The self-equilibrium conditions are equivalent to vanishing of static components of the average virial stress for the set of atoms (Huang 1950; Zhou 2003). When atomic interactions are harmonic, equilibrium demands that $\mathbf{F}^{\mathbf{I}}$ as defined in Section 7.3 should reduce to the unit tensor. In the more general case of anharmonic interactions that may be physically significant in the vicinity of defect cores where large atomic displacements arise, the derivations in Section 7.3 suggest that $\mathbf{F}^{\mathbf{I}}$ could be non-negligible.

In Section 7.4, average deformations of an element of crystal containing a distribution of point defects are addressed. Multiplicative decomposition (3.128) applies, $\mathbf{F}^{\mathbf{L}} = \mathbf{F}^{\mathbf{E}}\mathbf{F}^{\mathbf{V}}$, with $\mathbf{F}^{\mathbf{V}}$ accounting for volume changes from point defects and $\mathbf{F}^{\mathbf{L}}$ the total lattice deformation. The total volume change per point defect is derived by combining the volume change per defect predicted by the linear elastic sphere-in-hole model of Section C.3 of Appendix C (Bitter 1931; Teodosiu 1982) with a correction for nonlinear elasticity (Eshelby 1954; Holder and Granato 1969). Analytical solutions are considered with experimental data (Nilan and Granato 1965) to confirm accuracy of the theory for predicting residual volume changes associated with vacancies.

7.1 Multiplicative Kinematics

Consider a volume element of a crystal containing lattice defects. This element is larger than the average atomic spacing, but may be of smaller dimensions than the entire crystal. Static (i.e., null inertia) and isothermal conditions are assumed. Deformation of the element is described by mappings between tangent spaces of configurations, as shown in Fig. 7.1.

Reference configuration B_0 is treated as a perfect lattice. The position vector $\mathbf{R}_{\langle j \rangle}$ of atom j (e.g., the equilibrium position of its nucleus) relative to the origin of a Cartesian coordinate system in an infinite lattice in the reference configuration is given by periodicity relations (3.4) and (B.38):

$$\mathbf{R}_{\langle j \rangle} = \mathbf{R}\begin{pmatrix} l \\ k \end{pmatrix} = \mathbf{R}\begin{pmatrix} 0 \\ k \end{pmatrix} + \mathbf{R}(l) = \sum_{i=1}^{3} (m^i + l^i)\mathbf{A}_i , \ (l^i \in \mathbb{Z}, 0 \le m^i < 1). \quad (7.1)$$

In (7.1), $\mathbf{R}\begin{pmatrix} 0 \\ k \end{pmatrix}$ is a basis vector for atom k of the basis at each Bravais lattice point, $\mathbf{R}(l)$ is a Bravais lattice vector denoting the position of primitive unit cell l, and $\mathbf{A}_i$ is a primitive Bravais lattice vector. Recall that in a monatomic lattice with one atom per unit cell, basis vectors are redundant and $\mathbf{R}\begin{pmatrix} 0 \\ k \end{pmatrix} = 0$, though the treatment of Chapter 7 is not restricted to monatomic crystal structures.
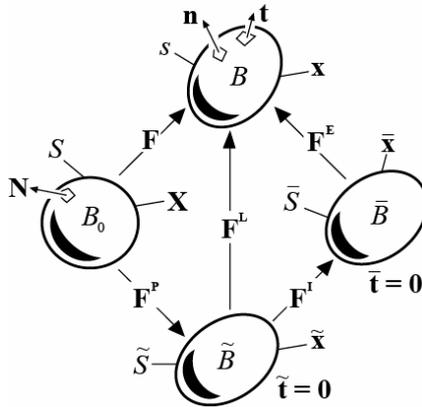
Fig. 7.1 Configurations, surface coordinates and tractions, and tangent maps

7.1.1 Plastic Deformation

Intermediate configuration $\tilde{B}$ in Fig. 7.1 differs from B_0 as a result of influences of cumulative motion of lattice defects and perturbations of atomic positions resulting from these defects. Configuration $\tilde{B}$ is by definition free of external traction ($\tilde{\mathbf{t}} = 0$) and free of internal stresses. For a crystal containing a single dislocation, a singular plastic deformation map can be defined as in (3.85):

$$\mathbf{F}^P = \mathbf{1} + \tilde{\mathbf{b}} \otimes \mathbf{M} \delta \langle \mathbf{X}, \mathbf{M} \rangle \chi , \quad (7.2)$$

where $\mathbf{1}$ is the unit tensor, $\tilde{\mathbf{b}}$ is the Burgers vector, $\mathbf{M}$ is the normal to the slip surface in the reference configuration, $\delta(.)$ is Dirac's delta function, and χ is the characteristic function that is unity at reference coordinates $\mathbf{X}$ on slipped surface Σ and zero elsewhere. The Cartesian coordinate sys-

tem for $\mathbf{X}$ is chosen with its origin in the slip plane. A singular dislocation density tensor corresponding to (7.2) and first listed in (3.86) is

$$\boldsymbol{\alpha}_0 = \tilde{\mathbf{b}} \otimes \boldsymbol{\xi}_0 \delta(L), \tag{7.3}$$

where $\boldsymbol{\xi}_0$ is the unit tangent to dislocation line of length L in the reference configuration. For a collection of j straight stationary dislocation line populations of density (length per unit reference volume) ρ_0^i, Burgers vector $\tilde{\mathbf{b}}^i$, and unit tangent $\boldsymbol{\xi}_0^i$, dislocation density (7.3) can be extended to

$$\boldsymbol{\alpha}_0 = V^{-1} \int_L \tilde{\mathbf{b}} \otimes \boldsymbol{\xi}_0 dL = \sum_{i=1}^{j} \rho_0^i \tilde{\mathbf{b}}^i \otimes \boldsymbol{\xi}_0^i , \tag{7.4}$$

as indicated in (3.87). The total volume occupied by the crystal element in the reference configuration is denoted by V. The second of (7.4) pertains to a total of j dislocation populations with the same tangent line and local Burgers vector for each value of i.

   A more general definition, first listed in (3.97), of average plastic deformation accounts for the history of generation and motion of defects within a material element, in which case

$$\dot{\mathbf{F}}^{\mathbf{P}} = \mathbf{L}^{\mathbf{P}} \mathbf{F}^{\mathbf{P}} , \ \ \mathbf{F}^{\mathbf{P}} \big|_{t=0} = \mathbf{1} . \tag{7.5}$$

The average plastic velocity gradient $\mathbf{L}^{\mathbf{P}}$ is dictated by the flux $\tilde{\boldsymbol{\varsigma}}$ of mobile dislocations as in (3.98)-(3.99), written in indicial notation as

$$L^{P\alpha}_{.\beta} = \varsigma^{\alpha\chi\delta} \varepsilon_{\chi\delta\beta} , \ \ \varsigma^{\alpha\chi\delta} = V^{-1} \int_L \tilde{b}^{i\alpha} \tilde{\xi}^{i\chi} \tilde{v}^{i\delta} dL = \sum_{i=1}^{j} \tilde{\rho}^i \tilde{b}^{i\alpha} \tilde{\xi}^{i\chi} \tilde{v}^{i\delta} , \tag{7.6}$$

where $\tilde{\boldsymbol{\xi}}^i$ and $\tilde{\mathbf{v}}^i$ are respectively the uniform tangent line and velocity of every dislocation in population i. Since dislocation segments have perpendicular velocities and tangent lines, the isochoric plastic deformation conditions $\dot{J}^P = J^P \mathrm{tr}(\mathbf{L}^{\mathbf{P}}) = 0$ and $J^P = 1$ follow automatically from (7.6). Introducing two quantities—$\tilde{\mathbf{m}}^i$, the unit normal to the slip plane and $\tilde{\mathbf{s}}^i$, a unit vector in the direction of slip—(7.6) reduces to (3.100), as typically encountered in crystal plasticity theory of Sections 3.2.6 and 6.3:

$$\mathbf{L}^{\mathbf{P}} = \sum_i \tilde{\rho}^i \tilde{b}^i \tilde{v}^i \tilde{\mathbf{s}}^i \otimes \tilde{\mathbf{m}}^i = \sum_i \dot{\gamma}^i \tilde{\mathbf{s}}^i \otimes \tilde{\mathbf{m}}^i . \tag{7.7}$$

Since $\tilde{\mathbf{s}}^i \perp \tilde{\mathbf{m}}^i$, again $\dot{J}^P = 0$ and $J^P = 1$. In summary, according to descriptions in terms of single dislocations (7.2), dislocation flux (7.6), or crystal plasticity (7.7), plastic deformation is always isochoric.

7.1.2 Lattice Deformation

Let $\mathbf{F^E}$ denote the tangent map to externally stressed configuration B, as denoted generally by $\mathbf{t} \neq 0$ in Fig. 7.1, from self-equilibrated configuration $\overline{B}$, with $\overline{\mathbf{t}} = 0$ in Fig. 7.1. Let $\overline{\mathbf{a}}_i$ denote a primitive Bravais lattice vector of (7.1) mapped to intermediate tangent bundle $T\overline{B}$:

$$\overline{\mathbf{a}}_i = \mathbf{F^I A}_i, \ \overline{a}_i^\alpha = F^{I\alpha}_{.\beta} g^\beta_{.A} A_i^A \tag{7.8}$$

with $g^\beta_{.A}$ the shifter between coordinate frames in B_0 and $\tilde{B}$, omitted in the direct tensor notation in the first of (7.8). When coincident coordinate systems are used in these two configurations, $g^\beta_{.A} = \delta^\beta_{.A}$. Note that lattice vectors are not affected by $\mathbf{F^P}$, in accordance with (3.107). Lattice vectors deform from $T\overline{B}$ to TB according to (3.109):

$$\mathbf{a}_i = \mathbf{F^E}\overline{\mathbf{a}}_i = \mathbf{F^L A}_i, \ a_i^a = F^{Ea}_{.\alpha}\overline{a}_i^\alpha = F^{L\alpha}_{.\beta} g^\beta_{.A} A_i^A. \tag{7.9}$$

where the total lattice deformation for the volume element is $\mathbf{F^L} = \mathbf{F^E F^I}$. Under a homogeneous deformation, basis vectors $\mathbf{R}\binom{0}{k}$ in (7.1) deform similarly to primitive Bravais lattice vectors $\mathbf{A}_i$ in (7.8) and (7.9), and the final position of atom j may also change by a translation that is uniform for each species in the basis but that may differ among species (Born and Huang 1954). This translation may be due, for example, to polarization in an applied electric field or inner displacements among sub-lattices in a non-centrosymmetric polyatomic crystal (Cousins 1978). Relations (7.8) and (7.9) generalize the Cauchy-Born hypothesis (Born and Huang 1954) of Section 3.1.2, distinguishing effects of recoverable ($\mathbf{F^E}$) and residual ($\mathbf{F^I}$) deformations. Rigid body rotations of the element are included in the rotational part of the polar decomposition of $\mathbf{F^L}$, denoted by $\mathbf{R^L}$.

Reference Bravais lattice vectors $\mathbf{A}_i$ are uniform with respect to position in a sample of a perfect single crystal. However, when defects are contained within the volume, deformed primitive lattice vectors $\mathbf{a}_i$ and $\overline{\mathbf{a}}_i$ represent suitable averages of local lattice vectors $\mathbf{a}'_i$ and $\overline{\mathbf{a}}'_i$ that may not be spatially constant, just as in (3.111):

$$\mathbf{a}_i = V^{-1}\int_V \mathbf{a}'_i dV, \ \overline{\mathbf{a}}_i = V^{-1}\int_V \overline{\mathbf{a}}'_i dV. \tag{7.10}$$

By cutting the volume element out of the stressed body thereby relieving the external traction, relaxing any possible internal viscous and inertial forces, and then rotating this element by $\mathbf{R^{E-1}}$, configuration $\overline{B}$ can be obtained from spatial configuration B. If experiments could be performed in which the average lattice vectors were measured in each of configurations

B_0, $\bar{B}$, and B, then (7.8) and the first of (7.9) would each provide nine equations involving nine unknown components of $\mathbf{F^I}$ or $\mathbf{F^E}$. However, configuration $\tilde{B}$ can only be realized for a solid with a heterogeneous internal stress field by removing all traction from the surface of each microscopic, residually stressed sub-element within that solid, physically corresponding to cutting or breaking it into small parts (Eckart 1948), in practice a prohibitively destructive laboratory experiment. In Sections 7.2 and 7.3, theoretical methods are offered for computing $\mathbf{F^I}$ that, in principle, would alleviate the need for such difficult experiments.

7.1.3 Multiplicative Decomposition of Total Deformation

The total deformation $\mathbf{F}$ is defined by the surface integral (Hill 1972, 1984; Clayton and McDowell 2004)

$$\mathbf{F} = V^{-1}\int_S \mathbf{x} \otimes \mathbf{N}dS \,, \tag{7.11}$$

where $\mathbf{x}$ are spatial coordinates of the deformed image of reference surface S enclosing the volume element with unit outward reference normal $\mathbf{N}$, as illustrated in Fig. 7.1. The volume element may contain discontinuities in the internal displacement field and gradients of displacement; when such discontinuities are absent and after Gauss's theorem (2.194) is applied, (7.11) reduces to $F^a_{.A} = V^{-1}\int x^a_{.,A}dV$, where $x^a = x^a(X^A,t)$ are now differentiable functions of reference position X within volume element of reference volume V. In contrast to notation used in Chapter 2, capital symbols are reserved in Chapter 7 for the total (average) deformation gradient $\mathbf{F}$ for a volume element and its constituents: $\mathbf{F^E}$, $\mathbf{F^I}$, $\mathbf{F^L}$, and $\mathbf{F^P}$. In contrast, the local deformation gradient within the volume element is written in Chapter 7 as $x^a_{.,A}$.

Assume that the total deformation gradient $\mathbf{F}$ is imposed on a volume element of material via (7.11), and that the decomposition

$$\mathbf{F} = \mathbf{F^E F^I F^P} = \mathbf{F^L F^P} \tag{7.12}$$

applies, as implied by Fig. 7.1. Plastic deformation $\mathbf{F^P}$ is known from integration of (7.5) with (7.6) or (7.7), presuming kinetic laws are available for the mobile dislocation velocity, for example those described in Section 6.2, or slip rates on each slip system, for example those described in Section 6.3. Under isothermal conditions, the crystal in a particular orientation responds to applied loading elastically such that

$$\bar{\boldsymbol{\Sigma}} = \bar{\boldsymbol{\Sigma}}\left(\mathbf{U^E}\right) \Leftrightarrow \mathbf{U^E} = \mathbf{U^E}\left(\bar{\boldsymbol{\Sigma}}\right), \tag{7.13}$$

where stretch tensor $\mathbf{U}^{\mathbf{E}} = \mathbf{R}^{\mathbf{E}-1}\mathbf{F}^{\mathbf{E}} = (\mathbf{F}^{\mathbf{E}T}\mathbf{F}^{\mathbf{E}})^{1/2}$ is an invertible function of conjugate stress measure $\overline{\Sigma}$ that vanishes when the traction $\mathbf{t} = 0$ along deformed surface s of the element in Fig. 7.1. The particular form of (7.13) will depend upon the orientation of the lattice in $\overline{B}$ (e.g., choice of coordinate system with respect to orientation of the sample) because of anisotropy. For example, for a hyperelastic-plastic solid with non-vanishing second- and third-order elastic constants, (7.13) can be inter-preted as a version of (6.56) pushed forward to configuration $\overline{B}$, in the ab-sence of temperature changes.

Henceforth in Chapter 7 it is assumed that

$$\mathbf{F}^{\mathbf{L}} = \mathbf{R}^{\mathbf{E}}\mathbf{U}^{\mathbf{E}}\mathbf{F}^{\mathbf{I}} = \mathbf{R}^{\mathbf{L}}\mathbf{U}^{\mathbf{E}}\mathbf{U}^{\mathbf{I}}, \ \mathbf{F}^{\mathbf{I}} = \mathbf{U}^{\mathbf{I}}, \tag{7.14}$$

meaning that $\mathbf{F}^{\mathbf{I}}$ is a stretch (e.g., a symmetric tensor with six independent entries in covariant Cartesian coordinates) and that all lattice rotation is embedded in $\mathbf{R}^{\mathbf{E}}$. The objective of Sections 7.2 and 7.3 is determination of analytical approaches to obtain $\mathbf{F}^{\mathbf{I}}$. If $\mathbf{F}^{\mathbf{P}}$ is also known at a particular instant, $\mathbf{F}^{\mathbf{E}} = \mathbf{F}\mathbf{F}^{\mathbf{P}-1}\mathbf{F}^{\mathbf{I}-1}$ can then be found from (7.12) and the average ex-ternal stress supported by the element can be updated according to elastic constitutive relation (7.13).

7.2 Nonlinear Elastic Interpretation of Residual Elasticity

The dimensional changes of a nonlinear elastic body in a state of self-stress, i.e., a self-equilibrated body with internal residual stresses but no traction applied to its external boundaries, are derived in Sections 7.2.1-7.2.3. The body may contain one or more internal surfaces across which traction is continuous but tangential displacements are not. The treatment is specialized in Section 7.2.4 to address volume changes in cubic crystals and isotropic materials. Formulae for volume changes attributed to local elastic stress fields of line defects are derived in the isotropic approxima-tion in Section 7.2.5. Derivations and discussion in Sections 7.2.1-7.2.5 consolidate and extend prior work of a number of authors (Zener 1942; Seeger and Haasen 1958; Toupin and Rivlin 1960; Holder and Granato 1969; Teodosiu 1982; Clayton and Bammann 2009). Additional analysis and examples follow in Sections 7.2.6 and 7.2.7. Since the derivations frequently involve integration of vector and tensor fields over regions of space occupied by the body, coincident Cartesian coordinates are used throughout the remainder of Chapter 7 unless noted otherwise. The proce-dure of Toupin (1956) outlined in (3.95) and (3.96) could be used instead

if curvilinear coordinates are desired, but such steps are omitted in order to provide a more concise presentation.

7.2.1 Self-equilibrium Conditions

Local balance of linear momentum (4.21) is written in rectangular Cartesian coordinates as

$$P^{aA}_{\;\;,A} + \bar{B}^a = \rho_0 A^a, \qquad (7.15)$$

with $\bar{B}^a$ the body force per unit reference volume, ρ_0 the reference mass density, and A^a the material acceleration. In reference coordinates X^A, application of the product rule then provides the local relation

$$(X^A P^{aB})_{,B} = P^{aA} + (\rho_0 A^a - \bar{B}^a)X^A. \qquad (7.16)$$

Consider a body of reference volume V with external surface S. The body may contain internal surfaces across which the motion $x^a(X,t)$ from the reference state (e.g., a perfect lattice), deformation gradient $x^a_{\;,A}(X,t)$, and stress components are generally discontinuous, but traction per unit reference area t^a_0 of (4.4) across internal surfaces is continuous:

$$\left[\!\left[t^a_0\right]\!\right] = t^{+a}_0 - t^{-a}_0 = (P^{+aA} - P^{-aA})M_A = 0, \text{ (on } \Sigma\text{)}, \qquad (7.17)$$

where $+$ and $-$ denote limiting values of a quantity near the surface as it is approached from either side, M_A is a unit normal covariant vector to an internal surface, and Σ denotes the union of such internal surfaces. The source of displacement discontinuities across Σ is arbitrary in (7.17); for the particular case of dislocation(s) within V, jump(s) in displacement across slip planes comprising Σ are attributed to Burgers vector(s) introduced in (7.2). Integrating (7.16) over V and applying the divergence theorem,

$$\int_V P^{aA} dV = \int_S X^A P^{aB} N_B dS + \int_\Sigma X^A (P^{+aB} - P^{-aB})M_B d\Sigma$$
$$+ \int_V X^A (\bar{B}^a - \rho_0 A^a) dV, \qquad (7.18)$$

where N_B are components of the external normal to V along S as introduced in (7.11). Applying (4.4) and (7.17) and considering a body in static equilibrium,

$$\int_V P^{aA} dV = \int_S X^A P^{aB} N_B dS = \int_S t^a_0 X^A dS. \qquad (7.19)$$

For a self-equilibrated body, $t^a_0 = 0$ by definition, and (7.19) reduces to

$$V^{-1}\int_V P^{aA}dV = 0\,,\tag{7.20}$$

meaning that the volume-averaged first Piola-Kirchhoff stress vanishes over the reference volume.

Now consider the spatial balance of linear momentum

$$\sigma^{ab}_{..,b}+\bar{b}^a = \rho a^a\,,\tag{7.21}$$

with $\sigma^{ab}=\det(X^A_{.,a})P^{aA}x^b_{.,A}$ the symmetric local Cauchy stress tensor, $\bar{b}^a$ the body force per current volume, $\rho = \rho_0\det(X^A_{.,a})$ the current mass density, and a^a the spatial acceleration. Spatial analogs of (7.16)-(7.18) are

$$(x^b\sigma^{ac})_{,c}= \sigma^{ab}+(\rho a^a-\bar{b}^a)x^b\,,\tag{7.22}$$

$$\left[\!\left[t^a\right]\!\right]=t^{+a}-t^{-a}=(\sigma^{+ab}-\sigma^{-ab})m_b = 0\,,\text{(on }\sigma\text{)},\tag{7.23}$$

$$\int_v\sigma^{ab}dv = \int_s x^b\sigma^{ac}n_c ds + \int_\sigma x^b(\sigma^{+ac}-\sigma^{-ac})m_c d\sigma + \int_v x^b(\bar{b}^a-\rho a^a)dv\,,\tag{7.24}$$

with $x^a = x^a(X,t)$ spatial coordinates, t^a the traction per unit current area of (4.3), σ the union of internal surfaces across which reference coordinates $X^A(x,t)$ may be discontinuous functions of spatial position and inverse deformation gradient $X^A_{.,a}$ may be singular, m_a the unit normal covector to such surfaces, n_a the unit normal covector to external surface s (Fig. 7.1), and v the spatial volume of the body enclosed by s. For a body in static equilibrium, (7.24) becomes

$$\int_v\sigma^{ab}dv = \int_s x^b\sigma^{ac}n_c ds = \int_s t^a x^b ds\,,\tag{7.25}$$

and for a self-equilibrated body , by definition $t^a = 0$ along s, and hence the average Cauchy stress vanishes by (7.25):

$$v^{-1}\int_v\sigma^{ab}dv = 0\,.\tag{7.26}$$

Relation (7.26) was derived by Toupin and Rivlin (1960) and Hoger (1986) in the context of residually stressed bodies.

7.2.2 Hyperelasticity

In the present treatment, the local, mechanically reversible part of the constitutive response of the material is assumed hyperelastic of grade one, with effects of temperature change neglected. Let $\Psi_0 = \Psi_0(E_{AB})$ denote the strain energy per unit reference volume of the solid, with the symmetric right Cauchy-Green strain of (2.156) in Cartesian coordinates

$$E_{AB} = \frac{1}{2}(x^a_{.,A}\delta_{ab}x^b_{.,B} - \delta_{AB}) = \delta^a_{.A}u_{(a,B)} + \frac{1}{2}u_{c,A}u^c_{.,B}, \qquad (7.27)$$

where $u^a = x^a - \delta^a_{.A}X^A$ is the local displacement of (2.137) when coincident coordinate systems are used in each configuration. Let

$$\Psi_0 = \frac{1}{2}\overline{\mathbb{C}}^{ABCD}E_{AB}E_{CD} + \frac{1}{6}\overline{\mathbb{C}}^{ABCDEF}E_{AB}E_{CD}E_{EF} + ..., \qquad (7.28)$$

where second- and third-order elastic constants are evaluated from a series expansion of the energy density about the unstrained state as in (5.65) and (5.66). The local first Piola-Kirchhoff stress, from (5.45) and (7.28), is computed as

$$
\begin{aligned}
P^{aA} &= \frac{\partial \Psi_0}{\partial x_{a,A}} = x^a_{.,B}\frac{\partial \Psi_0}{\partial E_{BA}} = x^a_{.,B}\frac{\partial \Psi_0}{\partial E_{AB}} \\
&= x^a_{.,B}\left(\overline{\mathbb{C}}^{ABCD}E_{CD} + \frac{1}{2}\overline{\mathbb{C}}^{ABCDEF}E_{CD}E_{EF} + ...\right).
\end{aligned}
\qquad (7.29)
$$

Using symmetry properties in (5.57) and (5.58) and omitting terms of degree higher than three in referential displacement gradient (i.e., distortion) $u_{A,B} = \delta^b_{.A}u_{b,B}$, strain energy function (7.29) can be written (Toupin and Rivlin 1960)

$$\Psi_0 = \frac{1}{2}\overline{\mathbb{C}}^{ABCD}u_{A,B}u_{C,D} + \frac{1}{2}\overline{\mathbb{C}}^{ABCD}u_{A,B}u_{E,C}u^E_{.,D} + \frac{1}{6}\overline{\mathbb{C}}^{ABCDEF}u_{A,B}u_{C,D}u_{E,F}. \quad (7.30)$$

7.2.3 Average Residual Elastic Strain

Consider the externally unloaded configuration of the volume element labeled $\overline{B}$ in Fig. 7.1. This configuration corresponds to the deformed but self-equilibrated body obeying (7.20) and (7.26). The reference configuration with internal displacement discontinuities described in (7.2)-(7.4) now corresponds to stress-free intermediate configuration $\tilde{B}$ of Fig. 7.1. As discussed in detail in Section C.1 of Appendix C and noted by De Wit (1973), displacement discontinuities attributed to Volterra dislocations lead to discontinuities or singularities in local plastic strain and rotation fields across the slip planes or internal surfaces Σ within the volume, which owing to the isochoric nature of slip, is preserved via $\tilde{V} = J^P V = V$. Such effects are quantified according to (3.85)-(3.90) and (7.2)-(7.4), wherein discontinuities or singularities are introduced by plastic deformation $\mathbf{F}^P$ between configurations B_0 and $\tilde{B}$. Residual deformations are introduced within the element from the mapping between configurations $\tilde{B}$

and $\bar{B}$. Locally[1], such deformations are treated as differentiable and elastic between $\tilde{B}$ and $\bar{B}$, with corresponding local displacement gradient and Lagrangian strain fields (i.e., eigenstrains) within the element denoted by $u_{A,B}$ and E_{AB}, respectively.

The corresponding definition for the average residual elastic deformation gradient entering (7.12) and (7.14) is, in Cartesian coordinates (Clayton and Bammann 2009)

$$F^I{}_{AB} = V^{-1} \int_V x_{(A,B)} dV = \delta_{AB} + V^{-1} \int_V u_{(A,B)} dV . \qquad (7.31)$$

Singular surfaces Σ and singular lines (e.g., defect cores) are excluded from the domain of integration V in (7.31). Contributions to **F** from singular surfaces (e.g., plastic slip) are incorporated via plastic deformation map $\mathbf{F}^P$, not $\mathbf{F}^I$. Relation (7.31) is a key definition used often later. In generalized coordinates,

$$\mathbf{F}^I = F^I{}_{AB}\mathbf{G}^A \otimes \mathbf{G}^B = F^I{}_{AB}(g^{A\alpha}\tilde{\mathbf{g}}_\alpha \otimes g^B_{.\beta}\tilde{\mathbf{g}}^\beta) = F^I{}_{.\beta}{}^\alpha\tilde{\mathbf{g}}_\alpha \otimes \tilde{\mathbf{g}}^\beta . \qquad (7.32)$$

Mapping self-equilibrium conditions (7.26) to the reference configuration and substituting from (7.29),

$$\delta^A_{.a}\delta^B_{.b}\int_v \sigma^{ab} dv = \delta^A_{.a}\delta^B_{.b}\int_V x^b_{.,C} P^{aC} dV = \int_V (\delta^B_{.C} + u^B_{.,C})\frac{\partial \Psi_0}{\partial u_{A,C}} dV = 0 . \qquad (7.33)$$

The integral on the right side of (7.33) becomes, upon substitution of (7.30) and omission of terms higher than second order in displacement gradients in the expression for the stress,

$$0 = \int_V (\delta^B_{.C} + u^B_{.,C})\frac{\partial \Psi_0}{\partial u_{A,C}} dV = \int_V \overline{\mathbb{C}}^{ABCD} u_{C,D} dV$$

$$+ \int_V (\overline{\mathbb{C}}^{AECD} u^B_{.,E} + \overline{\mathbb{C}}^{BECD} u^A_{.,E}) u_{C,D} dV \qquad (7.34)$$

$$+ \frac{1}{2}\int_V \overline{\mathbb{C}}^{ABCD} u_{E,C} u^E_{.,D} dV + \frac{1}{2}\int_V \overline{\mathbb{C}}^{ABCDEF} u_{C,D} u_{E,F} dV.$$

When products of order two in displacement gradients are omitted, as would be the case for a linear elastic body with spatially constant moduli, (7.34) reduces to

$$\overline{\mathbb{C}}^{ABCD} \int_V u_{C,D} dV = 0 \Rightarrow \int_V u_{(C,D)} dV = 0 \Rightarrow F^I{}_{CD} = \delta_{CD} \qquad (7.35)$$

---

[1] In configuration $\tilde{B}$, if defects are envisioned within the element, $u_A(X,t)$ is a discontinuous function of position X across singular surfaces, and hence $u_{A,B}$ is singular along such surfaces (recall Fig. 3.11). Thus u_A is globally discontinuous.

since $\overline{\mathbb{C}}^{ABCD}$ is assumed positive definite. The linear elastic approximation (7.35) states that no average elastic shape or volume change occurs in a self-equilibrated body with homogeneous elastic properties. The latter would be true even if the local elastic dilatation from defects does not vanish, as is exhibited in straight line edge dislocation and wedge and twist disclination solutions in (C.35), (C.107), and (C.140) for linear elastic isotropic bodies.

On the other hand, for a nonlinear elastic body with spatially constant moduli, components of the integrated symmetric displacement gradient are given by the six independent integral equations

$$
\overline{\mathbb{C}}^{ABCD}\int_V u_{(C,D)}dV = -\overline{\mathbb{C}}^{AECD}\int_V u^B_{,E}u_{C,D}dV - \overline{\mathbb{C}}^{BECD}\int_V u^A_{,E}u_{C,D}dV
$$
$$
-\frac{1}{2}\overline{\mathbb{C}}^{ABCD}\int_V u_{E,C}u^E_{,D}dV - \frac{1}{2}\overline{\mathbb{C}}^{ABCDEF}\int_V u_{C,D}u_{E,F}dV. \tag{7.36}
$$

Hence, from (7.31) and (7.36), components of $\mathbf{F}^I$ may be non-negligible:

$$
F^I_{\,MN} = \delta_{MN} - V^{-1}\overline{S}_{MNAB}\left[\overline{\mathbb{C}}^{AECD}\int_V u^B_{,E}u_{C,D}dV + \overline{\mathbb{C}}^{BECD}\int_V u^A_{,E}u_{C,D}dV\right.
$$
$$
\left. +\frac{1}{2}\overline{\mathbb{C}}^{ABCD}\int_V u_{E,C}u^E_{,D}dV + \frac{1}{2}\overline{\mathbb{C}}^{ABCDEF}\int_V u_{C,D}u_{E,F}dV\right]. \tag{7.37}
$$

The rank four compliance constants at the reference state, $\overline{S}_{MNAB}$ in (7.37), satisfy conditions listed in (5.149):

$$
2\overline{\mathbb{C}}^{CDAB}\overline{S}_{ABMN} = \delta^C_{.M}\delta^D_{.N} + \delta^D_{.M}\delta^C_{.N}. \tag{7.38}
$$

By introducing the quantity

$$
\hat{\mathbb{C}}^{CDABEF} = \overline{\mathbb{C}}^{AFCD}\delta^{BE} + \overline{\mathbb{C}}^{BFCD}\delta^{AE} + \overline{\mathbb{C}}^{EFAD}\delta^{BC}
$$
$$
+ \overline{\mathbb{C}}^{EFBD}\delta^{AC} + \overline{\mathbb{C}}^{ABFD}\delta^{CE} + \overline{\mathbb{C}}^{ABED}\delta^{CF} \tag{7.39}
$$
$$
- \overline{\mathbb{C}}^{ABCD}\delta^{EF} - \overline{\mathbb{C}}^{ABEF}\delta^{CD} + \overline{\mathbb{C}}^{ABCDEF},
$$

integral equations (7.36) and (7.37) are written more compactly as (Toupin and Rivlin 1960)

$$
\overline{\mathbb{C}}^{ABCD}\int_V u_{(C,D)}dV = \frac{1}{2}\overline{\mathbb{C}}^{ABCD}\int_V u_{C,E}u^E_{,D}dV - \overline{\mathbb{C}}^{ABCD}\int_V u^E_{,E}u_{C,D}dV
$$
$$
-\frac{1}{2}\hat{\mathbb{C}}^{CDABEF}\int_V u_{C,D}u_{E,F}dV, \tag{7.40}
$$

$$F^I{}_{MN} = \delta_{MN} + V^{-1}\overline{\mathrm{S}}_{MNAB}\left[\frac{1}{2}\overline{\mathbb{C}}^{ABCD}\int_V u_{C,E}u^E_{,D}dV\right.$$

$$\left.-\overline{\mathbb{C}}^{ABCD}\int_V u^E_{,E}u_{C,D}dV - \frac{1}{2}\hat{\mathbb{C}}^{CDABEF}\int_V u_{C,D}u_{E,F}dV\right]. \tag{7.41}$$

Notice from (7.37) and (7.41) that both geometric nonlinearity (i.e., quadratic terms in displacement gradients) and material nonlinearity (i.e., third-order elastic constants) contribute to $\mathbf{F}^I$, and that $\mathbf{F}^I$ does not necessarily reduce to the unit tensor when third-order elastic constants vanish. If the strain energy density in (7.30) is extended to incorporate products of displacement gradients of order higher than three, e.g., fourth-order elastic constants such as those in (5.67), then effects of these higher-order terms will likewise enter the right sides of (7.37) and (7.41). When elastic moduli are not spatially constant, for example in a multi-phase composite or body with foreign inclusions, (7.37) and (7.41) do not strictly apply since in that case elastic coefficients cannot be brought outside the volume integrals. If V is the initial volume of a polycrystal with randomly oriented grains, then uniform isotropic elastic properties (i.e., effective moduli) can be assigned to the volume element as an approximation. According to (7.27)-(7.30), when the (residual) displacement gradient $u_{A,B}$ vanishes at a material point, strain E_{AB} and (residual) stress vanish at that point. In an isotropic homogeneous elastic body that is regular (i.e., no defects or discontinuities in displacements and displacement gradients), local residual stress must vanish everywhere (Hoger 1985), regardless of the particular form of the strain energy function.

Because the average residual elastic deformation results from nonlinear elastic effects, i.e., products of displacement gradients of order two in (7.37) and (7.41), the contribution of the average residual elastic deformation $\mathbf{F}^I$ to the total deformation gradient $\mathbf{F}$ of (7.12) will generally be small in conventional engineering applications wherein defect densities are low to moderate. For example, linear elasticity theory is generally deemed valid beyond some cut-off distance on the order of one to ten lattice parameters from the dislocation core (Teodosiu 1982; Hull and Bacon 1984), beyond which magnitudes of elastic displacement gradients are small, say $\|u_{A,B}\| \lesssim 0.1$, so that contributions from such linear-elastic regions to terms in braces in (7.41) will be small. Contrarily, for materials with very large dislocation densities in which core regions comprise a substantial fraction of the volume element, nonlinear elastic contributions could be substantial, in which case the difference $\mathbf{F}^I - \mathbf{1}$ would be non-negligible. The contri-

bution of tensile volumetric and deviatoric parts of local elastic displacement gradients to $\mathbf{F}^I$ would also be limited by the theoretical strength of the crystal, typically on the order of 10% of an elastic shear modulus (see (C.209) of Section C.4.1), since the material would tend to fracture at elastic strains producing tensile or shear stresses in excess of the theoretical strength. On the other hand, large elastic volumetric compressions are usually sustainable in crystals, as noted in Section 5.3. The effect of residual elasticity would be greatest in materials whose third-order elastic constants are substantially larger than second-order constants; in some crystalline solids, representative third-order constants can exceed second-order constants by an order of magnitude or more (Teodosiu 1982).

7.2.4 Residual Elastic Volume Changes

Now consider the average volume change of the body resulting from the field of local residual elastic distortion $u_{A,B}$. The preceding derivations (and those that follow in Section 7.2.4) apply regardless of whether or not the average shape change resulting from $u_{A,B}$ vanishes. However, for a crystal containing a large number of randomly oriented defects (e.g., dislocation and disclination lines and loops), it may be reasonable to assume that the change in dimensions of the crystal imparted by local stress fields of defects exhibits no preferred directions, implying that the crystal undergoes only a volume change and no shape change (Clayton 2009a, c). The average residual elastic volume change is also of perhaps greater interest than the shape change because the former can be easily measured experimentally for plastically deformed crystals, with results then available to validate the theory. The residual elastic deviatoric shape change, on the other hand, cannot be obtained simply from the deformed shape of a sample of material since the residual elastic shape change cannot be easily delineated from the shape change resulting from dislocation glide.

The change in a differential volume of a body in coincident spatial and reference coordinate systems is given by (2.147):

$$dv/dV = \det(\delta^A_{.B} + u^A_{.,B}) = \frac{1}{6}\left[(x^A_{.,A})^3 - 3x^A_{.,A}x^B_{.,C}x^C_{.,B} + 2x^B_{.,C}x^C_{.,A}x^A_{.,B}\right]$$
$$\approx 1 + u^A_{.,A} + \frac{1}{2}(u^A_{.,A})^2 - \frac{1}{2}u^A_{.,B}u^B_{.,A}, \tag{7.42}$$

where products of order three in referential displacement gradients are omitted in the final expression. In the context of Fig. 7.1, dv is the volume of a differential sub-element of the body in configuration $\bar{B}$, and

dV is the volume of that sub-element in $\tilde{B}$. Integrating (7.42), a second-order accurate measure of the net volume change attributed to residual elastic deformation within the crystal is

$$\Delta V = v - V = \int_V u^A_{,A} dV + \frac{1}{2} \int_V \left[(u^A_{,A})^2 - u^A_{,B} u^B_{,A} \right] dV \; . \tag{7.43}$$

Right sides of (7.37), (7.41), and (7.43) depend on the local residual elastic displacement gradient fields in the body. For crystals of high symmetry, these relations can be further reduced by appealing to particular forms of the elastic coefficients. Specifically, for cubic crystal systems of the highest symmetry (Laue group CI of Table A.1 in Appendix A), the second-order moduli consist of three independent coefficients and the third-order moduli of six independent coefficients, as is clear from Tables A.8 and A.9, respectively. Consider a coordinate system with axes parallel to the cube axes of the crystal. In Voigt's notation (A.10), pairs of indices $11 \rightarrow 1$, $22 \rightarrow 2$, $33 \rightarrow 3$, $23 \rightarrow 4$, $13 \rightarrow 5$, $12 \rightarrow 6$, $2E_{AB} \rightarrow E_{\bar{A}}(1 + \delta_{AB})$, barred indices span $\bar{A} = 1, 2, ..., 6$, and nonzero second-order elastic constants of a cubic crystal are

$$\overline{\mathbb{C}}^{11} = \overline{\mathbb{C}}^{22} = \overline{\mathbb{C}}^{33},$$
$$\overline{\mathbb{C}}^{12} = \overline{\mathbb{C}}^{13} = \overline{\mathbb{C}}^{23}, \tag{7.44}$$
$$\overline{\mathbb{C}}^{44} = \overline{\mathbb{C}}^{55} = \overline{\mathbb{C}}^{66}.$$

Nonzero third-order constants of a cubic crystal of Laue group CI are

$$\overline{\mathbb{C}}^{111} = \overline{\mathbb{C}}^{222} = \overline{\mathbb{C}}^{333}, \qquad\qquad \overline{\mathbb{C}}^{144} = \overline{\mathbb{C}}^{255} = \overline{\mathbb{C}}^{366},$$
$$\overline{\mathbb{C}}^{112} = \overline{\mathbb{C}}^{113} = \overline{\mathbb{C}}^{122} = \overline{\mathbb{C}}^{223} = \overline{\mathbb{C}}^{133} = \overline{\mathbb{C}}^{233}, \qquad \overline{\mathbb{C}}^{123}, \tag{7.45}$$
$$\overline{\mathbb{C}}^{155} = \overline{\mathbb{C}}^{166} = \overline{\mathbb{C}}^{244} = \overline{\mathbb{C}}^{266} = \overline{\mathbb{C}}^{344} = \overline{\mathbb{C}}^{355}, \qquad \overline{\mathbb{C}}^{456}.$$

The following notation is common, as indicated in (A.17) and (A.19) of Appendix A:

$$3K = \overline{\mathbb{C}}^{11} + 2\overline{\mathbb{C}}^{12},$$
$$2\mu = \overline{\mathbb{C}}^{11} - \overline{\mathbb{C}}^{12}, \tag{7.46}$$
$$2\mu' = 2\overline{\mathbb{C}}^{44} - (\overline{\mathbb{C}}^{11} - \overline{\mathbb{C}}^{12}),$$

where K is the bulk modulus at the reference state and μ and μ' are shear moduli at the reference state. In a cubic crystal, the first term on the right side of strain energy function (7.30) can be written by linearizing (A.17), i.e., replacing the right Cauchy-Green strain in (A.17) with the symmetric part of the displacement gradient (Toupin and Rivlin 1960):

$$W = \frac{1}{2}\overline{\mathbb{C}}^{ABCD}u_{A,B}u_{C,D}$$

$$= \frac{1}{2}K(u^A_{,A})^2 + \mu\left[\frac{1}{2}(u^A_{,B}u^B_{,A} + u^A_{,B}u^{,B}_A) - \frac{1}{3}(u^A_{,A})^2\right]$$

$$+ \mu'\left[\frac{1}{2}(u^A_{,B}u^B_{,A} + u^A_{,B}u^{,B}_A) - (u^1_{,1})^2 - (u^2_{,2})^2 - (u^3_{,3})^2\right]$$

$$= W_D + W_S + W'_S,$$

(7.47)

where W_D is the strain energy of dilatation and W_S and W'_S result from elastic shape changes. In an isotropic material such as a polycrystal with no preferred orientations, the number of constants in (7.44) is further reduced to two according to Table A.8 as

$$2\overline{\mathbb{C}}^{44} = \overline{\mathbb{C}}^{11} - \overline{\mathbb{C}}^{12},$$

(7.48)

and in (7.45) reduced to three according to Table A.9 as

$$2\overline{\mathbb{C}}^{144} = \overline{\mathbb{C}}^{112} - \overline{\mathbb{C}}^{123},\quad 4\overline{\mathbb{C}}^{155} = \overline{\mathbb{C}}^{111} - \overline{\mathbb{C}}^{112},$$

$$8\overline{\mathbb{C}}^{456} = \overline{\mathbb{C}}^{111} - 3\overline{\mathbb{C}}^{112} + 2\overline{\mathbb{C}}^{123}.$$

(7.49)

Thus for isotropy, coefficients K and μ of (7.46) and energy densities W_D and W_S of (7.47) are identical, but $\mu' = 0$ in (7.46) and $W'_S = 0$ in (7.47).

Summation over the first two indices of (7.36) and using the first of (7.47) results in the integral equation

$$\overline{\mathbb{C}}^{A.CD}_{.A}\int_V u_{(C,D)}dV = -4\int_V WdV - \frac{1}{2}\overline{\mathbb{C}}^{A.CD}_{.A}\int_V u_{E,C}u^E_{,D}dV$$

$$- \frac{1}{2}\overline{\mathbb{C}}^{A.CDEF}_A\int_V u_{C,D}u_{E,F}dV.$$

(7.50)

Appealing to (7.40),

$$\overline{\mathbb{C}}^{A.CD}_{.A}\int_V u_{(C,D)}dV = -3\int_V WdV + \frac{1}{2}\overline{\mathbb{C}}^{A.CD}_{.A}\int_V (u_{C,E}u^E_{,D} - u_{C,D}u^E_{,E})dV$$

$$- \frac{1}{2}\hat{\mathbb{C}}^{A.CDEF}_A\int_V u_{C,D}u_{E,F}dV.$$

(7.51)

For a cubic crystal satisfying (7.44)-(7.46), equality (7.51) reduces to

$$3K\int_V u^D_{,D}dV = -3\int_V WdV - \frac{3}{2}K\int_V \left[(u^A_{,A})^2 - u^A_{,B}u^B_{,A}\right]dV$$

$$- \frac{1}{2}\hat{\mathbb{C}}^{A.CDEF}_A\int_V u_{C,D}u_{E,F}dV.$$

(7.52)

Then from (7.43), the net volume change for the element of reference volume V is

$$\Delta V = -\frac{1}{K}\int_V WdV - \frac{1}{6K}\hat{\mathbb{C}}_A^{A.CDEF}\int_V u_{C,D}u_{E,F}dV. \tag{7.53}$$

Letting $j = \det(x^a_{.A})$, where $j > 0$, the rightmost term of (7.53) can be written for a cubic crystal that remains cubic during deformation as (Toupin and Rivlin 1960)

$$\frac{1}{6}\hat{\mathbb{C}}_A^{A.CDEF}\int_V u_{C,D}u_{E,F}dV$$

$$= \frac{j}{K}\frac{\partial\overline{K}}{\partial j}\int_V W_D dV + \frac{j}{\mu}\frac{\partial\overline{\mu}}{\partial j}\int_V W_S dV + \frac{j}{\mu'}\frac{\partial\overline{\mu}'}{\partial j}\int_V W'_S dV \tag{7.54}$$

$$= \frac{\partial\ln\overline{K}}{\partial\ln j}\int_V W_D dV + \frac{\partial\ln\overline{\mu}}{\partial\ln j}\int_V W_S dV + \frac{\partial\ln\overline{\mu}'}{\partial\ln j}\int_V W'_S dV,$$

where $\overline{K}$, $\overline{\mu}$, and $\overline{\mu}'$ are tangent elastic coefficients for a cubic crystal with respective constant values K, μ, and μ' in the reference state. Volume derivatives of elastic coefficients are evaluated at the reference state in the last of (7.54). Following (5.188)-(5.193) and (5.205),

$$\frac{\partial(.)}{\partial j} = \frac{\partial p}{\partial j}\frac{\partial(.)}{\partial p} = -\frac{K}{j}\frac{\partial(.)}{\partial p}, \tag{7.55}$$

where $p = -\sigma^a_{.a}/3$ is the Cauchy pressure. Substituting (7.47) and (7.54)-(7.55) into (7.53), the residual volume change is

$$\Delta V = \frac{1}{K}\left[\left(\frac{\partial\overline{K}}{\partial p} - 1\right)\int_V W_D dV + \left(\frac{K}{\mu}\frac{\partial\overline{\mu}}{\partial p} - 1\right)\int_V W_S dV\right.$$

$$\left. + \left(\frac{K}{\mu'}\frac{\partial\overline{\mu}'}{\partial p} - 1\right)\int_V W'_S dV\right], \tag{7.56}$$

where derivatives with respect to pressure of $\overline{K}$, $\overline{\mu}$, and $\overline{\mu}'$ are evaluated at a stress-free reference state. In particular, recall that the pressure derivative of the bulk modulus can be estimated from the Gruneisen parameter using (5.237). After defining average strain energies on a per unit reference volume basis as

$$\overline{W}_D = V^{-1}\int_V W_D dV, \quad \overline{W}_S = V^{-1}\int_V W_S dV, \quad \overline{W}'_S = V^{-1}\int_V W'_S dV, \tag{7.57}$$

and the quantity

$$\overline{J} = 1 + \frac{\Delta V}{V} = \frac{v}{V}, \tag{7.58}$$

the normalized volume change for a self-equilibrated, cubic nonlinear elastic solid of grade one is

$$\bar{J} = 1 + \frac{1}{K}\left[\left(\frac{\partial K}{\partial p} - 1\right)\bar{W}_D + \left(\frac{K}{\mu}\frac{\partial \mu}{\partial p} - 1\right)\bar{W}_S\right.$$

$$\left. + \left(\frac{K}{\mu'}\frac{\partial \mu'}{\partial p} - 1\right)\bar{W}_S'\right]$$

$$= 1 + \left[\left(\frac{\partial \ln K}{\partial p} - \frac{1}{K}\right)\bar{W}_D + \left(\frac{\partial \ln \mu}{\partial p} - \frac{1}{K}\right)\bar{W}_S\right.$$

$$\left. + \left(\frac{\partial \ln \mu'}{\partial p} - \frac{1}{K}\right)\bar{W}'\right].$$

(7.59)

In (7.59) and henceforward, over-bars on tangent elastic coefficients are dropped, and it is understood that all elastic constants and their pressure derivatives are evaluated at the reference state. If the cubic second-order elastic coefficients, their pressure derivatives, and each of the average strain energy densities of (7.57) are known, the volumetric deformation can be computed from (7.59). So long as strain energy densities in (7.57) are always positive, if coefficients of the energy densities in (7.59) are all of the same algebraic sign, then the overall volume change will be of that sign. If only the total strain energy density $\bar{W} = \bar{W}_D + \bar{W}_S + \bar{W}_S'$ is known, for example from experiments (Clarebrough et al. 1957; Wright 1982), then (7.47) and (7.59) can be combined to establish bounds on the normalized volume change (Toupin and Rivlin 1960). Bounds of this sort have been validated by experimental data for several polycrystalline cubic metals (Wright 1982), wherein the volume changes induced by defects such as dislocations and stacking faults were always found to be positive by theory and experiment.

For an isotropic solid, (7.59) reduces to

$$\bar{J} = 1 + \frac{1}{K}\left(\frac{\partial K}{\partial p} - 1\right)\bar{W}_D + \frac{1}{\mu}\left(\frac{\partial \mu}{\partial p} - \frac{\mu}{K}\right)\bar{W}_S$$

$$= 1 + \left(\frac{\partial \ln K}{\partial p} - \frac{1}{K}\right)\bar{W}_D + \left(\frac{\partial \ln \mu}{\partial p} - \frac{1}{K}\right)\bar{W}_S.$$

(7.60)

In an isotropic body, pressure derivatives of tangent bulk and shear moduli K and μ are related to third-order elastic constants in (A.26).

Formula (7.59) for cubic crystals is attributed to Toupin and Rivlin (1960), while (7.60) was developed earlier by Zener (1942) using nonlinear isotropic elasticity and thermodynamic arguments. Isotropic formula (7.60) for the case when the dilatational energy vanishes agrees with that of Holder and Granato (1969) obtained from thermodynamic arguments:

$$\frac{\Delta V}{V} = \frac{\partial G_e(p,\theta)}{\partial p} = \frac{1}{\mu_e}\left(\frac{\partial \mu_e}{\partial p} - \frac{\mu_e}{K}\right)G_e = \frac{1}{\mu_e}\left(\frac{\partial \mu_e}{\partial p} - \frac{\mu_e}{K}\right)E\rho_{T0}, \quad (7.61)$$

where G_e is the Gibbs free energy change from defects, per unit reference volume that depends on pressure p and temperature θ, and μ_e is an effective elastic coefficient that depends upon the mathematical form of the strain energy of the particular defect. In the final term of (7.61), E is the elastic strain energy per unit length of the defect and ρ_{T0} is the total length per unit reference volume of the defect. For a number of kinds of crystals, Holder and Granato (1969) found that delineation between dilatational and deviatoric energies and incorporation of effects of cubic anisotropy had little influence on volume changes from straight dislocations predicted using (7.61).

The source of the local displacement gradient and residual strain energy in the body to this point has been arbitrary, so long as (7.23), (7.26), and (7.30) apply, that is, traction is continuous across internal surfaces, the body is self-equilibrated, and the local constitutive response is described by hyperelasticity with terms of order higher than three in referential displacement gradients omitted in the strain energy. Defects induce such displacement gradients and residual strain energies. These may include, for example, dislocation and disclination lines and loops, stacking faults, grain boundaries, twin boundaries, and slip bands. Volume changes attributed to point defects (e.g., substitutional atoms, interstitials, and vacancies), phase transformations, voids, and open cracks are not considered in the present treatment, since dimensional changes computed according to the present theory account only for volume and shape changes resulting from stress fields of defects and not volume and shape changes associated with defects themselves. However, the additional volume change induced by a point defect—for example the volume change in addition to the misfit dilatation in a sphere-in-hole model—attributed to elastic nonlinearity can be estimated from (7.61) for an isotropic elastic body (Eshelby 1954; Holder and Granato 1969), as illustrated later in Section 7.4. Anisotropy cannot be directly addressed in (7.59) when tangent elastic moduli may change with position, for example grain boundaries and twin boundaries across which lattice orientations may differ. However, isotropic approximation (7.60) could still be used as an estimate in these cases, as in previous applications towards polycrystals (Seeger and Haasen 1958) and single crystals of lower symmetry (Clayton 2009a). The isotropic approach is further developed for line defects in Sections 7.2.5 and 7.2.7.

Also neglected in the foregoing continuum elastic analysis are explicit effects of defect cores on the residual deformation of the body. For exam-

ple, elastic strain, stress, and strain energies imparted by Volterra line de-
fects diverge as the radial distance from the line shrinks to zero, as is clear
from linear elastic solutions given in Sections C.1 and C.2, and even
nonlinear elasticity is inadequate for describing non-convex energy distri-
butions imparted by highly distorted crystal structures within defect cores.
In the present continuum treatment, one can imagine each defect line to be
surrounded by a traction-free cylindrical boundary delineating the core re-
gion from the surrounding elastic continuum of reference volume V. In
linear elasticity, stresses and strains resulting from traction acting on the
cylindrical boundary of the core decay as R^{-3}, where R is the distance
from the defect line, and hence are usually neglected (Teodosiu 1982).
The elastic continuum is thus self-equilibrated in this approximation, and
(7.26) applies.

7.2.5 Straight Edge and Screw Dislocations

Consider volume changes imparted by dislocation lines in the isotropic ap-
proximation. The energy per unit length (linear elastic energy plus core
and interaction energies) of a straight dislocation embedded in an infinite
isotropic medium, with elastic energies given in (C.48) and (C.69), is

$$E = \frac{\mu b^2}{4\pi k} \ln\left(\frac{R}{R_C}\right) + \hat{E} , \quad k = \begin{cases} 1-\nu & \text{(edge dislocation)} \\ 1 & \text{(screw dislocation)} \end{cases} \quad (7.62)$$

where b is the magnitude of the Burgers vector that is treated as a constant,
$\nu = (3K - 2\mu)/(6K + 2\mu)$ is Poisson's ratio (see Table A.10), R is the ra-
dial distance from the dislocation core, R_C is the radius of the dislocation
core, and $\hat{E}$ is a correction to the linear elastic solutions that accounts for
core energy, line curvature, interaction energies from other defects and
boundaries, and stacking faults associated with partial dislocations.

Denoted by $E^E = E - \hat{E}$ is the elastic strain energy density per unit line
length L of straight, non-interacting edge dislocations, separated into di-
latational and shear contributions as in (C.49) and (C.50):

$$E_D^E = \frac{\mu b^2}{12\pi} \frac{1 - \nu - 2\nu^2}{(1-\nu)^2} \ln\left(\frac{R}{R_C}\right), \quad E_S^E = \frac{\mu b^2}{12\pi} \frac{2 - 2\nu + 2\nu^2}{(1-\nu)^2} \ln\left(\frac{R}{R_C}\right), \quad (7.63)$$

where superscript E refers to an edge dislocation. Relating energies per
unit reference volume to energies per unit length using the equalities

$$\bar{W}_D V = E_D^E L , \quad \bar{W}_S V = E_S^E L , \quad (7.64)$$

and multiplying (7.60) by V/L, the volume change per unit length of edge
dislocation line is (Seeger and Haasen 1958; Teodosiu 1982)

$$\left.\frac{\Delta V}{L}\right|_{Edge} = \frac{1}{K}\left(\frac{\partial K}{\partial p}-1\right)E_D^E + \frac{1}{\mu}\left(\frac{\partial \mu}{\partial p}-\frac{\mu}{K}\right)E_S^E$$

$$= \frac{E^E}{3}\left[\frac{1-\nu-2\nu^2}{(1-\nu)K}\left(\frac{\partial K}{\partial p}-1\right)+\frac{2-2\nu+2\nu^2}{(1-\nu)\mu}\left(\frac{\partial \mu}{\partial p}-\frac{\mu}{K}\right)\right], \tag{7.65}$$

where $E^E = E_D^E + E_S^E$ is the total elastic line energy of an edge dislocation.

Analogously, denote by $E^S = E - \hat{E}$ the strain energy per unit line length L of straight, non-interacting screw dislocations, partitioned as in (C.68) and (C.69):

$$E_D^S = 0, \quad E_S^S = \frac{\mu b^2}{4\pi}\ln\left(\frac{R}{R_C}\right), \tag{7.66}$$

Setting the deviatoric energy in the second of (7.57) equal to the product of the line length and energy per unit length (7.66) gives

$$\overline{W}_S V = E_S^S L = E^S L, \tag{7.67}$$

where E^S is the total elastic line energy of a screw dislocation. Multiplying (7.60) by V/L, the volume change per unit length of straight screw dislocation lines is (Seeger and Haasen 1958; Teodosiu 1982)

$$\left.\frac{\Delta V}{L}\right|_{Screw} = \frac{E^S}{\mu}\left(\frac{\partial \mu}{\partial p}-\frac{\mu}{K}\right). \tag{7.68}$$

Now let the total dislocation line density per unit reference volume be given by the sum

$$\rho_{T0} = L/V = \rho_{E0} + \rho_{S0}, \tag{7.69}$$

where now L is the total length of edge and screw dislocations in volume V, ρ_{E0} is the density of edge dislocations, and ρ_{S0} is the density of screw dislocations, both measured per unit reference volume. Define from (7.62) an energy per unit length

$$E_T = kE^E = E^S = \frac{\mu b^2}{4\pi}\ln\left(\frac{R}{R_C}\right), \tag{7.70}$$

and let $\chi = \rho_{E0}/\rho_{T0}$ be the fraction of pure edge dislocations in the total dislocation density. Superposing volume changes from (7.65) and (7.68) and using (7.58), (7.60) becomes

$$\bar{J} = 1 + \rho_{E0} \left. \frac{\Delta V}{L} \right|_{Edge} + \rho_{S0} \left. \frac{\Delta V}{L} \right|_{Screw}$$

$$= 1 + \left\{ \frac{\chi}{3k} \left[\frac{1-\nu-2\nu^2}{(1-\nu)K} \left(\frac{\partial K}{\partial p} - 1 \right) + \frac{2-2\nu+2\nu^2}{(1-\nu)\mu} \left(\frac{\partial \mu}{\partial p} - \frac{\mu}{K} \right) \right] \right.$$

$$\left. + \frac{1-\chi}{\mu} \left(\frac{\partial \mu}{\partial p} - \frac{\mu}{K} \right) \right\} E_T \rho_{T0}. \qquad (7.71)$$

Relation (7.71) yields the volume change associated with straight, non-interacting pure screw and edge dislocation lines in an isotropic body with homogeneous elastic properties. While terms in braces in (7.71) include nonlinear elastic effects (i.e., pressure derivatives of the elastic moduli or third-order elastic constants), dislocation line energy E_T does not account explicitly for nonlinearity or energy of dislocation cores. Thus, (7.71) represents the product of third-order nonlinear elasticity (terms in braces) and linear elasticity (defect energy E_T). Products of purely linear elastic origin would yield null volume change, as implied by (7.35), while higher-order products of nonlinear origin (e.g., products of pressure derivatives of moduli with contributions of nonlinear elasticity to dislocation energies) are neglected. Relation (7.71) can be used directly to estimate the volume change of a (poly)crystal if line densities of edge and screw dislocations, their energies per unit length, and the requisite elastic constants are known.

The preceding analysis assumes that defect densities are negligible in the reference configuration. When dislocation densities are substantial in the initial state, the predicted volume change between initial and final configurations corresponds only to the change in defect density that occurs during deformation between initial and final states, rather than that associated with the absolute density of dislocations. Viewed another way, if the absolute defect density is used in the calculation, then the computed volume change will be measured from a stress-free reference configuration B_0 in which the dislocation line density and residual elastic energy vanish.

Dislocation line densities in the preceding developments are defined per unit reference volume $V = \tilde{V}$, equivalent in configurations B_0 and $\tilde{B}$ of Fig. 7.1 because $J^P = 1$. When the dislocation line density is measured in the externally unloaded but internally stressed configuration $\bar{B}$ as $\bar{\rho}_T$, then $\rho_{T0} = \bar{J} \bar{\rho}_T$ in (7.71) such that

$$
\begin{aligned}
\bar{J}^{-1} = 1 - \Bigg\{ &\frac{\chi}{3k}\Bigg[\frac{1-\nu-2\nu^2}{(1-\nu)K}\bigg(\frac{\partial K}{\partial p}-1\bigg) + \frac{2-2\nu+2\nu^2}{(1-\nu)\mu}\bigg(\frac{\partial \mu}{\partial p}-\frac{\mu}{K}\bigg)\Bigg] \\
&+ \frac{1-\chi}{\mu}\bigg(\frac{\partial \mu}{\partial p}-\frac{\mu}{K}\bigg)\Bigg\} E_T \bar{\rho}_T .
\end{aligned}
\tag{7.72}
$$

However, the distinction between configurations used to define the dislocation line density will have a trivial effect on computed values of $\bar{J}$ for small volume changes ($1+\Delta V/V \approx 1/(1-\Delta V/V)$), and in these cases preferential use of (7.72) over (7.71) is probably not justified considering uncertainty in dislocation densities that can be measured experimentally. The elastic dislocation line energy depends on the core radius R_C and the cutoff radius R. A standard approximation, also listed in (6.118), is (Kocks et al. 1975; Hull and Bacon 1984)

$$
E_T = \Lambda\mu b^2 , \; 0.5 \lesssim \Lambda = \frac{1}{4\pi}\ln\bigg(\frac{R}{R_C}\bigg) \lesssim 1.0 .
\tag{7.73}
$$

Introducing the dimensionless quantities

$$
A_E = \frac{E_T \rho_{T0}}{3k}\Bigg[\frac{1-\nu-2\nu^2}{(1-\nu)K}\bigg(\frac{\partial K}{\partial p}-1\bigg) + \frac{2-2\nu+2\nu^2}{(1-\nu)\mu}\bigg(\frac{\partial \mu}{\partial p}-\frac{\mu}{K}\bigg)\Bigg],
\tag{7.74}
$$

$$
A_S = \frac{E_T \rho_{T0}}{\mu}\bigg(\frac{\partial \mu}{\partial p}-\frac{\mu}{K}\bigg),
\tag{7.75}
$$

the volume change in (7.71) becomes

$$
\Delta V/V = \bar{J}-1 = A_E \chi + A_S (1-\chi) .
\tag{7.76}
$$

Thus, $\Delta V/V$ for a mixture of straight, non-interacting edge and screw dislocations will fall between volume change A_E resulting from the same density of pure edge dislocations and volume change A_S resulting from the same density of pure screw dislocations.

7.2.6 Approximate Volume Changes

Returning to the overall dimensional changes of the body induced by averaged local displacement gradients, consider (7.31). Defining the quantities

$$
\bar{\alpha} = V^{-1}\int_V u^A_{,A}dV , \;\; \bar{\beta}^2 = V^{-2}\int_V u^A_{,B}dV \int_V u^B_{,A}dV ,
\tag{7.77}
$$

and, to second-order accuracy in referential displacement gradients, the analog of (7.42) is

$$\det(\mathbf{F^I}) = 1 + \bar{\alpha} + \frac{1}{2}\bar{\alpha}^2 - \frac{1}{2}\bar{\beta}^2 . \tag{7.78}$$

Recall from (7.42) and (7.58) that the true volume change satisfies, to second order in the local distortion,

$$\bar{J} = 1 + \bar{\alpha} + \frac{1}{2}\int_V \left[(u_{,A}^A)^2 - u_{,B}^A u_{,A}^B \right] dV . \tag{7.79}$$

Therefore quantities in (7.78) and (7.79) are related as follows:

$$\bar{J} = \det(\mathbf{F^I}) - \frac{1}{2}(\bar{\alpha}^2 - \bar{\beta}^2) + \frac{1}{2}\int_V \left[(u_{,A}^A)^2 - u_{,B}^A u_{,A}^B \right] dV . \tag{7.80}$$

At least to first-order accuracy in displacement gradients, $\bar{J} = \det(\mathbf{F^I})$. Possible differences between $\bar{J}$ and $\det(\mathbf{F^I})$ may arise because the determinant operation and volume integration do not commute. When products of distortions and their averages are small, $\mathrm{tr}(\mathbf{F^I}) = \bar{\alpha} + 3 \approx \det(\mathbf{F^I}) + 2$ and $\bar{J} \approx \det(\mathbf{F^I})$. Recall from (7.14) and (7.31) that $F^I{}_{AB} = F^I{}_{(AB)}$ as defined in Chapter 7 is a stretch with no rotation. Even though in some cases defects impart no local dilatation in the linear elastic approximation (e.g., Volterra screw dislocations in isotropic solids as in (C.59)), a volume change can still result (e.g., (7.79) with $\bar{J} \neq 1$) because of nonlinear elastic effects.

7.2.7 Examples: Dislocations and Disclinations in Copper

Table 7.1 lists strain energies per unit line length E of a number of defects whose elasticity solutions are described in detail in Appendix C: straight edge and screw dislocations discussed already in Section 7.2.5; circular screw and prismatic dislocation loops; and straight wedge disclinations and circular twist and wedge disclination loops of Frank vector ω. In each case, the core radius, i.e., inner radial coordinate at which the elastic solution is truncated, is labeled R_C. For straight line defects, the radial distance from the core is labeled R; for defect loops, the radius of the circular loop is labeled A, as in Fig. C.3. Energies all correspond to defects in infinitely extended, isotropic linear elastic solids. Analytical formulae for defect line energies follow from references quoted in Table 7.1 and corresponding equations of Appendix C, while normalized volume changes $\Delta V / V \div \rho_{T0} \mathrm{a}^2$ computed for copper follow from (7.65) for edge dislocations and from (7.61) for the other defects, using properties listed in Tables 7.2 and 7.3.

Table 7.1 Line defect energies and residual volume changes in copper

Line defect	Equation in Appendix C	Energy/length E [eV/Å]	Volume change $\Delta V/V \div \rho_{T0}a^2$
Edge dislocation[1] $$E = \frac{\mu b^2}{4\pi(1-\nu)} \ln \frac{R}{R_C}$$	(C.48)	3.30	0.89
Screw dislocation[1] $$E = \frac{\mu b^2}{4\pi} \ln \frac{R}{R_C}$$	(C.67)	2.12	0.51
Screw dislocation loop[2] $$E \approx \frac{\mu b^2}{12\pi(1-\nu)} \times \left[3(1-\nu)\ln \frac{8A}{R_C} - 9 + 10\nu \right]$$	(C.160)	2.00	0.49
Prismatic dislocation loop[2] $$E \approx \frac{\mu b^2}{4\pi(1-\nu)} \left[\ln \frac{8A}{R_C} - 2 \right]$$	(C.162)	3.32	0.81
Wedge disclination[3] $$E = \frac{\mu \omega^2 R^2}{16\pi(1-\nu)} \times \left[1 - \left(\frac{R_C}{R}\right)^2 - 4\left(\frac{R_C}{R}\right)^2 \left(1-\left(\frac{R_C}{R}\right)^2\right)^{-1} \ln^2\left(\frac{R_C}{R}\right) \right]$$	(C.149)	2.65	0.64
Twist disclination loop[3] $$E \approx \frac{\mu \omega^2 R^2}{4\pi} \left[\ln \frac{8A}{R_C} - \frac{8}{3} \right]$$	(C.167)	9.86	2.4
Wedge disclination loop[4] $$E \approx \frac{\mu \omega^2 R^2}{8\pi(1-\nu)} \left[\ln \frac{8A}{R_C} - \frac{8}{3} \right]$$	(C.170)	7.74	1.9
Experiment[5]	-	-	0.8-1.1

[1] Hirth and Lothe (1982)
[2] Owen and Mura (1967)
[3] Huang and Mura (1970)
[4] Liu and Li (1971); Kuo and Mura (1972)
[5] Clarebrough et al. (1957)

Table 7.2 Properties for line defects in copper

a [Å][1]	b [Å]	ω^*	A [Å]	R_C [Å]	R/R_C, A/R_C[**]	R/R_C, A/R_C[***]
3.62	2.56	$\pi/2$	10.0	10.0	10^6	10

[1]Rounded up from 3.61496 Å at a temperature of 291 K (Wyckoff 1963)
[*]Full disclination in cubic crystal (Li 1972)
[**]Dislocation lines and loops
[***] Disclination lines and loops

Table 7.3 Elastic properties for polycrystalline copper [1]

μ [GPa]	K [GPa]	ν	$\partial\mu/\partial p$	$\partial K/\partial p$
47	152	0.36	0.8	4.4

[1] Seeger and Haasen (1958)

For defects besides edge dislocations, the strain energy density is treated as deviatoric, leading to the linear relationship between volume change and defect density given in (7.61). This is a rigorous assertion for screw dislocation loops and twist disclination loops but not for prismatic loops or wedge disclinations, though it has been used elsewhere for these defects (Li and Gilman 1970; Liu and Li 1971) and should provide a reasonable approximation to volume change predictions for many metals (Holder and Granato 1969), including Cu. Again, ρ_{T0} is the line length per unit reference volume of the defect, and a is the lattice parameter of the conventional FCC unit cell in a perfect crystal at room temperature, as defined generically in (3.2). The magnitude of the Burgers vector, treated as a constant, is $b = a\sqrt{2}/2$ from Table 3.4. Experimental results for polycrystalline Cu are provided for comparison (Clarebrough et al. 1957); the range of volume changes reported in Table 7.1 for the experiments corresponds to estimates of dislocation line length from energy measurements after plastic compressive strains ranging from 0.3 to 0.7. The character of the defects (e.g., edge versus screw, straight lines versus loops) was not reported in that experimental investigation.

From Table 7.1, normalized volume changes predicted for various kinds of dislocations agree with the experimental findings within a factor of ~2 and are very close for edge dislocations and prismatic loops. Volume changes per unit defect length in Cu are positive (i.e., defects cause expansion) and small. For example, a 1% volume increase would require a very high density of edge dislocations on the order of $\rho_{T0} \approx 0.01a^{-2} \approx 10^{17}\,\mathrm{m}^{-2}$, corresponding to an average dislocation spacing on the order of 10a. For small volume changes ($\Delta V/V \lesssim 0.01$), the value of $\det(\mathbf{F^I})$ is expected

provide an accurate approximation of $\bar{J}$ according to (7.80). Disclination energies and volume changes are comparable to those for dislocations for the small cut-off radii or small loops considered here (i.e., $R = 10R_C$ or $A = 10R_C$ in Table 7.2) but would diverge quickly at large distances R from the core of straight disclinations or for larger disclination loops. Elastic anisotropy of grains within the polycrystal, defect core energies, and interaction energies among defects and between defects and the external boundary of the body (e.g., image forces) are omitted in this application of the model; such effects presumably contribute to discrepancies between theory and experiment.

Results of Table 7.1, along with experimental data summarized by Wright (1982), suggest that volume changes resulting from residual elasticity associated with dislocations should be relatively small in metallic crystals of cubic symmetry deformed in compression or shear to strains on the order of unity, under quasi-static conditions. Experimental results in the final row of Table 7.1 (Clarebrough et al. 1957) correspond to dislocation densities on the order of $\rho_{T0} \approx 10^{15}\,\mathrm{m}^{-2}$, leading to volume changes on the order of $\Delta V / V \approx 10^{-4}$. Such small volume changes would seem inconsequential in the context of measured yield properties of materials in unconfined loading, when specimens are free to expand or contract laterally. However, under lateral confinement, for example uniaxial strain conditions occurring in shock loading (Rohatgi and Vecchio 2002; Clayton 2009a), small volume changes can noticeably affect the measured hydrostatic pressure. Volume changes cannot be accommodated by dislocation glide as noted in Section 7.1.1; hence, any residual volume increase from defects must be compensated by an elastic volume decrease and corresponding hydrostatic pressure. Extremely high dislocation densities, $\rho_{T0} \approx 10^{16}\,\mathrm{m}^{-2}$, have been observed for metals such as Cu deformed in shock conditions (Rohatgi and Vecchio 2002). A dislocation density of $10^{16}\,\mathrm{m}^{-2}$ would lead to an expansion on the order of 0.1%, which would in turn require an offsetting pressure on the order of 0.1% of the bulk modulus, around 150 MPa in Cu. Such contributions of defects to pressure or volume change would manifest implicitly in the measured equation of state (i.e., pressure-volume-temperature relationship—see Section 5.3), bulk modulus, and pressure derivatives of the bulk modulus obtained from shock physics experiments. Substantial effects of large dislocation densities on tangent elastic moduli of metallic single crystals deformed in uniaxial strain have also been predicted using atomistic methods (Clayton and Chung 2006). Very large dislocation densities comprising dislocation walls in subdivided grains have been observed in metals subject to severe

plastic deformation (Hughes et al. 2003); presumably, residual elastic volume changes could be significant in highly defective regions of such materials.

While closed-form analytical solutions are not available for the deviatoric part of $\mathbf{F}^{\mathbf{I}}$ in terms of stored energy and elastic constants, magnitudes of its deviatoric components are expected to be of the same order as its volumetric part, i.e., small except in cases where defect densities are extremely large. Meant by small are conditions $F^{I}{}_{AB} - \delta_{AB} \lesssim 0.001$ for defect densities $\rho_{T0} \lesssim 10^{15} \, \text{m}^{-2}$ in cubic metals such as copper, though larger average residual elastic deformations would be conceivable in crystals that feature stronger pressure sensitivity of the elastic coefficients. Because deviatoric deformation can be accommodated by plastic slip, there seems to be no capacity available to delineate contributions from residual elasticity versus dislocation flux to the plastic properties of materials (e.g., yield and flow properties) measured in experiments on single- or poly-crystals. The effect of $\mathbf{F}^{\mathbf{I}}$ is implicitly included in such experimental measurements. Notice that $\mathbf{F}^{\mathbf{I}}$ and its spatial gradient implicitly affect defect density measures defined in Section 3.3 in terms of the lattice deformation $\mathbf{F}^{\mathbf{L}}$, e.g., (3.214), since $\mathbf{F}^{\mathbf{L}} = \mathbf{F}^{\mathbf{E}}\mathbf{F}^{\mathbf{I}}$ by (7.14).

7.3 Atomistic Interpretation of Residual Elasticity

The volume element of crystalline solid is treated in what follows in Section 7.3 as an ensemble $\mathscr{L}$ of discrete atoms rather than a (nonlinear) elastic continuum. Relevant background discussions pertinent to atomic-scale stress measures and atomic interactions are provided in Sections 7.3.1 and 7.3.2, respectively, in the context of discrete lattice statics. Additional, more extensive background treatment of lattice statics is contained in Section B.2 of Appendix B. Section 7.3.3 describes the self-equilibrated, relaxed intermediate configuration of an element of a crystal from an atomistic perspective and suggests a means to compute $\mathbf{F}^{\mathbf{I}}$ entering (7.12) from atomic quantities. The atomic-scale derivation of $\mathbf{F}^{\mathbf{I}}$ that follows in Section 7.3.3 may prove useful in the context of multiscale computations of nonlinear elastic and plastic properties of crystals (Horstemeyer and Baskes 1999; Clayton and Chung 2006) and offers a more accurate treatment of defect cores than classical continuum elasticity used in Section 7.2.

7.3.1 Atomic Stress Measures

A number definitions of stress based on atomic level quantities have been suggested, as discussed in Section B.2.2. In the context of lattice statics (i.e., null atomic velocities and accelerations), the average virial stress for a group of atoms is often considered equivalent to the average Cauchy stress, the former defined according to (B.35):

$$\boldsymbol{\sigma} = \frac{1}{2\Omega} \sum_{i \ne j} \mathbf{r}_{\langle ij \rangle} \otimes \mathbf{f}_{\langle ij \rangle} \,, \tag{7.81}$$

where Ω is the total volume occupied by the group $\mathscr{L}$ of atoms, i.e., the sum of all atomic volumes, in spatial configuration B. The summation convention written in (7.81) is a compact notation that replaces the explicit double sum used in (B.35); that used here proceeds over all pairs of distinct $(i \ne j)$ atoms. The factor of two arises in (7.81) because summation proceeds over all $i \ne j$, and because $\mathbf{r}_{\langle ij \rangle} = -\mathbf{r}_{\langle ji \rangle}$, and $\mathbf{f}_{\langle ij \rangle} = -\mathbf{f}_{\langle ji \rangle}$. Spatial coordinates of atoms in a fixed, rectilinear coordinate frame are written as $\mathbf{r}_{\langle i \rangle}$, and interatomic separations in the current configuration are defined as in (B.20):

$$\mathbf{r}_{\langle ij \rangle} = \mathbf{r}_{\langle j \rangle} - \mathbf{r}_{\langle i \rangle} \,. \tag{7.82}$$

Interatomic forces arise from potential energy Φ as in (B.21) and (B.22):

$$\mathbf{f}_{\langle ij \rangle} = \frac{\partial \Phi}{\partial \mathbf{r}_{\langle ij \rangle}} \,, \quad \Phi = \Phi\left(\mathbf{r}_{\langle ij \rangle}\right)_{\substack{i,j \in \mathscr{L} \\ i \ne j}} \,. \tag{7.83}$$

Now consider a homogeneous deformation $\mathbf{F}$ as in (B.37) and (B.43), applied to all atoms in $\mathscr{L}$, leading to $\mathbf{r}_{\langle ij \rangle} = \mathbf{F} \mathbf{R}_{\langle ij \rangle}$ (Huang 1950; Born and Huang 1954), with $\mathbf{R}_{\langle ij \rangle} = \mathbf{R}_{\langle j \rangle} - \mathbf{R}_{\langle i \rangle}$ fixed separations between atoms of the reference lattice as in (B.41). The discrete analog of continuum hyperelastic relation (7.29) is given by (B.54):

$$P^{aA} = \frac{1}{2\Omega_0} \sum_{i \ne j} \frac{\partial \Phi}{\partial r^b_{\langle ij \rangle}} \frac{\partial r^b_{\langle ij \rangle}}{\partial F_{aA}} = \frac{1}{2\Omega_0} \sum_{i \ne j} \delta^{ab} \frac{\partial \Phi}{\partial r^b_{\langle ij \rangle}} R^A_{\langle ij \rangle} \,, \tag{7.84}$$

with Ω_0 (italic font) the total volume of the atomic ensemble in B_0. Atomic volume Ω_0 (non-italic font) introduced in Section 3.1.1 is equal to Ω_0 divided by the number of atoms in $\mathscr{L}$. When $\mathscr{L}$ is a primitive cell of a monatomic crystal, $\Omega_0 = \Omega_0$, but in general $\Omega_0 \ll \Omega_0$. Relation (7.84) is a consequence of affine deformation of all atoms resulting in

$\partial r_{\langle ij \rangle}^b / \partial F_{aA} = \delta^{ab} R_{\langle ij \rangle}^A$. The average atomic Cauchy stress or average static virial stress is

$$\sigma^{ab} = \det(F_{.a}^{-1A}) P^{bA} F_{.A}^a$$

$$= \frac{\Omega_0}{\Omega} \left(\frac{1}{2\Omega_0} \sum_{i \neq j} \delta^{bc} \frac{\partial \Phi}{\partial r_{\langle ij \rangle}^c} R_{\langle ij \rangle}^A \right) F_{.A}^a = \frac{1}{2\Omega} \sum_{i \neq j} r_{\langle ij \rangle}^a \delta^{bc} \frac{\partial \Phi}{\partial r_{\langle ij \rangle}^c}, \tag{7.85}$$

in agreement with (7.81). The present analysis applies only to materials described by atomic force potentials of the general form (7.83) and for which stress definitions (7.81), (7.84), and (7.85) are appropriate. For example, metals that can be modeled by combinations of pair potentials and multi-body potentials such as the embedded atom method (Daw and Baskes 1983, 1984) are included. Not admitted are piezoelectric crystals (e.g., non-centrosymmetric ionic solids), some of whose atoms (sub-lattices) may display a relative shift when polarized, and for which hypere-lastic relation (7.84) may not be sufficient. In these cases, lattice vibra-tions may provide insight into origins of stress and material coefficients (Huang 1950; Born and Huang 1954; Mindlin 1968, 1972). Also excluded from the present treatment are non-centrosymmetric polyatomic lattices such as diamond and silicon that may incur inner displacements (Cousins 1978; Tadmor et al. 1999).

7.3.2 Harmonic and Anharmonic Interactions

Expanding the potential energy of (7.83) in a series about the reference state,

$$\Phi = \Phi_0 + \sum_{i \neq j} \left. \frac{\partial \Phi}{\partial r_{\langle ij \rangle}^a} \right|_{\mathbf{r}=\mathbf{R}} q_{\langle ij \rangle}^a + \frac{1}{2} \sum_{\substack{i \neq j \\ k \neq l}} \left. \frac{\partial^2 \Phi}{\partial r_{\langle ij \rangle}^a \partial r_{\langle kl \rangle}^b} \right|_{\mathbf{r}=\mathbf{R}} q_{\langle ij \rangle}^a q_{\langle kl \rangle}^b$$

$$+ \frac{1}{6} \sum_{\substack{i \neq j \\ k \neq l \\ m \neq n}} \left. \frac{\partial^3 \Phi}{\partial r_{\langle ij \rangle}^a \partial r_{\langle kl \rangle}^b \partial r_{\langle mn \rangle}^c} \right|_{\mathbf{r}=\mathbf{R}} q_{\langle ij \rangle}^a q_{\langle kl \rangle}^b q_{\langle mn \rangle}^c + ... \tag{7.86}$$

where Φ_0 is a cohesive or total ground state energy (i.e., zero-point kinetic and potential energies of electrons and nuclei) of the reference lattice, con-ventionally negative in sign and $\mathbf{q}_{\langle ij \rangle} = \mathbf{r}_{\langle ij \rangle} - \mathbf{R}_{\langle ij \rangle}$ is the relative displace-ment for an atomic pair. Henceforward it is assumed that the second term vanishes, meaning that the reference configuration B_0 is explicitly chosen (or approximated) as free of external and internal forces:

$$H_{\langle ij\rangle}^{a} = \delta^{ab} \left.\frac{\partial \Phi}{\partial r_{\langle ij\rangle}^{b}}\right|_{\mathbf{r}=\mathbf{R}} = 0, \qquad (7.87)$$

though such a condition need not strictly apply in all cases[2]. Following the scheme used in (7.81) and Section B.2.5, repeated use of the summation symbol is omitted in (7.86). Hence, the summation in the second term on the right of (7.86) applies over two sets of repeated atomic labels, that in the third term over four sets, and that in the fourth term over six sets. The energy per unit reference volume Φ / Ω_0 differs from the strain energy per reference volume Ψ_0 used in Section 7.2 by the additive constant Φ_0 / Ω_0, since the continuum strain energy (7.28) vanishes in the undistorted reference state. Introducing the matrix notation for atomic stiffness coefficients

$$H_{\langle ijkl\rangle}^{ab} = \delta^{ac}\delta^{bd} \left.\frac{\partial^{2}\Phi}{\partial r_{\langle ij\rangle}^{c}\partial r_{\langle kl\rangle}^{d}}\right|_{\mathbf{r}=\mathbf{R}} \;,\; H_{\langle ijklmn\rangle}^{abc} = \delta^{ad}\delta^{be}\delta^{cf} \left.\frac{\partial^{3}\Phi}{\partial r_{\langle ij\rangle}^{d}\partial r_{\langle kl\rangle}^{e}\partial r_{\langle mn\rangle}^{f}}\right|_{\mathbf{r}=\mathbf{R}} \;,\; (7.88)$$

and noting $\partial q_{\langle kl\rangle}^{a} / \partial r_{\langle kl\rangle}^{b} = \delta_{.b}^{a}$, the stress of (7.81) and (7.85) becomes

$$\sigma^{ab} = \frac{1}{2\Omega}\sum_{\substack{i\neq j\\k\neq l}} r_{\langle ij\rangle}^{a} H_{\langle ijkl\rangle}^{bc}\delta_{cd}q_{\langle kl\rangle}^{d} + \frac{1}{4\Omega}\sum_{\substack{i\neq j\\k\neq l\\m\neq n}} r_{\langle ij\rangle}^{a} H_{\langle ijklmn\rangle}^{bce}\delta_{cd}q_{\langle kl\rangle}^{d}\delta_{ef}q_{\langle mn\rangle}^{f} + ... \quad (7.89)$$

Under a homogeneous deformation $\mathbf{q}_{\langle ij\rangle} = (\mathbf{F}-\mathbf{1})\mathbf{R}_{\langle ij\rangle}$, the two-point stress tensor of (7.84) is

$$P^{aA} = \frac{1}{2\Omega_0}\sum_{\substack{i\neq j\\k\neq l}} H_{\langle ijkl\rangle}^{ab}\delta_{bc}q_{\langle kl\rangle}^{c}R_{\langle ij\rangle}^{A} + \frac{1}{4\Omega_0}\sum_{\substack{i\neq j\\k\neq l\\m\neq n}} H_{\langle ijklmn\rangle}^{abc}\delta_{bd}q_{\langle kl\rangle}^{d}\delta_{ce}q_{\langle mn\rangle}^{e}R_{\langle ij\rangle}^{A} + ... \quad (7.90)$$

In the harmonic approximation (Maradudin et al. 1971), products of order higher than two in atomic displacements are dropped from the crystal's potential energy, leading to the linear force-displacement relationship

$$f_{\langle ij\rangle}^{a} = \sum_{k\neq l} H_{\langle ijkl\rangle}^{ab}\delta_{bc}q_{\langle kl\rangle}^{c}, \qquad (7.91)$$

and to resulting stress measures

$$\sigma^{ab} = \frac{1}{2\Omega}\sum_{\substack{i\neq j\\k\neq l}} r_{\langle ij\rangle}^{a} H_{\langle ijkl\rangle}^{bc}\delta_{cd}q_{\langle kl\rangle}^{d} \;,\; P^{aA} = \frac{1}{2\Omega_0}\sum_{\substack{i\neq j\\k\neq l}} H_{\langle ijkl\rangle}^{ab}\delta_{bc}q_{\langle kl\rangle}^{c}R_{\langle ij\rangle}^{A}. \quad (7.92)$$

Second- and third-order elastic constants derived from an atomic potential in Appendix B, (B.75) and (B.77), are repeated here as, respectively,

---

[2] When (7.87) does not apply and $H_{\langle ij\rangle}^{a} \neq 0$, this term's contribution to forces, stresses, and energy can be incorporated in a straightforward manner.

$$\overline{\mathbb{C}}^{ABCD} = \frac{1}{2\Omega_0} \sum_{\substack{i \neq j \\ k \neq l}} H^{ab}_{\langle ijkl \rangle} \delta^A_{.a} R^B_{\langle ij \rangle} \delta^C_{.b} R^D_{\langle kl \rangle} , \tag{7.93}$$

$$\begin{aligned}
\overline{\mathbb{C}}^{ABCDEF} &= \frac{1}{2\Omega_0} \sum_{\substack{i \neq j \\ k \neq l \\ m \neq n}} H^{abc}_{\langle ijklmn \rangle} R^A_{\langle ij \rangle} R^C_{\langle kl \rangle} R^E_{\langle mn \rangle} \delta^B_{.a} \delta^D_{.b} \delta^F_{.c} \\
&\quad - \frac{1}{2\Omega_0} \sum_{\substack{i \neq j \\ k \neq l}} H^{ab}_{\langle ijkl \rangle} \delta^A_{.a} R^C_{\langle ij \rangle} \delta^E_{.b} R^F_{\langle kl \rangle} \delta^{BD} \\
&\quad - \frac{1}{2\Omega_0} \sum_{\substack{i \neq j \\ k \neq l}} H^{ab}_{\langle ijkl \rangle} \delta^A_{.a} R^E_{\langle ij \rangle} \delta^C_{.b} R^D_{\langle kl \rangle} \delta^{BF} \\
&\quad - \frac{1}{2\Omega_0} \sum_{\substack{i \neq j \\ k \neq l}} H^{ab}_{\langle ijkl \rangle} \delta^A_{.a} R^B_{\langle ij \rangle} \delta^C_{.b} R^E_{\langle kl \rangle} \delta^{DF} .
\end{aligned} \tag{7.94}$$

Relation (7.94) indicates that third- (and higher-order) elastic constants depend in part on anharmonic terms in the potential, as noted by Thurston and Brugger (1964) and Maugin (1999). Derivations (7.89), (7.90), (7.92), (7.93), and (7.94) rely on uniformity of the atomistic deformation (Huang 1950; Born and Huang 1954) such that the relationship between current position vector **r** and reference position vector **R** is linear in the mapping **F**. In this atomistic context, **F** is regarded as a linear transformation for the primitive Bravais lattice vectors similar to $\mathbf{F^L}$ in (7.9), and though it acts uniformly over atoms in an individual volume element, neither **F** nor $\mathbf{F^L}$ need be the gradient of any macroscopic vector field spanning neighboring volume elements (Clayton and Chung 2006).

Expansion (7.86), while generic in the sense that many types of interactions (e.g., pair-wise and multi-body, central and non-central force) are admitted, may be cumbersome for computation of elastic constants for specific potentials that are not typically expressed explicitly in terms of interatomic separation vectors. For example, explicit expressions for second- and third-order elastic constants are given in Section B.2.6 of Appendix B for pair potentials and embedded atom potentials.

7.3.3 Residual Deformation in a Self-equilibrated Lattice

Now consider the self-equilibrated configuration $\overline{B}$ of Fig. 7.1. Slip may have occurred in achieving this configuration from the reference state, but the atoms occupy perfect lattice sites apart from the effects of any defects

remaining within the element that either (i) are also present in reference configuration B_0 or (ii) are generated during the course of plastic deformation. Not considered in Section 7.3 is the (former) class of defects present initially in B_0. Although positions of specific atoms may differ in configurations B_0 and $\tilde{B}$ as a result of translations by Burgers vectors of dislocations that have passed through the volume element, coordinates $\mathbf{R}_{\langle i \rangle}$ can still be used to identify positions of atoms occupying perfect lattice sites in $\tilde{B}$, as discussed in Section 3.2.10. The volume element may either be treated as an isolated ensemble of atoms with free boundaries or as part of an infinite medium with a periodic defect distribution. The former case is more consistent with the fundamental definition of the isolated unloaded configuration given in Section 7.1 (Eckart 1948), although free surfaces can give rise to atomic or ionic displacements (and corresponding surface energy contributions), even for otherwise perfect and undeformed crystal structures. Such free surface effects are usually considered negligible when the crystal volume element contains a sufficiently large number of atoms; correspondingly, such surface effects are not considered in the context of usual continuum nonlinear elasticity of Section 7.2. The latter case—which implicitly includes effects of image forces of defects in neighboring volume elements—may be more practical from the standpoint of lattice statics calculations with periodic boundary conditions (Chung and Clayton 2007). Previous definitions for achieving the slipped configuration $\tilde{B}$ discussed in Section 7.1.2 still apply here, but dislocation fluxes contributing to plastic deformation are interpreted in terms of velocities of atoms comprising each line defect rather than as continuum quantities. External forces vanish by definition in $\bar{B}$, as do dynamics (i.e., atomic velocities and accelerations), so lattice statics relations (B.16) and (7.81) apply for a self-equilibrated lattice. However, because of the presence of defects, the total energy of the ensemble $\mathcal{L}$ of atoms in $\bar{B}$ is a local minimum (Gallego and Ortiz 1993; Chung and Clayton 2007) as opposed to the global minimum corresponding to the perfect reference lattice in B_0. This implies that some atoms occupy metastable positions; some interatomic forces do not vanish within the element in $\bar{B}$ as they do in B_0 via (7.87); and the potential energy of the ensemble of atoms in $\bar{B}$ exceeds Φ_0.

The position of atom i in configuration $\bar{B}$ is denoted by $\bar{\mathbf{r}}_{\langle i \rangle}$. Because $\bar{B}$ is self-equilibrated, average static atomic stress measures vanish by definition:

$$\bar{\sigma}^{ab} = \frac{1}{2\bar{\Omega}} \sum_{i \neq j} \bar{r}^{a}_{\langle ij \rangle} \delta^{bc} \frac{\partial \Phi}{\partial \bar{r}^{c}_{\langle ij \rangle}} = 0 \, , \ \ \bar{P}^{aA} = \frac{1}{2\Omega_0} \sum_{i \neq j} \delta^{ab} \frac{\partial \Phi}{\partial \bar{r}^{b}_{\langle ij \rangle}} R^{A}_{\langle ij \rangle} = 0 \, . \quad (7.95)$$

with $\bar{\Omega} = \bar{J}\Omega_0$ the system volume in $\bar{B}$, Φ the potential energy of (7.83), and $\bar{\mathbf{r}}_{\langle ij \rangle} = \bar{\mathbf{r}}_{\langle j \rangle} - \bar{\mathbf{r}}_{\langle i \rangle}$. Because atomic coordinates are not mapped homogeneously from their positions in B_0 to their positions in $\bar{B}$, the average first Piola-Kirchhoff stress measure in the second of (7.95) does not follow from a linear transformation such as used in the chain rule in (7.84); it is instead introduced in (7.95) as a fundamental definition. Equation (7.95) contains discrete analogs of continuum self-equilibrium conditions (7.20) and (7.26). As in (7.86), the potential energy is expanded in a series about a perfect reference configuration:

$$\Phi = \Phi_0 + \frac{1}{2} \sum_{\substack{i \neq j \\ k \neq l}} H^{ab}_{\langle ijkl \rangle} \delta_{ac} \bar{q}^{c}_{\langle ij \rangle} \delta_{bd} \bar{q}^{d}_{\langle kl \rangle}$$

$$+ \frac{1}{6} \sum_{\substack{i \neq j \\ k \neq l \\ m \neq n}} H^{abc}_{\langle ijklmn \rangle} \delta_{ad} \bar{q}^{d}_{\langle ij \rangle} \delta_{be} \bar{q}^{e}_{\langle kl \rangle} \delta_{cf} \bar{q}^{f}_{\langle mn \rangle} + ..., \quad (7.96)$$

with $\bar{\mathbf{q}}_{\langle ij \rangle} = \bar{\mathbf{r}}_{\langle ij \rangle} - \mathbf{R}_{\langle ij \rangle}$ the displacement difference between two atoms in the defective self-equilibrated lattice, and where (7.88) has been used to define atomic stiffness coefficients. Substituting (7.96) into the first of (7.95) and multiplying through by $\bar{J}$, the null average atomic stress relation becomes

$$0 = \bar{J}\bar{\sigma}^{fa} = \frac{1}{2\Omega_0} \sum_{\substack{i \neq j \\ k \neq l}} \bar{r}^{f}_{\langle ij \rangle} H^{ab}_{\langle ijkl \rangle} \delta_{bc} \bar{q}^{c}_{\langle kl \rangle}$$

$$+ \frac{1}{4\Omega_0} \sum_{\substack{i \neq j \\ k \neq l \\ m \neq n}} \bar{r}^{f}_{\langle ij \rangle} H^{abc}_{\langle ijklmn \rangle} \delta_{bd} \bar{q}^{d}_{\langle kl \rangle} \delta_{ce} \bar{q}^{e}_{\langle mn \rangle} + ... \quad (7.97)$$

As in (7.33)-(7.37), vanishing of the average symmetric stress measured in the reference configuration leads by definition to six equations for six unknown components of symmetric deformation map $\mathbf{F}^{\mathbf{I}}$. Identifying harmonic terms in the atomic definition of the average stress with linear terms in the continuum elastic definition of the average stress:

$$\underbrace{\frac{1}{V} \int_V \bar{\mathbb{C}}^{ABCD} u_{C,D} dV}_{\text{continuum elasticity}} \Leftrightarrow \underbrace{\frac{1}{2\Omega_0} \delta^{A}_{.f} \delta^{B}_{.a} \sum_{\substack{i \neq j \\ k \neq l}} \bar{r}^{f}_{\langle ij \rangle} H^{ab}_{\langle ijkl \rangle} \delta_{bc} \bar{q}^{c}_{\langle kl \rangle}}_{\text{discrete lattice statics}} \, , \quad (7.98)$$

the following definition emerges (Clayton and Bammann 2009):

$$\overline{\mathbb{C}}^{ABCD}(F^I{}_{CD} - \delta_{CD}) = \frac{1}{2\Omega_0}\delta^A_{.f}\delta^B_{.a}\sum_{\substack{i \ne j \\ k \ne l}}\overline{r}^f_{\langle ij \rangle}H^{ab}_{\langle ijkl \rangle}\delta_{bc}\overline{q}^c_{\langle kl \rangle}$$

$$= -\frac{1}{4\Omega_0}\delta^A_{.f}\delta^B_{.a}\sum_{\substack{i \ne j \\ k \ne l \\ m \ne n}}\overline{r}^f_{\langle ij \rangle}H^{abc}_{\langle ijklmn \rangle}\delta_{bd}\overline{q}^d_{\langle kl \rangle}\delta_{ce}\overline{q}^e_{\langle mn \rangle} - ..., \tag{7.99}$$

with the second equality in (7.99) following directly from (7.97). Assuming as usual that the reference stiffness of the perfect lattice $\overline{\mathbb{C}}^{ABCD}$ is positive definite,

$$F^I{}_{CD} = \delta_{CD} - \frac{1}{\Omega_0}\overline{S}_{CDAB}[(\frac{1}{4}\delta^A_{.f}\delta^B_{.a})\sum_{\substack{i \ne j \\ k \ne l \\ m \ne n}}\overline{r}^f_{\langle ij \rangle}H^{abc}_{\langle ijklmn \rangle}\delta_{bd}\overline{q}^d_{\langle kl \rangle}\delta_{ce}\overline{q}^e_{\langle mn \rangle} + ...], \tag{7.100}$$

where second-order elastic compliance $\overline{S}_{CDAB}$ satisfies (7.38) and can be found from inverting the second-order reference moduli (7.93). The series in brackets on the right of (7.100) accounts for anharmonic interactions, and includes terms of orders two and higher in relative atomic displacements $\overline{q}^a_{\langle ij \rangle}$ in the locally deformed, yet self-equilibrated, defective lattice. For harmonic lattice statics, in which case $H^{abc}_{\langle ijklmn \rangle} = 0$ and/or quadratic and higher-order terms in $\overline{q}^a_{\langle ij \rangle}$ are dropped from (7.100), the bracketed series degenerates to zero and $F^I{}_{CD} = \delta_{CD}$, analogously to linear continuum description (7.35). The definition for $F^I{}_{CD}$ implied by the first of (7.99), while not unique, is motivated by its analogous continuum definition $F^I{}_{CD} = V^{-1}\int x_{(C,D)}dV = V^{-1}\overline{S}_{CDAB}\overline{\mathbb{C}}^{ABEF}\int x_{(E,F)}dV$ in (7.31).

Following Section 7.2.6, the first-order accurate residual volume change is $\overline{J} = \overline{\Omega}/\Omega_0 \approx \det(\mathbf{F}^I) \approx \text{tr}(\mathbf{F}^I) - 2$, where continuum and discrete measures of reference and intermediate volumes are related, respectively, by $\Omega_0 = V$ and $\overline{\Omega} = V + \Delta V$. Calculation of this volume change does not require identification of a bounding surface delineating the volume occupied by the atoms in configuration $\overline{B}$; i.e., the atoms can occupy an arbitrary shape so long as their interaction forces self-equilibrate. If such a surface can be identified in a lattice statics calculation, for example an ensemble of atoms in a defective state contained within a hexahedral bounding box, it should be possible to compute $\overline{\Omega}$ trivially (i.e., $\overline{\Omega}$ is then the volume of the box) and then compare results with predictions of (7.100), so long as the average static virial stress vanishes over the defective ensemble of atoms. An apparent advantage of the atomistic approach of Section 7.3 over

the continuum approach of Section 7.2 is that effects of defect cores are accurately incorporated in the former, presuming that the atomic potential is sufficiently robust to model defect core structures. An apparent disadvantage is that solutions to (7.100) must be computed numerically, while the continuum approach pioneered by Zener (1942), Seeger and Haasen (1958), Toupin and Rivlin (1960), and Holder and Granato (1969) provides convenient analytical formulae for volume changes such as (7.59)-(7.61).

7.4 Point Defects and Residual Elasticity

In continuum and solid state physics, point defects are often idealized as spheres embedded in an elastic medium (Bitter 1931; Eshelby 1954, 1956; Holder and Granato 1969). Since spheres have finite volume, formation of such defects necessarily involves a volume change, regardless of the rigidity of the surrounding medium. This situation is in contrast to idealized line defects of the sort addressed in Section 7.2, e.g., dislocation and disclination lines, which have no intrinsic volume, though the surrounding elastic medium can still undergo dilatation as a result of the presence of such line defects. In Section 7.4.1, a model for the deformation gradient contribution resulting from generation of a point defect and its elastic fields is suggested, combining results of Sections 3.2.8, 7.2, and C.4 of Appendix C. In Section 7.4.2, the particular example of a monovacancy in copper is discussed and predictions are compared with experimental observations.

7.4.1 Spherical Deformation from a Point Defect

Recall from Section 3.2.8 that the total lattice deformation gradient for an elastic body with an isotropic distribution of spherical point defects can be written as

$$\mathbf{F^L} = \mathbf{F^E}\mathbf{F^V} , \tag{7.101}$$

where the residual volumetric deformation from defects is

$$F^{V\,\alpha}_{\ \ .\beta} = (1-\bar{\phi})^{-1/3}\delta^{\alpha}_{\beta} = J^{V1/3}\delta^{\alpha}_{\beta} , \quad J^V = \det(\mathbf{F^V}) . \tag{7.102}$$

As shown in Fig. 3.10, $\mathbf{F^V} : T\tilde{B} \to T\overline{B}$, where externally unloaded configuration $\overline{B}$ is analogous to that in Fig. 7.1. From (3.133)-(3.135), the volume fraction of point defects per unit volume in $\overline{B}$ is

$$\bar{\phi} = \alpha\bar{\xi} = \left[\pm\Omega_0 + (1+\Gamma)\Delta v\right]\bar{\xi} , \tag{7.103}$$

where $\bar{\xi}$ is the number of defects per unit volume in $\bar{B}$ and α is the net volume change per defect. When $\mathbf{F} = \mathbf{F}^{\mathbf{L}}$, (7.103) can also be written as

$$\phi_0 = \alpha \xi_0 = \left[\pm \Omega_0 + (1 + \Gamma) \Delta v \right] \xi_0 , \qquad (7.104)$$

where $\phi_0 = J^V \bar{\phi}$ and $\xi_0 = J^V \bar{\xi}$ are defined per unit reference volume. Recall from Section 3.2.8 that $\pm \Omega_0 \to \Omega_0$ in (7.103)-(7.104) when a vacancy enters the volume element (e.g., via diffusion at a free surface) and free volume of the crystal increases by atomic volume Ω_0, while $\pm \Omega_0 \to -\Omega_0$ in (7.103)-(7.104) when an atom moves from a lattice site to an interstitial position in the idealized situation when no vacancy is left behind. For a substitutional atom, the $\pm \Omega_0$ term is omitted, and $\alpha = (1 + \Gamma) \Delta v$. The algebraic sign of Δv is positive for an interstitial or a substitutional atom of larger size than the atom it replaces. The algebraic sign of Δv is negative for a vacancy or a substitutional atom smaller than the atom it replaces. In a polyatomic crystal, the magnitude and sign of Δv will generally depend on the atomic species of the defect under consideration, as well as any possible electric charge associated with the defect (e.g., in an ionic crystal).

The magnitude of relaxation volume Δv depends on the interaction of the point defect with the surrounding crystalline medium. In the linear elastic approximation, idealizing the surrounding crystalline material as isotropic and the point defect as a rigid sphere, analytical solutions are available, as presented in Sections C.3.1 and C.3.2, respectively, for an infinitely extended elastic medium and an elastic medium of finite dimensions. An analytical solution is also available for a deformable elastic sphere embedded in a finite medium (Section C.3.3 of Appendix C), but such a model is not invoked here in the context of point defects because assignment of continuum elastic constants to a sphere of dimensions of a single atom is deemed too severe an assumption.

The simplest model, discussed in Section C.3.1, idealizes the defect as a rigid sphere and the surrounding medium as infinitely extended. The relaxation volume is given by (C.188):

$$\Delta v = \delta V = 4 \pi A , \qquad (7.105)$$

where A is a misfit parameter that must be determined from experiments or atomic scale calculations. The average strain energy density of the elastic medium surrounding a single defect is purely deviatoric, as listed in (C.187):

$$\bar{W}_S = \frac{6\mu A^2}{(R_0^3 - r_0^3)r_0^3}\left[1 - \left(\frac{r_0}{R_0}\right)^3\right] \approx \frac{6\mu A^2}{(R_0^3/r_0^3 - 1)r_0^6}$$

$$\approx \frac{6\mu A^2}{R_0^3 r_0^3} = \frac{8\pi\mu A^2}{[(4\pi/3)r_0^3]R_0^3} = \frac{(32/3)\pi^2\mu A^2}{\Omega_0(4\pi/3)R_0^3} = \frac{(2/3)\mu(\delta V)^2}{\Omega_0(4\pi/3)R_0^3}. \tag{7.106}$$

The radius of the spherical point defect is r_0, and the radius of a spherical region of the surrounding medium is R_0. Successive approximations in (7.106) correspond to $R_0^3/r_0^3 \gg 1$, i.e., a very small defect in a much larger sample of material. For N dilute defects in the case where interactions among defects are reasonably omitted, (7.106) is extended to

$$\bar{W}_S \approx \frac{2\mu}{3\Omega_0}(\delta V)^2 \frac{N}{(4\pi/3)R_0^3} = \frac{2\mu}{3\Omega_0}(\delta V)^2 \xi_0, \tag{7.107}$$

with $\xi_0 = N/V$ the number of defects per unit reference volume as in (7.104). The relaxation volume can then be estimated by equating the product of (7.107) and the reference volume V with formation energy E_F of a single ($N = 1$) point defect:

$$E_F = \frac{4\pi}{3}R_0^3\bar{W}_S = \frac{2\mu}{3\Omega_0}(\delta V)^2 \Rightarrow \delta V = \pm\left(\frac{3\Omega_0 E_F}{2\mu}\right)^{1/2} = \Delta v. \tag{7.108}$$

The description of Section C.3.2 treats the defect as a rigid sphere embedded in a finite volume of isotropic elastic material. The volume change, from (C.195), is

$$\Delta v = 4\pi A\left[1 + \frac{4\mu}{3K}\right] = 4\pi A\left[\frac{3(1-\nu)}{1+\nu}\right], \tag{7.109}$$

where the misfit parameter

$$A = \frac{\delta V}{4\pi}\left[1 + \frac{4\mu}{3K}\left(\frac{r_0}{R_0}\right)^3\right]^{-1}. \tag{7.110}$$

The radius of the spherical point defect is r_0, and the traction-free external surface of the surrounding crystal is located at radial coordinate R_0. For $R_0^3/r_0^3 \gg 1$,

$$\Delta v = \left[\frac{3(1-\nu)}{1+\nu}\right]\left[1 + \frac{4\mu}{3K}\left(\frac{r_0}{R_0}\right)^3\right]^{-1}\delta V \approx \left[\frac{3(1-\nu)}{1+\nu}\right]\delta V = c\delta V, \tag{7.111}$$

where the dimensionless elastic constant $c = 3(1-\nu)/(1+\nu)$. The strain energy density is not purely deviatoric, since local pressure and elastic

dilatation are nonzero in (C.194). However, inserting (7.111) into (7.108) as an approximation, the relaxation volume is estimated as

$$\Delta v = c\delta V = \pm c\left(\frac{3\Omega_0 E_F}{2\mu}\right)^{1/2} = \pm\left[\frac{3(1-\nu)}{1+\nu}\right]\left(\frac{3\Omega_0 E_F}{2\mu}\right)^{1/2}. \quad (7.112)$$

The additional volume change resulting from nonlinear elastic effects is estimated using (7.60), assuming the strain energy density is deviatoric, following Eshelby (1954):

$$\frac{\Delta V}{V} \approx \frac{1}{\mu}\left(\frac{\partial\mu}{\partial p} - \frac{\mu}{K}\right)\overline{W}_S \approx \left(\frac{\partial\mu}{\partial p} - \frac{\mu}{K}\right)\left[\frac{2}{3\Omega_0}(\delta V)^2\,\xi_0\right]$$
$$= \frac{1}{\mu}\left(\frac{\partial\mu}{\partial p} - \frac{\mu}{K}\right)E_F\xi_0. \quad (7.113)$$

Thus, in (7.103) and (7.104), the additional volume change per defect resulting from nonlinearity is estimated as

$$\Gamma\Delta v = \frac{\Delta V/V}{\xi_0} = \frac{1}{\mu}\left(\frac{\partial\mu}{\partial p} - \frac{\mu}{K}\right)E_F. \quad (7.114)$$

When point defects are embedded in an infinite medium, (7.108) gives

$$\Gamma = \frac{\Delta V/V}{\xi_0\Delta v} = \left(\frac{\partial\mu}{\partial p} - \frac{\mu}{K}\right)\frac{E_F}{\mu\Delta v} = \pm\left(\frac{\partial\mu}{\partial p} - \frac{\mu}{K}\right)\left(\frac{2E_F}{3\mu\Omega_0}\right)^{1/2}. \quad (7.115)$$

When point defects are embedded in a finite medium, (7.112) gives

$$\Gamma = \pm\frac{1}{c}\left(\frac{\partial\mu}{\partial p} - \frac{\mu}{K}\right)\left(\frac{2E_F}{3\mu\Omega_0}\right)^{1/2} = \pm\left[\frac{1+\nu}{3(1-\nu)}\right]\left(\frac{\partial\mu}{\partial p} - \frac{\mu}{K}\right)\left(\frac{2E_F}{3\mu\Omega_0}\right)^{1/2}. \quad (7.116)$$

Algebraic signs for the $\pm$ symbols in (7.115) and (7.116) match those of corresponding relaxation volume Δv. Correction factor Γ can be positive or negative in sign depending on algebraic signs of Δv and the term $\partial\mu/\partial p - \mu/K$.

7.4.2 Example: Vacancies in Copper

Representative results of the theory outlined in Section 7.4.1 are listed in Table 7.5 for copper, applied to single point vacancies (i.e., mono-vacancies). Properties used in the calculations correspond to those listed in Tables 7.3 and 7.4. The atomic volume for a monatomic FCC crystal (four atoms per conventional unit cell) is $\Omega_0 = a^3/4 = b^3/\sqrt{2}$. Poisson's ratio ν used to obtain elastic constant c is listed in Table 7.3. The vacancy formation energy E_F and defect energy per atomic volume change

$E_F \Omega_0 / \alpha$ were obtained from independent experiments (Simmons and Balluffi 1963; Nilan and Granato 1965). The experimental value of E_F listed in Table 7.4 is used, however, in the model predictions of relaxation volume Δv, nonlinear elastic corrector Γ, and total volume change α listed in columns 2-4 of Table 7.5.

Table 7.4 Properties for copper

Atomic volume Ω_0 [Å^3]	$c = \dfrac{3-3\nu}{1+\nu}$	Vacancy formation energy $E_F{}^{(1)}$ [eV/atom]
11.81	1.41	1.17

$^{(1)}$ Simmons and Balluffi (1963)

Table 7.5 Volume changes from vacancies in copper

Model or experiment	Relaxation $\Delta v / \Omega_0$	Nonlinear correction Γ	Total volume change α / Ω_0	$E_F \Omega_0 / \alpha$ [eV/atom]
Infinite medium	-0.71	-0.23	0.45	2.6
Finite medium	-1.01	-0.16	0.16	7.3
Experiment$^{(1)}$	-	-	0.32	3.7

$^{(1)}$ Nilan and Granato (1965)

Values in the first row of results in Table 7.5 correspond to the model of a point defect in an infinitely extended elastic body of the sort described in Section C.3.1, specifically relations (7.108) and (7.115). Values in the second row of results in Table 7.5 correspond to the model of a point defect in a finite elastic body with traction free outer surface as addressed in Section C.3.2, specifically (7.111) and (7.116). Negative algebraic signs apply for Δv and hence Γ, since the relaxation volume is negative for a vacancy (i.e., surrounding atoms are pulled towards the vacant lattice site) and since $\partial \mu / \partial p - \mu / K = 0.49 > 0$ for copper. The total normalized volume change from (7.103) or (7.104) applied to a vacancy is then computed, per atomic volume, as

$$\frac{\alpha}{\Omega_0} = 1 + (1 + \Gamma)\frac{\Delta v}{\Omega_0}. \tag{7.117}$$

Experimental results listed in Table 7.5 are obtained from measurements of volume changes and energy released during annealing of deuteron-irradiated, i.e., radiation-damaged, copper foils (Nilan and Granato 1965). The total volume changes predicted by the two continuum models bound the experimental results from above and below, and all predictions agree with model results within a factor of two. Predicted relaxation volumes

are on the order of the atomic volume, and nonlinear elastic effects are non-negligible since $|\Gamma|$ is not small compared to unity.

8 Mechanical Twinning in Crystal Plasticity

Twinning in a general sense may encompass a variety of energy-invariant transformations of a crystal structure. A twin in a crystalline solid is usually defined as two regions of a crystal separated by a coherent planar interface called a twin boundary, though interpenetrating twins with irregular interfaces are also possible. Limiting values of deformation gradients in each region, on either side of the interface, differ by a simple shear. Twinning can be induced by a variety of mechanical, thermal, electrical, or chemical stimuli. Annealing twins or growth twins emerge during growth of a crystal. Another notable example is a set of finely twinned layers or lamina associated with kinematically compatible, low energy configurations emerging at or near the transformation temperature in the crystallographic theory of martensite (Ball and James 1987; Bhattacharya 1991), i.e., solid-solid polymorphic phase transformations. The present Chapter does not address such phase transformations, annealing, or crystal growth. Rather, the focus of Chapter 8 is a particular kind of twinning labeled mechanical twinning, which by definition is induced by mechanical stresses (Kosevich and Boiko 1971; James 1981). The part of the mechanical stress tensor responsible for twinning is most typically a resolved shear stress acting on the normal to the plane of the twin, in the direction of twinning shear or twin propagation. The term deformation twinning (Christian and Mahajan 1995) is used interchangeably with mechanical twinning.

When subjected to large deformations or large mechanical stresses, crystalline solids may deform via a number of mechanisms. As discussed in Chapter 6, when dislocation mobility is sufficiently high in an adequate number of directions, dislocation glide is the predominant accommodation mode for deviatoric deformations in ductile crystals at stresses above the elastic limit. On the other hand, depending on the particular kind of crystal and the loading conditions, inelastic deformation may be supported by other mechanisms such as deformation twinning.

As reviewed by Christian and Mahajan (1995), a number of theories, some complementary and some competing, exist that describe twin nucleation and propagation. Differences in twinning behaviors, or lack thereof, among crystals of various compositions and structures inhibit the formula-

tion of a universal theory for kinetics of deformation twinning in crystals of arbitrary composition and structure. In treatments of thermodynamics and kinetics that follow later in Chapter 8, deformation twinning is associated with thermodynamically irreversible shape deformation in correspondence with collective motion of partial dislocations and formation of stacking faults (Bilby and Crocker 1965; Christian and Mahajan 1995).

Deformation twinning is thought to be preferred over slip in cases wherein resistances to dislocation glide are very large in certain directions (Hirth and Lothe 1982), such as often occurs in crystal systems of non-cubic symmetry. For example, in hexagonal crystals, twinning is often favored over slip in directions not contained within the basal plane. In certain hexagonal or rhombohedral ceramics such as alumina (i.e., sapphire or corundum), slip-mediated shearing on basal and prismatic planes is often the preferred inelastic deformation mechanism, with slip resistances in directions normal to the basal plane extremely high (Veit 1921; Kronberg 1957; Bourne et al. 2007; Clayton 2009a). This phenomena occurs similarly in many hexagonal metals, including certain alloys of zirconium (Tome et al. 1991; Kalidindi 1998), titanium (Schoenfeld and Kad 2002), and magnesium (Staroselsky and Anand 2003), though secondary slip on pyramidal systems is sometimes possible. In many cases, deformation twinning, as opposed to slip, may be the only viable mechanism for accommodating deformation normal to the basal plane, in lieu of fracture. Twinning is often preferable to slip at lower temperatures in crystals with cubic symmetry, especially those with low stacking fault energy (Meyers et al. 2001; Bernstein and Tadmor 2004). For example, it has been observed that aluminum (stacking fault energy $\simeq 170$ mJ/m^2) is less likely to twin than copper (stacking fault energy $\simeq 60$ mJ/m^2).

The description set forth in Chapter 8 accounts for mechanisms of elasticity, plastic slip, and deformation twinning in single crystals. Each mechanism is addressed independently via an individual term within a three-term multiplicative decomposition of the deformation gradient. According to this representation, plastic deformation is deemed lattice-preserving (i.e., dislocation glide does not affect the Bravais lattice vectors or stored elastic energy of the crystal), following treatments of Chapter 3 (Section 3.2) and Chapter 6. In contrast, twinning is modeled here distinctly from dislocation plasticity via the use of an intermediate term in the deformation gradient decomposition. Three-term decompositions were suggested by Kratochvil (1972) and Clayton et al. (2005), who introduced intermediate terms within three-term decompositions to account for irreversible deformations distinct from those arising from dislocation glide. Following the scheme of continuum crystal plasticity theory of Sections

3.2.6 and 6.3, plastic deformation takes place via slip on one or more discrete systems. Twinning takes place via shears of predefined magnitude, with the rate of shearing determined by the rate of increase in volume fraction of the twin relative to the parent crystal (Chin et al. 1969; Van Houtte 1978; Kalidindi 1998; Staroselsky and Anand 1998, 2003). Microscopic strain fields associated with lattice defects may also contribute to irreversible deformation. In particular, net volume changes associated with residual strain fields of defects, as derived in Section 7.2.4, are directly incorporated into the extended crystal plasticity theory of Chapter 8. Finally, thermomechanically reversible deformation of the lattice is addressed via the elastic term in the decomposition, encompassing both the recoverable deformation associated with mechanical stresses and thermal expansion or contraction associated with temperature changes.

A constitutive framework based on internal state variable theory provides thermodynamic relationships among independent and dependent state variables as well as appropriate driving forces for evolution of internal state variables and rates of inelastic deformations. Here, internal state variables consist of dislocation and twin boundary densities, and inelastic deformation rates include rates of slip and of twinned volume fractions. Dislocation densities are partitioned into geometrically necessary dislocations associated with slip gradients and statistically stored dislocations associated with homogeneous plastic flow and dislocation loops. Recall that formal definitions of dislocation densities are given in Section 3.3.2. Interface partial dislocations at propagating twin boundaries (Scott and Orr 1983) are demonstrated to contribute to the geometrically necessary dislocation density tensor. Thermodynamic restrictions on kinetic relations follow naturally from energy conservation requirements and the entropy production inequality. Averaging concepts are invoked to describe effects of twinning on the thermoelastic response of an element of crystal containing one or more twins, leading to effective anisotropic moduli and dissipation rates that depend upon volume fractions of twins in the crystal.

In Section 8.1, brief physical descriptions of elasticity, plasticity, and twinning in crystalline solids are provided, with a focus on twinning. These descriptions serve to clarify the distinctions among the three deformation mechanisms and provide sufficient physical basis for the corresponding model framework that follows in Section 8.2. The framework of Section 8.2 may be applied to describe any crystalline solid that undergoes large deformations via elasticity, plasticity, and/or twinning, including many metallic and ceramic crystals and crystalline minerals.

8.1 Mechanisms: Elasticity, Slip, and Twinning

Elasticity, slip, and twinning are described in Sections 8.1.1, 8.1.2, and 8.1.3, respectively. Regarding elasticity and slip, some redundancy with previous descriptions given in Sections 3.1 and 3.2 is unavoidable, but necessary, in order to enable a complete description of mechanical twinning.
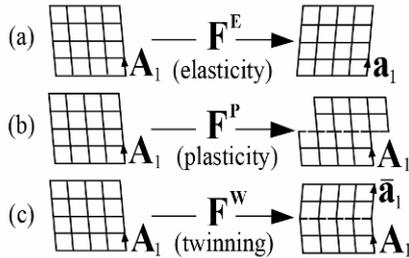
8.1.1 Elasticity

Elastic deformation is addressed in detail in Chapter 3 (Section 3.1) and Chapter 5. A crystal is said to deform elastically in the absence of generation or motion of defects. At the atomic scale, elastic deformation alters distances and/or orientations between neighboring atoms within each crystallographic unit cell. The resulting changes in inter-atomic forces produce mechanical stresses when the crystal is viewed as a continuous solid. Removal of mechanical stresses restores the original lattice without any dissipation of energy; hence, according to the usual idealization, such elastic deformation is said to be thermodynamically reversible. Elastic deformation as defined in Chapter 8 also includes changes in inter-atomic bond vectors induced by changes in temperature. At the atomistic scale of resolution, increases in local thermal vibration of atoms about their reference positions (i.e., phonons), result in expansion of the lattice in the absence of mechanical stresses. Such thermal deformations are also idealized as reversible, since presumably, in the absence of other applied stimuli, atoms of the crystal will return to their reference mean or equilibrium arrangement as the temperature is reduced to its original value.

Let $\mathbf{F}^{\mathbf{E}}(X,t)$ denote the two-point tensor of large (i.e., geometrically nonlinear) thermoelastic deformation, simply referred to as the elastic deformation in Chapter 8. When the crystal contains defects (e.g., dislocations), the elastic deformation will generally not be associated with the true derivative of any displacement field, and correspondingly, the compatibility conditions $F^{E-1\alpha}{}_{\cdot[a,b]} = 0$ are not satisfied in general, in contrast to (2.203) which apply for the total deformation gradient $\mathbf{F}(X,t)$. Let $\mathbf{A}_i$ ($i = 1,2,3$) denote primitive Bravais lattice vectors of (3.1). Then according to the Cauchy-Born hypothesis (Born and Huang 1954; Ericksen 1984) of Section 3.1.2 and (3.17), when the total deformation is elastic,

$$\mathbf{a}_i = \mathbf{F}^{\mathbf{E}}\mathbf{A}_i , \ (i = 1,2,3), \tag{8.1}$$

with $\mathbf{a}_i$ the primitive Bravais lattice vectors in the deformed crystal. Elastic deformation of a primitive non-cubic lattice is illustrated in Fig. 8.1(a); note the deformation of a representative primitive Bravais lattice vector $\mathbf{a}_1 = \mathbf{F}^E \mathbf{A}_1$.

Fig. 8.1 Deformation mechanisms and lattice vectors: (a) elasticity, (b) plastic slip, (c) twinning

Let ψ denote the Helmholtz free energy per unit mass of the crystal, as first introduced in Table 4.2. This energy is postulated, for illustrative purposes in Section 8.1, to depend only on the elastic deformation at particular material location X and at a given time t. Then the free energy satisfies the usual constraints imposed by invariance and material symmetry:

$$\psi\left(\mathbf{F}^E, X\right) = \psi\left(\hat{\mathbf{Q}} \mathbf{F}^E \breve{\mathbf{H}}, X\right) \geq \psi\left(\mathbf{1}, X\right) = \psi\left(\hat{\mathbf{Q}} \breve{\mathbf{H}}, X\right). \qquad (8.2)$$

In (8.2), $\mathbf{1}$ is the unit tensor, $\hat{\mathbf{Q}} = \hat{\mathbf{Q}}^{-T}$ represents any rigid body rotation of the spatial coordinate frame with $\det \hat{\mathbf{Q}} = +1$, and $\breve{\mathbf{H}} \in \mathbf{H}$ is any member of the group $\mathbf{H}$ of affine transformations of the Bravais lattice that does not affect its free energy. The point group $\mathbb{Q}$ of symmetry operations (i.e., rotations, reflections, and inversions) for the crystal class to which the material belongs is a subset of this potentially larger group of energy invariant transformations, i.e., $\mathbb{Q} \in \mathbf{H}$. The first of (8.2) corresponds to (A.1) of Appendix A when $\mathbf{F}^E = \mathbf{F}$ and $\breve{\mathbf{H}} = \breve{\mathbf{Q}} \in \mathbb{Q}$, where $\breve{\mathbf{Q}}$ is a member of the point group as introduced in Section 5.1.5 in the context of elastic symmetry. Point groups and crystal classes are discussed in more detail in Section A.1 of Appendix A. Matrix $\breve{\mathbf{H}}$ is not necessarily orthogonal and hence may fall outside the point group, as demonstrated explicitly later in Section 8.1.3 wherein $\breve{\mathbf{H}}$ is associated with twinning shear. Relation (8.2) implies that the state characterized by null elastic deformation, $\mathbf{F}^E = \mathbf{1}$, correlates with a local minimum of the free energy density ψ at point X.

8.1.2 Plastic Slip

Plastic deformation is discussed at length in Section 3.2 of Chapter 3 from the perspective of kinematics and in Chapter 6 from the perspective of thermomechanics and kinetics. Plastic deformation as addressed in this context occurs via glide of dislocations of edge, screw, and/or mixed character, including loops, and encompassing cross-slip but not dislocation climb. As discussed in Section 3.2.2, as full dislocations travel through a region of the lattice, the shape of the material will change, but the inter-atomic bond vectors remain the same (upon translation of planes by an integer multiple of the Burgers vector), so long as no defects are left behind within the region. In this sense, the plastic deformation is said to be lattice-preserving. Collective motion of leading and trailing partial dislocations is also lattice-preserving, since trailing partial(s) erase the stacking faults left in the wake of leading partials and hence restore the lattice periodicity. Mechanical stresses are conventionally required to enact glide of dislocations, apart from random thermal fluctuations such as occurring in kink migration. For example, according to Schmid's law, resolved shear stresses in (6.70) or (6.86) must exceed a threshold stress consisting of superposition of the Peierls barrier (C.248) and influences from other defects as in (6.99). Plastic deformation is thermomechanically irreversible, since the reference shape of the material is not recovered upon removal of mechanical stresses, and since heat is dissipated by moving dislocations as a result of lattice friction, phonon drag, and other mechanisms (Kocks et al. 1975; Gilman 1979). Plastic dissipation converted to temperature rise is evident from (6.43) and (6.45)-(6.47). Because the crystal lattice remains unchanged apart from steps on its surface, plastic deformation itself does not affect the strain energy of the crystal. However, defects generated during the course of plastic deformation that remain within the material lead to energy storage as a result of the local stress fields supported by these defects. Such effects are captured in continuum theories by internal state variables, leading for example to a Taylor-Quinney parameter $\beta' < 1$ in (6.46) during some part of the deformation history.

Let $\mathbf{F^P}(X,t)$ denote the two-point tensor of potentially large plastic deformation. The plastic deformation will generally not be the derivative (i.e., true material gradient) of a displacement function, and correspondingly, compatibility conditions $F^{P\alpha}_{\ \ [A,B]} = 0$ are not always satisfied, implying existence of geometrically necessary dislocations in the crystal, as is evident from kinematic relations (3.217)-(3.227) of Section 3.3.2. Plastic deformation is illustrated conceptually for a non-cubic lattice in Fig. 8.1(b). On the right side of the figure, the slip plane is denoted by the

dashed line. Note that the lattice vector $\mathbf{A}_1$ is unchanged by the action of the plastic deformation, in agreement with (3.107). As demonstrated in (3.116) the corresponding implication in crystal plasticity theory is that slip directions and slip plane normal vectors are unaffected by $\mathbf{F}^\mathbf{P}$. Since plastic deformation is lattice-preserving and consists of shearing in one or more directions, the volume of the material remains unaffected, and hence $J^P = 1$, as emphasized in Section 7.1.1. Furthermore, because the (continuum) plastic deformation by definition consists only of relative shear displacements of crystallographic planes in integer multiples of the Burgers vector, the free energy density of the crystal cannot depend explicitly on $\mathbf{F}^\mathbf{P}$:

$$\left. \frac{\partial \psi}{\partial \mathbf{F}^\mathbf{P}} \right|_{\mathbf{F}^\mathbf{E}, \theta, \alpha} = 0, \tag{8.3}$$

where elastic deformation, temperature, and internal state variable(s) are held fixed in the partial derivative. At the atomic scale, slip can be further understood by considering the generalized stacking fault energy (Vitek 1966; Zimmerman et al. 2000; Ogata et al. 2005):

$$E_{GSF}(\Delta \mathbf{x}) = E_{GSF}(\Delta \mathbf{x} + l_i \mathbf{b}), \; E_{GSF}(0) = E_{GSF}(l_i \mathbf{b}) = 0, \; (l_i \in \mathbb{Z}). \tag{8.4}$$

The relative shear displacement between two neighboring crystallographic planes is denoted by $\Delta \mathbf{x}$, l_i is any integer, and $\mathbf{b}$ is the Burgers vector of a full dislocation. The energy in (8.4) is minimal at null relative displacement, corresponding to a perfect reference lattice, and exhibits periodic total minima for rigid translations of planes by integer multiples of the Burgers vector. Local minima in generalized stacking fault energy surfaces, often called γ-surfaces, can be associated with metastable stacking faults, i.e., partial dislocations. The total energy of the atomic ensemble also includes energies of defect cores and residual stress fields of defects; in complementary continuum treatments such energetic contributions are measured by internal state variables, as discussed in Section 4.2.1.

8.1.3 Deformation Twinning

Deformation twinning results in two connected regions in the lattice separated by a twin boundary (i.e., the dotted line on the right side of Fig. 1 (c)) whose shape deformations differ by a simple shear. The original region of the crystal is termed the parent, while the sheared region is termed the twin. According to the classical definition of a deformation twin, atomic positions, and hence primitive Bravais lattice vectors and basis vectors, within each region differ by a proper or improper rotation, typically either

a reflection or 180° rotation (Christian and Mahajan 1995), though more general relationships are possible. The stacking sequence of atomic planes in the twin is altered or reversed with respect to that in the parent, and hence crystals with low stacking fault energies are usually more prone to twin formation than those with high stacking fault energies. Nucleation and propagation of deformation twins are though to take place by one or more mechanisms, often involving the formation and motion of partial dislocations (e.g., dissociation of full dislocations into partials) and possible atomic shuffles needed to maintain the orientation relationships between the twin and parent (Cottrell and Bilby 1951; Bilby and Crocker 1965; Hirth and Lothe 1982; Pirouz 1987; Zanzotto 1996; Lagerlof et al. 2002). Partial dislocations associated with twin growth are often labeled as twinning dislocations, and these twinning dislocations often have Burgers vectors whose magnitudes are very small fractions of full dislocations in the same crystal structure. In some cases, e.g., the standard twinning modes for BCC and FCC crystals listed in Table 8.1, twins can be formed by simple shearing of the Bravais lattice vectors alone. In other cases, atomic shuffles, i.e., additional displacements of only some of the atoms in the twin, are required in order to maintain the orientation relationship among all atoms in twin and parent. Such shuffles or relative displacements are usually mandatory in polyatomic crystals, i.e., those with a basis of more than one atom per primitive unit cell.

Twinning is not regarded as lattice-preserving in the sense of slip, since twinning involves rotation of the lattice, as evidenced by crystallographic texture measurements (Van Houtte 1978; Tome et al. 1991). The involvement of partial dislocations and atomic shuffles, for example, induces the rotational change of the twinned lattice relative to that of the parent. Such changes in the lattice orientation do not occur under plastic deformation arising from the slip of full dislocations, as shown in Fig. 8.1(b). Deformation twinning is also distinguished from plastic slip in that the former occurs by collective motion of defects, resulting in a quantized amount of shear, denoted by γ^j on twin system j, that preserves a particular orientation relationship between the twin and parent. In contrast, plastic deformation may conceivably result in shearing of any maximum magnitude, with the lower limit of relative displacement between two lattice planes limited by the Burgers vector for slip. The shear strain associated with deformation twinning is usually mechanically irreversible, since fully formed twins remain in single crystals after mechanical stresses are removed[1]. Twins of-

---

[1] Elastic twinning is physically possible (Cooper 1962; Kosevich and Boiko 1971). Elastic twins partially or fully disappear upon load relaxation, though dissipation associated with hysteresis can still be significant if the loading is cyclical.

ten seem to propagate very rapidly relative to slipped regions or slip bands (Christian and Mahajan 1995), even in low strain rate experiments as evidenced by load drops in the stress-strain response (Kronberg 1968; Scott and Orr 1983). When driving stresses are sufficiently large, tapered twin lamellae can extend or grow at velocities exceeding the elastic shear wave speed of the crystal, though the velocity of the twin resolved in the direction normal to its boundary surface must remain subsonic (Rosakis and Tsai 1995). Much slower twin growth kinetics has also been reported. Cooper (1962) measured velocities in transparent calcite that were only a small fraction of the elastic wave speed and were not strongly dependent on the applied shear stress. Another difference between slip and twinning is that twinning is polarized while slip is not. Geometry of the lattice tends to prevent twinning shears of equal magnitude and opposite directions on the same plane, while typically slip may initiate in opposite directions on the same plane. In typical crystal plasticity models, the initial resistance to slip is assumed the same in forward and reverse directions, though this assumption is not always warranted in BCC crystals (Vitek 1976; Lee et al. 1999) or in nonmetals such as low-symmetry ceramics (Clayton 2009a, 2010c). Dislocation motion resulting in shear deformation in the opposite direction to the twinning direction on the same set of planes is known as anti-twinning, and is physically possible. However, the mechanical resistance, in terms of shear stress, to anti-twinning, can be several times greater than the resistance to twinning (Paxton et al. 1991).
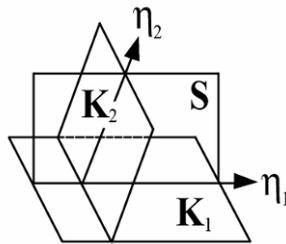
Fig. 8.2 Twin geometry and notation (Christian and Mahajan 1995)

Wedge-shaped elastic twins have been observed experimentally in semi-infinite crystals subjected to concentrated surface forces, for example knife-edge loading. If the region of the parent (matrix) is plastically deformed, then such an induced twin will not be elastic, but will instead remain present in the material upon unloading as a result of the constraint of the surrounding plastically deformed matrix. Thus, elastic twinning appears more common in certain nonmetals such as calcite wherein twinning is much easier than slip, and less common in metals that tend to undergo plastic slip and twinning simultaneously (Cooper 1962).

A geometric depiction of twinning is provided in Fig. 8.2, following the classical notational scheme of Bilby and Crocker (1965) and Christian and Mahajan (1995). The geometry of the twin is characterized by the four twinning elements $\{\mathbf{K}_1, \mathbf{K}_2, \mathbf{\eta}_1, \mathbf{\eta}_2\}$. The surface of composition separating parent and twinned regions of crystal is often called the habit plane and is labeled $\mathbf{K}_1$. The direction of relative shear is $\mathbf{\eta}_1$. The plane $\mathbf{S}$, called the plane of shear, contains both $\mathbf{\eta}_1$ and the normal to $\mathbf{K}_1$. Plane $\mathbf{K}_2$ is called the second undistorted plane, and contains those vectors that are only rotated, but not stretched, by the simple shearing operation associated with twinning. Vector $\mathbf{\eta}_2$, referred to as the conjugate shear direction, is the intersection of planes $\mathbf{S}$ and $\mathbf{K}_2$. A twinning mode can be defined by values of either the pair $\{\mathbf{K}_1, \mathbf{\eta}_2\}$ or the pair $\{\mathbf{K}_2, \mathbf{\eta}_1\}$, though it is customary to specify all four elements plus the magnitude of shear γ^j. When components of $\{\mathbf{K}_1, \mathbf{\eta}_2\}$ in Miller index notation—see Section 3.1.1—consist of rational numbers, the twin is said to be of type I, while when components $\{\mathbf{K}_2, \mathbf{\eta}_1\}$ are rational in Miller index notation, the twin is said to be of type II. When components of all four elements $\{\mathbf{K}_1, \mathbf{K}_2, \mathbf{\eta}_1, \mathbf{\eta}_2\}$ are rational, the twin is said to be compound. Primitive Bravais lattice vectors in the twin and parent in a type I twin are related by either a reflection in $\mathbf{K}_1$ (type Ia) or rotation of 180° about the direction normal to $\mathbf{K}_1$ (type Ib). For a type II twin, the lattice vectors are related by either a rotation of 180° about $\mathbf{\eta}_1$ (type IIa) or a reflection in the plane normal to $\mathbf{\eta}_1$ (type IIb). Mathematically, in Cartesian coordinates, the orthogonal transformations

$$\overline{\mathbf{Q}} = \begin{cases} \mathbf{1} - 2\mathbf{m}_0 \otimes \mathbf{m}_0, & \text{(type Ia)}, \\ 2\mathbf{m}_0 \otimes \mathbf{m}_0 - \mathbf{1}, & \text{(type Ib)}, \\ 2\mathbf{s}_0 \otimes \mathbf{s}_0 - \mathbf{1}, & \text{(type IIa)}, \\ \mathbf{1} - 2\mathbf{s}_0 \otimes \mathbf{s}_0, & \text{(type IIb)} \end{cases} \tag{8.5}$$

relate a primitive Bravais lattice vector in the parent, $\mathbf{A}_i$, to a vector in the twin $\overline{\mathbf{a}}_i$, via $\overline{\mathbf{a}}_i = \overline{\mathbf{Q}}\mathbf{A}_i$, as shown in Fig. 8.1(c) for $i = 1$. A unit vector normal to the habit plane $\mathbf{K}_1$ is denoted by $\mathbf{m}_0$. A unit vector parallel to the shear direction $\mathbf{\eta}_1$ is denoted by $\mathbf{s}_0$. Transformations for types Ib and IIa are rotations or proper orthogonal transformations, while transformations for types Ia and IIb are reflections or improper orthogonal transfor-

mations[2]. All transformation matrices listed in (8.5) will generally have different numerical components. However, in centrosymmetric crystal structures, types Ia and Ib are crystallographically equivalent, and types IIa and IIb are crystallographically equivalent (Christian and Mahajan 1995), since the point group of a centrosymmetric crystal class includes the inversion (see Table A.1 for specifics). In more complex crystal structures without a center of symmetry, the reflection and rotation operations listed in (8.5) all result in different configurations of the atomic structure, and hence four distinct transformation matrices need be considered (i.e., two for each type of twin). In a compound twin in a centrosymmetric crystal of the type shown in Fig. 8.1(c), all four definitions in (8.5) are crystallographically equivalent.

   Alternative (i.e., non-classical) descriptions of twinning kinematics are also possible. For example, Bevis and Crocker (1968) developed a generalized mathematical treatment of twinned lattices that encompasses non-conventional or degenerate twinning modes not addressed by (8.5).

Table 8.1 Representative twin systems in crystals (Christian and Mahajan 1995)

Crystal	$\mathbf{K}_1$	$\mathbf{K}_2$	$\boldsymbol{\eta}_1$	$\boldsymbol{\eta}_2$	$\mathbf{S}$	Shear γ^j	Partial $\mathbf{b}_P$
BCC	$\{112\}$	$\{\bar{1}\bar{1}2\}$	$\langle\bar{1}\bar{1}1\rangle$	$\langle 111\rangle$	$\{1\bar{1}0\}$	$1/\sqrt{2}$	$1/6\langle\bar{1}\bar{1}1\rangle$
FCC	$\{111\}$	$\{11\bar{1}\}$	$\langle 11\bar{2}\rangle$	$\langle 112\rangle$	$\{1\bar{1}0\}$	$1/\sqrt{2}$	$1/6\langle 11\bar{2}\rangle$
HCP	$\{10\bar{1}2\}$	$\{\bar{1}012\}$	$\langle 10\bar{1}\bar{1}\rangle$	$\langle\bar{1}01\bar{1}\rangle$	$\{1\bar{2}10\}$	$\dfrac{c^2/a^2-3}{\sqrt{3}\,c/a}$	$A\langle 10\bar{1}\bar{1}\rangle$*

*$A = [3-(c/a)^2]/[3+(c/a)^2]$

   Table 8.1 lists common twin systems in metallic crystals with cubic and hexagonal structures. The complete twinning elements $\{\mathbf{K}_1, \mathbf{K}_2, \boldsymbol{\eta}_1, \boldsymbol{\eta}_2\}$, the plane of shear $\mathbf{S}$, the magnitude of shear deformation γ^j, and the partial Burgers vector $\mathbf{b}_P$ of dislocations whose collective motion is thought to account for the twinning shear are all listed in Table 8.1. Shear $\gamma^j \geq 0$ is always non-negative by definition. Hence, twinning does not occur on the same plane in opposite directions. Care must be taken to ensure the correct directional sense of twinning is prescribed; Table 8.2 lists individual planes and directions for families of twin systems in Table 8.1.

---

   [2] An orthogonal transformation satisfies $\bar{\mathbf{Q}}^T = \bar{\mathbf{Q}}^{-1}$, with $\det\bar{\mathbf{Q}} = +1$ for a proper transformation and $\det\bar{\mathbf{Q}} = -1$ for an improper transformation. Since matrices in (8.5) are symmetric and orthogonal, $\bar{\mathbf{Q}} = \bar{\mathbf{Q}}^T = \bar{\mathbf{Q}}^{-1} = \bar{\mathbf{Q}}^{-T}$.

All twinning elements are rational for the twin systems listed in Table 8.1; hence all describe compound twins. No atomic shuffles are required for monatomic BCC and FCC crystals undergoing those particular twinning modes listed in Table 8.1. The list of twin systems in Table 8.1 is far from comprehensive, as numerous other systems have been observed in various alloys, polyatomic lattices, and crystal structures of lower symmetry (Schmid and Boas 1950; Christian and Mahajan 1995). Table 8.1 can be compared with Table 3.4 that lists slip systems and full Burgers vectors for dislocation glide in cubic and hexagonal crystal structures.

In hexagonal crystals (labeled HCP in Table 8.1, as in Table 3.4, though the c/a ratio may deviate from the ideal value of 1.633), the direction of shear $\boldsymbol{\eta}_1$ is reversed for ratios of lattice parameters $c^2/a^2 < 3$ and twinning does not occur for $c/a \approx 3^{1/2} \simeq 1.732$, as has been observed experimentally (Christain and Mahajan 1995). For $c^2/a^2 > 3$, twinning occurs when a single crystal is compressed parallel to the c-axis, while for $c^2/a^2 < 3$, twinning occurs when a crystal is stretched in tension parallel to the c-axis.

Table 8.2 Twinning planes and directions

BCC[1]	FCC[2]	HCP[3]
$(\bar{1}\bar{1}2)[111]$	$(111)[11\bar{2}]$	$(10\bar{1}2)[10\bar{1}\bar{1}]$
$(\bar{1}2\bar{1})[111]$	$(111)[1\bar{2}1]$	$(01\bar{1}2)[01\bar{1}\bar{1}]$
$(2\bar{1}\bar{1})[111]$	$(111)[\bar{2}11]$	$(\bar{1}102)[\bar{1}10\bar{1}]$
$(\bar{2}1\bar{1})[\bar{1}\bar{1}1]$	$(\bar{1}\bar{1}1)[2\bar{1}1]$	$(\bar{1}012)[\bar{1}01\bar{1}]$
$(12\bar{1})[\bar{1}\bar{1}1]$	$(\bar{1}\bar{1}1)[\bar{1}21]$	$(0\bar{1}12)[0\bar{1}1\bar{1}]$
$(112)[\bar{1}\bar{1}1]$	$(\bar{1}\bar{1}1)[\bar{1}1\bar{2}]$	$(1\bar{1}02)[1\bar{1}0\bar{1}]$
$(\bar{2}\bar{1}1)[\bar{1}11]$	$(\bar{1}11)[211]$	
$(12\bar{1})[\bar{1}11]$	$(\bar{1}11)[\overline{12}1]$	
$(1\bar{1}2)[\bar{1}11]$	$(\bar{1}11)[\bar{1}1\bar{2}]$	
$(21\bar{1})[1\bar{1}1]$	$(1\bar{1}1)[\bar{2}\bar{1}1]$	
$(\overline{12}\bar{1})[1\bar{1}1]$	$(1\bar{1}1)[121]$	
$(\bar{1}12)[1\bar{1}1]$	$(1\bar{1}1)[1\bar{1}\bar{2}]$	

[1]Subhash et al. (1994)
[2]Van Houtte (1978); Staroselsky and Anand (1998)
[3]Wu et al. (2007)

The partial dislocation for the $(112)[\bar{1}\bar{1}1]$ twinning mode in a BCC crystal can be formed from the dissociation (Hull and Bacon 1984)

$$\frac{1}{2}[\bar{1}\,\bar{1}1] \rightarrow \frac{1}{6}[\bar{1}\,\bar{1}1] + \frac{1}{6}[\bar{1}\,\bar{1}1] + \frac{1}{6}[\bar{1}\,\bar{1}1], \tag{8.6}$$

where only one of the three partials with identical Burgers vector moves at a time in the (112) plane to form the twin, the other two remaining temporarily sessile. According to the pole mechanism theory of Cottrell and Bilby (1951), as an alternative to (8.6), the following reaction is proposed to take place in the context of twin nucleation and growth in BCC crystals:

$$\frac{1}{2}[\bar{1}\,\bar{1}\,\bar{1}] \rightarrow \frac{1}{3}[\bar{1}\,\bar{1}2] + \frac{1}{6}[\bar{1}\,\bar{1}1]. \tag{8.7}$$

The first dislocation on the right side of (8.7) is a sessile pole dislocation normal to the (112) habit plane, while the second is the glissile partial dislocation lying in the (112) plane as listed in Table 8.1.

The partial dislocation typically involved in twinning of FCC crystals is the Shockley partial, which can be produced from the dissociation reaction

$$\frac{1}{2}[10\bar{1}] \rightarrow \frac{1}{6}[11\bar{2}] + \frac{1}{6}[2\,\bar{1}\,\bar{1}]. \tag{8.8}$$

Partial dislocations on the right side of (8.8) enter the double-cross-slip theory of twinning (Pirouz 1987; Lagerlof et al. 2002). In this theory, the full dislocation on the left side of (8.8) is a screw dislocation, the first partial dislocation on the right is a mobile twinning partial on a (111) plane as listed in Table 8.1, and the second dislocation on the right is sessile.

Unstressed twinned regions of the crystal far from internal boundaries or defects possess the same strain energy density as the unstressed parent (James 1981; Zanzotto 1996); hence, twinning shears are said to be energy invariant. However, the local strain energy density is increased relative to that of a perfect lattice in the vicinity of twin boundaries as a result of non-zero stacking fault or twin boundary energies. Mechanical work done during deformation twinning is dissipative, resulting from defect motion associated with shearing. Possible energy storage is associated only with defects left behind in the crystal, for example those comprising the twin boundary. From continuum thermomechanical considerations, the driving force for twin propagation is the resolved shear stress on the surface of composition (e.g., the habit plane) in the direction of twinning shear, as will be demonstrated explicitly in Section 8.2.3. The resistance to deformation twinning is typically modeled analogously to slip, that is, twinning proceeds when the resolved stress attains a critical value that may depend on temperature (Lagerlof et al. 1994; Kalidindi 1998; Staroselsky and Anand 2003). However, reservations regarding the validity of a Schmid-type law for twinning have been forwarded (Christian and Mahajan 1995). With accumulated slip and deformation twinning, strain hardening of the crystal may take place via interactions between different twins in the crys-

tal, interactions among different slip systems, and interactions between mobile dislocations and twins. For example, twin boundaries may serve as barriers to dislocation glide and hence twin propagation may block slip systems that are not coplanar with a given twin. Twins may also nucleate cracks, and vice-versa (Christian and Mahajan 1995). Vacancy or void formation is also common in some kinds of twinning (Seeger 2007). Detwinning, i.e., restoration of the twinned lattice to its original orientation, is possible, though is often more applicable to phase transformation phenomena (Bhattacharya 1991) and less applicable to mechanical twinning deemed here as thermodynamically irreversible. In some ionic crystals such as calcite (Kaga and Gilman 1969) and in some metals such as Mg (Proust et al. 2009), stress-induced detwinning has been observed to occur readily during strain path changes, without a phase transformation.

The mechanics of twinning can be described, in part, in the context of geometrically nonlinear elasticity. Let two regions of the crystal, denoted by subscripts 1 and 2 in what follows, be separated by a surface Σ across which displacements of the material are continuous but gradients of displacement are not. James (1981) calls this a surface of composition, which need not be planar, though it does correspond to the habit plane $\mathbf{K}_1$ in the traditional description of mechanical twinning (Bilby and Crocker 1965). Let $\mathbf{F}^- = \partial \mathbf{x}_1(\Sigma)/\partial \mathbf{X}$ and $\mathbf{F}^+ = \partial \mathbf{x}_2(\Sigma)/\partial \mathbf{X}$ denote constant limiting values of deformation gradients in each region the vicinity of surface Σ, where $\mathbf{x}_1(X,t)$ and $\mathbf{x}_2(X,t)$ are continuously differentiable coordinates of the material in parent and twin respectively, and where $\mathbf{X}$ are reference coordinates of the original, untwinned crystal. Requiring that volumes and masses remain positive implies that $\det \mathbf{F}^- > 0$ and $\det \mathbf{F}^+ > 0$. Let $\mathbf{m}_0$ be a unit normal vector to Σ, pointing from the – side to the + side. The compatibility requirement that the interface be coherent (i.e., continuous coordinates $\mathbf{x}_1(\Sigma) = \mathbf{x}_2(\Sigma)$ along the surface of composition) necessitates that Hadamard's jump conditions apply (James 1981; Bhattacharya 1991):

$$\llbracket \mathbf{F} \rrbracket = \mathbf{F}^+ - \mathbf{F}^- = \overline{\mathbf{a}} \otimes \mathbf{m}_0, \quad \mathbf{F}^+ = \mathbf{F}^- + \gamma^j \overline{\mathbf{s}} \otimes \mathbf{m}_0, \qquad (8.9)$$

where γ^j is a scalar magnitude of the twinning deformation, $\overline{\mathbf{s}} = \overline{\mathbf{a}}/\gamma^j$ is a unit vector, and $\hat{\mathbf{Q}}$ in (8.9) is a proper orthogonal transformation differing from the unit tensor[3] (i.e., $\hat{\mathbf{Q}} \neq \mathbf{1}$). Treating $\mathbf{F}^-$ and $\mathbf{F}^+$ as elastic de-

---

[3] When $\hat{\mathbf{Q}} = \mathbf{1}$ then $\mathbf{F}^+ = \mathbf{F}^- \breve{\mathbf{M}}$ for some matrix $\breve{\mathbf{M}} \in \mathbf{H}$. In that case, the elastic response (e.g., the stress state) of the twin is indistinguishable from that of the parent when each are subjected to the same further deformation, and the twin is said to be a false twin (James 1981). True twins satisfy (8.9) and demonstrate dif-

formations in strain energy density function (8.2) for illustrative purposes[4], consider the conditions $\psi(\mathbf{F}^+) = \psi(\hat{\mathbf{Q}}\mathbf{F}^-\breve{\mathbf{H}}) = \psi(\mathbf{F}^-)$, meaning that strain energy densities in the twin and parent regions are presumed identical in this particular case.   Hence, in addition to (8.9), it follows that $\mathbf{F}^+ = \hat{\mathbf{Q}}\mathbf{F}^-\breve{\mathbf{H}}$, where $\breve{\mathbf{H}} \in \mathbf{H}$ is an energy invariant transformation, not necessarily an orthogonal tensor (James 1981). Choosing a single global Cartesian coordinate system, and assuming that $\breve{\mathbf{H}}$ does not induce volume changes (i.e., $\breve{\mathbf{H}}$ is unimodular with $\det \breve{\mathbf{H}} = 1$, since the converse assertion would permit the strain energy of a sample of fixed mass to remain constant as the volume of the sample is increased without bound), the following identities apply[5]:

$$\det \mathbf{F}^+ = \det(\hat{\mathbf{Q}}\mathbf{F}^-\breve{\mathbf{H}}) = \det \mathbf{F}^- = \det(\mathbf{F}^- + \overline{\mathbf{a}} \otimes \mathbf{m}_0)$$
$$= \det \mathbf{F}^- \det(\mathbf{1} + \gamma^j (\mathbf{F}^-)^{-1}\overline{\mathbf{s}} \otimes \mathbf{m}_0) = \det \mathbf{F}^-[1 + \gamma^j \langle \mathbf{s}_0, \mathbf{m}_0 \rangle].$$

(8.10)

Since $\det \mathbf{F}^- > 0$ and $\gamma^j > 0$, it follows from (8.10) that the pull back of $\overline{\mathbf{s}}$ must be orthogonal to unit normal $\mathbf{m}_0$ in the reference configuration:

$$\langle (\mathbf{F}^-)^{-1}\overline{\mathbf{s}}, \mathbf{m}_0 \rangle = \langle \mathbf{s}_0, \mathbf{m}_0 \rangle = 0, \ \mathbf{s}_0 = (\mathbf{F}^-)^{-1}\overline{\mathbf{s}}. \quad (8.11)$$

When region 1 (parent) is taken as a perfect reference lattice with $\mathbf{F}^- = \mathbf{1}$, then $\mathbf{s}_0 = \overline{\mathbf{s}}$ and $\langle \overline{\mathbf{s}}, \mathbf{m}_0 \rangle = 0$. Since $\overline{\mathbf{s}} \perp \mathbf{m}_0$, $\mathbf{F}^+ = \mathbf{1} + \gamma^j \overline{\mathbf{s}} \otimes \mathbf{m}_0$ is a simple shear. In that case, $\mathbf{F}^+ = \hat{\mathbf{Q}}\breve{\mathbf{H}}$ is also a simple shear, possibly of large magnitude, that shifts the perfect crystal to another minimum energy configuration, with the strain energy density of this configuration equivalent to that of the (original) parent. The associated strain energy density function can be interpreted as a multi-well potential, with global minima corresponding to conditions $\psi(\mathbf{1}) = \psi(\hat{\mathbf{Q}}\breve{\mathbf{H}}) = 0$. The preceding treatment

---

ferent responses, for example anisotropic elastic constants defined with respect to a global coordinate system will differ on either side of the twin boundary.

[4] A twinned crystal remains elastic only when defect (i.e., dislocation) motion within the twin and surrounding material does not occur (Christian and Mahajan 1995). In many cases, elasticity theory may apply (Parry 1980; James 1981) to describe the reversible response of a crystal that has already twinned. In other cases, dislocation plasticity may render application of elasticity alone inappropriate. In the theory developed in Section 8.2, twin propagation itself is not regarded as an elastic deformation mechanism, but rather a thermodynamically irreversible process dictated by collective motion of partial dislocations and atomic shuffles.

[5] Identities $\det \mathbf{A} \det \mathbf{B} = \det(\mathbf{AB})$ and $\det(\mathbf{1} + \mathbf{a} \otimes \mathbf{b}) = 1 + \mathbf{a} \cdot \mathbf{b}$ for two matrices $\mathbf{A}$ and $\mathbf{B}$ and two vectors $\mathbf{a}$ and $\mathbf{b}$ are used. Recall also that matrix $\mathbf{A}$ is said to be unimodular when $\det \mathbf{A} = \pm 1$.

does not account for any (surface) energy associated with defects along the boundary of the twin, which can be reflected in continuum theories via augmentation of the free energy function with internal state variables. Recall also that the preceding analysis restricts the boundary to be coherent, in contrast to more general treatments permitting discontinuous displacements across interfaces that may occur in some kinds of phase transformations or in solids with other kinds of defects (Cermelli and Gurtin 1994).

8.2 Crystal Plasticity with Twins and Inelastic Volume Changes

A constitutive framework for crystals undergoing large thermoelastic, plastic, and twinning deformations is developed in what follows. The treatment of Section 8.2 extends those of geometrically nonlinear crystal plasticity of Sections 3.2.6 and 6.3 to incorporate kinematics, mechanics, thermodynamics, and kinetics of twinning. Residual elastic volume changes discussed in Sections 7.2.4-7.2.7 are also incorporated in the model framework of Section 8.2, as are geometrically necessary dislocations and statistically stored dislocations of Section 3.3.2. Plastic deformation is limited to that resulting from dislocation glide, and twinning deformation is limited to mechanical twinning.

8.2.1 Kinematics

Deformation gradient $\mathbf{F}(X,t)$ for an element of crystalline material, as defined in (2.112), is decomposed multiplicatively into the following series of terms:

$$\mathbf{F} = \mathbf{F}^{\mathbf{E}}\mathbf{F}^{\mathbf{I}}\mathbf{F}^{\mathbf{W}}\mathbf{F}^{\mathbf{P}} = \mathbf{F}^{\mathbf{E}}\overline{\mathbf{F}} = \mathbf{F}^{\mathbf{L}}\hat{\mathbf{F}} = \mathbf{F}^{\mathbf{E}}\overline{\mathbf{F}}^{\mathbf{W}}\mathbf{F}^{\mathbf{P}} , \tag{8.12}$$

with the notation

$$\mathbf{F}^{\mathbf{L}} = \mathbf{F}^{\mathbf{E}}\overline{J}^{1/3}, \qquad \overline{\mathbf{F}} = \overline{\mathbf{F}}^{\mathbf{W}}\mathbf{F}^{\mathbf{P}}, \qquad \hat{\mathbf{F}} = \mathbf{F}^{\mathbf{W}}\mathbf{F}^{\mathbf{P}},$$
$$\mathbf{F}^{\mathbf{I}} = \overline{J}^{1/3}\mathbf{1}, \qquad \overline{\mathbf{F}}^{\mathbf{W}} = \overline{J}^{1/3}\mathbf{F}^{\mathbf{W}}. \tag{8.13}$$

Elastic deformation $\mathbf{F}^{\mathbf{E}}$ accounts for recoverable thermoelastic deformation, as discussed in Section 8.1.1, and also includes any rigid body rotation of the element. Spherical tensor $\mathbf{F}^{\mathbf{I}}$ accounts for residual elastic volume changes associated with defects. Specifically, such volume changes are addressed by the Jacobian determinant $\overline{J}$, as discussed in Chapter 7. Plastic deformation $\mathbf{F}^{\mathbf{P}}$ accounts for lattice-preserving slip resulting from dislocation glide, as discussed in Section 8.1.2. Contributions to the de-

formation gradient from twinning shears are addressed by the term $\mathbf{F^W}$. (The W superscript is chosen to denote contributions from twinning rather than the T superscript, to avoid confusion with the transpose (2.125)). The total irreversible deformation is $\bar{\mathbf{F}}$. The total elastic lattice deformation (recoverable and residual) is denoted by $\mathbf{F^L} = \mathbf{F^E}\mathbf{F^I} = \mathbf{F^E}\bar{J}^{1/3}$, and the total deformation resulting from defect motion (i.e., both dislocation glide and twinning) is denoted by $\hat{\mathbf{F}} = \mathbf{F^W}\mathbf{F^P}$.

Residual elastic deformation $\mathbf{F^I}$ arising from distributed defects such as dislocation lines follows from the assertion that in continuum nonlinear elasticity, the average strain of a body containing residual stress fields arising from internal displacement discontinuities need not vanish even if traction on its external surfaces vanishes (Toupin and Rivlin 1960). Presently, only volume changes ($\bar{J}$) are considered, e.g., corresponding to random defect distributions imparting no preferred directions in average residual elastic strains, though shape changes are not precluded in the general treatment of Section 7.2.3, specifically (7.31), (7.37), and (7.41). The relationship between $\bar{J}$ and defect densities is given later in Section 8.2.4, implementing earlier derivations of Section 7.2.4. In the present context, $\mathbf{F^P}$ and $\mathbf{F^W}$ account for isochoric (shape) deformations resulting from respective motions of slip dislocations and twinning partials, while $\bar{J}$ accounts for volume changes resulting from the residual stress fields of the defects themselves.

In the model developed in the present Section, individual twins within the volume element of crystal are not modeled explicitly, nor are shapes and sizes of twinned regions. Rather, $\mathbf{F^W}$ accounts for the sum of shears resulting from evolving volume fractions of the material occupying each twin system (Chin et al. 1969; Kalidindi 1998). In this sense, $\mathbf{F^W}$ is a kind of average irreversible shape deformation acting over the volume element of crystal. Geometries of individual twin boundaries are likewise not represented, but the total twin boundary area density per unit volume is represented with an internal state variable. The resolution of twinning in Section 8.2 is thus comparable to that of slip in crystal plasticity of Section 6.3, wherein velocities of individual dislocations are not resolved explicitly, but the cumulative shearing on each slip system results in plastic deformation $\mathbf{F^P}$. Line densities of dislocations per unit volume are also represented by internal state variables.

Introduced next are sets of contravariant and covariant vectors denoting directions and planes, respectively, for slip and twinning. When referred to the reference lattice prior to any reorientation by twinning, these are de-

noted by $\{\mathbf{s}_0^i, \mathbf{m}_0^i\}$ for each slip system i, and $\{\mathbf{s}_0^j, \mathbf{m}_0^j\}$ for each twin system j. The total number of slip systems is denoted by n, and the total number of twin systems is denoted by w. Recall that for metallic crystals of high symmetry, typical slip systems are listed in Table 3.4, and typical twin systems are listed in Table 8.1, all in Miller index notation. Reference directions and plane normals are all of unit length, and each pair of contravariant shear direction and covariant plane normal is orthogonal:

$$\left\langle \mathbf{s}_0^i, \mathbf{m}_0^i \right\rangle = 0, \; \left| \mathbf{s}_0^i \right| = \left| \mathbf{m}_0^i \right| = 1, \; (\forall i = 1, \dots n);$$
$$\left\langle \mathbf{s}_0^j, \mathbf{m}_0^j \right\rangle = 0, \; \left| \mathbf{s}_0^j \right| = \left| \mathbf{m}_0^j \right| = 1, \; (\forall j = 1, \dots w). \tag{8.14}$$

During the course of twinning deformation, one or more parts (i.e., twins) of the volume element of crystal undergoes a rotation relative to the parent. In a volume fraction of the crystal undergoing twinning via mode j, slip directions and slip plane normals transform in the reference configuration according to the usual rules for contravariant and covariant vectors:

$$\mathbf{s}_{0j}^i = \overline{\mathbf{Q}}^j \mathbf{s}_0^i, \; \mathbf{m}_{0j}^i = \mathbf{m}_0^i \overline{\mathbf{Q}}^{jT}, \; (\forall i = 1, \dots n; \; \forall j = 1, \dots w), \tag{8.15}$$

where $\overline{\mathbf{Q}}^j$ is the reflection or rotation found from (8.5) corresponding to particular twin system j; e.g., if j is a type Ia twin, $\overline{\mathbf{Q}}^j = \mathbf{1} - 2\mathbf{m}_0^j \otimes \mathbf{m}_0^j$, or if j is a type IIa twin, $\overline{\mathbf{Q}}^j = 2\mathbf{s}_0^j \otimes \mathbf{s}_0^j - \mathbf{1}$. Notice from (8.15) that, within each twin volume, updated slip directions $\mathbf{s}_{0j}^i$ and slip plane normals $\mathbf{m}_{0j}^i$ remain orthogonal and of unit length for each i, since from (8.14),

$$\left\langle \mathbf{s}_{0j}^i, \mathbf{m}_{0j}^i \right\rangle = \left\langle \overline{\mathbf{Q}}^j \mathbf{s}_0^i, \mathbf{m}_0^i \overline{\mathbf{Q}}^{jT} \right\rangle = \overline{Q}_{.B}^{jA} s_0^{iB} m_{0C}^i \overline{Q}_{.A}^{j-1C} = s_0^{iA} m_{0A}^i = 0. \tag{8.16}$$

For simplicity, successive twinning (including detwinning as a particular example) is not considered; the present theory can readily be extended to address such phenomena via addition of appropriate kinematics and kinetics. Hence, secondary twins that could form within already twinned regions, leading to reorientation of sets $\{\mathbf{s}_0^j, \mathbf{m}_0^j\}$, are not represented here. Further reorientation of transformed directors in (8.15) is likewise prohibited once a twin is fully formed. Rotations (8.15) do not apply to the volume of crystal comprising the parent. Elastic twinning phenomena are also not addressed in the present theory.

Plastic deformation $\mathbf{F}^{\mathbf{P}}$ and twinning deformation $\mathbf{F}^{\mathbf{W}}$ do not directly alter directions associated with slip and twinning. The former is lattice-preserving, as discussed in Section 8.1.2, while the latter only affects lattice orientation indirectly via (8.15) and evolution of the twin volume frac-

tion for each system j to be discussed later. However, thermoelastic deformation and residual elastic volume change do affect the directors[6]:

$$\left.\begin{array}{ll} \mathbf{s}^i = \mathbf{F}^{\mathbf{L}}\mathbf{s}_0^i, & \mathbf{m}^i = \mathbf{m}_0^i\mathbf{F}^{\mathbf{L}-1} \\ \overline{\mathbf{s}}_0^i = \overline{J}^{1/3}\mathbf{s}_0^i, & \overline{\mathbf{m}}_0^i = \mathbf{m}_0^i\overline{J}^{-1/3} \end{array}\right\}(\forall i=1,...n \in \text{ parent});$$

$$\left.\begin{array}{ll} \mathbf{s}_j^i = \mathbf{F}^{\mathbf{L}}\mathbf{s}_{0j}^i, & \mathbf{m}_j^i = \mathbf{m}_{0j}^i\mathbf{F}^{\mathbf{L}-1} \\ \overline{\mathbf{s}}_{0j}^i = \overline{J}^{1/3}\mathbf{s}_{0j}^i, & \overline{\mathbf{m}}_{0j}^i = \mathbf{m}_{0j}^i\overline{J}^{-1/3} \end{array}\right\}(\forall i=1,...n \in \text{ twins } j=1,...w); \quad (8.17)$$

$$\left.\begin{array}{ll} \mathbf{s}^j = \mathbf{F}^{\mathbf{L}}\mathbf{s}_0^j, & \mathbf{m}^j = \mathbf{m}_0^j\mathbf{F}^{\mathbf{L}-1} \\ \overline{\mathbf{s}}_0^j = \overline{J}^{1/3}\mathbf{s}_0^j, & \overline{\mathbf{m}}_0^j = \mathbf{m}_0^j\overline{J}^{-1/3} \end{array}\right\}(\forall j=1,...w \in \text{ parent}).$$

Figure 8.3 depicts the physics underlying (8.12)-(8.17) for an element of crystal with a single slip system and a single twin. Multiplicative decomposition (8.12) implies a series of configurations of the material element. The reference configuration is labeled B_0 with corresponding coordinates **X**, the spatial configuration is labeled B with corresponding coordinates **x**, and the elastically unloaded intermediate configuration is labeled $\overline{B}$, as in Fig. 7.1 of Chapter 7. Since $\mathbf{F}^{\mathbf{E}-1}$ and $\overline{\mathbf{F}}$ are in general not integrable, continuous coordinates spanning anholonomic configuration $\overline{B}$ do not exist, following arguments in Sections 2.8 and 3.2.2. However, elastic and inelastic deformations act as tangent mappings between configurations via $\mathbf{F}^{\mathbf{E}}:T\overline{B} \to TB$ and $\overline{\mathbf{F}}:TB_0 \to T\overline{B}$. In Fig. 8.3, mappings $\overline{\mathbf{F}}^{\mathbf{W}}$ and $\mathbf{F}^{\mathbf{P}}$ constituting $\overline{\mathbf{F}}$ cannot be separately resolved because of the implicit effect of twinning on the orientation of the reference lattice. Another intermediate configuration, not shown in Fig. 8.3, is labeled $\tilde{B}$, attained via the tangent mappings $\mathbf{F}^{\mathbf{L}}:T\tilde{B} \to TB$ and $\hat{\mathbf{F}}:TB_0 \to T\tilde{B}$.

---

[6] The effect of $\overline{J}$ on the slip director vectors and slip plane normal covectors was omitted in earlier work (Clayton 2009a).
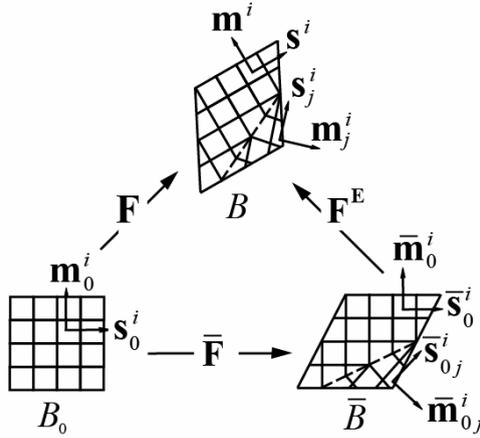
Fig. 8.3 Deformations and slip system geometry for crystal element deforming by elasticity, slip, and twinning

The spatial velocity gradient of (2.176) is expanded via application of the product rule, (8.12), and (8.13) as

$$\mathbf{L} = \dot{\mathbf{F}}\mathbf{F}^{-1}$$

$$= \dot{\mathbf{F}}^{\mathbf{E}}\mathbf{F}^{\mathbf{E}-1} + \mathbf{F}^{\mathbf{E}}\dot{\mathbf{F}}^{\mathbf{W}}\mathbf{F}^{\mathbf{W}-1}\mathbf{F}^{\mathbf{E}-1} + \mathbf{F}^{\mathbf{E}}\mathbf{F}^{\mathbf{W}}\dot{\mathbf{F}}^{\mathbf{P}}\mathbf{F}^{\mathbf{P}-1}\mathbf{F}^{\mathbf{W}-1}\mathbf{F}^{\mathbf{E}-1} + (1/3)\dot{\overline{JJ}}^{-1}\mathbf{1}. \tag{8.18}$$

The inelastic velocity gradient referred to configuration $\overline{B}$ is

$$\dot{\overline{\mathbf{F}}}\overline{\mathbf{F}}^{-1} = \dot{\mathbf{F}}^{\mathbf{W}}\mathbf{F}^{\mathbf{W}-1} + \mathbf{F}^{\mathbf{W}}\dot{\mathbf{F}}^{\mathbf{P}}\mathbf{F}^{\mathbf{P}-1}\mathbf{F}^{\mathbf{W}-1} + (1/3)\dot{\overline{JJ}}^{-1}\mathbf{1}$$

$$= \mathbf{L}^{\mathbf{W}} + \overline{\mathbf{L}}^{\mathbf{P}} + (1/3)\dot{\overline{JJ}}^{-1}\mathbf{1}, \tag{8.19}$$

where

$$\mathbf{L}^{\mathbf{W}} = \dot{\mathbf{F}}^{\mathbf{W}}\mathbf{F}^{\mathbf{W}-1} = \underbrace{\sum_{j=1}^{w} \dot{f}^{j}\gamma^{j}\overline{\mathbf{s}}_{0}^{j} \otimes \overline{\mathbf{m}}_{0}^{j}}_{\text{twinning in parent crystal}} \tag{8.20}$$

results from twinning shears, and

$$\overline{\mathbf{L}}^{\mathbf{P}} = \mathbf{F}^{\mathbf{W}}\mathbf{L}^{\mathbf{P}}\mathbf{F}^{\mathbf{W}-1} = \underbrace{(1-f_{T})\sum_{i=1}^{n} \dot{\gamma}^{i}\overline{\mathbf{s}}_{0}^{i} \otimes \overline{\mathbf{m}}_{0}^{i}}_{\text{slip in parent crystal}} + \underbrace{\sum_{j=1}^{w}\left(f^{j}\sum_{i=1}^{n} \dot{\gamma}_{j}^{i}\overline{\mathbf{s}}_{0j}^{i} \otimes \overline{\mathbf{m}}_{0j}^{i} \right)}_{\text{slip in twinned crystal}} \tag{8.21}$$

accounts for slip in the parent and in twinned regions. The usual plastic velocity gradient is written $\mathbf{L}^{\mathbf{P}} = \dot{\mathbf{F}}^{\mathbf{P}}\mathbf{F}^{\mathbf{P}-1}$, as in (3.58). In (8.20), $\gamma^{j} > 0$ is the predefined shear deformation associated with twin system j, a positive scalar that is fixed for all twins belonging to a given family of twin systems. Recall that magnitudes of γ^{j} are listed in Table 8.1 for BCC, FCC,

and hexagonal crystal structures. In (8.21), $\dot{\gamma}^i$ is the slip rate on system i in the parent, and $\dot{\gamma}^i_j$ is the slip rate on system i within reoriented twin fraction j. The volume fraction of crystal occupied by twin j, e.g., measured per unit volume in configuration $\bar{B}$, is labeled by scalar $f^j \geq 0$, with time rate $\dot{f}^j$ (Chin et al. 1969; Van Houtte 1978). The total volume fraction of twinned crystal is $f_T = \sum_{j=1}^{w} f^j$, subject to restriction $0 \leq f_T \leq 1$. Since detwinning is not considered in the present theory, $\dot{f}^j \geq 0$. In the inner sum within the rightmost term of (8.21), slip directors and plane normals in twinned regions are obtained from (8.15), where the particular form of rotation or reflection $\bar{\mathbf{Q}}^j$ corresponds to twin with associated volume fraction f^j in the outer sum. Because twinning is isochoric (see (8.22)), f^j is also equivalent to the mass fraction of an element of material occupied by twin system j.

Since for each slip or twin system, shear directions and plane normals are orthogonal,

$$\dot{J}^W = J^W \text{tr}(\mathbf{L}^W) = 0 \Rightarrow J^W = 1, \; J^P \text{tr}(\bar{\mathbf{L}}^P) = 0 \Rightarrow J^P = 1, \quad (8.22)$$

upon assuming that at $t = 0$, $\mathbf{F}^W = \mathbf{1}$ and $\mathbf{F}^P = \mathbf{1}$. Thus, (8.20)-(8.22) properly reflect the isochoric nature of slip and twinning, and together with (8.12) and (8.13), require that all volume changes be accommodated thermoelastically via J^E and/or by defect generation via $\bar{J}$, such that

$$J = \sqrt{g/G} \det \mathbf{F} = \sqrt{g/G} \det \mathbf{F}^E \det \bar{\mathbf{F}} = J^E \bar{J} = J^L. \quad (8.23)$$

When $\bar{J} = 1$ and $\dot{f}^j = 0$ for all j, then $\mathbf{F}^W = \mathbf{1}$, $\mathbf{F}^E = \mathbf{F}^L$, $\bar{\mathbf{F}} = \mathbf{F}^P$, and $\mathbf{L}^P = \bar{\mathbf{L}}^P$ in (8.21) reduces to its usual definition from crystal plasticity theory, (3.120). In this situation, all inelastic deformation occurs via slip, $\bar{\mathbf{F}}$ is lattice-preserving, and slip directors and slip plane normals remain unchanged between configurations B_0 and $\bar{B}$. On the other hand, when twinning does takes place, $\mathbf{F}^W$ does not act as a true elastic lattice deformation in the sense of (3.17), (8.1), and Born and Huang (1954). Rather, only that part of the lattice within the twinned volume undergoes a transformation, and this transformation occurs via improper rotation (8.15) and does not include any stretch of the lattice directors, even though shearing associated with $\mathbf{F}^W$ involves both stretch and rotation.

Extending (3.217)-(3.222), defect content in the crystal is measured, in part, by the second-order, two-point geometrically necessary dislocation tensor $\boldsymbol{\alpha}_0(X,t)$ satisfying

$$\tilde{B}^{\alpha} = -\int_{c} F^{L-1\alpha}_{\quad .a} dx^{a} = -\int_{C} \hat{F}^{\alpha}_{.A} dX^{A} = \int_{A} \alpha_{0}^{\alpha A} N_{A} dA \,, \qquad (8.24)$$

where $\tilde{B}^{\alpha}$ are components of a total Burgers vector associated with circuit c in the spatial frame or circuit C in the reference frame, A is the area enclosed by C with unit normal N_{A}, ε^{ABC} are components of permutation tensor (2.64), and

$$\alpha_{0}^{\alpha A} = \varepsilon^{ABC} \hat{F}^{\alpha}_{.B,C} = \varepsilon^{ABC} \hat{F}^{\alpha}_{[.B,C]} = \varepsilon^{ABC} \hat{F}^{\alpha}_{[B;C]} = \varepsilon^{ABC} \hat{F}^{\alpha}_{[B:C]} \,. \qquad (8.25)$$

Stokes's theorem of Section 2.7.2 is used to convert from the line integral to the area integral in the third equality of (8.24). Then from (8.12), (8.13), and the product rule,

$$\alpha_{0}^{\alpha A} = \varepsilon^{ABC} \hat{F}^{\alpha}_{.B,C} = \underbrace{\varepsilon^{ABC} F^{W\alpha}_{\quad .\beta} F^{P\beta}_{\quad .B,C}}_{\text{slip gradients}} + \underbrace{\varepsilon^{ABC} F^{W\alpha}_{\quad .\beta,C} F^{P\beta}_{\quad .B}}_{\text{twin gradients}} \,. \qquad (8.26)$$

Contributions of plastic slip gradients to the geometrically necessary dislocation density tensor, corresponding to the first term following the second equality in (8.26), are well documented in the continuum theory of dislocations (Ashby 1970; Teodosiu 1970; Fleck et al. 1994; Arsenlis and Parks 1999; Voyiadjis and Abu Al-Rub 2005, 2007; Rezvanian et al. 2007), as discussed at length in Section 3.3.2. The second term in the sum on the right in (8.26) arises from gradients of twinning deformation, for example gradients of twin volume fractions arising during propagation of tapered twins (Scott and Orr 1983; Christian and Mahajan 1995); the contribution to the dislocation density tensor in this context would be partial dislocations at interfaces between the twin and parent or at interfaces between intersecting twins (Kosevich and Boiko 1971).

Applying Nanson's formula (2.227) to (8.24):

$$\tilde{B}^{\alpha} = \int_{A} \alpha_{0}^{\alpha A} N_{A} dA = \int_{\tilde{a}} \alpha_{0}^{\alpha A} (\hat{J}^{-1} \hat{F}^{\beta}_{.A} \tilde{n}_{\beta}) d\tilde{a} = \int_{\tilde{a}} \hat{\alpha}^{\alpha\beta} \tilde{n}_{\beta} d\tilde{a} \,, \qquad (8.27)$$

a geometrically necessary dislocation tensor referred to intermediate configuration $\tilde{B}$, labeled $\hat{\alpha}$, is found as

$$\hat{\alpha}^{\alpha\beta} = \hat{J}^{-1} \hat{F}^{\beta}_{.A} \alpha_{0}^{\alpha A} = J^{L} F^{L-1\beta}_{\quad .a} \varepsilon^{abc} F^{L\alpha}_{\quad .[b,c]}$$
$$= \tilde{V}^{-1} \int \tilde{b}^{\alpha} \tilde{\xi}^{\beta} dL = \sum_{k} \tilde{\rho}^{k} \tilde{b}^{k\alpha} \tilde{\xi}^{k\beta} \,, \qquad (8.28)$$

where $\hat{J} = J^{W} J^{P} = 1$ by (8.22), and the second equality in (8.28) follows from (3.225). The integral following the third equality in (8.28) is carried out over all dislocation lines of length L, local Burgers vector $\tilde{b}$, and orientation $\tilde{\xi}$ in intermediate volume element $\tilde{V}$. Finally, the final sum on the right of (8.28) is the discrete form of this integral similar to (3.226), where $\tilde{\rho}^{k}$ is the length per unit intermediate volume of dislocation seg-

ments with unit tangent line vector $\tilde{\boldsymbol{\xi}}^k$ and Burgers vector $\tilde{\mathbf{b}}^k$. In (8.24)-(8.28), sufficient smoothness (i.e., differentiability) of $\mathbf{F}^L$, $\mathbf{F}^W$, and $\mathbf{F}^P$ has been assumed. Discontinuities in the deformation gradient of the lattice at the microscale, for example singularities across slipped regions as in (3.85) and jumps in microscopic deformation gradient across twin boundaries as discussed in Section 8.1.3 are not resolved explicitly in the present continuum framework that addresses defects via continuous distributions.

Two non-dimensional internal state variables are introduced to represent energetic changes associated with other kinds of defects in the crystal. The first internal state variable is a measure of the density of statistically stored dislocations (see (3.238)-(3.240)) that accumulate with homogeneous slip,

$$\alpha = b\sqrt{\overline{\rho}_S} \,, \tag{8.29}$$

where b is a scalar magnitude of the Burgers vector—or a constant on the order of a lattice parameter when the crystal exhibits slip on systems with different Burgers vectors—and $\overline{\rho}_S(X,t)$ is the length of such dislocations per unit volume in configuration $\overline{B}$. Statistically stored dislocations include closed loops and dipoles that do not contribute to the total Burgers vector $\tilde{B}^\alpha$ in (8.24). The second internal state variable measures the total density of twin boundaries,

$$\beta = \sqrt{b\overline{\eta}_W} \,, \tag{8.30}$$

with $\overline{\eta}_W(X,t)$ the area of twin boundaries measured per unit volume in configuration $\overline{B}$.

8.2.2 Constitutive Assumptions

Let $\rho(x,t)$ and $\rho_0(X)$ denote the mass density of the solid in current and reference configurations, respectively, related by $\rho_0 = \rho J$ as in (4.10), recalling from (8.23) that $J = J^L$ in the present context. Let

$$\overline{\rho} = \rho J^E = \rho_0 \overline{J}^{-1} \tag{8.31}$$

denote the mass density in configuration $\overline{B}$. The forthcoming thermodynamic analysis is conducted in $\overline{B}$, the intermediate configuration that serves as an evolving reference configuration for the instantaneous thermoelastic response of the crystal, analogous to the role of configuration $\tilde{B}$ in the thermodynamic treatment of finite elastoplasticity in Section 6.1. Because $\mathbf{F}^L = \overline{J}^{1/3}\mathbf{F}^E$, configurations $\tilde{B}$ and $\overline{B}$ differ by the residual elastic volume change $\overline{J}$. When explicit delineation of residual elasticity is

omitted, then $\mathbf{F}^{\mathbf{L}} = \mathbf{F}^{\mathbf{E}}$ and configurations $\tilde{B}$ of Chapter 6 and $\bar{B}$ of Chapter 8 coincide.

The Helmholtz free energy per unit volume in configuration $\bar{B}$ is written as

$$\bar{\Psi} = \bar{\rho}\psi = \bar{J}^{-1}\Psi_0 = J^E\Psi \,, \tag{8.32}$$

where ψ is the free energy per unit mass. The free energy is assumed to exhibit the dependencies

$$\bar{\Psi} = \bar{\Psi}\left(\mathbf{E^E},\theta,\hat{\boldsymbol{\alpha}},\alpha,\beta,\{f^j\},X,\bar{\mathbf{g}}_\alpha\right), \tag{8.33}$$

where $\theta(X,t)$ is the absolute temperature and $\bar{\mathbf{g}}_\alpha(X)$ are coordinate basis vectors on configuration $\bar{B}$. Variables $\hat{\boldsymbol{\alpha}}$, α, and β are respectively related to densities of geometrically necessary dislocations, statistically stored dislocations, and twin boundaries, as discussed in Section 8.2.1. The set $\{f^j\}$ includes each of the twin fractions $j = 1, 2, ...w$, and

$$E_{\alpha\beta}^E = \frac{1}{2}(C_{\alpha\beta}^E - \bar{g}_{\alpha\beta}) = \frac{1}{2}(F^{Ea}_{.\alpha}g_{ab}F^{Eb}_{.\beta} - \bar{g}_{\alpha\beta}) \tag{8.34}$$

is a finite elastic strain tensor associated with the covariant elastic deformation tensor $\mathbf{C^E}$. Components of the metric tensor in anholonomic configuration $\bar{B}$ are denoted by $\bar{g}_{\alpha\beta} = \bar{\mathbf{g}}_\alpha \cdot \bar{\mathbf{g}}_\beta$, and are assumed stationary with respect to time. In agreement with physical arguments of Sections 8.1.2 and 8.1.3, the free energy does not depend explicitly on plastic deformation gradient $\mathbf{F^P}$ or the contribution from twinning shear $\mathbf{F^W}$. Notice that each of the independent state variables entering the function (8.33) is invariant with respect to rigid body motions of the spatial coordinate frame. In particular, the scalars are always invariant and tensors $\mathbf{E^E}$ and $\hat{\boldsymbol{\alpha}}$ have all indicial components referred to intermediate configurations $\bar{B}$ and $\tilde{B}$, respectively.

Dependence of free energy on elastic strain $\mathbf{E^E}$ accounts for energy storage in stretched or misaligned atomic bonds, in association with mechanical stresses. The free energy depends on temperature for the same reasons discussed in Chapters 5 and 6, e.g., to account for specific heat capacity and thermal expansion, among other phenomena. A dependence on $\hat{\boldsymbol{\alpha}}$, α, and β accounts for line, surface, and/or interaction energies of dislocations and twin boundaries. The rationale for inclusion of $\{f^j\}$ in the list of state variables will become clear in Section 8.2.4, wherein effective elastic coefficients of the volume element depend explicitly on volume fractions of twins, with each twin exhibiting its own local anisotropic elastic coefficients. Dependence on X accounts for possibly heterogeneous

material properties, while $\overline{\mathbf{g}}_\alpha$ are included to reflect anisotropy, e.g., elastic constants of the parent dependent upon orientation of the sample of material with respect to a global coordinate system. Analogous functional forms to (8.33) can be written for entropy, stress, and time rates of internal state variables. An expression for the heat flux can also be written, incorporating dependence of temperature gradient. Dependence of the Helmholtz free energy on the temperature gradient has been omitted a priori in (8.33), but such dependence could be included and then eliminated by exercising thermodynamic arguments, as was done in Sections 5.1.2 and 6.1.2.

8.2.3 Thermodynamics

Local forms of the balance of energy and dissipation inequality, each referred to the reference configuration, are given respectively by (4.39) and (4.71), repeated below:

$$\rho_0 \dot{e} = \mathbf{\Sigma} : \dot{\mathbf{E}} - \left\langle \overset{G}{\nabla}, \mathbf{Q} \right\rangle + \rho_0 r, \ \mathbf{\Sigma} : \dot{\mathbf{E}} - \rho_0(\dot{\psi} + \eta\dot{\theta}) - \frac{1}{\theta}\left\langle \overset{G}{\nabla}\theta, \mathbf{Q} \right\rangle \ge 0. \quad (8.35)$$

Recall that $e = \psi + \theta\eta$ is the internal energy per unit mass, with η the entropy per unit mass. The symmetric second Piola-Kirchhoff stress $\mathbf{\Sigma}$ is related to the first Piola-Kirchhoff stress $\mathbf{P}$ and the symmetric Cauchy stress $\mathbf{\sigma}$ by equalities listed in Table 4.1:

$$\Sigma^{AB} = F^{-1A}_{\ \ \ a}P^{aB} = JF^{-1A}_{\ \ \ a}\sigma^{ab}F^{-1B}_{\ \ \ b}. \quad (8.36)$$

The symmetric tensor $\mathbf{E} = (1/2)(\mathbf{F}^T\mathbf{F} - \mathbf{G})$ is the right Cauchy-Green strain of (2.156), $\mathbf{Q}$ is the heat flux vector referred to the reference configuration B_0, and scalar r denotes other heat sources of energy per unit mass. The stress power per unit intermediate volume in configuration $\overline{B}$ can be written, similarly to (6.15), as

$$\overline{J}^{-1}\Sigma^{AB}\dot{E}_{AB} = J^E\sigma^{ab}L_{ab} = (J^E F^{E-1\beta}_{\ \ \ .b}\sigma^{.b}_a F^{Ea}_{\ \ \ .\alpha})(F^{E-1\alpha}_{\ \ \ .e}L^e_{.d}F^{Ed}_{\ \ \ .\beta})$$
$$= \overline{M}^{.\beta}_\alpha \overline{L}^\alpha_{.\beta}, \quad (8.37)$$

where a version of Mandel's stress (Mandel 1974) and symmetric elastic second Piola-Kirchhoff stress are, respectively,

$$\overline{\mathbf{M}} = \mathbf{C}^{\mathbf{E}}\overline{\mathbf{\Sigma}}, \ \overline{\mathbf{\Sigma}} = J^E\mathbf{F}^{\mathbf{E}-1}\mathbf{\sigma}\mathbf{F}^{\mathbf{E}-T}, \quad (8.38)$$

or in indicial notation,

$$\overline{M}^{.\beta}_\alpha = J^E F^{Ea}_{\ \ \ .\alpha}\sigma^{.b}_a F^{E-1\beta}_{\ \ \ .b} = C^E_{\alpha\delta}\overline{\Sigma}^{\delta\beta}, \ \overline{\Sigma}^{\alpha\beta} = J^E F^{E-1\alpha}_{\ \ \ .a}\sigma^{ab}F^{E-1\beta}_{\ \ \ .b}. \quad (8.39)$$

The total velocity gradient of (8.18) pulled back to configuration $\overline{B}$ is

$$\overline{\mathbf{L}} = \mathbf{F}^{E-1}\mathbf{L}\mathbf{F}^{E} = \mathbf{F}^{E-1}\dot{\mathbf{F}}^{E} + \mathbf{L}^{W} + \overline{\mathbf{L}}^{P} + \frac{1}{3\overline{J}}\dot{\overline{J}}\mathbf{1}. \tag{8.40}$$

The time rate of free energy change per unit intermediate configuration volume is, similarly to (6.19),

$$\dot{\overline{\Psi}} = \frac{d}{dt}(\overline{\rho}\psi) = \overline{J}^{-1}\rho_0(\dot{\psi} - \dot{F}^{\alpha}_{.A}\overline{F}^{-1A}_{.\alpha}\psi)$$
$$= \overline{\rho}\dot{\psi} - \overline{\Psi}(\dot{\overline{J}}\overline{J}^{-1} + \dot{J}^{W}J^{W-1} + \overline{L}^{P\alpha}_{.\alpha}) = \overline{\rho}\dot{\psi} - \overline{\Psi}\dot{\overline{J}}\overline{J}^{-1}, \tag{8.41}$$

where (8.22), (8.31), and (8.32) have been used. Following from (8.37), (8.40), and the symmetry of $\overline{\Sigma}$ and $\dot{\mathbf{E}}^{E}$,

$$\overline{M}^{.\beta}_{\alpha}\overline{L}^{\alpha}_{.\beta} = \overline{\Sigma}^{\beta\delta}\dot{E}^{E}_{\delta\beta} + \overline{M}^{.\beta}_{\alpha}L^{W\alpha}_{.\beta} + \overline{M}^{.\beta}_{\alpha}\overline{L}^{P\alpha}_{.\beta} + \frac{1}{3\overline{J}}\dot{\overline{J}}\overline{M}^{.\alpha}_{\alpha}. \tag{8.42}$$

Expanding the rate of free energy $\overline{\Psi}$ of (8.33) using the chain rule (Coleman and Noll 1963; Coleman and Gurtin 1967),

$$\dot{\overline{\Psi}} = \frac{\partial \overline{\Psi}}{\partial \mathbf{E}^{E}} : \dot{\mathbf{E}}^{E} + \frac{\partial \overline{\Psi}}{\partial \theta}\dot{\theta} + \frac{\partial \overline{\Psi}}{\partial \hat{\boldsymbol{\alpha}}} : \dot{\hat{\boldsymbol{\alpha}}} + \frac{\partial \overline{\Psi}}{\partial \alpha}\dot{\alpha} + \frac{\partial \overline{\Psi}}{\partial \beta}\dot{\beta} + \frac{\partial \overline{\Psi}}{\partial f^{j}}\dot{f}^{j}, \tag{8.43}$$

with summation implied over w twin fractions j, the entropy inequality in (8.35) can be written

$$\left(\overline{\Sigma} - \frac{\partial \overline{\Psi}}{\partial \mathbf{E}^{E}}\right) : \dot{\mathbf{E}}^{E} - \left(\overline{N} + \frac{\partial \overline{\Psi}}{\partial \theta}\right)\dot{\theta} + \overline{\Pi} : \left(\mathbf{L}^{W} + \overline{\mathbf{L}}^{P} + \frac{\dot{\overline{J}}}{3\overline{J}}\mathbf{1}\right)$$
$$- \frac{\partial \overline{\Psi}}{\partial \hat{\boldsymbol{\alpha}}} : \dot{\hat{\boldsymbol{\alpha}}} - \frac{\partial \overline{\Psi}}{\partial \alpha}\dot{\alpha} - \frac{\partial \overline{\Psi}}{\partial \beta}\dot{\beta} - \frac{\partial \overline{\Psi}}{\partial f^{j}}\dot{f}^{j} - \frac{1}{\theta}\langle\overline{\nabla}\theta, \overline{\mathbf{q}}\rangle \geq 0. \tag{8.44}$$

As introduced in (8.44), $\overline{N} = \overline{\rho}\eta$ is the entropy per unit intermediate volume, $\overline{\nabla}_{\alpha}\theta = \theta_{,A}\overline{F}^{-1A}_{.\alpha} = \theta_{,a}F^{Ea}_{.\alpha}$ is an anholonomic intermediate temperature gradient similar to (6.6), $\overline{\mathbf{q}} = \overline{J}^{-1}\overline{\mathbf{F}}\mathbf{Q} = J^{E}\mathbf{F}^{E-1}\mathbf{q}$ is the intermediate heat flux similar to (6.7), and

$$\overline{\Pi} = \overline{\mathbf{M}} - \overline{\Psi}\mathbf{1} \tag{8.45}$$

is a (negative) version of Eshelby's elastic energy-momentum tensor (see Section 6.6) pushed forward to configuration $\overline{B}$, similar to (6.33). Following arguments akin to those used in Sections 5.1.2 and 6.1.2, admissible stress-elastic strain and entropy-temperature relations are deduced as

$$\overline{\Sigma}^{\alpha\beta} = \frac{\partial \overline{\Psi}}{\partial E^{E}_{\alpha\beta}}, \quad \overline{N} = -\frac{\partial \overline{\Psi}}{\partial \theta}, \quad \sigma^{ab} = J^{E-1}F^{Ea}_{.\alpha}\frac{\partial \overline{\Psi}}{\partial E^{E}_{\alpha\beta}}F^{Eb}_{.\beta}, \quad \eta = -\frac{1}{\overline{\rho}}\frac{\partial \overline{\Psi}}{\partial \theta}. \tag{8.46}$$

Angular momentum balance (4.26) is satisfied consistently: $\sigma^{ab} = \sigma^{ba}$.

The final term on the left of (8.44) always contributes positively to dissipation upon prescription of a conduction law similar to (6.30):

$$\bar{\mathbf{q}} = -\bar{\mathbf{K}}\bar{\nabla}\theta \,, \ -\langle\bar{\nabla}\theta,\bar{\mathbf{q}}\rangle = \langle\bar{\nabla}\theta,\bar{\mathbf{K}}\bar{\nabla}\theta\rangle \geq 0 \,, \tag{8.47}$$

where $\bar{\mathbf{K}}(X,t)$ is a symmetric and positive semi-definite matrix of thermal conductivity. Applying (8.46) and (8.47),

$$\bar{\mathbf{\Pi}}:\mathbf{L}^{\mathbf{W}} + \bar{\mathbf{\Pi}}:\bar{\mathbf{L}}^{\mathbf{P}} + (1/3)\dot{\bar{J}}J^{-1}\mathrm{tr}(\bar{\mathbf{\Pi}})$$

$$\geq \frac{\partial\bar{\Psi}}{\partial\hat{\mathbf{a}}}:\dot{\hat{\mathbf{a}}} + \frac{\partial\bar{\Psi}}{\partial\alpha}\dot{\alpha} + \frac{\partial\bar{\Psi}}{\partial\beta}\dot{\beta} + \frac{\partial\bar{\Psi}}{\partial f^{j}}\dot{f}^{j} - \frac{1}{\theta}\langle\bar{\nabla}\theta,\bar{\mathbf{K}}\bar{\nabla}\rangle\theta \tag{8.48}$$

is the reduced dissipation inequality. In the absence of temperature gradients (e.g., an adiabatic process), (8.48) requires that the energy dissipated by twinning, slip, and residual volume changes must exceed the rate of energy storage associated with defects, specifically geometrically necessary and statistically stored dislocations, twin boundaries, and twin fractions.

From (8.17)-(8.22) and (8.39), dissipated energies from slip and twinning, respectively, can be written

$$\bar{\mathbf{\Pi}}:\bar{\mathbf{L}}^{\mathbf{P}} = (1-f_T)\sum_{i=1}^{n}\bar{\tau}^{i}\dot{\gamma}^{i} + \sum_{j=1}^{w}\left(f^{j}\sum_{i=1}^{n}\bar{\tau}_{j}^{i}\dot{\gamma}_{j}^{i}\right), \ \bar{\mathbf{\Pi}}:\mathbf{L}^{\mathbf{W}} = \sum_{j=1}^{w}\bar{\tau}^{j}\dot{f}^{j}\gamma^{j} \,, \tag{8.49}$$

where the driving forces are resolved stresses on each twin (habit) plane or slip plane, acting in the direction of shear:

$$\bar{\tau}^{i} = \bar{s}_{0}^{i\alpha}\bar{\Pi}_{\alpha}^{\cdot\beta}\bar{m}_{0\beta}^{i} = J^{E}s^{ia}\sigma_{a}^{\cdot b}m_{\cdot b}^{i} \,, \text{ (slip in parent);}$$

$$\bar{\tau}_{j}^{i} = \bar{s}_{0j}^{i\ \alpha}\bar{\Pi}_{\alpha}^{\cdot\beta}\bar{m}_{0j\beta}^{i} = J^{E}s_{j}^{ia}\sigma_{a}^{\cdot b}m_{jb}^{i} \,, \text{ (slip in twins);} \tag{8.50}$$

$$\bar{\tau}^{j} = \bar{s}_{0}^{j\alpha}\bar{\Pi}_{\alpha}^{\cdot\beta}\bar{m}_{0\beta}^{j} = J^{E}s^{ja}\sigma_{a}^{\cdot b}m_{\cdot b}^{j} \,, \text{ (twinning);}$$

since twinning and slip are isochoric. Resolved shear stress $\bar{\tau}^{i}$ is related to $\tilde{\tau}^{i}$ of crystal plasticity theory introduced in (6.85)-(6.86) by $\tilde{\tau}^{i} = \bar{J}\bar{\tau}^{i}$.

The specific heat capacity at constant elastic strain and internal state variables, measured per unit volume in configuration $\bar{B}$, is introduced as

$$\bar{C}(X,t) = \left.\frac{\partial\bar{E}}{\partial\theta}\right|_{\mathbf{E}^{\mathbf{E}},\hat{\mathbf{a}},\alpha,\beta,\{f^{j}\}} = -\theta\frac{\partial^{2}\bar{\Psi}}{\partial\theta^{2}} \,. \tag{8.51}$$

where (8.46) has been used and $\bar{E} = \bar{\rho}e$ is the internal energy per intermediate volume. Multiplying the first of (8.35) by $\bar{J}^{-1}$, and following a procedure analogous to that of (6.36)-(6.43), the energy balance can be written in the relaxed intermediate configuration $\bar{B}$ as[7]

---

[7] The factor of 3 preceding the term $\theta(\partial\bar{\Psi}/\partial\theta) = -\theta\bar{N}$ in (8.52) was incorrectly omitted in (3.29) and (3.43) of a previous article (Clayton 2009a). This misprint is corrected in (8.52) of the present text.

$$
\underbrace{\bar{C}\dot{\theta}}_{\substack{\text{temperature} \\ \text{change}}} = \underbrace{\bar{\Pi}:\left(\mathbf{L^W}+\bar{\mathbf{L}}^{\mathbf{P}}\right)}_{\text{dissipation from slip and twinning}} + \underbrace{\left(\operatorname{tr}(\bar{\Pi})+3\theta\frac{\partial\bar{\Psi}}{\partial\theta}\right)\frac{\dot{J}}{3\bar{J}}}_{\text{dissipation from defect generation}}
$$

$$
-\underbrace{\theta\bar{\beta}:\dot{\mathbf{E}}^{\mathbf{E}}}_{\substack{\text{thermoelastic} \\ \text{coupling}}} -\underbrace{\left(\frac{\partial\bar{\Psi}}{\partial\hat{\mathbf{a}}}-\theta\frac{\partial^2\bar{\Psi}}{\partial\theta\partial\hat{\mathbf{a}}}\right):\dot{\hat{\mathbf{a}}}}_{\substack{\text{strain energy of geometrically} \\ \text{necessary dislocations}}}
$$

$$
-\underbrace{\left(\frac{\partial\bar{\Psi}}{\partial\alpha}-\theta\frac{\partial^2\bar{\Psi}}{\partial\theta\partial\alpha}\right)\dot{\alpha}}_{\substack{\text{strain energy of statistically} \\ \text{stored dislocations}}} - \underbrace{\left(\frac{\partial\bar{\Psi}}{\partial\beta}-\theta\frac{\partial^2\bar{\Psi}}{\partial\theta\partial\beta}\right)\dot{\beta}}_{\text{surface energy of twin boundaries}}
$$

$$
-\underbrace{\left(\frac{\partial\bar{\Psi}}{\partial f^j}-\theta\frac{\partial^2\bar{\Psi}}{\partial\theta\partial f^j}\right)\dot{f}^j}_{\text{energy of lattice reorientation from twinning}} + \underbrace{\left\langle\hat{\nabla},\bar{\mathbf{K}}\bar{\nabla}\theta\right\rangle}_{\substack{\text{heat} \\ \text{conduction}}} + \underbrace{\bar{\rho}r}_{\substack{\text{heat} \\ \text{supply}}}.
$$

(8.52)

Stress-temperature coefficients in (8.52) are defined according to

$$
\bar{\beta}^{\alpha\beta} = -\frac{\partial^2\bar{\Psi}}{\partial\theta\partial E_{\alpha\beta}^E}\bigg|_{\hat{\mathbf{a}},\alpha,\beta,\{f^j\}}
\tag{8.53}
$$

and the anholonomic covariant derivative in (8.52) is performed similarly to that of (6.38) and (6.39):

$$
\hat{\nabla}_\alpha(.) = \bar{\nabla}_\alpha(.)+\bar{J}^{-1}(.)\bar{F}_{.A}^\beta\bar{\nabla}_\beta(\bar{J}F_{.\alpha}^{-1A})
$$
$$
= (.)_{:A}\bar{F}_{.\alpha}^{-1A}+\bar{J}^{-1}(.)(\bar{J}F_{.\alpha}^{-1A})_{:A}.
\tag{8.54}
$$

Notice that $\hat{\nabla}_\alpha = \bar{\nabla}_\alpha$ when compatibility conditions $\bar{F}_{[A:B]}^\alpha = 0$ apply, in which case Piola's identity (2.146) gives $(\bar{J}F_{.\alpha}^{-1A})_{:A} = (\partial\bar{J}/\partial\bar{F}_{.A}^\alpha)_{:A} = 0$.

8.2.4 Representative Free Energy

A particular form of (8.33) is now introduced for anisotropic single crystals that may undergo large elastic deformations, temperature changes, twinning, and dislocation accumulation. The free energy is decomposed additively as

$$
\bar{\Psi} = \bar{\Psi}^E\left(\mathbf{E^E},\theta,\{f^j\},X,\bar{\mathbf{g}}_\alpha\right)+\bar{\Psi}^R\left(\hat{\mathbf{a}},\alpha,\beta,\theta,X,\bar{\mathbf{g}}_\alpha\right),
\tag{8.55}
$$

where, as in (6.48), $\bar{\Psi}^E$ accounts for the thermoelastic response and $\bar{\Psi}^R$ accounts for residual free energy of lattice defects. As in Section 6.1.3, effects of defect densities besides twin volume fractions on the thermoelastic

energy are neglected, implying that the thermoelastic coefficients do not depend explicitly on dislocation density or twin boundary area.

The thermoelastic energy is expanded in a Taylor series about a reference state characterized by $E_{\alpha\beta}^E = 0$ and $\Delta\theta = \theta - \theta_0$, and here consists of four terms, similarly to (6.49):

$$\bar{\Psi}^E = \frac{1}{2}\bar{\mathbb{C}}^{\alpha\beta\chi\delta} E_{\alpha\beta}^E E_{\chi\delta}^E + \frac{1}{6}\bar{\mathbb{C}}^{\alpha\beta\chi\delta\varepsilon\phi} E_{\alpha\beta}^E E_{\chi\delta}^E E_{\varepsilon\phi}^E$$
$$- \bar{\beta}^{\alpha\beta} E_{\alpha\beta}^E \Delta\theta - \bar{C}\theta\ln\frac{\theta}{\theta_0}.$$

(8.56)

The first term on the right side of (8.56) accounts for materially linear, but geometrically nonlinear, mechanical effects. The second accounts for materially nonlinear elastic effects important at high pressures, and the third accounts for thermoelastic coupling. Constant θ_0 is a positive temperature at which the lattice parameters exhibit their reference values in a defect-free crystal, and the remaining coefficients in (8.56) consist of partial derivatives of the thermoelastic part of the free energy per unit intermediate volume at null elastic strain and at the reference temperature:

$$\bar{\mathbb{C}}^{\alpha\beta\chi\delta} = \left.\frac{\partial^2\bar{\Psi}^E}{\partial E_{\alpha\beta}^E \partial E_{\chi\delta}^E}\right|_{\substack{\mathbf{E}^E=0\\\theta=\theta_0}}, \quad \bar{\mathbb{C}}^{\alpha\beta\chi\delta\varepsilon\phi} = \left.\frac{\partial^3\bar{\Psi}^E}{\partial E_{\alpha\beta}^E \partial E_{\chi\delta}^E \partial E_{\varepsilon\phi}^E}\right|_{\substack{\mathbf{E}^E=0\\\theta=\theta_0}}, \quad (8.57)$$

$$\bar{\beta}^{\alpha\beta} = -\left.\frac{\partial^2\bar{\Psi}^E}{\partial\theta\partial E_{\alpha\beta}^E}\right|_{\substack{\mathbf{E}^E=0\\\theta=\theta_0}}, \quad \bar{C} = -\left(\theta\frac{\partial^2\bar{\Psi}^E}{\partial\theta^2}\right)\bigg|_{\substack{\mathbf{E}^E=0\\\theta=\theta_0}}. \quad (8.58)$$

The usual symmetry relations $\bar{\mathbb{C}}^{\alpha\beta\chi\delta} = \bar{\mathbb{C}}^{(\alpha\beta)(\chi\delta)}$, $\bar{\mathbb{C}}^{\alpha\beta\chi\delta\varepsilon\phi} = \bar{\mathbb{C}}^{(\alpha\beta)(\chi\delta)(\varepsilon\phi)}$, and $\bar{\beta}^{\alpha\beta} = \bar{\beta}^{(\alpha\beta)}$ follow automatically from (8.57) and (8.58). Thermoelastic constants and specific heat constant in (8.58) are particular values of coefficients introduced already in (8.53) and (8.51), respectively. Similarly to (6.52)-(6.55), coefficients in (8.57) and (8.58) are related to those of nonlinear elasticity theory introduced in (5.66) and (5.85) at the same material point X as

$$\bar{\mathbb{C}}^{\alpha\beta\chi\delta} = \bar{J}^{-1}\bar{\mathbb{C}}^{ABCD} g_{.A}^{\alpha} g_{.B}^{\beta} g_{.C}^{\chi} g_{.D}^{\delta}, \quad (8.59)$$

$$\bar{\mathbb{C}}^{\alpha\beta\chi\delta\varepsilon\phi} = \bar{J}^{-1}\bar{\mathbb{C}}^{ABCDEF} g_{.A}^{\alpha} g_{.B}^{\beta} g_{.C}^{\chi} g_{.D}^{\delta} g_{.E}^{\varepsilon} g_{.F}^{\phi}, \quad (8.60)$$

$$\bar{\beta}^{\alpha\beta} = \bar{J}^{-1}\bar{\beta}^{AB} g_{.A}^{\alpha} g_{.B}^{\beta}, \quad (8.61)$$

$$\bar{C} = \bar{\rho}\bar{c} = \bar{J}^{-1}\rho_0\bar{c} = \bar{J}^{-1}\bar{C}_0. \quad (8.62)$$

Since $\dot{\bar{\mathbf{g}}}_\alpha = 0$ and $\dot{\mathbf{G}}_A = 0$ (e.g., see discussion in Section 2.5.1), the shifter $g_{.A}^{\alpha} = \langle\bar{\mathbf{g}}^\alpha, \mathbf{G}_A\rangle$ at X does not depend on time. When residual elastic vol-

ume changes vanish ($\bar{J} = 1$) and when coincident coordinate systems are used in reference and intermediate configurations so that $g^{\alpha}_{.A} = \delta^{\alpha}_{.A}$, numerical values of material coefficients on left and right sides of each of (8.59)-(8.62) are equal. When $\dot{\bar{J}}(X,t) \neq 0$, then coefficients on both sides of (8.59)-(8.62) cannot all be constant for all $t > 0$. If the left sides are taken as constant in time, then the elastic coefficients and specific heat per unit reference volume on the right sides increase with increases in residual volume change. In that case, if the elastic strain is held fixed, an increase in residual elastic volume would have no effect on the measured Cauchy stress $\boldsymbol{\sigma}(x,t)$ or on the intermediate symmetric stress $\bar{\boldsymbol{\Sigma}}$ as will be clear in (8.65) and (8.69), but would affect the stresses $\boldsymbol{\Sigma}(X,t)$ and $\mathbf{P}(X,t)$ referred to the reference configuration, the latter evident from (8.70). Since $\bar{J}$ resulting from dislocations is expected to be very close to unity for most situations, i.e., $\bar{J} - 1 \lesssim 10^{-3}$ for dislocation densities $\lesssim 10^{15}\,\mathrm{m}^{-2}$ as explained in Section 7.2.7, differences among definitions of material coefficients listed in (8.59)-(8.62) will be trivial in such cases, i.e., less than ~0.1% error, and presumably will be much smaller than uncertainties in experimental measurements of such constants.

Possible influences of the dislocation densities ($\hat{\boldsymbol{\alpha}}$ and α) and twin boundaries (β) on the effective elastic moduli that may emerge in crystals at large defect densities (Smith 1953; Clayton and Chung 2006; Chung and Clayton 2007) are precluded by (8.55) since couplings between elastic strain $\mathbf{E}^{\mathbf{E}}$ and defects ($\hat{\boldsymbol{\alpha}}, \alpha, \beta$) are not included. Such effects could be incorporated by generalization of (8.55) if deemed relevant for applications of interest (Clayton et al. 2004a, b), as demonstrated in Section 9.4.6 of Chapter 9. The present assumption that elastic strain and defect densities are decoupled in the free energy would become suspect at large defect densities wherein the residual volume change $\bar{J}$ could have a noticeable effect on elastic and thermal coefficients measured per unit reference volume, i.e., the right sides of (8.59)-(8.62).

In anisotropic solids, tensor-valued coefficients in (8.56) depend upon the orientation of the lattice in configuration $\bar{B}$, via dependence of these coefficients on $\{f^{j}\}$ and $\bar{\mathbf{g}}_{\alpha}$. When twinning takes place, orientations of the original Bravais lattice (parent) and each twinned region differ. A straightforward averaging method is used to define the effective material coefficients for a volume element consisting of the parent and one or more twins. It is assumed that elastic deformation $\mathbf{F}^{\mathbf{E}}$ and elastic strain $\mathbf{E}^{\mathbf{E}}$ act uniformly over the parent and twins comprising this volume element. The

thermoelastic free energy density of (8.55) is thus partitioned into contributions from the parent and each twin:

$$\bar{\Psi}^E = \frac{1}{2}(1-f_T)E^E_{\alpha\beta}\bar{\mathbb{C}}^{\alpha\beta\chi\delta}_0 E^E_{\chi\delta} + \frac{1}{6}(1-f_T)E^E_{\alpha\beta}\bar{\mathbb{C}}^{\alpha\beta\chi\delta\varepsilon\phi}_0 E^E_{\chi\delta}E^E_{\varepsilon\phi}$$
$$- (1-f_T)\bar{\beta}^{\alpha\beta}_0 E^E_{\alpha\beta}\Delta\theta \qquad\qquad (8.63)$$
$$+ \sum_{j=1}^{w} f^j\left(\frac{1}{2}E^E_{\alpha\beta}\bar{\mathbb{C}}^{\alpha\beta\chi\delta}_j E^E_{\chi\delta} + \frac{1}{6}E^E_{\alpha\beta}\bar{\mathbb{C}}^{\alpha\beta\chi\delta\varepsilon\phi}_j E^E_{\chi\delta}E^E_{\varepsilon\phi} - \bar{\beta}^{\alpha\beta}_j E^E_{\alpha\beta}\Delta\theta\right),$$

where $\bar{\mathbb{C}}^{\alpha\beta\chi\delta}_0$, $\bar{\mathbb{C}}^{\alpha\beta\chi\delta\varepsilon\phi}_0$, and $\bar{\beta}^{\alpha\beta}_0$ refer to material constants corresponding to the orientation of the parent lattice relative to the external coordinate system, and where for each twin j (Van Houtte 1978; Kalidindi 1998) the elastic coefficients are mapped from original to twinned orientation via

$$\bar{\mathbb{C}}^{\alpha\beta\chi\delta}_j = \bar{Q}^{j\alpha}_{.\varepsilon}\bar{Q}^{j\beta}_{.\phi}\bar{Q}^{j\chi}_{.\varphi}\bar{Q}^{j\delta}_{.\gamma}\bar{\mathbb{C}}^{\varepsilon\phi\varphi\gamma}_0, \quad \bar{\beta}^{\alpha\beta}_j = \bar{Q}^{j\alpha}_{.\chi}\bar{Q}^{j\beta}_{.\delta}\bar{\beta}^{\chi\delta}_0,$$
$$\bar{\mathbb{C}}^{\alpha\beta\chi\delta\varepsilon\phi}_j = \bar{Q}^{j\alpha}_{.\varphi}\bar{Q}^{j\beta}_{.\gamma}\bar{Q}^{j\chi}_{.\eta}\bar{Q}^{j\delta}_{.\iota}\bar{Q}^{j\varepsilon}_{.\kappa}\bar{Q}^{j\phi}_{.\lambda}\bar{\mathbb{C}}^{\varphi\gamma\eta\iota\kappa\lambda}_0. \qquad (8.64)$$

Components of $\bar{\mathbf{Q}}$ in (8.64) are related to those used in (8.16) by the shifter: $\bar{Q}^{j\alpha}_{.\beta} = \bar{Q}^{jA}_{.B}g^{\alpha}_{.A}g^{B}_{.\beta}$. Since transformation matrix $\bar{\mathbf{Q}}$ always occurs in pairs in even rank coefficients of (8.64), the choice of reflection or rotation in (8.5) is irrelevant; i.e., $\bar{\mathbf{Q}}$ and $-\bar{\mathbf{Q}}$ will give the same updated coefficients in (8.64). The coefficients will differ, however, when computed for a type I versus type II twin, unless of course the twin is compound. The same considerations regarding symmetry of reference material coefficients discussed in Section 5.1.5 and Appendix A hold for referential thermoelastic constants $\bar{\mathbb{C}}^{\alpha\beta\chi\delta}_0$, $\bar{\mathbb{C}}^{\alpha\beta\chi\delta\varepsilon\phi}_0$, and $\bar{\beta}^{\alpha\beta}_0$. To convert symmetry relations in Section 5.1.5 and Appendix A to the present context, reference indices in capital Roman font are replaced with intermediate indices in Greek font.

Stress-strain-temperature relations following from (8.46), (8.55), (8.56), and (8.63) are

$$\bar{\Sigma}^{\alpha\beta} = \bar{\mathbb{C}}^{\alpha\beta\chi\delta}E^E_{\chi\delta} + \frac{1}{2}\bar{\mathbb{C}}^{\alpha\beta\chi\delta\varepsilon\phi}E^E_{\chi\delta}E^E_{\varepsilon\phi} - \bar{\beta}^{\alpha\beta}\Delta\theta$$
$$= (1-f_T)\bar{\mathbb{C}}^{\alpha\beta\chi\delta}_0 E^E_{\chi\delta} + \frac{1}{2}(1-f_T)\bar{\mathbb{C}}^{\alpha\beta\chi\delta\varepsilon\phi}_0 E^E_{\chi\delta}E^E_{\varepsilon\phi} - (1-f_T)\bar{\beta}^{\alpha\beta}_0\Delta\theta \quad (8.65)$$
$$+ \sum_{j=1}^{w} f^j\left(\bar{\mathbb{C}}^{\alpha\beta\chi\delta}_j E^E_{\chi\delta} + \frac{1}{2}\bar{\mathbb{C}}^{\alpha\beta\chi\delta\varepsilon\phi}_j E^E_{\chi\delta}E^E_{\varepsilon\phi} - \bar{\beta}^{\alpha\beta}_j\Delta\theta\right),$$

implying that the elastic stress $\bar{\Sigma}$ for a heterogeneous (twinned) crystal is equivalent to the volume average of the local stresses supported by the parent and each twin. Effective thermoelastic coefficients for the volume element entering (8.56), (8.63), and (8.65) are thus

$$\overline{\mathbb{C}}^{\alpha\beta\chi\delta}\left(\{f^j\},X,\overline{\mathbf{g}}_\alpha\right)=(1-f_T)\overline{\mathbb{C}}_0^{\alpha\beta\chi\delta}+\sum_{j=1}^{w}f^j\overline{\mathbb{C}}_j^{\alpha\beta\chi\delta},$$

$$\overline{\mathbb{C}}^{\alpha\beta\chi\delta\varepsilon\phi}\left(\{f^j\},X,\overline{\mathbf{g}}_\alpha\right)=(1-f_T)\overline{\mathbb{C}}_0^{\alpha\beta\chi\delta\varepsilon\phi}+\sum_{j=1}^{w}f^j\overline{\mathbb{C}}_j^{\alpha\beta\chi\delta\varepsilon\phi}, \qquad (8.66)$$

$$\overline{\beta}^{\alpha\beta}\left(\{f^j\},X,\overline{\mathbf{g}}_\alpha\right)=(1-f_T)\overline{\beta}_0^{\alpha\beta}+\sum_{j=1}^{w}f^j\overline{\beta}_j^{\alpha\beta}.$$

Coefficients in (8.66) can be interpreted as Voigt averages (see generic definition (A.33) of Appendix A) and hence provide upper bounds on the elastic stiffness (Hill 1952; Mura 1982). From (8.63), the necessity of inclusion of twin fractions $\{f^j\}$ in free energy function (8.33) is evident, since the effective thermoelastic moduli (8.66) depend on evolving twin fractions. In the absence of twinning, (8.66) reduces to the coefficients of the parent crystal. The symmetry exhibited by coefficients on the left of (8.66) is minimally triclinic; the averaging process used to compute effective coefficients generally does not preserve the symmetry properties of the parent and each individual twin. Anisotropic thermal conductivity of (8.47) for a twinned element of material can be defined in the same way as the thermal stress coefficients in the last of (8.66). The associated time rate of thermoelastic free energy change from the rates of twin fractions is

$$\frac{\partial \overline{\Psi}^E}{\partial f^j}\dot{f}^j = \overline{A}_j\dot{f}^j, \text{ (summed over } j=1,2,...w), \qquad (8.67)$$

where for each twin system, the quantity

$$\overline{A}_j = \frac{1}{2}E_{\alpha\beta}^E(\overline{\mathbb{C}}_j^{\alpha\beta\chi\delta}-\overline{\mathbb{C}}_0^{\alpha\beta\chi\delta})E_{\chi\delta}^E+\frac{1}{6}E_{\alpha\beta}^E(\overline{\mathbb{C}}_j^{\alpha\beta\chi\delta\varepsilon\phi}-\overline{\mathbb{C}}_0^{\alpha\beta\chi\delta\varepsilon\phi})E_{\chi\delta}^E E_{\varepsilon\phi}^E \qquad (8.68)$$
$$-(\overline{\beta}_j^{\alpha\beta}-\overline{\beta}_0^{\alpha\beta})E_{\alpha\beta}^E\Delta\theta.$$

From (8.65), the Cauchy stress and first Piola-Kirchhoff stress are, respectively,

$$\sigma^{ab} = J^{E-1}F_{.\alpha}^{Ea}F_{.\beta}^{Eb}\left(\overline{\mathbb{C}}^{\alpha\beta\chi\delta}E_{\chi\delta}^E+\frac{1}{2}\overline{\mathbb{C}}^{\alpha\beta\chi\delta\varepsilon\phi}E_{\chi\delta}^E E_{\varepsilon\phi}^E-\overline{\beta}^{\alpha\beta}\Delta\theta\right), \qquad (8.69)$$

$$P^{aA} = \overline{J}^{2/3}F_{.\gamma}^{P-1A}F_{.\beta}^{W-1\gamma}F_{.\alpha}^{Ea}\left(\overline{\mathbb{C}}^{\alpha\beta\chi\delta}E_{\chi\delta}^E+\frac{1}{2}\overline{\mathbb{C}}^{\alpha\beta\chi\delta\varepsilon\phi}E_{\varepsilon\phi}^E E_{\chi\delta}^E-\overline{\beta}^{\alpha\beta}\Delta\theta\right). \qquad (8.70)$$

As noted previously, if the residual volume change measured by $\overline{J}$ is increased (decreased) at fixed elastic strain and temperature, the Cauchy stress of (8.69) remains fixed but the first Piola-Kirchhoff stress of (8.70) will increase (decrease).

Consider a situation in which strains $E_{\alpha\beta}^E = \bar{\alpha}_{\alpha\beta}\Delta\theta$ arise from temperature change. The following relationship emerges between thermal stress, thermal expansion ($\bar{\alpha}_{\alpha\beta}$), and elasticity coefficients:

$$\bar{\beta}^{\alpha\beta} = \left(\overline{\mathbb{C}}^{\alpha\beta\chi\delta}\bar{\alpha}_{\chi\delta} + \overline{\mathbb{C}}^{\alpha\beta\chi\delta\varepsilon\phi}\bar{\alpha}_{\chi\delta}\bar{\alpha}_{\varepsilon\phi}\Delta\theta/2\right)\Big|_{\theta_0} = \overline{\mathbb{C}}^{\alpha\beta\chi\delta}\bar{\alpha}_{\chi\delta}\Big|_{\theta_0} . \qquad (8.71)$$

Relationship (8.71) is analogous to (5.161) of nonlinear thermoelasticity theory and (6.57) in the context of finite plasticity theory.

The residual Helmholtz free energy per unit intermediate volume of (8.55) is specified as the following polynomial form:

$$\bar{\Psi}^R = \frac{1}{2}\hat{K}\Big[\kappa_1\alpha^2 + \kappa_2\beta^2 + \kappa_3 l^{2N}(\hat{\mathbf{a}}:\hat{\mathbf{a}})^N + \kappa_4\alpha^2\beta^2$$
$$+ \kappa_5 l^{2N}(\hat{\mathbf{a}}:\hat{\mathbf{a}})^N\alpha^2 + \kappa_6 l^{2N}(\hat{\mathbf{a}}:\hat{\mathbf{a}})^N\beta^2\Big]. \qquad (8.72)$$

Energy factor $\hat{K}(\theta, X, \bar{\mathbf{g}}_\alpha)$ depends on anisotropic elastic constants, temperature, and orientation of the crystal relative to orientations of defects contained within. For straight dislocation lines whose energies are characterized via anisotropic linear elasticity solutions, $\hat{K}$ is defined in terms of second-order elastic constants in Appendix C, Section C.1.6. In an isotropic linear elastic body, $\hat{K}(\theta, X) = \mu(\theta, X)$, i.e., the elastic shear modulus that may depend on temperature. Denoted by κ_1, κ_2, κ_3, κ_4, κ_5, and κ_6 are dimensionless constants that scale energies in each internal variable and their pair-wise products. Also, l is a non-negative scalar with dimensions of length, required from dimensional considerations in gradient theories (Fleck et al. 1994; Regueiro et al. 2002; Clayton et al. 2004a, b; Voyiadjis and Abu Al-Rub 2005), and N is a constant. From (8.72), $\bar{\Psi}^R = 0$ when all defect densities vanish; this state of vanishing defects is always of minimum residual free energy when all coefficients κ_1, κ_2, κ_3, κ_4, κ_5, and κ_6 are non-negative.

Recalling from definition (8.29) that $\alpha = b\sqrt{\bar{\rho}_S}$, the first term on the right of (8.72) provides for a linear dependence of residual energy on the line density of statistically stored dislocations, following Regueiro et al. (2002) and Clayton et al. (2004b, 2006) and references therein. Assuming that energy per unit line length of statistically stored dislocations can be represented by linear elastic solutions (C.152) or (6.117), simple arguments then show that, similarly to (6.118) and (6.119),

$$\frac{\kappa_1}{2}\hat{K}\alpha^2 = \frac{\kappa_1}{2}\hat{K}b^2\bar{\rho}_S = \Lambda\hat{K}b^2\bar{\rho}_S, \; 0.5 \lesssim \Lambda \lesssim 1.0, \; 1.0 \lesssim \kappa_1 \lesssim 2.0 , \qquad (8.73)$$

where self- and interaction energies, core energy, and stacking fault energy if the dislocations are partial are absorbed into the constant κ_1. Recalling from (8.30) that $\beta = \sqrt{b\bar{\eta}_W}$, the second term in (8.72) provides for a linear dependence of residual energy on the area per unit volume of twin boundaries $\bar{\eta}_W$. Thus, letting $\bar{W}_W$ represent the twin boundary energy per unit area in configuration $\bar{B}$,

$$\frac{\kappa_2}{2}\hat{K}\beta^2 = \frac{\kappa_2}{2}\mu b\bar{\eta}_W = \bar{W}_W\bar{\eta}_W \approx \frac{\bar{W}_{SF}}{2}\bar{\eta}_W , \ \kappa_2 \approx \frac{\bar{W}_{SF}}{\mu b} . \tag{8.74}$$

where the approximation that holds for many crystals, $2\bar{W}_W \approx \bar{W}_{SF}$, has been used, with $\bar{W}_{SF}$ the intrinsic or extrinsic stacking fault energy (Hirth and Lothe 1982; Bernstein and Tadmor 2004). Energy factor $\hat{K}$ is set equal to the shear modulus in (8.74). The third term in (8.72) accounts for the energy of geometrically necessary dislocations, for which a number of forms for l, N, and κ_3 have been suggested for different crystal structures and different applications (Fleck et al. 1994; Regueiro et al. 2002; Clayton et al. 2004a, b; Voyiadjis and Abu Al-Rub 2005; Chung and Clayton 2007). The fifth term in (8.72) reflects possible interactions between statistically stored and geometrically necessary dislocations. The fourth and sixth terms in (8.72) reflect interaction energies between twin boundaries and dislocations, for example stress fields and strain energies of dislocation lines may be amplified at the stress concentration caused by a dislocation pile-up at a twin boundary (Christian and Mahajan 1995).

Methods for determining the content of geometrically necessary versus statistically stored dislocations have been forwarded in recent years (Arsenlis and Parks 1999; El-Dasher et al. 2003; Hughes et al. 2003). Such methods could facilitate unique selection of parameters in (8.72) if defect energies are known, for example, through measurements cold work (Clarebrough et al. 1957; Rosakis et al. 2000; Taheri et al. 2006) or atomic scale computer simulations of defect energy. However, in many cases, only the total scalar line density $\bar{\rho}_T$ of all dislocations, both geometrically necessary and statistically stored, may be known from historical data. In such cases, it becomes prudent to employ a simple form of (8.72) in terms of total line density per unit intermediate volume in configuration $\bar{B}$, denoted by $\bar{\rho}_T(X,t)$:

$$\bar{\Psi}^R = \frac{1}{2}\mu\left[\kappa_1\breve{\alpha}^2 + \kappa_2\beta^2 + \kappa_4\breve{\alpha}^2\beta^2\right], \tag{8.75}$$

where $\hat{K}(\theta, X) = \mu(\theta, X)$ has been used as an approximation, and where the dimensionless internal state variable $\breve{\alpha}(X,t)$ measures the total scalar dislocation density:

$$\breve{\alpha} = b\sqrt{\bar{\rho}_T} \ . \tag{8.76}$$

Internal state variable in (8.76) is analogous to that defined in (6.100). Comparison of (8.72) and (8.75) implies the following relationships:

$$\kappa_1 \breve{\alpha}^2 = \kappa_1 b^2 \bar{\rho}_T = \kappa_1 b^2 \bar{\rho}_S + \kappa_3 l^{2N} (\hat{\mathbf{a}} : \hat{\mathbf{a}})^N \ ; \tag{8.77}$$

$$\kappa_4 \breve{\alpha}^2 \beta^2 = \kappa_4 b^2 \bar{\rho}_T \beta^2 = \left[\kappa_4 b^2 \bar{\rho}_S + \kappa_6 l^{2N} (\hat{\mathbf{a}} : \hat{\mathbf{a}})^N \right] \beta^2 \ ; \tag{8.78}$$

$$\bar{\rho}_T = \bar{\rho}_S + \bar{\rho}_G \ , \ \bar{\rho}_G = b^{-1} (\hat{\mathbf{a}} : \hat{\mathbf{a}})^{1/2} \ ; \tag{8.79}$$

$$l = b \ , \ N = 1/2 \ , \ \kappa_1 = \kappa_3 \ , \ \kappa_4 = \kappa_6 \ , \ \kappa_5 = 0 \ . \tag{8.80}$$

Relations (8.75)-(8.80) provide for an equal contribution, per unit line length, of geometrically necessary and statistically stored dislocations to the residual free energy of the crystal. For uniform straight dislocation lines of density $\hat{\alpha}^{\alpha\beta} = \tilde{\rho} \tilde{b}^\alpha \tilde{\xi}^\beta$ in configuration $\tilde{B}$, (8.28) and the second of (8.79) consistently give

$$\bar{\rho}_G = b^{-1} (\tilde{\rho}^k \tilde{b}^\alpha \tilde{\xi}^\beta \tilde{\rho}^k \tilde{b}_\alpha \tilde{\xi}_\beta)^{1/2} = \tilde{\rho}^k (\tilde{b}/b) = \tilde{\rho}^k \bar{J}^{-1/3} \approx \tilde{\rho}^k \ . \tag{8.81}$$

Values of κ_1 and κ_2 in (8.75) can be approximated using (8.73) and (8.74), respectively.

Since the total dislocation density depends on geometrically necessary and statistically stored dislocations, i.e., $\breve{\alpha} = \breve{\alpha}(\hat{\mathbf{a}}, \alpha)$ from (8.76) and (8.79), terms entering (8.52) can be expressed as follows via the chain rule:

$$\begin{aligned}
\left(\frac{\partial \bar{\Psi}}{\partial \breve{\alpha}} - \theta \frac{\partial^2 \bar{\Psi}}{\partial \theta \partial \breve{\alpha}} \right) \dot{\breve{\alpha}} &= \left(\frac{\partial \bar{\Psi}}{\partial \breve{\alpha}} - \theta \frac{\partial^2 \bar{\Psi}}{\partial \theta \partial \breve{\alpha}} \right) \left(\frac{\partial \breve{\alpha}}{\partial \hat{\mathbf{a}}} : \dot{\hat{\mathbf{a}}} + \frac{\partial \breve{\alpha}}{\partial \alpha} \dot{\alpha} \right) \\
&= \left(\frac{\partial \bar{\Psi}}{\partial \hat{\mathbf{a}}} - \theta \frac{\partial^2 \bar{\Psi}}{\partial \theta \partial \hat{\mathbf{a}}} \right) : \dot{\hat{\mathbf{a}}} + \left(\frac{\partial \bar{\Psi}}{\partial \alpha} - \theta \frac{\partial^2 \bar{\Psi}}{\partial \theta \partial \alpha} \right) \dot{\alpha}.
\end{aligned} \tag{8.82}$$

Using (8.67), (8.75), and (8.82), the rate of temperature increase in (8.52) can then be written in this case as

$$\bar{C}\dot{\theta} = \beta' \dot{W}^P + \theta \left(\frac{\partial \bar{\Psi}}{\partial \theta} \frac{\dot{\bar{J}}}{\bar{J}} - \bar{\boldsymbol{\beta}} : \dot{\mathbf{E}}^E \right) + \left\langle \hat{\nabla}, \bar{\mathbf{K}} \bar{\nabla} \theta \right\rangle + \bar{\rho} r \ , \tag{8.83}$$

where

$$\beta' = 1 - \left\{ \left(\frac{\partial \bar{\Psi}}{\partial \bar{\alpha}} - \theta \frac{\partial^2 \bar{\Psi}}{\partial \theta \partial \bar{\alpha}} \right) \dot{\bar{\alpha}} - \left(\frac{\partial \bar{\Psi}}{\partial \beta} - \theta \frac{\partial^2 \bar{\Psi}}{\partial \theta \partial \beta} \right) \dot{\beta} \right.$$

$$\left. - \left(\frac{\partial \bar{\Psi}}{\partial f^j} - \theta \frac{\partial^2 \bar{\Psi}}{\partial \theta \partial f^j} \right) \dot{f}^j \right\} \dot{W}^{P-1}$$

$$= 1 - \left\{ \left(\mu - \theta \frac{\partial \mu}{\partial \theta} \right) \left[\frac{b^2}{2} \left(\kappa_1 + \kappa_4 \frac{\bar{\eta}_W}{\sqrt{\bar{\rho}_T}} \right) \dot{\bar{\rho}}_T + \right. \right.$$

$$\left. \left. \frac{b}{2} \left(\kappa_2 + \kappa_4 b^{3/2} \frac{\bar{\rho}_T}{\sqrt{\bar{\eta}_W}} \right) \dot{\bar{\eta}}_W \right] + \left(\bar{A}_j - \theta \frac{\partial \bar{A}_j}{\partial \theta} \right) \dot{f}^j \right\} \dot{W}^{P-1}.$$

(8.84)

is the Taylor-Quinney parameter similar to that in (6.47) and (6.120), such that $1 - \beta'$ is the ratio of inelastic stress power $\dot{W}^P$ converted to residual elastic energy. The inelastic stress power, per unit volume in configuration $\bar{B}$, is, from (8.49),

$$\dot{W}^P = \bar{\boldsymbol{\Pi}} : \left[\mathbf{L}^W + \bar{\mathbf{L}}^P + (1/3)\dot{\bar{J}}\bar{J}^{-1}\mathbf{1} \right]$$

$$= \sum_{j=1}^{w} \bar{\tau}^j \dot{f}^j \gamma^j + (1 - f_T) \sum_{i=1}^{n} \bar{\tau}^i \dot{\gamma}^i + \sum_{j=1}^{w} \left(f^j \sum_{i=1}^{n} \bar{\tau}_j^i \dot{\gamma}_j^i \right) + \frac{\dot{\bar{J}}}{3\bar{J}} \mathrm{tr}(\bar{\boldsymbol{\Pi}}).$$

(8.85)

Definition (8.84) is expressed in terms of the total dislocation density. A more specific form of (8.84) accounting for distinct contributions from geometrically necessary and statistically stored dislocations can be determined in a straightforward manner by substituting (8.72) into (8.52).

Consider next the energy of twin boundaries. Geometric arguments demonstrate that the area of twin boundaries per unit intermediate volume of lamellar twins can be approximated as

$$\bar{\eta}_W \approx 2 \sum_{j=1}^{w} f^j / t^j \,, \quad \dot{\bar{\eta}}_W \approx 2 \sum_{j=1}^{w} \left[\dot{f}^j / t^j - f^j \dot{t}^j / (t^j)^2 \right],$$

(8.86)

where t^j is the average thickness of a twin comprising fraction j with volume fraction f^j. From (8.84)-(8.86), β' depends on both the volume fraction and average thickness of each representative twin system.

The residual volume change $\bar{J}$ was introduced in Section 7.2.4 of Chapter 7, specifically following relations (7.43) and (7.58). An estimation of this quantity from nonlinear elasticity theory is given by (7.60):

$$\bar{J} = 1 + \frac{\Delta V}{V} = 1 + \frac{1}{K} \left(\frac{\partial K}{\partial p} - 1 \right) \bar{W}_D + \frac{1}{\mu} \left(\frac{\partial \mu}{\partial p} - \frac{\mu}{K} \right) \bar{W}_S,$$

(8.87)

where μ and K are isotropic shear and bulk moduli, $p = -\mathrm{tr}(\boldsymbol{\sigma})/3$ is the Cauchy pressure, and $\bar{W}_D$ and $\bar{W}_S$ are the dilatational and deviatoric strain energy densities per unit reference volume, respectively, associated with lattice defects. As an approximation, for anisotropic single crystals the bulk and shear elastic coefficients are defined as Voigt averages (A.36) and (A.38):

$$K = \frac{1}{9}\bar{\mathbb{C}}^{\alpha.\beta}_{.\alpha.\beta}, \quad \mu = \frac{1}{30}(3\bar{\mathbb{C}}^{\alpha\beta}_{..\alpha\beta} - \bar{\mathbb{C}}^{\alpha.\beta}_{.\alpha.\beta}). \tag{8.88}$$

Shear and bulk moduli in (8.88) do not depend on temperature since the right sides of (8.88) are evaluated at the reference state, according to (8.57). Pressure derivatives of bulk modulus and shear modulus in (8.87) are measured at the reference state and are treated as constants. The volume change in (8.87) is measured between reference and intermediate configurations: $\Delta V = \bar{V} - V$ with $\bar{V}$ the volume in $\bar{B}$. Setting the residual free energy of (8.75), measured per unit volume in the reference configuration, equal to the sum of defect energies (Kocks et al. 1975),

$$\bar{J}\bar{\Psi}^R = \bar{W}_D + \bar{W}_S = \frac{1}{2}\bar{J}\mu\left[\kappa_1\breve{\alpha}^2 + \kappa_2\beta^2 + \kappa_4\breve{\alpha}^2\beta^2\right]$$
$$= \frac{1}{2}\bar{J}\mu\left[\kappa_1 b^2\bar{\rho}_T + \kappa_2 b\bar{\eta}_W + \kappa_4 b^3\bar{\rho}_T\bar{\eta}_W\right] \approx \bar{W}_S, \tag{8.89}$$

where in the final equality, the energy is approximated as purely deviatoric. From (8.87),

$$\bar{J} \approx 1 + \frac{1}{2}\bar{J}\left(\frac{\partial\mu}{\partial p} - \frac{\mu}{K}\right)\left(\kappa_1 b^2\bar{\rho}_T + \kappa_2 b\bar{\eta}_W + \kappa_4 b^3\bar{\rho}_T\bar{\eta}_W\right)$$
$$= \left[1 - \frac{1}{2}\left(\frac{\partial\mu}{\partial p} - \frac{\mu}{K}\right)\left(\kappa_1 b^2\bar{\rho}_T + \kappa_2 b\bar{\eta}_W + \kappa_4 b^3\bar{\rho}_T\bar{\eta}_W\right)\right]^{-1} \tag{8.90}$$
$$\approx 1 + \frac{1}{2}\left(\frac{\partial\mu}{\partial p} - \frac{\mu}{K}\right)\left(\kappa_1 b^2\bar{\rho}_T + \kappa_2 b\bar{\eta}_W + \kappa_4 b^3\bar{\rho}_T\bar{\eta}_W\right),$$

where small residual volume changes $\bar{J} \approx (1 - \Delta V/V)^{-1}$ are assumed in the last expression, following discussion after (7.72). Dependence of residual volume change on twin boundary energy in (8.90) is similar to dependence of volume on generic grain boundaries derived by Holder and Granato (1969). Dilatancy from stacking faults (Kenway 1993) and twin boundaries (Yoo and Lee 1991) has been predicted by atomic simulations. The material time derivative of (8.90) is

$$\dot{J} \approx \frac{1}{2}\left(\frac{\partial \mu}{\partial p}-\frac{\mu}{K}\right)\left[(\kappa_1 b^2 + \kappa_4 b^3 \bar{\eta}_W)\dot{\bar{\rho}}_T + (\kappa_2 b + \kappa_4 b^3 \bar{\rho}_T)\dot{\bar{\eta}}_W\right]. \quad (8.91)$$

Expressions (8.86), (8.90) and (8.91) can be substituted into (8.85) and (8.84), which in turn enter the energy balance (8.83) and dissipation inequality (8.48). If the shear modulus used to scale the residual free energy in (8.75) is assumed independent of temperature following Voigt approximation (8.88), then $\theta \partial \mu / \partial \theta = 0$ in (8.84).

8.2.5 Kinetics

Rate dependent, i.e., viscoplastic, kinetic laws are often used to describe shearing associated with slip (Hutchinson 1976; Teodosiu and Sidoroff 1976; Asaro 1983) and twinning (Tome et al. 1991; Kalidindi 1998; Wu et al. 2007). Representative kinetic equations can be written as

$$\dot{\gamma}^i = \dot{\gamma}_0 \left|\frac{\bar{\tau}^i}{\hat{\tau}^i}\right|^m \frac{\bar{\tau}^i}{|\bar{\tau}^i|}, \quad (\forall i=1,...n \in \text{ parent}); \quad (8.92)$$

$$\dot{\gamma}^i_j = \dot{\gamma}_0 \left|\frac{\bar{\tau}^i_j}{\hat{\tau}^i_j}\right|^m \frac{\bar{\tau}^i_j}{|\bar{\tau}^i_j|}, \quad (\forall i=1,...n \in \text{ twins } j=1,...w); \quad (8.93)$$

$$\dot{f}^j = \frac{\dot{\gamma}_0}{\gamma^j}\left|\frac{\langle \bar{\tau}^j\rangle}{\hat{\tau}^j}\right|^p, \quad (\forall j=1,...w \in \text{ parent}; f_T < 1). \quad (8.94)$$

Kinetic equation (8.92) is similar to flow rule (6.106) of crystal plasticity theory, with the resolved shear stress $\bar{\tau}^i = J^E s^{ia}\sigma_a^b m^i_b$ in the first of (8.50) the thermodynamic work conjugate to slip rate $\dot{\gamma}^i$ in the dissipation inequality (8.49) and in the rate of plastic working (8.85). No backstress is included for slip or twin rate equations in (8.92)-(8.94), but a term such as $\hat{\chi}^i$ of (6.106) and (6.115) could be incorporated as appropriate. Relation (8.93) is a flow rule for $n \times w$ slip rates $\dot{\gamma}^i_j$ in reoriented regions of the twinned crystal. Resolved shear stress $\bar{\tau}^i_j = J^E s^{ia}_j \sigma_a^b m^i_{jb}$ in the second of (8.50) is the thermodynamic work conjugate to slip rate $\dot{\gamma}^i_j$ in the dissipation inequality (8.49) and in the plastic dissipation (8.85). Symbol $\dot{\gamma}_0 \geq 0$ denotes a material parameter with dimensions of inverse time that could depend on temperature (but is often taken as constant), and m is the rate sensitivity given by (6.90) in the context of single slip. Evolving resis-

tances to slip on system i in the parent and on system i in twin fraction j are denoted, respectively, by $\hat{\tau}^i(X,t)$ in (8.92) and $\hat{\tau}^i_j(X,t)$ in (8.93).

In (8.94), the rate of twinning shear $\dot{f}^j\gamma^j$ is dictated by the resolved shear stress component $\overline{\tau}^j = J^E s^{ja}\sigma^b_a m^j_{\ b}$, defined in the last of (8.50). This shear stress is a thermodynamic work conjugate to shearing rate $\dot{f}^j\gamma^j$ in the dissipation inequality (8.49) and in the inelastic power (8.85). The stress in Macaulay brackets satisfies $2\langle\overline{\tau}^j\rangle = \overline{\tau}^j + |\overline{\tau}^j| \geq 0$. Because $\dot{f}^j = 0$ for $\overline{\tau}^j \leq 0$, the unidirectional, i.e., polar, nature of twinning discussed in Section 8.1.3 is respected. The rate sensitivity parameter for twinning is written as p, and the resisting stress to twinning is $\hat{\tau}^j(X,t)$. Conceivably, a different value of $\dot{\gamma}_0$ could be used in each of (8.92)-(8.94); in the simple treatment suggested here, differences among kinetic behaviors are assumed to be addressed by different initial values of and evolution equations for the slip resistances. In the limit $m \to \infty$ or $p \to \infty$, rate independent behavior is attained for slip or twinning, respectively. Since detwinning and successive twinning are not considered here, the constraint $\dot{f}^j = 0$ applies when the crystal is fully twinned and $f_T = 1$. Special or alternative forms of (8.94) may be required to address load drops and serrated stress-strain responses observed for some twinned single-gle crystals. From (8.92)-(8.94), any nonzero contribution of slip and twinning to the rate of inelastic working (8.85) is always positive, since

$$\dot{W}^P - \frac{\dot{\overline{J}}}{3\overline{J}}\mathrm{tr}(\overline{\mathbf{\Pi}})$$

$$= \dot{\gamma}_0\left[\sum_{j=1}^{w}\overline{\tau}^j\left|\frac{\langle\overline{\tau}^j\rangle}{\hat{\tau}^j}\right|^p + (1-f_T)\sum_{i=1}^{n}|\overline{\tau}^i|\left|\frac{\overline{\tau}^i}{\hat{\tau}^i}\right|^m + \sum_{j=1}^{w}\left(f^j\sum_{i=1}^{n}|\overline{\tau}^i_j|\left|\frac{\overline{\tau}^i_j}{\hat{\tau}^i_j}\right|^m\right)\right] \geq 0. \tag{8.95}$$

Written generically, evolution equations for slip and twin resistances are expressed as

$$\dot{\hat{\tau}}^i = \dot{\hat{\tau}}^i\left(\mathbf{E}^{\mathbf{E}},\theta,\hat{\mathbf{a}},\alpha,\beta,\{f^j\},\{\hat{\tau}\},X,\overline{\mathbf{g}}_\alpha\right), \tag{8.96}$$

$$\dot{\hat{\tau}}^i_j = \dot{\hat{\tau}}^i_j\left(\mathbf{E}^{\mathbf{E}},\theta,\hat{\mathbf{a}},\alpha,\beta,\{f^j\},\{\hat{\tau}\},X,\overline{\mathbf{g}}_\alpha\right), \tag{8.97}$$

$$\dot{\hat{\tau}}^j = \dot{\hat{\tau}}^j\left(\mathbf{E}^{\mathbf{E}},\theta,\hat{\mathbf{a}},\alpha,\beta,\{f^j\},\{\hat{\tau}\},X,\overline{\mathbf{g}}_\alpha\right). \tag{8.98}$$

Hardening rates depend not only on the set of state variables that explicitly enter the free energy function (8.33), but also the set of hidden variables $\{\hat{\tau}\} = \{\hat{\tau}^i, \hat{\tau}^i_j, \hat{\tau}^j\}$ with $i = 1,...n$ and $j = 1,...w$, consisting of all possible

slip and twinning resistances. If the residual free energy depends only the total scalar dislocation density $\bar{\rho}_T = \breve{\alpha}^2 / b^2$ as in (8.75), it may be possible to replace (8.96)-(8.98) with

$$\dot{\hat{\tau}}^i = \dot{\hat{\tau}}^i \left(\mathbf{E}^{\mathbf{E}}, \theta, \breve{\alpha}, \beta, \{f^{\,j}\}, \{\hat{\tau}\}, X, \bar{\mathbf{g}}_\alpha \right), \tag{8.99}$$

$$\dot{\hat{\tau}}^i_j = \dot{\hat{\tau}}^i_j \left(\mathbf{E}^{\mathbf{E}}, \theta, \breve{\alpha}, \beta, \{f^{\,j}\}, \{\hat{\tau}\}, X, \bar{\mathbf{g}}_\alpha \right), \tag{8.100}$$

$$\dot{\hat{\tau}}^j = \dot{\hat{\tau}}^j \left(\mathbf{E}^{\mathbf{E}}, \theta, \breve{\alpha}, \beta, \{f^{\,j}\}, \{\hat{\tau}\}, X, \bar{\mathbf{g}}_\alpha \right). \tag{8.101}$$

Resistances to inelastic shearing modes can be described in terms of physical mechanisms by extending the treatments of dislocation kinetics in Sections 6.2 and 6.3 to include effects of twins. Following (6.99), resistance stresses $\{\hat{\tau}\}$ entering (8.96)-(8.101) are decomposed into sums of contributions of various mechanisms (Kocks et al. 1975; Clayton 2005a, b, 2009a):

$$\hat{\tau}^i = \hat{\tau}^i_P + \hat{\tau}^i_D, \ \hat{\tau}^i_j = (\hat{\tau}_P)^i_j + (\hat{\tau}_D)^i_j, \ \hat{\tau}^j = \hat{\tau}^j_W + \hat{\tau}^j_D. \tag{8.102}$$

In the first of (8.102), $\hat{\tau}^i_P$ reflects the initial yield stress in a defect-free crystal for slip on system i in the parent, and $\hat{\tau}^i_D$ reflects long range barriers associated with defects that accumulate during the deformation history. Analogous definitions apply for resistance to slip within the twins in the second of (8.102). Resistance to twin propagation in the third of (8.102) is likewise decomposed into a term $\hat{\tau}^j_W$ accounting for the initial resistance to twin nucleation and stress $\hat{\tau}^j_D$ due to interactions of twins with other twins and dislocations. Both terms in each sum in (8.102) depend on temperature. The initial yield stress (e.g., $\hat{\tau}^i_P$) depends on short range barriers such as Peierls barriers (see Section C.4.3) that may be significant at low temperatures or in crystals with low initial defect densities and non-metallic bonds (Friedel 1964; Farber et al. 1993), and at high dislocation velocities also accounts for viscous, phonon, and electron drag (Kocks et al. 1975; Gilman 1979).

An approximation often used for the twin nucleation stress follows from the energy required to translate a partial Burgers vector associated with a given twin system (Hirth and Lothe 1982):

$$\hat{\tau}^j_W \approx \bar{W}^j_{SF} / b^j_P, \tag{8.103}$$

where $\bar{W}^j_{SF}$ is the stacking fault energy associated with the movement of a twinning partial of Burgers magnitude b^j_P. The twin nucleation stress, like the slip resistance, can also depend on hydrostatic pressure, as indicated in atomic simulations (Xu et al. 2004). As noted in Section C.4.1, the theoretical strength (i.e., Frenkel's model) has been suggested as a stress crite-

rion for twin nucleation in metallic crystals (Bell and Cahn 1957; Paxton et al. 1991): $\hat{\tau}_W^j \approx \mu \gamma^j /(2\pi)$.

A number of analytical treatments of thermodynamics of twin nucleation have been forwarded (Price 1961; Lee and Yoo 1990; Yoo and Lee 1991; Lebensohn and Tome 1993; Meyers et al. 2001). Such theories often seek the minimum stable size and shape of a twin nucleus via consideration of stationary points in the total Gibbs free energy (including external work, elastic strain energy, and surface energy of the twin boundary), and many of these theories incorporate aspects of Eshelby's treatment of elastic inclusions and inhomogeneities (Eshelby 1961). In particular, Price (1961) and Lebensohn and Tome (1993) suggested formulae in which the twin nucleation stress is directly proportional to the twin boundary energy.

Conceivably, long range barriers in each of (8.102) could depend in a complex manner upon activity of the slip or twin system under consideration (i.e., self-hardening) as well as the activity of all other slip systems (i.e., latent hardening) and twinning systems (Christian and Mahajan 1995; Wu et al. 2007). Possible impedance or facilitation of slip or twinning via slip-slip interactions, slip-twin interactions, and twin-twin interactions depends in a complex manner on a number of factors, including geometrical relationships among interacting systems, temperature, crystal structure, and defect content (Christian and Mahajan 1995; Kalidindi 1998; Castaing et al. 2002; Wu et al. 2007). Experimental data enabling unique quantification of these effects is often scarce, and mechanisms responsible for hardening are not fully understood in many materials (Lagerlof et al. 1994; Kalidindi 1998). Because of the large number of parameters required for a complete description of the interactions among individual deformation mechanisms, many experiments may be required, with delineation of effects of a particular mechanism difficult. Initial values of hardness in (8.102) may differ among different slip and twin families in a crystal, and account for periodic lattice resistance in an initially perfect lattice (Peierls 1940; Nabarro 1947), friction stress (Beltz et al. 1996), and other initial barriers, for example those resulting from interstitials in crystals with impurities (Kocks et al. 1975). Short range barriers to dislocation motion are often strongly temperature dependent (Kuhlmann-Wilsdorf 1960; Kocks et al. 1975), since increases in temperature correlate with increased probability of dislocations overcoming such barriers via thermal activation, as discussed in Section 6.2. Long range barriers typically arise from interactions of local stress fields among defects, and generally increase with defect densities that accumulate with strain until saturation. Twinning resistance is often affected by temperature, but at low temperatures may increase less steeply than slip resistance as the temperature is decreased (Christian and

Mahajan 1995). This phenomenon explains the tendency for many solids to favor twinning over slip at low temperatures. The resistance to twinning may even decrease with decreasing temperature (Christian and Mahajan 1995). Twinning is observed frequently in shock-loaded metallic and ceramic crystals (Rohatgi and Vecchio 2002; Bourne et al. 2007).

Evolution equations for variables α and β, respectively reflecting densities of statistically stored dislocations and twin boundaries as indicated in (8.29) and (8.30), complete the model. A separate evolution equation for the geometrically necessary dislocation density tensor is not needed since $\hat{\boldsymbol{\alpha}}$ is obtained directly from kinematic relations (8.24)-(8.28), leading to the rate equation

$$
\begin{aligned}
\dot{\hat{\alpha}}^{\alpha\beta} &= \frac{d}{dt}\Big[F^{W\beta}_{.\chi} F^{P\chi}_{.A} \varepsilon^{ABC} (F^{W\alpha}_{.\beta} F^{P\beta}_{.B,C} + F^{W\alpha}_{.\beta,C} F^{P\beta}_{.B}) \Big] \\
&= (\dot{F}^{W\beta}_{.\chi} F^{P\chi}_{.A} + F^{W\beta}_{.\chi} \dot{F}^{P\chi}_{.A}) \varepsilon^{ABC} (F^{W\alpha}_{.\beta} F^{P\beta}_{.B,C} + F^{W\alpha}_{.\beta,C} F^{P\beta}_{.B}) \\
&\quad + F^{W\beta}_{.\chi} F^{P\chi}_{.A} \varepsilon^{ABC} \\
&\quad \times (\dot{F}^{W\alpha}_{.\beta} F^{P\beta}_{.B,C} + \dot{F}^{W\alpha}_{.\beta,C} F^{P\beta}_{.B} + F^{W\alpha}_{.\beta} \dot{F}^{P\beta}_{.B,C} + F^{W\alpha}_{.\beta,C} \dot{F}^{P\beta}_{.B}).
\end{aligned}
\tag{8.104}
$$

Terms entering (8.104) are obtained from updated plastic and twinning deformations, their rates in (8.20) and (8.21), and their partial derivatives taken with respect to material coordinates X^A. Analogously to hardening evolution laws listed in (8.96)-(8.101), defect densities may depend upon the history of slip and twin activity, as well as crystal structure and material composition. Generic evolution equations are written for statistically stored dislocations and the twin boundary area density, respectively as

$$
\dot{\bar{\rho}}_S = \dot{\bar{\rho}}_S \left(\mathbf{E}^{\mathbf{E}}, \theta, \hat{\boldsymbol{\alpha}}, \alpha, \beta, \{f^j\}, \{\hat{\tau}\}, X, \overline{\mathbf{g}}_\alpha \right),
\tag{8.105}
$$

$$
\dot{\bar{\eta}}_W = \dot{\bar{\eta}}_W \left(\mathbf{E}^{\mathbf{E}}, \theta, \hat{\boldsymbol{\alpha}}, \alpha, \beta, \{f^j\}, \{\hat{\tau}\}, X, \overline{\mathbf{g}}_\alpha \right).
\tag{8.106}
$$

From (8.105) and (8.106), Helmholtz free energy (8.33) depends on the shear resistances (i.e., hidden variables) $\{\hat{\tau}\}$ implicitly, via their influence on the evolution of the internal state variables. Kinetic equation (8.106) becomes redundant if, instead, an equation for thickness of each twin t^j in (8.86) is prescribed. If the residual free energy depends only the total scalar dislocation density as in (8.75), (8.104) need not be exercised, and (8.105) and (8.106) can be replaced with

$$
\dot{\bar{\rho}}_T = \dot{\bar{\rho}}_T \left(\mathbf{E}^{\mathbf{E}}, \theta, \breve{\alpha}, \beta, \{f^j\}, \{\hat{\tau}\}, X, \overline{\mathbf{g}}_\alpha \right),
\tag{8.107}
$$

$$
\dot{\bar{\eta}}_W = \dot{\bar{\eta}}_W \left(\mathbf{E}^{\mathbf{E}}, \theta, \breve{\alpha}, \beta, \{f^j\}, \{\hat{\tau}\}, X, \overline{\mathbf{g}}_\alpha \right).
\tag{8.108}
$$

Since a consensus on appropriate functional forms of evolution laws for hardening, (8.96)-(8.101), and defect densities, (8.105)-(8.108), for generic

crystalline solids undergoing simultaneous slip and twinning does not seem to exist, more specific forms of these equations are not included in this text. Examples of kinetic relations are available in the literature for certain metals (Van Houtte 1978; Tome et al. 1991; Kalidindi 1998; Staroselsky and Anand 2003; Wu et al. 2007; Proust et al. 2009) and ceramics (Scott and Orr 1983; Lagerlof et al. 1994; Castaing et al. 2002; Clayton 2009a, 2010c, d). The kinetic relations offered in Section 8.2.5 make no attempt to model geometry of twins (apart from simple relation (8.86)), nor do they capture interface morphology. A more refined treatment of thermodynamics and interface kinetics is required to address such aspects of microstructure evolution (Rosakis and Tsai 1995; Hou et al. 1999).

9 Generalized Inelasticity

The two-term multiplicative decomposition of the deformation gradient used in Chapter 6 does not explicitly account for residual deformation of the lattice, or in other words, does not account for irreversible deformations that are not lattice-preserving. Recall from Section 3.2 that the lattice-preserving part of the deformation gradient is attributed to plasticity from crystal dislocations, specifically dislocation glide and relative shearing of crystallographic planes in increments of the Burgers vector for slip. Residual deformations that are not explicitly addressed in the definition of plastic deformation used in this text may emerge from the following physical mechanisms: residual elastic deformation and residual volume changes associated with self-equilibrated stress fields of defects (Section 3.2.9 and Chapter 7), lattice rotations and reflections associated with twinning (Chapter 8), volumetric deformation associated with voids and point defects (Sections 3.2.8 and 7.4), and anisotropic damage mechanisms such as ductile or brittle fracture and material rupture. When treated distinctly from mechanically reversible elastic deformation as in the non-standard model of thermoelasticity of Section 5.5, deformation associated with thermal strains can also be categorized as a residual deformation mode distinct from plastic deformation.

Inelastic deformations accommodated by damage mechanisms are commonplace in brittle crystals, in which dislocations may be scarce, or in which barriers to dislocation motion and twinning may be very large. Large deformations of an element of a brittle solid may be sustained by generation of surfaces within the element and subsequent local motions of these surfaces. The term damage is used in this text to denote generic mechanisms of generation, growth, and motion of such internal surfaces whose creation requires breaking of atomic bonds. Often these surfaces support no mechanical forces, i.e., they are free of mechanical traction, and hence labeled free surfaces. However, damage surfaces are not always required to be traction free; for example, frictional forces may be supported at crack faces in sliding contact. Regardless of the ductility of the crystal, volumetric strains cannot be sustained by dislocation glide since such dislocation motion is conservative, as discussed in Sections 3.2.2, 3.2.5, and 7.1.1. Nor can volumetric strains be accommodated by deformation twin-

ning, which is also isochoric, as discussed in Sections 8.1.3 and 8.2.1. Hence, inelastic tensile volumetric deformations are accommodated, out of geometric necessity, through damage mechanisms or increases in free volume, even in ductile crystals[1]. On the other hand, as discussed in Section 5.3, large compressive volume changes are often accommodated elastically, commensurate with large compressive pressures that suppress damage modes such as void growth or crack opening.

Constitutive formulations described in Chapter 9 account explicitly for residual lattice deformations. A generic three-term decomposition for the deformation gradient, written as $\mathbf{F} = \mathbf{F}^E \mathbf{F}^R \mathbf{F}^P$, is used, as proposed by Kratochvil (1972) in a generalized, geometrically nonlinear kinematic and thermodynamic treatment of elastic-plastic crystalline solids. The intermediate or generic residual deformation (tangent map), denoted in Chapter 9 as $\mathbf{F}^R(X,t)$, accounts for all mechanically irreversible deformations that are not lattice-preserving, and may encompass thermal deformations as a particular case. Accordingly, such thermal deformations are not deemed mechanically reversible, but may be reversed by restoration of a crystal to its reference temperature. Intermediate term $\mathbf{F}^R$ is able to account for porosity increase or reduction, deformation resulting from isotropic or anisotropic damage mechanisms, and residual elastic lattice deformation associated with microscopic stress fields of individual lattice defects or their heterogeneous distributions within a volume element of material whose centroid is located at X. Furthermore, $\mathbf{F}^R$ encompasses deformations associated with vacancies and twins, as addressed already in Chapters 7 and 8, respectively.

In what follows first in Chapter 9, a general thermodynamic analysis is conducted wherein $\mathbf{F}^R$ is defined in a generic, fully anisotropic sense. The Helmholtz free energy of a volume element of fixed mass of the solid is assumed to depend minimally upon strain associated with the recoverable elastic deformation $\mathbf{F}^E$, temperature, position and orientation of the element (i.e., heterogeneity and anisotropy), and a generic internal state variable. This internal state variable could reflect residual stress fields associated with defects or tangent elastic stiffness reduction associated with damage. An explicit dependence of free energy density on $\mathbf{F}^R$ can be used (Clayton and McDowell 2003a; Clayton et al. 2004b), or temperature and internal state variables can be assumed to encompass free energy variations and constitutive dependencies implicitly associated with variations of $\mathbf{F}^R$.

---

[1] Volume changes in crystals can also occur during phase transformations, but the topic of phase transitions falls outside the scope of this text.

Particular forms of $\mathbf{F^R}$ corresponding, respectively, to isotropic porosity in the context of the kinematic description of Section 3.2.8 and residual elastic lattice deformation in the context of the kinematic description of Section 3.2.9, are considered in turn in Sections 9.2 and 9.3. Finally, a constitutive framework for thermomechanical behavior of elastoplastic crystals, explicitly incorporating residual elasticity and internal variables of the higher gradient type (Clayton et al. 2004b, 2006), is presented in Section 9.4. Specifically, this framework accounts for continuous distributions of geometrically necessary and statistically stored dislocation and disclination lines, complementing the differential-geometric description of micropolar kinematics of defective crystals of Section 3.3.3.

9.1 Three-term Elastoplasticity: General Principles

The following topics are addressed in Section 9.1. A kinematic description of solids involving a three-term multiplicative decomposition of the total deformation gradient for a volume element of material is given, with special reference to specific mechanisms encompassed by each term. Constitutive assumptions and thermodynamic implications then follow, the latter implementing balance relations of traditional continua described in Chapter 4.

9.1.1 Kinematics and Summary of Physical Mechanisms

Multiplicative elastoplasticity in the context of a three-term multiplicative decomposition (Kratochvil 1972; Clayton and McDowell 2003a),

$$\mathbf{F} = \mathbf{F^E}\mathbf{F^R}\mathbf{F^P} , \tag{9.1}$$

is now considered. The following notation is also used to denote pairs of mappings in (9.1):

$$\mathbf{F^L} = \mathbf{F^E}\mathbf{F^R} , \ \overline{\mathbf{F}} = \mathbf{F^R}\mathbf{F^P} . \tag{9.2}$$

Decomposition (9.1) implies the existence of two generally anholonomic intermediate configurations $\tilde{B}$ and $\overline{B}$, as shown in Fig. 9.1. Tangent mappings entering (9.1) and (9.2) are then $\mathbf{F^E} : T\overline{B} \to TB$, $\mathbf{F^R} : T\tilde{B} \to T\overline{B}$, $\mathbf{F^P} : TB_0 \to T\tilde{B}$, $\mathbf{F^L} : T\tilde{B} \to TB$, and $\overline{\mathbf{F}} : TB_0 \to T\overline{B}$. A time-independent metric tensor $\overline{\mathbf{g}}(X)$ with components $\overline{g}_{\alpha\beta} = \overline{\mathbf{g}}_\alpha \cdot \overline{\mathbf{g}}_\beta = \overline{g}_{\beta\alpha}$ and determinant $\overline{g} = \det \overline{\mathbf{g}}$ is introduced on configuration $\overline{B}$ and is assigned to every material element whose reference position is X.
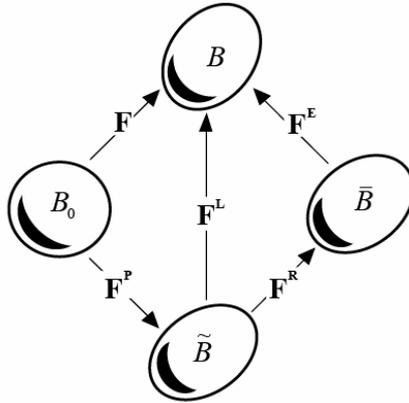
Fig. 9.1 Configurations and tangent maps

Recall from Section 7.1.2 that $\mathbf{F^E}(X,t) = \mathbf{V^E R^E} = \mathbf{R^E U^E}$ accounts for reversible elastic deformation attributed to mechanical loading, in particular left stretch $\mathbf{V^E}$ or right stretch $\mathbf{U^E}$, as well as rigid-body rotation of the solid, in particular proper orthogonal rotation $\mathbf{R^E}$. Elastic deformation $\mathbf{F^E}$ also includes thermal deformation when a standard treatment of thermoelasticity is adopted, as in Section 5.1. Plastic tangent map $\mathbf{F^P}(X,t)$ retains definitions used previously in Chapters 3 and 6-8, and specifically (6.1) in the context of two-term elastoplasticity: the plastic deformation accounts for dissipative, mechanically irreversible, lattice-preserving mechanisms. As discussed in Sections 3.2.5 and 7.1.1, $\mathbf{F^P}$ is associated with glide of mobile dislocations in ductile crystals and in such cases is isochoric; however, the mathematical treatment that follows in Chapter 9 does not formally impose plastic incompressibility constraint $J^P = 1$ unless noted otherwise. Term $\mathbf{F^R}(X,t)$, with volume ratio $J^R = \det \mathbf{F^R}\sqrt{g/\tilde{g}} = d\bar{V}/d\tilde{V}$, accounts for all other residual or mechanically irreversible deformation mechanisms that are not lattice-preserving. The total residual deformation, including lattice-preserving and lattice-altering parts, is $\bar{\mathbf{F}}(X,t) = \mathbf{F^R F^P}$. Jacobian determinant $\bar{J} = \det \bar{\mathbf{F}}\sqrt{g/G} = d\bar{V}/dV$ provides a relationship between volume elements $d\bar{V}$ in $\bar{B}$ and dV in B_0. The total lattice deformation is $\mathbf{F^L}(X,t) = \mathbf{F^E F^R}$, with $J^L = J^E J^R = \det \mathbf{F^L}\sqrt{g/\tilde{g}} = dv/d\tilde{V}$. The total volume change then satisfies, from (9.1) and (9.2),

$$J = J^E J^R J^P = J^E \bar{J} = J^L J^P . \qquad (9.3)$$

Physical examples of deformation mechanisms encompassed by $\mathbf{F^R}$ are listed in Table 9.1. In the analysis that follows in Sections 9.1.2 and 9.1.3, the generic case is considered, whereby $\mathbf{F^R}$ may be anisotropic (i.e., non-spherical) and may induce any admissible volume change, $0 < J^R < \infty$. Subsequently in Chapter 9, some particular cases listed in rows of Table 9.1—void nucleation and growth, pore compaction, and multiscale residual elasticity—are addressed via a reduction of the general theory to the more specific physics involved in each case.

Table 9.1 Possible physics represented by residual deformation $\mathbf{F^R}$

Behavior	Equations in text	Deformation	Volume change
Residual elasticity from defects	(7.31), (7.41), (7.100)	$\mathbf{F^R} = \mathbf{F^I}$	$J^I > 0$
Residual elastic volume change	(7.59)-(7.61), (8.87)	$\mathbf{F^R} = \overline{J}^{1/3}\mathbf{1}$	$\overline{J} > 0$
Spherical point defects	(3.129)-(3.136), (7.102)-(7.104)	$\mathbf{F^R} = \mathbf{F^V} = \overline{\upsilon}\mathbf{1}$	$J^V = (1 - \overline{\phi})^{-1} > 0$
Void nucleation and growth	(3.129)-(3.133), (9.48)-(9.53)	$\mathbf{F^R} = \mathbf{F^V} = \overline{\upsilon}\mathbf{1}$	$J^V = (1 - \overline{\phi})^{-1} \geq 1$
Pore compaction	(3.129), (9.94)-(9.97)	$\mathbf{F^R} = J^{C1/3}\mathbf{1}$	$J^C = (1 + \vartheta)^{-1} \leq 1$
Multiscale residual elasticity	(3.137), (3.148), (9.107)	$\mathbf{F^R} = \mathbf{F^I}$	$J^I > 0$
Mechanical twinning	(8.12), (8.13), (8.20)	$\mathbf{F^R} = \mathbf{F^W}$	$J^W = 1$
Disclination rotation	(3.280)-(3.281)	$\mathbf{F^R} = \mathbf{F^I}$	$J^I \approx 1$
Explicit thermal strain	(5.324)-(5.326)	$\mathbf{F^R} = \mathbf{F^0}$	$J^\theta > 0$

9.1.2 Constitutive Assumptions

Thermodynamic analysis of three-term multiplicative elastoplasticity proceeds in a manner similar to that of two-term elastoplasticity of Section 6.1. In the present context of (9.1)-(9.2) and Fig. 9.1, intermediate configuration $\overline{B}$ serves as an evolving reference configuration for mechanical loading by the elastic tangent map $\mathbf{F^E}$, and hence acts as a reference configuration for the instantaneous elastic response. The following variables referred to configuration $\overline{B}$ are introduced:

$$\overline{\rho} = \rho_0 \overline{J}^{-1} = \rho J^E, \tag{9.4}$$

$$\overline{\Psi} = \overline{\rho}\psi, \ \overline{E} = \overline{\rho}e, \ \overline{N} = \overline{\rho}\eta, \tag{9.5}$$

$$2E_{\alpha\beta}^E = C_{\alpha\beta}^E - \overline{g}_{\alpha\beta}, \ C_{\alpha\beta}^E = F_{.\alpha}^{Ea} g_{ab} F_{.\beta}^{Eb}, \tag{9.6}$$

$$\overline{\Sigma}^{\alpha\beta} = \overline{J}^{-1}\overline{F}^{\alpha}_{.A}\Sigma^{AB}\overline{F}^{\beta}_{.B} = J^E F^{E-1\alpha}_{.a}\sigma^{ab}F^{E-1\beta}_{.b}, \tag{9.7}$$

$$\theta_{,\alpha} = \theta_{,A}\overline{F}^{-1A}_{.\alpha} = \theta_{,a}F^{Ea}_{.\alpha} = \overline{\nabla}_{\alpha}\theta, \tag{9.8}$$

$$\overline{q}^{\alpha} = \overline{J}^{-1}\overline{F}^{\alpha}_{.A}Q^{A} = J^E F^{E-1\alpha}_{.a}q^{a}. \tag{9.9}$$

Mass density per unit intermediate volume in $\overline{B}$ is written as $\overline{\rho}$ in (9.4). Helmholtz free energy $\overline{\Psi}$, internal energy $\overline{E}$, and entropy $\overline{N}$ are each defined on a per unit intermediate configuration volume basis in (9.5). Definitions used in (9.6) for the symmetric covariant elastic deformation $\mathbf{C^E}$ and strain $\mathbf{E^E}$ referred to $T^*\overline{B}\times T^*\overline{B}$ are identical to those of (5.331) and (8.34). Relationships among the contravariant elastic stress $\overline{\Sigma} \in T\overline{B}\times T\overline{B}$ (symmetric by (4.26) and (9.7)), the symmetric second Piola-Kirchhoff stress Σ, and the symmetric Cauchy stress σ are analogous to those between the latter two in Table 4.1. The temperature gradient $\overline{\nabla}\theta$ in (9.8) is consistent with the definition of the anholonomic partial derivative listed in (2.206). In (9.9), the heat flux vector follows Piola transformations akin to those of (4.36), (6.7), and (8.44).

Under rigid body motions of the spatial frame $\mathbf{x} \to \hat{\mathbf{Q}}\mathbf{x} + \mathbf{c}$, where $\hat{\mathbf{Q}}(t)$ is a spatially constant rotation matrix and $\mathbf{c}(t)$ is a spatially constant translation vector, kinematic variables in decomposition (9.1) transform as

$$\mathbf{F} \to \hat{\mathbf{Q}}\mathbf{F}, \ \mathbf{F^E} \to \hat{\mathbf{Q}}\mathbf{F^E}, \ \mathbf{F^R} \to \mathbf{F^R}, \ \mathbf{F^P} \to \mathbf{F^P}, \tag{9.10}$$

and obviously, $J^E \to J^E$ and $J^R \to J^R$, for example since $\det\hat{\mathbf{Q}} = +1$. Notice that (9.10) is consistent with (6.8). From (9.10), variables defined with regards to the intermediate configuration $\overline{B}$ in (9.4)-(9.9) all remain invariant under such motions. Specifically, (trivial) invariance of scalar quantities in (9.4) and (9.5) can be confirmed by the conservation of mass, i.e., invariance of the scalar reference mass density, and invariance of the absolute scalar $\overline{J} = J^R J^P$. Invariance of $\mathbf{C^E}$ and $\mathbf{E^E}$ follows from direct calculation using the second of (9.10) in a procedure similar to (4.50). Invariance of $\overline{\Sigma}$, $\overline{\nabla}\theta$, and $\overline{q}$ follows, respectively, from invariance of reference quantities Σ, $\theta_{,A}$, and $\mathbf{Q}$ entering (9.7)-(9.9) and from invariance of $\overline{F} = F^R F^P$ implied by the last two parts of (9.10).

From the above considerations, objective forms of general constitutive assumptions (4.45)-(4.49) are specified as follows for three-term multiplicative elastoplasticity:

$$\overline{\Psi} = \overline{\Psi}\left(E^E_{\alpha\beta}, F^{R\alpha}_{.\beta}, \alpha, \theta, \overline{\nabla}_{\alpha}\theta, X, \overline{\mathbf{g}}_{\alpha}\right); \tag{9.11}$$

$$\overline{N} = \overline{N}\left(E^E_{\alpha\beta}, F^{R\alpha}_{.\beta}, \alpha, \theta, \overline{\nabla}_{\alpha}\theta, X, \overline{\mathbf{g}}_{\alpha}\right); \tag{9.12}$$

$$\bar{\Sigma}^{\alpha\beta} = \bar{\Sigma}^{\alpha\beta}\left(E_{\alpha\beta}^{E}, F^{R\alpha}_{\ .\beta}, \alpha, \theta, \bar{\nabla}_{\alpha}\theta, X, \bar{\mathbf{g}}_{\alpha}\right); \qquad (9.13)$$

$$\bar{q}^{\alpha} = \bar{q}^{\alpha}\left(E_{\alpha\beta}^{E}, F^{R\alpha}_{\ .\beta}, \alpha, \theta, \bar{\nabla}_{\alpha}\theta, X, \bar{\mathbf{g}}_{\alpha}\right); \qquad (9.14)$$

$$\dot{\alpha} = \dot{\alpha}\left(E_{\alpha\beta}^{E}, F^{R\alpha}_{\ .\beta}, \alpha, \theta, \bar{\nabla}_{\alpha}\theta, X, \bar{\mathbf{g}}_{\alpha}\right). \qquad (9.15)$$

As in Chapters 4 and 6, $\alpha(X,t)$ denotes a scalar internal state variable, accounting here in Chapter 9 for changes in energy or response functions of the crystalline solid attributed to sources other than the elastic strain, residual deformation measure $\mathbf{F^R}$, temperature, and temperature gradient. For simplicity of presentation, a single scalar internal state variable is considered in Section 9.1, though (tensor-valued) internal state variables of higher rank can be included without conceptual difficulty, as can multiple internal state variables, as demonstrated by example in Section 9.4. Though not listed in (9.11)-(9.15), additional relationships are typically required to control evolution of plastic deformation $\mathbf{F^P}(X,t)$ and residual deformation $\mathbf{F^R}(X,t)$. These often assume the form of kinetic equations similar in functional dependency to (9.15), though more general relationships are not prohibited by the laws of thermodynamics. As was the case in Chapters 5, 6, and 8, a dependence on material particle X accounts for heterogeneous properties, while a dependence on basis vectors (here $\bar{\mathbf{g}}_{\alpha}(X)$) is written to explicitly denote an anisotropic material, the norm for single crystals.

No explicit dependence of the free energy, entropy, stress, or other response functions upon plastic deformation is prescribed explicitly, in agreement with the philosophy of Chapter 6 (Section 6.1.1). Deformation map $\mathbf{F^P}$ is excluded from the list of independent variables entering (9.11)-(9.15) for exactly the same reasons as given in the discussion immediately following (6.9)-(6.13). Defects such as dislocations may naturally be associated with residual strain energy of the lattice and may accumulate with plastic deformation; in such cases, the corresponding variation of thermodynamic state of the solid is reflected by variations of the internal state variable α. As discussed in more detail in Section 9.3, a measurable correlation may exist between the residual lattice deformation $\mathbf{F^R}$ and the stored energy in the (poly)crystalline solid (Clayton and McDowell 2003a, 2004b), in which case it may be logical to include $\mathbf{F^R}$ in the list of independent variables in (9.11)-(9.15). However, in other cases it may be possible to implicitly include effects of $\mathbf{F^R}$ on the response functions via the elastic strain, temperature, and judicious choices of internal state variables. In such cases, $\mathbf{F^R}$ need not be included in the list of independent variables entering the response functions (9.11)-(9.15), since its inclusion would be

redundant. In the forthcoming thermodynamic analysis, $\mathbf{F^R}$ is maintained in the list of independent variables, following the treatment of Kratochvil (1972).

9.1.3 Thermodynamics

When referred to the reference configuration B_0, the entropy production inequality can be written according to (4.71) as

$$\Sigma^{AB}\dot{E}_{AB} - \rho_0(\dot{\psi}+\eta\dot{\theta}) - \theta^{-1}Q^A\theta_{,A} \geq 0 . \qquad (9.16)$$

Stress power per unit reference volume can be written, similarly to (6.15), as follows:

$$\Sigma^{AB}\dot{E}_{AB} = J\sigma_a^{\cdot b}L_{\cdot b}^a = \bar{J}(J^E F_{\cdot\alpha}^{Ea}\sigma_a^{\cdot b}F_{\cdot b}^{E-1\beta})(F_{\cdot e}^{E-1\alpha}L_{\cdot d}^e F_{\cdot\beta}^{Ed})$$
$$= \bar{J}\bar{M}_\alpha^{\cdot\beta}\bar{L}_{\cdot\beta}^\alpha. \qquad (9.17)$$

Quantity $\bar{\mathbf{M}}$ is a version of the Mandel stress (Mandel 1974), defined along with the velocity gradient pulled back to intermediate configuration $\bar{B}$ by

$$\bar{M}_\alpha^{\cdot\beta} = J^E F_{\cdot\alpha}^{Ea}\sigma_a^{\cdot b}F_{\cdot b}^{E-1\beta} = C_{\alpha\delta}^E\bar{\Sigma}^{\delta\beta} , \quad \bar{L}_{\cdot\beta}^\alpha = F_{\cdot a}^{E-1\alpha}L_{\cdot b}^a F_{\cdot\beta}^{Eb} , \qquad (9.18)$$

where (9.6) and (9.7) have been consulted. The stress tensor $\bar{\mathbf{M}}$ is generally not symmetric. The total velocity gradient of (3.58) is

$$\mathbf{L} = \overset{\mathrm{g}}{\nabla}\mathbf{v} = \dot{\mathbf{F}}\mathbf{F}^{-1} = \dot{\mathbf{F}}^{\mathbf{L}}\mathbf{F}^{\mathbf{L}-1} + \mathbf{F}^{\mathbf{L}}\dot{\mathbf{F}}^{\mathbf{P}}\mathbf{F}^{\mathbf{P}-1}\mathbf{F}^{\mathbf{L}-1}$$
$$= \dot{\mathbf{F}}^{\mathbf{E}}\mathbf{F}^{\mathbf{E}-1} + \mathbf{F}^{\mathbf{E}}\dot{\bar{\mathbf{F}}}\bar{\mathbf{F}}^{-1}\mathbf{F}^{\mathbf{E}-1}, \qquad (9.19)$$

leading to

$$\bar{\mathbf{L}} = \mathbf{F}^{\mathbf{E}-1}\dot{\mathbf{F}}^{\mathbf{E}} + \dot{\bar{\mathbf{F}}}\bar{\mathbf{F}}^{-1} = \mathbf{F}^{\mathbf{E}-1}\dot{\mathbf{F}}^{\mathbf{E}} + \dot{\mathbf{F}}^{\mathbf{R}}\mathbf{F}^{\mathbf{R}-1} + \mathbf{F}^{\mathbf{R}}\dot{\mathbf{F}}^{\mathbf{P}}\mathbf{F}^{\mathbf{P}-1}\mathbf{F}^{\mathbf{R}-1}$$
$$= \mathbf{F}^{\mathbf{E}-1}\dot{\mathbf{F}}^{\mathbf{E}} + \mathbf{L}^{\mathbf{R}} + \mathbf{F}^{\mathbf{R}}\mathbf{L}^{\mathbf{P}}\mathbf{F}^{\mathbf{R}-1} = \mathbf{F}^{\mathbf{E}-1}\dot{\mathbf{F}}^{\mathbf{E}} + \mathbf{L}^{\mathbf{R}} + \bar{\mathbf{L}}^{\mathbf{P}}. \qquad (9.20)$$

The notation for inelastic velocity gradient contributions $\mathbf{L}^{\mathbf{R}} = \dot{\mathbf{F}}^{\mathbf{R}}\mathbf{F}^{\mathbf{R}-1}$, $\mathbf{L}^{\mathbf{P}} = \dot{\mathbf{F}}^{\mathbf{P}}\mathbf{F}^{\mathbf{P}-1}$, and $\bar{\mathbf{L}}^{\mathbf{P}} = \mathbf{F}^{\mathbf{R}}\mathbf{L}^{\mathbf{P}}\mathbf{F}^{\mathbf{R}-1}$ is used in (9.20) and henceforth in Chapter 9. The material time derivative of the free energy per unit intermediate volume in configuration $\bar{B}$ is, from (9.3)-(9.5),

$$\dot{\bar{\Psi}} = \frac{d}{dt}(\bar{\rho}\psi) = \bar{\rho}\dot{\psi} + \dot{\bar{\rho}}\psi = \bar{J}^{-1}\rho_0\dot{\psi} - \dot{\bar{J}}\bar{J}^{-2}\rho_0\psi$$
$$= \bar{\rho}(\dot{\psi} - \dot{\bar{F}}_{\cdot A}^\alpha\bar{F}_{\cdot\alpha}^{-1A}\psi) = \bar{\rho}\dot{\psi} - \bar{\Psi}\dot{\bar{J}}\bar{J}^{-1}. \qquad (9.21)$$

Substituting (9.4), (9.5), (9.7), (9.8), (9.9), (9.17), (9.20), and (9.21) into (9.16) and multiplying the result by $\bar{J}^{-1}$ yields a local entropy production inequality referred to intermediate configuration $\bar{B}$:

$$\bar{M}_\alpha^{\cdot\beta}\bar{L}_{\cdot\beta}^\alpha - \bar{\Psi}\dot{\bar{F}}_{\cdot A}^\alpha \bar{F}_{\cdot\beta}^{-1A}\delta_{\cdot\alpha}^\beta - \dot{\bar{\Psi}} - \bar{N}\dot{\theta} - \theta^{-1}\bar{q}^\alpha\theta_{,\alpha} \geq 0 \ . \tag{9.22}$$

Using (9.17)-(9.20), the stress power can be expressed as

$$\begin{aligned}
\bar{M}_\alpha^{\cdot\beta}\bar{L}_{\cdot\beta}^\alpha &= \bar{M}_\alpha^{\cdot\beta}F_{\cdot a}^{E-1\alpha}\dot{F}_{\cdot\beta}^{Ea} + \bar{M}_\alpha^{\cdot\beta}\dot{\bar{F}}_{\cdot A}^\alpha\bar{F}_{\cdot\beta}^{-1A} \\
&= (F_{\cdot a}^{E-1\delta a}F_{\cdot a}^{E-1\alpha}\bar{M}_\alpha^{\cdot\beta})(F_{\ b\delta}^E\dot{F}_{\cdot\beta}^{Eb}) + \bar{M}_\alpha^{\cdot\beta}\dot{\bar{F}}_{\cdot A}^\alpha\bar{F}_{\cdot\beta}^{-1A} \\
&= C^{E-1\delta a}C_{\alpha\chi}^E\bar{\Sigma}^{\beta\chi}\dot{E}_{\delta\beta}^E + \bar{M}_\alpha^{\cdot\beta}\dot{\bar{F}}_{\cdot A}^\alpha\bar{F}_{\cdot\beta}^{-1A} \\
&= \bar{\Sigma}^{\beta\delta}\dot{E}_{\delta\beta}^E + \bar{M}_\alpha^{\cdot\beta}L_{\cdot\beta}^{R\alpha} + \bar{M}_\alpha^{\cdot\beta}\bar{L}_{\cdot\beta}^{P\alpha} \ ,
\end{aligned} \tag{9.23}$$

where $\dot{\bar{g}}_{\alpha\beta} = d(\bar{g}_\alpha \cdot \bar{g}_\beta)/dt = 0$ is assumed. From (9.11) with $\dot{\bar{g}}_\alpha = 0$,

$$\dot{\bar{\Psi}} = \frac{\partial\bar{\Psi}}{\partial E_{\alpha\beta}^E}\dot{E}_{\alpha\beta}^E + \frac{\partial\bar{\Psi}}{\partial F_{\cdot\beta}^{R\alpha}}\dot{F}_{\cdot\beta}^{R\alpha} + \frac{\partial\bar{\Psi}}{\partial\theta}\dot{\theta} + \frac{\partial\bar{\Psi}}{\partial\theta_{,\alpha}}\bar{\gamma}_\alpha + \frac{\partial\bar{\Psi}}{\partial\alpha}\dot{\alpha} \ , \tag{9.24}$$

where the intermediate rate of temperature gradient obeys the identities

$$\begin{aligned}
\bar{\gamma}_\alpha &= d(\theta_{,\alpha})/dt = d(\theta_{,A}\bar{F}_{\cdot\alpha}^{-1A})/dt \\
&= \dot{\theta}_{,\alpha} + \theta_{,\beta}\bar{F}_{\cdot A}^\beta\dot{\bar{F}}_{\cdot\alpha}^{-1A} = \dot{\theta}_{,\alpha} - \theta_{,\beta}\dot{\bar{F}}_{\cdot A}^\beta\bar{F}_{\cdot\alpha}^{-1A} \ .
\end{aligned} \tag{9.25}$$

Inserting (9.23) and (9.24) into (9.22), the dissipation inequality becomes

$$\begin{aligned}
&\left(\bar{\Sigma}^{\alpha\beta} - \frac{\partial\bar{\Psi}}{\partial E_{\alpha\beta}^E}\right)\dot{E}_{\alpha\beta}^E - \left(\bar{N} + \frac{\partial\bar{\Psi}}{\partial\theta}\right)\dot{\theta} - \frac{\partial\bar{\Psi}}{\partial\theta_{,\alpha}}\bar{\gamma}_\alpha \\
&-\frac{\partial\bar{\Psi}}{\partial F_{\cdot\delta}^{R\alpha}}F_{\cdot\delta}^{R\beta}\dot{F}_{\cdot\chi}^{R\alpha}F_{\cdot\beta}^{R-1\chi} + \left(\bar{M}_\alpha^{\cdot\beta} - \bar{\Psi}\delta_{\cdot\alpha}^\beta\right)\dot{F}_{\cdot\chi}^{R\alpha}F_{\cdot\beta}^{R-1\chi} \\
&+\left(\bar{M}_\alpha^{\cdot\beta} - \bar{\Psi}\delta_{\cdot\alpha}^\beta\right)\bar{L}_{\cdot\beta}^{P\alpha} - \frac{\partial\bar{\Psi}}{\partial\alpha}\dot{\alpha} - \theta^{-1}\bar{q}^\alpha\theta_{,\alpha} \geq 0.
\end{aligned} \tag{9.26}$$

It is assumed that coefficients of $\dot{\mathbf{E}}^{\mathbf{E}}$, $\dot{\theta}$, and $\bar{\gamma}$ should vanish identically in (9.26) to ensure thermodynamic admissibility. The following constitutive relations are then deduced:

$$\bar{\Sigma} = \frac{\partial\bar{\Psi}}{\partial\mathbf{E}^{\mathbf{E}}} = \frac{\partial\bar{\Psi}}{\partial\mathbf{E}^{\mathbf{E}T}} = \bar{\Sigma}^T \ , \quad \bar{N} = -\frac{\partial\bar{\Psi}}{\partial\theta} \ , \quad \frac{\partial\bar{\Psi}}{\partial(\bar{\nabla}\theta)} = 0 \ , \tag{9.27}$$

and it follows that the free energy, entropy, and stress do not depend explicitly on the temperature gradient:

$$\begin{aligned}
\bar{\Psi} &= \bar{\Psi}\left(\mathbf{E}^{\mathbf{E}}, \mathbf{F}^{\mathbf{R}}, \alpha, \theta, X, \bar{\mathbf{g}}_\alpha\right), \quad \bar{N} = \bar{N}\left(\mathbf{E}^{\mathbf{E}}, \mathbf{F}^{\mathbf{R}}, \alpha, \theta, X, \bar{\mathbf{g}}_\alpha\right), \\
\bar{\Sigma} &= \bar{\Sigma}\left(\mathbf{E}^{\mathbf{E}}, \mathbf{F}^{\mathbf{R}}, \alpha, \theta, X, \bar{\mathbf{g}}_\alpha\right).
\end{aligned} \tag{9.28}$$

The Cauchy stress tensor and specific entropy per unit mass are then obtained, respectively, from (9.7) and (9.5):

$$\sigma^{ab} = J^{E-1} F^{Ea}_{.\alpha} \frac{\partial \overline{\Psi}}{\partial E^E_{\alpha\beta}} F^{Eb}_{.\beta} \,, \quad \eta = -\frac{1}{\rho} \frac{\partial \overline{\Psi}}{\partial \theta} \,. \tag{9.29}$$

Using the chain rule and the functional dependency $C^E_{\alpha\beta} = C^E_{\alpha\beta}(F^{Ea}_{.\alpha}, g_{ab})$,

$$2\frac{\partial \overline{\Psi}}{\partial g_{ab}} = 2\frac{\partial \overline{\Psi}}{\partial C^E_{\alpha\beta}} \frac{\partial C^E_{\alpha\beta}}{\partial g_{ab}} = F^{Ea}_{.\alpha} \frac{\partial \overline{\Psi}}{\partial E^E_{\alpha\beta}} F^{Eb}_{.\beta} \,. \tag{9.30}$$

Following a similar calculation as that listed in (6.29), a relation similar to Doyle-Ericksen formula (5.36) of nonlinear elasticity is obtained:

$$\sigma^{ab} = 2\rho\frac{\partial \psi}{\partial g_{ab}} = 2\rho\frac{\partial \psi}{\partial g_{ba}} = \sigma^{ba} \,. \tag{9.31}$$

Dissipation associated with heat conduction can be prescribed non-negative by assuming a Fourier-type conduction law analogous to (5.48), (6.30), and (8.47):

$$\overline{\mathbf{q}} = -\overline{\mathbf{K}}\overline{\nabla}\theta \,, \quad \overline{q}^\alpha = -\overline{K}^{\alpha\beta}\theta_{,\beta} = -\overline{K}^{\alpha\beta}\theta_{,b}F^{Eb}_{.\beta} = -\overline{K}^{\alpha\beta}\theta_{,B}\overline{F}^B_{.\beta} \,, \tag{9.32}$$

with $\overline{\mathbf{K}}(X,t)$ a symmetric positive semi-definite matrix of thermal conductivity that, like $\mathbf{K}$ of (5.48), may generally depend on temperature and other state variables:

$$-\frac{1}{\theta}\langle\overline{\nabla}\theta,\overline{\mathbf{q}}\rangle = \frac{1}{\theta}\langle\overline{\nabla}\theta,\overline{\mathbf{K}}\overline{\nabla}\theta\rangle \geq 0 \,. \tag{9.33}$$

Implementing (9.27), the dissipation inequality consists of the remaining terms in (9.26):

$$\overline{\Pi}^{.\beta}_\alpha \overline{L}^{P\alpha}_{.\beta} + \left(\overline{\Pi}^{.\beta}_\alpha - \frac{\partial \overline{\Psi}}{\partial F^{R\alpha}_{.\delta}}F^{R\beta}_{.\delta}\right)L^{R\alpha}_{.\beta} - \frac{\partial \overline{\Psi}}{\partial \alpha}\dot{\alpha} + \frac{1}{\theta}\overline{K}^{\alpha\beta}\theta_{,\alpha}\theta_{,\beta} \geq 0 \,, \tag{9.34}$$

where

$$\overline{\mathbf{\Pi}} = \overline{\mathbf{M}} - \overline{\Psi}\mathbf{1}, \quad \overline{\Pi}^{.\beta}_\alpha = \overline{M}^{.\beta}_\alpha - \overline{\Psi}\delta^{.\beta}_\alpha \,. \tag{9.35}$$

Stress measure $\overline{\mathbf{\Pi}}$ is similar to $\tilde{\mathbf{\Pi}}$ of (6.33), and is related to a quantity introduced by Eshelby (1975) whose divergence represents a kind of force on arbitrary heterogeneities in elastic solids, as discussed in Section 6.6. The scalar quantity

$$\begin{aligned}
\dot{\overline{W}}^P &= \overline{\mathbf{\Pi}}:\overline{\mathbf{L}}^P = \overline{\Pi}^{.\beta}_\alpha \overline{L}^{P\alpha}_{.\beta} = \overline{\Pi}^{.\beta}_\alpha F^{R\alpha}_{.\chi}L^{P\chi}_{.\delta}F^{R-1\delta}_{.\beta} \\
&= J^E F^{Ea}_{.\alpha}F^{R\alpha}_{.\chi}\sigma^b_a F^{R-1\delta}_{.\beta}F^{E-1\beta}_{.b}L^{P\chi}_{.\delta} - \overline{\Psi}\delta^\beta_\alpha F^{R\alpha}_{.\chi}F^{R-1\delta}_{.\beta}L^{P\chi}_{.\delta} \\
&= J^{R-1}\left[(J^L F^{La}_{.\chi}\sigma^b_a F^{L-1\delta}_{.b}) - J^R\overline{\Psi}\delta^\delta_{.\chi}\right]L^{P\chi}_{.\delta} \\
&= J^{R-1}\left[\tilde{M}^{.\delta}_\chi - \tilde{\Psi}\delta^\delta_{.\chi}\right]L^{P\chi}_{.\delta} = J^{R-1}\tilde{\Pi}^{.\delta}_\chi L^{P\chi}_{.\delta} = J^{R-1}\dot{W}^P \,,
\end{aligned} \tag{9.36}$$

is referred to in Chapter 9 as the plastic dissipation or the rate of plastic work, and is related to the plastic work rate per unit volume in configura-

tion $\tilde{B}$, first defined as $\dot{W}^P$ in (6.34), as indicated in the final expression of (9.36). Therefore, the first term on the left side of inequality (9.34) represents the effect of the plastic velocity gradient, i.e., plastic dissipation, on the rate of temperature increase. The second term, in parentheses on the left of (9.34), accounts for possible dissipation and free energy storage associated with residual deformation contribution $\mathbf{F^R}$, and is thermodynamically conjugate to the time rate of change of $\mathbf{F^R}$. The third term on the left of (9.34) represents energetic changes attributed to the rate of the internal state variable α, for example residual elastic energy accumulation with increases in defect densities, or decreases in recoverable elastic energy commensurate with damage mechanisms, e.g., strain energy release rates during fracture. The last term on the left of (9.34) accounts for heat conduction.

A specific heat parameter at constant elastic strain, constant residual deformation, and constant internal variable α, measured as energy per degree per unit intermediate volume, is introduced as

$$\overline{C} = \left.\frac{\partial \overline{E}}{\partial \theta}\right|_{\mathbf{E^E},\mathbf{F^R},\alpha} = \left[\frac{\partial \overline{E}}{\partial \overline{N}}\right]\left[\frac{\partial \overline{N}}{\partial \theta}\right]$$

$$= \left[\theta + \frac{\partial \theta}{\partial \overline{N}}\left(\overline{N} + \frac{\partial \overline{\varPsi}}{\partial \theta}\right)\right]\left[-\frac{\partial^2 \overline{\varPsi}}{\partial \theta^2}\right] = -\theta\frac{\partial^2 \overline{\varPsi}}{\partial \theta^2},$$

(9.37)

where (9.27) has been used. Multiplying (4.39) by $\overline{J}^{-1}$, the local balance of energy per unit volume in configuration $\overline{B}$ is

$$\overline{\rho}\dot{e} = \dot{\overline{E}} - \dot{\overline{\rho}}e = \dot{\overline{E}} - \overline{J}^{-1}\rho_0 e$$

$$= \dot{\overline{E}} + \dot{\overline{J}}\overline{J}^{-1}\overline{E} = \overline{M}_\alpha^{\ \beta}\overline{L}_{\cdot\beta}^\alpha - \overline{J}^{-1}Q_{;A}^A + \overline{\rho}r.$$

(9.38)

Substituting from (9.24) and the second of (9.27), the rate of internal energy can be written as

$$\dot{\overline{E}} = \dot{\overline{\varPsi}} + \dot{\theta}\overline{N} + \theta\dot{\overline{N}}$$

$$= \frac{\partial \overline{\varPsi}}{\partial E_{\alpha\beta}^E}\dot{E}_{\alpha\beta}^E + \frac{\partial \overline{\varPsi}}{\partial F_{\cdot\beta}^{R\alpha}}\dot{F}_{\cdot\beta}^{R\alpha} + \frac{\partial \overline{\varPsi}}{\partial \alpha}\dot{\alpha} + \theta\dot{\overline{N}}$$

(9.39)

$$= \overline{M}_\alpha^{\ \beta}\overline{L}_{\cdot\beta}^\alpha - \dot{\overline{J}}\overline{J}^{-1}\overline{E} - \hat{\nabla}_\alpha\overline{q}^\alpha + \overline{\rho}r.$$

The anholonomic covariant derivative of the heat flux is defined as in (8.54):

$$\hat{\nabla}_\alpha(.) = (.)_{:A}\overline{F}_{\cdot\alpha}^{-1A} + \overline{J}^{-1}(.)(\overline{JF}_{\cdot\alpha}^{-1A})_{:A},$$

(9.40)

such that

$$\overline{J}^{-1}Q_{;A}^A = \overline{J}^{-1}(\overline{JF}_{\cdot\alpha}^{-1A}\overline{q}^\alpha)_{;A} = (\overline{q}^\alpha)_{:A}\overline{F}_{\cdot\alpha}^{-1A} + \overline{J}^{-1}\overline{q}^\alpha(\overline{JF}_{\cdot\alpha}^{-1A})_{:A} = \hat{\nabla}_\alpha\overline{q}^\alpha.$$ (9.41)

From (2.226), the term $(\overline{J}F_{.\alpha}^{-1A})_{:A} = 0$ when $\overline{F}_{[A:B]}^{\alpha} = 0$. Rearranging (9.39) for the rate of entropy production and using (9.27),

$$
\theta \dot{\overline{N}} = \overline{M}_{\alpha}^{.\beta} \overline{L}_{.\beta}^{\alpha} - \frac{\partial \overline{\Psi}}{\partial E_{\alpha\beta}^{E}} \dot{E}_{\alpha\beta}^{E} - \frac{\partial \overline{\Psi}}{\partial F_{.\beta}^{R\alpha}} \dot{F}_{.\beta}^{R\alpha}
$$

$$
- \frac{\partial \overline{\Psi}}{\partial \alpha} \dot{\alpha} - \dot{\overline{J}} J^{-1} \overline{E} - \hat{\nabla}_{\alpha} \overline{q}^{\alpha} + \overline{\rho} r \tag{9.42}
$$

$$
= \left(\overline{\Pi}_{\alpha}^{.\beta} + \delta_{.\alpha}^{\beta} \theta \frac{\partial \overline{\Psi}}{\partial \theta} \right) \dot{F}_{.A}^{\alpha} \overline{F}_{.\beta}^{-1A} - \frac{\partial \overline{\Psi}}{\partial F_{.\beta}^{R\alpha}} \dot{F}_{.\beta}^{R\alpha} - \frac{\partial \overline{\Psi}}{\partial \alpha} \dot{\alpha} - \hat{\nabla}_{\alpha} \overline{q}^{\alpha} + \overline{\rho} r.
$$

Entropy production can also be expressed analogously to (5.50) and (6.41):

$$
\theta \dot{\overline{N}} = -\theta \frac{d}{dt} \left(\frac{\partial \overline{\Psi}}{\partial \theta} \right)
$$

$$
= -\theta \left(\frac{\partial^{2} \overline{\Psi}}{\partial \theta^{2}} \dot{\theta} + \frac{\partial^{2} \overline{\Psi}}{\partial \theta \partial E_{\alpha\beta}^{E}} \dot{E}_{\alpha\beta}^{E} + \frac{\partial^{2} \overline{\Psi}}{\partial \theta \partial F_{.\beta}^{R\alpha}} \dot{F}_{.\beta}^{R\alpha} + \frac{\partial^{2} \overline{\Psi}}{\partial \theta \partial \alpha} \dot{\alpha} \right) \tag{9.43}
$$

$$
= \overline{C} \dot{\theta} + \theta \overline{\beta}^{\alpha\beta} \dot{E}_{\alpha\beta}^{E} - \theta \frac{\partial^{2} \overline{\Psi}}{\partial \theta \partial F_{.\beta}^{R\alpha}} \dot{F}_{.\beta}^{R\alpha} - \theta \frac{\partial^{2} \overline{\Psi}}{\partial \theta \partial \alpha} \dot{\alpha},
$$

where stress-temperature coefficients in the intermediate configuration are

$$
\overline{\beta} = -\frac{\partial^{2} \overline{\Psi}}{\partial \theta \partial \mathbf{E}^{E}} \Bigg|_{\mathbf{F}^{R},\alpha}. \tag{9.44}
$$

Equating (9.42) and (9.43) and using (9.32), the temperature rate becomes

$$
\overline{C} \dot{\theta} = \left(\overline{\Pi}_{\alpha}^{.\beta} + \delta_{.\alpha}^{\beta} \theta \frac{\partial \overline{\Psi}}{\partial \theta} \right) \dot{F}_{.A}^{\alpha} \overline{F}_{.\beta}^{-1A} - \left(\frac{\partial \overline{\Psi}}{\partial F_{.\beta}^{R\alpha}} - \theta \frac{\partial^{2} \overline{\Psi}}{\partial \theta \partial F_{.\beta}^{R\alpha}} \right) \dot{F}_{.\beta}^{R\alpha}
$$

$$
- \left(\frac{\partial \overline{\Psi}}{\partial \alpha} - \theta \frac{\partial^{2} \overline{\Psi}}{\partial \theta \partial \alpha} \right) \dot{\alpha} - \theta \overline{\beta}^{\alpha\beta} \dot{E}_{\alpha\beta}^{E} + \hat{\nabla}_{\alpha} (\overline{K}^{\alpha\beta} \theta_{,\beta}) + \overline{\rho} r
$$

$$
= \dot{\overline{W}}^{P} + \theta \frac{\partial \overline{\Psi}}{\partial \theta} L_{.\alpha}^{P\alpha} - \left(\frac{\partial \overline{\Psi}}{\partial \alpha} - \theta \frac{\partial^{2} \overline{\Psi}}{\partial \theta \partial \alpha} \right) \dot{\alpha} + \hat{\nabla}_{\alpha} (\overline{K}^{\alpha\beta} \theta_{,\beta}) + \overline{\rho} r \tag{9.45}
$$

$$
- \theta \overline{\beta}^{\alpha\beta} \dot{E}_{\alpha\beta}^{E} + \left(\overline{\Pi}_{\alpha}^{.\beta} + \delta_{.\alpha}^{\beta} \theta \frac{\partial \overline{\Psi}}{\partial \theta} - \frac{\partial \overline{\Psi}}{\partial F_{.\delta}^{R\alpha}} F_{.\delta}^{R\beta} + \theta \frac{\partial^{2} \overline{\Psi}}{\partial \theta \partial F_{.\delta}^{R\alpha}} F_{.\delta}^{R\beta} \right) L_{.\beta}^{R\alpha}.
$$

The first two terms on the right side of the final equality in (9.45) represent, respectively, plastic dissipation and entropy production associated with plastic volume change:

$$
\dot{\overline{W}}^{P} + \theta \frac{\partial \overline{\Psi}}{\partial \theta} L_{.\alpha}^{P\alpha} = J^{R-1} \tilde{\Pi}_{\chi}^{.\delta} L_{.\delta}^{P\chi} + \frac{\dot{J}^{P}}{J^{P}} \frac{\partial \overline{\Psi}}{\partial \ln \theta}. \tag{9.46}
$$

Notice that when the plastic deformation is isochoric, as required for lattice-preserving slip in the present context, then $\dot{J}^P = J^P L^{P\alpha}_{.\alpha} = 0$. The next term on the right of (9.45) represents energetic changes attributed to the rate of change of the internal state variable α, for example energy accumulation or release with changes in defect density. The subsequent two terms on the right of (9.45) account for heat conduction and non-mechanical heat sources, respectively. The next term represents contributions from thermoelastic coupling. The final term,

$$
\begin{aligned}
&\left(\bar{\Pi}^{.\beta}_{\alpha} + \delta^{\beta}_{.\alpha}\theta\frac{\partial \bar{\Psi}}{\partial \theta} - \frac{\partial \bar{\Psi}}{\partial F^{R\alpha}_{.\delta}}F^{R\beta}_{.\delta} + \theta\frac{\partial^2 \bar{\Psi}}{\partial \theta \partial F^{R\alpha}_{.\delta}}F^{R\beta}_{.\delta} \right)L^{R\alpha}_{.\beta} \\
&= \left(\bar{\Pi}^{.\beta}_{\alpha}F^{R-1\delta}_{.\beta} - \frac{\partial \bar{\Psi}}{\partial F^{R\alpha}_{.\delta}} \right)\dot{F}^{R\alpha}_{.\delta} + \frac{1}{J^R}\frac{\partial \bar{\Psi}}{\partial \ln \theta}\dot{J}^R + \frac{\partial^2 \bar{\Psi}}{\partial F^{R\alpha}_{.\delta}\partial \ln \theta}\dot{F}^{R\alpha}_{.\delta}
\end{aligned}
\tag{9.47}
$$

accounts for energy storage and release associated with the time rate of change of residual deformation $\mathbf{F^R}$. Notice that because the value of free energy $\bar{\Psi}$ itself enters stress measure $\bar{\Pi}$ in (9.34) and (9.45), this free energy per unit intermediate volume cannot always be prescribed arbitrarily to within an additive constant.

In what follows in Sections 9.2-9.4, the framework of Section 9.1, i.e., (9.1)-(9.47), is specialized to describe different classes of behavior in deformable solids. Specific forms of $\mathbf{F^R}$, e.g., those listed in Table 9.1, along with specific forms of $\bar{\Psi}$ of (9.28), enable descriptions of crystalline solids containing, in addition to dislocations, a number of other kinds of defects, including voids, point defects, mechanical twins, and disclinations.

9.2 Porous Elastoplasticity

Constitutive frameworks for classes of solids exhibiting two different isotropic residual deformation mechanisms are considered in Section 9.2: volumetric expansion attributed to void nucleation and growth, and volumetric contraction attributed to pore collapse. The constitutive framework for the former case (i.e., expansion) described in Section 9.2.1 exhibits similarities to continuum damage mechanics theories (Lemaitre 1985; Krajcinovic 1996). These similarities are briefly discussed in Section 9.2.2, prior to presentation of the framework for pore collapse given in Section 9.2.3.

9.2.1 Void Nucleation and Growth

Consider first materials that undergo expansion as a result of void nucleation and growth, following the kinematic description given in Section 3.2.8 and the fourth row of Table 9.1. Many ductile metals demonstrate such phenomena when subjected to large tensile pressures; voids may also nucleate during creep processes wherein dislocation climb and vacancy migration and coalescence are prevalent (McClintock 1968; Rice and Tracey 1969; Gurson 1977; Bammann and Aifantis 1989). Void nucleation and growth also are known to contribute to spall fracture in ductile metals, with such damage the result of high rate inertial loading and wave reverberations (Antoun et al. 2003; Wright and Ramesh 2008). In Section 9.2, $\mathbf{F}^E$ of (9.1) accounts for both mechanical elastic deformation and thermal deformation.

Residual deformation attributed to an isotropic distribution of spherical defects is, from (3.129)-(3.131),

$$\mathbf{F}^R = \mathbf{F}^V = \bar{\upsilon}\mathbf{1} = \frac{1}{(1-\bar{\phi})^{1/3}}\mathbf{1}, \ F^{R\alpha}_{.\beta} = F^{V\alpha}_{.\beta} = \bar{\upsilon}\delta^{\alpha}_{.\beta} = \frac{1}{(1-\bar{\phi})^{1/3}}\delta^{\alpha}_{.\beta}, \quad (9.48)$$

where the Jacobian determinant is $J^V = \bar{\upsilon}^3$, and where the quantity

$$\bar{\phi} = (d\bar{V} - d\tilde{V})/d\bar{V} = 1 - J^{V-1}, \quad (9.49)$$

is the volume fraction of voids or pores per unit volume in configuration $\bar{B}$. Let $r_0(X,t) \geq 0$ be the typical radius of a void contained in a volume element of material at reference location X; this radius may evolve with time as voids shrink or expand. Then

$$\bar{\phi} = \frac{4}{3}\pi r_0^3 \bar{\xi}, \ \phi_0 = \frac{4}{3}\pi r_0^3 \xi_0, \ \xi_0 = J^V \bar{\xi}, \ \phi_0 = J^V \bar{\phi}, \quad (9.50)$$

where ϕ_0 is the fraction of voids per unit reference volume in B_0, $\bar{\xi}$ is the number of voids per unit intermediate volume in $\bar{B}$, and $\xi_0(X,t) \geq 0$ is the number of voids per unit reference volume. In the present treatment, the material is assumed fully dense in the initial state, hence $r_0(X,0) = 0$ and $\xi_0(X,0) = 0$. Since void radii and number densities are always nonnegative, and since the total volume occupied by the material and voids remains bounded,

$$0 \leq \bar{\phi} < 1, \ 1 \leq J^V < \infty. \quad (9.51)$$

From (9.48), the deformation rate contribution attributed to defect-induced volumetric expansion is

$$\mathbf{L}^R = \mathbf{L}^V = \dot{\mathbf{F}}^V \mathbf{F}^{V-1} = \frac{\dot{\bar{\phi}}}{3 - 3\bar{\phi}}\mathbf{1}, \ L^{R\alpha}_{.\beta} = \frac{\dot{\bar{\phi}}}{3 - 3\bar{\phi}}\delta^{\alpha}_{.\beta}, \ L^{R\alpha}_{.\alpha} = \frac{\dot{\bar{\phi}}}{1 - \bar{\phi}}, \quad (9.52)$$

where from (9.50), the porosity rate per unit intermediate volume is

$$\dot{\bar{\phi}} = 4\pi r_0^{\;2}\left(\frac{r_0}{3}\dot{\bar{\xi}} + \dot{r}_0\bar{\xi}\right). \tag{9.53}$$

An illustrative form of free energy function (9.11) and (9.28) for the present class of defective solids is

$$\bar{\Psi} = \bar{\Psi}\left(\mathbf{E}^{\mathbf{E}},\bar{\phi},\alpha,\theta,X,\bar{\mathbf{g}}_\alpha\right), \tag{9.54}$$

where $\alpha(X,t)$ accounts for effects of other internal variables distinct from the void concentration $\bar{\phi}(X,t)$, e.g., dislocations or other defects. Notice that $\mathbf{F^R}$ need not be included in the list of independent variables, since $\mathbf{F^R}$ of (9.48) can be expressed directly in terms of $\bar{\phi}$. Using (9.52) and (9.54), dissipation inequality (9.34) and energy balance (9.45) reduce to

$$\bar{\varPi}_\alpha^{.\beta}L^{P\alpha}_{.\beta} + \left(\frac{1}{3-3\bar{\phi}}\bar{\varPi}_\alpha^{.\alpha} - \frac{\partial\bar{\Psi}}{\partial\bar{\phi}}\right)\dot{\bar{\phi}} - \frac{\partial\bar{\Psi}}{\partial\alpha}\dot{\alpha} + \frac{1}{\theta}\bar{K}^{\alpha\beta}\theta_{,\alpha}\theta_{,\beta} \geq 0, \tag{9.55}$$

$$\bar{C}\dot{\theta} = \dot{\bar{W}}^P + \theta\frac{\partial\bar{\Psi}}{\partial\theta}L^{P\alpha}_{.\alpha} - \left(\frac{\partial\bar{\Psi}}{\partial\alpha} - \theta\frac{\partial^2\bar{\Psi}}{\partial\theta\partial\alpha}\right)\dot{\alpha} + \hat{\nabla}_\alpha(\bar{K}^{\alpha\beta}\theta_{,\beta}) + \bar{\rho}r$$

$$ - \theta\bar{\beta}^{\alpha\beta}\dot{E}^E_{\alpha\beta} + \left(\frac{1}{3-3\bar{\phi}}\bar{\varPi}_\alpha^{.\alpha} + \frac{\theta}{1-\bar{\phi}}\frac{\partial\bar{\Psi}}{\partial\theta} - \frac{\partial\bar{\Psi}}{\partial\bar{\phi}} + \theta\frac{\partial^2\bar{\Psi}}{\partial\theta\partial\bar{\phi}}\right)\dot{\bar{\phi}}. \tag{9.56}$$

Since $\mathbf{F^R}$ is spherical, $\bar{\mathbf{L}}^{\mathbf{P}} = \mathbf{L^P} = \dot{\mathbf{F}}^{\mathbf{P}}\mathbf{F}^{\mathbf{P}-1}$ is the purely plastic velocity gradient of (3.58).

A more specific form of (9.54) is

$$\bar{\Psi} = \bar{\Psi}^E\left(\mathbf{E}^{\mathbf{E}},\bar{\phi},\theta,X,\bar{\mathbf{g}}_\alpha\right) + \bar{\Psi}^R\left(\bar{\phi},\alpha,\theta,X,\bar{\mathbf{g}}_\alpha\right), \tag{9.57}$$

where $\bar{\Psi}^E$ accounts for the thermoelastic response (with material coefficients affected by porosity) and $\bar{\Psi}^R$ accounts for energy associated with defects. Assuming a materially linear hyperelastic response along the lines of (5.84), the thermoelastic part of the free energy is expanded about a reference state in which $\Delta\theta = \theta - \theta_0 = 0$ and $E^E_{\alpha\beta} = 0$:

$$\bar{\Psi}^E = \frac{1}{2}\hat{\mathbb{C}}^{\alpha\beta\chi\delta}E^E_{\alpha\beta}E^E_{\chi\delta} - \hat{\beta}^{\alpha\beta}E^E_{\alpha\beta}\Delta\theta - \hat{C}\theta\ln\frac{\theta}{\theta_0}, \tag{9.58}$$

where the effective thermoelastic coefficients depend on orientation, position, and void volume fraction, and are not constants at a point X:

$$\hat{\mathbb{C}}^{\alpha\beta\chi\delta}\left(\bar{\phi},X,\bar{\mathbf{g}}_\alpha\right) = \left.\frac{\partial^2\bar{\Psi}^E}{\partial E^E_{\alpha\beta}\partial E^E_{\chi\delta}}\right|_{\substack{\mathbf{E^E}=0 \\ \theta=\theta_0}}, \quad \hat{\beta}^{\alpha\beta}\left(\bar{\phi},X,\bar{\mathbf{g}}_\alpha\right) = -\left.\frac{\partial^2\bar{\Psi}^E}{\partial\theta\partial E^E_{\alpha\beta}}\right|_{\substack{\mathbf{E^E}=0 \\ \theta=\theta_0}}, \tag{9.59}$$

$$\hat{C}(\overline{\phi}, X) = -\left(\theta \frac{\partial^2 \overline{\varPsi}^E}{\partial \theta^2}\right)\bigg|_{\substack{\mathbf{E}^E=0 \\ \theta=\theta_0}}. \tag{9.60}$$

A number of specific forms for effective material coefficients, in particular effective moduli of (9.59), in terms of void volume fraction can be found in texts on micromechanics (Nemat-Nasser and Hori 1999). Perhaps the simplest physically realistic assumption is that each term in the thermoelastic energy (9.58) degrades linearly with increasing void volume fraction:

$$\overline{\varPsi}^E = \frac{1}{2}\overline{\mathbb{C}}^{\alpha\beta\chi\delta}(1-\overline{\phi})E_{\alpha\beta}^E E_{\chi\delta}^E - \overline{\beta}^{\alpha\beta}(1-\overline{\phi})E_{\alpha\beta}^E \Delta\theta - \overline{C}(1-\overline{\phi})\theta\ln\frac{\theta}{\theta_0}, \tag{9.61}$$

where the thermoelastic constants for a fully dense (poly)crystalline element of material are defined as

$$\overline{\mathbb{C}}^{\alpha\beta\chi\delta} = \hat{\mathbb{C}}^{\alpha\beta\chi\delta}(0, X, \overline{\mathbf{g}}_\alpha), \ \overline{\beta}^{\alpha\beta} = \hat{\beta}^{\alpha\beta}(0, X, \overline{\mathbf{g}}_\alpha), \ \overline{C} = \hat{C}(0, X). \tag{9.62}$$

Effective elastic coefficients $\overline{\mathbb{C}}^{\alpha\beta\chi\delta}$ are thus interpreted as Voigt averages (see (A.33) of Appendix A) over the volume element since the energy density vanishes inside the free space occupied by the voids. Since voids are assumed to affect the material response in an isotropic manner, their presence does not alter the symmetry properties of the material. Thus, the degraded coefficients exhibit the same material symmetries as the thermoelastic coefficients of the fully dense material in (9.62), with symmetries of the latter discussed in Section 5.1.5 of Chapter 5 and in Appendix A for specific crystal classes.

For an isotropic material, e.g., a polycrystal with randomly oriented grains, (9.58) reduces to

$$\overline{\varPsi}^E = \frac{1}{2}\left[\hat{\mu}(\overline{g}^{\alpha\chi}\overline{g}^{\beta\delta} + \overline{g}^{\alpha\delta}\overline{g}^{\chi\beta}) + \hat{\lambda}\overline{g}^{\alpha\beta}\overline{g}^{\chi\delta}\right]E_{\alpha\beta}^E E_{\chi\delta}^E$$

$$- \hat{\beta}\overline{g}^{\alpha\beta}E_{\alpha\beta}^E \Delta\theta - \hat{C}\theta\ln\frac{\theta}{\theta_0} \tag{9.63}$$

$$= \frac{1}{2}\hat{K}(E_{\cdot\alpha}^{E\alpha})^2 + \hat{\mu}E_{\alpha\beta}'^E E'^{E\alpha\beta} - \hat{\beta}\overline{g}^{\alpha\beta}E_{\alpha\beta}^E \Delta\theta - \hat{C}\theta\ln\frac{\theta}{\theta_0},$$

where the deviatoric part of the elastic strain is $E_{\alpha\beta}'^E = E_{\alpha\beta}^E - E_{\cdot\chi}'^{E\chi}/3$, the effective thermal stress coefficient is $\hat{\beta}$, and the effective shear modulus, Lamé coefficient, and bulk modulus are $\hat{\mu}$, $\hat{\lambda}$, and $\hat{K}$, respectively. For linear degradation of coefficients with porosity as in (9.61), the effective elastic coefficients are

$$\hat{\mu} = (1-\overline{\phi})\mu, \ \hat{\lambda} = (1-\overline{\phi})\lambda, \ \hat{K} = (1-\overline{\phi})K, \tag{9.64}$$

with μ, λ, and K elastic constants of the fully dense material. Using Table A.10, an effective Young's modulus and Poisson ratio are, respectively

$$\widehat{E} = \frac{\widehat{\mu}(2\widehat{\mu}+3\widehat{\lambda})}{\widehat{\mu}+\widehat{\lambda}} = (1-\overline{\phi})\frac{\mu(2\mu+3\lambda)}{\mu+\lambda} = (1-\overline{\phi})E , \qquad (9.65)$$

$$\widehat{v} = \frac{\widehat{\lambda}}{2(\widehat{\mu}+\widehat{\lambda})} = \frac{\lambda}{2(\mu+\lambda)} = v . \qquad (9.66)$$

Thus, Poisson's ratio remains unaffected by porosity according to the simple model of (9.64). Notice that for small volume fractions of defects, the following approximations can be substituted into (9.61) and (9.64)-(9.66):

$$1-\overline{\phi} \approx \frac{1}{1+\overline{\phi}} \approx 1-\phi_0 \approx \frac{1}{1+\phi_0} . \qquad (9.67)$$

An alternative set of expressions to (9.64), widely used, for effective isotropic elastic constants of solids with voids was derived by Mackenzie (1950) using a self-consistent approach:

$$\widehat{\mu} = \mu\left[1-5\left(\frac{3K+4\mu}{9K+8\mu}\right)\overline{\phi}\right], \ \widehat{K} = \frac{4\mu K(1-\overline{\phi})}{4\mu+3K\overline{\phi}} . \qquad (9.68)$$

Now consider the contribution of lattice defects to the free energy (9.57). For illustrative purposes, let α represent a normalized total dislocation density as in (6.100):

$$\alpha = \overline{b}\sqrt{\overline{\rho}_T} , \qquad (9.69)$$

with $\overline{b}$ a constant magnitude of Burgers vector and $\overline{\rho}_T(X,t)$ the line length of dislocations per unit volume in configuration $\overline{B}$. Furthermore let $\overline{\gamma}(\theta,X)$ denote a scalar energy per unit area associated with possible surface tension in each void (Huo et al. 1999). The residual free energy for non-interacting defects can be approximated by

$$\overline{\Psi}^R = \Lambda\mu\alpha^2 + 4\pi\overline{\gamma}r_0^2\overline{\xi} = \Lambda\mu\overline{b}^2\overline{\rho}_T + 3\overline{\gamma}r_0^{-1}\overline{\phi} , \qquad (9.70)$$

where Λ is a constant on the order of unity as introduced in (6.118) that scales the energy per unit length of dislocation lines and μ is an elastic shear modulus of the crystalline matrix.

A kinetic equation is required to specify the time rate of porosity, $\dot{\overline{\phi}}$, following the general form of (9.15), for example. A number of kinetic laws for void nucleation, growth, and/or coalescence have been suggested from experimental evidence and results of numerical studies for plastically deforming metallic solids subjected to various loading conditions (Gurson 1977; Cocks and Ashby 1980; Budianski et al. 1982; Becker and Needle-

man 1986; Bammann and Aifantis 1989; Rajendran et al. 1989; McDowell et al. 1993; Marin and McDowell 1996; Horstemeyer et al. 2000). A kinetic relation can be posited directly as an explicit evolution law (Cocks and Ashby 1980; Bammann et al. 1993) or implicitly as the volumetric part of the derivative of a dissipation potential with respect to some measure of stress (Gurson 1977; Tvergaard 1981; Becker 1987). The former class of models often falls into the category of non-associative plasticity (see Section 6.4) if the rate of porosity is labeled as a plastic volume change, while the latter class of models corresponds to associative plasticity. From the perspective of dissipation inequality (9.55), it may be desirable to require

$$\frac{1}{3-3\bar{\phi}}\bar{\Pi}_\alpha^{\,\alpha}\dot{\bar{\phi}} = -\bar{p}\dot{\bar{\phi}} \geq 0 \,, \;\; 3\bar{p} = \frac{1}{\bar{\phi}-1}\operatorname{tr}\bar{\mathbf{\Pi}}\,. \tag{9.71}$$

where $\bar{p}$ is an effective pressure, the spherical part of the Eshelby-type stress in configuration $\bar{B}$, negative in algebraic sign in tension. Evolution laws requiring $\bar{p}$ and $\dot{\bar{\phi}}$ to exhibit opposite algebraic signs (when both are nonzero) will automatically result in $-\bar{p}\dot{\bar{\phi}} \geq 0$. This is a physically realistic requirement, since void growth is usually accelerated by tensile hydrostatic stress, and void collapse promoted by compressive hydrostatic stress. Under adiabatic loading conditions, energy dissipated in (9.71) would contribute to a temperature change in (9.56), for example via heat generated from local plastic deformation in the vicinity of expanding voids.

As discussed in Section 6.4 of Chapter 6, kinetic relations for macroscopic plasticity (i.e., a description wherein each material element consists of a large number of single crystals), are often expressed in the spatial configuration B as opposed to an intermediate configuration. In the context of a spatial description, the spatial velocity gradient (9.19) is used as the primary descriptor of kinematics:

$$\mathbf{L} = \dot{\mathbf{F}}^{\mathbf{E}}\mathbf{F}^{\mathbf{E}-1} + \mathbf{F}^{\mathbf{E}}\mathbf{F}^{\mathbf{R}}\dot{\mathbf{F}}^{\mathbf{P}}\mathbf{F}^{\mathbf{P}-1}\mathbf{F}^{\mathbf{R}-1}\mathbf{F}^{\mathbf{E}-1} + \mathbf{F}^{\mathbf{E}}\dot{\mathbf{F}}^{\mathbf{R}}\mathbf{F}^{\mathbf{R}-1}\mathbf{F}^{\mathbf{E}-1}$$
$$= \mathbf{L}^{\mathbf{E}} + \hat{\mathbf{L}}^{\mathbf{P}} + \hat{\mathbf{L}}^{\mathbf{R}}, \tag{9.72}$$

where

$$\mathbf{L}^{\mathbf{E}} = \dot{\mathbf{F}}^{\mathbf{E}}\mathbf{F}^{\mathbf{E}-1}\,, \;\; \hat{\mathbf{L}}^{\mathbf{P}} = \mathbf{F}^{\mathbf{E}}\mathbf{F}^{\mathbf{R}}\dot{\mathbf{F}}^{\mathbf{P}}\mathbf{F}^{\mathbf{P}-1}\mathbf{F}^{\mathbf{R}-1}\mathbf{F}^{\mathbf{E}-1}\,, \;\; \hat{\mathbf{L}}^{\mathbf{R}} = \mathbf{F}^{\mathbf{E}}\dot{\mathbf{F}}^{\mathbf{R}}\mathbf{F}^{\mathbf{R}-1}\mathbf{F}^{\mathbf{E}-1}\,. \tag{9.73}$$

Substituting from (9.48) and (9.52), the symmetric deformation rate $\mathbf{D}$ and skew spin $\mathbf{W}$ are

$$\mathbf{D} = \mathbf{L}_{symm} = \left(\dot{\mathbf{F}}^{\mathbf{E}}\mathbf{F}^{\mathbf{E}-1}\right)_{symm} + \left(\mathbf{F}^{\mathbf{E}}\dot{\mathbf{F}}^{\mathbf{P}}\mathbf{F}^{\mathbf{P}-1}\mathbf{F}^{\mathbf{E}-1}\right)_{symm} + \dot{\mathbf{F}}^{\mathbf{V}}\mathbf{F}^{\mathbf{V}-1}$$
$$= \mathbf{D}^{\mathbf{E}} + \hat{\mathbf{D}}^{\mathbf{P}} + \frac{\dot{\bar{\phi}}}{3-3\bar{\phi}}\mathbf{1}, \tag{9.74}$$

$$\mathbf{W} = \mathbf{L}_{skew} = \left(\dot{\mathbf{F}}^{\mathbf{E}} \mathbf{F}^{\mathbf{E}-1} \right)_{skew} + \left(\mathbf{F}^{\mathbf{E}} \dot{\mathbf{F}}^{\mathbf{P}} \mathbf{F}^{\mathbf{P}-1} \mathbf{F}^{\mathbf{E}-1} \right)_{skew} = \mathbf{W}^{\mathbf{E}} + \hat{\mathbf{W}}^{\mathbf{P}} . \qquad (9.75)$$

A standard assumption used to denote plastic incompressibility of the fully dense material (i.e., the matrix) is that $\hat{\mathbf{D}}^{\mathbf{P}}$ is traceless: $\hat{D}_{\cdot a}^{Pa} = 0$. Kinetic equations provide the plastic strain rate $\hat{\mathbf{D}}^{\mathbf{P}}$, plastic spin $\hat{\mathbf{W}}^{\mathbf{P}}$, and rate of porosity change $\dot{\bar{\phi}}$.

Consider first a direct approach wherein kinetic equations are supplied explicitly rather than defined as derivatives of a dissipation potential. One example of such a model is that of Bammann et al. (1993). In this plasticity model intended for metals, $\hat{\mathbf{W}}^{\mathbf{P}}$ is specified by (6.129), which remains unchanged in form when the material contains voids. Viscoplastic flow rule (6.130) is modified, however, to account for porosity:

$$\hat{\mathbf{D}}^{\mathbf{P}} = \begin{cases} \hat{f} \sinh \left[\dfrac{|\hat{\xi}| - \hat{k} - \hat{Y}(1 - \bar{\phi})}{\hat{V}(1 - \bar{\phi})} \right] \dfrac{\hat{\xi}}{|\hat{\xi}|} & \text{for } |\hat{\xi}| = (\hat{\xi} : \hat{\xi})^{1/2} \geq \hat{k} + \hat{Y}(1 - \bar{\phi}), \\ 0 & \text{for } |\hat{\xi}| = (\hat{\xi} : \hat{\xi})^{1/2} < \hat{k} + \hat{Y}(1 - \bar{\phi}), \end{cases} \qquad (9.76)$$

where terms in (9.76) are defined in Section 6.4, immediately following (6.130). The presence of voids degrades the effective yield strength of the material by a factor of $1 - \bar{\phi}$, increasing the rate of plastic deformation at a fixed level of applied stress, as explained by Bammann et al. (1993). The porosity evolution equation used by Bammann et al. (1993), similar to a model by Cocks and Ashby (1980), is

$$\dot{\bar{\phi}} = \left[\frac{1}{(1 - \bar{\phi})^m} - (1 - \bar{\phi}) \right] \sinh \left[\frac{2(1 - 2m)p}{(2m + 1)\bar{\sigma}} \right] (\hat{\mathbf{D}}^{\mathbf{P}} : \hat{\mathbf{D}}^{\mathbf{P}})^{1/2}, \qquad (9.77)$$

with m a constant, p the usual Cauchy pressure (positive in compression), and $\bar{\sigma}$ the Von Mises effective stress of (6.137). The triaxiality ratio $-p/\bar{\sigma}$ dictates the rate of porosity evolution; tensile pressure accelerates void growth for $m > 1/2$.

Another typical approach specifies kinetics of plasticity and porosity evolution via the associated flow concept:

$$\mathbf{D} - \mathbf{D}^{\mathbf{E}} = \hat{\mathbf{D}}^{\mathbf{P}} + \frac{\dot{\bar{\phi}}}{3 - 3\bar{\phi}} \mathbf{1} = \hat{\lambda}^P \frac{\partial \hat{F}}{\partial \boldsymbol{\sigma}} , \qquad (9.78)$$

where the inelastic volume change arises only from the time rate of void fraction:

$$\left(\hat{\mathbf{D}}^{\mathbf{P}} + \frac{\dot{\bar{\phi}}}{3 - 3\bar{\phi}} \mathbf{1} \right) : \mathbf{1} = \frac{\dot{\bar{\phi}}}{1 - \bar{\phi}} . \qquad (9.79)$$

In (9.78), $\hat{\lambda}^P \geq 0$ is a scalar plastic multiplier, and for a typical isotropic material, the flow potential is

$$\hat{F} = \hat{F}\left(I_1, J_2, \hat{R}, \bar{\phi}\right), \ I_1 = \text{tr}\boldsymbol{\sigma} = -3p \,, \ J_2 = \frac{1}{2}\boldsymbol{\sigma}':\boldsymbol{\sigma}' \,, \qquad (9.80)$$

with $\hat{R}$ an evolving scalar function representing the yield strength of the matrix material. Isosurfaces of $\hat{F}$ demarcate elastic ($\hat{F} < 0$) and inelastic ($\hat{F} = 0$) regimes; hence inelastic deformation is associative since yield and flow functions coincide. A number of functional forms for $\hat{F}$ have been posited, as summarized, for example, by Marin and McDowell (1996). A popular function originated by Gurson (1977) and refined by Tvergaard (1981) and Tvergaard and Needleman (1984) is usually referred to as the Gurson potential:

$$\hat{F} = \frac{3J_2}{\hat{R}^2} + 2q_1\bar{\phi}\cosh\left(\frac{q_2 I_1}{2\hat{R}}\right) - q_3\bar{\phi}^2 - 1 \,, \qquad (9.81)$$

where q_1, q_2, and q_3 are constants. In particular, Gurson (1977) posited the constants $q_1 = q_2 = q_3 = 1$, while Tvergaard (1981) suggested $q_1 = 1.5$, $q_2 = 1$, and $q_3 = (q_1)^2$. When $q_1 = q_3 = 0$, the flow function reduces to that of standard J_2-plasticity of (6.140), with $\hat{R}^2 = 3\hat{k}^2$. When the matrix material is viscoplastic, an effective scalar plastic strain rate can be introduced as the function (Becker 1987)

$$\dot{\bar{\varepsilon}}^P = \dot{\bar{\varepsilon}}^P\left(\bar{\sigma}, \hat{R}\right). \qquad (9.82)$$

Relating rates of plastic work in the voided material and matrix,

$$\boldsymbol{\sigma}:\left(\hat{\mathbf{D}}^{\mathbf{P}} + \frac{\dot{\bar{\phi}}}{3-3\bar{\phi}}\mathbf{1}\right) = \boldsymbol{\sigma}:\hat{\mathbf{D}}^{\mathbf{P}} - \frac{p\dot{\bar{\phi}}}{1-\bar{\phi}} = (1-\bar{\phi})\hat{R}\dot{\bar{\varepsilon}}^P \,, \qquad (9.83)$$

the plastic multiplier in flow rule (9.78) becomes

$$\hat{\lambda}^P = \frac{(1-\bar{\phi})\hat{R}\dot{\bar{\varepsilon}}^P}{\boldsymbol{\sigma}:(\partial\hat{F}/\partial\boldsymbol{\sigma})} \,. \qquad (9.84)$$

The volumetric part of (9.78) can be obtained from differentiation of (9.81), leading to (Marin and McDowell 1996)

$$\dot{\bar{\phi}} = \sqrt{\frac{3}{2}}q_1 q_2 \bar{\phi}(1-\bar{\phi})\frac{\hat{R}}{\sqrt{3J_2}}\sinh\left[\frac{q_2 I_1}{2\hat{R}}\right](\hat{\mathbf{D}}^{\mathbf{P}}:\hat{\mathbf{D}}^{\mathbf{P}})^{1/2} \,. \qquad (9.85)$$

Finally consider dissipation in the context of the spatial description of (9.72)-(9.75). From (9.18), (9.36), and (9.55),

$$\dot{\bar{W}}^P + \frac{\dot{\bar{\phi}}}{3-3\bar{\phi}}\bar{\Pi}_\alpha^{\cdot\alpha} = J^E \sigma_a^{\cdot b} \hat{L}_{\cdot b}^{Pa} + \frac{1}{3-3\bar{\phi}}(J^E \sigma_a^{\cdot a} - 3\bar{\Psi})\dot{\bar{\phi}}$$

$$= J^E \sigma^{ab} \hat{D}_{ab}^P - \frac{1}{1-\bar{\phi}}(J^E p + \bar{\Psi})\dot{\bar{\phi}}.$$

(9.86)

The sum in (9.86) represents the combined rate of working from plastic deformation from dislocations and volumetric deformation from voids.

A novel theory for elastic materials containing voids, differing entirely from the preceding treatment of Section 9.2.1, was developed by Nunziato and Cowin (Nunziato and Cowin 1979; Cowin and Nunziato 1983). According to their generalized continuum theory, the energy balance is augmented with additional terms not appearing in classical continuum mechanics (Chapter 4) or standard nonlinear elasticity (Chapter 5). Their internal energy density e is permitted to depend on the material gradient of the void volume fraction, e.g., $\bar{\phi}_{,A}$, in addition to the porosity itself and the usual independent variables of nonlinear elasticity of (5.39). Furthermore, an additional force equilibrium equation incorporating the derivative of the strain energy density with respect to $\bar{\phi}_{,A}$ was suggested by these authors. Apparently, the theory of Nunziato and Cowin does not require specification of kinetic equations for temporal evolution of voids or postulation of effective elastic coefficients. Rather, solution of the set of equilibrium equations for a given history of boundary conditions provides the void fraction distribution over the body for that history. However, additional boundary conditions must be supplied, in addition to the usual traction ((4.3)-(4.4)) or displacement boundary conditions of traditional continuum mechanics, in that theory (Nunziato and Cowin 1979; Cowin and Nunziato 1983).

9.2.2 Continuum Damage Mechanics

Relations (9.57)-(9.66) exhibit certain parallels to isotropic continuum damage mechanics (Lemaitre 1985; Krajcinovic 1996). In isotropic damage mechanics theories, a scalar internal state variable, denoted here by D:

$$\alpha = D(X,t), \ 0 \le D \le 1, \tag{9.87}$$

is often introduced to depict degradation of material integrity commensurate with micro-cracking or other damage mechanisms. The dependence of effective elastic moduli on micro-cracks has been a focus of numerous experimental and theoretical studies (Bristow 1960; Budianski and O'Connell 1976; Margolin 1983, 1984; Kachanov 1992; Nemat-Nasser and Hori 1999).

Omitting thermal effects and other internal state variables besides damage for illustrative purposes, the strain energy density is of the form

$$\overline{\Psi} = \overline{\Psi}^E\left(\mathbf{E}^\mathbf{E}, D, X, \overline{\mathbf{g}}_\alpha\right) + \overline{\Psi}^R\left(D, X\right). \tag{9.88}$$

A typical simple prescription for the recoverable strain energy density is, for a materially linear hyperelastic response in the absence of damage,

$$\overline{\Psi}^E = \frac{1}{2}\breve{\mathbb{C}}^{\alpha\beta\chi\delta} E^E_{\alpha\beta} E^E_{\chi\delta} = \frac{1}{2}(1-D)\overline{\mathbb{C}}^{\alpha\beta\chi\delta} E^E_{\alpha\beta} E^E_{\chi\delta}, \tag{9.89}$$

where second-order elastic constants of the undamaged material and effective elastic coefficients of the damaged material are, respectively,

$$\overline{\mathbb{C}}^{\alpha\beta\chi\delta}\left(X, \overline{\mathbf{g}}_\alpha\right) = \left.\frac{\partial^2 \overline{\Psi}^E}{\partial E^E_{\alpha\beta} \partial E^E_{\chi\delta}}\right|_{\substack{\mathbf{E}^\mathbf{E}=0 \\ D=0}}, \quad \breve{\mathbb{C}}^{\alpha\beta\chi\delta}\left(D, X, \overline{\mathbf{g}}_\alpha\right) = \overline{\mathbb{C}}^{\alpha\beta\chi\delta}(1-D). \tag{9.90}$$

For an isotropic response,

$$\breve{\mathbb{C}}^{\alpha\beta\chi\delta} = (1-D)\left[\mu(\overline{g}^{\alpha\chi}\overline{g}^{\beta\delta} + \overline{g}^{\alpha\delta}\overline{g}^{\chi\beta}) + \lambda\overline{g}^{\alpha\beta}\overline{g}^{\chi\delta}\right], \tag{9.91}$$

with μ and λ elastic constants of the undamaged solid. Similarities with the treatment of porous solids in Section 9.2.1 are now apparent: D replaces $\overline{\phi}$ in expressions for effective elastic coefficients. Hence, from comparison with (9.64)-(9.66), the effective bulk modulus and Young's modulus degrade linearly with damage, and Poisson's ratio is unaffected by D. It should be noted, however, that Mackenzie's formulae (9.68) do not apply for cracked solids. Furthermore, unlike the void volume fraction, D does not explicitly enter the kinematic description, i.e., expressions for deformation gradient or velocity gradient do not contain D or its time rate of change. Residual energy density $\overline{\Psi}^R(D, X)$, often omitted in continuum damage mechanics theories, can be used to reflect surface energy required to extend cracks or create new cracks (Grinfeld and Wright 2004), or residual elastic energy that is dissipated in conjunction with crack generation and growth (Clayton 2008). It is noted that (9.89)-(9.91) may be inappropriate for solids with micro-cracks subjected to generic loading regimes. For example, the bulk modulus of a cracked solid might not be significantly reduced relative to that of its undamaged counterpart during hydrostatic compression if the cracks are fully closed.

A generic kinetic law for the damage rate in the athermal case is

$$\dot{D} = \dot{D}\left(\mathbf{E}^\mathbf{E}, D, X, \overline{\mathbf{g}}_\alpha\right) \geq 0. \tag{9.92}$$

The restriction that the time rate of damage be non-negative ensures that the material does not heal. The dissipation associated with the damage rate following from (9.88) is

$$-\frac{\partial \bar{\Psi}}{\partial D}\dot{D} = -\frac{\partial \bar{\Psi}^E}{\partial D}\dot{D} - \frac{\partial \bar{\Psi}^R}{\partial D}\dot{D} = \left(\frac{\bar{\Psi}^E}{1-D} - \frac{\partial \bar{\Psi}^R}{\partial D}\right)\dot{D} . \qquad (9.93)$$

In the absence of other dissipative mechanisms, the term in parentheses in (9.93) should remain non-negative to ensure thermodynamic admissibility. Dissipation potentials (Lemaitre 1985) may be useful for construction of thermodynamically consistent rate equations, i.e., (9.92), describing the evolution of damage, following the general scheme of Section 4.3.

   Some general remarks regarding continuum damage theories are now in order. Deterioration of material strength resulting from separation or rupture of material—for example attributed to cracking, void coalescence, or spall fracture—has been the focus of numerous investigations within the context of continuum damage mechanics (Kachanov 1958; Murakami 1983; Lemaitre 1985; Krajcinovic 1996). As discussed in Section 9.2.1, scalar damage descriptions measuring porosity and reflecting inelastic volume changes have received a great deal of attention for modeling failure in ductile polycrystalline metals (Gurson 1977; Cocks and Ashby 1980, 1982; Tvergaard 1981; Becker 1987; Bammann and Aifantis 1989; Bammann et al. 1993; Needleman and Tvergaard 1991; Reusch et al. 2003). Representations based on effective configurations with reduced material strength have also demonstrated utility, including models featuring scalar damage variables (Kachanov 1958; Lemaitre 1985; Johnson and Cook 1985) or vector- or higher-order tensor-based damage variables (Murakami 1983; Steinmann and Carol 1998; Voyiadjis and Park 1999; Menzel and Steinmann 2003; Voyiadjis et al. 2004). In brittle ceramic polycrystals, scalar damage variables are often implemented (Rajendran 1994; Rajendran and Grove 1996; Johnson et al. 2003). Methods have been forwarded to account for anisotropic strain rate accommodation due to distributed micro-cracking (Espinosa 1995; Espinosa et al. 1998). Nonlocal or gradient-based measures have also been proposed for damage evolution in ductile polycrystals (Hall and Hayhurst 1991; Tvergaard and Needleman 1997; Reusch et al. 2003; Voyiadjis et al. 2004; Abu Al-Rub and Kim 2009) and brittle solids (Pijaudiercabot and Bazant 1987; Bazant 1991; Lacy et al. 1999). Frameworks accounting for anisotropic strain accommodation due to shear localization in metals have been developed (Pecherski 1998; Longere et al. 2003). Ahzi and Schoenfeld (1997) formulated a polycrystal plasticity theory capturing evolution of crystallographic texture in conjunction with a scalar porosity description. Zubelewicz (1993) proposed a model accounting for anisotropic inelastic deformation resulting from grain boundary sliding and migration in creep processes. Descriptions of anisotropic damage incorporating additive (Zhou and Zhai 2000; Clayton 2006b, 2010a) or hybrid additive-multiplicative (Clayton and McDowell

2003b, 2004) decompositions of the total deformation gradient **F** of an element of material containing displacement discontinuities associated with pores and cracks have been forwarded.

Even though micromechanics-based treatments characterizing anisotropic damage have been postulated and implemented with some success (Espinosa 1995; Clayton 2006b, 2010a; Ghosh et al. 2007), these models still have yet to surpass, in practical or commercial applications, empirical scalar-based models that tend to feature fewer material parameters and typically require less effort to implement in a numerical setting. However, detailed multiscale models of damage with explicit links between microstructural properties—for example grain size distributions, crystallographic texture, and grain boundary character—and macroscopic strength degradation are anticipated to become commonplace in future numerical simulations of structures undergoing yielding and failure, enabling design of materials for enhanced performance during failure processes (Watanabe 1989; McDowell 2001). Such processes quite often involve high rates of deformation, and include energy absorption in vehicular impact (Bammann et al. 1993) or ballistic performance of armor (Schoenfeld and Kad 1998; Clayton 2009c) and projectiles (Clayton 2005a, b, 2006a, b; Vogler and Clayton 2008). Considering improvements in computational methods that have become available during the past two decades for modeling defects in microstructures (Ortiz 1996; Needleman 2000; McDowell 2008), along with improvements in experimental capabilities for characterizing material behavior at increasingly fine length scales (Espinosa et al. 1998; Humphreys 2001; McDowell 2001), multiscale micromechanics-based approaches towards modeling plasticity and damage appear increasingly promising.

9.2.3 Volumetric Compaction and Pore Collapse

Consider situations in which the material contains initial porosity in the reference state. For example, materials of this sort, often of geological origin, include sandstone and granite (Sano et al. 1992; Rubin and Lomov 2003) and urban structural materials such as cement, mortar, and concrete (Clayton 2008). At a microscopic scale of observation, rocks are typically composed of a number of minerals of various chemical compositions and crystal structures (Goodman 1989). Many industrial-grade polycrystalline ceramics also contain substantial porosity. Under compressive loading, pores or voids within individual crystals or at grain or phase boundaries may be compacted, resulting in an increase in mass density of the material.

Pore collapse can be an important consideration in ductile metals subjected to shock compression (Herrmann 1969).

Isotropic kinematics of pore compaction, i.e., reduction in size or number of voids, can be represented by the deformation gradient term

$$\mathbf{F}^{\mathbf{R}} = J^{C1/3}\mathbf{1} = (1+\mathcal{9})^{-1/3}\mathbf{1}, \ J^C = (1+\mathcal{9})^{-1} > 0. \tag{9.94}$$

following row five of Table 9.1. Scalar field $\mathcal{9}(X,t)$ satisfies

$$\mathcal{9} = (d\tilde{V} - d\overline{V})/d\overline{V} = J^{C-1} - 1. \tag{9.95}$$

Thus $\mathcal{9}(X,t)$ represents the reduction in volume fraction of the material occupied by pores in configuration $\overline{B}$. Whereas $\overline{\phi}$ of (9.48) is a positive quantity associated with expansion of an element of material from voids, $\mathcal{9}$ of (9.94) is positive when changes in defect structure or concentration result in contraction of the volume element. Restricting the present description to compaction only provides the inequalities

$$0 < J^C \leq 1, \ 0 \leq \mathcal{9} < \infty. \tag{9.96}$$

From (9.94), the deformation rate contribution from pore collapse is

$$\mathbf{L}^{\mathbf{R}} = \dot{\mathbf{F}}^{\mathbf{R}}\mathbf{F}^{\mathbf{R}-1} = -\frac{\dot{\mathcal{9}}}{3+3\mathcal{9}}\mathbf{1}, \ L^{R\alpha}_{.\beta} = -\frac{\dot{\mathcal{9}}}{3+3\mathcal{9}}\delta^{\alpha}_{.\beta}, \ L^{R\alpha}_{.\alpha} = -\frac{\dot{\mathcal{9}}}{1+\mathcal{9}}. \tag{9.97}$$

An illustrative form of free energy function (9.11) and (9.28) is

$$\overline{\Psi} = \overline{\Psi}\left(\mathbf{E}^{\mathbf{E}}, \mathcal{9}, \alpha, \theta, X, \overline{\mathbf{g}}_{\alpha}\right), \tag{9.98}$$

where $\alpha(X,t)$ accounts for effects of other internal state variables apart from pore compaction $\mathcal{9}$, e.g., dislocations and twin boundaries. Notice that $\mathbf{F}^{\mathbf{R}}$ need not be included in the list of independent state variables in (9.98), since $\mathbf{F}^{\mathbf{R}}$ of (9.94) can be written directly in terms of $\mathcal{9}$. Substituting from (9.97) and (9.98), dissipation inequality (9.34) and energy balance (9.45) reduce, respectively, to the following:

$$\overline{\Pi}^{.\beta}_{\alpha}L^{P\alpha}_{.\beta} - \left(\frac{1}{3+3\mathcal{9}}\overline{\Pi}^{.\alpha}_{\alpha} + \frac{\partial\overline{\Psi}}{\partial\mathcal{9}}\right)\dot{\mathcal{9}} - \frac{\partial\overline{\Psi}}{\partial\alpha}\dot{\alpha} + \frac{1}{\theta}\overline{K}^{\alpha\beta}\theta_{,\alpha}\theta_{,\beta} \geq 0, \tag{9.99}$$

$$\overline{C}\dot{\theta} = \dot{\overline{W}}^P + \theta\frac{\partial\overline{\Psi}}{\partial\theta}L^{P\alpha}_{.\alpha} - \left(\frac{\partial\overline{\Psi}}{\partial\alpha} - \theta\frac{\partial^2\overline{\Psi}}{\partial\theta\partial\alpha}\right)\dot{\alpha} + \hat{\nabla}_{\alpha}(\overline{K}^{\alpha\beta}\theta_{,\beta}) + \overline{\rho}r$$

$$-\theta\overline{\beta}^{\alpha\beta}\dot{E}^E_{\alpha\beta} - \left(\frac{1}{3+3\mathcal{9}}\overline{\Pi}^{.\alpha}_{\alpha} + \frac{\theta}{1+\mathcal{9}}\frac{\partial\overline{\Psi}}{\partial\theta} + \frac{\partial\overline{\Psi}}{\partial\mathcal{9}} - \theta\frac{\partial^2\overline{\Psi}}{\partial\theta\partial\mathcal{9}}\right)\dot{\mathcal{9}}. \tag{9.100}$$

Since $\mathbf{F}^{\mathbf{R}}$ is spherical, $\overline{\mathbf{L}}^{\mathbf{P}} = \mathbf{L}^{\mathbf{P}} = \dot{\mathbf{F}}^{\mathbf{P}}\mathbf{F}^{\mathbf{P}-1}$, with plastic velocity gradient $\mathbf{L}^{\mathbf{P}}$ first introduced in (3.58).

A more specific form of (9.98), analogous to (9.57), is

$$\overline{\Psi} = \overline{\Psi}^E\left(\mathbf{E}^{\mathbf{E}}, \mathcal{9}, \theta, X, \overline{\mathbf{g}}_{\alpha}\right) + \overline{\Psi}^R\left(\mathcal{9}, \alpha, \theta, X, \overline{\mathbf{g}}_{\alpha}\right), \tag{9.101}$$

where $\bar{\Psi}^E$ accounts for the thermoelastic response, incorporating coefficients affected by porosity, and $\bar{\Psi}^R$ accounts for energy associated with defects. In porous materials, the effective second-order elastic moduli

$$\tilde{\mathbb{C}}^{\alpha\beta\chi\delta}\left(\vartheta, X, \bar{\mathbf{g}}_\alpha\right) = \left.\frac{\partial^2 \bar{\Psi}^E}{\partial E^E_{\alpha\beta} \partial E^E_{\chi\delta}}\right|_{\substack{\mathbf{E}^\mathbf{E}=\mathbf{0} \\ \theta=\theta_0}}, \tag{9.102}$$

may depend on the magnitude of pore compaction. For example, the effective bulk modulus is known to increase with increasing ϑ above some threshold pressure in concrete (Clayton 2008), beyond which pores are irreversibly crushed. Elastic coefficients similarly increase as open cracks initially present in hard crystalline rocks such as granite (Brace et al. 1966; Goodman 1989) close reversibly as a result of applied compressive stress. The rate of energy dissipated from pore collapse can be written

$$-\left(\frac{1}{3+3\vartheta}\bar{\Pi}_\alpha^{\;\alpha}\right)\dot{\vartheta} = \bar{p}\dot{\vartheta}, \tag{9.103}$$

where $\bar{p} = -(3+3\vartheta)^{-1}\operatorname{tr}\bar{\mathbf{\Pi}}$ is an effective pressure, positive in compression. A generic kinetic law for pore collapse is

$$\dot{\vartheta} = \dot{\vartheta}\left(\mathbf{E}^\mathbf{E}, \vartheta, \alpha, \theta, X, \bar{\mathbf{g}}_\alpha\right) \geq 0, \tag{9.104}$$

with the restriction of non-negativity applicable when pore crushing is irreversible. Kinetic equations requiring that $\dot{\vartheta}$ and $\bar{p}$ share the same algebraic sign (when both variables are nonzero) will automatically result in $\bar{p}\dot{\vartheta} \geq 0$, a physically realistic requirement since compressive stress is generally required to enact void closure or pore collapse. Positive energy dissipated in (9.103) would contribute, via (9.100), to temperature rise in an adiabatic event. This temperature rise could result from local plastic dissipation in the material in the vicinity of crushed pores as well as heat generated by compression of any fluid (e.g., air) contained within the pores. Such temperature increases can be significant in shock compression events (Herrmann 1969; Graham 1992). Specific free energy functions and kinetic relations ensuring that the dissipation from pore collapse exceeds the rate of free energy increase associated with increasing bulk modulus are available for selected crushable solids (Clayton 2008). Evolution equations for inelastic volume changes are widely available in the context of macroscopic plasticity with pressure-sensitive yield (Lubliner 1990). Such relations are usually formulated in terms of spatial variables and Cauchy stress, similarly to (9.72)-(9.86). Crystalline rocks may also undergo dilatancy, defined as volumetric expansion from opening of microcracks induced by frictional sliding of microcrack faces with mismatched asperities (Brace et al. 1966). When such materials also exhibit pore compaction

(Goodman 1989), superposition of approaches of Sections 9.2.1 and 9.2.3 may be in order.

9.3 Multiscale Description of Residual Elasticity

Consider the case whereby $\mathbf{F^R} = \mathbf{F^I}$ accounts for residual elastic lattice deformation, as discussed in Section 3.2.9 and Chapter 7. In general, such deformation may be attributed to microscopic heterogeneities such as dislocation networks, sub-grain boundaries, disclinations, or deformation twins. Recall that in contrast to $\mathbf{F^P}$, deformation $\mathbf{F^I}$ is not lattice-preserving. Tangent map $\mathbf{F^I}$ is generally anisotropic as opposed to spherical as was the case for voids or pores in Section 9.2. As explained in Sections 7.2.4-7.2.7, the volumetric part ($J^I \approx \bar{J}$) of the residual lattice deformation correlates with dislocations contained in metallic crystals and the stored energy of cold working (Toupin and Rivlin 1960; Wright 1982).

Because $\mathbf{F^I}(X,t)$ is of arbitrary anisotropy in the present context, and because the Helmholtz free energy density of the crystal could conceivably depend on $\mathbf{F^I}$, no immediate simplification of the thermodynamic treatment of (9.1)-(9.47) of Section 9.1 is possible. A possible free energy function satisfying (9.28) is

$$\bar{\varPsi} = \bar{\varPsi}^E\left(\mathbf{E^E}, \theta, X, \overline{\mathbf{g}}_\alpha\right) + \bar{\varPsi}^R\left(\mathbf{F^I}, \alpha, \theta, X, \overline{\mathbf{g}}_\alpha\right), \tag{9.105}$$

where thermoelastic part $\bar{\varPsi}^E$ can be formulated analogously to (6.49):

$$\begin{aligned}\bar{\varPsi}^E = &\frac{1}{2}\overline{\mathbb{C}}^{\alpha\beta\chi\delta}E_{\alpha\beta}^E E_{\chi\delta}^E + \frac{1}{6}\overline{\mathbb{C}}^{\alpha\beta\chi\delta\varepsilon\phi}E_{\alpha\beta}^E E_{\chi\delta}^E E_{\varepsilon\phi}^E \\ &- \bar{\beta}^{\alpha\beta}E_{\alpha\beta}^E \Delta\theta - \bar{C}\theta\ln\frac{\theta}{\theta_0},\end{aligned} \tag{9.106}$$

with usual definitions for second- and third-order elastic constants, thermal stress coefficients, and specific heat, all referred to configuration $\bar{B}$. Residual free energy $\bar{\varPsi}^R$ depends on temperature, residual lattice deformation, and internal state variable α. This internal variable is needed to reflect defect-induced changes in the residual Helmholtz free energy not represented by $\mathbf{F^I}$.

One interpretation of the deformation map $\mathbf{F^I}$ can be obtained following multiscale averaging concepts according to (3.137)-(3.148) and row six of Table 9.1. In this interpretation,

$$\mathbf{F^I} = \frac{1}{V}\left[\int_V \overline{\mathbf{f}}^E \overline{\mathbf{f}}^P dV\right]\mathbf{F^{P-1}}, \tag{9.107}$$

where V is the reference volume of an element of crystalline material undergoing average macroscopic plastic deformation $\mathbf{F^P}$. Recall that residual, microscopic elastic and plastic deformation fields within the volume element are denoted respectively by $\overline{\mathbf{f}}^E$ and $\overline{\mathbf{f}}^P$. Mapping $\mathbf{F^I}$ in (9.107) thus represents a volume average of the microscopic residual elastic deformation $\overline{\mathbf{f}}^E$, respectively weighted and normalized by local and average measures of the plastic deformation $\overline{\mathbf{f}}^P$ and $\mathbf{F^P}$. Finite element calculations, with crystal plasticity theory used to determine the evolution of local fields $\overline{\mathbf{f}}^E$ and $\overline{\mathbf{f}}^P$ within polycrystalline volumes subjected to macroscopic deformation $\mathbf{F}$, have demonstrated a positive correlation between a scalar invariant of the stretch associated with $\mathbf{F^I}$ and $\overline{\varPsi}^R$ (Clayton and McDowell 2003a, 2004; Clayton et al. 2004b).

Although more general forms may be appropriate, for illustrative purposes let the residual energy be further decomposed as

$$\overline{\varPsi}^R = \overline{\varPsi}_1^R\left(J^I, \varepsilon^I\right) + \Lambda\mu\overline{b}^2\overline{\rho}_T, \tag{9.108}$$

where the term $\Lambda\mu\alpha^2 = \Lambda\mu\overline{b}^2\overline{\rho}_T$ accounts for the line energy of the scalar density of dislocations as in (6.118) or (9.70). From (9.107), the Jacobian determinant representing residual elastic volume changes is

$$J^I(X,t) = \sqrt{\overline{g}/\tilde{g}}\,\det\mathbf{F^I} = V^{-1}\sqrt{\overline{g}/G}\,\det\left[\int_V \overline{\mathbf{f}}^E \overline{\mathbf{f}}^P dV\right]J^{P-1}. \tag{9.109}$$

The scalar

$$\varepsilon^I(X,t) = \left[\frac{1}{6}(\overline{g}_{\alpha\beta} - F^{I-1\chi}_{.\alpha}F^{I-1}_{\chi\beta})(\overline{g}^{\alpha\beta} - F^{I-1\chi\alpha}F^{I-1,\beta}_{\chi})\right]^{1/2} \tag{9.110}$$

is a measure of the magnitude of macroscopic strain induced by $\mathbf{F^I}$ and referred to configuration $\overline{B}$. As shown in Figure 9.2, a linear dependence of $\overline{\varPsi}_1^R$ on the product $J^{I-1}\varepsilon^I$ has been observed in finite element simulations (Clayton and McDowell 2003a) of volume elements of polycrystalline copper, first deformed to large logarithmic total strains on the order of unity, and then externally relaxed to a macroscopically unloaded configuration $\overline{B}$. In some simulations, initial grain orientations were assigned randomly, while in others, grain orientations were constrained such that initial misorientations remained less than 15°, the latter following the usual definition of a low-angle grain boundary (Brandon 1966). Notice that ε^I and $\overline{\varPsi}_1^R$ both attain larger values in polycrystals with random as opposed

to low-angle grain boundaries. This phenomenon occurs because larger misorientations correlate with larger residual stress and strain fields in the vicinity of grain boundaries and triple points in the randomly oriented polycrystals. Notice also that $\bar{\Psi}_1^R$, in this context, only accounts for a fraction of the total energy associated with cold work. The remaining stored energy is captured in (9.108) by the term $\Lambda\mu\bar{b}^2\bar{\rho}_T$ that is generally nonzero even when $\mathbf{F}^{\mathbf{I}}(t > 0) \approx \mathbf{1}$. The energy $\bar{\Psi}_1^R$, on the other hand, can be associated with residual stresses and heterogeneous elastic strain fields in the vicinity of grain and subgrain boundaries. While more extensive studies are needed for various classes of materials and various loading regimes, the results in Fig. 9.2 suggest

$$\bar{\Psi}_1^R \approx \frac{A_1}{J^I}\varepsilon^I,\tag{9.111}$$

where A_1 is a constant with dimensions of energy per unit volume.
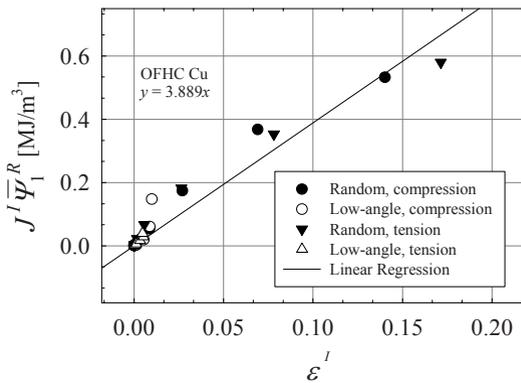
Fig. 9.2 Results from crystal plasticity simulations of uniaxial tensile and compressive deformations of polycrystalline copper (Clayton and McDowell 2003a). A scalar measure of the magnitude of residual lattice strain is ε^I, and stored energy per unit intermediate volume associated with residual lattice strain is $\bar{\Psi}_1^R$.

9.4 Inelasticity with Dislocations and Disclinations

A description of thermomechanics of crystalline solids containing dislocation and disclination defects is presented in Section 9.4, refining and extending several previous frameworks of micropolar elastoplasticity of crys-

tals (Clayton et al. 2004b, 2006, 2008a). The model presented here, like grade two elasticity and elastoplasticity theories of Sections 5.7 and 6.7, is an example of a generalized continuum theory, though some notable differences appear between the theory of Section 9.4 and those of Sections 5.7 and 6.7. Relevant background information is provided in Section 9.4.1 to lend context to the theory developed subsequently in Sections 9.4.2-9.4.7. Section 9.4.8 describes reduction of the general theory to cases wherein disclinations and micropolar rotations vanish by definition, leaving only dislocations as the defects of formal consideration in the theory.

9.4.1 Background

Theories describing behavior of what are referred to in this text as generalized continua differ from classical continua in one or more of the following ways: generalized continua may contain additional degrees of freedom beyond the usual motion $x^a = x^a(X,t)$ of (2.1); may support additional mechanical stresses beyond the usual symmetric Cauchy stress tensor σ^{ab} (or its counterparts in Table 4.1); may exhibit deviations from the usual balances of momentum and energy presented in Sections 4.1.3 and 4.1.4; and/or may contain dependencies of constitutive response functions (e.g., thermodynamic potentials) and/or kinetic relations upon higher-order deformation gradients or nonlocal measures of field variables. In particular, in generalized continua the stress tensor may be non-symmetric, the material may support higher-order stresses such as couple stresses (Cosserat and Cosserat 1909; Toupin 1962), and in such cases the usual balance laws of mechanics and thermodynamics, i.e., those of Chapter 4, may not apply in full.

Perhaps the most well known, and one of the earliest, generalized continuum theories is the oriented director theory of the Cosserats (Cosserat and Cosserat 1909). Generalized continuum theories witnessed a resurgence in popularity in the mid-20th century (Ericksen and Truesdell 1958; Gunther 1958; Kroner 1960, 1963b; Toupin 1962, 1964; Green and Rivlin 1964b; Mindlin 1964; Truesdell and Noll 1965; Fox 1966, 1968; Teodosiu 1967a, b; Eringen and Claus 1970; Eringen 1972) and again in the 1990s and early 2000s (Fleck and Hutchinson 1993; Naghdi and Srinivasa 1993; Fleck et al. 1994; Le and Stumpf 1996b, c, 1998; Steinmann 1996; Shizawa and Zbib 1999; Gurtin 2000, 2002; Acharya 2001; Bammann 2001). Additional degrees of freedom associated with rotation and possibly stretch of a set of director vectors attached to each material point X are often introduced to describe effects of finer-scale microstructure on the material's response, for example effects of crystal structure and long-range

atomic interactions or effects of lattice curvature associated with dislocations (Nye 1953; Ashby 1970). Mindlin (1968a, 1972) discussed relationships between discrete interatomic forces and hyperstresses in the context of lattice dynamics in the geometrically linear regime. In many cases, a description of so-called length scale effects absent in classical continuum mechanics is afforded, for example effects of specimen size on the material's strength and ductility.

In contrast to the governing equations of classical continua (i.e., traditional continuum mechanics) listed in Chapter 4 that are almost uniformly accepted in the mechanics community, no standardized framework for generalized continua exists. Discrepancies emerge among various theories with regards to the presence of higher-order stresses, symmetry or lack thereof of the Cauchy stress tensor, and the role of higher-order stresses in the balance of energy and in the entropy inequality. Some theories propose additional degrees of freedom that are work conjugate to higher-order stresses (Eringen and Claus 1970; Eringen 1972), while others do not and instead impose work conjugate higher-order deformation gradients to higher-order stresses (i.e., hyperstresses). The latter case applies in second-grade treatments of hyperelasticity (Toupin 1964; Teodosiu 1967a), as discussed in Sections 5.7 and 6.7 of the present text. In some theories (Gurtin 2000, 2002), inelastic deformation rates are work conjugate to traction measures distinct from those associated with Cauchy's theorem of (4.3). Generalized theories can become quite complex for addressing geometrically nonlinear elastic and inelastic regimes, wherein balance equations and stress measures can be introduced in various configurations of the deforming body and/or at multiple length scales (Le and Stumpf 1996b, c; Steinmann 1996; Bammann 2001; Regueiro et al. 2002; Clayton et al. 2006; Epstein and Elzanowski 2007; Regueiro 2009, 2010).

A number of single and polycrystal plasticity models have been developed that incorporate higher than first-order deformation gradients—for example strain gradients, lattice curvature measures, and other gradient-based dislocation density measures—in the material response functions. Early models of this sort were developed some 40 years ago (Fox 1966, 1968; Berdichevski and Sedov 1967; Teodosiu 1967a, 1970; Lardner 1969; Dillon and Kratochvil 1970, Dillon and Perzyna 1972). The presence of higher-order gradients in the response functions renders these classes of models nonlocal, as discussed in Section 4.2.1 (see e.g., (4.52)-(4.56)).

Higher-order deformation gradients have been included in plasticity theories for a number of reasons. Their inclusion permits resolution of numerical difficulties (e.g., mesh dependent solutions) associated with boundary value problems of strain softening materials in which strain lo-

calization occurs (Zbib and Aifantis 1992; Menzel and Steinmann 2000; Voyiadjis et al. 2004). Gradient-based approaches have been used to model dislocation dynamics and pattern formation (Holt 1970; Bammann and Aifantis 1982; Aifantis 1987) and to describe single and periodically distributed shear bands in single crystals (Gurtin 2000) and polycrystals (Aifantis 1987). Other applications of nonlocal theories include characterization of stress and strain fields, without singularities in field variables, at dislocation cores and crack tips (Eringen 1984; Aifantis 1999) and modeling evolution of the plastic spin in finite deformation plasticity (Shizawa and Zbib 1999). More recently, generalized crystal mechanics theories incorporating higher-order strain gradients and/or higher-order stresses have become popular for describing size effects on hardness in metals (Fleck and Hutchinson 1993; Fleck et al. 1994; Gao et al. 1999; Abu Al-Rub and Voyiadjis 2006). Such theories have also been used to supplement descriptions of physics of lattice defect populations, for example via internal force balances (Eringen and Claus 1970; Gurtin 2000; Bammann 2001).

A fundamental physical motivation for use of gradient plasticity theories has been representation of the observed trend of increasing strength with decreasing size of considered volume or microstructural features. Often quoted is the Hall-Petch relation, in which mechanical strength properties such as yield stress or cleavage strength increase with decreasing grain size in polycrystals, specifically an inverse square-root dependence (Hall 1951; Petch 1953), a phenomenon that classical local plasticity theory, being devoid of a material length scale, is unable to capture. Couple stress theories (Cosserat and Cosserat 1909) have been used to characterize Hall-Petch behavior in bicrystals (Shu and Fleck 1999) and in polycrystals (Forest et al. 2000). Fleck et al. (1994) employed a couple stress model of strain gradient plasticity to describe an increase in flow stress with decreasing diameter of twisted thin copper wires. Shu and Fleck (1998) and Hwang et al. (2002) used variations of strain gradient-couple stress theory to capture an observed increase in hardness with decreasing indentor size in pure metals.

Composite models wherein walled cellular dislocation structures, represented by hard and soft regions of relatively high and low defect densities, respectively, have been posited to explain effects of evolving populations of dislocation substructures on flow stress in ductile metallic crystals (Mughrabi 1983; Berveiller et al. 1993; Zaiser 1998). Composite models featuring grain boundary layers of relatively high dislocation density have been used to explain grain size influences on yielding (Meyers and Ashworth 1982; Benson et al. 2001). Models have been developed that embed grain subdivision and related dislocation substructure effects into the kinematics of crystal plasticity theory (Leffers 1994; Butler and

McDowell 1998) and the hardening and intergranular interaction laws of polycrystal plasticity (Horstemeyer and McDowell 1998; Horstemeyer et al. 1999). Composite models have also been applied to describe the breakdown of the Hall-Petch effect in nanocrystals (Capolungo et al. 2005). Zubelewicz et al. (2005) developed a nonlocal incompatibility-based theory to address dislocation pattern formation in metals deformed at extreme loading rates that occur in shock physics experiments.

In what follows in the remainder of Section 9.4, the disclination concept is used to describe rotational defects in crystals, as introduced already from a purely kinematic perspective in Section 3.3.3. The theory described in Section 9.4 may naturally be used to describe ductile metallic crystals that exhibit heterogeneous dislocation accumulation and grain subdivision, for example when subjected to severe plastic deformation (Stout and Rollett 1990; Butler and McDowell 1994; Pantleon 1996; Hughes et al. 1997, 1998; Valiev et al. 2002; Clayton et al. 2006). Other, perhaps more general, applications in which residual lattice deformation mechanisms emerge at multiple length scales are also conceivable. For example, aspects of the theory have been applied towards dielectric crystals containing dislocations, point defects, and micro-rotations associated with polarized subdomains (Clayton et al. 2008a).

9.4.2 Kinematics

The kinematic description follows from a combination of assumptions introduced in Sections 3.2.9, 3.3.3, and 9.1.1. The deformation gradient is decomposed multiplicatively into three terms according to (9.1):

$$\mathbf{F} = \mathbf{F}^{\mathbf{E}}\mathbf{F}^{\mathbf{I}}\mathbf{F}^{\mathbf{P}}, \; F_{.A}^{a} = F_{.\alpha}^{Ea} F_{.\beta}^{I\alpha} F_{.B}^{P\beta}, \tag{9.112}$$

with $\mathbf{F}^{\mathbf{R}} = \mathbf{F}^{\mathbf{I}}$. Consistent with (9.2), and Fig. 9.1, the following notation applies:

$$\mathbf{F}^{\mathbf{L}} = \mathbf{F}^{\mathbf{E}}\mathbf{F}^{\mathbf{I}}, \; \overline{\mathbf{F}} = \mathbf{F}^{\mathbf{I}}\mathbf{F}^{\mathbf{P}}. \tag{9.113}$$

Decomposition (9.112) implies the existence of two generally anholonomic intermediate configurations, labeled $\tilde{B}$ and $\overline{B}$. Deformation gradients act as global tangent mappings according to the following scheme: $\mathbf{F}^{\mathbf{E}} : T\overline{B} \to TB$, $\mathbf{F}^{\mathbf{I}} : T\tilde{B} \to T\overline{B}$, $\mathbf{F}^{\mathbf{P}} : TB_0 \to T\tilde{B}$, $\mathbf{F}^{\mathbf{L}} : T\tilde{B} \to TB$, and $\overline{\mathbf{F}} : TB_0 \to T\overline{B}$. Recall that $\mathbf{F}^{\mathbf{E}} = \mathbf{V}^{\mathbf{E}}\mathbf{R}^{\mathbf{E}}$ accounts for reversible elastic strain ($\mathbf{V}^{\mathbf{E}}$) resulting from mechanical loading of the lattice, as well as rigid body rotation ($\mathbf{R}^{\mathbf{E}}$). Plastic tangent map $\mathbf{F}^{\mathbf{P}}$ accounts for irreversible but lattice-preserving inelastic deformation. When the lattice-preserving deformation is associated with glide of mobile dislocations, it is considered

isochoric. However, the mathematical treatment that follows does not impose $J^P = 1$ until single crystal plasticity kinematics are formally adopted in Section 9.4.7. The remaining term in (9.112), $\mathbf{F^I}$, accounts for residual or mechanically irreversible deformations that are not lattice-preserving. Here $\mathbf{F^I}(X,t)$ manifests from defects such as dislocations and disclinations embedded within the local volume element at X of a crystalline material under consideration, as discussed in Section 3.2.9 and Chapter 7. Specifically, $\mathbf{F^I}$ accounts for residual elastic volume and shape changes associated with residual strain energies of defects (Section 7.2) in addition to effects of defect cores. When temperature changes result in lattice expansion or contraction, the thermoelastic part of the deformation gradient, $\mathbf{F^E}$, also accounts for these effects following traditional thermoelasticity of Sections 5.1-5.4; no additional term accounting for purely thermal deformation is introduced into decomposition (9.112), in contrast to the theory of Section 5.5.

Accompanying (9.112) and (9.113) is a microscopic description of spatial gradients of a field of lattice director vectors, following relations (3.166)-(3.168) and (3.243)-(3.269). Connection coefficients defining covariant derivatives of the lattice directors are

$$\hat{\Gamma}_{.cb}^{..a} = F_{.\alpha}^{La} F_{.b,c}^{L-1\alpha} + Q_{cb}^{.a} = -F_{.\alpha,\beta}^{La} F_{.c}^{L-1\beta} F_{.b}^{L-1\alpha} + Q_{cb}^{.a} , \qquad (9.114)$$

where $Q_{cb}^{.a}(x,t)$ represents generalized degrees of freedom satisfying antisymmetry constraints (3.243):

$$Q_{cba} = Q_{cb}^{.d} C_{da}^{L} = -Q_{cab} = Q_{c[ba]} , \qquad (9.115)$$

with $C_{da}^{L} = F_{.d}^{L-1\alpha} \tilde{g}_{\alpha\beta} F_{.a}^{L-1\beta}$. Thus, $\mathbf{Q}$ consists of nine independent components. Spatial defect density tensors constructed from connection coefficients (9.114) are, as in (3.253),

$$\alpha^{af} = \varepsilon^{fbc} \hat{T}_{cb}^{..a} , \quad 4\theta^{gf} = \varepsilon^{gde} \varepsilon^{fbc} \hat{R}_{cbde} , \qquad (9.116)$$

where the rank three torsion tensor $\hat{\mathbf{T}}$ and rank four curvature tensor $\hat{\mathbf{R}}$ are computed from the connection coefficients via (3.249) and (3.250), respectively. As discussed in Section 3.3.3, the quantity $\boldsymbol{\alpha} \in T_x B \times T_x B$ represents the geometrically necessary dislocation density of a material element with spatial position x, and the quantity $\boldsymbol{\theta} \in T_x B \times T_x B$ represents the geometrically necessary disclination density of that material element at x.

Paralleling the analysis of generic three-term multiplicative inelasticity in Section 9.1, the thermodynamic analysis that follows in Section 9.4 is conducted prominently in unloaded configuration $\bar{B}$, which serves here as

the evolving reference state for the instantaneous thermoelastic response of the crystal. Pre-multiplying (3.257) and (3.258) by $J^{I-1}\mathbf{F^I}$ and post-multiplying (3.257) and (3.258) by $\mathbf{F}^{IT}$ gives the defect density tensors of (9.116) mapped to configuration $\bar{B}$:

$$\bar{\alpha}^{\alpha\beta} = J^{I-1}F^{I\alpha}_{.\chi}\tilde{\alpha}^{\chi\delta}F^{I\beta}_{.\delta} = J^E F^{E-1\alpha}_{.a}\alpha^{ab}F^{E-1\beta}_{.b}, \qquad (9.117)$$

$$\bar{\theta}^{\alpha\beta} = J^{I-1}F^{I\alpha}_{.\chi}\tilde{\theta}^{\chi\delta}F^{I\beta}_{.\delta} = J^E F^{E-1\alpha}_{.a}\theta^{ab}F^{E-1\beta}_{.b}. \qquad (9.118)$$

Notice that defect density tensors $\bar{\alpha}$ and $\bar{\theta}$ remain invariant under rigid body rotations of the form $\mathbf{F^E} \to \hat{\mathbf{Q}}\mathbf{F^E}$ considered in (9.10).

9.4.3 Constitutive Assumptions

Definitions and relationships introduced in (9.4)-(9.9) apply. Objective forms of constitutive assumptions (9.11)-(9.15) are extended as follows:

$$\bar{\Psi} = \bar{\Psi}\left(\mathbf{E^E}, \mathbf{F^I}, \theta, \bar{\nabla}\theta, \bar{\alpha}, \bar{\theta}, \bar{\varepsilon}_\rho, \bar{\varepsilon}_\eta, X, \bar{\mathbf{g}}_\alpha\right), \qquad (9.119)$$

$$\bar{N} = \bar{N}\left(\mathbf{E^E}, \mathbf{F^I}, \theta, \bar{\nabla}\theta, \bar{\alpha}, \bar{\theta}, \bar{\varepsilon}_\rho, \bar{\varepsilon}_\eta, X, \bar{\mathbf{g}}_\alpha\right), \qquad (9.120)$$

$$\bar{\Sigma} = \bar{\Sigma}\left(\mathbf{E^E}, \mathbf{F^I}, \theta, \bar{\nabla}\theta, \bar{\alpha}, \bar{\theta}, \bar{\varepsilon}_\rho, \bar{\varepsilon}_\eta, X, \bar{\mathbf{g}}_\alpha\right), \qquad (9.121)$$

$$\bar{\mathbf{q}} = \bar{\mathbf{q}}\left(\mathbf{E^E}, \mathbf{F^I}, \theta, \bar{\nabla}\theta, \bar{\alpha}, \bar{\theta}, \bar{\varepsilon}_\rho, \bar{\varepsilon}_\eta, X, \bar{\mathbf{g}}_\alpha\right), \qquad (9.122)$$

$$\dot{\mathbf{F}}^\mathbf{I} = \dot{\mathbf{F}}^\mathbf{I}\left(\mathbf{E^E}, \mathbf{F^I}, \theta, \bar{\nabla}\theta, \bar{\alpha}, \bar{\theta}, \bar{\varepsilon}_\rho, \bar{\varepsilon}_\eta, X, \bar{\mathbf{g}}_\alpha\right), \qquad (9.123)$$

$$\dot{\bar{\varepsilon}}_\rho = \dot{\bar{\varepsilon}}_\rho\left(\mathbf{E^E}, \mathbf{F^I}, \theta, \bar{\nabla}\theta, \bar{\alpha}, \bar{\theta}, \bar{\varepsilon}_\rho, \bar{\varepsilon}_\eta, X, \bar{\mathbf{g}}_\alpha\right), \qquad (9.124)$$

$$\dot{\bar{\varepsilon}}_\eta = \dot{\bar{\varepsilon}}_\eta\left(\mathbf{E^E}, \mathbf{F^I}, \theta, \bar{\nabla}\theta, \bar{\alpha}, \bar{\theta}, \bar{\varepsilon}_\rho, \bar{\varepsilon}_\eta, X, \bar{\mathbf{g}}_\alpha\right). \qquad (9.125)$$

Covariant elastic strain tensor $E^E_{\alpha\beta}$ of (9.6) is included in the list of independent variables in (9.119)-(9.125) to account for changes of elastic strain energy density with changes in external loads as well as thermoelastic coupling. Deformation measure $F^{I\alpha}_{.\beta}$ is incorporated to reflect contributions to response functions from residual microelasticity within a volume element at centroidal position X as explained in Section 9.3 and demonstrated in Fig. 9.2, and may be non-negligible when deformation within the volume element is heterogeneous (Clayton and McDowell 2003a). Absolute temperature θ and anholonomic temperature gradient $\bar{\nabla}\theta$ are included in the list of independent variables following arguments akin to those for (6.9)-(6.13). An evolution equation for $\mathbf{F^I}$, whose rate may contribute to both energy storage and to dissipation according to inequality (9.34), is explicitly listed in (9.123). Not shown is the kinetic equation for

the purely dissipative time rate of $\mathbf{F^P}$, a kinetic equation that is not formally restricted to the functional dependencies of the other response functions in (9.119)-(9.125).

In lieu of the generic approach outlined in Section 9.1, internal state variables are defined explicitly in Section 9.4. These internal state variables consist of the defect density tensors $\bar{\boldsymbol{\alpha}}(X,t)$ and $\bar{\boldsymbol{\theta}}(X,t)$ of (9.117) and (9.118) and scalar defect measures $\bar{\varepsilon}_\rho(X,t)$ and $\bar{\varepsilon}_\eta(X,t)$ that are defined as

$$\bar{\varepsilon}_\rho = \bar{b}\sqrt{\bar{\rho}_S} \ , \ \ \bar{\varepsilon}_\eta = \bar{r}\bar{\omega}\sqrt{\bar{\eta}_S} \ . \tag{9.126}$$

Subscripts on scalars in (9.126) do not denote covariant vector indices and hence are not subject to the summation convention. A constant scalar magnitude of the typical Burgers vector is $\bar{b}$, as in (9.70). The statistically stored dislocation density, in terms of line length per unit volume in configuration $\bar{B}$, is defined by

$$\bar{\rho}_S = J^{I-1}\tilde{\rho}_S \ , \tag{9.127}$$

where $\tilde{\rho}_S$ is defined in (3.240). Similarly to the treatment of Section 3.2.5 and (3.104), $\bar{r}$ denotes a typical (constant) disclination radius, and $\bar{\omega}$ denotes the constant magnitude of a typical Frank vector. The statistically stored disclination density, measured in terms of line length per unit volume in configuration $\bar{B}$, is defined by

$$\bar{\eta}_S = J^{I-1}\tilde{\eta}_S \ , \tag{9.128}$$

with $\tilde{\eta}_S$ defined in (3.266).

Residual elastic energies attributed to lattice curvatures in the volume element induced by geometrically necessary dislocations and disclinations are reflected, respectively, by inclusion of $\bar{\boldsymbol{\alpha}}$ and $\bar{\boldsymbol{\theta}}$ in the thermodynamic potentials. As a point of clarification, recall that the total dislocation density tensor $\tilde{\boldsymbol{\alpha}}_\mathbf{T}^i$, whose glissile constituents contribute to the plastic velocity gradient, was introduced in (3.105). The net or geometrically necessary dislocation density tensor $\boldsymbol{\alpha}$ (or its elastic pull-back $\bar{\boldsymbol{\alpha}}$) differs from the total dislocation density, and may include both glissile and sessile dislocations, as noted in (3.235)-(3.237). Notice that when $\mathbf{Q} = 0$ (implying no associated Riemann-Christoffel curvature tensor according to (3.250) and hence no geometrically necessary disclinations) and when $\mathbf{F^I} = \mathbf{1}$, identity $\bar{\alpha}^{\alpha\beta} = J^E \varepsilon^{abc} F^{E-1\alpha}_{.b,c} F^{E-1\beta}_{.a} = J^{P-1}\varepsilon^{ABC} F^{P\alpha}_{.B,C} F^{P\beta}_{.A}$ from (3.225) holds, meaning that (9.119) is consistent with constitutive assumptions made in previous gradient-based dislocation theories from the plasticity literature (Teodosiu 1970; Steinmann 1996; Regueiro et al. 2002). From (9.116) and

supporting developments in Section 3.3.3, state variables $\bar{\boldsymbol{\alpha}}$ and $\bar{\boldsymbol{\theta}}$ are constructed, respectively and in part, from spatial gradients of the inverse of the lattice deformation $\mathbf{F}^{\mathbf{L}}$ and spatial gradients of $\mathbf{Q}$. Hence, the geometrically necessary defect density tensors can be regarded as internal variables of the higher-order gradient type or the nonlocal type, following philosophical arguments of (4.52)-(4.56) in Section 4.2.1.

Since, as mentioned already in Sections 3.3.2 and 3.3.3, the second-order tensors $\bar{\boldsymbol{\alpha}}$ and $\bar{\boldsymbol{\theta}}$ entering (9.119)-(9.125) do not include a measure of the total length of all dislocation and disclination lines within a given volume element—examples of such excluded defects include statistically stored defects consisting of closed loops and full dipoles—non-dimensional scalars $\bar{\varepsilon}_\rho$ and $\bar{\varepsilon}_\eta$ are incorporated in the list of independent state variables. These two internal state variables account, respectively, for contributions of elastic self-energy of the statistically stored dislocations of line density $\bar{\rho}_S$ and statistically stored disclinations of line density $\bar{\eta}_S$ to the Helmholtz free energy and other response functions. One may regard $\bar{\varepsilon}_\rho$ and $\bar{\varepsilon}_\eta$ as microscopic residual lattice strain measures associated with these defects (Bammann 2001).

Heterogeneity of lattice deformation, reflected in (9.119) by the energetic dependence on $\mathbf{F}^{\mathbf{I}}$, $\bar{\boldsymbol{\alpha}}$, and $\bar{\boldsymbol{\theta}}$, is not essential to engender substantial energy storage associated with defects, since $\bar{\varepsilon}_\rho$ and $\bar{\varepsilon}_\eta$ can account for a large fraction of the observed stored energy of cold working under conditions of homogeneous plastic flow and the increase in its magnitude with the accumulation of plastic deformation $\mathbf{F}^{\mathbf{p}}$. Rather, these tensor state variables tend to reflect length scale effects, particularly the latter two ($\bar{\boldsymbol{\alpha}}$ and $\bar{\boldsymbol{\theta}}$). Additionally, $\mathbf{F}^{\mathbf{I}}$ in (9.119)-(9.125) may be used to account for higher-order moments of distributions of lattice defects within the volume element that lead to internal heterogeneity (Kroner 1963b, 1973). Such higher-order moments may reflect dislocation pile-ups that are not accounted for by geometrically necessary and statistically stored defect densities that by definition are first-order averages of defect fields (i.e., weighted sums of outer products of tangent lines and Burgers or Frank vectors, normalized per unit volume) over the volume element, as indicated in (3.255). The presence of $\mathbf{F}^{\mathbf{I}}$, $\bar{\boldsymbol{\alpha}}$, and $\bar{\boldsymbol{\theta}}$ in the free energy function allows for contribution of surface or interfacial energy of grain boundaries, for example, in manifesting certain length scale (surface area to bulk volume) effects on flow stress, provided the dislocation-disclination content of such boundaries is described by these kinematics-based state variables. Such effects are thought important for describing

microstructures in nanocrystalline materials (Konstantinidis and Aifantis 1998), for example those undergoing grain size refinement in conjunction with severe plastic deformation (Valiev et al. 2002).

9.4.4 Thermodynamics

Traditional conservation laws of mass, momentum, and energy of Chapter 4 apply, to be augmented later in Section 9.4.5 with additional equilibrium equations for internal forces thermodynamically conjugate to defect density tensors. The treatment of Section 9.1 applies, with the substitutions $\mathbf{F}^{R} \to \mathbf{F}^{I}$ following from (9.112) and the set of internal state variables $\alpha \to \{\overline{\boldsymbol{\alpha}}, \overline{\boldsymbol{\theta}}, \overline{\varepsilon}_{\rho}, \overline{\varepsilon}_{\eta}\}$ following from (9.119)-(9.125). The key results of these substitutions are now listed.

The following constitutive relations are deduced as in (9.27):

$$\overline{\boldsymbol{\Sigma}} = \frac{\partial \overline{\Psi}}{\partial \mathbf{E}^{\mathbf{E}}}, \ \overline{N} = -\frac{\partial \overline{\Psi}}{\partial \theta}, \ \frac{\partial \overline{\Psi}}{\partial (\overline{\nabla} \theta)} = 0, \tag{9.129}$$

and since the temperature gradient does not explicitly affect the free energy,

$$\begin{aligned}
\overline{\Psi} &= \overline{\Psi}\left(\mathbf{E}^{\mathbf{E}}, \mathbf{F}^{\mathbf{I}}, \overline{\boldsymbol{\alpha}}, \overline{\boldsymbol{\theta}}, \overline{\varepsilon}_{\rho}, \overline{\varepsilon}_{\eta}, \theta, X, \overline{\mathbf{g}}_{\alpha}\right), \\
\overline{N} &= \overline{N}\left(\mathbf{E}^{\mathbf{E}}, \mathbf{F}^{\mathbf{I}}, \overline{\boldsymbol{\alpha}}, \overline{\boldsymbol{\theta}}, \overline{\varepsilon}_{\rho}, \overline{\varepsilon}_{\eta}, \theta, X, \overline{\mathbf{g}}_{\alpha}\right), \\
\overline{\boldsymbol{\Sigma}} &= \overline{\boldsymbol{\Sigma}}\left(\mathbf{E}^{\mathbf{E}}, \mathbf{F}^{\mathbf{I}}, \overline{\boldsymbol{\alpha}}, \overline{\boldsymbol{\theta}}, \overline{\varepsilon}_{\rho}, \overline{\varepsilon}_{\eta}, \theta, X, \overline{\mathbf{g}}_{\alpha}\right).
\end{aligned} \tag{9.130}$$

Heat conduction is assumed to obey (9.32). The local form of the dissipation inequality, (9.34), is

$$\overline{\Pi}_{\alpha}^{\cdot\beta} \overline{L}_{.\beta}^{P\alpha} + \left(\overline{\Pi}_{\alpha}^{\cdot\beta} - \frac{\partial \overline{\Psi}}{\partial F_{.\delta}^{I\alpha}} F_{.\delta}^{I\beta} \right) L_{.\beta}^{I\alpha}$$

$$- \left(\frac{\partial \overline{\Psi}}{\partial \overline{\alpha}^{\alpha\beta}} \dot{\overline{\alpha}}^{\alpha\beta} + \frac{\partial \overline{\Psi}}{\partial \overline{\theta}^{\alpha\beta}} \dot{\overline{\theta}}^{\alpha\beta} + \frac{\partial \overline{\Psi}}{\partial \overline{\varepsilon}_{\rho}} \dot{\overline{\varepsilon}}_{\rho} + \frac{\partial \overline{\Psi}}{\partial \overline{\varepsilon}_{\eta}} \dot{\overline{\varepsilon}}_{\eta} \right) + \frac{1}{\theta} \overline{K}^{\alpha\beta} \theta_{,\alpha} \theta_{,\beta} \geq 0, \tag{9.131}$$

with

$$L_{.\beta}^{I\alpha} = \dot{F}_{.\delta}^{I\alpha} F_{.\beta}^{I-1\delta}. \tag{9.132}$$

The local energy balance expressed as a temperature rate, (9.45), becomes

$$\bar{C}\dot{\theta} = \dot{\bar{W}}^P + \theta \frac{\partial \bar{\Psi}}{\partial \theta} L^{P\alpha}_{.\alpha} - \theta \bar{\beta}^{\alpha\beta} \dot{E}^E_{\alpha\beta} + \hat{\nabla}_\alpha (\bar{K}^{\alpha\beta} \theta_{,\beta}) + \bar{\rho} r$$

$$- \left[\left(\frac{\partial \bar{\Psi}}{\partial \bar{\alpha}^{\alpha\beta}} - \theta \frac{\partial^2 \bar{\Psi}}{\partial \theta \partial \bar{\alpha}^{\alpha\beta}} \right) \dot{\bar{\alpha}}^{\alpha\beta} + \left(\frac{\partial \bar{\Psi}}{\partial \bar{\theta}^{\alpha\beta}} - \theta \frac{\partial^2 \bar{\Psi}}{\partial \theta \partial \bar{\theta}^{\alpha\beta}} \right) \dot{\bar{\theta}}^{\alpha\beta} \right.$$

$$\left. + \left(\frac{\partial \bar{\Psi}}{\partial \bar{\varepsilon}_\rho} - \theta \frac{\partial^2 \bar{\Psi}}{\partial \theta \partial \bar{\varepsilon}_\rho} \right) \dot{\bar{\varepsilon}}_\rho + \left(\frac{\partial \bar{\Psi}}{\partial \bar{\varepsilon}_\eta} - \theta \frac{\partial^2 \bar{\Psi}}{\partial \theta \partial \bar{\varepsilon}_\eta} \right) \dot{\bar{\varepsilon}}_\eta \right] \qquad (9.133)$$

$$+ \left(\bar{\Pi}^{.\beta}_\alpha + \delta^\beta_{.\alpha} \theta \frac{\partial \bar{\Psi}}{\partial \theta} - \frac{\partial \bar{\Psi}}{\partial F^{I\alpha}_{.\delta}} F^{I\beta}_{.\delta} + \theta \frac{\partial^2 \bar{\Psi}}{\partial \theta \partial F^{I\alpha}_{.\delta}} F^{I\beta}_{.\delta} \right) L^{I\alpha}_{.\beta}.$$

Contributions to the temperature rate from geometrically necessary and statistically stored defect densities are enclosed in square braces in (9.133). Terms within the final set of parentheses in (9.133) account for temperature changes associated with the contribution of residual elastic deformation $F^{I\alpha}_{.\beta}$ to the deformation gradient and to the Helmholtz free energy density.

9.4.5 Macroscopic and Microscopic Momentum Balances

The general philosophy adopted in Section 9.4 is prescription of balance laws for the following thermodynamic forces: $\bar{\Sigma}$, the macroscopic elastic stress supported by a volume element at X, conjugate to the macroscopic elastic strain; $\bar{\sigma}$, a microscopic force conjugate to the density of geometrically necessary dislocations within that volume element; and $\bar{\mu}$, a microscopic force conjugate to the density of geometrically necessary disclinations within that volume element:

$$\bar{\Sigma}^{\alpha\beta} = \frac{\partial \bar{\Psi}}{\partial E^E_{\alpha\beta}} = J^E F^{E-1\alpha}_{.a} \sigma^{ab} F^{E-1\beta}_{.b}, \quad \bar{\sigma}_{\alpha\beta} = \frac{\partial \bar{\Psi}}{\partial \bar{\alpha}^{\alpha\beta}}, \quad \bar{\mu}_{\alpha\beta} = \frac{\partial \bar{\Psi}}{\partial \bar{\theta}^{\alpha\beta}}. \qquad (9.134)$$

Additional evolution equations, i.e., kinetic laws, are required to specify the time histories of dissipative kinematic variables $\mathbf{F^I}$ and $\mathbf{F^P}$ and scalar internal state variables $\bar{\varepsilon}_\rho$ and $\bar{\varepsilon}_\eta$, as described in Section 9.4.7.

Cauchy stress $\boldsymbol{\sigma}(x,t)$ obeys standard linear and angular momentum balances and reflects average traction $\mathbf{t}$ carried by an oriented surface of a volume element in the current configuration by (4.3), (4.17), and (4.26). These laws can be expressed in terms of elastic second Piola-Kirchhoff stress $\bar{\boldsymbol{\Sigma}}(X,t)$ as follows:

$$(J^{E-1} F^{Ea}_{.\alpha} \bar{\Sigma}^{\alpha\beta} F^{Eb}_{.\beta})_{;b} + \bar{b}^a = \rho a^a, \qquad (9.135)$$

$$J^{E-1}F^{Ea}_{.\alpha}\bar{\Sigma}^{\alpha\beta}F^{Eb}_{.\beta} = J^{E-1}F^{Eb}_{.\alpha}\bar{\Sigma}^{\alpha\beta}F^{Ea}_{.\beta} \Leftrightarrow \bar{\Sigma}^{\alpha\beta} = \bar{\Sigma}^{\beta\alpha}, \quad (9.136)$$

$$t^a = J^{E-1}F^{Ea}_{.\alpha}\bar{\Sigma}^{\alpha\beta}F^{Eb}_{.\beta}n_b. \quad (9.137)$$

Recall from (4.17) that $\bar{b}^a$, ρ, and a^a are components of the vector body force density per unit spatial volume, the scalar current mass density, and components of the spatial acceleration vector, respectively.

Microforces $\bar{\sigma}(X,t)$ and $\bar{\mu}(X,t)$ reflect higher-order moments of the microscopic traction distribution supported by the volume element (Kroner 1963b) and by definition do not explicitly enter macroscopic momentum balances (9.135) and (9.136). Instead, contravariant mixed-configurational versions of these forces,

$$\tilde{\sigma}^{ab} = J^{E-1}F^{I-1\alpha}_{.\varepsilon}(\bar{g}^{\varepsilon\chi}\bar{\sigma}_{\chi\delta}\bar{g}^{\delta\beta})F^{Eb}_{.\beta} = J^{E-1}F^{I-1\alpha}_{.\varepsilon}\bar{\sigma}^{\varepsilon\beta}F^{Eb}_{.\beta}, \quad (9.138)$$

$$\tilde{\mu}^{ab} = J^{E-1}F^{I-1\alpha}_{.\varepsilon}(\bar{g}^{\varepsilon\chi}\bar{\mu}_{\chi\delta}\bar{g}^{\delta\beta})F^{Eb}_{.\beta} = J^{E-1}F^{I-1\alpha}_{.\varepsilon}\bar{\mu}^{\varepsilon\beta}F^{Eb}_{.\beta}, \quad (9.139)$$

satisfy coupled microscopic momentum balances independent from (4.17) and (4.26), as will be presented shortly in (9.142). Indices of tensor objects defined in (9.138) and (9.139) are referred to the product of tangent bundles $T\tilde{B} \times TB$. These microscopic balances are intended to apply over sub-volumes within the considered volume element of size pertinent to the macroscopic momentum balance relations in (9.135) and (9.136). At these finer (sub-volume) scales, heterogeneous features such as grain boundaries, domain walls, second phases, sub-grains, or dislocation substructures are expected to engender spatial gradients of average defect density measures $\bar{\alpha}$ and $\bar{\theta}$. Higher-order stresses in (9.138) and (9.139) can be associated with residual elastic stress field distributions induced by their work conjugate defect density measures.

The present theory falls into the category of generalized continua. Notice that $\tilde{\sigma}$ is a first-order moment stress (i.e., hyperstress or couple stress) with dimensions of force per length or energy per area in physical components, since $\bar{\alpha}$ is of dimensions of inverse length. Quantity $\tilde{\mu}$ is a second-order moment stress with dimensions of force or energy per length, since $\bar{\theta}$ is of dimensions of inverse length squared. Static equilibrium of the first-order moment stress implies the following global force conservation law and traction boundary conditions for $\tilde{\sigma}$:

$$\int_s \tilde{t}^\alpha ds = \int_s \tilde{\sigma}^{\alpha b}n_b ds = 0,$$
$$\tilde{t}^\alpha(x,t) = \tilde{\sigma}^{\alpha b}n_b, \quad (9.140)$$

where $\tilde{t}(x,t)$ is a first-order hypertraction vector acting on spatial surface s with outward unit normal $\mathbf{n}$. The first of (9.140) is analogous to (4.15)

when body forces and inertial forces vanish; the second is analogous to Cauchy's theorem (4.4). Prescribing a global angular momentum balance in the absence of microscopic body forces or microscopic inertial forces, similarly that of the couple stress theory outlined by Malvern (1969),

$$\int_s (\varepsilon_{\alpha\beta\chi}\tilde{x}^\beta\tilde{t}^\chi + \tilde{h}_\alpha)ds = \int_s (\varepsilon_{\alpha\beta\chi}\tilde{x}^\beta\tilde{\sigma}^{\chi b}n_b + \tilde{\mu}_\alpha^{\cdot b}n_b)ds = 0,$$

(9.141)

$$\tilde{h}_\alpha(x,t) = \tilde{\mu}_\alpha^{\cdot b}n_b,$$

where $\tilde{\mathbf{h}}(x,t)$ is a second-order hypertraction vector acting on spatial surface s, $\mu_\alpha^{\cdot b} = \tilde{g}_{\alpha\beta}\tilde{\mu}^{\beta b}$, and $\tilde{\mathbf{x}} = \mathbf{F}^{\mathbf{L}^{-1}}\mathbf{x}$ are spatial coordinates pulled back to configuration $\tilde{B}$ under the Cauchy-Born approximation of Section 3.1.2. Local forms of balance laws in (9.140) and (9.141) then follow directly from the divergence theorem:

$$\tilde{\sigma}_{:b}^{\alpha b} = 0,$$

(9.142)

$$\varepsilon_{\alpha\chi\beta}\tilde{\sigma}^{\chi b}F_{.b}^{L-1\beta} - \tilde{\mu}_{\alpha:b}^{\cdot b} = 0,$$

(9.143)

since by (9.142) and the definition $\tilde{x}_{:a}^\alpha = F_{.a}^{L-1\alpha}$,

$$\varepsilon_{\alpha\beta\chi}(\tilde{x}^\beta\tilde{\sigma}^{\chi b})_{:b} = \varepsilon_{\alpha\beta\chi}\tilde{\sigma}^{\chi b}F_{.b}^{L-1\beta} + \varepsilon_{\alpha\beta\chi}\tilde{\sigma}_{:b}^{\chi b}\tilde{x}^\beta = \varepsilon_{\alpha\beta\chi}\tilde{\sigma}^{\chi b}F_{.b}^{L-1\beta}.$$

(9.144)

A subscripted colon denotes a total covariant derivative of a two-point tensor, similar to (4.20) and (6.217):

$$\tilde{\sigma}_{:b}^{\alpha b} = \tilde{\sigma}_{...,b}^{\alpha b} + \overset{g}{\Gamma}{}_{bc}^{\cdot\cdot b}\tilde{\sigma}^{\alpha c} + \tilde{\Gamma}_{\beta\chi}^{\cdot\cdot\alpha}\tilde{\sigma}^{\chi b}F_{.b}^{L-1\beta},$$

(9.145)

$$\tilde{\mu}_{\alpha:b}^{\cdot b} = \tilde{\mu}_{\alpha,b}^{\cdot b} + \overset{g}{\Gamma}{}_{bc}^{\cdot\cdot b}\tilde{\mu}_\alpha^{\cdot c} - \tilde{\Gamma}_{\beta\alpha}^{\cdot\cdot\chi}\tilde{\mu}_\chi^{\cdot b}F_{.b}^{L-1\beta},$$

(9.146)

where $\overset{g}{\Gamma}{}_{bc}^{\cdot\cdot b} = \overset{g}{\Gamma}{}_{cb}^{\cdot\cdot b} = (\ln\sqrt{g})_{,b}$ by an identity analogous to (2.73), and $\tilde{\Gamma}_{\beta\chi}^{\cdot\cdot\alpha}$ are Christoffel symbols of the extrinsic coordinate system in configuration $\tilde{B}$, as discussed in Sections 3.2.2 and 3.2.3, typically assumed to vanish. Viewing (9.142) and (9.143) as spatial balances, only one partial (spatial) derivative is included in each total covariant derivative defined in (9.145) and (9.146), as in (2.116) and (4.20). Notice that second-order hyperstress $\tilde{\mu}^{ab}$ does not enter the first micro-force balance (9.142).

   The local forms of microscopic force balances in (9.142) and (9.143) are similar to equilibrium equations of second grade elasticity of Section 5.7 and second grade elastoplasticity of Section 6.7. When body forces $\bar{b}^a$ vanish, microscopic momentum balance (9.142) is analogous to static linear momentum balance (5.433) in elasticity of grade two, and is also analogous to static linear momentum balance (6.245) of elastoplasticity of grade two. Microscopic angular momentum balance (9.143) is similar to angular momentum balance (5.441) of grade two elasticity and to (6.253)

of grade two elastoplasticity. Angular momentum balance (9.143) is also similar to that encountered in couple stress theories (Cosserat and Cosserat 1909; Toupin 1962; Malvern 1969). Relations (9.142)-(9.143) are analogous to micropolar equilibrium equations suggested in disclination theories of Minagawa (1979, 1981) and Eringen and Claus (1970). It is emphasized, however, that in the present theory, microscopic equilibrium equations coexist independently from macroscopic momentum balances (9.135) and (9.136), in contrast to grade two elasticity (Section 5.7 and Toupin (1964)), grade two elastoplasticity (Section 6.7 and Teodosiu (1967a)), and many kinds of couple stress theories (Cosserat and Cosserat 1909; Toupin 1962; Malvern 1969), wherein the latter, a couple stress or hyperstress enters the macroscopic angular momentum balance and the macroscopic Cauchy stress may be non-symmetric. A set of decoupled macroscopic and microscopic balance equations was suggested by Bammann (2001), similar to that developed in the present Section.

Boundary conditions on external surface s of the body are specified as follows. Let the boundary surface be partitioned as $s = s_1 \cup s_2$ and $s_1 \cap s_2 = \varnothing$, where s_1 is that part of the boundary over which stresses are prescribed, and s_2 is that part of the boundary over which kinematic variables are prescribed:

$$\left.\begin{array}{c} t^a \\ \tilde{t}^\alpha \\ \tilde{h}^\alpha \end{array}\right\} \text{prescribed on } s_1 \; ; \quad \left.\begin{array}{c} x^a \\ F^{Ea}_{.\alpha}, F^{I\alpha}_{.\beta} \\ F^{Ea}_{.\alpha,b}, F^{I\alpha}_{.\beta,b} \\ Q^{.a}_{bc} \end{array}\right\} \text{prescribed on } s_2. \quad (9.147)$$

Though more general boundary conditions are conceivable, particularly physically relevant sets of conditions correspond to null applied external forces, as would arise in a self-equilibrated body, and null applied deformations, as would occur for a full clamped, i.e., rigid, boundary:

$$\left.\begin{array}{c} t^a = 0 \\ \tilde{t}^\alpha = 0 \\ \tilde{h}^\alpha = 0 \end{array}\right\} \begin{array}{c} \text{self-equilibrated} \\ \text{(on } s_1); \end{array} \quad \left.\begin{array}{c} x^a = g^a_{.A} X^A \\ F^{Ea}_{.\alpha} = g^a_{.\alpha}, F^{I\alpha}_{.\beta} = \delta^\alpha_{.\beta} \\ F^{Ea}_{.\alpha,b} = 0, F^{I\alpha}_{.\beta,b} = 0 \\ Q^{.a}_{bc} = 0 \end{array}\right\} \begin{array}{c} \text{fully clamped} \\ \text{(on } s_2). \end{array} \quad (9.148)$$

9.4.6 Representative Free Energy

A more descriptive form of the free energy per unit intermediate volume in (9.119) and (9.130) is considered for illustrative purposes. The following additive decomposition is suggested:

$$\bar{\varPsi} = \bar{\varPsi}^E\left(\mathbf{E^E},\mathbf{F^I},\theta,\bar{\boldsymbol{\alpha}},\bar{\boldsymbol{\theta}},\bar{\varepsilon}_\rho,\bar{\varepsilon}_\eta,X,\bar{\mathbf{g}}_\alpha\right)$$
$$+ \bar{\varPsi}^R\left(\mathbf{E^E},\mathbf{F^I},\theta,\bar{\boldsymbol{\alpha}},\bar{\boldsymbol{\theta}},\bar{\varepsilon}_\rho,\bar{\varepsilon}_\eta,X,\bar{\mathbf{g}}_\alpha\right), \tag{9.149}$$

where $\bar{\varPsi}^E$ accounts for the thermoelastic response and $\bar{\varPsi}^R$ accounts for energy associated with defects in the absence of external mechanical loading. Because each term on the right of (9.149) depends on same list of arguments, specific forms of $\bar{\varPsi}^E$ and $\bar{\varPsi}^R$ are required in order to provide an improved description over the first of (9.130), for example. Such specific forms are developed below.

Energy density $\bar{\varPsi}^E$ is expanded in a series about a reference state at which the following conditions hold: $\mathbf{E^E}=0$, $\Delta\theta=\theta-\theta_0=0$. The thermoelastic part of the free energy is written similarly to (6.49):

$$\bar{\varPsi}^E = \frac{1}{2}\breve{\mathbb{C}}^{\alpha\beta\chi\delta}E_{\alpha\beta}^E E_{\chi\delta}^E + \frac{1}{6}\breve{\mathbb{C}}^{\alpha\beta\chi\delta\varepsilon\phi}E_{\alpha\beta}^E E_{\chi\delta}^E E_{\varepsilon\phi}^E$$
$$- \breve{\beta}^{\alpha\beta}E_{\alpha\beta}^E\Delta\theta - \breve{C}\theta\ln\frac{\theta}{\theta_0}. \tag{9.150}$$

Second-order isothermal elastic coefficients, third-order isothermal elastic coefficients, thermal stress coefficients, and specific heat at constant elastic strain, all referred to configuration $\bar{B}$, are defined as follows:

$$\breve{\mathbb{C}}^{\alpha\beta\chi\delta}\left(\mathbf{F^I},\bar{\boldsymbol{\alpha}},\bar{\boldsymbol{\theta}},\bar{\varepsilon}_\rho,\bar{\varepsilon}_\eta,X,\bar{\mathbf{g}}_\alpha\right) = \frac{\partial^2\bar{\varPsi}^E}{\partial E_{\alpha\beta}^E\partial E_{\chi\delta}^E}\bigg|_{\substack{\mathbf{E^E}=0\\\theta=\theta_0}}, \tag{9.151}$$

$$\breve{\mathbb{C}}^{\alpha\beta\chi\delta\varepsilon\phi}\left(\mathbf{F^I},\bar{\boldsymbol{\alpha}},\bar{\boldsymbol{\theta}},\bar{\varepsilon}_\rho,\bar{\varepsilon}_\eta,X,\bar{\mathbf{g}}_\alpha\right) = \frac{\partial^3\bar{\varPsi}^E}{\partial E_{\alpha\beta}^E\partial E_{\chi\delta}^E\partial E_{\varepsilon\phi}^E}\bigg|_{\substack{\mathbf{E^E}=0\\\theta=\theta_0}}, \tag{9.152}$$

$$\breve{\beta}^{\alpha\beta}\left(\mathbf{F^I},\bar{\boldsymbol{\alpha}},\bar{\boldsymbol{\theta}},\bar{\varepsilon}_\rho,\bar{\varepsilon}_\eta,X,\bar{\mathbf{g}}_\alpha\right) = -\frac{\partial^2\bar{\varPsi}^E}{\partial\theta\partial E_{\alpha\beta}^E}\bigg|_{\substack{\mathbf{E^E}=0\\\theta=\theta_0}}, \tag{9.153}$$

$$\breve{C}\left(\mathbf{F^I},\bar{\boldsymbol{\alpha}},\bar{\boldsymbol{\theta}},\bar{\varepsilon}_\rho,\bar{\varepsilon}_\eta,X\right) = -\left(\theta\frac{\partial^2\bar{\varPsi}^E}{\partial\theta^2}\right)\bigg|_{\substack{\mathbf{E^E}=0\\\theta=\theta_0}}. \tag{9.154}$$

Notice that material coefficients entering (9.150) are permitted to depend on residual lattice deformation and defect densities, as well as on lo-

cation X and orientation of the element of crystalline solid, via $\bar{\mathbf{g}}_\alpha(X)$. Dependence of material coefficients on defect densities was omitted in Chapters 6 and 8; the present description permits changes in elastic coefficients and specific heat that may appear in highly defective crystals with very large defect densities, wherein $\mathbf{F}^I$ could differ substantially from the unit tensor and whereby $\bar{J} = J^I J^P$ could differ substantially from unity. For example, changes in elastic modulus with dislocation line density have been observed for metallic crystals, both experimentally (Smith 1953; Simmons and Balluffi 1963; Lebedev 1996) and from atomistic models (Clayton and Chung 2006). Bell (1968) describes experimental evidence of variations in elastic coefficients of metallic crystals subjected to finite inelastic deformation. Dependence of elastic coefficients on residual stress is discussed by Johnson and Hoger (1993). As noted by Kocks et al. (1975), dislocations can also affect the specific heat capacity (Gottstein 1973).

Material coefficients at null defect densities and null residual lattice deformation are related to those of (5.65), (5.66), (5.68), and (5.85) at the same material point X as follows:

$$\breve{\mathbb{C}}^{\alpha\beta\chi\delta}\left(\mathbf{1},0,0,0,0,X,\bar{\mathbf{g}}_\alpha\right) = \bar{J}^{-1}\overline{\mathbb{C}}^{ABCD}g^\alpha_{.A}g^\beta_{.B}g^\chi_{.C}g^\delta_{.D}, \qquad (9.155)$$

$$\breve{\mathbb{C}}^{\alpha\beta\chi\delta\varepsilon\phi}\left(\mathbf{1},0,0,0,0,X,\bar{\mathbf{g}}_\alpha\right) = \bar{J}^{-1}\overline{\mathbb{C}}^{ABCDEF}g^\alpha_{.A}g^\beta_{.B}g^\chi_{.C}g^\delta_{.D}g^\varepsilon_{.E}g^\phi_{.F}, \qquad (9.156)$$

$$\breve{\beta}^{\alpha\beta}\left(\mathbf{1},0,0,0,0,X,\bar{\mathbf{g}}_\alpha\right) = \bar{J}^{-1}\overline{\beta}^{AB}g^\alpha_{.A}g^\beta_{.B}, \qquad (9.157)$$

$$\breve{C}\left(\mathbf{1},0,0,0,0,X\right) = \overline{\rho c} = \bar{J}^{-1}\rho_0\bar{c} = \bar{J}^{-1}\overline{C}_0. \qquad (9.158)$$

Since $\dot{\bar{\mathbf{g}}}_\alpha = 0$ and $\dot{\mathbf{G}}_A = 0$, the coordinate shifter $g^\alpha_{.A} = \left\langle\bar{\mathbf{g}}^\alpha,\mathbf{G}_A\right\rangle$ at X does not depend on time. When plastic deformation is isochoric ($J^P = 1$), and when coincident coordinate systems are used in reference and intermediate configurations so that $g^\alpha_{.A} = \delta^\alpha_{.A}$, numerical values of material coefficients on left and right sides of each of (9.155)-(9.158) are the same. Hence, considerations regarding symmetry of reference material coefficients discussed in Section 5.1.5 and Appendix A apply for the intermediate elasticity tensors on the left of (9.155)-(9.158). Contrarily, defects may affect the symmetry properties of the effective coefficients in (9.151)-(9.153); hence, these coefficients may not exhibit the same natural symmetries corresponding to the crystal class of the non-defective crystal. Stress-strain-temperature relations following from (9.129), (9.149), and (9.150) become

$$\overline{\Sigma}^{\alpha\beta} = \breve{\mathbb{C}}^{\alpha\beta\chi\delta}E^E_{\chi\delta} + \frac{1}{2}\breve{\mathbb{C}}^{\alpha\beta\chi\delta\varepsilon\phi}E^E_{\chi\delta}E^E_{\varepsilon\phi} - \breve{\beta}^{\alpha\beta}\Delta\theta + \frac{\partial\overline{\Psi}^R}{\partial E^E_{\alpha\beta}}. \qquad (9.159)$$

A physically viable (but not the most general) form of residual energy $\overline{\Psi}^R$ is now considered for illustrative purposes. Omitting possible energetic couplings among defect densities (e.g., as in (8.72)), let this energy be expressed as the sum

$$\overline{\Psi}^R = \overline{\Psi}_1^R(\mathbf{F}^{\mathbf{I}}) + \frac{1}{2}\Big[\overline{\kappa}_1\overline{\varepsilon}_\rho{}^2 + \overline{\kappa}_2\overline{\varepsilon}_\eta{}^2 + \overline{\kappa}_3\overline{\alpha}^{\alpha\beta}\overline{\alpha}_{\alpha\beta} + \overline{\kappa}_4\overline{\theta}^{\alpha\beta}\overline{\theta}_{\alpha\beta}$$
$$+\overline{\kappa}_5\overline{\alpha}^{\alpha\beta}\overline{\alpha}_{\alpha\beta}E_{\chi\delta}^E E^{E\chi\delta} + \overline{\kappa}_6\overline{\theta}^{\alpha\beta}\overline{\theta}_{\alpha\beta}E_{\chi\delta}^E E^{E\chi\delta}\Big], \tag{9.160}$$

where the scalar material coefficients

$$\overline{\kappa}_i = \overline{\kappa}_i\left(\theta, X, \overline{\mathbf{g}}_\alpha\right) \geq 0, \; (i = 1, 2...6), \tag{9.161}$$

generally can depend on temperature, position, and lattice orientation. The first term on the right of (9.160), $\overline{\Psi}_1^R$, accounts for the explicit contribution of residual elastic lattice deformation, and can be assigned following the treatment of Section 9.3, for example, and results from computational crystal mechanics (Clayton and McDowell 2003a, 2004). The second term accounts for the energy of statistically stored dislocations, approximated as in (8.73):

$$\frac{1}{2}\overline{\kappa}_1\overline{\varepsilon}_\rho{}^2 = \frac{1}{2}\overline{\kappa}_1\overline{b}^2\overline{\rho}_S = \Lambda\hat{K}(\theta, X, \overline{\mathbf{g}}_\alpha)\overline{b}^2\overline{\rho}_S \approx \mu\overline{b}^2\overline{\rho}_S, \tag{9.162}$$

where $\hat{K}$ is the energy factor of (C.152) and the last approximation corresponds to screw dislocations embedded in a linear isotropic elastic medium with shear modulus[2] μ. The rightmost expression in (9.162) would apply for a dilute distribution of non-interacting straight screw dipoles, for example. Core energies and interaction energies among statistically dislocations are absorbed into the constant $\overline{\kappa}_1$. All line defect loops considered in Section C.2 of Appendix C—screw loops, prismatic loops, and shear loops—are statistically stored dislocations because they produce no net contribution to the geometrically necessary dislocation density tensor. Hence, $\overline{\kappa}_1$ could alternatively be prescribed from the appropriate combination of elastic constants and geometric parameters of pertinent dislocation loops in the material, following the elasticity solutions (C.160), (C.162), and (C.165).

The third term on the right of (9.160) accounts for the energy of statistically stored disclinations. Considering a dilute distribution of straight wedge disclinations, (C.149) gives

---

[2] In an anisotropic single crystal, Voigt averages (A.36) and (A.38) can be used to provide estimates of isotropic second-order elastic constants.

$$\frac{1}{2}\overline{\kappa}_2\overline{\varepsilon}_\eta{}^2 = \frac{1}{2}\overline{\kappa}_2\overline{r}^2\overline{\omega}^2\overline{\eta}_S \approx \frac{\mu}{16\pi(1-\nu)}\overline{r}^2\overline{\omega}^2\overline{\eta}_S, \qquad (9.163)$$

where ν is Poisson's ratio and $\overline{r}$ is treated as a constant radius of influence of the disclination in a given material. Because the energy diverges as $\overline{r} \to \infty$, disclinations tend to arrange in configurations for which their long-range stress fields cancel, leading to a finite value of $\overline{r}$. Recall also from the discussion in Section C.1.4 that full disclinations tend to dissociate into partials with small Frank vectors $\overline{\omega}$ to minimize their total elastic energy; hence, $\overline{\kappa}_2$ of (9.163) implicitly accounts for stacking fault or surface energies associated with partial disclinations, in addition to core and interaction energies. If statistically stored disclinations are arranged as wedge dipoles, then (9.163) is replaced with (Li 1972)

$$\frac{1}{2}\overline{\kappa}_2\overline{\varepsilon}_\eta{}^2 = \frac{1}{2}\overline{\kappa}_2\overline{r}^2\overline{\omega}^2\overline{\eta}_S \approx \left[\frac{\mu R^2\overline{\omega}^2}{\pi(1-\nu)}\ln\left(\frac{\overline{r}}{2R}\right) + 2R\overline{\gamma}_\eta\right]\overline{\eta}_S, \quad (9.164)$$

where $\overline{\gamma}_\eta$ is the surface energy per unit area of formation of the partial disclination (akin to a stacking fault energy) and $2R$ is an equilibrium dipole separation distance as shown in Fig. 3.16. This gives

$$\overline{\kappa}_2 \approx 2\left[\frac{R^2}{\overline{r}^2}\frac{\mu}{\pi(1-\nu)}\ln\left(\frac{\overline{r}}{2R}\right) + \frac{2R\overline{\gamma}_\eta}{\overline{r}^2\overline{\omega}^2}\right]. \qquad (9.165)$$

When completely enclosed by the volume element centered at X, closed disclination loops of the kinds considered in Section C.2—twist and wedge loops—are also statistically stored. Hence, solutions (C.167) and (C.170) can be used to provide alternative definitions of $\overline{\kappa}_2$, with the particular choice depending on the particular kind of disclination line or loop most prevalent in the material.

Geometrically necessary defects contribute to the total Burgers vector of (3.251) and (3.252). From (3.235) and (3.261) respectively, geometrically necessary dislocations and disclinations consist of excess defects of a particular sign and direction in a volume element centered at X. These may include straight lines, portions of loops not completely contained in the element, excess partial dislocations and excess partial disclinations, and single defect lines of a dipole (with the second defect of the dipole contained outside the volume element). Grain boundaries, domain walls, and subgrain boundaries may all be addressed in terms of geometrically necessary dislocations and disclinations, as discussed in Section 3.3.3. Depending on the spatial arrangement of partial disclination dipoles in the material relative to the choice of volume element, partial disclination dipoles can

also be treated as geometrically necessary, since they contribute to a rotational closure failure (Clayton et al. 2006, 2008a).

Energies of geometrically necessary dislocations and disclinations in (9.160) are expressed, respectively, as

$$\frac{1}{2}\Big[\,\overline{\kappa}_3 + \overline{\kappa}_5 E^E_{\chi\delta} E^{E\chi\delta}\Big]\overline{\alpha}^{\alpha\beta}\overline{\alpha}_{\alpha\beta} = \frac{1}{2}l_\rho^{\,2}\mu\Big[1 + c_5 E^E_{\chi\delta} E^{E\chi\delta}\Big]\overline{\alpha}^{\alpha\beta}\overline{\alpha}_{\alpha\beta}, \quad (9.166)$$

$$\frac{1}{2}\Big[\,\overline{\kappa}_4 + \overline{\kappa}_6 E^E_{\chi\delta} E^{E\chi\delta}\Big]\overline{\theta}^{\alpha\beta}\overline{\theta}_{\alpha\beta} = \frac{1}{2}l_\eta^{\,4}\mu\Big[1 + c_6 E^E_{\chi\delta} E^{E\chi\delta}\Big]\overline{\theta}^{\alpha\beta}\overline{\theta}_{\alpha\beta}, \quad (9.167)$$

where μ is an elastic shear modulus, $c_5 \geq 0$ and $c_6 \geq 0$ are dimensionless constants, and $l_\rho \geq 0$ and $l_\eta \geq 0$ are material parameters with dimensions of length. The proportionality relationship between defect energy and shear modulus is expected following the isotropic elastic solutions of dislocation and disclination lines and loops listed in Sections C.1 and C.2 of Appendix C. For greater accuracy, the isotropic shear modulus in relations (9.166) and (9.167) would need to be replaced by the appropriate combination of elastic coefficients to account for anisotropy, following (C.152) and the treatment of Section C.1.6 for dislocations, for example.

The two parameters with dimensions of length are required on dimensional grounds. A large body of research has sought to determine physical justifications for selection of values of length scale parameters of this sort for ductile crystalline solids (Fleck et al. 1994; Stolken and Evans 1998; Voyiadjis and Abu Al-Rub 2005; Abu Al-Rub and Voyiadjis 2006; Chung and Clayton 2007). Relations (9.166) and (9.167) suggest quadratic dependencies of free energy upon geometrically necessary defect densities. Steinmann (1996), Bammann (2001), Gurtin (2002), and Regueiro et al. (2002) similarly postulated quadratic dependencies of free energy upon the geometrically necessary dislocation density tensor. Previous investigations involving on physical experiments or computational models of lattice defects indicate that internal stress fields associated with defects may be amplified by external loads (Gibeling and Nix 1980; Argon and Takeuchi 1981; Kassner et al. 2002; Chung and Clayton 2007). Nonzero constants c_5 and c_6 enable description of such effects, following Clayton et al. (2004a, b)[3]. Berdichevski and Sedov (1967) also suggested an internal energy function for crystals incorporating a scalar product of elastic strain and dislocation density. A linear dependence of residual energy $\overline{\Psi}^R$ on

---

[3] In previous work (Clayton 2004a), an expression involving the metric $C^E_{\alpha\beta}$ of (9.6) was suggested to account for the coupled defect-elastic energy analogous to the sum in (9.166). The present treatment provides amplification of defect energy regardless of the algebraic sign of components of elastic strain.

elastic strain is prohibited by the assertion that the stress (9.159) should vanish when the elastic strain vanishes at the reference temperature.

The contribution from defect density tensors to the second Piola-Kirchhoff stress in the final term on the right of (9.159) becomes

$$\frac{\partial \bar{\Psi}^R}{\partial E_{\alpha\beta}^E} = \mu \left[l_\rho^2 c_5 \bar{\alpha}^{\chi\delta} \bar{\alpha}_{\chi\delta} + l_\eta^4 c_6 \bar{\theta}^{\chi\delta} \bar{\theta}_{\chi\delta} \right] E^{E\alpha\beta} . \tag{9.168}$$

The contribution of these defects to the second-order tangent mechanical stiffness is, from (9.166)-(9.168),

$$\frac{\partial^2 \bar{\Psi}^R}{\partial E_{\alpha\beta}^E \partial E_{\chi\delta}^E} = \frac{\mu}{2} \left[l_\rho^2 c_5 \bar{\alpha}^{\chi\delta} \bar{\alpha}_{\chi\delta} + l_\eta^4 c_6 \bar{\theta}^{\chi\delta} \bar{\theta}_{\chi\delta} \right] \left[\bar{g}^{\alpha\chi} \bar{g}^{\beta\delta} + \bar{g}^{\alpha\delta} \bar{g}^{\beta\chi} \right]. \tag{9.169}$$

Notice that the residual free energy in (9.160) features a quadratic dependence in each of the defect density measures. As demonstrated by simple example by Clayton et al. (2006), such dependencies do not always guarantee that $\bar{\Psi}^R$ is a convex function of the total deformation gradient or the inelastic strain. As a result, metastable, local minimum energy configurations of the crystal may correspond to heterogeneous deformation patterns and heterogeneous defect distributions, even when the solid is subjected to affine boundary conditions. Energy arguments have likewise been used elsewhere to account for the emergence of heterogeneous deformation patterns in the context of martensitic phase transformations (Ball and James 1987; Bhattacharya 1991), emergence of slip patterns and dislocation substructures (Ortiz and Repetto 1999; Ortiz et al. 2000; Conti and Ortiz 2005), and geometrically nonlinear plasticity (Carstensen et al. 2002).

The microscopic first-order couple stress and second-order hyperstress are, from the second and third of (9.134), (9.150), (9.166), and (9.167),

$$\bar{\sigma}_{\alpha\beta} = \frac{1}{2} \frac{\partial \breve{\mathbb{C}}^{\chi\delta\varepsilon\phi}}{\partial \bar{\alpha}^{\alpha\beta}} E_{\chi\delta}^E E_{\varepsilon\phi}^E + \frac{1}{6} \frac{\partial \breve{\mathbb{C}}^{\chi\delta\varepsilon\phi\varphi\gamma}}{\partial \bar{\alpha}^{\alpha\beta}} E_{\chi\delta}^E E_{\varepsilon\phi}^E E_{\varphi\gamma}^E - \frac{\partial \breve{\beta}^{\chi\delta}}{\partial \bar{\alpha}^{\alpha\beta}} E_{\chi\delta}^E \Delta\theta$$
$$- \frac{\partial \breve{C}}{\partial \bar{\alpha}^{\alpha\beta}} \theta \ln \frac{\theta}{\theta_0} + \mu l_\rho^2 \left[1 + c_5 E_{\chi\delta}^E E^{E\chi\delta} \right] \bar{\alpha}_{\alpha\beta}, \tag{9.170}$$

$$\bar{\mu}_{\alpha\beta} = \frac{1}{2} \frac{\partial \breve{\mathbb{C}}^{\chi\delta\varepsilon\phi}}{\partial \bar{\theta}^{\alpha\beta}} E_{\chi\delta}^E E_{\varepsilon\phi}^E + \frac{1}{6} \frac{\partial \breve{\mathbb{C}}^{\chi\delta\varepsilon\phi\varphi\gamma}}{\partial \bar{\theta}^{\alpha\beta}} E_{\chi\delta}^E E_{\varepsilon\phi}^E E_{\varphi\gamma}^E - \frac{\partial \breve{\beta}^{\chi\delta}}{\partial \bar{\theta}^{\alpha\beta}} E_{\chi\delta}^E \Delta\theta$$
$$- \frac{\partial \breve{C}}{\partial \bar{\theta}^{\alpha\beta}} \theta \ln \frac{\theta}{\theta_0} + \mu l_\eta^4 \left[1 + c_6 E_{\chi\delta}^E E^{E\chi\delta} \right] \bar{\theta}_{\alpha\beta}. \tag{9.171}$$

It follows that microforce balances (9.142) and (9.143) respectively include terms representing spatial gradients of geometrically necessary dislocations pertaining to stress fields/concentrations at dislocation pile-ups,

and gradients of disclinations contributing to possible anti-symmetry of moment stress $\tilde{\boldsymbol{\sigma}}$.

In the particular case when effects of geometrically necessary defects on elastic coefficients are omitted, (9.170) and (9.171) reduce to the linear relationships

$$\bar{\sigma}_{\alpha\beta} = \mu l_\rho^{\;2} \bar{\alpha}_{\alpha\beta}, \;\; \bar{\mu}_{\alpha\beta} = \mu l_\eta^{\;4} \bar{\theta}_{\alpha\beta}. \tag{9.172}$$

Furthermore, when (9.172) applies, (9.138) and (9.139) produce

$$\tilde{\sigma}^{ab} = \mu l_\rho^{\;2} J^{E-1} F^{I-1\alpha}_{\quad.\varepsilon} \bar{\alpha}^{\varepsilon\beta} F^{Eb}_{\;.\beta}, \;\; \tilde{\mu}^{ab} = \mu l_\eta^{\;4} J^{E-1} F^{I-1\alpha}_{\quad.\varepsilon} \bar{\theta}^{\varepsilon\beta} F^{Eb}_{\;.\beta}. \tag{9.173}$$

Assuming shear modulus μ is spatially constant and also assuming that the second of (6.218) applies, the spatial divergence of the couple stress entering microscopic linear momentum balance (9.142) becomes

$$
\begin{aligned}
\tilde{\sigma}^{ab}_{:b} &= (\mu l_\rho^{\;2} J^{E-1} F^{I-1\alpha}_{\quad.\varepsilon} \bar{\alpha}^{\varepsilon\beta} F^{Eb}_{\;.\beta})_{:b} \\
&= \mu l_\rho^{\;2} \left[J^{E-1} F^{I-1\alpha}_{\quad.\varepsilon} (J^E F^{E-1\varepsilon}_{\quad.c} \alpha^{cd} F^{E-1\beta}_{\quad.d}) F^{Eb}_{\;.\beta} \right]_{:b} \\
&= \mu l_\rho^{\;2} \left[F^{I-1\alpha}_{\quad.\varepsilon} F^{E-1\varepsilon}_{\quad.c} \alpha^{cb} \right]_{:b} \\
&= \mu l_\rho^{\;2} \varepsilon^{bfe} \left[F^{L-1\alpha}_{\quad.c} \hat{T}^{..c}_{ef} \right]_{:b} = \mu l_\rho^{\;2} \varepsilon^{bfe} \left[F^{L-1\alpha}_{\quad.c} \hat{\Gamma}^{..c}_{ef} \right]_{:b} \\
&= \mu l_\rho^{\;2} \varepsilon^{bfe} \left[F^{L-1\alpha}_{\quad.f:eb} + (F^{L-1\alpha}_{\quad.c} Q^{.c}_{ef})_{:b} \right] \\
&= \mu l_\rho^{\;2} \varepsilon^{bfe} (F^{L-1\alpha}_{\quad.c} Q^{.c}_{ef})_{:b} = \mu l_\rho^{\;2} \varepsilon^{bfe} (F^{L-1\alpha}_{\quad.c:b} Q^{.c}_{ef} + F^{L-1\alpha}_{\quad.c} Q^{.c}_{ef:b}),
\end{aligned}
\tag{9.174}
$$

leading to the three kinematic equations

$$\varepsilon^{bfe} F^{L-1\alpha}_{\quad.c:b} Q^{.c}_{ef} = \varepsilon^{bfe} F^{L-1\alpha}_{\quad.c} Q^{.c}_{fe:b}. \tag{9.175}$$

With these same assumptions, terms on the left side of microscopic momentum balance (9.143) become

$$
\begin{aligned}
\varepsilon_{\alpha\chi\delta} \tilde{\sigma}^{\chi b} F^{L-1\delta}_{\quad.b} &= \mu l_\rho^{\;2} \varepsilon_{\alpha\chi\delta} J^{E-1} F^{I-1\chi}_{\quad.\varepsilon} \bar{\alpha}^{\varepsilon\beta} F^{Eb}_{\;.\beta} F^{L-1\delta}_{\quad.b} \\
&= \mu l_\rho^{\;2} \varepsilon_{\alpha\chi\delta} \left[J^{E-1} F^{I-1\chi}_{\quad.\varepsilon} (J^E F^{E-1\varepsilon}_{\quad.c} \alpha^{cd} F^{E-1\beta}_{\quad.d}) F^{Eb}_{\;.\beta} F^{L-1\delta}_{\quad.b} \right] \\
&= \mu l_\rho^{\;2} \varepsilon_{\alpha\chi\delta} \left[F^{L-1\chi}_{\quad.c} \alpha^{cb} F^{L-1\delta}_{\quad.b} \right] \\
&= \mu l_\rho^{\;2} \varepsilon_{\alpha\chi\delta} \varepsilon^{bfe} \left[F^{L-1\chi}_{\quad.c} \hat{T}^{..c}_{ef} F^{L-1\delta}_{\quad.b} \right] \\
&= \mu l_\rho^{\;2} \varepsilon_{\alpha\chi\delta} \varepsilon^{bfe} \left[F^{L-1\chi}_{\quad.c} \hat{\Gamma}^{..c}_{ef} F^{L-1\delta}_{\quad.b} \right] \\
&= \mu l_\rho^{\;2} \varepsilon_{\alpha\chi\delta} \varepsilon^{bfe} \left[F^{L-1\chi}_{\quad.c} (F^{Lc}_{\;.\beta} F^{L-1\beta}_{\quad.f,e} + Q^{.c}_{ef}) F^{L-1\delta}_{\quad.b} \right],
\end{aligned}
\tag{9.176}
$$

and

$$\tilde{\mu}^{b}_{\alpha:b} = \mu l_{\eta}^{4}(J^{E-1}F^{I-1}{}_{\alpha\varepsilon}\overline{\theta}^{\varepsilon\beta}F^{Eb}{}_{.\beta})_{:b}$$

$$= \mu l_{\eta}^{4}\Big[J^{E-1}F^{I-1}{}_{\alpha\varepsilon}(J^{E}F^{E-1\varepsilon}{}_{.a}\theta^{ac}F^{E-1\beta}{}_{.c})F^{Eb}{}_{.\beta}\Big]_{:b}$$

$$= \mu l_{\eta}^{4}\tilde{g}_{\alpha\beta}\Big[F^{L-1\beta}{}_{.a}\theta^{ab}\Big]_{:b} \qquad (9.177)$$

$$= \mu l_{\eta}^{4}\tilde{g}_{\alpha\beta}\Big[F^{L-1\beta}{}_{.a:b}\theta^{ab} + F^{L-1\beta}{}_{.a}\theta^{ab}_{;b}\Big]$$

$$= \frac{1}{4}\mu l_{\eta}^{4}\tilde{g}_{\alpha\beta}\varepsilon^{acd}\varepsilon^{bef}\Big[F^{L-1\beta}{}_{.a:b}\hat{R}_{fecd} + F^{L-1\beta}{}_{.a}\hat{R}_{fecd;b}\Big],$$

where from the identity in (3.250), the rank four curvature tensor satisfies

$$\hat{R}_{fecd} = 2\hat{\nabla}_{[f}Q_{e][cd]} + 2\hat{T}^{.a}_{[fe]}Q_{a[cd]}. \qquad (9.178)$$

Microscopic angular momentum balance (9.143) then becomes the kinematic equality

$$4l_{\rho}^{2}\varepsilon_{\alpha\chi\delta}\varepsilon^{bfe}\Big[F^{L-1\chi}{}_{.c}(F^{Lc}{}_{.\beta}F^{L-1\beta}{}_{.f,e} + Q^{.c}_{ef})F^{L-1\delta}{}_{.b}\Big]$$

$$= l_{\eta}^{4}\tilde{g}_{\alpha\beta}\varepsilon^{acd}\varepsilon^{bef}\Big[F^{L-1\beta}{}_{.a:b}\hat{R}_{fecd} + F^{L-1\beta}{}_{.a}\hat{R}_{fecd;b}\Big]. \qquad (9.179)$$

9.4.7 Kinetics and Evolution Equations

The theory is complete upon prescription of evolution laws for the internal state variables, (9.124)-(9.125), and kinetic equations for the time rates of plastic flow and residual lattice deformation, the latter via (9.123). Collectively, these should be formulated so that the dissipation inequality (9.131) is satisfied at all times. Consider first the plastic deformation, which to this point in Section 9.4 has been addressed generically, but is henceforth constrained to follow the kinematic relations of crystal plasticity theory of Section 3.2.6, i.e.,

$$\mathbf{L}^{\mathbf{P}} = \dot{\mathbf{F}}^{\mathbf{P}}\mathbf{F}^{\mathbf{P}-1} = \sum_{i=1}^{n}\dot{\gamma}^{i}\tilde{\mathbf{s}}^{i}\otimes\tilde{\mathbf{m}}^{i}, \qquad (9.180)$$

where i denotes a slip system with shearing rate $\dot{\gamma}^{i}$, reference slip direction vector $\tilde{\mathbf{s}}^{i}(X)\in T\tilde{B}$, and reference slip plane normal covariant vector $\tilde{\mathbf{m}}^{i}(X)\in T^{*}\tilde{B}$. The total number of slip systems is denoted by the scalar constant n. Slip directions and slip plane normals are updated with the total lattice deformation of the first of (9.113), as in (3.118):

$$s^{ia} = F^{La}{}_{.\alpha}\tilde{s}^{i\alpha} = F^{Ea}{}_{.\beta}F^{I\beta}{}_{.\alpha}\tilde{s}^{i\alpha}, \quad m^{i}_{a} = F^{L-1\alpha}{}_{.a}\tilde{m}^{i}_{\alpha} = F^{I-1\alpha}{}_{.\beta}F^{E-1\beta}{}_{.a}\tilde{m}^{i}_{\alpha}. \qquad (9.181)$$

Since from (9.180), $\text{tr}(\mathbf{L}^{\mathbf{P}}) = 0$; hence volume changes are measured by

$$J = J^{E}\overline{J} = J^{E}J^{I} = J^{L}, \quad \overline{J} = J^{I}, \quad J^{P} = 1. \qquad (9.182)$$

Plastic dissipation per unit volume in configuration $\overline{B}$ resulting directly from the slip rates is, from (6.85), (9.36), and (9.180),

$$\dot{\tilde{W}}^{P} = J^{I-1}\left[\tilde{M}_{\chi}^{\delta} - \tilde{\Psi}\delta_{\cdot\chi}^{\delta}\right]L_{.\delta}^{P\chi} = J^{I-1}\tilde{M}_{\chi}^{\delta}L_{.\delta}^{P\chi} = \sum_{i}\overline{\tau}^{i}\dot{\gamma}^{i}\,, \qquad (9.183)$$

where the resolved elastic Kirchhoff stress

$$\overline{\tau}^{i} = \overline{J}^{-1}\tilde{\tau}^{i} = J^{E}\sigma^{ab}s_{a}^{i}m_{b}^{i}\,. \qquad (9.184)$$

Viscoplastic flow rules for slip are then posited to exhibit the general form

$$\dot{\gamma}^{i} = \overline{f}^{i}\left(\overline{\tau}^{i},\mathbf{F^{I}},\overline{\mathbf{\alpha}},\overline{\mathbf{\theta}},\overline{\varepsilon}_{\rho},\overline{\varepsilon}_{\eta},\theta,X\right)\frac{\overline{\tau}^{i}}{|\overline{\tau}^{i}|}\,, \qquad (9.185)$$

where the following constraints on the flow rate are prescribed:

$$\overline{f}^{i} \geq 0\,,\ \overline{f}^{i}\left(0,\mathbf{F^{I}},\overline{\mathbf{\alpha}},\overline{\mathbf{\theta}},\overline{\varepsilon}_{\rho},\overline{\varepsilon}_{\eta},\theta,X\right) = 0\,. \qquad (9.186)$$

Scalar function $\overline{f}^{i}$ imposes that the rate of working $\overline{\tau}^{i}\dot{\gamma}^{i} = |\overline{\tau}^{i}|\overline{f}^{i}$ on each slip system always remains non-negative. Specific guidelines describing how dislocation densities may participate in the flow rule (i.e., strain hardening) can be found in a number of works (Bammann 2001; Regueiro et al. 2002; Clayton et al. 2004b; Rezvanian et al. 2007).

In the context of a viscoplastic flow rule such as (6.106), it has been widely suggested in the literature that statistically stored defect densities contribute to the shearing resistance on each system, while geometrically necessary defect densities contribute to a backstress on each system, though such a distinction may not always be immediately clear from experimental data. In particular, from canonical decomposition (3.226) and (3.235), the magnitude of the projection of the dislocation density on each slip plane i,

$$\left|\tilde{\alpha}^{\alpha\beta}\tilde{m}_{\beta}^{i}\right| = \left|\overline{J}F_{\cdot\chi}^{I-1\alpha}\overline{\alpha}^{\chi\delta}F_{.\delta}^{I-1\beta}\tilde{m}_{\beta}^{i}\right| = \left|\overline{J}F_{\cdot\chi}^{I-1\alpha}\overline{\alpha}^{\chi\delta}\overline{m}_{\delta}^{i}\right| = \left|\sum_{k}\tilde{\rho}^{k}\tilde{b}^{k\alpha}\tilde{\xi}^{k\beta}\tilde{m}_{\beta}^{i}\right|\,, \quad (9.187)$$

may provide a measure of dislocations threading that slip plane. Index k runs over all populations of straight line segments with the same Burgers vector and tangent line. So-called forest dislocations measured by (9.187) are thought to give rise to strain hardening in crystals (Kuhlmann-Wilsdorf 1989; Acharya and Beaudoin 2000), particularly latent hardening as discussed in Section 6.3. The scalar quantity

$$\left|\tilde{m}_{\alpha}^{i}\tilde{\alpha}^{\alpha\beta}\tilde{m}_{\beta}^{i}\right| = \left|\sum_{k}\tilde{m}_{\alpha}^{i}\tilde{\rho}^{k}\tilde{b}^{k\alpha}\tilde{\xi}^{k\beta}\tilde{m}_{\beta}^{i}\right| \qquad (9.188)$$

provides a measure of the distortion of the slip plane (Cermelli and Gurtin 2001; Gurtin 2002), and when the dislocations are pure screw with Burgers

magnitude $\tilde{b}$, yields a measure of the density of geometrically necessary screw dislocations threading the slip plane:

$$\left| \tilde{m}_\alpha^i \tilde{\alpha}^{\alpha\beta} \tilde{m}_\beta^i \right| = \tilde{b} \left| \sum_k \tilde{\rho}^k \tilde{m}_\alpha^i \tilde{\xi}^{k\alpha} \tilde{\xi}^{k\beta} \tilde{m}_\beta^i \right| = \tilde{b} \sum_k \rho^k (\tilde{m}_\alpha^i \tilde{\xi}^{k\alpha})^2 = \tilde{b} \sum_k \rho^k . \quad (9.189)$$

Disclination densities may contribute to hardening and/or geometrical softening depending upon the particular material under consideration and its deformation history, as discussed by Pecherski (1983, 1985) and Seefeldt and co-workers (Seefeldt and Klimanek 1997, 1998; Seefeldt 2001). Two-point tensor $\mathbf{F^I}$ is included in (9.186) to account for contributions of heterogeneity of inelastic deformation within the local volume not engendered by that volume's (average) statistically stored and geometrically necessary defect densities, such as higher-order moments of dislocation densities (Kroner 1973, 1992; Hartley 1975) contained within the volume. For example, a backstress may arise in conjunction with piled-up geometrically dislocations at a misoriented subgrain boundary or domain wall. The corresponding inhibiting effect on plastic flow would then manifest in (9.186) through the inclusion of $\bar{\boldsymbol{\theta}}$ and $\mathbf{F^I}$, the former reflecting the misorientation boundary itself (see Fig. 3.18 and (3.282)-(3.285)) and the latter accounting for microscopic elastic stress fields associated with a spatial gradient of dislocation density.

Statistically stored defects accumulate in response to the motion of defects and interactions with each other and other obstacles (Ashby 1970; Kocks et al. 1975). Evolution equations for the statistically stored dislocation rate $\dot{\bar{\varepsilon}}_\rho$ and statistically stored disclination rate $\dot{\bar{\varepsilon}}_\eta$ are assigned here the generic constitutive dependencies of (9.124) and (9.125), respectively. Kinetic relations such these are strongly material dependent. More specific equations dealing with coupled evolution of dislocation and disclination densities—which may be considered as particular implementations of general relations (9.124) and (9.125)—are available in the literature (Pecherski 1983, 1985; Seefeldt and Klimanek 1997, 1998; Seefeldt 2001). Note that these evolution equations need not reflect positive dissipation associated with time rates of the defect densities; on the other hand, an increase in free energy associated with these rates provides the stored energy of cold working under conditions wherein homogeneous plastic deformation occurs. One example of an evolution equation for statistically stored dislocations given by Regueiro et al. (2002) is

$$\dot{\bar{\rho}}_S = \frac{2}{\tilde{b}} \dot{\bar{\varepsilon}}_\rho \sqrt{\bar{\rho}_S} = \left[a_1 \sqrt{\bar{\rho}_S} - a_2 \bar{\rho}_S \right] \dot{\bar{\varepsilon}}^P - a_3 \bar{\rho}_S \sinh\left(a_4 \sqrt{\bar{\rho}_S} \right), \quad (9.190)$$

where a_1 is a scalar constant; scalar functions a_2, a_3, and a_4 depend on temperature; and the scalar effective plastic strain rate is

$$\dot{\bar{\varepsilon}}^P = \sqrt{2/3}\ \bar{L}^{P(\alpha\beta)}\bar{L}^P_{(\alpha\beta)}, \tag{9.191}$$

where, in the context of crystal plasticity kinematics (9.180),

$$\bar{L}^P_{\alpha\beta} = F^I{}_{\alpha\chi}L^{P\chi}_{.\delta}F^{I-1\delta}_{.\beta} = \sum_i \dot{\gamma}^i(F^I{}_{\alpha\chi}\tilde{s}^{i\chi})(\tilde{m}^i_\delta F^{I-1\delta}_{.\beta}) = \sum_i \dot{\gamma}^i\bar{s}^i_\alpha\bar{m}^i_\beta . \tag{9.192}$$

Relation (9.190) combines thermally activated hardening and dynamic recovery mechanisms addressed by Kocks and Mecking (1979) via nonzero a_1 and a_2, and static recovery from thermal diffusion mechanisms addressed by Nes (1995) via nonzero a_3 and a_4. Evolution equations similar to (9.190) have also been extended to include influences of geometrically necessary dislocations (Acharya and Beaudoin 2000; Bammann 2001).

A generic functional form is given for $\dot{\mathbf{F}}^I = \mathbf{L}^I\mathbf{F}^I$ in (9.123). The net dissipation (i.e., rate of working less free energy storage) from the residual lattice deformation in the dissipation inequality (9.131) is of the form

$$\left(\bar{\Pi}^{.\beta}_\alpha - \frac{\partial\bar{\Psi}}{\partial F^{I\alpha}_{.\delta}}F^{I\beta}_{.\delta} \right)L^{I\alpha}_{.\beta} = \bar{Z}^{.\beta}_\alpha L^{I\alpha}_{.\beta}, \tag{9.193}$$

with $\bar{Z}^{.\beta}_\alpha$ the conjugate thermodynamic force to $L^{I\alpha}_{.\beta}$. While not necessary, it may be advantageous to postulate evolution laws for the rate quantity $\mathbf{L}^I$ that render the scalar product $\bar{Z}^{.\beta}_\alpha L^{I\alpha}_{.\beta}$ unconditionally nonnegative. This can be accomplished in practicality by use of a dissipation potential, as outlined in a general way in Section 4.3. As intended in (9.112), $\mathbf{F}^I(X,t)$ accounts for heterogeneity of microscopic residual elastic deformation within the crystalline volume element at X and also dictates the change of orientation of slip planes and slip directions arising from lattice defects, the latter effects manifesting through the presence of $\mathbf{F}^I$ in (9.181). As a result, such rotations of slip planes and directions can presumably account for the diffusion of crystallographic texture observed as subgrain cells emerge and then rotate relative to one another in severely deforming metallic crystals (Butler and McDowell 1998; Peeters et al. 2001; Hughes et al. 2003).

The specific form of the constitutive equation, e.g., a dissipation potential, for $\mathbf{F}^I$ for a given material and scale of resolution depends upon the particular arrangement of defects within the crystal and how their local lattice strain fields interact and contribute to the motion of the crystal element's external boundary. If the rotational part of $\mathbf{F}^I$, denoted by $\mathbf{R}^I$, is assumed to manifest solely as a result of geometrically necessary disclina-

tions within the element, then (3.281) can be used to define $\mathbf{R}^{\mathbf{I}}$. Given an evolution equation for the (rate of) rotation $\mathbf{R}^{\mathbf{I}}$, an evolution equation for the (rate of) stretch $\mathbf{U}^{\mathbf{I}} = \mathbf{R}^{\mathbf{I}^{-1}}\mathbf{F}^{\mathbf{I}}$ is still needed. If this stretch, i.e., the symmetric part of $\mathbf{F}^{\mathbf{I}}$, is assumed to manifest from local residual elastic displacement gradient fields within the volume element, then this symmetric tensor can be expressed via methods outlined in Chapter 7, e.g., integral equations (7.31), (7.37), and (7.41). If a further simplification is made that deviatoric shape changes associated with $\mathbf{F}^{\mathbf{I}}$ may be omitted, e.g., as might occur for an element of material containing many randomly oriented defects, then

$$\mathbf{F}^{\mathbf{I}} \approx \bar{J}^{1/3}\mathbf{R}^{\mathbf{I}}, \tag{9.194}$$

with $\mathbf{R}^{\mathbf{I}}$ defined as in (3.281) and the residual elastic volume change $\bar{J}$ derived via analytical methods in Section 7.2.4, e.g., (7.59) for a cubic crystal or (7.60) when the isotropic elastic approximation is used. Treating all defect energy as deviatoric in (9.160), similarly to (8.89)-(8.90), the defect energy per unit reference volume $\bar{W}_S$ and residual elastic volume change $\bar{J}$ are estimated, respectively, as

$$\bar{W}_S \approx \frac{1}{2}\bar{J}\Big[\bar{\kappa}_1\bar{\varepsilon}_\rho{}^2 + \bar{\kappa}_2\bar{\varepsilon}_\eta{}^2 + \bar{\kappa}_3\bar{\alpha}^{\alpha\beta}\bar{\alpha}_{\alpha\beta} + \bar{\kappa}_4\bar{\theta}^{\alpha\beta}\bar{\theta}_{\alpha\beta}$$
$$+\bar{\kappa}_5\bar{\alpha}^{\alpha\beta}\bar{\alpha}_{\alpha\beta}E^E_{\chi\delta}E^{E\chi\delta} + \bar{\kappa}_6\bar{\theta}^{\alpha\beta}\bar{\theta}_{\alpha\beta}E^E_{\chi\delta}E^{E\chi\delta}\Big], \tag{9.195}$$

$$\bar{J} \approx 1 + \frac{\bar{J}}{2\mu}\left(\frac{\partial\mu}{\partial p} - \frac{\mu}{K}\right)\Big[\bar{\kappa}_1\bar{\varepsilon}_\rho{}^2 + \bar{\kappa}_2\bar{\varepsilon}_\eta{}^2 + \bar{\kappa}_3\bar{\alpha}^{\alpha\beta}\bar{\alpha}_{\alpha\beta} + \bar{\kappa}_4\bar{\theta}^{\alpha\beta}\bar{\theta}_{\alpha\beta}$$
$$+\bar{\kappa}_5\bar{\alpha}^{\alpha\beta}\bar{\alpha}_{\alpha\beta}E^E_{\chi\delta}E^{E\chi\delta} + \bar{\kappa}_6\bar{\theta}^{\alpha\beta}\bar{\theta}_{\alpha\beta}E^E_{\chi\delta}E^{E\chi\delta}\Big]$$
$$\approx 1 + \frac{1}{2\mu}\left(\frac{\partial\mu}{\partial p} - \frac{\mu}{K}\right)\Big[\bar{\kappa}_1\bar{\varepsilon}_\rho{}^2 + \bar{\kappa}_2\bar{\varepsilon}_\eta{}^2 + \bar{\kappa}_3\bar{\alpha}^{\alpha\beta}\bar{\alpha}_{\alpha\beta} + \bar{\kappa}_4\bar{\theta}^{\alpha\beta}\bar{\theta}_{\alpha\beta}$$
$$+\bar{\kappa}_5\bar{\alpha}^{\alpha\beta}\bar{\alpha}_{\alpha\beta}E^E_{\chi\delta}E^{E\chi\delta} + \bar{\kappa}_6\bar{\theta}^{\alpha\beta}\bar{\theta}_{\alpha\beta}E^E_{\chi\delta}E^{E\chi\delta}\Big], \tag{9.196}$$

where small residual elastic volume changes, $\bar{J} \approx (1-\Delta V/V)^{-1}$ are assumed in the last expression of (9.196), following discussion after (7.72). Bulk modulus K, like shear modulus μ, can be estimated from second-order elastic constants of an anisotropic crystal via (8.88), for example. The pressure derivative of the shear modulus, $\partial\mu/\partial p$, is evaluated in a defect-free crystal in the undistorted reference configuration, i.e., at null strain and at the reference temperature. Since coefficients $\bar{\kappa}_i$ ($i = 1,2,...6$) introduced to scale energies of defect densities in (9.162)-(9.167) are usually proportional the shear modulus, the shear modulus in the denominator

of (9.196) will generally cancel with that entering each $\bar{\kappa}_i$. With (9.194) and (9.196) prescribed, relations (3.281), (9.142), and (9.143) then provide nine coupled differential equations for the nine independent components of micropolar rotation $Q_{a[bc]}$ of (9.115).

9.4.8 Dislocation Theory

When micropolar rotations associated with geometrically necessary disclinations are absent, the number of degrees of freedom of the general theory of Section 9.4 is reduced by nine, through imposition that the microrotation variable

$$Q_{abc} = Q_{a[bc]} = 0 \tag{9.197}$$

in (9.114), leading to the following linear connection, i.e., the crystal connection of Section 3.3.2:

$$\hat{\Gamma}^{..a}_{cb} = F^{La}_{.\alpha} F^{L-1\alpha}_{.b,c} = -F^{La}_{.\alpha,c} F^{L-1\alpha}_{.b} = \bar{\Gamma}^{..a}_{cb}. \tag{9.198}$$

From (9.116), spatial dislocation density tensor α^{ab} is defined as follows, while the disclination density tensor vanishes identically:

$$\alpha^{af} = \varepsilon^{fbc} \bar{T}^{..a}_{cb} = \varepsilon^{fbc} F^{La}_{.\alpha} F^{L-1\alpha}_{.b,c}, \quad \theta^{gf} = 0. \tag{9.199}$$

Kinematic relations (9.117) and (9.118) become, respectively,

$$\bar{\alpha}^{\alpha\beta} = J^E F^{E-1\alpha}_{.a} \alpha^{ab} F^{E-1\beta}_{.b} = J^E \varepsilon^{bcd} F^{I\alpha}_{.\chi} F^{L-1\chi}_{.c,d} F^{E-1\beta}_{.b}, \tag{9.200}$$

$$\bar{\theta}^{\alpha\beta} = 0. \tag{9.201}$$

Omitting disclinations from the constitutive assumptions of Section 9.4.3, assumptions (9.119)-(9.125) are replaced with

$$\bar{\Psi} = \bar{\Psi}\left(\mathbf{E}^{\mathbf{E}}, \mathbf{F}^{\mathbf{I}}, \theta, \bar{\nabla}\theta, \bar{\mathbf{a}}, \bar{\varepsilon}_\rho, X, \bar{\mathbf{g}}_\alpha\right), \tag{9.202}$$

$$\bar{N} = \bar{N}\left(\mathbf{E}^{\mathbf{E}}, \mathbf{F}^{\mathbf{I}}, \theta, \bar{\nabla}\theta, \bar{\mathbf{a}}, \bar{\varepsilon}_\rho, X, \bar{\mathbf{g}}_\alpha\right), \tag{9.203}$$

$$\bar{\mathbf{\Sigma}} = \bar{\mathbf{\Sigma}}\left(\mathbf{E}^{\mathbf{E}}, \mathbf{F}^{\mathbf{I}}, \theta, \bar{\nabla}\theta, \bar{\mathbf{a}}, \bar{\varepsilon}_\rho, X, \bar{\mathbf{g}}_\alpha\right), \tag{9.204}$$

$$\bar{\mathbf{q}} = \bar{\mathbf{q}}\left(\mathbf{E}^{\mathbf{E}}, \mathbf{F}^{\mathbf{I}}, \theta, \bar{\nabla}\theta, \bar{\mathbf{a}}, \bar{\varepsilon}_\rho, X, \bar{\mathbf{g}}_\alpha\right), \tag{9.205}$$

$$\dot{\mathbf{F}}^{\mathbf{I}} = \dot{\mathbf{F}}^{\mathbf{I}}\left(\mathbf{E}^{\mathbf{E}}, \mathbf{F}^{\mathbf{I}}, \theta, \bar{\nabla}\theta, \bar{\mathbf{a}}, \bar{\varepsilon}_\rho, X, \bar{\mathbf{g}}_\alpha\right), \tag{9.206}$$

$$\dot{\bar{\varepsilon}}_\rho = \dot{\bar{\varepsilon}}_\rho\left(\mathbf{E}^{\mathbf{E}}, \mathbf{F}^{\mathbf{I}}, \theta, \bar{\nabla}\theta, \bar{\mathbf{a}}, \bar{\varepsilon}_\rho, X, \bar{\mathbf{g}}_\alpha\right). \tag{9.207}$$

The constitutive relations presented already in (9.129) still hold:

$$\bar{\mathbf{\Sigma}} = \frac{\partial \bar{\Psi}}{\partial \mathbf{E}^{\mathbf{E}}}, \bar{N} = -\frac{\partial \bar{\Psi}}{\partial \theta}, \frac{\partial \bar{\Psi}}{\partial(\bar{\nabla}\theta)} = 0, \tag{9.208}$$

leading to

$$\bar{\varPsi} = \bar{\varPsi}\left(\mathbf{E^E}, \mathbf{F^I}, \bar{\boldsymbol{\alpha}}, \bar{\varepsilon}_\rho, \theta, X, \bar{\mathbf{g}}_\alpha\right), \quad \bar{N} = \bar{N}\left(\mathbf{E^E}, \mathbf{F^I}, \bar{\boldsymbol{\alpha}}, \bar{\varepsilon}_\rho, \theta, X, \bar{\mathbf{g}}_\alpha\right),$$

$$\bar{\boldsymbol{\Sigma}} = \bar{\boldsymbol{\Sigma}}\left(\mathbf{E^E}, \mathbf{F^I}, \bar{\boldsymbol{\alpha}}, \bar{\varepsilon}_\rho, \theta, X, \bar{\mathbf{g}}_\alpha\right). \tag{9.209}$$

The reduced dissipation inequality (9.131) becomes, from (9.209),

$$\bar{\varPi}_\alpha^{\cdot\beta} \bar{L}_{.\beta}^{P\alpha} + \left(\bar{\varPi}_\alpha^{\cdot\beta} - \frac{\partial \bar{\varPsi}}{\partial F_{.\delta}^{I\alpha}} F_{.\delta}^{I\beta}\right) L_{.\beta}^{I\alpha}$$

$$- \left(\frac{\partial \bar{\varPsi}}{\partial \bar{\alpha}^{\alpha\beta}} \dot{\bar{\alpha}}^{\alpha\beta} + \frac{\partial \bar{\varPsi}}{\partial \bar{\varepsilon}_\rho} \dot{\bar{\varepsilon}}_\rho\right) + \frac{1}{\theta} \bar{K}^{\alpha\beta} \theta_{,\alpha} \theta_{,\beta} \geq 0. \tag{9.210}$$

Local energy balance in the form of temperature rate, (9.133), becomes

$$\bar{C}\dot{\theta} = \left(\bar{\varPi}_\alpha^{\cdot\beta} + \delta_{.\alpha}^\beta \theta \frac{\partial \bar{\varPsi}}{\partial \theta}\right) \dot{F}_{.A}^\alpha \bar{F}_{.\beta}^{-1A} - \left(\frac{\partial \bar{\varPsi}}{\partial F_{.\beta}^{I\alpha}} - \theta \frac{\partial^2 \bar{\varPsi}}{\partial \theta \partial F_{.\beta}^{I\alpha}}\right) \dot{F}_{.\beta}^{I\alpha}$$

$$- \left[\left(\frac{\partial \bar{\varPsi}}{\partial \bar{\alpha}^{\alpha\beta}} - \theta \frac{\partial^2 \bar{\varPsi}}{\partial \theta \partial \bar{\alpha}^{\alpha\beta}}\right) \dot{\bar{\alpha}}^{\alpha\beta} + \left(\frac{\partial \bar{\varPsi}}{\partial \bar{\varepsilon}_\rho} - \theta \frac{\partial^2 \bar{\varPsi}}{\partial \theta \partial \bar{\varepsilon}_\rho}\right) \dot{\bar{\varepsilon}}_\rho\right]$$

$$- \theta \bar{\beta}^{\alpha\beta} \dot{E}_{\alpha\beta}^E + \hat{\nabla}_\alpha(\bar{K}^{\alpha\beta} \theta_{,\beta}) + \bar{\rho} r$$

$$= \dot{\bar{W}}^P + \theta \frac{\partial \bar{\varPsi}}{\partial \theta} L_{.\alpha}^{P\alpha} - \theta \bar{\beta}^{\alpha\beta} \dot{E}_{\alpha\beta}^E + \hat{\nabla}_\alpha(\bar{K}^{\alpha\beta} \theta_{,\beta}) + \bar{\rho} r \tag{9.211}$$

$$- \left[\left(\frac{\partial \bar{\varPsi}}{\partial \bar{\alpha}^{\alpha\beta}} - \theta \frac{\partial^2 \bar{\varPsi}}{\partial \theta \partial \bar{\alpha}^{\alpha\beta}}\right) \dot{\bar{\alpha}}^{\alpha\beta} + \left(\frac{\partial \bar{\varPsi}}{\partial \bar{\varepsilon}_\rho} - \theta \frac{\partial^2 \bar{\varPsi}}{\partial \theta \partial \bar{\varepsilon}_\rho}\right) \dot{\bar{\varepsilon}}_\rho\right]$$

$$+ \left(\bar{\varPi}_\alpha^{\cdot\beta} + \delta_{.\alpha}^\beta \theta \frac{\partial \bar{\varPsi}}{\partial \theta} - \frac{\partial \bar{\varPsi}}{\partial F_{.\delta}^{I\alpha}} F_{.\delta}^{I\beta} + \theta \frac{\partial^2 \bar{\varPsi}}{\partial \theta \partial F_{.\delta}^{I\alpha}} F_{.\delta}^{I\beta}\right) L_{.\beta}^{I\alpha}.$$

Macroscopic momentum balances and boundary conditions (9.135)-(9.137) remain unchanged. However, since in this restricted case corresponding to (9.197), the body is not a micropolar medium, the microscopic momentum balances considered in (9.140)-(9.144), are, by assertion or postulate, not invoked. In particular, (9.142) and (9.143) are redundant because their imposition, in general, over-constrains the model, providing more six more equations than unknowns. Definitions (9.134) and (9.138) for microscopic moment stresses $\bar{\sigma}^{\alpha\beta}$ and $\tilde{\sigma}^{ab}$ are still relevant; second-order hyperstresses thermodynamically conjugate to disclination densities, $\bar{\mu}^{\alpha\beta}$ and $\tilde{\mu}^{ab}$, vanish identically. The higher-order boundary condition associated with the couple stress, $\tilde{t}^\alpha = \tilde{\sigma}^{ab} n_b$, is still admitted in the non-polar situation, while $\tilde{h}^\alpha = \tilde{\mu}^{ab} n_b = 0$ identically. Generic boundary conditions of (9.147) become

$$\left.\begin{array}{c} t^a \\ \tilde{t}^\alpha \end{array}\right\} \text{prescribed on } s_1 \, ; \quad \left.\begin{array}{c} x^a \\ F^{Ea}_{.\alpha}, F^{I\alpha}_{.\beta} \end{array}\right\} \text{prescribed on } s_2 \, . \qquad (9.212)$$

Particular boundary conditions (9.148) in turn reduce to

$$\left.\begin{array}{c} t^a = 0 \\ \tilde{t}^\alpha = 0 \end{array}\right\} \begin{array}{c} \text{self-equilibrated} \\ \text{(on } s_1); \end{array} \quad \left.\begin{array}{c} x^a = g^a_{.A} X^A \\ F^{Ea}_{.\alpha} = g^a_{.\alpha}, F^{I\alpha}_{.\beta} = \delta^\alpha_{.\beta} \end{array}\right\} \begin{array}{c} \text{fully clamped} \\ \text{(on } s_2). \end{array} \qquad (9.213)$$

A representative free energy function can be constructed just as in Section 9.4.6, but because disclinations are absent here, all dependencies on $\bar{\boldsymbol{\theta}}$ and ε_η are omitted. In cases wherein defects and elastic coefficients are decoupled in the free energy, (9.172) applies:

$$\bar{\sigma}_{\alpha\beta} = \mu l_\rho^{\,2} \bar{\alpha}_{\alpha\beta} = \mu l_\rho^{\,2} J^E F^I_{\,\alpha\chi} \varepsilon^{bcd} F^{L-1\chi}_{\quad .c,d} F^{E-1}_{\quad \beta b} \, , \qquad (9.214)$$

and further assuming that the second of (6.218) holds, microscopic momentum balance (9.174) is then satisfied identically (Clayton et al. 2006):

$$\tilde{\sigma}^{ab}_{\,:b} = (\mu l_\rho^{\,2} J^{E-1} F^{I-1\alpha}_{\quad .\varepsilon} \bar{\alpha}^{\varepsilon\beta} F^{Eb}_{\quad .\beta})_{,b} = \mu l_\rho^{\,2} \varepsilon^{bfe} (F^{L-1\alpha}_{\quad .c} \bar{T}^{.c}_{ef})_{:b}$$

$$= \mu l_\rho^{\,2} \varepsilon^{bfe} F^{L-1\alpha}_{\quad .f:eb} = \mu l_\rho^{\,2} \varepsilon^{f[eb]} F^{L-1\alpha}_{\quad .f:(eb)} = 0. \qquad (9.215)$$

Kinetics can be addressed as in Section 9.4.7, but because disclinations are absent, all dependencies on $\bar{\boldsymbol{\theta}}$ and ε_η are now omitted. Kinetic equations are only required for $\dot{F}^{I\alpha}_{.\beta}$ (or $L^{I\alpha}_{.\beta}$) in (9.206), $\dot{\bar{\varepsilon}}_\rho$ in (9.207), and the slip rates $\dot{\gamma}^i$ entering crystal plasticity kinematic relation (9.180), repeated here in indicial notation:

$$L^{P\alpha}_{.\beta} = \sum_{i=1}^{n} \dot{\gamma}^i \tilde{s}^{i\alpha} \tilde{m}^i_\beta \, . \qquad (9.216)$$

Since (9.216) is traceless, (9.182) again applies. No separate kinetic equation is required for the geometrically necessary dislocation tensor (nor were separate evolution equations required for dislocation or disclination density tensors in the dislocation-disclination theory of previous Sections 9.4.1-9.4.7). In particular, it follows from kinematic identity (3.225), (9.182), and (9.200) that the dislocation density tensor satisfies

$$\tilde{\alpha}^{\alpha\beta} = J^L F^{L-1\alpha}_{\quad .a} \alpha^{ab} F^{L-1\beta}_{\quad .b} = \bar{J} F^{I-1\alpha}_{\quad .\chi} \bar{\alpha}^{\chi\delta} F^{I-1\beta}_{\quad .\chi}$$

$$= J^{P-1} \varepsilon^{ABC} F^{P\alpha}_{\quad .B,C} F^{P\beta}_{\quad .A} = \varepsilon^{ABC} F^{P\alpha}_{\quad .B,C} F^{P\beta}_{\quad .A}. \qquad (9.217)$$

Thus, noting from the chain rule that

$$L^{P\alpha}_{.\beta,C} = \dot{F}^{P\alpha}_{.A,C} F^{P-1A}_{\quad .\beta} + \dot{F}^{P\alpha}_{.A} F^{P-1A}_{\quad .\beta,C}$$

$$= \dot{F}^{P\alpha}_{.A,C} F^{P-1A}_{\quad .\beta} - \dot{F}^{P\alpha}_{.A} F^{P-1A}_{\quad .\chi} F^{P\chi}_{\quad .B,C} F^{P-1B}_{\quad .\beta}$$

$$= (\dot{F}^{P\alpha}_{.B,C} - L^{P\alpha}_{.\chi} F^{P\chi}_{\quad .B,C}) F^{P-1B}_{\quad .\beta}, \qquad (9.218)$$

the rate of the dislocation density tensor in (9.217) becomes, using (9.216),

$$
\begin{aligned}
\dot{\tilde{\alpha}}^{\alpha\beta} &= \varepsilon^{ABC}\left[\dot{F}^{P\alpha}_{.B,C}F^{P\beta}_{.A} + F^{P\alpha}_{.B,C}\dot{F}^{P\beta}_{.A}\right] \\
&= \varepsilon^{ABC}\left[(L^{P\alpha}_{.\chi,C}F^{P\chi}_{.B} + L^{P\alpha}_{.\chi}F^{P\chi}_{.B,C})F^{P\beta}_{.A} + F^{P\alpha}_{.B,C}L^{P\beta}_{.\chi}F^{P\chi}_{.A}\right] \\
&= \varepsilon^{ABC}L^{P\alpha}_{.\chi,C}F^{P\chi}_{.B}F^{P\beta}_{.A} + L^{P\alpha}_{.\chi}\tilde{\alpha}^{\chi\beta} + L^{P\beta}_{.\chi}\tilde{\alpha}^{\alpha\chi} \\
&= \varepsilon^{ABC}F^{P\chi}_{.B}F^{P\beta}_{.A}\sum_{i}\dot{\gamma}^{i}_{,C}\tilde{s}^{i\alpha}\tilde{m}^{i}_{\chi} + \tilde{\alpha}^{\chi\beta}\sum_{i}\dot{\gamma}^{i}\tilde{s}^{i\alpha}\tilde{m}^{i}_{\chi} + \tilde{\alpha}^{\alpha\chi}\sum_{i}\dot{\gamma}^{i}\tilde{s}^{i\beta}\tilde{m}^{i}_{\chi}.
\end{aligned}
\tag{9.219}
$$

From (9.219), the time rate of dislocation density $\tilde{\alpha}^{\alpha\beta}$ depends on material gradients of slip rates, $\dot{\gamma}^{i}_{,C}$, as well as current values of $\tilde{\alpha}^{\alpha\beta}$ and the slip rates. The last of (9.219) applies only over regions of a homogeneous single crystal wherein reference slip directions and slip plane normals are independent of position X. The time rate of $\overline{\alpha}^{\chi\delta}$ can be obtained by substituting (9.219) into the material time derivative of (9.200):

$$
\dot{\overline{\alpha}}^{\alpha\beta} = \frac{1}{J}\left[\dot{\tilde{\alpha}}^{\chi\delta}F^{I\alpha}_{.\chi}F^{I\beta}_{.\delta} + \tilde{\alpha}^{\chi\delta}\frac{d}{dt}(F^{I\alpha}_{.\chi}F^{I\beta}_{.\delta})\right] - \overline{\alpha}^{\alpha\beta}L^{I\chi}_{.\chi}.
\tag{9.220}
$$

10 Dielectrics and Piezoelectricity

A dielectric material by definition is an insulator, i.e., a non-conductor of electricity associated with mobile free charges, which can exhibit polarization in the presence of an electric field. Chapter 10 provides an introduction to dielectric material behavior in the context of geometrically nonlinear continuum mechanics. Electromechanical behaviors of general interest include piezoelectricity, pyroelectricity, and ferroelectricity. Piezoelectricity may refer to the coupling between electric field or polarization and stress or deformation. Specifically, the direct piezoelectric effect refers to electric polarization induced by mechanical strain, while the inverse piezoelectric effect refers to mechanical strain induced proportionately to an electric field (Maugin 1988). In continuum theories, piezoelectricity of first order is attributed to the particular choice of thermodynamic potential (e.g., free energy or internal energy) for the body that may depend, for example, on a scalar product of elastic strain and electric polarization or electric field. Since the first-order piezoelectric effect can be associated with a rank three polar tensor of material coefficients, first-order piezoelectricity can only occur in crystal classes that lack a center of symmetry (Landau and Lifshitz 1960; Thurston 1974), as noted in Appendix A. On the other hand, certain higher-order electromechanical effects, e.g., strains induced by products of electrical field variables, can arise in dielectrics or non-conductors of all crystal classes as a result of quadratic influences of the electric field. This phenomenon is called electrostriction (Devonshire 1954; Maugin 1988; Damjanovic 1998). Pyroelectric crystals exhibit surface charges when uniformly heated or cooled; such crystals feature energetic coupling between polarization and temperature. The pyroelectric effect is revealed by heating a crystal to induce a change in its polarization. Because pyroelectricity is associated with a rank one set of material coefficients, it too is absent in centrosymmetric crystals. Ferroelectric crystals comprise a subset of pyroelectric crystals, the former exhibiting spontaneous polarity that can be reversed by an applied electric field. Ferroelectric crystals may exhibit a transition temperature, called the Curie point, above which they are not spontaneously polarized; the loss of polarity may often accompany a polymorphic phase transition from a non-centrosymmetric to a centrosymmetric structure, for example.

A number of theories of geometrically and materially nonlinear electromechanics of dielectric solids have appeared in historic and more recent literature, often with differences among representations of nonlinear effects. Stratton (1941) and Landau and Lifshitz (1960) described electrostatics and electrodynamics of deformable media, though without emphasis towards large deformations of the material. Devonshire (1954) developed a continuum thermodynamic theory of ferroelectric crystals accounting for material nonlinearity, e.g., a higher than quadratic dependence of the free energy upon polarization, but not geometric nonlinearity. Toupin (1956), Eringen (1962, 1963), and Tiersten (1971) formulated theories of elastic dielectric bodies subjected to arbitrarily large deformations. Tiersten (1971) also considered thermal effects and material inertia. Mindlin (1972) developed frameworks accounting for spatial gradients of both mechanical strain and electric polarization and demonstrated correlation between higher-order continuum theory and discrete lattice dynamics in the limit of long wavelength behavior. Chowdhury et al. (1979) formulated a nonlinear theory for thermoelastic dielectrics with effects of polarization gradients. Fully dynamical theories of insulators were postulated by Toupin (1963) and Tiersten and Tsai (1972), the latter also accounting for magnetization. Geometrically nonlinear theories of electromechanics were also posited by Maugin (1978a, b, 1988), Ani and Maugin (1988), Hadjigeorgiou et al. (1999), Dorfmann and Ogden (2005), McMeeking and Landis (2005), McMeeking et al. (2007), Vu and Steinmann (2007), and Bustamante et al. (2009). Xiao and Bhattacharya (2008) formulated a nonlinear continuum theory of semiconducting ferroelectric crystals.

In some dielectrics, large strains are feasible via domain switching (Bhattacharya and Ravichandran 2003; Zhang and Bhattacharya 2005), necessitating use of a geometrically nonlinear theory. Large deformations are also attained when pressures are significant enough to suppress fracture, for example in shock physics or impact applications (Allison 1965; Graham et al. 1965; Hauver 1965; Graham 1972; Chen et al. 1976; Ani and Maugin 1988; Maugin 1988; Clayton 2010b).

Detailed descriptions of atomic origins of electromechanical phenomena such as piezoelectricity are beyond the scope of this text. Representative treatments of molecular or electronic origins of continuum electromechanical properties of condensed matter are provided by Huang (1950), Wooster (1953), Born and Huang (1954), Lax and Nelson (1971, 1976a), Maradudin et al. (1971), Tiersten (1971), Martin (1972), Tiersten and Tsai (1972), Maugin (1988), and Jackson (1999).

Chapter 10 begins, in Section 10.1, with presentation of Maxwell's equations of electromagnetism. For completeness, the entire set of electrodynamic equations is listed, including classical forms, definitions enter-

ing Lorentz invariant representations (Stratton 1941), and definitions accurate to terms linear in the ratio of particle velocity to the speed of light. Reduction of Maxwell's equations to quasi-electrostatics, often deemed applicable for studies of dielectrics in the absence of optical phenomena, is then presented in Section 10.2. Governing relationships for geometrically nonlinear continuum electromechanics—momentum and energy balances and the dissipation inequality in the context of large deformations—are then described.

Section 10.3 presents a geometrically nonlinear theory for crystalline thermoelastic dielectrics, i.e., dielectric crystals whose macroscopic deformations result only from mechanical elastic deformation of the crystal structure and thermal expansion or contraction. Constitutive relations for elastic dielectric solids emerge, following consideration of local forms of the energy balance and dissipation inequality (Chowdhury et al. 1979; Hadjigeorgiou et al. 1999; McMeeking et al. 2007). A detailed treatment of material coefficients—e.g., elastic, dielectric, pyroelectric, and piezoelectric coefficients of various orders—is provided, along with transformation equations describing their relationships as derived from thermostatics. Phase transformations, e.g., those often associated with ferroelectric materials (Devonshire 1954), are not addressed. Reduction of the nonlinear theory to the geometrically and materially linear regime is presented for completeness in Section 10.4, which also includes the standard constitutive equations of linear piezoelectricity (Bond et al. 1949; Haskins and Hickman 1950). Deformations resulting from defect motion (e.g., dislocation plasticity, void growth, vacancy migration, or fracture) are not addressed, nor are explicit effects of defects on properties of dielectric solids.

While the intent of Chapter 10 is to provide a rigorous treatment of electromechanics of dielectric solids, the content of Chapter 10 is not a comprehensive treatment of electromagnetism. Relevant texts with supporting information include those of Stratton (1941), Landau and Lifshitz (1960), Eringen (1962), Thurston (1974), Maugin (1988), and Jackson (1999).

10.1 Maxwell's Equations

Local forms of Maxwell's equations of classical electromagnetism are given in Section 10.1. Representations of field variables and Maxwell's equations applicable at velocities substantial with respect to the speed of light are then discussed for completeness, though these representations are not used in treatments that follow in Sections 10.2-10.4 wherein material velocities are assumed small relative to light speed in vacuum. Reduced

forms of Maxwell's equations for the case of quasi-electrostatics, deemed adequate for particular (restricted) descriptions of deformable dielectric media in subsequent Sections 10.2-10.4, then follow. Global forms of Maxwell's equations and jump conditions at surfaces of discontinuity are also addressed for the quasi-electrostatic case.

10.1.1 Classical Electrodynamics

Local forms of Maxwell's field equations of electromagnetics can be written as (Stratton 1941; Thurston 1974; Maugin 1988)[1]

$$\overset{\text{g}}{\nabla} \times \hat{\mathbf{e}} = -\frac{\partial \hat{\mathbf{b}}}{\partial t}, \quad \varepsilon^{abc}\hat{e}_{c;b} = -\frac{\partial \hat{b}^a}{\partial t}; \tag{10.1}$$

$$\overset{\text{g}}{\nabla} \times \hat{\mathbf{h}} = \frac{\partial \hat{\mathbf{d}}}{\partial t} + \hat{\mathbf{j}}, \quad \varepsilon^{abc}\hat{h}_{c;b} = \frac{\partial \hat{d}^a}{\partial t} + \hat{j}^a; \tag{10.2}$$

$$\left\langle \overset{\text{g}}{\nabla}, \hat{\mathbf{b}} \right\rangle = 0, \quad \hat{b}^a_{;a} = 0; \tag{10.3}$$

$$\left\langle \overset{\text{g}}{\nabla}, \hat{\mathbf{d}} \right\rangle = \hat{\rho}, \quad \hat{d}^a_{;a} = \hat{\rho}. \tag{10.4}$$

Field quantities in (10.1)-(10.4) are referred to current (spatial) configuration B, from the perspective of a fixed observer, and are presumed at least C^1-continuous. Vector fields are labeled as follows: electric field $\hat{\mathbf{e}}(x,t)$, magnetic flux density or magnetic induction $\hat{\mathbf{b}}(x,t)$, magnetic intensity or magnetic field $\hat{\mathbf{h}}(x,t)$, electric displacement $\hat{\mathbf{d}}(x,t)$, and electric current density $\hat{\mathbf{j}}(x,t)$. The scalar electric free charge density is $\hat{\rho}(x,t)$. Relation (10.1) is often called Faraday's law, (10.2) is often called Ampere's law, (10.3) reflects the solenoidal (i.e., divergence-free) character of the magnetic flux density, and (10.4) is often called Gauss's law. Supplementing (10.1)-(10.4) are the definitions

$$\hat{\mathbf{p}} = \hat{\mathbf{d}} - \varepsilon_0\hat{\mathbf{e}}, \quad \hat{p}^a = \hat{d}^a - \varepsilon_0\hat{e}^a; \tag{10.5}$$

$$\hat{\mathbf{m}} = \frac{1}{\mu_0}\hat{\mathbf{b}} - \hat{\mathbf{h}}, \quad \hat{m}^a = \frac{1}{\mu_0}\hat{b}^a - \hat{h}^a. \tag{10.6}$$

---

[1] In Chapter 10, $\partial(\cdot)/\partial t = \partial(\cdot)/\partial t\big|_x$ denotes partial time differentiation with spatial position x fixed, while $d(\cdot)/dt$ and superposed dots denote material time derivatives (i.e., material particle at X fixed). See Section 2.6.1 for additional discussion of time differentiation in continuum mechanics.

Polarization density per unit spatial volume, also called the electric moment or simply the polarization, is the vector $\hat{\mathbf{p}}(x,t)$ often associated with relative displacements of ions and centers of electron clouds comprising a dielectric, and may also result from a permanent molecular dipole moment (Pauling and Wilson 1935; Maugin 1988). The magnetization or magnetic moment per unit spatial volume is written $\hat{\mathbf{m}}(x,t)$. Electric current, free charge density, polarization, and magnetization can exist only within certain kinds of matter but vanish in pure vacuum (i.e., space devoid of all mass and all charges). The other fields in (10.1)-(10.6) may exist in vacuum as well as certain kinds of matter. In particular, in vacuum the relations $\hat{\mathbf{d}} = \varepsilon_0 \hat{\mathbf{e}}$ and $\hat{\mathbf{b}} = \mu_0 \hat{\mathbf{h}}$ apply.

The SI system of units (international standard) is used in (10.1)-(10.6), as described more fully Appendix E. Other systems of units exist in which various scaling factors appear or disappear in Maxwell's equations (Stratton 1941; Maugin 1988; Jackson 1999). In the SI system of units, the dimensional constants

$$\varepsilon_0 = \frac{10^7}{4\pi c^2}\, \text{F m/s}^2 \approx 8.854 \times 10^{-12}\, \text{F/m} , \tag{10.7}$$

$$\mu_0 = \frac{1}{c^2 \varepsilon_0} = 4\pi \times 10^{-7}\, \text{H/m} , \tag{10.8}$$

are respectively called the permittivity and permeability of vacuum (in classical electrodynamics), where $c \approx 3 \times 10^8\, \text{m/s}$ is the speed of light in vacuum. From (10.8), dimensional constants of electromagnetism, in SI units, are related by

$$\frac{1}{\mu_0 \varepsilon_0} = c^2 . \tag{10.9}$$

The free charge density per unit spatial volume can be defined as the following sum of contributions of charge populations:

$$\hat{\rho} = \sum_i \hat{n}^{(i)} q^{(i)} = \sum_i \hat{n}^{(i)} e z^{(i)} , \tag{10.10}$$

with $\hat{n}^{(i)}$ the number of charge carriers per unit spatial volume of charge $q^{(i)} = e z^{(i)}$, where e is the charge magnitude of an electron $(1.602 \times 10^{-19}\, \text{C})$ and $z^{(i)}$ is the valence of each member of charge carrier population i. For example, for excess electrons $z = -1$, while for holes or missing electrons $z = +1$. Excess or missing ions can also contribute to (10.10); the effective valence $z^{(i)}$ of such defects (e.g., interstitials, vacancies, or substitutional ions) need not be of unit magnitude and need not be an integer.

In the context of two stationary point charges in vacuum, the spatial electric field $\hat{\mathbf{e}}$ describes the static Lorentz force $\hat{\mathbf{F}}$ between the charges arising from Coulomb's law:

$$\hat{\mathbf{F}} = q\hat{\mathbf{e}} = \frac{q^{(1)}q^{(2)}}{4\pi\varepsilon_0}\frac{\mathbf{r}}{r^3}, \; \mathbf{r} = \mathbf{x}^{(1)} - \mathbf{x}^{(2)}, \; r = |\mathbf{r}|, \tag{10.11}$$

where r is the distance between the two point charges with spatial coordinates $\mathbf{x}^{(1)}$ and $\mathbf{x}^{(2)}$. It follows from (10.11) that the electric field induced by a point charge of magnitude q is

$$\hat{\mathbf{e}} = \frac{q}{4\pi\varepsilon_0}\frac{\mathbf{r}}{r^3}. \tag{10.12}$$

Some classifications of different kinds of matter are in order. A material is said to be electrically polarized if $\hat{\mathbf{p}} \neq 0$ at the instant of time t under consideration and at one or more locations x; otherwise it is said to be non-polarized or non-polar. A material is said to be magnetized if $\hat{\mathbf{m}} \neq 0$; otherwise it is said to be non-magnetized. A material is said to be an electrical conductor if $\hat{\mathbf{j}} \neq 0$; otherwise, it is said to be an insulator. A material is formally said to be a dielectric if it is an insulator (electric current $\hat{\mathbf{j}} = 0$) with no free charges (charge density $\hat{\rho} = 0$) capable of exhibiting electric polarization (electric polarization $\hat{\mathbf{p}} \neq 0$ for some electromechanical loading condition) (Maugin 1988). Sometimes this strict definition is relaxed, so that a dielectric may support (excess) free charge density at certain material points (Eringen 1962, 1963; Chowdhury et al. 1979; Jackson 1999; McMeeking and Landis 2005; McMeeking et al. 2007; Clayton et al. 2008a, b; Clayton 2010b). A semiconductor may act either as an electrical conductor or as an insulator (e.g., a dielectric) depending on its environment; for example, the electrical resistivity of a semiconductor may depend on temperature, applied electric field, and/or mechanical stress.

As will be demonstrated later in Section 10.2.1, a dielectric can sustain an effective "displacement current" resulting from the time rate of change of electric displacement (Allison 1965; Graham et al. 1965; Hauver 1965; Graham 1972; Clayton 2010b). Hence, $\hat{\mathbf{j}}$ is sometimes labeled a free current density—for example an electric current resulting from fluxes of free electrons or holes in a conductor, or from mobile ions or other charged defects in an ionic crystal—to distinguish it from displacement current which can exist even if all charges are bound, as in an insulator, or even in vacuum.

The preceding discussion and definitions have been framed in the context of traditional forms of Maxwell's equations. Mathematically alterna-

tive, yet physically equivalent, representations of Maxwell's electrodynamic equations are also possible[2], but will not be used explicitly in Chapter 10.

10.1.2 Lorentz and Galilean Invariance

Maxwell's equations (10.1)-(10.4) apply for a fixed observer in the context of a stationary coordinate frame. An invariant representation of the laws of electromagnetism should apply for any choice of inertial frame of reference. Fields denoted in what follows by primes are those observed with respect to a coordinate system moving with constant velocity $\mathbf{v}$ and enter Lorentz invariant theories of electrodynamics in the context of special relativity (Stratton 1941; Thurston 1974), accounting for the absolute propagation velocity c of electromagnetic waves in vacuum in all inertial coordinate frames:

$$\hat{\mathbf{e}}'_{\parallel} = \hat{\mathbf{e}}_{\parallel}, \; \hat{\mathbf{e}}'_{\perp} = \Xi(\hat{\mathbf{e}} + \mathbf{v} \times \hat{\mathbf{b}})_{\perp}, \tag{10.13}$$

$$\hat{\mathbf{d}}'_{\parallel} = \hat{\mathbf{d}}_{\parallel}, \; \hat{\mathbf{d}}'_{\perp} = \Xi(\hat{\mathbf{d}} + \mathbf{v} \times \hat{\mathbf{h}}/c^2)_{\perp}, \tag{10.14}$$

$$\hat{\mathbf{b}}'_{\parallel} = \hat{\mathbf{b}}_{\parallel}, \; \hat{\mathbf{b}}'_{\perp} = \Xi(\hat{\mathbf{b}} - \mathbf{v} \times \hat{\mathbf{e}}/c^2)_{\perp}, \tag{10.15}$$

$$\hat{\mathbf{h}}'_{\parallel} = \hat{\mathbf{h}}_{\parallel}, \; \hat{\mathbf{h}}'_{\perp} = \Xi(\hat{\mathbf{h}} - \mathbf{v} \times \hat{\mathbf{d}})_{\perp}, \tag{10.16}$$

$$\hat{\mathbf{p}}'_{\parallel} = \hat{\mathbf{p}}_{\parallel}, \; \hat{\mathbf{p}}'_{\perp} = \Xi(\hat{\mathbf{p}} - \mathbf{v} \times \hat{\mathbf{m}}/c^2)_{\perp}, \tag{10.17}$$

$$\hat{\mathbf{m}}'_{\parallel} = \hat{\mathbf{m}}_{\parallel}, \; \hat{\mathbf{m}}'_{\perp} = \Xi(\hat{\mathbf{m}} + \mathbf{v} \times \hat{\mathbf{p}})_{\perp}, \tag{10.18}$$

$$\hat{\mathbf{j}}'_{\parallel} = \Xi(\hat{\mathbf{j}} - \hat{\rho}\mathbf{v})_{\parallel}, \; \hat{\mathbf{j}}'_{\perp} = \hat{\mathbf{j}}_{\perp}, \tag{10.19}$$

$$\hat{\rho}' = \Xi(\hat{\rho} - \mathbf{v} \bullet \hat{\mathbf{j}}/c^2). \tag{10.20}$$

The scalar factor accounting for special relativistic effects is

$$\Xi = \left[\frac{1}{1 - (\mathbf{v} \bullet \mathbf{v})/c^2} \right]^{1/2}, \tag{10.21}$$

and subscripts $\parallel$ and $\perp$ denote respective components of a vector parallel and perpendicular to velocity vector $\mathbf{v}$. For example,

---

[2] For example, so-called Maxwell-Lorentz forms of Ampere's law (10.2) and Gauss's law (10.4) can be written, respectively, as (Lax and Nelson 1971)

$$\overset{g}{\nabla} \times \frac{\hat{\mathbf{b}}}{\mu_0} - \varepsilon_0 \frac{\partial \hat{\mathbf{e}}}{\partial t} = \breve{\mathbf{j}} = \hat{\mathbf{j}} + \frac{\partial \hat{\mathbf{p}}}{\partial t} + \overset{g}{\nabla} \times \hat{\mathbf{m}}, \; \varepsilon_0 \left\langle \overset{g}{\nabla}, \hat{\mathbf{e}} \right\rangle = \breve{\rho} = \hat{\rho} - \left\langle \overset{g}{\nabla}, \hat{\mathbf{p}} \right\rangle,$$

where by definition, $\breve{\mathbf{j}}$ and $\breve{\rho}$ are total (as opposed to free) current density and total charge density, respectively.

$$\hat{\mathbf{e}}_{\parallel} = (\hat{\mathbf{e}} \cdot \boldsymbol{\xi})\boldsymbol{\xi}, \ \ \hat{\mathbf{e}}_{\perp} = \boldsymbol{\xi} \times (\hat{\mathbf{e}} \times \boldsymbol{\xi}), \ \ \boldsymbol{\xi} = \mathbf{v}/(\mathbf{v} \cdot \mathbf{v})^{1/2}. \tag{10.22}$$

For $(\mathbf{v} \cdot \mathbf{v})/c^2 \ll 1$, special relativistic effects are considered unimportant, $\Xi \approx 1$, and the following definitions apply in lieu of (10.13)-(10.20):

$$\hat{\mathbf{e}}' = \hat{\mathbf{e}} + \mathbf{v} \times \hat{\mathbf{b}}, \tag{10.23}$$

$$\hat{\mathbf{d}}' = \hat{\mathbf{d}} + \mathbf{v} \times \hat{\mathbf{h}}/c^2, \tag{10.24}$$

$$\hat{\mathbf{b}}' = \hat{\mathbf{b}} - \mathbf{v} \times \hat{\mathbf{e}}/c^2, \tag{10.25}$$

$$\hat{\mathbf{h}}' = \hat{\mathbf{h}} - \mathbf{v} \times \hat{\mathbf{d}}, \tag{10.26}$$

$$\hat{\mathbf{p}}' = \hat{\mathbf{p}} - \mathbf{v} \times \hat{\mathbf{m}}/c^2, \tag{10.27}$$

$$\hat{\mathbf{m}}' = \hat{\mathbf{m}} + \mathbf{v} \times \hat{\mathbf{p}}, \tag{10.28}$$

$$\hat{\mathbf{j}}' = \hat{\mathbf{j}} - \hat{\rho}\mathbf{v}, \tag{10.29}$$

$$\hat{\rho}' = \hat{\rho} - \mathbf{v} \cdot \hat{\mathbf{j}}/c^2. \tag{10.30}$$

Using (10.23) and (10.26), Maxwell's equations can be expressed in terms of electric and magnetic fields and current perceived at each material particle at x moving with velocity field $\mathbf{v}(x,t)$ of (2.168) as (Thurston 1974)

$$\overset{\mathbf{g}}{\nabla} \times \hat{\mathbf{e}}' = -\overset{*}{\hat{\mathbf{b}}}, \ \ \varepsilon^{abc}\hat{e}'_{c;b} = -\left[\frac{\partial \hat{b}^a}{\partial t} + \varepsilon^{abc}(\varepsilon_{cde}\hat{b}^d v^e)_{;b} + v^a \hat{b}^b_{;b}\right]; \tag{10.31}$$

$$\overset{\mathbf{g}}{\nabla} \times \hat{\mathbf{h}}' = \overset{*}{\hat{\mathbf{d}}} + \hat{\mathbf{j}}', \ \ \varepsilon^{abc}\hat{h}'_{c;b} = \left[\frac{\partial \hat{d}^a}{\partial t} + \varepsilon^{abc}(\varepsilon_{cde}\hat{d}^d v^e)_{;b} + v^a \hat{d}^b_{;b}\right] + \hat{j}'^a; \tag{10.32}$$

$$\left\langle \overset{\mathbf{g}}{\nabla}, \hat{\mathbf{b}} \right\rangle = 0, \ \ \hat{b}^a_{;a} = 0; \tag{10.33}$$

$$\left\langle \overset{\mathbf{g}}{\nabla}, \hat{\mathbf{d}} \right\rangle = \hat{\rho}, \ \ \hat{d}^a_{;a} = \hat{\rho}. \tag{10.34}$$

Notice that (10.31) and (10.32) replace, respectively, (10.1) and (10.2), while (10.33) and (10.34) are identical to (10.3) and (10.4). Differentiation in (10.31)-(10.34) is expressed in the usual fixed space-time coordinates. As used in (10.31) and (10.32), the convected time derivative of a continuous vector field $A^a(x,t)$ is defined as follows (Toupin 1963; Lax and Nelson 1976b):

$$\overset{*}{A}{}^{a} = J^{-1} F^{a}_{.A} \frac{d}{dt} (J F^{-1A}_{.b} A^{b})$$

$$= \dot{A}^{a} - v^{a}_{;b} A^{b} + A^{a} v^{b}_{;b}$$

$$= \frac{\partial A^{a}}{\partial t} + A^{a}_{;b} v^{b} - v^{a}_{;b} A^{b} + A^{a} v^{b}_{;b}$$

$$= (\mathcal{L}_{\mathbf{v}} A)^{a} + J^{-1} A^{a} (\mathcal{L}_{\mathbf{v}} J) \tag{10.35}$$

$$= \frac{\partial A^{a}}{\partial t} + (A^{a} v^{b} - A^{b} v^{a})_{;b} + A^{b}_{;b} v^{a}$$

$$= \frac{\partial A^{a}}{\partial t} + \varepsilon^{abc} (\varepsilon_{cde} A^{d} v^{e})_{;b} + A^{b}_{;b} v^{a},$$

recalling the definition of the Lie derivative $\mathcal{L}_{\mathbf{v}}$ in (2.178)-(2.181). To the same order of approximation of (10.23)-(10.30), (10.5) and (10.6) become

$$\hat{\mathbf{p}}' = \hat{\mathbf{d}} - \varepsilon_{0} \hat{\mathbf{e}} - \mathbf{v} \times \hat{\mathbf{m}} / c^{2}, \quad \hat{p}'^{a} = \hat{d}^{a} - \varepsilon_{0} \hat{e}^{a} - \varepsilon^{abc} v_{b} \hat{m}_{c} / c^{2}; \tag{10.36}$$

$$\hat{\mathbf{m}}' = \hat{\mathbf{b}} / \mu_{0} - \hat{\mathbf{h}} + \mathbf{v} \times \hat{\mathbf{p}}, \quad \hat{m}'^{a} = \hat{b}^{a} / \mu_{0} - \hat{h}^{a} + \varepsilon^{abc} v_{b} \hat{p}_{c}. \tag{10.37}$$

In a plane electromagnetic wave in vacuum (Thurston 1974), the following equalities and approximations apply, appealing to (10.9):

$$\frac{|\hat{\mathbf{e}}|}{|\hat{\mathbf{h}}|} = \left(\frac{\mu_{0}}{\varepsilon_{0}} \right)^{1/2} = \mu_{0} c, \tag{10.38}$$

$$|\hat{\mathbf{h}}| \sim \frac{|\hat{\mathbf{e}}|}{\mu_{0} c} = |\hat{\mathbf{d}}| c, \quad |\hat{\mathbf{b}}| = |\hat{\mathbf{h}}| \mu_{0} \sim \frac{|\hat{\mathbf{e}}|}{c}, \quad |\hat{\mathbf{d}}| \sim \frac{|\hat{\mathbf{h}}|}{c}. \tag{10.39}$$

It follows that in situations involving electromagnetic wave propagation, differences between primed and unprimed values of electric field, electric displacement, magnetic induction, and magnetic field in (10.23)-(10.26) are all of order $(\mathbf{v} \cdot \mathbf{v})^{1/2} / c$. Following Tiersten (1971), Chowdhury et al. (1979), and McMeeking et al. (2007), such differences are overlooked in the treatment of deformable elastic dielectrics that follows in the remainder of Chapter 10. For example, in an acoustic wave propagating through an elastic solid, typically $(\mathbf{v} \cdot \mathbf{v})^{1/2} / c \lesssim 10^{-7}$ (Thurston 1974).

Lorentz invariance of Maxwell's equations demands that (10.1)-(10.4) apply with primed quantities of (10.13)-(10.20) replacing unprimed ones and differentiation performed with respect to the moving space-time coordinate system (Stratton 1941). Maxwell's equations (10.1)-(10.6) are Gali-

lean invariant[3], i.e., remain fundamentally unchanged in form under Galilean transformations, only in the limit $(\mathbf{v}\bullet\mathbf{v})/c^2 \to 0$ and $(\mathbf{v}\bullet\mathbf{v})^{1/2}/c^2 \to 0$. In other words, Galilean invariance of Maxwell's equations corresponds to a relativity principle applied in the limit of infinite propagation velocities of electromagnetic disturbances. Approximations such as (10.23)-(10.30) are accurate to terms linear in the ratio of material velocity to speed of light, with inaccuracies relative to Lorentz invariant theory on the order of $(\mathbf{v}\bullet\mathbf{v})/c^2$ (Toupin 1963; Tiersten and Tsai 1972; Maugin 1988).

10.2 Electrostatics of Dielectric Media

Reduced representations of Maxwell's field equations are applicable towards dielectric solids when electromagnetic waves of high frequencies or short wavelengths (e.g., those associated with optical phenomena) are of no concern. These equations are listed in global and local forms in both spatial (Section 10.2.1) and material (Section 10.2.2) configurations. Governing relations of continuum mechanics for dielectric media are then presented: balances of linear and angular momentum, the balance of energy, and the dissipation inequality. Only stationary coordinate systems are considered. Differences arise among the governing equations listed in what follows in Section 10.2 for nonlinear electromechanics and those of Chapter 4 wherein electromechanical phenomena were not addressed.

10.2.1 Maxwell's Equations of Electrostatics

Treatments of dielectric elastic solids wherein electromagnetic wave propagation is not of interest often follow a quasi-electrostatic approximation[4]. In one kind of quasi-electrostatic approximation (Tiersten 1971; Ani

---

[3] Under a generic Galilean transformation (Truesdell and Toupin 1960; Maugin 1988), $x'^a = \hat{Q}^a_b x^b - v^a t + C^a$ and $t' = t + C$, where $\hat{\mathbf{Q}}$ is a constant proper orthogonal matrix, $\mathbf{v}$ is the constant velocity of the origin of the primed coordinate system relative to that of the unprimed system, and C^a and C are constants.

[4] Since material accelerations and mechanical wave propagation are admitted, the quasi-electrostatic approximation does enable accurate depiction of acoustic modes (i.e., stress waves with typical frequencies $\ll 1$ GHz (Maugin 1988)). Studies of optical modes (specifically, electromagnetic waves with wavelengths on the order of the specimen size or smaller), in contrast, require application of Maxwell's fully electrodynamic equations. In the quasi-electrostatic approximation,

and Maugin 1988; Maugin 1988), magnetic flux density at any spatial point x is treated as constant in time (i.e., $\partial \hat{\mathbf{b}} / \partial t = 0$), so that the first of Maxwell's equations, (10.1), becomes

$$\overset{g}{\nabla} \times \hat{\mathbf{e}} = 0 , \; \varepsilon^{abc} \hat{e}_{c;b} = 0 . \tag{10.40}$$

Relations (10.3) and (10.4) are unchanged in the quasi-electrostatic approximation; the latter (i.e., Gauss's law) is of particular importance in the present context for applications in dielectric solids and is repeated here:

$$\left\langle \overset{g}{\nabla}, \hat{\mathbf{d}} \right\rangle = \hat{\rho} , \; \hat{d}^a_{;a} = \hat{\rho} . \tag{10.41}$$

Relations (10.40) and (10.41) are referred to as Maxwell's equations of electrostatics. In the remainder of Chapter 10, only permanently non-magnetic materials are considered. Recalling from Section 10.1.1 that in non-magnetized materials, $\hat{\mathbf{m}} = 0$ by definition, and taking the curl of spatial equality (10.6),

$$\overset{g}{\nabla} \times \hat{\mathbf{h}} = \overset{g}{\nabla} \times \left[\frac{1}{\mu_0} \hat{\mathbf{b}} - \hat{\mathbf{m}} \right] = \frac{1}{\mu_0} \overset{g}{\nabla} \times \hat{\mathbf{b}} . \tag{10.42}$$

Recall also that in a dielectric material, electric current density $\hat{\mathbf{j}} = 0$ by definition, implying that free electrons, holes, and other charge carriers, if they exist at all, are treated as immobile. Thus, the second of Maxwell's classical equations, i.e., Ampere's law (10.2), becomes the following expression for the displacement current density $\hat{\mathbf{i}}(x,t)$ in non-magnetic materials under a quasi-electrostatic approximation[5]:

$$\hat{\mathbf{i}} = \overset{g}{\nabla} \times \hat{\mathbf{h}} = \frac{1}{\mu_0} \overset{g}{\nabla} \times \hat{\mathbf{b}} = \frac{\partial \hat{\mathbf{d}}}{\partial t} , \; \hat{i}^a = \varepsilon^{abc} \hat{h}_{c;b} = \frac{1}{\mu_0} \varepsilon^{abc} \hat{b}_{c;b} = \frac{\partial \hat{d}^a}{\partial t} . \tag{10.43}$$

---

the electric field, electric displacement, and polarization vector are permitted to vary (slowly) with time, e.g., within the acoustic range of frequencies (Maugin 1988). From the partial time derivative of (10.43) and (10.1), strict consistency of (10.40), (10.42), and (10.43) requires $\mu_0 \partial^2 \hat{\mathbf{d}} / \partial t^2 = \overset{g}{\nabla} \times \partial \hat{\mathbf{b}} / \partial t = -\overset{g}{\nabla} \times (\overset{g}{\nabla} \times \hat{\mathbf{e}}) = 0$.

[5] In previous work (Clayton 2010b), the notation $\hat{j}^a$ was used to represent the negative of the displacement current density. An alternative quasi-electrostatic approximation obeying (10.40) is also possible, whereby $\hat{\mathbf{j}} \neq 0$ but $\hat{\mathbf{b}} = \text{constant}$.

In this context of quasi-electrostatics, the rate of change of electric field energy contained within a spatial volume can then be represented using a simple form of Poynting's theorem[6] (Tiersten 1971; Maugin 1988).

Substituting (10.4) into the divergence of (10.2) and using (2.169), the following charge conservation law emerges, applicable in any regime (i.e., not restricted to non-magnetic materials or quasi-electrostatics):

$$\hat{j}^a_{;a} = \varepsilon^{abc} \hat{h}_{c;ba} - \left(\frac{\partial \hat{d}^a}{\partial t} \right)_{;a} = -\frac{\partial}{\partial t}(\hat{d}^a_{;a}) = -\frac{\partial \hat{\rho}}{\partial t} = -\dot{\hat{\rho}} + \hat{\rho}_{,a} v^a . \qquad (10.44)$$

For a non-conducting (e.g., dielectric) material, since free electric current density vanishes identically, (10.44) then reduces to

$$\hat{j}^a_{;a} = -\frac{\partial \hat{\rho}}{\partial t} = 0 \Leftrightarrow \dot{\hat{\rho}} = \hat{\rho}_{,a} v^a . \qquad (10.45)$$

For a dielectric in the strict sense (Ani and Maugin 1988; Maugin 1988), free charge density also vanishes by definition, so that (10.45) reduces to $\dot{\hat{\rho}} = 0$ identically, though more general relations (10.41) and (10.45) are used in Chapter 10 unless noted otherwise.

Relation (10.5) also applies verbatim in electrostatics:

$$\hat{\mathbf{d}} = \varepsilon_0 \hat{\mathbf{e}} + \hat{\mathbf{p}} , \quad \hat{d}^a = \varepsilon_0 \hat{e}^a + \hat{p}^a . \qquad (10.46)$$

Substitution of (10.46) into (10.43) leads to $\hat{\mathbf{i}} = \varepsilon_0 \partial \hat{\mathbf{e}} / \partial t + \partial \hat{\mathbf{p}} / \partial t$, where the term $\varepsilon_0 \partial \hat{\mathbf{e}} / \partial t$ can exist in non-polar materials or even in vacuum, and where the polarization current $\partial \hat{\mathbf{p}} / \partial t$ exists only within the dielectric. Relation (10.6) is not needed or used explicitly in the remainder of Chapter 10 since the treatment henceforth is restricted to non-magnetic materials.

Maxwell's equations of electrostatics can be expressed globally as the following integral relations in the spatial frame:

$$\int_c \hat{\mathbf{e}} \cdot d\mathbf{x} = 0 , \quad \int_s \langle \hat{\mathbf{d}}^- , \mathbf{n} \rangle ds = \int_v \hat{\rho} dv . \qquad (10.47)$$

In (10.47) and henceforward in Chapter 10, superscripts + and – denote respective limiting values of a quantity at locations outside and inside the body as s is approached from the corresponding side, and **n** is the unit

---

[6] Specifically, using (10.40), (10.43), (10.49), and the divergence theorem, and letting $\hat{\mathbf{s}} = \hat{\mathbf{e}} \times \hat{\mathbf{h}}$ denote the Poynting vector, the flow rate of quasi-static electric field energy out of surface s enclosing volume v is (Tiersten 1971; Jackson 1999)

$$\int_s \hat{s}^a n_a ds = \int_v \hat{s}^a_{;a} dv = \int_v (\varepsilon^{abc} \hat{e}_b \hat{h}_c)_{;a} dv = \int_v \varepsilon^{bac} \hat{\phi}_{;ba} \hat{h}_c dv + \int_v \varepsilon^{bac} \hat{h}_{c;a} \hat{\phi}_{,b} dv = -\int_v \hat{e}_b \hat{i}^b dv$$

$$= \int_v \hat{\phi}_{,b} \hat{i}^b dv = \int_v [(\hat{\phi} \hat{i}^b)_{;b} - \hat{\phi} \hat{i}^b_{;b}] dv = \int_v [(\hat{\phi} \hat{i}^b)_{;b} + \hat{\phi}(\varepsilon^{abc} \hat{h}_{c;ab})] dv = \int_s \hat{\phi} \hat{i}^b n_b ds.$$

normal to s directed from the – side to the + side (i.e., directed from the inside to the outside of the dielectric body).

The first of Maxwell's electrostatic equations in (10.47) states that the line integral of the electric field along an arbitrary closed curve c vanishes. From Stokes's theorem (2.197), the first of Maxwell's global equations of electrostatics in (10.47) can be written

$$\int_c \hat{e}_a dx^a = \int_s \varepsilon^{abc} \hat{e}_{b;a} n_c ds = 0 . \tag{10.48}$$

A vector field in a simply connected domain whose skew covariant derivative (i.e., curl) vanishes can be represented as the gradient of a scalar potential. In the context of electrostatics, scalar potential $\hat{\phi}(x,t)$ is called the electrostatic potential or electric potential and is continuous throughout space (Eringen 1963), except at point charges (e.g., (10.12)), line charges, or dipole layers (Jackson 1999). The local form of (10.48) is

$$\varepsilon^{abc} \hat{e}_{b;a} = \varepsilon^{abc} \hat{e}_{b,a} = 0 \Leftrightarrow \hat{e}_{[b,a]} = -\hat{\phi}_{[,ba]} = 0 \Leftrightarrow \hat{e}_b = -\hat{\phi}_{,b} . \tag{10.49}$$

Within the domain of (10.48), C^1-continuity of $\hat{\mathbf{e}}(x,t)$ is assumed; finite (i.e., bounded) jumps in the normal component of $\hat{\mathbf{e}}$ are admitted across surfaces of discontinuity, but tangential jumps vanish across such surfaces:

$$[\![\hat{\mathbf{e}}]\!] \times \mathbf{n} = 0 , \; \varepsilon^{abc} [\![\hat{e}_b]\!] n_c = \varepsilon^{acb} [\![\hat{\phi}_{,b}]\!] n_c = 0 , \tag{10.50}$$

an identity that follows from the first of (10.47) and application of Stokes's theorem in (10.48) to regions on either side of the discontinuity and subsequent addition of the results (Eringen 1963). The jump in a vector-valued quantity across a surface s is defined by

$$[\![\mathbf{A}]\!] = \mathbf{A}^+ - \mathbf{A}^- , \; [\![A^a]\!] = A^{+a} - A^{-a} . \tag{10.51}$$

The second of Maxwell's static equations establishes a conservation law among surface and volumetric charges. Applying the divergence theorem to the second of (10.47) and localizing the result, (10.41) is recovered:

$$\hat{d}^a_{;a} = \hat{\rho} . \tag{10.52}$$

In arriving at (10.52) from the second of (10.47), C^1-continuity of electric displacement $\hat{\mathbf{d}}$ is assumed within the domain of integration. When $\hat{\mathbf{d}}$ is discontinuous across a surface, the normal component of a jump in $\hat{\mathbf{d}}$ across that surface is given by the surface free charge density $\hat{\sigma}(x,t)$:

$$\hat{\sigma} = [\![\hat{d}^a]\!] n_a = \hat{d}^{+a} n_a - \hat{d}^{-a} n_a . \tag{10.53}$$

Definition (10.53) follows from the following charge conservation requirement (Toupin 1956; Eringen 1962):

$$\hat{Q} = \int_v \hat{\rho}\,dv + \int_a \hat{\sigma}\,da = \int_s \hat{d}^{-a} n_a\,ds \ , \qquad (10.54)$$

where $\hat{Q}$ is the total free charge contained in a volume v with internal surface of discontinuity a and external boundary s. Application of the divergence theorem (2.193) to the rightmost term of (10.54) with consideration of the jump in electric displacement over internal surface a gives

$$\int_s \hat{d}^{-a} n_a\,ds = \int_v \hat{d}^a_{;a}\,dv + \int_a \left[\!\left[\hat{d}^a\right]\!\right] n_a\,da \ , \qquad (10.55)$$

which, upon comparison with the first equality in (10.54), is consistent with (10.52) and (10.53).

Multiplying (10.52) by $\hat{\phi}$, integrating over volume v enclosed by surface s, and applying the divergence theorem with (10.49) and (10.53) yields

$$\int_v \mathbf{\hat{d}}\!\cdot\!\mathbf{\hat{e}}\,dv = \int_v \hat{\rho}\hat{\phi}\,dv + \int_s \hat{\omega}\hat{\phi}\,ds \ , \quad \hat{\omega} = -\hat{d}^{-a} n_a \ , \qquad (10.56)$$

where $\hat{\omega}(x,t)$ measures the contribution from the inside of s to the free charge density in (10.53). Now extend the domain of volume integration in (10.56) to an infinite region containing possible dielectric matter and vacuum, and let a denote the union of enclosed surfaces over which $\mathbf{\hat{d}}$ (and hence $\hat{\omega}$) is discontinuous. Integral expression (10.56) then becomes (Eringen 1962, 1963; Clayton et al. 2008a)

$$\int_v \mathbf{\hat{d}}\!\cdot\!\mathbf{\hat{e}}\,dv = \int_v \hat{\rho}\hat{\phi}\,dv \pm \int_a \left|\hat{\sigma}\right|\hat{\phi}\,da \ , \qquad (10.57)$$

where $\hat{\phi} \to 0$ as $|\mathbf{x}| \to \infty$ has been assumed, and where the algebraic sign on the rightmost term in (10.57) depends on the sense of normal $\mathbf{n}$ and designation of interior and exterior sides of surface a used to define $\hat{\sigma}$. A deforming material element of a dielectric body with a number of corresponding electromechanical quantities is illustrated in Fig. 10.1.
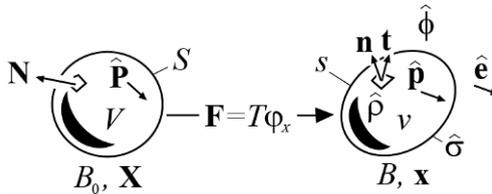
Fig. 10.1 Deforming dielectric material element in an electric field

10.2.2 Material Forms of Maxwell's Equations

Spatial relations of Section 10.2.1 can be mapped to their counterparts in the reference configuration[7] in various ways (Thurston 1974; Lax and Nelson 1976b; Ani and Maugin 1988; Dorfmann and Ogden 2005; Vu and Steinmann 2007). In particular, from (2.115), the first of Maxwell's global (i.e., integral) equations of electrostatics in (10.47) becomes

$$\int_c \hat{\mathbf{e}} \cdot d\mathbf{x} = \int_C \hat{\mathbf{e}} \cdot \mathbf{F} d\mathbf{X} = \int_C \mathbf{F}^T \hat{\mathbf{e}} \cdot d\mathbf{X} = \int_C \hat{\mathbf{E}} \cdot d\mathbf{X} = 0 , \qquad (10.58)$$

or in indicial notation,

$$\int_c \hat{e}_a dx^a = \int_C \hat{e}_a F^a_{.A} dX^A = \int_C F^{TA}_{.a} \hat{e}^a dX_A = \int_C \hat{E}_A dX^A = 0 , \qquad (10.59)$$

where C is a closed reference curve and referential electric field $\hat{\mathbf{E}}(X,t)$ is

$$\hat{\mathbf{E}} = \mathbf{F}^T \hat{\mathbf{e}} , \quad \hat{E}_A = F^a_{.A} \hat{e}_a = x^a_{.A} \hat{e}_a , \qquad (10.60)$$

with covariant components listed in the second of (10.60). Applying Stokes's theorem to (10.59), relations analogous to (10.49) then emerge:

$$\varepsilon^{ABC} \hat{E}_{B;A} = \varepsilon^{ABC} \hat{E}_{B,A} = 0 \Leftrightarrow \hat{E}_{[B,A]} = -\hat{\Phi}_{[,BA]} = 0 \Leftrightarrow \hat{E}_B = -\hat{\Phi}_{,B} , \qquad (10.61)$$

where the referential electrostatic potential is $\hat{\Phi} = \hat{\phi} \circ \varphi$. It follows that $\hat{\Phi}(X,t) = \hat{\phi}(\varphi(X,t),t)$ and $\hat{\Phi}_{,A} = \hat{\phi}_{,a} x^a_{.A}$. Sufficient differentiability of the referential electric field has been assumed in localizing (10.59) to arrive at (10.61); in the converse situation, a jump condition analogous to (10.50) applies in the reference configuration.

The second of Maxwell's electrostatic equations in (10.47) becomes

$$\int_s \hat{d}^{-a} n_a ds = \int_s \hat{d}^{-a} (J F^{-1A}_{.a} N_A dS) = \int_S \hat{D}^{-A} N_A dS \qquad (10.62)$$

upon application of Nanson's formula (2.148). Then from (2.141),

$$\int_v \hat{\rho} dv = \int_V \hat{\rho}(J dV) = \int_V \hat{\rho}_0 dV , \qquad (10.63)$$

leading to the referential definitions of electric displacement $\hat{\mathbf{D}} \in TB_0$:

$$\hat{\mathbf{D}} = J \mathbf{F}^{-1} \hat{\mathbf{d}} , \quad \hat{D}^A = J F^{-1A}_{.a} \hat{d}^a , \qquad (10.64)$$

and free charge density $\hat{\rho}_0(X,t)$:

$$\hat{\rho}_0 = \hat{\rho} J . \qquad (10.65)$$

Maxwell's equation of charge conservation is then, in global form,

---

[7] Definitions in this Section are unambiguous for material elements, but are not always so for regions of vacuum or aether wherein deformation gradients are not defined. A natural assumption is to let $\mathbf{F} = \mathbf{1} = g^a_{.A} \mathbf{g}_a \otimes \mathbf{G}^A$ in vacuum.

$$\int_S \hat{D}^{-A} N_A dS = \int_V \hat{\rho}_0 dV \,, \tag{10.66}$$

with S the surface enclosing reference volume V. The analog of (10.52) is then obtained directly from (10.65) and the divergence theorem:

$$\hat{D}^A_{;A} = \hat{\rho}_0 \,. \tag{10.67}$$

Notice also from Piola's identity (2.146) that (10.64) and (10.67) are consistent: $\hat{D}^A_{;A} = (JF^{-1A}_{.a}\hat{d}^a)_{;A} = JF^{-1A}_{.a}\hat{d}^a_{;A} = J\hat{d}^a_{;a} = J\hat{\rho} = \hat{\rho}_0$. Differentiability of the referential electric displacement field has been assumed in deriving (10.67); in the converse situation, a surface charge density similar to (10.53) can be introduced at reference surfaces over which $\hat{\mathbf{D}}(X,t)$ exhibits jump discontinuities. Multiplying both sides of (10.67) by potential $\hat{\Phi}$, integrating over V, and using (10.61) gives the identity

$$\int_V \hat{\mathbf{D}} \cdot \hat{\mathbf{E}} dV = \int_V \hat{\rho}_0 \hat{\Phi} dV - \int_S \hat{\Phi} \langle \hat{\mathbf{D}}^-, \mathbf{N} \rangle dS \,. \tag{10.68}$$

No natural definition exists for the reference analog of spatial polarization $\hat{\mathbf{p}}(x,t)$. One obvious assumption is, analogous to (10.60),

$$\hat{\mathbf{P}} = \mathbf{F}^T \hat{\mathbf{p}} \,, \quad \hat{P}_A = F^a_{.A} \hat{p}_a = x^a_{.,A} \hat{p}_a \,, \tag{10.69}$$

leaving the following referential version of (10.5) and (10.46):

$$\hat{\mathbf{D}} = J\mathbf{C}^{-1}(\varepsilon_0 \hat{\mathbf{E}} + \hat{\mathbf{P}}) \,, \quad \hat{D}^A = JC^{-1AB}(\varepsilon_0 \hat{E}_B + \hat{P}_B) \,. \tag{10.70}$$

Symmetric right Cauchy-Green deformation $C_{AB} = F_{aA} F^a_{.B} = x_{a,A} x^a_{.,B}$ is defined in (2.153), with inverse $C^{-1AB} = F^{-1Aa} F^{-1B}_{.a} = X^{A,a} X^B_{.,a}$. Other definitions of the reference polarization (e.g., $JF^{-1A}_{.a}\hat{p}^a$ analogous to (10.64)) have been suggested by various authors (Toupin 1963; Lax and Nelson 1976b; Ani and Maugin 1988).

10.2.3 Momentum Conservation

Electromechanical interactions induce modifications to balances of momentum of classical nonlinear continuum mechanics presented in Chapter 4. Such interactions can be addressed in the balance of linear momentum via an electromechanical body force. In the context of continuum electrostatics, i.e., for negligible electrodynamic contributions from $\hat{\mathbf{j}} \times \hat{\mathbf{b}}$, this force, per unit spatial volume, is

$$\hat{f}^a = \hat{p}^b \hat{e}^a_{;b} + \hat{\rho} \hat{e}^a \,, \tag{10.71}$$

where the first term on the right is attributed to short range interaction of the polarization with the electric field[8] (Toupin 1956; Tiersten 1971), and the second term arises from static Lorentz forces acting on non-vanishing free charges. From (10.46), (10.49), and (10.52), and assuming sufficient differentiability of the spatial electric field and spatial polarization, body force $\hat{\mathbf{f}}(x,t)$ can be expressed as the divergence of a rank two contravariant tensor known as the Maxwell stress $\hat{\boldsymbol{\tau}}(x,t)$:

$$\hat{\boldsymbol{\tau}} = \hat{\mathbf{e}} \otimes \hat{\mathbf{d}} - \frac{\varepsilon_0}{2}(\hat{\mathbf{e}} \cdot \hat{\mathbf{e}})\mathbf{g}^{-1} = \hat{\mathbf{e}} \otimes \hat{\mathbf{p}} + \varepsilon_0 \hat{\mathbf{e}} \otimes \hat{\mathbf{e}} - \frac{\varepsilon_0}{2}(\hat{\mathbf{e}} \cdot \hat{\mathbf{e}})\mathbf{g}^{-1}, \quad (10.72)$$

or in index notation,

$$\hat{\tau}^{ab} = \hat{e}^a \hat{d}^b - \frac{\varepsilon_0}{2}\hat{e}^c \hat{e}_c g^{ab} = \hat{e}^a \hat{p}^b + \varepsilon_0 \hat{e}^a \hat{e}^b - \frac{\varepsilon_0}{2}\hat{e}^c \hat{e}_c g^{ab}, \quad (10.73)$$

with spatial divergence

$$\begin{aligned}
\hat{\tau}^{ab}_{;b} &= (\hat{e}^a \hat{d}^b)_{;b} - \frac{\varepsilon_0}{2}\hat{e}^c_{;b}\hat{e}_c g^{ab} - \frac{\varepsilon_0}{2}\hat{e}^c \hat{e}_{c;b} g^{ab} \\
&= \hat{d}^b \hat{e}^a_{;b} - \varepsilon_0 \hat{e}^{b;a}\hat{e}_b + \hat{e}^a \hat{d}^b_{;b} \\
&= \hat{p}^b \hat{e}^a_{;b} + \varepsilon_0 \hat{e}^b \hat{e}^a_{;b} - \varepsilon_0 \hat{e}^{b;a}\hat{e}_b + \hat{e}^a \hat{d}^b_{;b} \\
&= \hat{p}^b \hat{e}^a_{;b} + \varepsilon_0 \hat{e}_b(\hat{e}^{a;b} - \hat{e}^{b;a}) + \hat{e}^a \hat{\rho} \\
&= \hat{p}^b \hat{e}^a_{;b} - \varepsilon_0 \hat{e}_b \hat{\phi}^{[;ab]} + \hat{e}^a \hat{\rho} \\
&= \hat{p}^b \hat{e}^a_{;b} + \hat{\rho}\hat{e}^a \\
&= \hat{f}^a.
\end{aligned} \quad (10.74)$$

With the inclusion of electrostatic body force $\hat{\mathbf{f}}$, the global balance of linear momentum for dielectric solids, which replaces (4.15)-(4.16), is[9]

---

[8] Physically, let the electric polarization vector be defined as $\hat{p}^a = \hat{\rho}\delta r^a$, where $\hat{\rho}$ is a bound, partial charge density (e.g., associated either with ions of the crystal lattice or with bound electrons) and δr^a a (microscopic) dipole separation vector (Tiersten 1971; Tiersten and Tsai 1972). The force contribution from the first term on the right in (10.71) is then $\hat{f}^a - \hat{\rho}\hat{e}^a = \hat{p}^b \hat{e}^a_{;b} = \hat{\rho}\hat{e}^a_{;b}\delta r^b = \hat{\rho}\delta\hat{e}^a$.

[9] Though curvilinear coordinates are used throughout Chapter 10 for generality, Cartesian indices are implied for integral equations involving vector and tensor fields. Alternatively, following Toupin (1956) and the discussion in Section 3.2.5, all quantities entering a vector-valued integrand could be parallel transported to a single point using the shifter, and the resultant integral evaluated at that point.

$$\frac{d}{dt}\int_v \rho v^a dv = \int_s t^a ds + \int_v (\bar{b}^a + \hat{f}^a) dv$$
$$= \int_v (\sigma^{ab}_{;b} + \bar{b}^a + \hat{f}^a) dv,$$

(10.75)

with $t^a = \sigma^{ab} n_b$ the mechanical traction vector and n_b covariant components of the unit outward normal to surface s. The Cauchy stress is denoted by $\boldsymbol{\sigma}(x,t)$, and $\bar{\mathbf{b}}(x,t)$ is the mechanical body force per unit current volume as introduced in (4.15). In application of the divergence theorem in the second equality of (10.75), the Cauchy stress is assumed to exhibit C^1-continuity within v. Noting from (10.74) and the distributive property of the covariant derivative that

$$\sigma^{ab}_{;b} + \hat{f}^a = \sigma^{ab}_{;b} + (\hat{p}^b \hat{e}^a_{;b} + \hat{\rho}\hat{e}^a)_{;b}$$
$$= \sigma^{ab}_{;b} + \hat{\tau}^{ab}_{;b} = (\sigma^{ab} + \hat{\tau}^{ab})_{;b} = T^{ab}_{;b},$$

(10.76)

and using Reynolds transport theorem (4.14), the local form of linear momentum balance (10.75) can be written as

$$T^{ab}_{;b} + \bar{b}^a = \rho a^a,$$

(10.77)

where $a^a(x,t) = \dot{v}^a(x,t)$ is the spatial acceleration of (2.173) and $T^{ab}(x,t)$ are contravariant components of the total stress tensor:

$$\mathbf{T} = \boldsymbol{\sigma} + \hat{\boldsymbol{\tau}}, \ T^{ab} = \sigma^{ab} + \hat{\tau}^{ab},$$

(10.78)

i.e., the sum of the Cauchy and Maxwell stresses. Because electric field and electric polarization vectors may exhibit jump discontinuities in directions normal to surface s, electromechanical traction boundary conditions are

$$T^a = T^{ab} n_b = t^{-a} - [\![\hat{\tau}^{ab}]\!] n_b$$
$$= \sigma^{-ab} n_b + \hat{\tau}^{-ab} n_b - \hat{\tau}^{+ab} n_b$$
$$= \sigma^{+ab} n_b = t^{+a},$$

(10.79)

where $T^a(x,t)$ are components of the net applied traction (Toupin 1956), which can be assigned as $T^a = t^{+a}$ (Tiersten 1971) as indicated in the final equality. From (10.79), the total traction continuity condition can also be expressed

$$[\![T^{ab}]\!] n_b = (\sigma^{+ab} - \sigma^{-ab} + \hat{\tau}^{+ab} - \hat{\tau}^{-ab}) n_b$$
$$= [\![t^a]\!] + [\![\hat{\tau}^{ab}]\!] n_b = 0.$$

(10.80)

Traditional continuity of the mechanical traction vector $\mathbf{t}$ in the context of Cauchy's theorem (4.3) is recovered when the Maxwell stress is continu-

ous normal to s, i.e., $[\![\hat{\tau}^{ab}]\!]n_b = 0$ leads to $[\![t^a]\!] = 0$. As was the case in Chapter 4, shock waves associated with discontinuities in particle velocity have not been considered in (10.77) and (10.80).

Electromechanical body force $\hat{\mathbf{f}}$ of (10.71) and (10.74) likewise enters the balance of moment of momentum, along with an additional moment contribution attributed to interaction between electric polarization and electric field[10] (Toupin 1956; Tiersten 1971). Traditional angular momentum balance (4.23) is replaced with the following for dielectric solids:

$$
\begin{aligned}
\frac{d}{dt}\int_v \varepsilon_{abc} x^b \rho v^c \, dv &= \int_v \varepsilon_{abc} x^b \overline{b}^c \, dv + \int_s \varepsilon_{abc} x^b t^c \, ds \\
&+ \int_v \varepsilon_{abc} x^b \hat{f}^c \, dv + \int_v \varepsilon_{abc} \hat{e}^c \hat{p}^b \, dv.
\end{aligned}
\tag{10.81}
$$

Application of the divergence theorem and Reynolds transport theorem (4.14) along with (10.74) leads to

$$
\int_v \varepsilon_{abc} x^b (\rho a^c - \overline{b}^c - T^{cd}_{;d}) \, dv = \int_v \varepsilon_{abc}(\sigma^{cb} + \rho v^c v^b + \hat{\tau}^{cb}) \, dv .
\tag{10.82}
$$

The left side of (10.82) vanishes by linear momentum balance (10.77), and the second term in the integrand on the right vanishes from the natural symmetry of the dyad $\mathbf{v} \otimes \mathbf{v}$. The local balance of angular momentum is, from the remaining terms in (10.82),

$$
\begin{aligned}
\varepsilon_{abc}(\sigma^{cb} + \hat{\tau}^{cb}) &= \varepsilon_{abc} T^{cb} = 0 \Leftrightarrow T^{ab} = T^{ba} = T^{(ab)}, \\
\sigma^{[ab]} &= \hat{\tau}^{[ba]} = \hat{e}^{[b} \hat{p}^{a]},
\end{aligned}
\tag{10.83}
$$

meaning that total stress tensor $\mathbf{T}$ of (10.78) is symmetric, but the Cauchy stress tensor $\boldsymbol{\sigma}$ entering (10.75) need not be, for example, when spatial electric field and electric polarization vectors are not parallel. The final equality in (10.83) follows from the skew part of (10.73). In non-polarized media, $\hat{e}^{[a} \hat{p}^{b]} = 0$, implying that the classical balance of angular momentum $\sigma^{[ab]} = 0$ of (4.26) applies in the non-polar case. However, even if not polarized, if a material supports both an electric field and a non-vanishing free charge density, the balance of linear momentum (10.77) will be affected by the contribution of the product of charge density and electric field in (10.74). In vacuum, the Cauchy stress vanishes, and linear momentum balance (10.77) reduces to $\hat{\tau}^{ab}_{;b} = \hat{f}^a = 0$, satisfied identically since polarization and free charge density vanish by definition in vacuum.

---

[10] Physically, let $\hat{p}^a = \widetilde{\rho}\delta r^a$ again. Then the moment contribution from the rightmost term in (10.81) is the vector cross product $\hat{\mathbf{p}} \times \hat{\mathbf{e}} = \delta\mathbf{r} \times \widetilde{\rho}\hat{\mathbf{e}}$.

10.2.4 Energy Conservation

A number of methods, some similar and others very different[11], have been set forth to account for energy conservation in dielectric solids (Devonshire 1954; Toupin 1956, 1963; Eringen 1962, 1963; Lax and Nelson 1971; Tiersten 1971; Tiersten and Tsai 1972; Maugin 1978a, b, 1988; Chowdhury et al. 1979; McMeeking and Landis 2005; Vu and Steinmann 2007; Clayton 2009b). Variational principles akin to those of Section 5.6 can provide insight into field equations and boundary conditions for static and non-dissipative processes (Toupin 1956; Eringen 1962, 1963), while rate forms of the energy balance are useful for situations involving mechanical inertia and dissipation (Tiersten 1971; McMeeking et al. 2007; Clayton 2010b). Prescribed here is a global balance among time rates of internal energy, kinetic energy, external work, and heat input:

$$\frac{d}{dt}\left(\mathcal{E}+\mathcal{K}\right)=\mathcal{P}+\mathcal{Q}\,,\tag{10.84}$$

with contributions from kinetic energy $\mathcal{K}$ and extrinsic thermal (heat) energy rate $\mathcal{Q}$ given by

$$\mathcal{K}=\int_{v}\frac{\rho}{2}\mathbf{v}\cdot\mathbf{v}\,dv\,,\tag{10.85}$$

$$\mathcal{Q}=\int_{v}\rho r\,dv-\int_{s}\left\langle\mathbf{q}^{-},\mathbf{n}\right\rangle ds\,,\tag{10.86}$$

and where a dielectric body occupying spatial volume v with oriented surface element $\mathbf{n}ds$ is considered. Field variables are assumed to exhibit continuous space-time derivatives of sufficiently high order within v to enable use of Maxwell's equations (10.49) and (10.52), momentum balances (10.77) and (10.83), and the divergence theorem for conversion from surface to volume integrals. Electric field and electric polarization may exhibit finite jumps normal to external surface s. In the present thermodynamic analysis, the dielectric body is treated as an open region, meaning that surface terms are evaluated as s is approached from the inside of the body. In (10.86), scalar $r(x,t)$ denotes sources of heat energy per unit mass as introduced in (4.32), and $\mathbf{q}(x,t)$ is the heat flux vector presumed continuous normal to interfaces, i.e., $[\![q^{a}]\!]n_{a}=0$ and $q^{+a}n_{a}=q^{-a}n_{a}$ along s (Tiersten 1971).

---

[11] Similarities and differences among the present theory and other geometrically nonlinear treatments of electromechanics of dielectric solids from the literature are discussed in Section 10.3.7.

Thermodynamic relations (10.84)-(10.86), to this point, are identical to (4.28), (4.30), and (4.32). However, the total internal energy and rate of external working in a dielectric solid differ from those of classical continuum mechanics given in (4.29) and (4.31), respectively. For a dielectric solid, or more generally a body with nonzero electric field, the total internal energy is defined by

$$\mathcal{E} = \int_v \rho e \, dv + \frac{\varepsilon_0}{2} \int_v \hat{\mathbf{e}} \cdot \hat{\mathbf{e}} \, dv. \tag{10.87}$$

The first term on the right accounts for the (stored) internal energy of the material body, denoted locally per unit mass by $e(x,t)$. The second term on the right side of (10.87) represents the potential energy of the electric field that permeates the body and underlying vacuum, often called the aether. The combined electromechanical rate of working on the right side of (10.84) is defined as (Clayton 2009b)

$$\mathcal{P} = \int_s \mathbf{t} \cdot \mathbf{v} \, ds + \int_v (\overline{\mathbf{b}} + \hat{\mathbf{f}}) \cdot \mathbf{v} \, dv + \int_s \hat{\omega} \dot{\hat{\phi}} \, ds + \int_v \hat{\rho} \dot{\hat{\phi}} \, dv + \int_v \Omega \, dv. \tag{10.88}$$

The first term on the right of (10.88) accounts for the mechanical traction, the second term accounts for body forces, the third term accounts for the work done by the surface charge density, and the fourth for the work of the bulk (volume) charge density. The final term is prescribed in part such that throughout all space (i.e., within both moving dielectric and vacuum) the balance of energy is satisfied identically:

$$\Omega = -\hat{\phi}_{,a} \dot{\hat{d}}^a + \dot{\hat{\phi}}_{,a} \hat{d}^a + \frac{\varepsilon_0}{2} \hat{\phi}_{,a} \hat{\phi}^{,a} v^b_{;b}$$

$$= \hat{e}_a \dot{\hat{d}}^a - (\dot{\hat{e}}_a + \hat{e}_b v^b_{;a}) \hat{d}^a + \frac{\varepsilon_0}{2} \hat{e}_a \hat{e}^a v^b_{;b}, \tag{10.89}$$

where application of the chain rule, (2.176), and (10.49) yields the identity

$$\dot{\hat{e}}_a = -\frac{d}{dt}(\hat{\phi}_{,A} F^{-1A}_{.a}) = -\dot{\hat{\phi}}_{,A} F^{-1A}_{.a} - \hat{\phi}_{,A} \dot{F}^{-1A}_{.a}$$

$$= -\dot{\hat{\phi}}_{,a} + \hat{\phi}_{,A} F^{-1A}_{.b} \dot{F}^b_{.B} F^{-1B}_{.a} = -\dot{\hat{\phi}}_{,a} + \hat{\phi}_{,b} v^b_{;a}. \tag{10.90}$$

Substituting (10.85)-(10.89) into (10.84) and then converting all surface integrals to volume integrals using the second of (10.56) and the divergence theorem, the global balance of energy becomes

$$\left[\int_v \rho\dot{e}dv + \int_v \rho\dot{v}^a v_a dv - \int_v \hat{e}_a\dot{\hat{p}}^a dv\right] + \int_v \hat{e}_a\dot{\hat{d}}^a dv + \frac{\varepsilon_0}{2}\int_v \hat{e}_a\hat{e}^a v^b_{;b}dv =$$

$$\left[\int_v \rho r dv - \int_v q^b_{;b}dv + \int_s (\sigma^{ab}_{;b}v_a + \sigma^{ab}v_{a;b})dv + \int_v (\bar{b}^a + \hat{f}^a)v_a dv\right] \quad (10.91)$$

$$+\int_v \hat{e}_a\dot{\hat{d}}^a dv + \frac{\varepsilon_0}{2}\int_v \hat{\phi}_{,a}\hat{\phi}^{,a}v^b_{;b}dv + \int_v (\dot{\hat{e}}_a + \hat{e}_b v^b_{;a} + \dot{\hat{\phi}}_{,a})\hat{d}^a dv.$$

The integrand of the last term on the right side of (10.91) vanishes identically from (10.90). Terms in square braces vanish identically in vacuum, and the remaining terms not in square braces cancel. Collecting the terms in braces, localizing the result, and applying (10.76) gives

$$\rho\dot{e} = (T^{ab}_{;b} + \bar{b}^a - \rho\dot{v}^a)v_a + \sigma^{ab}v_{a;b} - q^a_{;a} + \rho r + \hat{e}_a\dot{\hat{p}}^a. \quad (10.92)$$

Then after using (2.176) and (10.77), the local balance of energy for dielectric solids in the quasi-electrostatic approximation remains:

$$\rho\dot{e} = \langle\boldsymbol{\sigma}, \mathbf{L}^T\rangle - \left\langle\overset{\mathbf{g}}{\nabla}, \mathbf{q}\right\rangle + \rho r + \langle\hat{\mathbf{e}}, \dot{\hat{\mathbf{p}}}\rangle, \quad (10.93)$$

or in index notation,

$$\rho\dot{e} = \sigma^{ab}L_{ab} - q^a_{;a} + \rho r + \hat{e}_a\dot{\hat{p}}^a. \quad (10.94)$$

Notice that (10.93)-(10.94) differ from the traditional energy balance for non-polar continua, (4.34)-(4.35), in two ways. Firstly, from (10.83), the Cauchy stress is not necessarily symmetric in (10.93)-(10.94), so that the spin (i.e., the skew part) of $\mathbf{L}$ can contribute to the local stress power $\langle\boldsymbol{\sigma}, \mathbf{L}^T\rangle = \boldsymbol{\sigma}:\mathbf{L} = \sigma^{ab}L_{ab} = \sigma^{ab}v_{a;b}$. Secondly, the final term on the right side of (10.94) is absent in non-polarized solids[12]. Recall also that in the present Section, along the lines of previous theories for dielectric media in the quasi-electrostatic approximation (Tiersten 1971; Chowdhury et al. 1979; McMeeking et al. 2007), purely mechanical dynamic effects are considered (i.e., finite spatial velocity of the material $\mathbf{v}$), but electrodynamics are not. Explicit contributions to the balance of energy from fluxes of free electrons/holes that may result in Joule heating in conductors (those

---

[12] Physically, let $\hat{p}^a = \tilde{\rho}\delta r^a$ as in previous footnotes. Then the rightmost contribution to (10.94) is $\hat{e}_a\dot{\hat{p}}^a = \tilde{\rho}\hat{e}_a\delta\dot{r}^a + \dot{\tilde{\rho}}\delta\hat{\phi}$, where $\tilde{\rho}\hat{e}_a\delta\dot{r}^a$ is the scalar product of Lorentz force density $\tilde{\rho}\hat{e}_a$ and effective charge velocity $\delta\dot{r}^a$, and $\delta\hat{\phi} = \hat{e}_a\delta r^a$ is an effective potential work conjugate to the rate of change of effective charge density $\tilde{\rho}$ associated with polarization. Such developments ultimately provide additional physical motivation for the definition of Ω introduced in (10.89).

with non-negligible electrical resistance) or semiconductors, for example, are not included in the present version of the energy balance (10.94). However, the rightmost term of (10.94), when (10.43) applies, does provide a contribution from the electric displacement current $\hat{i}^a$:

$$
\begin{aligned}
\hat{e}_a \dot{\hat{p}}^a = \hat{e}_a \left[\dot{\hat{d}}^a - \varepsilon_0 \dot{\hat{e}}^a \right] &= \hat{e}_a \left[\frac{\partial \hat{d}^a}{\partial t} - \varepsilon_0 \frac{\partial \hat{e}^a}{\partial t} + (\hat{d}^a_{;b} - \varepsilon_0 \hat{e}^a_{;b}) v^b \right] \\
&= \hat{e}_a \hat{i}^a - \varepsilon_0 \hat{e}_a \frac{\partial \hat{e}^a}{\partial t} + \hat{e}_a \hat{p}^a_{;b} v^b = -\hat{i}^a \hat{\phi}_{,a} - \hat{\phi}_{,a} \left(\hat{p}^a_{;b} v^b + \varepsilon_0 \frac{\partial \hat{\phi}^{,a}}{\partial t} \right).
\end{aligned}
\tag{10.95}
$$

Notice that the electric displacement current density is work conjugate to the spatial electric field in (10.95).

10.2.5 Entropy Production

The global form of the Clausius-Duhem inequality is written as in (4.57) of Chapter 4 (Tiersten 1971):

$$
\frac{d}{dt} \int_v \rho \eta \, dv \geq \int_v \frac{\rho r}{\theta} \, dv - \int_s \frac{\langle \mathbf{q}^-, \mathbf{n} \rangle}{\theta} \, ds,
\tag{10.96}
$$

where η is the entropy per unit mass and $\theta > 0$ is the absolute temperature. Application of the divergence theorem and differentiation of the Helmholtz free energy per unit mass $\psi = e - \theta \eta$ provides a local form of (10.96), identical to (4.63):

$$
\rho(\dot{e} - \dot{\psi} - \dot{\theta}\eta - r) + q^a_{;a} - \theta^{-1} q^a \theta_{,a} \geq 0.
\tag{10.97}
$$

The local entropy inequality following from insertion of (10.94) into (10.97) is

$$
\left\langle \boldsymbol{\sigma}, \mathbf{L}^T \right\rangle + \left\langle \hat{\mathbf{e}}, \dot{\hat{\mathbf{p}}} \right\rangle - \rho(\dot{\psi} + \dot{\theta}\eta) - \frac{1}{\theta} \left\langle \overset{\mathbf{g}}{\nabla} \theta, \mathbf{q} \right\rangle \geq 0,
\tag{10.98}
$$

or in index notation, using (10.83),

$$
\sigma^{(ab)} D_{ab} - \hat{e}^{[a} \hat{p}^{b]} W_{ab} + \hat{e}^a \dot{\hat{p}}_a - \rho(\dot{\psi} + \dot{\theta}\eta) - \theta^{-1} q^a \theta_{,a} \geq 0.
\tag{10.99}
$$

The covariant velocity gradient $\mathbf{L}$ is decomposed in (10.99) into a symmetric part $\mathbf{D}$ and skew part $\mathbf{W}$, as formally defined in Section 2.6.3. In the non-polar case, Maxwell's stress is symmetric and $\hat{\tau}^{[ba]} = 0$, so that in non-polarized media, the skew spin tensor $W_{ab} = v_{[a,b]}$ does not contribute to the dissipation inequality (or, for that matter, the energy balance (10.94)). Moreover, for permanently non-polarized materials, the rate of electric po-

larization $\dot{p}^a = 0$, and (10.99) reduces to the familiar dissipation inequality (4.64) of Section 4.2.2.

10.3 Elastic Dielectric Solids

Recall that a dielectric material by definition is able to exhibit electric polarization when immersed in an electric field. Conductors such as typical metals, on the other hand, are not dielectrics since they cannot exhibit electric polarization. In contrast to a dielectric whose charges are primarily bound and hence may contribute to electric polarization, in a conductor the majority of charges are mobile and give rise to electric current when immersed in an electric field. Examples of dielectric crystalline solids (i.e., insulators) include the alkali halides, quartz, topaz, Rochelle salt, and many engineering ceramics, including those with a perovskite structure such as barium titanate and lead titanate. Piezoelectrics, pyroelectrics, and ferroelectrics are classified as subsets of dielectric materials. Semiconductors can be treated within the framework of Section 10.3 under conditions wherein electrodynamic effects (e.g., dissipative free electric current) are negligible. Examples of semiconductors include gallium arsenide, germanium, selenium, silicon, and silicon carbide. In what follows in Section 10.3, and as noted in Section 10.1.2, no attempt is made here towards construction of a Galilean or Lorentz invariant constitutive theory.

10.3.1 Constitutive Assumptions

Elastic dielectrics considered in the present Section, by definition, exhibit negligible contributions to their deformation from defects. Possible effects of defects on mechanical properties are also not addressed explicitly. Such materials obey the Cauchy-Born hypothesis of Section 3.1.2 (Born and Huang 1954; Ericksen 1984): both the material and the primitive Bravais lattice vectors of the crystal structure deform via the deformation gradient $\mathbf{F}(X,t)$ of (2.112). Under a homogeneous deformation in the sense of Born and Huang (1954), a polarized dielectric may also exhibit a relative translation among different atomic species (e.g., positively and negatively charged ions) comprising the basis of the crystal structure. As remarked in Section 3.1.2 and Section B.2.3 of Appendix B, in non-centrosymmetric crystals with a basis, additional inner displacements—not associated with electric polarization—among atoms are also possible under macroscopi-

cally homogeneous deformation $\mathbf{F}$. As in classical nonlinear thermoelasticity, the deformation gradient for elastic dielectric solids obeys (5.1):

$$\mathbf{F} = \mathbf{F^L} , \ F_{.A}^{a} = x_{.,A}^{a} = F_{.\alpha}^{La} g_{.A}^{\alpha} = F_{.A}^{La} , \quad (10.100)$$

meaning that lattice deformation gradient $\mathbf{F^L}$ and total deformation gradient $\mathbf{F}$ coincide. Mass conservation law (4.10) is then

$$\rho_0 = \rho J = \rho J^L = \rho \sqrt{g/G} \det \mathbf{F} , \ J = J^L > 0 . \quad (10.101)$$

Henceforward in Section 10.3, the superscript L is omitted from the deformation gradient and its Jacobian determinant without consequence, paralleling the treatment of nonlinear thermoelasticity of Section 5.1.

Constitutive response functions analogous to (4.45)-(4.49) are assumed to exhibit the following dependencies, prior to consideration of objectivity and material symmetry requirements:

$$\psi = \psi\left(\mathbf{F}, \hat{\mathbf{p}}, \theta, \overset{\mathbf{g}}{\nabla}\theta, X, \mathbf{G}_A \right), \ \psi = \psi\left(F_{.A}^{a}, \hat{p}_a, \theta, \theta_{,a}, X, \mathbf{G}_A \right); \quad (10.102)$$

$$\eta = \eta\left(\mathbf{F}, \hat{\mathbf{p}}, \theta, \overset{\mathbf{g}}{\nabla}\theta, X, \mathbf{G}_A \right), \ \eta = \eta\left(F_{.A}^{a}, \hat{p}_a, \theta, \theta_{,a}, X, \mathbf{G}_A \right); \quad (10.103)$$

$$\boldsymbol{\sigma} = \boldsymbol{\sigma}\left(\mathbf{F}, \hat{\mathbf{p}}, \theta, \overset{\mathbf{g}}{\nabla}\theta, X, \mathbf{G}_A \right), \ \sigma^{ab} = \sigma^{ab}\left(F_{.A}^{a}, \hat{p}_a, \theta, \theta_{,a}, X, \mathbf{G}_A \right); \quad (10.104)$$

$$\mathbf{q} = \mathbf{q}\left(\mathbf{F}, \hat{\mathbf{p}}, \theta, \overset{\mathbf{g}}{\nabla}\theta, X, \mathbf{G}_A \right), \ q^{a} = q^{a}\left(F_{.A}^{a}, \hat{p}_a, \theta, \theta_{,a}, X, \mathbf{G}_A \right); \quad (10.105)$$

$$\hat{\mathbf{e}} = \hat{\mathbf{e}}\left(\mathbf{F}, \hat{\mathbf{p}}, \theta, \overset{\mathbf{g}}{\nabla}\theta, X, \mathbf{G}_A \right), \ \hat{e}^{a} = \hat{e}^{a}\left(F_{.A}^{a}, \hat{p}_a, \theta, \theta_{,a}, X, \mathbf{G}_A \right). \quad (10.106)$$

Constitutive assumptions (10.102)-(10.106) differ from the constitutive assumptions of nonlinear thermoelasticity in (5.2)-(5.5) via the addition of the spatial polarization (covariant) vector $\hat{\mathbf{p}}(x,t)$ to the list of independent state quantities and the spatial electric field vector $\hat{\mathbf{e}}(x,t)$ in the list of dependent response functions.

Use of a version of the polarization as an independent variable and a version of the electric field as a dependent variable follows general schemes of Devonshire (1954), Toupin (1956), Eringen (1962, 1963), Tiersten (1971), and Shu and Bhattacharya (2001). However, the alternative choice of electric field as independent variable and electric polarization as dependent variable is also possible (Maugin 1988; Dorfmann and Ogden 2005; Vu and Steinmann 2007). Furthermore, via use of (10.46), electric displacement $\hat{\mathbf{d}}(x,t)$ could be used as a substitute for either of the electric field or polarization vectors in the thermodynamic potentials, as illustrated by Thurston (1974). Use of the polarization as an independent

state variable for a dielectric material seems most natural since electric polarization vanishes, by definition, outside matter, in contrast to the electric field or electric displacement, either of which can exist in vacuum. However, in experiments, the electric field or electric displacement may be easier to control than the polarization, via application of short-circuit or open-circuit boundary conditions, for example (Bond et al. 1949; Graham 1972). Thus, transformation formulae are required to relate coefficients measured experimentally at constant electric field or constant electric displacement to those defined at constant polarization, as discussed later in Section 10.3.3. Regardless of the choice of independent and dependent electrical field variables, frame indifferent theories quoted above and in what follows are necessarily formulated in terms of objective transformations of spatial electric polarization, electric field, and electric displacement.

Consider rigid body motions of the form $\mathbf{x} \to \hat{\mathbf{Q}}\mathbf{x} + \mathbf{c}$, where $\hat{\mathbf{Q}}(t) = \hat{\mathbf{Q}}^{-T}(t)$ is a spatially constant rotation tensor with $\det \hat{\mathbf{Q}} = +1$ and $\mathbf{c}(t)$ is a spatially constant translation vector. Under such motions, the following transformations listed in (5.6) apply:

$$F_{.A}^{a} \to \hat{Q}_{.b}^{a} F_{.A}^{b}, \ \sigma^{ab} \to \hat{Q}_{.c}^{a} \sigma^{cd} \hat{Q}_{.d}^{b}, \ q^{a} \to \hat{Q}_{.b}^{a} q^{b}, \ \theta^{.a} \to \hat{Q}_{.b}^{a} \theta^{.b}, \quad (10.107)$$

along with the following vector transformations of spatial electric field and polarization that apply in the non-relativistic or quasi-electrostatic limit:

$$\hat{e}^{a} \to \hat{Q}_{.b}^{a} \hat{e}^{b}, \ \hat{p}^{a} \to \hat{Q}_{.b}^{a} \hat{p}^{b}. \quad (10.108)$$

On the other hand, the referential polarization and electric field vectors of (10.60) and (10.69) are invariant under such rigid body motions:

$$\hat{\mathbf{E}} = \mathbf{F}^{T} \hat{\mathbf{e}} \to \mathbf{F}^{T} \hat{\mathbf{Q}}^{T} \hat{\mathbf{Q}} \hat{\mathbf{e}} = \hat{\mathbf{E}}, \ \hat{\mathbf{P}} = \mathbf{F}^{T} \hat{\mathbf{p}} \to \mathbf{F}^{T} \hat{\mathbf{Q}}^{T} \hat{\mathbf{Q}} \hat{\mathbf{p}} = \hat{\mathbf{P}}, \quad (10.109)$$

and thus are valid candidates for use in frame-indifferent constitutive relations. Analogously to (5.15)-(5.18), the following objective forms of (10.102)-(10.106) are suggested:

$$\psi = \psi \left(\mathbf{E}, \hat{\mathbf{P}}, \theta, \overset{\mathbf{G}}{\nabla} \theta, X, \mathbf{G}_{A} \right), \ \psi = \psi \left(E_{AB}, \hat{P}_{A}, \theta, \theta_{,A}, X, \mathbf{G}_{A} \right); \quad (10.110)$$

$$\eta = \eta \left(\mathbf{E}, \hat{\mathbf{P}}, \theta, \overset{\mathbf{G}}{\nabla} \theta, X, \mathbf{G}_{A} \right), \ \eta = \eta \left(E_{AB}, \hat{P}_{A}, \theta, \theta_{,A}, X, \mathbf{G}_{A} \right); \quad (10.111)$$

$$\boldsymbol{\Sigma} = \boldsymbol{\Sigma} \left(\mathbf{E}, \hat{\mathbf{P}}, \theta, \overset{\mathbf{G}}{\nabla} \theta, X, \mathbf{G}_{A} \right), \ \Sigma^{AB} = \Sigma^{AB} \left(E_{AB}, \hat{P}_{A}, \theta, \theta_{,A}, X, \mathbf{G}_{A} \right); \quad (10.112)$$

$$\mathbf{Q} = \mathbf{Q} \left(\mathbf{E}, \hat{\mathbf{P}}, \theta, \overset{\mathbf{G}}{\nabla} \theta, X, \mathbf{G}_{A} \right), \ Q^{A} = Q^{A} \left(E_{AB}, \hat{P}_{A}, \theta, \theta_{,A}, X, \mathbf{G}_{A} \right); \quad (10.113)$$

$$\hat{\mathbf{E}} = \hat{\mathbf{E}} \left(\mathbf{E}, \hat{\mathbf{P}}, \theta, \overset{\mathbf{G}}{\nabla} \theta, X, \mathbf{G}_{A} \right), \ \hat{E}^{A} = \hat{E}^{A} \left(E_{AB}, \hat{P}_{A}, \theta, \theta_{,A}, X, \mathbf{G}_{A} \right); \quad (10.114)$$

where the right Cauchy-Green strain tensor of (2.156) and second Piola-Kirchhoff stress of (4.7) are, respectively,

$$E_{AB} = \frac{1}{2}(C_{AB} - G_{AB}), \ \Sigma^{AB} = JF^{-1A}_{\ \ .a}\sigma^{ab}F^{-1B}_{\ \ .b}. \qquad (10.115)$$

The referential heat flux vector of (4.36), and the referential temperature gradient of (4.51), are respectively,

$$Q^A = JF^{-1A}_{\ \ .a}q^a, \ \theta_{,A} = \theta_{,a}F^a_{.A}. \qquad (10.116)$$

As noted in Section 5.1, each of the quantities in (10.115) and (10.116) is referred to a reference coordinate system and is invariant under rigid body motions of the spatial frame (see e.g., (4.50)-(4.51) and (5.19)). Notice that in contrast to the second of (4.27), the second Piola-Kirchhoff stress is not necessarily symmetric in polarized dielectric solids, since by (10.83),

$$\begin{aligned}
\Sigma^{[AB]} &= JF^{-1[A}_{\ \ .a}\sigma^{ab}F^{-1B]}_{\ \ .b} = JF^{-1A}_{\ \ .a}\sigma^{[ab]}F^{-1B}_{\ \ .b} \\
&= JF^{-1A}_{\ \ .a}\hat{\tau}^{[ba]}F^{-1B}_{\ \ .b} = JF^{-1A}_{\ \ .a}\hat{e}^{[b}\hat{p}^{a]}F^{-1B}_{\ \ .b} = JF^{-1[A}_{\ \ .a}\hat{p}^a\hat{e}^b F^{-1B]}_{\ \ .b}.
\end{aligned} \qquad (10.117)$$

The rationale for inclusion of particular independent state variables in (10.110)-(10.114) is now discussed. Reasoning behind inclusion of all variables except polarization is given in Section 5.1.1, following (5.2)-(5.5). Succinctly, dependence on strain provides for the elastic strain energy of a crystal, e.g., internal energy and forces associated with changes in interatomic bond lengths and angles. Temperature is incorporated to account for the specific heat capacity of the material as well as thermoelastic effects such as thermal expansion. Temperature gradients permit conduction laws such as Fourier-type relations (4.62) or (4.69); however, the thermodynamic analysis that follows in Section 10.3.2 will eliminate the dependence on temperature gradient from all response functions except the heat flux. Material position X permits a dependence of properties on location in a heterogeneous specimen, while reference basis vectors $\mathbf{G}_A(X)$ are included to denote a specific relationship between the reference coordinate system and orientation of the Bravais lattice used to describe anisotropic material properties (Eringen 1962, 1963). Incorporation of the polarization and electric field as independent and dependent variables, respectively, enables description of the stored electrostatic field energy of a dielectric or electrical insulator (e.g., a capacitor). Couplings among polarization and strain or temperature in the thermodynamic potentials enable description of other physical phenomena observed in dielectric crystals such as piezoelectricity, pyroelectricity, and electrostriction. Following the same arguments given in Section 5.1.1, inner displacements (i.e., internal displacements) not associated with electric polarization are not viewed as independent state variables because inner displacements are assumed obtainable (e.g., via energy minimization of the crystal structure) when the

independent state variables are known; in polyatomic dielectric crystals, inner displacements and electric polarization may be strongly coupled since both can involve relative translations of atoms comprising sub-lattices.

10.3.2 Thermodynamics

The governing equations presented in Section 10.2—Maxwell's equations in the quasi-electrostatic approximation, balances of linear and angular momentum, the balance of energy, and the dissipation inequality—are deemed valid for elastic dielectric solids under conditions considered presently in Section 10.3. The stress power entering (10.94) and (10.98) can be written

$$\sigma^{ab} L_{ab} = J^{-1}(JF^{-1A}_{\quad .b}\sigma^{cb}g_{ac})\dot{F}^{a}_{.A} = J^{-1}P^{A}_{a}\dot{F}^{a}_{.A}, \qquad (10.118)$$

where $\mathbf{P}(X,t)$ is the first Piola-Kirchhoff stress:

$$P^{aA} = J\sigma^{ab}F^{-1A}_{\quad .b}. \qquad (10.119)$$

Expanding the time derivative of the free energy using (10.110) gives

$$\dot{\psi} = \frac{\partial\psi}{\partial E_{AB}}\dot{E}_{AB} + \frac{\partial\psi}{\partial\hat{P}_{A}}\dot{\hat{P}}_{A} + \frac{\partial\psi}{\partial\theta}\dot{\theta} + \frac{\partial\psi}{\partial\theta_{,A}}\gamma_{0A}, \qquad (10.120)$$

where from (4.66) and (5.29),

$$\gamma_{0A} = F^{a}_{.A}\gamma_{a} = F^{a}_{.A}\frac{d}{dt}(\theta_{,a}) = F^{a}_{.A}(\dot{\theta}_{,a} - \theta_{,b}v^{b}_{;a}) = \dot{\theta}_{,a}F^{a}_{.A} - \theta_{,a}\dot{F}^{a}_{.A}. \qquad (10.121)$$

From the chain rule, (10.69), and (10.115),

$$\frac{\partial\psi}{\partial E_{AB}}\dot{E}_{AB} = F^{a}_{.B}\frac{\partial\psi}{\partial E_{AB}}\dot{F}_{aA}, \quad \frac{\partial\psi}{\partial\hat{P}_{A}}\dot{\hat{P}}_{A} = \frac{\partial\psi}{\partial\hat{P}_{A}}\hat{p}^{a}\dot{F}_{aA} + \frac{\partial\psi}{\partial\hat{P}_{A}}F^{a}_{.A}\dot{\hat{p}}_{a}. \qquad (10.122)$$

Substitution of (10.118)-(10.122) into dissipation inequality (10.98) then leads to

$$\left(J^{-1}P^{aA} - \rho F^{a}_{.B}\frac{\partial\psi}{\partial E_{AB}} - \rho\hat{P}_{B}F^{-1Ba}\frac{\partial\psi}{\partial\hat{P}_{A}}\right)\dot{F}_{aA} + \left(\hat{e}^{a} - \rho F^{a}_{.A}\frac{\partial\psi}{\partial\hat{P}_{A}}\right)\dot{\hat{p}}_{a}$$

$$- \rho\left(\frac{\partial\psi}{\partial\theta} + \eta\right)\dot{\theta} - \rho\left(\frac{\partial\psi}{\partial\theta_{,A}}\right)\gamma_{0A} - J^{-1}\theta^{-1}Q^{A}\theta_{,A} \geq 0. \qquad (10.123)$$

Invoking arguments similar to those used in the Coleman-Noll procedure (Chowdhury et al. 1979; McMeeking et al. 2007; Clayton et al. 2008a; Clayton 2009b) and analogous to those following (5.22), thermodynamic admissibility is ensured if coefficients (in parentheses) of time rates of $\mathbf{F}$, $\hat{\mathbf{p}}$, and θ, and the coefficient of γ_{0}, all vanish identically in (10.123), leading to the following constitutive equations:

$$\hat{e}^a = \rho F^a_{.A} \frac{\partial \psi}{\partial \hat{P}_A} = \rho F^a_{.A} \frac{\partial \psi}{\partial \hat{p}_b} \frac{\partial \hat{p}_b}{\partial \hat{P}_A} = \rho F^a_{.A} \frac{\partial \psi}{\partial \hat{p}_b} \frac{\partial (F^{-1B}_{.b} \hat{P}_B)}{\partial \hat{P}_A} = \rho \frac{\partial \psi}{\partial \hat{p}_a}, \quad (10.124)$$

$$P^{aA} = \rho_0 \left(F^a_{.B} \frac{\partial \psi}{\partial E_{BA}} + F^{-1Ba} \hat{P}_B \frac{\partial \psi}{\partial \hat{P}_A} \right), \quad \eta = -\frac{\partial \psi}{\partial \theta}, \quad \frac{\partial \psi}{\partial \theta_{,A}} = 0. \quad (10.125)$$

It follows from the third of (10.125) that free energy, entropy, stress, and electric field do not depend explicitly on the temperature gradient:

$$\psi = \psi \left(E_{AB}, \hat{P}_A, \theta, X, \mathbf{G}_A \right), \quad \eta = \eta \left(E_{AB}, \hat{P}_A, \theta, X, \mathbf{G}_A \right), \quad (10.126)$$

$$\Sigma^{AB} = \Sigma^{AB} \left(E_{AB}, \hat{P}_A, \theta, X, \mathbf{G}_A \right), \quad \hat{E}^A = \hat{E}^A \left(E_{AB}, \hat{P}_A, \theta, X, \mathbf{G}_A \right). \quad (10.127)$$

The electric field referred to the reference configuration is, from the first of (10.124) and definition (10.60),

$$\hat{E}_A = F_{aA} \hat{e}^a = F_{aA} F^a_{.B} \rho \frac{\partial \psi}{\partial \hat{P}_B} = C_{AB} \rho \frac{\partial \psi}{\partial \hat{P}_B}. \quad (10.128)$$

Substituting (10.124) into the first of (10.125), the first Piola-Kirchhoff stress is computed as

$$P^{aA} = \rho_0 F^a_{.B} \frac{\partial \psi}{\partial E_{BA}} + F^{-1Ba} \hat{P}_B J F^{-1A}_{.b} \hat{e}^b = \rho_0 F^a_{.B} \frac{\partial \psi}{\partial E_{BA}} + J \hat{p}^a \hat{e}^b F^{-1A}_{.b}. \quad (10.129)$$

From (10.115) and (10.119), second Piola-Kirchhoff and Cauchy stresses become, respectively,

$$\Sigma^{AB} = F^{-1A}_{.a} P^{aB} = \rho_0 \frac{\partial \psi}{\partial E_{AB}} + J F^{-1A}_{.a} F^{-1Ca} \hat{P}_C F^{-1B}_{.b} \hat{e}^b$$
$$= \rho_0 \frac{\partial \psi}{\partial E_{AB}} + J C^{-1AC} \hat{P}_C C^{-1BD} \hat{E}_D, \quad (10.130)$$

$$\sigma^{ab} = J^{-1} P^{aB} F^b_{.B} = J^{-1} (\rho_0 F^a_{.C} \frac{\partial \psi}{\partial E_{CB}} F^b_{.B}) + J^{-1} (J \hat{p}^a \hat{e}^c F^{-1B}_{.c}) F^b_{.B}$$
$$= 2\rho F^a_{.C} \frac{\partial \psi}{\partial C_{CB}} F^b_{.B} + \hat{p}^a \hat{e}^b = 2\rho \frac{\partial \psi}{\partial g_{ab}} + \hat{p}^a \hat{e}^b. \quad (10.131)$$

The second terms on each of the right sides of (10.130) and (10.131) account for possibly non-symmetric parts of the second Piola-Kirchhoff and Cauchy stress tensors. These terms arise from nonlinear electromechanical interactions. Since the spatial metric tensor is symmetric by definition, $g_{[ab]} = 0$, and consistency of skew-symmetric parts of (10.131) and the Maxwell stress entering (10.83) is revealed by

$$\sigma^{[ab]} = 2\rho \frac{\partial \psi}{\partial g_{[ab]}} + \hat{p}^{[a} \hat{e}^{b]} = \hat{p}^{[a} \hat{e}^{b]} = \hat{e}^{[b} \hat{p}^{a]} = \hat{\tau}^{[ba]}. \quad (10.132)$$

Combining (10.72) and (10.131), the symmetric total stress of (10.78) for an elastic dielectric solid becomes

$$\mathbf{T} = 2\rho \frac{\partial \psi}{\partial \mathbf{g}} + \hat{\mathbf{p}} \otimes \hat{\mathbf{e}} + \hat{\mathbf{e}} \otimes \hat{\mathbf{p}} + \varepsilon_0 \hat{\mathbf{e}} \otimes \hat{\mathbf{e}} - \frac{\varepsilon_0}{2}(\hat{\mathbf{e}} \cdot \hat{\mathbf{e}})\mathbf{g}^{-1}. \qquad (10.133)$$

The first term on the right of (10.133) is recognizable as the Doyle-Ericksen formula for hyperelastic solids (Doyle and Ericksen 1956; Marsden and Hughes 1983), as appearing in (5.36). The final two terms on the right side of (10.133) can contribute to electrostriction, even in non-polarized solids.

From (10.124) and (10.125), the local entropy production rate of (4.61) vanishes identically in an elastic dielectric:

$$\theta \Gamma_L = \rho \theta \dot{\eta} + q^a_{;a} - \rho r = \rho(\dot{e} - \dot{\psi} - \dot{\theta}\eta) + q^a_{;a} - \rho r$$

$$= \sigma^{ab} L_{ab} + \hat{e}^a \dot{\hat{p}}_a - \rho \dot{\psi} - \rho \dot{\theta}\eta = 0, \qquad (10.134)$$

leaving the conduction inequality

$$J\theta\Gamma = J\theta\Gamma_C = -\frac{1}{\theta}\theta_{,A}Q^A \geq 0. \qquad (10.135)$$

When a referential version of Fourier's Law applies such as in (5.48), then

$$Q^A = -K^{AB}\theta_{,B}, \quad -Q^A\theta_{,A} = K^{AB}\theta_{,A}\theta_{,B} \geq 0, \qquad (10.136)$$

where the thermal conductivity $\mathbf{K}(X,t)$ is presumed symmetric and positive semi-definite.

The local energy balance is now revisited. The specific heat capacity c at constant strain and polarization is introduced, from (10.125) satisfying

$$c = \frac{\partial e}{\partial \theta}\bigg|_{\mathbf{E},\hat{\mathbf{P}}} = \frac{\partial e}{\partial \eta}\frac{\partial \eta}{\partial \theta}$$

$$= \left[\frac{\partial}{\partial \eta}(\psi + \theta\eta)\right]\left[\frac{\partial}{\partial \theta}\left(-\frac{\partial \psi}{\partial \theta}\right)\right] = -\theta\frac{\partial^2 \psi}{\partial \theta^2}\bigg|_{\mathbf{E},\hat{\mathbf{P}}}. \qquad (10.137)$$

Multiplying (10.134) by J and using (4.37) and (10.136),

$$\rho_0 \theta \dot{\eta} = -\theta\frac{d}{dt}\left(\rho_0 \frac{\partial \psi}{\partial \theta}\right) = (K^{AB}\theta_{,B})_{;A} + \rho_0 r. \qquad (10.138)$$

Carrying out the time derivative of the temperature derivative of the free energy using (10.120), and substituting with (10.137), results in

$$-\theta\frac{d}{dt}\left(\rho_0 \frac{\partial \psi}{\partial \theta}\right) = -\rho_0\theta\left(\frac{\partial^2 \psi}{\partial \theta^2}\dot{\theta} + \frac{\partial^2 \psi}{\partial \theta \partial E_{AB}}\dot{E}_{AB} + \frac{\partial^2 \psi}{\partial \theta \partial \hat{P}_A}\dot{\hat{P}}_A\right) \qquad (10.139)$$

$$= \rho_0 c\dot{\theta} + \theta\beta^{AB}\dot{E}_{AB} + \theta\chi^A\dot{\hat{P}}_A,$$

where cross-derivatives account for thermoelastic and thermoelectric coupling, respectively:

$$\boldsymbol{\beta} = -\rho_0 \left.\frac{\partial^2 \psi}{\partial \theta \partial \mathbf{E}}\right|_{\hat{\mathbf{P}}} , \quad \boldsymbol{\chi} = -\rho_0 \left.\frac{\partial^2 \psi}{\partial \theta \partial \hat{\mathbf{P}}}\right|_{\mathbf{E}} . \tag{10.140}$$

Coefficients β^{AB} are often called thermal stress coefficients, while χ^A are referred to as pyroelectric coefficients. Equating (10.138) and (10.139), a rate equation for the temperature emerges:

$$\rho_0 c \dot{\theta} = (K^{AB} \theta_{,B})_{,A} - \theta(\beta^{AB} \dot{E}_{AB} + \chi^A \dot{\hat{P}}_A) + \rho_0 r , \tag{10.141}$$

with the first term on the right capturing heat conduction, the second and third terms capturing thermomechanical and thermoelectrical couplings, respectively, and the final term capturing non-mechanical sources of heat energy. In the absence of pyroelectric effects, (10.141) is identical to (5.51) of traditional, non-polar thermoelastic solids.

10.3.3 Material Coefficients

Partial derivatives of thermodynamic or thermostatic potentials with respect to field variables enable definitions of various material coefficients. Thermostatic relationships along the lines of those discussed in Section 5.2 can be constructed, as discussed by Thurston (1974). The number of possible material coefficients becomes immense, however, because any of electric field, electric displacement, or electric polarization can be held fixed during differentiation of a given energy potential, as can temperature or entropy and strain or stress. A number of material coefficients encountered in practical applications are defined in what follows in Section 10.3.3. A complete list of interrelationships among all possible coefficients for thermoelastic dielectric solids is beyond the scope of the present Section; however, relationships among other material coefficients not listed here may be derived following procedures similar to those used in the forthcoming examples.

Second- and third-order elastic coefficients at fixed electric polarization can be defined as partial derivatives of the Helmholtz free energy of (10.126) as, respectively,

$$\mathbb{C}^{ABCD} = \rho_0 \left.\frac{\partial^2 \psi}{\partial E_{AB} \partial E_{CD}}\right|_{\hat{\mathbf{P}},\theta} = \left.\frac{\partial^2 \Psi_0}{\partial E_{AB} \partial E_{CD}}\right|_{\hat{\mathbf{P}},\theta} , \tag{10.142}$$

$$\mathbb{C}^{ABCDEF} = \left.\frac{\partial^3 \Psi_0}{\partial E_{AB} \partial E_{CD} \partial E_{EF}}\right|_{\hat{\mathbf{P}},\theta} = \left.\frac{\partial \mathbb{C}^{ABCD}}{\partial E_{EF}}\right|_{\hat{\mathbf{P}},\theta} . \tag{10.143}$$

Recall from definitions in (4.9) that the Helmholtz free energy per unit reference volume is $\Psi_0(X,t) = \rho_0 \psi$. Coefficients in (10.142)-(10.143) are

called isothermal tangent moduli when evaluated at particular values of the state variables. Owing to their definitions, these coefficients exhibit the same symmetries as those listed in (5.57) and (5.58): $\mathbb{C}^{ABCD}$ consists of up to 21 independent entries and $\mathbb{C}^{ABCDEF}$ consists of up to 56 independent entries.

Second- and third-order derivatives of free energy density with respect to material polarization at fixed strain and temperature lead to the following coefficients, labeled isothermal inverse dielectric susceptibilities:

$$\Lambda^{AB} = \rho_0 \left. \frac{\partial^2 \psi}{\partial \hat{P}_A \partial \hat{P}_B} \right|_{\mathbf{E},\theta} = \left. \frac{\partial^2 \Psi_0}{\partial \hat{P}_A \partial \hat{P}_B} \right|_{\mathbf{E},\theta}, \qquad (10.144)$$

$$\Lambda^{ABC} = \left. \frac{\partial^3 \Psi_0}{\partial \hat{P}_A \partial \hat{P}_B \partial \hat{P}_C} \right|_{\mathbf{E},\theta} = \left. \frac{\partial \Lambda^{AB}}{\partial \hat{P}_C} \right|_{\mathbf{E},\theta}. \qquad (10.145)$$

The following symmetry relations emerge naturally:

$$\Lambda^{AB} = \Lambda^{BA}, \ \Lambda^{ABC} = \Lambda^{ACB} = \Lambda^{BAC}, \qquad (10.146)$$

implying Λ^{AB} consists of at most 6 independent entries and Λ^{ABC} at most 10 independent entries.

The following mixed derivatives, at constant temperature, of free energy density with respect to strain and polarization give rise to electromechanical coupling:

$$\Delta^{ABC} = \rho_0 \left. \frac{\partial^2 \psi}{\partial \hat{P}_A \partial E_{BC}} \right|_\theta = \left. \frac{\partial^2 \Psi_0}{\partial \hat{P}_A \partial E_{BC}} \right|_\theta, \qquad (10.147)$$

$$\Delta^{ABCD} = \rho_0 \left. \frac{\partial^3 \psi}{\partial \hat{P}_A \partial \hat{P}_B \partial E_{CD}} \right|_\theta = \left. \frac{\partial \Lambda^{AB}}{\partial E_{CD}} \right|_\theta = \left. \frac{\partial \Delta^{BCD}}{\partial \hat{P}_A} \right|_\theta, \qquad (10.148)$$

$$\Delta^{ABCDE} = \rho_0 \left. \frac{\partial^3 \psi}{\partial \hat{P}_A \partial E_{BC} \partial E_{DE}} \right|_\theta = \left. \frac{\partial \mathbb{C}^{BCDE}}{\partial \hat{P}_A} \right|_\theta = \left. \frac{\partial \Delta^{ABC}}{\partial E_{DE}} \right|_\theta. \qquad (10.149)$$

From (10.147), second-order piezoelectric coefficients consist of up to 18 independent entries:

$$\Delta^{ABC} = \Delta^{ACB}. \qquad (10.150)$$

Symmetry properties of mixed third-order coefficients can be deduced straightforwardly; Δ^{ABCD} of (10.148) consists of up to 36 independent coefficients, while Δ^{ABCDE} of (10.149) consists of up to 63.

Other material coefficients include the second-order thermal stress and pyroelectric coefficients introduced in (10.140) and the specific heat at constant strain and polarization of (10.137), the latter denoted on a per unit reference volume basis as C_E:

$$\beta^{AB} = -\frac{\partial^2 \Psi_0}{\partial \theta \partial E_{AB}}\bigg|_{\hat{\mathbf{P}}} \ , \ \chi^A = -\frac{\partial^2 \Psi_0}{\partial \theta \partial \hat{P}_A}\bigg|_{\mathbf{E}} \ , \ C_E = \frac{\partial E_0}{\partial \theta}\bigg|_{\mathbf{E},\hat{\mathbf{P}}} = -\theta \frac{\partial^2 \Psi_0}{\partial \theta^2}\bigg|_{\mathbf{E},\hat{\mathbf{P}}} \ . \quad (10.151)$$

None of the coefficients in (10.142)-(10.151) are necessarily constants; instead, these coefficients generally may depend on state variables, position, and orientation of the volume element of material under consideration.

From (10.128), the material electric field satisfies

$$\hat{E}_A = J^{-1} C_{AC} \rho_0 \frac{\partial \psi}{\partial \hat{P}_C}$$

$$\Rightarrow \frac{\partial \hat{E}_A}{\partial \hat{P}_B}\bigg|_{\mathbf{E},\theta} = J^{-1} C_{AC} \frac{\partial^2 \Psi_0}{\partial \hat{P}_C \partial \hat{P}_B}\bigg|_{\mathbf{E},\theta} = J^{-1} C_{AC} \Lambda^{CB}, \quad (10.152)$$

which, since (10.144) is symmetric and assumed non-singular (and more often in dielectrics presumed positive definite), can be inverted to give

$$\frac{\partial \hat{P}_B}{\partial \hat{E}_A}\bigg|_{\mathbf{E},\theta} = J \Lambda^{-1}_{BC} C^{-1CA} = J C^{-1AC} \Lambda^{-1}_{CB}. \quad (10.153)$$

Then from (10.70), the dielectric permittivity tensor ε^{AB} is defined according to

$$\varepsilon^{AB} = \frac{\partial \hat{D}^A}{\partial \hat{E}_B}\bigg|_{\mathbf{E},\theta} = J C^{-1AC} \left(\frac{\partial(\varepsilon_0 \hat{E}_C + \hat{P}_C)}{\partial \hat{E}_B} \right)\bigg|_{\mathbf{E},\theta}$$

$$= J C^{-1AC} \left(\varepsilon_0 \delta^B_{.C} + \frac{\partial \hat{P}_C}{\partial \hat{E}_B}\bigg|_{\mathbf{E},\theta} \right)$$

$$= J C^{-1AB} \varepsilon_0 + J^2 C^{-1AC} C^{-1BD} \Lambda^{-1}_{CD} \quad (10.154)$$

$$= \varepsilon_0 (J C^{-1AB} + \varepsilon_0^{-1} J^2 C^{-1AC} C^{-1BD} \Lambda^{-1}_{CD})$$

$$= \varepsilon_0 (\varepsilon_R)^{AB},$$

where $\boldsymbol{\varepsilon_R}$ is the symmetric, dimensionless relative permittivity tensor that depends on the state variables, position, and orientation of the crystal element. In vacuum, it follows that $\Lambda^{-1A}_{.B} = 0$ in (10.154) because $(\varepsilon_R)^A_{.B} = \delta^A_{.B}$ in vacuum. Notice that symmetry conditions $\Lambda^{-1AB} = \Lambda^{-1BA}$ and $\varepsilon^{AB} = \varepsilon^{BA}$ apply.

Elastic and piezoelectric coefficients are often measured as derivatives with respect to electric displacement or electric field as opposed to electric polarization (Bond et al. 1949; Thurston 1974). First consider the second-order piezoelectric coefficients of (10.147). At constant strain and at con-

stant temperature, let $\hat{P}_A = \hat{P}_A(\hat{E}_A)$ or $\hat{P}_A = \hat{P}_A(\hat{D}_A)$. Then two additional sets of piezoelectric coefficients can be defined using (10.153) as

$$e^{ABC} = -\frac{\partial^2 \Psi_0}{\partial \hat{E}_A \partial E_{BC}}\bigg|_\theta = -\frac{\partial^2 \Psi_0}{\partial \hat{P}_D \partial E_{BC}}\bigg|_\theta \frac{\partial \hat{P}_D}{\partial \hat{E}_A}\bigg|_{\mathbf{E},\theta} = -JC^{-1AE} \Lambda_{ED}^{-1} \Delta^{DBC}, \quad (10.155)$$

$$h^{ABC} = -\frac{\partial^2 \Psi_0}{\partial \hat{D}_A \partial E_{BC}}\bigg|_\theta = -\frac{\partial^2 \Psi_0}{\partial \hat{P}_D \partial E_{BC}}\bigg|_\theta \frac{\partial \hat{P}_D}{\partial \hat{D}_A}\bigg|_{\mathbf{E},\theta} = -\Delta^{ABC} + \varepsilon_{R\ .D}^{-1A} \Delta^{DBC}, \quad (10.156)$$

since from (10.154),

$$\frac{\partial \hat{P}_D}{\partial \hat{D}_A}\bigg|_{\mathbf{E},\theta} = \frac{\partial(\hat{D}_D - \varepsilon_0 \hat{E}_D)}{\partial \hat{D}_A}\bigg|_{\mathbf{E},\theta} = \delta_{.D}^A - \varepsilon_{R\ .D}^{-1A}. \quad (10.157)$$

At constant strain and constant temperature, piezoelectric coefficients of (10.156) and (10.157) are related by

$$e^{ABC} = -\frac{\partial^2 \Psi_0}{\partial \hat{E}_A \partial E_{BC}}\bigg|_\theta = -\frac{\partial^2 \Psi_0}{\partial \hat{D}_D \partial E_{BC}}\bigg|_\theta \frac{\partial \hat{D}_D}{\partial \hat{E}_A}\bigg|_{\mathbf{E},\theta} = h^{DBC} \varepsilon_D^{\ A} = \varepsilon^{AD} h_D^{\ BC}. \quad (10.158)$$

Following a similar procedure, higher-order piezoelectric coefficients in (10.148) and (10.149) can be transformed to their counterparts differentiated with respect to electric field or electric displacement as follows:

$$e^{ABCD} = -\frac{\partial^3 \Psi_0}{\partial \hat{E}_A \partial \hat{E}_B \partial E_{CD}}\bigg|_\theta = -\frac{\partial^3 \Psi_0}{\partial \hat{P}_E \partial \hat{P}_F \partial E_{CD}}\bigg|_\theta \frac{\partial \hat{P}_E}{\partial \hat{E}_A}\bigg|_{\mathbf{E},\theta} \frac{\partial \hat{P}_F}{\partial \hat{E}_B}\bigg|_{\mathbf{E},\theta} \quad (10.159)$$

$$= -J^2 C^{-1AG} \Lambda_{EG}^{-1} C^{-1BH} \Lambda_{FH}^{-1} \Delta^{EFCD},$$

$$e^{ABCDE} = -\frac{\partial^3 \Psi_0}{\partial \hat{E}_A \partial E_{BC} \partial E_{DE}}\bigg|_\theta = -\frac{\partial^3 \Psi_0}{\partial \hat{P}_F \partial E_{BC} \partial E_{DE}}\bigg|_\theta \frac{\partial \hat{P}_F}{\partial \hat{E}_A}\bigg|_{\mathbf{E},\theta} \quad (10.160)$$

$$= -JC^{-1AG} \Lambda_{FG}^{-1} \Delta^{FBCDE},$$

$$h^{ABCD} = -\frac{\partial^3 \Psi_0}{\partial \hat{D}_A \partial \hat{D}_B \partial E_{CD}}\bigg|_\theta = -\frac{\partial^3 \Psi_0}{\partial \hat{P}_E \partial \hat{P}_F \partial E_{CD}}\bigg|_\theta \frac{\partial \hat{P}_E}{\partial \hat{D}_A}\bigg|_{\mathbf{E},\theta} \frac{\partial \hat{P}_F}{\partial \hat{D}_B}\bigg|_{\mathbf{E},\theta} \quad (10.161)$$

$$= -\Delta^{EFCD}(\delta_{.E}^A - \varepsilon_{R\ .E}^{-1A})(\delta_{.F}^B - \varepsilon_{R\ .F}^{-1B}),$$

$$h^{ABCDE} = -\frac{\partial^3 \Psi_0}{\partial \hat{D}_A \partial E_{BC} \partial E_{DE}}\bigg|_\theta = -\frac{\partial^3 \Psi_0}{\partial \hat{P}_F \partial E_{BC} \partial E_{DE}}\bigg|_\theta \frac{\partial \hat{P}_F}{\partial \hat{D}_A}\bigg|_{\mathbf{E},\theta} \quad (10.162)$$

$$= -\Delta^{ABCDE} + \varepsilon_{R\ .F}^{-1A} \Delta^{FBCDE}.$$

Consider now the second-order elastic coefficients. Letting $\mathbb{C}_{\hat{E}}^{ABCD}$ denote tangent isothermal elastic moduli measured at constant electric field,

$$\mathbb{C}_{\hat{E}}^{ABCD} = \left.\frac{\partial^2 \Psi_0}{\partial E_{AB} \partial E_{CD}}\right|_{\hat{\mathbf{E}},\theta} = \left.\frac{\partial^2 \Psi_0}{\partial E_{AB} \partial E_{CD}}\right|_{\hat{\mathbf{P}},\theta} + \left.\frac{\partial \Sigma^{AB}}{\partial \hat{P}_E}\right|_{\mathbf{E},\theta} \left.\frac{\partial \hat{P}_E}{\partial E_{CD}}\right|_{\hat{\mathbf{E}},\theta}$$

$$= \mathbb{C}^{ABCD} - \Delta^{EAB} \Lambda_{GE}^{-1} \tag{10.163}$$

$$\times \left[\Delta^{GCD} + J(2C^{-1CG}C^{-1DF} - C^{-1CD}C^{-1GF})\hat{E}_F \right],$$

since from (2.158), (2.160), (10.147), and (10.153),

$$\left.\frac{\partial \hat{P}_E}{\partial E_{CD}}\right|_{\hat{\mathbf{P}},\theta} = 0 = \left.\frac{\partial \hat{P}_E}{\partial E_{CD}}\right|_{\hat{\mathbf{E}},\theta} + \left.\frac{\partial \hat{P}_E}{\partial \hat{E}_F}\right|_{\mathbf{E},\theta} \left.\frac{\partial \hat{E}_F}{\partial E_{CD}}\right|_{\hat{\mathbf{P}},\theta}$$

$$= \left.\frac{\partial \hat{P}_E}{\partial E_{CD}}\right|_{\hat{\mathbf{E}},\theta} + JC^{-1FG}\Lambda_{GE}^{-1} \frac{\partial}{\partial E_{CD}}\left(J^{-1}C_{FA} \left.\frac{\partial \Psi_0}{\partial \hat{P}_A}\right) \right|_{\hat{\mathbf{P}},\theta} \tag{10.164}$$

$$= \left.\frac{\partial \hat{P}_E}{\partial E_{CD}}\right|_{\hat{\mathbf{E}},\theta} + \Lambda_{GE}^{-1}\left[\Delta^{GCD} + J(2C^{-1CG}C^{-1DB} - C^{-1CD}C^{-1GB})\hat{E}_B \right].$$

Second-order isothermal moduli measured at fixed electric displacement are related to those measured at fixed electric field by (Thurston 1974)

$$\mathbb{C}_{\hat{D}}^{ABCD} = \left.\frac{\partial^2 \Psi_0}{\partial E_{AB} \partial E_{CD}}\right|_{\hat{\mathbf{D}},\theta} = \left.\frac{\partial^2 \Psi_0}{\partial E_{AB} \partial E_{CD}}\right|_{\hat{\mathbf{E}},\theta} + \left.\frac{\partial \Sigma^{AB}}{\partial \hat{E}_E}\right|_{\mathbf{E},\theta} \left.\frac{\partial \hat{E}_E}{\partial E_{CD}}\right|_{\hat{\mathbf{D}},\theta} \tag{10.165}$$

$$= \mathbb{C}_{\hat{E}}^{ABCD} + e^{EAB}h_E^{CD}.$$

Next consider the pyroelectric coefficients, which can be introduced as follows as cross derivatives with respect to electric field (ς^A) or electric displacement (ι^A) when the strain **E** is held constant:

$$\varsigma^A = -\left.\frac{\partial^2 \Psi_0}{\partial \theta \partial \hat{E}_A}\right|_{\mathbf{E}} = -\left.\frac{\partial^2 \Psi_0}{\partial \theta \partial \hat{P}_B}\right|_{\mathbf{E}} \left.\frac{\partial \hat{P}_B}{\partial \hat{E}_A}\right|_{\mathbf{E},\theta} \tag{10.166}$$

$$= JC^{-1AC}\Lambda_{CB}^{-1}\chi^B,$$

$$\iota^A = -\left.\frac{\partial^2 \Psi_0}{\partial \theta \partial \hat{D}_A}\right|_{\mathbf{E}} = -\left.\frac{\partial^2 \Psi_0}{\partial \theta \partial \hat{E}_B}\right|_{\mathbf{E}} \left.\frac{\partial \hat{E}_B}{\partial \hat{D}_A}\right|_{\mathbf{E},\theta} \tag{10.167}$$

$$= \varepsilon_{.B}^{-1A}\varsigma^B = JC^{-1BC}\varepsilon_{.B}^{-1A}\Lambda_{CD}^{-1}\chi^D.$$

Similarly, thermal stress coefficients can be introduced at fixed electric field:

$$\beta_{\hat{E}}^{AB} = -\frac{\partial^2 \Psi_0}{\partial \theta \partial E_{AB}}\bigg|_{\hat{\mathbf{E}}} = -\left[\frac{\partial^2 \Psi_0}{\partial \theta \partial E_{AB}}\bigg|_{\hat{\mathbf{P}}} - \frac{\partial N_0}{\partial \hat{P}_C}\bigg|_{\mathbf{E}} \frac{\partial \hat{P}_C}{\partial E_{AB}}\bigg|_{\hat{\mathbf{E}},\theta}\right]$$

$$= \beta^{AB} + \chi^C \frac{\partial \hat{P}_C}{\partial E_{AB}}\bigg|_{\hat{\mathbf{E}},\theta} \tag{10.168}$$

$$= \beta^{AB} - \chi^C \Lambda_{GC}^{-1}\left[\Delta^{GAB} + J(2C^{-1AG}C^{-1BF} - C^{-1AB}C^{-1GF})\hat{E}_F\right],$$

and at fixed electric displacement:

$$\beta_{\hat{D}}^{AB} = -\frac{\partial^2 \Psi_0}{\partial \theta \partial E_{AB}}\bigg|_{\hat{\mathbf{D}}} = -\left[\frac{\partial^2 \Psi_0}{\partial \theta \partial E_{AB}}\bigg|_{\hat{\mathbf{E}}} - \frac{\partial N_0}{\partial \hat{E}_C}\bigg|_{\mathbf{E}} \frac{\partial \hat{E}_C}{\partial E_{AB}}\bigg|_{\hat{\mathbf{D}},\theta}\right]$$

$$= \beta_{\hat{E}}^{AB} + \varsigma^C \frac{\partial \hat{E}_C}{\partial E_{AB}}\bigg|_{\hat{\mathbf{D}},\theta} = \beta_{\hat{E}}^{AB} - \varsigma^C h_C^{AB} \tag{10.169}$$

$$= \beta_{\hat{E}}^{AB} - \iota^D \varepsilon_{CD} h^{CAB} = \beta_{\hat{E}}^{AB} - \iota^C e_C^{AB}.$$

In deriving (10.168) and (10.169), use has been made of (10.158) and (10.164)-(10.167) as well as the usual entropy per unit reference volume relationship

$$N_0 = \rho_0 \eta = -\frac{\partial \Psi_0}{\partial \theta} \tag{10.170}$$

that follows from the second of (10.125).

Specific heats can be defined with electric field or electric displacement held fixed as opposed to electric polarization. The specific heat at fixed strain and electric field is related to that of the last of (10.151) by

$$C_{E,\hat{E}} = \frac{\partial E_0}{\partial \theta}\bigg|_{\mathbf{E},\hat{\mathbf{E}}} = \frac{\partial E_0}{\partial \theta}\bigg|_{\mathbf{E},\hat{\mathbf{P}}} - \theta \frac{\partial^2 \Psi_0}{\partial \theta \partial \hat{P}_A}\bigg|_{\mathbf{E}} \frac{\partial \hat{P}_A}{\partial \theta}\bigg|_{\mathbf{E},\hat{\mathbf{E}}} \tag{10.171}$$

$$= C_E + \theta \Lambda_{AB}^{-1} \chi^A \chi^B,$$

since from the second of (10.151) and (10.153),

$$
\begin{aligned}
\left.\frac{\partial \hat{P}_A}{\partial \theta}\right|_{\mathbf{E},\hat{\mathbf{P}}} &= 0 = \left.\frac{\partial \hat{P}_A}{\partial \theta}\right|_{\mathbf{E},\hat{\mathbf{E}}} + \left.\frac{\partial \hat{P}_A}{\partial \hat{E}_B}\right|_{\mathbf{E},\theta} \left.\frac{\partial \hat{E}_B}{\partial \theta}\right|_{\mathbf{E},\hat{\mathbf{P}}} \\
&= \left.\frac{\partial \hat{P}_A}{\partial \theta}\right|_{\mathbf{E},\hat{\mathbf{E}}} + JC^{-1BC}\Lambda_{CA}^{-1}\left.\frac{\partial \hat{E}_B}{\partial \theta}\right|_{\mathbf{E},\hat{\mathbf{P}}} \\
&= \left.\frac{\partial \hat{P}_A}{\partial \theta}\right|_{\mathbf{E},\hat{\mathbf{E}}} + JC^{-1BC}\Lambda_{CA}^{-1}J^{-1}C_{BD}\frac{\partial^2 \Psi_0}{\partial\theta\partial\hat{P}_D} \\
&= \left.\frac{\partial \hat{P}_A}{\partial \theta}\right|_{\mathbf{E},\hat{\mathbf{E}}} - \Lambda_{CA}^{-1}\chi^C.
\end{aligned}
\tag{10.172}
$$

Similarly, relating specific heats at fixed electric field and fixed electric displacement (Thurston 1974),

$$
\begin{aligned}
C_{E,\hat{E}} &= \left.\frac{\partial E_0}{\partial \theta}\right|_{\mathbf{E},\hat{\mathbf{E}}} = \left.\frac{\partial E_0}{\partial \theta}\right|_{\mathbf{E},\hat{\mathbf{D}}} - \theta\left.\frac{\partial^2 \Psi_0}{\partial\theta\partial\hat{D}_A}\right|_{\mathbf{E}}\left.\frac{\partial \hat{D}_A}{\partial \theta}\right|_{\mathbf{E},\hat{\mathbf{E}}} \\
&= C_{E,\hat{D}} + \theta\varepsilon_{AB}\iota^A\iota^B \\
&= C_{E,\hat{D}} + \theta\iota^A\varsigma_B \\
&= C_{E,\hat{D}} + \theta\varepsilon_{AB}^{-1}\varsigma^A\varsigma^B.
\end{aligned}
\tag{10.173}
$$

Formulae from Section 5.2 of Chapter 5 can be used to relate isentropic and isothermal material coefficients when the same electric variable ($\hat{\mathbf{P}}$, $\hat{\mathbf{E}}$, or $\hat{\mathbf{D}}$) is held constant in definitions of all relevant quantities. For example, relationships among thermal stress coefficients, elastic coefficients, and thermal expansion coefficients $\boldsymbol{\alpha}_T$ are, from (5.161),

$$
\beta^{AB} = \mathbb{C}^{ABCD}(\alpha_T)_{CD}, \quad \beta_{\hat{E}}^{AB} = \mathbb{C}_{\hat{E}}^{ABCD}(\alpha_{T,\hat{E}})_{CD},
$$
$$
\beta_{\hat{D}}^{AB} = \mathbb{C}_{\hat{D}}^{ABCD}(\alpha_{T,\hat{D}})_{CD}.
\tag{10.174}
$$

Similarly, differences between specific heats at constant stress and constant strain are, from (5.165),

$$
C_\Sigma - C_E = \theta\beta^{AB}(\alpha_T)_{AB}, \quad C_{\Sigma,\hat{E}} - C_{E,\hat{E}} = \theta\beta_{\hat{E}}^{AB}(\alpha_{T,\hat{E}})_{AB},
$$
$$
C_{\Sigma,\hat{D}} - C_{E,\hat{D}} = \theta\beta_{\hat{D}}^{AB}(\alpha_{T,\hat{D}})_{AB}.
\tag{10.175}
$$

From (5.166), isentropic second-order elastic moduli are related to their isothermal counterparts via

$$\underline{\mathbb{C}}^{ABCD} = \mathbb{C}^{ABCD} + (\theta / C_E)\beta^{AB}\beta^{CD},$$

$$\underline{\mathbb{C}}_{\hat{E}}^{ABCD} = \mathbb{C}_{\hat{E}}^{ABCD} + (\theta / C_{E,\hat{E}})\beta_{\hat{E}}^{AB}\beta_{\hat{E}}^{CD}, \qquad (10.176)$$

$$\underline{\mathbb{C}}_{\hat{D}}^{ABCD} = \mathbb{C}_{\hat{D}}^{ABCD} + (\theta / C_{E,\hat{D}})\beta_{\hat{D}}^{AB}\beta_{\hat{D}}^{CD}.$$

Isentropic piezoelectric coefficients can be introduced as follows:

$$\underline{\Delta}^{ABC} = \left.\frac{\partial^2 \Psi_0}{\partial \hat{P}_A \partial E_{BC}}\right|_{N_0} = \left.\frac{\partial^2 \Psi_0}{\partial \hat{P}_A \partial E_{BC}}\right|_{\theta} + \left.\frac{\partial \Sigma^{BC}}{\partial \theta}\right|_{\hat{\mathbf{P}}} \left.\frac{\partial \theta}{\partial \hat{P}_A}\right|_{N_0} \qquad (10.177)$$

$$= \Delta^{ABC} + (\theta / C_E)\beta^{BC}\chi^A,$$

$$\underline{e}^{ABC} = -\left.\frac{\partial^2 \Psi_0}{\partial \hat{E}_A \partial E_{BC}}\right|_{N_0} = -\left[\left.\frac{\partial^2 \Psi_0}{\partial \hat{E}_A \partial E_{BC}}\right|_{\theta} + \left.\frac{\partial \Sigma^{BC}}{\partial \theta}\right|_{\hat{\mathbf{E}}} \left.\frac{\partial \theta}{\partial \hat{E}_A}\right|_{N_0}\right] \qquad (10.178)$$

$$= e^{ABC} - (\theta / C_{E,\hat{E}})\beta_{\hat{E}}^{BC}\varsigma^A,$$

$$\underline{h}^{ABC} = -\left.\frac{\partial^2 \Psi_0}{\partial \hat{D}_A \partial E_{BC}}\right|_{N_0} = -\left[\left.\frac{\partial^2 \Psi_0}{\partial \hat{D}_A \partial E_{BC}}\right|_{\theta} + \left.\frac{\partial \Sigma^{BC}}{\partial \theta}\right|_{\hat{\mathbf{D}}} \left.\frac{\partial \theta}{\partial \hat{D}_A}\right|_{N_0}\right] \qquad (10.179)$$

$$= h^{ABC} - (\theta / C_{E,\hat{D}})\beta_{\hat{D}}^{BC}t^A,$$

Relationships between isothermal and isentropic dielectric permittivity tensors and their inverses can be derived in a similar manner. Specifically, differences between isothermal and isentropic dielectric coefficients at constant strain or stress involve the dyadic product of pyroelectric coefficients.

Finally consider the strain derivative of the second-order dielectric permittivity of (10.154) at fixed temperature. From (2.158) and (2.160),

$$\frac{\partial \varepsilon^{AB}}{\partial E_{FG}} = \varepsilon_0 \frac{\partial}{\partial E_{FG}}(JC^{-1AB} + \varepsilon_0^{-1}J^2 C^{-1AC}C^{-1BD}\Lambda_{CD}^{-1})$$

$$= \varepsilon_0\left(\frac{\partial J}{\partial E_{FG}}C^{-1AB} + J\frac{\partial C^{-1AB}}{\partial E_{FG}}\right) + 2J\frac{\partial J}{\partial E_{FG}}C^{-1AC}C^{-1BD}\Lambda_{CD}^{-1} \qquad (10.180)$$

$$+ J^2\left(\frac{\partial C^{-1AC}}{\partial E_{FG}}C^{-1BD}\Lambda_{CD}^{-1} + \frac{\partial C^{-1BD}}{\partial E_{FG}}C^{-1AC}\Lambda_{CD}^{-1} + C^{-1AC}C^{-1BD}\frac{\partial \Lambda_{CD}^{-1}}{\partial E_{FG}}\right),$$

which, from (10.148), is related to third-order piezoelectric coefficients:

$$\frac{\partial \varepsilon^{AB}}{\partial E_{FG}} = -\varDelta^{HIFG} J^2 C^{-1AC} C^{-1BD} \varLambda_{CH}^{-1} \varLambda_{DI}^{-1}$$

$$+\varepsilon_0 J(C^{-1FG}C^{-1AB} - 2C^{-1AF}C^{-1GB}) \qquad (10.181)$$

$$+2J^2 \varLambda_{CD}^{-1}(C^{-1FG}C^{-1AC}C^{-1BD}$$

$$-C^{-1AF}C^{-1CG}C^{-1BD} - C^{-1BF}C^{-1DG}C^{-1AC}).$$

In arriving at (10.181), the first two of the following three identities have been used, all three of which can be derived via the chain rule (Eringen 1962; Chowdhury and Glockner 1976):

$$\frac{\partial C_{CD}^{-1}}{\partial E_{EF}} = -2C_{.C}^{-1E}C_{.D}^{-1F}, \quad \frac{\partial \varLambda_{CD}^{-1}}{\partial E_{EF}} = -\varLambda_{CA}^{-1}\frac{\partial \varLambda^{AB}}{\partial E_{EF}}\varLambda_{BD}^{-1},$$

$$\frac{\partial F_{.b}^{-1B}}{\partial F_{.A}^{a}} = \frac{\partial X_{.,b}^{B}}{\partial x_{.,A}^{a}} = -X_{.,a}^{B}X_{.,b}^{A} = -F_{.a}^{-1B}F_{.b}^{-1A}.$$

$$(10.182)$$

As noted in Section 2.5.2 of Chapter 2, the third identity of (10.182) follows from $\partial(F_{.A}^{a}F_{.b}^{-1A})/\partial F_{.C}^{c} = \partial(x_{.,A}^{a}X_{.,b}^{A})/\partial x_{.,C}^{c} = \partial(\delta_{.b}^{a})/\partial x_{.,C}^{c} = 0$.

10.3.4 Representative Free Energy

Expanding the free energy function in the first of (10.126) of a hyperelastic dielectric material with thermal effects in a Taylor series about a reference state wherein $F_{.A}^{a} = g_{.A}^{a}$, $C_{AB} = G_{AB}$, $E_{AB} = 0$, $\hat{P}_A = 0$, and $\theta = \theta_0 > 0$ produces the following result per unit reference volume, where material coefficients corresponding to derivatives of up to order three are retained:

$$\begin{aligned}
\Psi_0 &= \rho_0 \psi \left(E_{AB}, \hat{P}_A, \theta, X, \mathbf{G}_A \right) \\
&= \bar{\Psi}_0 + \bar{\mathbb{C}}^{AB} E_{AB} + \bar{\varLambda}^{A} \hat{P}_A + Y_0(\theta, X) \\
&\quad + \frac{1}{2!} \bar{\mathbb{C}}^{ABCD} E_{AB} E_{CD} + \frac{1}{3!} \bar{\mathbb{C}}^{ABCDEF} E_{AB} E_{CD} E_{EF} \\
&\quad + \frac{1}{2!} \bar{\varLambda}^{AB} \hat{P}_A \hat{P}_B + \frac{1}{3!} \bar{\varLambda}^{ABC} \hat{P}_A \hat{P}_B \hat{P}_C \\
&\quad + \bar{\varDelta}^{ABC} \hat{P}_A E_{BC} + \frac{1}{2!} \bar{\varDelta}^{ABCD} \hat{P}_A \hat{P}_B E_{CD} + \frac{1}{2!} \bar{\varDelta}^{ABCDE} \hat{P}_A E_{BC} E_{DE} \\
&\quad - \bar{\beta}^{AB} E_{AB} \Delta\theta - \frac{1}{2!} \bar{\beta}^{ABCD} E_{AB} E_{CD} \Delta\theta - \frac{1}{2!} \bar{\beta}'^{AB} E_{AB} (\Delta\theta)^2 \\
&\quad - \bar{\chi}^{A} \hat{P}_A \Delta\theta - \frac{1}{2!} \bar{\chi}^{AB} \hat{P}_A \hat{P}_B \Delta\theta - \frac{1}{2!} \bar{\chi}'^{A} \hat{P}_A (\Delta\theta)^2.
\end{aligned}$$

$$(10.183)$$

Temperature change from the reference state $\Delta\theta = \theta - \theta_0$ can be positive, zero, or negative. The remaining quantities or material coefficients introduced in (10.183) are defined as follows:

$$\Psi_0\left(0,0,\theta_0,X,\mathbf{G}_A\right) = \overline{\Psi}_0\left(X\right) + Y_0\left(\theta_0,X\right) = 0 , \tag{10.184}$$

$$\overline{\mathbb{C}}^{AB}\left(X,\mathbf{G}_A\right) = \left.\frac{\partial\Psi_0}{\partial E_{AB}}\right|_{\substack{\mathbf{E}=0\\\hat{\mathbf{P}}=0\\\theta=\theta_0}} = 0 , \tag{10.185}$$

$$\overline{\Lambda}^{A}\left(X,\mathbf{G}_A\right) = \left.\frac{\partial\Psi_0}{\partial\hat{P}_A}\right|_{\substack{\mathbf{E}=0\\\hat{\mathbf{P}}=0\\\theta=\theta_0}} = 0 , \tag{10.186}$$

$$\overline{\mathbb{C}}^{ABCD}\left(X,\mathbf{G}_A\right) = \left.\frac{\partial^2\Psi_0}{\partial E_{AB}\partial E_{CD}}\right|_{\substack{\mathbf{E}=0\\\hat{\mathbf{P}}=0\\\theta=\theta_0}} , \tag{10.187}$$

$$\overline{\mathbb{C}}^{ABCDEF}\left(X,\mathbf{G}_A\right) = \left.\frac{\partial^3\Psi_0}{\partial E_{AB}\partial E_{CD}\partial E_{EF}}\right|_{\substack{\mathbf{E}=0\\\hat{\mathbf{P}}=0\\\theta=\theta_0}} , \tag{10.188}$$

$$\overline{\Lambda}^{AB}\left(X,\mathbf{G}_A\right) = \left.\frac{\partial^2\Psi_0}{\partial\hat{P}_A\partial\hat{P}_B}\right|_{\substack{\mathbf{E}=0\\\hat{\mathbf{P}}=0\\\theta=\theta_0}} , \tag{10.189}$$

$$\overline{\Lambda}^{ABC}\left(X,\mathbf{G}_A\right) = \left.\frac{\partial^3\Psi_0}{\partial\hat{P}_A\partial\hat{P}_B\partial\hat{P}_C}\right|_{\substack{\mathbf{E}=0\\\hat{\mathbf{P}}=0\\\theta=\theta_0}} , \tag{10.190}$$

$$\overline{\varDelta}^{ABC}\left(X,\mathbf{G}_A\right) = \left.\frac{\partial^2\Psi_0}{\partial\hat{P}_A\partial E_{BC}}\right|_{\substack{\mathbf{E}=0\\\hat{\mathbf{P}}=0\\\theta=\theta_0}} , \tag{10.191}$$

$$\overline{\varDelta}^{ABCD}\left(X,\mathbf{G}_A\right) = \left.\frac{\partial^3\Psi_0}{\partial\hat{P}_A\partial\hat{P}_B\partial E_{CD}}\right|_{\substack{\mathbf{E}=0\\\hat{\mathbf{P}}=0\\\theta=\theta_0}} , \tag{10.192}$$

$$\overline{\varDelta}^{ABCDE}\left(X,\mathbf{G}_A\right) = \left.\frac{\partial^3\Psi_0}{\partial\hat{P}_A\partial E_{BC}\partial E_{DE}}\right|_{\substack{\mathbf{E}=0\\\hat{\mathbf{P}}=0\\\theta=\theta_0}} , \tag{10.193}$$

$$\overline{\beta}^{AB}\left(X,\mathbf{G}_A\right) = -\left.\frac{\partial^2\Psi_0}{\partial\theta\partial E_{AB}}\right|_{\substack{\mathbf{E}=0\\\hat{\mathbf{P}}=0\\\theta=\theta_0}} , \tag{10.194}$$

$$\overline{\beta}^{ABCD}\left(X,\mathbf{G}_A\right)=-\left.\frac{\partial^3\Psi_0}{\partial\theta\partial E_{AB}\partial E_{CD}}\right|_{\substack{\mathbf{E}=0\\\hat{\mathbf{P}}=0\\\theta=\theta_0}}, \tag{10.195}$$

$$\overline{\beta}'^{AB}\left(X,\mathbf{G}_A\right)=-\left.\frac{\partial^3\Psi_0}{\partial\theta^2\partial E_{AB}}\right|_{\substack{\mathbf{E}=0\\\hat{\mathbf{P}}=0\\\theta=\theta_0}}, \tag{10.196}$$

$$\overline{\chi}^A\left(X,\mathbf{G}_A\right)=-\left.\frac{\partial^2\Psi_0}{\partial\theta\partial\hat{P}_A}\right|_{\substack{\mathbf{E}=0\\\hat{\mathbf{P}}=0\\\theta=\theta_0}}, \tag{10.197}$$

$$\overline{\chi}^{AB}\left(X,\mathbf{G}_A\right)=-\left.\frac{\partial^3\Psi_0}{\partial\theta\partial\hat{P}_A\partial\hat{P}_B}\right|_{\substack{\mathbf{E}=0\\\hat{\mathbf{P}}=0\\\theta=\theta_0}}, \tag{10.198}$$

$$\overline{\chi}'^A\left(X,\mathbf{G}_A\right)=-\left.\frac{\partial^3\Psi_0}{\partial\theta^2\partial\hat{P}_A}\right|_{\substack{\mathbf{E}=0\\\hat{\mathbf{P}}=0\\\theta=\theta_0}}. \tag{10.199}$$

The total free energy at the reference state is chosen as zero in (10.184) for convenience (implying $\overline{\Psi}_0=-Y_0(\theta_0)$ at each material point X), since from the derivations in Section 10.3.2, the dependent variables stress, electric field, entropy, and heat flux only depend on derivatives of the free energy and not its absolute value. First-order elastic constants $\overline{\mathbb{C}}^{AB}$ and dielectric constants $\overline{\Lambda}^A$ are zero by definition in (10.185) and (10.186), so that by (10.128)-(10.133), the total stress, Maxwell stress, and electric field all vanish in the reference state. Coefficients in (10.187) and (10.188) are referred to, respectively, as isothermal second-order elastic constants and isothermal third-order elastic constants at constant polarization. Coefficients in (10.189) and (10.190) are second- and third-order isothermal, inverse dielectric susceptibilities. Coefficients in (10.190)-(10.192) are second- and third-order isothermal piezoelectric coefficients. Stress-temperature coefficients at constant polarization of second and third orders are defined in (10.194)-(10.196). Pyroelectric coefficients of second and third orders are defined in (10.197)-(10.199). Strain dependence of pyroelectric coefficients (i.e., temperature dependence of piezoelectric coefficients) is omitted in (10.183), but could be included via addition of a term linear in each of polarization, strain, and temperature change. While coefficients in (10.187)-(10.199) depend possibly on position X in a heterogeneous body and orientation via $\mathbf{G}_A(X)$, they are usually referred to as material constants because they have fixed values at each material point or particle at X. Coefficients in (10.187)-(10.199) can be related to others

measured at the reference state using the results of Section 10.3.3 by setting $C_{AB} = G_{AB}$, $E_{AB} = 0$, $\hat{P}_A = 0$, $\hat{E}_A = 0$, and $\theta = \theta_0$. The thermal part of the free energy Y_0 can be defined as discussed in Section 5.1.3. Ferroelectric behavior, e.g., spontaneous polarization below a characteristic temperature according to the Curie-Weiss law (Maugin 1988), is not addressed by (10.183).

The referential electric field becomes, from (10.128) and (10.183),

$$
\begin{aligned}
\hat{E}_A &= J^{-1} C_{AB} \frac{\partial \Psi_0}{\partial \hat{P}_B} \\
&= J^{-1} C_{AB} \left[\overline{A}^{BC} \hat{P}_C + \frac{1}{2} \overline{A}^{BCD} \hat{P}_C \hat{P}_D + \overline{A}^{BCD} E_{CD} + \overline{A}^{BCDE} \hat{P}_C E_{DE} \right. \\
&\quad \left. + \frac{1}{2} \overline{A}^{BCDEF} E_{CD} E_{EF} - \overline{\chi}^B \Delta\theta - \overline{\chi}^{BC} \hat{P}_C \Delta\theta - \frac{1}{2} \overline{\chi}'^B (\Delta\theta)^2 \right].
\end{aligned}
\tag{10.200}
$$

The second Piola-Kirchhoff stress tensor becomes, from (10.130) and (10.183),

$$
\begin{aligned}
\Sigma^{AB} &= \frac{\partial \Psi_0}{\partial E_{AB}} + J C^{-1AC} \hat{P}_C C^{-1BD} \hat{E}_D \\
&= \overline{\mathbb{C}}^{ABCD} E_{CD} + \frac{1}{2} \overline{\mathbb{C}}^{ABCDEF} E_{CD} E_{EF} + \overline{A}^{CAB} \hat{P}_C + \frac{1}{2} \overline{A}^{CDAB} \hat{P}_C \hat{P}_D \\
&\quad + \overline{A}^{CABDE} \hat{P}_C E_{DE} - \overline{\beta}^{AB} \Delta\theta - \overline{\beta}^{ABCD} E_{CD} \Delta\theta - \frac{1}{2} \overline{\beta}'^{AB} (\Delta\theta)^2 \\
&\quad + C^{-1AC} \hat{P}_C \frac{\partial \Psi_0}{\partial \hat{P}_B},
\end{aligned}
\tag{10.201}
$$

where the contribution from $\partial \Psi_0 / \partial \hat{P}_B$ is given by the term in braces in (10.200). Total stress tensor **T** of (10.133) can then be computed from (10.124)-(10.131), (10.200), and (10.201) in a straightforward manner, noting that the Maxwell stress of (10.73) satisfies

$$
\begin{aligned}
\hat{\tau}^{ab} &= \hat{e}^a \hat{p}^b + \varepsilon_0 \hat{e}^a \hat{e}^b - \frac{\varepsilon_0}{2} \hat{e}^c \hat{e}_c g^{ab} \\
&= F^{-1Aa} F^{-1Bb} (\hat{E}_A \hat{P}_B + \varepsilon_0 \hat{E}_A \hat{E}_B) - \frac{\varepsilon_0}{2} C^{-1AB} \hat{E}_A \hat{E}_B g^{ab}.
\end{aligned}
\tag{10.202}
$$

Finally, the entropy per unit reference volume becomes, using (10.170),

$$
\begin{aligned}
N_0 &= -\frac{\partial \Psi_0}{\partial \theta} = -\frac{\partial Y_0}{\partial \theta} + \overline{\beta}^{AB} E_{AB} + \frac{1}{2} \overline{\beta}^{ABCD} E_{AB} E_{CD} + \overline{\beta}'^{AB} E_{AB} \Delta\theta \\
&\quad + \overline{\chi}^A \hat{P}_A + \frac{1}{2} \overline{\chi}^{AB} \hat{P}_A \hat{P}_B + \overline{\chi}'^A \hat{P}_A \Delta\theta.
\end{aligned}
\tag{10.203}
$$

10.3.5 Materially Linear Electroelasticity

Now consider free energy polynomial (10.183) of a hyperelastic dielectric material with thermal effects, truncated after derivatives of second order:

$$
\begin{aligned}
\Psi_0 = {}&\frac{1}{2}\overline{\mathbb{C}}^{ABCD} E_{AB} E_{CD} + \frac{1}{2}\overline{\Lambda}^{AB}\hat{P}_A\hat{P}_B + \overline{\Lambda}^{ABC}\hat{P}_A E_{BC} \\
&- \overline{\beta}^{AB} E_{AB}\Delta\theta - \overline{\chi}^A \hat{P}_A \Delta\theta - \overline{C}_E \theta\ln\frac{\theta}{\theta_0},
\end{aligned}
\tag{10.204}
$$

where all terms have the same meanings as those introduced in Section 10.3.4,

$$
\overline{\mathbb{C}}^{ABCD} = \left.\frac{\partial^2\Psi_0}{\partial E_{AB}\partial E_{CD}}\right|_{\substack{\mathbf{E}=0\\\hat{\mathbf{P}}=0\\\theta=\theta_0}} , \quad \overline{\Lambda}^{AB} = \left.\frac{\partial^2\Psi_0}{\partial\hat{P}_A\partial\hat{P}_B}\right|_{\substack{\mathbf{E}=0\\\hat{\mathbf{P}}=0\\\theta=\theta_0}} , \quad \overline{\Lambda}^{ABC} = \left.\frac{\partial^2\Psi_0}{\partial\hat{P}_A\partial E_{BC}}\right|_{\substack{\mathbf{E}=0\\\hat{\mathbf{P}}=0\\\theta=\theta_0}} , \tag{10.205}
$$

$$
\overline{\beta}^{AB} = -\left.\frac{\partial^2\Psi_0}{\partial\theta\partial E_{AB}}\right|_{\substack{\mathbf{E}=0\\\hat{\mathbf{P}}=0\\\theta=\theta_0}} , \quad \overline{\chi}^A = -\left.\frac{\partial^2\Psi_0}{\partial\theta\partial\hat{P}_A}\right|_{\substack{\mathbf{E}=0\\\hat{\mathbf{P}}=0\\\theta=\theta_0}} , \tag{10.206}
$$

and the thermal energy and specific heat constant at constant strain and polarization are defined, respectively, as

$$
Y_0 = -\overline{C}_E\theta\ln\frac{\theta}{\theta_0} , \quad \overline{C}_E = -\left.\left(\theta\frac{\partial^2\Psi_0}{\partial\theta^2}\right)\right|_{\substack{\mathbf{E}=0\\\hat{\mathbf{P}}=0\\\theta=\theta_0}} . \tag{10.207}
$$

For illustrative purposes, coefficients in (10.205)-(10.207) are related to those defined with electric field as an independent variable as follows. First, from (10.154), the second-order dielectric constants at the reference state are

$$
\overline{\varepsilon}_{AB} = \varepsilon_0 G_{AB} + \overline{\Lambda}_{AB}^{-1} \Leftrightarrow \overline{\Lambda}^{AB} = \varepsilon_0^{-1}(\overline{\varepsilon}_R - G)^{-1AB} . \tag{10.208}
$$

Then, from (10.155), piezoelectric coefficients defined with respect to electric field are

$$
\overline{e}^{ABC} = -G^{-1AE}\overline{\Lambda}_{ED}^{-1}\overline{\Lambda}^{DBC} = -\varepsilon_0\left[(\overline{\varepsilon}_R)^A_{.D} - \delta^A_{.D}\right]\overline{\Lambda}^{DBC} . \tag{10.209}
$$

From (10.163) and (10.208), second-order elastic constants at fixed electric field are related to those of (10.205) by the equalities

$$
\begin{aligned}
\overline{\mathbb{C}}_{\hat{E}}^{ABCD} &= \overline{\mathbb{C}}^{ABCD} - \overline{\Lambda}^{EAB}\overline{\Lambda}_{EF}^{-1}\overline{\Lambda}^{FCD} \\
&= \overline{\mathbb{C}}^{ABCD} - \varepsilon_0\overline{\Lambda}^{EAB}\left[(\overline{\varepsilon}_R)_{EF} - G_{EF}\right]\overline{\Lambda}^{FCD} .
\end{aligned}
\tag{10.210}
$$

From (10.166) pyroelectric constants defined with respect to electric field or polarization are related by

$$
\overline{\varsigma}^A = \overline{\Lambda}_{.B}^{-1A}\overline{\chi}^B = \varepsilon_0\left[(\overline{\varepsilon}_R)^A_{.B} - \delta^A_{.B}\right]\overline{\chi}^B , \tag{10.211}
$$

while from (10.168), thermal stress constants measured at fixed electric field and fixed polarization are related by

$$\bar{\beta}_{\hat{E}}^{AB} = \bar{\beta}^{AB} - \bar{\chi}^C \bar{\Lambda}_{GC}^{-1} \bar{A}^{GAB} = \bar{\beta}^{AB} - \varepsilon_0 \bar{\chi}^C \left[(\bar{\varepsilon}_R)_{CG} - G_{CG} \right] \bar{A}^{GAB}. \quad (10.212)$$

Finally, specific heat constants at fixed electric field and fixed polarization are related by (10.171), specifically in the reference state as

$$\bar{C}_{E,\hat{E}} = \bar{C}_E + \theta_0 \bar{\Lambda}_{AB}^{-1} \bar{\chi}^A \bar{\chi}^B. \quad (10.213)$$

From (10.130) and the strain derivative of (10.204), the second Piola-Kirchhoff stress becomes

$$\Sigma^{AB} = \frac{\partial \Psi_0}{\partial E_{AB}} + JC^{-1AC} \hat{P}_C C^{-1BD} \hat{E}_D$$

$$= \bar{\mathbb{C}}^{ABCD} E_{CD} + \bar{A}^{CAB} \hat{P}_C - \bar{\beta}^{AB} \Delta\theta + C^{-1AC} \hat{P}_C \frac{\partial \Psi_0}{\partial \hat{P}_B}. \quad (10.214)$$

The first three terms on the right side of the final equality of (10.214) are symmetric contributions to the second Piola-Kirchhoff stress. The first term on the right side accounts for materially linear hyperelasticity, the second term accounts for the inverse piezoelectric effect, the third accounts for thermoelasticity, and the final term, not necessarily symmetric when electric field and electric polarization are not parallel, is a nonlinear electromechanical effect.

From (10.128) and (10.204), the referential electric field is

$$\hat{E}_A = J^{-1} C_{AB} \frac{\partial \Psi_0}{\partial \hat{P}_B} = J^{-1} C_{AB} \left[\bar{A}^{BC} \hat{P}_C + \bar{A}^{BCD} E_{CD} - \bar{\chi}^B \Delta\theta \right]. \quad (10.215)$$

The first term on the right side of (10.215) accounts for the dielectric permittivity, the second accounts for the direct piezoelectric effect or the induction of an electric field by the mechanical strain, and the third term accounts for the pyroelectric effect resulting from the coupling of polarization and temperature in the free energy function.

The electric displacement referred to the reference configuration, from (10.70), can then be written

$$\hat{D}^A = JC^{-1AB} \varepsilon_0 \hat{E}_B + JC^{-1AB} \hat{P}_B$$

$$= \varepsilon_0 (\bar{A}^{AD} \hat{P}_D + \bar{A}^{ADE} E_{DE} - \bar{\chi}^A \Delta\theta) + JC^{-1AB} \hat{P}_B \quad (10.216)$$

$$= (\varepsilon_0 \bar{A}^{AB} + JC^{-1AB}) \hat{P}_B + \varepsilon_0 \bar{A}^{ADE} E_{DE} - \varepsilon_0 \bar{\chi}^A \Delta\theta.$$

Assuming that $\bar{A}^{AB}$ is non-singular and inverting (10.215), the polarization can be written in terms of the electric field as

$$\hat{P}_B = (J \bar{A}_{BD}^{-1} C^{-1DC}) \hat{E}_C - (\bar{A}_{BC}^{-1} \bar{A}^{CDE}) E_{DE} + (\bar{A}_{BC}^{-1} \bar{\chi}^C) \Delta\theta$$

$$= \hat{A}_B^C \hat{E}_C + \bar{e}_B^{DE} E_{DE} + \bar{\varsigma}_B \Delta\theta, \quad (10.217)$$

where $\hat{A}_B^C$ depends on strain and where $\overline{e}_B^{\cdot DE}$ and $\overline{\varsigma}_B$ are piezoelectric and pyroelectric constants defined as derivatives with respect to the electric field, as in (10.155) and (10.166) or (10.209) and (10.211). Substitution of (10.217) into (10.216) provides the following relationship between material electric displacement, material electric field, strain, and temperature change:

$$
\begin{aligned}
\hat{D}^A &= \left[\varepsilon_0 \overline{A}^{AB} + JC^{-1AB} \right] \left[\hat{A}_B^C \hat{E}_C + \overline{e}_B^{\cdot DE} E_{DE} + \overline{\varsigma}_B \Delta\theta \right] \\
&\quad + \varepsilon_0 \overline{A}^{ADE} E_{DE} - \varepsilon_0 \overline{\chi}^A \Delta\theta \\
&= (JC^{-1AB} \hat{A}_B^C + \varepsilon_0 \overline{A}^{AB} \hat{A}_B^C) \hat{E}_C + JC^{-1AB} (\overline{e}_B^{\cdot DE} E_{DE} + \overline{\varsigma}_B \Delta\theta) \qquad (10.218) \\
&= (J^2 C^{-1AB} \overline{A}_{BD}^{-1} C^{-1CD} + \varepsilon_0 JC^{-1AC}) \hat{E}_C + JC^{-1AB} (\overline{e}_B^{\cdot DE} E_{DE} + \overline{\varsigma}_B \Delta\theta) \\
&= \varepsilon^{AC} \hat{E}_C + JC^{-1AB} (\overline{e}_B^{\cdot DE} E_{DE} + \overline{\varsigma}_B \Delta\theta).
\end{aligned}
$$

The permittivity tensor ε^{AC}, defined more generally in (10.154), may depend here on strain as indicated, but not on temperature or polarization. The first term on the right of (10.218) accounts for the purely dielectric effect, the second term accounts for piezoelectric coupling, and the third term accounts for pyroelectric coupling. When higher-order terms in the polarization are retained in the free energy, e.g., (10.183) with nonzero coefficients (10.190), the effective permittivity will depend upon polarization or electric field (Johnson 1962), in which case (10.218) obtained from the second-order Taylor series expansion of (10.204) does not apply.

10.3.6 Symmetry

Two topics regarding material symmetry are discussed in what follows in Section 10.3.6. The first is Voigt's notation that follows from natural symmetries of material coefficients defined as derivatives of thermodynamic potentials with respect to symmetric independent state variables or pairs of independent state variables, regardless of the symmetry of a given material (e.g., regardless of a crystal's point group). The second topic concerns the reduction in number of constant material coefficients arising because of the particular symmetry or structure of a material in its undistorted reference state, i.e., specific symmetries of vectors and tensors of material coefficients emerging because of a crystal's point group.

Consider the materially linear theory of Section 10.3.5. Following from (10.205) and (10.206), matrices of second-order elastic constants $\overline{\overline{\mathbb{C}}}^{ABCD}$, dielectric constants $\overline{A}^{AB}$, piezoelectric constants $\overline{A}^{ABC}$, and thermal stress constants $\overline{\beta}^{AB}$ exhibit the following symmetries:

$$\overline{\mathbb{C}}^{ABCD} = \overline{\mathbb{C}}^{BACD} = \overline{\mathbb{C}}^{ABDC} = \overline{\mathbb{C}}^{CDAB}, \qquad (10.219)$$

$$\overline{\varLambda}^{AB} = \overline{\varLambda}^{BA}, \; \overline{\varLambda}^{ABC} = \overline{\varLambda}^{ACB}, \; \overline{\beta}^{AB} = \overline{\beta}^{BA}. \qquad (10.220)$$

meaning that $\overline{\mathbb{C}}^{ABCD}$ contains up to 21 independent entries, $\overline{\varLambda}^{ABC}$ contains up to 18 independent entries, and $\overline{\varLambda}^{AB}$ and $\overline{\beta}^{AB}$ each contain up to 6 independent entries.

Voigt's notation (Voigt 1928) is often used in mixed form to describe piezoelectric solids. Nine components of symmetric pairs of indices reduce to six according to the usual correspondence of (5.93):

$$11 \sim 1, \qquad 22 \sim 2, \qquad 33 \sim 3,$$
$$23 = 32 \sim 4, \quad 31 = 13 \sim 5, \quad 12 = 21 \sim 6. \qquad (10.221)$$

In the notation scheme of Brugger (1964), Thurston (1974), and Teodosiu (1982), components of the symmetric total stress and material coefficients are re-written to take advantage of these symmetries:

$$T^{(AB)} \sim T^{\overline{A}}, \; \overline{\mathbb{C}}^{(AB)(CD)} \sim \overline{\mathbb{C}}^{\overline{AB}}, \; \overline{\beta}^{AB} \sim \overline{\beta}^{\overline{A}}, \; \overline{\varLambda}^{AB} \sim \overline{\varLambda}^{\overline{A}}. \quad (10.222)$$

Barred indices span $1,2,\dots 6$ and correspond to unbarred pairs of indices as indicated in (10.221). Symmetric strain tensor **E** in Voigt's notation becomes

$$2E_{(AB)} = (1 + \delta_{AB})E_{\overline{A}}. \qquad (10.223)$$

As a consequence of hyperelasticity, second-order elastic constants have the remaining symmetries of (5.96):

$$\overline{\mathbb{C}}^{\overline{AB}} = \overline{\mathbb{C}}^{(\overline{AB})}. \qquad (10.224)$$

The 18 independent piezoelectric constants can only be partially converted to Voigt's notation, since symmetry conditions exist only over one pair of indices:

$$\overline{\varLambda}^{A(BC)} \sim \overline{\varLambda}^{A\overline{B}}. \qquad (10.225)$$

In matrix notation, the right side of (10.225) corresponds to a 3×6 matrix:

$$\begin{bmatrix} \overline{\varLambda}^{11} = \overline{\varLambda}^{111} & \overline{\varLambda}^{12} = \overline{\varLambda}^{122} & \overline{\varLambda}^{13} = \overline{\varLambda}^{133} & \overline{\varLambda}^{14} = \overline{\varLambda}^{123} & \overline{\varLambda}^{15} = \overline{\varLambda}^{131} & \overline{\varLambda}^{16} = \overline{\varLambda}^{112} \\ \overline{\varLambda}^{21} = \overline{\varLambda}^{211} & \overline{\varLambda}^{22} = \overline{\varLambda}^{222} & \overline{\varLambda}^{23} = \overline{\varLambda}^{233} & \overline{\varLambda}^{24} = \overline{\varLambda}^{223} & \overline{\varLambda}^{25} = \overline{\varLambda}^{231} & \overline{\varLambda}^{26} = \overline{\varLambda}^{212} \\ \overline{\varLambda}^{31} = \overline{\varLambda}^{311} & \overline{\varLambda}^{32} = \overline{\varLambda}^{322} & \overline{\varLambda}^{33} = \overline{\varLambda}^{333} & \overline{\varLambda}^{34} = \overline{\varLambda}^{323} & \overline{\varLambda}^{35} = \overline{\varLambda}^{331} & \overline{\varLambda}^{36} = \overline{\varLambda}^{312} \end{bmatrix}. \quad (10.226)$$

Using (10.222)-(10.225), the Helmholtz free energy density in the materially linear case (10.204) is written compactly as

$$\varPsi_0 = \frac{1}{2}\overline{\mathbb{C}}^{\overline{AB}} E_{\overline{A}} E_{\overline{B}} + \frac{1}{2}\overline{\varLambda}^{AB} \hat{P}_A \hat{P}_B + \overline{\varLambda}^{A\overline{B}} \hat{P}_A E_{\overline{B}}$$
$$- \overline{\beta}^{\overline{A}} E_{\overline{A}} \Delta\theta - \overline{\chi}^A \hat{P}_A \Delta\theta - \overline{C}_E \theta \ln \frac{\theta}{\theta_0}. \qquad (10.227)$$

Voigt's notation can be applied in a similar manner towards other material coefficients with natural symmetries introduced in Sections 10.3.4 and

10.3.5. For example, the other piezoelectric coefficients introduced in (10.155), (10.156), and (10.209) can all be written in 3×6 matrix forms akin to (10.225) and (10.226).

When the reference coordinate system and the crystallographic axes used to define material coefficients do not coincide, a rotation operation is needed to transform dielectric, piezoelectric, and pyroelectric coefficients into their representations in the reference coordinate system, analogously to operations described for the elastic and thermal stress constants in (5.100) that still apply here. Let X'^A denote coordinates in the crystallographic frame, and let X^A denote coordinates in the reference configuration. The orthogonal transformation

$$X^A = \breve{Q}_{.B}^A X'^B \tag{10.228}$$

describes the relationship between crystallographic coordinates and the reference frame, with $\hat{Q}_{.B}^{TA} = \hat{Q}_{.B}^{-1A}$ and $|\det \hat{Q}_{.B}^A| = 1$. To apply this transformation to dielectric and piezoelectric coefficients, the reduced Voigt notation is not applied; e.g., the piezoelectric moduli are written in rank three form. Dielectric, piezoelectric, and pyroelectric coefficients transform according to

$$\overline{A}^{AB} = \breve{Q}_{.C}^A \breve{Q}_{.D}^B \overline{A}'^{CD} , \quad \overline{A}^{ABC} = \breve{Q}_{.D}^A \breve{Q}_{.E}^B \breve{Q}_{.F}^C \overline{A}'^{DEF} , \quad \overline{\chi}^A = \breve{Q}_{.B}^A \overline{\chi}'^B , \tag{10.229}$$

where primed quantities are defined with respect to the crystallographic coordinates and unprimed quantities are referred to the reference coordinate system.

Arguments regarding material symmetry presented in Section 5.1.5 for hyperelastic materials in the absence of electromechanical effects also apply for hyperelastic dielectric materials. One notable distinction arises: dielectric materials contain a dependence of response functions on polarization $\hat{P}_A$, a rank one tensor (i.e., a vector). Under a change of reference coordinate system as shown in (10.228), the referential polarization and electric field transform as

$$\hat{P}_A \to \breve{Q}_{.A}^B \hat{P}_B , \quad \hat{E}_A \to \breve{Q}_{.A}^B \hat{E}_B . \tag{10.230}$$

For all rotations and reflections $\breve{Q} \in \mathbb{Q}$ (i.e., within symmetry group $\mathbb{Q}$) of the considered material, the following identities replace (5.110)-(5.113):

$$\psi\left(\mathbf{C}, \hat{\mathbf{P}}, \theta, X\right) = \psi\left(\breve{\mathbf{Q}}^T \mathbf{C} \breve{\mathbf{Q}}, \breve{\mathbf{Q}}^T \hat{\mathbf{P}}, \theta, X\right), \tag{10.231}$$

$$\eta\left(\mathbf{C}, \hat{\mathbf{P}}, \theta, X\right) = \eta\left(\breve{\mathbf{Q}}^T \mathbf{C} \breve{\mathbf{Q}}, \breve{\mathbf{Q}}^T \hat{\mathbf{P}}, \theta, X\right), \tag{10.232}$$

$$\breve{\mathbf{Q}} \mathbf{\Sigma}\left(\mathbf{C}, \hat{\mathbf{P}}, \theta, X\right) \breve{\mathbf{Q}}^T = \mathbf{\Sigma}\left(\breve{\mathbf{Q}}^T \mathbf{C} \breve{\mathbf{Q}}, \breve{\mathbf{Q}}^T \hat{\mathbf{P}}, \theta, X\right), \tag{10.233}$$

$$\breve{\mathbf{Q}}\mathbf{Q}\left(\mathbf{C},\hat{\mathbf{P}},\theta,\overset{\mathbf{G}}{\nabla}\theta,X\right)=\mathbf{Q}\left(\breve{\mathbf{Q}}^{T}\mathbf{C}\breve{\mathbf{Q}},\breve{\mathbf{Q}}^{T}\hat{\mathbf{P}},\theta,\breve{\mathbf{Q}}^{T}\overset{\mathbf{G}}{\nabla}\theta,X\right),\quad(10.234)$$

$$\breve{\mathbf{Q}}^{T}\hat{\mathbf{E}}\left(\mathbf{C},\hat{\mathbf{P}},\theta,X\right)=\hat{\mathbf{E}}\left(\breve{\mathbf{Q}}^{T}\mathbf{C}\breve{\mathbf{Q}},\breve{\mathbf{Q}}^{T}\hat{\mathbf{P}},\theta,X\right).\qquad(10.235)$$

Dependence of response functions on right Cauchy-Green deformation tensor $\mathbf{C}$ can readily be exchanged for a dependence on strain tensor $\mathbf{E}$, which itself transforms the same way as $\mathbf{C}$ under a change of reference co-ordinates.

The particular crystal class of the crystal structure of a dielectric solid determines the symmetries of its material coefficients evaluated in an un-distorted reference state. Thirty-two crystal classes exist for natural crystal structures, each falling into one of eleven Laue groups. While mechanical elastic properties such as second- and third-order elastic constants depend only on the Laue group of the crystal, other material coefficients such as vectors and tensors of odd rank, including various piezoelectric and py-roelectric constants, may generally depend on the particular crystal class within a Laue group. Symmetries of crystals in the context of material co-efficients are discussed in Appendix A. Tables A.3-A.7 list independent material coefficients for tensors of orders one, two, three, and four, while Tables A.8 and A.9 list second- and third-order elastic constants for all Laue groups.

As remarked in Section A.2, material coefficients of odd rank vanish identically for crystals with a center of symmetry. Coefficients of odd rank include the piezoelectric ($\overline{\Delta}^{ABC}$) and pyroelectric ($\overline{\chi}^{A}$) constants of (10.205) and (10.206), respectively, as well as more general electrome-chanical and electrothermal coefficients of ranks one, three, and five de-fined in Sections 10.3.3 and 10.3.4. Recall that centrosymmetric crystals have an inversion center, meaning that the material representation of the response is invariant under an inversion transformation of the form $X^{A}\rightarrow-X^{A}$. Consider the pyroelectric effect in a rigid body as an exam-ple. Since under an inversion of reference coordinates, $\overline{\chi}^{A}\rightarrow\overline{\chi}^{A}$ in a cen-trosymmetric crystal, it follows from (10.215) that the electric field gener-ated by a temperature change is

$$\hat{E}_{A}=-\overline{\chi}^{A}\Delta\theta\rightarrow-\hat{E}_{A}=-\overline{\chi}^{A}\Delta\theta\Leftrightarrow\overline{\chi}^{A}=-\overline{\chi}^{A}=0,\qquad(10.236)$$

implying that since the pyroelectric constants are equal to their negatives, they must vanish identically when the crystal has a center of symmetry. Similar arguments can be used to show that the piezoelectric constants $\overline{\Delta}^{ABC}$ of (10.191) and (10.205) must vanish identically for centrosymmet-ric crystals, noting that the right Cauchy-Green strain tensor $E_{AB}\rightarrow E_{AB}$ under such an inversion. Higher-order piezoelectric constants of even rank

(e.g., electrostriction coefficients of rank four such as those in (10.192)) need not always vanish in centrosymmetric dielectric solids.

The piezoelectric effect is present in 20 of the 21 non-centrosymmetric crystallographic point groups (Landau and Lifshitz 1960; Damjanovic 1998). Of these piezoelectric materials, 10 crystallographic point groups are generally pyroelectric. Ferroelectric crystals are a subset of pyroelectric materials whose direction of spontaneous polarization may be switched by the action of an external electric field. It is noted that the framework of Section 10.3.5 is insufficient to fully address ferroelectric behavior, which requires a more detailed total energy function to accurately account for transition temperatures and higher-order influences of polarization on the thermodynamic response functions (Devonshire 1954).

When the symmetry group $\mathbb{Q}$ of the material contains all orthogonal transformations, the response is independent of the choice of reference coordinate basis vectors $\mathbf{G}_A(X)$, and the material behavior is isotropic. While isotropy is extremely rare among single crystalline solids, the response of polycrystals containing a large number of randomly oriented grains is often idealized as isotropic. For example, polycrystalline dielectric ceramics are often treated as perfectly isotropic in aggregate form, even though their constituent single crystals may be anisotropic. Isotropy implies a center of symmetry. Thus, isotropic dielectric materials cannot display piezoelectric or pyroelectric effects, leading automatically to vanishing of the corresponding piezoelectric coefficients, $\bar{\Delta}^{ABC} = 0$, and pyroelectric coefficients, $\bar{\chi}^A = 0$. For an isotropic, materially linear dielectric, free energy (10.204) reduces to

$$\Psi_0 = \frac{1}{2}\Big[\mu(G^{AC}G^{BD} + G^{AD}G^{CB}) + \lambda G^{AB}G^{CD}\Big]E_{AB}E_{CD}$$
$$+ \frac{1}{2}\bar{\Lambda}\hat{P}_A\hat{P}^A - \bar{\beta}E^A_{.A}\Delta\theta - \bar{C}_E\theta\ln\frac{\theta}{\theta_0}, \tag{10.237}$$

where μ and λ are elastic coefficients as in (5.121), and $\bar{\Lambda}$ and $\bar{\beta}$ are scalar dielectric and thermal stress constants, respectively.

10.3.7 Comparison with Other Theories

Differences exist among various nonlinear continuum theories of elastic dielectric solids. A few of these differences are noted in Section 10.3.7, along with a brief justification for assumptions made in the present theory.

Some authors partition the electric field vector or scalar electrostatic potential into additive contributions from various internal and external

sources (Toupin 1956; Eringen 1962, 1963; Bustamante et al. 2009).   In the notational scheme of the present work, a single electric field and electrostatic potential are used in the governing equations (when mapped to a particular spatial or material configuration), following Tiersten (1971), Thurston (1974), and McMeeking and Landis (2005).   However, a more detailed decomposition, while not necessary, is physically and mathematically admissible.   The electric field used here can be thought of as the quasi-static (total) Maxwell-Faraday electric field $\hat{\mathbf{e}}_{\mathbf{M}}$, equal in magnitude and opposite in sign (i.e., direction) to an effective local electric field $\hat{\mathbf{e}}_{\mathbf{L}}$ associated with interactions between electrons and ions, for example (Tiersten 1971).   The electric field used throughout Sections 10.2 and 10.3 thus satisfies $\hat{\mathbf{e}} = \hat{\mathbf{e}}_{\mathbf{M}} = \hat{\mathbf{e}}_{\mathbf{MS}} + \hat{\mathbf{e}}_0 = -\hat{\mathbf{e}}_{\mathbf{L}} = -\overset{\mathbf{g}}{\nabla}\hat{\phi}$, where $\hat{\mathbf{e}}_{\mathbf{MS}}$ is the Maxwell self electric field and $\hat{\mathbf{e}}_0$ is the extrinsic or external electric field (Toupin 1956; Eringen 1962).   In the present theory, the electric field and electrostatic potential also have naturally different representations in the spatial configuration (e.g., as in (10.49)) and reference configuration (e.g., as in (10.61)).

Various definitions have been postulated for mechanical stress and Maxwell stress tensors, as discussed by Eringen (1962, 1963) and Bustamante et al. (2009).   The definition used in the present work for the Cauchy stress tensor, i.e., σ^{ab} entering (10.75), corresponds to the local stress of Toupin (1956) and is the transpose of the mechanical stress of Tiersten (1971).   The definition used in the present work for the Maxwell stress tensor, i.e., $\hat{\tau}^{ab}$ of (10.72), is consistent with the sum of contributions of the Maxwell self electric field and the external electric field of Toupin (1956) entering his static balances of linear and angular momentum in the absence of free charge density (i.e., a strict dielectric).   The present definition of Maxwell's stress is equal to the transpose of the Maxwell stress of Tiersten (1971) in the absence of free charge density.   Notice that in Chapter 10, the index of the traction vector corresponds to the first index of the corresponding stress tensor ($t^a = \sigma^{ab} n_b$), following the notation scheme of previous Chapters in this book and Toupin (1956), but opposite to notations of Eringen (1963), Tiersten (1971), and McMeeking et al. (2007), wherein the traction is defined via contraction of the first index of the mechanical stress with the unit normal.   Because in physical experiments one cannot easily distinguish between contributions of Maxwell stress and Cauchy stress to the symmetric total stress (e.g., T^{ab} of (10.78)), different theories can provide identical equations for the total stress while partitioning it into Maxwell and Cauchy stresses in various ways (Eringen 1962; Nelson and Lax 1976; McMeeking et al. 2007).   Ad-

ditional considerations regarding momentum conservation and symmetry properties, or lack thereof, of the stress tensor were offered by Nelson and Lax (1976).

Various forms of the balance of energy have been suggested for dielectric solids (Eringen 1962, 1963; Toupin 1963; Tiersten 1971; Maugin 1988; Clayton 2009b). Regarding (10.88)-(10.89), some authors subtract part or all of the contribution of the volumetric electromechanical work rate term Ω from the rate of total internal energy rather than incorporate it in the external power. Identical quantities can be represented in a vast number of ways via manipulation of Maxwell's equations and use of vector identities and theorems of Gauss and Stokes, so complications arise in discerning among forms of the energy balance used in different theories. The local balance of energy in (10.94) matches that of Tiersten (1971), except for Tiersten's use of polarization per unit mass $\hat{\pi}^a = \hat{p}^a / \rho$ rather than polarization per unit volume $\hat{p}^a$. In Tiersten's theory, $\hat{e}_a \dot{\hat{p}}^a$ of (10.94) is replaced with $\hat{e}_a \rho \dot{\hat{\pi}}^a = \hat{e}_a (\dot{\hat{p}}^a + \hat{p}^a v^b_{;b})$. The difference $\hat{e}_a \hat{p}^a v^b_{;b}$ vanishes if the material is incompressible. In the theory of Toupin (1963), the convected time derivative of spatial polarization per unit volume does work against a particular form of the electric field. Polarization gradients may be important for describing some phenomena (Mindlin 1968b, 1972; Chowdhury and Glockner 1976; Chowdhury et al. 1979; Maugin 1988); in such cases, augmentation of the energy balance and thermodynamic potentials to account for effects of polarization gradients may be prudent.

The energy balance and dissipation inequality have been used in combination in Section 10.3.2 of this text to obtain constitutive equations for elastic dielectrics. Other valid methods used to obtain constitutive equations include variational principles for static and non-dissipative systems (Toupin 1956; Eringen 1962, 1963; Mindlin 1968b, 1972), as well as consideration of pair-wise terms in the energy balance for conditions wherein the local entropy production rate of (4.61) vanishes (Tiersten and Tsai 1972; Thurston 1974). Alternatively, constitutive equations such as those of (10.124)-(10.131) can simply be assumed to hold from the outset as fundamental definitions. As remarked in the introduction of Chapter 10, atomistic or molecular arguments can also be used to provide insight into physical origins of various constitutive relationships and material coefficients, as well as terms entering the balance of energy (Born and Huang 1954; Lax and Nelson 1971; Martin 1972; Mindlin 1972; Tiersten and Tsai 1972; Maugin 1988). One benefit of the extended Coleman-Noll kind of procedure used in Section 10.3.2 is that such a procedure can readily be extended to address dielectric crystals with mobile defects or other sources

of dissipation distinct from heat conduction, e.g., viscosity or internal state variables (Tiersten 1971; McMeeking et al. 2007; Clayton et al. 2008a, b; Xiao and Bhattacharya 2008; Clayton 2009b, 2010b).

The present theory reduces to the expected equations in the absence of matter, i.e., when the domain simply consists of vacuum. In that case, all material coefficients in (10.183) are presumed to vanish identically, as does the polarization. The stress $\Sigma^{AB} = 0$ in (10.130) and (10.201), and the Cauchy stress $\sigma^{ab} = 0$ in (10.131). The total stress of (10.78) reduces, in vacuum, to the usual quasi-electrostatic Maxwell stress in the absence of polarization (Jackson 1999): $T^{ab} = \hat{\tau}^{ab} = \varepsilon_0 \hat{e}^a \hat{e}^b - (\varepsilon_0 / 2)\hat{e}^c \hat{e}_c g^{ab}$, which in turn is identically divergence-free ($T^{ab}_{;b} = 0$) and symmetric ($T^{ab} = T^{ba}$), thereby identically satisfying balances of linear (10.77) and angular (10.83) momentum. As remarked already in Section 10.2.4, energy balance (10.91) is satisfied identically in vacuum. In the absence of material, relationship (10.218) becomes $\hat{D}_A = -\varepsilon_0 \hat{\Phi}_{,A}$, analogous to standard aether relation (10.46) for vacuum $\hat{d}_a = -\varepsilon_0 \hat{\phi}_{,a}$. Certain relationships that rely on invertibility of (10.144), e.g., (10.153), break down when material coefficients (10.144) all vanish.

When the dependence of response functions on polarization vanishes, representative free energy of (10.183) corresponds to that of a traditional nonlinear thermoelastic material as considered in Section 5.1.3. In that case, all dielectric, piezoelectric, and pyroelectric coefficients vanish identically, and the second Piola-Kirchhoff stress of (10.201) becomes identical to that of (5.74), while the entropy of (10.203) becomes identical to that of (5.75), up to the same orders of coefficients retained in the Taylor series expansion of the free energy. The electric field then vanishes in a non-polar material according to (10.200), e.g., within a conductor in the absence of electric current. It is emphasized that neither electric field nor electric displacement need always vanish in vacuum.

The theory enables description of nonlinear phenomena such as Maxwell's stress, electrostriction, and effects of higher-order material coefficients, as discussed in Section 10.3.4. Transformation formulae among material coefficients listed in Section 10.3.3 are consistent with other nonlinear theories of thermoelectroelasticity for dielectric solids (Thurston 1974). As demonstrated later in Section 10.4, linearization of the theory of Section 10.3 recovers the standard constitutive equations of linear piezoelectric solids (Bond et al. 1949), as well as standard governing equations and relationships among material coefficients (Mindlin 1972).

While defects are not addressed explicitly in the theory of Chapter 10, a few remarks regarding defective dielectric crystals are merited. Lattice defects are known to strongly affect electromechanical behavior of dielectric solids and hence performance of engineering devices fabricated from such materials. For example, dislocations accommodate misfit strains between dielectric thin films and substrates in electronic devices (Speck and Pompe 1994). In crystals with ionic bonding such as corundum and sodium chloride, consideration of charge distributions and effects of electric fields becomes necessary for describing details of dislocation motion and dislocation reactions (Kronberg 1957; Kliewer and Koehler 1965; Nabarro 1967; Hirth and Lothe 1982; Hull and Bacon 1984). Polarized domains and domain walls affect hysteresis and performance of ferroelectric-based actuator systems (Zhang and Bhattacharya 2005). Dislocations (Bommel et al. 1955, 1956) and vacancies (Brice 1985) are often important in quartz, a piezoelectric crystal used frequently for pressure transducers, resonators, and stress gauges (Graham et al. 1965). Continuum elastoplasticity theories for dielectric and piezoelectric crystals have been formulated in terms of small (Clayton et al. 2008a) and large (Clayton 2010b) strain measures, the latter incorporating multiplicative deformation gradient kinematics.

Vacancies are observed in a number of dielectric materials, and have been addressed in theories based on continuum physics (Xiao et al. 2005; Xiao and Bhattacharya 2008; Clayton et al. 2008a, b; Clayton 2009b, 2010b). Mobile vacancies, in conjunction with climbing dislocations, can dominate creep deformation, often preferentially to glide-controlled inelasticity at high temperatures (Weertman 1955; Chang 1960). In ionic crystals, vacancies typically carry an electric charge (Jamnik and Raj 1996; Conrad 2001). Charged interstitial ions and vacancies, when the crystal is held at a temperature enabling their mobility (i.e., diffusion), can contribute directly to electric current in ionic crystals such as alkali halides (Mott and Gurney 1948). Charged point defects can influence dielectric properties and electrical loss characteristics of capacitors, oscillators, and tunable filters (Damjanovic 1998), for example those comprised of perovskite ceramic crystals such as barium titanate and strontium titanate (Cole et al. 2003; Nothwang et al. 2005). Impurities and associated lattice defects often strongly affect the availability of free electrons and holes that enable free electric current conduction in semiconductors. For example, electronically active Si and C vacancies are important in silicon carbide (Bernstein et al. 2005; Clayton 2010b), a wide band-gap semiconductor.

10.4 Linear Elastic Dielectric Solids

Two approximations are often made to simplify the governing equations of deformable dielectrics. The first is the assumption of geometric linearity, i.e., small deformations. The second approximation is the assumption that terms on the order of the product of the electric field and polarization, as well as those on the order of the square of the electric field, can be omitted in the momentum balances.

Geometrically linear mechanics is often sufficient and relevant because dielectric solids are non-metallic and hence often brittle, for example engineering ceramics under tensile loading. In such materials, when subjected to large mechanical stresses, fracture precludes attainment of large deformations that require use of a geometrically nonlinear continuum theory. In the geometrically linear regime, Section 10.2.2 is unnecessary, since the distinction between undeformed and deformed configurations is not made explicitly, and displacements are measured with respect to a single (possibly curvilinear) coordinate system with fixed origin, as discussed in Section 2.5.3. Linear and angular momentum balances (10.77) and (10.83) are unchanged as a result of the assumption of geometric linearity. However, the local energy balance of the nonlinear theory, i.e., (10.94), reduces to $\rho \dot{e} = \sigma^{ab} \dot{u}_{a;b} - q^a_{;a} + \rho r + \hat{e}_a \dot{p}^a$, with **u** the displacement, in the geometrically linear regime.

Linear electrostatics is deemed valid when terms on the order of the square of the electric field and the product of electric field and polarization entering Maxwell's stress tensor are all small. In that case, body force (10.71) and Maxwell stress (10.72) are omitted, and local linear and angular momentum balances (10.77) and (10.83) reduce to those of classical continua of Chapter 4, i.e., (4.17) and (4.26) respectively. With these reductions, the term in parentheses in (10.92) still vanishes, and the final form of the local energy balance, (10.94), remains unchanged. However, the stress tensor is now symmetric, and hence the skew part of the velocity gradient does not contribute to the time rate of change of internal energy. The framework of linear electrostatics is very often used out of mathematical convenience and practicality, since in linear elastic dielectric bodies, the Cauchy stress tensor exhibits the usual symmetry and divergence properties of the stress tensor of its representation in classical linear elasticity.

The theory described in what follows in Section 10.4 combines the aforementioned assumptions of geometric linearity and linear electrostatics, i.e., vanishing of Maxwell's stress tensor. The forthcoming treatment thus reduces to a standard framework for linear elastic dielectric and piezoelectric crystals (Bond et al. 1949; Haskins and Hickman 1950; Mindlin

1972; Pan 2001) in the absence of electrodynamic effects, i.e., in the quasi-electrostatic approximation.

10.4.1 Governing Equations

Governing equations of linear dielectrics in the context of the quasi-electrostatic approximation of Section 10.2.1 are summarized as follows. Maxwell's equations (10.49) and (10.52) remain valid:

$$\hat{e}_a = -\hat{\phi}_{,a}, \ \hat{d}^a_{;a} = \hat{\rho}, \tag{10.238}$$

and referential analogs (10.61) and (10.67) are not needed. Maxwell's stress of (10.72) is omitted by definition, such that the balances of linear and angular momentum exhibit their traditional forms of Section 4.1.3:

$$\sigma^{ab}_{;b} + \overline{b}^a = \rho a^a, \ \sigma^{[ab]} = 0. \tag{10.239}$$

The local balance of energy of (10.93)-(10.94) reduces as follows for a linear elastic dielectric:

$$\rho \dot{e} = \sigma^{ab} \dot{\varepsilon}_{ab} - q^a_{;a} + \rho r + \hat{e}^a \dot{\hat{p}}_a, \tag{10.240}$$

where $\dot{\varepsilon}_{ab} = \dot{u}_{(a;b)}$ is the symmetric strain rate of (2.191). The analog of (10.100) implies that the total distortion is thermoelastic, as in (5.254):

$$u_{a;b} = \beta^L_{ab} = \varepsilon^L_{ab} + \Omega^L_{ab} = \varepsilon_{ab} + \Omega_{ab},$$
$$\varepsilon_{ab} = u_{(a;b)} = \varepsilon^L_{ab} = \beta^L_{(ab)}, \tag{10.241}$$
$$\Omega_{ab} = u_{[a,b]} = \Omega^L_{ab} = \beta^L_{[ab]}.$$

The entropy inequality of (10.98)-(10.99) reduces to

$$\langle \boldsymbol{\sigma}, \dot{\boldsymbol{\varepsilon}} \rangle + \langle \hat{\mathbf{e}}, \dot{\hat{\mathbf{p}}} \rangle - \rho(\dot{\psi} + \dot{\theta}\eta) - \frac{1}{\theta} \langle \nabla \theta, \mathbf{q} \rangle \geq 0, \tag{10.242}$$

or in index notation,

$$\sigma^{ab} \dot{u}_{(a;b)} + \hat{e}^a \dot{\hat{p}}_a - \rho(\dot{\psi} + \dot{\theta}\eta) - \theta^{-1} q^a \theta_{,a} \geq 0. \tag{10.243}$$

10.4.2 Constitutive Assumptions

In lieu of (10.110)-(10.114) that apply for the geometrically nonlinear regime, the following constitutive functions are suggested for linear elastic dielectric solids:

$$\psi = \psi\left(\boldsymbol{\varepsilon}, \hat{\mathbf{p}}, \theta, \nabla \theta, x, \mathbf{g}_a\right), \ \psi = \psi\left(\varepsilon_{ab}, \hat{p}_a, \theta, \theta_{,a}, x, \mathbf{g}_a\right); \tag{10.244}$$

$$\eta = \eta\left(\boldsymbol{\varepsilon}, \hat{\mathbf{p}}, \theta, \nabla \theta, x, \mathbf{g}_a\right), \ \eta = \eta\left(\varepsilon_{ab}, \hat{p}_a, \theta, \theta_{,a}, x, \mathbf{g}_a\right); \tag{10.245}$$

$$\boldsymbol{\sigma} = \boldsymbol{\sigma}\left(\boldsymbol{\varepsilon}, \hat{\mathbf{p}}, \theta, \nabla\theta, x, \mathbf{g}_a\right), \; \sigma^{ab} = \sigma^{ab}\left(\varepsilon_{ab}, \hat{p}_a, \theta, \theta_{,a}, x, \mathbf{g}_a\right); \qquad (10.246)$$

$$\mathbf{q} = \mathbf{q}\left(\boldsymbol{\varepsilon}, \hat{\mathbf{p}}, \theta, \nabla\theta, x, \mathbf{g}_a\right), \; q^a = q^a\left(\varepsilon_{ab}, \hat{p}_a, \theta, \theta_{,a}, x, \mathbf{g}_a\right); \qquad (10.247)$$

$$\hat{\mathbf{e}} = \hat{\mathbf{e}}\left(\boldsymbol{\varepsilon}, \hat{\mathbf{p}}, \theta, \nabla\theta, x, \mathbf{g}_a\right), \; \hat{e}^a = \hat{e}^a\left(\varepsilon_{ab}, \hat{p}_a, \theta, \theta_{,a}, x, \mathbf{g}_a\right). \qquad (10.248)$$

Notice that (10.244)-(10.248) differ from the constitutive assumptions of linear thermoelasticity in (5.262)-(5.265) only via addition of the polarization $\hat{\mathbf{p}}$ as an independent state variable and prescription of electric field $\hat{\mathbf{e}}$ as a dependent response function. Incorporation of polarization as an independent variable in the thermodynamic response functions enables description of energies associated with the dielectric permittivity, the piezoelectric effect, and the pyroelectric effect. The rationale for inclusion of particular variables other than $\hat{\mathbf{p}}$ in the response functions (e.g., thermodynamic potentials) is explained in Section 5.4.1 in the context of linear thermoelasticity of non-polarized solids.

10.4.3 Thermodynamics

From the chain rule and (10.244), the time rate of change of the free energy is

$$\dot{\psi} = \frac{\partial\psi}{\partial\varepsilon_{ab}}\dot{\varepsilon}_{ab} + \frac{\partial\psi}{\partial\hat{p}_a}\dot{\hat{p}}_a + \frac{\partial\psi}{\partial\theta}\dot{\theta} + \frac{\partial\psi}{\partial\theta_{,a}}\gamma_a, \qquad (10.249)$$

where $\gamma_a = d(\theta_{,a})/dt$. Substitution of (10.249) into dissipation inequality (10.243) then gives

$$\left(\sigma^{ab} - \rho\frac{\partial\psi}{\partial\varepsilon_{ab}}\right)\dot{\varepsilon}_{ab} + \left(\hat{e}^a - \rho\frac{\partial\psi}{\partial\hat{p}_a}\right)\dot{\hat{p}}_a$$
$$- \rho\left(\eta + \frac{\partial\psi}{\partial\theta}\right)\dot{\theta} - \rho\left(\frac{\partial\psi}{\partial\theta_{,a}}\right)\gamma_a - \frac{q^a\theta_{,a}}{\theta} \geq 0. \qquad (10.250)$$

Arguments analogous to those following (10.123) then result in vanishing of terms in parentheses in (10.250). The following stress-strain, electric field-polarization, and entropy-temperature relations emerge:

$$\boldsymbol{\sigma} = \rho\frac{\partial\psi}{\partial\boldsymbol{\varepsilon}}, \; \hat{\mathbf{e}} = \rho\frac{\partial\psi}{\partial\hat{\mathbf{p}}}, \; \eta = -\frac{\partial\psi}{\partial\theta}. \qquad (10.251)$$

The dependence of free energy on temperature gradient vanishes:

$$\frac{\partial\psi}{\partial\theta_{,a}} = 0, \qquad (10.252)$$

leading to reduced forms of constitutive functions (10.244)-(10.246) and (10.248):

$$\psi = \psi\left(\boldsymbol{\varepsilon}, \hat{\mathbf{p}}, \theta, x, \mathbf{g}_a\right), \ \eta = \eta\left(\boldsymbol{\varepsilon}, \hat{\mathbf{p}}, \theta, x, \mathbf{g}_a\right), \tag{10.253}$$

$$\boldsymbol{\sigma} = \boldsymbol{\sigma}\left(\boldsymbol{\varepsilon}, \hat{\mathbf{p}}, \theta, x, \mathbf{g}_a\right), \ \hat{\mathbf{e}} = \hat{\mathbf{e}}\left(\boldsymbol{\varepsilon}, \hat{\mathbf{p}}, \theta, x, \mathbf{g}_a\right). \tag{10.254}$$

The rate of local entropy production vanishes identically:

$$\theta\Gamma_L = \rho\theta\dot{\eta} + q^a_{;a} - \rho r = \rho(\dot{e} - \dot{\psi} - \dot{\theta}\eta) + q^a_{;a} - \rho r$$
$$= \sigma^{ab}\dot{\varepsilon}_{ab} + \hat{e}^a\dot{\hat{p}}_a - \rho\dot{\psi} - \rho\dot{\theta}\eta = 0, \tag{10.255}$$

and the conduction inequality remains:

$$\theta\Gamma_C = -q^a\theta_{,a} \geq 0 . \tag{10.256}$$

The conduction inequality can be satisfied unconditionally, for example, by applying Fourier's law of (5.277), with k^{ab} a symmetric and positive semi-definite matrix of thermal conductivity:

$$q^a = -k^{ab}\theta_{,b}, \ -\theta^{-1}q^a\theta_{,a} = \theta^{-1}k^{ab}\theta_{,a}\theta_{,b} \geq 0 . \tag{10.257}$$

From (10.251), (10.255), and (10.257), the local energy balance can be expressed as

$$\rho\theta\dot{\eta} = -\rho\theta\frac{d}{dt}\left(\frac{\partial\psi}{\partial\theta}\right) = (k^{ab}\theta_{,b})_{;a} + \rho r . \tag{10.258}$$

By the chain rule as in (10.249),

$$-\rho\theta\frac{d}{dt}\left(\frac{\partial\psi}{\partial\theta}\right) = -\rho\theta\frac{\partial}{\partial\theta}\left(\frac{\partial\psi}{\partial\varepsilon_{ab}}\dot{\varepsilon}_{ab} + \frac{\partial\psi}{\partial\hat{p}_a}\dot{\hat{p}}_a + \frac{\partial\psi}{\partial\theta}\dot{\theta}\right)$$
$$= \theta\beta^{ab}\dot{\varepsilon}_{ab} + \theta\chi^a\dot{\hat{p}}_a + \rho c\dot{\theta}, \tag{10.259}$$

where thermal stress coefficients, pyroelectric coefficients, and specific heat per unit mass at constant strain and constant polarization are, respectively,

$$\beta^{ab} = -\rho\frac{\partial^2\psi}{\partial\theta\partial\varepsilon_{ab}}\bigg|_{\hat{\mathbf{p}}}, \ \chi^a = -\rho\frac{\partial^2\psi}{\partial\theta\partial\hat{p}_a}\bigg|_{\boldsymbol{\varepsilon}}, \ c = \frac{\partial e}{\partial\theta}\bigg|_{\hat{\mathbf{p}},\boldsymbol{\varepsilon}} = -\theta\frac{\partial^2\psi}{\partial\theta^2}\bigg|_{\hat{\mathbf{p}},\boldsymbol{\varepsilon}} . \tag{10.260}$$

Equating (10.258) and (10.259) results in the temperature rate equation

$$\rho c\dot{\theta} = (k^{ab}\theta_{,b})_{;a} - \theta(\beta^{ab}\dot{\varepsilon}_{ab} + \chi^a\dot{\hat{p}}_a) + \rho r . \tag{10.261}$$

10.4.4 Representative Free Energy

Conceivably, the free energy potential of the first of (10.253) could be expanded in a Taylor series about a reference state, with such an expansion incorporating material coefficients corresponding to derivatives of the potential of arbitrary order, as was demonstrated in Section 5.4.3 in the con-

text of thermoelasticity. However, as explained following (5.300), coefficients defined as derivatives of orders three and higher in strain should consistently be omitted from the energy potential, since second- and higher-order products of displacement gradients are omitted implicitly in the stress and strain of the first of (10.251) via the assumption of geometric linearity. Similarly, when the Maxwell stress is omitted as in the present case of electric linearity, material coefficients defined as derivatives of orders three and higher in polarization should be omitted from the energy potential for consistency. Piezoelectric coefficients consisting of derivatives of higher than first order in either of polarization or strain should also be omitted in the linear case. Thus, the following linearized form of (10.204) suffices for linear elastic dielectrics:

$$
\rho_0 \psi = \frac{1}{2} \overline{\mathbb{C}}^{abcd} \varepsilon_{ab} \varepsilon_{cd} + \frac{1}{2} \overline{\Lambda}^{ab} \hat{p}_a \hat{p}_b + \overline{\Delta}^{abc} \hat{p}_a \varepsilon_{bc}
$$
$$
- \overline{\beta}^{ab} \varepsilon_{ab} \Delta\theta - \overline{\chi}^a \hat{p}_a \Delta\theta - \overline{C}_\varepsilon \theta \ln \frac{\theta}{\theta_0},
$$

(10.262)

where the expansion is about a strain-free, non-polar reference state at the reference temperature, with $u_{a;b} = \varepsilon_{ab} = 0$, $\hat{p}_a = 0$, and $\theta = \theta_0 > 0$ in this reference state.

Material constants in (10.262) are defined as follows. Isothermal second-order elastic and dielectric constants, respectively, are

$$
\overline{\mathbb{C}}^{abcd} = \rho_0 \left. \frac{\partial^2 \psi}{\partial \varepsilon_{ab} \partial \varepsilon_{cd}} \right|_{\substack{\varepsilon=0 \\ \hat{\mathbf{p}}=0 \\ \theta=\theta_0}} , \quad \overline{\Lambda}^{ab} = \rho_0 \left. \frac{\partial^2 \psi}{\partial \hat{p}_a \partial \hat{p}_b} \right|_{\substack{\varepsilon=0 \\ \hat{\mathbf{p}}=0 \\ \theta=\theta_0}} .
$$

(10.263)

Piezoelectric and pyroelectric constants are defined, respectively, as

$$
\overline{\Delta}^{abc} = \rho_0 \left. \frac{\partial^2 \psi}{\partial \hat{p}_a \partial \varepsilon_{bc}} \right|_{\substack{\varepsilon=0 \\ \hat{\mathbf{p}}=0 \\ \theta=\theta_0}} , \quad \overline{\chi}^a = -\rho_0 \left. \frac{\partial^2 \psi}{\partial \theta \partial \hat{p}_a} \right|_{\substack{\varepsilon=0 \\ \hat{\mathbf{p}}=0 \\ \theta=\theta_0}} ,
$$

(10.264)

and thermal stress coefficients and specific heat per unit volume at constant strain and polarization are

$$
\overline{\beta}^{ab} = -\rho_0 \left. \frac{\partial^2 \psi}{\partial \theta \partial \varepsilon_{ab}} \right|_{\substack{\varepsilon=0 \\ \hat{\mathbf{p}}=0 \\ \theta=\theta_0}} , \quad \overline{C}_\varepsilon = -\rho_0 \theta_0 \left. \frac{\partial^2 \psi}{\partial \theta^2} \right|_{\substack{\varepsilon=0 \\ \hat{\mathbf{p}}=0 \\ \theta=\theta_0}} .
$$

(10.265)

Analogously to (10.219)-(10.220), the following symmetries emerge for elastic, dielectric, piezoelectric, and thermal stress coefficients:

$$
\overline{\mathbb{C}}^{abcd} = \overline{\mathbb{C}}^{bacd} = \overline{\mathbb{C}}^{abdc} = \overline{\mathbb{C}}^{cdab} ,
$$

(10.266)

$$
\overline{\Lambda}^{ab} = \overline{\Lambda}^{ba} , \quad \overline{\Delta}^{abc} = \overline{\Delta}^{acb} , \quad \overline{\beta}^{ab} = \overline{\beta}^{ba} ,
$$

(10.267)

meaning that $\overline{\mathbb{C}}^{abcd}$ contains up to 21 independent entries, $\overline{A}^{abc}$ contains up to 18 independent entries, and $\overline{A}^{ab}$ and $\overline{\beta}^{ab}$ each contain up to 6 independent entries.

From the first of (10.251) and (10.262), the stress tensor is

$$\sigma^{ab} = J\tau^{ab} \approx \tau^{ab} = \rho_0 \frac{\partial \psi}{\partial \varepsilon_{ab}} = \overline{\mathbb{C}}^{abcd} \varepsilon_{cd} + \overline{A}^{cab} \hat{p}_c - \overline{\beta}^{ab} \Delta\theta, \qquad (10.268)$$

where, as in the geometrically linear theory of elasticity in (5.301), the difference between Kirchhoff and Cauchy stresses is typically omitted, and will be omitted henceforth, such that $\sigma^{ab} \approx \tau^{ab}$. The first term in the final expression of (10.268) is attributed to mechanical strain, the second to the inverse piezoelectric effect, and the third to thermoelastic coupling.

To the same order of approximation, from the second of (10.251) and (10.262), the electric field satisfies

$$\hat{e}^a = \rho \frac{\partial \psi}{\partial \hat{p}_a} \approx \rho_0 \frac{\partial \psi}{\partial \hat{p}_a} = \overline{A}^{ab} \hat{p}_b + \overline{A}^{abc} \varepsilon_{bc} - \overline{\chi}^a \Delta\theta , \qquad (10.269)$$

where the first term on the far right is attributed to the electric polarization, the second to the direct piezoelectric effect, and the third to thermoelectric coupling, i.e., pyroelectricity. The electric displacement in terms of polarization, strain, and temperature is then, from (10.46),

$$\hat{d}^a = \varepsilon_0 \hat{e}^a + \hat{p}^a = (\varepsilon_0 \overline{A}^{ab} + g^{ab})\hat{p}_b + \varepsilon_0 \overline{A}^{abc} \varepsilon_{bc} - \varepsilon_0 \overline{\chi}^a \Delta\theta . \qquad (10.270)$$

Upon inverting (10.269), the polarization vector can be written in terms of the electric field as

$$\begin{aligned} \hat{p}_b &= \overline{A}_{ba}^{-1} \hat{e}^a - \overline{A}_{ba}^{-1} \overline{A}^{acd} \varepsilon_{cd} + \overline{A}_{ba}^{-1} \overline{\chi}^a \Delta\theta \\ &= \overline{A}_{ba}^{-1} \hat{e}^a + \overline{e}_b^{.cd} \varepsilon_{cd} + \overline{\varsigma}_b \Delta\theta, \end{aligned} \qquad (10.271)$$

where piezoelectric and pyroelectric coefficients, analogously to (10.209) and (10.211), are defined as

$$\overline{e}_a^{.bc} = \overline{A}_{ab}^{-1} \overline{A}^{bcd} , \quad \overline{\varsigma}_a = \overline{A}_{ab}^{-1} \overline{\chi}^b . \qquad (10.272)$$

Substitution of (10.271) into (10.270) then provides a constitutive relationship between electric displacement and electric field:

$$\begin{aligned} \hat{d}^a &= (\varepsilon_0 \overline{A}^{ab} + g^{ab})(\overline{A}_{bc}^{-1} \hat{e}^c - \overline{A}_{bc}^{-1} \overline{A}^{cde} \varepsilon_{de} + \overline{A}_{bc}^{-1} \overline{\chi}^c \Delta\theta) \\ &\quad + \varepsilon_0 \overline{A}^{abc} \varepsilon_{bc} - \varepsilon_0 \overline{\chi}^a \Delta\theta \\ &= (\overline{A}_{.b}^{-1a} + \varepsilon_0 \delta_{.b}^a)\hat{e}^b - \overline{A}_{.c}^{-1a} \overline{A}^{cde} \varepsilon_{de} + \overline{A}_{.c}^{-1a} \overline{\chi}^c \Delta\theta \\ &= \overline{\varepsilon}^{ab} \hat{e}_b + \overline{e}^{abc} \varepsilon_{bc} + \overline{\varsigma}^a \Delta\theta, \end{aligned} \qquad (10.273)$$

with the permittivity tensor $\overline{\varepsilon}^{ab}$ and dimensionless relative permittivity tensor $\overline{\varepsilon}_R^{ab}$

$$\bar{\varepsilon}^{ab} = \bar{\Lambda}^{-1ab} + \varepsilon_0 g^{ab} = \varepsilon_0 \bar{\mathcal{E}}_R^{ab},$$

$$\bar{\mathcal{E}}_R^{ab} = \frac{1}{\varepsilon_0} \bar{\varepsilon}^{ab} = (\varepsilon_0 \bar{\Lambda})^{-1ab} + g^{ab}. \tag{10.274}$$

Now consider the stress tensor of (10.268), which can be expressed in components using (10.271) as

$$\sigma^{ab} = \bar{\mathbb{C}}^{abcd}\varepsilon_{cd} + \bar{\Lambda}^{cab}(\bar{\Lambda}_{cd}^{-1}\hat{e}^d + \bar{e}_c^{.de}\varepsilon_{de} + \bar{\varsigma}_c\Delta\theta) - \bar{\beta}^{ab}\Delta\theta$$

$$= (\bar{\mathbb{C}}^{abcd} + \bar{\Lambda}^{eab}\bar{e}_e^{.cd})\varepsilon_{cd} + (\bar{\Lambda}^{cab}\bar{\Lambda}_{cd}^{-1})\hat{e}^d + (\bar{\Lambda}^{cab}\bar{\varsigma}_c - \bar{\beta}^{ab})\Delta\theta$$

$$= (\bar{\mathbb{C}}^{abcd} - \bar{\Lambda}^{eab}\bar{\Lambda}_{ef}^{-1}\bar{\Lambda}^{fcd})\varepsilon_{cd} - \bar{e}^{cab}\hat{e}_c - (\bar{\Lambda}^{cd}e_d^{.ab}\bar{\varsigma}_c + \bar{\beta}^{ab})\Delta\theta$$

$$= \bar{\mathbb{C}}_{\hat{e}}^{abcd}\varepsilon_{cd} - \bar{e}^{cab}\hat{e}_c - (\bar{e}_d^{.ab}\bar{\chi}^d + \bar{\beta}^{ab})\Delta\theta, \tag{10.275}$$

where second-order isothermal, linear elastic constants at fixed electric field are, similarly to (10.210),

$$\bar{\mathbb{C}}_{\hat{e}}^{abcd} = \bar{\mathbb{C}}^{abcd} + \bar{\Lambda}^{eab}\bar{e}_e^{.cd} = \bar{\mathbb{C}}^{abcd} - \bar{\Lambda}^{eab}\bar{\Lambda}_{ef}^{-1}\bar{\Lambda}^{fcd}. \tag{10.276}$$

Following similar arguments used to obtain (5.302) and (5.303), the following relationships emerge among second-order material coefficients of Section 10.3.5 and those of the geometrically linear theory of (10.263)-(10.265):

$$\bar{\mathbb{C}}^{abcd} = \bar{\mathbb{C}}^{ABCD}\delta_{(A}^{(a}\delta_{.B)}^{b)}\delta_{(C}^{(c}\delta_{.D)}^{d)}, \quad \bar{\Lambda}^{ab} = \bar{\Lambda}^{AB}\delta_{(A}^{(a}\delta_{.B)}^{b)}, \tag{10.277}$$

$$\bar{\Lambda}^{abc} = \bar{\Lambda}^{ABC}\delta_{.A}^a\delta_{(B}^{(b}\delta_{.C)}^{c)}, \quad \bar{\chi}^a = \bar{\chi}^A\delta_{.A}^a, \quad \bar{\beta}^{ab} = \bar{\beta}^{AB}\delta_{(A}^{(a}\delta_{.B)}^{b)}. \tag{10.278}$$

Similarly, for the other material coefficients introduced in Section 10.4.4,

$$\bar{\mathbb{C}}_{\hat{e}}^{abcd} = \bar{\mathbb{C}}_{\hat{E}}^{ABCD}\delta_{(A}^{(a}\delta_{.B)}^{b)}\delta_{(C}^{(c}\delta_{.D)}^{d)}, \quad \bar{\mathcal{E}}^{ab} = \bar{\mathcal{E}}^{AB}\delta_{(A}^{(a}\delta_{.B)}^{b)}, \tag{10.279}$$

$$\bar{e}^{abc} = \bar{e}^{ABC}\delta_{.A}^a\delta_{(B}^{(b}\delta_{.C)}^{c)}, \quad \bar{\varsigma}^a = \bar{\varsigma}^A\delta_{.A}^a. \tag{10.280}$$

Thus, all arguments regarding symmetry of material coefficients discussed in Section 10.3.6 and Appendix A apply identically for material coefficients of the linear theory. For example, linear piezoelectric and pyroelectric coefficients of (10.264) vanish identically in centrosymmetric crystals. Voigt's notation can be used in the linear theory in a similar fashion to that of (10.221)-(10.227). For example, in Voigt's notation with barred lowercase indices spanning $1, 2, \ldots 6$, free energy (10.262) becomes

$$\rho_0\psi = \frac{1}{2}\bar{\mathbb{C}}^{\bar{a}\bar{b}}\varepsilon_{\bar{a}}\varepsilon_{\bar{b}} + \frac{1}{2}\bar{\Lambda}^{ab}\hat{p}_a\hat{p}_b + \bar{\Lambda}^{a\bar{b}}\hat{p}_a\varepsilon_{\bar{b}}$$

$$- \bar{\beta}^{\bar{a}}\varepsilon_{\bar{a}}\Delta\theta - \bar{\chi}^a\hat{p}_a\Delta\theta - \bar{C}_\varepsilon\theta\ln\frac{\theta}{\theta_0}. \tag{10.281}$$

All material coefficients introduced to this point in Section 10.4 are isothermal coefficients. Transformation formulae between these coefficients

and their isentropic counterparts can be obtained by substitution of (10.277)-(10.280) into (10.176)-(10.179), for example.

Substituting (10.273) and (10.275) into the second of (10.238) and the first of (10.239), and using the first of (10.238) and the definition $\varepsilon_{ab} = u_{(a;b)}$, the following relationships are obtained for a linear elastic dielectric with homogeneous material properties:

$$\overline{e}^{abc} u_{b;ca} - \overline{\varepsilon}^{ab} \hat{\phi}_{,ba} + \overline{\varsigma}^a \theta_{,a} = \hat{\rho}, \tag{10.282}$$

$$\overline{\mathbb{C}}_{\hat{e}}^{abcd} u_{c;db} + \overline{e}^{cab} \hat{\phi}_{,cb} - (\overline{e}_d^{\,ab} \overline{\chi}^d + \overline{\beta}^{ab}) \theta_{,b} = \rho \ddot{u}^a - \overline{b}^a. \tag{10.283}$$

Energy balance (10.261) becomes, with (10.271) and the approximation $\rho \approx \rho_0$ used for the specific heat:

$$\dot{\theta} = \frac{1}{\overline{C}_\varepsilon} \left\{ k^{ab} \theta_{;ba} - \theta \left[\beta^{ab} \dot{u}_{a;b} - \chi^a (\overline{\Lambda}_{ab}^{-1} \dot{\hat{\phi}}^{,b} - \overline{e}_a^{\,cd} \dot{u}_{c;d} - \overline{\varsigma}_a \dot{\theta}) \right] + \rho r \right\}. \tag{10.284}$$

Equalities (10.282)-(10.284) represent 5 coupled differential equations in 5 unknowns—three components of displacement $u_a(x,t)$, electrostatic potential $\hat{\phi}(x,t)$, and temperature $\theta(x,t)$ —presuming that free charge density $\hat{\rho}(x,t)$, mechanical body force $\overline{b}^a(x,t)$, and heat source $r(x,t)$ are either prescribed via independent equations or vanish identically. In the absence of temperature effects and free charges, (10.282) and (10.283) are identical to a standard set of linear piezoelectric relations listed by Mindlin (1972).

10.4.5 Constitutive Equations of Linear Piezoelectricity

In the classical theory of linear piezoelectricity (Bond et al. 1949), the mechanical field variables are stress σ^{ab} and strain ε_{ab}, either of which may be assigned as the independent variable, and the electrical field variables are electric field $\hat{e}_a$ and electric displacement $\hat{d}_a$, either of which may be assigned as the independent variable. Constitutive equations at a fixed temperature (i.e., omitting pyroelectricity and thermal expansion) are written in the following four equivalent sets (Bond et al. 1949; Thurston 1974):

$$\sigma^{ab} = \overline{\mathbb{C}}_{\hat{e}}^{abcd} \varepsilon_{cd} - \overline{e}^{cab} \hat{e}_c, \ \hat{d}^a = \overline{e}^{abc} \varepsilon_{bc} + \overline{\varepsilon}^{ab} \hat{e}_b; \tag{10.285}$$

$$\sigma^{ab} = \overline{\mathbb{C}}_{\hat{d}}^{abcd} \varepsilon_{cd} - \overline{h}^{cab} \hat{d}_c, \ \hat{e}^a = -\overline{h}^{abc} \varepsilon_{bc} + \overline{\varepsilon}^{-1ab} \hat{d}_b; \tag{10.286}$$

$$\varepsilon_{ab} = (\overline{S}_{\hat{d}})_{abcd} \sigma^{cd} + \overline{g}_{cab} \hat{d}^c, \ \hat{e}^a = -\overline{g}_{.bc}^a \sigma^{bc} + \overline{\varepsilon}_\sigma^{-1ab} \hat{d}_b; \tag{10.287}$$

$$\varepsilon_{ab} = (\overline{S}_{\hat{e}})_{abcd} \sigma^{cd} + \overline{d}_{cab} \hat{e}^c, \ \hat{d}^a = \overline{d}_{.bc}^a \sigma^{bc} + \overline{\varepsilon}_\sigma^{ab} \hat{e}_b. \tag{10.288}$$

Relationships among material coefficients entering (10.285)-(10.288) are listed in Table 10.1. Notice that (10.285) is consistent with (10.273) and (10.275) at the reference temperature, implying that the constitutive theory of Sections 10.4.1-10.4.4, derived via linearization of the nonlinear continuum theory of elastic dielectrics of Section 10.3, is consistent with standard linear piezoelectricity (Bond et al. 1949; Haskins and Hickman 1950; Mindlin 1972). Relationships between coefficients introduced in (10.262) with polarization as the independent electrical field variable and those entering (10.285) are given in (10.272), (10.274), and (10.276).

Table 10.1 Coefficient relationships in linear piezoelectricity (Bond et al. 1949)

Inversions	Differences	Piezoelectric coefficients
$2\overline{\mathbb{C}}_{\hat{d}}^{abcd}(\overline{S}_{\hat{d}})_{cdef} = \delta_{.e}^{a}\delta_{.f}^{b} + \delta_{.e}^{b}\delta_{.f}^{a}$	$(\overline{\varepsilon}_{\sigma})_{ab} - \overline{\varepsilon}_{ab} = \overline{e}_{a}^{.cd}\,\overline{d}_{bcd}$	$\overline{d}_{abc} = (\overline{\varepsilon}_{\sigma})_{ad}\,\overline{g}_{.bc}^{d} = \overline{e}_{ade}(\overline{S}_{\hat{e}})_{..bc}^{de}$
$2\overline{\mathbb{C}}_{\hat{e}}^{abcd}(\overline{S}_{\hat{e}})_{cdef} = \delta_{.e}^{a}\delta_{.f}^{b} + \delta_{.e}^{b}\delta_{.f}^{a}$	$\overline{\varepsilon}_{ab}^{-1} - (\overline{\varepsilon}_{\sigma}^{-1})_{ab} = \overline{g}_{a}^{.cd}\overline{h}_{bcd}$	$\overline{e}_{abc} = \overline{\varepsilon}_{ad}\overline{h}_{.bc}^{d} = \overline{d}_{ade}(\overline{\mathbb{C}}_{\hat{e}})_{..bc}^{de}$
$\overline{\varepsilon}^{-1ac}\overline{\varepsilon}_{cb} = \delta_{.b}^{a}$	$(\overline{\mathbb{C}}_{\hat{d}} - \overline{\mathbb{C}}_{\hat{e}})^{abcd} = \overline{e}_{f}^{.ab}\overline{h}^{fcd}$	$\overline{g}_{abc} = (\overline{\varepsilon}_{\sigma}^{-1})_{ad}\,\overline{d}_{.bc}^{d} = \overline{h}_{ade}(\overline{S}_{\hat{d}})_{..bc}^{de}$
$\overline{\varepsilon}_{\sigma}^{-1ac}(\overline{\varepsilon}_{\sigma})_{cb} = \delta_{.b}^{a}$	$(\overline{S}_{\hat{e}} - \overline{S}_{\hat{d}})_{abcd} = \overline{d}_{.ab}^{f}\overline{g}_{fcd}$	$\overline{h}_{abc} = (\overline{\varepsilon}^{-1})_{ad}\overline{e}_{.bc}^{d} = \overline{g}_{ade}(\overline{\mathbb{C}}_{\hat{d}})_{..bc}^{de}$

Often in practice, low deformation rate (i.e., mechanically quasi-static) experiments are idealized as isothermal, while mechanical stress wave propagation (i.e., acoustic) experiments are idealized as adiabatic or isentropic. Thus in such cases, (10.285)-(10.288) can be used verbatim for isothermal conditions, while these same equations can be used for isentropic conditions by replacing all isothermal material coefficients with their isentropic counterparts (Bond et al. 1949; Thurston 1974).

Appendix A: Crystal Symmetries and Elastic Constants

In anisotropic materials, constitutive relations and corresponding material coefficients depend on the orientation of the body with respect to the reference coordinate system. This Appendix discusses symmetry operations for point groups and Laue groups comprising the seven crystal systems first introduced in Chapter 3. Requisite terminology and definitions are given in Section A.1. Listed in Section A.2 are matrix forms of generic polar tensors (i.e., material coefficients) of orders one, two, three, and four for each Laue group, and forms for individual crystal classes comprising each Laue group for polar tensors of odd rank. Second- and third-order elastic constants are given particular attention in Section A.3. The content generally applies to materials whose elastic behavior is independent of deformation gradients of orders higher than one, more specifically hyperelastic materials of grade one. The discussion and tabular results of Appendix A summarize a number of previous descriptions (Hearmon 1946, 1956; Bond et al. 1949; Schmid and Boas 1950; Landau and Lifshitz 1959; Brugger 1964, 1965; Truesdell and Noll 1965; Thurston 1974; Teodosiu 1982).

A.1 Crystal Classes, Point Groups, and Laue Groups

Under an orthogonal transformation of Cartesian reference coordinates $\mathbf{X} \rightarrow \breve{\mathbf{Q}}\mathbf{X}$, deformation gradient $\mathbf{F} = \partial \mathbf{x} / \partial \mathbf{X}$ and right Cauchy-Green strain $\mathbf{E} = (\mathbf{F}^T \mathbf{F} - \mathbf{1}) / 2$ transform as $\mathbf{F} \rightarrow \mathbf{F}\breve{\mathbf{Q}}$ and $\mathbf{E} \rightarrow \breve{\mathbf{Q}}^T \mathbf{E}\breve{\mathbf{Q}}$, respectively. Consider the free energy density in the first of (5.6) for an elastic crystal at fixed temperature, i.e., the strain energy density. The specific form of the elastic mechanical response function, in this case the strain energy density, respects the symmetry, or lack thereof, of the material:

$$\psi\left(\breve{\mathbf{Q}}^T \mathbf{E}\breve{\mathbf{Q}}\right) = \psi\left(\mathbf{E}\right). \tag{A.1}$$

The set $\mathbb{Q}$ of all orthogonal tensors $\breve{\mathbf{Q}}$ that leave the mechanical response function unaffected, i.e., those operations for which (A.1) is satisfied, is

called the symmetry group or isotropy group for the material. For two transformations $\breve{\mathbf{Q}}_1, \breve{\mathbf{Q}}_2 \in \mathbb{Q}$, their product $\breve{\mathbf{Q}}_1 \breve{\mathbf{Q}}_2 \in \mathbb{Q}$. Furthermore, $\breve{\mathbf{Q}} \in \mathbb{Q}$ implies $\breve{\mathbf{Q}}^T = \breve{\mathbf{Q}}^{-1} \in \mathbb{Q}$. Every isotropy group contains the identity map $\breve{\mathbf{Q}} = \mathbf{1}$ and the inversion $\breve{\mathbf{Q}} = -\mathbf{1}$. Subgroups consisting of all proper orthogonal tensors ($\det \breve{\mathbf{Q}} = +1$) of the isotropy groups comprise the rotation groups $\mathbb{Q}^+$. Any member of particular group $\mathbb{Q}^+$ can be created by a product of rotation matrices called generators of that group, labeled $\mathbf{R}_N^n$. Any entry of $\mathbb{Q}$ for that group can then be obtained from entries of $\mathbb{Q}^+$ via use of the inversion. The group of all rotations, reflections, and translations that leave a structure invariant is called the space group. A space group can include combinations of translations, rotations, and reflections (i.e., screw and glide operations) individually not contained in that space group (Chaikin and Lubensky 1995). The set of all rotations and reflections that preserve a structure at a point is called the point group. Crystals sharing the same point group are said to belong to the same crystal class. In three dimensions, the number of distinct space groups is 230, and the number of distinct point groups or crystal classes is thirty-two.

Every crystal class falls into one of eleven Laue groups. Each Laue group corresponds to a different set of rotations $\mathbb{Q}^+$ to which elastic mechanical response functions in the context of (A.1) are invariant. Table A.1 lists Laue groups, point groups, and generators for all crystal classes, following Thurston (1974). The notation $\mathbf{R}_N^n$ denotes a right-handed rotation by angle $2\pi/n$ about an axis in the direction of unit vector $\mathbf{N}$. Boldface indices $\mathbf{i}$, $\mathbf{j}$, and $\mathbf{k}$ denote unit vectors of a right-handed orthonormal basis for $\mathbf{X}$, and $\mathbf{m} = 3^{-1/2}(\mathbf{i} + \mathbf{j} + \mathbf{k})$. Also denoted by asterisk in Table A.1 are the eleven crystal point groups—one per Laue group—with an inversion center or center of symmetry (i.e., those that are centrosymmetric). The seven crystal systems of Fig. 3.1 whose symmetry elements are listed in Table A.2 are recovered from the eleven Laue groups, since two Laue groups comprise each of the cubic, tetragonal, rhombohedral, and hexagonal crystal systems. The alpha-numeric notation used to label each point group gives details about symmetries of crystals in that group, and a number of different notational schemes exist in crystallography for labeling point (and space) groups. The reader is referred to Thurston (1974), Rohrer (2001), and references therein for a more detailed explanation. Modern Hermann-Mauguin international symbols are used in column five of Table A.1, following Rohrer (2001). Columns six and seven of Table A.1 follow the scheme of Thurston (1974), who in turn cites Groth (1905).

Table A.1 Laue groups, generators, point groups, and crystal classes

Crystal system	Laue group	#	Generators	Point group	Crystal class	#
Triclinic	N	1	$\mathbf{1}$	1	triclinic asymmetric	1
				$\overline{1}$	triclinic pinacoidal*	2
Mono-clinic	M	2	$\mathbf{R}_k^2$	2	monoclinic sphenoidal	3
				m	monoclinic domatic	4
				$2/m$	monoclinic prismatic*	5
Ortho-rhombic	O	3	$\mathbf{R}_i^2$, $\mathbf{R}_j^2$	222	orthorhombic disphenoidal	6
				$mm2$	orthorhombic pyramidal	7
				mmm	orthorhombic dipyramidal*	8
Tetrago-nal	TII	4	$\mathbf{R}_k^4$	4	tetragonal pyramidal	10
				$\overline{4}$	tetragonal disphenoidal	9
				$4/m$	tetragonal dipyramidal*	13
Tetrago-nal	TI	5	$\mathbf{R}_k^4$, $\mathbf{R}_i^2$	422	tetragonal trapezohedral	12
				$4mm$	ditetragonal pyramidal	14
				$\overline{4}2m$	tetragonal scalenohedral	11
				$4/mmm$	ditetragonal dipyramidal*	15
Rhom-bohedral	RII	6	$\mathbf{R}_k^3$	3	trigonal pyramidal	16
				$\overline{3}$	trigonal rhombohedral*	17
Rhom-bohedral	RI	7	$\mathbf{R}_k^3$, $\mathbf{R}_i^2$	32	trigonal trapezohedral	18
				$3m$	ditrigonal pyramidal	20
				$\overline{3}m$	ditrigonal scalenohedral*	21
Hexago-nal	HII	8	$\mathbf{R}_k^6$	6	hexagonal pyramidal	23
				$\overline{6}$	trigonal dipyramidal	19
				$6/m$	hexagonal dipyramidal*	25
Hexago-nal	HI	9	$\mathbf{R}_k^6$, $\mathbf{R}_i^2$	622	hexagonal trapezohedral	24
				$6mm$	dihexagonal pyramidal	26
				$\overline{6}m2$	ditrigonal dipyramidal	22
				$6/mmm$	dihexagonal dipyramidal*	27
Cubic	CII	10	$\mathbf{R}_i^2$, $\mathbf{R}_j^2$, $\mathbf{R}_m^3$	23	cubic tetartoidal	28
				$m\overline{3}$	cubic diploidal*	30
Cubic	CI	11	$\mathbf{R}_i^4$, $\mathbf{R}_j^4$, $\mathbf{R}_k^4$	432	cubic gyroidal	29
				$4\overline{3}m$	cubic hextetrahedral	31
				$m\overline{3}m$	cubic hexoctahedral*	32
Transversely iso-tropic**		12	$\mathbf{R}_k^\varphi$, $0 < \varphi < 2\pi$			
Isotropic**		13	all proper rotations			

*Denotes a point group with an inversion center   **Not a natural crystal system

Particular aspects of each Laue group are discussed next. The reader is referred to Bond et al. (1949), Landau and Lifshitz (1959), and Teodosiu (1982) for additional details. Formal standards on terminology and assignment of coordinate systems for crystalline solids are given by Bond et al. (1949).

The triclinic crystal system contains Laue group N or 1. This system has the lowest material symmetry; a triclinic crystal has no symmetry axes or planes. Though the coordinate system corresponding to $\mathbf{R}_{N}^{n}$ in Table A.1 may be chosen arbitrarily (Landau and Lifshitz 1959), standard conventions do exist for selecting $\mathbf{i}$, $\mathbf{j}$, and $\mathbf{k}$ for a given specimen (Bond et al. 1949).

Monoclinic crystals belong to Laue group M or 2 in the numbering scheme of Table A.1. Crystals of this system possess at any point, an axis of symmetry of second order, a single plane of reflection symmetry, or both. The coordinate system corresponding to $\mathbf{R}_{N}^{n}$ is chosen such that $\mathbf{k}$ is aligned along the axis of symmetry or is perpendicular to the plane of symmetry.

The orthorhombic system includes Laue group O or 3. It describes crystals with three mutually perpendicular twofold axes, two mutually perpendicular planes of reflection symmetry, or both. The coordinate system corresponding to $\mathbf{R}_{N}^{n}$ is chosen such that $\mathbf{i}$ and $\mathbf{j}$ are aligned along the twofold axes or perpendicular to the planes of symmetry. If in this case $\mathbf{k}$ is also a plane of symmetry, then the orthorhombic crystal is also orthotropic.

The tetragonal system includes Laue groups TII (4) and TI (5). Crystals of group TII have a single axis of fourfold symmetry. The $\mathbf{k}$ axis is chosen parallel to this axis. Crystals of the tetragonal subsystem TI possess, in addition to this fourfold axis, an axis of twofold symmetry along vector $\mathbf{i}$.

The rhombohedral system includes Laue groups RII (6) and RI (7). Crystals of these groups have an axis of threefold symmetry, conventionally called the c-axis when the Bravais-Miller system is used. For this reason, sometimes the rhombohedral system is referred to as the trigonal system. Furthermore, sometimes groups 6 and 7 are labeled as belonging to the hexagonal system, even though crystals of these groups do not possess an axis of sixfold symmetry. The unit vector $\mathbf{k}$ is taken parallel to the axis of symmetry, that is, parallel to the c-axis. Crystals of group RI also possess an axis of twofold symmetry parallel to unit vector $\mathbf{i}$.

The hexagonal system contains Laue groups HII (8) and HI (9). These crystals have an axis of sixfold symmetry, conventionally labeled the c-axis. According to the notation in Table A.1, unit vector $\mathbf{k}$ is aligned parallel to the axis of sixfold symmetry. Crystals of group HI also possess an axis of twofold symmetry parallel to unit vector $\mathbf{i}$.

The cubic crystal system includes Laue groups CII (10) and CI (11). Cubic crystals have three twofold axes of symmetry. The coordinate system is chosen such that **i**, **j**, and **k** are each parallel to one of these cube axes. Groups CII and CI are distinguished by their generators as is clear from Table A.1.

Two other forms of symmetry not corresponding to any natural crystal class arise often: transverse isotropy and isotropy. The rotation group $\mathbb{Q}^+$ for transverse isotropy, i.e., group 12 in Table A.1, includes the unit tensor and all rotations $\mathbf{R}_{\mathbf{k}}^{n}$ where **k** is normal to the plane of isotropy and $1 < n < \infty$. When $\mathbb{Q}^+$ consists of all proper orthogonal tensors, the material is isotropic; otherwise, it is anisotropic (i.e., aleotropic). The rotation group for isotropy is labeled 13. Isotropic materials are always centrosymmetric.

Table A.2 Symmetry elements of crystal systems, after Thurston (1974)

Crystal system	Essential symmetry
Triclinic	None
Monoclinic	One 2-fold axis or one plane
Orthorhombic	Three orthogonal 2-fold axes or 2 planes intersecting via a 2-fold axis
Tetragonal	Either a 4-fold rotation axis or a 4-fold rotation-inversion axis
Rhombohedral	One 3-fold axis but no 6-fold rotation or 6-fold rotation-inversion axis
Hexagonal	Either a 6-fold rotation axis or a 6-fold rotation-inversion axis
Cubic	Four 3-fold rotation axes which also implies three 2-fold axes

A.2 Generic Material Coefficients

Material coefficients are listed in matrix form in Tables A.3-A.7 for each of the thirty-two point groups, following Thurston (1974), who in turn refers to Mason (1966). The point group numbers used in Tables A.3 and A.6 correspond to those in the rightmost column of Table A.1. The Laue group numbers used in Tables A.4, A.5, and A.7 correspond to those in the third column of Table A.1. Tensors of rank (i.e., order) one are given in Table A.3, of rank two in Tables A.4 and A.5, of rank three in Table A.6, and of rank four in Table A.7. These are all so-called polar tensors of Thurston (1974), defined as derivatives of thermodynamic potentials with respect to state variables measured in some thermoelastically undistorted state. This undistorted state could be the stress-free reference configuration of thermoelasticity (Chapter 5 and Chapter 10), or the stress-free intermediate configuration(s) of finite elastoplasticity (Chapter 6-Chapter 9). State variables in these contexts of geometrically nonlinear mechanics

must have components referred to the coordinate system corresponding to the undistorted state, and not referred to the deformed spatial configuration, for example. Obviously, the state variables and resulting material coefficients must also be referred to a single consistent configuration; e.g., two-point tensors of material coefficients may not always exhibit the symmetries evident in Tables A.3-A.7. Material coefficients as defined in the present context are constants at an undistorted reference state wherein vector- and tensor-valued independent thermodynamic state variables such as electric polarization and strain vanish, and wherein the material exhibits the full symmetry of its original crystal structure. Tangent material coefficients do not necessarily obey the definition of a polar tensor used here in Appendix A and may have different symmetries than those listed in the forthcoming tables. For example, the matrix of isotropic tangent elastic moduli in (5.119) depends on up to eight independent scalar functions and does not generally exhibit the same symmetries as the matrix formed from two independent second-order elastic constants in (5.121) and (5.122).

Examples of polar tensors of rank one include pyroelectric coefficients of (10.197), (10.206), and (10.211). Examples of polar tensors of rank two include thermal stress coefficients of (5.68), (5.85), and (5.201); second-order thermal expansion coefficients of (5.201); Gruneisen's tensor entering (5.223); dielectric susceptibilities of (10.189) and (10.205); and the dielectric permittivity tensor of (10.208). Examples of polar tensors of rank three include piezoelectric coefficients of (10.191), (10.205), and (10.209). Polar tensors of rank four include the second-order elastic stiffness tensor of (5.65), (5.85), and (5.90), as well as its inverse, i.e., the tensor of second-order compliance constants measured in an undistorted reference state.

Coefficients of polar tensors of odd rank vanish identically for all eleven classes of centrosymmetric crystals. Coefficients of polar tensors of rank three also vanish for non-centrosymmetric crystal class 432 (point group 29) because of other symmetry properties of this cubic structure (Thurston 1974). Tensors of rank one, e.g., pyroelectric coefficients, vanish in all but ten of the twenty-one crystal classes lacking an inversion center.

Indices of coefficients listed in Tables A.3-A.7 are referred to rectangular Cartesian axes X^1, X^2, X^3. Care must be taken to properly account for the relationship between these axes and the crystallographic axes, especially when interpreting experimental data for elastic constants of materials of less than cubic symmetry. Standards exist for various crystal classes (Bond et al. 1949), though in some cases ambiguities arise leading to different sign conventions for the coefficients (Winey et al. 2001). Methods for identifying material symmetry of a substance given the values of second-order elastic constants referred to a known—but otherwise arbitrary

with respect to material structure—coordinate system have been developed (Cowin and Mehrabadi 1987).

Tensors of rank two are written first in Table A.4 without presuming symmetry a priori; symmetric forms are then indicated in Table A.5, corresponding for example to thermal stress or thermal expansion coefficients. Notably, symmetric polar tensors of rank two are diagonal in form for crystals of all Laue groups that are not triclinic or monoclinic. Furthermore, for cubic crystals (and for isotropic solids), polar tensors of rank two are spherical with only one unique entry.

Table A.3 Forms of rank one polar tensors (Thurston 1974)

Point groups:	1	3	4	7,10,14,16,20,23,26	Others
Components	1	0	1	0	0
	2	2	0	0	0
	3	0	3	3	0
No. constants:	3	1	2	1	0

Table A.4 Forms of rank two polar tensors (Thurston 1974)

Laue groups*:	1	2	3	4,6,8	5,7,9,12	10,11,13
Components	11	11	11	11	11	11
	12	0	0	12	0	0
	13	13	0	0	0	0
	21	0	0	-12	0	0
	22	22	22	11	11	11
	23	0	0	0	0	0
	31	31	0	0	0	0
	32	0	0	0	0	0
	33	33	33	33	33	11
No. constants:	9	5	3	3	2	1

*Includes transversely isotropic (12) and isotropic (13)

Table A.5 Forms of symmetric rank two polar tensors (Thurston 1974)

Laue groups*:	1	2	3	4,6,8	5,7,9,12	10,11,13
Components	11	11	11	11	11	11
	12	0	0	0	0	0
	13	13	0	0	0	0
	12	0	0	0	0	0
	22	22	22	11	11	11
	23	0	0	0	0	0
	13	13	0	0	0	0
	23	0	0	0	0	0
	33	33	33	33	33	11
No. constants:	6	4	3	2	2	1

*Includes transversely isotropic (12) and isotropic (13)

Tensors of orders three and four, on the other hand, are written for conciseness by assuming additional symmetries. Specifically in Table A.6, the last two indices are reduced to one according to the Voigt (1928) notation, assuming that these indices correspond to differentiation of the thermodynamic potential with respect to a symmetric variable. For example, the nine components of a symmetric second-order tensor reduce to six according to the correspondence

$$11 \sim 1, \qquad 22 \sim 2, \qquad 33 \sim 3,$$
$$23 = 32 \sim 4, \quad 31 = 13 \sim 5, \quad 12 = 21 \sim 6. \tag{A.2}$$

In Table A.6, the first index spanning 1,2,3 which varies among the three rows of that matrix corresponds to the component of the polar tensor arising from differentiation of a thermodynamic potential with respect to a vector. The second index spanning 1,2,…6 which varies among six columns corresponds to differentiation with respect to a symmetric second order tensor. When this polar tensor describes piezoelectric-type coefficients, for example, the vector is the electrical variable and the tensor is the symmetric elastic strain or stress. The convention used here is consistent with that of Section 10.3.6.

Table A.6 Forms of rank three polar tensors (Thurston 1974)

Point groups:	1	3	4	6	7	9	10,23	11
Components	11	0	11	0	0	0	0	0
	12	0	12	0	0	0	0	0
	13	0	13	0	0	0	0	0
	14	14	0	14	0	14	14	14
	15	0	15	0	15	0	0	0
	16	16	0	0	0	15	0	0
	21	21	0	0	0	0	0	0
	22	22	0	0	0	0	0	0
	23	23	0	0	0	0	0	0
	24	0	24	0	24	-15	0	0
	25	25	0	25	0	14	-14	14
	26	0	26	0	0	0	0	0
	31	0	31	0	31	31	0	0
	32	0	32	0	32	-31	0	0
	33	0	33	0	33	0	0	0
	34	34	0	0	0	0	0	0
	35	0	35	0	0	0	0	0
	36	36	0	36	0	36	0	36
No. constants:	18	8	10	3	5	4	1	2

Table A.6 (Continued)

Point groups:	12,24	14,26*	16	18	19	20	22	28,31
Components	0	0	11	11	11	0	11	0
	0	0	-11	-11	-11	0	-11	0
	0	0	0	0	0	0	0	0
	14	0	14	14	0	0	0	14
	0	15	15	0	0	15	0	0
	0	0	-22	0	-22	-22	0	0
	0	0	-22	0	-22	-22	0	0
	0	0	22	0	22	22	0	0
	0	0	0	0	0	0	0	0
	0	15	15	0	0	15	0	0
	-14	0	-14	-14	0	0	0	14
	0	0	-11	-11	-11	0	-11	0
	0	31	31	0	0	31	0	0
	0	31	31	0	0	31	0	0
	0	33	33	0	0	33	0	0
	0	0	0	0	0	0	0	0
	0	0	0	0	0	0	0	0
	0	0	0	0	0	0	0	14
No. constants:	1	3	6	2	2	4	1	1

*Includes transversely isotropic

The coefficients in Table A.7 are written assuming symmetry with respect to each individual pair of indices, consistent with Section 5.1.5. This symmetry reduces the maximum number of independent coefficients from $3^4=81$ to $6\times6=36$. For example, for the case of elastic moduli, each index spanning 1,2,…6 corresponds to differentiation of the strain energy density with respect to an independent component of strain. However, the matrices listed in Table A.7 are more generic than elastic moduli that result from the assumption of hyperelasticity, and do not require that the 6×6 matrix of coefficients is symmetric. Thus Table A.7 admits coefficients defined via differentiation of a thermodynamic potential with respect to two different symmetric, second-order tensors. The additional symmetry that would arise from differentiation with respect to the same symmetric second-order tensor further reduces the maximum number of independent coefficients to 21. This is discussed by example in the context of second-order elastic constants in Section A.3.

Table A.7 Forms of rank four polar tensors (Thurston 1974)

1	2	3	4	5	6	7	8	9	10	11	12	13
N	M	O	TII	TI	RII	RI	HII	HI	CII	CI	t-i	iso
11	11	11	11	11	11	11	11	11	11	11	11	11
12	12	12	12	12	12	12	12	12	12	12	12	12
13	13	13	13	13	13	13	13	13	13	12	13	12
14	0	0	0	0	14	14	0	0	0	0	0	0
15	15	0	0	0	-25	0	0	0	0	0	0	0
16	0	0	16	0	2×62	0	2×61	0	0	0	0	0
21	21	21	12	12	12	12	12	12	13	12	12	12
22	22	22	11	11	11	11	11	11	11	11	11	11
23	23	23	13	13	13	13	13	13	12	12	13	12
24	0	0	0	0	-14	-14	0	0	0	0	0	0
25	25	0	0	0	25	0	0	0	0	0	0	0
26	0	0	-16	0	-2×62	0	-2×61	0	0	0	0	0
31	31	31	31	31	31	31	31	31	12	12	31	12
32	32	32	31	31	31	31	31	31	13	12	31	12
33	33	33	33	33	33	33	33	33	11	11	33	11
34	0	0	0	0	0	0	0	0	0	0	0	0
35	35	0	0	0	0	0	0	0	0	0	0	0
36	0	0	0	0	0	0	0	0	0	0	0	0
41	0	0	0	0	41	41	0	0	0	0	0	0
42	0	0	0	0	-41	-41	0	0	0	0	0	0
43	0	0	0	0	0	0	0	0	0	0	0	0
44	44	44	44	44	44	44	44	44	44	44	44	A*
45	0	0	45	0	45	0	45	0	0	0	0	0
46	46	0	0	0	2×52	0	0	0	0	0	0	0
51	51	0	0	0	-52	0	0	0	0	0	0	0
52	52	0	0	0	52	0	0	0	0	0	0	0
53	53	0	0	0	0	0	0	0	0	0	0	0
54	0	0	-45	0	-45	0	-45	0	0	0	0	0
55	55	55	44	44	44	44	44	44	44	44	44	A*
56	0	0	0	0	2×41	2×41	0	0	0	0	0	0
61	0	0	61	0	-62	0	61	0	0	0	0	0
62	0	0	-61	0	62	0	-61	0	0	0	0	0
63	0	0	0	0	0	0	0	0	0	0	0	0
64	64	0	0	0	25	0	0	0	0	0	0	0
65	0	0	0	0	14	14	0	0	0	0	0	0
66	66	66	66	66	A*	A*	A*	A*	44	44	A*	A*
36	20	12	10	7	12	8	8	6	4	3	6	2

* $A = 11 - 12$

The discussion in Section A.1 pertains to a geometrically nonlinear response, as implied by (A.1). For geometrically linear or small-strain representations, the same symmetries in material coefficients listed in Tables A.3-A.7 still apply, following from appropriate linearization of the finite deformation descriptions.

As implied in the discussion of polar tensors above, (A.1) can be extended to apply when the free energy density (or another thermodynamic potential such as internal energy density) depends on other state variables, for example temperature in thermoelastic bodies or electric polarization in dielectric bodies. However, as noted by Thurston (1974), when polar tensors of odd rank are involved (e.g., piezoelectric constants in electromechanical theories), the number of operations needed to describe all kinds of symmetry in the response functions requires extension beyond those generators shared by all crystal classes within a given Laue group listed in Table A.1. This is evident from Table A.6, wherein sixteen different forms of rank three polar tensors are required to address the non-centrosymmetric point groups. Put another way, polar tensors of odd rank require precise consideration of which of the thirty-two point groups a crystal structure belongs, not just which of the eleven Laue groups it falls into. Delineation of symmetries of magnetic properties, outside the scope of this text, evidently requires introduction of ninety magnetic crystal classes (Thurston 1974).

A.3 Elastic Constants

Consider a hyperelastic body with a strain energy density function expressed in polynomial form as

$$
\Psi_0\left(E_{AB}\right) = \rho_0 \psi = \frac{1}{2!}\overline{\mathbb{C}}^{ABCD} E_{AB} E_{CD} + \frac{1}{3!}\overline{\mathbb{C}}^{ABCDEF} E_{AB} E_{CD} E_{EF}
$$
$$
+ \frac{1}{4!}\overline{\mathbb{C}}^{ABCDEFGH} E_{AB} E_{CD} E_{EF} E_{GH} + ...
$$
(A.3)

Strain energy per unit reference volume is Ψ_0, strain energy per unit mass is ψ, mass density is ρ_0, and elastic constants at null elastic strain (i.e., in the undistorted state) satisfy

$$
\overline{\mathbb{C}}^{ABCD} = \left.\frac{\partial^2 \Psi_0}{\partial E_{AB} \partial E_{CD}}\right|_{\mathbf{E}=0} , \text{ (second-order elastic constants);} \quad (A.4)
$$

$$
\overline{\mathbb{C}}^{ABCDEF} = \left.\frac{\partial^3 \Psi_0}{\partial E_{AB} \partial E_{CD} \partial E_{EF}}\right|_{\mathbf{E}=0} , \text{ (third-order constants);} \quad (A.5)
$$

$$
\overline{\mathbb{C}}^{ABCDEFGH} = \left.\frac{\partial^4 \Psi_0}{\partial E_{AB} \partial E_{CD} \partial E_{EF} \partial E_{GH}}\right|_{\mathbf{E}=0} , \text{ (fourth-order constants);} \quad (A.6)
$$

and so forth for elastic constants of orders higher than four. Recall from (5.10) that in a hyperelastic material of grade one, the second Piola-Kirchhoff stress tensor satisfies

$$\Sigma^{AB} = \rho_0 \frac{\partial \psi}{\partial E_{AB}} = \frac{\partial \Psi_0}{\partial E_{AB}} = \frac{\partial \Psi_0}{\partial E_{BA}} = \Sigma^{BA}, \tag{A.7}$$

leading to

$$\Sigma^{AB} = \overline{\mathbb{C}}^{ABCD} E_{CD} + \frac{1}{2} \overline{\mathbb{C}}^{ABCDEF} E_{CD} E_{EF}, \tag{A.8}$$

where terms of orders four and higher in the strain **E** are dropped from (A.3) henceforth. From the symmetry of strain tensor **E** and the hyperelastic definitions of the elastic moduli in (A.4) and (A.5),

$$\overline{\mathbb{C}}^{ABCD} = \overline{\mathbb{C}}^{(AB)(CD)} = \overline{\mathbb{C}}^{(CD)(AB)},$$
$$\overline{\mathbb{C}}^{ABCDEF} = \overline{\mathbb{C}}^{(AB)(CD)(EF)} = \overline{\mathbb{C}}^{(AB)(EF)(CD)}..., \tag{A.9}$$

implying that the tensor of second-order elastic constants contains at most 21 independent entries, and the tensor of third-order elastic constants at most 56 independent entries.

In the compact notation of Brugger (1964), Thurston (1974), and Teodosiu (1982), components of the stress and moduli are re-written to take advantage of these symmetries:

$$\Sigma^{(AB)} \sim \Sigma^{\overline{A}}, \ \overline{\mathbb{C}}^{(AB)(CD)} \sim \overline{\mathbb{C}}^{\overline{A}\overline{B}}, \ \overline{\mathbb{C}}^{(AB)(CD)(EF)} \sim \overline{\mathbb{C}}^{\overline{A}\overline{B}\overline{C}}. \tag{A.10}$$

Barred indices span 1,2,…6 and correspond to unbarred pairs of indices as indicated in (A.2). Consistent with (A.10), strains and second-order elastic compliances are re-written as

$$2E_{(AB)} = (1 + \delta_{AB})E_{\overline{A}}, \ 4\overline{\mathbb{S}}_{(AB)(CD)} = (1 + \delta_{AB})(1 + \delta_{CD})\overline{\mathbb{S}}_{\overline{A}\overline{B}}, \tag{A.11}$$

recalling from (5.148) that elastic moduli and compliances are inverses of each other:

$$2\overline{\mathbb{S}}_{ABCD}\overline{\mathbb{C}}^{CDEF} = \delta_{.A}^{E}\delta_{.B}^{F} + \delta_{.A}^{F}\delta_{.B}^{E}, \ \overline{\mathbb{S}}_{\overline{A}\overline{B}}\overline{\mathbb{C}}^{\overline{B}\overline{C}} = \delta_{.\overline{A}}^{\overline{C}}. \tag{A.12}$$

As a consequence of hyperelasticity, the elastic coefficients exhibit the remaining symmetries

$$\overline{\mathbb{C}}^{\overline{A}\overline{B}} = \overline{\mathbb{C}}^{(\overline{A}\overline{B})}, \ \overline{\mathbb{C}}^{\overline{A}\overline{B}\overline{C}} = \overline{\mathbb{C}}^{\overline{B}\overline{A}\overline{C}} = \overline{\mathbb{C}}^{\overline{A}\overline{C}\overline{B}} = \overline{\mathbb{C}}^{\overline{C}\overline{A}\overline{B}}, \ \overline{\mathbb{S}}_{\overline{A}\overline{B}} = \overline{\mathbb{S}}_{(\overline{A}\overline{B})}. \tag{A.13}$$

Using (A.10) and (A.11), the strain energy density of (A.3) is

$$\Psi_0\left(E_{\overline{A}}\right) = \frac{1}{2!} \overline{\mathbb{C}}^{\overline{A}\overline{B}} E_{\overline{A}} E_{\overline{B}} + \frac{1}{3!} \overline{\mathbb{C}}^{\overline{A}\overline{B}\overline{C}} E_{\overline{A}} E_{\overline{B}} E_{\overline{C}} + ..., \tag{A.14}$$

and the stress tensor of (A.8) is written compactly in Voigt's notation as

$$\Sigma^{\overline{A}} = \overline{\mathbb{C}}^{\overline{A}\overline{B}} E_{\overline{B}} + \frac{1}{2} \overline{\mathbb{C}}^{\overline{A}\overline{B}\overline{C}} E_{\overline{B}} E_{\overline{C}}. \tag{A.15}$$

Other condensed notations exist for elastic coefficients (Birch 1947; Murnaghan 1951; Hearmon 1953; Toupin and Bernstein 1961); transformation formulae among several notations are given by Brugger (1964).

The number of independent elastic coefficients for a given substance may be further reduced because of material symmetry associated with the structure of the substance. Specifically, the strain energy density Ψ_0 for crystals of a particular Laue group is invariant with respect to rotations of reference coordinates belonging to the proper rotation group $\mathbb{Q}^+$ of that Laue group. This requires that the strain energy density depend only on certain scalar functions, called invariants, of $\mathbf{E}$ (or of the symmetric deformation tensor $\mathbf{C} = \mathbf{F}^T\mathbf{F}$) that leave the energy unchanged with respect to such rotations (Smith and Rivlin 1958). Scalar invariants of $\mathbf{E}$ are labeled as $I_1, I_2, ... I_P$. The stress (A.7) can then be found as

$$\Sigma^{AB} = \sum_{\lambda=1}^{P} \frac{\partial \Psi_0}{\partial I_\lambda} \frac{\partial I_\lambda}{\partial E_{AB}}. \tag{A.16}$$

Lists of invariants for each Laue group are given by Truesdell and Noll (1965) and Teodosiu (1982) and are not repeated here. Consideration of the list of invariants for each Laue group enables deduction of the independent elastic coefficients for that group, as explained for example by Teodosiu (1982). Alternative arguments providing the independent elastic constants for various Laue groups are provided by Landau and Lifshitz (1959).

Tables A.8 and A.9 list independent second- and third-order elastic constants, respectively, for the eleven Laue groups of crystals, for transversely isotropic materials, and for isotropic bodies. The bottom row in each column provides the total number of independent coefficients. The reduced notation of Brugger (1964) explained in (A.10)-(A.15) is used in Tables A.8 and A.9. Table A.8 applies for (second-order) elastic compliance as well as elastic stiffness constants, while Table A.9 applies only for (third-order) elastic stiffness constants. As a result of (A.11), differences in factors of two arise among some entries of Tables A.7 and A.8. Notice that footnotes for Table A.9 continue onto the following page.

Second- and third-order elastic constants are often obtained from experimental measurements of sound velocities in stress-free and homogeneously stressed crystals, respectively (Thurston and Brugger 1964; Thomas 1968; Thurston 1974; Hiki 1981). Constants of orders four and higher, not listed here, may be important in some shock compression events (Graham 1992) and can be estimated from temperature dependence of lower-order elastic coefficients or deviations from a linear relationship between sound velocity and initial stress (Markenscoff 1977; Hiki 1981).

Table A.8 Second-order elastic constants (Brugger 1965; Teodosiu 1982)

1	2	3	4	5	6	7	8	9	10	11	12	13
N	M	O	TII	TI	RII	RI	HII	HI	CII	CI	t-i	iso
11	11	11	11	11	11	11	11	11	11	11	11	11
12	12	12	12	12	12	12	12	12	12	12	12	12
13	13	13	13	13	13	13	13	13	12	12	13	12
14	0	0	0	0	14	14	0	0	0	0	0	0
15	15	0	0	0	15	0	0	0	0	0	0	0
16	0	0	16	0	0	0	0	0	0	0	0	0
22	22	22	11	11	11	11	11	11	11	11	11	11
23	23	23	13	13	13	13	13	13	12	12	13	12
24	0	0	0	0	-14	-14	0	0	0	0	0	0
25	25	0	0	0	-15	0	0	0	0	0	0	0
26	0	0	-16	0	0	0	0	0	0	0	0	0
33	33	33	33	33	33	33	33	33	11	11	33	11
34	0	0	0	0	0	0	0	0	0	0	0	0
35	35	0	0	0	0	0	0	0	0	0	0	0
36	0	0	0	0	0	0	0	0	0	0	0	0
44	44	44	44	44	44	44	44	44	44	44	44	B^*
45	0	0	0	0	0	0	0	0	0	0	0	0
46	46	0	0	0	-15	0	0	0	0	0	0	0
55	55	55	44	44	44	44	44	44	44	44	44	B^*
56	0	0	0	0	14	14	0	0	0	0	0	0
66	66	66	66	66	A^*	A^*	A^*	A^*	44	44	A^*	A^*
21	13	9	7	6	7	6	5	5	3	3	5	2

$* \ A: 2\overline{\mathbb{C}}^{66} = \overline{\mathbb{C}}^{11} - \overline{\mathbb{C}}^{12}; \ \overline{S}_{66} = 2(\overline{S}_{11} - \overline{S}_{12})$

$B: 2\overline{\mathbb{C}}^{44} = \overline{\mathbb{C}}^{11} - \overline{\mathbb{C}}^{12}; \ \overline{S}_{44} = 2(\overline{S}_{11} - \overline{S}_{12})$

Table A.9 Third-order stiffness constants (Brugger 1965)

1 N	2 M	3 O	4 TII	5 TI	6 RII	7 RI	8 HII	9 HI	10 CII	11 CI	12 t-i	13 iso
111	111	111	111	111	111	111	111	111	111	111	111	111
112	112	112	112	112	112	112	112	112	112	112	112	112
113	113	113	113	113	113	113	113	113	113	112	113	112
114	0	0	0	0	114	114	0	0	0	0	0	0
115	115	0	0	0	115	0	0	0	0	0	0	0
116	0	0	116	0	116	0	0	0	0	0	0	0
122	122	122	112	112	A*	A*	A*	A*	113	112	112	112
123	123	123	123	123	123	123	123	123	123	123	123	123
124	0	0	0	0	124	124	0	0	0	0	0	0
125	125	0	0	0	125	0	0	0	0	0	0	0
126	0	0	0	0	-116	0	-116	0	0	0	0	0
133	133	133	133	133	133	133	133	133	112	112	133	112
134	0	0	0	0	134	134	0	0	0	0	0	0
135	135	0	0	0	135	0	0	0	0	0	0	0
136	0	0	136	0	0	0	0	0	0	0	0	0
144	144	144	144	144	144	144	144	144	144	144	144	L*
145	0	0	145	0	145	0	145	0	0	0	0	0
146	146	0	0	0	B*	0	0	0	0	0	0	0
155	155	155	155	155	155	155	155	155	155	155	155	M*
156	0	0	0	0	C*	C*	0	0	0	0	0	0
166	166	166	166	166	D*	D*	D*	D*	166	155	M*	M*
222	222	222	111	111	222	222	222	222	111	111	111	111
223	223	223	113	113	113	113	113	113	112	112	113	112
224	0	0	0	0	E*	E*	0	0	0	0	0	0
225	225	0	0	0	F*	0	0	0	0	0	0	0
226	0	0	-116	0	116	0	116	0	0	0	0	0
233	233	233	133	133	133	133	133	133	113	112	133	112
234	0	0	0	0	-134	-134	0	0	0	0	0	0
235	235	0	0	0	-135	0	0	0	0	0	0	0
236	0	0	-136	0	0	0	0	0	0	0	0	0
244	244	244	155	155	155	155	155	155	166	155	155	M*
245	0	0	-145	0	-145	0	-145	0	0	0	0	0
246	246	0	0	0	G*	0	0	0	0	0	0	0
255	255	255	144	144	144	144	144	144	144	144	144	L*
256	0	0	0	0	H*	H*	0	0	0	0	0	0
266	266	266	166	166	I*	I*	I*	I*	155	155	M*	M*
333	333	333	333	333	333	333	333	333	111	111	333	111
334	0	0	0	0	0	0	0	0	0	0	0	0
335	335	0	0	0	0	0	0	0	0	0	0	0
336	0	0	0	0	0	0	0	0	0	0	0	0
344	344	344	344	344	344	344	344	344	155	155	344	M*
345	0	0	0	0	0	0	0	0	0	0	0	0
346	346	0	0	0	-135	0	0	0	0	0	0	0
355	355	355	344	344	344	344	344	344	166	155	344	M*
356	0	0	0	0	134	134	0	0	0	0	0	0
366	366	366	366	366	J*	J*	J*	J*	144	144	J*	L*
444	0	0	0	0	444	444	0	0	0	0	0	0
445	445	0	0	0	445	0	0	0	0	0	0	0
446	0	0	446	0	145	0	145	0	0	0	0	0
455	0	0	0	0	-444	-444	0	0	0	0	0	0
456	456	456	456	456	K*	K*	K*	K*	456	456	K*	N*
466	0	0	0	0	124	124	0	0	0	0	0	0
555	555	0	0	0	-445	0	0	0	0	0	0	0
556	0	0	-446	0	-145	0	-145	0	0	0	0	0
566	566	0	0	0	125	0	0	0	0	0	0	0
666	0	0	0	0	-116	0	-116	0	0	0	0	0
56	32	20	16	12	20	14	12	10	8	6	9	3

Table A.9 (Continued)

*$A = 111 + 112 - 222$	$E = -114 - 2 \times 124$	$I = (2 \times 111 - 112 - 222)/4$	$M = (111 - 112)/4$
$B = -(115 + 3 \times 125)/2$	$F = -115 - 2 \times 125$	$J = (113 - 123)/2$	$N = (111 - 3 \times 112 + 2 \times 123)/8$
$C = (114 + 3 \times 124)/2$	$G = -(115 - 125)/2$	$K = -(144 - 155)/2$	
$D = -(2 \times 111 + 112 - 3 \times 222)/4$	$H = (114 - 124)/2$	$L = (112 - 123)/2$	

Highly symmetric materials are given special consideration in the text that follows. Specifically considered are cubic crystals, transversely isotropic materials, and isotropic materials.

A.3.1 Cubic Symmetry

Cubic crystals include Laue group numbers 10 and 11 in the notation of Table A.1. Both groups exhibit three independent second-order elastic constants. Group 10 exhibits eight independent third-order elastic constants, while group 11 exhibits six independent third-order elastic constants. All second rank polar tensors (e.g., thermal expansion coefficients) are spherical or diagonal in cubic crystals, as is clear from Table A.4. Neglecting third- and higher-order elastic coefficients, and when the coordinate system is chosen coincident with the cube axes, strain energy density (A.3) can be written as (Thurston 1974)

$$
\begin{aligned}
\Psi_0 &= \frac{1}{2}\overline{\mathbb{C}}^{12}(E_{.A}^{A})^2 + \overline{\mathbb{C}}^{44}E_{AB}E^{AB} \\
&\quad + \frac{1}{2}(\overline{\mathbb{C}}^{11} - \overline{\mathbb{C}}^{12} - 2\overline{\mathbb{C}}^{44})\left[(E_{11})^2 + (E_{22})^2 + (E_{33})^2\right] \\
&= \frac{1}{2}K(E_{.A}^{A})^2 + \overline{\mathbb{C}}^{44}E'_{AB}E'^{AB} - \mu'\left[(E'_{11})^2 + (E'_{22})^2 + (E'_{33})^2\right] \\
&= \frac{1}{2}K(E_{.A}^{A})^2 + 2\overline{\mathbb{C}}^{44}\left[(E_{12})^2 + (E_{23})^2 + (E_{31})^2\right] \\
&\quad + \frac{1}{2}(\overline{\mathbb{C}}^{11} - \overline{\mathbb{C}}^{12})\left[(E'_{11})^2 + (E'_{22})^2 + (E'_{33})^2\right] \\
&= \frac{1}{2}K(E_{.A}^{A})^2 + 2\overline{\mathbb{C}}^{44}\left[(E_{12})^2 + (E_{23})^2 + (E_{31})^2\right] \\
&\quad + \mu\left\{E'_{AB}E'^{AB} - 2\left[(E_{12})^2 + (E_{23})^2 + (E_{31})^2\right]\right\} \\
&= \frac{1}{2}K(E_{.A}^{A})^2 + \mu E'_{AB}E'^{AB} + 2\mu'\left[(E_{12})^2 + (E_{23})^2 + (E_{31})^2\right],
\end{aligned}
\tag{A.17}
$$

where $E'_{AB} = E_{AB} - \delta_{AB}E_{.C}^{C}/3$ is the deviatoric part of the strain tensor, satisfying the identity

$$E'^{AB} E'_{AB} = (E_{11})^2 + (E_{22})^2 + (E_{33})^2 + 2\left[(E_{12})^2 + (E_{23})^2 + (E_{31})^2\right]. \quad (A.18)$$

Second-order bulk modulus K and shear moduli μ and μ' are defined, respectively, in terms of cubic second-order elastic constants as

$$K = \frac{1}{3}(\overline{\mathbb{C}}^{11} + 2\overline{\mathbb{C}}^{12}), \ \mu = \frac{1}{2}(\overline{\mathbb{C}}^{11} - \overline{\mathbb{C}}^{12}), \ \mu' = \overline{\mathbb{C}}^{44} - \frac{1}{2}(\overline{\mathbb{C}}^{11} - \overline{\mathbb{C}}^{12}). \quad (A.19)$$

When $\mu' = 0$, the material becomes isotropic in the materially linear approximation of (A.17). An anisotropy ratio A (Zener 1948) measuring the deviation from isotropy is typically defined according to the formula $A = 2\overline{\mathbb{C}}^{44}/(\overline{\mathbb{C}}^{11} - \overline{\mathbb{C}}^{12}) = \overline{\mathbb{C}}^{44}/\mu$. When anisotropy ratio $A = 1$, the solid is perfectly isotropic. To ensure that the elastic strain energy density of (A.17) remains positive for any nonzero strain, the second-order cubic elastic constants are constrained by $K > 0$, $\mu > 0$, and $\overline{\mathbb{C}}^{44} > 0$.

When the deformation is spherical, the deformation gradient becomes $F^a_{.A} = J^{1/3}\delta^a_{.A}$ in Cartesian coordinates with strain $E_{AB} = (1/2)(J^{2/3} - 1)\delta_{AB}$, so that $E^A_{.A} = (3/2)(J^{2/3} - 1)$ and $E'_{AB} = 0$. In that case, all but the first term vanish on the right side of the final equality in (A.17), and the stress state is purely hydrostatic. The second Piola-Kirchhoff stress tensor becomes $\Sigma^{AB} = (3K/2)(J^{2/3} - 1)\delta^{AB}$ for spherical deformation, the Cauchy stress tensor becomes $\sigma^{ab} = (3K/2)(J^{1/3} - J^{-1/3})\delta^{ab}$, and the Cauchy pressure becomes $p = (3K/2)(J^{-1/3} - J^{1/3})$.

Elastic stress wave propagation (i.e., acoustic waves) and methods of determination of elastic constants in cubic crystals from ultrasonic measurements are discussed in detail by Thurston (1974). A procedure for determining cubic elastic constants at high pressures from sound wave velocities is outlined by Dandekar (1970).

A.3.2 Transverse Isotropy

Materials with transverse isotropy, belonging to rotation group 12 of Table A.1, exhibit five independent second-order elastic constants. Thus, the second-order moduli of transversely isotropic solids exhibit the same form as those of hexagonal crystals of Laue groups 8 and 9, as is clear from Table A.8. However, transversely isotropic materials have only nine independent third-order elastic constants. This is in contrast to hexagonal crystals which exhibit twelve independent constants (group 8) or ten constants (group 9). Transverse isotropy does not correspond to naturally occurring, single crystal Bravais lattices, but can emerge in polycrystalline samples

via texturing. It is also commonly used to describe properties of certain kinds of fiber-reinforced composite materials, for example those with randomly or periodically distributed cylindrical fibers oriented perpendicular to a plane of symmetry.

A.3.3 Isotropy

Isotropic solids exhibit two second-order elastic constants and three third-order elastic constants. The second-order elasticity tensor is constructed from two independent constants in Cartesian reference coordinates as

$$\overline{\mathbb{C}}^{ABCD} = \mu(\delta^{AC}\delta^{BD} + \delta^{AD}\delta^{BC}) + \lambda\delta^{AB}\delta^{CD}, \tag{A.20}$$

where μ is the shear modulus and λ is Lamé's constant. The third-order elastic constants of an isotropic elastic body can be written as (Toupin and Bernstein 1961; Teodosiu 1982)

$$\overline{\nu}_1 = \overline{\mathbb{C}}^{123}, \ \overline{\nu}_2 = \overline{\mathbb{C}}^{144}, \ \overline{\nu}_3 = \overline{\mathbb{C}}^{456}, \tag{A.21}$$

leading to the following representation of the third-order elastic moduli:

$$\begin{aligned}
\overline{\mathbb{C}}^{ABCDEF} = &\overline{\nu}_1\left[\delta^{AB}\delta^{CD}\delta^{EF}\right] \\
&+ \overline{\nu}_2\left[\delta^{AB}(\delta^{CE}\delta^{DF} + \delta^{CF}\delta^{DE}) + \delta^{CD}(\delta^{AE}\delta^{BF} + \delta^{AF}\delta^{BE})\right. \\
&\left. \quad + \delta^{EF}(\delta^{AC}\delta^{BD} + \delta^{AD}\delta^{BC})\right] \\
&+ \overline{\nu}_3\left[\delta^{AC}(\delta^{BE}\delta^{DF} + \delta^{BF}\delta^{DE}) + \delta^{BD}(\delta^{AE}\delta^{CF} + \delta^{AF}\delta^{CE})\right. \\
&\left. \quad + \delta^{AD}(\delta^{BE}\delta^{CF} + \delta^{BF}\delta^{CE}) + \delta^{BC}(\delta^{AE}\delta^{DF} + \delta^{AF}\delta^{DE})\right].
\end{aligned} \tag{A.22}$$

In the absence of material nonlinearity (i.e., omitting the third-order elastic constants), the strain energy density and stress-strain relations are simply

$$\Psi_0 = \frac{1}{2}\lambda(E_{.A}^A)^2 + \mu E_{AB}E^{AB}, \tag{A.23}$$

$$\Sigma^{AB} = \lambda E_{.C}^C\delta^{AB} + 2\mu E^{AB}. \tag{A.24}$$

Three other elastic constants are often introduced to describe the isotropic mechanical behavior demonstrated in (A.23): elastic modulus E, Poisson's ratio ν, and bulk modulus K. Relationships among the five isotropic second-order elastic constants are listed in Table A.10. To ensure that the elastic strain energy density of (A.23) remains positive for all non-zero strains, isotropic elastic constants are restricted to $\mu > 0$, $E > 0$, $K > 0$, and $-1 < \nu \leq 1/2$. When $\nu = 1/2$, then $\mu = E/3$, $1/K = 0$, $K \to \infty$, and the material is elastically incompressible.

Using definitions in Table A.10, stress-strain relations (A.24) become

$$\Sigma'_{AB} = 2\mu E'_{AB}, \ \Sigma^A_{.A} = 3KE^A_{.A}. \tag{A.25}$$

The first of (A.25) relates the deviatoric (i.e., traceless) parts of second Piola-Kirchhoff stress and right Cauchy-Green strain, and the second relates spherical parts of stress and strain measures. When the deformation is spherical with $F^a_{.A} = J^{1/3}\delta^a_{.A}$, the stress state is hydrostatic, with Cauchy pressure $p = (3K/2)(J^{-1/3} - J^{1/3})$; the same relationship is observed for materials with cubic symmetry as mentioned already in Section A.3.1.

Returning now to the materially nonlinear case, third-order elastic constants can be related to pressure derivatives of tangent bulk and shear moduli, $\bar{K}$ and $\bar{\mu}$ respectively, at an undistorted stress-free state as (Teodosiu 1982)

$$-K\frac{\partial \bar{K}}{\partial p}\bigg|_{p=0} = \bar{\nu}_1 + 2\bar{\nu}_2 + \frac{8}{9}\bar{\nu}_3, \ -K\frac{\partial \bar{\mu}}{\partial p}\bigg|_{p=0} = K + \frac{1}{3}\mu + \bar{\nu}_2 + \frac{4}{3}\bar{\nu}_3. \tag{A.26}$$

A more in-depth treatment of pressure derivatives of elastic coefficients, including those of anisotropic crystals, is given by Thurston (1974).

Table A.10 Relationships among second-order elastic constants of isotropic solids

	E	ν	μ	K	λ
E,ν	-	-	$\dfrac{E}{2(1+\nu)}$	$\dfrac{E}{3(1-2\nu)}$	$\dfrac{E\nu}{(1+\nu)(1-2\nu)}$
E,μ	-	$\dfrac{E-2\mu}{2\mu}$	-	$\dfrac{E\mu}{3(3\mu-E)}$	$\dfrac{\mu(E-2\mu)}{3\mu-E}$
E,K	-	$\dfrac{3K-E}{6K}$	$\dfrac{3EK}{9K-E}$	-	$\dfrac{3K(3K-E)}{9K-E}$
E,λ *	-	$\dfrac{2\lambda}{E+\lambda+A}$	$\dfrac{E-3\lambda+A}{4}$	$\dfrac{E+3\lambda+A}{6}$	-
ν,μ	$2\mu(1+\nu)$	-	-	$\dfrac{2\mu(1+\nu)}{3(1-2\nu)}$	$\dfrac{2\nu\mu}{1-2\nu}$
ν,K	$3K(1-2\nu)$	-	$\dfrac{3K(1-2\nu)}{2(1+\nu)}$	-	$\dfrac{3\nu K}{1+\nu}$
ν,λ	$\dfrac{\lambda(1+\nu)(1-2\nu)}{\nu}$	-	$\dfrac{\lambda(1-2\nu)}{2\nu}$	$\dfrac{\lambda(1+\nu)}{3\nu}$	-
μ,K	$\dfrac{9\mu K}{\mu+3K}$	$\dfrac{3K-2\mu}{6K+2\mu}$	-	-	$\dfrac{3K-2\mu}{3}$
μ,λ	$\dfrac{\mu(2\mu+3\lambda)}{\mu+\lambda}$	$\dfrac{\lambda}{2(\mu+\lambda)}$	-	$\dfrac{2\mu+3\lambda}{3}$	-
λ,K	$\dfrac{9K(K-\lambda)}{3K-\lambda}$	$\dfrac{\lambda}{3K-\lambda}$	$\dfrac{3(K-\lambda)}{2}$	-	-

* $A = (E^2 + 2E\lambda + 9\lambda^2)^{1/2}$

In many applications, the effect of elastic material nonlinearity on deviatoric stresses may be negligible. For example, in ductile metallic crystals, plastic yielding (i.e., dislocation glide) may take place before large deviatoric elastic strains are attained. However, because dislocation glide is isochoric as discussed in Section 3.2 of Chapter 3, volumetric strains cannot be accommodated inelastically in the absence of defects (e.g., in the absence of vacancy formation, void growth, or fracture). In such cases, it may be prudent discard from (A.3) only terms of order greater than two in the deviatoric strains:

$$\Psi_0 = \frac{1}{2}\overline{\mathbb{C}}^{ABCD}E_{AB}E_{CD} - \frac{1}{3}K_1\delta^{AB}\delta^{CD}\delta^{EF}E_{AB}E_{CD}E_{EF} , \qquad (A.27)$$

where for an isotropic solid, setting $E_{AB} \propto \delta_{AB}$ in (A.22) and (A.27) gives

$$K_1 = -\overline{\nu}_1 - 2\overline{\nu}_2 - \frac{8}{9}\overline{\nu}_3 . \qquad (A.28)$$

The bulk modulus usually increases with increasing (compressive) pressure, in which case from (A.26) and (A.28), $K_1 > 0$. The first term in (A.27) can be anisotropic; for the particular case of isotropic second-order elasticity (Clayton 2005b)

$$\Psi_0 = \frac{1}{2}K(E^A_{.A})^2 + \mu E'_{AB}E'^{AB} - \frac{1}{3}K_1(E^A_{.A})^3 , \qquad (A.29)$$

resulting in the stress-strain relations

$$\Sigma^{AB} = \overline{K}E^C_{.C}\delta^{AB} + 2\mu E'^{AB} , \qquad (A.30)$$

where the apparent bulk modulus is

$$\overline{K} = K - K_1 E^A_{.A} . \qquad (A.31)$$

Deviatoric and spherical parts of the second Piola-Kirchhoff stress are then, respectively,

$$\Sigma'^{AB} = 2\mu E'^{AB} , \quad \Sigma^A_{.A} = 3\overline{K}E^A_{.A} . \qquad (A.32)$$

The approach taken in (A.27)-(A.32) is comparable to that of Murnaghan (1944), who assumed a bulk modulus linearly dependent on pressure.

Naturally occurring isotropic single crystals are rare, a notable exception being tungsten single crystals at room temperature and small deformations (Hirth and Lothe 1982). The isotropic description is often used for aggregates of a large number of polycrystals with random texture and for amorphous solids such as non-crystalline polymers and glasses. Though typically the (isotropic) elastic constants of polycrystals are measured directly using mechanical testing or ultrasonic techniques, theoretical methods exist for estimating effective isotropic elastic constants of an aggregate from anisotropic elastic constants of its constituents. A number of methods based on various averaging or self-consistent assumptions have been de-

veloped, as can be found in texts on micromechanics (Mura 1982; Nemat-Nasser and Hori 1993; Buryachenko 2007). The two simplest, yet still physically realistic, methods are referred to as Voigt's approximation and Reuss's approximation.

In Voigt's approximation, all single crystals of the volume element of a polycrystalline are assigned the same strain $\mathbf{E}$, and the total stress supported by the polycrystal is taken as the volume average of the stresses in each crystal. This leads to the definition of the Voigt average second-order elastic constants

$$\overline{\mathbb{C}}_V^{ABCD} = V^{-1} \int_V \overline{\mathbb{C}}^{ABCD}(X) dV \,, \tag{A.33}$$

where the average components $\overline{\mathbb{C}}_V^{ABCD}$ and the local single crystal constants $\overline{\mathbb{C}}^{ABCD}$, the latter listed in Table A.8 for crystals of different Laue groups, are all referred to the same global Cartesian coordinate system. The reference volume of the aggregate is denoted by V. Omitting elastic constants of orders three and higher, the average second Piola-Kirchhoff stress is

$$\Sigma_V^{AB} = \overline{\mathbb{C}}_V^{ABCD} E_{CD} \,, \tag{A.34}$$

where $\overline{\mathbb{C}}_V^{ABCD}$ is assumed in the present application to exhibit isotropic symmetry of the form in (A.20). For an imposed spherical strain tensor $E_{CD} = E_{.F}^F \delta_{CD}/3$, substituting (A.33) into the trace of (A.34) gives

$$3(\Sigma_V)_{.A}^A = (\overline{\mathbb{C}}_V)_{.A}^{A.CD} E_{.F}^F \delta_{CD} = \frac{1}{V} E_{.F}^F \int_V \overline{\mathbb{C}}_{.A.C}^{A.C} dV$$

$$= \overline{\mathbb{C}}_{.A.C}^{A.C} E_{.F}^F = 9 K_V E_{.F}^F \,, \tag{A.35}$$

since the integrand in (A.35) is a scalar invariant. The Voigt average bulk modulus K_V follows in full tensor notation and reduced Voigt notation, respectively, as

$$K_V = \frac{1}{9} \overline{\mathbb{C}}_{.A.B}^{A.B} = \frac{1}{9} \left[\overline{\mathbb{C}}^{1111} + \overline{\mathbb{C}}^{2222} + \overline{\mathbb{C}}^{3333} + 2(\overline{\mathbb{C}}^{1122} + \overline{\mathbb{C}}^{2233} + \overline{\mathbb{C}}^{3311}) \right]$$

$$= \frac{1}{9} \left[\overline{\mathbb{C}}^{11} + \overline{\mathbb{C}}^{22} + \overline{\mathbb{C}}^{33} + 2(\overline{\mathbb{C}}^{12} + \overline{\mathbb{C}}^{23} + \overline{\mathbb{C}}^{13}) \right]. \tag{A.36}$$

When single crystals of the aggregate are cubic, comparison with (A.19) demonstrates that (A.36) is exact. For an imposed shear strain E_{12}, relation (A.34) gives

$$\Sigma_V^{12} = 2\overline{\mathbb{C}}_V^{1212} E_{12} = 2\mu_V E_{12} \,, \tag{A.37}$$

where the Voigt average shear modulus μ_V is given by (Hill 1952)

$$\mu_V = \frac{1}{30}\left[3\overline{\mathbb{C}}^{AB}_{..AB} - \overline{\mathbb{C}}^{A.B}_{.A.B}\right] = \frac{1}{10}\left[\overline{\mathbb{C}}^{AB}_{..AB} - 3K_V\right]$$

$$= \frac{1}{15}\left[(\overline{\mathbb{C}}^{11} + \overline{\mathbb{C}}^{22} + \overline{\mathbb{C}}^{33}) - (\overline{\mathbb{C}}^{12} + \overline{\mathbb{C}}^{23} + \overline{\mathbb{C}}^{13}) + 3(\overline{\mathbb{C}}^{44} + \overline{\mathbb{C}}^{55} + \overline{\mathbb{C}}^{66})\right]. \quad (A.38)$$

For an aggregate composed of cubic single crystals with elastic constants of the form listed in (A.19), the final expression in (A.38) reduces to

$$\mu_V = \frac{1}{5}(\overline{\mathbb{C}}^{11} - \overline{\mathbb{C}}^{12}) + \frac{3}{5}\overline{\mathbb{C}}^{44} = \frac{2}{5}\mu + \frac{3}{5}(\mu + \mu'). \quad (A.39)$$

In the Reuss approximation, all single crystals of the element of polycrystal are assigned the same stress $\mathbf{\Sigma}$, and the strain $\mathbf{E}$ supported by the polycrystal is taken as the volume average of the strains in each crystal. This leads to the definition of Reuss average second-order elastic compliance

$$(\overline{S}_R)_{ABCD} = V^{-1}\int_V S_{ABCD}(X)dV, \quad (A.40)$$

where average components $(\overline{S}_R)_{ABCD}$ and local single crystal constants $\overline{S}_{ABCD}$ are all referred to the same global Cartesian coordinate system. Recall that general forms of single crystal compliance tensors are listed in Table A.8 for crystal classes of each of the eleven Laue groups. The Reuss average bulk modulus K_R is found, using a procedure similar to (A.35), as (Hill 1952; Mura 1982)

$$K_R = 1/\overline{S}^{A.B}_{.A.B} = \left[\overline{S}_{11} + \overline{S}_{22} + \overline{S}_{33} + 2(\overline{S}_{12} + \overline{S}_{23} + \overline{S}_{13})\right]^{-1}. \quad (A.41)$$

The Reuss average shear modulus μ_R is (Hill 1952)

$$\mu_R = \left\{\frac{1}{15}\left[4(\overline{S}_{11} + \overline{S}_{22} + \overline{S}_{33}) - 4(\overline{S}_{12} + \overline{S}_{23} + \overline{S}_{13})\right.\right.$$

$$\left.\left. + 3(\overline{S}_{44} + \overline{S}_{55} + \overline{S}_{66})\right]\right\}^{-1}. \quad (A.42)$$

For cubic single crystals, the Reuss average shear modulus reduces to

$$\mu_R = \left[\frac{4}{5(\overline{\mathbb{C}}^{11} - \overline{\mathbb{C}}^{12})} + \frac{3}{5\overline{\mathbb{C}}^{44}}\right]^{-1} = \left[\frac{2}{5\mu} + \frac{3}{5(\mu + \mu')}\right]^{-1}. \quad (A.43)$$

The Reuss average bulk modulus is exact, and is the same as the Voigt average bulk modulus, when single crystals of the aggregate are cubic in symmetry. The difference between polycrystalline shear moduli computed using Voigt and Reuss averaging when single crystals of the aggregate are cubic is

$$\mu_V - \mu_R = \frac{3}{5}\frac{[2\overline{\mathbb{C}}^{44} - (\overline{\mathbb{C}}^{11} - \overline{\mathbb{C}}^{12})]^2}{[4\overline{\mathbb{C}}^{44} + 3(\overline{\mathbb{C}}^{11} - \overline{\mathbb{C}}^{12})]}. \quad (A.44)$$

It is noted that Voigt and Reuss averaged bulk moduli depend only on six of the up to 21 independent single crystal elastic constants. Voigt and Reuss averaged shear moduli depend only on nine of up to 21 independent single crystal elastic constants.

It can be shown (Hill 1952; Mura 1982; Nemat-Nasser and Horii 1999) that Voigt average (A.33) provides an upper bound to the exact effective elastic stiffness constants of a heterogeneous polycrystal, and the inverse of the Reuss average (A.40) provides a lower bound for the elastic stiffness. For the true effective bulk modulus K_E and shear modulus μ_E, the following bounds apply, for example:

$$K_R \leq K_E \leq K_V , \ \mu_R \leq \mu_E \leq \mu_V . \tag{A.45}$$

Voigt and Reuss definitions of effective elastic constants in (A.33) and (A.40) also can be prescribed when the overall behavior of the material is anisotropic, though in that case (A.24) does not strictly apply.

Appendix B: Lattice Statics and Dynamics

A brief overview of the governing equations of classical mechanics of discrete (e.g., particle or atomic) systems is given. This overview provides insight into general methods often used in mechanics, in an analogous fashion, to describe behavior of continuous bodies, e.g., Hamilton's principle and the Euler-Lagrange equations. A description of lattice statics then offers insight into atomic-scale origins of stress tensors and elastic coefficients. This account is not comprehensive; areas not explicitly addressed are relativistic effects, lattice vibrations, electronic structure, thermal, optical, and electrical properties of matter, or topics in quantum and statistical mechanics. While terms lattice statics and lattice dynamics are used often, unless noted otherwise the description applies to any discrete particle system with conservative internal forces, regardless of whether or not such particles occupy positions on a regular lattice.

B.1 Dynamics

Governing equations of classical mechanics of discrete particle systems are now surveyed briefly. Successively discussed are Newton's equations of motion, Lagrange's equations, and equations of motion in Hamiltonian form. Much of the survey follows from Pauling and Wilson (1935) and Born (1960). Terms particle and atom are often used interchangeably.

B.1.1 Newton's Equations

Newton's equations of motion for a discrete particle system are written in indicial notation as

$$m_{\langle i \rangle} \ddot{r}_{\langle i \rangle}^a = \hat{f}_{\langle i \rangle}^a + f_{\langle i \rangle}^a,$$

(B.1)

Angled brackets denote atomic labels. In (B.1), $m_{\langle i \rangle}$ and $\mathbf{r}_{\langle i \rangle}$ are the constant mass of atom i and the spatial position vector of (the nucleus) of atom i. Atomic nuclei are treated as ideal rigid point masses. The non-

conservative force acting on particle i is written $\hat{\mathbf{f}}_{\langle i \rangle}$, and the conservative force acting on particle i is written $\mathbf{f}_{\langle i \rangle}$. Relation (B.1) is expressed in the spatial (i.e., current) configuration spanned by constant orthonormal basis vectors in an inertial frame, e.g., Cartesian coordinates. The conservative force by definition is the position gradient of an energy potential:

$$f_{\langle i \rangle}^a = -\delta^{ab} \frac{\partial \Phi}{\partial r_{\langle i \rangle}^b} . \tag{B.2}$$

If instead curvilinear coordinates are used, the appropriate particle acceleration[1] must be incorporated in (B.1), and contravariant components of (the inverse of the) metric tensor replace δ^{ab} in (B.2). Potential energy Φ depends, by definition, only on nuclear coordinates, i.e.,

$$\Phi = \Phi\left(\mathbf{r}_{\langle i \rangle} \right)_{i \in N} , \tag{B.3}$$

where N denotes the set of atoms comprising the system. Forces of mechanical, electrostatic, and/or gravitational origin can be expressed using (B.2). Dependence on species of each atom i is implicit in (B.3), which is applicable for systems with multiple atomic species. Non-conservative forces include time-dependent external forces and forces that depend explicitly on velocity, e.g., certain electromagnetic, viscous, and other dissipative forces.

B.1.2 Lagrange's Equations

Hamilton's principle can be used to obtain equations of motion for a conservative system that apply in any coordinate system (e.g., curvilinear coordinates). A scalar Lagrangian function $\mathcal{L}$ is introduced as

$$\mathcal{L} = \mathcal{L}\left(\mathbf{r}_{\langle i \rangle}, \dot{\mathbf{r}}_{\langle i \rangle} \right)_{i \in N} = \mathcal{K} - \Phi , \tag{B.4}$$

where $\mathcal{K}$ is the kinetic energy of the system. Positions and velocities can be expressed in generalized coordinates in (B.4). Hamilton's principle is stated as

$$\int_{t_1}^{t_2} \mathcal{L} dt = \text{constant} , \tag{B.5}$$

---

[1] For example, denoting by $\left\{ {}^{\ .a}_{bc} \right\}$ the Christoffel symbols of the second kind,

$$A_{\langle i \rangle}^a = \frac{D}{Dt}(\dot{r}_{\langle i \rangle}^a) + \left\{ {}^{\ .a}_{bc} \right\} \dot{r}_{\langle i \rangle}^b \dot{r}_{\langle i \rangle}^c .$$

meaning that the motion of the atoms or particles over the (arbitrary) interval $t_1 \le t \le t_2$ results a stationary value of the integrated Lagrangian, i.e., the action integral. This stationary value can correspond to a maximum, minimum, or saddle point. Equations of motion consistent with (B.5) are obtained as general solutions of the following variational problem:

$$\delta \int_{t_1}^{t_2} \mathcal{L} dt = 0 , \tag{B.6}$$

where δ is the first variation. Using (B.4) and integrating by parts,

$$\delta \int_{t_1}^{t_2} \mathcal{L} dt = \int_{t_1}^{t_2} \sum_{i=1}^{N} \left[\frac{\partial \mathcal{L}}{\partial \mathbf{r}_{\langle i \rangle}} \bullet \delta \mathbf{r}_{\langle i \rangle} + \frac{\partial \mathcal{L}}{\partial \dot{\mathbf{r}}_{\langle i \rangle}} \bullet \delta \dot{\mathbf{r}}_{\langle i \rangle} \right] dt$$

$$= \int_{t_1}^{t_2} \sum_{i=1}^{N} \left[\left(\frac{\partial \mathcal{L}}{\partial \mathbf{r}_{\langle i \rangle}} - \frac{d}{dt} \frac{\partial \mathcal{L}}{\partial \dot{\mathbf{r}}_{\langle i \rangle}} \right) \bullet \delta \mathbf{r}_{\langle i \rangle} \right] dt, \tag{B.7}$$

where admissible variation $\delta \mathbf{r}_{\langle i \rangle}$ presumably vanishes (e.g., by definition) at endpoints t_1 and t_2. Substituting (B.7) into (B.6), the resulting Euler-Lagrange equations are

$$\frac{\partial \mathcal{L}}{\partial \mathbf{r}_{\langle i \rangle}} - \frac{d}{dt} \frac{\partial \mathcal{L}}{\partial \dot{\mathbf{r}}_{\langle i \rangle}} = 0 , \; (i = 1, 2, ... N) . \tag{B.8}$$

Prescribing the total kinetic energy as the sum $\mathcal{K} = (1/2) \sum_{i=1}^{N} m_{\langle i \rangle} \dot{\mathbf{r}}_{\langle i \rangle} \bullet \dot{\mathbf{r}}_{\langle i \rangle}$ and using (B.2) and (B.4), Newton's laws (B.1) are recovered from (B.8) when forces are conservative, i.e., when $\hat{\mathbf{f}}_{\langle i \rangle} = 0$ in (B.1). However, particle coordinates and velocities need not always be referred to a Cartesian frame in (B.4)-(B.8); $\mathbf{r}_{\langle i \rangle}$ can represent a triplet of generalized scalar (curvilinear) coordinates of particle i as opposed to its position vector in Cartesian space (Pauling and Wilson 1935). A more general derivation treating non-conservative and non-holonomic systems is given by Synge (1960). By an analogous procedure, as discussed in Section 5.6.2, Hamilton's principle can be used to obtain the local balance of momentum and constitutive laws for a non-dissipative continuous body, e.g., a hyperelastic solid.

B.1.3 Hamilton's Equations

The Euler-Lagrange equations for a discrete system in (B.8) are second-order differential equations in time. These can be expressed in so-called

canonical form as a system of first-order differential equations by introducing, via a Legendre transformation, the Hamiltonian $\mathcal{H}$:

$$\mathcal{H}(q_k, p_k) = \sum_{k=1}^{3N} p_k \dot{q}_k - \mathcal{L}(q_k, \dot{q}_k);$$

$$\dot{q}_k = \dot{q}_k(q_l, p_l), \ \det\left(\frac{\partial^2 \mathcal{L}}{\partial \dot{q}_k \partial \dot{q}_l}\right) \neq 0.$$

(B.9)

A change of notation for kinematic variables is used: triplets of generalized coordinates $\mathbf{r}_{\langle 1 \rangle}, \mathbf{r}_{\langle 2 \rangle}, ... \mathbf{r}_{\langle N \rangle}$ are expressed as scalars $q_1, q_2, ... q_{3N}$, and similarly generalized velocities are expressed as scalars $\dot{q}_1, \dot{q}_2, ... \dot{q}_{3N}$. Generalized momenta are defined as the scalars

$$p_k = \frac{\partial \mathcal{L}}{\partial \dot{q}_k}, \ (k = 1, 2, ... 3N).$$

(B.10)

Noting that in the differential

$$d\mathcal{H} = \sum_{k=1}^{3N} \left[\dot{q}_k dp_k - \frac{\partial \mathcal{L}}{\partial q_k} dq_k + \left(p_k - \frac{\partial \mathcal{L}}{\partial \dot{q}_k} \right) d\dot{q}_k \right],$$

(B.11)

the inner term in parentheses vanishes by (B.10), canonical equations of motion are deduced as

$$\dot{q}_k = \frac{\partial \mathcal{H}}{\partial p_k}, \ \dot{p}_k = -\frac{\partial \mathcal{H}}{\partial q_k}, \ (k = 1, 2, ... 3N).$$

(B.12)

Since for the conservative systems considered here, the Hamiltonian in (B.9) does not depend explicitly on time,

$$\frac{d\mathcal{H}}{dt} = \sum_{k=1}^{3N} \left[\frac{\partial \mathcal{H}}{\partial q_k} \dot{q}_k + \frac{\partial \mathcal{H}}{\partial p_k} \dot{p}_k \right] = 0.$$

(B.13)

Noting that in conservative systems with a stationary coordinate frame,

$$\sum_{k=1}^{3N} p_k \dot{q}_k = \sum_{k=1}^{3N} \frac{\partial \mathcal{K}}{\partial \dot{q}_k} \dot{q}_k = 2\mathcal{K},$$

(B.14)

the Hamiltonian becomes

$$\mathcal{H} = 2\mathcal{K} - \mathcal{L} = \mathcal{K} + \Phi.$$

(B.15)

Together, (B.13) and (B.15) express that the sum of kinetic and potential energies of the system remains constant. This is analogous to the energy balance (4.44) for insulated, continuous bodies subjected only to conservative body forces and subjected to no surface forces. A more general derivation of the canonical equations of classical dynamics valid for nonconservative systems is given by Synge (1960).

B.2 Statics

Successively discussed next are governing equations, interatomic potentials, atomic stress measures, and atomic origins of elasticity coefficients. The interpretation of stress and elastic coefficients is restricted to solids that deform homogeneously without inner translations, for example centrosymmetric crystals deforming according to the Cauchy-Born hypothesis (Born and Huang 1950) in the absence of lattice vibrations and ionic polarization. Example formulae for stresses and second- and third-order elastic coefficients are given for systems described by pair potentials and the embedded atom method, with Cauchy's symmetry restrictions demonstrated in the former case. The forthcoming treatment of lattice statics is restricted to coincident Cartesian coordinate systems in referential and deformed configurations of the atomic ensemble. By definition, nuclear vibrations associated with zero-point, thermal, acoustic, and/or electromagnetic phenomena are omitted in the context of molecular or lattice statics. Hence, contributions of such vibrations to the free energy are excluded in what follows. Zero-point kinetic energy (particularly of electrons) implicitly affects bonding energies and hence atomic force interactions, but such effects are incorporated implicitly in what follows via prescription of empirical interatomic force potentials.

B.2.1 Governing Equations

Governing equations of motion for molecular or lattice statics are those of (B.1) in the absence of atomic velocities and accelerations:

$$\hat{f}^a_{\langle i \rangle} + f^a_{\langle i \rangle} = 0 , \tag{B.16}$$

where again non-conservative and conservative forces acting on particle i are respectively denoted by $\hat{\mathbf{f}}_{\langle i \rangle}$ and $\mathbf{f}_{\langle i \rangle}$. Statics corresponds to a system at null kinetic energy, as is clear from (B.14), and also corresponds to a system at null absolute temperature (i.e., $\theta = 0$ K) if temperature θ is assumed to depend only on kinetic energy of the nuclei in the atomic system. For example, $3N k_B \theta = 2\mathcal{K}$ for N atoms of an ideal gas with random velocities, where k_B is Boltzmann's constant. Balance relations (B.16) can be obtained from a variational principle incorporating external forces:

$$-\delta\mathcal{L} = \delta\Phi = \sum_{i=1}^{N} \hat{\mathbf{f}}_{\langle i \rangle} \cdot \delta\mathbf{r}_{\langle i \rangle} , \tag{B.17}$$

whence from (B.3),

$$\delta \Phi = \sum_{i=1}^{N} \frac{\partial \Phi}{\partial \mathbf{r}_{\langle i \rangle}} \cdot \delta \mathbf{r}_{\langle i \rangle} = -\sum_{i=1}^{N} \mathbf{f}_{\langle i \rangle} \cdot \delta \mathbf{r}_{\langle i \rangle} \ . \qquad (B.18)$$

B.2.2 Interatomic Potentials and Forces

Interatomic force potentials are often expressed as a series of terms of the general format

$$\Phi = \sum_{i=1}^{N} \Phi_1\left(\mathbf{r}_{\langle i \rangle}\right) + \sum_{i=1}^{N}\sum_{j=1}^{N} \Phi_2\left(\mathbf{r}_{\langle ij \rangle}\right) + \sum_{i=1}^{N}\sum_{j=1}^{N}\sum_{k=1}^{N} \Phi_3\left(\mathbf{r}_{\langle ij \rangle}, \mathbf{r}_{\langle jk \rangle}, \mathbf{r}_{\langle ki \rangle}\right) + \dots , \quad (B.19)$$

where the vector describing the spatial separation between two atoms is

$$\mathbf{r}_{\langle ij \rangle} = \mathbf{r}_{\langle j \rangle} - \mathbf{r}_{\langle i \rangle} \ . \qquad (B.20)$$

In (B.19), Φ_1 is a one-body potential that can represent conservative forces arising from an external field such as gravity. In the second term on the right side of (B.19), Φ_2 accounts for pairwise interactions, while in the third term Φ_3 accounts for three-body interactions, and so forth implied for higher-order terms in the series. Also implied in (B.19) is vanishing of the contribution to the potential energy for a particular term when atomic indices are repeated, e.g., $\Phi_2(\mathbf{r}_{\langle ij \rangle}) = 0$ for $i = j$. Some redundancy is included in the notation (B.19) since arguments of each function are not independent: $\mathbf{r}_{\langle ij \rangle} = -\mathbf{r}_{\langle ji \rangle}$ and $\mathbf{r}_{\langle ij \rangle} + \mathbf{r}_{\langle jk \rangle} = \mathbf{r}_{\langle ik \rangle}$. Because of this redundancy, potentials are often recast such that summation proceeds over reduced numbers of pairs and triplets of atoms, for example.

Henceforth the term Φ_1 is not considered, and effects of all conservative and non-conservative external forces are simultaneously incorporated in vector $\hat{\mathbf{f}}_{\langle i \rangle}$. With this change in notation, variations of potential energy result only from interactions among two or more atoms (e.g., from bond cohesion or repulsion). This is reflected by

$$\Phi = \Phi\left(\mathbf{r}_{\langle ij \rangle}\right)_{\substack{i,j \in N \\ i \neq j}} = \sum_{i=1}^{N}\sum_{j=1}^{N} \Phi_2\left(\mathbf{r}_{\langle ij \rangle}\right) + \sum_{i=1}^{N}\sum_{j=1}^{N}\sum_{k=1}^{N} \Phi_3\left(\mathbf{r}_{\langle ij \rangle}, \mathbf{r}_{\langle jk \rangle}, \mathbf{r}_{\langle ki \rangle}\right) + \dots . \quad (B.21)$$

Relation (B.21), unlike (B.19), is invariant under rigid spatial translations of the system. Potentials incorporating additional degrees of freedom in the form of angular coordinates are also possible. For example, rotational degrees of freedom may be used to model molecules as single particles, or to address aspects of electric polarization. Incorporation of rotational degrees of freedom and conjugate interatomic moments are not considered here, though their inclusion can provide insight into origins of couple

stresses in generalized continuum theories (Zhou and McDowell 2002). Note also that electronic degrees of freedom are not explicitly addressed in (B.3) or (B.19), following the Born-Oppenheimer approximation that presumes that electrons follow ions adiabatically, remaining in their ground states for instantaneous positions of the nuclei (Nielsen and Martin 1985).

A conservative interatomic force can be introduced as

$$f_{\langle ij \rangle}^a = \delta^{ab} \frac{\partial \Phi}{\partial r_{\langle ij \rangle}^b} = -\delta^{ab} \frac{\partial \Phi}{\partial r_{\langle ji \rangle}^b} = -f_{\langle ji \rangle}^a . \tag{B.22}$$

The static equilibrium equations (B.16) then become, from (B.21),

$$\hat{f}_{\langle i \rangle}^a = \delta^{ab} \sum_{j=1}^{N} \left(\sum_{k=1}^{N} \frac{\partial \Phi}{\partial r_{\langle jk \rangle}^c} \frac{\partial r_{\langle jk \rangle}^c}{\partial r_{\langle i \rangle}^b} \right) = \delta^{ab} \sum_{j=1}^{N} \frac{\partial \Phi}{\partial r_{\langle ji \rangle}^b} = -\delta^{ab} \sum_{j=1}^{N} \frac{\partial \Phi}{\partial r_{\langle ij \rangle}^b} , \tag{B.23}$$

implying that the total interaction force is

$$f_{\langle i \rangle}^a = \delta^{ab} \sum_{j=1}^{N} \frac{\partial \Phi}{\partial r_{\langle ij \rangle}^b} = -\sum_{j=1}^{N} f_{\langle ij \rangle}^a . \tag{B.24}$$

Potential Φ in (B.21) may generally depend upon interactions between two (Φ_2), three (Φ_3), and more atoms, and hence on distances and orientations among multiple atoms. A more specific form of potential energy (B.21) depending only on scalar interatomic distances is

$$\Phi = \Phi \left(r_{\langle ij \rangle} \right)_{\substack{i, j \in N \\ i \neq j}} , \tag{B.25}$$

where the distance between atoms i and j is written as follows:

$$r_{\langle ij \rangle} = (\mathbf{r}_{\langle ij \rangle} \bullet \mathbf{r}_{\langle ij \rangle})^{1/2} = r_{\langle ji \rangle} , \quad \frac{\partial r_{\langle ij \rangle}}{\partial \mathbf{r}_{\langle ij \rangle}} = \frac{\mathbf{r}_{\langle ij \rangle}}{r_{\langle ij \rangle}} = -\frac{\mathbf{r}_{\langle ji \rangle}}{r_{\langle ij \rangle}} . \tag{B.26}$$

Notice that (B.25) is not restricted to two-body interactions. The interatomic force resulting from (B.25), in this case called a central force, and the total internal force are then found, respectively, for the particular case of exclusively central forces as

$$\mathbf{f}_{\langle ij \rangle} = \frac{\partial \Phi}{\partial r_{\langle ij \rangle}} \frac{\mathbf{r}_{\langle ij \rangle}}{r_{\langle ij \rangle}} , \quad \mathbf{f}_{\langle i \rangle} = -\sum_{j=1}^{N} \frac{\partial \Phi}{\partial r_{\langle ij \rangle}} \frac{\mathbf{r}_{\langle ij \rangle}}{r_{\langle ij \rangle}} . \tag{B.27}$$

A vast number of different potentials have been developed for various substances by physics, chemistry, materials science, and engineering communities over the previous century; a few specific potentials are described here for illustrative purposes. The Lennard-Jones pair potential obeys (Lennard-Jones 1924; see also extension for ionic crystals by Lennard-Jones (1925))

$$\Phi = \sum_{i=1}^{N}\sum_{j=1}^{N}\Phi_2\left(r_{\langle ij\rangle}\right) = \frac{1}{2}\sum_{i=1}^{N}\sum_{j=1}^{N}\phi\left(r_{\langle ij\rangle}\right)$$

$$= \sum_{i=1}^{N}\sum_{j=1}^{N}4\varepsilon\left[\left(\frac{\sigma}{r_{\langle ij\rangle}}\right)^{12} - \left(\frac{\sigma}{r_{\langle ij\rangle}}\right)^{6}\right],$$

(B.28)

where $\phi(r)$ is the local pair potential and ε and σ are scalar constants. Interatomic force vector (B.27) for a Lennard-Jones system is then

$$\mathbf{f}_{\langle ij\rangle} = \frac{\partial\phi}{\partial r_{\langle ij\rangle}}\frac{\mathbf{r}_{\langle ij\rangle}}{r_{\langle ij\rangle}} = 24\frac{\varepsilon}{\sigma}\left[2\left(\frac{\sigma}{r_{\langle ij\rangle}}\right)^{13} - \left(\frac{\sigma}{r_{\langle ij\rangle}}\right)^{7}\right]\frac{\mathbf{r}_{\langle ij\rangle}}{r_{\langle ij\rangle}}.$$

(B.29)

Obviously, (B.28) and (B.29) only account for pairwise interactions. Such pair potentials alone are usually insufficient for modeling behavior of anisotropic crystalline solids, including the full set of independent elastic constants, as will be demonstrated by example later in Section B.2.6. The Lennard-Jones potential is often used to address dipole interactions in atomic models of noble gas crystals and molecular crystals (Gilman 2003).

Popular potentials for solids incorporating interactions among more than two atoms (i.e., three-body and higher-order terms) include those of Daw and Baskes (1983, 1984), Finnis and Sinclair (1984), Stillinger and Weber (1985), Tersoff (1988), and Brenner (1990). For metallic solids, a potential is often written as a sum of a pairwise interaction term and an *N*-body term accounting for the embedding energy (Daw and Baskes 1983, 1984; Finnis and Sinclair 1984). For certain materials such as many pure metals and covalent solids without long-range (e.g., unscreened Coulomb) forces between nuclei, interaction forces between an atom and its neighbors often decay rapidly for separation distances beyond some cut-off radius, often on the order of several lattice parameters.

In the embedded atom method of Daw and Baskes (1983, 1984), all forces are of central type, and the form of (B.25) is

$$\Phi = \Phi\left(r_{\langle ij\rangle}\right) = \sum_{i=1}^{N}U^{\langle i\rangle}\left(\rho_{\langle i\rangle}\right) + \frac{1}{2}\sum_{i=1}^{N}\sum_{j=1}^{N}\phi\left(r_{\langle ij\rangle}\right),$$

(B.30)

where the second term on the right side of the final equality is recognizable as a pair potential. The first term U on the right of (B.30), called the embedding function, is generally a nonlinear function of

$$\rho_{\langle i\rangle} = \sum_{j=1}^{N}g^{\langle j\rangle}\left(r_{\langle ij\rangle}\right), \ (j \neq i),$$

(B.31)

where $g^{\langle j\rangle}$ is the electron density function. Interatomic force (B.27) is

$$\mathbf{f}_{\langle ij\rangle} = \frac{\partial \Phi}{\partial r}\frac{\mathbf{r}_{\langle ij\rangle}}{r} = \left[\sum_{i=1}^{N} U' \frac{\partial \rho_{\langle i\rangle}}{\partial r} + \frac{\phi'}{2}\right]\frac{\mathbf{r}_{\langle ij\rangle}}{r} = \left[\sum_{i=1}^{N} U' \sum_{j=1}^{N} g' + \frac{\phi'}{2}\right]\frac{\mathbf{r}_{\langle ij\rangle}}{r}, \quad \text{(B.32)}$$

where the following compact notation is used for derivatives of functions and for scalar atomic separation distance:

$$U' = \frac{\partial U^{\langle i\rangle}}{\partial \rho_{\langle i\rangle}}, \; \phi' = \frac{\partial \phi}{\partial r}, \; g' = \frac{\partial g}{\partial r}, \; r = r_{\langle ij\rangle} = \left|\mathbf{r}_{\langle ij\rangle}\right|. \quad \text{(B.33)}$$

Functions U, g, and ϕ, often very complex, can be deduced and parameterized for different materials via calibration to properties obtained independently from physical experiments or quantum mechanical calculations. Even though the potential energy (B.30) depends only on interatomic distances (i.e., r), the first sum on the right side of (B.30) implicitly accounts for bond angle effects associated with electron density because the double sum incorporating embedding function U generally involves relative separation distances among more than two atoms taken at a time. This is in contrast to pair potentials which do not address bond angle changes.

Various interpretations of stress have been proposed in the context of discrete atomic systems (Nielsen and Martin 1983, 1985; Zhou 2003; Chen and Lee 2005). The stress (or traction) concept traditionally describes directional forces, normalized per unit area, acting on internal or external surfaces of continuous bodies in the context of continuum mechanics and Cauchy's theorem, e.g., (4.2)-(4.5). Ambiguities can arise when attempts are made to extract the stress tensor from discrete dynamic systems (Tsai 1979; Nielsen and Martin 1985; Lutsko 1988; Cheung and Yip 1991; Zhou 2003, 2005; Zimmerman et al. 2004; Chen and Lee 2005). For static systems considered here, momentum associated with particle velocities is excluded, the definition of a stress tensor is more straightforward. A local singular stress tensor $\mathbf{s}$ is defined on a per atom basis as (Zhou 2003)

$$\mathbf{s}(\mathbf{r}) = \frac{1}{2}\sum_{i=1}^{N}\sum_{j=1}^{N} \mathbf{r}_{\langle ij\rangle} \otimes \mathbf{f}_{\langle ij\rangle} \delta(\mathbf{r} - \mathbf{r}_{\langle ij\rangle}), \quad \text{(B.34)}$$

where $\delta(.)$ is Dirac's delta function. Integration over a spatial volume Ω then provides the atomistic analog of the continuum Cauchy stress tensor supported by that volume:

$$\boldsymbol{\sigma} = \int_{\Omega} \mathbf{s}(\mathbf{r})d\Omega = \frac{1}{2\Omega}\sum_{i=1}^{N}\sum_{j=1}^{N} \mathbf{r}_{\langle ij\rangle} \otimes \mathbf{f}_{\langle ij\rangle}. \quad \text{(B.35)}$$

Definition (B.34) is considered equivalent to the virial stress (Tsai 1979) when atomic velocities vanish, and its spatial average in (B.35) has been used to interpret results in the context of pair potentials (Born and Huang 1954) and the embedded atom method (Horstemeyer and Baskes 1999).

Stress tensor (B.35) can also be expressed directly in terms of atomic co-ordinates[2] $\mathbf{r}_{\langle i \rangle}$ (Nielsen and Martin 1985). For exclusively central force interactions, symmetry of stress tensor (B.34) follows trivially from (B.27):

$$\sigma^{ab} = \frac{1}{2\Omega} \sum_{i=1}^{N} \sum_{j=1}^{N} \frac{r_{\langle ij \rangle}^{a} r_{\langle ij \rangle}^{b}}{r_{\langle ij \rangle}} \frac{\partial \Phi}{\partial r_{\langle ij \rangle}} = \sigma^{ba}. \tag{B.36}$$

B.2.3 Kinematics of Homogeneous Deformation

Now consider a collection N of discrete atoms that occupy a regular lattice in an undeformed reference configuration B_0. The position of atom i in configuration B_0 is denoted by vector $\mathbf{R}_{\langle i \rangle}$. The position of atom i in current configuration B is again denoted by spatial vector $\mathbf{r}_{\langle i \rangle}$. First consider a crystal structure with a monatomic basis. Under a homogeneous deformation in the sense of Born and Huang (1954), the kinematic relationship between reference and deformed atomic coordinates, in the absence of rigid body translations, is

$$\mathbf{r}_{\langle i \rangle} = \mathbf{F} \mathbf{R}_{\langle i \rangle}, \ r_{\langle i \rangle}^{a} = F_{.A}^{a} R_{\langle i \rangle}^{A}, \tag{B.37}$$

where $\mathbf{F}$ is a 3×3 matrix with positive determinant, analogous to the deformation gradient of continuum mechanics introduced in (2.112), though here $\mathbf{F}$ need not be a gradient of any vector field. Next consider a crystal structure with a polyatomic basis, that is, a lattice with multiple atoms per point on a Bravais lattice. In the reference configuration,

$$\mathbf{R}\binom{l}{k} = \mathbf{R}(l) + \mathbf{R}\binom{0}{k}, \tag{B.38}$$

where notation $\binom{l}{k}$ denotes atom k within primitive unit cell l. The notation $\binom{0}{k}$ denotes the basis vector for atom k within cell zero. The notation (l) denotes the Bravais lattice vector for unit cell l, that is

---

[2] In the absence of applied torques, $\sigma^{ab} = \sigma^{ba}$, and using (B.2) and (B.24),

$$\Omega \sigma^{ab} = \frac{1}{2} \sum_{i=1}^{N} \sum_{j=1}^{N} r_{\langle ij \rangle}^{a} f_{\langle ij \rangle}^{b} = \frac{1}{2} (r_{\langle 12 \rangle}^{a} f_{\langle 12 \rangle}^{b} + \dots + r_{\langle 21 \rangle}^{a} f_{\langle 21 \rangle}^{b} + \dots)$$

$$= -[r_{\langle 1 \rangle}^{a} (f_{\langle 12 \rangle}^{b} + f_{\langle 13 \rangle}^{b} \dots) + r_{\langle 2 \rangle}^{a} (f_{\langle 21 \rangle}^{b} + f_{\langle 23 \rangle}^{b} \dots) + \dots]$$

$$= -\sum_{i=1}^{N} r_{\langle i \rangle}^{a} \sum_{j=1}^{N} f_{\langle ij \rangle}^{b} = \sum_{i=1}^{N} r_{\langle i \rangle}^{a} f_{\langle i \rangle}^{b} = -\sum_{i=1}^{N} r_{\langle i \rangle}^{a} \delta^{bc} \frac{\partial \Phi}{\partial r_{\langle i \rangle}^{c}}$$

$$\mathbf{R}\left(l\right)=\sum_{i=1}^{3}l^{i}\mathbf{A}_{i}=l^{1}\mathbf{A}_{1}+l^{2}\mathbf{A}_{2}+l^{3}\mathbf{A}_{3},\ (l^{1},l^{2},l^{3}\in\mathbb{Z}),\qquad\text{(B.39)}$$

with $\mathbf{A}_{i}$ the primitive Bravais lattice vectors and l^{i} integers. A homogeneous deformation for a crystal with a polyatomic basis, in the sense of Born and Huang (1954), is expressed as the vector sum

$$\mathbf{r}\left(\begin{smallmatrix}l\\k\end{smallmatrix}\right)=\mathbf{q}\left(\begin{smallmatrix}0\\k\end{smallmatrix}\right)+\mathbf{F}\mathbf{R}\left(\begin{smallmatrix}l\\k\end{smallmatrix}\right).\qquad\text{(B.40)}$$

Vector $\mathbf{q}(\begin{smallmatrix}0\\k\end{smallmatrix})$ represents a uniform displacement (i.e., translation) of all atoms of particular type k, as might occur for example when an ionic crystal becomes polarized under an electric field. Vector $\mathbf{q}(\begin{smallmatrix}0\\k\end{smallmatrix})$ can also be used to represent an inner displacement for a sub-lattice of a crystal with a polyatomic basis wherein each atom does not occupy a center of inversion symmetry (Wallace 1972; Cousins 1978; Tadmor et al. 1999), for example diamond or silicon. When such crystals are subjected to affine far-field boundary conditions, inner displacements result in a lower potential energy than would arise if inner translations were absent.

Henceforward in Appendix B, considered are conditions for which inner displacements vanish, i.e., $\mathbf{q}(\begin{smallmatrix}0\\k\end{smallmatrix})=0$ for all atoms $k=1,2,...K$ in the basis. Under these conditions, (B.37) can be used in place of (B.40) for crystal structures with polyatomic bases since there is no distinction among motions of atoms or ions of different types k. Additional discussion of homogeneous deformations in the context of the Cauchy-Born hypothesis is given in Section 3.1.2 of Chapter 3. Various definitions exist for atomic-level representations of first- and higher-order deformation gradients for ensembles of atoms deforming heterogeneously (Zimmerman et al. 2009); such locally heterogeneous deformations are not addressed in Appendix B. As discussed by Wallace (1972), when the ensemble of atoms (i.e., the crystal) is of finite dimensions, non-homogeneous deformations can emerge locally where external forces are applied along the boundary. Deviations from perfect periodicity can also occur at free boundary surfaces.

The following notation for referential interatomic separation vectors and spatial interatomic displacement vectors, respectively, is introduced:

$$\mathbf{R}_{\langle ij\rangle}=\mathbf{R}_{\langle j\rangle}-\mathbf{R}_{\langle i\rangle},\qquad\text{(B.41)}$$

$$\mathbf{q}_{\langle ij\rangle}=\mathbf{r}_{\langle ij\rangle}-\mathbf{R}_{\langle ij\rangle}=(\mathbf{F}-\mathbf{1})\mathbf{R}_{\langle ij\rangle},\qquad\text{(B.42)}$$

with the second of (B.42) applicable under homogeneous deformations of the kind in (B.37). Following from (B.20), (B.37), and (B.41),

$$\mathbf{r}_{\langle ij\rangle}=\mathbf{F}\mathbf{R}_{\langle ij\rangle},\ r_{\langle ij\rangle}^{a}=F_{.A}^{a}R_{\langle ij\rangle}^{A}.\qquad\text{(B.43)}$$

For homogeneous deformation, $\mathbf{r}_{\langle ij\rangle}=\mathbf{r}_{\langle ij\rangle}\left(\mathbf{F},\mathbf{R}_{\langle ij\rangle}\right)$ with $\mathbf{R}_{\langle ij\rangle}$ constants, so

$$\frac{\partial r^a_{\langle ij\rangle}}{\partial F^b_{.A}} = \delta^a_{.b} R^A_{\langle ij\rangle}, \quad \frac{\partial q^a_{\langle ij\rangle}}{\partial F^b_{.A}} = \delta^a_{.b} R^A_{\langle ij\rangle}, \quad \frac{\partial q^a_{\langle ij\rangle}}{\partial r^b_{\langle ij\rangle}} = \delta^a_{.b}.$$ (B.44)

The analog of the right Cauchy-Green strain of (2.156) is introduced as

$$E_{AB} = \frac{1}{2}(F^a_{.A}\delta_{ab}F^b_{.B} - \delta_{AB}).$$ (B.45)

The following notation is used for magnitudes of reference interatomic separation vectors, analogous to (B.26):

$$R_{\langle ij\rangle} = (\mathbf{R}_{\langle ij\rangle} \bullet \mathbf{R}_{\langle ij\rangle})^{1/2} = R_{\langle ji\rangle}, \quad \frac{\partial R_{\langle ij\rangle}}{\partial \mathbf{R}_{\langle ij\rangle}} = \frac{\mathbf{R}_{\langle ij\rangle}}{R_{\langle ij\rangle}} = -\frac{\mathbf{R}_{\langle ji\rangle}}{R_{\langle ij\rangle}}.$$ (B.46)

Then the difference in squared lengths of spatial and reference atomic position vectors, analogous to (2.157), is

$$r_{\langle ij\rangle}{}^2 - R_{\langle ij\rangle}{}^2 = 2R^A_{\langle ij\rangle}E_{AB}R^B_{\langle ij\rangle}.$$ (B.47)

Noting that

$$r_{\langle ij\rangle} = (F^a_{.A}R^A_{\langle ij\rangle}\delta_{ab}F^b_{.B}R^B_{\langle ij\rangle})^{1/2},$$ (B.48)

the following identities that are particularly useful for describing systems with central force interactions can be derived (Tadmor et al. 1996; Chung and Namburu 2003):

$$\frac{\partial r_{\langle ij\rangle}}{\partial F^a_{.A}} = \frac{\partial r_{\langle ij\rangle}}{\partial r^b_{\langle ij\rangle}}\frac{\partial r^b_{\langle ij\rangle}}{\partial F^a_{.A}} = \delta_{ab}\frac{r^b_{\langle ij\rangle}}{r_{\langle ij\rangle}}R^A_{\langle ij\rangle} = \delta_{ab}\frac{r^b_{\langle ij\rangle}r^c_{\langle ij\rangle}}{r_{\langle ij\rangle}}F^{-1A}_{.c},$$ (B.49)

$$\frac{\partial^2 r_{\langle ij\rangle}}{\partial F^a_{.A}\partial F^b_{.B}} = \frac{\partial^2 r_{\langle ij\rangle}}{\partial r^c_{\langle ij\rangle}\partial r^d_{\langle ij\rangle}}\frac{\partial r^c_{\langle ij\rangle}}{\partial F^a_{.A}}\frac{\partial r^d_{\langle ij\rangle}}{\partial F^b_{.B}} = \left(\frac{\delta_{cd}}{r_{\langle ij\rangle}} - \delta_{ce}\delta_{df}\frac{r^e_{\langle ij\rangle}r^f_{\langle ij\rangle}}{r_{\langle ij\rangle}^3}\right)\delta^c_a R^A_{\langle ij\rangle}\delta^d_b R^B_{\langle ij\rangle}$$

$$= \left(\delta_{ab}\frac{r^c_{\langle ij\rangle}r^d_{\langle ij\rangle}}{r_{\langle ij\rangle}} - \delta_{ae}\delta_{bf}\frac{r^e_{\langle ij\rangle}r^f_{\langle ij\rangle}r^c_{\langle ij\rangle}r^d_{\langle ij\rangle}}{r_{\langle ij\rangle}^3}\right)F^{-1A}_{.c}F^{-1B}_{.d},$$ (B.50)

$$\frac{\partial r_{\langle ij\rangle}}{\partial E_{AB}} = \frac{\partial}{\partial E_{AB}}\left[(2R^C_{\langle ij\rangle}E_{CD}R^D_{\langle ij\rangle} + R^C_{\langle ij\rangle}\delta_{CD}R^D_{\langle ij\rangle})^{1/2}\right] = \frac{R^A_{\langle ij\rangle}R^B_{\langle ij\rangle}}{r_{\langle ij\rangle}},$$ (B.51)

$$\frac{\partial^2 r_{\langle ij\rangle}}{\partial E_{AB}\partial E_{CD}} = \frac{\partial}{\partial E_{AB}}\left(\frac{R^C_{\langle ij\rangle}R^D_{\langle ij\rangle}}{r_{\langle ij\rangle}}\right) = -\frac{R^C_{\langle ij\rangle}R^D_{\langle ij\rangle}}{r_{\langle ij\rangle}^2}\frac{\partial r_{\langle ij\rangle}}{\partial E_{AB}} = -\frac{R^A_{\langle ij\rangle}R^B_{\langle ij\rangle}R^C_{\langle ij\rangle}R^D_{\langle ij\rangle}}{r_{\langle ij\rangle}^3}.$$ (B.52)

B.2.4 Stresses and Moduli for Homogeneous Deformations

At null temperature and when all atomic coordinates undergo homogeneous deformation, the free energy density Ψ_0 (or equivalently, the internal

energy density or strain energy density) of the solid in a continuum sense can be equated in a straightforward manner with the potential energy normalized per unit reference volume:

$$\Psi_0(\mathbf{F}) = \frac{1}{\Omega_0}\left[\Phi\left(\mathbf{r}_{\langle ij\rangle}\right) - \Phi\left(\mathbf{R}_{\langle ij\rangle}\right)\right]$$
$$= \frac{1}{\Omega_0}\left[\Phi\left(\mathbf{F}\mathbf{R}_{\langle ij\rangle}\right) - \Phi\left(\mathbf{R}_{\langle ij\rangle}\right)\right], \tag{B.53}$$

where the volume of the atomic system in the reference configuration is denoted by $\Omega_0 = N\Omega_0$, with Ω_0 (non-italic font) the average atomic volume occupied by each atom of the unit cell as defined in Section 3.1.1, and N is the total number of atoms in the system. When the system consists of but a single primitive unit cell, then $\Omega_0 = \Omega_P = K\Omega_0$, where Ω_P is the volume of the primitive cell and K is the number of atoms in the basis of the crystal structure. Consideration of a single unit cell subjected to periodic boundary conditions is a standard means of analyzing an infinitely repeating, perfect crystal structure, thereby accounting for all pertinent interactions among atoms within the unit cell and those comprising the surrounding (infinite) crystal. The cohesive energy of the crystal in the reference configuration, $\Phi(\mathbf{R}_{\langle ij\rangle})$, is subtracted from the right of (B.53) such that by the usual convention of continuum elasticity theory, the strain energy vanishes at null deformation, i.e., $\Psi_0(\mathbf{1}) = 0$. However $\Psi_0(\mathbf{1}) = 0$ is not mandatory; for example, the reference configuration can include defects. Because only derivatives of energy with respect to $\mathbf{r}_{\langle ij\rangle}$ enter relationships that follow for stresses and tangent moduli, the magnitude of additive constant $\Phi(\mathbf{R}_{\langle ij\rangle})$, consisting of the total ground state energy at null temperature, is inconsequential. Such ground state total energy of the atoms comprising the reference crystal includes zero-point kinetic and potential (e.g., electrostatic interaction) energies of electrons and nuclei when the latter occupy regular sites in a perfect undeformed crystal.

Using (B.53) and recalling that reference interatomic separation vectors are fixed during deformation $(\partial\mathbf{R}_{\langle ij\rangle} / \partial\mathbf{F} = 0)$, stresses and elastic coefficients can be computed using the chain rule of differentiation along with formulae (B.43)-(B.52) if the behavior of the solid is assumed hyperelastic. An atomic measure of the first Piola-Kirchhoff stress for homogeneous deformations is

$$P^{aA} = \frac{\partial \Psi_0}{\partial F_{aA}} = \frac{1}{\Omega_0} \frac{\partial}{\partial F_{aA}} \Phi\left(r_{\langle ij \rangle}^a\right)$$

$$= \frac{1}{\Omega_0} \sum_{j>i}^{N} \sum_{i=1}^{N} \delta^{ab} \frac{\partial \Phi}{\partial r_{\langle ij \rangle}^b} R_{\langle ij \rangle}^A = \frac{1}{2\Omega_0} \sum_{i=1}^{N} \sum_{j=1}^{N} \delta^{ab} \frac{\partial \Phi}{\partial r_{\langle ij \rangle}^b} R_{\langle ij \rangle}^A. \tag{B.54}$$

Notice that in the first double sum in (B.54), the summation proceeds only over independent atomic position vectors, i.e., over $\mathbf{r}_{\langle ij \rangle}$ with $j > i$. The factor of two arises in the denominator of the term following the final equality in (B.54) because in the final double sum, summation proceeds over all possible pairs satisfying $i \neq j$ with $\partial / \partial \mathbf{r}_{\langle ij \rangle} = -\partial / \partial \mathbf{r}_{\langle ji \rangle}$. Definition (B.54) is not restricted exclusively to pair potentials. For example, using (B.21) and writing out explicitly the contributions of the three-body potential,

$$P^{aA} = \frac{1}{\Omega_0} \frac{\partial}{\partial F_{aA}} \left[\sum_{i=1}^{N} \sum_{j=1}^{N} \Phi_2\left(\mathbf{r}_{\langle ij \rangle}\right) + \sum_{i=1}^{N} \sum_{j=1}^{N} \sum_{k=1}^{N} \Phi_3\left(\mathbf{r}_{\langle ij \rangle}, \mathbf{r}_{\langle jk \rangle}, \mathbf{r}_{\langle ki \rangle}\right) + \dots \right]$$

$$= \frac{\delta^{ab}}{2\Omega_0} \times \left[\sum_{i=1}^{N} \sum_{j=1}^{N} \frac{\partial \Phi_2}{\partial r_{\langle ij \rangle}^b} R_{\langle ij \rangle}^A + \left(\sum_{i=1}^{N} \sum_{j=1}^{N} \frac{\partial \Phi_3}{\partial r_{\langle ij \rangle}^b} R_{\langle ij \rangle}^A \right. \right. \tag{B.55}$$

$$\left. \left. + \sum_{j=1}^{N} \sum_{k=1}^{N} \frac{\partial \Phi_3}{\partial r_{\langle jk \rangle}^b} R_{\langle jk \rangle}^A + \sum_{k=1}^{N} \sum_{i=1}^{N} \frac{\partial \Phi_3}{\partial r_{\langle ki \rangle}^b} R_{\langle ki \rangle}^A \right) + \dots \right].$$

The term in parentheses in the rightmost expression in (B.55) is the three-body contribution to the double sum in (B.54). Average atomic Cauchy stress, i.e., static virial stress, then obeys, following (4.26) and Table 4.1[3],

$$\sigma^{ab} = \det(F_{.a}^{-1A}) P^{bA} F_{.A}^a = \frac{\Omega_0}{\Omega} \left(\frac{1}{2\Omega_0} \sum_{i=1}^{N} \sum_{j=1}^{N} \delta^{bc} \frac{\partial \Phi}{\partial r_{\langle ij \rangle}^c} R_{\langle ij \rangle}^A \right) F_{.A}^a$$

$$= \frac{1}{2\Omega} \sum_{i=1}^{N} \sum_{j=1}^{N} r_{\langle ij \rangle}^a \delta^{bc} \frac{\partial \Phi}{\partial r_{\langle ij \rangle}^c} = \frac{1}{2\Omega} \sum_{i=1}^{N} \sum_{j=1}^{N} r_{\langle ij \rangle}^a f_{\langle ij \rangle}^b, \tag{B.56}$$

---

[3] In Table 4.1, $\sigma^{ba} = \det(F_{.a}^{-1A}) P^{bA} F_{.A}^a$, but in (B.56), $\sigma^{ab} = \det(F_{.a}^{-1A}) P^{bA} F_{.A}^a$. The difference is inconsequential in the case of symmetric Cauchy stresses as would arise from central forces, i.e., (B.36), or when the atomic system supports no externally supplied torque (Nielsen and Martin 1985). Consistency could be obtained by defining the average atomic Cauchy stress as the transpose of that in (B.35) (Nielsen and Martin 1985), though in that case the definition of stress would become inconsistent with the convention adopted by Zhou (2003) and references therein.

in agreement with (B.35).

Tangent elastic coefficients follow from additional differentiation of the strain energy per unit reference volume with respect to macroscopic deformation **F** or macroscopic strain **E**. A two-point tensor of second-order elastic moduli is, analogous to (5.53),

$$
A^{aAbB} = \frac{\partial P^{aA}}{\partial F_{bB}} = \frac{\partial^2 \Psi_0}{\partial F_{aA}\partial F_{bB}} = \frac{1}{2\Omega_0}\sum_{\substack{i\neq j\\ k\neq l}}\frac{\partial^2 \Phi}{\partial r^c_{\langle ij\rangle}\partial r^d_{\langle kl\rangle}}\frac{\partial r^c_{\langle ij\rangle}}{\partial F_{aA}}\frac{\partial r^d_{\langle kl\rangle}}{\partial F_{bB}}
$$

$$
= \frac{1}{2\Omega_0}\sum_{\substack{i\neq j\\ k\neq l}}\frac{\partial^2 \Phi}{\partial r^c_{\langle ij\rangle}\partial r^d_{\langle kl\rangle}}\delta^{ac} R^A_{\langle ij\rangle}\delta^{bd} R^B_{\langle kl\rangle}. \tag{B.57}
$$

Repeated use of the summation symbol is omitted in the abbreviated notation of (B.57). Hence, summation applies over four sets of repeated atomic labels, as should be clear from the context. Recalling from (5.60), in Cartesian coordinates,

$$
\mathbb{C}^{ABCD} = \frac{\partial^2 \Psi_0}{\partial E_{AB}\partial E_{CD}} = \left(A^{aBcD} - \frac{\partial \Psi_0}{\partial E_{BD}}\delta^{ac}\right)F^{-1A}_{.a}F^{-1C}_{.c}, \tag{B.58}
$$

the tangent second-order elasticity tensor referred to the reference configuration is

$$
\mathbb{C}^{ABCD} = \frac{1}{2\Omega_0}F^{-1A}_{.a}F^{-1C}_{.c} \times
$$

$$
\left(\sum_{\substack{i\neq j\\ k\neq l}}\frac{\partial^2 \Phi}{\partial r^e_{\langle ij\rangle}\partial r^f_{\langle kl\rangle}}\delta^{ae} R^B_{\langle ij\rangle}\delta^{cf} R^D_{\langle kl\rangle} - F^{-1B}_{.e}\sum_{i\neq j}\delta^{eb}\frac{\partial \Phi}{\partial r^b_{\langle ij\rangle}} R^D_{\langle ij\rangle}\delta^{ac}\right). \tag{B.59}
$$

A two-point tensor of third-order elastic stiffness coefficients is, similarly to (5.55),

$$
A^{aAbBcC} = \frac{\partial^2 P^{aA}}{\partial F_{bB}\partial F_{cC}} = \frac{\partial^3 \Psi_0}{\partial F_{aA}\partial F_{bB}\partial F_{cC}}
$$

$$
= \frac{1}{2\Omega_0}\sum_{\substack{i\neq j\\ k\neq l\\ m\neq n}}\frac{\partial^3 \Phi}{\partial r^d_{\langle ij\rangle}\partial r^e_{\langle kl\rangle}\partial r^f_{\langle mn\rangle}}\delta^{ad} R^A_{\langle ij\rangle}\delta^{be} R^B_{\langle kl\rangle}\delta^{cf} R^C_{\langle mn\rangle}. \tag{B.60}
$$

Similarly to (B.58) and recalling from (5.61), in Cartesian coordinates,

$$
\mathbb{C}^{AEBDCG} = \frac{\partial^3 \Psi_0}{\partial E_{AE}\partial E_{BD}\partial E_{CG}} = (A^{aAbBcC} - \mathbb{C}^{ABCF}\delta^{ab}F^c_{.F} - \mathbb{C}^{ACBF}\delta^{ac}F^b_{.F}
$$

$$
- \mathbb{C}^{AFBC}\delta^{bc}F^a_{.F})F^{-1E}_{.a}F^{-1D}_{.b}F^{-1G}_{.c}. \tag{B.61}
$$

Substitution of (B.59) and (B.60) into (B.61) then provides the third-order tangent elastic stiffness coefficients $\mathbb{C}^{ABCDEF}$ in terms of atomic coordinates and derivatives of the interatomic potential. Note that (B.57)-(B.61) evolve with deformation or strain. Tangent moduli for a particular (un)strained configuration are evaluated using the corresponding values of $\mathbf{r}_{\langle ij \rangle}$ and $\mathbf{F}$ in that configuration.

As discussed in Section 5.1.3, elastic constants are typically introduced as derivatives of the strain energy density at the reference configuration, with that energy expressed as a Taylor series about the undistorted reference state. Elastic constants evaluated at the reference state corresponding to an undeformed lattice are found simply by setting $\mathbf{r}_{\langle ij \rangle} = \mathbf{R}_{\langle ij \rangle}$, $\mathbf{F} = \mathbf{1}$, and evaluating derivatives of the potential at $\mathbf{r}_{\langle ij \rangle} = \mathbf{R}_{\langle ij \rangle}$. These reference elastic constants are denoted with an over-bar in the following expressions:

$$\overline{\mathbf{A}}^{aAbB} = \frac{1}{2\Omega_0} \sum_{\substack{i \neq j \\ k \neq l}} \left. \frac{\partial^2 \Phi}{\partial r^c_{\langle ij \rangle} \partial r^d_{\langle kl \rangle}} \right|_{\mathbf{r=R}} \delta^{ac} R^A_{\langle ij \rangle} \delta^{bd} R^B_{\langle kl \rangle}, \tag{B.62}$$

$$\overline{\mathbb{C}}^{ABCD} = \frac{1}{2\Omega_0} \sum_{\substack{i \neq j \\ k \neq l}} \left. \frac{\partial^2 \Phi}{\partial r^e_{\langle ij \rangle} \partial r^f_{\langle kl \rangle}} \right|_{\mathbf{r=R}} \delta^{Ae} R^B_{\langle ij \rangle} \delta^{Cf} R^D_{\langle kl \rangle}, \tag{B.63}$$

$$\overline{\mathbf{A}}^{aAbBcC} = \frac{1}{2\Omega_0} \sum_{\substack{i \neq j \\ k \neq l \\ m \neq n}} \left. \frac{\partial^3 \Phi}{\partial r^d_{\langle ij \rangle} \partial r^e_{\langle kl \rangle} \partial r^f_{\langle mn \rangle}} \right|_{\mathbf{r=R}} \delta^{ad} R^A_{\langle ij \rangle} \delta^{be} R^B_{\langle kl \rangle} \delta^{cf} R^C_{\langle mn \rangle}, \tag{B.64}$$

$$\overline{\mathbb{C}}^{ABCDEF} = \overline{\mathbf{A}}^{aAbCcE} \delta^B_{.a} \delta^D_{.b} \delta^F_{.c} - \overline{\mathbb{C}}^{ACEF} \delta^{BD} - \overline{\mathbb{C}}^{AECD} \delta^{BF} - \overline{\mathbb{C}}^{ABCE} \delta^{DF}$$

$$= \frac{1}{2\Omega_0} \sum_{\substack{i \neq j \\ k \neq l \\ m \neq n}} \left. \frac{\partial^3 \Phi}{\partial r^d_{\langle ij \rangle} \partial r^e_{\langle kl \rangle} \partial r^f_{\langle mn \rangle}} \right|_{\mathbf{r=R}} \delta^{ad} \delta^{eb} \delta^{fc} R^A_{\langle ij \rangle} R^C_{\langle kl \rangle} R^E_{\langle mn \rangle} \delta^B_{.a} \delta^D_{.b} \delta^F_{.c}$$

$$- \frac{1}{2\Omega_0} \sum_{\substack{i \neq j \\ k \neq l}} \left. \frac{\partial^2 \Phi}{\partial r^d_{\langle ij \rangle} \partial r^e_{\langle kl \rangle}} \right|_{\mathbf{r=R}} \delta^{ad} \delta^{eb} \delta^A_{.a} R^C_{\langle ij \rangle} \delta^E_{.b} R^F_{\langle kl \rangle} \delta^{BD} \tag{B.65}$$

$$- \frac{1}{2\Omega_0} \sum_{\substack{i \neq j \\ k \neq l}} \left. \frac{\partial^2 \Phi}{\partial r^d_{\langle ij \rangle} \partial r^e_{\langle kl \rangle}} \right|_{\mathbf{r=R}} \delta^{ad} \delta^{eb} \delta^A_{.a} R^E_{\langle ij \rangle} \delta^C_{.b} R^D_{\langle kl \rangle} \delta^{BF}$$

$$- \frac{1}{2\Omega_0} \sum_{\substack{i \neq j \\ k \neq l}} \left. \frac{\partial^2 \Phi}{\partial r^d_{\langle ij \rangle} \partial r^e_{\langle kl \rangle}} \right|_{\mathbf{r=R}} \delta^{ad} \delta^{eb} \delta^A_{.a} R^B_{\langle ij \rangle} \delta^C_{.b} R^E_{\langle kl \rangle} \delta^{DF}.$$

Second-order elastic constants $\overline{\mathbb{C}}^{ABCD}$ depend on second-order derivatives of energy potential Φ with respect to atomic coordinates, and third-order elastic constants $\overline{\mathbb{C}}^{ABCDEF}$ depend on second- and third-order derivatives of the potential energy. Tangent moduli (under homogeneous deformations) and reference elastic constants of orders four and higher can be obtained by further differentiation and use of the chain rule.

Use of (B.53)-(B.65) does not necessarily require that the reference configuration correspond to a perfect lattice, merely that atomic bond vectors deform homogeneously according to (B.37) from the (possibly defective) state at which the elasticity coefficients are measured[4]. The crystal need not deform homogeneously in the process of achieving this original defective state. Stresses and tangent moduli for a defective crystal at a particular value of macroscopic deformation $\mathbf{F}$ can be obtained using (B.55)-(B.61). For example, Dienes (1952) computed elasticity coefficients of copper and sodium crystals containing vacancies and interstitials using the atomic model of Fuchs (1936). Chung and Namburu (2003) and Chung (2004) computed tangent moduli of graphene with vacancies and interstitials using the multi-body potential of Brenner (1990). Clayton and Chung (2006) and Chung and Clayton (2007) calculated effects on tangent elastic moduli of vacancies, screw dislocations, screw dislocation dipoles, and twist disclinations in BCC tungsten single crystals, using the multi-body atomic potential of Finnis and Sinclair (1984).

B.2.5 Harmonic and Anharmonic Interactions

In what follows next, the potential energy is expressed in generalized polynomial form about a perfect reference state, leading to relations for stress and elastic stiffness tensors in terms of harmonic (i.e., linear force-displacement) and anharmonic (i.e., nonlinear force-displacement) parts of the potential energy. Anharmonic interactions must be incorporated to properly account for third-order elastic constants, and are also important in the vicinity of defect cores wherein large atomic displacements arise (Gallego and Ortiz 1993; Yavari et al. 2007). Anharmonicity must also be considered to address thermal expansion and temperature dependent elastic moduli in the context of thermoelasticity (Thomsen 1970; Phillips 2001); such dynamic effects are not formally considered here, however, in the

---

[4] If the reference configuration includes defects, then by definition $\mathbf{R}_{\langle i \rangle}$ does not correspond to atomic coordinates in a perfect crystal structure for all i. In such cases, interatomic forces will not always vanish in the reference configuration.

context of lattice statics. Relationships among atomic force coefficients, lattice vibrational frequencies, and continuum thermomechanical properties (e.g., temperature-dependent elastic coefficients, thermal expansion coefficients, and strain-dependent Gruneisen parameters) in the context of finite deformation theory are outlined by Thomsen (1970).

Expanding the potential energy of (B.21) in a series about the reference state in a polynomial of interatomic displacements $\mathbf{q}_{\langle ij \rangle} = \mathbf{r}_{\langle ij \rangle} - \mathbf{R}_{\langle ij \rangle}$,

$$
\Phi = \Phi_0 + \sum_{i \neq j} \left. \frac{\partial \Phi}{\partial r^a_{\langle ij \rangle}} \right|_{\mathbf{r}=\mathbf{R}} q^a_{\langle ij \rangle} + \frac{1}{2} \sum_{\substack{i \neq j \\ k \neq l}} \left. \frac{\partial^2 \Phi}{\partial r^a_{\langle ij \rangle} \partial r^b_{\langle kl \rangle}} \right|_{\mathbf{r}=\mathbf{R}} q^a_{\langle ij \rangle} q^b_{\langle kl \rangle}
$$
$$
+ \frac{1}{6} \sum_{\substack{i \neq j \\ k \neq l \\ m \neq n}} \left. \frac{\partial^3 \Phi}{\partial r^a_{\langle ij \rangle} \partial r^b_{\langle kl \rangle} \partial r^c_{\langle mn \rangle}} \right|_{\mathbf{r}=\mathbf{R}} q^a_{\langle ij \rangle} q^b_{\langle kl \rangle} q^c_{\langle mn \rangle} + ...
$$

(B.66)

Repeated use of the summation symbol is again omitted in the abbreviated notation of (B.66). Summation in the second term on the right of (B.66) applies over two sets of repeated atomic labels, that in the third term over four sets, and that in the fourth term over six sets. The second term on the right side of (B.66) vanishes identically if, as assumed henceforth in Section B.2.5 for simple illustrative purposes (Clayton and Bammann 2009), atoms in reference state B_0 are free of external and internal forces[5]:

$$
H^a_{\langle ij \rangle} = \delta^a_{.b} \left(\partial \Phi / \partial r^b_{\langle ij \rangle} \right) \Big|_{\mathbf{r}=\mathbf{R}} = 0 .
$$

(B.67)

Denoted by Φ_0 is a cohesive or total ground state energy of the reference lattice or crystal structure, conventionally negative in algebraic sign.

Introducing matrix notation for interatomic stiffness coefficients:

$$
H^{ab}_{\langle ijkl \rangle} = \delta^{ac} \delta^{bd} \left. \frac{\partial^2 \Phi}{\partial r^c_{\langle ij \rangle} \partial r^d_{\langle kl \rangle}} \right|_{\mathbf{r}=\mathbf{R}} , \quad H^{abc}_{\langle ijklmn \rangle} = \delta^{ad} \delta^{be} \delta^{cf} \left. \frac{\partial^3 \Phi}{\partial r^d_{\langle ij \rangle} \partial r^e_{\langle kl \rangle} \partial r^f_{\langle mn \rangle}} \right|_{\mathbf{r}=\mathbf{R}} , \quad
$$

(B.68)

the potential energy in (B.66) becomes

$$
\Phi = \Phi_0 + \frac{1}{2} \sum_{\substack{i \neq j \\ k \neq l}} H^{cd}_{\langle ijkl \rangle} \delta_{ca} \delta_{db} q^a_{\langle ij \rangle} q^b_{\langle kl \rangle}
$$
$$
+ \frac{1}{6} \sum_{\substack{i \neq j \\ k \neq l \\ m \neq n}} H^{def}_{\langle ijklmn \rangle} \delta_{da} \delta_{eb} \delta_{fc} q^a_{\langle ij \rangle} q^b_{\langle kl \rangle} q^c_{\langle mn \rangle} + ...
$$

(B.69)

---

[5] Condition (B.67) is an approximation that need not hold for arbitrary potentials; contributions of nonzero $H^a_{\langle ij \rangle}$ could affect subsequently derived quantities.

Since $\mathbf{r}_{\langle ij \rangle} = -\mathbf{r}_{\langle ji \rangle}$, the atomic stiffness matrix in the first of (B.68) exhibits the natural symmetries

$$H^{ab}_{\langle ijkl \rangle} = H^{ab}_{\langle jilk \rangle} = H^{ba}_{\langle klij \rangle} = -H^{ab}_{\langle jikl \rangle} = -H^{ab}_{\langle ijlk \rangle} = -H^{ba}_{\langle klji \rangle}. \qquad (B.70)$$

Other forms and symmetries of harmonic stiffness coefficients are listed by Maradudin et al. (1971). Symmetries can be deduced for anharmonic coefficients $H^{abc}_{\langle ijklmn \rangle}$ via (B.68).

Noting from (B.44) that $\partial q^a_{\langle kl \rangle} / \partial r^b_{\langle kl \rangle} = \delta^a_{.b}$, the average spatial (e.g., mechanical Cauchy) stress of (B.36) and (B.56) becomes

$$\sigma^{ab} = \frac{1}{2\Omega} \sum_{\substack{i \neq j \\ k \neq l}} r^a_{\langle ij \rangle} H^{bc}_{\langle ijkl \rangle} \delta_{cd} q^d_{\langle kl \rangle}$$

$$+ \frac{1}{4\Omega} \sum_{\substack{i \neq j \\ k \neq l \\ m \neq n}} r^a_{\langle ij \rangle} H^{bce}_{\langle ijklmn \rangle} \delta_{cd} q^d_{\langle kl \rangle} \delta_{ef} q^f_{\langle mn \rangle} + ..., \qquad (B.71)$$

and under likewise conditions of homogeneous deformation, the two-point stress tensor (B.55) is

$$P^{aA} = \frac{1}{2\Omega_0} \sum_{\substack{i \neq j \\ k \neq l}} H^{ab}_{\langle ijkl \rangle} \delta_{bc} q^c_{\langle kl \rangle} R^A_{\langle ij \rangle}$$

$$+ \frac{1}{4\Omega_0} \sum_{\substack{i \neq j \\ k \neq l \\ m \neq n}} H^{abc}_{\langle ijklmn \rangle} \delta_{bd} q^d_{\langle kl \rangle} \delta_{ce} q^e_{\langle mn \rangle} R^A_{\langle ij \rangle} + ... \qquad (B.72)$$

In the harmonic approximation, products of order higher than two in interatomic displacements are dropped from (B.69), leading to the following expressions for interatomic forces, Cauchy stress, and first Piola-Kirchhoff stress:

$$\left. \begin{array}{l} f^a_{\langle ij \rangle} = \sum_{k \neq l} H^{ab}_{\langle ijkl \rangle} \delta_{bc} q^c_{\langle kl \rangle}, \\[3mm] \sigma^{ab} = \dfrac{1}{2\Omega} \sum_{\substack{i \neq j \\ k \neq l}} r^a_{\langle ij \rangle} H^{bc}_{\langle ijkl \rangle} \delta_{cd} q^d_{\langle kl \rangle}, \\[4mm] P^{aA} = \dfrac{1}{2\Omega_0} \sum_{\substack{i \neq j \\ k \neq l}} H^{ab}_{\langle ijkl \rangle} \delta_{bc} q^c_{\langle kl \rangle} R^A_{\langle ij \rangle}. \end{array} \right\} \begin{array}{l} \text{harmonic} \\ \text{approximation} \end{array} \qquad (B.73)$$

Returning now to the general case admitting anharmonic terms, second- and third-order elastic constants at the reference state first introduced in (B.62)-(B.65) can be rewritten as

$$\overline{\mathbb{A}}^{aAbB} = \frac{1}{2\Omega_0} \sum_{\substack{i \neq j \\ k \neq l}} H^{ab}_{\langle ijkl \rangle} R^A_{\langle ij \rangle} R^B_{\langle kl \rangle}, \tag{B.74}$$

$$\overline{\mathbb{C}}^{ABCD} = \frac{1}{2\Omega_0} \sum_{\substack{i \neq j \\ k \neq l}} H^{ac}_{\langle ijkl \rangle} \delta^A_{.a} R^B_{\langle ij \rangle} \delta^C_{.c} R^D_{\langle kl \rangle}, \tag{B.75}$$

$$\overline{\mathbb{A}}^{aAbBcC} = \frac{1}{2\Omega_0} \sum_{\substack{i \neq j \\ k \neq l \\ m \neq n}} H^{abc}_{\langle ijklmn \rangle} R^A_{\langle ij \rangle} R^B_{\langle kl \rangle} R^C_{\langle mn \rangle}, \tag{B.76}$$

$$\begin{aligned}
\overline{\mathbb{C}}^{ABCDEF} =\ & \frac{1}{2\Omega_0} \sum_{\substack{i \neq j \\ k \neq l \\ m \neq n}} H^{abc}_{\langle ijklmn \rangle} R^A_{\langle ij \rangle} R^C_{\langle kl \rangle} R^E_{\langle mn \rangle} \delta^B_{.a} \delta^D_{.b} \delta^F_{.c} \\[2mm]
& - \frac{1}{2\Omega_0} \sum_{\substack{i \neq j \\ k \neq l}} H^{ab}_{\langle ijkl \rangle} \delta^A_{.a} R^C_{\langle ij \rangle} \delta^E_{.b} R^F_{\langle kl \rangle} \delta^{BD} \\[2mm]
& - \frac{1}{2\Omega_0} \sum_{\substack{i \neq j \\ k \neq l}} H^{ab}_{\langle ijkl \rangle} \delta^A_{.a} R^E_{\langle ij \rangle} \delta^C_{.b} R^D_{\langle kl \rangle} \delta^{BF} \\[2mm]
& - \frac{1}{2\Omega_0} \sum_{\substack{i \neq j \\ k \neq l}} H^{ab}_{\langle ijkl \rangle} \delta^A_{.a} R^B_{\langle ij \rangle} \delta^C_{.b} R^E_{\langle kl \rangle} \delta^{DF}.
\end{aligned} \tag{B.77}$$

Clearly third- (and higher-order) elastic constants depend on anharmonic terms in the potential energy, as noted by Thurston and Brugger (1964), Kaga (1968), and Maugin (1999). On the other hand, third-order (and higher-order) interatomic stiffness coefficients $H^{abc}_{\langle ijklmn \rangle}$ do not affect the second-order elastic constants.

Expansion (B.69), while generic in the sense that many types of interactions (e.g., pair-wise and multi-body, central and non-central force) are admitted, may be cumbersome for computation of elastic constants for specific potentials that are not expressed explicitly in terms of interatomic separation vectors. For example, expressions for second- and third-order elastic constants for cubic crystals obtained from the embedded atom method are given by Chantasiriwan and Milstein (1996) in terms of derivatives with respect to scalar interatomic distances r as opposed to derivatives with respect to interatomic separation vectors. As will be demonstrated explicitly in Section B.2.6, such expressions (Chantasiriwan and Milstein 1996) for second- and third-order elastic constants analogously contain derivatives of up to orders two and three, respectively, of the potential energy function with respect to scalar atomic separation distance.

B.2.6 Examples: Pair Potential and Embedded Atom Method

For illustrative purposes, stresses and tangent elasticity coefficients are computed for pair potentials and embedded atom potentials. First consider a generic pair potential ϕ of the type following the first equality in (B.28), for example. The two-point stress tensor can be found using (B.51) as

$$P^{aA} = F_{.B}^{a}\frac{\partial \Psi_0}{\partial E_{AB}} = \frac{1}{2\Omega_0}\sum_{i=1}^{N}\sum_{j=1}^{N}\phi'\frac{r_{\langle ij\rangle}^{a}R_{\langle ij\rangle}^{A}}{r_{\langle ij\rangle}}, \tag{B.78}$$

where $\phi' = \partial\phi/\partial r$ with the appropriate atomic subscripts implied. The average atomic Cauchy stress is then

$$\sigma^{ab} = \det(F_{.a}^{-1A})F_{.A}^{a}P^{bA} = \frac{1}{2\Omega}\sum_{i=1}^{N}\sum_{j=1}^{N}\phi'\frac{r_{\langle ij\rangle}^{a}r_{\langle ij\rangle}^{b}}{r_{\langle ij\rangle}}. \tag{B.79}$$

Second-order tangent elastic moduli are found as

$$\begin{aligned}
\mathbb{C}^{ABCD} &= \frac{\partial^2\Psi_0}{\partial E_{AB}\partial E_{CD}} = \frac{1}{2\Omega_0}\sum_{i=1}^{N}\sum_{j=1}^{N}R_{\langle ij\rangle}^{A}R_{\langle ij\rangle}^{B}\frac{\partial}{\partial E_{CD}}\left(\frac{\phi'}{r_{\langle ij\rangle}}\right) \\
&= \frac{1}{2\Omega_0}\sum_{i=1}^{N}\sum_{j=1}^{N}\left(\frac{\phi''}{r_{\langle ij\rangle}^2} - \frac{\phi'}{r_{\langle ij\rangle}^3}\right)R_{\langle ij\rangle}^{A}R_{\langle ij\rangle}^{B}R_{\langle ij\rangle}^{C}R_{\langle ij\rangle}^{D}.
\end{aligned} \tag{B.80}$$

Third-order tangent moduli resulting from a pair potential are obtained from further differentiation as

$$\begin{aligned}
\mathbb{C}^{ABCDEF} &= \frac{1}{2\Omega_0}\sum_{i=1}^{N}\sum_{j=1}^{N}R_{\langle ij\rangle}^{A}R_{\langle ij\rangle}^{B}R_{\langle ij\rangle}^{C}R_{\langle ij\rangle}^{D}\frac{\partial}{\partial E_{EF}}\left(\frac{\phi''}{r_{\langle ij\rangle}^2} - \frac{\phi'}{r_{\langle ij\rangle}^3}\right) \\
&= \frac{1}{2\Omega_0}\sum_{i=1}^{N}\sum_{j=1}^{N}\left(\frac{\phi'''}{r_{\langle ij\rangle}^3} - \frac{3\phi''}{r_{\langle ij\rangle}^4} + \frac{3\phi'}{r_{\langle ij\rangle}^5}\right)R_{\langle ij\rangle}^{A}R_{\langle ij\rangle}^{B}R_{\langle ij\rangle}^{C}R_{\langle ij\rangle}^{D}R_{\langle ij\rangle}^{E}R_{\langle ij\rangle}^{F}.
\end{aligned} \tag{B.81}$$

For a stress-free reference configuration, by definition $r_{\langle ij\rangle} = R_{\langle ij\rangle}$, $F = 1$, and $\Omega = \Omega_0$. In that case, (B.78)-(B.81) become, using over-bars to denote quantities in the undistorted state,

$$\bar{P}^{aA} = \frac{1}{2\Omega_0}\delta_{.B}^{a}\sum_{i=1}^{N}\sum_{j=1}^{N}\phi'\big|_{r=R}\frac{R_{\langle ij\rangle}^{B}R_{\langle ij\rangle}^{A}}{R_{\langle ij\rangle}} = 0, \tag{B.82}$$

$$\bar{\sigma}^{ab} = \frac{1}{2\Omega_0}\delta_{.A}^{a}\delta_{.B}^{b}\sum_{i=1}^{N}\sum_{j=1}^{N}\phi'\big|_{r=R}\frac{R_{\langle ij\rangle}^{A}R_{\langle ij\rangle}^{B}}{R_{\langle ij\rangle}} = 0, \tag{B.83}$$

$$\overline{\mathbb{C}}^{ABCD} = \frac{1}{2\Omega_0} \sum_{i=1}^{N} \sum_{j=1}^{N} \left(\frac{\phi''}{R_{\langle ij \rangle}^{\;2}} - \frac{\phi'}{R_{\langle ij \rangle}^{\;3}} \right) \Bigg|_{\mathbf{r=R}} R_{\langle ij \rangle}^{A} R_{\langle ij \rangle}^{B} R_{\langle ij \rangle}^{C} R_{\langle ij \rangle}^{D}, \qquad (B.84)$$

$$\overline{\mathbb{C}}^{ABCDEF} = \frac{1}{2\Omega_0} \sum_{i=1}^{N} \sum_{j=1}^{N} \left(\frac{\phi'''}{R_{\langle ij \rangle}^{\;3}} - \frac{3\phi''}{R_{\langle ij \rangle}^{\;4}} + \frac{3\phi'}{R_{\langle ij \rangle}^{\;5}} \right) \Bigg|_{\mathbf{r=R}} R_{\langle ij \rangle}^{A} R_{\langle ij \rangle}^{B} R_{\langle ij \rangle}^{C} R_{\langle ij \rangle}^{D} R_{\langle ij \rangle}^{E} R_{\langle ij \rangle}^{F}. (B.85)$$

Average stress measures vanish by definition in (B.82) and (B.83), second-order elastic constants in (B.84) depend on first and second derivatives of the potential energy with respect to atomic separation distance r, and third-order elastic constants in (B.85) depend on first, second, and third derivatives of the potential energy with respect to r.

Notice from (B.80) and (B.81) that tangent moduli (and consequently, the elastic constants in (B.84) and (B.85)) exhibit peculiar symmetries as a consequence of exclusive use of a pair potential to describe interatomic forces in crystals without inner displacements (i.e., non-polarized centro-symmetric crystals). These symmetries are often referred to as Cauchy's relations (Love 1927; Born and Huang 1954). In addition to the usual symmetries for hyperelastic moduli listed in (5.57) and (A.9), for a material obeying Cauchy's relations, the second-order elastic moduli obey

$$\mathbb{C}^{ABCD} = \mathbb{C}^{ACBD} = \mathbb{C}^{ADCB}, \qquad (B.86)$$

or in Voigt's notation (A.2),

$$\mathbb{C}^{12} = \mathbb{C}^{66}, \; \mathbb{C}^{13} = \mathbb{C}^{55}, \; \mathbb{C}^{23} = \mathbb{C}^{44},$$
$$\mathbb{C}^{14} = \mathbb{C}^{56}, \; \mathbb{C}^{25} = \mathbb{C}^{46}, \; \mathbb{C}^{36} = \mathbb{C}^{45}. \qquad (B.87)$$

Cauchy's relations reduce the maximum number of independent second-order elastic coefficients for a material of arbitrary anisotropy from 21 to 15. For cubic crystals (Section A.3.1), since $\overline{\mathbb{C}}^{12} = \overline{\mathbb{C}}^{13} = \overline{\mathbb{C}}^{23}$, the number of independent second-order constants is reduced from three to two via

$$\overline{\mathbb{C}}^{12} = \overline{\mathbb{C}}^{44}. \qquad (B.88)$$

Cauchy's relations for second-order constants are not physically realistic for most crystalline solids. However, they can be reasonably appropriate in some cubic ionic crystals, e.g., certain alkali halides, whose long-range pairwise interactions are primarily of the Coulomb type (i.e., (10.11)), with attractive forces emerging between alkali and halide ions and repulsive forces emerging between ions of the same kind. Each ion of an alkali halide crystal (rock salt structure) lies at a center of symmetry (Born and Huang 1954; Maradudin et al. 1971). The Coulomb potential energy of a pair of ions decays with separation distance only as $1/r$ and accounts for most of the cohesive energy of the lattice. Incorporation of other shorter-range interactions in the total potential energy (Mott and Gurney 1948) can account for other pairwise and/or multi-body atomic force interactions

(e.g., repulsive overlap forces and/or attractive and repulsive van der Waals forces) and enables deviation from Cauchy's relations.

In an isotropic solid (Section A.3.3) obeying Cauchy's relations, the number of independent second-order elastic constants is reduced from two to one via the restriction $\lambda = \mu$, implying that Poisson's ratio is $\nu = 1/4$ for an isotropic elastic body whose atoms interact only via a pair potential. Also in this case, the ratio of shear modulus to bulk modulus is $\mu / K = 3/5$. Cauchy's restrictions do not, however, render a cubic crystal structure isotropic because μ' can still be nonzero in (A.19).

Cauchy's relations for third-order constants can be derived from (B.85) in a similar manner. For cubic crystals of the highest elastic symmetry (i.e., those of Laue group CI of Table A.1), the number of independent third-order elastic constants is reduced from six to three. Cauchy's relations for the third-order elastic constants in this case are (Chantasiriwan and Milstein 1996)

$$\overline{\mathbb{C}}^{112} = \overline{\mathbb{C}}^{166}, \ \overline{\mathbb{C}}^{123} = \overline{\mathbb{C}}^{144} = \overline{\mathbb{C}}^{456}. \tag{B.89}$$

Contributions from vibrational free energy can affect the elastic constants: even when atomic interactions are described by pair potentials, Cauchy's relations do not necessarily apply at finite temperatures (Kaga 1968) or even at absolute zero (i.e., null temperature), with the latter deviations a result of zero-point kinetic energy contributions (Wallace 1972).

Now consider the embedded atom potential (Daw and Baskes 1983, 1984) of (B.30)-(B.33), consisting of an N-body term U and a generic pair potential ϕ. The two-point stress tensor **P** found using identity (B.51) is

$$P^{aA} = F^a_{.B} \frac{\partial \Psi_0}{\partial E_{AB}}$$
$$= \frac{1}{\Omega_0} \sum_{i=1}^{N} U' \sum_{j=1}^{N} g' \frac{r^a_{\langle ij \rangle} R^A_{\langle ij \rangle}}{r_{\langle ij \rangle}} + \frac{1}{2\Omega_0} \sum_{i=1}^{N} \sum_{j=1}^{N} \phi' \frac{r^a_{\langle ij \rangle} R^A_{\langle ij \rangle}}{r_{\langle ij \rangle}}, \tag{B.90}$$

where the compact notation $U' = \partial U / \partial \rho$, $g' = \partial g / \partial r$, and $\phi' = \partial \phi / \partial r$ is used. The average spatial stress tensor (i.e., akin to the mechanical Cauchy stress) is

$$\sigma^{ab} = \det(F^{-1A}_{.a}) F^a_{.A} P^{bA}$$
$$= \frac{1}{\Omega} \sum_{i=1}^{N} U' \sum_{j=1}^{N} g' \frac{r^a_{\langle ij \rangle} r^b_{\langle ij \rangle}}{r_{\langle ij \rangle}} + \frac{1}{2\Omega} \sum_{i=1}^{N} \sum_{j=1}^{N} \phi' \frac{r^a_{\langle ij \rangle} r^b_{\langle ij \rangle}}{r_{\langle ij \rangle}}. \tag{B.91}$$

Second-order tangent elastic moduli are found as

$$\mathbb{C}^{ABCD} = \frac{\partial^2 \Psi_0}{\partial E_{AB} \partial E_{CD}}$$

$$= \frac{1}{\Omega_0} \frac{\partial}{\partial E_{CD}} \left(\sum_{i=1}^{N} U' \sum_{j=1}^{N} g' \frac{R_{\langle ij \rangle}^A R_{\langle ij \rangle}^B}{r_{\langle ij \rangle}} \right) + \frac{1}{2\Omega_0} \sum_{i=1}^{N} \sum_{j=1}^{N} R_{\langle ij \rangle}^A R_{\langle ij \rangle}^B \frac{\partial}{\partial E_{CD}} \left(\frac{\phi'}{r_{\langle ij \rangle}} \right)$$

$$= \frac{1}{\Omega_0} \sum_{i=1}^{N} U'' \left(\sum_{j=1}^{N} \frac{g'}{r_{\langle ij \rangle}} R_{\langle ij \rangle}^A R_{\langle ij \rangle}^B \right) \left(\sum_{k=1}^{N} \frac{g'}{r_{\langle ik \rangle}} R_{\langle ik \rangle}^C R_{\langle ik \rangle}^D \right) \qquad\text{(B.92)}$$

$$+ \frac{1}{\Omega_0} \sum_{i=1}^{N} U' \sum_{j=1}^{N} \left(\frac{g''}{r_{\langle ij \rangle}^2} - \frac{g'}{r_{\langle ij \rangle}^3} \right) R_{\langle ij \rangle}^A R_{\langle ij \rangle}^B R_{\langle ij \rangle}^C R_{\langle ij \rangle}^D$$

$$+ \frac{1}{2\Omega_0} \sum_{i=1}^{N} \sum_{j=1}^{N} \left(\frac{\phi''}{r_{\langle ij \rangle}^2} - \frac{\phi'}{r_{\langle ij \rangle}^3} \right) R_{\langle ij \rangle}^A R_{\langle ij \rangle}^B R_{\langle ij \rangle}^C R_{\langle ij \rangle}^D.$$

The third-order tangent moduli resulting from the embedded atom potential are calculated, after further differentiation, as (Chantasiriwan and Milstein 1996)

$$\mathbb{C}^{ABCDEF} = \frac{\partial^3 \Psi_0}{\partial E_{AB} \partial E_{CD} \partial E_{EF}}$$

$$= \frac{1}{\Omega_0} \sum_{i=1}^{N} U''' \left(\sum_{j=1}^{N} \frac{g'}{r_{\langle ij \rangle}} R_{\langle ij \rangle}^A R_{\langle ij \rangle}^B \right) \left(\sum_{k=1}^{N} \frac{g'}{r_{\langle ik \rangle}} R_{\langle ik \rangle}^C R_{\langle ik \rangle}^D \right) \left(\sum_{l=1}^{N} \frac{g'}{r_{\langle il \rangle}} R_{\langle il \rangle}^E R_{\langle il \rangle}^F \right)$$

$$+ \frac{1}{\Omega_0} \sum_{i=1}^{N} U'' \left(\sum_{j=1}^{N} \frac{g'}{r_{\langle ij \rangle}} R_{\langle ij \rangle}^A R_{\langle ij \rangle}^B \right) \left[\sum_{k=1}^{N} \left(\frac{g''}{r_{\langle ik \rangle}^2} - \frac{g'}{r_{\langle ik \rangle}^3} \right) R_{\langle ik \rangle}^C R_{\langle ik \rangle}^D R_{\langle ik \rangle}^E R_{\langle ik \rangle}^F \right]$$

$$+ \frac{1}{\Omega_0} \sum_{i=1}^{N} U'' \left(\sum_{j=1}^{N} \frac{g'}{r_{\langle ij \rangle}} R_{\langle ij \rangle}^C R_{\langle ij \rangle}^D \right) \left[\sum_{k=1}^{N} \left(\frac{g''}{r_{\langle ik \rangle}^2} - \frac{g'}{r_{\langle ik \rangle}^3} \right) R_{\langle ik \rangle}^A R_{\langle ik \rangle}^B R_{\langle ik \rangle}^E R_{\langle ik \rangle}^F \right]$$

$$+ \frac{1}{\Omega_0} \sum_{i=1}^{N} U'' \left(\sum_{j=1}^{N} \frac{g'}{r_{\langle ij \rangle}} R_{\langle ij \rangle}^E R_{\langle ij \rangle}^F \right) \left[\sum_{k=1}^{N} \left(\frac{g''}{r_{\langle ik \rangle}^2} - \frac{g'}{r_{\langle ik \rangle}^3} \right) R_{\langle ik \rangle}^C R_{\langle ik \rangle}^D R_{\langle ik \rangle}^A R_{\langle ik \rangle}^B \right]$$

$$+ \frac{1}{\Omega_0} \sum_{i=1}^{N} U' \sum_{j=1}^{N} \left(\frac{g'''}{r_{\langle ij \rangle}^3} - \frac{3g''}{r_{\langle ij \rangle}^4} + \frac{3g'}{r_{\langle ij \rangle}^5} \right) R_{\langle ij \rangle}^A R_{\langle ij \rangle}^B R_{\langle ij \rangle}^C R_{\langle ij \rangle}^D R_{\langle ij \rangle}^E R_{\langle ij \rangle}^F$$

$$+ \frac{1}{2\Omega_0} \sum_{i=1}^{N} \sum_{j=1}^{N} \left(\frac{\phi'''}{r_{\langle ij \rangle}^3} - \frac{3\phi''}{r_{\langle ij \rangle}^4} + \frac{3\phi'}{r_{\langle ij \rangle}^5} \right) R_{\langle ij \rangle}^A R_{\langle ij \rangle}^B R_{\langle ij \rangle}^C R_{\langle ij \rangle}^D R_{\langle ij \rangle}^E R_{\langle ij \rangle}^F. \qquad\text{(B.93)}$$

For a reference configuration free of both internal and external forces, $\mathbf{r}_{\langle ij \rangle} = \mathbf{R}_{\langle ij \rangle}$, $\mathbf{F} = \mathbf{1}$, and $\Omega = \Omega_0$. In this case, (B.90)-(B.93) degenerate to

$$\bar{P}^{aA} = \frac{1}{\Omega_0} \delta^a_{.B} \left[\sum_{i=1}^{N} U' \sum_{j=1}^{N} g' \big|_{\mathbf{r}=\mathbf{R}} \frac{R^B_{\langle ij \rangle} R^A_{\langle ij \rangle}}{R_{\langle ij \rangle}} + \sum_{i=1}^{N} \sum_{j=1}^{N} \phi' \big|_{\mathbf{r}=\mathbf{R}} \frac{R^B_{\langle ij \rangle} R^A_{\langle ij \rangle}}{2R_{\langle ij \rangle}} \right] = 0 , \quad \text{(B.94)}$$

$$\bar{\sigma}^{ab} = \frac{1}{\Omega_0} \delta^a_{.A} \delta^b_{.B} \left[\sum_{i=1}^{N} U' \sum_{j=1}^{N} g' \big|_{\mathbf{r}=\mathbf{R}} \frac{R^A_{\langle ij \rangle} R^B_{\langle ij \rangle}}{R_{\langle ij \rangle}} + \sum_{i=1}^{N} \sum_{j=1}^{N} \phi' \big|_{\mathbf{r}=\mathbf{R}} \frac{R^A_{\langle ij \rangle} R^B_{\langle ij \rangle}}{2R_{\langle ij \rangle}} \right] = 0 , \quad \text{(B.95)}$$

$$\overline{\mathbb{C}}^{ABCD} = \frac{1}{\Omega_0} \sum_{i=1}^{N} U'' \left(\sum_{j=1}^{N} \frac{g' \big|_{\mathbf{r}=\mathbf{R}}}{R_{\langle ij \rangle}} R^A_{\langle ij \rangle} R^B_{\langle ij \rangle} \right) \left(\sum_{k=1}^{N} \frac{g' \big|_{\mathbf{r}=\mathbf{R}}}{R_{\langle ik \rangle}} R^C_{\langle ik \rangle} R^D_{\langle ik \rangle} \right)$$

$$+ \frac{1}{\Omega_0} \sum_{i=1}^{N} U' \sum_{j=1}^{N} \left(\frac{g'' \big|_{\mathbf{r}=\mathbf{R}}}{R_{\langle ij \rangle}^2} - \frac{g' \big|_{\mathbf{r}=\mathbf{R}}}{R_{\langle ij \rangle}^3} \right) R^A_{\langle ij \rangle} R^B_{\langle ij \rangle} R^C_{\langle ij \rangle} R^D_{\langle ij \rangle} \quad \text{(B.96)}$$

$$+ \frac{1}{2\Omega_0} \sum_{i=1}^{N} \sum_{j=1}^{N} \left(\frac{\phi'' \big|_{\mathbf{r}=\mathbf{R}}}{R_{\langle ij \rangle}^2} - \frac{\phi' \big|_{\mathbf{r}=\mathbf{R}}}{R_{\langle ij \rangle}^3} \right) R^A_{\langle ij \rangle} R^B_{\langle ij \rangle} R^C_{\langle ij \rangle} R^D_{\langle ij \rangle} ,$$

$$\overline{\mathbb{C}}^{ABCDEF} = \frac{1}{\Omega_0} \times$$

$$\left\{ \sum_{i=1}^{N} U''' \left(\sum_{j=1}^{N} \frac{g' \big|_{\mathbf{r}=\mathbf{R}}}{R_{\langle ij \rangle}} R^A_{\langle ij \rangle} R^B_{\langle ij \rangle} \right) \left(\sum_{k=1}^{N} \frac{g' \big|_{\mathbf{r}=\mathbf{R}}}{R_{\langle ik \rangle}} R^C_{\langle ik \rangle} R^D_{\langle ik \rangle} \right) \left(\sum_{l=1}^{N} \frac{g' \big|_{\mathbf{r}=\mathbf{R}}}{R_{\langle il \rangle}} R^E_{\langle il \rangle} R^F_{\langle il \rangle} \right) \right.$$

$$+ \sum_{i=1}^{N} U'' \left(\sum_{j=1}^{N} \frac{g' \big|_{\mathbf{r}=\mathbf{R}}}{R_{\langle ij \rangle}} R^A_{\langle ij \rangle} R^B_{\langle ij \rangle} \right) \left[\sum_{k=1}^{N} \left(\frac{g'' \big|_{\mathbf{r}=\mathbf{R}}}{R_{\langle ik \rangle}^2} - \frac{g' \big|_{\mathbf{r}=\mathbf{R}}}{R_{\langle ik \rangle}^3} \right) R^C_{\langle ik \rangle} R^D_{\langle ik \rangle} R^E_{\langle ik \rangle} R^F_{\langle ik \rangle} \right]$$

$$+ \sum_{i=1}^{N} U'' \left(\sum_{j=1}^{N} \frac{g' \big|_{\mathbf{r}=\mathbf{R}}}{R_{\langle ij \rangle}} R^C_{\langle ij \rangle} R^D_{\langle ij \rangle} \right) \left[\sum_{k=1}^{N} \left(\frac{g'' \big|_{\mathbf{r}=\mathbf{R}}}{R_{\langle ik \rangle}^2} - \frac{g' \big|_{\mathbf{r}=\mathbf{R}}}{R_{\langle ik \rangle}^3} \right) R^A_{\langle ik \rangle} R^B_{\langle ik \rangle} R^E_{\langle ik \rangle} R^F_{\langle ik \rangle} \right]$$

$$+ \sum_{i=1}^{N} U'' \left(\sum_{j=1}^{N} \frac{g' \big|_{\mathbf{r}=\mathbf{R}}}{R_{\langle ij \rangle}} R^E_{\langle ij \rangle} R^F_{\langle ij \rangle} \right) \left[\sum_{k=1}^{N} \left(\frac{g'' \big|_{\mathbf{r}=\mathbf{R}}}{R_{\langle ik \rangle}^2} - \frac{g' \big|_{\mathbf{r}=\mathbf{R}}}{R_{\langle ik \rangle}^3} \right) R^C_{\langle ik \rangle} R^D_{\langle ik \rangle} R^A_{\langle ik \rangle} R^B_{\langle ik \rangle} \right]$$

$$+ \sum_{i=1}^{N} U' \sum_{j=1}^{N} \left(\frac{g''' \big|_{\mathbf{r}=\mathbf{R}}}{R_{\langle ij \rangle}^3} - \frac{3 g'' \big|_{\mathbf{r}=\mathbf{R}}}{R_{\langle ij \rangle}^4} + \frac{3 g' \big|_{\mathbf{r}=\mathbf{R}}}{R_{\langle ij \rangle}^5} \right) R^A_{\langle ij \rangle} R^B_{\langle ij \rangle} R^C_{\langle ij \rangle} R^D_{\langle ij \rangle} R^E_{\langle ij \rangle} R^F_{\langle ij \rangle}$$

$$+ \left. \sum_{i=1}^{N} \sum_{j=1}^{N} \left(\frac{\phi''' \big|_{\mathbf{r}=\mathbf{R}}}{2R_{\langle ij \rangle}^3} - \frac{3 \phi'' \big|_{\mathbf{r}=\mathbf{R}}}{2R_{\langle ij \rangle}^4} + \frac{3 \phi' \big|_{\mathbf{r}=\mathbf{R}}}{2R_{\langle ij \rangle}^5} \right) R^A_{\langle ij \rangle} R^B_{\langle ij \rangle} R^C_{\langle ij \rangle} R^D_{\langle ij \rangle} R^E_{\langle ij \rangle} R^F_{\langle ij \rangle} \right\} . \quad \text{(B.97)}$$

While interatomic (internal) forces from N-body and two-body terms need not vanish in this configuration, i.e., $g'|_{r=R} \neq 0$ and $\phi'|_{r=R} \neq 0$ in general, average stresses in (B.94) and (B.95) still vanish for a crystal lattice in static equilibrium (Huang 1950) in the absence of external forces.

Second-order elastic constants in (B.96) depend on first and second derivatives (with respect to atomic separation distance r) of the potential energy functions g and ϕ; third-order constants in (B.97) depend on first, second, and third derivatives of these functions with respect to r. The embedded atom method can be used to reproduce second- and third-order elastic constants of cubic crystals without imposition of Cauchy's symmetries. However, when a linear embedding function is used such that $U = U(0) + U'\rho$ with $U' = \text{constant}$, the embedded atom method degenerates to a pair potential of the form $\Phi_2(r) = \phi(r)/2 + U'g(r)$, as noted by Daw and Baskes (1984). In that degenerate case, Cauchy's relations are recovered, e.g., (B.88) and (B.89) for a cubic crystal of Laue group CI.

Relations (B.78)-(B.97) are limited to central force interactions of the type described by (B.27). Explicit methods of computation of elastic coefficients of crystalline solids exhibiting non-central force interactions can be found in representative works of Chung and Namburu (2003) and Oh and Slattery (2008), for example.

The preceding treatment in Appendix B did not consider explicitly the origin of mechanical properties from the perspective of electronic structure (e.g., quantum mechanical principles governing atomic bonding); however, electronic structure does implicitly affect all functional forms and parameters entering the (empirical) interatomic potentials considered thus far. Gilman (2003) discusses the electronic basis of mechanical properties of solids, including elastic coefficients, plastic properties such as dislocation mobility, and surface properties such as surface energy and fracture resistance. Wallace (1972) provides an exhaustive mathematical treatment of atomic origins of thermoelastic behavior of crystals, including lattice statics and dynamics of polyatomic structures (e.g., those undergoing inner displacements); large deformations; harmonic and anharmonic effects; surface effects; explicit electronic contributions; and sample calculations using various potentials, with comparisons of theoretical results to experimental data for a number of different crystalline materials.

Appendix C: Discrete Defects in Linear Elasticity

The focus of much of this text—specifically parts of Chapters 3 and Chapters 6, 7, 8, and 9—has centered on continuum models of crystalline solids containing continuous distributions of lattice defects. Effects of individual, i.e., discrete, defects on the response of an otherwise elastic solid are considered in Appendix C. These effects are quantified via solutions of boundary value problems obtained using continuum elasticity theory. Elasticity solutions for line and point defects provide insight into stored energies addressed elsewhere via internal state variables in continuum constitutive models, as discussed in Chapters 6, 8, and 9; stored energies of lattice defects also enter expressions for residual volume changes as discussed in Chapter 7. Fundamental concepts of theoretical strength and Peierls stress that can provide insight into failure and yielding, respectively, of crystalline solids are also presented in this Appendix.

Most solutions presented in Appendix C follow from treating the body containing the defect as isotropic and linear elastic, though some anisotropic elasticity solutions are provided for energies of dislocations of orientations that arise frequently in cubic and hexagonal crystals. Compact closed-form solutions do not seem to exist for nonlinear elastic solids (i.e., large deformations and/or higher-order elastic constants), and lengthy nonlinear elasticity solutions for field variables of crystals with discrete defects, often obtained via iterative methods (Willis 1967; Teodosiu 1982) fall outside the scope of this Appendix.

Linear elastic solutions offer quantitative accuracy for field variables such as stress, strain, and strain energy density far from the defect core, which itself cannot be treated accurately via linear or even nonlinear elasticity (Teodosiu 1982), since the non-convex energy density of the highly distorted crystal structure is not addressed by standard continuum elasticity theories. The core region surrounding a line defect extends on the order of one to ten lattice parameters and typically accounts for on the order of ten percent of the total energy per unit length of the dislocation line (Teodosiu 1982; Hull and Bacon 1984). The size of the dislocation core, and its effect on slip resistance, is treated in an approximate sense in the final Section of Appendix C by the Peierls model (Peierls 1940; Nabarro 1947; Eshelby 1949b; Foreman et al. 1951). Very accurate studies of defect core

structures and properties require fully resolved atomic/molecular statics calculations or possibly even quantum mechanical treatments.

No new derivations or new solutions are developed in this Appendix. Instead, existing formulae are collected from a number of sources (Frenkel 1926; Peierls 1940; Cottrell 1953; Eshelby 1949b, 1954, 1956; Eshelby et al. 1953; Foreman 1955; Seeger and Haasen 1958; Nabarro 1967; Owen and Mura 1967; Huang and Mura 1970; Li and Gilman 1970; Liu and Li 1971; Kuo and Mura 1972; Li 1972; De Wit 1973; Steeds 1973; Hirth and Lothe 1982; Teodosiu 1982; Hull and Bacon 1984; Phillips 2001).

C.1 Volterra Defects

Volterra (1907) determined field variables (i.e., displacements, strains, and stresses) for a hollow isotropic, linear elastic cylinder subjected to the following process: cutting a plane passing from the axis of the cylinder through one side, rigidly translating or rotating one face of the cut with respect to the other, joining the material together via removal or insertion of the appropriate amount of the same kind of matter, and then removing external forces from the cylinder. Love (1927) used the term "dislocation" to describe Volterra's solutions, and Taylor (1934) suggested use of Volterra's solutions to describe real line defects observed experimentally in crystalline solids. In the modern literature, Volterra's elastic defects corresponding to translational displacement discontinuities are labeled simply as "dislocations", while Volterra's elastic defects corresponding to rotational discontinuities are usually called "disclinations", the latter as termed by Frank (1958).
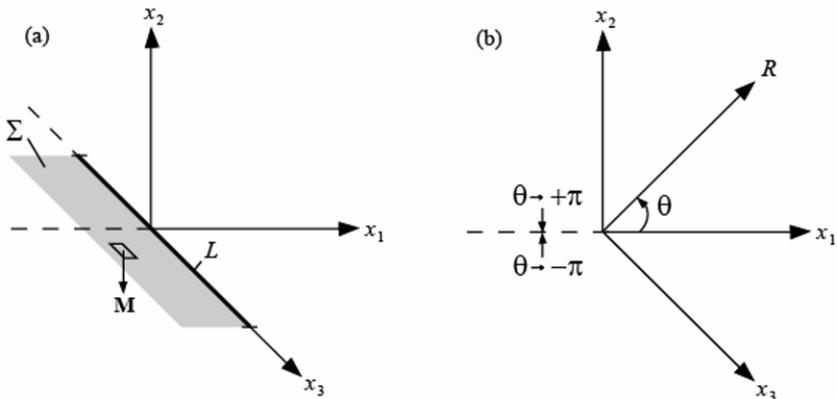
Fig. C.1 Cartesian coordinate system (a) and cylindrical coordinate system (b)

The present treatment is restricted to small deformations (i.e., geometrically linear theory) in elastic bodies of infinite dimensions. Hence, there is no need to consider changes in defect geometry (e.g., Burgers vectors and tangent lines) associated with changes in configuration of the body. Cartesian and cylindrical coordinate systems are shown in Fig. C.1(a) and Fig. C.1(b), respectively. Straight line defects are considered in Section C.1, with unit tangent line $\boldsymbol{\xi} = \xi \mathbf{e}_3$ always oriented parallel to the x_3-axis, as shown in Fig. C.2(a). The dislocation line itself, and the total length of this line, are simply labeled L. The surface across which displacements are discontinuous is denoted by Σ, with unit normal vector $\mathbf{M} = -\mathbf{e}_2$.

Following De Wit (1973), the special cylindrical coordinates of Fig. C.1(b) are related to Cartesian coordinates via

$$R = [(x_1)^2 + (x_2)^2]^{1/2}, \tag{C.1}$$

$$\theta = \tan^{-1}(x_2 / x_1) + \pi H(-x_1)\left[H(x_2) - H(-x_2)\right], \tag{C.2}$$

$$x_3 = x_3. \tag{C.3}$$

The range of $\tan^{-1}$ in (C.2) is limited to principle values $(-\pi/2, \pi/2)$; hence the angular coordinate is restricted to the range $-\pi < \theta < \pi$. Coordinate θ is multi-valued across the half-plane $\pm\pi$, with a jump of magnitude 2π. Heaviside (step) function $H(.)$ in (C.2) satisfies

$$H(x - a) = \begin{cases} 0 \,\forall\, x < a, \\ 1 \,\forall\, a < x. \end{cases} \tag{C.4}$$

Discontinuities in displacement and rotation of the material occur across the semi-infinite plane Σ. Specifically, jumps in displacement vector $\mathbf{u}$ and rotation vector $\mathbf{w}$ for an elastic body containing a Volterra line defect with an axis of rotation passing through the origin $\mathbf{x} = 0$ are (De Wit 1973)

$$\llbracket u_a \rrbracket = b_a + \varepsilon_{abc}\omega^b x^c, \tag{C.5}$$

$$\llbracket w_a \rrbracket = -\frac{1}{2}\varepsilon_{abc}\llbracket \Omega^{bc} \rrbracket = \omega_a, \tag{C.6}$$

where $\mathbf{b}$ and $\boldsymbol{\omega}$ are the Burgers vector and Frank vector, respectively, and the jump in an arbitrary quantity a across singular surface Σ satisfies

$$\llbracket a \rrbracket = a^+ - a^- = a(R, x_3)\big|_{\theta \to \pi} - a(R, x_3)\big|_{\theta \to -\pi}. \tag{C.7}$$

The notion that $\mathbf{b}$ and $\boldsymbol{\omega}$ are spatially constant for Volterra line defects follows from Weingarten's theorem (Weingarten 1901), as explained in detail by De Wit (1973) and Teodosiu (1982).

The following relationships for displacement gradients (i.e., distortions), strains, and rotations from Section 3.2.4 apply in the context of geometric linearity:

$$u_{a;b} = \beta_{ab} = \beta_{ab}^L + \beta_{ab}^P; \qquad (C.8)$$

$$\varepsilon_{ab} = \varepsilon_{ab}^L + \varepsilon_{ab}^P, \;\; \Omega_{ab} = \Omega_{ab}^L + \Omega_{ab}^P; \qquad (C.9)$$

$$\beta_{ab}^L = \varepsilon_{ab}^L + \Omega_{ab}^L, \;\; \varepsilon_{ab}^L = \beta_{(ab)}^L, \;\; \Omega_{ab}^L = \beta_{[ab]}^L; \qquad (C.10)$$

$$\beta_{ab}^P = \varepsilon_{ab}^P + \Omega_{ab}^P, \;\; \varepsilon_{ab}^P = \beta_{(ab)}^P, \;\; \Omega_{ab}^P = \beta_{[ab]}^P. \qquad (C.11)$$

The elastic or lattice displacement gradient is denoted by $\boldsymbol{\beta}^L$ and the plastic displacement gradient is denoted by $\boldsymbol{\beta}^P$. An additive decomposition of the total displacement gradient applies as is clear from (C.8). The displacement gradients on the right of (C.8) are sometimes called distortions, whose elastic and plastic parts are further separated into skew rotation and symmetric strain tensors in (C.10) and (C.11). Some authors (De Wit 1973; Mura 1982) use transposes of the quantities in (C.8)-(C.11) for definitions of distortions and rotations.

In contrast to the theory of elastoplasticity with continuous distributions of defects described in much of Chapters 3 and 6-9, in the context of discrete defects the plastic distortion is discontinuous. More specifically, plastic distortion is singular along Σ, as implied by (3.85) in the context of finite deformations (Rice 1971). Furthermore, since displacement (C.5) is discontinuous across Σ, (C.8) results in singular values of total distortion $u_{a;b}$ at Σ. On the other hand, as will be demonstrated later, elastic strain ε_{ab}^L is defined to be continuous and non-singular everywhere except at the core of the defect, i.e., except along the line $\boldsymbol{\xi} = \xi \mathbf{e}_3$. Physically, one can imagine the cutting and rigid translation and rotation processes of Volterra's construction as the source of plastic distortion, and the residual deformation remaining in the body after the material is joined across the cut as the source of elastic distortion.

Gradients of rotation are also important for describing kinematics of line defects. In the geometrically linear theory, the gradient of the rotation vector $\mathbf{w}$ is decomposed into an elastic and plastic part:

$$\kappa_{ab} = w_{a,b} = \kappa_{ab}^L + \kappa_{ab}^P, \qquad (C.12)$$

$$\kappa_{ab}^L = -\frac{1}{2}\varepsilon_{acd}\Omega_{..,b}^{Lcd} - \varphi_{ab}, \;\; \kappa_{ab}^P = -\frac{1}{2}\varepsilon_{acd}\Omega_{..,b}^{Pcd} + \varphi_{ab}. \qquad (C.13)$$

De Wit (1973) labels the transposes of $\boldsymbol{\kappa}$, $\boldsymbol{\kappa}^L$, and $\boldsymbol{\kappa}^P$ the total bend-twist, elastic bend-twist, and plastic bend-twist, respectively. The term φ is a contribution from disclinations to the elastic or plastic bend-twist not

arising from gradients of the rotation vector or the distortion. Hence φ contributes nine independent micropolar degrees of freedom. The micro-rotation in (C.13) is related to the micropolar rotation introduced in the continuum dislocation-disclination theory of Section 3.3.3 and (3.275) as follows:

$$\varphi_{ab} = \frac{1}{2}\varepsilon_{acd}Q_b^{[cd]}.$$

(C.14)

Analogously to the distortion, total and plastic bend-twists exhibit singularities along Σ, while the elastic bend-twist is defined to be continuous and non-singular except at the core of the defect. Notice in (C.12) and (C.13) that the rotation gradients (i.e., bend-twists) and micropolar rotation are all transposes of definitions used by De Wit (1973).

For traditional (i.e., translational) dislocations, $\varphi = 0$ and it is possible to divide the total distortion $\boldsymbol{\beta}$ and total rotation $\mathbf{w}$ into sums of (i) elastic parts that are non-singular except at the core and (ii) plastic parts that are singular on Σ and vanish elsewhere. For disclinations (i.e., rotational defects), $\varphi \neq 0$ and it is not possible to define an elastic distortion and elastic rotation that are non-singular everywhere except at the core. However, for disclinations it is still possible to define a (symmetric) elastic strain and an elastic bend-twist that are non-singular everywhere except along the disclination line. Relation (C.8) still applies in such cases, but the elastic distortion is not defined uniquely when discrete disclinations are present.

Shown in Fig. C.2(b) and C.2(c) are edge dislocations defined according to $\mathbf{b} \perp \boldsymbol{\xi}$. Shown in Fig. C.2(d) is a screw dislocation defined by $\mathbf{b} \parallel \boldsymbol{\xi}$. Shown in Fig. C.2(e) and C.2(f) are twist disclinations defined according to $\boldsymbol{\omega} \perp \boldsymbol{\xi}$. Shown in Fig. C.2(d) is a wedge disclination defined by $\boldsymbol{\omega} \parallel \boldsymbol{\xi}$.

Formulae for displacements, distortions, rotations, bend-twists, stresses, and strain energies resulting from each kind of defect in Fig. C.2 are given later in Sections C.1.1-C.1.4. In each case, the defect is contained within an isotropic linear elastic body of infinite extent. Unless noted otherwise, formulae are obtained from De Wit (1973) with minor differences in notation, some of which have been explained already following (C.8) and (C.12). Defects of mixed character are discussed in Section C.1.5. Strain energies of dislocation lines of particular orientations in anisotropic bodies are provided in Section C.1.6, primarily following from derivations of Foreman (1955).
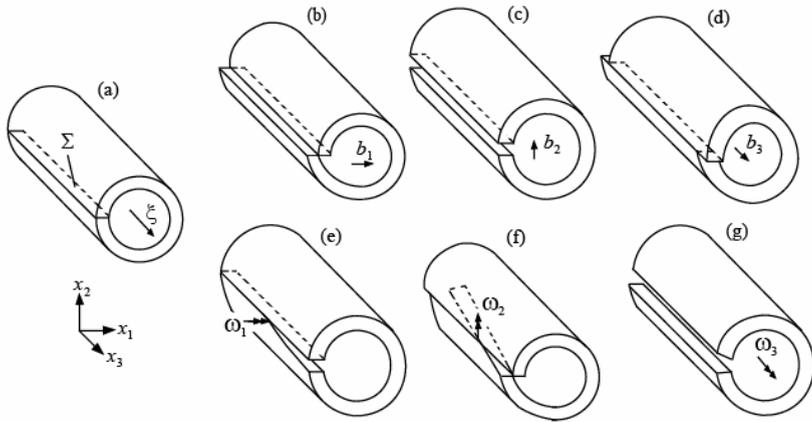
Fig. C.2 Volterra's line defects: defect line (a); edge dislocations (b), (c); screw dislocation (d); twist disclinations (e), (f); wedge disclination (g)

C.1.1 Edge Dislocation

The Burgers vector and its magnitude for an edge dislocation with superposed components of Fig. C.2(b) and Fig. C.2(c) are, respectively,

$$\mathbf{b} = b_1 \mathbf{e}_1 + b_2 \mathbf{e}_2, \ b = \left[(b_1)^2 + (b_2)^2 \right]^{1/2}. \tag{C.15}$$

Corresponding non-vanishing components of the plastic distortion tensor are

$$\beta_{12}^P = b_1 H(-x_1)\delta(x_2), \ \beta_{22}^P = b_2 H(-x_1)\delta(x_2), \tag{C.16}$$

with $\delta(.)$ Dirac's delta function and $H(.)$ the Heaviside step function. The first index of the plastic distortion corresponds to the Burgers vector, the second to the normal to the slip plane or surface of discontinuity Σ.

The linearized dislocation density tensor $\boldsymbol{\alpha}$ introduced in (3.230) in the context of continuum plasticity theory is written again in the present context of discrete defects as

$$\alpha^{da} = \varepsilon^{abc} \beta^{Pd}_{.b,c}, \tag{C.17}$$

with non-vanishing Cartesian components

$$\alpha_{13} = b_1 \delta(x_1)\delta(x_2), \ \alpha_{23} = b_2 \delta(x_1)\delta(x_2). \tag{C.18}$$

The first index of the dislocation density corresponds to the Burgers vector, the second to the tangent line. For consistency with Chapter 3, distortions and dislocation densities as defined here are transposes of those used by De Wit (1973). The notation convention used here, on the other hand, is the same as that used by Nye (1953).

Displacements induced by the edge dislocation in an isotropic elastic solid of infinite dimensions and Poisson's ratio v are

$$u_1 = b_1 \left[\frac{\theta}{2\pi} + \frac{x_1 x_2}{4\pi(1-v)R^2} \right] + \frac{b_2}{4\pi(1-v)} \left[(1-2v)\ln R + \frac{(x_2)^2}{R^2} \right], \quad \text{(C.19)}$$

$$u_2 = -\frac{b_1}{4\pi(1-v)} \left[(1-2v)\ln R + \frac{(x_1)^2}{R^2} \right] + b_2 \left[\frac{\theta}{2\pi} - \frac{x_1 x_2}{4\pi(1-v)R^2} \right], \quad \text{(C.20)}$$

$$u_3 = 0. \quad \text{(C.21)}$$

Non-vanishing parts of the total distortion $\beta_{a,b} = u_{a,b}$ in rectangular coordinates are

$$
\begin{aligned}
\beta_{11} = &-\frac{b_1}{4\pi(1-v)} \left[(1-2v)\frac{x_2}{R^2} + 2\frac{(x_1)^2 x_2}{R^4} \right] \\
&+ \frac{b_2}{4\pi(1-v)} \left[(1-2v)\frac{x_1}{R^2} - 2\frac{x_1(x_2)^2}{R^4} \right],
\end{aligned} \quad \text{(C.22)}
$$

$$
\begin{aligned}
\beta_{12} = &\frac{b_1}{4\pi(1-v)} \left[(3-2v)\frac{x_1}{R^2} - 2\frac{x_1(x_2)^2}{R^4} \right] \\
&+ \frac{b_2}{4\pi(1-v)} \left[(1-2v)\frac{x_2}{R^2} + 2\frac{(x_1)^2 x_2}{R^4} \right] + b_1 H(-x_1)\delta(x_2),
\end{aligned} \quad \text{(C.23)}
$$

$$
\begin{aligned}
\beta_{21} = &-\frac{b_1}{4\pi(1-v)} \left[(1-2v)\frac{x_1}{R^2} + 2\frac{x_1(x_2)^2}{R^4} \right] \\
&- \frac{b_2}{4\pi(1-v)} \left[(3-2v)\frac{x_2}{R^2} - 2\frac{(x_1)^2 x_2}{R^4} \right],
\end{aligned} \quad \text{(C.24)}
$$

$$
\begin{aligned}
\beta_{22} = &-\frac{b_1}{4\pi(1-v)} \left[(1-2v)\frac{x_2}{R^2} - 2\frac{(x_1)^2 x_2}{R^4} \right] \\
&+ \frac{b_2}{4\pi(1-v)} \left[(1-2v)\frac{x_1}{R^2} + 2\frac{x_1(x_2)^2}{R^4} \right] + b_2 H(-x_1)\delta(x_2).
\end{aligned} \quad \text{(C.25)}
$$

Elastic distortions are defined as those parts of β that are nonsingular everywhere except at the dislocation core, i.e., except at radial coordinate $R = 0$:

$$
\begin{aligned}
\beta_{11}^L = &-\frac{b_1}{4\pi(1-v)} \left[(1-2v)\frac{x_2}{R^2} + 2\frac{(x_1)^2 x_2}{R^4} \right] \\
&+ \frac{b_2}{4\pi(1-v)} \left[(1-2v)\frac{x_1}{R^2} - 2\frac{x_1(x_2)^2}{R^4} \right],
\end{aligned} \quad \text{(C.26)}
$$

$$\beta_{12}^{L} = \frac{b_1}{4\pi(1-v)}\left[(3-2v)\frac{x_1}{R^2} - 2\frac{x_1(x_2)^2}{R^4}\right]$$

$$+ \frac{b_2}{4\pi(1-v)}\left[(1-2v)\frac{x_2}{R^2} + 2\frac{(x_1)^2 x_2}{R^4}\right],$$

(C.27)

$$\beta_{21}^{L} = -\frac{b_1}{4\pi(1-v)}\left[(1-2v)\frac{x_1}{R^2} + 2\frac{x_1(x_2)^2}{R^4}\right]$$

$$- \frac{b_2}{4\pi(1-v)}\left[(3-2v)\frac{x_2}{R^2} - 2\frac{(x_1)^2 x_2}{R^4}\right],$$

(C.28)

$$\beta_{22}^{L} = -\frac{b_1}{4\pi(1-v)}\left[(1-2v)\frac{x_2}{R^2} - 2\frac{(x_1)^2 x_2}{R^4}\right]$$

$$+ \frac{b_2}{4\pi(1-v)}\left[(1-2v)\frac{x_1}{R^2} + 2\frac{x_1(x_2)^2}{R^4}\right],$$

(C.29)

$$\beta_{13}^{L} = \beta_{31}^{L} = \beta_{23}^{L} = \beta_{32}^{L} = \beta_{33}^{L} = 0.$$

(C.30)

Elastic strain components $\varepsilon_{ab}^{L} = \beta_{(ab)}^{L}$ are then obtained as follows:

$$\varepsilon_{11}^{L} = -\frac{b_1}{4\pi(1-v)}\left[(1-2v)\frac{x_2}{R^2} + 2\frac{(x_1)^2 x_2}{R^4}\right]$$

$$+ \frac{b_2}{4\pi(1-v)}\left[(1-2v)\frac{x_1}{R^2} - 2\frac{x_1(x_2)^2}{R^4}\right],$$

(C.31)

$$\varepsilon_{12}^{L} = \frac{b_1}{4\pi(1-v)}\left[\frac{x_1}{R^2} - 2\frac{x_1(x_2)^2}{R^4}\right] - \frac{b_2}{4\pi(1-v)}\left[\frac{x_2}{R^2} - 2\frac{(x_1)^2 x_2}{R^4}\right],$$

(C.32)

$$\varepsilon_{22}^{L} = -\frac{b_1}{4\pi(1-v)}\left[(1-2v)\frac{x_2}{R^2} - 2\frac{(x_1)^2 x_2}{R^4}\right]$$

$$+ \frac{b_2}{4\pi(1-v)}\left[(1-2v)\frac{x_1}{R^2} + 2\frac{x_1(x_2)^2}{R^4}\right],$$

(C.33)

$$\varepsilon_{13}^{L} = \varepsilon_{23}^{L} = \varepsilon_{33}^{L} = 0.$$

(C.34)

The elastic dilatation, i.e., elastic volume change in the context of geometric linearity, is

$$\varepsilon_{11}^{L} + \varepsilon_{22}^{L} + \varepsilon_{33}^{L} = -\frac{1-2v}{2\pi(1-v)R^2}(b_1 x_2 - b_2 x_1).$$

(C.35)

An elastic rotation $\mathbf{w^L}$ can be defined as that part of the total rotation non-singular except at the defect core, with components $w_a^L = -\varepsilon_{abc}(\Omega^L)^{bc}/2$ given for an edge dislocation by

$$w_1^L = w_2^L = 0, \ w_3^L = -\frac{1}{2\pi R^2}(b_1 x_1 + b_2 x_2) . \tag{C.36}$$

The micropolar rotation tensor vanishes by definition for an edge dislocation: $\varphi_{ab} = 0$. Elastic bend-twist components are

$$\kappa_{31}^L = \frac{1}{\pi}(b_1 x_1 + b_2 x_2)\frac{x_1}{R^4} - \frac{b_1}{2\pi R^2} , \tag{C.37}$$

$$\kappa_{32}^L = \frac{1}{\pi}(b_1 x_1 + b_2 x_2)\frac{x_2}{R^4} - \frac{b_2}{2\pi R^2} , \tag{C.38}$$

$$\kappa_{33}^L = \frac{1}{\pi}(b_1 x_1 + b_2 x_2)\frac{x_3}{R^4} , \tag{C.39}$$

$$\kappa_{11}^L = \kappa_{12}^L = \kappa_{13}^L = \kappa_{21}^L = \kappa_{22}^L = \kappa_{23}^L = 0 . \tag{C.40}$$

The stress field of an edge dislocation, using isotropic linear elasticity relation (see e.g., Sections 5.4 and A.3.3)

$$\sigma_{ab} = 2\mu\left[\varepsilon_{ab}^L + \left(\frac{\nu}{1-2\nu}\varepsilon_{.c}^{Lc}\right)\delta_{ab}\right] \tag{C.41}$$

is calculated as

$$\sigma_{11} = -\frac{\mu}{2\pi(1-\nu)}\left\{b_1\left[\frac{x_2}{R^2} + 2\frac{(x_1)^2 x_2}{R^4}\right] - b_2\left[\frac{x_1}{R^2} - 2\frac{x_1(x_2)^2}{R^4}\right]\right\}, \tag{C.42}$$

$$\sigma_{22} = -\frac{\mu}{2\pi(1-\nu)}\left\{b_1\left[\frac{x_2}{R^2} - 2\frac{(x_1)^2 x_2}{R^4}\right] - b_2\left[\frac{x_1}{R^2} + 2\frac{x_1(x_2)^2}{R^4}\right]\right\}, \tag{C.43}$$

$$\sigma_{33} = -\frac{\mu\nu}{\pi(1-\nu)}\left\{b_1\frac{x_2}{R^2} - b_2\frac{x_1}{R^2}\right\}, \tag{C.44}$$

$$\sigma_{12} = \frac{\mu}{2\pi(1-\nu)}\left\{b_1\left[\frac{x_1}{R^2} - 2\frac{x_1(x_2)^2}{R^4}\right] - b_2\left[\frac{x_2}{R^2} - 2\frac{(x_1)^2 x_2}{R^4}\right]\right\}, \tag{C.45}$$

$$\sigma_{13} = \sigma_{23} = 0 . \tag{C.46}$$

One can verify that the stress field of (C.42)-(C.46) satisfies the static equilibrium equations in the absence of body forces: $\sigma_{..,b}^{ab} = 0$ (De Wit 1973). The strain energy density is expressed most easily in cylindrical coordinates in terms of the magnitude b of the Burgers vector (Teodosiu 1982):

$$W = \frac{1}{2}\sigma^{ab}\varepsilon_{ab}^{L} = \frac{\mu b^2}{8\pi^2(1-\nu)^2 R^2}(1 - 2\nu\sin^2\theta).\qquad(\text{C.47})$$

The strain energy per unit length of an isotropic linear elastic cylinder containing the defect is

$$E = \int_{-\pi}^{\pi}\int_{R_C}^{R} W(R)(dR)(d\theta) = \frac{\mu b^2}{4\pi(1-\nu)}\ln\left(\frac{R}{R_C}\right),\qquad(\text{C.48})$$

where R_C is the radius of the dislocation core. The strain energy per unit length can be decomposed into dilatational and deviatoric parts as (Seeger and Haasen 1958)

$$E_D = \int_{-\pi}^{\pi}\int_{R_C}^{R} W_D(R)(dR)(d\theta) = \frac{\mu b^2}{12\pi}\frac{1-\nu-2\nu^2}{(1-\nu)^2}\ln\left(\frac{R}{R_C}\right),\qquad(\text{C.49})$$

$$E_S = \int_{-\pi}^{\pi}\int_{R_C}^{R} W_S(R)(dR)(d\theta) = \frac{\mu b^2}{6\pi}\frac{1-\nu+\nu^2}{(1-\nu)^2}\ln\left(\frac{R}{R_C}\right),\qquad(\text{C.50})$$

where the volumetric strain energy per unit volume is $W_D = K(\varepsilon_{.a}^{La})^2/2$, the deviatoric strain energy is $W_S = \mu(\varepsilon_{.b}^{La} - \delta_b^a\varepsilon_{.c}^{Lc}/3)(\varepsilon_{.a}^{Lb} - \delta_a^b\varepsilon_{.d}^{Ld}/3)$, and the bulk modulus is $K = 2\mu(1+\nu)/(3-6\nu)$. The core energy cannot be adequately described by continuum elasticity theory and is not explicitly included in the derivation of (C.48)-(C.50). However, if the core energy is known a priori, a value of R_C can be defined such that E implicitly contains both the core energy and the elastic strain energy, as explained in Section C.4.3 in the context of the Peierls model (Peierls 1940; Nabarro 1947).

Non-vanishing stress components in (C.42)-(C.45) decay as $1/R$ with increasing distance from the core. As the core ($R = 0$) is approached, elastic strains in excess of 10% are achieved for $R \lesssim b$, and hence linear elasticity theory is not valid in close vicinity of the dislocation line, i.e., within the core region. At distances far from the dislocation line, stresses and elastic strains decay to zero as $R \to \infty$, but the energy per unit length E of (C.48) decays only logarithmically and hence diverges (i.e., is unbounded) in the limit $R \to \infty$.

C.1.2 Screw Dislocation

The Burgers vector and its magnitude for a screw dislocation shown in Fig. C.2(d) are

$$\mathbf{b} = b_3\mathbf{e}_3, \quad b = b_3.\qquad(\text{C.51})$$

The non-vanishing component of the plastic distortion is

$$\beta_{32}^P = b_3 H(-x_1)\delta(x_2). \tag{C.52}$$

The non-vanishing part of the dislocation density (C.17) is

$$\alpha_{33} = b_3\delta(x_1)\delta(x_2). \tag{C.53}$$

Displacements induced by an isolated screw dislocation in an isotropic elastic solid of infinite dimensions and Poisson ratio ν are

$$u_1 = 0, \ u_2 = 0, \ u_3 = \frac{b_3\theta}{2\pi}. \tag{C.54}$$

Non-vanishing parts of the total distortion are

$$\beta_{31} = -\frac{b_3 x_2}{2\pi R^2}, \ \beta_{32} = \frac{b_3 x_1}{2\pi R^2} + b_3 H(-x_1)\delta(x_2). \tag{C.55}$$

Elastic distortion components are

$$\beta_{31}^L = -\frac{b_3 x_2}{2\pi R^2}, \ \beta_{32}^L = \frac{b_3 x_1}{2\pi R^2}, \tag{C.56}$$

$$\beta_{11}^L = \beta_{12}^L = \beta_{21}^L = \beta_{22}^L = \beta_{13}^L = \beta_{23}^L = \beta_{33}^L = 0. \tag{C.57}$$

Elastic strain components are

$$\varepsilon_{13}^L = -\frac{b_3 x_2}{4\pi R^2}, \ \varepsilon_{23}^L = \frac{b_3 x_1}{4\pi R^2}. \tag{C.58}$$

The elastic dilatation vanishes:

$$\varepsilon_{11}^L + \varepsilon_{22}^L + \varepsilon_{33}^L = 0. \tag{C.59}$$

An elastic rotation $w_a^L = -\varepsilon_{abc}(\Omega^L)^{bc}/2$ can be introduced:

$$w_1^L = \frac{b_3 x_1}{4\pi R^2}, \ w_2^L = \frac{b_3 x_2}{4\pi R^2}, \ w_3^L = 0. \tag{C.60}$$

The micropolar rotation $\varphi_{ab} = 0$ identically for a screw dislocation. Elastic bend-twist components are

$$\kappa_{11}^L = \frac{b_3}{4\pi R^2}\left[1 - \frac{2(x_1)^2}{R^2}\right], \ \kappa_{22}^L = \frac{b_3}{4\pi R^2}\left[1 - \frac{2(x_2)^2}{R^2}\right], \tag{C.61}$$

$$\kappa_{12}^L = \kappa_{21}^L = -\frac{b_3 x_1 x_2}{2\pi R^4}, \ \kappa_{13}^L = -\frac{b_3 x_1 x_3}{2\pi R^4}, \ \kappa_{23}^L = -\frac{b_3 x_1 x_2}{2\pi R^4}, \tag{C.62}$$

$$\kappa_{31}^L = \kappa_{32}^L = \kappa_{33}^L = 0. \tag{C.63}$$

The stress field of a screw dislocation aligned along the x_3-axis, obtained using isotropic linear elasticity relation (C.41) is

$$\sigma_{13} = -\frac{\mu b_3}{2\pi}\frac{x_2}{R^2}, \ \sigma_{23} = \frac{\mu b_3}{2\pi}\frac{x_1}{R^2}, \tag{C.64}$$

$$\sigma_{11} = \sigma_{12} = \sigma_{22} = \sigma_{33} = 0. \tag{C.65}$$

One can verify that (C.64) satisfies the static equilibrium equations $\sigma^{ab}_{\ ,b} = 0$ (De Wit 1973). The elastic strain energy density is

$$W = \frac{1}{2}\sigma^{ab}\varepsilon^{L}_{ab} = \frac{\mu b^2}{8\pi^2 R^2} \,. \tag{C.66}$$

The strain energy per unit length of the cylinder containing the defect is

$$E = \int_{-\pi}^{\pi}\int_{R_C}^{R} W(R)(dR)(d\theta) = \frac{\mu b^2}{4\pi}\ln\left(\frac{R}{R_C}\right), \tag{C.67}$$

with R_C the dislocation core radius. Strain energy is purely deviatoric:

$$E_D = \int_{-\pi}^{\pi}\int_{R_C}^{R} W_D(R)(dR)(d\theta) = 0 \,, \tag{C.68}$$

$$E_S = \int_{-\pi}^{\pi}\int_{R_C}^{R} W_S(R)(dR)(d\theta) = \frac{\mu b^2}{4\pi}\ln\left(\frac{R}{R_C}\right). \tag{C.69}$$

As was observed for edge dislocations, non-vanishing stress and strain components decay as $1/R$ for an isolated screw dislocation, and thus for $R \lesssim b$ strains are large and linear elasticity theory is no longer valid. At distances far from the dislocation line, stresses and elastic strains decay to zero as $R \to \infty$, but the energy per unit length E again decays only logarithmically with increasing R.

C.1.3 Twist Disclination

The combined Frank vector, and its magnitude, for a twist disclination passing through the origin with components shown in Fig. C.2(e) and C.2(f) are, respectively,

$$\boldsymbol{\omega} = \omega_1 \mathbf{e}_1 + \omega_2 \mathbf{e}_2 \,, \quad \omega = \left[(\omega_1)^2 + (\omega_2)^2\right]^{1/2}. \tag{C.70}$$

Non-vanishing components of the plastic distortion are

$$\beta^{P}_{12} = \omega_2 x_3 H(-x_1)\delta(x_2), \tag{C.71}$$

$$\beta^{P}_{22} = -\omega_1 x_3 H(-x_1)\delta(x_2), \tag{C.72}$$

$$\beta^{P}_{32} = -\omega_2 x_1 H(-x_1)\delta(x_2). \tag{C.73}$$

Non-vanishing components of the micro-rotation tensor are

$$\varphi_{12} = \omega_1 H(-x_1)\delta(x_2), \quad \varphi_{22} = \omega_2 H(-x_1)\delta(x_2). \tag{C.74}$$

The nonzero plastic strain components are

$$\varepsilon^{P}_{12} = \frac{\omega_2}{2} x_3 H(-x_1)\delta(x_2), \tag{C.75}$$

$$\varepsilon_{22}^{P} = -\omega_1 x_3 H(-x_1)\delta(x_2),$$

(C.76)

$$\varepsilon_{23}^{P} = -\frac{\omega_2}{2} x_1 H(-x_1)\delta(x_2).$$

(C.77)

Non-vanishing components of the plastic bend-twist are

$$\kappa_{11}^{P} = -\frac{\omega_2}{2} H(-x_1)\delta(x_2),$$

(C.78)

$$\kappa_{12}^{P} = -\frac{\omega_2}{2} x_1 H(-x_1)\delta'(x_2) + \omega_1 H(-x_1)\delta(x_2),$$

(C.79)

$$\kappa_{22}^{P} = \omega_2 H(-x_1)\delta(x_2),$$

(C.80)

$$\kappa_{31}^{P} = \frac{\omega_2}{2} x_3 \delta(x_1)\delta(x_2),$$

(C.81)

$$\kappa_{32}^{P} = -\frac{\omega_2}{2} x_3 H(-x_1)\delta'(x_2),$$

(C.82)

$$\kappa_{33}^{P} = -\frac{\omega_2}{2} H(-x_1)\delta(x_2).$$

(C.83)

The dislocation density tensor in the geometrically linear micropolar theory is defined as follows (De Wit 1973), consistent with (3.276):

$$\alpha^{da} = \varepsilon^{abc}(\beta_{.b,c}^{Pd} + \delta_{bf}\varepsilon^{fde}\varphi_{ec}) = \varepsilon^{abc}(\varepsilon_{.b,c}^{Pd} + \delta_{bf}\varepsilon^{fde}\kappa_{ec}^{P}),$$

(C.84)

and reduces to (C.17) in the absence of micro-rotation φ. The disclination density tensor in the geometrically linear theory is

$$\theta^{ab} = \varepsilon^{bcd}\varphi_{.c,d}^{a} = \varepsilon^{bcd}(\kappa^{P})_{.c,d}^{a}.$$

(C.85)

This is the transpose of the disclination density tensor defined by De Wit (1973), but it is consistent with the notation of Chapter 3 of the present text. Using (C.14), definition (C.85) is found to be consistent with the linearization of the disclination density tensor given in (3.277):

$$\theta^{ab} = \frac{1}{2}\varepsilon^{aef}\varepsilon^{bcd}Q_{cef,d}.$$

(C.86)

In particular, for a twist disclination, non-vanishing components of (C.84) are

$$\alpha_{13} = \omega_2 x_3 \delta(x_1)\delta(x_2), \quad \alpha_{23} = -\omega_1 x_3 \delta(x_1)\delta(x_2),$$

(C.87)

implying that the straight disclination line imparts a contribution to the dislocation density tensor. This is analogous to the contribution from micropolar rotation $\mathbf{Q}$ to torsion tensor $\hat{\mathbf{T}}$ in the theory of Section 3.3.3 in (3.249) and (3.272). The disclination density tensor (C.85) has nonzero components

$$\theta_{13} = \omega_1 \delta(x_1)\delta(x_2), \quad \theta_{23} = \omega_2 \delta(x_1)\delta(x_2).$$

(C.88)

The first index of the disclination tensor in (C.88) corresponds to the Frank vector, the second to the tangent line.

The displacement field of a twist disclination is

$$u_1 = -\frac{\omega_1 x_3}{4\pi(1-\nu)}\left[(1-2\nu)\ln R + \frac{(x_2)^2}{R^2}\right] + \omega_2 x_3\left[\frac{\theta}{2\pi} + \frac{x_1 x_2}{4\pi(1-\nu)R^2}\right], \quad \text{(C.89)}$$

$$u_2 = -\omega_1 x_3\left[\frac{\theta}{2\pi} - \frac{x_1 x_2}{4\pi(1-\nu)R^2}\right] - \frac{\omega_2 x_3}{4\pi(1-\nu)}\left[(1-2\nu)\ln R + \frac{(x_1)^2}{R^2}\right], \quad \text{(C.90)}$$

$$u_3 = \omega_1\left[\frac{x_2\theta}{2\pi} - \frac{(1-2\nu)x_1}{4\pi(1-\nu)}(\ln R - 1)\right] - \omega_2\left[\frac{x_1\theta}{2\pi} - \frac{(1-2\nu)x_2}{4\pi(1-\nu)}(\ln R - 1)\right]. \quad \text{(C.91)}$$

Cartesian distortion (i.e., displacement gradient) components are

$$\beta_{11} = -\frac{\omega_1 x_3}{4\pi(1-\nu)}\left[(1-2\nu)\frac{x_1}{R^2} - 2\frac{x_1(x_2)^2}{R^4}\right]$$
$$-\frac{\omega_2 x_3}{4\pi(1-\nu)}\left[(1-2\nu)\frac{x_2}{R^2} + 2\frac{(x_1)^2 x_2}{R^4}\right], \quad \text{(C.92)}$$

$$\beta_{12} = -\frac{\omega_1 x_3}{4\pi(1-\nu)}\left[(1-2\nu)\frac{x_2}{R^2} + 2\frac{(x_1)^2 x_2}{R^4}\right]$$
$$+\frac{\omega_2 x_3}{4\pi(1-\nu)}\left[(3-2\nu)\frac{x_1}{R^2} - 2\frac{x_1(x_2)^2}{R^4}\right] + \omega_2 x_3 H(-x_1)\delta(x_2), \quad \text{(C.93)}$$

$$\beta_{13} = -\frac{\omega_1}{4\pi(1-\nu)}\left[(1-2\nu)\ln R + \frac{(x_2)^2}{R^2}\right] + \omega_2\left[\frac{\theta}{2\pi} + \frac{x_1 x_2}{4\pi(1-\nu)R^2}\right], \quad \text{(C.94)}$$

$$\beta_{21} = \frac{\omega_1 x_3}{4\pi(1-\nu)}\left[(3-2\nu)\frac{x_2}{R^2} - 2\frac{(x_1)^2 x_2}{R^4}\right]$$
$$-\frac{\omega_2 x_3}{4\pi(1-\nu)}\left[(1-2\nu)\frac{x_1}{R^2} + 2\frac{x_1(x_2)^2}{R^4}\right], \quad \text{(C.95)}$$

$$\beta_{22} = -\frac{\omega_1 x_3}{4\pi(1-\nu)}\left[(1-2\nu)\frac{x_1}{R^2} + 2\frac{x_1(x_2)^2}{R^4}\right] - \omega_1 x_3 H(-x_1)\delta(x_2)$$
$$-\frac{\omega_2 x_3}{4\pi(1-\nu)}\left[(1-2\nu)\frac{x_2}{R^2} - 2\frac{(x_1)^2 x_2}{R^4}\right], \quad \text{(C.96)}$$

$$\beta_{23} = -\omega_1\left[\frac{\theta}{2\pi} - \frac{x_1 x_2}{4\pi(1-\nu)R^2}\right] - \frac{\omega_2}{4\pi(1-\nu)}\left[(1-2\nu)\ln R + \frac{(x_1)^2}{R^2}\right], \quad \text{(C.97)}$$

$$\beta_{31} = -\frac{\omega_1}{4\pi(1-v)}\left[(1-2v)\ln R + \frac{(x_2)^2}{R^2}\right] - \omega_2\left[\frac{\theta}{2\pi} - \frac{x_1x_2}{4\pi(1-v)R^2}\right], \quad \text{(C.98)}$$

$$\beta_{32} = \omega_1\left[\frac{\theta}{2\pi} + \frac{x_1x_2}{4\pi(1-v)R^2}\right]$$
$$-\frac{\omega_2}{4\pi(1-v)}\left[(1-2v)\ln R + \frac{(x_1)^2}{R^2}\right] - \omega_2 x_1 H(-x_1)\delta(x_2), \quad \text{(C.99)}$$

$$\beta_{33} = 0. \quad \text{(C.100)}$$

Because the total distortion $\boldsymbol{\beta}$ contains terms linear in θ, and because angular coordinate θ is discontinuous (i.e., multi-valued) with a jump of magnitude 2π as half-plane $\pm\pi$ ($x_2 = 0$, $x_1 < 0$) is traversed (Fig. C.1), an elastic distortion that is non-singular (i.e., simultaneously continuous and bounded or finite) except at the core $R = 0$ cannot be extracted naturally from (C.92)-(C.100). On the other hand, an elastic strain tensor that is non-singular except at the core can be extracted from the symmetric part of the total distortion:

$$\varepsilon_{11}^L = -\frac{\omega_1 x_3}{4\pi(1-v)}\left[(1-2v)\frac{x_1}{R^2} - 2\frac{x_1(x_2)^2}{R^4}\right]$$
$$-\frac{\omega_2 x_3}{4\pi(1-v)}\left[(1-2v)\frac{x_2}{R^2} + 2\frac{(x_1)^2 x_2}{R^4}\right], \quad \text{(C.101)}$$

$$\varepsilon_{12}^L = \frac{\omega_1 x_3}{4\pi(1-v)}\left[\frac{x_2}{R^2} - 2\frac{(x_1)^2 x_2}{R^4}\right] + \frac{\omega_2 x_3}{4\pi(1-v)}\left[\frac{x_1}{R^2} - 2\frac{x_1(x_2)^2}{R^4}\right], \quad \text{(C.102)}$$

$$\varepsilon_{22}^L = -\frac{\omega_1 x_3}{4\pi(1-v)}\left[(1-2v)\frac{x_1}{R^2} + 2\frac{x_1(x_2)^2}{R^4}\right]$$
$$-\frac{\omega_2 x_3}{4\pi(1-v)}\left[(1-2v)\frac{x_2}{R^2} - 2\frac{(x_1)^2 x_2}{R^4}\right], \quad \text{(C.103)}$$

$$\varepsilon_{13}^L = -\frac{\omega_1}{4\pi(1-v)}\left[(1-2v)\ln R + \frac{(x_2)^2}{R^2}\right] + \frac{\omega_2 x_1 x_2}{4\pi(1-v)R^2}, \quad \text{(C.104)}$$

$$\varepsilon_{23}^L = \frac{\omega_1 x_1 x_2}{4\pi(1-v)R^2} - \frac{\omega_2}{4\pi(1-v)}\left[(1-2v)\ln R + \frac{(x_1)^2}{R^2}\right], \quad \text{(C.105)}$$

$$\varepsilon_{33}^L = 0. \quad \text{(C.106)}$$

The remaining (plastic) parts of the symmetric displacement gradient tensor $\varepsilon_{ab}^P = \beta_{(ab)} - \varepsilon_{ab}^L$ correspond to (C.75)-(C.77). The elastic dilatation is

$$\varepsilon_{11}^{L} + \varepsilon_{22}^{L} + \varepsilon_{33}^{L} = -\frac{(1-2v)x_3}{2\pi(1-v)R^2}\left[\omega_1 x_1 + \omega_2 x_2\right]. \tag{C.107}$$

The total rotation vector $w_a = -\varepsilon_{abc}\beta^{bc}/2$ is

$$w_1 = \frac{\omega_1\theta}{2\pi} - \frac{1}{2}\omega_2 x_1 H(-x_1)\delta(x_2), \tag{C.108}$$

$$w_2 = \frac{\omega_2\theta}{2\pi}, \tag{C.109}$$

$$w_3 = \frac{x_3}{2\pi R^2}\left[\omega_1 x_2 - \omega_2 x_1\right] - \frac{1}{2}\omega_2 x_3 H(-x_1)\delta(x_2). \tag{C.110}$$

Because the total rotation $\mathbf{w}$, like $\boldsymbol{\beta}$, contains terms linear in θ, an elastic rotation that is non-singular except at the disclination core (i.e., at $R = 0$) cannot be extracted naturally from (C.108)-(C.110). However, an elastic bend-twist that is non-singular except at the core can be extracted from the gradient of the rotation vector:

$$\kappa_{11}^{L} = \frac{-\omega_1 x_2}{2\pi R^2}, \; \kappa_{12}^{L} = \frac{\omega_1 x_1}{2\pi R^2}, \; \kappa_{21}^{L} = -\frac{\omega_2 x_2}{2\pi R^2}, \; \kappa_{22}^{L} = \frac{\omega_2 x_1}{2\pi R^2}, \tag{C.111}$$

$$\kappa_{31}^{L} = -\frac{\omega_1 x_1 x_2 x_3}{\pi R^4} - \frac{\omega_2 x_3}{2\pi}\left[\frac{1}{R^2} - 2\frac{(x_1)^2}{R^4} + \pi\delta(R)\right], \tag{C.112}$$

$$\kappa_{32}^{L} = \frac{\omega_1 x_3}{2\pi}\left[\frac{1}{R^2} - 2\frac{(x_2)^2}{R^4} + \pi\delta(R)\right] - \frac{\omega_2 x_1 x_2 x_3}{\pi R^4}, \tag{C.113}$$

$$\kappa_{33}^{L} = \frac{1}{2\pi R^2}\left[\omega_1 x_2 - \omega_2 x_1\right], \tag{C.114}$$

$$\kappa_{13}^{L} = \kappa_{23}^{L} = 0. \tag{C.115}$$

The remaining (plastic) parts of the bend twist $\kappa_{ab}^{P} = \kappa_{ab} - \kappa_{ab}^{L}$ correspond to (C.78)-(C.83).

The stresses obtained from linear isotropic elasticity theory[1] (C.41) and the elastic strains (C.101)-(C.106) are

$$\sigma_{11} = -\frac{\mu x_3}{2\pi(1-v)}\left\{\omega_1\left[\frac{x_1}{R^2} - 2\frac{x_1(x_2)^2}{R^4}\right] + \omega_2\left[\frac{x_2}{R^2} + 2\frac{(x_1)^2 x_2}{R^4}\right]\right\}, \tag{C.116}$$

---

[1] Generalized continuum elasticity theories, for example those admitting couple stresses, are popular for describing elastic fields of discrete disclination and dislocation lines (Minagawa 1977; Lazar and Maugin 2005) but such applications of these theories are not addressed in Appendix C.

$$\sigma_{12} = \frac{\mu x_3}{2\pi(1-v)}\left\{\omega_1\left[\frac{x_2}{R^2} - 2\frac{(x_1)^2 x_2}{R^4}\right] + \omega_2\left[\frac{x_1}{R^2} - 2\frac{x_1(x_2)^2}{R^4}\right]\right\}, \quad \text{(C.117)}$$

$$\sigma_{13} = -\frac{\mu\omega_1}{2\pi(1-v)}\left[(1-2v)\ln R + \frac{(x_2)^2}{R^2}\right] + \frac{\mu\omega_2 x_1 x_2}{2\pi(1-v)R^2}, \quad \text{(C.118)}$$

$$\sigma_{22} = -\frac{\mu x_3}{2\pi(1-v)}\left\{\omega_1\left[\frac{x_1}{R^2} + 2\frac{x_1(x_2)^2}{R^4}\right] + \omega_2\left[\frac{x_2}{R^2} - 2\frac{(x_1)^2 x_2}{R^4}\right]\right\}, \quad \text{(C.119)}$$

$$\sigma_{23} = \frac{\mu\omega_1 x_1 x_2}{2\pi(1-v)R^2} - \frac{\mu\omega_2}{2\pi(1-v)}\left[(1-2v)\ln R + \frac{(x_1)^2}{R^2}\right], \quad \text{(C.120)}$$

$$\sigma_{33} = -\frac{\mu v x_3}{\pi(1-v)R^2}\left[\omega_1 x_1 + \omega_2 x_2\right]. \quad \text{(C.121)}$$

One can verify that the (Cauchy) stress components of (C.116)-(C.121) satisfy the static equilibrium equations in the absence of body forces: $\sigma^{ab}_{\ ,b} = 0$ (De Wit 1973).

Stress components are singular at $R = 0$; hence, linear elasticity theory breaks down at small distances from the disclination line. At distances far from the disclination line, stresses and elastic strains decay only logarithmically with R and hence diverge as $R \to \infty$. The elastic strain energy density $W = \sigma^{ab}\varepsilon^L_{ab}/2$ of the defect likewise diverges at large distances from the core of the defect.

C.1.4 Wedge Disclination

The Frank vector and its magnitude for an isolated wedge disclination passing through the origin as shown in Fig. C.2(g) are

$$\boldsymbol{\omega} = \omega_3 \mathbf{e}_3, \quad \omega = \omega_3. \quad \text{(C.122)}$$

Notice that ω_3 can be positive or negative in algebraic sign, corresponding in Volterra's construction to removal or insertion of a wedge of matter. The non-vanishing component of the plastic distortion is

$$\beta^P_{22} = \omega_3 x_1 H(-x_1)\delta(x_2). \quad \text{(C.123)}$$

The non-vanishing component of the micro-rotation is

$$\varphi_{32} = \omega_3 H(-x_1)\delta(x_2). \quad \text{(C.124)}$$

The nonzero plastic strain component is

$$\varepsilon^P_{22} = \omega_3 x_1 H(-x_1)\delta(x_2). \quad \text{(C.125)}$$

The non-vanishing component of the plastic bend-twist is

$$\kappa_{32}^{P} = \omega_{3}H\left(-x_{1}\right)\delta\left(x_{2}\right). \tag{C.126}$$

For a wedge disclination, (C.84) vanishes. The disclination density defined in (C.85) has the nonzero component

$$\theta_{33} = \omega_{3}\delta\left(x_{1}\right)\delta\left(x_{2}\right). \tag{C.127}$$

The displacement field of a wedge disclination is

$$u_{1} = -\omega_{3}\left[\frac{x_{2}\theta}{2\pi} - \frac{(1-2v)x_{1}}{4\pi(1-v)}(\ln R - 1)\right], \tag{C.128}$$

$$u_{2} = \omega_{3}\left[\frac{x_{1}\theta}{2\pi} + \frac{(1-2v)x_{2}}{4\pi(1-v)}(\ln R - 1)\right], \tag{C.129}$$

$$u_{3} = 0. \tag{C.130}$$

Displacement gradient (i.e., distortion) components in Cartesian coordinates are

$$\beta_{11} = \frac{\omega_{3}}{4\pi(1-v)}\left[(1-2v)\ln R + \frac{(x_{2})^{2}}{R^{2}}\right], \tag{C.131}$$

$$\beta_{12} = -\omega_{3}\left[\frac{\theta}{2\pi} + \frac{x_{1}x_{2}}{4\pi(1-v)R^{2}}\right], \tag{C.132}$$

$$\beta_{21} = \omega_{3}\left[\frac{\theta}{2\pi} - \frac{x_{1}x_{2}}{4\pi(1-v)R^{2}}\right], \tag{C.133}$$

$$\beta_{22} = \frac{\omega_{3}}{4\pi(1-v)}\left[(1-2v)\ln R + \frac{(x_{1})^{2}}{R^{2}}\right] + \omega_{3}x_{1}H\left(-x_{1}\right)\delta\left(x_{2}\right), \tag{C.134}$$

$$\beta_{13} = \beta_{23} = \beta_{31} = \beta_{32} = \beta_{33} = 0. \tag{C.135}$$

Because the total distortion $\boldsymbol{\beta}$ contains terms linear in θ, an elastic distortion that is non-singular except at $R = 0$ cannot be extracted naturally from (C.131)-(C.135). However, an elastic strain tensor that is non-singular except at the core can be extracted from the symmetric part of the total distortion as follows:

$$\varepsilon_{11}^{L} = \frac{\omega_{3}}{4\pi(1-v)}\left[(1-2v)\ln R + \frac{(x_{2})^{2}}{R^{2}}\right], \tag{C.136}$$

$$\varepsilon_{12}^{L} = -\frac{\omega_{3}x_{1}x_{2}}{4\pi(1-v)R^{2}}, \tag{C.137}$$

$$\varepsilon_{22}^{L} = \frac{\omega_{3}}{4\pi(1-v)}\left[(1-2v)\ln R + \frac{(x_{1})^{2}}{R^{2}}\right], \tag{C.138}$$

$$\varepsilon_{13}^{L} = \varepsilon_{23}^{L} = \varepsilon_{33}^{L} = 0. \tag{C.139}$$

The remaining (plastic) part of the symmetric displacement gradient $\varepsilon^P_{ab} = \beta_{(ab)} - \varepsilon^L_{ab}$ corresponds to (C.125). The elastic dilatation is

$$\varepsilon^L_{11} + \varepsilon^L_{22} + \varepsilon^L_{33} = \frac{\omega_3}{4\pi(1-v)}\left[2(1-2v)\ln R - 1\right]. \tag{C.140}$$

The total rotation vector $w_a = -\varepsilon_{abc}\beta^{bc}/2$ is

$$w_1 = w_2 = 0, \quad w_3 = \frac{\omega_3\theta}{2\pi}. \tag{C.141}$$

Because the total rotation $\mathbf{w}$, like $\boldsymbol{\beta}$, contains a term linear in θ, an elastic rotation that is non-singular except at $R = 0$ cannot be extracted naturally from (C.141). However, an elastic bend-twist that is non-singular except at the core can be extracted from the gradient of the rotation vector:

$$\kappa^L_{31} = -\frac{\omega_3 x_2}{2\pi R^2}, \quad \kappa^L_{32} = \frac{\omega_3 x_1}{2\pi R^2}, \tag{C.142}$$

$$\kappa^L_{11} = \kappa^L_{12} = \kappa^L_{13} = \kappa^L_{21} = \kappa^L_{22} = \kappa^L_{23} = \kappa^L_{33} = 0. \tag{C.143}$$

The remaining (plastic) part of the bend twist $\kappa^P_{ab} = \kappa_{ab} - \kappa^L_{ab}$ corresponds to (C.126). Stress components obtained from linear isotropic elasticity theory (C.41) and elastic strains (C.136)-(C.139) are

$$\sigma_{11} = \frac{\mu\omega_3}{2\pi(1-v)}\left[\ln R + \frac{(x_2)^2}{R^2} + \frac{v}{1-2v}\right], \tag{C.144}$$

$$\sigma_{12} = -\frac{\mu\omega_3 x_1 x_2}{2\pi(1-v)R^2}, \tag{C.145}$$

$$\sigma_{22} = \frac{\mu\omega_3}{2\pi(1-v)}\left[\ln R + \frac{(x_1)^2}{R^2} + \frac{v}{1-2v}\right], \tag{C.146}$$

$$\sigma_{33} = \frac{\mu\omega_3}{2\pi(1-v)}\left[2v\ln R + \frac{v}{1-2v}\right], \tag{C.147}$$

$$\sigma_{13} = \sigma_{23} = 0. \tag{C.148}$$

One can verify that stresses of (C.145)-(C.148) satisfy the static equilibrium equations in the absence of body forces (De Wit 1973). The algebraic sign of the disclination (i.e., positive or negative value of ω_3) dictates the sign of each of the nonzero stress components.

Some stress components are singular at $R = 0$; hence, linear elasticity theory is not valid within the core. At distances far from the disclination line, stresses and elastic strains decay only logarithmically with R and hence diverge as $R \to \infty$. The elastic strain energy density $W = \sigma^{ab}\varepsilon^L_{ab}/2$ of the defect likewise diverges at large distances from the core.

The strain energy per unit length of an elastic cylinder containing a wedge disclination line with Frank vector magnitude $\omega = \omega_3$ is (Huang and Mura 1970)

$$
E = \int_{-\pi}^{\pi} \int_{R_C}^{R} W(R)(dR)(d\theta)
$$

$$
= \frac{\mu \omega^2 R^2}{16\pi(1-\nu)} \left[1 - \left(\frac{R_C}{R} \right)^2 - 4 \left(\frac{R_C}{R} \right)^2 \left(1 - \left(\frac{R_C}{R} \right)^2 \right)^{-1} \ln^2 \left(\frac{R_C}{R} \right) \right].
$$
(C.149)

The energy per unit length E diverges at distances away from the defect at a rate of $\omega^2 R^2$, demonstrating the high energy of uncompensated wedge disclination lines. In crystal lattices, full wedge disclinations can exhibit Frank vectors of magnitude $\omega = \pi/2$ for cubic crystals with the tangent line parallel to a cube axis, and $\omega = \pi/3$ for hexagonal crystals with the tangent line parallel to the c-axis of the conventional unit cell (De Wit 1971; Li 1972). In either case, because the product $\mu \omega^2 R^2$ becomes large at even moderate distances away from the core, disclinations tend to form partial dipole configurations to minimize their total elastic strain energy (Li 1972; Seefeldt 2001).

C.1.5 Mixed Line Defects

Straight line defects of mixed character are easily represented by superposition of the results of Sections C.1.1-C.1.4. A mixed dislocation with unit tangent line ξ and Burgers vector $\mathbf{b}$ can be decomposed into the sum of a screw dislocation with Burgers vector $\mathbf{b_S}$ and edge dislocation with Burgers vector $\mathbf{b_E}$ using basic vector mathematics (Hirth and Lothe 1982):

$$
\mathbf{b} = \mathbf{b_S} + \mathbf{b_E}, \quad \mathbf{b_S} = (\mathbf{b} \cdot \xi)\xi, \quad \mathbf{b_E} = \xi \times (\mathbf{b} \times \xi).
$$
(C.150)

Similarly, a mixed disclination aligned along unit tangent vector ξ can be expressed as the sum of a wedge disclination with Frank vector $\boldsymbol{\omega_W}$ and a twist disclination of Frank vector $\boldsymbol{\omega_T}$ via the vector addition relation $\boldsymbol{\omega} = \boldsymbol{\omega_W} + \boldsymbol{\omega_T} = (\boldsymbol{\omega} \cdot \xi)\xi + \xi \times (\boldsymbol{\omega} \times \xi)$.

Upon selection of a Cartesian coordinate system with $\xi \| \mathbf{e}_3$, the displacement, displacement gradient, rotation, and rotation gradient fields can then be superposed for a generic line defect with both a Burgers vector of mixed character (screw and edge) and a Frank vector of mixed character (wedge and twist). Jumps in displacement and rotation in (C.5) and (C.6) demonstrate such a superposition. When superposing fields of dislocations

and disclinations, an elastic rotation cannot be defined that is non-singular except at the core of the mixed defect, since the elastic rotation is undefined for the disclination alone. Because the results of Sections C.1.1-C.1.4 are obtained using linear isotropic elasticity, stress fields and strain energy densities can be superposed to determine the fields of mixed straight line defects.

In particular, the elastic strain energy per unit length of a straight dislocation line of possibly mixed character in the linear isotropic approximation is

$$E = \int\limits_{-\pi}^{\pi} \int\limits_{R_C}^{R} W(R)(dR)(d\theta) = \frac{\mu b^2}{4\pi}\left[\cos^2\phi + \frac{1}{1-\nu}\sin^2\phi\right]\ln\left(\frac{R}{R_C}\right), \quad \text{(C.151)}$$

where $\phi = \cos^{-1}|\mathbf{b}\cdot\boldsymbol{\xi}/b|$ is the angle between the Burgers vector and tangent line. When $\phi = 0$, (C.151) reduces to formula (C.67) for a screw dislocation; when $\phi = \pi/2$, (C.151) reduces to formula (C.48) for an edge dislocation. The superposition procedure outlined above is rigorous only for a single line defect, and does not account for interactions that would arise between two different defects with distinct tangent lines and the same total Burgers and Frank vectors.

C.1.6 Dislocation Energies in Anisotropic Crystals

For anisotropic crystals, field variables such as stress, strain, and strain energy density depend on the orientation of the defect and its Burgers or Frank vector with respect to directions in the crystal lattice. Methods for obtaining solutions for dislocations in anisotropic linear elasticity theory are outside the scope of this Appendix, but are described elsewhere in a number of references (Eshelby 1949b; Eshelby et al. 1953; Foreman 1955; Stroh 1958; Head 1964; Steeds 1973; Bacon et al. 1979; Hirth and Lothe 1982; Teodosiu 1982). Listed next are strain energies per unit length of Volterra dislocation lines in particular orientations, with emphasis directed towards configurations found in cubic and hexagonal lattices for which concise analytical solutions exist. Disclinations in anisotropic media are not considered.

The strain energy per unit length of a straight dislocation line in an infinite linear elastic body can be written in the general form

$$E = \int\limits_{-\pi}^{\pi} \int\limits_{R_C}^{R} W(R)(dR)(d\theta) = \hat{K}\frac{b^2}{4\pi}\ln\left(\frac{R}{R_C}\right), \quad \text{(C.152)}$$

where $b = (\mathbf{b} \cdot \mathbf{b})^{1/2}$ is the magnitude of the Burgers vector, R is the radial distance from the dislocation core, and R_C is the cut-off radius from the core. The tangent line is again oriented along the x_3-axis: $\boldsymbol{\xi} = \xi \mathbf{e}_3$. The strain energy E is then determined by the energy factor $\hat{K}$, with dimensions of stress or energy per unit volume, that depends upon the orientation of the defect and the symmetry of the crystal. Let the Burgers vector be decomposed into an edge component $\mathbf{b}_E = b_1 \mathbf{e}_1 + b_2 \mathbf{e}_2$ and a screw component $\mathbf{b}_S = b_3 \mathbf{e}_3$ via (C.150), consistent with Fig. C.2. In an isotropic body, the energy factor reduces to $\hat{K} = \mu / (1 - \nu)$ for a straight edge dislocation in (C.48) and to $\hat{K} = \mu$ (i.e., the elastic shear modulus) for a straight screw dislocation in (C.69).

Analytical solutions are available for $\hat{K}$ when either of the following conditions is satisfied (Foreman 1955): (i) each axis of the Burgers vector of the dislocation (x_1, x_2, and x_3) falls along an axis of two-fold symmetry or (ii) any axis of the Burgers vector of the dislocation (x_1, x_2, or x_3) is an axis of six-fold symmetry. From Table A.2, Table A.8, and the analysis of Foreman (1955), such results are available for dislocations of particular orientations in elastic solids belonging to Laue groups TI, HII, HI, CII, and CI, i.e., high-symmetry tetragonal, hexagonal, and cubic crystals. The energy factor in these cases can be written as (Foreman 1955)

$$\hat{K} = \frac{1}{b^2} \left[\hat{K}_1 (b_1)^2 + \hat{K}_2 (b_2)^2 + \hat{K}_3 (b_3)^2 \right], \tag{C.153}$$

with

$$\hat{K}_1 = (\hat{C} + \overline{\mathbb{C}}^{12}) \left[\frac{\overline{\mathbb{C}}^{66} (\hat{C} - \overline{\mathbb{C}}^{12})}{\overline{\mathbb{C}}^{22} (\hat{C} + \overline{\mathbb{C}}^{12} + 2\overline{\mathbb{C}}^{66})} \right]^{1/2}, \tag{C.154}$$

$$\hat{K}_2 = \hat{K}_1 \left(\frac{\overline{\mathbb{C}}^{22}}{\overline{\mathbb{C}}^{11}} \right)^{1/2}, \quad \hat{K}_3 = \left(\overline{\mathbb{C}}^{44} \overline{\mathbb{C}}^{55} \right)^{1/2}, \quad \hat{C} = \left(\overline{\mathbb{C}}^{11} \overline{\mathbb{C}}^{22} \right)^{1/2}. \tag{C.155}$$

Independent second-order elastic constants $\overline{\mathbb{C}}^{\overline{AB}}$ (in Voigt's notation of (A.2)) are listed in Table A.8 for crystals of each Laue group, where barred indices span $\overline{A} = 1, 2, ...6$. Elastic constants must be expressed in the same Cartesian coordinate system used to describe the dislocation line and Burgers vector, in some cases requiring a change of coordinates such as in (5.99)-(5.100).

First consider cubic crystals with the cube axes ($[100],[010],[001]$) aligned coincident with the Cartesian coordinate system (x_1, x_2, x_3). In this case, (C.154) and (C.155) reduce to

$$\hat{K}_1 = \hat{K}_2 = (\overline{\mathbb{C}}^{11} + \overline{\mathbb{C}}^{12})\left[\frac{\overline{\mathbb{C}}^{44}(\overline{\mathbb{C}}^{11} - \overline{\mathbb{C}}^{12})}{\overline{\mathbb{C}}^{11}(\overline{\mathbb{C}}^{11} + \overline{\mathbb{C}}^{12} + 2\overline{\mathbb{C}}^{44})}\right]^{1/2}, \quad \hat{K}_3 = \overline{\mathbb{C}}^{44}. \quad (C.156)$$

Substitution of (C.156) into (C.153) provides the energy factor for a dislocation with tangent line along a [001] direction in a cubic lattice, i.e., $\xi\|[001]$. Table C.1 lists reduced representations of energy factor $\hat{K}$ for such dislocations with Burgers vectors **b** in $\langle 100 \rangle$, $\langle 110 \rangle$, and $\langle 111 \rangle$ directions.

Table C.1 Energy factors for dislocations in cubic crystals (Foreman 1955)

Dislocation type	Line	Slip plane	Burgers vector	$\hat{K}$
Screw	[001]	-	[001]	$\hat{K}_3$ *
Edge	[001]	{100}	[100]	$\hat{K}_1$ *
Mixed	[001]	{100}	1/2 [101]	$(\hat{K}_1 + \hat{K}_3)/2$ *
Edge	[001]	{110}	1/2 [110]	$(\hat{K}_1 + \hat{K}_2)/2$ *
Mixed	[001]	{110}	1/2 [111]	$(\hat{K}_1 + \hat{K}_2 + \hat{K}_3)/3$ *
Screw	[101]	-	1/2 [101]	$\hat{K}_3$ **
Edge	[101]	{100}	$1/2[10\overline{1}]$	$\hat{K}_1$ **
Mixed	[101]	{100}	[100]	$(\hat{K}_1 + \hat{K}_3)/2$ **
Edge	[101]	{110}	[010]	$\hat{K}_2$ **
Mixed	[101]	{110}	1/2 [111]	$(\hat{K}_2 + 2\hat{K}_3)/3$ **
Mixed	[101]	{111}	1/2 [110]	$(\hat{K}_1 + 2\hat{K}_2 + \hat{K}_3)/4$ **
Edge	[101]	{112}	$1/2[\overline{1}11]$	$(2\hat{K}_1 + \hat{K}_2)/3$ **

*Equations (C.156)   **Equations (C.154), (C.155), (C.157), and (C.158)

A cubic crystal with crystallographic axes ($[10\overline{1}],[010],[101]$) parallel to respective Cartesian axes (x_1, x_2, x_3) also fulfills symmetry condition (i) listed above. For a cubic crystal containing a dislocation line aligned along a [101] direction, the following transformation formulae apply:

$$2\overline{\mathbb{C}}^{11} = \overline{\mathbb{C}}'^{11} + \overline{\mathbb{C}}'^{12} + 2\overline{\mathbb{C}}'^{44}, \quad \overline{\mathbb{C}}^{22} = \overline{\mathbb{C}}'^{11}, \qquad (C.157)$$
$$\overline{\mathbb{C}}^{12} = \overline{\mathbb{C}}'^{12}, \quad \overline{\mathbb{C}}^{44} = \overline{\mathbb{C}}^{66} = \overline{\mathbb{C}}'^{44}, \quad 2\overline{\mathbb{C}}^{55} = \overline{\mathbb{C}}'^{11} - \overline{\mathbb{C}}'^{12}, \qquad (C.158)$$

with $\overline{\mathbb{C}}'^{\overline{AB}}$ the (three independent) elastic constants in the original crystallographic coordinate system. Unprimed elastic constants from (C.157) and (C.158) are then substituted into (C.153)-(C.155) to obtain the energy factor $\hat{K}$ for a dislocation line along a [101] direction in a cubic crystal, i.e., $\xi \parallel [101]$. Table C.1 lists reduced representations of $\hat{K}$ for such dislocations with Burgers vectors **b** parallel to $\langle 100 \rangle$, $\langle 110 \rangle$, and $\langle 111 \rangle$ directions.

Finally consider hexagonal crystals, again with the dislocation line parallel to the x_3-axis. Consider dislocations for which any one of the coordinate directions x_1, x_2, or x_3 and the c-axis [0001] coincide. Since the c-axis is an axis of six-fold symmetry and since second-order elastic constants of hexagonal crystals are invariant for any rotations about the c-axis, condition (ii) mentioned above is satisfied and (C.153)-(C.155) can be used directly, without a coordinate transformation. Particular forms of $\hat{K}$ for screw dislocations oriented along [0001] and edge dislocations on basal {0001} and first-order prism $\{1\overline{1}00\}$ planes are listed in Table C.2.

Table C.2 Energy factors for dislocations in hexagonal crystals (Foreman 1955)

Dislocation type	Slip plane	Burgers vector	$\hat{K}$
Screw	-	*	$[(\overline{\mathbb{C}}^{44}/2)(\overline{\mathbb{C}}^{11} - \overline{\mathbb{C}}^{12})]^{1/2}$
Edge	{0001}	$1/3\,[11\overline{2}0]$	$\left[(\overline{\mathbb{C}}^{11}\overline{\mathbb{C}}^{33})^{1/2} + \overline{\mathbb{C}}^{13} \right]$
			$\times\left\{ \dfrac{\overline{\mathbb{C}}^{44}[(\overline{\mathbb{C}}^{11}\overline{\mathbb{C}}^{33})^{1/2} - \overline{\mathbb{C}}^{13}]}{\overline{\mathbb{C}}^{33}[(\overline{\mathbb{C}}^{11}\overline{\mathbb{C}}^{33})^{1/2} + \overline{\mathbb{C}}^{13} + 2\overline{\mathbb{C}}^{44}]} \right\}^{1/2}$
Edge	$\{1\overline{1}00\}$	$1/3\,[11\overline{2}0]$	$[(\overline{\mathbb{C}}^{11})^2 - (\overline{\mathbb{C}}^{12})^2]/(2\overline{\mathbb{C}}^{11})$

*Any **b** parallel or perpendicular to the c-axis [0001]

C.2 Defect Loops

Lattice defects can often appear in crystals as closed loops rather than as straight lines. This occurs for several reasons. Firstly, dislocation lines cannot terminate abruptly within a crystal structure, but rather must terminate at external or internal (e.g., grain) boundaries, at intersections with other defects, or on themselves (i.e., loops). Secondly, dislocations often multiply or nucleate in the form of loops via Frank-Read sources (Read 1953; Kocks et al. 1975; Hirth and Lothe 1982; Hull and Bacon 1984). Considered in Section C.2 are dislocation and disclination loops whose

tangent lines lie completely within a single plane. Helical defects whose tangent lines are not confined to a single plane are possible (Owen and Mura 1967; Hull and Bacon 1984) but are not addressed here.

Consider a generic defect loop of radius A shown in Fig. C.3. The curved defect line L of total length $2\pi A$ lies within the plane $x_3 = 0$. Cylindrical coordinates R and θ are introduced, satisfying (C.1)-(C.3). The unit tangent vector to the defect is $\boldsymbol{\xi} = \xi \mathbf{e}_\theta$, with $\mathbf{e}_\theta$ a dimensionless unit vector in physical coordinates (Section 2.4.2). The Burgers vector or Frank vector of the defect, not shown in Fig. C.3, determines the type of loop. Specifically considered in what follows are screw dislocation loops, prismatic dislocation loops, circular dislocation loops with constant Burgers vector in the plane of the loop (i.e., shear dislocation loops), twist disclination loops, and wedge disclination loops. Defect energies are provided for each of these kinds of loops contained in isotropic linear elastic solids of infinite extent.
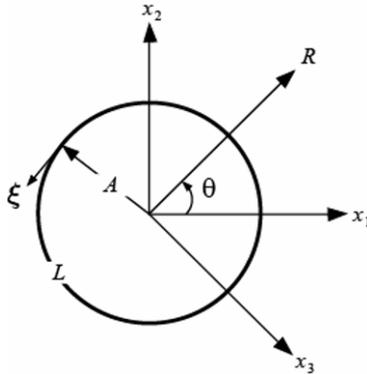
Fig. C.3 Defect loop and cylindrical and Cartesian coordinate systems

First consider a screw dislocation loop, for which the orientation of the Burgers vector varies spatially so that it always remains parallel to the dislocation line, leading to $\mathbf{b} = b\mathbf{e}_\theta$ where b is a constant. Owen and Mura (1967) call this a rotational dislocation loop. The only non-vanishing component of the dislocation density tensor of (C.17) in this case is, in cylindrical coordinates,

$$\alpha_{\theta\theta} = b\delta(R - A)\delta(x_3). \tag{C.159}$$

The stress field resulting from (C.159) in an infinitely extended, isotropic linear elastic body is given by Owen and Mura (1967) and is too lengthy to repeat here. The energy per unit length E is (Owen and Mura 1967)

$$E \approx \frac{\mu b^2}{12\pi(1-v)}\left[3(1-v)\ln\left(\frac{8A}{R_C}\right)-(9-10v)\right], \qquad \text{(C.160)}$$

where $R_C \ll A$ has been assumed, with R_C the radius of a curved tube (i.e., core region) of material encasing the dislocation line. Recall that μ is the elastic shear modulus and v is Poisson's ratio.

Next consider a prismatic dislocation loop, for which the orientation of the Burgers vector is constant and always perpendicular to the tangent line, leading to $\mathbf{b} = b\mathbf{e}_3$ where b is a constant. This is a circular edge dislocation. The only non-vanishing component of dislocation density tensor (C.17) is

$$\alpha_{3\theta} = b\delta(R-A)\delta(x_3). \qquad \text{(C.161)}$$

The energy per unit length E of a prismatic dislocation loop in an isotropic linear elastic body of infinite dimensions is (Owen and Mura 1967)

$$E \approx \frac{\mu b^2}{4\pi(1-v)}\left[\ln\left(\frac{8A}{R_C}\right)-2\right], \qquad \text{(C.162)}$$

where $R_C \ll A$ has been assumed.

Now consider a mixed dislocation loop, for which the orientation of the Burgers vector is constant and within the plane of the loop, leading to $\mathbf{b} = b_1\mathbf{e}_2 + b_2\mathbf{e}_2$, with constants b_1, b_2, and $b = [(b_1)^2 + (b_2)^2]^{1/2}$. This is often called a circular shear dislocation or shear dislocation loop (Hull and Bacon 1984). The only non-vanishing components of the dislocation density tensor (C.17) are

$$\alpha_{R\theta} = [b_1\cos\theta + b_2\sin\theta]\delta(R-A)\delta(x_3), \qquad \text{(C.163)}$$

$$\alpha_{\theta\theta} = [-b_1\sin\theta + b_2\cos\theta]\delta(R-A)\delta(x_3). \qquad \text{(C.164)}$$

The energy per unit length E in an infinitely extended, isotropic linear elastic solid is (Owen and Mura 1967)

$$E \approx \frac{\mu b^2}{8\pi(1-v)}\left[\left(\frac{5}{2}-v\right)\ln\left(\frac{8A}{R_C}\right)-\left(\frac{4\pi}{3}+\frac{23}{9}\right)+v(2-\pi)\right]. \qquad \text{(C.165)}$$

where $R_C \ll A$ has been assumed.

Next consider a twist disclination loop, for which the orientation of the Frank vector is constant and perpendicular to the tangent line, leading to $\boldsymbol{\omega} = \omega\mathbf{e}_3$, where ω is a constant. This is a circular edge disclination in the terminology of Huang and Mura (1970). The only non-vanishing component of the disclination density tensor of (C.85) is

$$\theta_{3\theta} = \omega\delta(R-A)\delta(x_3). \qquad \text{(C.166)}$$

The energy per unit length E of a twist disclination loop in a linear elastic isotropic body of infinite dimensions is (Huang and Mura 1970; Liu and Li 1971)

$$E \approx \frac{\mu \omega^2 R^2}{4\pi} \left[\ln\left(\frac{8A}{R_C}\right) - \frac{8}{3} \right], \tag{C.167}$$

where $R_C \ll A$ has been assumed.

Finally consider a wedge disclination loop, for which the orientation of the Frank vector is constant and within the plane of the loop, leading to $\boldsymbol{\omega} = \omega_1 \mathbf{e}_2 + \omega_2 \mathbf{e}_2$, with constants ω_1, ω_2, and $\omega = [(\omega_1)^2 + (\omega_2)^2]^{1/2}$. This is a circular wedge disclination with constant Frank vector. The only non-vanishing components of the disclination density tensor (C.85) are, in this case,

$$\theta_{R\theta} = [\omega_1 \cos\theta + \omega_2 \sin\theta] \delta(R - A) \delta(x_3), \tag{C.168}$$

$$\theta_{\theta\theta} = [-\omega_1 \sin\theta + \omega_2 \cos\theta] \delta(R - A) \delta(x_3). \tag{C.169}$$

The energy per unit length E of a circular wedge disclination loop in an isotropic linear elastic body of infinite dimensions is (Liu and Li 1971; Kuo and Mura 1972)

$$E \approx \frac{\mu \omega^2 R^2}{8\pi(1-\nu)} \left[\ln\left(\frac{8A}{R_C}\right) - \frac{8}{3} \right]. \tag{C.170}$$

where $R_C \ll A$ has been assumed.

Disclination loop energies in isotropic elastic bodies were also computed analytically by Li and Gilman (1970) at large distances away from the loop. Notice from (C.167) and (C.170) that disclination loop energies diverge at distances away from the core at a rate of $\omega^2 R^2$, similar to what was observed for straight disclination lines in (C.149). On the other hand, dislocation loop energies per unit line length in (C.160), (C.162), and (C.165) are constant for fixed values of A and R_C; i.e., the dislocation loop energies per unit line length do not depend on radial coordinate R.

C.3 Point Defects

The continuum model of a point defect considered in Section C.3 consists of a sphere of one material forced into a spherical hole of a different radius in a larger sample of a possibly different material. This type of model can be used to describe inclusions, interstitial atoms, and substitutional atoms of larger size than those of the sample when the radius of the inserted

sphere is larger than that of the hole in the surrounding medium. In that case, when the inserted sphere is rigid and the surrounding medium is of infinite extent, the radial strain in the vicinity of the sphere is compressive. This model can also be used to describe vacancies or substitutional atoms of smaller size than those of the surrounding medium, via insertion of a sphere of smaller radius than the radius of the hole, then contracting the boundary of the hole such that it is bound to the sphere, followed by removal of external forces. In that case, when the inserted sphere is rigid and the surrounding medium is of infinite extent, the radial strain in the vicinity of the sphere is tensile.

The spherically symmetric model of a point defect in an isotropic linear elastic medium has been considered by a number of authors (Bitter 1931; Eshelby 1954, 1956; Holder and Granato 1969; Hirth and Lothe 1982; Teodosiu 1982). The description below follows mainly from the presentation of Teodosiu (1982).

Spherical coordinates and generic problem geometry are shown in Fig. C.4(a) and Fig. C.4(b), respectively. Spherical coordinates are related to Cartesian coordinates as follows (see also Table 2.1):

$$x_1 = R\sin\theta\cos\varphi, \ x_2 = R\sin\theta\sin\varphi, \ x_3 = R\cos\theta; \quad \text{(C.171)}$$

$$R = [(x_1)^2 + (x_2)^2 + (x_3)^2]^{1/2}. \quad \text{(C.172)}$$

The radius of the inclusion prior to elastic relaxation is r_0, and the radius of the elastic body in which the inclusion is immersed is R_0. When the inclusion is rigid, its radius of course remains fixed at r_0. When the inclusion is deformable, on the other hand, its final radius may differ from r_0 after it is forced into or bonded to the surrounding medium via application of external forces, and then these external forces removed.
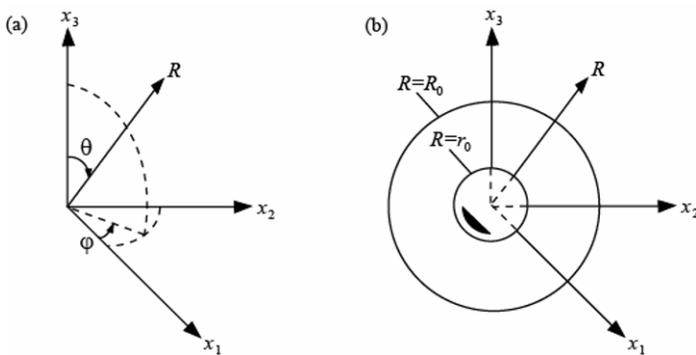
Fig. C.4 Coordinate systems (a) and geometry of spherical inclusion (b)

For spherically symmetric problems of the present kind, displacement field **u** is of the form

$$u_R = u_R(R) , \ u_\theta = u_\varphi = 0 . \tag{C.173}$$

Physical components of the small strain tensor (i.e., dimensionless strains in spherical coordinates of Section 2.4.3) then follow from differentiation of (C.173):

$$\varepsilon_{RR} = u_{R,R} , \ \varepsilon_{\theta\theta} = \varepsilon_{\varphi\varphi} = \frac{u_R}{R} , \ \varepsilon_{R\theta} = \varepsilon_{R\varphi} = \varepsilon_{\theta\varphi} = 0 . \tag{C.174}$$

All of the strains are considered elastic in the present treatment, e.g., plasticity is not considered.

Stresses, in physical components of spherical coordinates, in a linear isotropic elastic body with the above strain field are computed as follows using the linearized version of (A.24) or using (5.321) in the isothermal case:

$$\sigma_{RR} = (\lambda + 2\mu)u_{R,R} + 2\lambda\frac{u_R}{R} , \tag{C.175}$$

$$\sigma_{\theta\theta} = \sigma_{\varphi\varphi} = \lambda u_{R,R} + 2(\lambda + \mu)\frac{u_R}{R} , \tag{C.176}$$

$$\sigma_{R\theta} = \sigma_{R\varphi} = \sigma_{\theta\varphi} = 0 . \tag{C.177}$$

Substitution of this stress field into the static equilibrium equations (i.e., the first row of Table 5.2 with vanishing acceleration) in the absence of body forces provides the differential equation (Bitter 1931)

$$u_{R,RR} + 2\frac{u_{R,R}}{R} - 2\frac{u_R}{R^2} = 0 , \tag{C.178}$$

which has the general solution

$$u_R = \frac{A}{R^2} + BR , \tag{C.179}$$

with constants A and B whose values depend on the boundary conditions.

C.3.1 Rigid Defect in Infinite Body

First, let the body surrounding the spherical defect of radius r_0 be of infinite extent, i.e., $R_0 \to \infty$, and let the sphere be rigid. The corresponding boundary conditions are

$$u_R(\infty) \to 0 , \ u_R(r_0) = \frac{\delta V}{4\pi r_0^2} , \tag{C.180}$$

with δV the volume change resulting from the change in dimensions of the hole into which the sphere is inserted. Using (C.179), the constants are

$$A = \frac{\delta V}{4\pi}, \ B = 0. \tag{C.181}$$

Notice that A has dimensions of volume and measures the "strength" of the defect (Eshelby 1954). The displacement field is thus

$$u_a = AR^{-3}x_a = -A(R^{-1})_{,a}. \tag{C.182}$$

Non-vanishing strains and stresses are

$$\varepsilon_{RR} = -2AR^{-3}, \ \varepsilon_{\theta\theta} = \varepsilon_{\varphi\varphi} = AR^{-3}; \tag{C.183}$$

$$\sigma_{RR} = -4\mu AR^{-3}, \ \sigma_{\theta\theta} = \sigma_{\varphi\varphi} = 2\mu AR^{-3}. \tag{C.184}$$

The dilatation and pressure vanish identically:

$$\varepsilon_{RR} + \varepsilon_{\theta\theta} + \varepsilon_{\varphi\varphi} = 0, \ p = -\frac{1}{3}(\sigma_{RR} + \sigma_{\theta\theta} + \sigma_{\varphi\varphi}) = 0, \tag{C.185}$$

implying that the elastic medium is in a state of deviatoric stress. The strain energy density is

$$W = 6\mu A^2 R^{-6}, \tag{C.186}$$

and the average strain energy per unit volume $\overline{W}$ (and its equivalent average deviatoric energy density $\overline{W}_S$) of an elastic ball of radius R_0 surrounding the defect is obtained as

$$\begin{aligned}
\overline{W} = \overline{W}_S &= \left[\frac{4}{3}\pi(R_0^3 - r_0^3)\right]^{-1} \int_{r_0}^{R_0} 4\pi R^2 W dR \\
&= \frac{6\mu A^2}{(R_0^3 - r_0^3)r_0^3}\left[1 - \left(\frac{r_0}{R_0}\right)^3\right].
\end{aligned} \tag{C.187}$$

The total volume change Δv of any region of the medium containing the inclusion is, upon applying the divergence theorem (2.193),

$$\begin{aligned}
\Delta v &= \int_v u^a_{,a} dv = \int_s u^a n_a ds \\
&= \int_0^{2\pi}\int_0^\pi (AR^{-2})R^2(\sin\theta)(d\theta)(d\varphi) = 4\pi A = \delta V.
\end{aligned} \tag{C.188}$$

The final equality in (C.187) makes use of (C.188). The total volume change is positive and the radial stress is compressive when $A > 0$. This situation corresponds to a rigid interstitial atom imparting volume increase δV, or to a substitutional atom of volume larger by δV than an atom of the elastic medium. On the other hand, the volume change is negative and the radial stress tensile when $A < 0$. This situation corresponds to a missing atom (i.e., vacancy) of volume decrease δV, or to a substitutional atom of volume smaller by δV than an atom of the elastic medium. In a

polyatomic structure, the atomic species of the defect will generally affect the sign and magnitude of the volume change, as will the electric charge of the defect in an ionic solid. In such cases, it is possible for a vacancy to cause local expansion of the surrounding crystal, i.e., $A > 0$ (Mott and Littleton 1938; Sprackling 1976).

Volume change δV is often called the relaxation volume of a point defect, while the sum $\delta V \pm \Omega_0$ is often called the formation volume. The relaxation volume δV can be estimated by equating the normalized formation energy of the defect with the strain energy (C.187), as demonstrated in Section 7.4.1 of Chapter 7. Atomic lattice statics calculations can be used to more accurately determine relaxation and formation volumes, including effects of geometric and material nonlinearities[2], anisotropy, and boundary conditions (Garikipati et al. 2006). Effects of the defect on the surrounding elastic medium can also be represented by a force dipole tensor (Eshelby 1954, 1956; Teodosiu 1982; Garikipati et al. 2006).

C.3.2 Rigid Defect in Finite Body

Now let the isotropic elastic body surrounding the spherical defect of radius r_0 be of finite extent, i.e., R_0 is bounded, and let the sphere be rigid. The boundary conditions are

$$\sigma_{RR}(R_0) = 0, \; u_R(r_0) = \frac{\delta V}{4\pi r_0^2}, \tag{C.189}$$

with δV a constant with dimensions of volume. Using (C.175) and (C.179), the integration constants are

$$A = \frac{\delta V}{4\pi}\left[1 + \frac{4\mu}{3K}\left(\frac{r_0}{R_0}\right)^3\right]^{-1}, \; B = \frac{4\mu A}{3KR_0^3}, \tag{C.190}$$

with elastic bulk modulus $K = \lambda + 2\mu/3$. The nonzero part of the displacement field is

$$u_R = \frac{\delta V}{4\pi}\left[1 + \frac{4\mu}{3K}\left(\frac{r_0}{R_0}\right)^3\right]^{-1} R^{-2} + \frac{\mu \delta V}{3\pi KR_0^3}\left[1 + \frac{4\mu}{3K}\left(\frac{r_0}{R_0}\right)^3\right]^{-1} R. \tag{C.191}$$

Non-vanishing components of strain and stress are

---

[2] Section 7.4 of Chapter 7 also describes a means for accounting for effects of nonlinear elasticity, specifically a pressure-dependent shear modulus, on the overall volume change associated with a point defect in an isotropic elastic body.

$$\varepsilon_{RR} = -2AR^{-3}\left[1 - \frac{2\mu}{3K}\left(\frac{R}{R_0}\right)^3\right], \ \ \varepsilon_{\theta\theta} = \varepsilon_{\varphi\varphi} = AR^{-3}\left[1 + \frac{4\mu}{3K}\left(\frac{R}{R_0}\right)^3\right]; \ \ \text{(C.192)}$$

$$\sigma_{RR} = -4\mu AR^{-3}\left[1 - \left(\frac{R}{R_0}\right)^3\right], \ \ \sigma_{\theta\theta} = \sigma_{\varphi\varphi} = 2\mu AR^{-3}\left[1 + 2\left(\frac{R}{R_0}\right)^3\right]. \ \ \text{(C.193)}$$

The dilatation and pressure are nonzero but constant:

$$\varepsilon_{RR} + \varepsilon_{\theta\theta} + \varepsilon_{\varphi\varphi} = 3B = \frac{4\mu A}{KR_0^3}, \ \ p = -\frac{1}{3}(\sigma_{RR} + \sigma_{\theta\theta} + \sigma_{\varphi\varphi}) = -\frac{4\mu A}{R_0^3}. \ \ \text{(C.194)}$$

When $R_0 \gg R \gg r_0$, stress and strain fields of the solution outlined in Section C.3.1 are recovered.

The total volume change produced in the entire elastic sphere surrounding the inclusion is

$$\begin{aligned}\Delta v &= 4\pi R_0^2 u_R(R_0) = 4\pi A\left(1 + \frac{4\mu}{3K}\right) = 4\pi A\left[\frac{3(1-\nu)}{1+\nu}\right]\\ &= \delta V\left[\frac{3(1-\nu)}{1+\nu}\right]\left[1 + \frac{4\mu}{3K}\left(\frac{r_0}{R_0}\right)^3\right]^{-1}.\end{aligned} \quad \text{(C.195)}$$

Even when the defect is small relative to the medium (i.e., even when $R_0 \gg r_0$), relation (C.195) indicates that the volume change of the finite medium with a stress-free outer surface is increased over that of infinite body in (C.188) by a factor of $3(1-\nu)/(1+\nu)$, on the order of 1.6 when Poisson ratio $\nu = 0.3$.

The total volume change is positive and the pressure is tensile (i.e., p is negative in algebraic sign) when $A > 0$. This situation corresponds to a rigid interstitial atom imparting volume increase δV, or to a substitutional atom of volume larger by δV than an atom of the elastic medium. The total volume change is negative and the hydrostatic stress is compressive when $A < 0$. This situation corresponds to a missing atom (i.e., vacancy) imparting local volume change δV, or to a substitutional atom of volume smaller by δV than an atom of the surrounding medium. It is possible for the magnitude of the relaxation volume Δv of a point defect to exceed the atomic volume Ω_0 (Garikipati et al. 2006), in which case the net formation volume of a vacancy, i.e., the sum $\Delta v + \Omega_0$, will be negative in algebraic sign. As mentioned in Section C.3.1, it is also possible for a vacancy to induce local expansion ($\Delta v > 0$), e.g., as might occur for a charged defect in an ionic crystal with strong repulsive Coulomb forces arising among ions surrounding the defect.

C.3.3 Deformable Defect in Finite Body

Finally, let the body surrounding the spherical defect of radius r_0 be of finite extent, i.e., R_0 is bounded, and let the sphere be elastic and isotropic, with possibly different elastic constants than the surrounding medium. Generalizing (C.179), the radial displacement is bounded at the origin and satisfies

$$u_R = \begin{cases} AR^{-2} + BR & (r_0 < R \le R_0), \\ CR & (R \le r_0), \end{cases} \qquad \text{(C.196)}$$

with C a constant to be determined from additional boundary conditions. In this case, the boundary conditions are

$$\sigma_{RR}(r_0) = \sigma'_{RR}(r_0), \ \sigma_{RR}(R_0) = 0, \ u_R(r_0) - u'_R(r_0) = \frac{\delta V}{4\pi r_0^2}, \quad \text{(C.197)}$$

with δV the local volume change resulting from the sum of changes in dimensions of the hole and sphere when the sphere is inserted. In (C.197) and henceforth, primed quantities correspond to the inclusion, e.g., $u'_R = CR$, while unprimed quantities correspond to the surrounding medium, e.g., $u_R = AR^{-2} + BR$. Boundaries of the inclusion and medium are perfectly bonded at $R = r_0$, but the displacements of inclusion and surrounding medium may differ at r_0 since the initial radii of the sphere and hole differ. The integration constants in (C.196) are obtained using (C.197) as (Teodosiu 1982)

$$A = \frac{\delta V}{4\pi} \left\{ 1 + \frac{4\mu}{3K} \left(\frac{r_0}{R_0} \right)^3 + \frac{4\mu}{3K'} \left[1 - \left(\frac{r_0}{R_0} \right)^3 \right] \right\}^{-1}, \qquad \text{(C.198)}$$

$$B = \frac{4\mu A}{3K R_0^3}, \ C = \frac{4\mu A}{3K'} \left[\frac{1}{R_0^3} - \frac{1}{r_0^3} \right], \qquad \text{(C.199)}$$

with the elastic bulk modulus of the inclusion denoted by K'. Constants A and B degenerate to those of (C.190) when the inclusion becomes rigid and $K' \to \infty$.

Radial displacements in the body and inclusion are, henceforward presuming small defects in large bodies such that $(r_0/R_0)^3 \ll 1$,

$$u_R = AR^{-2} \left[1 + \frac{4\mu}{3K} \left(\frac{R}{R_0} \right)^3 \right], \ u'_R = -\frac{4\mu A}{3K'R_0^3} R. \qquad \text{(C.200)}$$

Non-vanishing stresses within the surrounding finite elastic body are

$$\sigma_{RR} = -4\mu A R^{-3}\left[1-\left(\frac{R}{R_0}\right)^3\right], \ \sigma_{\theta\theta} = \sigma_{\varphi\varphi} = 2\mu A R^{-3}\left[1+2\left(\frac{R}{R_0}\right)^3\right]. \quad \text{(C.201)}$$

Dilatation and hydrostatic pressure in the surrounding body are nonzero but constant:

$$\varepsilon_{RR} + \varepsilon_{\theta\theta} + \varepsilon_{\varphi\varphi} = \frac{4\mu A}{K R_0^3}, \ p = -\frac{1}{3}(\sigma_{RR} + \sigma_{\theta\theta} + \sigma_{\varphi\varphi}) = -\frac{4\mu A}{R_0^3}. \quad \text{(C.202)}$$

The only non-vanishing stress arising within the elastic inclusion is hydrostatic:

$$-\sigma'_{RR} = -\sigma'_{\theta\theta} = -\sigma'_{\varphi\varphi} = p' = 4\mu A r_0^{-3}, \quad \text{(C.203)}$$

meaning that the inclusion is subjected to uniform hydrostatic stress.

The net volume change in the elastic medium surrounding the inclusion is calculated as

$$\Delta v = 4\pi R_0^2 u_R\left(R_0\right) = 4\pi A\left(1+\frac{4\mu}{3K}\right)$$
$$= \delta V\left(1+\frac{4\mu}{3K}\right)\left(1+\frac{4\mu}{3K'}\right)^{-1}. \quad \text{(C.204)}$$

The volume change of the inclusion is

$$\Delta v' = 4\pi r_0^2 u'_R\left(r_0\right) = 4\pi C r_0^3 = -\delta V \frac{4\mu}{3K'}\left(1+\frac{4\mu}{3K'}\right)^{-1}. \quad \text{(C.205)}$$

The volume change of the medium is positive and the pressure in the medium is negative (tensile) when $\delta V > 0$. The volume change of the inclusion is negative and the pressure in the inclusion is positive (compressive) when $\delta V > 0$. This situation corresponds to an elastic interstitial atom of local volume increase δV, or to an elastic substitutional atom of initial volume larger by δV than an atom of the surrounding medium. The volume change of the medium is negative and the pressure positive (compressive), and the volume change of the inclusion is positive and the pressure in the inclusion negative (tensile), when $A < 0$. This scenario corresponds to an elastic substitutional atom of volume smaller by δV than an atom of the surrounding medium.

The use of continuum elastic properties (e.g., bulk modulus K') for an inclusion of atomic dimensions is a severe and questionable approximation. However, the results of Section C.3.3 would also apply for inclusions much larger than atomic dimensions, for which continuum elasticity theory is more applicable.

C.4 Dislocation Nucleation and Motion

Linear elastic models of dislocations, in some cases combined with simple discrete atomic representations of defect cores in the context of lattice statics, can provide insight into shear stresses required to enact dislocation nucleation, dislocation motion, or fracture. These models omit thermal effects that can dominate dislocation kinetics at moderate and high temperatures in many solids. Reviewed in Section C.4 are models based in part on linear elasticity: Frenkel's model of shear failure (Frenkel 1926), a model for homogeneous dislocation nucleation (Cottrell 1953), and the Peierls model of the dislocation core and dislocation glide resistance (Peierls 1940; Nabarro 1947; Eshelby 1949b).

C.4.1 Frenkel Model

Consider two regions of a crystal separated by a plane. Assume that one region is held fixed, while the other is displaced rigidly by an amount u in the direction of the Burgers vector $\mathbf{b}$ for slip, the latter which lies in the plane of separation (i.e., in the slip plane). Since the crystal structure is restored to an equilibrium configuration when the magnitude of displacement is $b = (\mathbf{b}\cdot\mathbf{b})^{1/2}$, the shear stress τ required to enact the relative displacement should vanish when u is an integer multiple of b. The simplest representation of the shear stress that satisfies this periodicity condition is

$$\tau = C\sin\left(2\pi\frac{u}{b}\right), \tag{C.206}$$

where C is a constant with dimensions of energy per unit volume or stress. In the context of atomic lattice statics (see Section B.2), (C.206) implies a sinusoidal interatomic force potential for relative displacements of atoms on either side of the slip plane if long-range forces associated with higher-order neighbors are omitted.

A scalar measure of shear strain associated with the displacement is $\varepsilon = u/(2d)$; for a linear elastic body, the resulting shear stress is

$$\tau = 2\mu\varepsilon = 2\mu\frac{u}{2d} = \mu\frac{u}{d}, \tag{C.207}$$

with μ the appropriate shear elastic constant for the plane and direction under consideration and d the separation distance between slip planes. The crystal need not have isotropic or cubic symmetry.

Equating (C.206) and (C.207), and assuming small strains such that $\sin(2\pi u/b) \approx 2\pi u/b$, results in the constant C and the shear stress τ:

$$C = \frac{\mu b}{2\pi d}, \quad \tau = \frac{\mu b}{2\pi d}\sin\left(2\pi\frac{u}{b}\right). \tag{C.208}$$

The maximum of the shear stress in (C.208) is called the theoretical stress or theoretical strength of the crystal:

$$\tau_T = \tau\big|_{u=b/4} = \frac{\mu b}{2\pi d} \approx \frac{\mu}{10}. \tag{C.209}$$

The derivation of (C.206)-(C.209) is often attributed to Frenkel (1926). The theoretical strength of (C.209) can be considered as an upper bound for the shear stress required for nucleation of a straight dislocation line within an otherwise perfect crystal. The theoretical strength is often used as an order of magnitude estimate of the maximum shear stress a crystal can support before fracture, and has been suggested as a failure criterion for high pressure loading of single crystals (Graham and Brooks 1971; Clayton 2009a). The assumption of linear elasticity entering the derivation is questionable, however, since the shear strain at the stress maximum is often fairly large: $b/(8d) = (3/2)^{1/2}/8 \approx 0.15$ for $\frac{1}{2} <110>\{1\bar{1}1\}$ shear in FCC crystals or $\frac{1}{2}<111>\{1\bar{1}0\}$ shear in BCC crystals. Analytical formulae such as (C.209) should be used with caution, especially in brittle and polyatomic structures, since certain crystallographic planes may be more or less prone to fracture as a result of atomic bonding (e.g., electrostatic charge imbalances) and crystal structure (Schultz et al. 1994). An analogous derivation in terms of separation distance and Young's modulus normal to the fracture plane can be used to estimate the stress and surface energy associated with tensile (i.e., cleavage) fracture on preferred planes in anisotropic single crystals (Gilman 1960; Mishra and Thomas 1977). Formula (C.209), with ratio b/d replaced with the magnitude of twinning shear γ^j, has been suggested as a criterion for twin nucleation stress (Bell and Cahn 1957), with such a criterion for the theoretical stress required for twinning in the null temperature limit verified for several cubic metals by quantum mechanical calculations (Paxton et al. 1991).

C.4.2 Loop Nucleation in a Perfect Crystal

Consider a shear dislocation loop of radius A in an isotropic linear elastic crystal with total strain energy given by (C.165):

$$(2\pi A)E \approx \frac{\mu b^2 A}{4(1-\nu)}\left[\left(\frac{5}{2}-\nu\right)\ln\left(\frac{8A}{R_C}\right)-\left(\frac{4\pi}{3}+\frac{23}{9}\right)+\nu(2-\pi)\right]$$

$$\approx \frac{\mu b^2 A}{2}\left[\ln\left(\frac{2A}{R_C}\right)\right]. \tag{C.210}$$

In the second approximation of (C.210), Poisson's ratio $\nu = 0$ has been assumed to simplify the derivations that follow. The work P done by the applied shear stress τ in creating the loop is that required to displace the area enclosed by the loop by the magnitude b of one Burgers vector:

$$P = \pi A^2 \tau b. \tag{C.211}$$

The net energy cost (enthalpy change, or equivalently, the change in Gibbs free energy in the athermal situation) $H(A)$ associated with loop formation is

$$H = 2\pi AE - P = \frac{\mu b^2 A}{2}\left[\ln\left(\frac{2A}{R_C}\right)\right] - \pi A^2 \tau b, \tag{C.212}$$

and is stationary (specifically, maximized) when

$$\frac{\partial H}{\partial A} = \frac{\mu b^2}{2}\left[\ln\left(\frac{2A}{R_C}\right)+1\right] - 2\pi A\tau b = 0. \tag{C.213}$$

Here H is measured in terms of absolute energy rather than energy per unit spatial volume as in (4.8).

Solving (C.213) for A, the critical radius for nucleation, denoted as A_N, satisfies

$$A_N = \frac{\mu b}{4\pi\tau}\left[\ln\left(\frac{2A_N}{R_C}\right)+1\right], \tag{C.214}$$

and the maximum of the enthalpy in (C.212) is then calculated to be

$$H_N = \frac{\mu b^2}{4}A_N\left[\ln\left(\frac{2A_N}{R_C}\right)-1\right]. \tag{C.215}$$

In the absence of thermal sources of energy, loop nucleation requires (Hull and Bacon 1984)

$$H_N = 0 \Leftrightarrow \ln\left(\frac{2A_N}{R_C}\right) = 1, \tag{C.216}$$

giving a nucleation radius of $A_N = [\exp(1)/2]R_C$. Then from (C.214), the critical nucleation stress is

$$\tau_N = \frac{\mu b}{2\pi A_N} = \frac{\mu b}{8.54 R_C} \approx \frac{\mu}{10}, \tag{C.217}$$

of the same order of magnitude of the theoretical shear stress (C.209). The preceding derivation is attributed to Cottrell (1953).

Even when thermal fluctuations are present enabling $H_N > 0$, energy of such thermal fluctuations is usually insufficient to permit homogeneous nucleation of dislocation loops in metals at experimentally measured yield stresses at room temperature (Hull and Bacon 1984). Instead, the extremely high values of theoretical stresses to create straight lines (C.209) and loops (C.217) relative to experimentally measured yield stresses in ductile crystalline solids—usually on the order of $10^{-4}\mu$–$10^{-2}\mu$ (Friedel 1964)—indicate that dislocation nucleation tends to take place at defects within the crystal or at its surface, e.g., at stress concentrators such as point defects, inclusions, or pre-existing dislocations.

C.4.3 Peierls Model

The treatment in Section C.4.1 offers an estimate for the stress needed to generate a dislocation line by merging descriptions motivated by both lattice statics (C.206) and continuum linear elasticity (C.207). A similar approach was initiated by Peierls (1940) to derive the shear stress required to move an existing line defect, rather than generate it. The treatment of Peierls (1940) offers an estimate of the width of the core of an edge dislocation line in a simple cubic crystal and the shear stress required to enact uniform glide of this dislocation.

The original analysis of Peierls—which addressed an edge dislocation in a simple cubic crystal with isotropic elastic properties—was refined and extended by Nabarro (1947, 1952), Foreman et al. (1951), and Huntington (1955). Elastic anisotropy was addressed by Eshelby (1949b) and Foreman (1955). Extensive descriptions of the Peierls model, some including its derivation, can be found in books on dislocations (Friedel 1964; Nabarro 1967; Hirth and Lothe 1982; Hull and Bacon 1984; Phillips 2001). The forthcoming description follows mainly from the text of Hirth and Lothe (1982), who in turn cite the aforementioned original authors.

Consider an edge dislocation in a cubic lattice of Burgers vector $\mathbf{b} = b\mathbf{e}_1$, tangent line $\boldsymbol{\xi} = \xi\mathbf{e}_3$, and slip plane $x_2 = 0$, as shown in Fig. C.5. Distance between slip planes is denoted by d. Displacements and strains do not vary with x_3, as was the case for Volterra edge dislocations of the same line orientation discussed in Section C.1.1, and the problem is therefore one of plane strain in the $x_1 x_2$-plane.

The displacements at the slip plane $x_2 = 0$ are assumed to satisfy[3]

$$\Delta u_1(x_1) = 2u_1(x_1,0) - \frac{b}{2}, \ (x_1 > 0);$$

$$\Delta u_1(x_1) = 2u_1(x_1,0) + \frac{b}{2}, \ (x_1 < 0);$$

(C.218)

where quantity Δu_1 describes the difference in displacements of two adjacent atoms immediately above and below the slip plane, sometimes called the disregistry. Specifically with regards to the configuration in Fig. C.5, $\Delta u_1 = u_1|_B - u_1|_A$, where subscripts A and B denote, respectively, adjacent atoms in rows above and below the plane $x_2 = 0$. Limiting values of the displacement in the slip plane are assumed to follow the equalities

$$u_1(x_1 \to \infty, x_2 = 0) = -u_1(x_1 \to -\infty, x_2 = 0) = \frac{b}{4}, \qquad \text{(C.219)}$$

meaning that the disregistry Δu_1 of (C.218) vanishes as $x_1 \to \pm\infty$. The solution $u_1(x_1,0)$ is not known a priori, but is instead determined simultaneously from atomic periodicity considerations and continuum elasticity theory as explained in what follows.
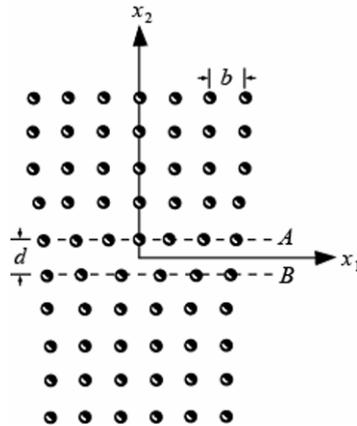
Fig. C.5 Edge dislocation in a cubic lattice

---

[3] This is the opposite of the sign convention used by Hirth and Lothe (1982), who insert the extra half plane of atoms of the dislocation in the region $x_2 < 0$.

Henceforward, consider the upper half of the crystal, for which $x_2 > 0$. Shear stresses in the slip plane are assumed to follow a periodic sinusoidal law of the same form as in (C.206):

$$\sigma_{12}(x_1,0) = -C\sin\left(\frac{2\pi(\Delta u_1)}{b}\right)$$

$$= -C\sin\left(\frac{4\pi u_1}{b} \mp \pi\right) = C\sin\left(\frac{4\pi u_1}{b}\right),$$

(C.220)

where (C.218) has been used. Applying continuum linear elasticity,

$$\sigma_{12}(x_1,0) = -\mu\frac{\Delta u_1}{d},$$

(C.221)

where the appropriate shear modulus is $\mu = \sigma_{12}/(2\varepsilon_{12})$, with ε_{12} the shear strain. Equating the first of (C.220) and (C.221) for small Δu_1, the solution for constant C is identical to that in (C.208), and the shear stress acting on the slip plane is

$$\sigma_{12}(x_1,0) = \frac{\mu b}{2\pi d}\sin\left(\frac{4\pi u_1}{b}\right).$$

(C.222)

A continuous distribution of infinitesimal edge dislocations, of the same line orientation as in Fig. C.5 but distributed along the x_1-axis, can be used to satisfy (C.218) and (C.219). The differential element of Burgers vector for each of these dislocations is denoted by $b'(x_1')dx_1'$ for the differential interval $x_1' < x_1 < x_1' + dx_1'$ along the x_1-axis. The cumulative Burgers vector resulting from this distribution is given by an integral over the slip plane:

$$b = \int_{-\infty}^{\infty} b'dx_1' = -2\int_{-\infty}^{\infty} u_{1,1}\big|_{x_1'} dx_1'.$$

(C.223)

The shear stress resulting from this distribution of infinitesimal edge dislocations in a linear elastic isotropic solid is calculated as (Peierls 1940; Eshelby 1949b)

$$\sigma_{12}(x_1,0) = -\frac{\mu}{2\pi(1-v)}\int_{-\infty}^{\infty}\frac{b'}{x_1 - x_1'}dx_1'$$

$$= \frac{\mu}{\pi(1-v)}\int_{-\infty}^{\infty}\frac{u_{1,1}\big|_{x_1'}}{x_1 - x_1'}dx_1'.$$

(C.224)

At equilibrium, the shear stress from the interaction of sheared atomic planes in (C.222) must balance the shear stress of the continuum elastic field of the dislocation in (C.224), i.e., their sums must vanish:

$$\frac{b(1-v)}{2d}\sin\left(\frac{4\pi u_1}{b}\right)+\int_{-\infty}^{\infty}\frac{u_{1,1}\big|_{x_1'}}{x_1-x_1'}dx_1'=0\,. \tag{C.225}$$

The solution of (C.225) is

$$u_1(x_1,0)=\frac{b}{2\pi}\tan^{-1}\left[\frac{2x_1(1-v)}{d}\right]=\frac{b}{2\pi}\tan^{-1}\left(\frac{x_1}{\zeta}\right), \tag{C.226}$$

where $\zeta=d/(2-2v)$. One can readily verify that (C.226) satisfies the end conditions (C.219). The disregistry (C.218) exhibits a maximum magnitude of $b/2$ as $x_1\to 0$.

The complete stress field of the Peierls edge dislocation with Burgers vector $\mathbf{b}=b\mathbf{e}_1$, tangent line $\boldsymbol{\xi}=\xi\mathbf{e}_3$, and slip plane $x_2=0$ is (Hirth and Lothe 1982)

$$\sigma_{11}=-\frac{\mu b}{2\pi(1-v)}\left\{\frac{3x_2\pm 2\zeta}{(x_1)^2+(x_2\pm\zeta)^2}-2\frac{x_2(x_2\pm\zeta)^2}{[(x_1)^2+(x_2\pm\zeta)^2]^2}\right\}, \tag{C.227}$$

$$\sigma_{22}=-\frac{\mu b}{2\pi(1-v)}\left\{\frac{x_2}{(x_1)^2+(x_2\pm\zeta)^2}-2\frac{(x_1)^2 x_2}{[(x_1)^2+(x_2\pm\zeta)^2]^2}\right\}, \tag{C.228}$$

$$\sigma_{33}=-\frac{\mu v b}{\pi(1-v)}\left\{\frac{x_2\pm\zeta}{(x_1)^2+(x_2\pm\zeta)^2}\right\}, \tag{C.229}$$

$$\sigma_{12}=\frac{\mu b}{2\pi(1-v)}\left\{\frac{x_1}{(x_1)^2+(x_2\pm\zeta)^2}-2\frac{x_1 x_2(x_2\pm\zeta)}{[(x_1)^2+(x_2\pm\zeta)^2]^2}\right\}, \tag{C.230}$$

$$\sigma_{13}=\sigma_{23}=0\,. \tag{C.231}$$

Above, $x_2\pm\zeta\to x_2+\zeta$ for $x_2>0$ and $x_2\pm\zeta\to x_2-\zeta$ for $x_2<0$. The stress field of the Peierls edge dislocation in (C.227)-(C.231) reduces to that of Volterra's model in (C.42)-(C.46) when $R=[(x_1)^2+(x_2)^2]^{1/2}\gg\zeta$, $\mathbf{b}=b\mathbf{e}_1=b_1\mathbf{e}_1$ and $b_2=0$ (Hirth and Lothe 1982). However, unlike Volterra's dislocation, the stress components are all non-singular along the dislocation line $R=0$ in the Peierls model. Strains are still large in the Peierls model as the defect line is approached, with a maximum of $\varepsilon_{11}(R=0)=2b/(\pi d)$, on the order of unity.

For a stationary edge dislocation, the strain energy per unit length according to the Peierls model is

$$E=\frac{\mu b^2}{4\pi(1-v)}\left[\ln\left(\frac{R}{2\zeta}\right)+\frac{1-2v}{4(1-v)}+1\right], \tag{C.232}$$

where the logarithmic term accounts for the elastic strain energy in the crystal. The second term in brackets accounts for stresses acting along the

surface of the cylinder of radius R enclosing the dislocation line (Hirth and Lothe 1982). The final term of unity in brackets accounts for the misfit energy stored in the stretched atomic bonds along the plane $x_2 = 0$ that follows from integration of the periodic shear stress law in (C.222).

Equating (C.48) and (C.232), an estimate of the core radius from the Peierls treatment is

$$R_C = 2\zeta \exp\left[\frac{6v-5}{4(1-v)}\right]. \tag{C.233}$$

The value $2\zeta = d/(1-v)$ is often called the width of the dislocation. The magnitude of the disregistry within the region $-\zeta < x_1 < \zeta$ exceeds $b/4$.

The misfit energy in (C.232) must be refined to account for movement of the dislocation. Let the dislocation line translate uniformly by a distance αb in the x_1-direction, where α is a scalar. After a rather lengthy series of mathematical operations not repeated here, it can be shown that the total energy per unit length of the dislocation can be expressed as follows (Peierls 1940; Nabarro 1947; Huntington 1955; Hirth and Lothe 1982):

$$E \simeq \frac{\mu b^2}{4\pi(1-v)}\left[\ln\left(\frac{R}{2\zeta}\right) + \frac{1-2v}{4(1-v)} + 1 + 2\exp\left(-\frac{4\pi\zeta}{b}\right)\cos(4\pi\alpha)\right], \tag{C.234}$$

where the energetic contribution depending on the dislocation's position α, i.e., the final term in brackets, is written

$$\left[\frac{\mu b^2}{2\pi(1-v)}\exp\left(-\frac{4\pi\zeta}{b}\right)\right]\cos(4\pi\alpha) = \frac{E_P}{2}\cos(4\pi\alpha), \tag{C.235}$$

with the periodic Peierls energy barrier to dislocation motion defined as

$$E_P = \frac{\mu b^2}{\pi(1-v)}\exp\left(-\frac{4\pi\zeta}{b}\right). \tag{C.236}$$

The shear stress required to surmount this barrier is defined as the maximum slope of $E(\alpha)$, normalized to dimensions of stress (i.e., energy per unit volume) via division by the square of the Burgers vector:

$$\tau_P = \frac{1}{b^2}\frac{\partial E}{\partial \alpha}\bigg|_{\sin(4\pi\alpha)=-1}$$

$$= \frac{2\mu}{1-v}\exp\left(-\frac{4\pi\zeta}{b}\right) \tag{C.237}$$

$$= \frac{2\mu}{1-v}\exp\left(-\frac{2\pi d}{b(1-v)}\right).$$

The shear stress τ_P in (C.237) is called the Peierls stress or, less commonly, the Peierls-Nabarro stress.

Now consider a screw dislocation in a cubic lattice with Burgers vector $\mathbf{b} = b\mathbf{e}_3$, tangent line $\boldsymbol{\xi} = \xi\mathbf{e}_3$, and slip plane $x_2 = 0$. The distance between slip planes is again denoted by d. Derivation of the displacement function and stress field follows a similar procedure as was used for the edge dislocation: the shear stresses at the slip plane arising from the elastic strain field of a distribution of infinitesimal screw dislocations balance those arising from the periodic forces associated with differences in displacements of adjacent atoms immediately above and below the slip plane. Isotropic linear elastic behavior is again assumed.

The non-zero component of displacement along the slip plane is

$$u_3(x_1,0) = \frac{b}{2\pi}\tan^{-1}\left(\frac{x_1}{\zeta}\right),\tag{C.238}$$

where the scalar $\zeta = d/2$. The stress field is

$$\sigma_{13} = -\frac{\mu b}{2\pi}\frac{x_2 \pm \zeta}{(x_1)^2 + (x_2 \pm \zeta)^2}, \quad \sigma_{23} = \frac{\mu b}{2\pi}\frac{x_1 \pm \zeta}{(x_1)^2 + (x_2 \pm \zeta)^2},\tag{C.239}$$

$$\sigma_{11} = \sigma_{12} = \sigma_{22} = \sigma_{33} = 0.\tag{C.240}$$

Above, $x_2 \pm \zeta \to x_2 + \zeta$ for $x_2 > 0$ and $x_2 \pm \zeta \to x_2 - \zeta$ for $x_2 < 0$. The stresses of the Peierls screw dislocation in (C.239) reduce to those of the Volterra screw dislocation in (C.64) when $R = [(x_1)^2 + (x_2)^2]^{1/2} \gg \zeta$ and $b = b_3$ (Hirth and Lothe 1982). However, unlike Volterra's solution, the stress components are non-singular along $R = 0$ in the Peierls model.

For a stationary screw dislocation, the strain energy per unit length according to the Peierls model is

$$E = \frac{\mu b^2}{4\pi}\left[\ln\left(\frac{R}{2\zeta}\right) + 1\right],\tag{C.241}$$

where the logarithmic term accounts for the elastic strain energy in the crystal. The final term of unity in brackets accounts for the misfit energy stored in the stretched atomic bonds along the plane $x_2 = 0$. There is no additional work of stresses at R in contrast to the edge dislocation in (C.232).

Equating (C.67) and (C.241), an estimate of the core radius from the Peierls treatment is

$$R_C = 2\zeta\exp(-1).\tag{C.242}$$

The value $2\zeta = d$ is the width of the screw dislocation. The width of the Peierls edge dislocation exceeds that of the Peierls screw dislocation by a factor of $1/(1-\nu)$, or ~1.4 for a typical Poisson's ratio ν of 0.3.

The misfit energy in (C.241) must be refined to account for movement of the dislocation. Let the dislocation line translate uniformly by a distance αb in the x_1-direction, where α is a scalar. The total energy per unit length becomes

$$E \simeq \frac{\mu b^2}{4\pi}\left[\ln\left(\frac{R}{2\zeta}\right)+1+2\exp\left(-\frac{4\pi\zeta}{b}\right)\cos(4\pi\alpha)\right], \qquad \text{(C.243)}$$

where the final term in brackets depending on the instantaneous position of the dislocation line is written

$$\left[\frac{\mu b^2}{2\pi(1-\nu)}\exp\left(-\frac{4\pi\zeta}{b}\right)\right]\cos(4\pi\alpha)=\frac{E_P}{2}\cos(4\pi\alpha), \qquad \text{(C.244)}$$

with the periodic Peierls energy barrier to dislocation motion

$$E_P = \frac{\mu b^2}{\pi}\exp\left(-\frac{4\pi\zeta}{b}\right). \qquad \text{(C.245)}$$

The Peierls stress τ_P for the screw dislocation is then defined as

$$\tau_P = \frac{1}{b^2}\frac{\partial E}{\partial \alpha}\Big|_{\sin(4\pi\alpha)=-1}$$

$$= 2\mu\exp\left(-\frac{4\pi\zeta}{b}\right) \qquad \text{(C.246)}$$

$$= 2\mu\exp\left(-\frac{2\pi d}{b}\right).$$

The preceding treatment of edge and screw dislocations assumed isotropic elastic behavior for each region of the crystalline body above and below the slip plane $x_2 = 0$. Effects of anisotropy can be incorporated by following analytical approaches of Eshelby (1949b) and Foreman (1955). Omitting effects of bulk continuum stresses at R for edge dislocations, energy per unit length and Peierls stress are written in a generic form that applies for edge or screw dislocations as

$$E = \frac{\hat{K}b^2}{4\pi}\left[\ln\left(\frac{R}{2\zeta}\right)+1+2\exp\left(-\frac{4\pi\zeta}{b}\right)\cos(4\pi\alpha)\right], \qquad \text{(C.247)}$$

$$\tau_P = 2\hat{K}\exp\left(-\frac{4\pi\zeta}{b}\right), \qquad \text{(C.248)}$$

where $\hat{K}$ is the anisotropic energy factor for the corresponding dislocation in Section C.1.6, with examples listed Tables C.1 or C.2. The dislocation width is

$$2\zeta = \frac{\hat{K}}{\hat{\mu}} d \,, \tag{C.249}$$

where $\hat{\mu}$ is the appropriate choice of shear elastic coefficient entering (C.221). For example, for the edge dislocation configuration in Fig. C.5 (specifically [100](010) slip with dislocation line [001]), $\hat{\mu} = \overline{\mathbb{C}}^{1212} = \overline{\mathbb{C}}^{66}$. For the screw dislocation considered previously with line along the x_3-axis and slip plane $x_2 = 0$ (specifically [001](010) slip with dislocation line [001]), the appropriate shear elastic constant is $\hat{\mu} = \overline{\mathbb{C}}^{2323} = \overline{\mathbb{C}}^{44}$.

While original derivations of Peierls (1940) and Nabarro (1947) considered simple cubic structures (i.e., $b = d = a$, where a is the lattice parameter of (3.2)), the same derivation has been applied to other cubic crystal structures (Eshelby 1949b). Recall from Section A.3.1 that cubic crystals exhibit three independent second-order elastic stiffness constants $\overline{\mathbb{C}}^{11}$, $\overline{\mathbb{C}}^{12}$, and $\overline{\mathbb{C}}^{44}$. Energy factors $\hat{K}$ for various kinds of dislocations in cubic crystals are listed in terms of these constants in Table C.1. To represent the effective shear modulus $\hat{\mu}$ in (C.249) for preferred directions in cubic lattices, it becomes prudent to introduce the three independent second-order elastic compliance coefficients for cubic solids (Steeds 1973):

$$\overline{S}_{11} = \frac{\overline{\mathbb{C}}^{11} + \overline{\mathbb{C}}^{12}}{(\overline{\mathbb{C}}^{11} - \overline{\mathbb{C}}^{12})(\overline{\mathbb{C}}^{11} + 2\overline{\mathbb{C}}^{12})} \,, \tag{C.250}$$

$$\overline{S}_{12} = \frac{-\overline{\mathbb{C}}^{12}}{(\overline{\mathbb{C}}^{11} - \overline{\mathbb{C}}^{12})(\overline{\mathbb{C}}^{11} + 2\overline{\mathbb{C}}^{12})} \,, \tag{C.251}$$

$$\overline{S}_{44} = \frac{1}{\overline{\mathbb{C}}^{44}} \,. \tag{C.252}$$

Coefficients in (C.250)-(C.252) are all referred to a Cartesian coordinate system with axes parallel to the cube axes of the crystal. Consider now the primary slip systems for simple cubic (SC), body centered cubic (BCC), and face centered cubic (FCC) crystals listed in Table 3.4.

For shearing in a <100> direction on a {010} plane, the primary slip mode for SC structures, the appropriate elastic constant is simply (Eshelby 1949b)

$$\hat{\mu}_{\{100\}} = \frac{1}{\overline{S}_{44}} = \overline{\mathbb{C}}^{44} \,. \tag{C.253}$$

For shearing in a <110> direction on a {111} plane, the primary slip mode for FCC structures, the shear constant is (Nabarro 1947)

$$\hat{\mu}_{\{111\}} = \frac{1}{(2/3)\overline{S}_{44} + (2/3)(\overline{S}_{11} - \overline{S}_{12})} = \frac{3\overline{\mathbb{C}}^{44}(\overline{\mathbb{C}}^{11} - \overline{\mathbb{C}}^{12})}{2(\overline{\mathbb{C}}^{44} + \overline{\mathbb{C}}^{11} - \overline{\mathbb{C}}^{12})}. \quad (C.254)$$

Gilman (2003) notes that in cubic crystals, the shear elastic constant should be independent of shearing direction on {100} or {111} families of planes. However, $\hat{\mu}$ does depend on direction for shearing on {110} planes. For example, for shearing in a <111> direction on a {110} plane, often the primary slip mode for BCC structures, the shear constant is (Eshelby 1949b)

$$\hat{\mu}_{\{110\}<1\bar{1}1>} = \frac{1}{(1/3)\overline{S}_{44} + (4/3)(\overline{S}_{11} - \overline{S}_{12})} = \frac{3\overline{\mathbb{C}}^{44}(\overline{\mathbb{C}}^{11} - \overline{\mathbb{C}}^{12})}{4\overline{\mathbb{C}}^{44} + \overline{\mathbb{C}}^{11} - \overline{\mathbb{C}}^{12}}. \quad (C.255)$$

For shearing in a <110> direction on a {110} plane (Gilman 2003), the shear elastic constant is

$$\hat{\mu}_{\{110\}<1\bar{1}0>} = \frac{1}{2(\overline{S}_{11} - \overline{S}_{12})} = \frac{\overline{\mathbb{C}}^{11} - \overline{\mathbb{C}}^{12}}{2}, \quad (C.256)$$

whereas along a <100> direction on a {110} plane, it is (Gilman 2003)

$$\hat{\mu}_{\{110\}<\bar{1}00>} = \frac{1}{\overline{S}_{44}} = \overline{\mathbb{C}}^{44}. \quad (C.257)$$

For the degenerate situation of isotropy, $\overline{S}_{11} - \overline{S}_{12} = \overline{S}_{44}/2$ and the coefficients computed via (C.253)-(C.257) all reduce to the isotropic shear modulus, i.e., $\hat{\mu} = \mu = (\overline{\mathbb{C}}^{11} - \overline{\mathbb{C}}^{12})/2 = \overline{\mathbb{C}}^{44}$.

The equations listed in Section C.4.3 for stress fields, energies, and slip resistance (i.e., Peierls stress) are regularly used as estimates of such quantities for non-cubic crystal structures and for polyatomic lattices. The theory has also been applied regularly to both metals and nonmetals. Limitations inherent in the simple sinusoidal atomic force law (C.220) will of course limit the accuracy of predictions; e.g., Coulomb interactions among ions of the same and different species in ionic crystals are not formally addressed. Additional refinements to atomic force interaction models used in Peierls-Nabarro treatments were made by Foreman et al. (1951) and Huntington (1955). Several variations of energy (C.247) accounting for different kinds of atomic force laws are listed by Foreman (1955).

The Peierls model suggests that the energy per unit length of the dislocation should decrease with increasing interplanar spacing d and increasing dislocation width 2ζ. It also suggests that edge dislocations should be more mobile than screw dislocations in most crystals, since typically Pois-

son's ratio $\nu > 0$. For example, $\tau_P = 3.6 \times 10^{-4}\,\mu$ for edge dislocations and $\tau_P = 3.7 \times 10^{-3}\,\mu$ for screw dislocations in an isotropic solid with $b = d$ and $\nu = 0.3$. Johnston and Gilman (1959) found that at a given applied stress, edge components of dislocation loops move considerably faster than screw components in lithium fluoride single crystals. This phenomenon (i.e., edge dislocation components more mobile than screw components) is known to occur similarly in many cubic metals.

The Peierls stress is thought to provide a more accurate measure of the shear yield stress in most crystals than does the theoretical stress (C.209). However, the Peierls stress neglects effects of temperature, correlated and uncorrelated atomic fluctuations (Kuhlmann-Wilsdorf 1960), and in metallic crystals above cryogenic temperatures the Peierls barrier is often easily overcome by thermal activation (Kocks et al. 1975; Hull and Bacon 1984). Possible velocity-dependent contributions to dislocation drag that may be important at high rates of deformation are also omitted, since the Peierls stress accounts only for the static component of lattice friction. Such contributions include viscous, phonon, and electron drag (Kocks et al. 1975; Gilman 1979). Resistances to slip arising from interaction forces, for example interactions among dislocations (Taylor 1934; Beltz et al. 1996), dislocations and point defects, and dislocations and inclusions or second-phase particles, often far exceed resistance from lattice friction. However, the Peierls stress may be significant relative to other sources of glide resistance in some cases. These include crystals with low defect densities deformed at very low temperatures wherein thermal effects and interaction forces between defects are small, and some ionic or covalent solids (Friedel 1964; Farber et al. 1993). Nabarro (1997) and Gilman (2003) provide more recent critical reviews of Peierls-type models of glide resistance, including comparisons with experimental data for solids with various crystal structures and various kinds of atomic bonding. It is possible for the dislocation glide resistance to approach the theoretical strength in very stiff or brittle solids (e.g., some nonmetals); in such cases, the theoretical stress (C.209) would provide a more accurate representation of the shear strength than the Peierls stress, with the latter underestimating the strength.

A key assumption implicit in (C.220) is that the shear stress at x_1 resulting from interatomic forces depends only on the local value of disregistry at x_1. A recent reformulation of the Peierls model relaxing this assumption to account for nonlocality (Miller et al. 1998) has been demonstrated to enable closer agreement with lattice statics calculations for dislocation energies.

Another limitation of the Peierls model is its presumption of linear elastic constitutive behavior for the bulk crystal. Extension of the derivation to account for general nonlinear elastic behavior does not appear straightforward. However, results of the original derivation can be extended—in a simple and physically plausible, if not completely rigorous manner—to consider effects of superposed hydrostatic stress (i.e., pressure p) in crystals of cubic symmetry. Recall that in cubic crystals, pressure results only in a volume change and imparts no shear deformation, with a reduction in the instantaneous lattice parameter occurring when pressure is compressive (i.e., when $p > 0$). Under an imposed pressure, the lattice parameter, Burgers vector magnitude b, and interplanar spacing d presumably all change by the same fraction, since b and d are proportional to the lattice parameter (see Section 3.1.1). Thus the ratio ζ/b is unchanged by effects of pressure, and the Peierls stress of (C.237), (C.246), and (C.248) is modified only by effects of pressure on the elastic coefficients entering these expressions. For example, in the isotropic elastic approximation for a screw dislocation, letting $\tilde{\mu}$ denote a pressure-dependent shear modulus (i.e., a tangent shear stiffness), (C.246) is replaced with

$$\tau_P = 2\tilde{\mu}\exp\left(-\frac{2\pi d}{b}\right), \ \tilde{\mu} = \tilde{\mu}(p). \tag{C.258}$$

Recall from (A.26) that, to first order in an isotropic material, the dependence of shear modulus on pressure depends on the material's second-order elastic constants and several of its third-order elastic constants. Chua and Ruoff (1975) found that yield and flow stresses for slip in polycrystalline potassium (body centered cubic structure (Wyckoff 1963)) increased with increasing hydrostatic pressure by about the same proportion as the elastic coefficients, justifying the use of (C.258). Effects of temperature θ on elastic properties can be incorporated following similar arguments, since thermal expansion is spherical in cubic crystals. In that case, the tangent shear modulus $\tilde{\mu} = \tilde{\mu}(p, \theta)$ in (C.258), for example. Such a description would not account for kinetics of thermally activated dislocation motion, however, whereby effects of temperature on glide resistance tend to be much greater than changes in shear modulus with temperature. Typically, the shear modulus increases with increasing pressure and decreases with increasing temperature, though exceptions are possible. The same arguments would apply towards estimates of the theoretical strength: μ in (C.209) can be replaced with its pressure- and temperature-dependent counterpart.

Appendix D: Kinematic Derivations

Appendix D provides an interpretation of the total covariant derivative of the deformation gradient in the context of deformation of a differential line element. Next, derivation of Piola's identity for the Jacobian determinant of the deformation gradient is given. Compatibility conditions for the deformation gradient and symmetric deformation tensor are addressed using convected basis vectors and geometric concepts. Finally, anholonomic connection coefficients are obtained via use of convected basis vectors.

D.1 Total Covariant Derivative of Deformation Gradient

Consider the Taylor-like series for deformed differential line element in the spatial configuration $d\mathbf{x} = dx^a \mathbf{g}_a \in T_x B$ given in (2.114). In what follows in (D.1), a second-order accurate approximation is used, meaning terms of orders three and higher in reference element $d\mathbf{X} = dX^A \mathbf{G}_A \in T_X B_0$ are truncated from the series expansion. In tensor form, (2.114) can then be written as follows, using (2.4), (2.56), (2.59), (2.112), and (2.116):

$$d\mathbf{x} = \left[\mathbf{F}|_X + \frac{1}{2} (\mathbf{F}|_X)_{,B} \left\langle \mathbf{G}^B, d\mathbf{X} \right\rangle \right] d\mathbf{X}$$

$$= \left[F^a_{.A}\big|_X \mathbf{g}_a \otimes \mathbf{G}^A + \frac{1}{2} (F^a_{.A} \mathbf{g}_a \otimes \mathbf{G}^A)_{,B} \left\langle \mathbf{G}^B, dX^C \mathbf{G}_C \right\rangle \right] dX^D \mathbf{G}_D$$

$$= \left[F^a_{.A}\big|_X \mathbf{g}_a \otimes \mathbf{G}^A + \frac{1}{2} (F^a_{.A} \mathbf{g}_a \otimes \mathbf{G}^A)_{,B} \delta^B_{.C} dX^C \right] dX^D \mathbf{G}_D$$

$$= F^a_{.A}\big|_X \mathbf{g}_a \left\langle \mathbf{G}^A, \mathbf{G}_D \right\rangle dX^D + \frac{1}{2} \left[(F^a_{.A} \mathbf{g}_a \otimes \mathbf{G}^A)_{,B} dX^B \right] dX^D \mathbf{G}_D$$

$$= F^a_{.A}\big|_X dX^A \mathbf{g}_a + \frac{1}{2} \left[F^a_{.A,B} \mathbf{g}_a \otimes \mathbf{G}^A + F^a_{.A} \mathbf{g}_{a,B} \otimes \mathbf{G}^A \right.$$

$$\left. + F^a_{.A} \mathbf{g}_a \otimes \mathbf{G}^A_{.,B} \right] dX^B dX^D \mathbf{G}_D$$

<div align="right">(continued...)</div>

$$
= F^a_{.A}\big|_X dX^A \mathbf{g}_a + \frac{1}{2}\Big[F^a_{.A,B}\mathbf{g}_a \otimes \mathbf{G}^A + F^a_{.A}F^b_{.B}\mathbf{g}_{a,b}\otimes\mathbf{G}^A
$$

$$
+ F^a_{.A}\mathbf{g}_a \otimes \mathbf{G}^A_{,B}\Big] dX^B dX^D \mathbf{G}_D
$$

$$
= F^a_{.A}\big|_X dX^A \mathbf{g}_a
$$

$$
+ \frac{1}{2}\Big[F^a_{.A,B}\mathbf{g}_a \otimes \mathbf{G}^A + F^a_{.A}F^b_{.B}\overset{g}{\Gamma}{}^{.c}_{ba}\mathbf{g}_c \otimes \mathbf{G}^A
$$

$$
- F^a_{.A}\overset{g}{\Gamma}{}^{.A}_{BC}\mathbf{g}_a \otimes \mathbf{G}^C \Big] dX^B dX^D \mathbf{G}_D
$$

$$
= F^a_{.A}\big|_X dX^A \mathbf{g}_a + \frac{1}{2}(F^a_{.A,B} + \overset{g}{\Gamma}{}^{.a}_{bc}F^c_{.A}F^b_{.B} - \overset{g}{\Gamma}{}^{.C}_{BA}F^a_{.C})\mathbf{g}_a
$$

$$
\times dX^B dX^D \big\langle \mathbf{G}^A , \mathbf{G}_D \big\rangle
$$

$$
= F^a_{.A}\big|_X dX^A \mathbf{g}_a + \frac{1}{2}(F^a_{.A,B} + \overset{g}{\Gamma}{}^{.a}_{bc}F^c_{.A}F^b_{.B} - \overset{g}{\Gamma}{}^{.C}_{BA}F^a_{.C})\mathbf{g}_a dX^A dX^B
$$

$$
= \Big(F^a_{.A}\big|_X + \frac{1}{2}F^a_{.A:B}\big|_X dX^B \Big) dX^A \mathbf{g}_a
$$

$$
= \Big(x^a_{,A}\big|_X + \frac{1}{2}x^a_{,AB}\big|_X dX^B \Big) dX^A \mathbf{g}_a . \tag{D.1}
$$

In a homogeneous deformation in the continuum sense, $F^a_{.A:B} = 0$ by definition (Truesdell and Toupin 1960), in which case $d\mathbf{x} = \mathbf{F}d\mathbf{X}$ is exact.

D.2 Piola's Identity for the Jacobian Determinant

Identity (2.145), most typically and compactly expressed as $(J^{-1}F^a_{.A})_{:a} = 0$, is derived in full below:

$$
\left(\frac{\partial J^{-1}}{\partial F^{-1A}_{.a}} \right)_{:a} = (J^{-1}F^a_{.A})_{:a} = (J^{-1}F^a_{.A})_{;a} - J^{-1}F^a_{.C}\overset{G}{\Gamma}{}^{.C}_{BA}F^{-1B}_{.a}
$$

$$
= (J^{-1}F^a_{.A})_{,a} + J^{-1}\overset{g}{\Gamma}{}^{.a}_{ab}F^b_{.A} - J^{-1}F^a_{.C}\overset{G}{\Gamma}{}^{.C}_{BA}F^{-1B}_{.a}
$$

$$
= (J^{-1}F^a_{.A})_{,a} + J^{-1}F^a_{.A}(\ln\sqrt{g})_{,a} - J^{-1}F^a_{.C}\overset{G}{\Gamma}{}^{.C}_{BA}F^{-1B}_{.a}
$$

$$
= (J^{-1}F^a_{.A})_{,a} + J^{-1}F^a_{.A}\frac{1}{\sqrt{g}}(\sqrt{g})_{,a} - J^{-1}F^a_{.C}\overset{G}{\Gamma}{}^{.C}_{BA}F^{-1B}_{.a}
$$

<div align="right">(continued...)</div>

$$= \sqrt[-1]{g}\left(\sqrt{g}\,J^{-1}F^a_{.A}\right)_{,a} - J^{-1}F^a_{.C}\,\overset{G}{\Gamma}{}^{.C}_{BA}F^{-1B}_{.a}$$

$$= J^{-1}F^a_{.A,B}F^{-1B}_{.a} + \sqrt[-1]{g}\left(\sqrt{g}\,J^{-1}\right)_{,a}F^a_{.A} - J^{-1}\overset{G}{\Gamma}{}^{.B}_{BA}$$

$$= J^{-1}F^a_{.A,B}F^{-1B}_{.a} + \sqrt[-1]{g}\left(\sqrt{G}\det\mathbf{F}^{-1}\right)_{,a}F^a_{.A} - J^{-1}\overset{G}{\Gamma}{}^{.B}_{BA}$$

$$= J^{-1}F^a_{.A,B}F^{-1B}_{.a} + \sqrt[-1]{g}\det\mathbf{F}^{-1}\left(\sqrt{G}\right)_{,a}F^a_{.A}$$

$$\quad + \sqrt[-1]{g}\sqrt{G}\left(\det\mathbf{F}^{-1}\right)_{,a}F^a_{.A} - J^{-1}\overset{G}{\Gamma}{}^{.B}_{BA}$$

$$= J^{-1}F^a_{.A,B}F^{-1B}_{.a} + \left[\sqrt[-1]{g}\sqrt{G}\det\mathbf{F}^{-1}\right]\left[\sqrt[-1]{G}\left(\sqrt{G}\right)_{,A}\right]$$

$$\quad - \sqrt[-1]{g}\sqrt{G}\left(\det\mathbf{F}\right)^{-2}\left(\det\mathbf{F}\right)_{,a}F^a_{.A} - J^{-1}\overset{G}{\Gamma}{}^{.B}_{BA}$$

$$= J^{-1}F^a_{.A,B}F^{-1B}_{.a} + J^{-1}\left(\ln\sqrt{G}\right)_{,A}$$

$$\quad - \sqrt[-1]{g}\sqrt{G}\left(\det\mathbf{F}\right)^{-2}\left(\partial\det\mathbf{F}/\partial F^b_{.B}\right)F^b_{.B,a}F^a_{.A} - J^{-1}\overset{G}{\Gamma}{}^{.B}_{BA}$$

$$= J^{-1}F^a_{.A,B}F^{-1B}_{.a} - \sqrt[-1]{g}\sqrt{G}\left(\det\mathbf{F}\right)^{-2}\left(\partial\det\mathbf{F}/\partial F^b_{.B}\right)F^b_{.B,A}$$

$$\quad + J^{-1}\left(\overset{G}{\Gamma}{}^{.B}_{BA} - \overset{G}{\Gamma}{}^{.B}_{BA}\right)$$

$$= J^{-1}F^a_{.A,B}F^{-1B}_{.a} - J^{-1}\left(\det\mathbf{F}^{-1}\right)\left(\partial\det\mathbf{F}/\partial F^a_{.B}\right)F^a_{.B,A}$$

$$= J^{-1}F^a_{.A,B}F^{-1B}_{.a} - J^{-1}J^{-1}\left(\partial J/\partial F^a_{.B}\right)F^a_{.B,A}$$

$$= J^{-1}\left[F^a_{.A,B}F^{-1B}_{.a} - J^{-1}\left(JF^{-1B}_{.a}\right)F^a_{.B,A}\right] \tag{D.2}$$

$$= J^{-1}F^{-1B}_{.a}\left[x^a_{.,AB} - x^a_{.,BA}\right]$$

$$= 0.$$

Relations (2.56), (2.59), (2.73), (2.112), (2.116), and (2.142)-(2.144) have been consulted in derivation (D.2). The inverse identity in (2.146), i.e., $(JF^{-1A}_{.a})_{.A} = 0$, can be derived using a completely analogous procedure. Truesdell and Toupin (1960) attribute these identities (i.e., (2.145), (2.146), and (D.2)) to Euler and Jacobi as well as Piola.

For completeness, identity (2.73) and its counterpart in the spatial configuration are derived below:

$$(\ln \sqrt{G})_{,A} = \sqrt[G]{G}(\sqrt{G})_{,A} = G^{-1/2}(G^{1/2})_{,A} = \frac{1}{2G}G_{,A}$$

$$= \frac{1}{2G}\frac{\partial \det \mathbf{G}}{\partial G_{BC}}G_{BC,A} = \frac{1}{2G}GG^{CB}\left(\overset{G}{\Gamma}{}^{..D}_{AC}G_{BD} + \overset{G}{\Gamma}{}^{..D}_{AB}G_{CD}\right)$$

$$= \frac{1}{2}\left(\overset{G}{\Gamma}{}^{..D}_{AC}\delta^{C}_{.D} + \overset{G}{\Gamma}{}^{..D}_{AB}\delta^{B}_{.D}\right) = \frac{1}{2}\left(\overset{G}{\Gamma}{}^{..D}_{AD} + \overset{G}{\Gamma}{}^{..D}_{AD}\right)$$

$$= \overset{G}{\Gamma}{}^{..D}_{AD} = \overset{G}{\Gamma}{}^{..D}_{DA},$$

(D.3)

$$(\ln \sqrt{g})_{,a} = \sqrt[g]{g}(\sqrt{g})_{,a} = g^{-1/2}(g^{1/2})_{,a} = \frac{1}{2g}g_{,a}$$

$$= \frac{1}{2g}\frac{\partial \det \mathbf{g}}{\partial g_{bc}}g_{bc,a} = \frac{1}{2g}gg^{cb}\left(\overset{g}{\Gamma}{}^{..d}_{ac}g_{bd} + \overset{g}{\Gamma}{}^{..d}_{ab}g_{cd}\right)$$

$$= \frac{1}{2}\left(\overset{g}{\Gamma}{}^{..d}_{ac}\delta^{c}_{.d} + \overset{g}{\Gamma}{}^{..d}_{ab}\delta^{b}_{.d}\right) = \frac{1}{2}\left(\overset{g}{\Gamma}{}^{..d}_{ad} + \overset{g}{\Gamma}{}^{..d}_{ad}\right)$$

$$= \overset{g}{\Gamma}{}^{..d}_{ad} = \overset{g}{\Gamma}{}^{..d}_{da}.$$

(D.4)

In deriving (D.3) and (D.4), (2.143) and symmetries of covariant indices of the Christoffel symbols have been used, along with identities (2.57) and (2.60), the latter two derived in full as follows. From (2.11) and (2.56), the partial derivative of the referential metric with components $G_{AB}(X)$ is

$$G_{AB,C} = (\mathbf{G}_{A}\cdot\mathbf{G}_{B})_{,C} = \mathbf{G}_{A,C}\cdot\mathbf{G}_{B} + \mathbf{G}_{A}\cdot\mathbf{G}_{B,C}$$

$$= \overset{G}{\Gamma}{}^{..D}_{CA}\mathbf{G}_{D}\cdot\mathbf{G}_{B} + \mathbf{G}_{A}\cdot\mathbf{G}_{D}\overset{G}{\Gamma}{}^{..D}_{CB}$$

$$= \overset{G}{\Gamma}{}^{..D}_{CA}G_{BD} + \overset{G}{\Gamma}{}^{..D}_{CB}G_{AD}.$$

(D.5)

Similarly, from (2.12) and (2.59), the partial derivative of spatial metric with components $g_{ab}(x)$ is

$$g_{ab,c} = (\mathbf{g}_{a}\cdot\mathbf{g}_{b})_{,c} = \mathbf{g}_{a,c}\cdot\mathbf{g}_{b} + \mathbf{g}_{a}\cdot\mathbf{g}_{b,c}$$

$$= \overset{g}{\Gamma}{}^{..d}_{ca}\mathbf{g}_{d}\cdot\mathbf{g}_{b} + \mathbf{g}_{a}\cdot\mathbf{g}_{d}\overset{g}{\Gamma}{}^{..d}_{cb}$$

$$= \overset{g}{\Gamma}{}^{..d}_{ca}g_{bd} + \overset{g}{\Gamma}{}^{..d}_{cb}g_{ad}.$$

(D.6)

Also for completeness, relationship (2.141) relating differential volumes and the Jacobian determinant is derived directly. With minor abuse of notation, letting dX^{A}, dX^{B}, and dX^{C} denote components of distinct vectors comprising edges of a differential element of reference volume dV,

$$dV = d\mathbf{X}_{1}\cdot(d\mathbf{X}_{2} \times d\mathbf{X}_{3}) = \varepsilon_{ABC}dX^{A}dX^{B}dX^{C} .$$

(D.7)

Similarly, for the current configuration,

$$dv = d\mathbf{x}_1 \bullet (d\mathbf{x}_2 \times d\mathbf{x}_3) = \varepsilon_{abc} dx^a dx^b dx^c . \tag{D.8}$$

It follows from the final identity in Table 2.3 that

$$6 dX^A dX^B dX^C = \varepsilon^{ABC} dV . \tag{D.9}$$

Finally, using (2.115), i.e., linear transformation $dx^a = x^a_{.,A} dX^A = F^a_{.A} dX^A$, along with (D.7)-(D.9),

$$
\begin{aligned}
\frac{dv}{dV} &= \frac{\varepsilon_{abc} dx^a dx^b dx^c}{dV} \\
&= \frac{\varepsilon_{abc} F^a_{.A} dX^A F^b_{.B} dX^B F^c_{.C} dX^C}{dV} \\
&= \varepsilon_{abc} F^a_{.A} F^b_{.B} F^c_{.C} \frac{dX^A dX^B dX^C}{dV} \\
&= \varepsilon_{abc} F^a_{.A} F^b_{.B} F^c_{.C} \frac{\varepsilon^{ABC}}{6} \\
&= J,
\end{aligned}
\tag{D.10}
$$

in agreement with the definition of Jacobian invariant J in (2.142):

$$J = \frac{1}{6} \varepsilon_{abc} \varepsilon^{ABC} F^a_{.A} F^b_{.B} F^c_{.C}, \ J^{-1} = \frac{1}{6} \varepsilon_{ABC} \varepsilon^{abc} F^{-1A}_{.a} F^{-1B}_{.b} F^{-1C}_{.c} . \tag{D.11}$$

In the common coordinate systems of Table 2.1, referential volume element $dV = \sqrt{G} dX^1 dX^2 dX^3$ is

$$
dV = \begin{cases}
(dX)(dY)(dZ) & \text{(Cartesian coordinates)}, \\
(R)(dR)(d\theta)(dZ) & \text{(cylindrical coordinates)}, \\
(R^2 \sin\theta)(dR)(d\theta)(d\varphi) & \text{(spherical coordinates)}.
\end{cases}
\tag{D.12}
$$

The following identities for the Jacobian or its inverse are also noted:

$$JF^{-1A}_{.a} = \frac{\partial J}{\partial F^a_{.A}} = \frac{1}{2} \varepsilon_{abc} \varepsilon^{ABC} F^b_{.B} F^c_{.C} ; \tag{D.13}$$

$$J^{-1} F^a_{.A} = \frac{\partial J^{-1}}{\partial F^{-1A}_{.a}} = \frac{1}{2} \varepsilon_{ABC} \varepsilon^{abc} F^{-1B}_{.b} F^{-1C}_{.c} ; \tag{D.14}$$

$$J \delta^A_{.B} = \frac{1}{2} \varepsilon_{acd} \varepsilon^{ACD} F^c_{.C} F^d_{.D} F^a_{.B}, \ J^{-1} \delta^a_{.b} = \frac{1}{2} \varepsilon_{ACD} \varepsilon^{acd} F^{-1C}_{.c} F^{-1D}_{.d} F^{-1A}_{.b} ; \tag{D.15}$$

$$J \varepsilon_{ABC} = \varepsilon_{abc} F^a_{.A} F^b_{.B} F^c_{.C}, \ J \varepsilon^{abc} = \varepsilon^{ABC} F^a_{.A} F^b_{.B} F^c_{.C} . \tag{D.16}$$

Truesdell and Toupin (1960) also attribute identities (D.15) to Piola. Nanson's formula (2.148) is easily derived after inverting the first of (D.16):

$$
\begin{aligned}
n_a ds &= \varepsilon_{abc} dx^b dx^c = (JF^{-1D}_{.a} F^{-1E}_{.b} F^{-1F}_{.c} \varepsilon_{DEF})(F^b_{.B} dX^B F^c_{.C} dX^C) \\
&= JF^{-1D}_{.a} \varepsilon_{DBC} dX^B dX^C = JF^{-1D}_{.a} N_D dS.
\end{aligned}
\tag{D.17}
$$

Squaring both sides of (D.17), dividing by dS^2, and then taking the square root of the result, the ratio of scalar area elements is then obtained:

$$\frac{ds}{dS} = J\sqrt{(F^{-1A}_{.a}g^{ab}F^{-1B}_{.b})N_A N_B} = J\sqrt{C^{-1AB}N_A N_B} \ . \tag{D.18}$$

Finally, material time derivatives of spatial volume element dv and oriented spatial surface element $n_a ds$ are computed, respectively, as follows:

$$\frac{d}{dt}(dv) = \frac{d}{dt}(JdV) = \dot{J}dV = \dot{J}J^{-1}dv \tag{D.19}$$
$$= (\dot{x}^a)_{;a}\,dv = v^a_{;a}dv = L^a_{.a}dv = D^a_{.a}dv,$$

$$\frac{d}{dt}(n_a ds) = \frac{d}{dt}(JF^{-1A}_{.a}N_A dS) = \frac{d}{dt}(JF^{-1A}_{.a})N_A dS$$
$$= (\dot{J}F^{-1A}_{.a} + J\dot{F}^{-1A}_{.a})N_A dS$$
$$= \dot{J}J^{-1}JF^{-1A}_{.a}N_A dS + J\dot{F}^{-1A}_{.a}N_A dS \tag{D.20}$$
$$= v^b_{;b}JF^{-1A}_{.a}N_A dS - v^b_{;a}JF^{-1A}_{.b}N_A dS$$
$$= (v^b_{;b}n_a - v^b_{;a}n_b)ds = (L^b_{.b}n_a - L^b_{.a}n_b)ds.$$

In derivation (D.19), relation (2.181) has been used. In derivation (D.20), relations (2.148), (2.176), and (2.181) have been used.

D.3 Compatibility Conditions via Convected Coordinates

Compatibility conditions for finite deformations are further examined in what follows. Consider again the deformation gradient $\mathbf{F}$ of (2.112). Assume spatial coordinates $x^a = x^a(X,t)$ are at least three times differentiable and one-to-one functions of reference coordinates X^A. Denote components of deformation gradient $\mathbf{F}$ and its inverse, respectively, by

$$F^a_{.A}(X,t) = x^a_{,A}, \ \ F^{-1A}_{.a}(x,t) = X^A_{,a} \ . \tag{D.21}$$

For mathematical convenience, constant orthonormal (i.e., Cartesian) basis vectors $\mathbf{g}_a = \mathbf{e}_a$ are selected in the current configuration such that

$$\mathbf{F}(X,t) = F^a_{.A}(X,t)\mathbf{e}_a \otimes \mathbf{G}^A(X), \tag{D.22}$$

where the scalar products

$$\mathbf{e}^a \bullet \mathbf{e}^b = \delta^{ab}, \ \ \mathbf{e}_a \bullet \mathbf{e}_b = \delta_{ab}, \ \ \langle \mathbf{e}^a, \mathbf{e}_b \rangle = \delta^a_{.b} \ . \tag{D.23}$$

Convected basis vectors and covectors are assigned, respectively, as

$$\mathbf{G}'^A(x,t) = F^{-1A}_{.a}(x,t)\mathbf{e}^a, \ \ \mathbf{G}'_A(X,t) = F^a_{.A}(X,t)\mathbf{e}_a \ . \tag{D.24}$$

Notice that the sets of basis and dual vectors in (D.24) are reciprocal to one another, i.e.,

$$\left\langle \mathbf{G}'^{A}, \mathbf{G}'_{B} \right\rangle = F^{-1A}_{.a} F^{b}_{.B} \left\langle \mathbf{e}^{a}, \mathbf{e}_{b} \right\rangle = F^{-1A}_{.a} F^{b}_{.B} \delta^{a}_{.b} = \delta^{A}_{.B}. \qquad (D.25)$$

From the second of (D.24), deformation gradient (D.22) can be written in convected coordinate form as

$$\mathbf{F} = F^{a}_{.A}(X,t) \mathbf{e}_{a} \otimes \mathbf{G}^{A}(X) = \delta^{B}_{.A} \mathbf{G}'_{B}(X,t) \otimes \mathbf{G}^{A}(X). \qquad (D.26)$$

Metric components formed from the convected basis vectors are components of the right Cauchy-Green deformation tensor $C_{AB}(X,t)$ of (2.153):

$$\mathbf{G}'_{A} \cdot \mathbf{G}'_{B} = F^{a}_{.A} F^{b}_{.B} (\mathbf{e}_{a} \cdot \mathbf{e}_{b}) = F^{a}_{.A} \delta_{ab} F^{b}_{.B} = C_{AB}. \qquad (D.27)$$

Now consider partial derivatives of the convected basis vectors:

$$\mathbf{G}'_{A,B} = (F^{a}_{.A} \mathbf{e}_{a})_{,B} = F^{a}_{.A,B} \mathbf{e}_{a} + F^{a}_{.A} \mathbf{e}_{a,b} F^{b}_{.B}$$

$$= F^{a}_{.A,B} \mathbf{e}_{a} = F^{-1D}_{.a} F^{a}_{.A,B} \mathbf{G}'_{D} \qquad (D.28)$$

$$= F^{-1D}_{.a} \partial_{B} F^{a}_{.A} \mathbf{G}'_{D} = \overset{C}{\Gamma}{}^{.D}_{BA} \mathbf{G}'_{D},$$

where $\overset{C}{\Gamma}{}^{.D}_{BA} = F^{-1D}_{.a} \partial_{B} F^{a}_{.A} = (\partial_{a} X^{D})(\partial_{B} \partial_{A} x^{a})$ are coefficients of a linear connection and the notation $\partial_{B}(\cdot) = \partial(\cdot)/\partial X^{B} = (\cdot)_{,B}$ is used interchangeably for partial differentiation with respect to reference coordinates. From the first of (2.203), or as a consequence of the first of (D.21), the torsion of this connection vanishes identically:

$$\overset{C}{T}{}^{.D}_{BA} = \overset{C}{\Gamma}{}^{.D}_{[BA]} = F^{-1D}_{.a} \partial_{[B} F^{a}_{.A]}$$

$$= X^{D}_{.,a} x^{a}_{.,[AB]} = (\partial_{a} X^{D})(\partial_{[B} \partial_{A]} x^{a}) = 0. \qquad (D.29)$$

Next, by inverting a derivation similar to (2.221) and using (D.29), the connection coefficients introduced in (D.28) are found to be equivalent to those of (2.213):

$$2\overset{C}{\Gamma}{}^{.A}_{BC} = 2\overset{C}{\Gamma}{}^{.A}_{(BC)} = 2F^{-1A}_{.a} F^{a}_{.(C,B)}$$

$$= 2F^{-1A}_{.a} F^{a}_{.(C,B)} + 2F^{-1A}_{.a} \delta^{ab} F^{-1D}_{.b} \left[F^{c}_{.B} F^{d}_{.[D,C]} + F^{c}_{.C} F^{d}_{.[D,B]} \right] \delta_{cd}$$

$$= F^{-1A}_{.a} \delta^{ab} F^{-1D}_{.b} \delta_{cd} \left[F^{c}_{.B,C} F^{d}_{.D} + F^{c}_{.C,B} F^{d}_{.D} \right.$$

$$\left. + F^{c}_{.B} F^{d}_{.D,C} - F^{c}_{.B} F^{d}_{.C,D} + F^{c}_{.C} F^{d}_{.D,B} - F^{c}_{.C} F^{d}_{.B,D} \right] \qquad (D.30)$$

$$= F^{-1A}_{.a} \delta^{ab} F^{-1D}_{.b} \left[F^{c}_{.B,C} F^{d}_{.D} + F^{c}_{.B} F^{d}_{.D,C} + F^{c}_{.C,B} F^{d}_{.D} + F^{c}_{.C} F^{d}_{.D,B} \right.$$

$$\left. - F^{c}_{.B,D} F^{d}_{.C} - F^{c}_{.B} F^{d}_{.C,D} \right] \delta_{cd}$$

$$= C^{-1AD} \left[C_{BD,C} + C_{CD,B} - C_{BC,D} \right].$$

Differentiation of the connection coefficients introduced in (D.28) yields

$$\partial_E (F^a_{.D}\, \overset{C}{\Gamma}{}^{.D}_{BA}) = \partial_E (F^a_{.D} F^{-1D}_{.b} \partial_B F^b_{.A})$$

$$= \partial_E \partial_B F^a_{.A} = \partial_B \partial_E F^a_{.A} \tag{D.31}$$

$$= \partial_E \partial_B \partial_A x^a.$$

Expanding the left side of (D.31) using the product rule of Leibniz gives

$$\partial_E (F^a_{.D}\, \overset{C}{\Gamma}{}^{.D}_{BA}) = F^a_{.D,E}\, \overset{C}{\Gamma}{}^{.D}_{BA} + F^a_{.D}\, \overset{C}{\Gamma}{}^{.D}_{BA,E}$$

$$= F^a_{.D} \left(\overset{C}{\Gamma}{}^{.D}_{EF} \overset{C}{\Gamma}{}^{.F}_{BA} + \partial_E\, \overset{C}{\Gamma}{}^{.D}_{BA} \right). \tag{D.32}$$

Skew covariant parts of (D.31) and (D.32) then provide the equalities

$$F^a_{.D} \left(\partial_{[E}\, \overset{C}{\Gamma}{}^{.D}_{B]A} + \overset{C}{\Gamma}{}^{.D}_{[E|F|}\, \overset{C}{\Gamma}{}^{.F}_{B]A} \right) = F^a_{.D} \left(\frac{1}{2} \overset{C}{R}{}^{.D}_{EBA} \right) = \partial_{[E} \partial_{B]} \partial_A x^a = 0. \tag{D.33}$$

Since $F^a_{.D}$ is non-singular, it follows from (D.33) that

$$\overset{C}{R}{}^{.D}_{EBA} = 0, \tag{D.34}$$

where $\overset{C}{R}{}^{.D}_{EBA}$ are components of the Riemann-Christoffel curvature tensor—defined generically in (2.34)—formed from connection coefficients $\overset{C}{\Gamma}{}^{.A}_{BC}$ of (D.30), the latter constructed from components of the right Cauchy-Green deformation tensor C_{AB} of (D.27).

The geometric interpretation of the compatibility conditions therefore emerges as follows: (i) the torsion tensor of the aforementioned connection coefficients vanishes as in (D.29) and (ii) the curvature tensor of these connection coefficients vanishes as in (D.34). Notice that (D.29) is necessary and sufficient for (D.21) to hold (Schouten 1954), as remarked following (2.205). Condition (D.34) then follows automatically as a consequence of (D.21) and (D.29).

By simply interchanging spatial and reference coordinates, an analogous procedure can be used to show that the Riemann-Christoffel curvature tensor arising from spatial metric $c_{ab}(x,t) = F^{-1A}_{.a} \delta_{AB} F^{-1B}_{.b} = X^A_{.,a} \delta_{AB} X^B_{.,b}$ associated with the inverse deformation must also vanish identically in Euclidean space.

D.4 Anholonomic Connection Coefficients

First consider the lattice deformation in the first equality of (3.34):

$$\mathbf{F^L} = F^{La}_{.\alpha}(x,t)\mathbf{g}_a \otimes \tilde{\mathbf{g}}^\alpha \, . \tag{D.35}$$

Convected anholonomic basis vectors and their reciprocals are introduced as in (3.53) and (3.54):

$$\tilde{\mathbf{g}}'_\alpha(x,t) = F^{La}_{.\alpha}\mathbf{g}_a \, , \ \tilde{\mathbf{g}}'^\alpha(x,t) = F^{L-1\alpha}_{.a}\mathbf{g}^a \, , \ \left\langle \tilde{\mathbf{g}}'^\alpha, \tilde{\mathbf{g}}'_\beta \right\rangle = F^{L-1\alpha}_{.a} F^{La}_{.\beta} = \delta^\alpha_{.\beta} \, . \tag{D.36}$$

The lattice deformation of (D.35) then follows, when expressed in convected coordinates, as

$$\mathbf{F^L} = (F^{La}_{.\alpha}\mathbf{g}_a) \otimes \tilde{\mathbf{g}}^\alpha = \delta^\beta_{.\alpha}\tilde{\mathbf{g}}'_\beta \otimes \tilde{\mathbf{g}}^\alpha \, . \tag{D.37}$$

The metric tensor corresponding to basis vectors (D.36) is identical to that of (3.52):

$$\tilde{g}'_{\alpha\beta} = \tilde{\mathbf{g}}'_\alpha \bullet \tilde{\mathbf{g}}'_\beta = F^{La}_{.\alpha}\mathbf{g}_a \bullet \mathbf{g}_b F^{Lb}_{.\beta} = F^{La}_{.\alpha} g_{ab} F^{Lb}_{.\beta} = \tilde{C}^L_{\alpha\beta} \, . \tag{D.38}$$

Calculation of the anholonomic partial derivative of the first of (D.36), using (3.36), results in the intermediate configuration connection coefficients first introduced in (3.39):

$$\begin{aligned}
\tilde{\mathbf{g}}'_{\alpha,\beta} &= F^{La}_{.\alpha}\mathbf{g}_{a,\beta} + F^{La}_{.\alpha,\beta}\mathbf{g}_a \\
&= F^{La}_{.\alpha}\mathbf{g}_{a,b}F^{Lb}_{.\beta} + F^{La}_{.\alpha,\beta}F^{L-1\chi}_{.a}\tilde{\mathbf{g}}_\chi \\
&= F^{La}_{.\alpha}F^{Lb}_{.\beta}\overset{g}{\Gamma}{}^{.c}_{ba}\mathbf{g}_c - F^{La}_{.\alpha}F^{L-1\chi}_{.a,\beta}\tilde{\mathbf{g}}_\chi \\
&= F^{La}_{.\alpha}F^{Lb}_{.\beta}F^{L-1\chi}_{.c}\overset{g}{\Gamma}{}^{.c}_{ba}\tilde{\mathbf{g}}_\chi - F^{La}_{.\alpha}F^{Lb}_{.\beta}F^{L-1\chi}_{.a,b}\tilde{\mathbf{g}}_\chi \\
&= \left(F^{Lb}_{.\beta}F^{La}_{.\alpha}F^{L-1\chi}_{.c}\overset{g}{\Gamma}{}^{.c}_{ba} - F^{Lb}_{.\beta}F^{La}_{.\alpha}F^{L-1\chi}_{.a,b} \right)\tilde{\mathbf{g}}_\chi \\
&= \tilde{\Gamma}^{..\chi}_{\beta\alpha}\tilde{\mathbf{g}}_\chi \, .
\end{aligned} \tag{D.39}$$

Next consider the plastic deformation gradient in the second equality of (3.34):

$$\mathbf{F^P} = F^{P\alpha}_{.A}(X,t)\tilde{\mathbf{g}}_\alpha \otimes \mathbf{G}^A \, . \tag{D.40}$$

Convected anholonomic basis vectors and their reciprocals are again introduced:

$$\tilde{\mathbf{g}}'_\alpha(X,t) = F^{P-1A}_{.\alpha}\mathbf{G}_A \, , \ \tilde{\mathbf{g}}'^\alpha(X,t) = F^{P\alpha}_{.A}\mathbf{G}^A \, , \ \left\langle \tilde{\mathbf{g}}'^\alpha, \tilde{\mathbf{g}}'_\beta \right\rangle = \delta^\alpha_{.\beta} \, . \tag{D.41}$$

The plastic deformation of (D.40) can then be expressed in convected coordinates as

$$\mathbf{F^P} = \tilde{\mathbf{g}}_\alpha \otimes (F^{P\alpha}_{.A}\mathbf{G}^A) = \delta^\alpha_{.\beta}\tilde{\mathbf{g}}_\alpha \otimes \tilde{\mathbf{g}}'^\beta \, . \tag{D.42}$$

The metric tensor corresponding to basis vectors (D.41) is identical to that of (3.56):

$$\tilde{g}'_{\alpha\beta} = \tilde{\mathbf{g}}'_\alpha \bullet \tilde{\mathbf{g}}'_\beta = F^{P-1A}_{.\alpha}\mathbf{G}_A \bullet \mathbf{G}_B F^{P-1B}_{.\beta} = F^{P-1A}_{.\alpha} G_{AB} F^{P-1B}_{.\beta} = \tilde{C}^P_{\alpha\beta} \, . \tag{D.43}$$

The anholonomic partial derivative of the first of (D.41), with (3.36), produces the intermediate configuration connection coefficients first introduced in (3.38):

$$
\begin{aligned}
\tilde{\mathbf{g}}'_{\alpha,\beta} &= F^{P-1A}_{.\alpha}\mathbf{G}_{A,\beta} + F^{P-1A}_{.\alpha,\beta}\mathbf{G}_A \\
&= F^{P-1A}_{.\alpha}F^{P-1B}_{.\beta}\mathbf{G}_{A,B} + F^{P-1A}_{.\alpha,\beta}F^{P\chi}_{.A}\tilde{\mathbf{g}}_\chi \\
&= F^{P-1A}_{.\alpha}F^{P-1B}_{.\beta}\overset{G}{\Gamma}{}^{.C}_{BA}\mathbf{G}_C - F^{P-1A}_{.\alpha}F^{P\chi}_{.A,\beta}\tilde{\mathbf{g}}_\chi \\
&= F^{P-1A}_{.\alpha}F^{P-1B}_{.\beta}F^{P\chi}_{.C}\overset{G}{\Gamma}{}^{.C}_{BA}\tilde{\mathbf{g}}_\chi - F^{P-1A}_{.\alpha}F^{P-1B}_{.\beta}F^{P\chi}_{.A,B}\tilde{\mathbf{g}}_\chi \\
&= \left(F^{P-1B}_{.\beta}F^{P-1A}_{.\alpha}F^{P\chi}_{.C}\overset{G}{\Gamma}{}^{.C}_{BA} - F^{P-1B}_{.\beta}F^{P-1A}_{.\alpha}F^{P\chi}_{.A,B} \right)\tilde{\mathbf{g}}_\chi \\
&= \tilde{\Gamma}^{..\chi}_{\beta\alpha}\tilde{\mathbf{g}}_\chi.
\end{aligned}
\tag{D.44}
$$

Connection coefficients $\tilde{\Gamma}^{..\chi}_{\beta\alpha}$ defined in (D.39) and (D.44) are generally different. However, from (2.203) and (3.31), it follows that their skew covariant components (i.e., torsion tensors) are identical:

$$
\begin{aligned}
\tilde{\Gamma}^{..\chi}_{[\beta\alpha]} &= F^{Lb}_{[\beta}F^{La}_{.\alpha]}F^{L-1\chi}_{.c}\overset{g}{\Gamma}{}^{.c}_{ba} - F^{Lb}_{[\beta}F^{La}_{.\alpha]}F^{L-1\chi}_{.a,b} \\
&= \frac{1}{2}\left[F^{Lb}_{.\beta}F^{La}_{.\alpha}F^{L-1\chi}_{.c}\overset{g}{\Gamma}{}^{.c}_{ba} - F^{Lb}_{.\alpha}F^{La}_{.\beta}F^{L-1\chi}_{.c}\overset{g}{\Gamma}{}^{.c}_{ba} \right] \\
&\quad -\frac{1}{2}\left[F^{Lb}_{.\beta}F^{La}_{.\alpha}F^{L-1\chi}_{.a,b} - F^{Lb}_{.\alpha}F^{La}_{.\beta}F^{L-1\chi}_{.a,b} \right] \\
&= F^{La}_{.\alpha}F^{Lb}_{.\beta}F^{L-1\chi}_{.c}\overset{g}{\Gamma}{}^{.c}_{[ba]} - F^{Lb}_{.\beta}F^{La}_{.\alpha}F^{L-1\chi}_{[a,b]} \\
&= -F^{Lb}_{.\beta}F^{La}_{.\alpha}F^{L-1\chi}_{[a,b]} = -F^{Lb}_{[\beta}F^{La}_{.\alpha]}F^{L-1\chi}_{.a,b} \\
&= -F^{b}_{.B}F^{a}_{.A}F^{P-1B}_{[\beta}F^{P-1A}_{.\alpha]}\left[(F^{P\chi}_{.C}F^{-1C}_{.a})_{,b} \right] \\
&= -F^{b}_{.B}F^{a}_{.A}F^{P-1B}_{[\beta}F^{P-1A}_{.\alpha]}\left[F^{P\chi}_{.C,b}F^{-1C}_{.a} + F^{P\chi}_{.C}F^{-1C}_{.a,b} \right] \\
&= -F^{P-1B}_{[\beta}F^{P-1A}_{.\alpha]}\left[F^{P\chi}_{.A,B} + F^{P\chi}_{.C}F^{-1C}_{.a,b}F^{b}_{.B}F^{a}_{.A} \right] \\
&= -F^{P-1B}_{[\beta}F^{P-1A}_{.\alpha]}F^{P\chi}_{.A,B} - \frac{1}{2}F^{P-1B}_{.\beta}F^{P-1A}_{.\alpha}F^{P\chi}_{.C}F^{-1C}_{.a,b}F^{b}_{.B}F^{a}_{.A} \\
&\quad +\frac{1}{2}F^{P-1A}_{.\alpha}F^{P-1B}_{.\beta}F^{P\chi}_{.C}F^{-1C}_{.b,a}F^{a}_{.A}F^{b}_{.B}
\end{aligned}
$$

(continued...)

$$= -F^{P-1B}{}_{[\beta}F^{P-1A}{}_{.\alpha]}F^{P\chi}{}_{.A,B} - F^{P-1B}{}_{.\beta}F^{P-1A}{}_{.\alpha}F^{P\chi}{}_{.C}F^{-1C}{}_{[a,b]}F^{b}{}_{.B}F^{a}{}_{.A}$$

$$= -F^{P-1B}{}_{[\beta}F^{P-1A}{}_{.\alpha]}F^{P\chi}{}_{.A,B} = -F^{P-1B}{}_{.\beta}F^{P-1A}{}_{.\alpha}F^{P\chi}{}_{[A,B]}$$

$$= -F^{P-1B}{}_{[\beta}F^{P-1A}{}_{.\alpha]}F^{P\chi}{}_{.A,B} + F^{P-1B}{}_{.\beta}F^{P-1A}{}_{.\alpha}F^{P\chi}{}_{.C}\overset{G}{\Gamma}{}^{..C}_{[BA]}$$

$$= -F^{P-1B}{}_{[\beta}F^{P-1A}{}_{.\alpha]}F^{P\chi}{}_{.A,B} + F^{P-1B}{}_{[\beta}F^{P-1A}{}_{.\alpha]}F^{P\chi}{}_{.C}\overset{G}{\Gamma}{}^{..C}_{BA}.$$

(D.45)

Symmetry properties of Levi-Civita connection coefficients in (2.55) and (2.58) have also been used in derivation (D.45). Thus, relation (3.41) is verified in derivation (D.45), where $\tilde{\kappa}^{..\chi}_{\beta\alpha}$ is the anholonomic object:

$$\tilde{\kappa}^{..\chi}_{\beta\alpha} = -\tilde{\Gamma}^{..\chi}_{[\beta\alpha]} = \tilde{\Gamma}^{..\chi}_{[\alpha\beta]}$$

$$= F^{Lb}{}_{.\beta}F^{La}{}_{.\alpha}F^{L-1\chi}{}_{[a,b]} = F^{P-1B}{}_{.\beta}F^{P-1A}{}_{.\alpha}F^{P\chi}{}_{[A,B]}.$$

(D.46)

Appendix E: SI Units and Fundamental Constants

Appendix E includes tables of units and fundamental constants relevant to disciplines of mechanics, physical chemistry, and solid state physics.

E.1 Units

Table E.1 lists base units, following the International System (SI) of units (Thompson and Taylor 2008). Frequently encountered units derived from base units follow in Tables E.2 (named units) and E.3 (unnamed units).

Table E.1 Base SI units of measure

Quantity	Unit	Symbol
Length	meter	m
Mass	kilogram	kg
Time	second	s
Electric current	ampere	A
Temperature	kelvin	K
Amount of substance	mole	mol
Luminous intensity	candela	cd

Table E.2 Some derived SI units of measure (named units)

Quantity	Name	Symbol	Relation	Relation to base units
Frequency	hertz	Hz	-	s^{-1}
Force	newton	N	-	$m\ kg\ s^{-2}$
Stress or pressure	pascal	Pa	N/m^2	$m^{-1}\ kg\ s^{-2}$
Energy	joule	J	N m	$m^2\ kg\ s^{-2}$
Power	watt	W	J/s	$m^2\ kg\ s^{-3}$
Electric charge	coulomb	C	-	s A
Electric potential	volt	V	W/A	$m^2\ kg\ s^{-3}\ A^{-1}$
Capacitance	farad	F	C/V	$m^{-2}\ kg^{-1}\ s^4\ A^2$
Electric resistance	ohm	Ω	V/A	$m^2\ kg\ s^{-3}\ A^{-2}$
Electric conductance	siemens	S	A/V	$m^{-2}\ kg^{-1}\ s^3\ A^2$
Magnetic flux	weber	Wb	V s	$m^2\ kg\ s^{-2}\ A^{-1}$
Magnetic flux density	tesla	T	Wb/m^2	$kg\ s^{-2}\ A^{-1}$
Inductance	henry	H	Wb/A	$m^2\ kg\ s^{-2}\ A^{-2}$

Table E.3 Some derived SI units of measure

Quantity	Relation to derived units	Relation to base units
Velocity	-	$m\ s^{-1}$
Acceleration	-	$m\ s^{-2}$
Mass density	-	$kg\ m^{-3}$
Dynamic viscosity	Pa s	$m^{-1}\ kg\ s^{-1}$
Torque or moment	N m	$m^2\ kg\ s^{-2}$
Surface tension	N/m	$kg\ s^{-2}$
Heat flux	W/m^2	$kg\ s^{-3}$
Heat capacity, entropy	J/K	$m^2\ kg\ s^{-2}\ K^{-1}$
Specific heat capacity	J/(kg K)	$m^2\ s^{-2}\ K^{-1}$
Specific energy	J/kg	$m^2\ s^{-2}$
Thermal conductivity	W/(m K)	$m\ kg\ s^{-3}\ K^{-1}$
Energy density	J/m^3	$m^{-1}\ kg\ s^{-2}$
Electric field	V/m	$m^2\ kg\ s^{-3}\ A^{-1}$
Electric charge density	C/m^3	$m^{-3}\ s\ A$
Surface charge density	C/m^2	$m^{-2}\ s\ A$
Electric displacement	C/m^2	$m^{-2}\ s\ A$
Electric permittivity	F/m	$m^{-3}\ kg^{-1}\ s^4\ A^2$
Magnetic permeability	H/m	$m^2\ kg\ s^{-2}\ A^{-2}$

Several frequently encountered non-SI units are listed in Table E.4. A comprehensive treatment of SI units can be found in the recent United States National Institute of Standards and Technology (NIST) report of Thompson and Taylor (2008).

Table E.4 Some named non-SI units of measure

Quantity	Name	Symbol	Relation to SI units
Length	angstrom	Å	$1\ \text{Å} = 10^{-10}\ m$
Force	dyne	dyn	$1\ dyn = 10^{-5}\ N$
Stress or pressure	bar	bar	$1\ bar = 10^5\ Pa$
Energy	erg	erg	$1\ erg = 10^{-7}\ J$
Electric charge	statcoulomb	esu	$1\ esu = 3.336 \times 10^{-10}\ C$

E.2 Fundamental Constants

Table E.5 lists a number of fundamental constants arising in the physical sciences, referred to the SI system of units.

Table E.5 Fundamental constants

Name	Symbol	Value in SI units
Light velocity in vacuum	c	$c = 2.998 \times 10^8$ m/s
Standard gravity	g	$g = 9.807$ m/s^2
Electronic mass	m_e	$m_e = 9.110 \times 10^{-31}$ kg
Electronic charge	e	$e = 1.602 \times 10^{-19}$ C
Electron volt	eV	1 eV $= 1.602 \times 10^{-19}$ J
Vacuum permittivity	ε_0	$\varepsilon_0 = 10^7/(4\pi c^2)$ F m/s^2 $= 8.854 \times 10^{-12}$ F/m
Vacuum permeability	μ_0	$\mu_0 = 1/(c^2\varepsilon_0) = 4\pi \times 10^{-7}$ H/m
Standard pressure	atm	1 atm $= 1.013 \times 10^5$ N/m^2 $= 1.013$ bar
Calorie	cal	1 cal $= 4.184$ J
Universal gas constant	R	$R = 8.314$ J/(mol K)
Avagadro's number	N_A	$N_A = 6.022 \times 10^{23}$ mol^{-1}
Atomic mass unit (dalton)	u	$u = 1$ g mol$^{-1}/N_A = 1.661 \times 10^{-27}$ kg $= 1823 m_e$
Boltzmann's constant	k_B	$k_B = 1.381 \times 10^{-23}$ J/K $= 8.617 \times 10^{-5}$ eV/K
Planck's constant	h	$h = 2\pi\hbar = 6.626 \times 10^{-34}$ J s
Bohr's radius	a_0	1 a$_0 = 4\pi\varepsilon_0\hbar^2/(m_e e^2) = 0.529 \times 10^{-10}$ m
Rydberg's constant	Ry	1 Ry $= m_e e^4/[8(\varepsilon_0 h)^2] = 2.180 \times 10^{-18}$ J

References

Abeyaratne R, Knowles JK (1993) A continuum model of a thermoelastic solid capable of undergoing phase transitions. J Mech Phys Solids 41: 541-571

Abu Al-Rub RK, Kim S-M (2009) Predicting mesh-independent ballistic limits for heterogeneous targets by a nonlocal damage computational framework. Composites B 40, 495-510

Abu Al-Rub RK, Voyiadjis GZ (2005) A direct finite element implementation of the gradient plasticity theory. Int J Numer Meth Eng 63: 603–629

Abu Al-Rub RK, Voyiadjis GZ (2006) A physically based gradient theory. Int J Plasticity 22: 654-684

Acharya A (2001) A model of crystal plasticity based on the theory of continuously distributed dislocations. J Mech Phys Solids 49: 761-784

Acharya A, Bassani JL (1995) Incompatible lattice deformations and crystal plasticity. In: Ghoniem N (ed) Plastic and Fracture Instabilities in Materials, AMD vol 200. ASME, New York, pp 75-80

Acharya A, Beaudoin AJ (2000) Grain size effects in viscoplastic polycrystals at moderate strains. J Mech Phys Solids 48: 2213-2230

Ahzi S, Schoenfeld SE (1998) Mechanics of porous polycrystals: a fully anisotropic flow potential. Int J Plasticity 14: 829-839

Aifantis EC (1987) The physics of plastic deformation. Int J Plasticity 3: 211-247

Allison FE (1965) Shock-induced polarization in plastics. I. Theory. J Appl Phys 36: 2111-2113

Amari S (1981) Dualistic theory of non-Riemannian material manifolds. Int J Eng Sci 19: 1581-1594

Anand L, Gurtin ME (2003) A theory of amorphous solids undergoing large deformations, with application to polymeric glasses. Int J Solids Structures 40: 1465-1487

Anand L, Kalidindi SR (1994) The process of shear-band formation in plane-strain compression of FCC metals – effects of crystallographic texture. Mech Mater 17: 223-243

Ani W, Maugin GA (1988) Basic equations for shocks in nonlinear electroelastic materials. J Acoust Soc Amer 85: 599-610

Anthony KH (1970) Die theorie der disklinationen. Arch Rat Mech Anal 39: 43-88

Anthony KH, Essmann U, Seeger A, Trauble H (1968) Disclinations and the Cosserat-continuum with incompatible rotations. In: Kroner E (ed) Mechanics of Generalized Continua. Springer-Verlag, New York, pp 354-358

Antoun T, Seaman L, Curran DR, Kanel GI, Razorenov SV, Utkin AV (2003) Spall Fracture. Springer, Berlin

Argon AS, Takeuchi S (1981) Internal stresses in power-law creep. Acta Metall 29: 1877-1884

Arroyo M, Belytschko T (2002) An atomistic-based finite deformation membrane for single layer crystalline films. J Mech Phys Solids 50: 1941-1977

Arsenlis A, Parks DM (1999) Crystallographic aspects of geometrically necessary and statistically stored dislocation density. Acta Mater 47: 1597-1611

Arsenlis A, Parks DM (2002) Modeling the evolution of crystallographic disloca-tion density in crystal plasticity. J Mech Phys Solids 50: 1979-2009

Asaro RJ (1976) Somigliana dislocations and internal stresses: with application to second phase hardening. Int J Eng Sci 13: 271-286

Asaro RJ (1983) Crystal plasticity. ASME J Appl Mech 50: 921-934

Asaro RJ, Needleman A (1985) Texture development and strain hardening in rate dependent polycrystals. Acta Metall 33: 923-953

Ashby MF (1970) The deformation of plastically non-homogeneous materials. Phil Mag 21: 399- 424

Bacon DJ, Barnett DM, Scattergood RO (1979) Anisotropic continuum theory of lattice defects. Prog Mater Sci 23: 51-262

Ball JM, James RD (1987) Fine phase mixtures as minimizers of energy. Arch Rat Mech Anal 100: 13-52

Balasubramanian S, Anand L (2002) Plasticity of initially textured hexagonal polycrystals at high homologous temperatures: application to titanium. Acta Mater 50: 133-148

Bammann DJ (2001) A model of crystal plasticity containing a natural length scale. Mater Sci Eng A 309-310: 406-410

Bammann DJ, Aifantis EC (1982) On a proposal for a continuum with microstruc-ture. Acta Mech 45: 91-121

Bammann DJ, Aifantis EC (1987) A model for finite-deformation plasticity. Acta Mech 69: 97-117

Bammann DJ, Aifantis EC (1989) A damage model for ductile metals. Nucl Eng Des 116: 355-362

Bammann DJ, Johnson GC (1987) On the kinematics of finite-deformation plastic-ity. Acta Mech 70: 1-13

Bammann DJ, Chiesa ML, Horstemeyer MF, Weingarten LI (1993) Failure in ductile materials using finite element methods. In: Jones N, Wierzbicki T (eds) Structural Crashworthiness and Failure. Elsevier, London, pp 1-53

Barton NR, Wenk H-R (2007) Dauphine twinning in polycrystalline quartz. Mod Sim Mater Sci Eng 15: 369-384

Barton NR, Winter NW, Reaugh JE (2009) Defect evolution and pore collapse in crystalline energetic materials. Mod Sim Mater Sci Eng 17: 035003

Bassani JL (2001) Incompatibility theory and a simple gradient theory of plastic-ity. J Mech Phys Solids 49: 1983-1996

Bazant ZP (1991) Why continuum damage mechanics is nonlocal—micromechanics arguments. ASCE J Eng Mech 117: 1070-1087

Becker R (1987) The effect of porosity distribution on ductile failure. J Mech Phys Solids 35: 577-599

Becker R (2004) Effects of crystal plasticity on materials loaded at high pressures and strain rates. Int J Plasticity 20: 1983-2006

Becker R, Needleman A (1986) Effect of yield surface curvature on necking and failure in porous plastic solids. ASME J Appl Mech 53: 491-499

Bejancu A (1990) Finsler Geometry and Applications. Ellis Horwood, New York

Bell JF (1968) The Physics of Large Deformation of Crystalline Solids. Springer-Verlag, New York

Bell RL, Cahn RW (1957) The dynamics of twinning and the interrelation of slip and twinning in zinc crystals. Proc R Soc Lond A 239: 494-521

Beltz GE, Rice JR, Shih CF, Xia L (1996) A self-consistent model for cleavage in the presence of plastic flow. Acta Metall 44: 3943-3954

Benson DJ, Fu H-H, Meyers MA (2001) On the effect of grain size on yield stress: extension into the nanocrystalline domain. Mater Sci Eng A 319-321: 854-861

Berdichevski VL, Sedov LI (1967) Dynamic theory of continuously distributed dislocations. Its relation to plasticity theory. J Appl Math Mech 31: 981-1000

Bernstein N, Tadmor EB (2004) Tight-binding calculations of stacking energies and twinnability in fcc metals. Phys Rev B 69: 094116

Bernstein N, Gostis HJ, Papaconstantopoulos DA, Mehl MJ (2005) Tight-binding calculations of the band structure and total energies of the various polytypes of silicon carbide. Phys Rev B 71: 075203

Berveiller M, Muller D, Kratochvil J (1993) Nonlocal versus local elastoplastic behavior of heterogeneous materials. Int J Plasticity 9: 633-652

Bevis M, Crocker AG (1968) Twinning shears in lattices. Proc R Soc Lond A 304: 123-134

Bhattacharya K (1991) Wedge-like microstructure in martensites. Acta Metall Mater 39: 2431-2444

Bhattacharya K, Ravichandran G (2003) Ferroelectric perovskites for electromechanical actuation. Acta Mater 51: 5941-5960

Bian Q, Bose SK, Shukla RC (2008) Vibrational and thermodynamic properties of metals from a model embedded-atom potential. J Phys Chem Solids 69: 168-181

Bilby BA, Crocker AG (1965) The theory of the crystallography of deformation twinning. Proc R Soc Lond A 288: 240-255

Bilby BA, Smith E (1956) Continuous distributions of dislocations III. Proc R Soc Lond A 232: 481-505

Bilby BA, Bullough R, Smith E (1955) Continuous distributions of dislocations: a new application of the methods of non-Riemannian geometry. Proc R Soc Lond A 231: 263-273

Bilby BA, Gardner LRT, Stroh AN (1957) Continuous distributions of dislocations and the theory of plasticity. In: Proc 9th Int Congr Appl Mech, vol 8. Univ de Bruxelles, Brussels, pp 35-44

Birch F (1947) Finite elastic strain of cubic crystals. Phys Rev 71: 809-824

Birch F(1978) Finite strain isotherm and velocities for single crystal and polycrystalline NaCl at high pressures and 300K. J Geophys Res 83: 1257-1268

Bishop JFW, Hill R (1951) A theory of the plastic distortion of a polycrystalline aggregate under combined stresses. Phil Mag 42: 414-427

Bitter F (1931) On impurities in metals. Phys Rev 37: 1527-1547

Bollmann W (1991) The stress field of a model triple line disclination. Mater Sci Eng A 136: 1-7

Bommel HE, Mason WP, Warner AW (1955) Experimental evidence for dislocations in crystalline quartz. Phys Rev 99: 1894-1896

Bommel HE, Mason WP, Warner AW (1956) Dislocations, relaxations, and anelasticity of crystal quartz. Phys Rev 102: 64-71

Bond WL et al (1949) Standards on piezoelectric crystals. Proc IRE 37: 1378-1395

Boothby WM (1975) An Introduction to Differentiable Manifolds and Riemannian Geometry. Elsevier Science, Academic Press, San Diego

Born M (1960) The Mechanics of the Atom. Frederick Ungar, New York

Born M, Huang K (1954) Dynamical Theory of Crystal Lattices. Oxford University Press, London

Bourne NK, Millett JCF, Chen M, McCauley JW, Dandekar DP (2007) On the Hugoniot elastic limit in polycrystalline alumina. J Appl Phys 102: 073514

Bowen RM (1967) Toward a thermodynamics and mechanics of mixtures. Arch Rat Mech Anal 24: 370-403

Brace WF, Paulding BW, Scholz C (1966) Dilatancy in the fracture of crystalline rocks. J Geophys Res 71: 3939-3953

Brandon DG (1966) Structure of high-angle grain boundaries. Acta Metall 14: 1479-1484

Brenner DW (1990) Empirical potential for hydrocarbons for use in simulating the chemical vapor deposition of diamond films. Phys Rev B 42: 9458-9471

Brice JC (1985) Crystals for quartz resonators. Rev Mod Phys 57: 105-147

Brillouin L (1964) Tensors in Mechanics and Elasticity. Academic Press, New York

Bristow JR (1960) Microcracks and the static and dynamic elastic constants of annealed and heavily cold-worked metals. British J Appl Phys 11: 81-85

Brugger K (1964) Thermodynamic definition of higher order elastic constants. Phys Rev 133: A1611-A1612

Brugger K (1965) Pure modes for elastic waves in crystals. J Appl Phys 36: 759-768

Budianski B, O'Connell RJ (1976) Elastic moduli of a cracked solid. Int J Solids Structures 12: 81-97

Budianski B, Hutchinson JW, Slutsky S (1982) Void growth and collapse in viscous solids. In: Hopkins HG, Sewell MJ (eds) Mechanics of Solids. Pergamon, Oxford, pp 13-45

Bueger MJ (1956) Elementary Crystallography: An Introduction to the Fundamental Geometrical Features of Crystals. John Wiley and Sons, New York

Bullough R, Bilby BA (1956) Continuous distributions of dislocations: surface dislocations and the crystallography of martensitic transformations. Proc Phys Soc Lond B 69: 1276-1286

Bunge H-J (1982) Texture Analysis in Materials Science: Mathematical Methods. Butterworths, London

Burgers JM (1939) Some considerations on the fields of stress connected with dislocations in a regular crystal lattice I. Proc Kon Nederl Akad Wetensch 42: 293-324

Buryachenko VA (2007) Micromechanics of Heterogeneous Materials. Springer, New York

Bustamante R, Dorfmann A, Ogden RW (2009) On electric body forces and Maxwell stresses in nonlinearly electroelastic solids. Int J Eng Sci 47: 1131-1141

Butler GC, McDowell DL (1998) Polycrystal constraint and grain subdivision. Int J Plasticity 14: 703-717

Capolungo L, Jochum C, Cherkaoui M, Qu J (2005) Homogenization method for strength and inelastic behavior of nanocrystalline materials. Int J Plasticity 21: 67-82

Carstensen C, Hackl K, Mielke A (2002) Non-convex potentials and microstructures in finite-strain plasticity. Proc R Soc Lond A 458: 299-317

Cartan E (1922) Sur une généralisation de la notion de courbure de Riemann et les espaces à torsion. CR 174: 593-575

Castaing J, Munoz A, Dominguez-Rodriguez A (2002) Hardening of rhombohedral twinning in sapphire (α-Al_2O_3) by basal slip dislocations. Phil Mag A 82: 1419-1431

Cermelli P, Fried E (1997) The influence of inertia on the configurational forces in a deformable solid. Proc R Soc Lond A 453 : 1915-1927

Cermelli P, Fried E (2002) The evolution equation for a disclination in a nematic liquid crystal. Proc R Soc Lond A 458: 1-20

Cermelli P, Gurtin ME (1994) On the kinematics of incoherent phase transformations. Acta Metall Mater 42: 3349-3359

Cermelli P, Gurtin ME (2001) On the characterization of geometrically necessary dislocations in finite plasticity. J Mech Phys Solids 49: 1539-1568

Cermelli P, Gurtin, ME (2002) Geometrically necessary dislocations in viscoplastic single crystals and bicrystals undergoing small deformations. Int J Solids Structures 39: 6281-6309

Chaikin PM, Lubensky TC (1995) Principles of Condensed Matter Physics. Cambridge University Press, Cambridge, UK

Chang R (1960) Creep of Al_2O_3 single crystals. J Appl Phys 31: 484-487

Chantasiriwan S, Milstein F (1996) Higher-order elasticity of cubic metals in the embedded-atom method. Phys Rev B 53: 14080-14088

Chen PJ, McCarthy MF, O'Leary TR (1976) One-dimensional shock and acceleration waves in deformable dielectric materials with memory. Arch Rat Mech Anal 62: 189-207

Chen Y, Lee J (2005) Atomistic formulation of a multiscale field theory for nano/micro solids. Phil Mag 85: 4095-4126

Cheung KS, Yip Y (1991) Atomic-level stress in an inhomogeneous system. J Appl Phys 70: 5688-5690

Chin GY, Hosford WF, Mendorf DR (1969) Accommodation of constrained deformation in FCC metals by slip and twinning. Proc R Soc Lond A 309: 433-456

Chowdhury KL, Glockner PG (1976) Constitutive equations for elastic dielectrics. Int J Non-Linear Mech 11: 315-324

Chowdhury KL, Epstein M, Glockner PG (1979) On the thermodynamics of nonlinear elastic dielectrics. Int J Non-Linear Mech 13, 311-322

Christian JW, Mahajan S (1995) Deformation twinning. Prog Mater Sci 39: 1-157

Chua JO, Ruoff AL (1975) Pressure dependence of the yield stress of potassium at low homologous temperature. J Appl Phys 46: 4659-4663

Chung PW (2004) Computational method for atomistic homogenization of nanopatterned point defect structures. Int J Numer Meth Eng 60: 833-859

Chung PW, Clayton JD (2007) Multiscale modeling of point and line defects in cubic lattices. Int J Multiscale Comp Eng 5: 203-226

Chung PW, Namburu RR (2003) On a formulation for a multiscale atomistic-continuum homogenization method. Int J Solids Structures 40: 2563-2588

Ciarlet PG (1998) Introduction to Linear Shell Theory. Elsevier, Paris

Clarebrough LM, Hargreaves ME, West GW (1957) The density of dislocations in compressed copper. Acta Metall. 5: 738-740

Clayton JD (2005a) Dynamic plasticity and fracture in high density polycrystals: constitutive modeling and numerical simulation. J Mech Phys Solids 53: 261-301

Clayton JD (2005b) Modeling dynamic plasticity and spall fracture in high density polycrystalline alloys. Int J Solids Structures 42: 4613-4640

Clayton JD (2006a) Plasticity and spall in high density polycrystals: modeling and simulation. In: Furnish MD, Elert M, Russell TP, White CT (eds) Shock Compression of Condensed Matter, AIP Press, Melville, New York, pp 311-314

Clayton JD (2006b) Continuum multiscale modeling of finite deformation plasticity and anisotropic damage in polycrystals. Theo Appl Fract Mech 45: 163-185

Clayton JD (2008) A model for deformation and fragmentation in crushable brittle solids. Int J Impact Eng 35: 269-289

Clayton JD (2009a) A continuum description of nonlinear elasticity, slip and twinning, with application to sapphire. Proc R Soc Lond A 465: 307-334

Clayton JD (2009b) A non-linear model for elastic dielectric crystals with mobile vacancies. Int J Non-Linear Mech 44: 675-688

Clayton JD (2009c) Modeling effects of crystalline microstructure, energy storage mechanisms, and residual volume changes on penetration resistance of precipitate-hardened aluminum alloys. Composites B 40: 443-450

Clayton JD (2010a) Deformation, fracture, and fragmentation in brittle geologic solids. Int J Fracture 163: 151-172

Clayton JD (2010b) Modeling nonlinear electromechanical behavior of shocked silicon carbide. J Appl Phys 107: 013520

Clayton JD (2010c) Modeling finite deformations in trigonal ceramic crystals with lattice defects. Int J Plasticity 26: 1357-1386

Clayton JD (2010d) A nonlinear thermomechanical model of spinel ceramics applied to aluminum oxynitride (AlON). ASME J Appl Mech: accepted for publication

Clayton JD, Bammann DJ (2009) Finite deformations and internal forces in elastic-plastic crystals: interpretations from nonlinear elasticity and anharmonic lattice statics. ASME J Eng Mater Tech 131: 041201

Clayton JD, Chung PW (2006) An atomistic-to-continuum framework for nonlinear crystal mechanics based on asymptotic homogenization. J Mech Phys Solids 54: 1604-1639

Clayton JD, McDowell DL (2003a) A multiscale multiplicative decomposition for elastoplasticity of polycrystals. Int J Plasticity 19: 1401-1444

Clayton JD, McDowell DL (2003b) Finite polycrystalline elastoplasticity and damage: multiscale kinematics. Int J Solids Structures 40: 5669-5688

Clayton JD, McDowell DL (2004) Homogenized finite elastoplasticity and damage: theory and computations. Mech Mater 36: 799-824

Clayton JD, Schroeter BM, Graham S, McDowell DL (2002) Distributions of stretch and rotation in polycrystalline OFHC Cu. ASME J Eng Mater Tech 124: 302-313

Clayton JD, Bammann DJ, McDowell DL (2004a) Anholonomic configuration spaces and metric tensors in finite strain elastoplasticity. Int J Non-Linear Mech 39: 1039-1049

Clayton JD, McDowell DL, Bammann DJ (2004b) A multiscale gradient theory for single crystalline elastoviscoplasticity. Int J Eng Sci 42: 427-457

Clayton JD, Bammann DJ, McDowell DL (2005) A geometric framework for the kinematics of crystals with defects. Phil Mag 85: 3983-4010

Clayton JD, McDowell DL, Bammann DJ (2006) Modeling dislocations and disclinations with finite micropolar elastoplasticity. Int J Plasticity 22: 210-256

Clayton JD, Chung PW, Grinfeld MA, Nothwang WD (2008a) Kinematics, electromechanics, and kinetics of dielectric and piezoelectric crystals with lattice defects. Int J Eng Sci 46:10-30

Clayton JD, Chung PW, Grinfeld MA, Nothwang WD (2008b) Continuum modeling of charged vacancy migration in elastic dielectric solids, with application to perovskite thin films. Mech Res Comm 35: 57-64

Clifton RJ (1972) On the equivalence of $F^e F^p$ and $F^p F^e$. ASME J Appl Mech 39: 287-289

Cocks ACF, Ashby MF (1980) Intergranular fracture during power-law creep under multiaxial stresses. Metal Sci 14: 395-402

Cocks ACF, Ashby MF (1982) Creep fracture by void growth. Prog Mater Sci 27: 189-244

Cole MW, Nothwang WD, Hubbard C, Ngo E, Ervin M (2003) Low dielectric loss and enhanced tunability of $Ba_{0.6}Sr_{0.4}TiO_3$ based thin films via material compositional design and optimized film processing methods. J Appl Phys 93: 9218-9225

Coleman BD (1964) Thermodynamics of material with memory. Arch Rat Mech Anal 17 : 1-46

Coleman BD, Gurtin ME (1967) Thermodynamics with internal state variables. J Chem Phys 17: 597-613

Coleman BD, Mizel VJ (1964) Existence of caloric equations of state in thermodynamics. J Chem Phys 40: 1116-1125

Coleman BD, Noll W (1963) The thermodynamics of elastic materials with heat conduction and viscosity. Arch Rat Mech Anal 13: 167-178

Conrad H (2001) Space charge and the dependence of the flow stress of ceramics on an applied electric field. Scripta Mater 44: 311-316

Conti S, Ortiz M (2005) Dislocation microstructures and the effective behavior of single crystals. Arch Rat Mech Anal 176: 103-147

Cooper RE (1962) Kinetics of elastic twinning in calcite. Proc R Soc Lond A 270: 525-537

Cosserat E, Cosserat F (1909) Théorie des corps déformables. Hermann, Paris

Cottrell AH (1953) Dislocations and Plastic Flow in Crystals. Oxford University Press, Oxford

Cottrell AH, Bilby BA (1951) A mechanism for the growth of deformation twins in crystals. Phil Mag 42: 573-581

Cousins CSG (1978) Inner elasticity. J Phys C 11: 4867-4879

Cowin SC, Mehrabadi MM (1987) On the identification of material symmetry for anisotropic elastic materials. Quart J Appl Math 40: 451-476

Cowin SC, Nunziato JW (1983) Linear elastic materials with voids. J Elasticity 13: 125-147

Curtin WA, Miller RE (2003) Atomistic/continuum coupling in computational materials science. Mod Sim Mater Sci Eng 11: R33-R68

Dafalias, YF (1998) Plastic spin: necessity or redundancy? Int J Plasticity 14: 909-931

Damjanovic D (1998) Ferroelectric, dielectric and piezoelectric properties of ferroelectric thin films and ceramics. Rep Prog Phys 61: 1267-1324

Dandekar DP (1970) Iterative procedure to estimate the values of elastic constants of a cubic solid at high pressures from the sound wave velocity measurements. J Appl Phys 41: 667-672

Das ESP, Marcinkowski MJ, Armstrong RW, De Wit R (1973) The movement of Volterra disclinations and the associated mechanical forces. Phil Mag 27: 369-391

Davison L (1995) Kinematics of finite elastoplastic deformation. Mech Mater 21: 73-88

Daw MS, Baskes MI (1984) Embedded atom method: derivation and application to impurities, surfaces, and other defects in metals. Phys Rev B 29: 6443-6453

Debye P (1912) Zur theorie der spezifischen warme. Ann Phys 39: 789-839

De Groot SR, Mazur P (1962) Non-Equilibrium Thermodynamics. North-Holland, Amsterdam

Deng S, Liu J, Liang N (2007) Wedge and twist disclinations in second strain gradient elasticity. Int J Solids Structures 44: 3646-3665

Devonshire AF (1954) Theory of ferroelectrics. Phil Mag 3: 85-130

De Wit R (1968) Differential geometry of a nonlinear continuum theory of dislocations. In: Kroner E (ed) Mechanics of Generalized Continua. Springer-Verlag, New York, pp 251-261

De Wit R (1971) Relation between dislocations and disclinations. J Appl Phys 42: 3304-3308

De Wit R (1973) Theory of disclinations II, III, IV. J Res Nat Bureau Standards A Phys Chem 77: 49-100, 359-368, 607-658

De Wit R (1981) A view of the relation between the continuum theory of lattice defects and non-Euclidean geometry in the linear approximation. Int J Eng Sci 19: 1475-1506

Dienes GJ (1952) A theoretical estimate of the effect of radiation on the elastic constants of simple metals. Phys Rev 86: 228-234

Dillon OW, Kratochvil J (1970) A strain gradient theory of plasticity. Int J Solids Structures 6: 1513-1533

Dillon OW, Perzyna P (1972) A gradient theory of materials with memory and internal changes. Arch Mech 24: 727-747

Dluzewksi P (1996) On geometry and continuum thermodynamics of movement of structural defects. Mech Mater 22: 23-41

Dorfmann A, Ogden RW (2005) Nonlinear electroelasticity. Acta Mech 174: 167-183

Doyle TC, Ericksen JL (1956) Nonlinear elasticity. In: Dryden HL, Von Karman T (eds) Adv Applied Mech IV. Academic Press, New York, pp 53-115

Drucker DC (1951) A more fundamental approach to plastic stress-strain relations. In: Proc 1st US Nat Congr Appl Mech. ASME, New York, pp 487-491

Dugdale JS, MacDonald DKC (1953) The thermal expansion of solids. Phys Rev 89: 832-834

Duszek M, Perzyna P (1991) The localization of plastic deformation in thermoplastic solids. Int J Solids Structures 27: 1419-1433

Eckart C (1940) The thermodynamics of irreversible processes I. The simple fluid. Phys Rev 58: 267-269

Eckart C (1948) The thermodynamics of irreversible processes IV. The theory of elasticity and anelasticity. Phys Rev 73: 373-382

Einstein A (1907) Plankshe theorie der strahlung und die theorie der spezifischen warme. Ann Phys 22: 180-190

Einstein A (1928) Riemann geometrie mit aufrechterhaltung des begriffes des fernparallelismus. SB Preuss Akad Wiss: 217-221, 224

Einstein A (1945) A generalization of the relativistic theory of gravitation. Ann Math 46: 578-584

Eisenhart LP (1926) Riemannian Geometry. Princeton University Press, Princeton

El-Dasher BS, Adams BL, Rollett AD (2003) Experimental recovery of geometrically necessary dislocation density in polycrystals. Scr Mater 48: 141-145

Epstein M, Elzanowski M (2007) Material Inhomogeneities and their Evolution: A Geometric Approach. Springer, Berlin

Epstein M, Maugin GA (1990) The energy-momentum tensor and material uniformity in finite elasticity. Acta Mech 83: 127-133

Ericksen JL (1960) Tensor fields. In: Flugge S (ed) Handbuch der Physik, vol III/1. Springer-Verlag, Berlin, pp 794-858

Ericksen JL (1970) Nonlinear elasticity of diatomic crystals. Int J Solids Structures 6: 951-957

Ericksen JL (1975) Equilibrium of bars. J Elasticity 5: 191-201

Ericksen JL (1984) The Cauchy and Born hypothesis for crystals. In: Gurtin ME (ed) Phase Transformations and Material Instabilities in Solids. Academic Press, New York, pp 61-78

Ericksen JL (1991) Introduction to the Thermodynamics of Solids. Chapman and Hall, London

Ericksen JL (2008) On the Cauchy-Born rule. Math Mech Solids 13: 199-220

Ericksen JL, Truesdell C (1958) Exact theory of stress and strain in rods and shells. Arch Rat Mech Anal 1: 296-323

Eringen AC (1962) Nonlinear Theory of Continuous Media. McGraw-Hill, New York

Eringen AC (1963) On the foundations of electroelastostatics. Int J Eng Sci 1: 127-153

Eringen AC (1968) Mechanics of micromorphic continua. In: Kroner E (ed) Mechanics of Generalized Continua. Springer-Verlag, New York, pp 18-35

Eringen AC (1972) Nonlocal polar elastic continua. Int J Eng Sci 10: 1-16

Eringen AC (1984) On continuous distributions of dislocations in nonlocal elasticity. J Appl Phys 56: 2675-2680

Eringen AC, Claus WD (1970) A micromorphic approach to dislocation theory and its relation to several existing theories. In: Simmons JA, De Wit R, Bullough R (eds) Fundamental Aspects of Dislocation Theory. US Govt Printing Office, Gaithersburg, MD, pp 1023-1040

Eringen AC, Suhubi ES (1964) Nonlinear theory of simple micro-elastic solids—I. Int J Eng Sci 2: 189-203

Eshelby JD (1949a) Uniformly moving dislocations. Proc Phys Soc Lond A 62: 307-314

Eshelby JD (1949b) Edge dislocations in anisotropic materials. Phil Mag 40: 903-912

Eshelby JD (1951) The force on an elastic singularity. Phil Trans R Soc Lond 244: 87-112

Eshelby JD (1954) Distortion of a crystal caused by point imperfections. J Appl Phys 25: 255-261

Eshelby JD (1956) The continuum theory of lattice defects. In: Seitz F, Turnbull D (eds) Solid State Physics 3. Academic Press, New York, pp 79-144

Eshelby JD (1961) Elastic inclusions and inhomogeneities. In Sneddon IN, Hill R (eds) Progress in Solid Mechanics 2. North-Holland, Amsterdam, pp 89-140

Eshelby JD (1973) Dislocation theory for geophysical applications. Phil Trans R Soc Lond A 274: 331-338

Eshelby JD (1975) The elastic energy-momentum tensor. J Elasticity 5: 321-335

Eshelby JD, Read WT, Shockley W (1953) Anisotropic elasticity with applications to dislocation theory. Acta Metall 1: 251-259

Espinosa HD (1995) On the dynamic shear resistance of ceramic composites and its dependence on applied multiaxial deformation. Int J Solids Structures 32: 3105-3128

Espinosa HD, Zavattieri PD, Dwivedi SK (1998) A finite deformation continuum discrete model for the description of fragmentation and damage in brittle materials. J Mech Phys Solids 46: 1909-1942

Farber YA, Yoon SY, Lagerlof KPD, Heuer AH (1993) Microplasticity during high temperature indentation and the Peierls potential of sapphire (α-Al$_2$O$_3$) single crystals. Phys Stat Solidi A 137: 485-498

Farren WS, Taylor GI (1925) The heat developed during plastic extension of metals. Proc R Soc Lond A 107: 422-451

Finnis MW, Sinclair JE (1984) A simple empirical N-body potential for transition metals. Phil Mag A 50: 45-55

Fleck NA, Hutchinson JW (1993) A phenomenological theory for strain gradient effects in plasticity. J Mech Phys Solids 41: 1825-1857

Fleck NA, Muller GM, Ashby MF, Hutchinson JW (1994) Strain gradient plasticity – theory and experiment. Acta Metall Mater 42: 475-487

Follansbee PS, Kocks UF (1988) A constitutive description of the deformation of copper based on the use of the mechanical threshold stress as an internal state variable. Acta Metall 36: 81-93

Foltz JV, Grace FI (1969) Theoretical Hugoniot stress-temperature-strain states for aluminum and copper. J Appl Phys 40: 4195-4199

Foreman AJE (1955) Dislocation energies in anisotropic crystals. Acta Metall 3: 322-330

Foreman AJE, Jawson MA, Wood JK (1951) Factors controlling dislocation widths. Proc Phys Soc Lond A 64: 156-163

Forest S, Barbe F, Cailletaud G (2000) Cosserat modelling of size effects in the mechanical behaviour of polycrystals and multi-phase materials. Int J Solids Structures 37: 7105-7126

Fosdick RL (1966) Remarks on compatibility. In: Eskinazi S (ed) Modern Developments in the Mechanics of Continua. Academic Press, New York, pp 109-127

Fox N (1966) A continuum theory of dislocations for polar elastic materials. Quart J Mech Appl Math 19: 343-355

Fox N (1968) On the continuum theory of dislocations and plasticity. Quart J Mech Appl Math 21: 67-75

Frank FC (1958) On the theory of liquid crystals. Disc Faraday Soc 25: 19-28

Frenkel J (1926) Zur theorie der elastizitatsgrenze und der festigkeit kristallinischer korper. Z Phys 37: 572-609

Friedel J (1964) Dislocations. Pergamon, Oxford

Fuchs K (1936) A quantum mechanical calculation of the elastic constants of monovalent metals. Proc R Soc Lond A 153: 622-639

Gallego R, Ortiz M (1993) A harmonic/anharmonic energy partition method for lattice statics computations. Mod Sim Mater Sci Eng 1: 417-436

Gao H, Huang Y, Nix WD, Hutchinson JW (1999) Mechanism-based strain gradient plasticity—I. Theory. J Mech Phys Solids 47: 1239-1263

Garikipati K (2003) Couple stresses in crystalline solids: origins from plastic slip gradients, dislocation core distortions, and three-body interatomic potentials. J Mech Phys Solids 51: 1189-1214

Garikipati K, Falk M, Bouville M, Puchala B, Narayanan H (2006) The continuum elastic and atomistic viewpoints on the formation volume and strain energy of a point defect. J Mech Phys Solids 54: 1929-1951

Gerken JM, Dawson PR (2008) A crystal plasticity model that incorporates stresses and strains due to slip gradients. J Mech Phys Solids 56: 1651-1672

Germain P, Lee EH (1973) On shock waves in elastic-plastic solids. J Mech Phys Solids 21: 359-382

Germain P, Nguyen QS, Suquet P (1983) Continuum thermodynamics. ASME J Appl Mech 50: 1010-1020

Gertsman VY, Nazarov AA, Romanov AE, Valiev RZ, Vladimirov VI (1989) Disclination-structural unit model of grain boundaries. Phil Mag A 59: 1113-1118

Ghosh S, Bai J, Raghavan P (2007) Concurrent multi-level model for damage evolution in microstructurally debonding composites. Mech Mater 39: 241-266

Gibeling JC, Nix WD (1980) A numerical study of long range internal stresses associated with subgrain boundaries. Acta Metall 28: 1743-1752

Gilman JJ (1960) Direct measurements of the surface energies of crystals. J Appl Phys 31: 2208-2218

Gilman JJ (1979) Resistance to shock-front propagation in solids. J Appl Phys 50: 4059-4064

Gilman JJ (2003) Electronic Basis of the Strength of Materials. Cambridge University Press, Cambridge

Goodman RE (1989) Introduction to Rock Mechanics. 2nd ed, John Wiley and Sons, New York

Gottstein G, Steffen H, Wollenberger H (1973) Discrepancy between specific heat and stored energy data for plastically deformed copper. Scripta Metall 7: 451-456

Graham RA (1972) Strain dependence of longitudinal piezoelectric, elastic, and dielectric constants of x-cut quartz. Phys Rev B 6: 4779-4792

Graham RA (1992) Solids Under High-Pressure Shock Compression. Springer-Verlag, New York

Graham RA, Brooks WP (1971) Shock-wave compression of sapphire from 15 to 420 kbar. The effects of large anisotropic compressions. J Phys Chem Solids 32: 2311-2330

Graham RA, Neilson FW, Benedick WB (1965) Piezoelectric current from shock-loaded quartz—a submicrosecond stress gauge. J Appl Phys 36: 1775-1783

Green AE, Naghdi PM (1995) A unified procedure for construction of theories of deformable media. II. Generalized continua. Proc R Soc Lond A 448: 357-377

Green AE, Rivlin RS (1964a) On Cauchy's equations of motion. J Appl Math Phys ZAMP 15: 290-292

Green AE, Rivlin RS (1964b) Simple forces and stress multipoles. Arch Rat Mech Anal 16: 325-353

Griffith AA (1921) The phenomena of rupture and flow in solids. Phil Trans R Soc Lond A 221: 163-198

Grinfeld M (1981) On heterogeneous equilibrium of nonlinear elastic phases and chemical potential tensors. Lett Appl Eng Sci 19: 1031-1039

Grinfeld M (1991) Thermodynamic Methods in the Theory of Heterogeneous Systems. Longman, Sussex

Grinfeld M, Wright TW (2004) Morphology of fractured domains in brittle fracture. Metall Mater Trans A 35: 2651-2661

Groth P (1905) Physikalische Kristallographie und Einleitung in die Kristallographische Kenntnis der wichtigsten Substanzen. 4th ed, Engelmann, Leipzig

Grunesien E (1926) Zustand des festen korpers. In: Geiger H, Scheel K (eds) Handbuch der Physik 10. Springer, Berlin, pp 1-59

Gumbsch P, Gao H (1999) Dislocations faster than the speed of sound. Science 283: 965-968

Gunther W (1958) Zur static und dynamik des Cosseratschen kontinuums. Abh Braunschw Wiss Ges 10: 195-213

Gunther H (1983) On the physical origin for the geometric theory of continuum mechanics. Ann der Physik 7: 220-226

Gupta A, Steigmann DJ, Stolken JS (2007) On the evolution of plasticity and incompatibility. Math Mech Solids 12: 583-610

Gurson AL (1977) Continuum theory of ductile rupture by void nucleation and growth: part 1—yield criteria and flow rules for porous ductile media. ASME J Eng Mater Tech 99: 2-15

Gurtin ME (1965) Thermodynamics and the possibility of spatial interaction in elastic materials. Arch Rat Mech Anal 19: 339-352

Gurtin ME (1981) An Introduction to Continuum Mechanics. Academic Press, New York

Gurtin ME (1995) The nature of configurational forces. Arch Rat Mech Anal 131: 67-100

Gurtin ME (2000) On the plasticity of single crystals: free energy, microforces, plastic strain gradients. J Mech Phys Solids 48: 989-1036

Gurtin ME (2002) A gradient theory of single-crystal viscoplasticity that accounts for geometrically necessary dislocations. J Mech Phys Solids 50: 5-32

Hadjigeorgiou EP, Kalpakides VK, Massalas CV (1999) A general theory for elastic dielectrics – part I. The vectorial approach. Int J Non-Linear Mech 34, 831-841

Hall EO (1951) The deformation and aging of mild steel. Part III: discussion of results. Proc Phys Soc Lond 64: 747-753

Hall FR, Hayhurst DR (1991) Modeling of grain size effects in creep crack growth using a nonlocal continuum damage approach. Proc R Soc Lond A 433: 405-421

Hanson RC, Helliwell K, Schwab C (1974) Anharmonicity in CuCl—elastic, dielectric, and piezoelectric constants. Phys Rev B 9: 2649-2654

Hartley CS (1975) Linear force and dislocation multipoles in anisotropic elasticity. J Appl Phys 41: 3197-3201

Hartley CS (2003) A method for linking thermally activated dislocation mechanisms of yielding with continuum plasticity theory. Phil Mag 83: 3783-3808

Hartley CS, Blachon DLA (1978) Reactions of slip dislocations at coherent twin boundaries in face-centered-cubic metals. J Appl Phys 49: 4788-4796

Haskins JF, Hickman JS (1950) A derivation and tabulation of the piezoelectric equations of state. J Acoust Soc Amer 22: 584-588

Hauver GE (1965) Shock-induced polarization in plastics. II. Experimental study of plexiglas and polystyrene. J Appl Phys 36: 2113-2118

Havner KS (1973) On the mechanics of crystalline solids. J Mech Phys Solids 21: 383-394

Havner KS (1986) Fundamental considerations in micromechanical modeling of polycrystalline metals at finite strain. In: Gittus J, Zarka J, Nemat-Nasser S (eds) Large Deformations of Solids: Physical Basis and Mathematical Modeling. Elsevier, Amsterdam, pp 243-265

Havner KS (1992) Finite Plastic Deformation of Crystalline Solids. Cambridge University Press, Cambridge

Head AK (1964) The [111] dislocation in a cubic crystal. Phys Stat Solidi 6: 461-465

Hearmon RFS (1946) The elastic constants of anisotropic materials. Rev Mod Phys 18: 409-440

Hearmon RFS (1953) Third-order elastic coefficients. Acta Cryst 6: 331-340

Hearmon RFS (1956) The elastic constants of anisotropic materials—II. Adv Phys 5: 323-382

Herrmann W (1969) Constitutive equation for the dynamic compaction of ductile porous materials. J Appl Phys 40: 2490-2499

Hiki Y (1981) Higher order elastic constants of solids. Ann Rev Mater Sci 11: 51-73

Hill R (1950) The Mathematical Theory of Plasticity. Oxford, New York

Hill R (1952) The elastic behavior of a crystalline aggregate. Proc Phys Soc Lond A 65: 349-354

Hill R (1963) Elastic properties of reinforced solids: some theoretical principles. J Mech Phys Solids 11: 357-372

Hill R (1972) On constitutive macro-variables for heterogeneous solids at finite strain. Proc R Soc Lond A 326: 131-147

Hill R (1984) On macroscopic effects of heterogeneity in elastoplastic media at finite strain. Math Proc Camb Phil Soc 95: 481-494

Hill R (1986) Energy-momentum tensors in elastostatics: some reflections on the general theory. J Mech Phys Solids 34: 305-317

Hill R, Rice JR (1972) Constitutive analysis of elastic-plastic crystals at arbitrary strain. J Mech Phys Solids 20: 401-413

Hill R, Rice JR (1973) Elastic potentials and the structure of inelastic constitutive laws. SIAM J Appl Math 25: 448-461

Hirth JP, Lothe J (1982) Theory of Dislocations. John Wiley and Sons, New York

Hoffman JD (1992) Numerical Methods for Engineers and Scientists. McGraw-Hill, New York

Hoger A (1985) On the residual stress possible in an elastic body with material symmetry. Arch Rat Mech Anal 88: 271-290

Hoger A (1986) On the determination of residual stress in an elastic body. J Elasticity 16: 303-324

Holder J, Granato AV (1969) Thermodynamic properties of solids containing defects. Phys Rev 182: 729-741

Holt DL (1970) Dislocation cell formation in metals. J Appl Phys 41: 3197-3201

Horstemeyer MF, Baskes MI (1999) Atomic finite deformation simulations: a discussion on length scale effects in relation to mechanical stress. ASME J Eng Mater Tech 121: 114-119

Horstemeyer MF, McDowell DL (1998) Modeling effects of dislocation substructure in polycrystal elastoviscoplasticity. Mech Mater 27: 145-163

Horstemeyer MF, McDowell DL, McGinty RD (1999) Design of experiments for constitutive model selection: application to polycrystal elastoviscoplasticity. Mod Sim Mater Sci Eng 7: 253-273

Horstemeyer MF, Lathrop J, Gokhale AM, Dighe M (2000) Modeling stress state dependent damage evolution in a cast Al-Si-Mg aluminum alloy. Theo Appl Fract Mech 33: 31-47

Hou B, Hou B (1997) Differential Geometry for Physicists. World Scientific, Singapore

Hou TY, Rosakis P, LeFloch P (1999) A level-set approach to the computation of twinning and phase-transition dynamics. J Comp Phys 150: 302-331

Huang K (1950) On the atomic theory of elasticity. Proc R Soc Lond A 203: 178-194

Huang W, Mura T (1970) Elastic fields and energies of a circular edge disclination and a straight screw disclination. J Appl Phys 41: 5175-5179

Hughes DA, Liu Q, Chrzan DC, Hansen N (1997) Scaling of microstructural parameters: misorientations of deformation induced boundaries. Acta Mater 45: 105-112

Hughes DA, Chrzan DC, Liu Q, Hansen N (1998) Scaling of misorientation angle distributions. Phys Rev Lett 81: 4664-4667

Hughes DA, Hansen N, Bammann DJ (2003) Geometrically necessary boundaries, incidental dislocation boundaries, and geometrically necessary dislocations. Scr Mater 48: 147-153

Hull D, Bacon DJ (1984) Introduction to Dislocations. 3rd ed, Butterworth-Heinemann, Oxford

Humphreys FJ (2001) Grain and subgrain characterisation by electron backscatter diffraction. J Mater Sci 36: 3833-3854

Huntington HB (1955) Modification of the Peierls-Nabarro model for edge dislocation core. Proc Phys Soc Lond B 68: 1043-1048

Huo B, Zheng Q-S, Huang Y (1999) A note on the effect of surface energy and void size to void growth. Eur J Mech A Solids 18: 987-994

Hutchinson JW (1976) Bounds and self-consistent estimates for creep of polycrystalline materials. Proc R Soc Lond A 348: 101-127

Hutchinson JW (2000) Plasticity at the micron scale. Int J Solids Structures 37: 225-238

Hwang KC, Jiang H, Huang Y, Gao H, Hu N (2002) A finite deformation theory of strain gradient plasticity. J Mech Phys Solids 50: 81-99

Ilyushin AA (1961) On a postulate of plasticity. Prikl Mat Meh 25: 503-507

Imam A, Johnson GC (1998) Decomposition of the deformation gradient in thermoelasticity. ASME J Appl Mech 65: 362-366

Jackson, JD (1999) Classical Electrodynamics. 3rd ed, John Wiley and Sons, New York

Jamnik J, Raj R (1996) Space-charge-controlled diffusional creep: volume diffusion case. J Amer Ceram Soc 79: 193-198

James RD (1981) Finite deformation by mechanical twinning. Arch Rat Mech Anal 77: 143-176

Johnson BE, Hoger A (1993) The dependence of the elasticity tensor on residual stress. J Elasticity 33: 145-165

Johnson KM (1962) Variation of dielectric constant with voltage in ferroelectrics and its application to parametric devices. J Appl Phys 33: 2826-2831

Johnson GR, Cook WH (1985) Fracture characteristics of three metals subjected to various strains, strain rates, temperatures, and pressures. Eng Fract Mech 21: 31-48

Johnson GR, Holmquist TJ, Beissel SR (2003) Response of aluminum nitride (including a phase change) to large strains, high strain rates, and high pressures. J Appl Phys 94: 1639-1646

Johnston WG, Gilman JJ (1959) Dislocation velocities, dislocation densities, and plastic flow in lithium fluoride crystals. J Appl Phys 30: 129-144

Kachanov LM (1958) On the time to failure under creep conditions. Izv An SSSR Otd Tekhn Nauk 8: 26-31

Kachanov M (1992) Effective elastic properties of cracked solids: critical review of some basic concepts. ASME Appl Mech Rev 45: 304-335

Kaga H (1968) Third-order elastic constants of calcite. Phys Rev 172: 900-919

Kaga H, Gilman JJ (1969) Twinning and detwinning in calcite. J Appl Phys 40: 3196-3207

Kalidindi SR (1998) Incorporation of deformation twinning in crystal plasticity models. J Mech Phys Solids 46: 267-290

Kalidindi SR, Bronkhorst CA, Anand L (1992) Crystallographic texture evolution in bulk deformation processing of FCC metals. J Mech Phys Solids 40: 537-569

Kassner ME, Perez-Prado MT, Long M, Vecchio KS (2002) Dislocation microstructure and internal-stress measurements by convergent-beam electron diffraction on creep-deformed Cu and Al. Metall Mater Trans A 33: 311-317

Kenway PR (1993) Calculated stacking-fault energies in α-Al$_2$O$_3$. Phil Mag B 68: 171-183

Kestin J (1992) Local equilibrium formalism applied to mechanics of solids. Int J Solids Structures 29: 1827-1836

Khan AS, Huang S (1995) Continuum Theory of Plasticity. John Wiley and Sons, New York

Kienzler R, Herrmann G (2000) Mechanics in Material Space. Springer-Verlag, Berlin

Kliewer KL, Koehler JS (1965) Space charge in ionic crystals. I. General approach with application to NaCl. Phys Rev 140: 1226-1240

Knap J, Ortiz M (2001) An analysis of the quasicontinuum method. J Mech Phys Solids 49: 1899-1923

Kocks UF (1970) The relation between polycrystal deformation and single-crystal deformation. Metall Trans 1: 1121-1143

Kocks UF, Mecking H (1979) A mechanism for static and dynamic recovery. In: Haasen P, Gerold V, Kostorz G (eds) Strength of Metals and Alloys. Pergamon, Oxford, pp 345-350

Kocks UF, Argon AS, Ashby MF (1975) Thermodynamics and kinetics of slip. Prog Mater Sci 19: 1-288

Kocks UF, Tome CN, Wenk HR (1998) Texture and Anisotropy. Cambridge University Press, Cambridge

Kondo K (1949) A proposal of a new theory concerning the yielding of materials based on Riemannian geometry. J Japan Soc Appl Mech 2: 123-128, 146-151

Kondo K (1953) On the geometrical and physical foundations of the theory of yielding. In: Proc 2nd Japan Congr Appl Mech Japan Nat Committee for Theoretical and Applied Mechanics, Science Council of Japan, Tokyo, pp 41-47

Kondo K (1963) Non-Riemannian and Finslerian approaches to the theory of yielding. Int J Eng Sci 1: 71-88

Kondo K (1964) On the analytical and physical foundations of the theory of dislocations and yielding by the differential geometry of continua. Int J Eng Sci 2: 219-251

Konstantinidis DA, Aifantis EC (1998) On the anomalous hardness of nanocrystalline materials. Nano Mater 10: 1111-1118

Kosevich AM, Boiko VS (1971) Dislocation theory of the elastic twinning of crystals. Sov Phys Uspek 14: 286-316

Kosinski AA (1993) Differentiable Manifolds. Academic Press, San Diego

Kossecka E, De Wit R (1977) Disclination kinematics. Arch Mech 29: 633-651

Krajcinovic D (1996) Damage Mechanics. North-Holland, Amsterdam

Kratochvil J (1971) Finite-strain theory of crystalline elastic-inelastic materials. J Appl Phys 42: 1104-1108

Kratochvil J (1972) Finite strain theory of inelastic behavior of crystalline solids. In: Sawczuk A (ed) Foundations of Plasticity. Noordhoff, Leyden, pp 401-415

Kronberg ML (1957) Plastic deformation of single crystals of sapphire: basal slip and twinning. Acta Metall 5: 507-524

Kronberg ML (1968) A structural mechanism for the twinning process on {1012} in hexagonal close packed metals. Acta Metall 16: 29-34

Kroner E (1960) Allgemeine kontinuumsthoerie der versetzungen und eigenspannungen. Arch Rat Mech Anal 4: 273-334

Kroner E (1963a) Dislocation: a new concept in the continuum theory of plasticity. J Math Phys 42: 27-37

Kroner E (1963b) On the physical reality of torque stresses in continuum mechanics. Int J Eng Sci 1: 261-278

Kroner E (1973) The rheological behaviour of metals. Rheol Acta 12: 374-392

Kroner E (1980) Description of dislocation distributions. In: Hartley CS, Hirth JP (eds) Dislocation Modelling of Physical Systems. Pergamon Press, Oxford, pp 285-303

Kroner E (1981) Differential geometry of defects in condensed systems of particles with only translational mobility. Int J Eng Sci 19: 1507-1515

Kroner E (1983) Field theory of defects in Bravais crystals. In: Paidar V, Lejcek L (eds) The Structure and Properties of Crystal Defects. Elsevier, Amsterdam, pp 357-369

Kroner E (1990) The differentiable geometry of elementary point and line defects in Bravais crystals. Int J Theo Phys 29: 1219-1237

Kroner E (1992) The internal mechanical state of solids with defects. Int J Solids Structures 29: 1849-1857

Kroner E, Lagoudas DC (1992) Gauge theory with disclinations. Int J Eng Sci 30: 47-53

Kroner E, Seeger A (1959) Nicht-lineare elastizitatstheorie der versetzungen und eigenspannungen. Arch Rat Mech Anal 3: 97-119

Kroupa F (1962) Continuous distribution of dislocation loops. Czech J Phys B 12: 191-201

Kuhlmann-Wildsorf D (1960) Frictional stress acting on a moving dislocation in an otherwise perfect crystal. Phys Rev 120: 773-781

Kuhlmann-Wilsdorf D (1989) Theory of plastic deformation: properties of low-energy dislocation structures. Mater Sci Eng A 113: 1-41

Kuhlmann-Wilsdorf D (1999) Theory of dislocation-based crystal plasticity. Phil Mag A 79: 955-1008

Kunin IA (1990) Kinematics of media with continuously changing topology. Int J Theo Phys 29: 1167-1176

Kuo HH, Mura T (1972) Elastic field and strain energy of a circular wedge disclination. J Appl Phys 43: 1454-1457

Lacy TE, McDowell DL, Talreja R (1999) Gradient concepts for evolution of damage. Mech Mater 31: 831-860

Lagerlof KPD, Heuer AH, Castaing J, Riviere JP, Mitchell TE (1994) Slip and twinning in sapphire (α-Al$_2$O$_3$). J Amer Ceram Soc 77: 385-397

Lagerlof KPD, Castaing J, Pirouz P, Heuer AH (2002) Nucleation and growth of deformation twins: a perspective based on the double-cross-slip mechanism of deformation twinning. Phil Mag A 82: 2841-2854

Landau LD, Lifshitz EM (1959) Theory of Elasticity. Pergamon Press, London

Landau LD, Lifshitz EM (1960) Electrodynamics of Continuous Media. Pergamon Press, Oxford

Lardner RW (1969) Dislocation dynamics and the theory of the plasticity of single crystals. Z Agnew Math Phys 20: 514-529

Lardner RW (1973) Foundations of the theory of disclinations. Arch Mech 25: 911-922

Lardner RW (1974) Mathematical Theory of Dislocations and Fracture. University of Toronto Press, Great Britain

Lax M, Nelson DF (1971) Linear and nonlinear electrodynamics in elastic anisotropic dielectrics. Phys Rev B 4: 3694-3731

Lax M, Nelson DF (1976a) Electrodynamics of elastic pyroelectrics. Phys Rev B 13: 1759-1769

Lax M, Nelson DF (1976b) Maxwell equations in material form. Phys Rev B 13: 1777-1784

Lazar M, Maugin GA (2004) Defects in gradient micropolar elasticity—II: edge dislocation and wedge disclination. J Mech Phys Solids 52: 2285-2307

Lazar M, Maugin GA (2005) Nonsingular stress and strain fields of dislocations and disclinations in first strain gradient elasticity. Int J Eng Sci 43: 1157-1184

Le KC, Stumpf H (1996a) On the determination of the crystal reference in nonlinear continuum theory of dislocations. Proc R Soc Lond A 452: 359-371

Le KC, Stumpf H (1996b) Nonlinear continuum theory of dislocations. Int J Eng Sci 34: 339-358

Le KC, Stumpf H (1996c) A model of elastoplastic bodies with continuously distributed dislocations. Int J Plasticity 12: 611-627

Le KC, Stumpf H (1998) Strain measures, integrability condition and frame indifference in the theory of oriented media. Int J Solids Structures 35: 783-798

Lebedev AB (1996) Amplitude-dependent decrement to modulus defect ratio in breakaway models of dislocation hysteresis. Phil Mag A 74: 137-150

Lebensohn RA, Tome CN (1993) A study of the stress state associated with twin nucleation and propagation in anisotropic materials. Phil Mag A 67: 187-206

Lee BJ, Vecchio KS, Ahzi S, Schoenfeld S (1997) Modeling the mechanical behavior of tantalum. Metall Mater Trans A 28: 113-122

Lee EH (1969) Elastic-plastic deformation at finite strains. ASME J Appl Mech 36: 1-6

Lee EH (1981) Some comments on elastic-plastic analysis. Int J Solids Structures 17: 859-872

Lee EH, Liu DT (1967) Elastic-plastic theory with application to plane-wave analysis. J Appl Phys 38: 19-27

Lee EH, Wierzbicki T (1967) Analysis of the propagation of plane elastic-plastic waves at finite strain. ASME J Appl Mech 34: 931-936

Lee JK, Yoo MH (1990) Elastic strain energy of deformation twinning in tetragonal crystals. Metall Trans A 21: 2521-2530

Lee YJ, Subhash G, Ravichandran G (1999) Constitutive modeling of textured body-centered-cubic (bcc) polycrystals. Int J Plasticity 15: 625-645

Leffers T (1994) Lattice rotations during plastic deformation with grain subdivision. Mater Sci Forum 157-162: 1815-1820

Lemaitre J (1985) A continuous damage mechanics model for ductile fracture. ASME J Eng Mater Tech 107: 83-89

Lempriere BM (1970) The relation of incompatibility and dislocation motion to plastic deformation. Metall Trans 1: 2695-2697

Lennard-Jones JE (1924) On the determination of molecular fields. I. From the variation of the viscosity of a gas with temperature. Proc R Soc Lond A 106: 441-462

Lennard-Jones JE (1925) On the forces between atoms and ions. Proc R Soc Lond A 109: 584-597

Li JCM (1960) Some elastic properties of an edge dislocation wall. Acta Metall 8: 563-574

Li JCM (1972) Disclination model of high angle grain boundaries. Surf Sci 31: 12-26

Li JCM, Gilman JT (1970) Disclination loops in polymers. J Appl Phys 41: 4248-4256

Lippmann H (1996) Averaging or distributing stress and strain? Eur J Mech A Solids 15: 749-759

Liu GCT, Li JCM (1971) Strain energies of disclination loops. J Appl Phys 42: 3313-3315

Longere P, Dragon A (2008) Plastic work induced heating evaluation under dynamic conditions: critical assessment. Mech Res Comm 35: 135-141

Longere P, Dragon A, Trumel H, De Resseguier T, Deprince X, Petitpas E (2003) Modelling adiabatic shear banding via damage mechanics approach. Arch Mech 55: 3-38

Love AEH (1927) A Treatise on the Mathematical Theory of Elasticity. 4th ed, Cambridge University Press, Cambridge

Lu SCH, Pister KS (1975) Decomposition of deformation and representation of the free energy function for isotropic thermoelastic solids. Int J Solids Structures 11: 927-934

Lubarda VA (1999) Duality in constitutive formulation of finite-strain elastoplasticity based on $F=F_eF_p$ and $F=F^pF^e$ decompositions. Int J Plasticity 15: 1277-1290

Lubliner J (1990) Plasticity Theory. Macmillan, New York

Lutsko JF (1988) Stress and elastic constants in anisotropic solids: molecular dynamics techniques. J Appl Phys 64: 1152-1154

Mackenzie JK (1950) The elastic constants of a solid containing spherical holes. Proc Phys Soc Lond B 63: 2-11

Maeda K, Suzuki K, Fujita S, Ichihara M, Hyodo S (1988) Defects in plastically deformed 6H SiC single crystals studied by transmission electron microscopy. Phil Mag A 57: 573-592

Makarov PV, Smolin IY, Prokopinsky IP, Stefanov YP (1999) Modeling of development of localized plastic deformation and prefracture stage in mesovolumes of heterogeneous media. Int J Fracture 100: 121-131

Malvern LE (1969) Introduction to the mechanics of a continuous medium. Prentice-Hall, Englewood Cliffs

Mandel J (1973) Equations constitutives et directeurs dans les milieux plastiques et viscoplastiques. Int J Solids Structures 9: 725-740

Mandel J (1974) Thermodynamics and plasticity. In: Delgado JJ (ed) Foundations of Continuum Thermodynamics. Macmillan, New York, pp 283-304

Many A, Rakavy G (1962) Theory of transient space-charge-limited currents in solids in the presence of trapping. Phys Rev 126: 1980-1988

Maradudin AA, Montroll EW, Weiss GH, Ipatova IP (1971) Theory of Lattice Dynamics in the Harmonic Approximation. Academic Press, New York

Marcinkowski MJ (1990) Inter-relationships between disclinations, surface dislocations, and grain boundaries. Phil Mag Lett 62: 19-23

Marcinkowski MJ, Sadananda K (1975) Unification of coincident-site-lattice and continuum theories of grain boundaries. Acta Cryst A 31: 280-292

Margolin LG (1983) Elastic moduli of a cracked body. Int J Fracture 22: 65-79

Margolin LG (1984) Microphysical models for inelastic material response. Int J Eng Sci 22: 1171-1179

Marin EB, McDowell DL (1996) Associative versus non-associative porous viscoplasticity based on internal state variable concepts. Int J Plasticity 12: 629-669

Markenscoff X (1977) On the determination of the fourth-order elastic constants. J Appl Phys 48: 3752-3755

Martin RM (1972) Piezoelectricity. Phys Rev B 5: 1607-1613

Marsden JE, Hughes TJR (1983) Mathematical Foundations of Elasticity. Prentice-Hall, Englewood Cliffs

Mason WP (1966) Crystal Physics of Interaction Processes. Academic Press, New York

Maugin GA (1978a) On the covariant equations of the relativistic electrodynamics of continua. I. General equations. J Math Phys 19: 1198-1205

Maugin GA (1978b) On the covariant equations of the relativistic electrodynamics of continua. III. Elastic solids. J Math Phys 19: 1212-1219

Maugin GA (1988) Continuum Mechanics of Electromagnetic Solids. North-Holland, Amsterdam

Maugin GA (1993) Material Inhomogeneities in Elasticity. Chapman and Hall, London

Maugin GA (1994) Eshelby stress in elastoplasticity and ductile fracture. Int J Plasticity 10: 393-408

Maugin GA (1995) Material forces: concepts and applications. ASME Appl Mech Rev 48: 213-245

Maugin GA (1999) Nonlinear Waves in Elastic Crystals. Oxford University Press, New York

Maugin GA, Epstein M (1991) The electroelastic energy-momentum tensor. Proc R Soc Lond A 433: 299-312

Maugin GA, Epstein M (1998) Geometric material structure of elastoplasticity. Int J Plasticity 14: 109-115

Maugin GA, Muschik W (1994a) Thermodynamics with internal variables. Part I. General concepts. J Non-Equil Thermo 19: 217-249

Maugin GA, Muschik W (1994b) Thermodynamics with internal variables. Part II. Applications. J Non-Equil Thermo 19: 250-289

McClintock FA (1968) A criterion for ductile rupture by the growth of holes. ASME J Appl Mech 35: 363-371

McDowell DL (2000) Modeling and experiments in plasticity. Int J Solids Structures 37: 293-309

McDowell DL (2005) Internal state variable theory. In: Yip S (ed) Handbook of Materials Modeling. Springer, The Netherlands, pp 1151-1169

McDowell DL (2008) Viscoplasticity of heterogeneous metallic materials. Mater Sci Eng R 62: 67-123

McDowell DL, Moosebrugger JC (1992) Continuum slip foundations of elasto-viscoplasticity. Acta Mech 93: 73-87

McDowell DL, Marin E, Bertoncelli C (1993) A combined kinematic-isotropic hardening theory for porous inelasticity of ductile metals. Int J Damage Mech 2: 137-161

McMeeking RM, Landis CM (2005) Electrostatic forces and stored energy for deformable dielectric materials. ASME J Appl Mech 72: 581-590

McMeeking RM, Landis CM, Jimenez, SMA (2007) A principle of virtual work for combined electrostatic and mechanical loading of materials. Int J Non-Linear Mech 42: 831-838

Menzel A, Steinmann P (2000) On the continuum formulation of higher gradient plasticity for single and polycrystals. J Mech Phys Solids 48: 1777-1796

Menzel A, Steinmann P (2003) Geometrically non-linear anisotropic inelasticity based on fictitious configurations: application to the coupling of continuum damage and multiplicative elasto-plasticity. Int J Numer Meth Eng 56: 2233-2266

Meyers MA, Ashworth E (1982) A model for the effect of grain size on the yield stress of metals. Phil Mag A 46: 737-759

Meyers MA, Vohringer O, Lubarda VA (2001) The onset of twinning in metals: a constitutive description. Acta Mater 49: 4025-4039

Miehe C (1998) A theoretical and computational model for isotropic elastoplastic stress analysis in shells at large strains. Comp Meth Appl Mech Eng 155: 193-233

Miller R, Phillips R, Beltz G, Ortiz M (1998) A non-local formulation of the Peierls dislocation model. J Mech Phys Solids 46: 1845-1867

Minagawa S (1977) Elastic fields of dislocations and disclinations in an isotropic micropolar continuum. Lett Appl Eng Sci 5: 85-94

Minagawa S (1979) A non-Riemannian geometrical theory of imperfections in a Cosserat continuum. Arch Mech 31: 783-792

Minagawa S (1981) Stress functions and stress-function spaces of non-metric connection for 3-dimensional micropolar elastostatics. Int J Eng Sci 19: 1705-1710

Mindlin RD (1964) Micro-structure in linear elasticity. Arch Rat Mech Anal 16: 51-78

Mindlin RD (1965) Second gradient of strain and surface tension in linear elasticity. Int J Solids Structures 1: 417-438

Mindlin RD (1968a) Theories of elastic continua and crystal lattice theories. In: Kroner E (ed) Mechanics of Generalized Continua. Springer-Verlag, New York, pp 312-320

Mindlin RD (1968b) Polarization gradient in elastic dielectrics. Int J Solids Structures 4: 637-642

Mindlin RD (1972) Elasticity, piezoelectricity, and crystal lattice dynamics. J Elasticity 2: 217-282

Mishra RK, Thomas G (1977) Surface energy of spinel. J Appl Phys 48: 4576-4580

Moran B, Ortiz M, Shih CF (1990) Formulation of implicit finite element methods for multiplicative finite deformation plasticity. Int J Numer Meth Eng 29: 483-514

Mott NF, Littleton MJ (1938) Conduction in polar crystals. I. Electrolytic conduction in solid salts. Trans Faraday Soc 34: 485-511

Mott NF, Gurney RW (1948) Electronic Processes in Ionic Crystals. 2nd ed, Oxford University Press, London

Mughrabi H (1983) Dislocation wall and cell structures and long-range internal stresses in deformed metal crystals. Acta Metall 31: 1367-1379

Mullner P, Romanov AE (1994) Between dislocation and disclination models for twins. Scr Metall Mater 31: 1657-1662

Mura T (1982) Micromechanics of Defects in Solids. Martinus Nijhoff, Dordrecht

Murakami S (1983) Notion of continuum damage mechanics and its application to anisotropic creep damage theory. ASME J Eng Mater Tech 105: 99-105

Murakami S (1988) Mechanical modeling of material damage. ASME J Appl Mech 55: 280-286

Murnaghan FD (1944) The compressibility of matter under extreme pressures. Proc Nat Acad Sci USA 30: 244-247

Murnaghan FD (1951) Finite Deformation of an Elastic Solid. John Wiley and Sons, New York

Nabarro FRN (1947) Dislocations in a simple cubic lattice. Proc Phys Soc Lond 59: 256-272

Nabarro FRN (1952) Mathematical theory of stationary dislocations. Adv Phys 1: 269-394

Nabarro FRN (1967) Theory of Crystal Dislocations. Oxford University Press, London

Nabarro FRN (1997) Theoretical and experimental estimates of the Peierls stress. Phil Mag A 75: 703-711

Nadai A (1950) Theory of Flow and Fracture of Solids. McGraw-Hill, New York

Nagdhi PM, Srinivasa AR (1993) A dynamic theory of structured solids. I. Basic developments. Phil Trans R Soc Lond A 345: 425-458

Nazarov AA, Romanov AE, Valiev RZ (1993) On the structure, stress fields, and energy of nonequilibrium grain boundaries. Acta Metall Mater 41: 1033-1040

Nazarov AA, Shenderova OA, Brenner DW (2000) Elastic models of symmetrical <001> and <011> tilt grain boundaries in diamond. Phys Rev B 61: 928-936

Needleman A (2000) Computational mechanics at the mesoscale. Acta Mater 48: 105-124

Needleman A, Tvergaard V (1991) A numerical study of void distribution effects on dynamic ductile crack growth. Eng Fract Mech 38: 157-173

Nelson DF, Lax M (1976) Asymmetric total stress tensor. Phys Rev B 13: 1770-1776

Nemat-Nasser S (1979) Decomposition of strain measures and their rates in finite deformation elastoplasticity. Int J Solids Struct 15: 155-166

Nemat-Nasser S (1999) Averaging theorems in finite deformation plasticity. Mech Mater 31: 493-523

Nemat-Nasser S (2004) Plasticity: A Treatise on Finite Deformation of Heterogeneous Inelastic Materials. Cambridge University Press, Cambridge

Nemat-Nasser S, Hori M (1999) Micromechanics: Overall Properties of Heterogeneous Materials. 2nd ed, Elsevier, North-Holland, Amsterdam

Nemat-Nasser S, Li YF (1994) An algorithm for large-scale computational finite-deformation plasticity. Mech Mater 18: 231-264

Nemat-Nasser S, Obata M (1986) Rate-dependent, finite elasto-viscoplastic deformation of polycrystals. Proc R Soc Lond A 407: 343-375

Nemat-Nasser S, Mehrabadi MM, Iwakuma T (1981) On certain macroscopic and microscopic aspects of plastic flow in ductile materials. In: Nemat-Nasser S (ed) Three-dimensional Constitutive Relations for Ductile Fracture. North-Holland, Amsterdam, pp 157-172

Nes E (1995) Recovery revisited. Acta Metall Mater 43: 2189-2207

Nielsen OH, Martin RM (1983) First-principles calculation of stress. Phys Rev Lett 50: 697-700

Nielsen OH, Martin RM (1985) Quantum-mechanical theory of stress and force. Phys Rev B 32: 3780-3791

Nilan TG, Granato AV (1965) Stored-energy release below 80°K in deuteron-irradiated copper. Phys Rev 137: A1233-A1249

Noll W (1958) A mathematical theory of the mechanical behavior of continuous media. Arch Rat Mech Anal 2: 197-226

Noll W (1967) Materially uniform simple bodies with inhomogeneities. Arch Rat Mech Anal 27: 1-32

Nothwang WD, Cole MW, Hirsch SG (2005) Grain growth and residual stress in BST thin films. Integrated Ferroelectrics 71: 107-113

Nunziato JW, Cowin SC (1979) A nonlinear theory of elastic materials with voids. Arch Rat Mech Anal 72: 175-201

Nye JF (1953) Some geometrical relations in dislocated crystals. Acta Metall 1: 153-162

Nye JF (1957) Physical Properties of Crystals: Their Representation by Tensors and Matrices. Clarendon, Oxford

Ogata S, Li J, Yip S (2005) Energy landscape of deformation twinning in bcc and fcc metals. Phys Rev B 71: 224102

Ogden RW (1997) Nonlinear Elastic Deformations. Dover, New York

Oh ES, Slattery JC (2008) Nanoscale thermodynamics of multicomponent, elastic, crystalline solids: diamond, silicon, and silicon carbide. Phil Mag 88: 427-440

Onsager L (1931a) Reciprocal relations in irreversible processes I. Phys Rev 37: 405-426

Onsager L (1931b) Reciprocal relations in irreversible processes II. Phys Rev 38: 2265-2279

Orowan E (1934) Zur krystallplastizitat, I, II, III. Z Phys 89: 605-659

Orowan E (1940) Problems of plastic gliding. Proc Phys Soc Lond 52: 8-22

Ortiz M (1996) Computational micromechanics. Comp Mech 18: 321-338

Ortiz M, Repetto EA (1999) Nonconvex energy minimization and dislocation structures in ductile single crystals. J Mech Phys Solids 47: 397-462

Ortiz M, Repetto EA, Stanier L (2000) A theory of subgrain dislocation structures. J Mech Phys Solids 48: 2077-2114

Owen DJR, Mura, T (1967) Dislocation configurations in cylindrical coordinates. J Appl Phys 38: 2818-2825

Pan E (1991) Dislocation in an infinite poroelastic medium. Acta Mech 87: 105-115

Pan E (2001) Mindlin's problem for an anisotropic piezoelectric half-space with general boundary conditions. Proc R Soc Lond A 458: 181-208

Panin VE (1998) Overview on mesomechanics of plastic deformation and fracture of solids. Theo Appl Fract Mech 30: 1-11

Pantleon W (1996) On the distribution function of disorientations in dislocation cell structures. Scr Mater 35: 511-515

Parry GP (1980) Twinning in nonlinearly elastic monatomic crystals. Int J Solids Structures 16: 275-281

Park T, Voyiadjis GZ (1998) Kinematic description of damage. ASME J Appl Mech 65: 93-98

Pauling L, Wilson EB (1935) Introduction to Quantum Mechanics. McGraw-Hill, New York

Paxton AT, Gumbsch P, Methfessel M (1991) A quantum mechanical calculation of the theoretical strength of metals. Phil Mag Lett 63: 267-274

Peach MO, Koehler JS (1950) The forces exerted on dislocations and the stress fields produced by them. Phys Rev 80: 436-439

Pecherski RB (1983) Relation of microscopic observations to constitutive modeling for advanced deformations and fracture initiation of viscoplastic materials. Arch Mech 35: 257-277

Pecherski RB (1985) Discussion of sufficient condition for plastic flow localization. Eng Fract Mech 21: 767-779

Pecherski RB (1998) Macroscopic effects of micro-shear banding in plasticity of metals. Acta Mech 131: 203-224

Peeters B, Seefeldt M, Van Houtte P, Aernoudt E (2001) Taylor ambiguity in BCC polycrystals: a non-problem if sub-structural anisotropy is considered. Scr Mater 45: 1349-1356

Peierls RE (1940) The size of a dislocation. Proc Phys Soc Lond 52: 34-37

Peirce D, Asaro RJ, Needleman A (1982) An analysis of nonuniform and localized deformation in ductile single crystals. Acta Metall 30: 1087-1119

Perzyna P (1963) The constitutive equations for rate sensitive plastic materials. Q Appl Math 20: 321-332

Petch NJ (1953) The cleavage strength of polycrystals. J Iron Steel Inst 174: 25-28

Phillips R (2001) Crystals, Defects and Microstructures. Cambridge University Press, Cambridge

Pijaudiercabot G, Bazant ZP (1987) Nonlocal damage theory. ASCE J Eng Mech 113: 1512-1533

Pirouz P (1987) Deformation mode in silicon: slip or twinning. Scr Metall 21: 1463-1468

Polanyi M (1934) Uber eine art gitterstorung, die einen kristall plastisch machen konnte. Z Phys 89: 660-664

Price PB (1961) Nucleation and growth of twins in dislocation-free zinc crystals. Proc R Soc Lond A 260: 251-262

Proust G, Tome CN, Jain A, Agnew SR (2009) Modeling the effect of twinning and detwinning during strain-path changes of magnesium alloy AZ31. Int J Plasticity 25: 861-880

Rajagopal KR, Srinivasa AR (1998) Mechanics of the inelastic behavior of materials—part I, theoretical underpinnings. Int J Plasticity 14: 945-967

Rajendran AM (1994) Modeling the impact behavior of AD85 ceramic under multiaxial loading. Int J Impact Eng 15: 749-768

Rajendran AM, Grove DJ (1996) Modeling the shock response of silicon carbide, boron carbide and titanium diboride. Int J Impact Eng 18: 611-631

Rajendran AM, Dietenberger MA, Grove DJ (1989) A void growth-based failure model to describe spallation. J Appl Phys 85: 1521-1527

Randle V, Engler O (2000) Introduction to Texture Analysis: Macrotexture, Microtexture, and Orientation Mapping. Gordon and Breach Scientific Publishers, Australia

Read WT (1953) Dislocations in Crystals. McGraw-Hill, New York

Regueiro RA (2009) Finite strain micromorphic pressure-sensitive plasticity. ASCE J Eng Mech 135: 178-191

Regueiro RA (2010) On finite strain micromorphic elastoplasticity. Int J Solids Structures 47: 786-800

Regueiro RA, Bammann DJ, Marin EB, Garikipati K (2002) A nonlocal phenomenological anisotropic finite deformation plasticity model accounting for dislocation defects. ASME J Eng Mater Tech 124: 380-387

Reusch F, Svendsen B, Klingbeil D (2003) Local and non-local Gurson-based ductile damage and failure modelling at large deformation. Eur J Mech A—Solids 22: 779-792

Rezvanian O, Zikry MA, Rajendran AM (2007) Statistically stored, geometrically necessary and grain boundary dislocation densities: microstructural representation and modelling. Proc R Soc Lond A 463: 2833-2853

Rice JR (1968) A path independent integral and approximate analysis of strain concentration by notches and cracks. ASME J Appl Mech 33: 379-386

Rice JR (1971) Inelastic constitutive relations for solids: an internal variable theory and its application to metal plasticity. J Mech Phys Solids 19: 433-455

Rice JR (1976) The localization of plastic deformation. In: Koiter WT (ed) Proc 14th Int Cong Theo Appl Mech. North-Holland, Amsterdam, pp 207-220

Rice JR, Tracey DM (1969) On the ductile enlargement of voids in triaxial stress fields. J Mech Phys Solids 17: 201-217

Rohatgi A, Vecchio KS (2002) The variation of dislocation density as a function of the stacking fault energy in shock-deformed FCC materials. Mater Sci Eng A 328: 256-266

Rohrer GS (2001) Structure and Bonding in Crystalline Materials. Cambridge University Press, Cambridge

Romanov AE (1993) Screened disclinations in solids. Mater Sci Eng A 164: 58-68

Rosakis P, Tsai H (1995) Dynamic twinning processes in crystals. Int J Solids Structures 32: 2711-2723

Rosakis P, Rosakis AJ, Ravichandran G, Hodowany J (2000) A thermodynamic internal variable model for the partition of plastic work into heat and stored energy in metals. J Mech Phys Solids 48: 581-607

Rubin MB, Lomov I (2003) A thermodynamically consistent large deformation elastic-viscoplastic model with directional tensile failure. Int J Solids Structures 40: 4299-4318

Rudnicki JW, Rice JR (1975) Conditions for the localization of deformation in pressure-sensitive dilatant materials. J Mech Phys Solids 23: 371-394

Rund H (1959) The Differential Geometry of Finsler Spaces. Springer-Verlag, Berlin

Sano O, Kudo Y, Yoshiaki M (1992) Experimental determination of elastic constants of Oshima granite, Barre granite, and Chelmsford granite. J Geophys Res 97: 3367-3379

Scheidler M, Wright TW (2001) A continuum framework for finite viscoplasticity. Int J Plasticity 17: 1033-1085

Scheidler M, Wright TW (2003) Classes of flow rules for finite viscoplasticity. Int J Plasticity 19: 1119-1165

Schmid E, Boas IW (1950) Plasticity of Crystals. Chapman and Hall, London

Schoenfeld SE (1998) Dynamic behaviour of polycrystalline tantalum. Int J Plasticity 14: 871-890

Schoenfeld SE, Kad B (2002) Texture effects on shear response in Ti-6Al-4V plates. Int J Plasticity 18: 461-486

Schoenfeld SE, Ahzi S, Asaro RJ (1995) Elastic-plastic crystal mechanics for low symmetry crystals. J Mech Phys Solids 43: 415-446

Schouten JA (1954) Ricci Calculus. Springer-Verlag, Berlin

Schultz RA, Jensen MC, Bradt RC (1994) Single crystal cleavage of brittle materials. Int J Fracture 65: 291-312

Scott WD, Orr KK (1983) Rhombohedral twinning in alumina. J Amer Ceram Soc 66: 27-32

Sedov LI (1966) Foundations of the Non-linear Mechanics of Continua. Pergamon, Oxford

Seefeldt M (2001) Disclinations in large-strain plastic deformation and work hardening. Rev Adv Mater Sci 2: 44-79

Seefeldt M, Klimanek P (1997) Interpretation of plastic deformation by means of dislocation-disclination reaction kinetics. Mater Sci Eng A 234-236, 758-761

Seefeldt M, Kimanek P (1998) Modelling of flow behaviour of metals by means of a dislocation-disclination reaction kinetics. Mod Sim Mater Sci Eng 6: 349-360

Seefeldt M, Delannay L, Peeters B, Kalidindi SR, Van Houtte P (2001) A disclination-based model for grain subdivision. Mater Sci Eng A 234-236: 758-761

Seeger A (2007) Production of lattice vacancies in metals by deformation twinning. Phil Mag Lett 87: 95-102

Seeger A, Haasen P (1958) Density changes of crystals containing dislocations. Phil Mag 3: 470-475

Segletes SB, Walters WP (1998) On theories of the Gruneisen parameter. J Phys Chem Solids 59: 425-433

Senechal M (1990) Crystalline Symmetries: An Informal Mathematical Introduction. Adam Hilger, Bristol

Shepherd JE, McDowell DL, Jacob KI (2006) Modeling morphology evolution and mechanical behavior during thermo-mechanical processing of semi-crystalline polymers. J Mech Phys Solids 54: 467-489

Shenderova OA, Brenner DW (1999) Atomistic simulations of structures and mechanical properties of <011> tilt grain boundaries and their triple junctions in diamond. Phys Rev B 60: 7053-7061

Shizawa K, Zbib H (1999) A thermodynamical theory of plastic spin and internal stress with dislocation density tensor. ASME J Eng Mater Tech 121: 247-253

Shu JY, Fleck NA (1999) Strain gradient crystal plasticity: size-dependent deformation of bicrystals. J Mech Phys Solids 47: 297-324

Shu YC, Bhattacharya K (2001) Domain patterns and macroscopic behaviour of ferroelectric materials. Phil Mag B 81: 2021-2054

Simmons RO, Balluffi RW (1963) Measurement of equilibrium concentrations of vacancies in copper. Phys Rev 129: 1533-1544

Simo JC (1988) A framework for finite strain elastoplasticity based on maximum plastic dissipation and the multiplicative decomposition: Part I. Continuum formulation. Comp Meth Appl Mech Eng 66: 199-219

Simo JC, Hughes TJR (1998) Computational Inelasticity. Springer-Verlag, New York

Simo JC, Ortiz M (1985) A unified approach to finite deformation elastoplastic analysis based on the use of hyperelastic constitutive equations. Comp Meth Appl Mech Eng 49: 221-245

Simo JC, Taylor RL, Pister KS (1985) Variational and projection methods for the volume constraint in finite deformation elasto-plasticity. Comp Meth Appl Mech Eng 51: 177-208

Slater JC (1939) Introduction to Chemical Physics. McGraw-Hill, New York

Slater JC (1940) Note on Gruneisen's constant for the incompressible metals. Phys Rev 57: 744-746

Slater JC (1955) Modern Physics. McGraw-Hill, New York

Smith ADN (1953) The effect of small amounts of cold work on Young's modulus of copper. Phil Mag A 44: 453-466

Smith GF, Rivlin RS (1958) The strain energy function for anisotropic elastic materials. Trans Amer Math Soc 88: 175-193

Somigliana C (1914) Sulla teoria delle distorsioni elastiche. Rend R Acc Lincei Ser 5 23: 463-472

Spearot DE, Jacob KI, McDowell DL (2005) Nucleation of dislocations from [001] bicrystal interfaces in aluminum. Acta Mater 53: 3579-3589

Speck JS, Pompe W (1994) Domain configurations due to multiple misfit relaxation mechanisms in epitaxial thin films. I. Theory. J Appl Phys 76: 466-476

Sprackling MT (1976) The Plastic Deformation of Simple Ionic Crystals. Academic Press, New York

Staroselsky A, Anand L (1998) Inelastic deformation of polycrystalline face centered cubic materials by slip and twinning. J Mech Phys Solids 46: 671-696

Staroselsky A, Anand L (2003) A constitutive model for hcp materials deforming by slip and twinning: application to magnesium alloy AZ31B. Int J Plasticity 19: 1843-1864

Steeds JW (1973) Introduction to Anisotropic Elasticity Theory of Dislocations. Clarendon Press, Oxford

Steinberg DJ, Cochran SG, Guinan MW (1980) A constitutive model for metals applicable at high-strain rate. J Appl Phys 51: 1498-1504

Steinmann P (1996) Views on multiplicative elastoplasticity and the continuum theory of dislocations. Int J Eng Sci 34: 1717-1735

Steinmann P, Carol I (1998) A framework for geometrically nonlinear continuum damage mechanics. Int J Eng Sci 36: 1793-1814

Stillinger FH, Weber TA (1985) Computer simulation of local order in condensed phases of silicon. Phys Rev B 31: 5262-5271

Stojanovitch R (1969) On the stress relation in non-linear thermoelasticity. Int J Non-Linear Mech 4, 217-233

Stolken JS, Evans AG (1998) A microbend test method for measuring the plasticity length scale. Acta Mater 46: 5109-5115

Stout MG, Rollett AD (1990) Large-strain Bauschinger effects in FCC metals and alloys. Metall Trans A 21: 3201-3213

Stratton JA (1941) Electromagnetic Theory. McGraw-Hill, New York

Stroh AN (1958) Dislocations and cracks in anisotropic elasticity. Phil Mag 3: 625-646

Stumpf H, Hoppe U (1997) The application of tensor algebra on manifolds to nonlinear continuum mechanics—invited survey article. Z Agnew Math Mech 76: 447-462

Subhash G, Lee YJ, Ravichandran G (1994) Plastic deformation of CVD textured tungsten—I. Constitutive response. Acta Metall Mater 42: 319-330

Suhubi ES, Eringen AC (1964) Nonlinear theory of micro-elastic solids—II. Int J Eng Sci 2: 389-404

Sunyk R, Steinmann P (2003) On higher gradients in continuum-atomistic modelling. Int J Solids Structures 40: 6877-6896

Svendsen B (2001) On the modeling of anisotropic elastic and inelastic material behaviour at large deformation. Int J Solids Structures 38: 9579-9599

Svendsen B (2002) Continuum thermodynamic models for crystal plasticity including the effects of geometrically-necessary dislocations. J Mech Phys Solids 50: 1297-1329

Synge JL (1960) Classical dynamics. In: Flugge S (ed) Handbuch der Physik, vol III/1. Springer-Verlag, Berlin, pp 1-225

Tadmor EB, Ortiz M, Phillips R (1996) Quasicontinuum analysis of defects in solids. Phil Mag A 73: 1529-1563

Tadmor EB, Smith GS, Bernstein N, Kaxiras E (1999) Mixed finite element and atomistic formulation for complex crystals. Phys Rev B 59: 235-245

Taheri M, Weiland H, Rollett A (2006) A method of measuring stored energy macroscopically using statistically stored dislocations in commercial purity aluminum. Metall Mater Trans A 37: 19-25

Taylor GI (1927) The distortion of crystals of aluminum under compression—Part II. Distortion by double slipping and changes in orientation of crystal axes during compression. Proc R Soc Lond A 116: 16-38

Taylor GI (1934) The mechanism of plastic deformation of crystals. Proc R Soc Lond A 145: 362-415

Taylor GI (1938) Plastic strain in metals. J Inst Metals 62: 307-324

Taylor GI, Elam CF (1923) The distortion of an aluminum crystal during a tensile test. Proc R Soc Lond A 102: 643-667

Taylor GI, Quinney H (1934) The latent energy remaining in a metal after cold working. Proc R Soc Lond A 143: 307-326

Teodosiu C (1967a) Contributions to the continuum theory of dislocations and initial stresses I. Rev Roum Sci Techn-Mec Appl 12: 961-977

Teodosiu C (1967b) Contributions to the continuum theory of dislocations and initial stresses III. Rev Roum Sci Techn-Mec Appl 12: 1291-1308

Teodosiu C (1968) Continuous distributions of dislocations in hyperelastic materials of grade 2. In: Kroner E (ed) Mechanics of Generalized Continua. Springer-Verlag, New York, pp 279-282

Teodosiu C (1970) A dynamic theory of dislocations and its application to the theory of elastic-plastic continuum. In: Simmons JA, De Wit R, Bullough R (eds) Fundamental Aspects of Dislocation Theory. US Govt Printing Office, Gaithersburg, MD, pp 837-876

Teodosiu C (1981) Somigliana dislocation in an anisotropic elastic medium. Int J Eng Sci 19: 1563-1571

Teodosiu C (1982) Elastic Models of Crystal Defects. Springer-Verlag, Berlin

Teodosiu C, Sidoroff F (1976) A finite theory of the elastoviscoplasticity of single crystals. Int J Eng Sci 14: 713-723

Tersoff J (1988) Empirical interatomic potential for carbon, with applications to amorphous carbon. Phys Rev Lett 61: 2879-2882

Thomas JF (1968) Third-order elastic constants of aluminum. Phys Rev 175: 955-962

Thomsen L (1970) On the fourth-order anharmonic equation of state of solids. J Phys Chem Solids 31: 2003-2016

Thompson A, Taylor BN (2008) Guide for the use of the International System of units (SI). NIST Special Publication 811, Gaithersburg, MD

Thurston RN (1974) Waves in solids. In: Truesdell C (ed) Handbuch der Physik, vol VIa/4. Springer-Verlag, Berlin, pp 109-308

Thurston RN, Brugger K (1964) Third-order elastic constants and the velocity of small amplitude elastic waves in homogeneously stressed media. Phys Rev 133: 1604-1612

Tiersten HF (1971) On the nonlinear equations of thermoelectroelasticity. Int J Eng Sci 9: 587-604

Tiersten HF, Tsai CF (1972) On the interaction of the electromagnetic field with heat conducting deformable insulators. J Math Phys 13: 361-378

Tigoiu SC, Soos E (1990) Elastoviscoplastic models with relaxed configurations and internal state variables. ASME Appl Mech Rev 43: 131-151

Tome C, Lebhenson RA, Kocks UF (1991) A model for texture development dominated by deformation twinning: application to zirconium alloys. Acta Metall 39: 2667-2680

Toupin RA (1956) The elastic dielectric. J Rat Mech Anal 5: 849-915

Toupin RA (1962) Elastic materials with couple stresses. Arch Rat Mech Anal 11: 385-414

Toupin RA (1963) A dynamical theory of elastic dielectrics. Int J Eng Sci 1: 101-126

Toupin RA (1964) Theories of elasticity with couple stress. Arch Rat Mech Anal 17: 85-112

Toupin RA (1968) Dislocated and oriented media. In: Kroner E (ed) Mechanics of Generalized Continua, Springer-Verlag, New York, pp 126-140

Toupin RA, Bernstein B (1961) Sound waves in deformed perfectly elastic materials. Acoustoelastic effect. J Acoust Soc Amer 33: 216-225

Toupin RA, Rivlin RS (1960) Dimensional changes in crystals caused by dislocations. J Math Phys 1: 8-15

Truesdell C, Noll W (1965) The nonlinear field theories of mechanics. In: Flugge S (ed) Handbuch der Physik, vol III/3. Springer-Verlag, Berlin, pp 1-602

Truesdell C, Toupin R (1960) The classical field theories. In: Flugge S (ed) Handbuch der Physik, vol III/1. Springer-Verlag, Berlin, pp 226-793

Tsai DH (1979) The virial theorem and stress calculation in molecular dynamics. J Chem Phys 70: 1375-1382

Tvergaard V (1981) Influence of voids on shear band instabilities under plane strain conditions. Int J Fracture 17: 389-407

Tvergaard V, Needleman A (1984) Analysis of the cup-cone fracture in a round tensile bar. Acta Metall 32: 157-169

Tvergaard V, Needleman A (1997) Nonlocal effects on localization in a void sheet. Int J Solids Structures 34: 2221-2238

Valiev RZ, Islamgaliev RK, Tumentsev AN (2002) The disclination approach for nanostructured SPD materials. Solid State Phenom 87: 255-264

Van der Giessen E, Kollmann FG (1996) On mathematical aspects of dual variables in continuum mechanics. Part I: mathematical principles. Z Agnew Math Mech 76: 447-462

Van Houtte P (1978) Simulation of the rolling and shear texture of brass by the Taylor theory adapted for mechanical twinning. Acta Metall 26: 591-604

Veit K (1921) Artificial deformations and transpositions in minerals. Neues Jahrb Miner 45: 121-148

Vinet P, Rose JH, Ferrante J, Smith JR (1989) Universal features of the equation of state of solids. J Phys Cond Matter 1: 1941-1963

Vitek V (1966) Thermally activated motion of screw dislocations in BCC metals. Phys Stat Solidi 18: 687-701

Vitek V (1976) Computer simulation of the screw dislocation motion in bcc metals under the effect of the external shear and uniaxial stresses. Proc R Soc Lond A 352: 109-124

Vogler TJ, Clayton JD (2008) Heterogeneous deformations and spall of an extruded tungsten alloy: plate impact experiments and crystal plasticity modeling. J Mech Phys Solids 56: 297-335

Voigt W (1928) Lehrbuch der Kristallphysik. Teubner, Leipzig

Volterra V (1907) Sur l'équilibre des carps élastiques multiplement connexes. Ann Ecole Norm Sup Paris 24: 401-517

Von Mises R (1913) Mechanik der festen korper im plastich-deformablen zustand. Natchr Ges Wiss Gott: 582-592

Voyiadjis GZ, Abu Al-Rub RK (2003) Thermodynamic based model for the evolution equation of the backstress in cyclic plasticity. Int J Plasticity 19: 2121-2147

Voyiadjis GZ, Abu Al-Rub RK (2005) Gradient plasticity with a variable length scale parameter. Int J Solids Structures 42: 3998-4029

Voyiadjis GZ, Abu Al-Rub RK (2007) Nonlocal gradient-dependent thermodynamics for modeling scale-dependent plasticity. Int J Multiscale Comp Eng 5: 295-323

Voyiadjis GZ, Deliktas B (2009) Theoretical and experimental characterization for the inelastic behavior of the micro-/nanostructured thin films using strain gradient plasticity with interface energy. ASME J Eng Mater Tech 131: 041202

Voyiadjis GZ, Park T (1999) The kinematics of damage for finite strain elasto-plastic solids. Int J Eng Sci 37: 803-830

Voyiadjis GZ, Abu Al-Rub RK, Palazotto AN (2004) Thermodynamic framework for coupling of non-local viscoplasticity and non-local anisotropic viscodamage for dynamic localization problems using gradient theory. Int J Plasticity 20: 981-1038

Vu DK, Steinmann P (2007) Nonlinear electro- and magneto-elastostatics: material and spatial settings. Int J Solids Structures 44: 7891-7905

Wallace DC (1972) Thermodynamics of Crystals. John Wiley and Sons, New York

Wang JN (1996) A microphysical model of Harper-Dorn creep. Acta Mater 44: 855-862

Wang C-C, Truesdell C (1973) Introduction to Rational Elasticity. Noordoff, Leyden

Watanabe T (1989) Grain boundary design for the control of intergranular fracture. Mater Sci Forum 46: 25-48

Weertman J (1955) Theory of steady-state creep based on dislocation climb. J Appl Phys 26: 1213-1217

Weingarten G (1901) Atti Accad naz Lincei Rc 10: 57

Wenk H-R, Canova G, Brechet Y, Flandin L (1997) A deformation-based model for recrystallization of anisotropic materials. Acta Mater 45: 3283-3296

Werne RW, Kelly JM (1978) A dislocation theory of isotropic polycrystalline plasticity. Int J Eng Sci 16: 951-965

Willis JR (1967) Second-order effects of dislocations in anisotropic crystals. Int J Eng Sci 5: 171-190

Winey JM, Gupta YM, Hare DE (2001) R-axis sound speed and elastic properties of sapphire single crystals. J Appl Phys 90: 3109-3111

Wooster WA (1953) Physical properties and atomic arrangements in crystals. Rep Prog Phys 16: 62-82

Wright TW (1982) Stored energy and plastic volume change. Mech Mater 1: 185-187

Wright TW (2002) The Physics and Mathematics of Adiabatic Shear Bands. Cambridge University Press, Cambridge

Wright TW, Ramesh KT (2008) Dynamic void nucleation and growth in solids: a self-consistent statistical theory. J Mech Phys Solids 56: 336-359

Wu X, Kalidindi SR, Necker C, Salem AA (2007) Prediction of crystallographic texture evolution and anisotropic stress-strain curves during large plastic strains in high purity α-titanium using a Taylor-type crystal plasticity model. Acta Mater 55: 423-432

Wyckoff RWG (1963) Crystal Structures. John Wiley and Sons, New York

Xiao, Y, Bhattacharya K (2008) A continuum theory of deformable, semiconducting ferroelectrics. Arch Rat Mech Anal 189: 59-95

Xiao Y, Shenoy VB, Bhattacharya K (2005) Depletion layers and domain walls in semiconducting ferroelectric thin films. Phys Rev Lett 95: 247603

Xie CL, Ghosh S, Groeber M (2004) Modeling cyclic deformation of HSLA steels using crystal plasticity. ASME J Eng Mater Tech 126: 339-352

Xu D-S, Chang J-P, Li J, Yang R, Li D, Yip S (2004) Dislocation slip or deformation twinning: confining pressure makes a difference. Mater Sci Eng A 387-389: 840-844

Yavari A, Marsden JE (2009) Covariant balance laws in continua with microstructure. Rep Math Phys 63: 1-42

Yavari A, Marsden JE, Ortiz M (2006) On spatial and material covariant balance laws in elasticity. J Math Phys 47: 042903

Yavari A, Ortiz M, Bhattacharya K (2007) A theory of anharmonic lattice statics for analysis of defective crystals. J Elasticity 86: 41-83

Yoo MH, Lee JK (1991) Deformation twinning in hcp metals and alloys. Phil Mag A 63: 987-1000

Zaiser M (1998) A generalized composite approach to the flow stress and strain hardening of crystals containing heterogeneous dislocation distributions. Mater Sci Eng A 249: 145-151

Zanzotto G (1992) On the material symmetry group of elastic crystals and the Born rule. Arch Rat Mech Anal 121: 1-36

Zanzotto G (1996) Nonlinear elasticity, the Cauchy-Born hypothesis, and mechanical twinning in crystals. Acta Cryst A 52: 839-849

Zbib HM, Aifantis EC (1992) On the gradient-dependent theory of plasticity and shear banding. Acta Mech 92: 209-225

Zbib HM, De La Rubia TD (2002) A multiscale model of plasticity. Int J Plasticity 18: 1133-1163

Zbib HM, Rhee M, Hirth JP (1998) On plastic deformation and the dynamics of 3D dislocations. Int J Mech Sci 40: 113-127

Zener C (1942) Theory of lattice expansion introduced by cold work. Trans Am Inst Mining Metall Engrs 147: 361-368

Zener C (1948) Elasticity and Anelasticity of Metals. Chicago University Press, Chicago

Zerilli F, Armstrong RW (1987) Dislocation mechanics-based constitutive relations for material dynamics calculations. J Appl Phys 61: 1817-1825

Zhang W, Bhattacharya K (2005) A computational model of ferroelectric domains. Part I: model formulation and domain switching. Acta Mater 53: 185-198

Zhou M (2003) A new look at the atomic level virial stress: on continuum-molecular system equivalence. Proc R Soc Lond A 459: 2347-2392

Zhou M (2005) Thermomechanical continuum representation of atomistic deformation at arbitrary size scales. Proc R Soc Lond A 461: 3437-3472

Zhou M, McDowell DL (2002) Equivalent continuum for dynamically deforming atomistic particle systems. Phil Mag A 82: 2547-2574

Zhou M, Zhai J (2000) Modelling of micromechanical fracture using a cohesive finite element method. In: Furnish MD, Chhabildas LC, Hixson RS (eds) Shock Compression of Condensed Matter, AIP Press, Melville, New York, pp 623-628

Zhou M, Clifton RJ, Needleman A (1994) Finite element simulations of shear localization in plate impact. J Mech Phys Solids 42: 423-458

Ziegler M (1963) Some extremum principles in irreversible thermodynamics, with application to continuum mechanics. In: Sneddon IN, Hill R (eds) Progress in Solid Mechanics, vol 4. North-Holland, Amsterdam, pp 91-193

Zikry MA, Kao M (1996) Inelastic microstructural failure mechanisms in crystalline solids with high angle grain boundaries. J Mech Phys Solids 44: 1765-1798

Zikry MA, Nemat-Nasser S (1990) High strain-rate localization and failure of crystalline materials. Mech Mater 10: 215-237

Zimmerman JA, Gao H, Abraham FF (2000) Generalized stacking fault energies for embedded atom FCC metals. Mod Sim Mater Sci Eng 8: 103-115

Zimmerman JA, Webb III EB, Hoyt JJ, Jones RE, Klein PA, Bammann DJ (2004) Calculation of stress in atomistic simulation. Mod Sim Mater Sci Eng 12: S319-S332

Zimmerman JA, Bammann DJ, Gao H (2009) Deformation gradients for continuum mechanical analysis of atomistic simulations. Int J Solids Structures 46: 238-253

Zorski H (1981) Force on a defect in non-linear elastic medium. Int J Eng Sci 19: 1573-1579

Zubelewicz A (1993) Micromechanical study of ductile polycrystalline metals. J Mech Phys Solids 41: 1711-1722

Zubelewicz A (2008) Metal behavior at extreme loading rates: thermodynamics. Phys Rev B 77: 214111

Zubelewicz A, Maudlin PJ, Gray GT, Zurek AK (2005) Formation of dynamic defect structure in metals subjected to extreme loading conditions. Phys Rev B 71: 104107

Zubov LM (1997) Nonlinear Theory of Dislocations and Disclinations in Elastic Bodies. Springer, Berlin

Index